N71-16538

NASA TECHNICAL MEMORANDUM

NASA TM X-2119

NASA TM X-2119

CASE FILE COPY

SUBSONIC AERODYNAMIC CHARACTERISTICS OF A MODEL OF THE HL-10 FLIGHT RESEARCH VEHICLE WITH BASIC AND MODIFIED TIP FINS

RECEIVED FEB 1971

by Linwood W. McKinney and Jarrett K. Huffman

Langley Research Center
Hampton, Va. 23365

NATIONAL AERONAUTICS AND SPACE ADMINISTRATION • WASHINGTON, D. C. • JANUARY 1971

1. Report No.	2. Government Accession No.	3. Recipient's Catalog No.
NASA TM X-2119		

4. Title and Subtitle	5. Report Date
SUBSONIC AERODYNAMIC CHARACTERISTICS OF A MODEL OF THE HL-10 FLIGHT RESEARCH VEHICLE WITH BASIC AND MODIFIED TIP FINS	January 1971
	6. Performing Organization Code

7. Author(s)	8. Performing Organization Report No.
Linwood W. McKinney and Jarrett K. Huffman	L-7430
	10. Work Unit No.
9. Performing Organization Name and Address	124-07-24-04
NASA Langley Research Center Hampton, Virginia 23365	11. Contract or Grant No.
	13. Type of Report and Period Covered
12. Sponsoring Agency Name and Address	Technical Memorandum
National Aeronautics and Space Administration Washington, D.C. 20546	14. Sponsoring Agency Code

15. Supplementary Notes

16. Abstract

A wind-tunnel investigation has been made at Mach numbers from 0.35 to 0.80 to determine the cause for the loss in lateral control experienced on the basic HL-10 during the first flight. The results of the study indicated that the loss in lateral control was associated with flow separation originating near the leading edge of the outboard fins and spreading over the inner fin surface and elevon controls with increasing angle of attack. Two modifications to the fin leading edge were tested and both modifications were effective in significantly reducing the amount of flow separation and, as a result, the lateral control characteristics were improved.

17. Key Words (Suggested by Author(s))	18. Distribution Statement
HL-10 research vehicle Fin modifications Subsonic performance	Unclassified – Unlimited

19. Security Classif. (of this report)	20. Security Classif. (of this page)	21. No. of Pages	22. Price*
Unclassified	Unclassified	560	$3.00

*For sale by the National Technical Information Service, Springfield, Virginia 22151

SUBSONIC AERODYNAMIC CHARACTERISTICS OF A MODEL OF THE HL-10 FLIGHT RESEARCH VEHICLE WITH BASIC AND MODIFIED TIP FINS

By Linwood W. McKinney and Jarrett K. Huffman
Langley Research Center

SUMMARY

The results of a wind-tunnel investigation of the aerodynamic characteristics of the basic HL-10 configuration and with two leading-edge camber modifications to the tip fins are presented. The investigation covered a Mach number range from 0.35 to 0.90.

The investigation showed that flow separation on the basic HL-10 model correlated to a reasonable degree with indications of flow separation on the basic HL-10 flight vehicle, with auxiliary flaps in the subsonic position. Significant reductions in the regions of flow separation were obtained for either of the two modifications to the tip fins. With the auxiliary flaps in the subsonic position, both fin modifications showed marked improvements in the roll characteristics at Mach numbers from 0.35 to 0.70.

The results of the investigation indicated that the overall static aerodynamic characteristics of the HL-10 with auxiliary flaps in the subsonic position were satisfactory with either of the two fin modifications over the Mach number range from 0.35 to 0.70. With the auxiliary flaps in the transonic position, the static aerodynamic characteristics for both fin modifications are generally equivalent to those of the basic HL-10.

INTRODUCTION

The results of development wind-tunnel tests of models of the HL-10 lifting reentry vehicle concept (ref. 1) indicated regions where the longitudinal stability and control at high subsonic and transonic speeds and the landing performance were marginal. These investigations (refs. 2 to 5) led to auxiliary two-position flaps on the tip fins and upper surface of the elevons and a split rudder on the center fin. These flaps are used to obtain maximum boattailing at landing approach speeds for drag reduction and are deflected outward at high subsonic and transonic speeds to control flow separation and to improve longitudinal stability. The results of wind-tunnel investigations (included in this paper) indicated satisfactory longitudinal characteristics with utilization of these flaps.

The first flight tests of the HL-10 vehicle, however, made with the flaps in the position that resulted in maximum boattailing indicated a deficiency in the lateral control characteristics at sideslip in the Mach number range from 0.50 to 0.65. Specifically, the flight record showed that during turn maneuvers in which a sideslip angle was allowed to develop, the aileron effectiveness decreased to near zero. Additional wind-tunnel tests were made to evaluate the roll control problems experienced on the flight vehicle.

This report presents the results of the wind-tunnel data on the basic HL-10 with two position auxiliary flaps, and the results of tests made with tip fins modified to alleviate the roll control problems experienced on the first flight. The tests were made on a 0.063-scale model and covered a Mach number range from 0.35 to 0.90.

SYMBOLS

The longitudinal data are presented about the stability axes and the lateral data are presented about the body axes. The reference dimensions used in computing the coefficients were model projected area, length, and span. The moment reference used corresponds to the nominal center-of-gravity location of 53-percent body length as shown in figure 1. The symbols used in the paper are defined as follows:

a	speed of sound, ft/sec (m/sec)
b	reference span for yawing- and rolling-moment coefficients
c	reference chord for pitching-moment coefficient
C_D	drag coefficient, $\frac{\text{Drag}}{qS}$
C_L	lift coefficient, $\frac{\text{Lift}}{qS}$
C_l	rolling-moment coefficient, $\frac{\text{Rolling moment}}{qSb}$
C_{l_β}	rolling moment due to sideslip, $\frac{\partial C_l}{\partial \beta}$, per degree
$C_{l_{\delta_a}}$	rolling moment due to aileron deflection, $\frac{\partial C_l}{\partial \delta_a}$, per degree
C_m	pitching-moment coefficient, $\frac{\text{Pitching moment}}{qSc}$
C_n	yawing-moment coefficient, $\frac{\text{Yawing moment}}{qSb}$

C_{n_β}	directional stability parameter, $\frac{\partial C_n}{\partial \beta}$, per degree
$C_{n_{\delta_a}}$	yawing moment due to aileron deflection, $\frac{\partial C_n}{\partial \delta_a}$, per degree
$C_{n_{\delta_r}}$	yawing moment due to rudder deflection, $\frac{\partial C_n}{\partial \delta_r}$, per degree
C_Y	side-force coefficient, $\frac{\text{Side force}}{qS}$
C_{Y_β}	side force due to sideslip, $\frac{\partial C_Y}{\partial \beta}$, per degree
L/D	lift-drag ratio
l	length of vehicle, ft (m)
M	free-stream Mach number, V/a
q	free-stream dynamic pressure, lb/sq in. (N/m^2)
R	Reynolds number
S	reference area, projected planform area of body with elevons, $0.357l^2$
V	free-stream velocity, ft/sec (m/sec)
X, Y, Z	coordinate axes
α	angle of attack, deg
β	angle of sideslip, deg
δ_a	aileron deflection angle, deg
δ_e	elevon deflection angle, positive with trailing edge down, deg
δ_{ef}	elevon flap deflection angle, deg
δ_{if}	tip-fin inner surface flap deflection angle, deg
δ_{of}	tip-fin outer surface flap deflection angle, deg

δ_r rudder deflection angle, deg

θ included angle of rudder cross section, positive when left and right surfaces are divergent, deg

Subscripts:

R right surface

L left surface

trim trimmed condition

MODEL

The model used in this investigation was a 0.063-scale model of the HL-10 lifting-body vehicle. Design concepts for the basic HL-10 are presented in reference 1. Geometric characteristics of the basic HL-10 model are presented in figure 1. In order to obtain improved stability characteristics in the transonic speed range and increased lift-drag ratio on the landing approach, the HL-10 employs two-position flaps on the tip fins and on the upper surface of the elevons and a split rudder on the center fin. Details of these flaps are given in figure 1(b). In the landing-approach configuration, hereafter referred to as the subsonic configuration, the movable surfaces are retracted to provide maximum boattailing on the aft section of the vehicle. Photographs showing the subsonic configuration with maximum boattailing are presented in figures 2(a) and 2(b). In the high subsonic and transonic speed range where the flow on the upper surface of the vehicle becomes sonic, the movable flaps are deflected to minimize flow separation in the region of the control surfaces. The HL-10 in this mode is hereafter referred to as the transonic configuration. Photographs showing the flaps in the transonic configuration are presented in figures 2(c) and 2(d).

In order to improve lateral control characteristics, particularly on the subsonic configuration, two modifications to the fin were tested. The first modification (Mod I) retained the original tip fin planform and outer surface and utilized a built-up inner fin surface to obtain a cambered section in the streamwise direction. A sketch of the Mod I fin section is shown in figure 3(a) and photographs of the fin are shown in figures 3(b) and 3(c). The second tip fin modification (Mod II) had an extended fin leading edge deflected outboard to achieve a cambered inner surface in the streamwise direction. A sketch of the Mod II fin section is shown in figure 4(a) and photographs are shown in figures 4(b) and 4(c).

TEST AND CORRECTIONS

The tests were made in the Langley high-speed 7- by 10-foot wind tunnel over a Mach range from 0.35 to 0.90. The test Reynolds number varied from 2.7×10^6 at a Mach number of 0.35 to 4.0×10^6 at a Mach number of 0.90. (See fig. 5.) All configurations were tested over an angle-of-attack range from 0° to 26° at 0° sideslip and selected configurations were tested at $\pm 5^\circ$ of sideslip over the angle-of-attack range and through a sideslip range from $+8^\circ$ to -8° at selected angles of attack. Corrections due to bending of the sting and balance support system under load have been applied to the angles of attack and sideslip. The jet-boundary corrections to the angles of attack were applied by the method of reference 6. The effect of model blockage was accounted for by the method of reference 7. The drag data presented are uncorrected for base pressure.

PRESENTATION OF RESULTS

The results of the investigation are presented in the following figures:

	Figure
Basic fin configuration:	
Auxiliary flaps in subsonic position:	
Longitudinal characteristics:	
Effect of elevon deflection	6
Effect of aileron deflection	7
Effect of deflecting inner fin surface flap	8
Effect of rudder deflection	9
Effect of combined rudder and sideslip	10
Lateral directional characteristics:	
Effect of aileron deflection	11
Effect of rudder deflection	12
Effect of sideslip	13
Effect of combined rudder and sideslip	14
Effect of sideslip (β sweeps)	15
Auxiliary flaps in transonic position:	
Longitudinal characteristics:	
Effect of elevon deflection	16
Lateral directional characteristics:	
Effect of sideslip angle	17
Effect of aileron deflection	18
Effect of rudder deflection	19

Figure

Modification I fin configuration:
Auxiliary flaps in subsonic position:
Longitudinal characteristics:
Effect of elevon deflection 20
Effect of sideslip angle 21
Effect of aileron deflection 22
Effect of combined aileron and sideslip 23
Lateral directional characteristics:
Effect of aileron deflection 24
Effect of sideslip angle 25
Effect of combined aileron and sideslip 26
Effect of sideslip (β sweep) 27, 28
Auxiliary flaps in transonic position:
Longitudinal characteristics:
Effect of elevon deflection 29
Effect of sideslip angle 30
Effect of aileron deflection 31
Effect of combined aileron and sideslip 32
Lateral directional characteristics:
Effect of aileron deflection 33
Effect of sideslip 34
Effect of combined aileron and sideslip 35
Modification II fin configuration:
Auxiliary flaps in subsonic position:
Longitudinal characteristics:
Effect of elevon deflection 36
Effect of sideslip angle 37
Effect of aileron deflection 38
Lateral directional characteristics:
Effect of aileron deflection 39
Effect of sideslip angle 40
Effect of combined aileron and sideslip 41
Effect of sideslip (β sweeps) 42, 43
Auxiliary flaps in transonic position:
Longitudinal characteristics:
Effect of elevon deflection 44
Effect of sideslip angle 45
Effect of aileron deflection 46
Effect of combined aileron and sideslip 47

Figure

Lateral directional characteristics:
Effect of aileron deflection 48
Effect of sideslip 49
Effect of combined aileron and sideslip 50
Asymmetric deflection of auxiliary flaps:
Longitudinal characteristics . . . . . 51 to 56
Lateral directional characteristics . . . . . 57 to 62
Summary results:
Auxiliary flaps in the subsonic position:
Variation of rolling-moment coefficient with sideslip angle for basic fin configuration 63
Variation of rolling- and yawing-moment coefficients with sideslip angle for modification I fin configuration 64, 65
Variation of rolling- and yawing-moment coefficients with sideslip angle for modification II fin configuration 66, 67
Comparison of the trimmed lateral control characteristics for the three tip fin configurations 68
Comparison of the trimmed lateral directional stability characteristics for the three tip fin configurations 69
Comparison of the trimmed longitudinal characteristics for the three tip fin configurations 70
Auxiliary flaps in the transonic position:
Variation of rolling- and yawing-moment coefficients with sideslip angle for modification I fin configuration 71
Variation of rolling- and yawing-moment coefficients with sideslip angle for modification II fin configuration 72
Comparison of the trimmed lateral directional stability characteristics for the three tip fin configurations 73
Comparison of the trimmed lateral control characteristics for the three tip fin configurations 74
Comparison of the trimmed longitudinal characteristics for the three tip fin configurations 75

DISCUSSION

This paper presents the results of wind-tunnel tests made to evaluate configuration changes for the HL-10 lifting-body research vehicle. These changes were aimed at aerodynamic refinements in three specific areas. These areas are (1) improvement of lift-drag ratio for landing approach (figs. 6 to 15), (2) improvement of longitudinal stability at

high subsonic speeds (figs. 16 to 19), and (3) improvement of lateral control characteristics (figs. 20 to 50).

The development of the two-position auxiliary flaps and the extent to which these flaps were effective in improving the lift-drag ratio for landing approach and the longitudinal stability at high subsonic speeds are discussed in detail in references 2 to 5. The discussion presented here is primarily concerned with the development of the fin modifications for improved lateral control.

Subsonic Configuration

Lateral directional characteristics.- As pointed out in the Introduction, the first flight tests of the HL-10 lifting-body research vehicle indicated a deficiency in the lateral control characteristics at sideslip with the flaps in the subsonic position (subsonic configuration) at Mach numbers from 0.50 to 0.65, at an angle of attack of approximately 17°. Wind-tunnel tests were made at an angle of attack of 17° through a range of sideslip angles for longitudinal control settings δ_e from -5° to -20° at Mach numbers from 0.35 to 0.80. The variation of C_l with β for these tests is shown in figure 63 for $\delta_a = 0^{\circ}$ and $\delta_a = 10^{\circ}$. The range of pitch control deflections δ_e are those required for trim at angles of attack from approximately -1° at $\delta_e = -5^{\circ}$ to 28° at $\delta_e = -20^{\circ}$. A value of $\delta_e = -15^{\circ}$ is near the required value for trim for the data of figure 63. Although a complete loss of roll control is not shown in the data of figure 63 at Mach numbers of 0.7 and below, irregularities in the rolling-moment characteristics are apparent at sideslip conditions. Visual observations of the boundary-layer flow by use of a fluorescent oil technique showed that regions of separated flow existed over the inner fin surface and pitch controls. Boundary-layer flow observations made during other tests indicated the separated flow originated near the fin leading edge and spread over nearly the entire inner surface of the tip fins as the angles of attack were increased to the moderately high angles of interest. It was also observed that the flow separation spread to envelop the elevons to a varying degree, dependent on the sideslip angle. Since the separated flow appeared to originate near the fin leading edge, two modifications to the tip-fin airfoil section which reduced the local slopes in the region of the fin leading edge were tested. (See figs. 3 and 4.) Both modifications were effective in significantly reducing the amount of flow separation on the inner fin surface and elevons.

The variations of rolling- and yawing-moment coefficient with sideslip angle at several elevon settings for fin modification I (Mod I) at an angle of attack of 17° are shown in figure 64. A comparison of the rolling-moment data of figure 64 with the data of figure 63 indicates improvements over the basic HL-10 in both rolling effectiveness of the ailerons and the linearity of the variation of C_l with β for Mach numbers from 0.35 to 0.70. The data also indicate satisfactory yawing-moment characteristics

(figs. 64(f) to 64(j)). The variation of C_l and C_n with β at $\alpha = 7^o$ for Mod I is shown in figure 65, for an elevon angle of $\delta_e = -10^o$ which is near the value required for trim at this angle of attack. Comparable data for the basic HL-10 were not obtained but the level of rolling effectiveness with sideslip appears to be satisfactory at Mach numbers of 0.70 and below.

The variation of rolling moment and yawing moment with sideslip for Mod II is shown in figures 66 and 67 for $\alpha = 17^o$ and $\alpha = 7^o$, respectively. A comparison of these data with the data of figure 63 indicates essentially the same level of improvement in rolling effectiveness with sideslip angle over the basic HL-10 configuration as did Mod I. The roll control effectiveness is unsatisfactory for both modifications at a Mach number of 0.80.

The effects of the fin modifications on lateral control characteristics through the angle-of-attack range are summarized in figure 68 as plots of $C_{l_{\delta_a}}$ and $C_{n_{\delta_a}}$ against trimmed angle of attack at $\beta = 0^o$ and $\pm 2.5^o$. Improvements in the lateral control effectiveness $C_{l_{\delta_a}}$ over the basic configuration are shown for both fin modifications at $\beta = 0^o$. The modified fin configurations show only small effects of sideslip on the roll control effectiveness at Mach numbers from 0.35 to 0.60. At a Mach number of 0.70, a significant reduction of roll control effectiveness at moderate angles of attack is noted, particularly at positive β. Mod II appears slightly superior to Mod I in this respect. Although the variation of $C_{l_{\delta_a}}$ just discussed appears to be satisfactory, examination of the basic data indicates that the value of $C_{l_{\delta_a}}$ depends on elevator angle, sideslip angle, and the range of aileron angles considered, and that localized regions of zero roll control effectiveness exist at $M = 0.70$ for both modifications at out-of-trim elevon settings. Comparable data for the basic HL-10 were not obtained.

The lateral directional stability parameters C_{l_β} and C_{n_β} of both modifications are compared with the basic HL-10 in figure 69 through the Mach number range as a function of trimmed angle of attack. The trends of C_{n_β} with angle of attack shown in the basic data are depicted in the fairing of the trimmed points. The lateral directional characteristics for the two modifications appear to be satisfactory. The characteristics of Mod II are roughly equivalent to those of the basic HL-10 whereas Mod I shows somewhat lower directional stability at low to moderate angles of attack. The trimmed points for the basic HL-10 are not sufficient for a detailed comparison.

Longitudinal characteristics.- The longitudinal characteristics are summarized as curves of trimmed values of L/D, C_L, and δ_e required for trim and are compared in figure 70. Both modifications resulted in higher maximum values of L/D, presumably because of reduced flow separation, although both modifications required larger trailing-edge-up elevon settings for trim than the basic fin configuration.

Transonic Configuration

Lateral directional characteristics.- The variation of C_l and C_n with β is shown in figure 71 at $\alpha = 7^o$ and $\alpha = 17^o$ for the Mod I fin configuration with the auxiliary flaps in the transonic position. The elevon settings were near trim for the respective angles of attack. The variations of rolling- and yawing-moment coefficients with β are linear and the roll control power appears to be adequate. Comparable data for the Mod II fin configuration are shown in figure 72 for $\alpha = 17^o$ and indicate about the same trends.

The lateral directional parameters as a function of trimmed angle of attack are summarized in figure 73. These data indicate that both fin modifications result in lateral directional characteristics for the transonic configuration that are about equivalent to the basic configuration. The Mod I configuration, however, generally has lower static directional stability. The lateral control parameters $C_{l_{\delta a}}$ and $C_{n_{\delta a}}$ are summarized in figure 74 for Mod I and Mod II, respectively. No significant effect of the fin modifications on $C_{l_{\delta a}}$ is shown at Mach numbers of 0.80 and below; however, at $M = 0.90$ the curve at $\beta = -2.5^o$ (fig. 74(a)) for Mod I appears to be somewhat low in the trimmed angle-of-attack range from about 10^o to 20^o.

Longitudinal characteristics.- The effects of fin modifications on the longitudinal characteristics of the transonic configuration are summarized in figure 75. No significant changes in L/D and trimmed C_L are shown as a result of fin modification. Both modifications require larger positive δ_e (trailing edge up) for trim.

SUMMARY OF RESULTS

A wind-tunnel investigation of the aerodynamic characteristics of the basic HL-10 configuration and with two leading-edge camber modifications to the tip fins has been made and the following results are indicated:

1. The basic HL-10 with auxiliary flaps in the subsonic position showed areas of flow separation which correlated to a reasonable degree with indications of flow separation on the basic HL-10 flight vehicle.

2. With the auxiliary flaps in the subsonic position, both fin modifications showed marked improvements in roll control effectiveness and the variation of rolling moment with sideslip for Mach numbers 0.35 to 0.70 compared with the basic HL-10. With either fin modification, however, the roll control effectiveness at a Mach number of 0.70 is considerably less than that at the lower Mach numbers. At a Mach number of 0.80, the roll control effectiveness is unsatisfactory with both modifications.

3. With the exception of directional stability, neither fin modification showed any degradation in static aerodynamic characteristics over the basic HL-10 for the auxiliary flaps in the subsonic position. In some cases, however, the data for the modifications are more complete than the data for the basic HL-10 and detailed comparisons are not possible.

4. The directional stability for fin modification II was essentially equivalent to that of the basic HL-10. Fin modification I caused some reduction in directional stability at low and moderate angles of attack.

5. Both of the fin modifications showed significant reductions of the regions of flow separation on the wind-tunnel model with auxiliary flaps in the subsonic position.

6. The static aerodynamic characteristics of the HL-10 with both modified fin configurations and the auxiliary flaps in the transonic position are generally equivalent to the basic HL-10 with the exception of roll control effectiveness. Fin modification I shows a loss in roll control effectiveness at a Mach number of 0.90 at negative sideslip angles. Modification II, however, shows no significant effect of sideslip on roll control effectiveness.

7. The overall static aerodynamic characteristics of the HL-10 with the auxiliary flaps in the subsonic position are indicated by the wind-tunnel results to be satisfactory with either of the two fin modifications over the Mach number range from 0.35 to 0.70. Modification II appears to be superior to modification I in several minor respects.

8. With the auxiliary flaps in the transonic position, the data indicate modification II to be superior to modification I in roll control effectiveness at Mach numbers from 0.60 to 0.90.

The fin modification designated herein as modification II has been incorporated on the HL-10 lifting-body flight research vehicle.

Langley Research Center,
National Aeronautics and Space Administration,
Hampton, Va., September 23, 1970.

REFERENCES

1. Rainey, Robert W.: Summary of an Advanced Manned Lifting Entry Vehicle Study. NASA TM X-1159, 1965.

2. Spencer, Bernard, Jr.: An Investigation of Methods of Improving Subsonic Performance of a Manned Lifting Entry Vehicle. NASA TM X-1157, 1965.

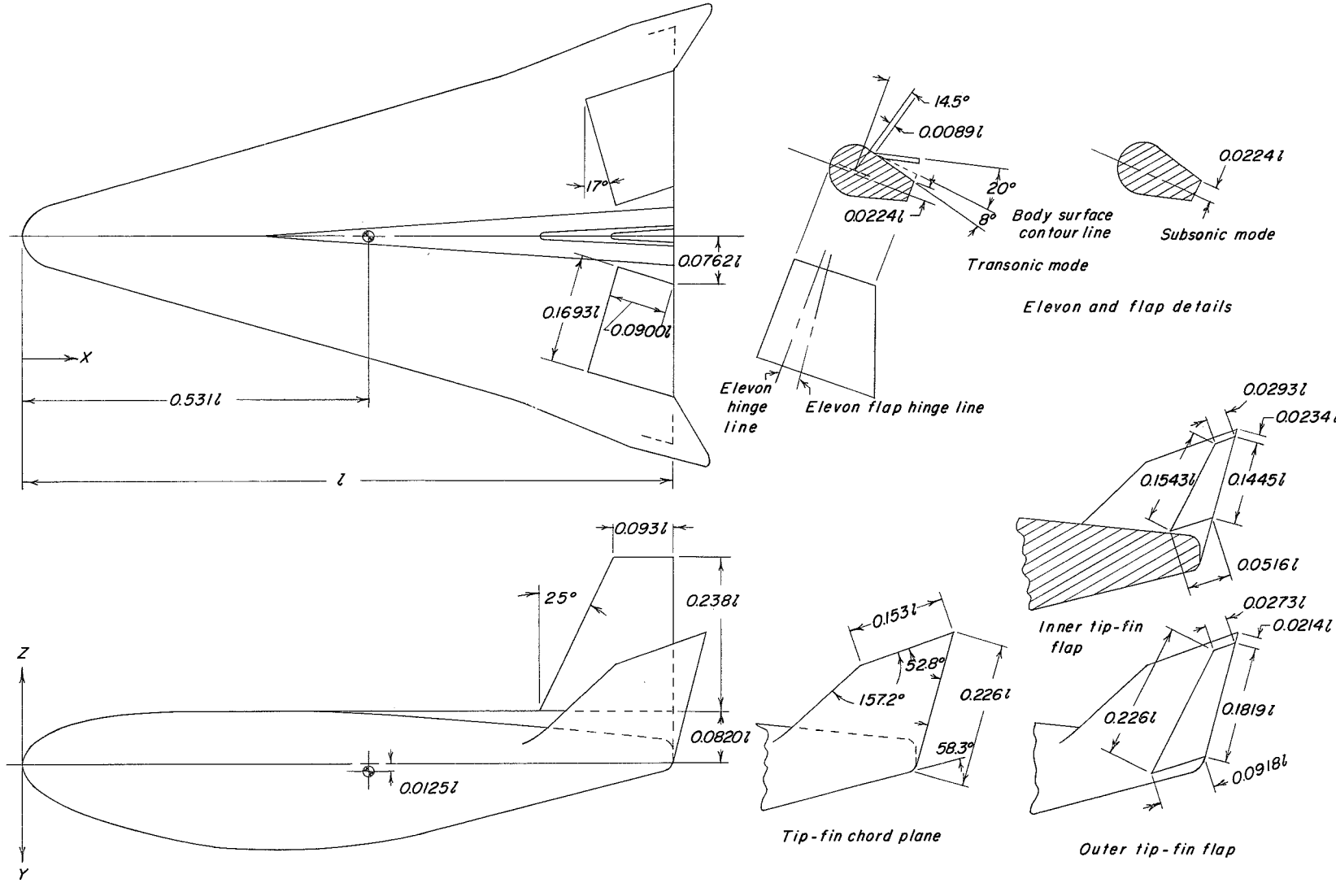
3. Spencer, Bernard, Jr.; and Fox, Charles H., Jr.: Subsonic Longitudinal Control Characteristics of Several Elevon Configurations for a Manned Lifting Entry Vehicle. NASA TM X-1227, 1966.

4. Spencer, Bernard, Jr.: Effects of Elevon Planform on Low-Speed Aerodynamic Characteristics of the HL-10 Manned Lifting Entry Vehicle. NASA TM X-1409, 1967.

5. Henderson, William P.: Static Stability Characteristics of a Manned Lifting Entry Vehicle at High Subsonic Speeds. NASA TM X-1349, 1967.

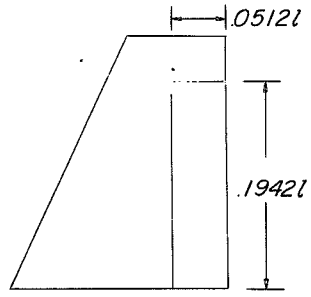
6. Gillis, Clarence L.; Polhamus, Edward C.; and Gray, Joseph L., Jr.: Charts for Determining Jet-Boundary Corrections for Complete Models in 7- by 10-Foot Closed Rectangular Wind Tunnels. NACA WR L-123, 1945. (Formerly NACA ARR L5G31.)

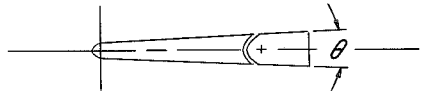
7. Herriot, John G.: Blockage Corrections for Three-Dimensional-Flow Closed-Throat Wind Tunnels With Consideration of the Effect of Compressibility. NACA Rep. 995, 1950. (Supersedes NACA RM A7B28.)



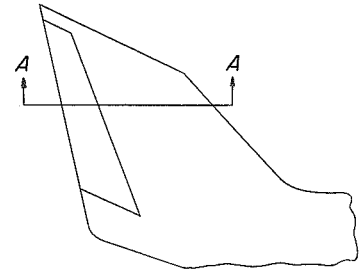
(a) Basic dimensions.

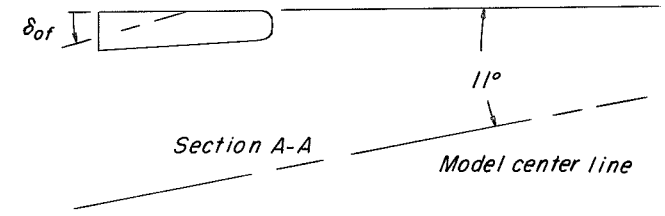
Figure 1.- Geometric characteristics of basic HL-10 model.



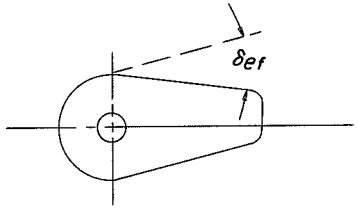


Rudder detail

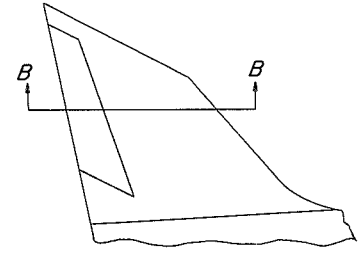


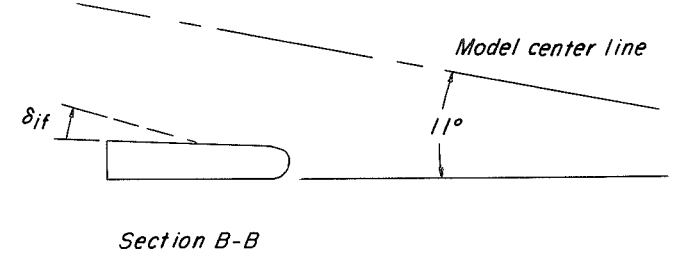


Tip-fin outer surface detail



Elevon flap detail



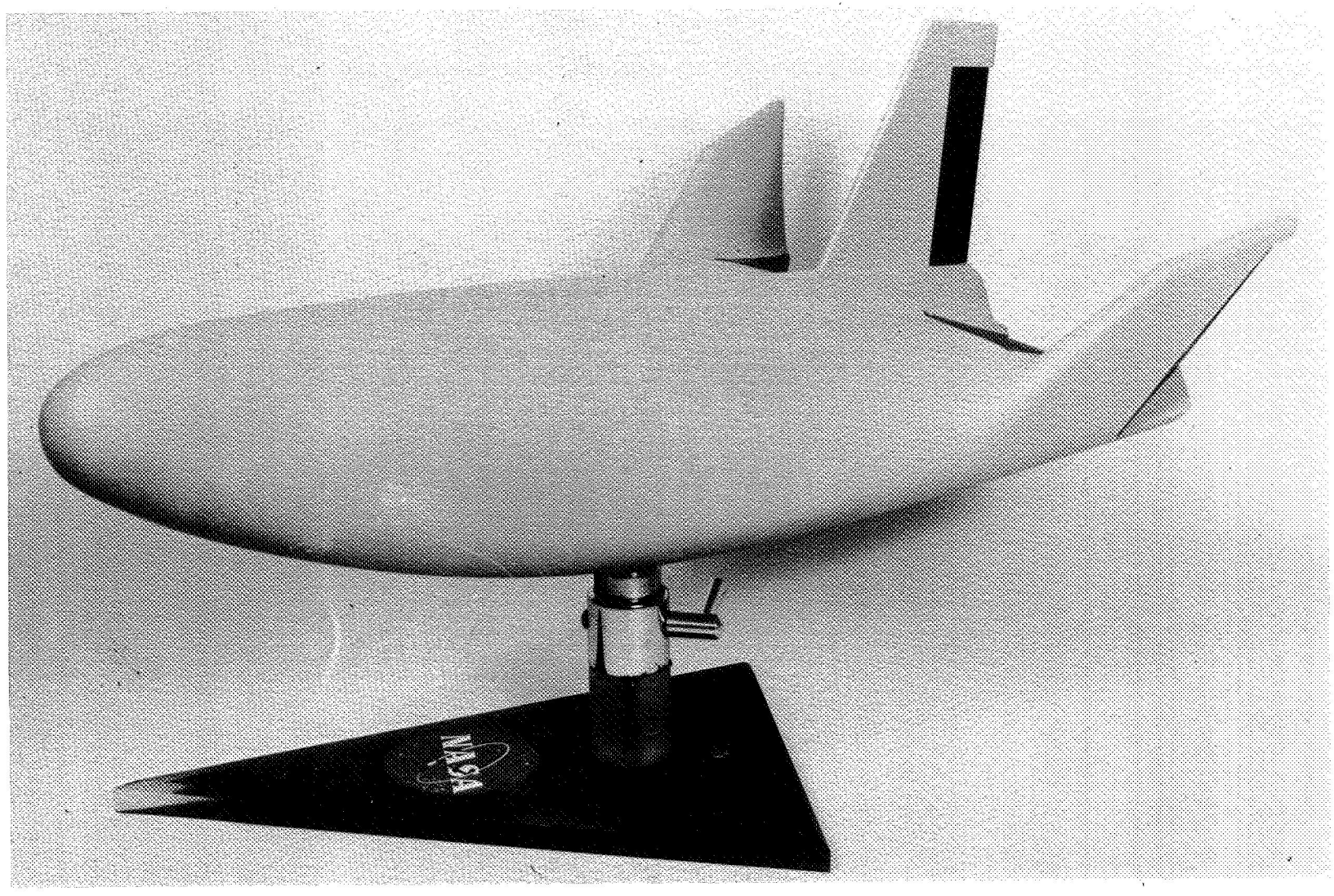


Tip-fin inner surface detail

Flap details

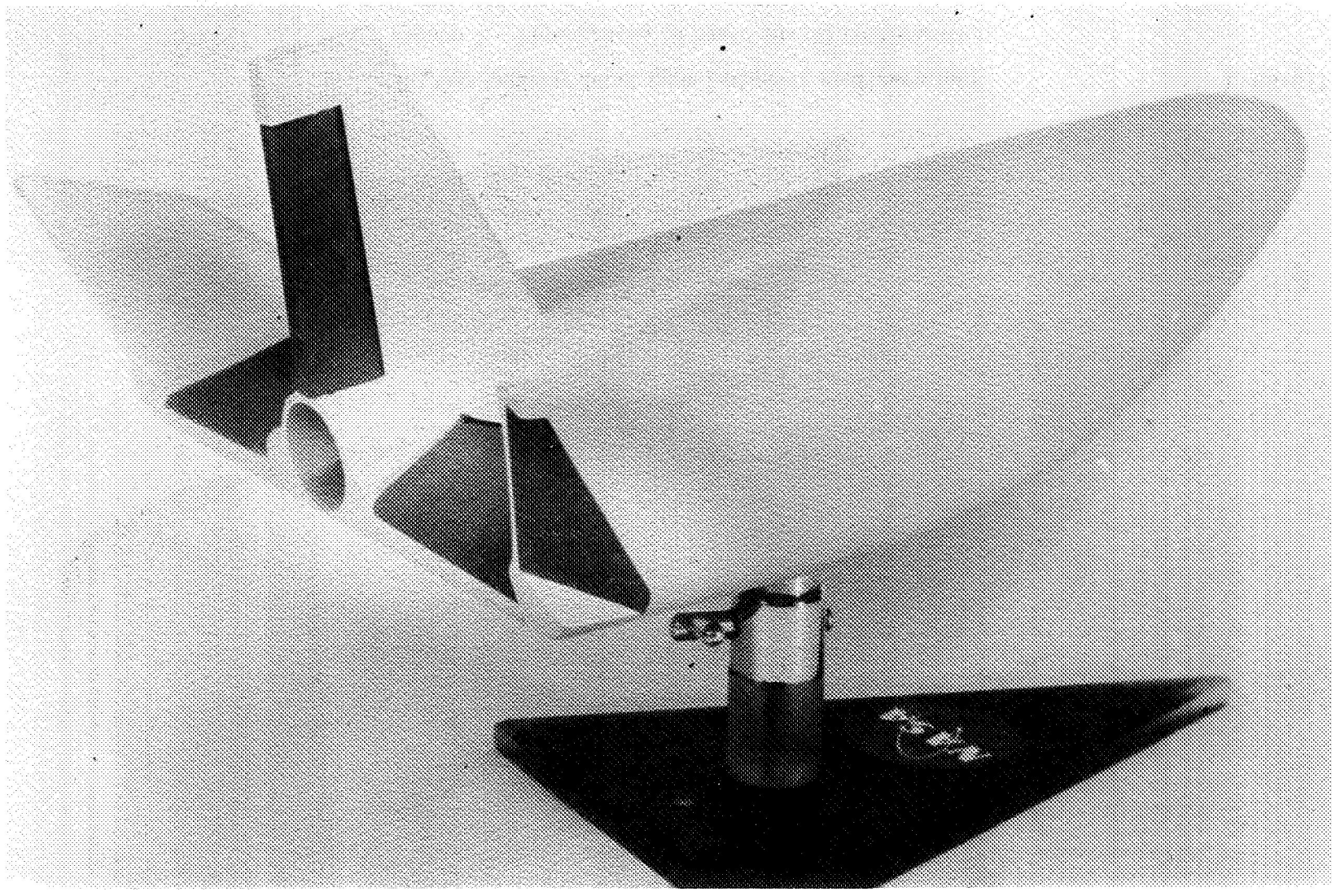
(b) Details of flap hinge lines.

Figure 1.- Concluded.



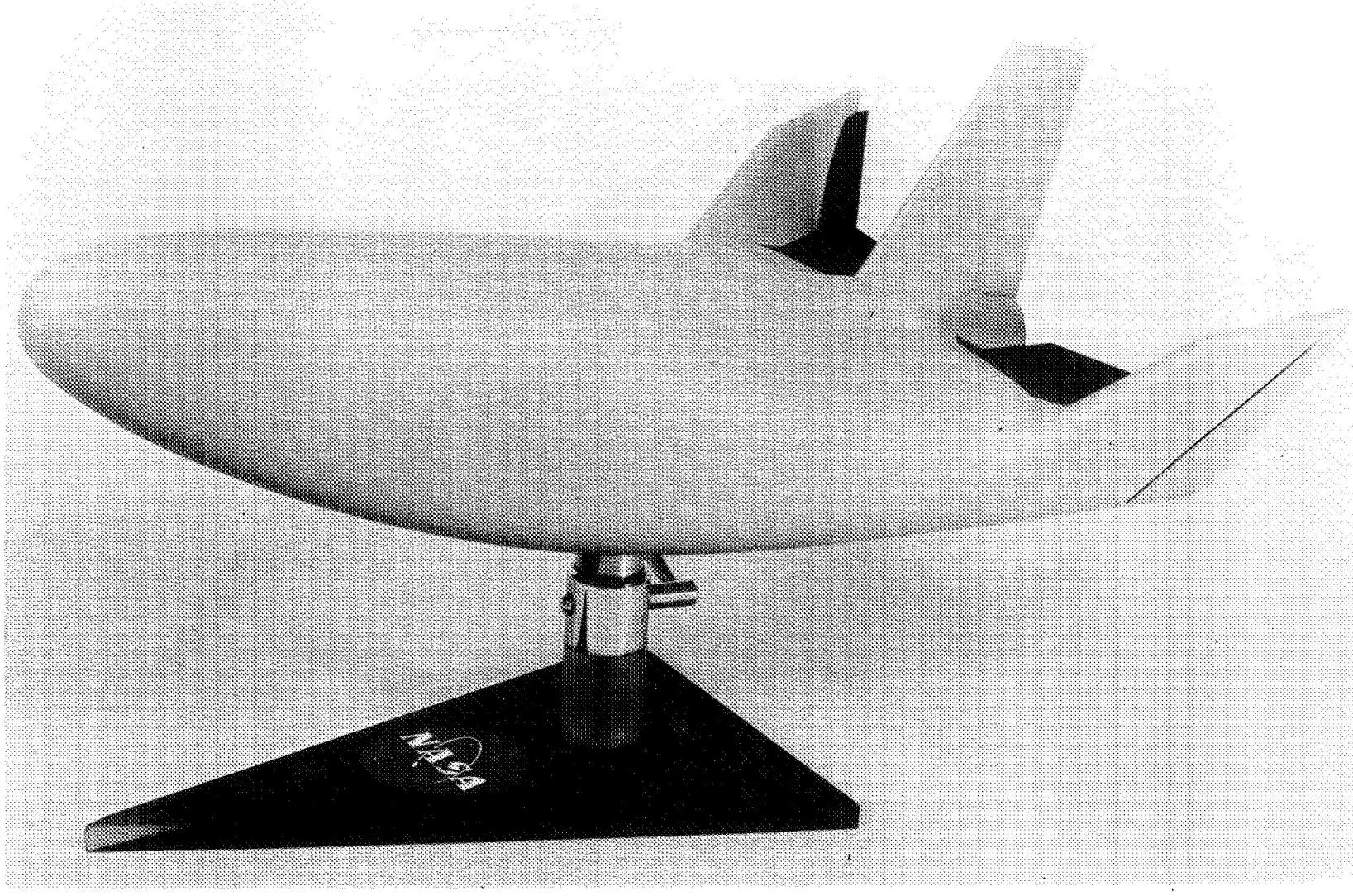
(a) One-quarter front view (subsonic configuration). L-65-6177

Figure 2.- Photographs of basic HL-10 configuration.



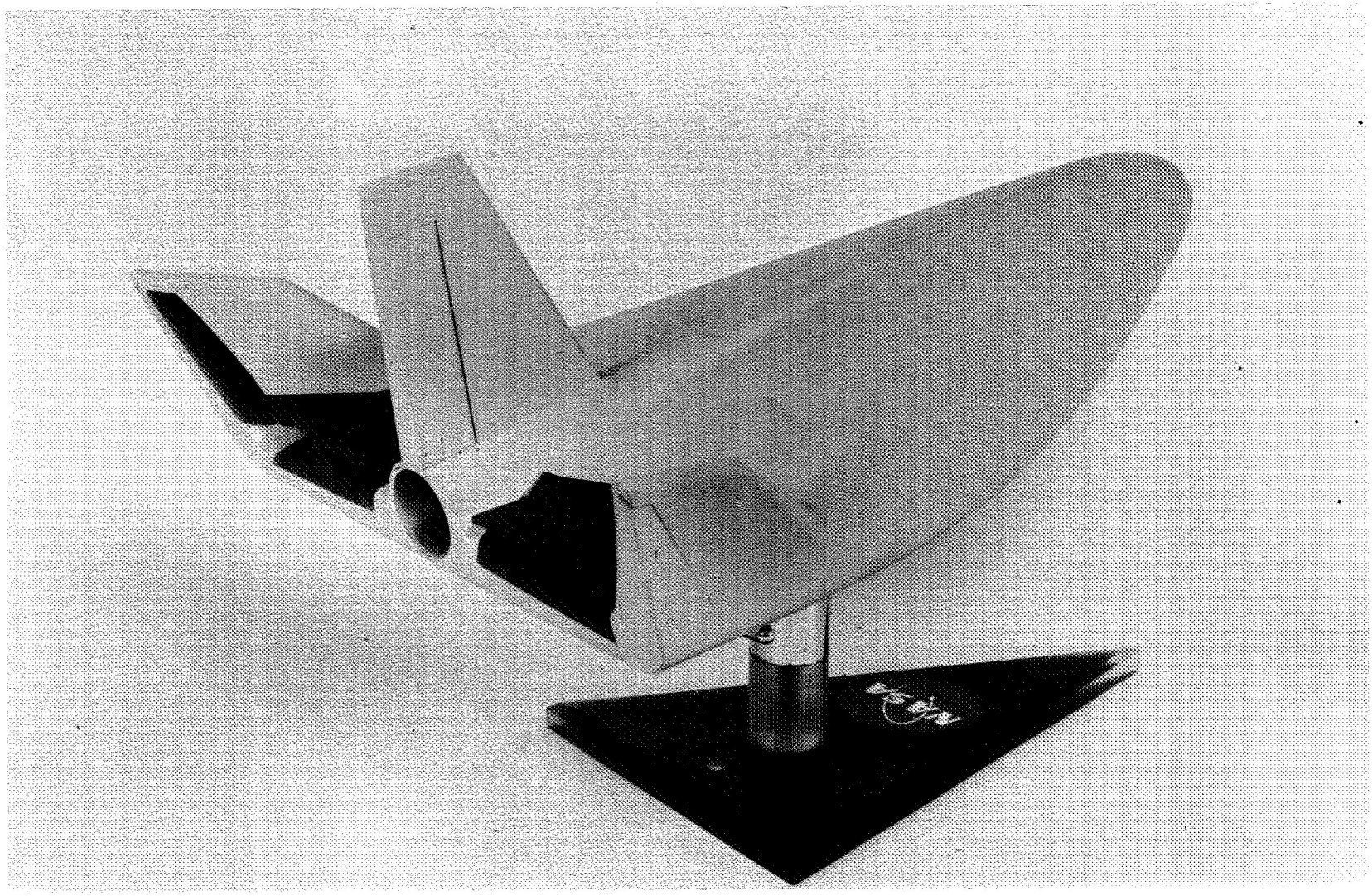
(b) Three-quarter rear view (subsonic configuration). L-65-6178

Figure 2.- Continued.



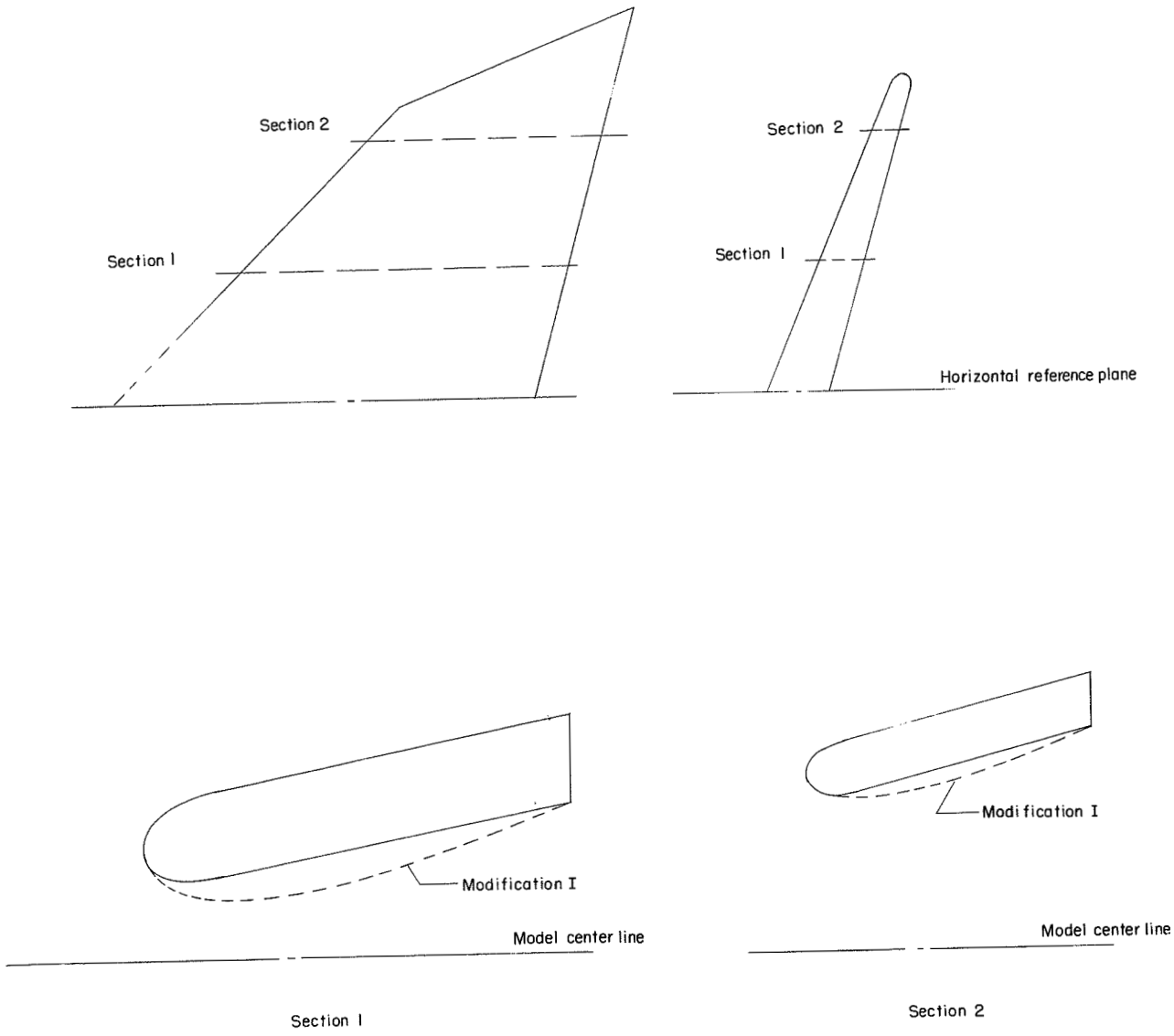
(c) One-quarter front view (transonic configuration). L-65-6175

Figure 2.- Continued.



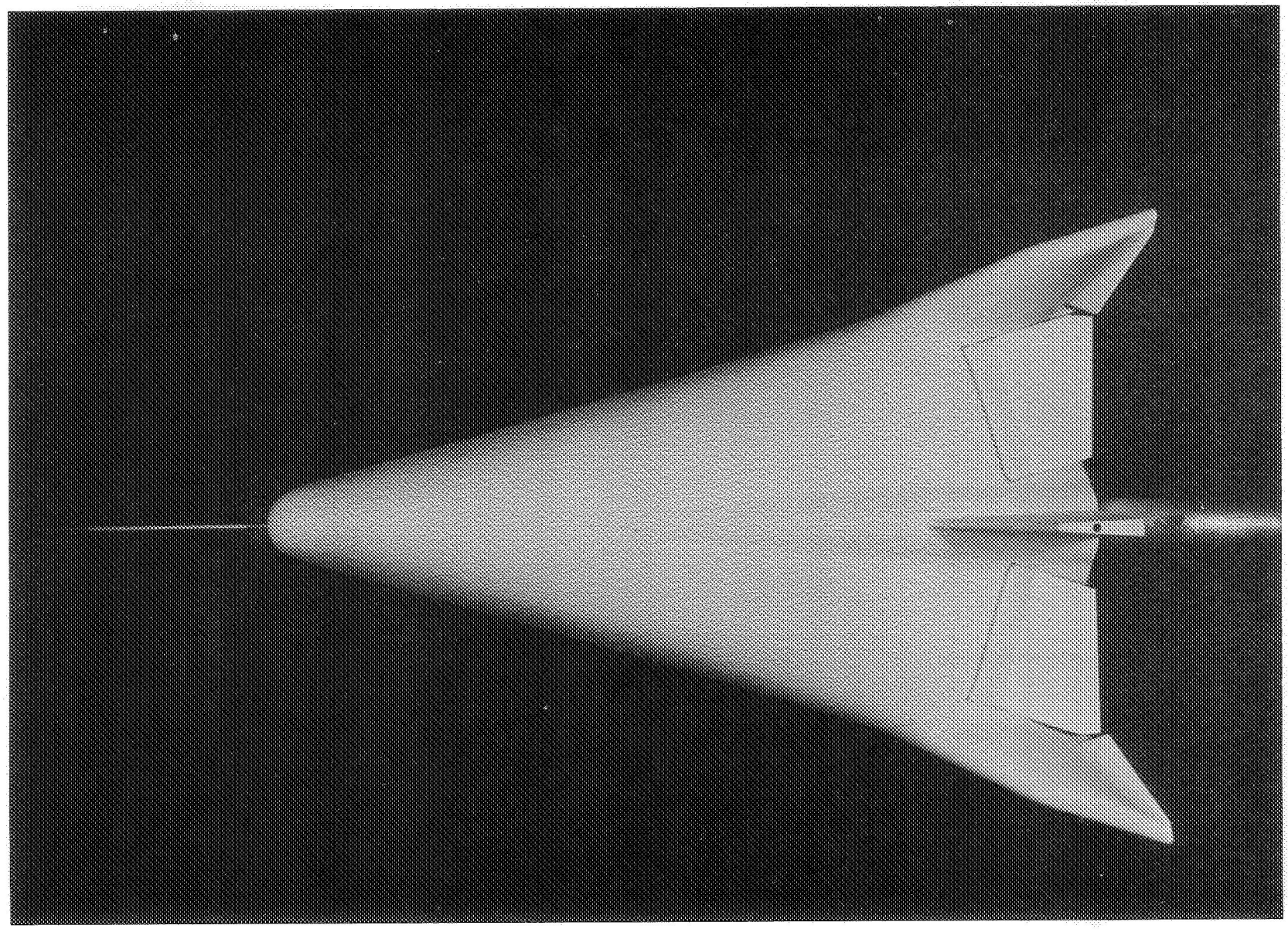
(d) Three-quarter rear view (transonic configuration). L-65-6176

Figure 2.- Concluded.



(a) Typical sections.

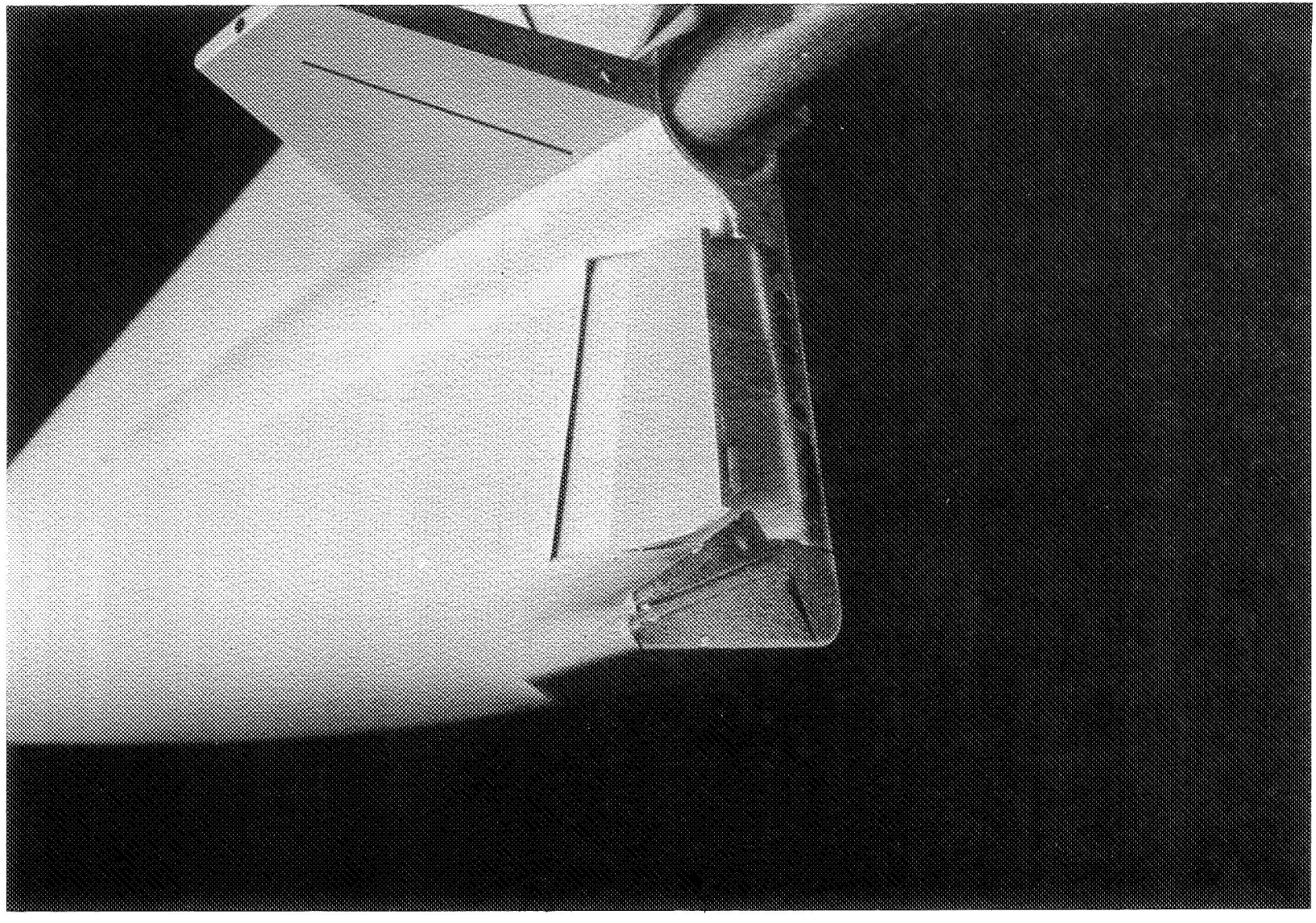
Figure 3.- HL-10 tip fin modification I.



L-68-5266

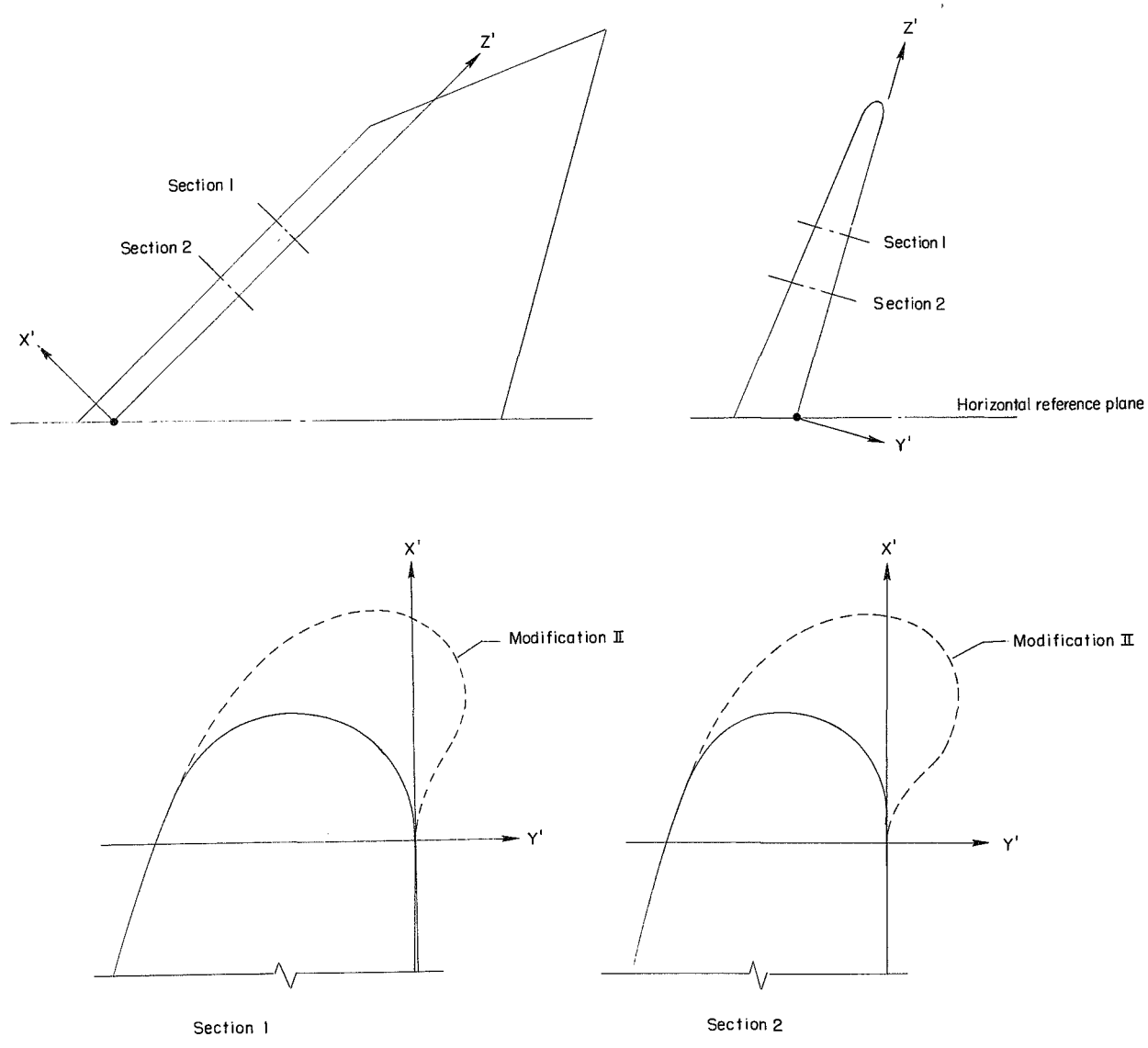
(b) HL-10 model with modification I fins.

Figure 3.- Continued.



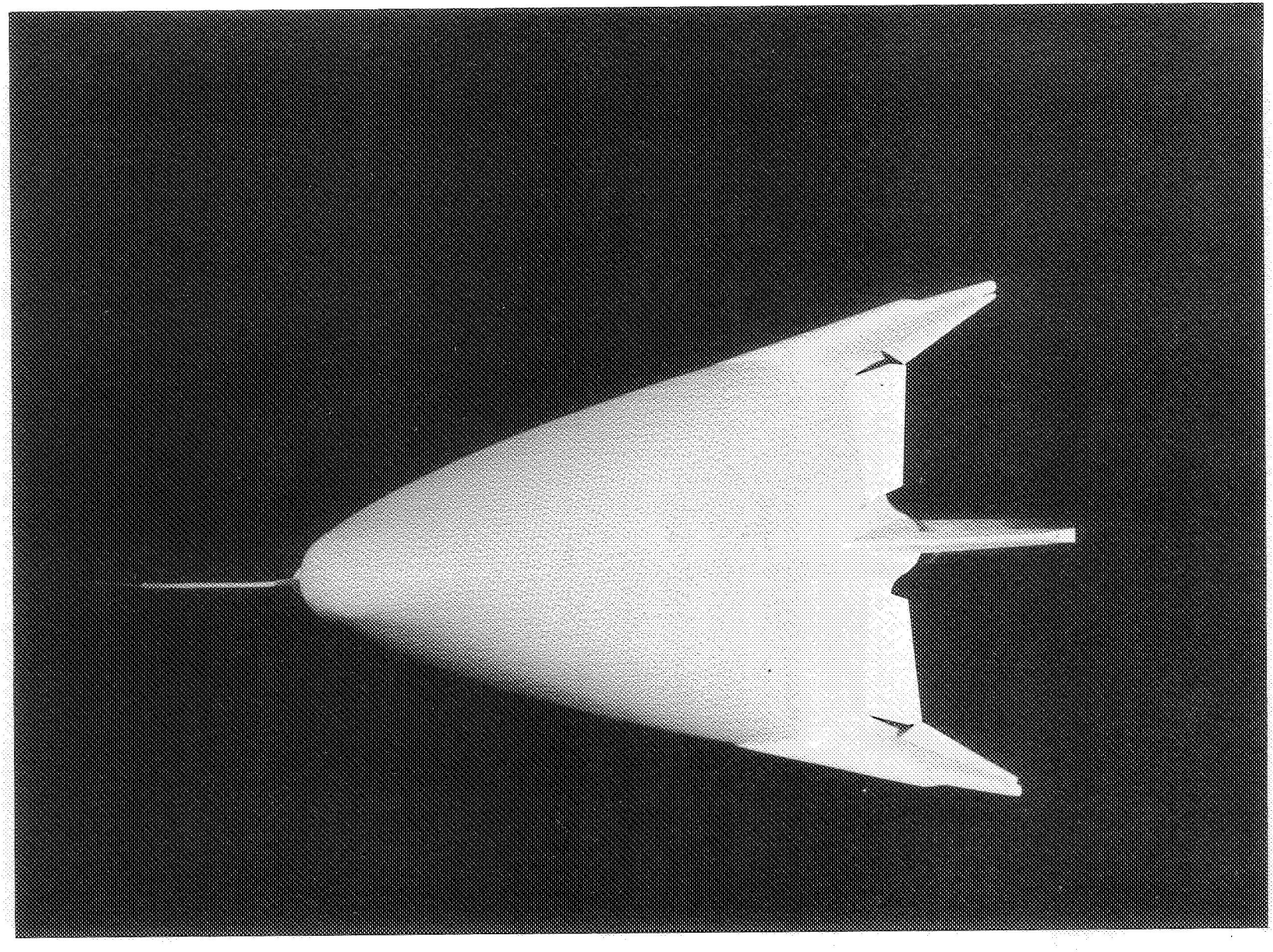
(c) Closeup of modification I fin. L-68-5269

Figure 3.- Concluded.



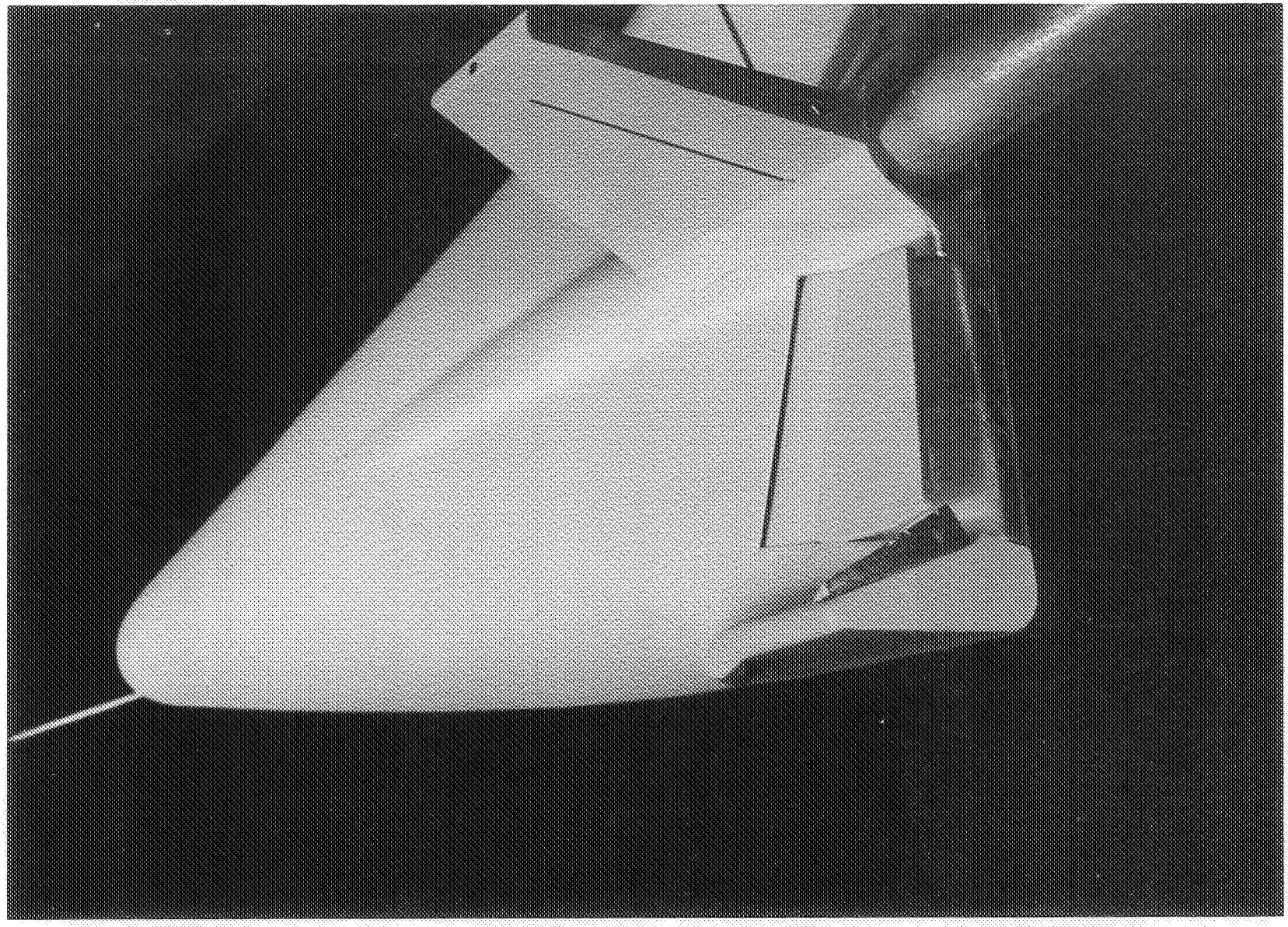
(a) Typical section.

Figure 4.- HL-10 tip fin modification II.



(b) HL-10 model with modification II fins. L-68-5268

Figure 4.- Continued.



(c) Closeup of modification II fins. L-70-4782

Figure 4.- Concluded.

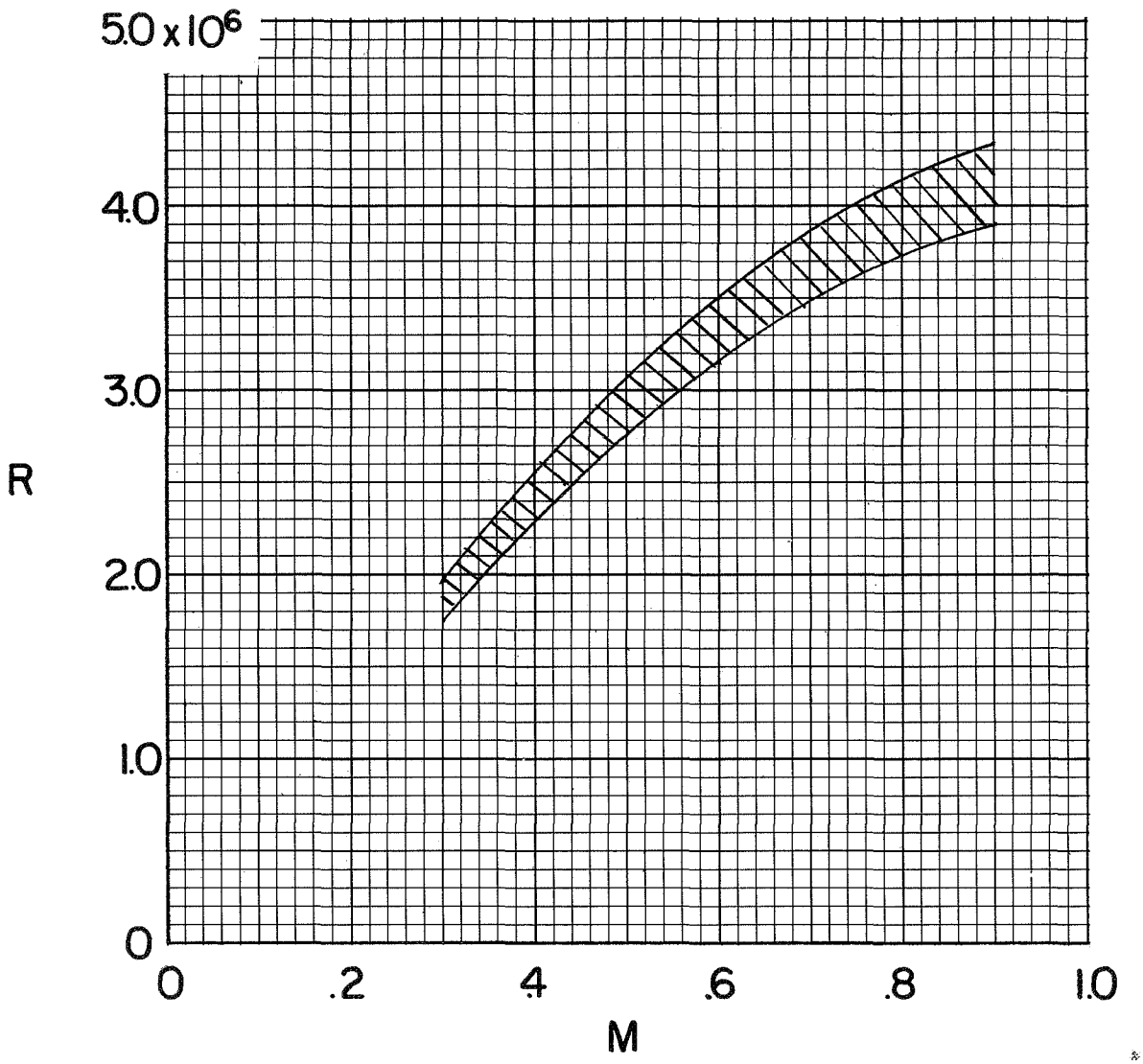
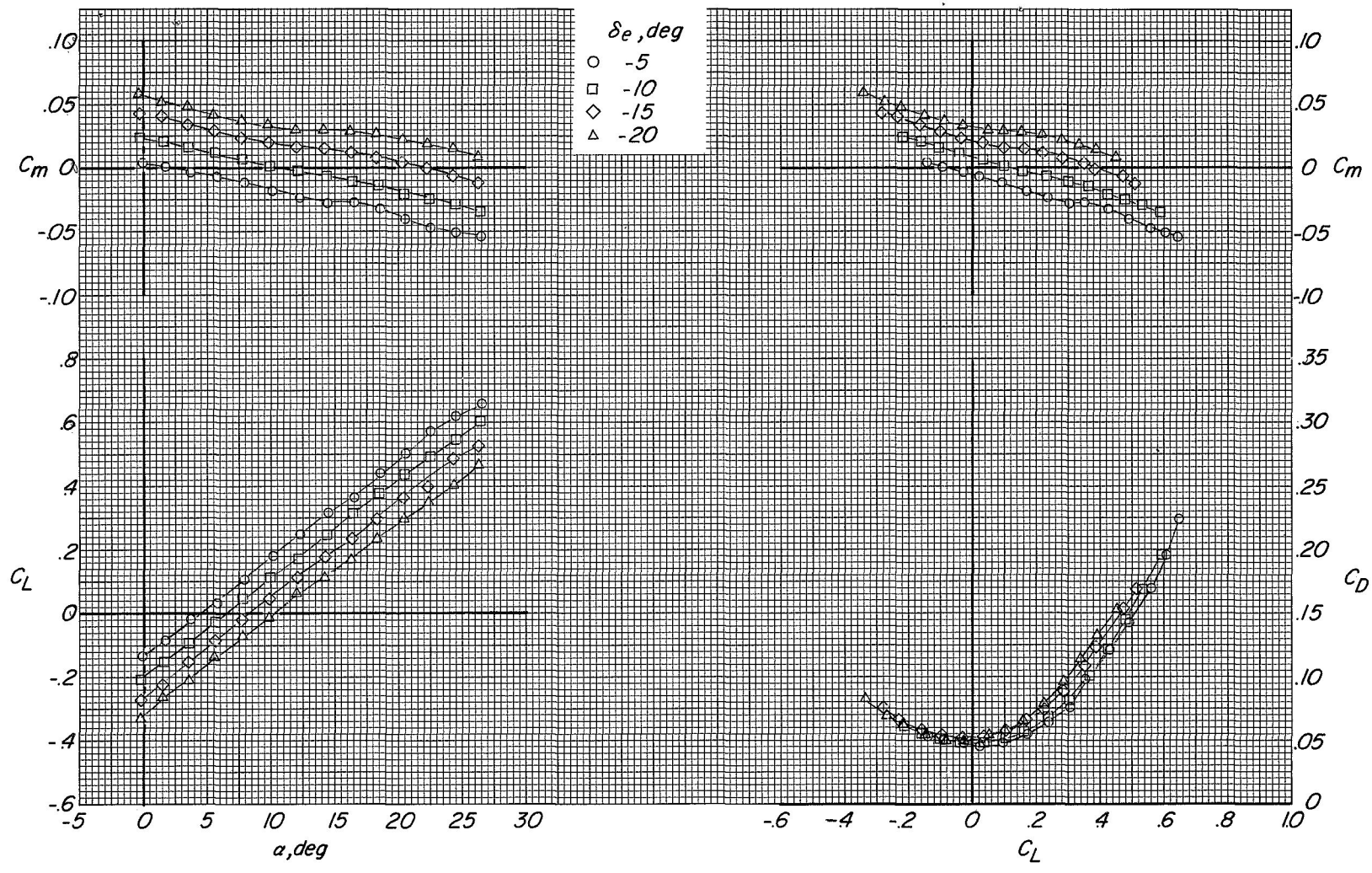
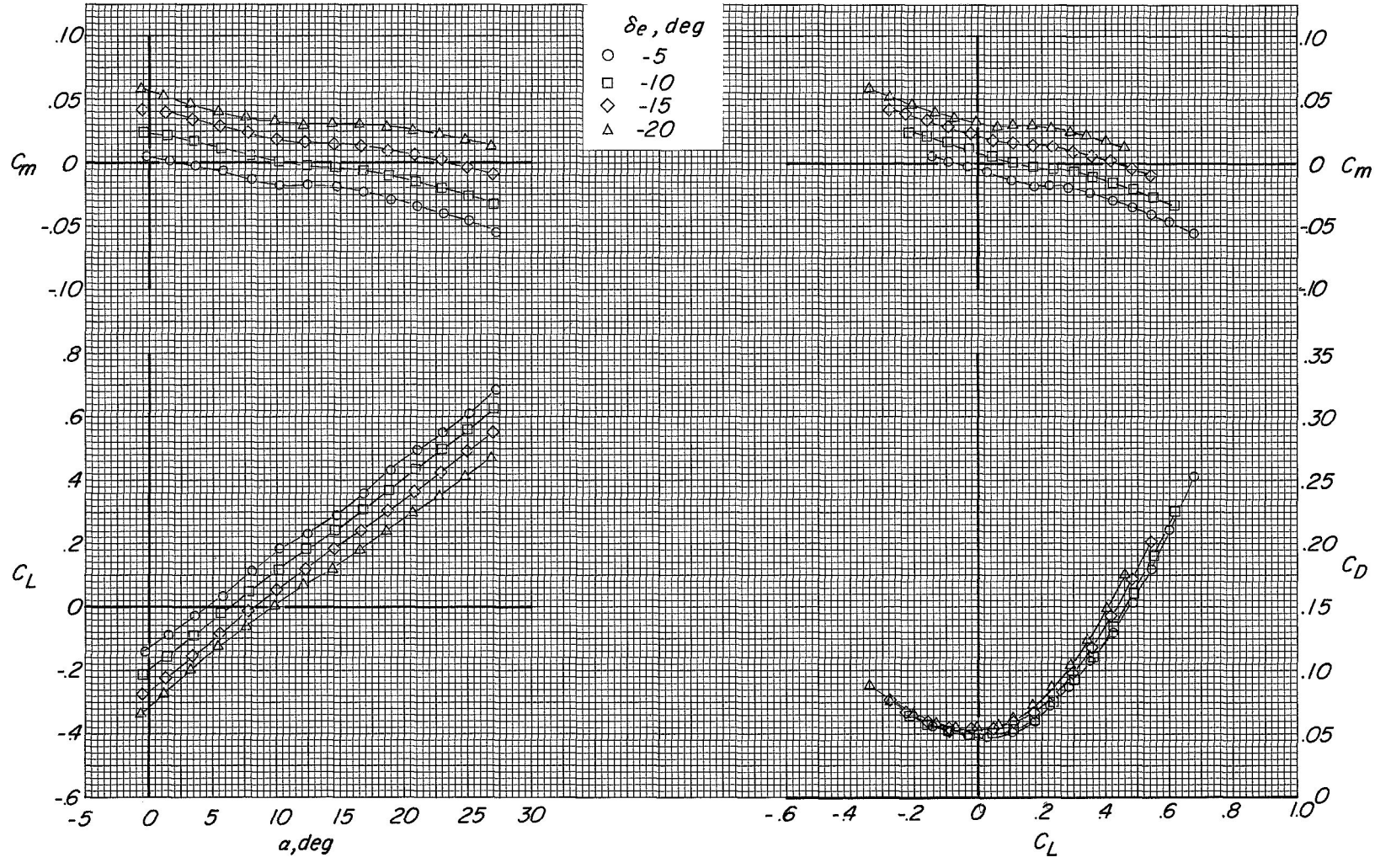


Figure 5.- Variation of test Reynolds number with Mach number.



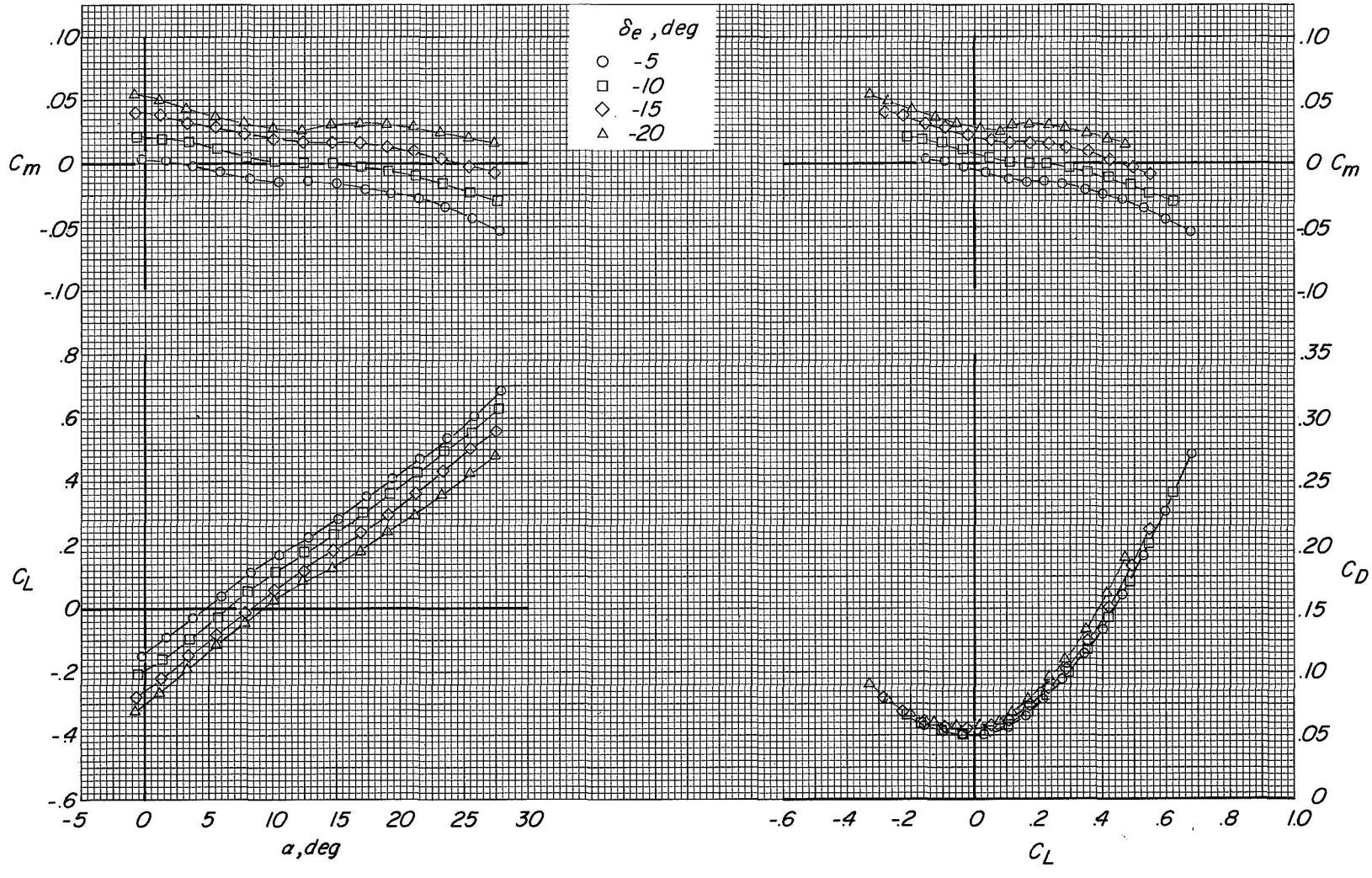
(a) M = 0.35.

Figure 6.- Longitudinal characteristics of the model with basic fin configuration. Auxiliary flaps in the subsonic position; $\delta_a = \beta = 0^o$.



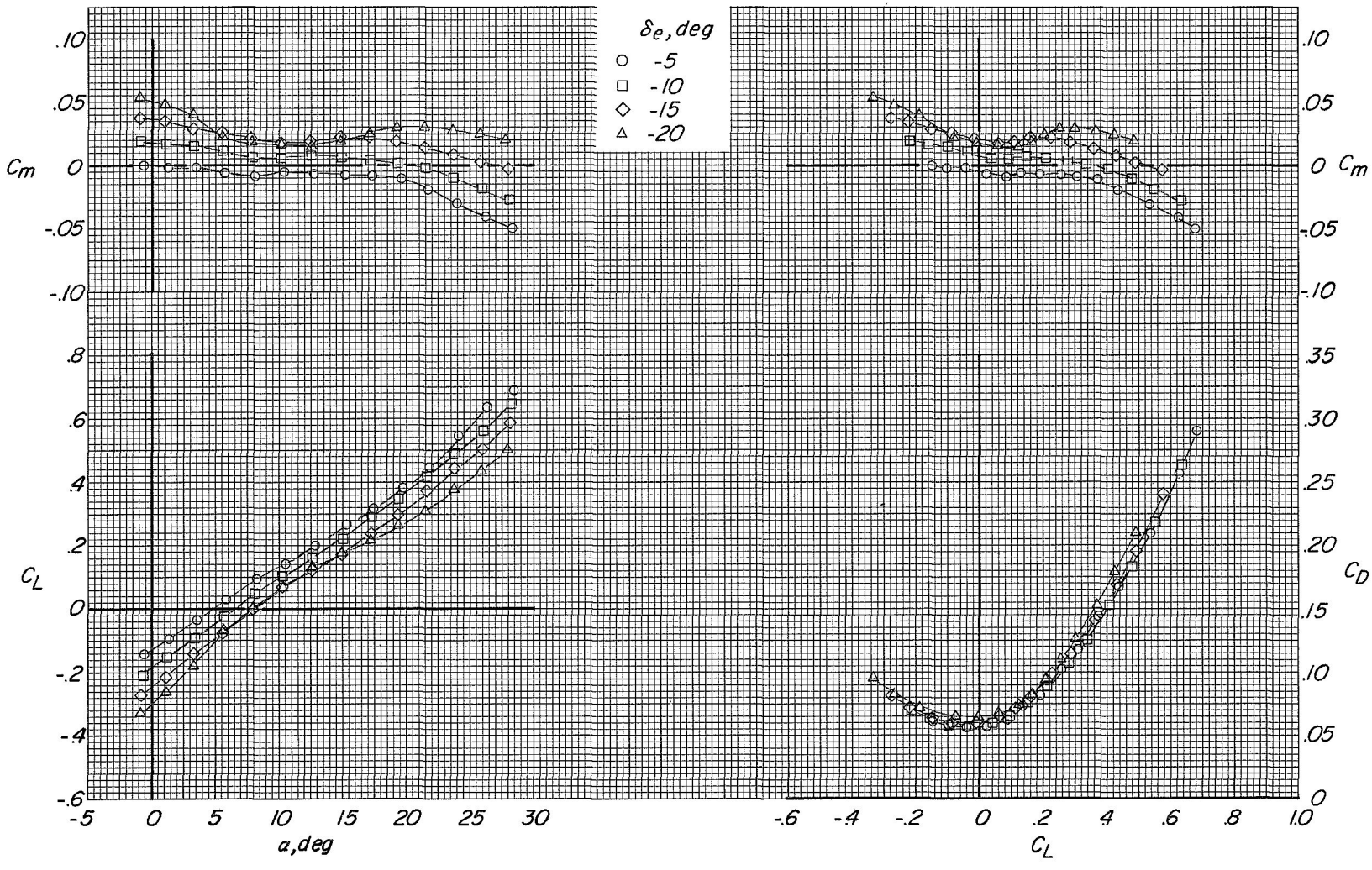
(b) M = 0.50.

Figure 6.- Continued.



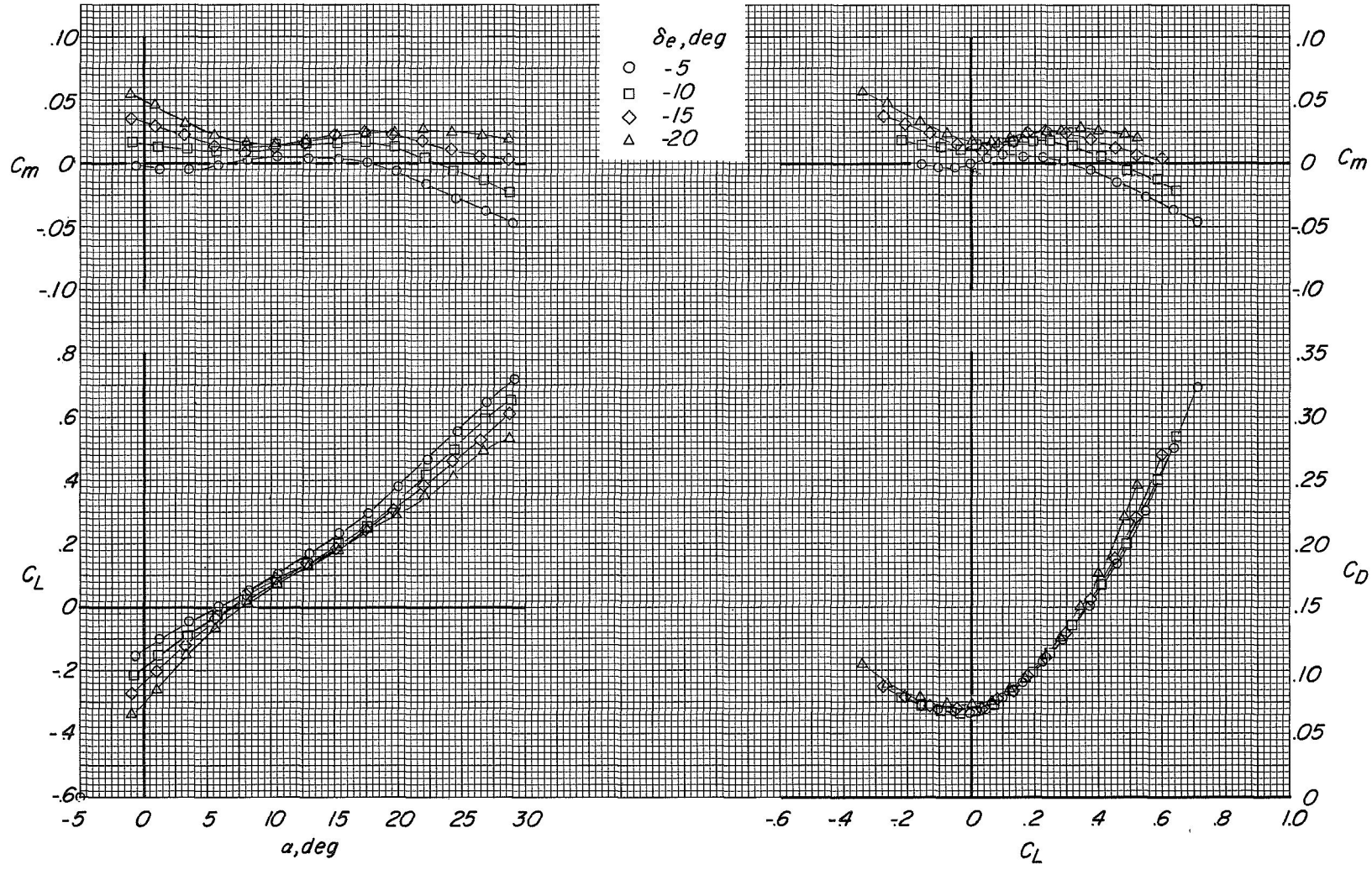
(c) M = 0.60.

Figure 6.- Continued.



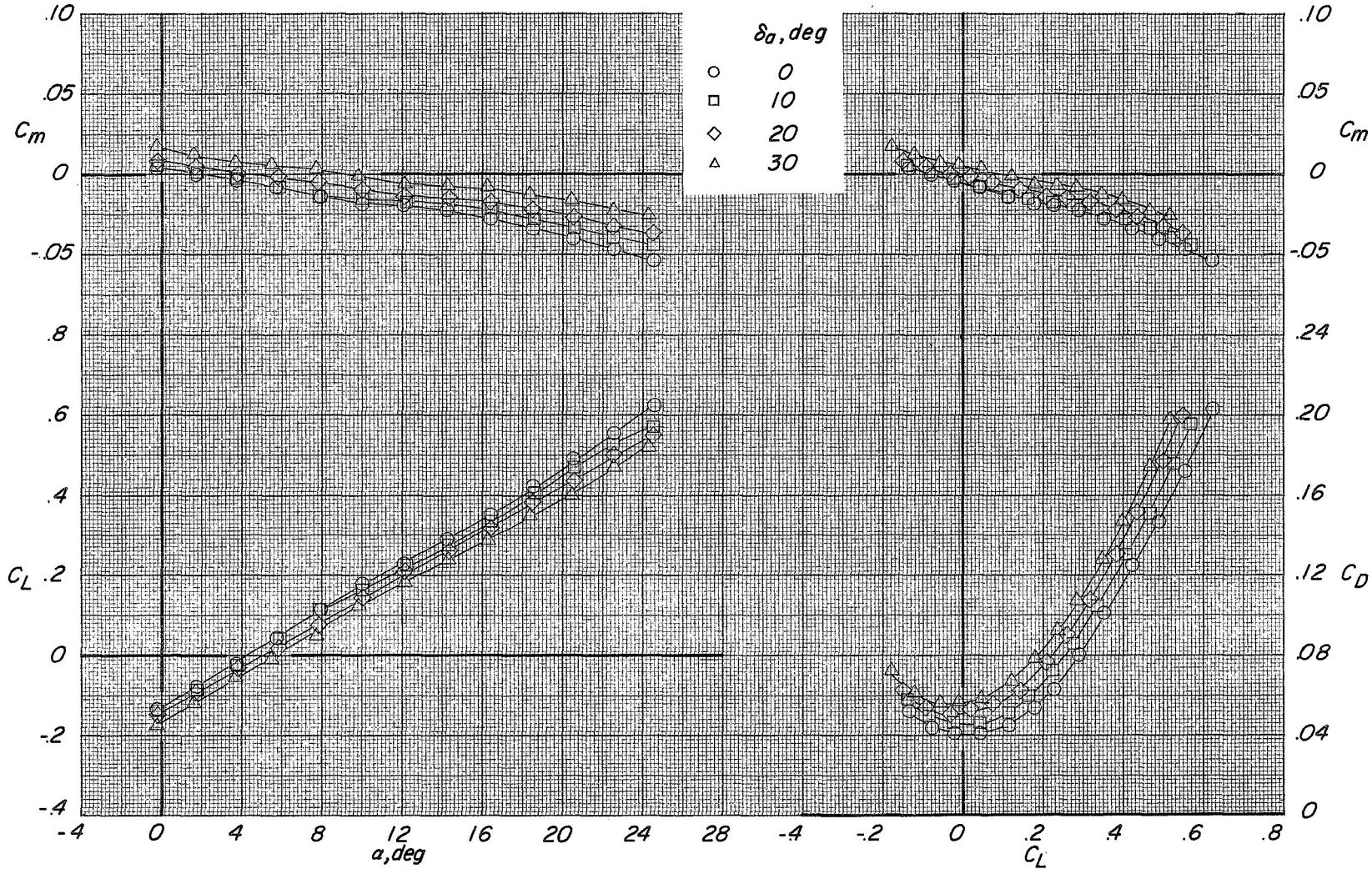
(d) M = 0.70.

Figure 6.- Continued.



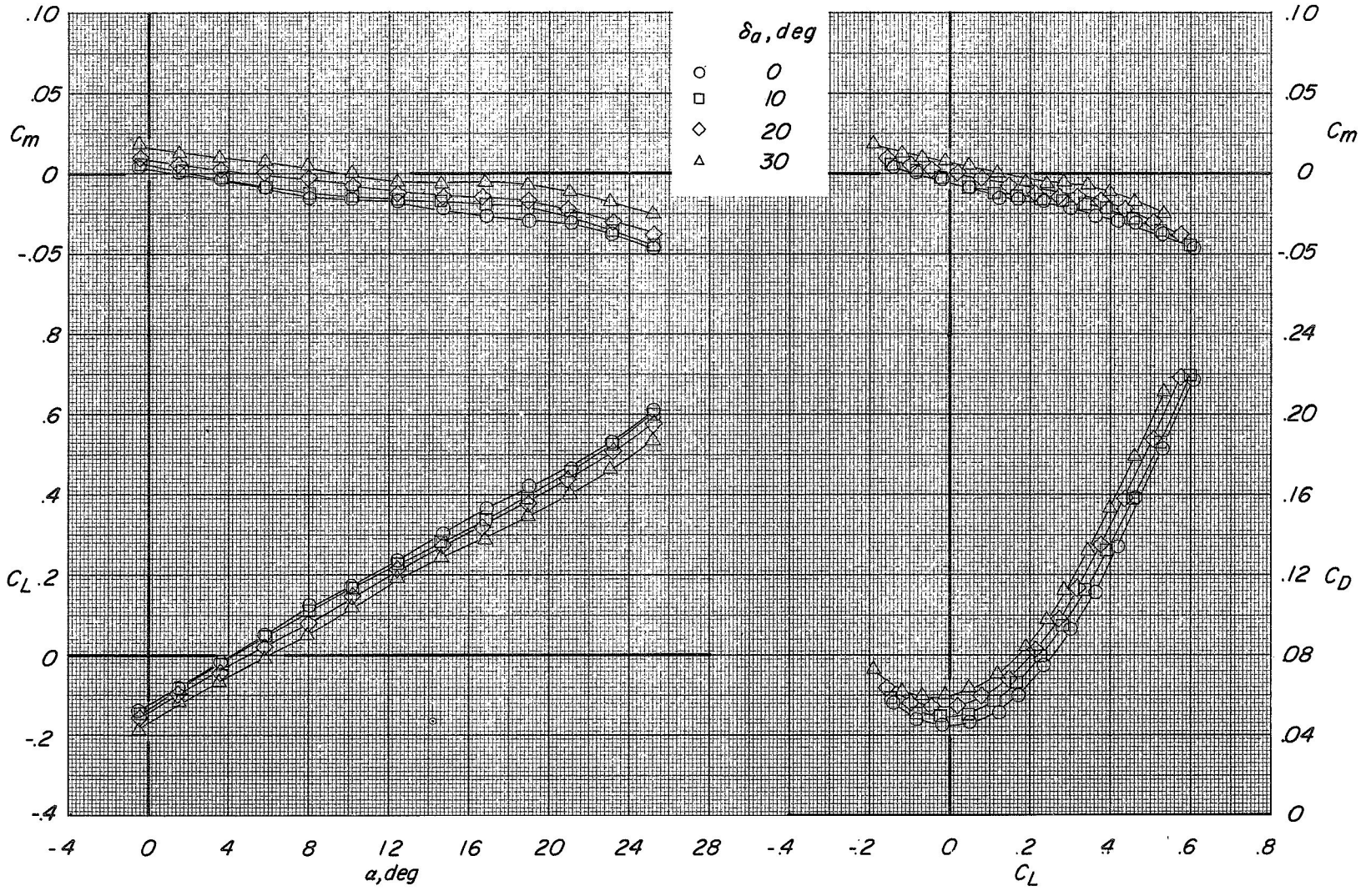
(e) M = 0.80.

Figure 6.- Concluded.



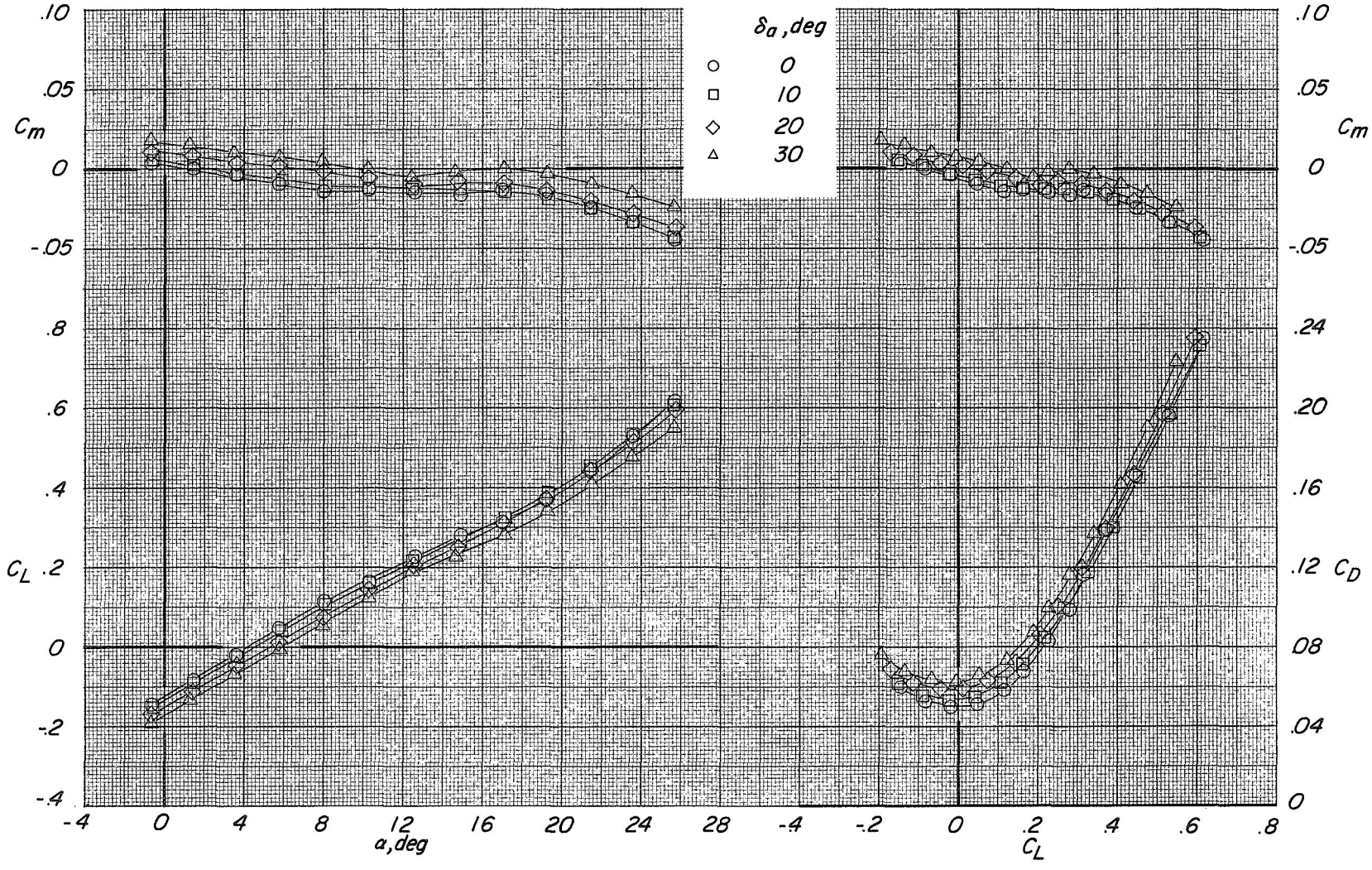
(a) $\delta_e = -5^o$; M = 0.35.

Figure 7.- Longitudinal characteristics with ailerons deflected. Basic fin configuration; auxiliary flaps in the subsonic position; $\beta = 0^o$.



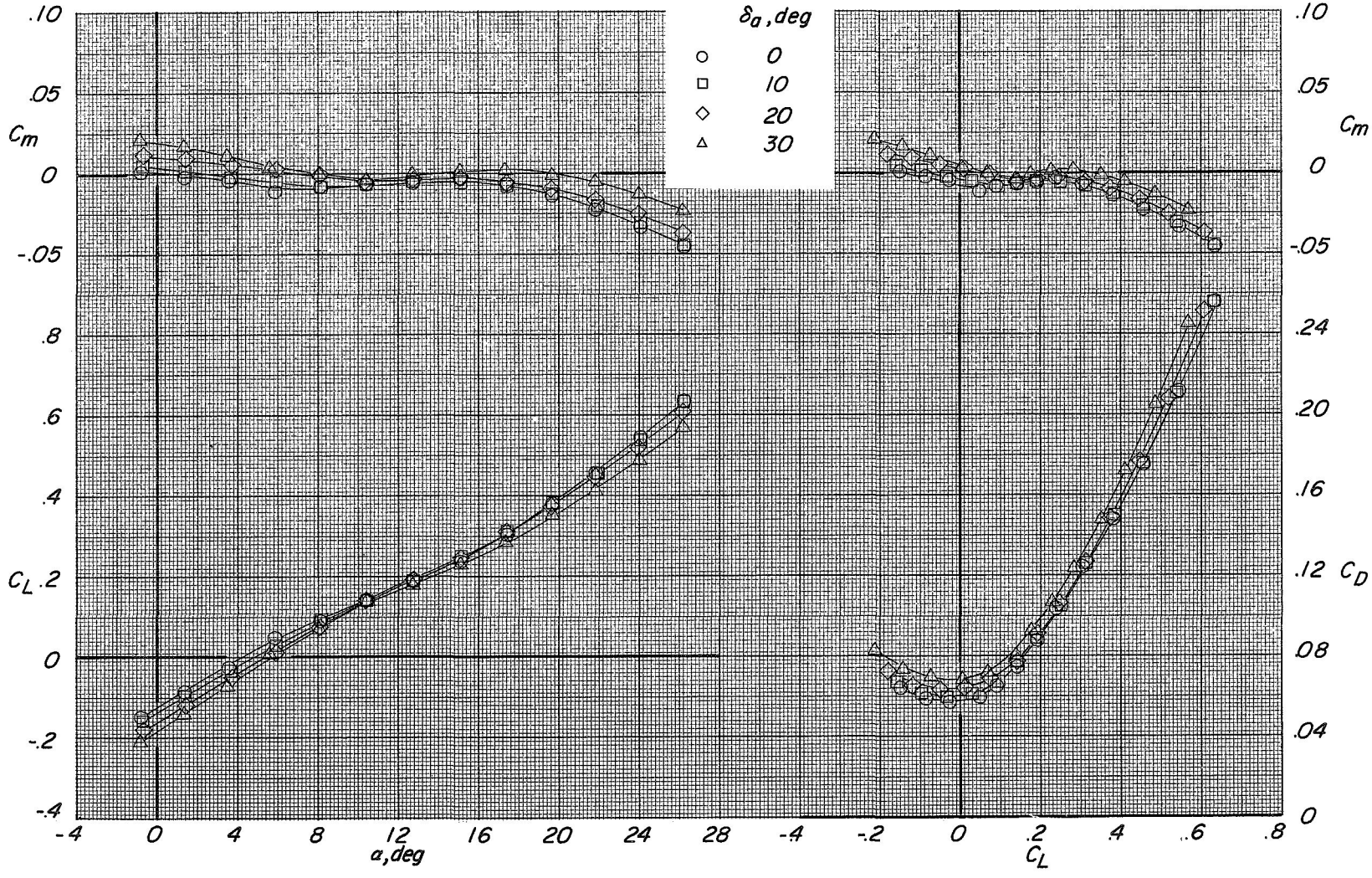
(b) $\delta_e = -5^o$; M = 0.50.

Figure 7.- Continued.



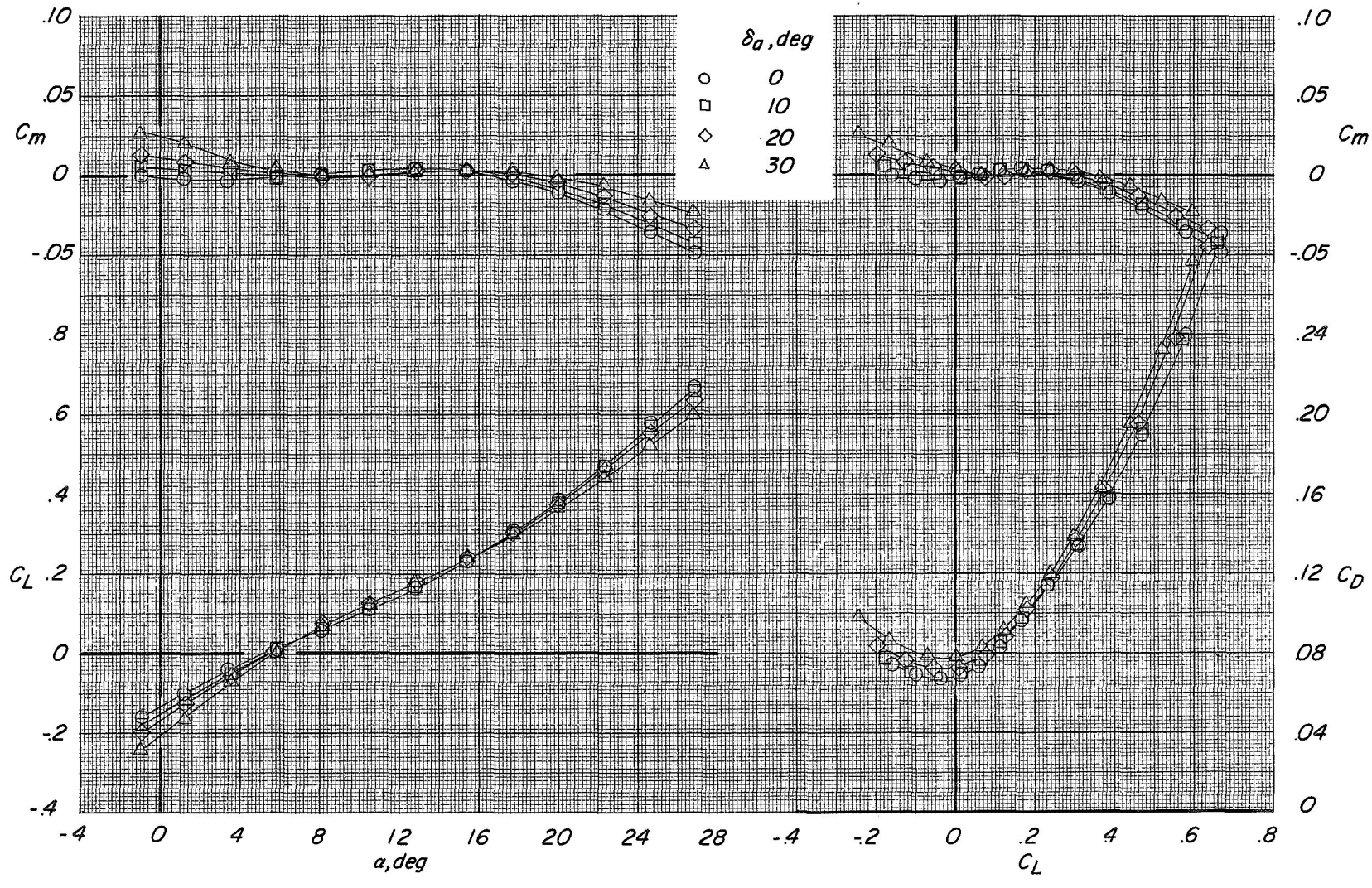
(c) $\delta_e = -5^o$; M = 0.60.

Figure 7.- Continued.



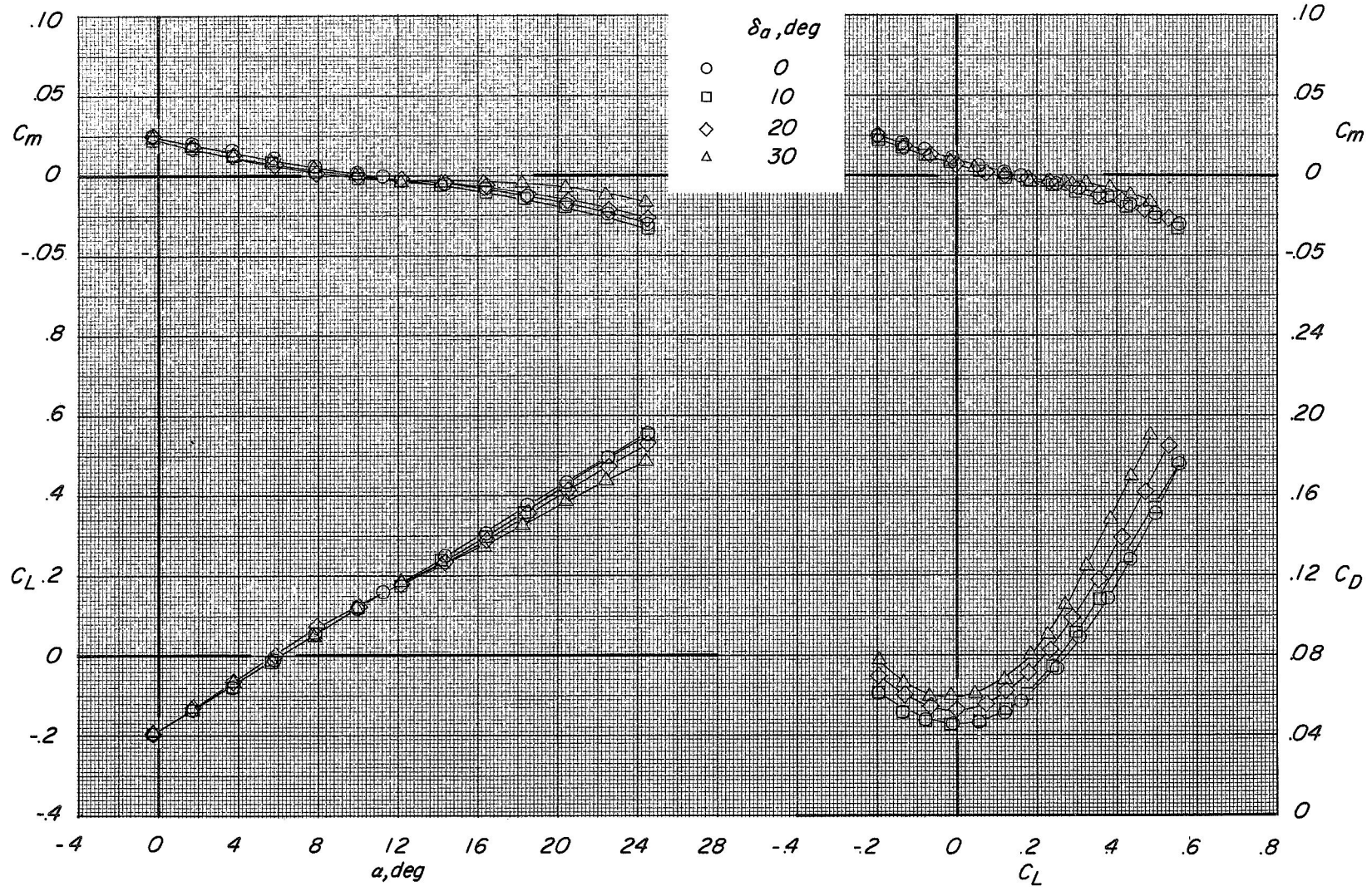
(d) $\delta_e = -5^o$; M = 0.70.

Figure 7.- Continued.



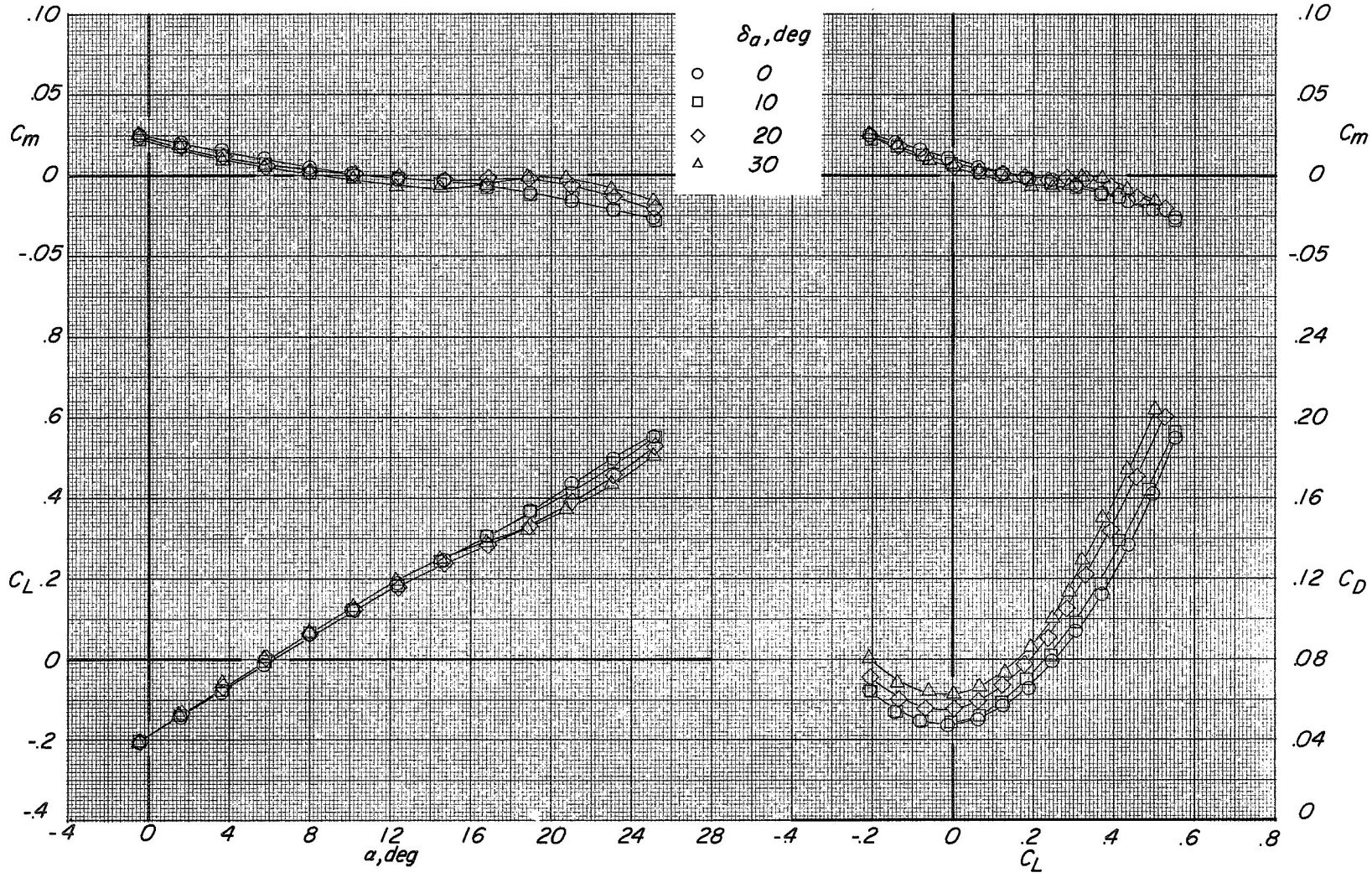
(e) $\delta_e = -5^o$; M = 0.80.

Figure 7.- Continued.



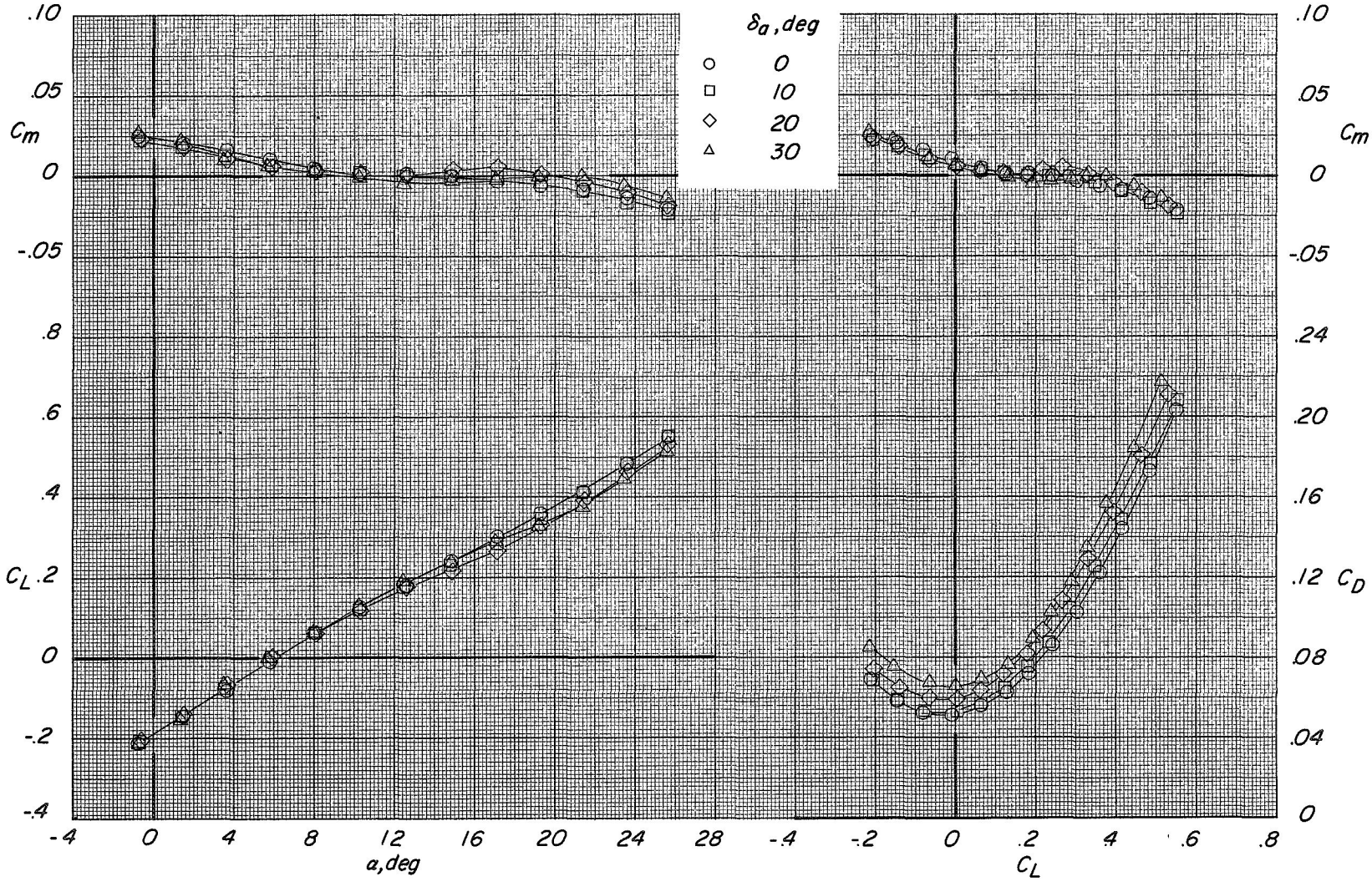
(f) $\delta_e = -10^o$; M = 0.35.

Figure 7.- Continued.



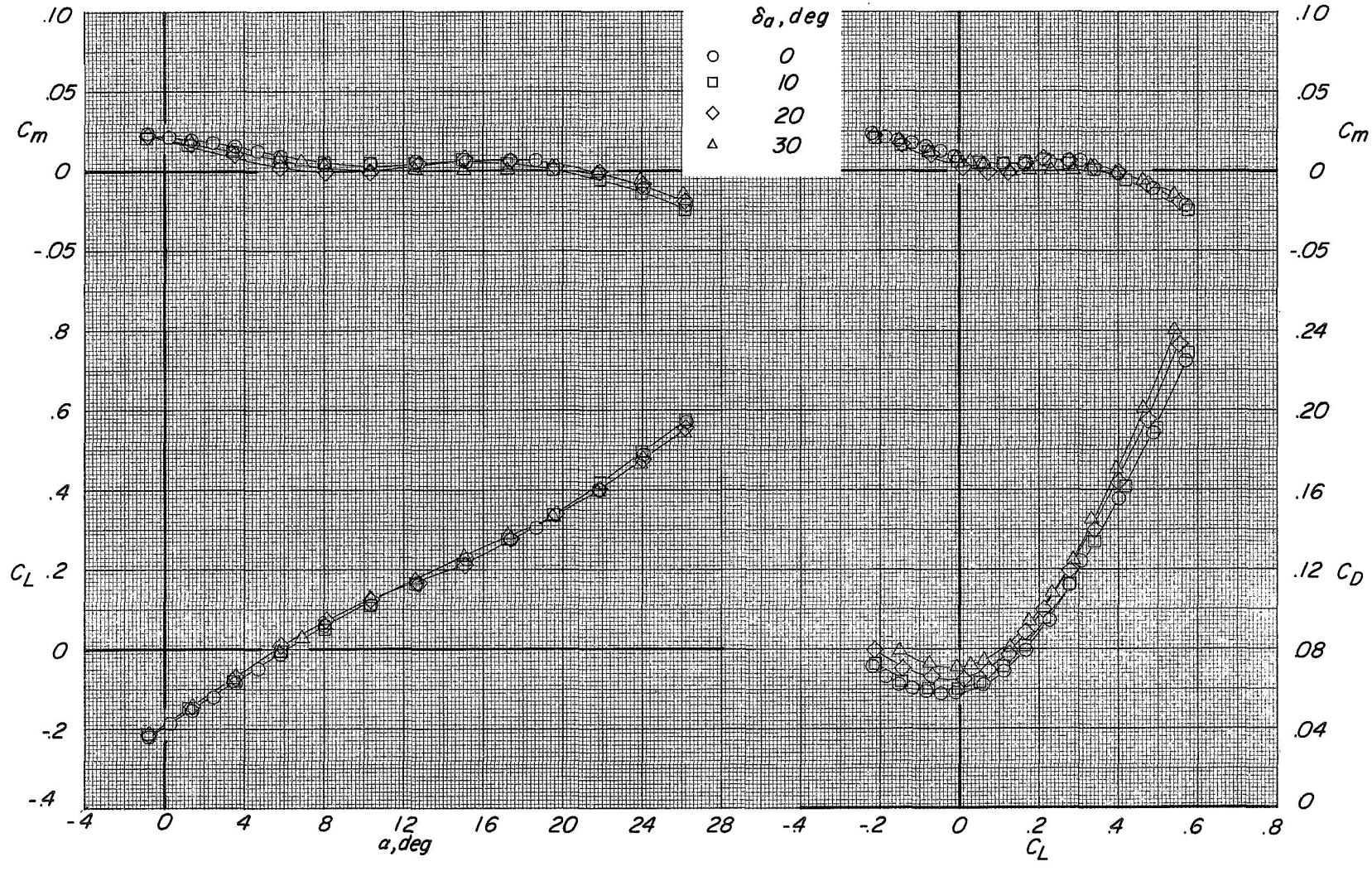
(g) $\delta_e = -10^o$; M = 0.50.

Figure 7.- Continued.



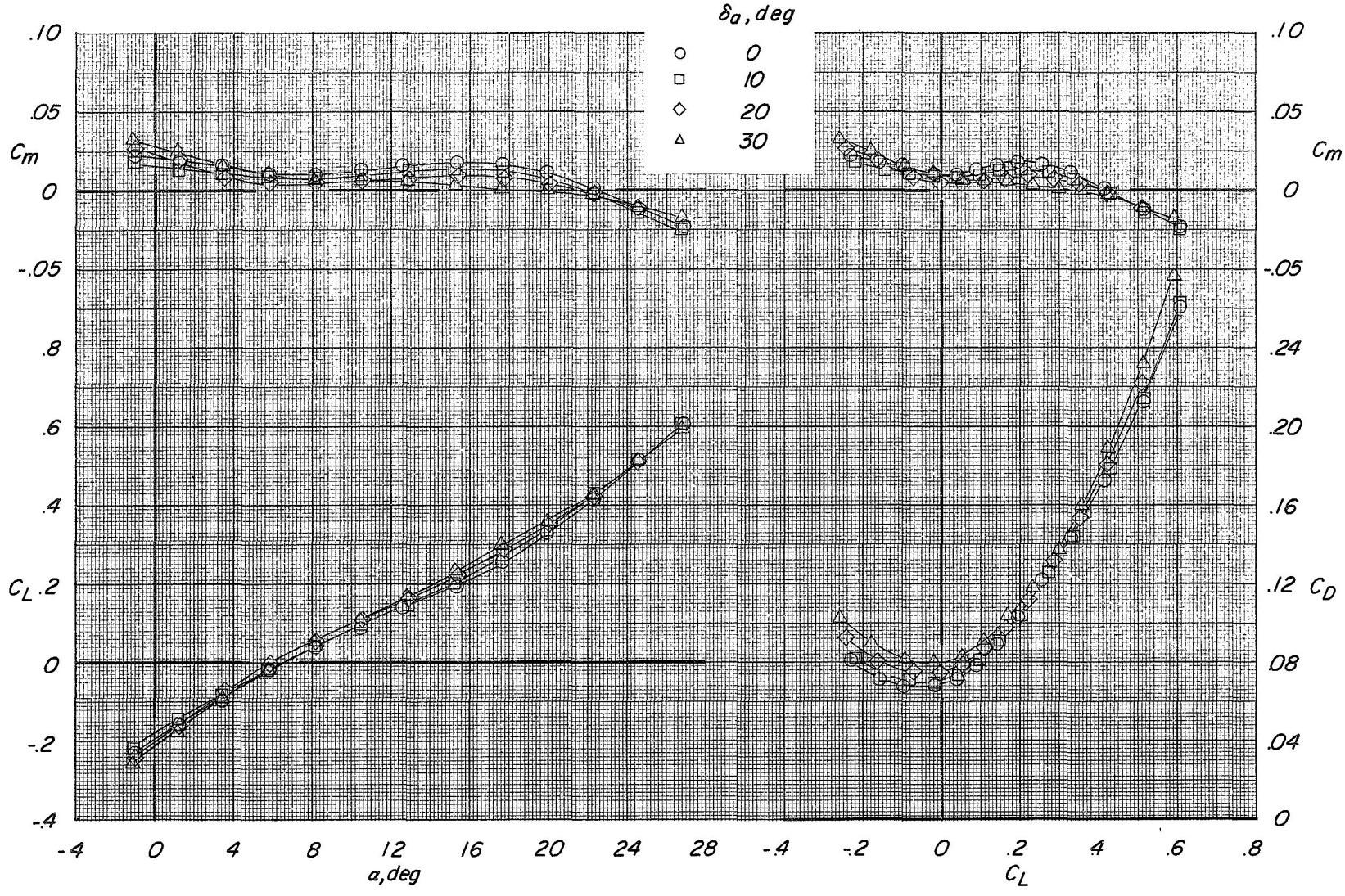
(h) $\delta_e = -10^o$; M = 0.60.

Figure 7.- Continued.



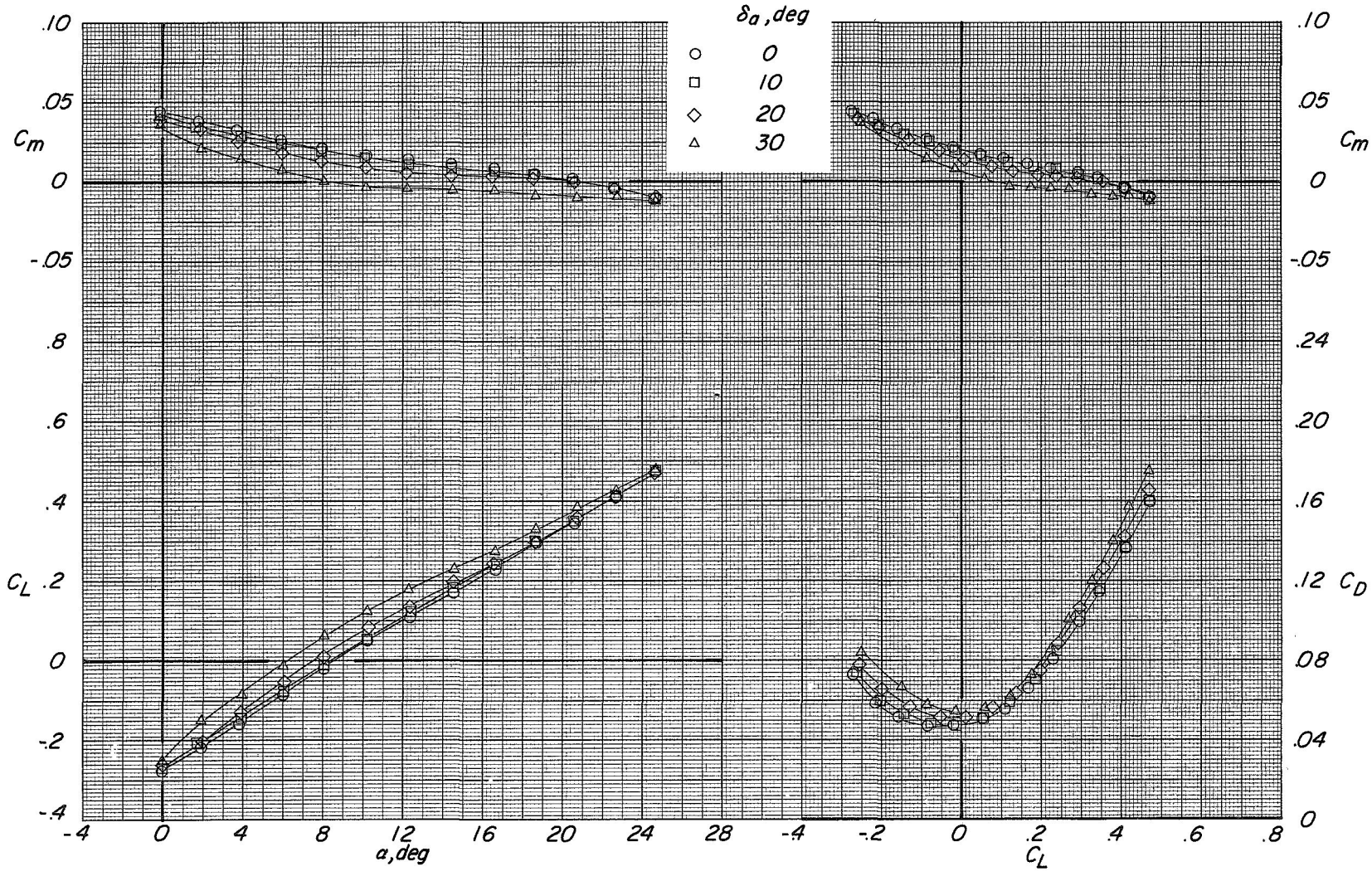
(i) $\delta_e = -10^o$; M = 0.70.

Figure 7.- Continued.



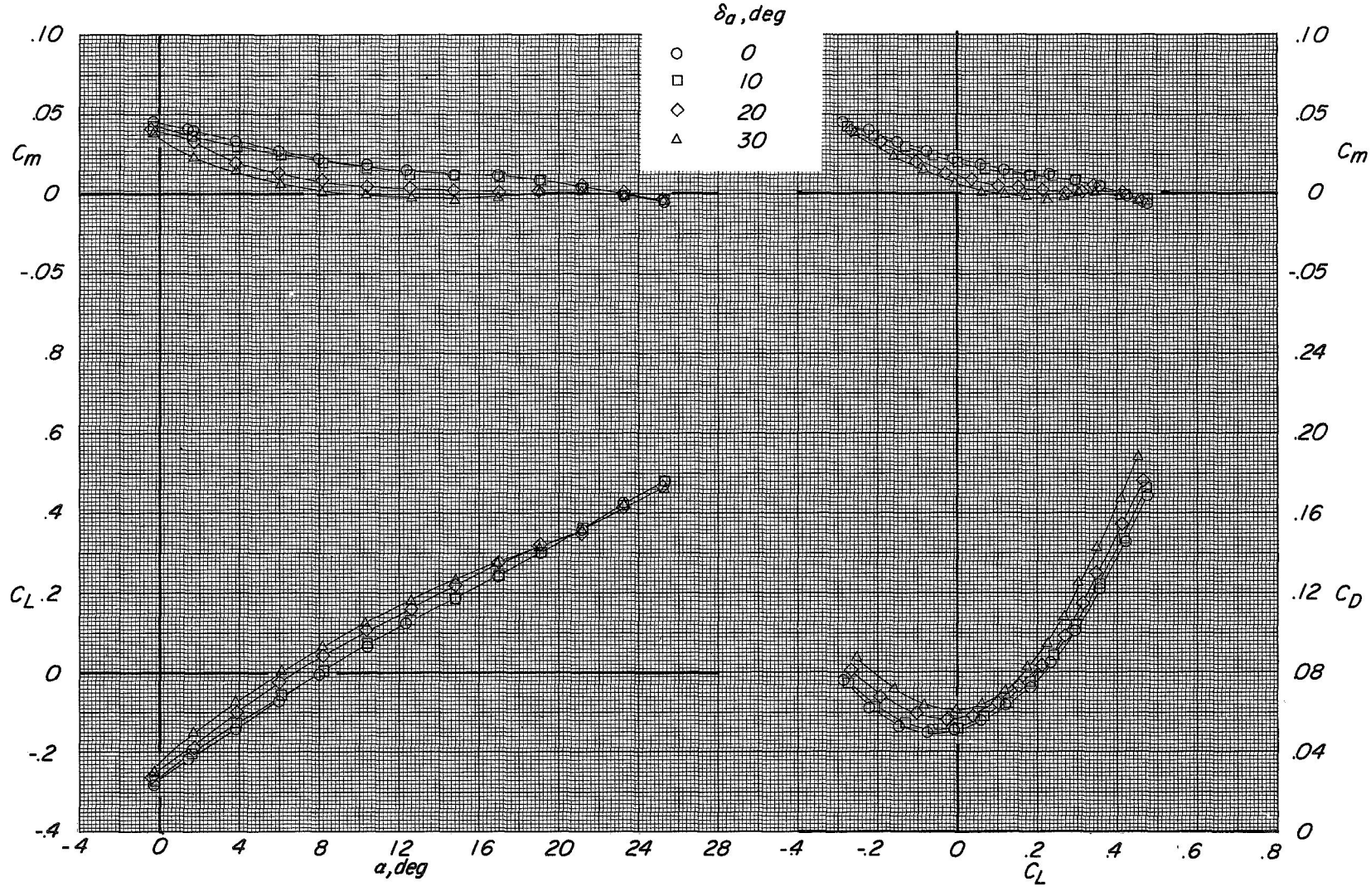
(j) $\delta_e = -10^o$; M = 0.80.

Figure 7.- Continued.



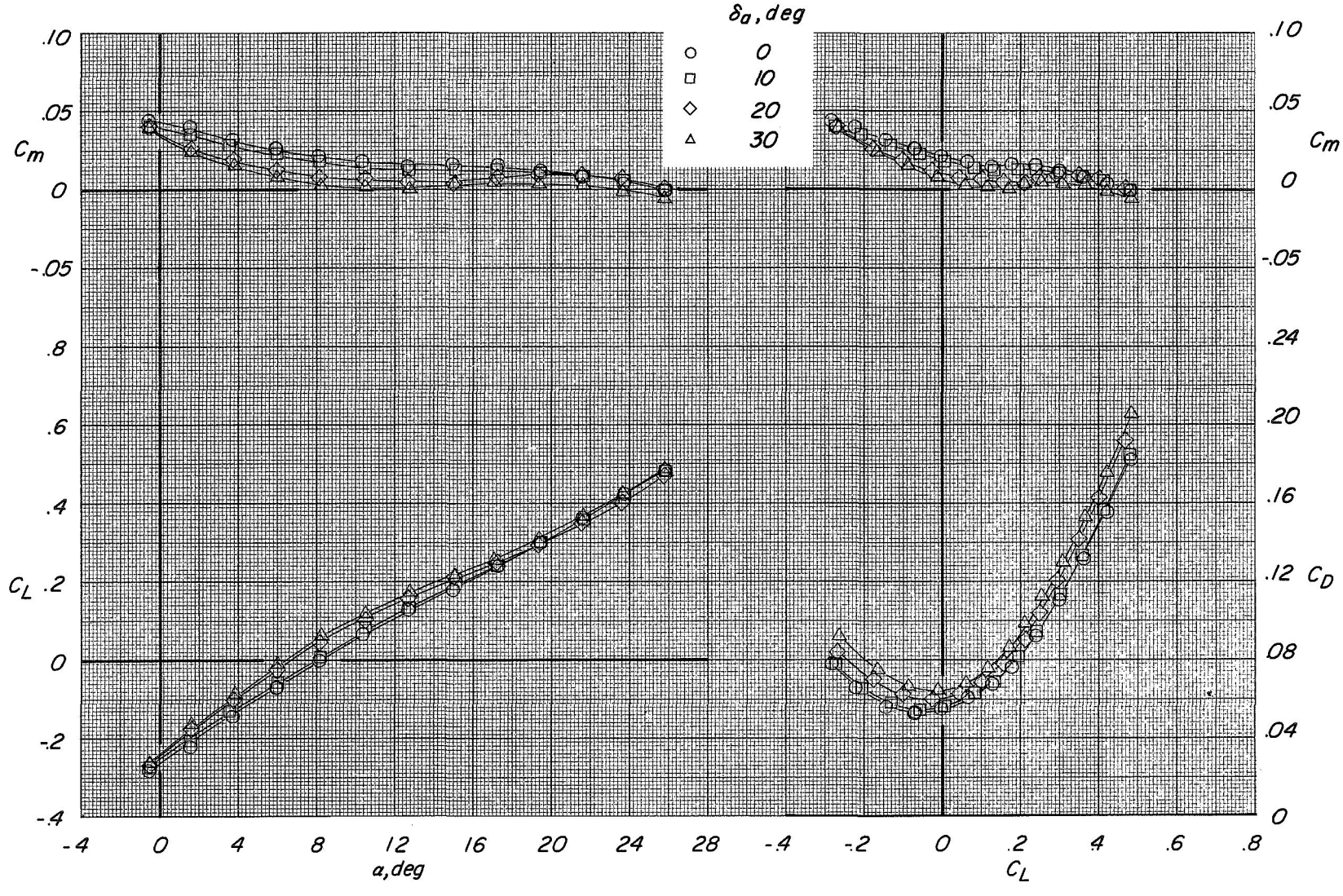
(k) $\delta_e = -15^o$; M = 0.35.

Figure 7.- Continued.



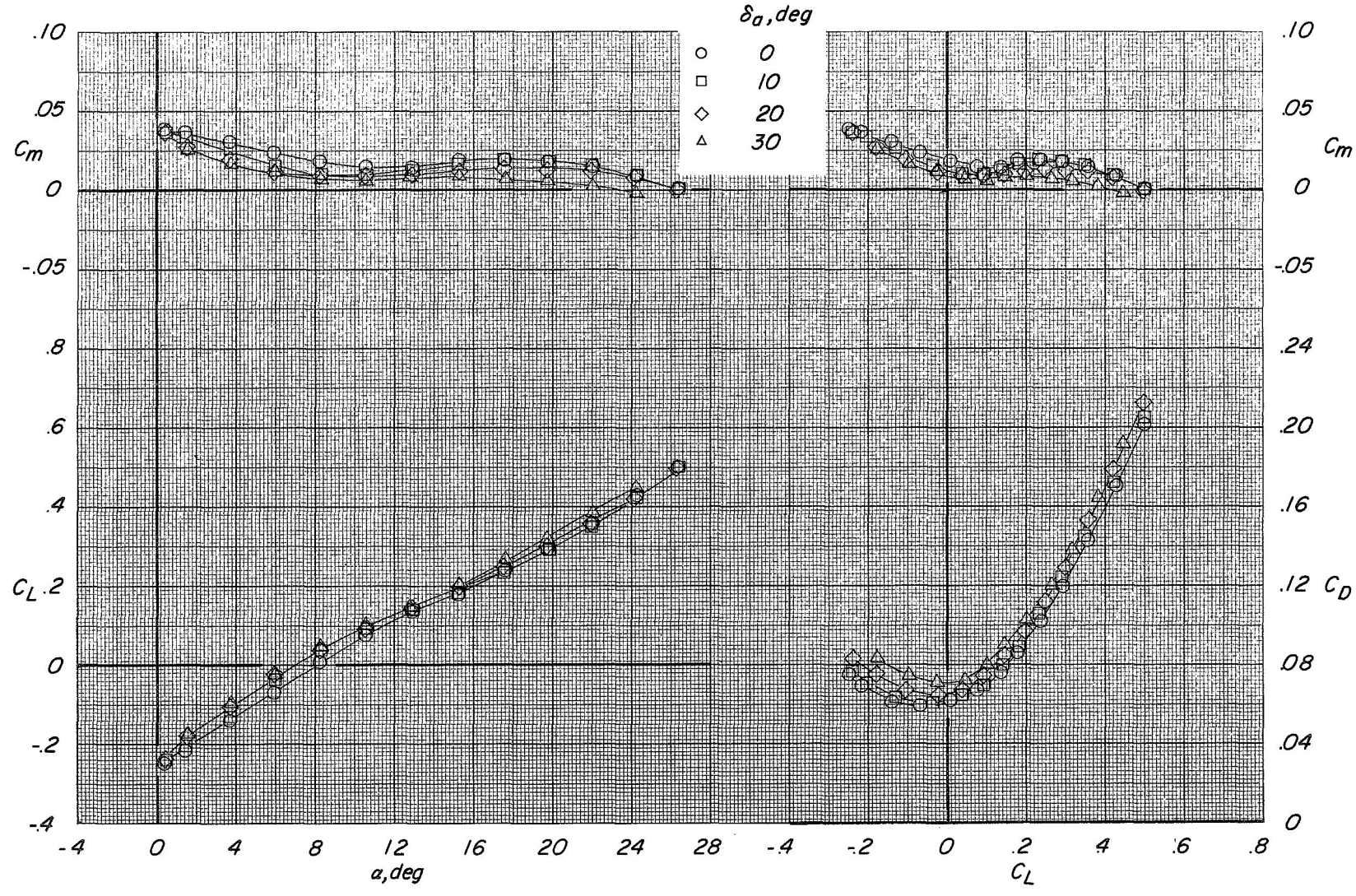
(l) $\delta_e = -15^o$; M = 0.50.

Figure 7.- Continued.



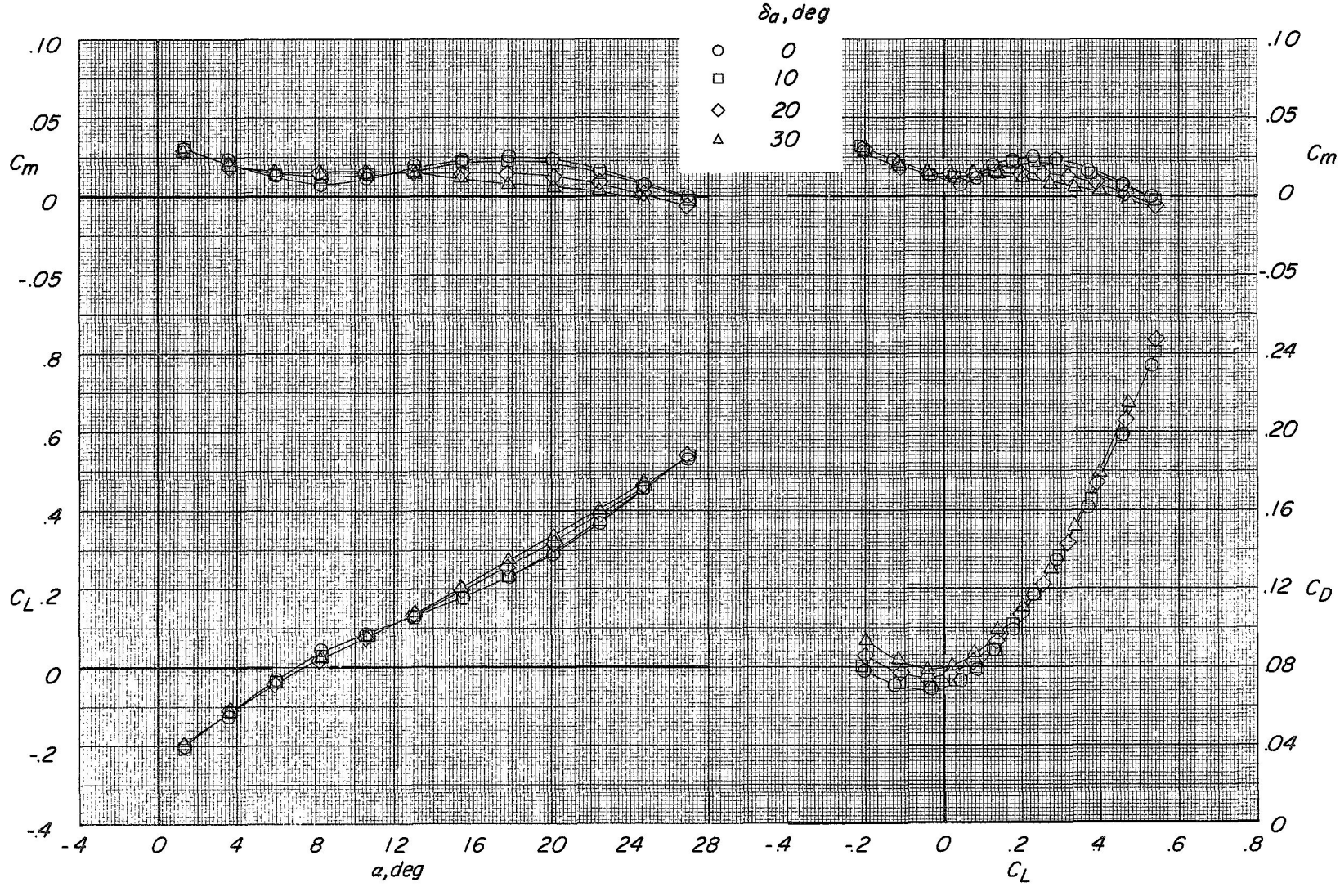
(m) $\delta_e = -15^o$; M = 0.60.

Figure 7.- Continued.



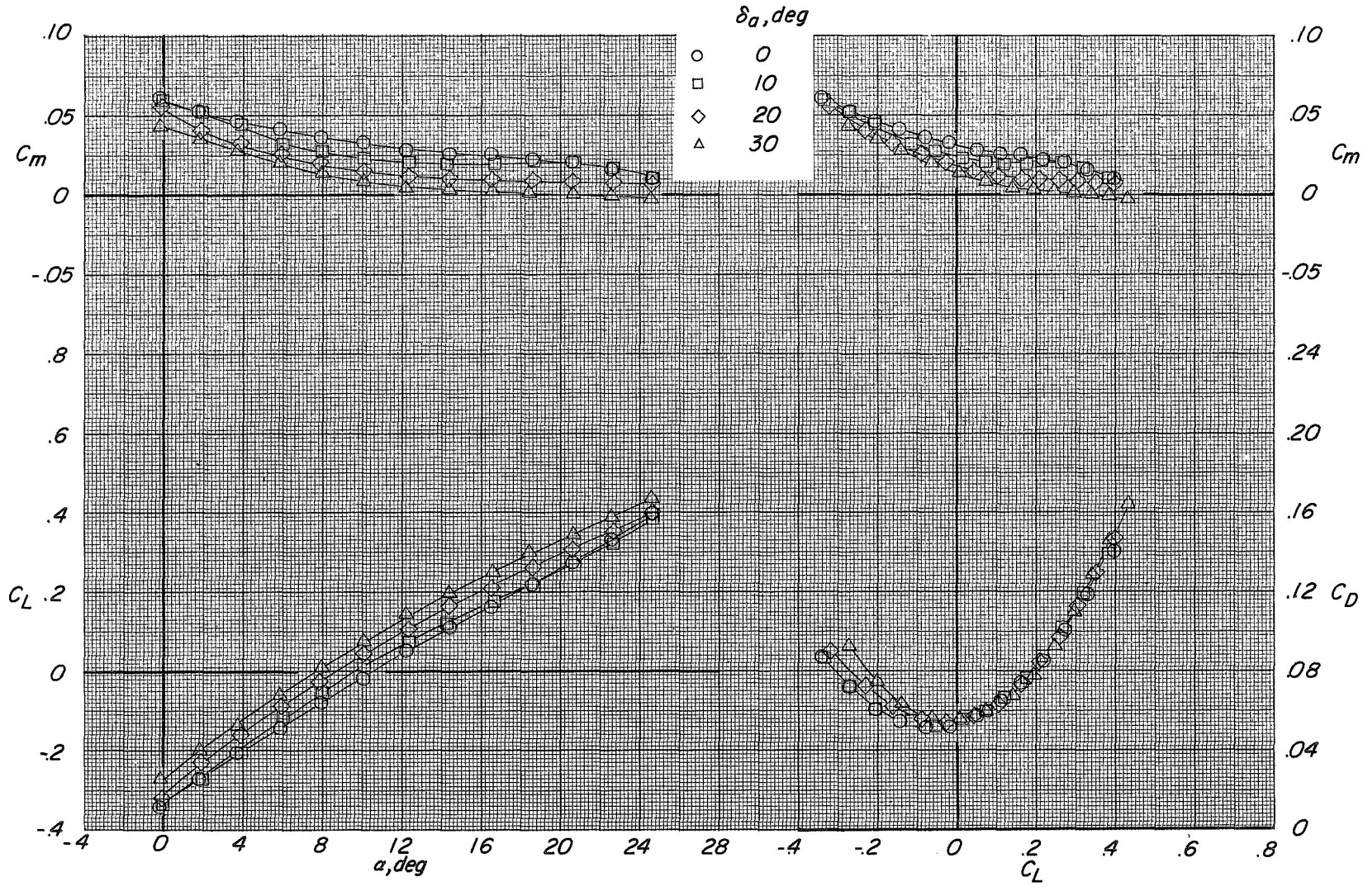
(n) $\delta_e = -15^o$; M = 0.70.

Figure 7.- Continued.



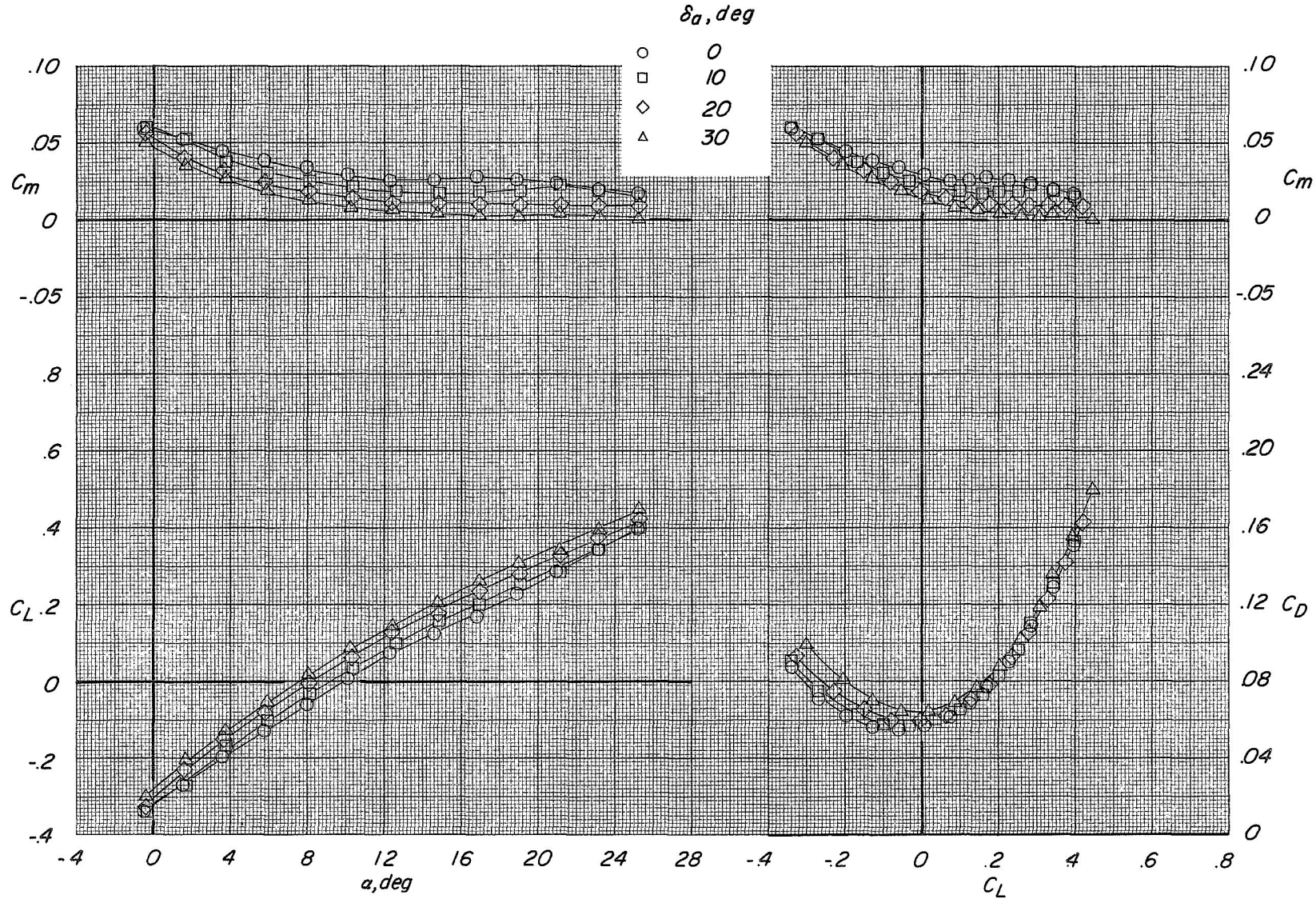
(o) $\delta_e = -15^o$; M = 0.80.

Figure 7.- Continued.



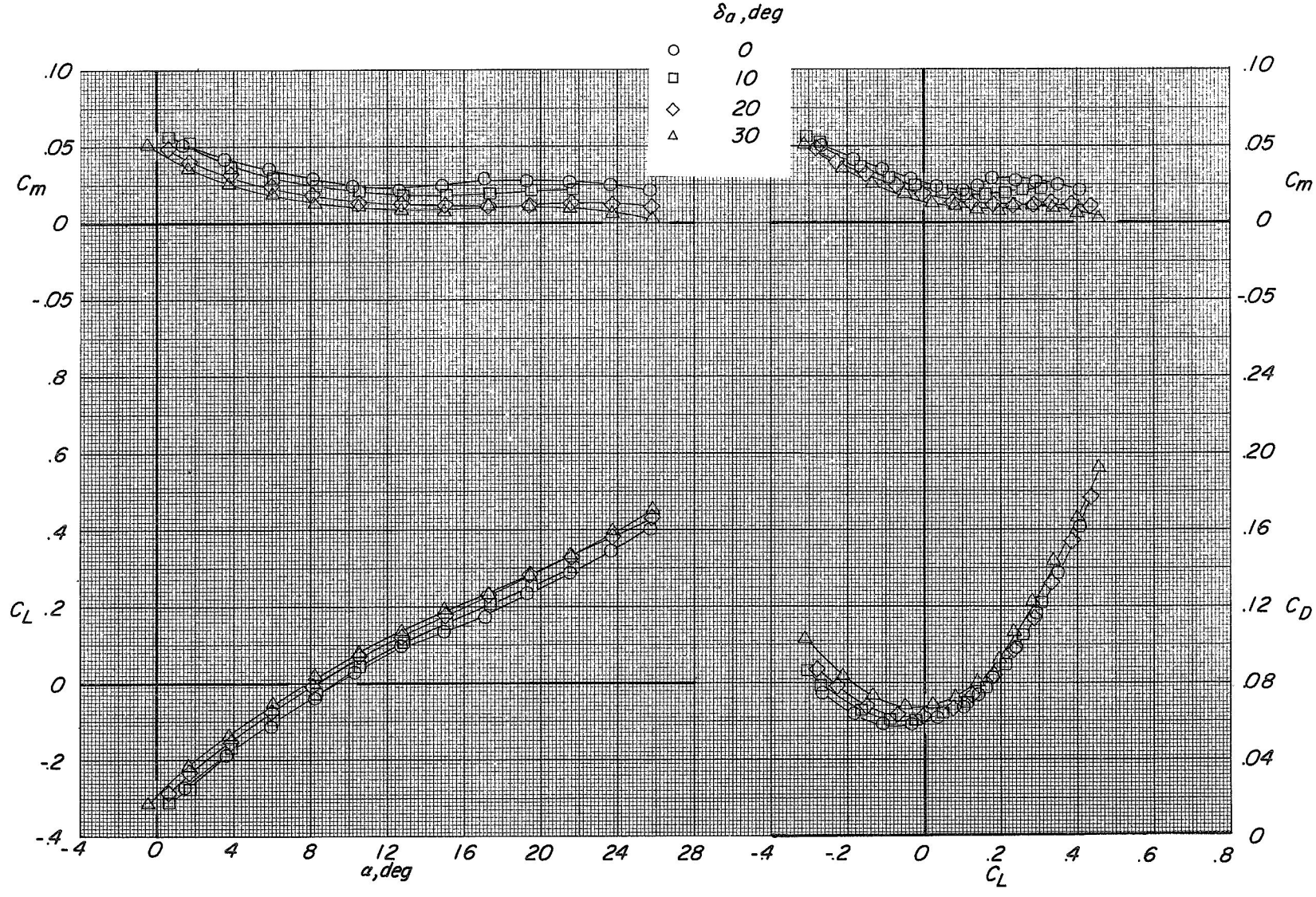
(p) $\delta_e = -20^o$; M = 0.35.

Figure 7.- Continued.



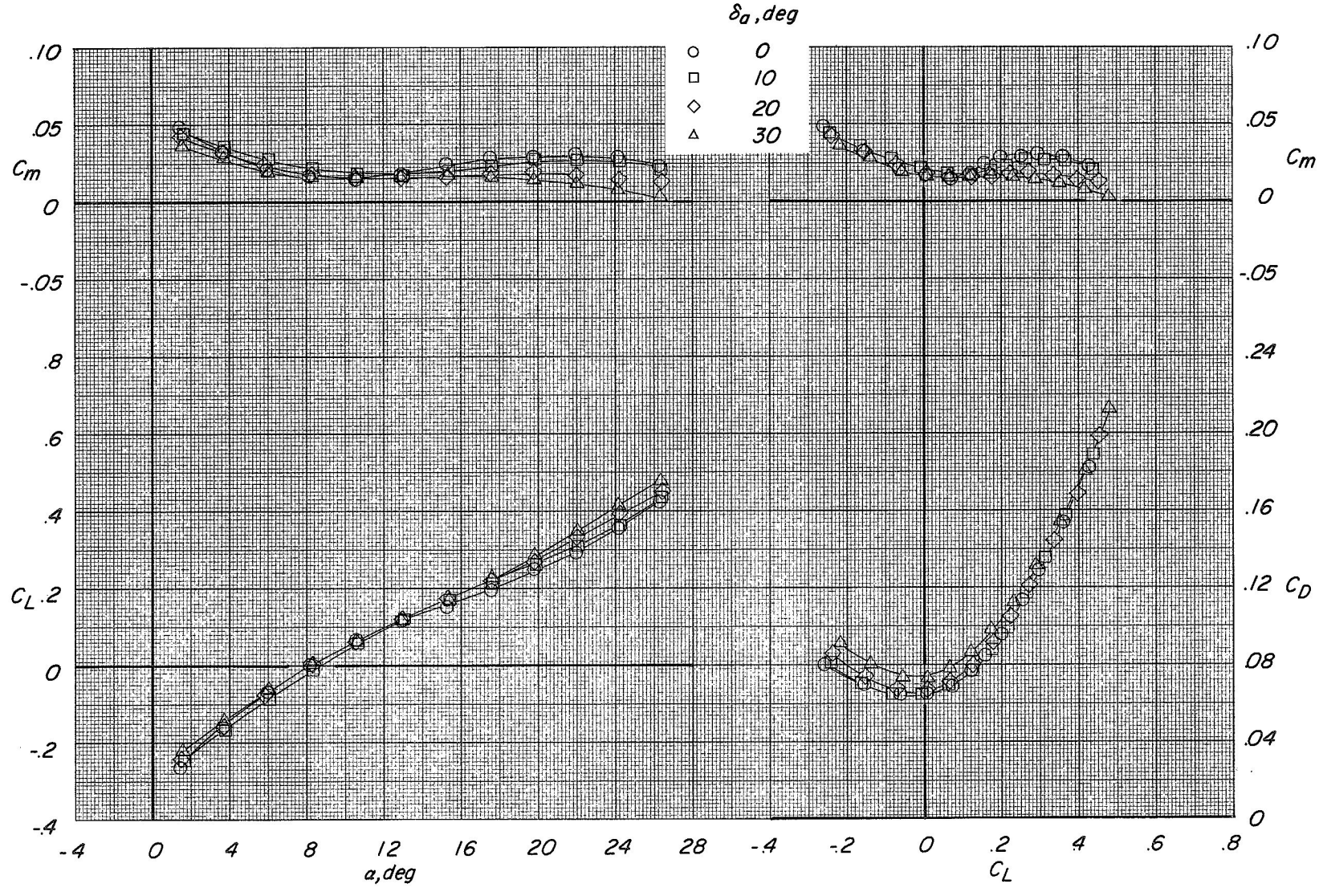
(q) $\delta_e = -20^o$; M = 0.50.

Figure 7.- Continued.



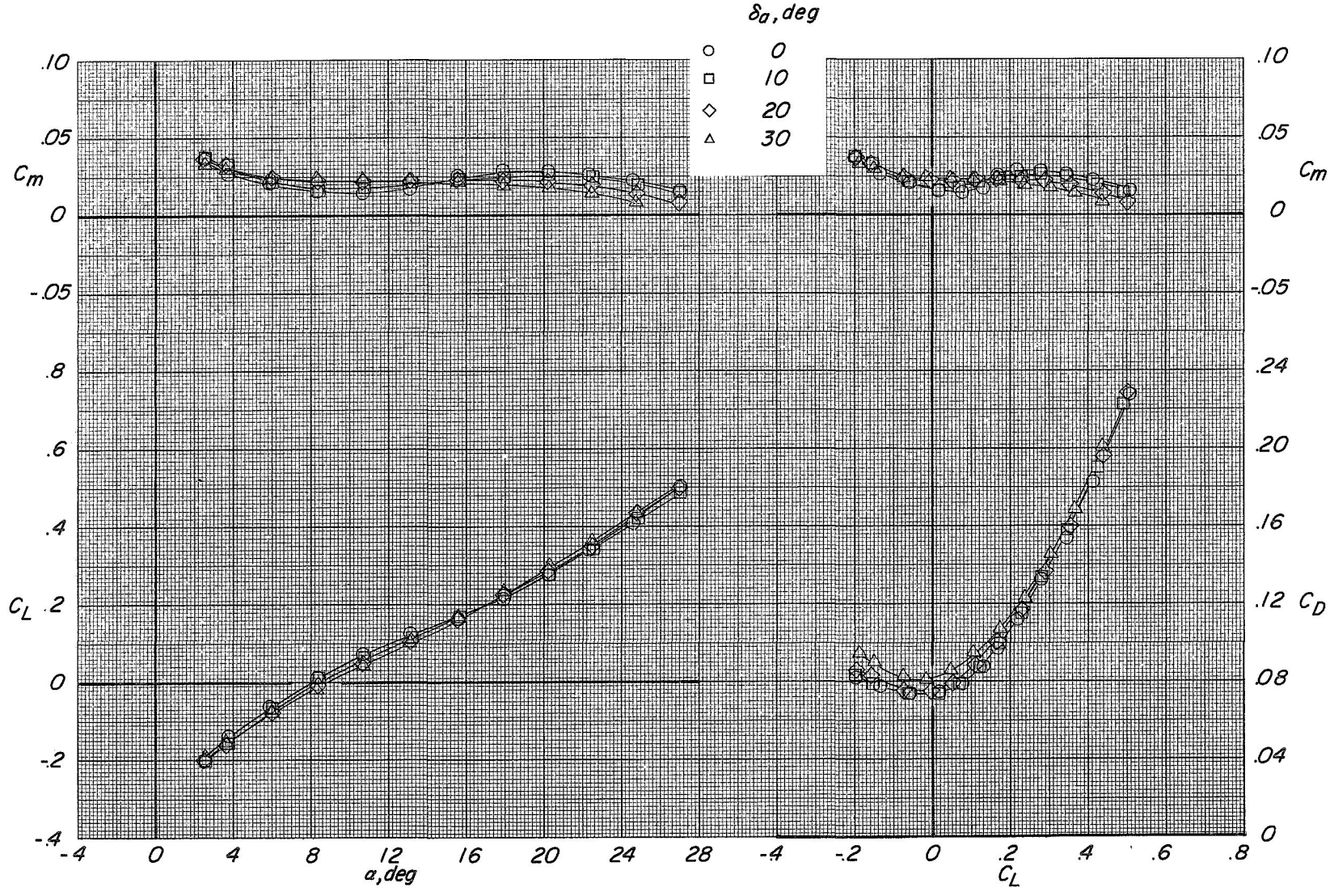
(r) $\delta_e = -20^o$; M = 0.60.

Figure 7.- Continued.



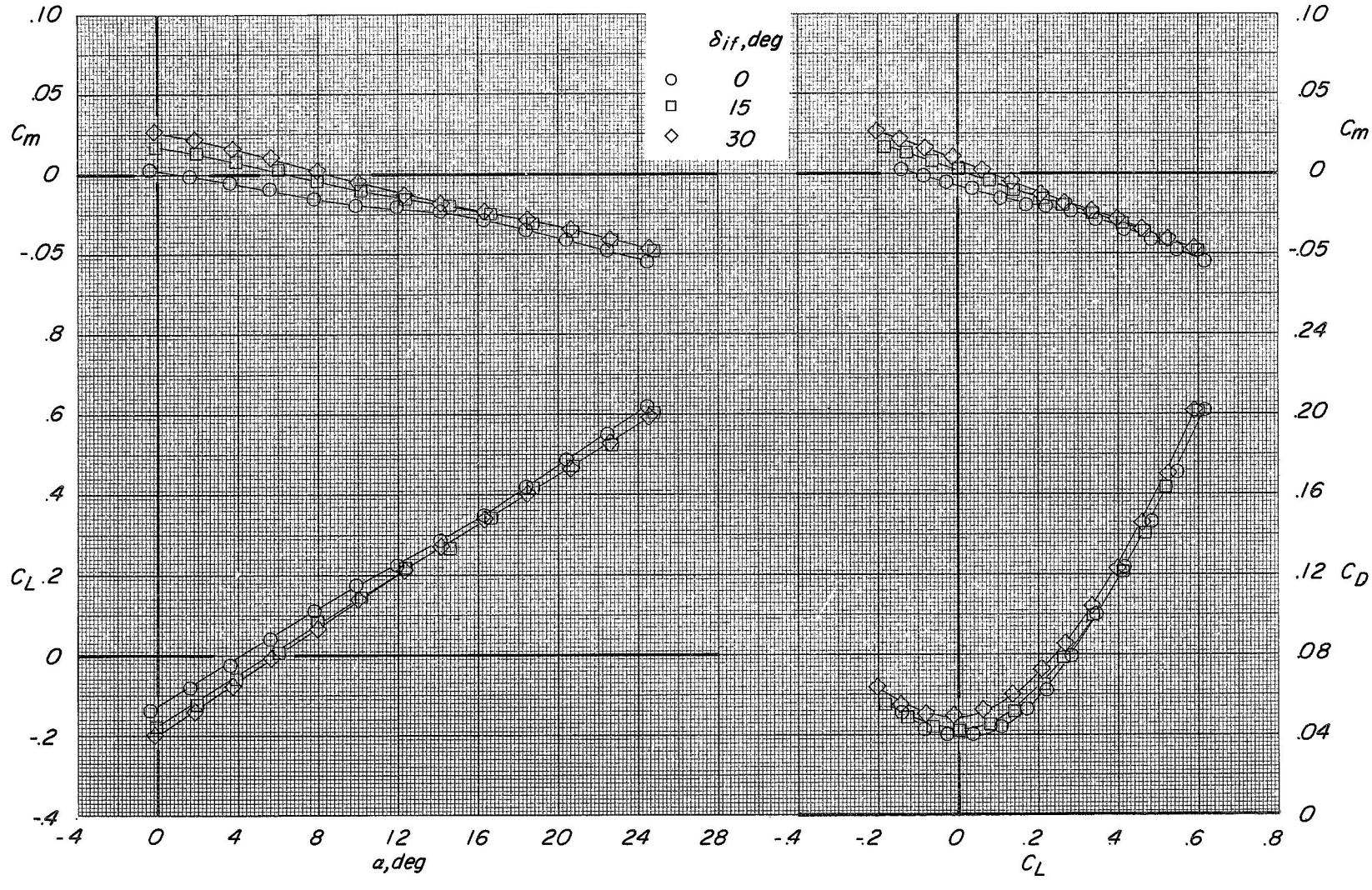
(s) $\delta_e = -20^o$; M = 0.70.

Figure 7.- Continued.



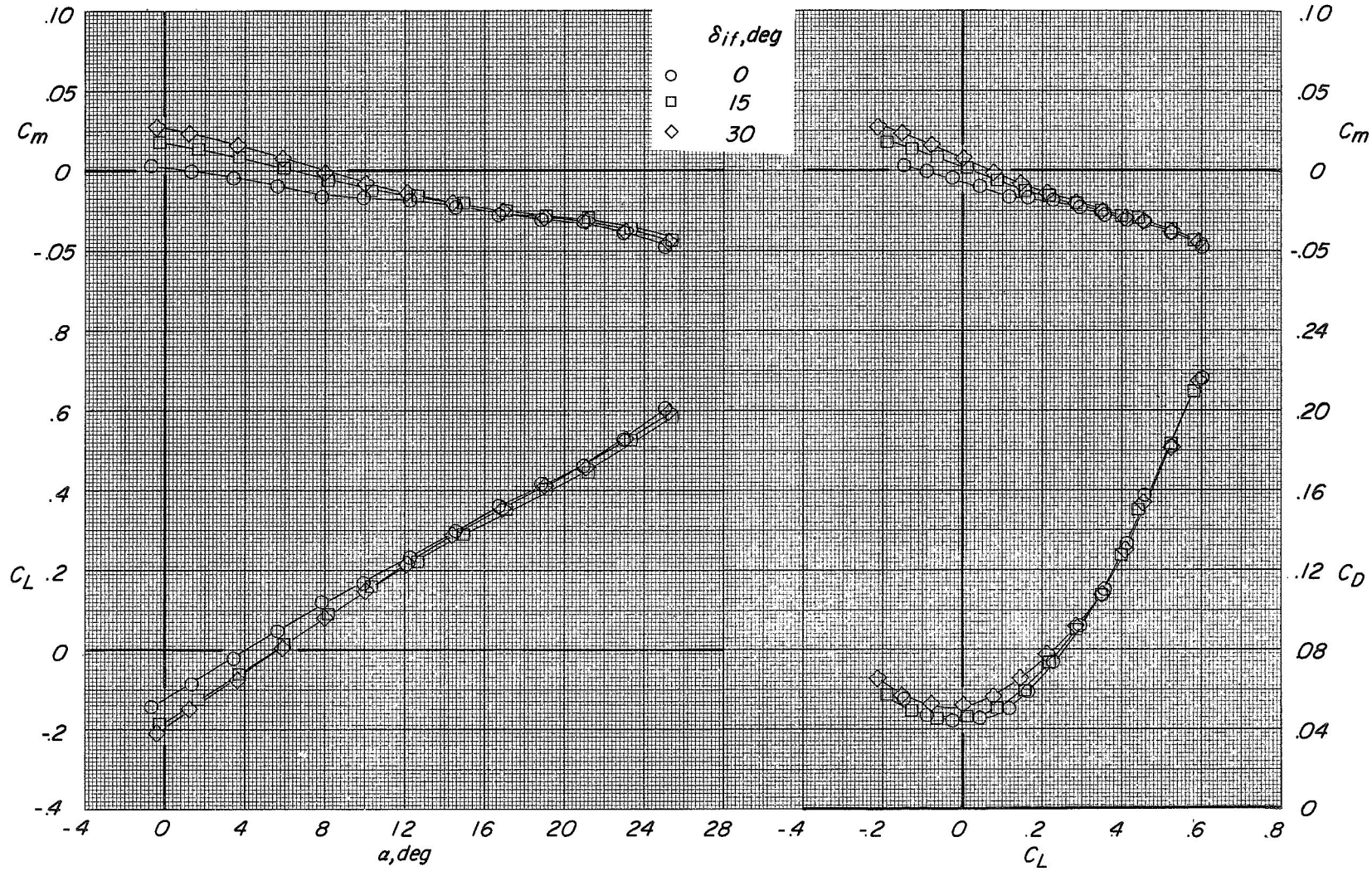
(t) $\delta_e = -20^o$; M = 0.80.

Figure 7.- Concluded.



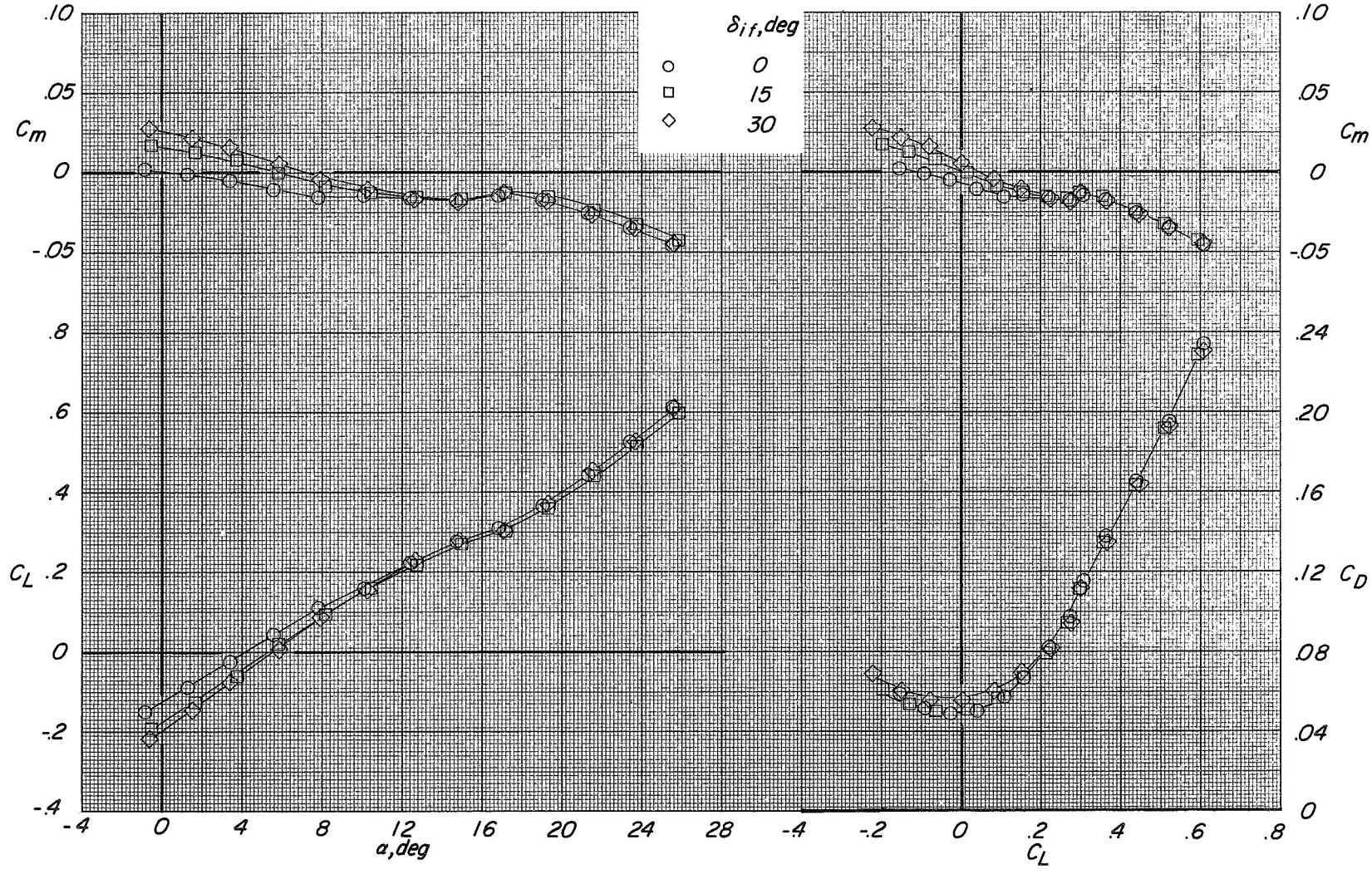
(a) $\delta_e = -5^o$; M = 0.35.

Figure 8.- Effect of tip fin inner surface flaps deflection δ_{if} on the longitudinal characteristics of the HL-10 with the basic fin configuration. Auxiliary flaps in the subsonic position; $\beta = 0^o$.



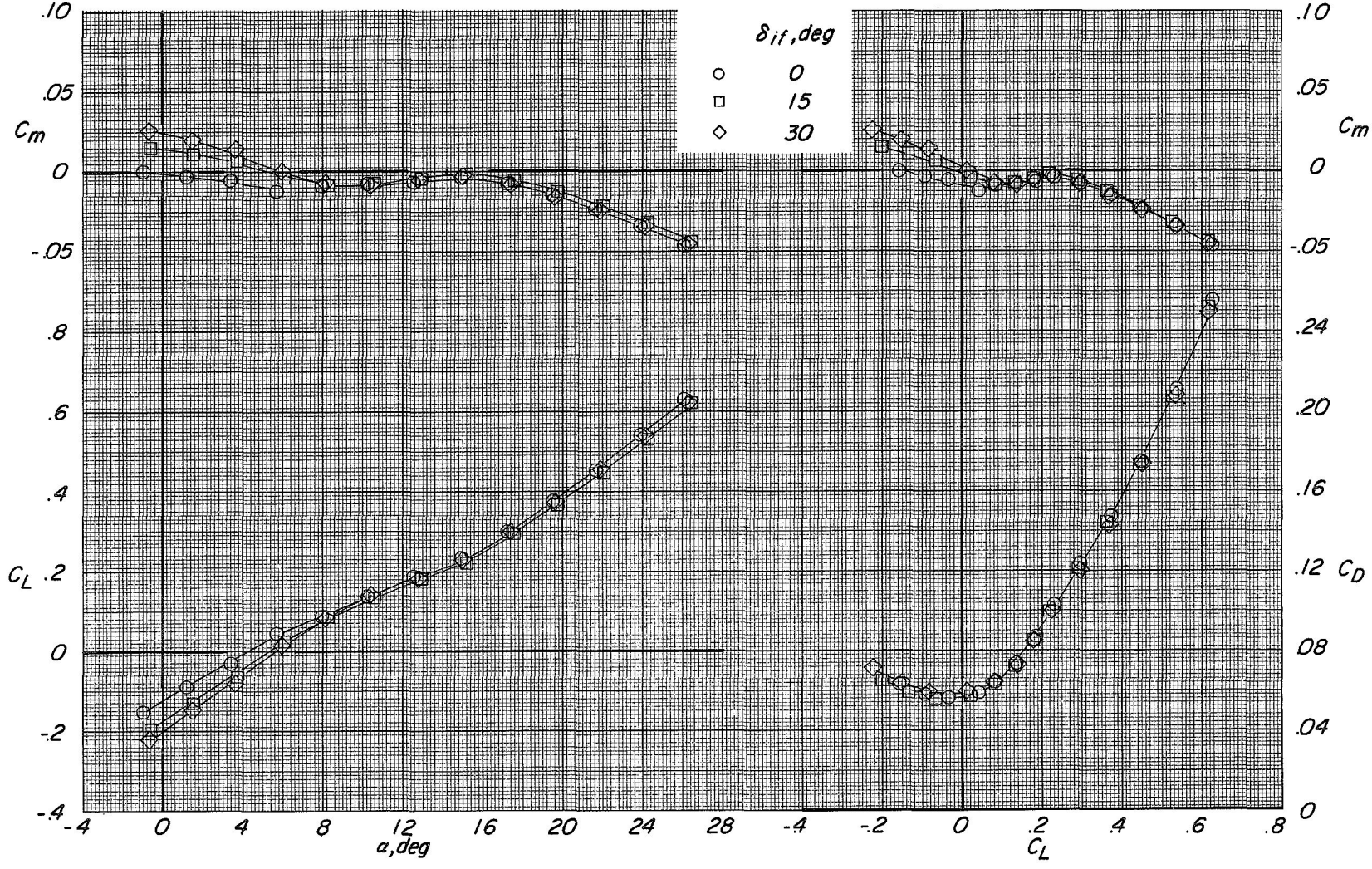
(b) $\delta_e = -5^o$; M = 0.50.

Figure 8.- Continued.



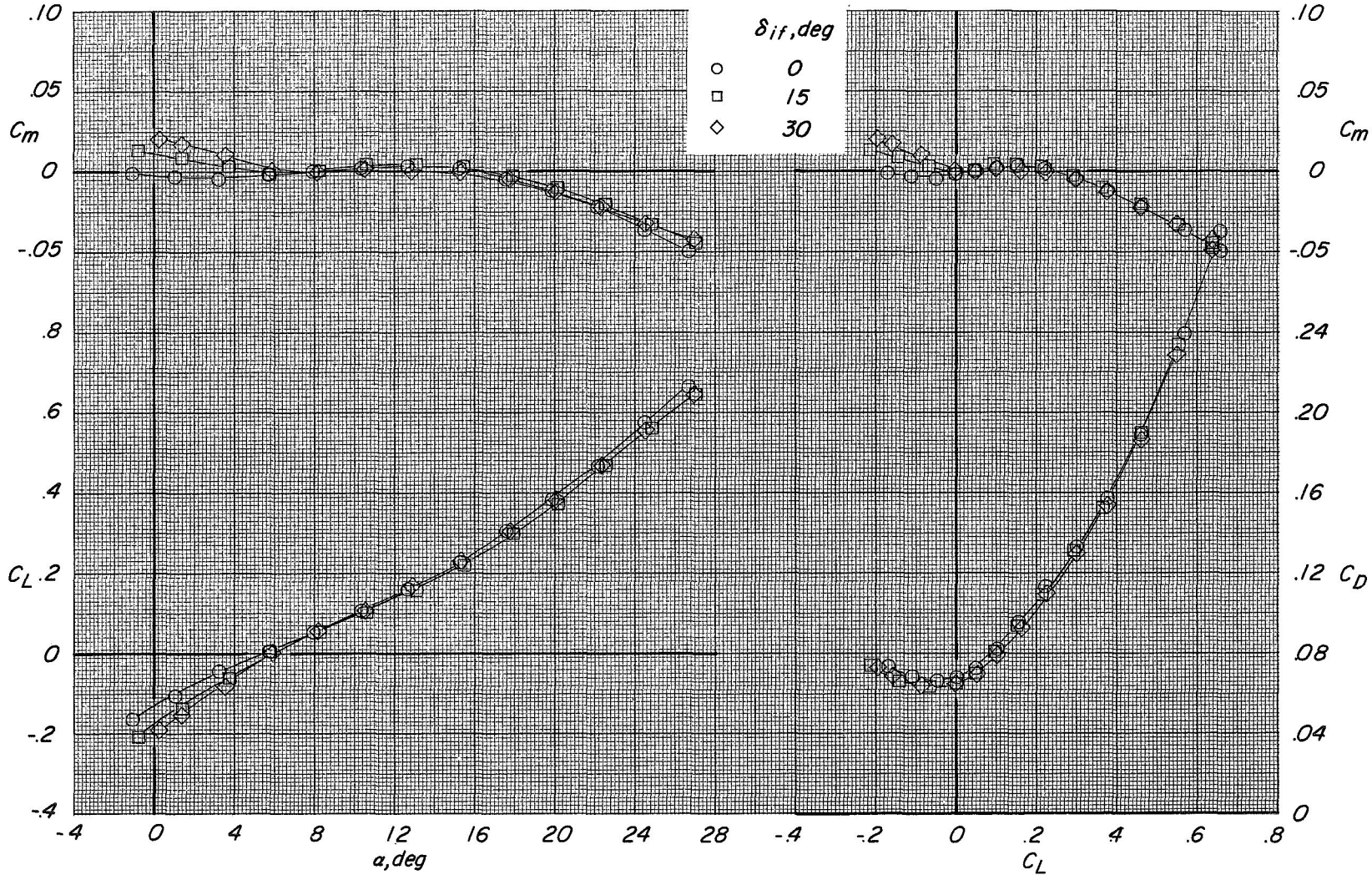
(c) $\delta_e = -5^o$; M = 0.60.

Figure 8.- Continued.



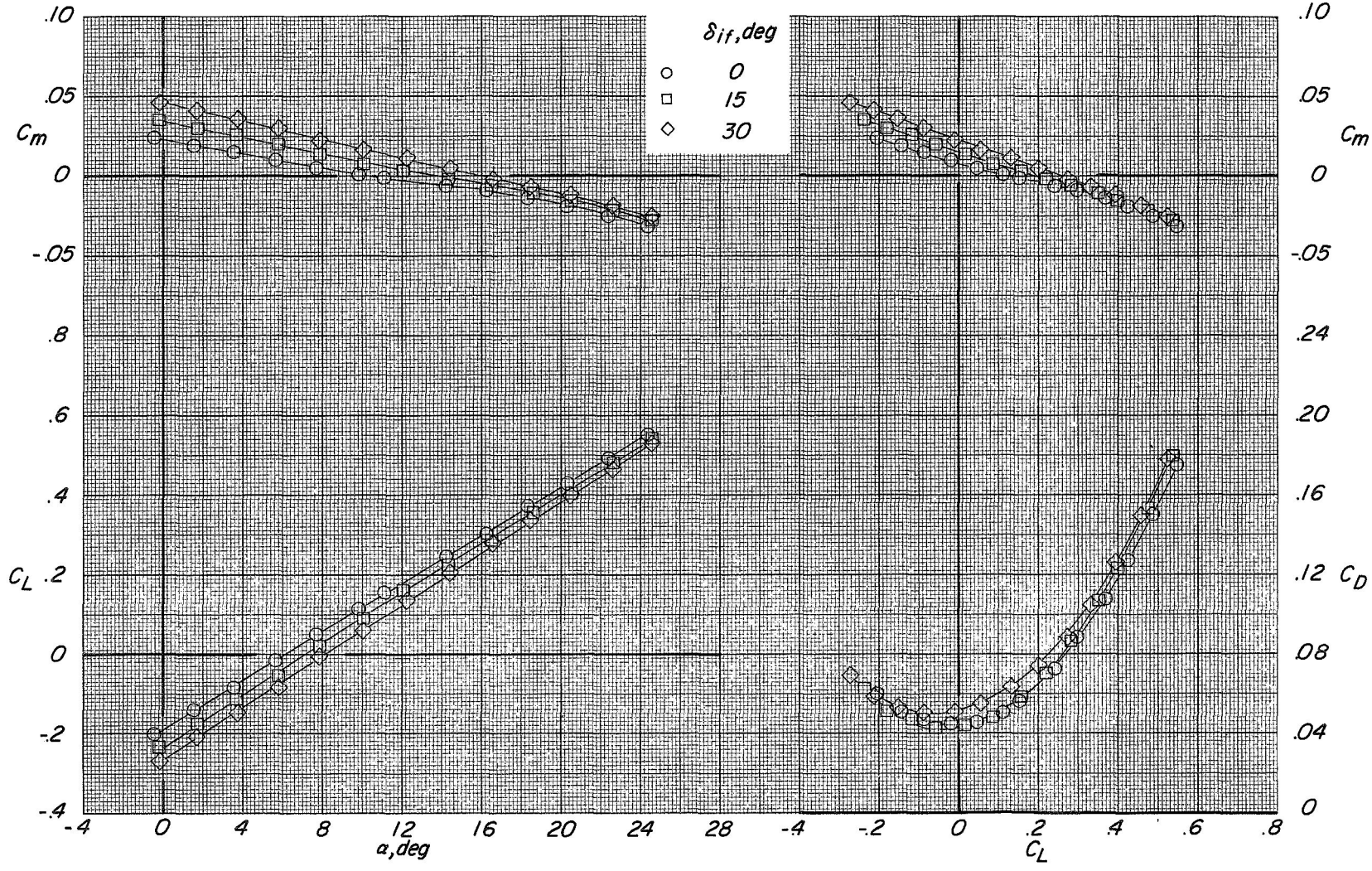
(d) $\delta_e = -5^o$; M = 0.70.

Figure 8.- Continued.



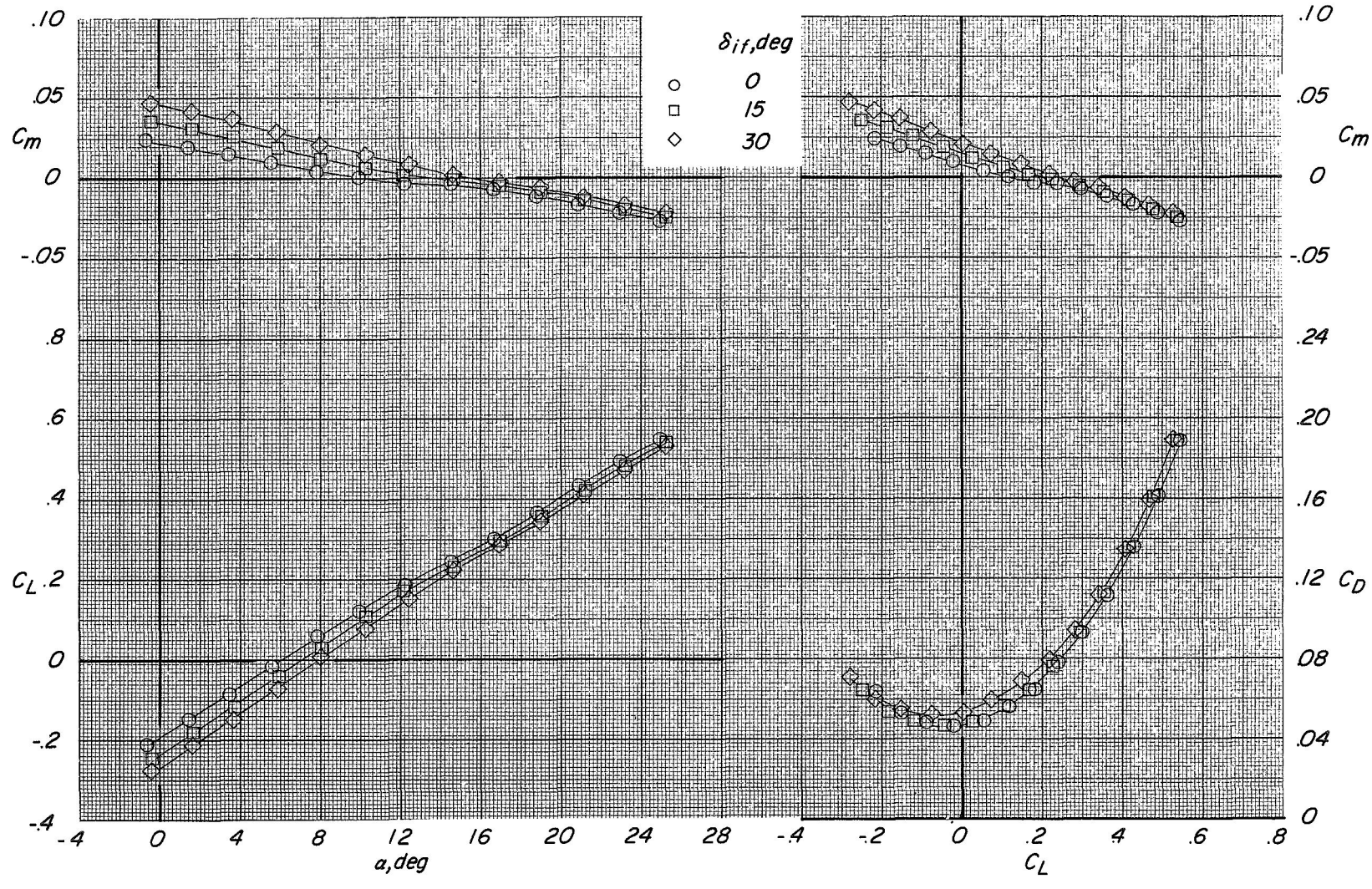
(e) $\delta_e = -5^o$; M = 0.80.

Figure 8.- Continued.



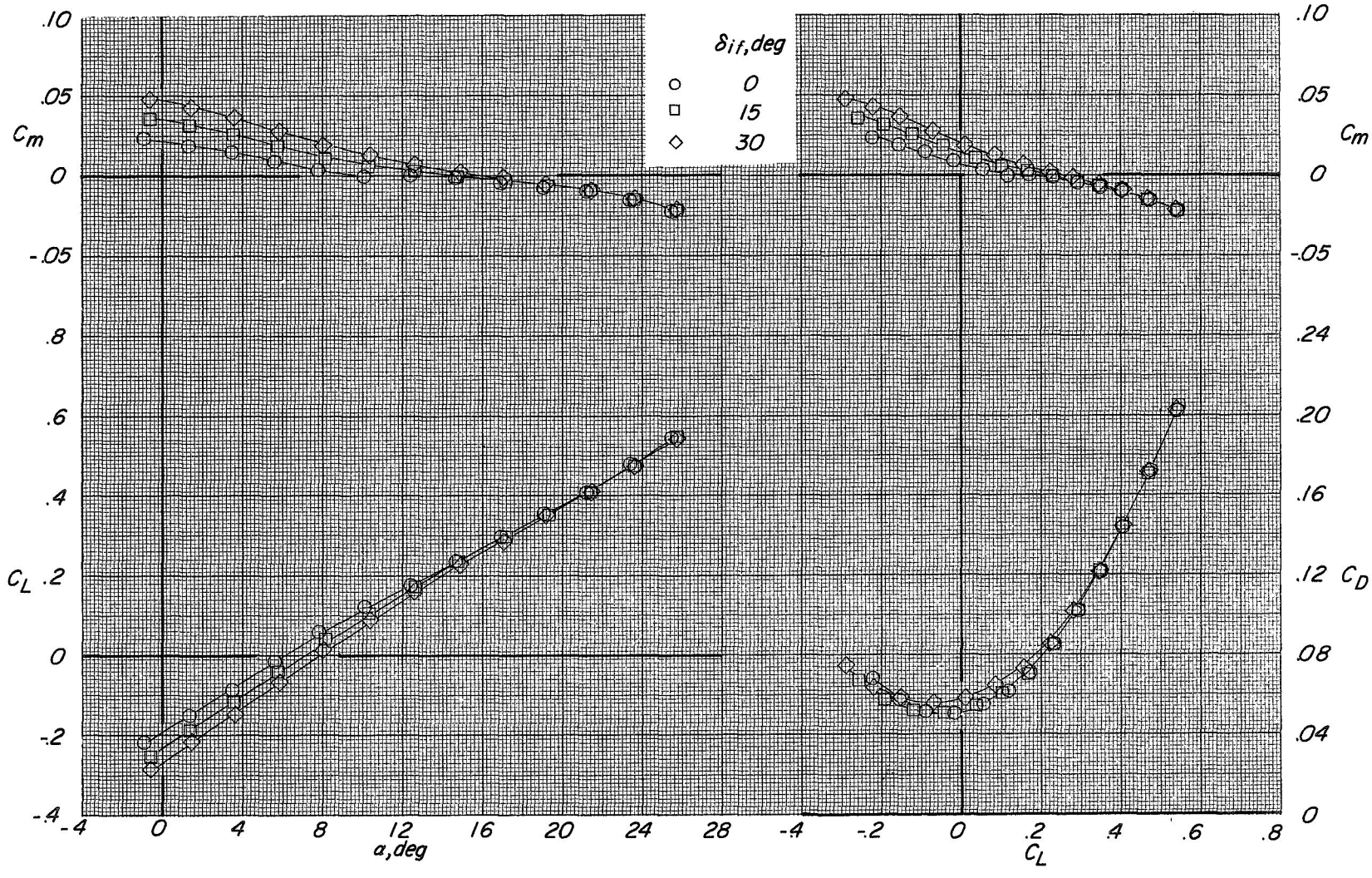
(f) $\delta_e = -10^o$; M = 0.35.

Figure 8.- Continued.



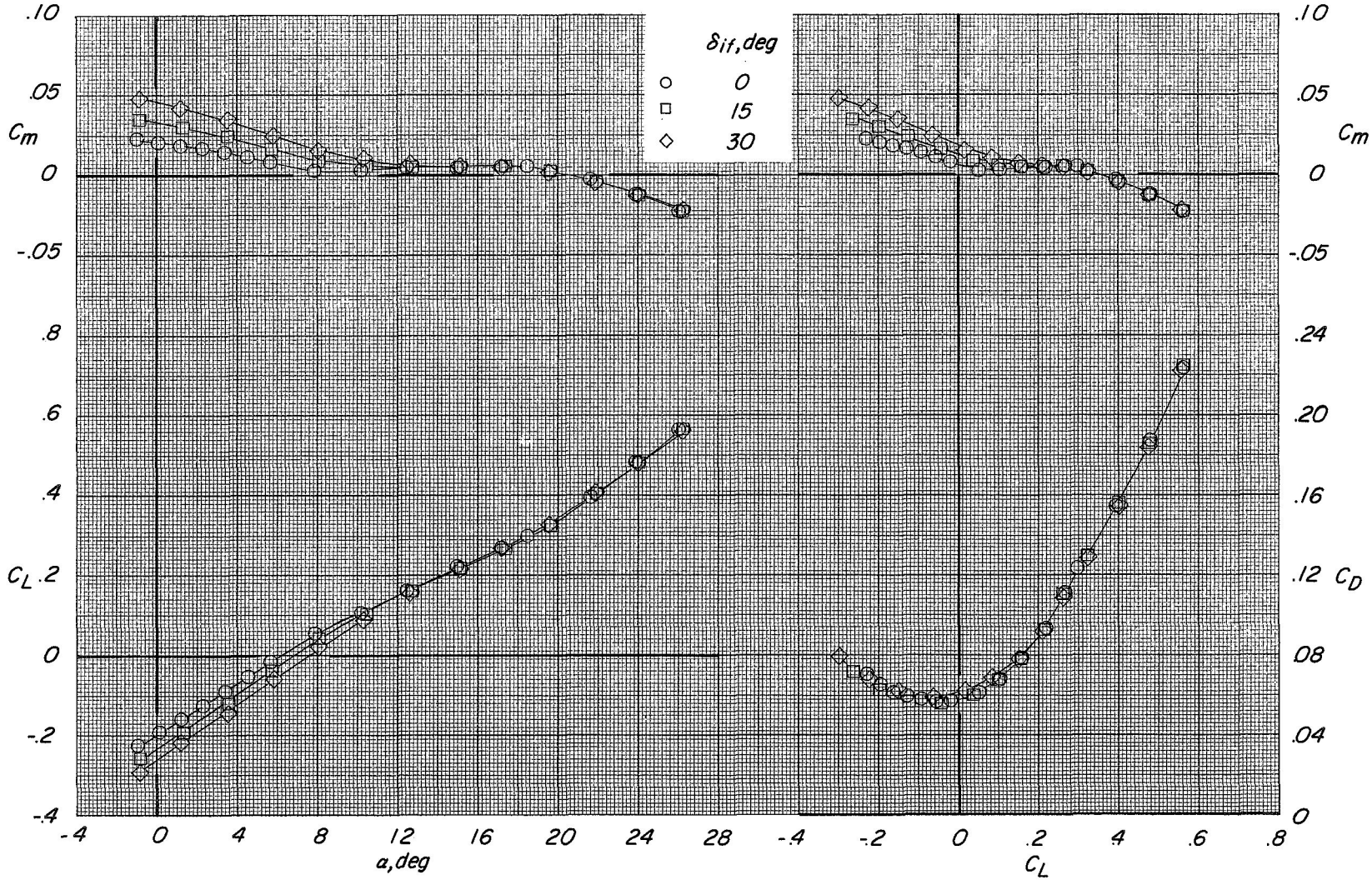
(g) $\delta_e = -10^o$; M = 0.50.

Figure 8.- Continued.



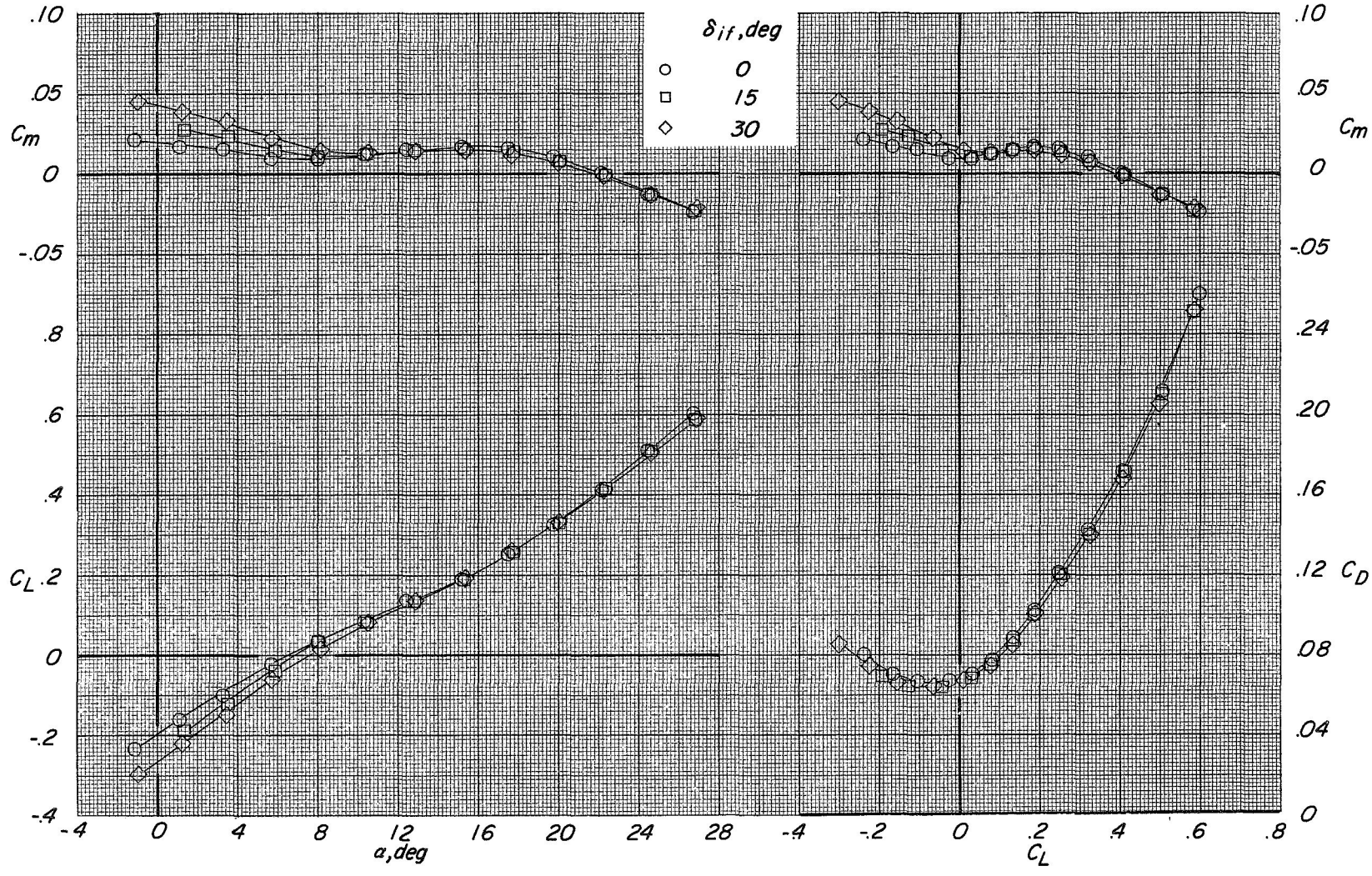
(h) $\delta_e = -10^o$; M = 0.60.

Figure 8.- Continued.



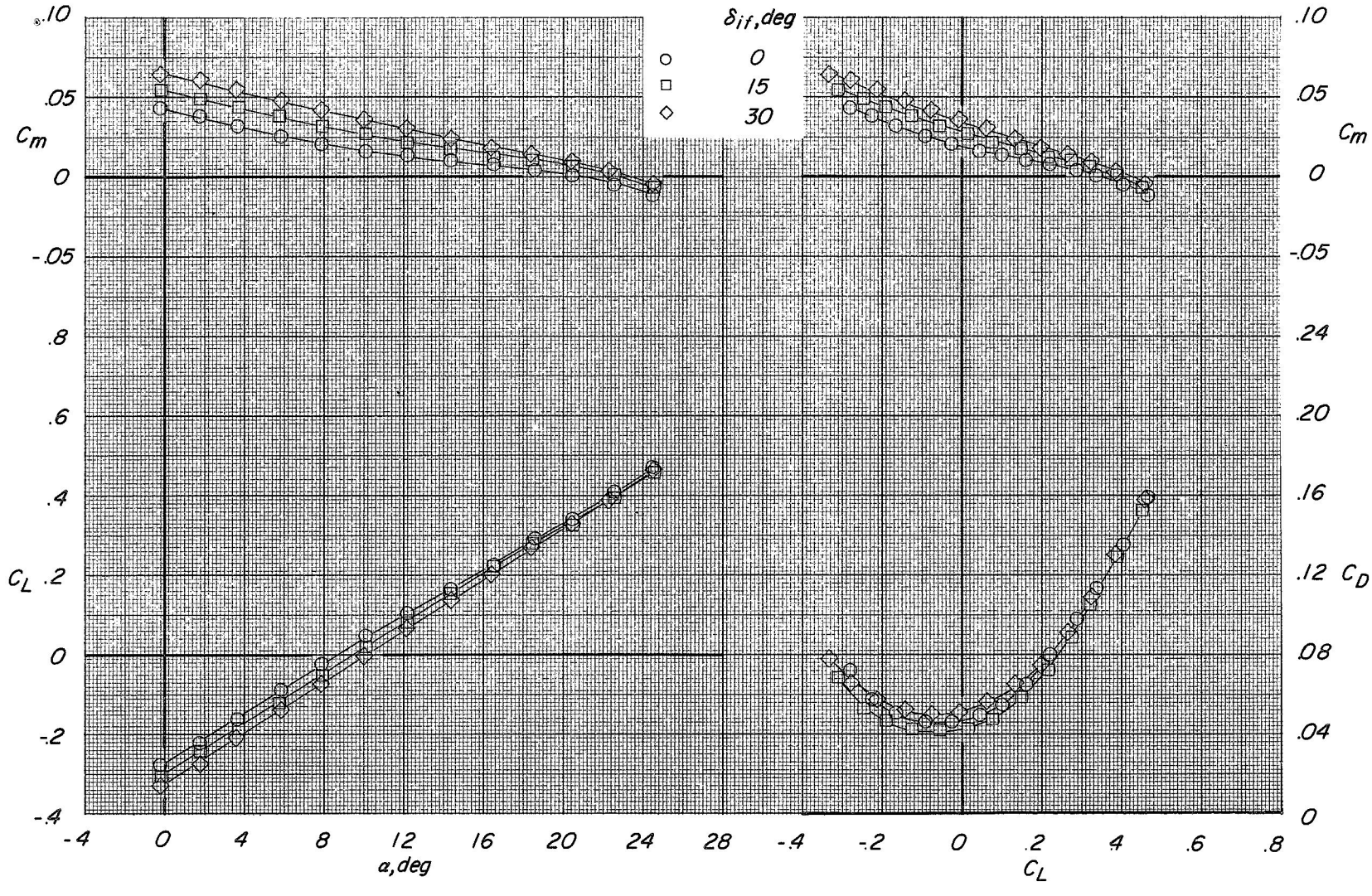
(i) $\delta_e = -10^o$; M = 0.70.

Figure 8.- Continued.



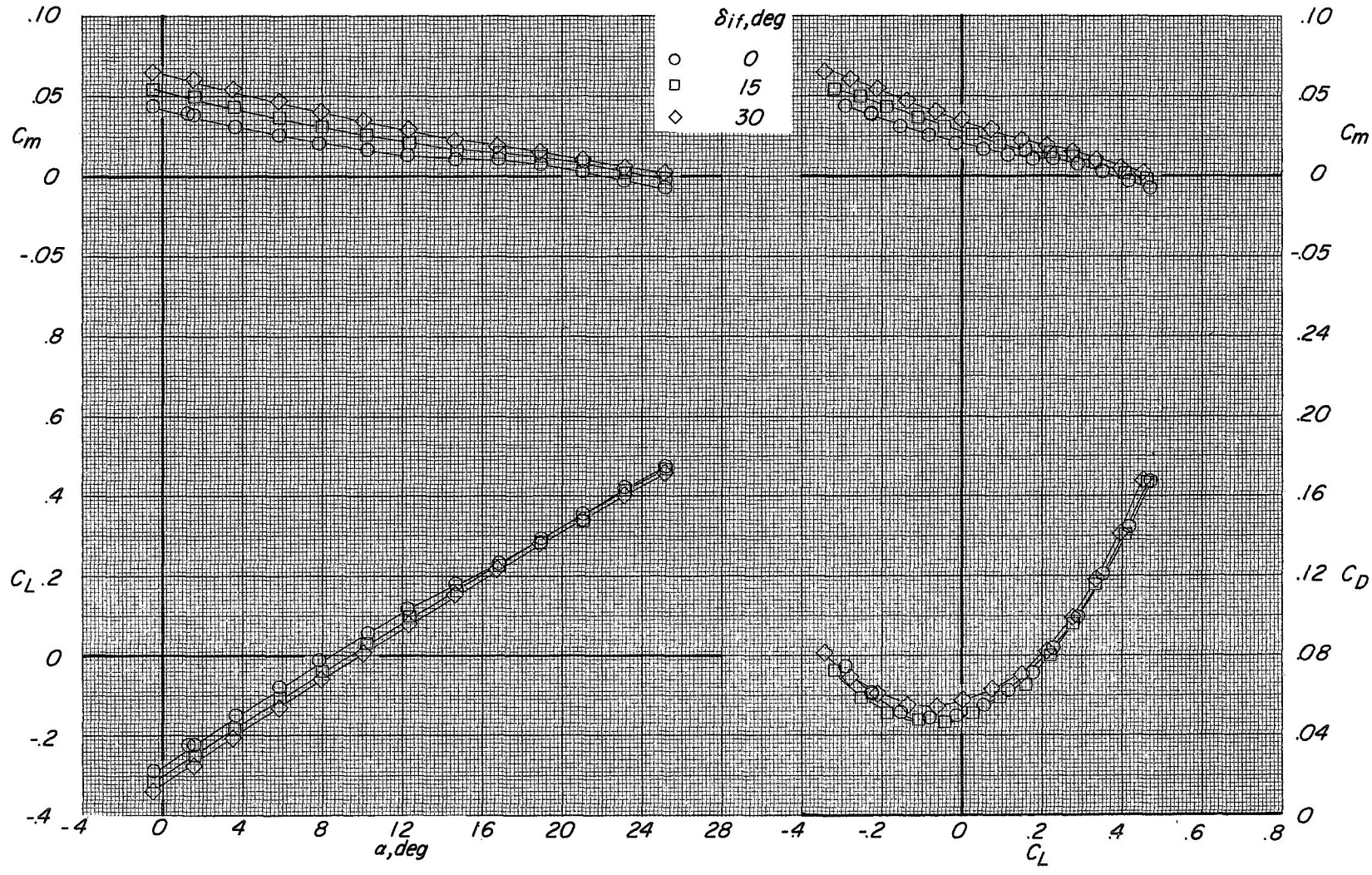
(j) $\delta_e = -10^o$; M = 0.80.

Figure 8.- Continued.



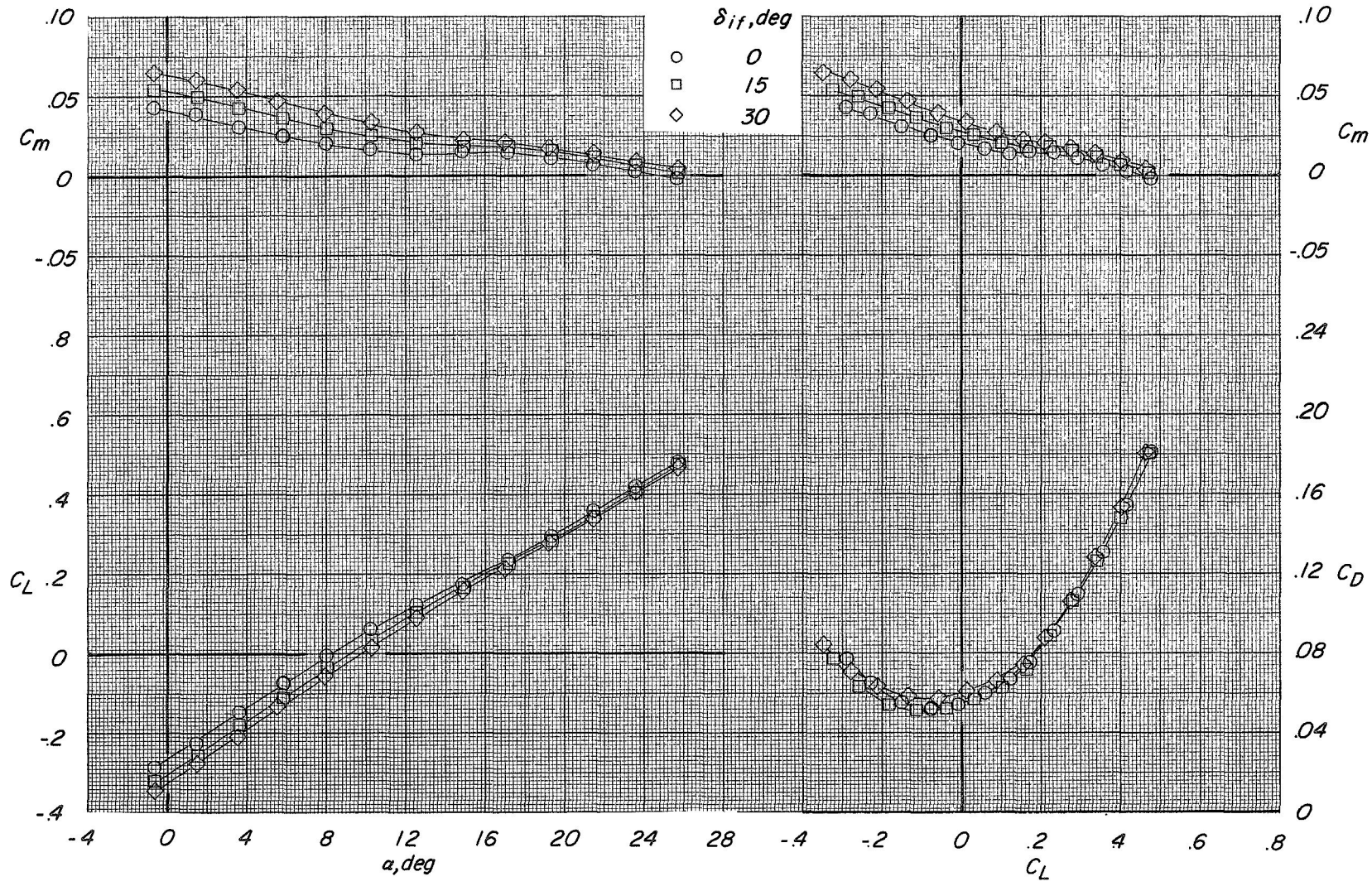
(k) $\delta_e = -15^o$; M = 0.35.

Figure 8.- Continued.



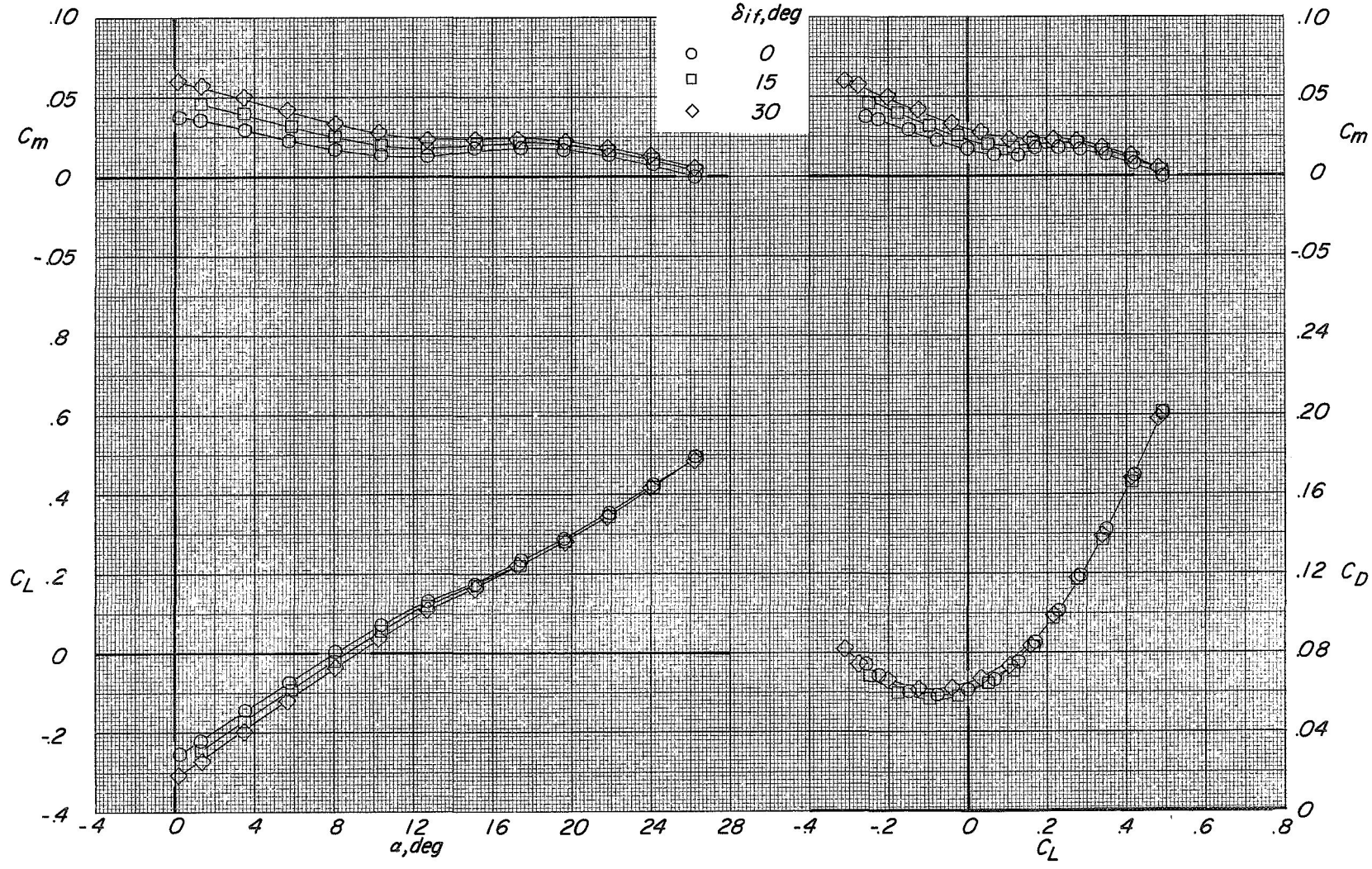
(l) $\delta_e = -15^o$; M = 0.50.

Figure 8.- Continued.



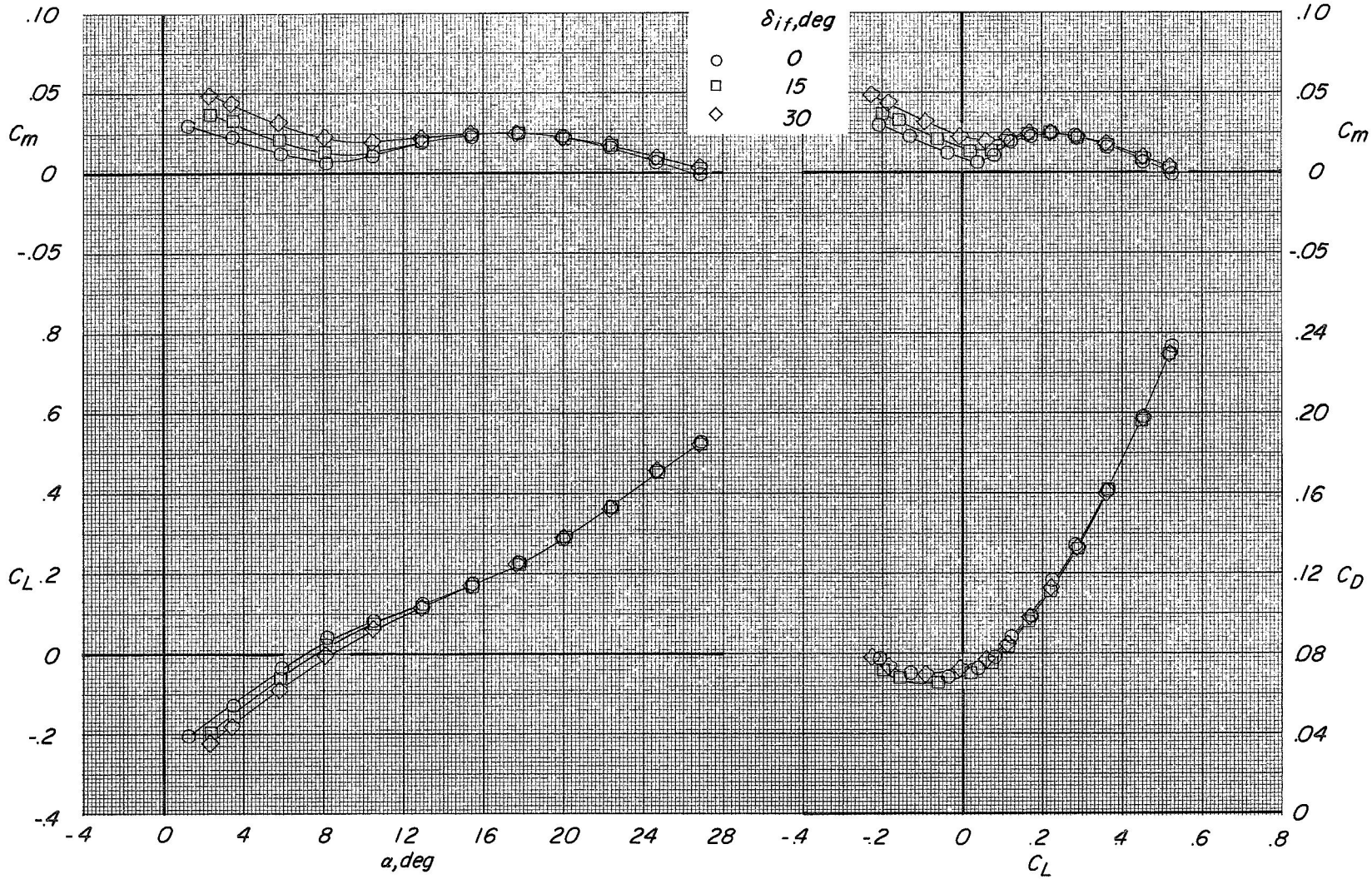
(m) $\delta_e = -15^o$; M = 0.60.

Figure 8.- Continued.



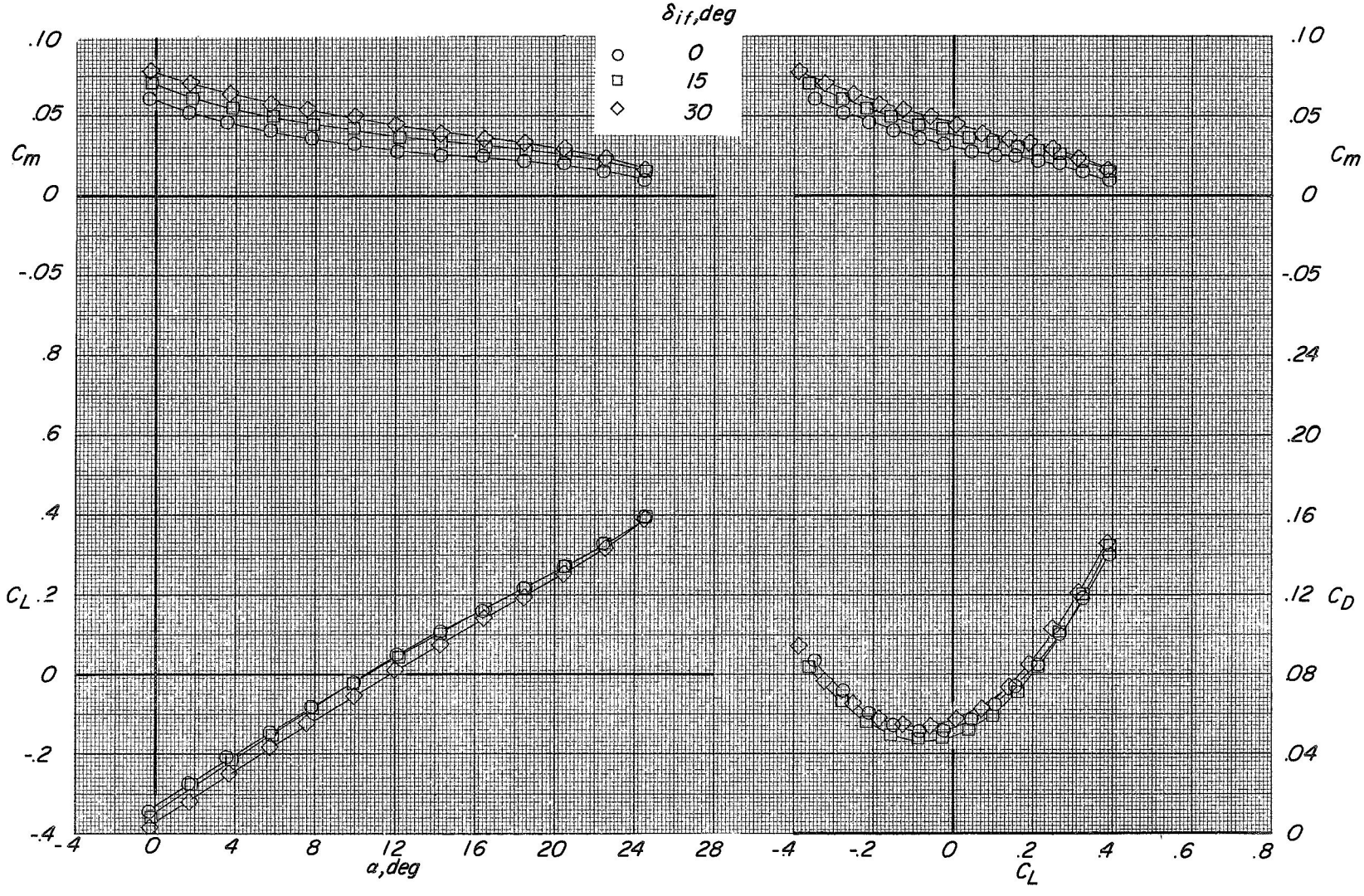
(n) $\delta_e = -15^o$; M = 0.70.

Figure 8.- Continued.



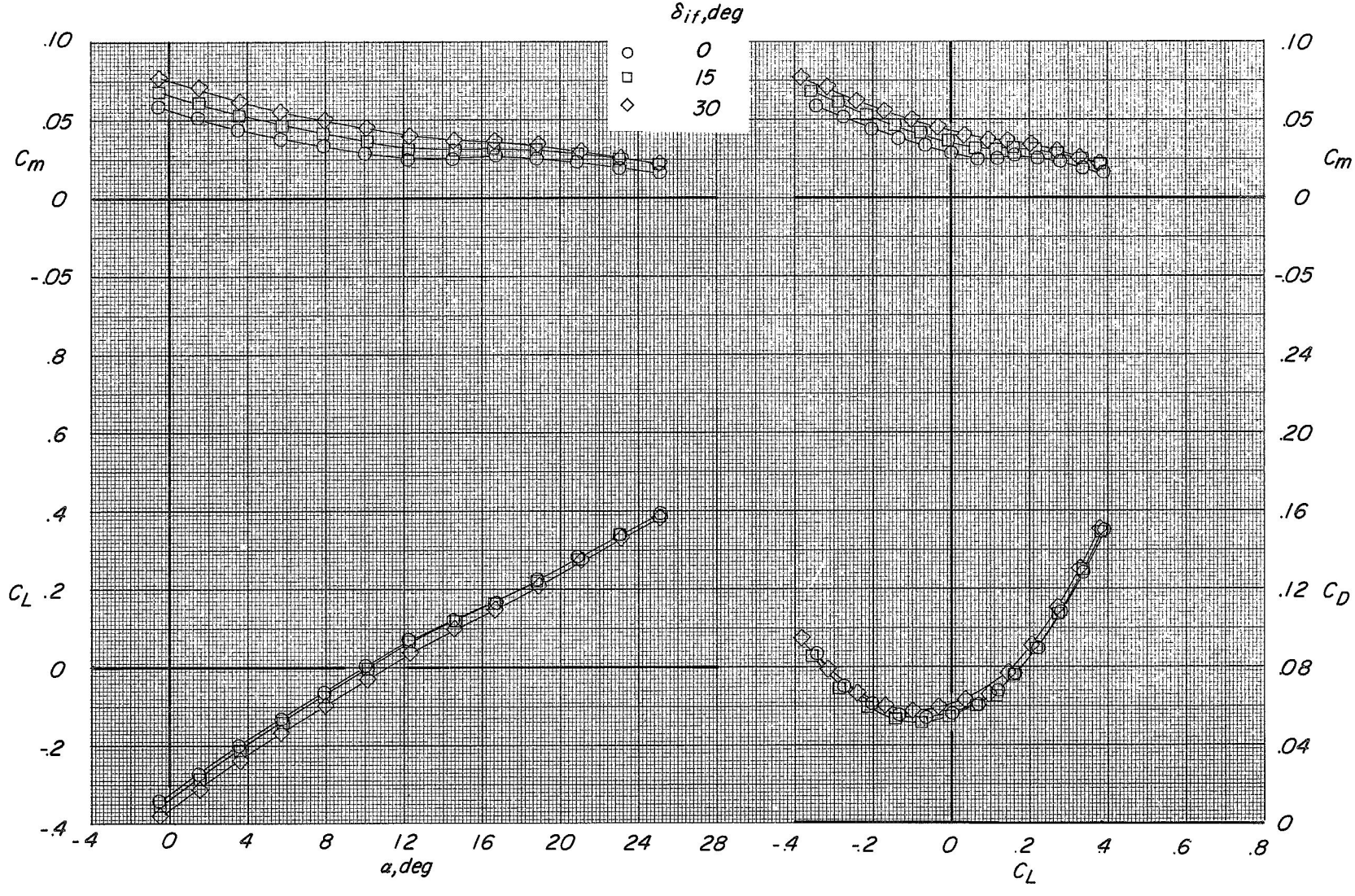
(o) $\delta_e = -15^o$; M = 0.80.

Figure 8.- Continued.



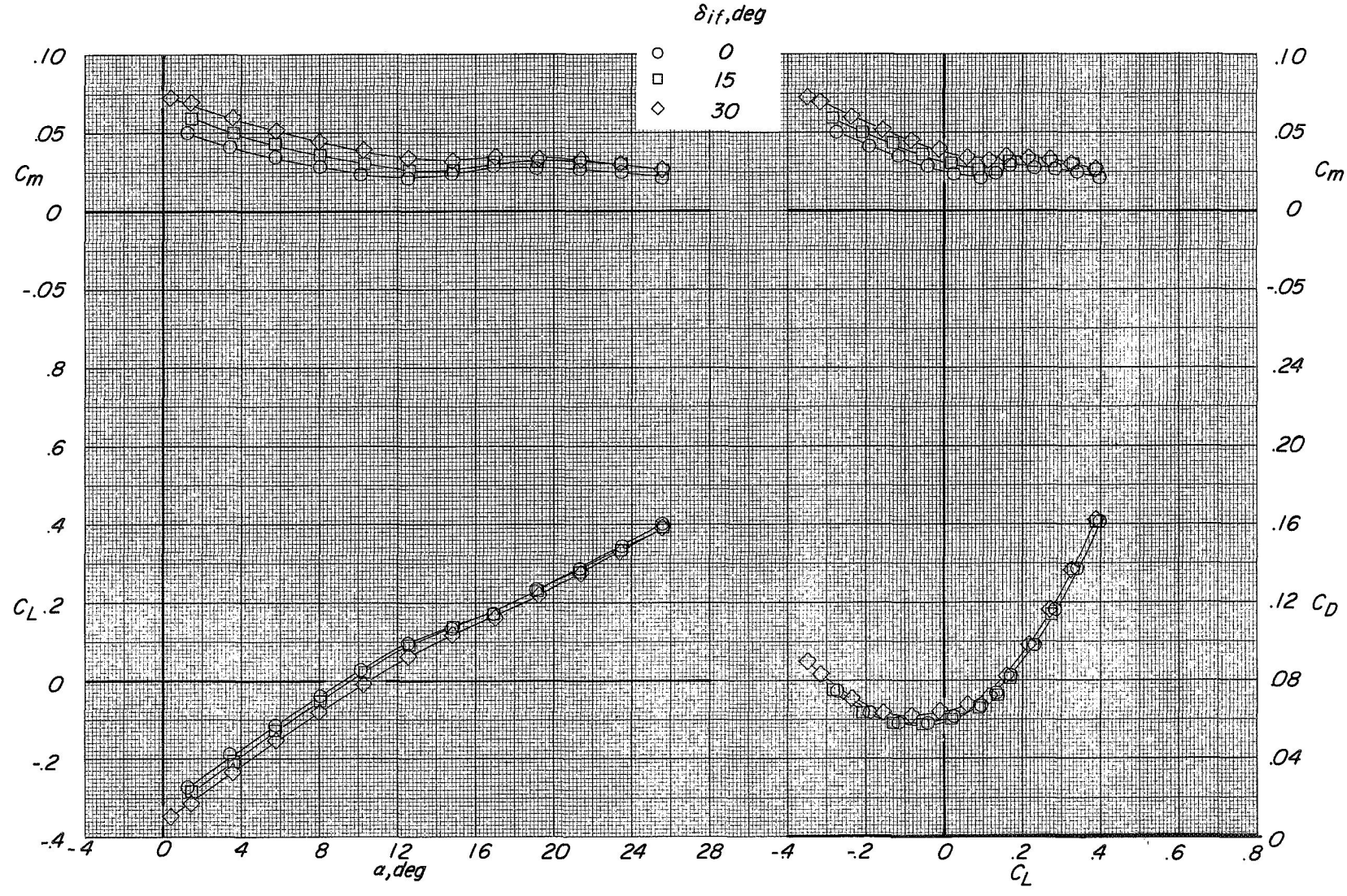
(p) $\delta_e = -20^o$; M = 0.35.

Figure 8.- Continued.



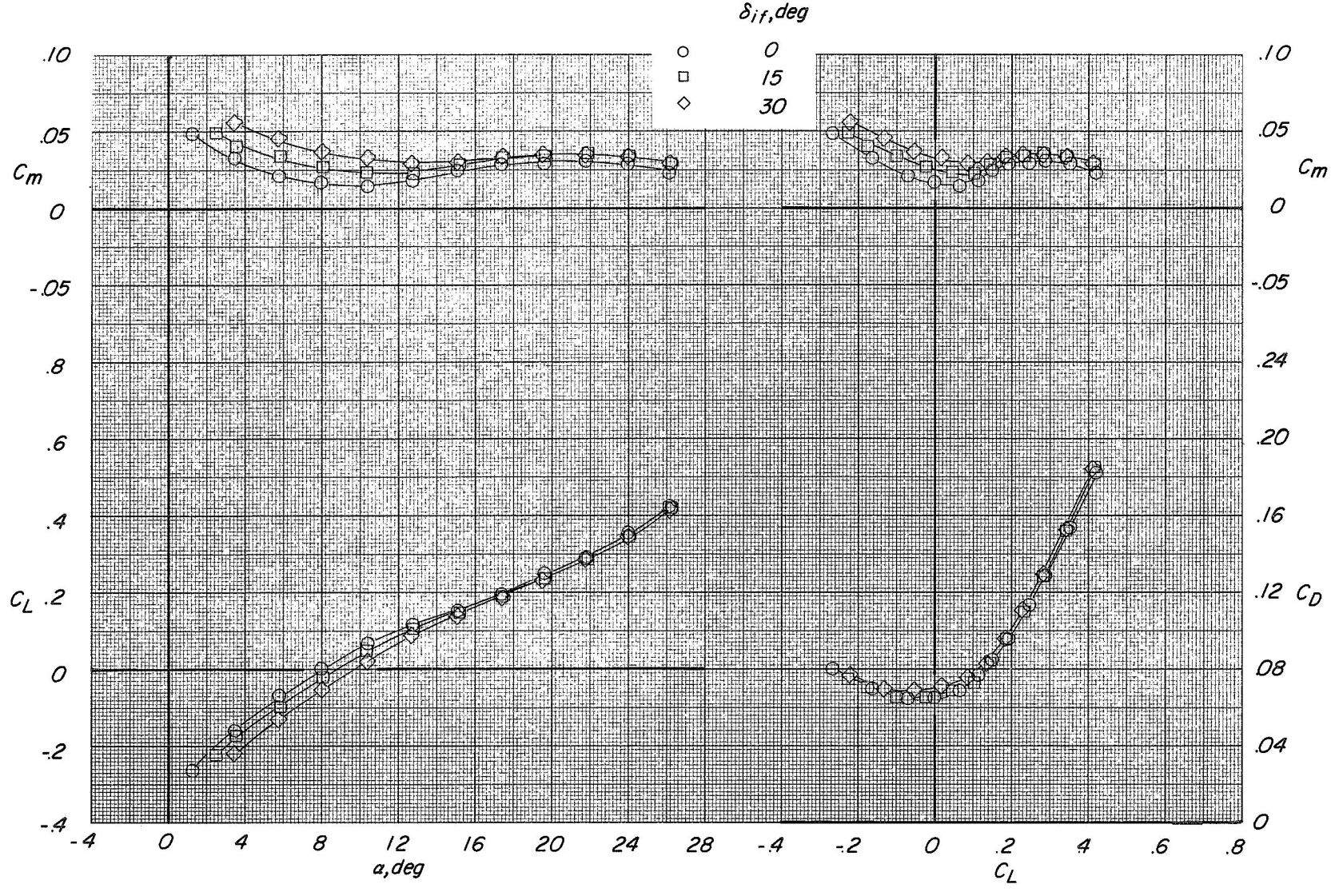
(q) $\delta_e = -20^o$; M = 0.50.

Figure 8.- Continued.



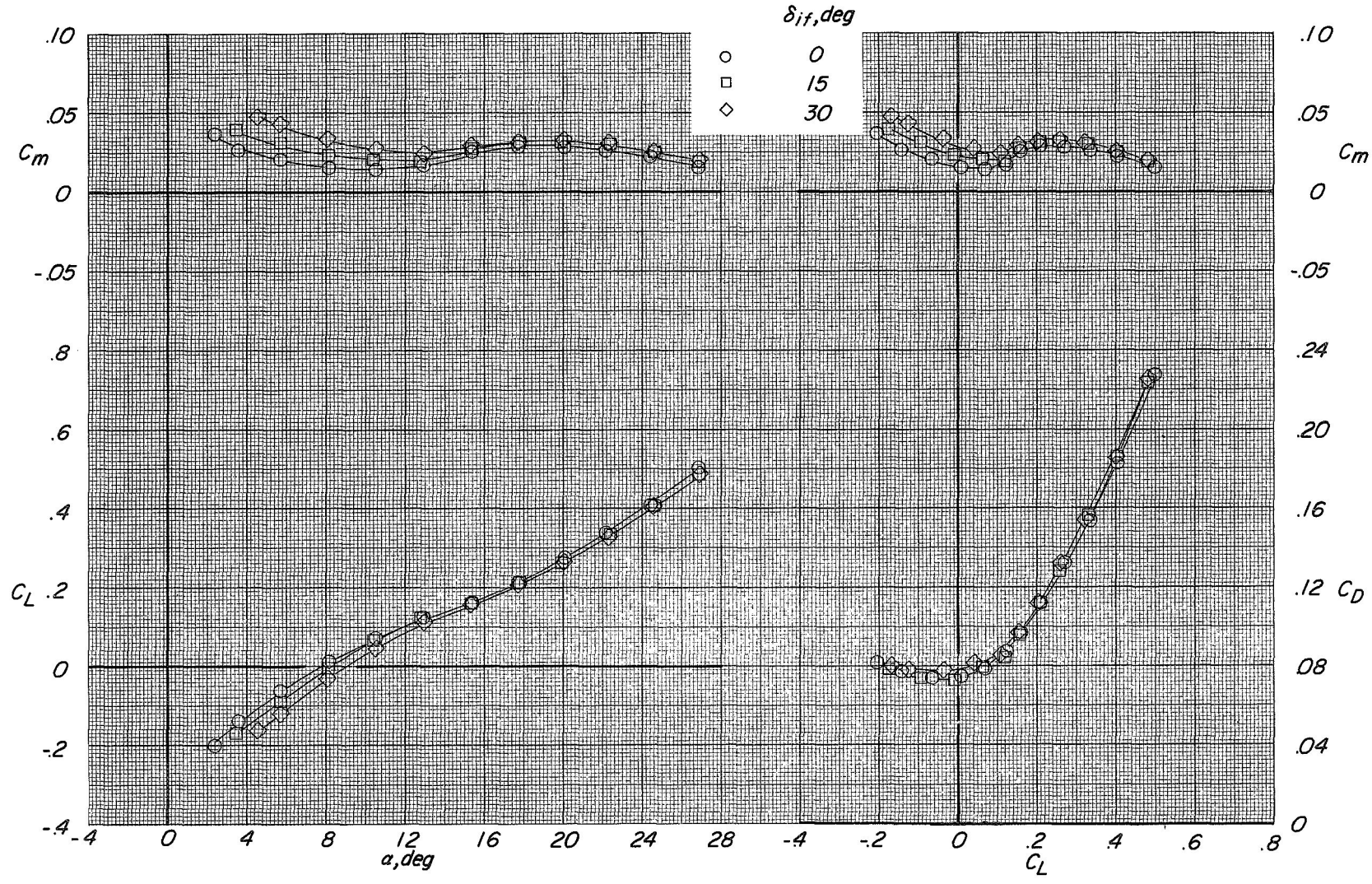
(r) $\delta_e = -20^o$; M = 0.60.

Figure 8.- Continued.



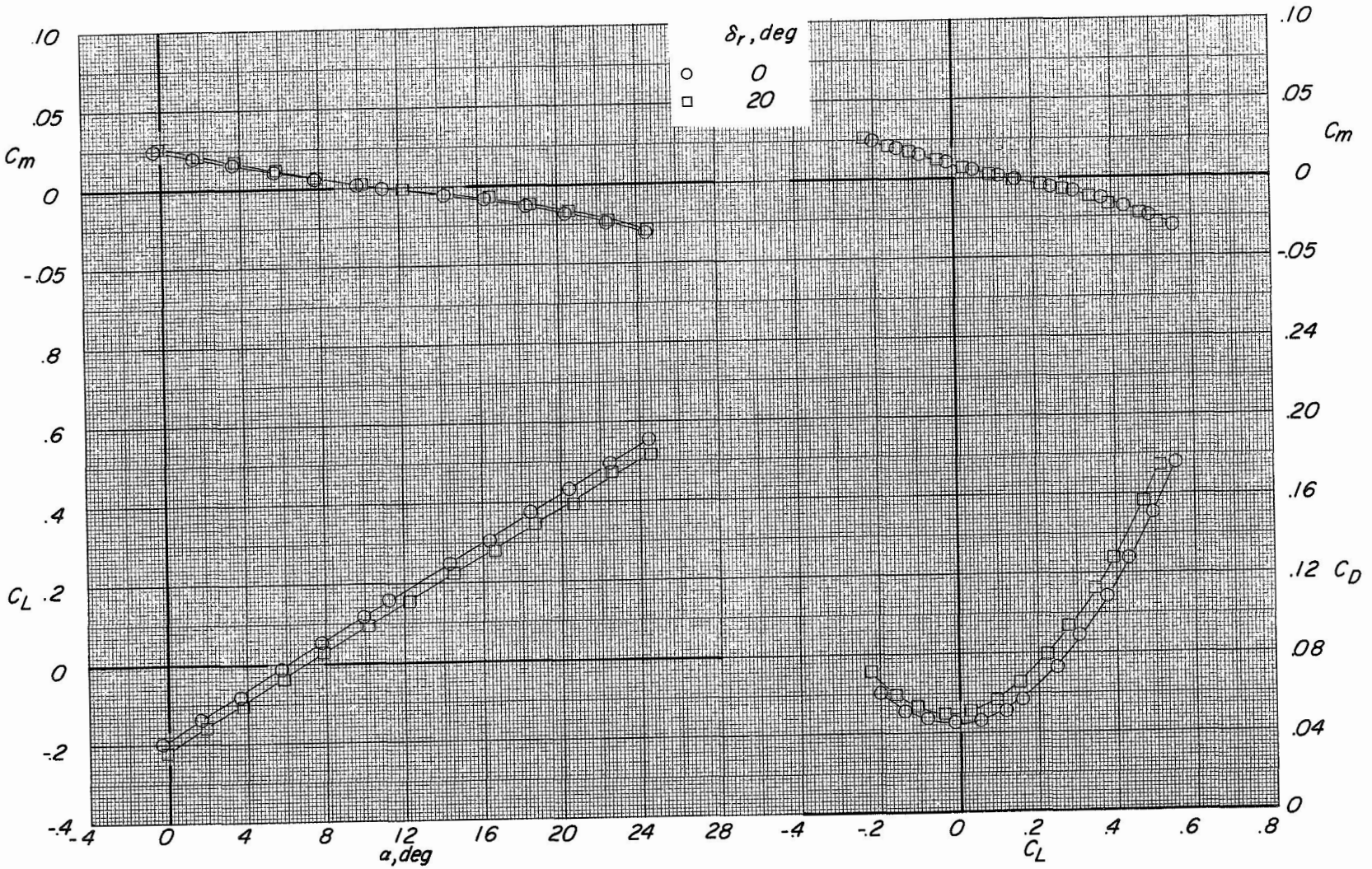
(s) $\delta_e = -20^o$; M = 0.70.

Figure 8.- Continued.



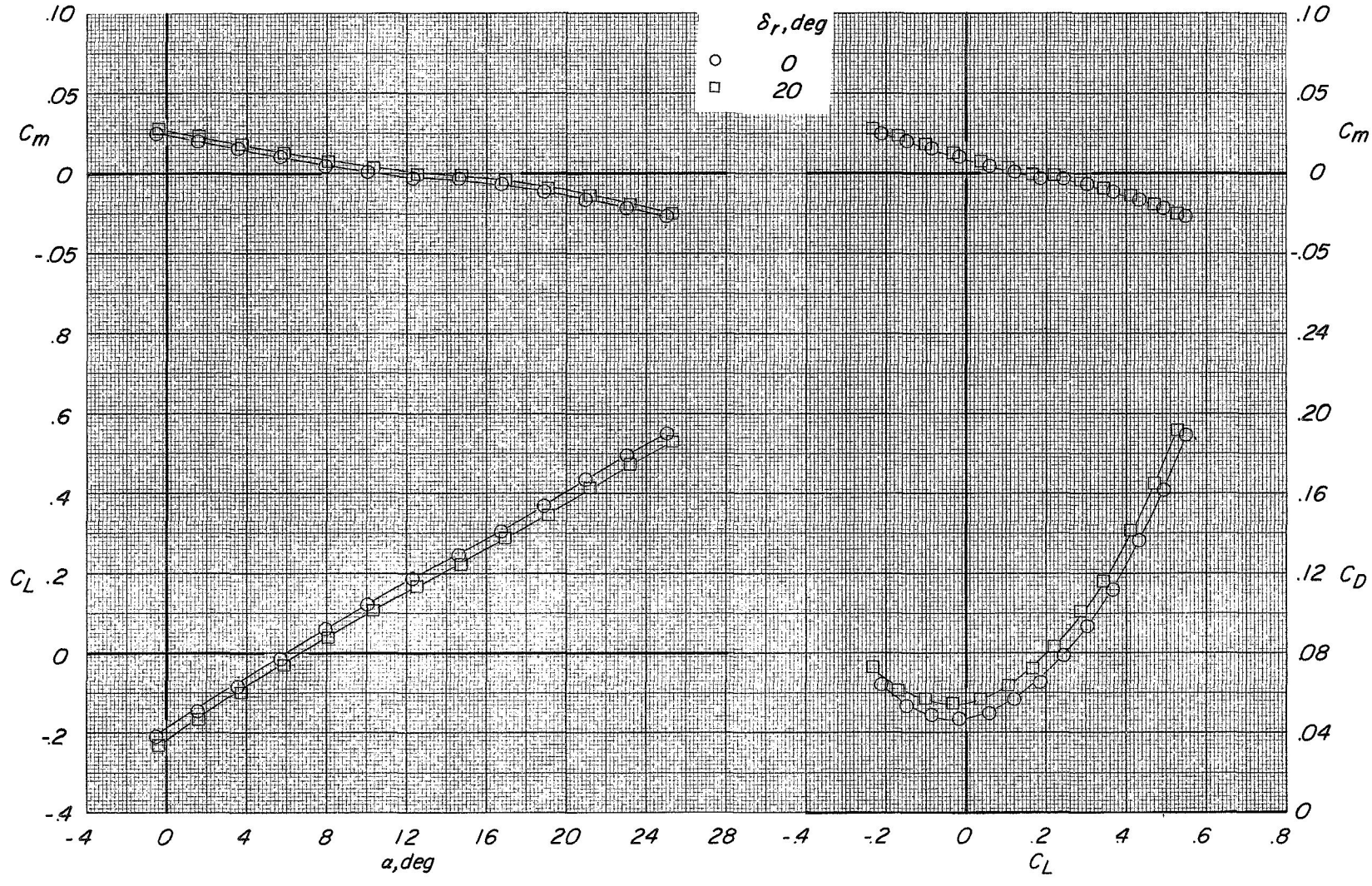
(t) $\delta_e = -20^o$; M = 0.80.

Figure 8.- Concluded.



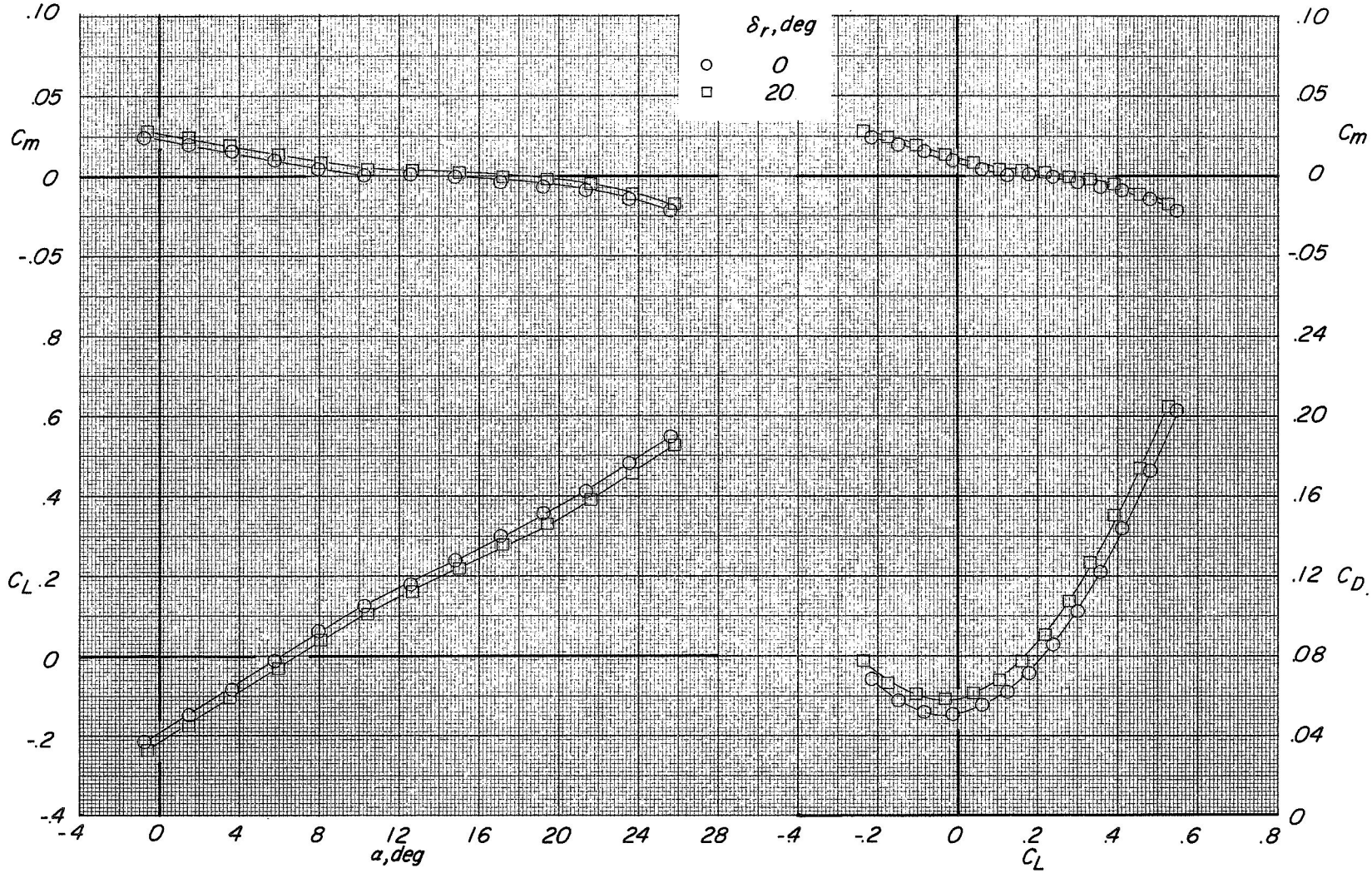
(a) $\delta_e = -10^o$; M = 0.35.

Figure 9.- Effect of rudder deflection δ_r on the longitudinal characteristics of the HL-10 with the basic fin configuration. Auxiliary flaps in the subsonic position; $\beta = \delta_a = 0^o$.



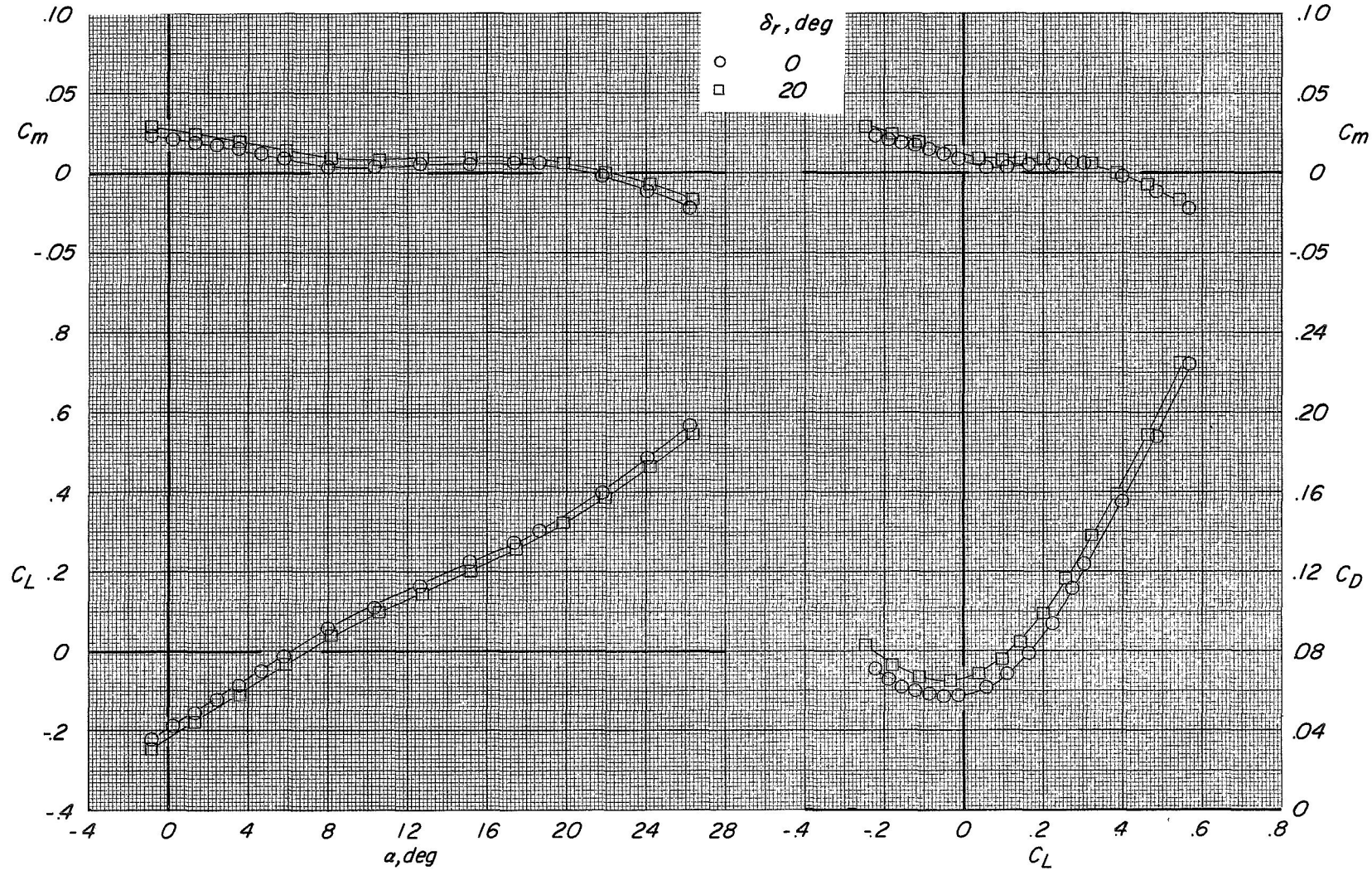
(b) $\delta_e = -10^o$; M = 0.50.

Figure 9.- Continued.



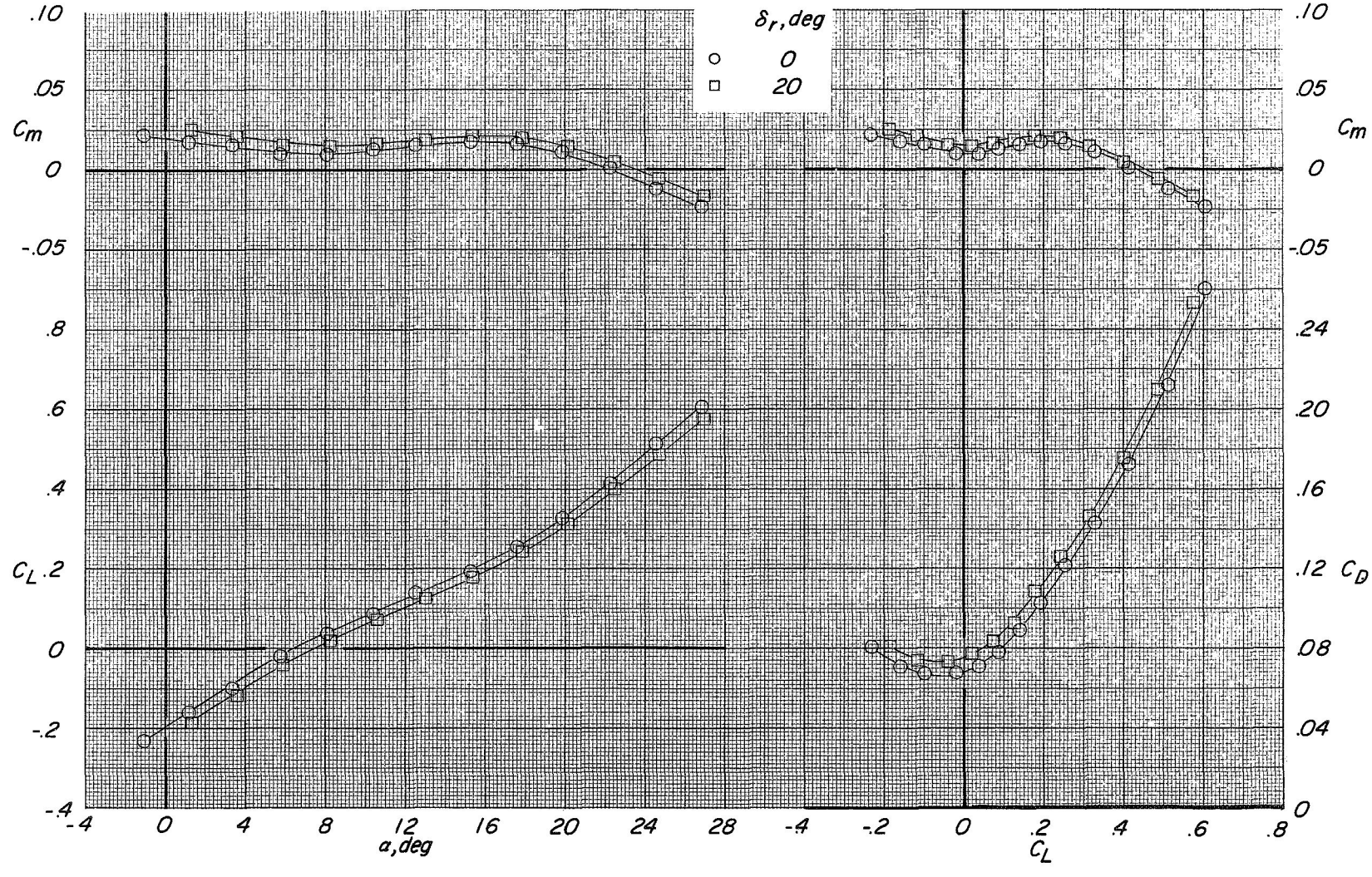
(c) $\delta_e = -10^o$; M = 0.60.

Figure 9.- Continued.



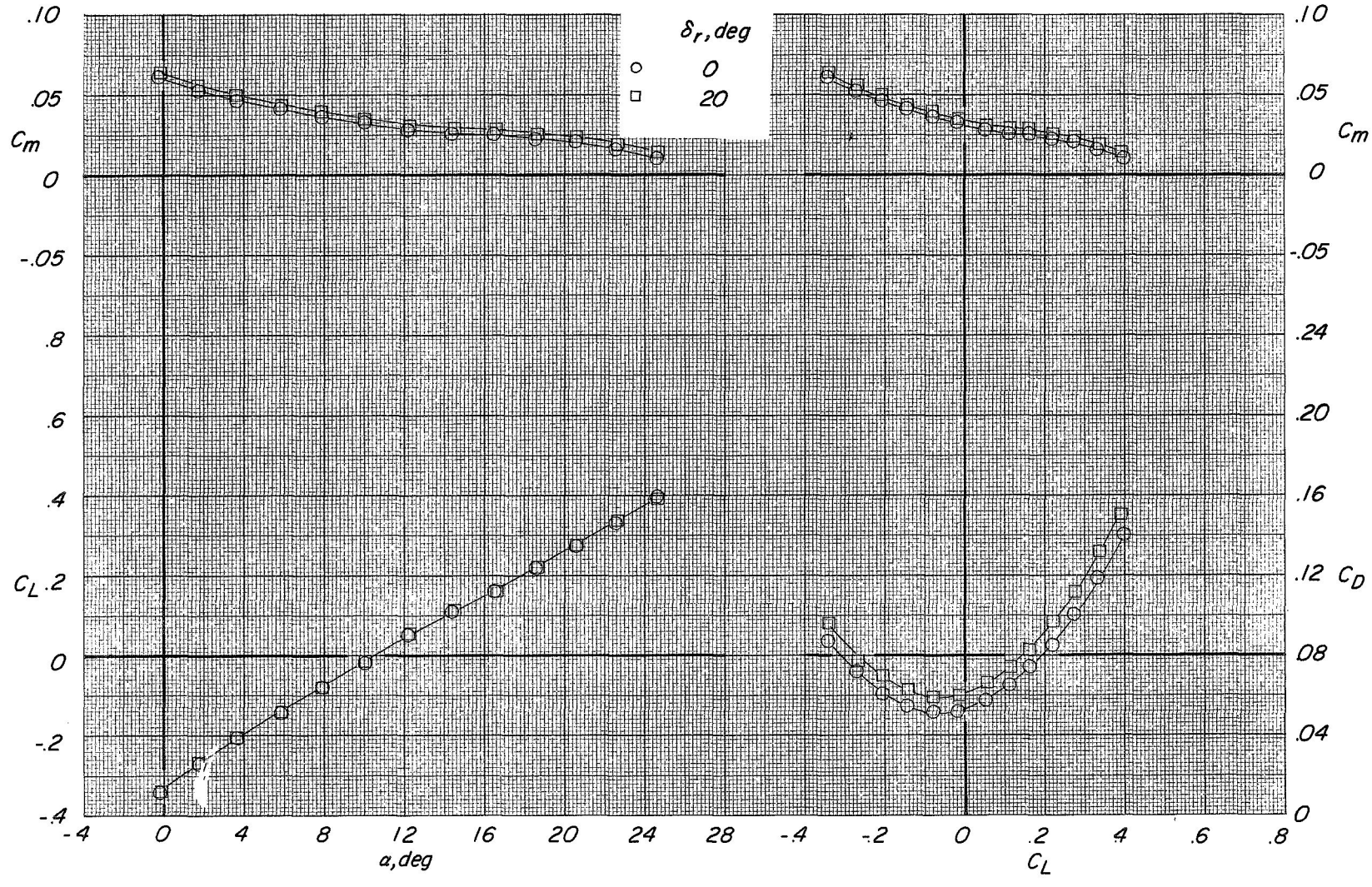
(d) $\delta_e = -10^o$; M = 0.70.

Figure 9.- Continued.



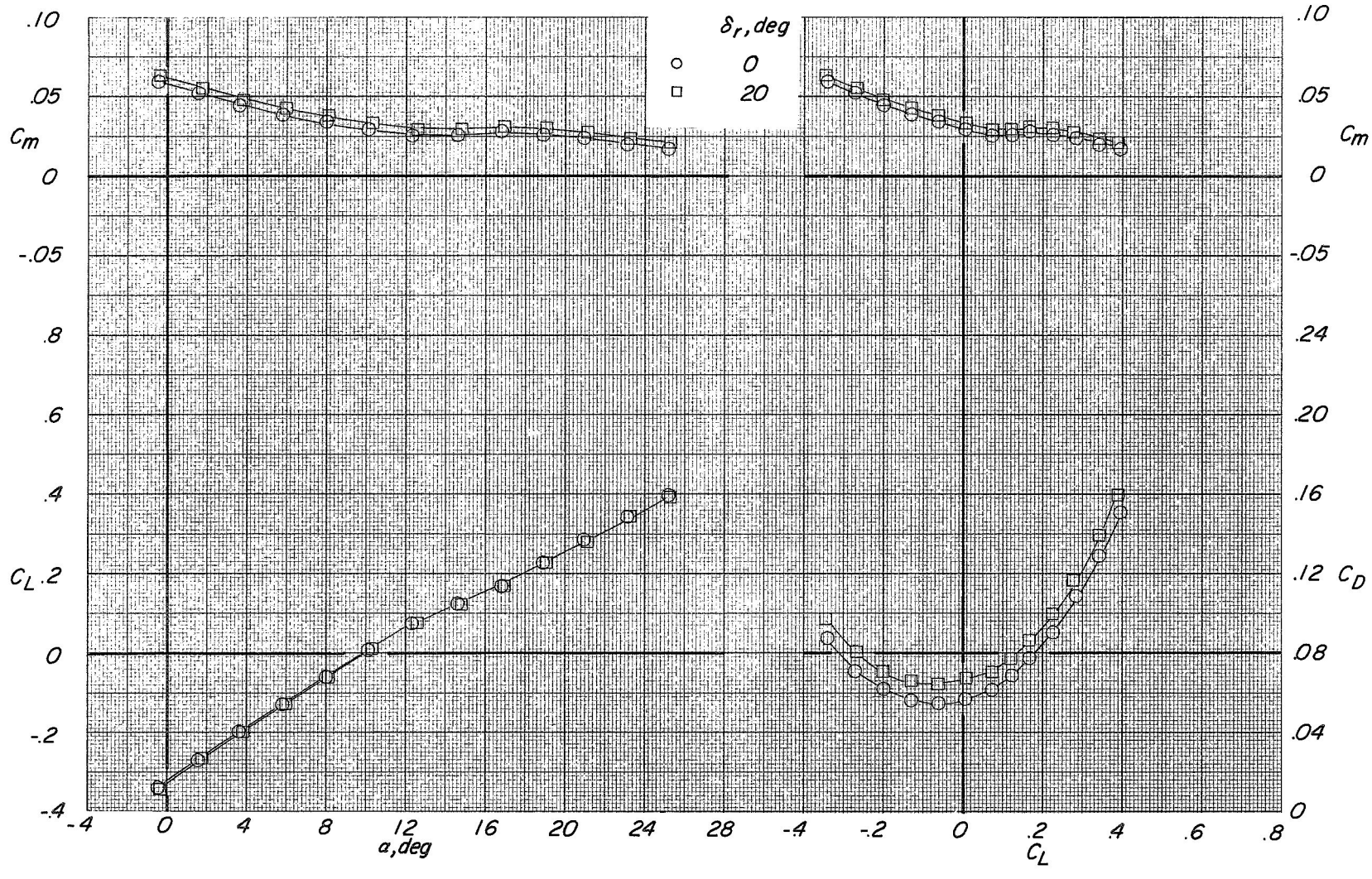
(e) $\delta_e = -10^o$; M = 0.80.

Figure 9.- Continued.



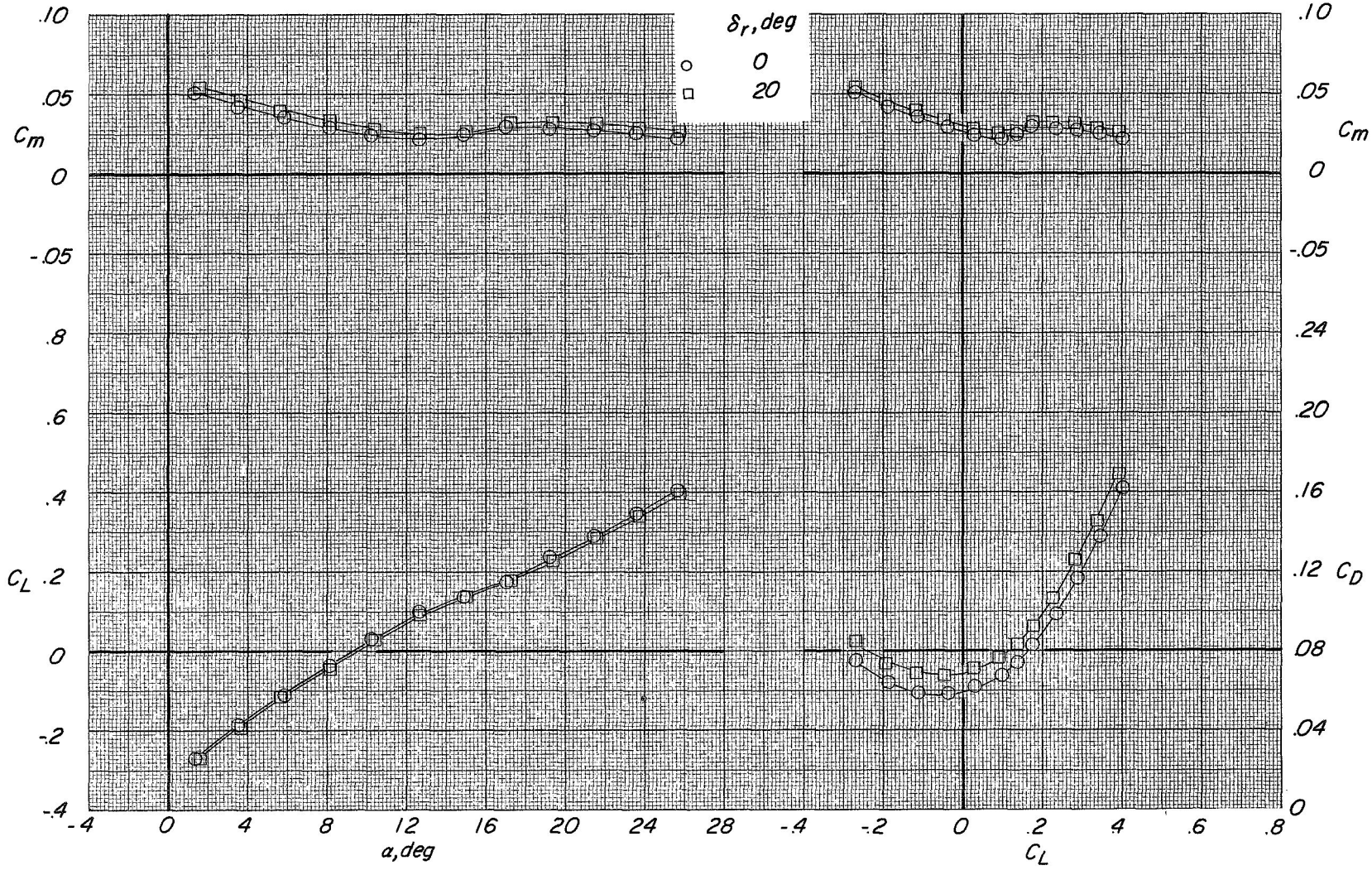
(f) $\delta_e = -10^o$; M = 0.35.

Figure 9.- Continued.



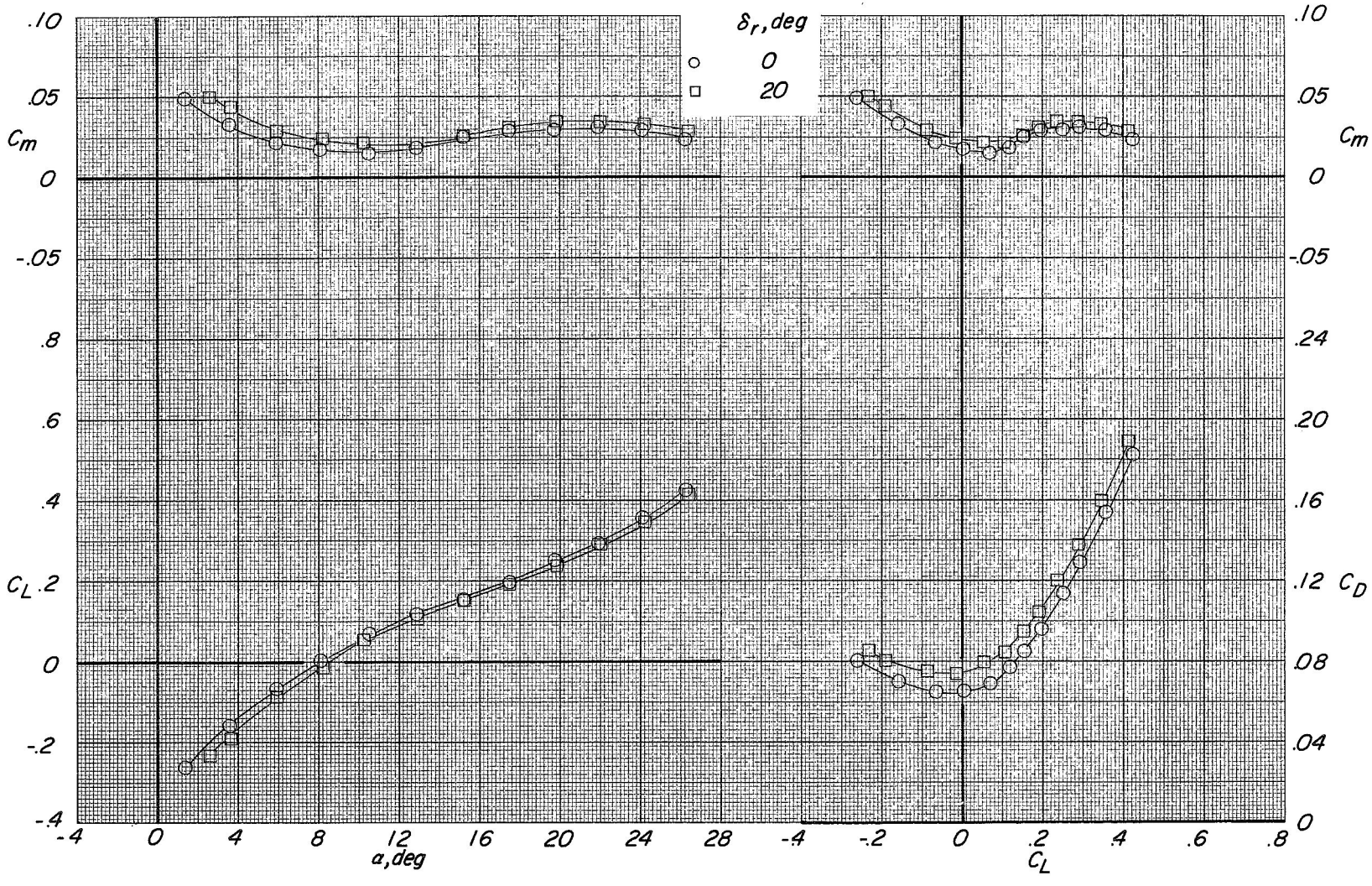
(g) $\delta_e = -10^o$; M = 0.50.

Figure 9.- Continued.



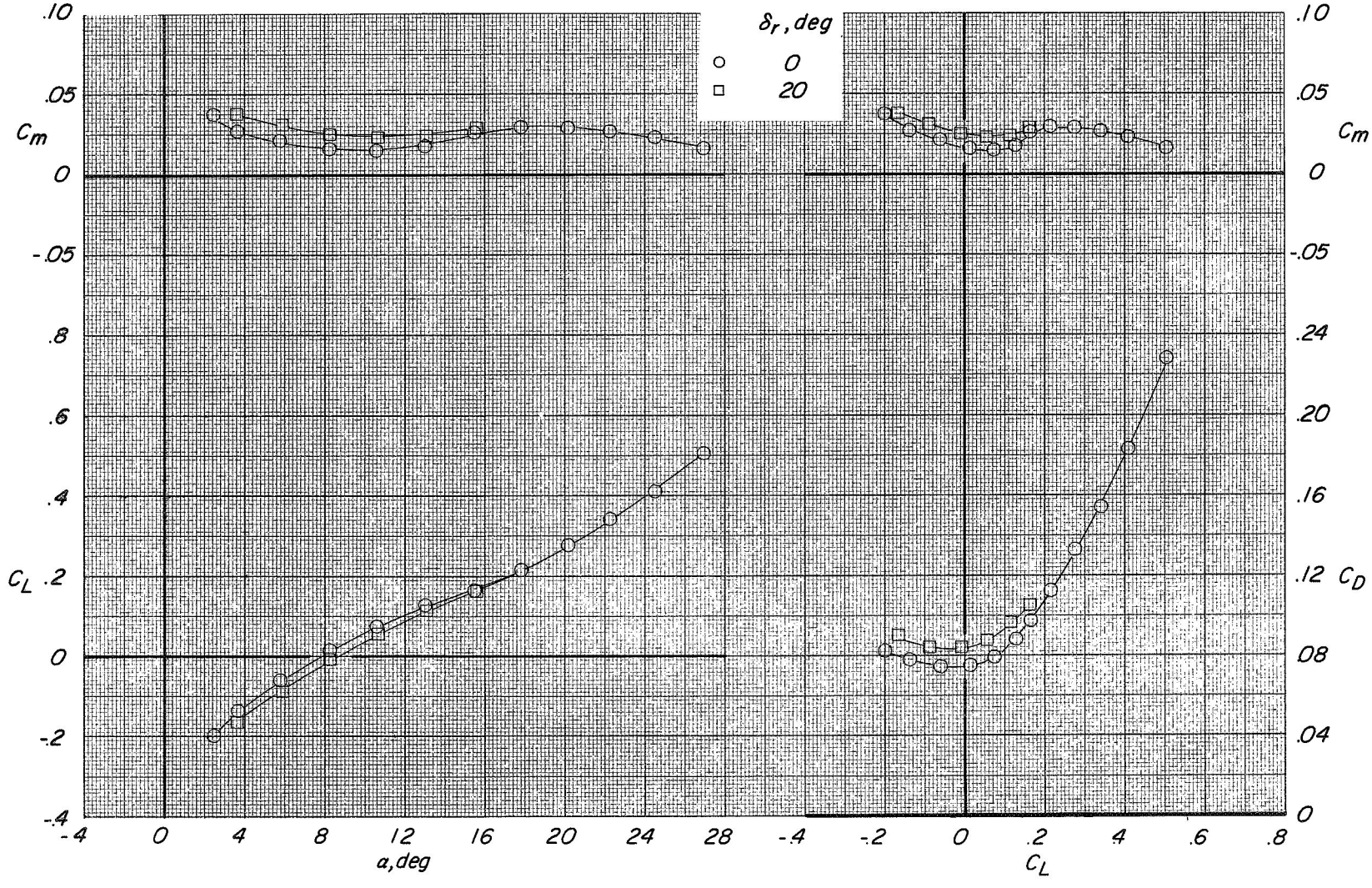
(h) $\delta_e = -10^o$; M = 0.60.

Figure 9.- Continued.



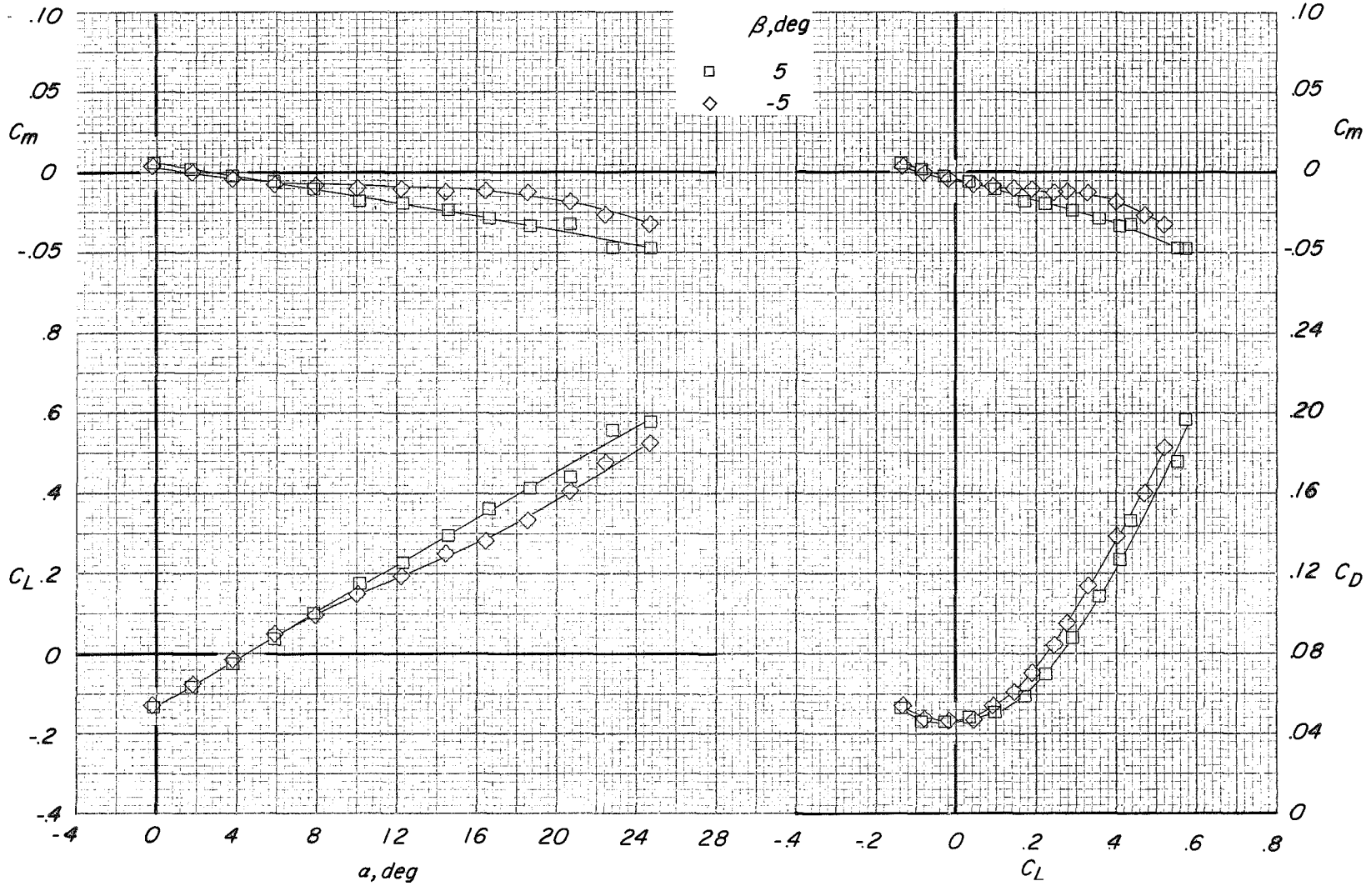
(i) $\delta_e = -10^o$; M = 0.70.

Figure 9.- Continued.



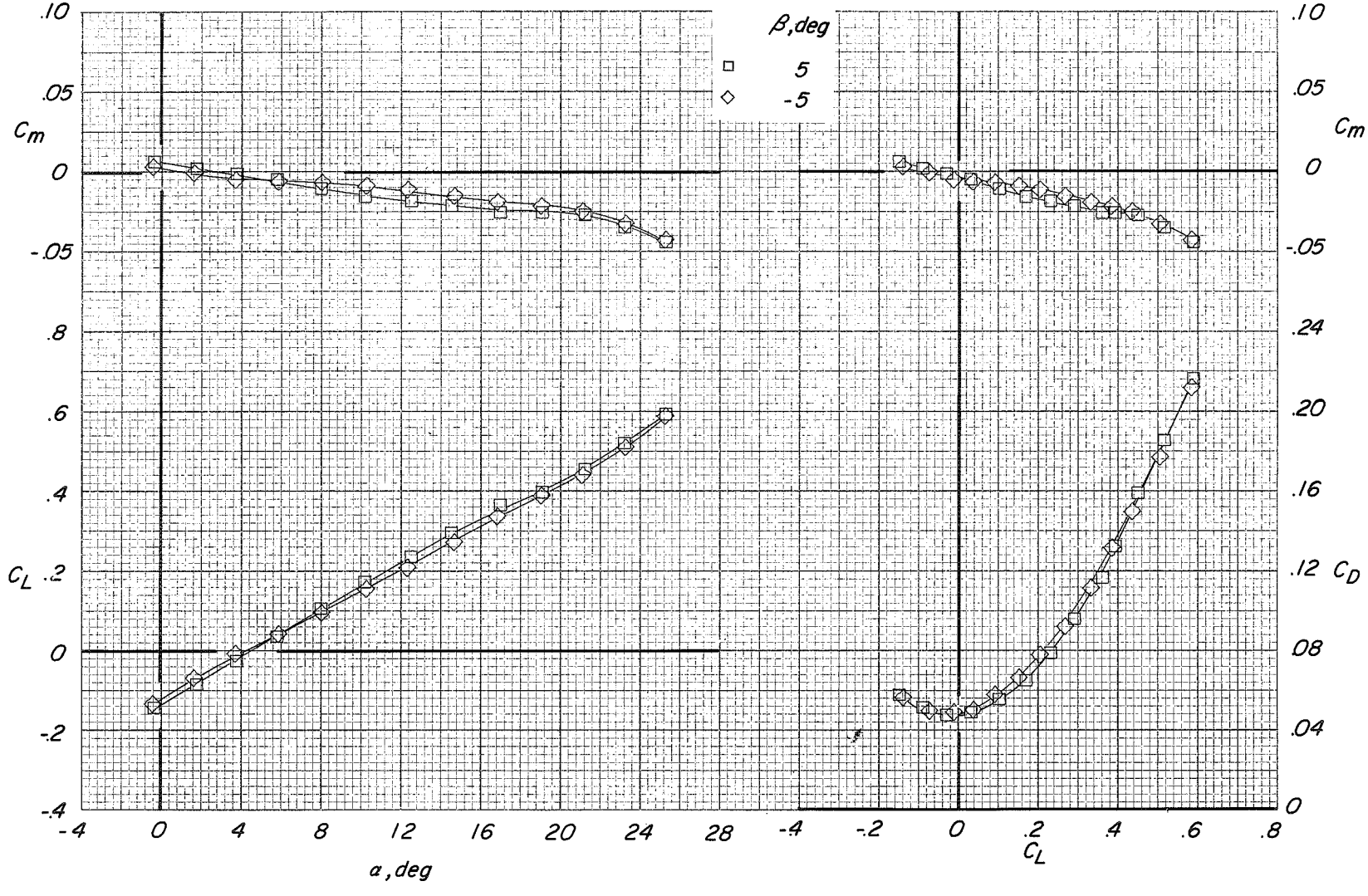
(j) $\delta_e = -10^o$; M = 0.80.

Figure 9.- Concluded.



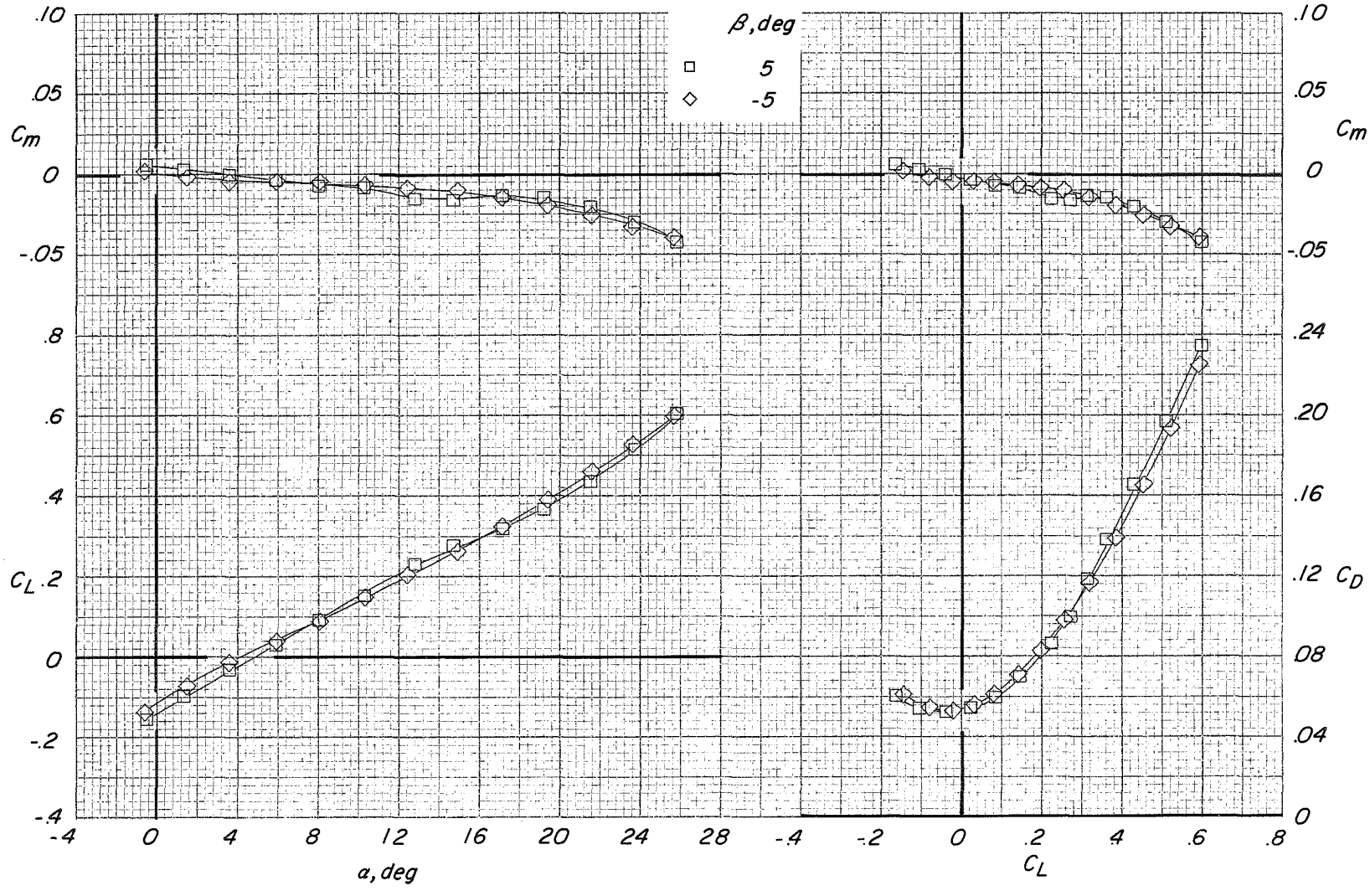
(a) $\delta_e = -5^o$; M = 0.35.

Figure 10.- Longitudinal characteristics with combined rudder deflection and sideslip. Basic fin configuration; auxiliary flap in the subsonic position; $\delta_a = 0^o$.



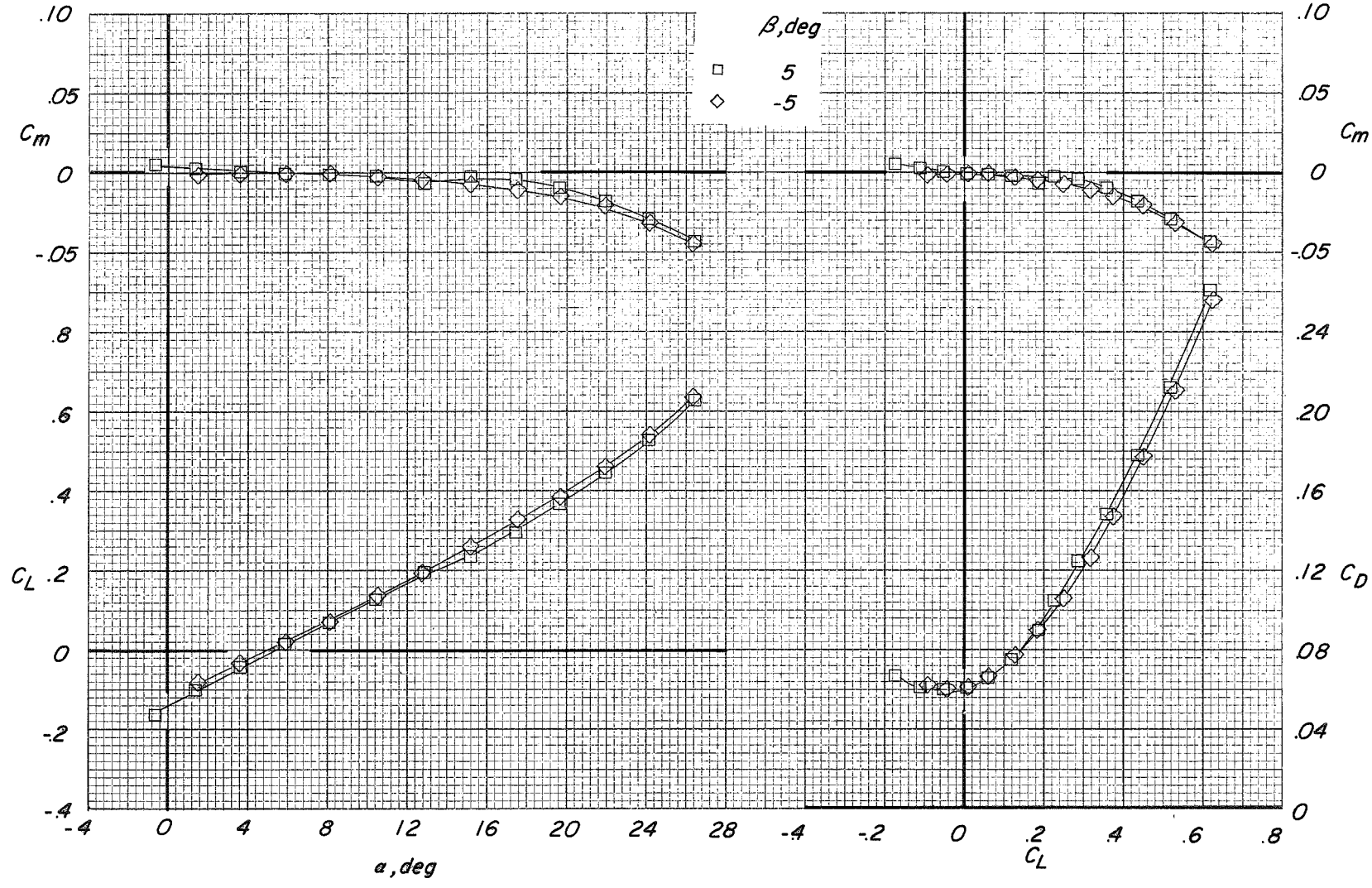
(b) $\delta_e = -5^o$; M = 0.50.

Figure 10.- Continued.



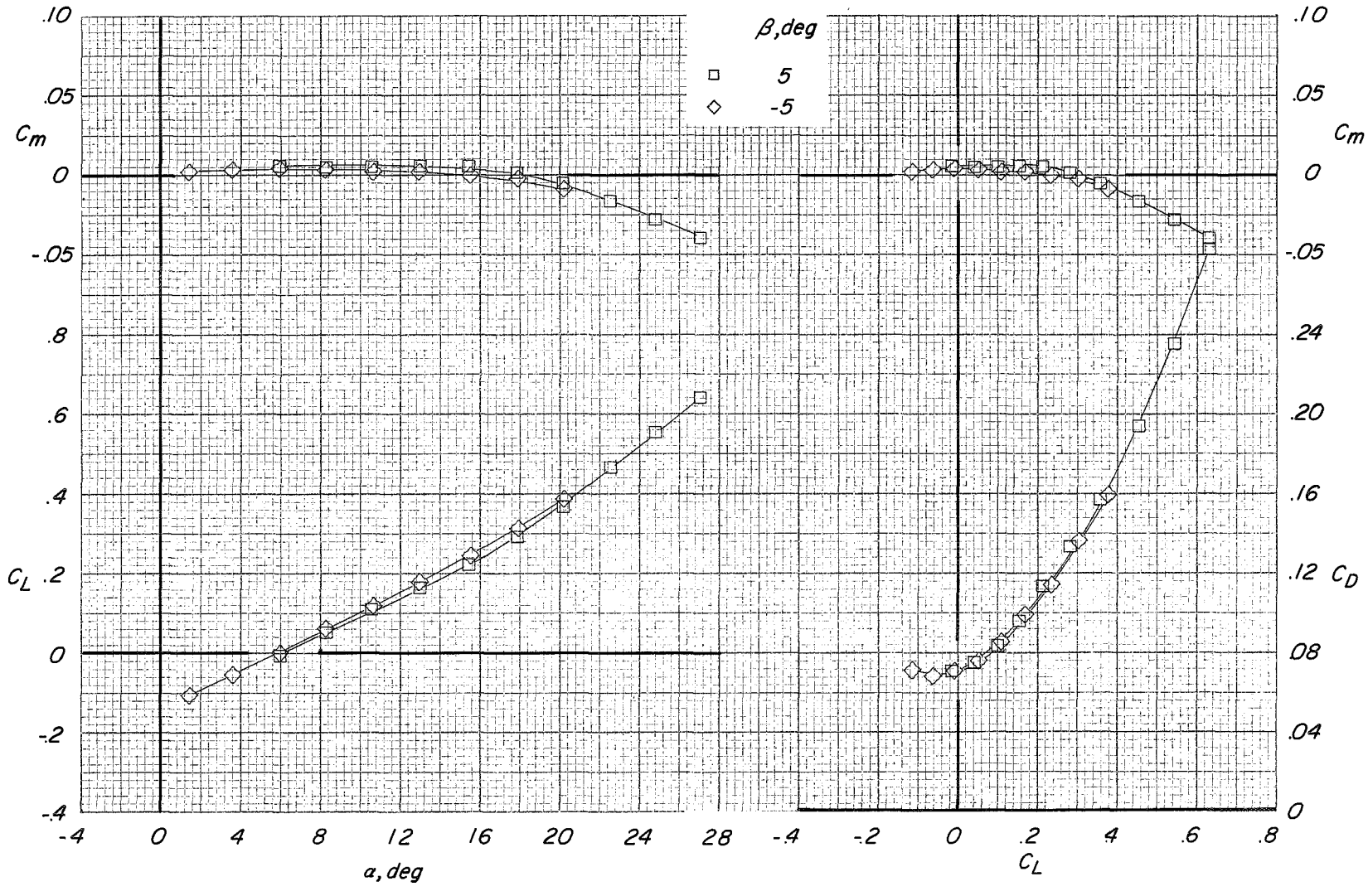
(c) $\delta_e = -5^o$; M = 0.60.

Figure 10.- Continued.



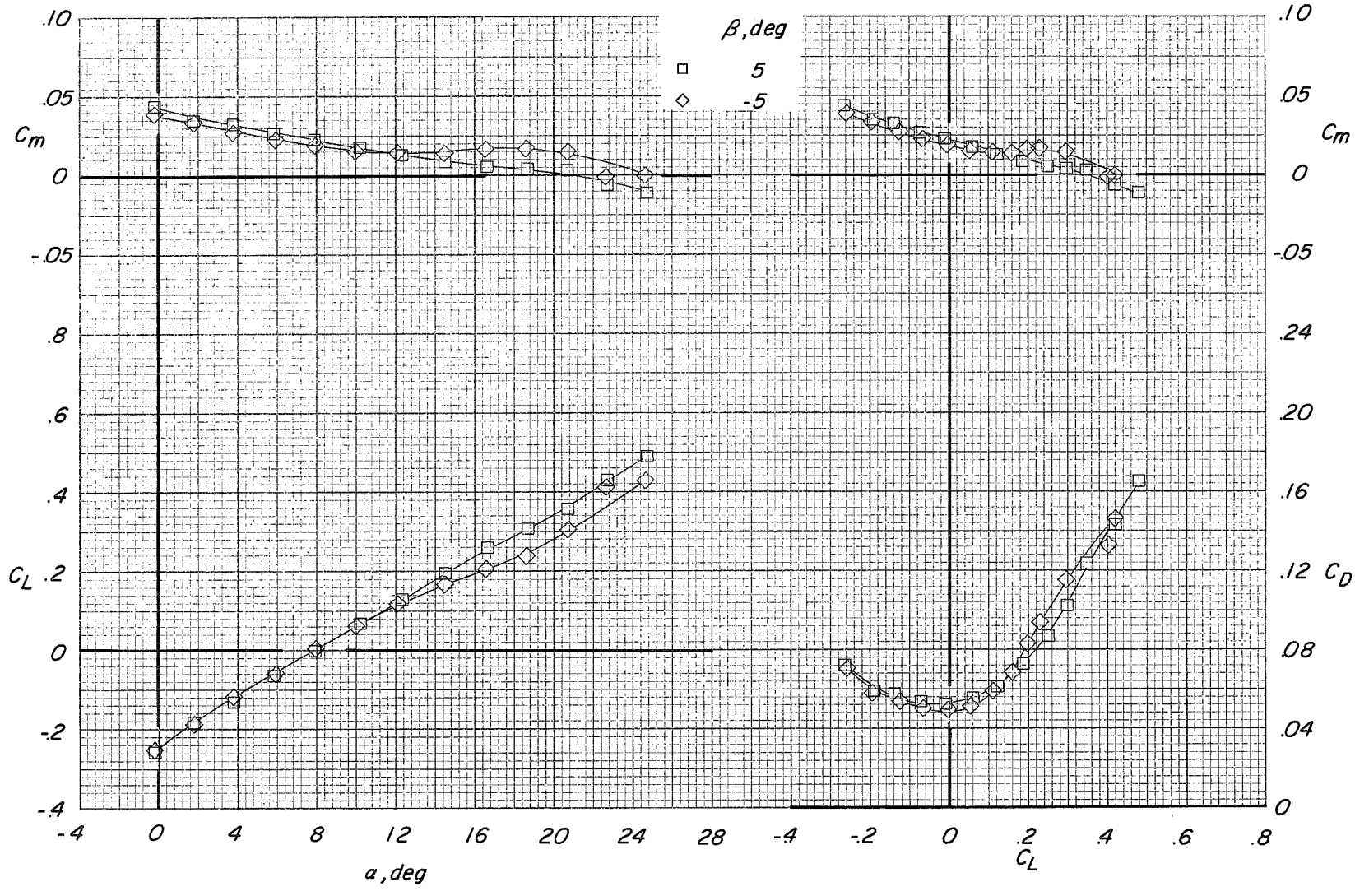
(d) $\delta_e = -5^o$; M = 0.70.

Figure 10.- Continued.



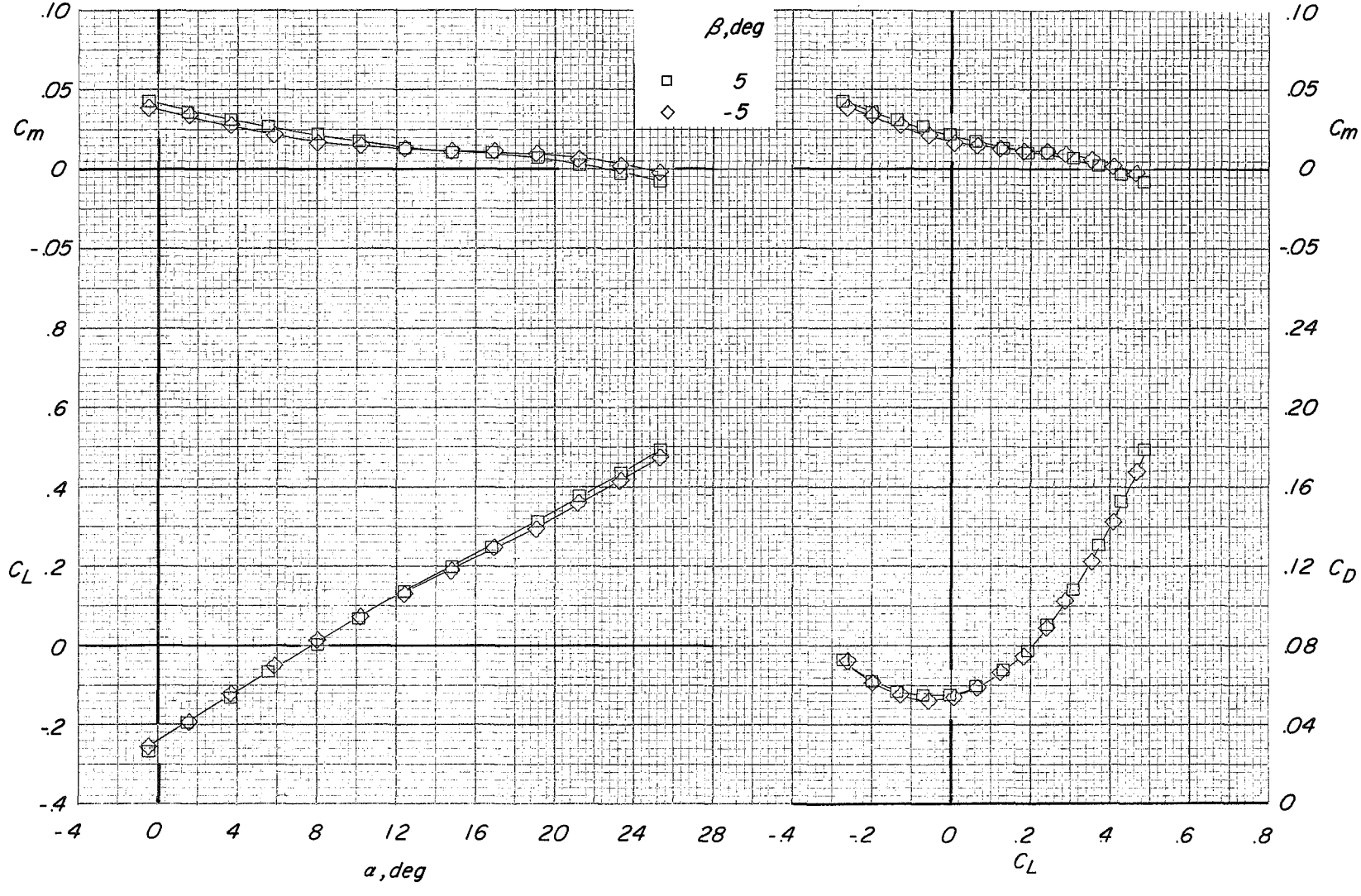
(e) $\delta_e = -5^o$; M = 0.80.

Figure 10.- Continued.



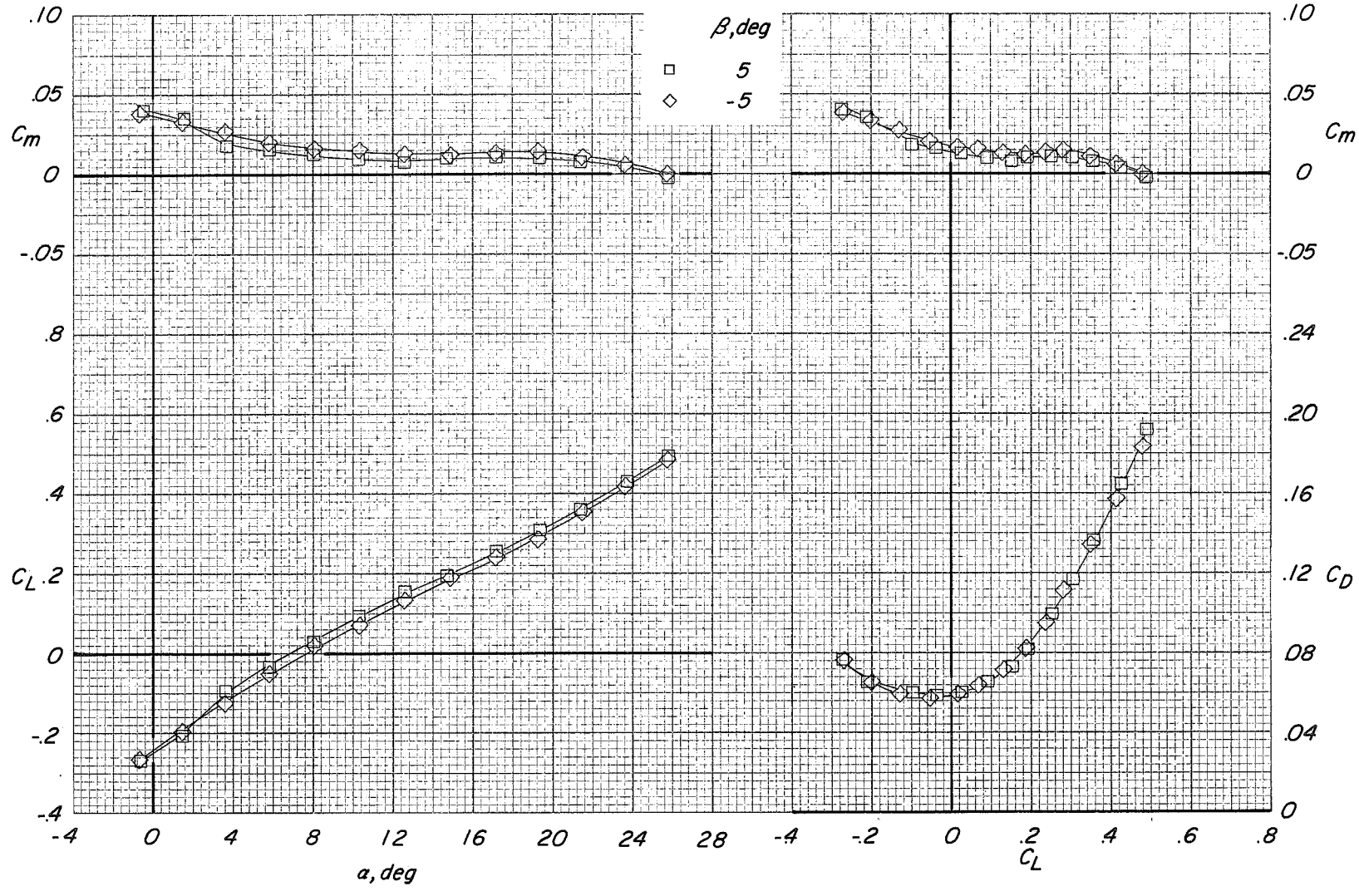
(f) $\delta_e = -15^o$; M = 0.35.

Figure 10.- Continued.



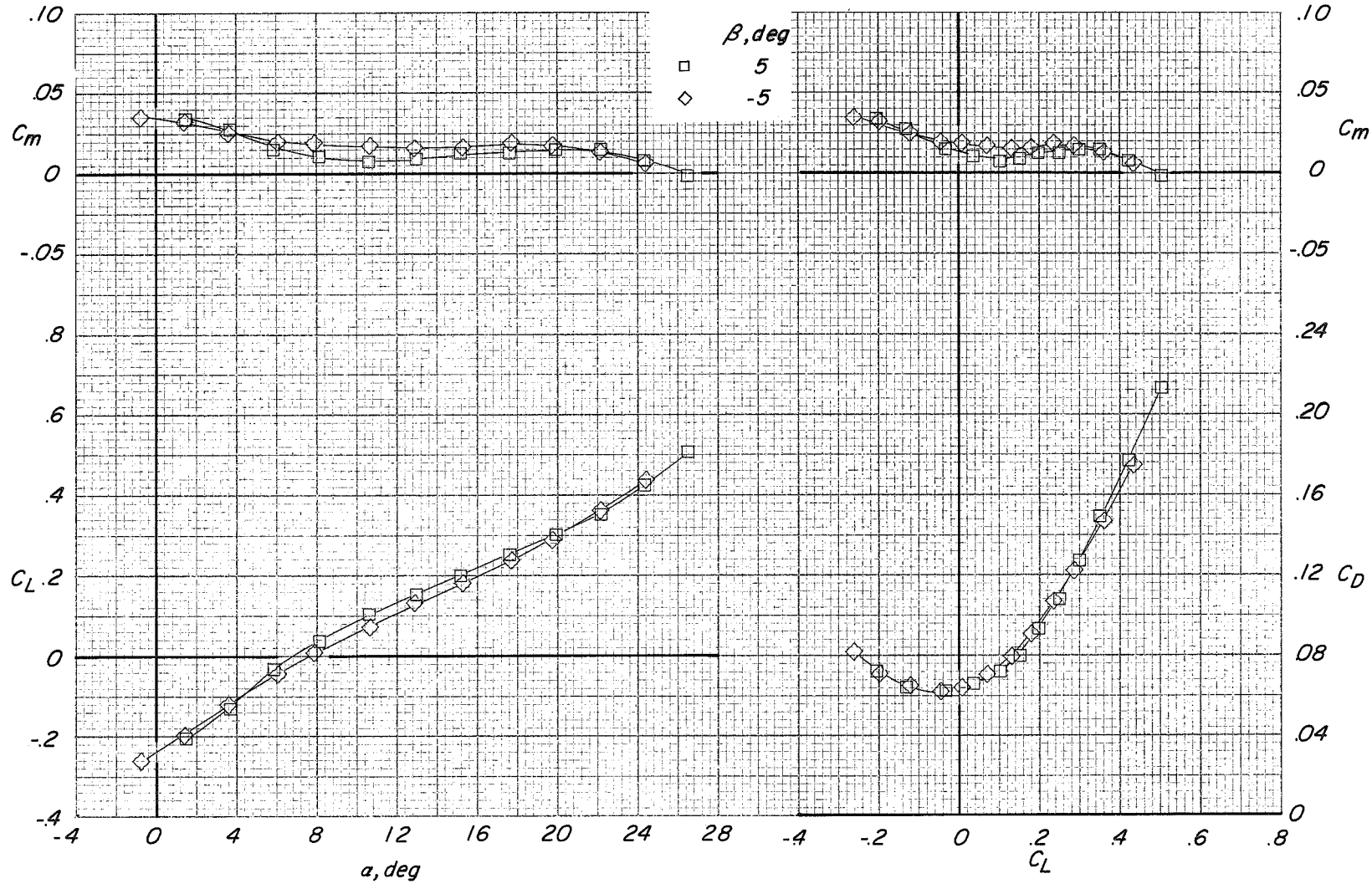
(g) $\delta_e = -15^o$; M = 0.50.

Figure 10.- Continued.



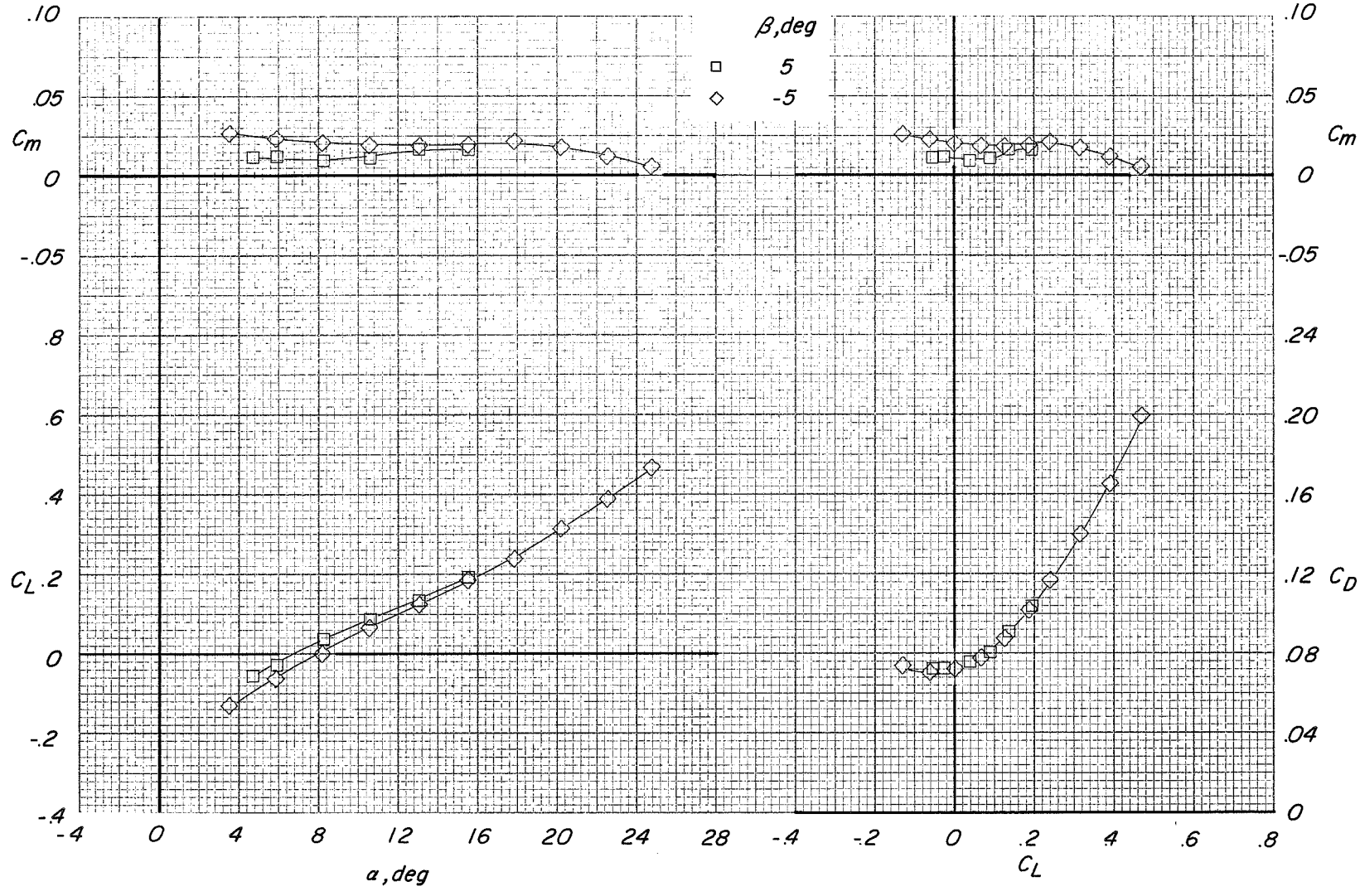
(h) $\delta_e = -15^o$; M = 0.60.

Figure 10.- Continued.



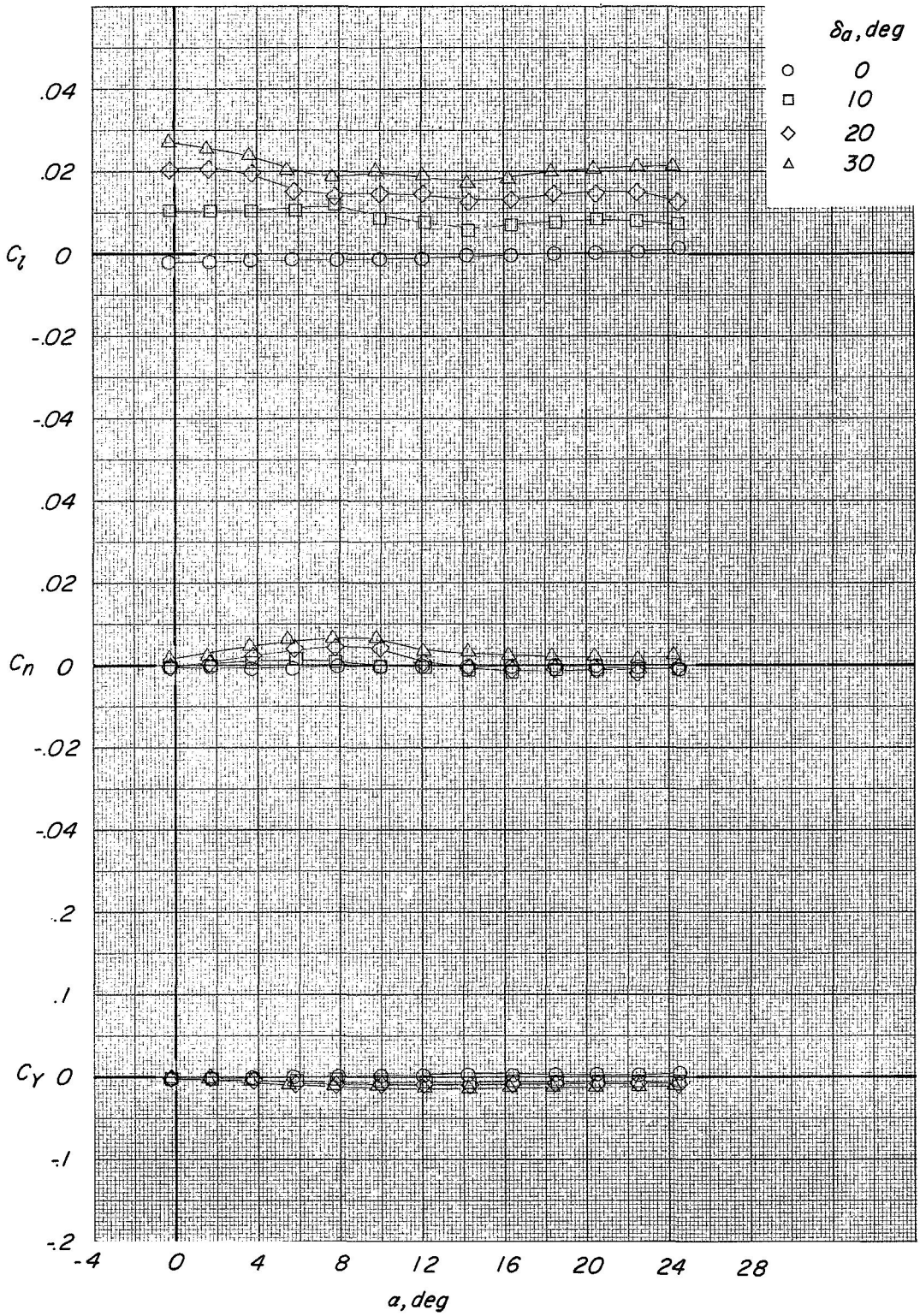
(i) $\delta_e = -15^o$; M = 0.70.

Figure 10.- Continued.



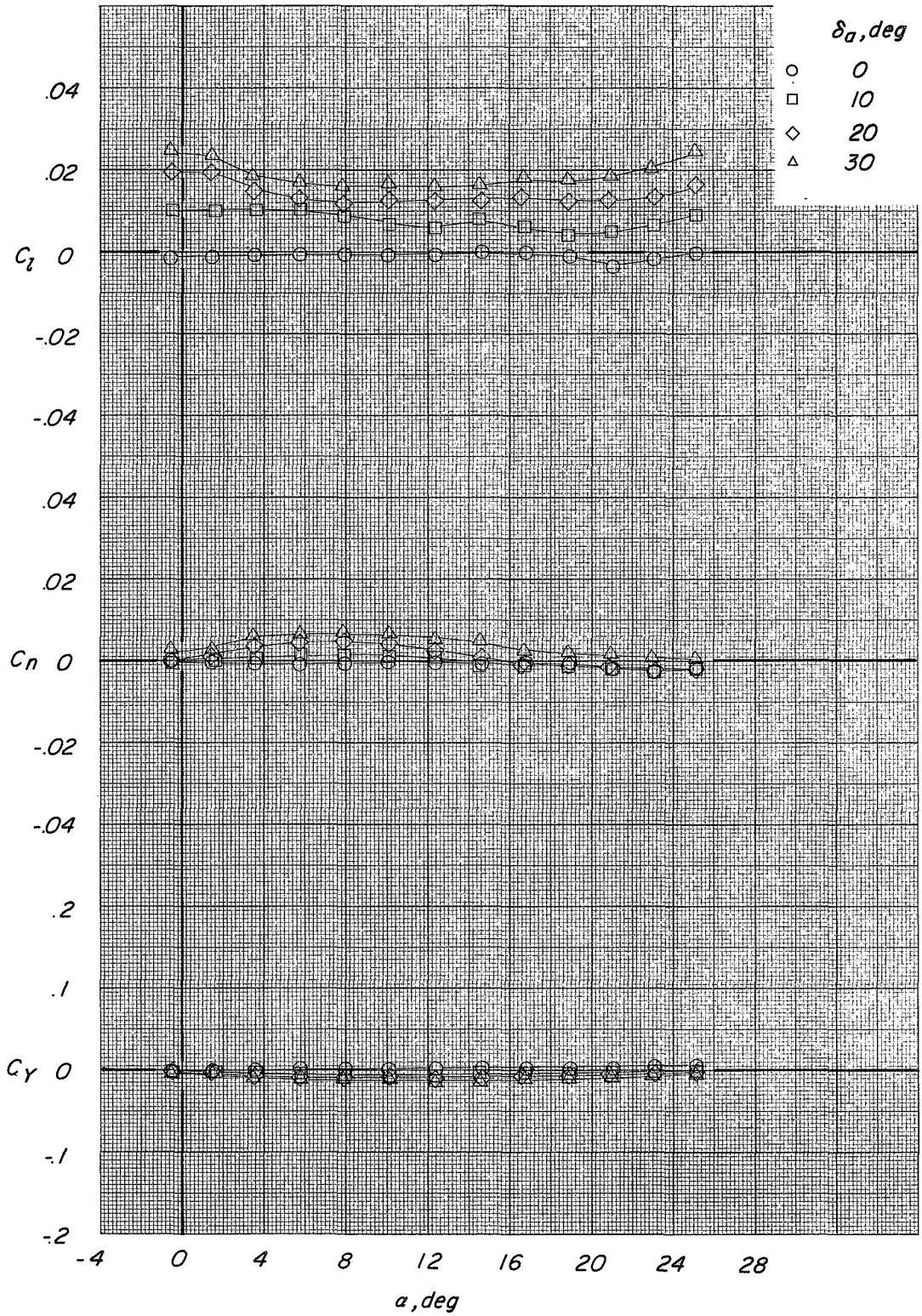
(j) $\delta_e = -15^o$; M = 0.80.

Figure 10.- Concluded.



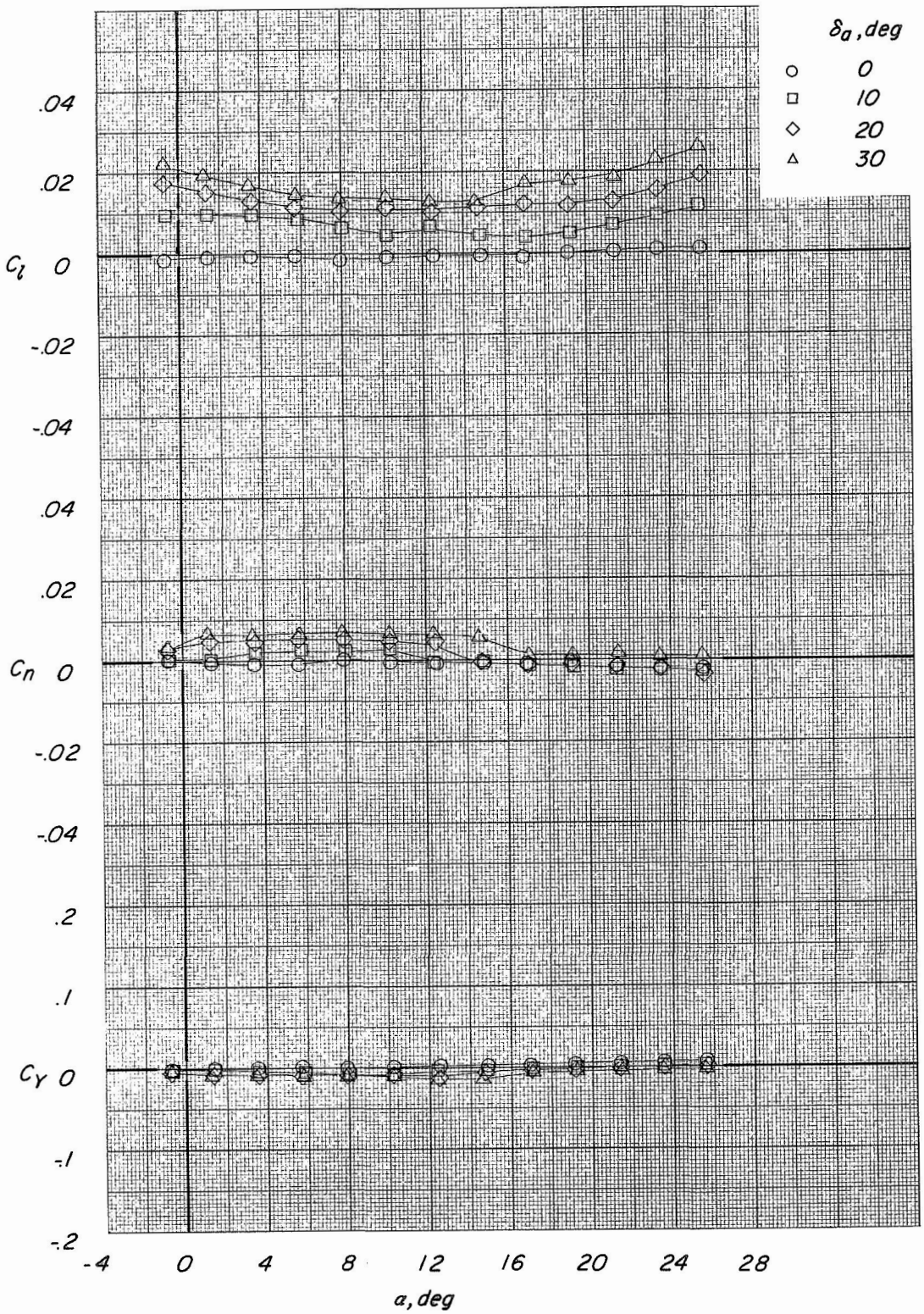
(a) $\delta_e = -5^o$; M = 0.35.

Figure 11.- Effect of aileron deflection on the lateral directional characteristics. Basic fin configuration; auxiliary flaps in subsonic position; $\beta = 0^o$.



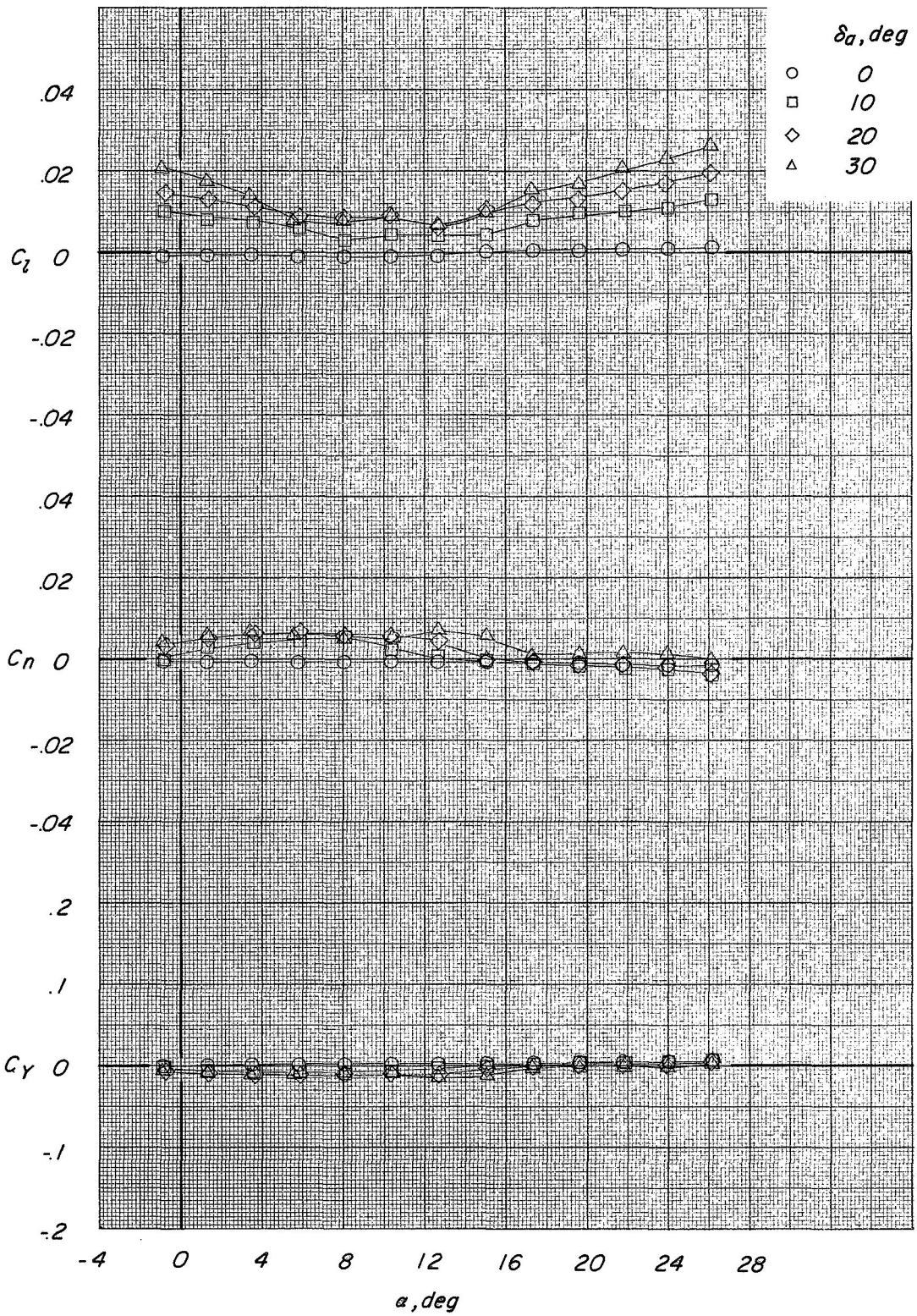
(b) $\delta_e = -5^o$; M = 0.50.

Figure 11.- Continued.



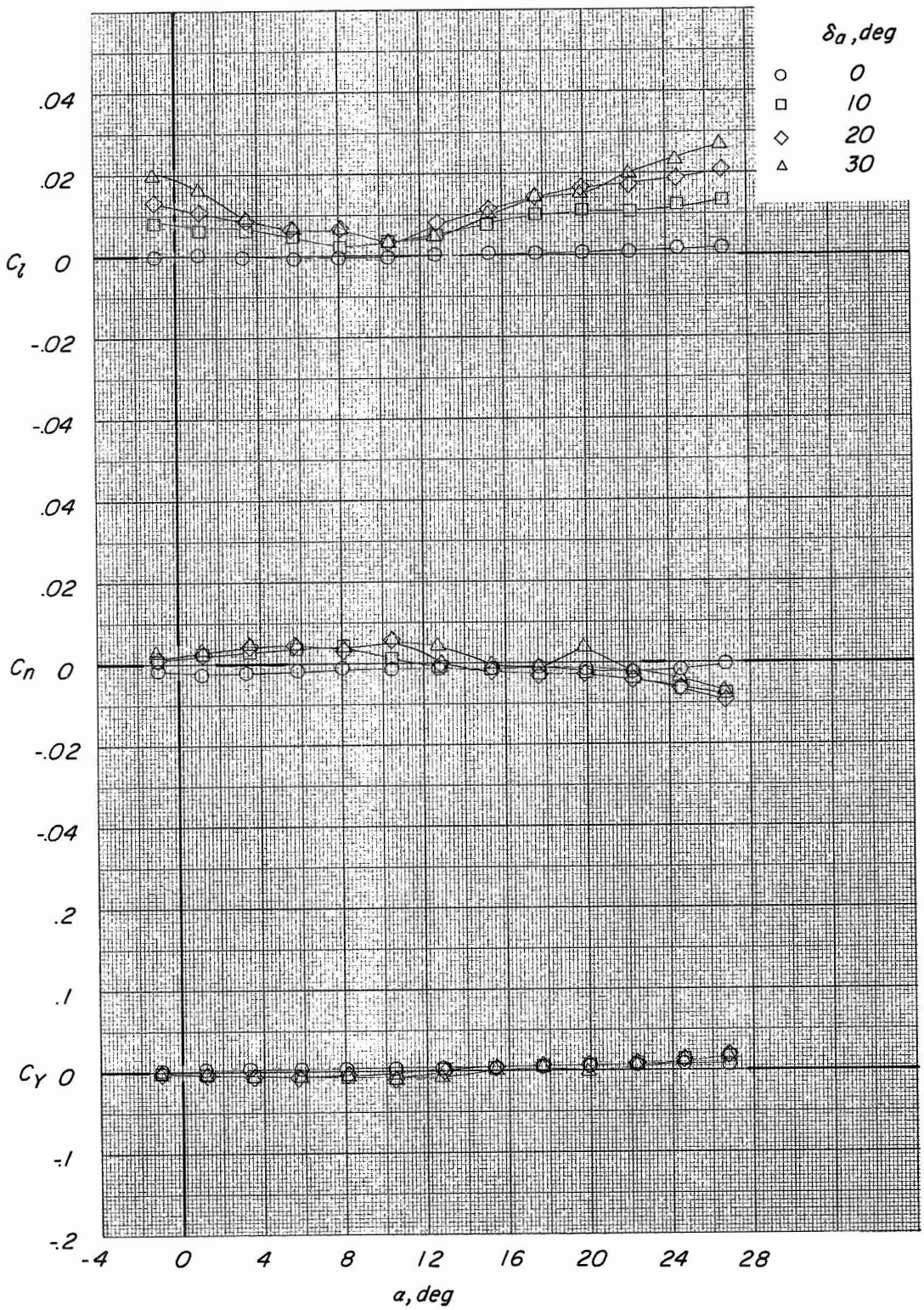
(c) $\delta_e = -5^o$; M = 0.60.

Figure 11.- Continued.



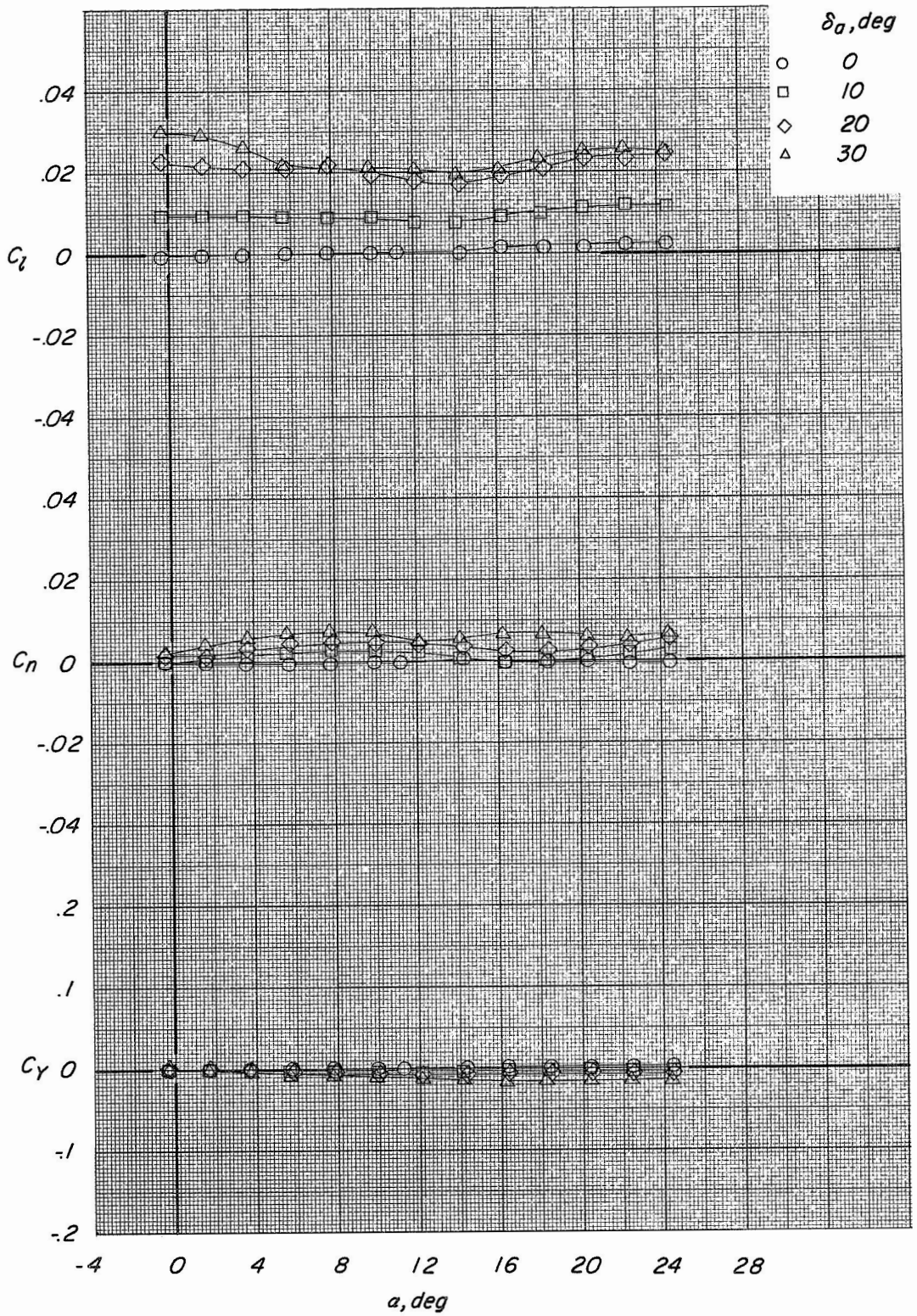
(d) $\delta_e = -5^o$; M = 0.70.

Figure 11.- Continued.



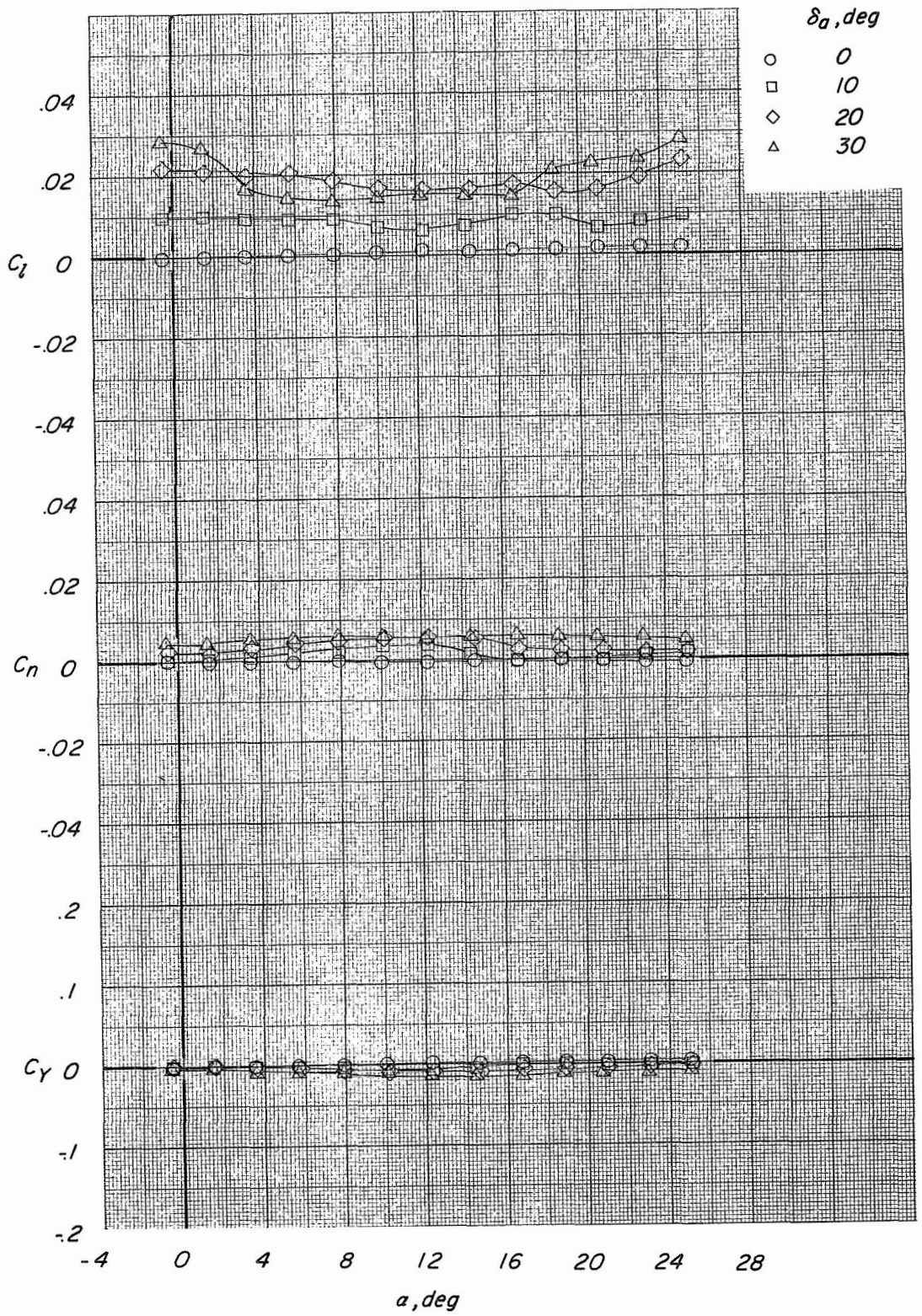
(e) $\delta_e = -5^o$; M = 0.80.

Figure 11.- Continued.



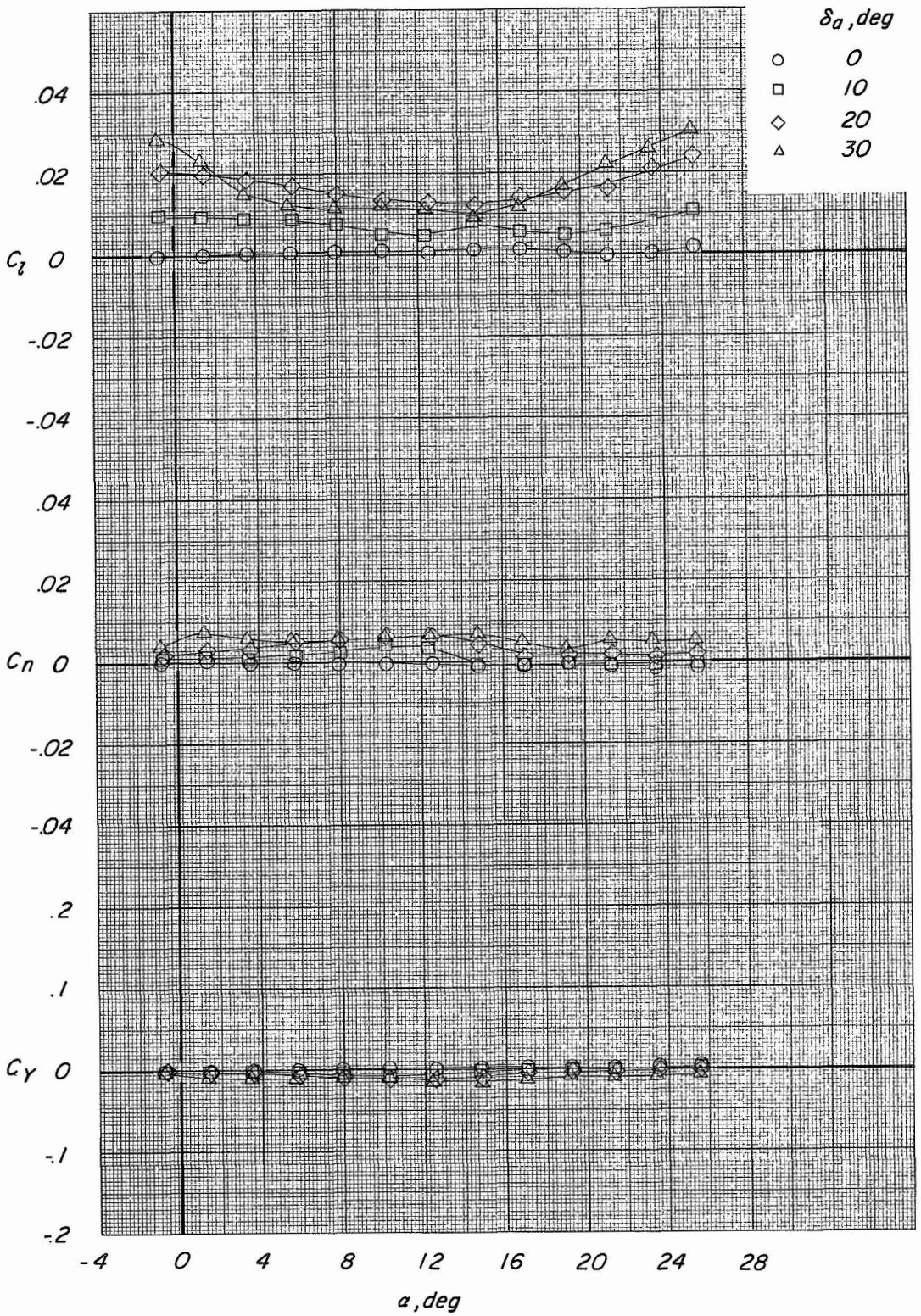
(f) $\delta_e = -10^o$; M = 0.35.

Figure 11.- Continued.



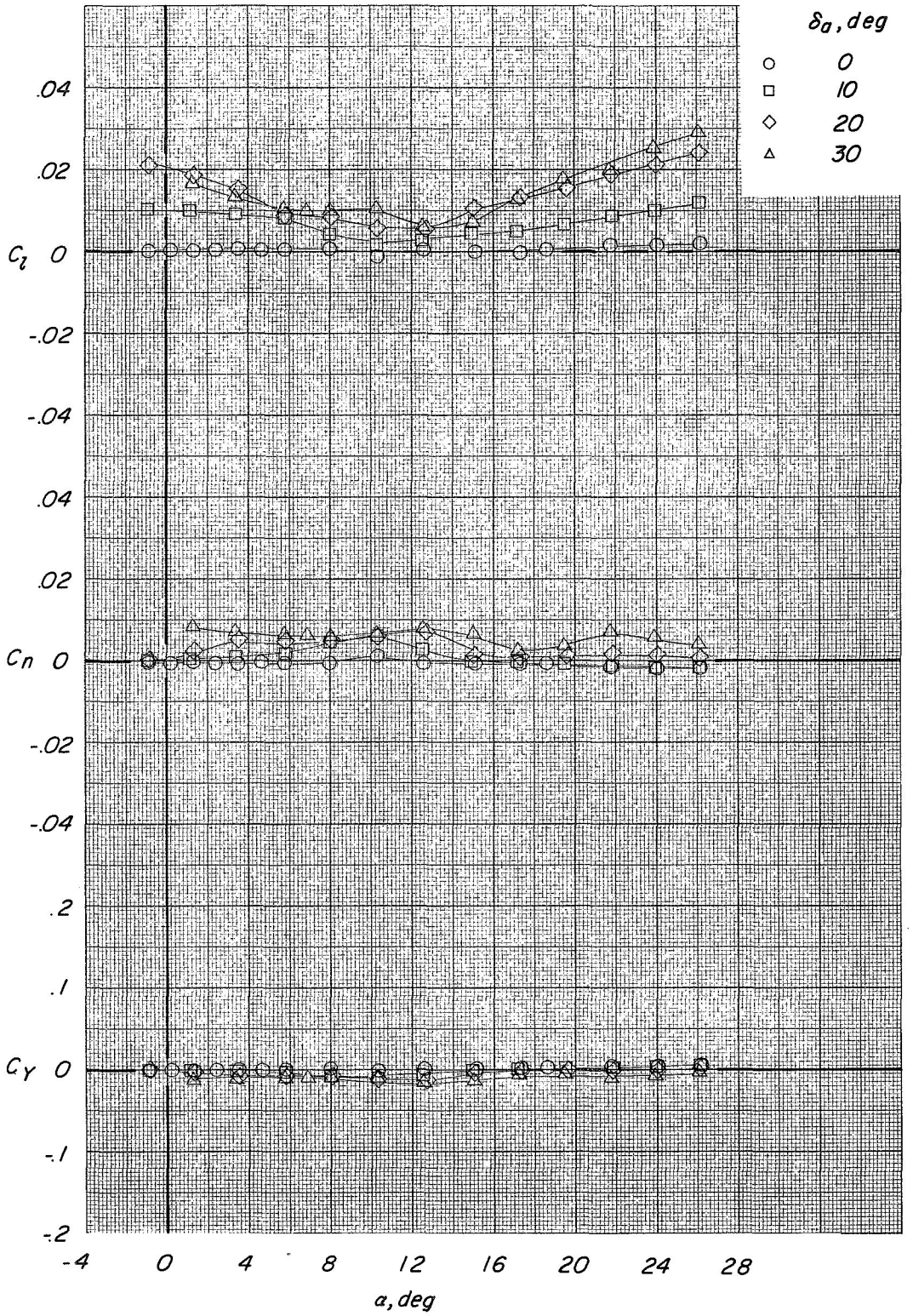
(g) $\delta_e = -10^o$; M = 0.50.

Figure 11.- Continued.



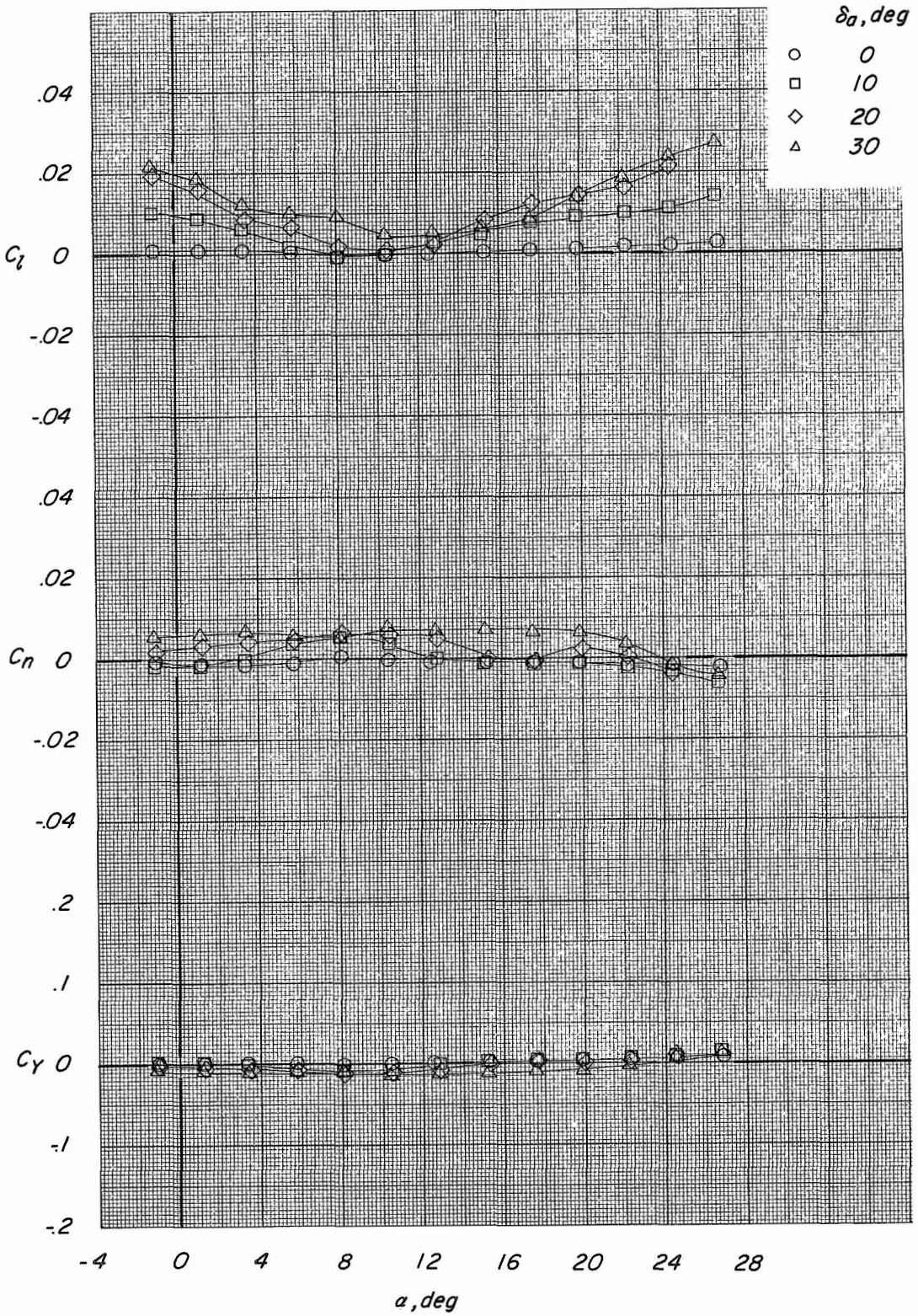
(h) $\delta_e = -10^o$; M = 0.60.

Figure 11.- Continued.



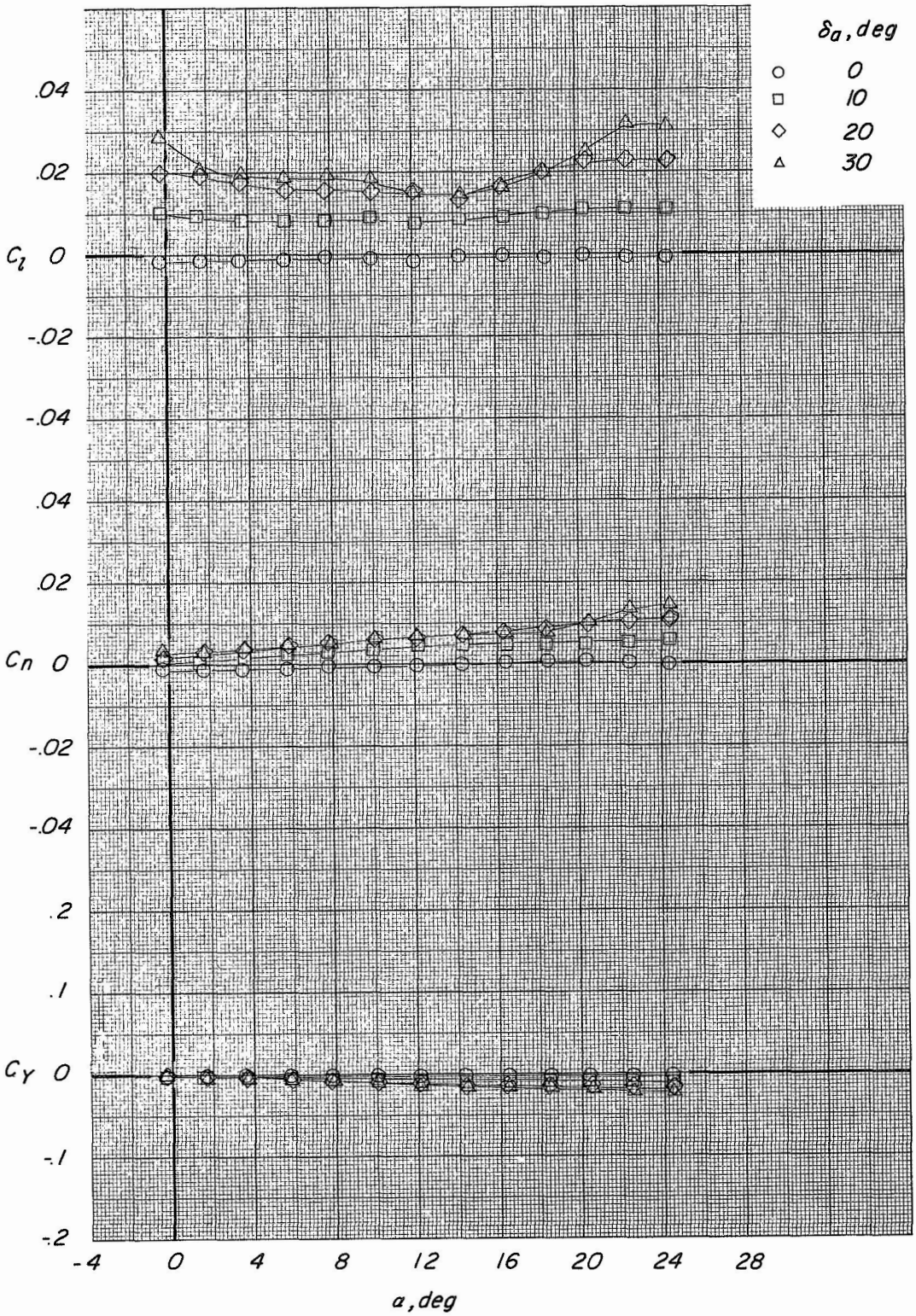
(i) $\delta_e = -10^o$; M = 0.70.

Figure 11.- Continued.



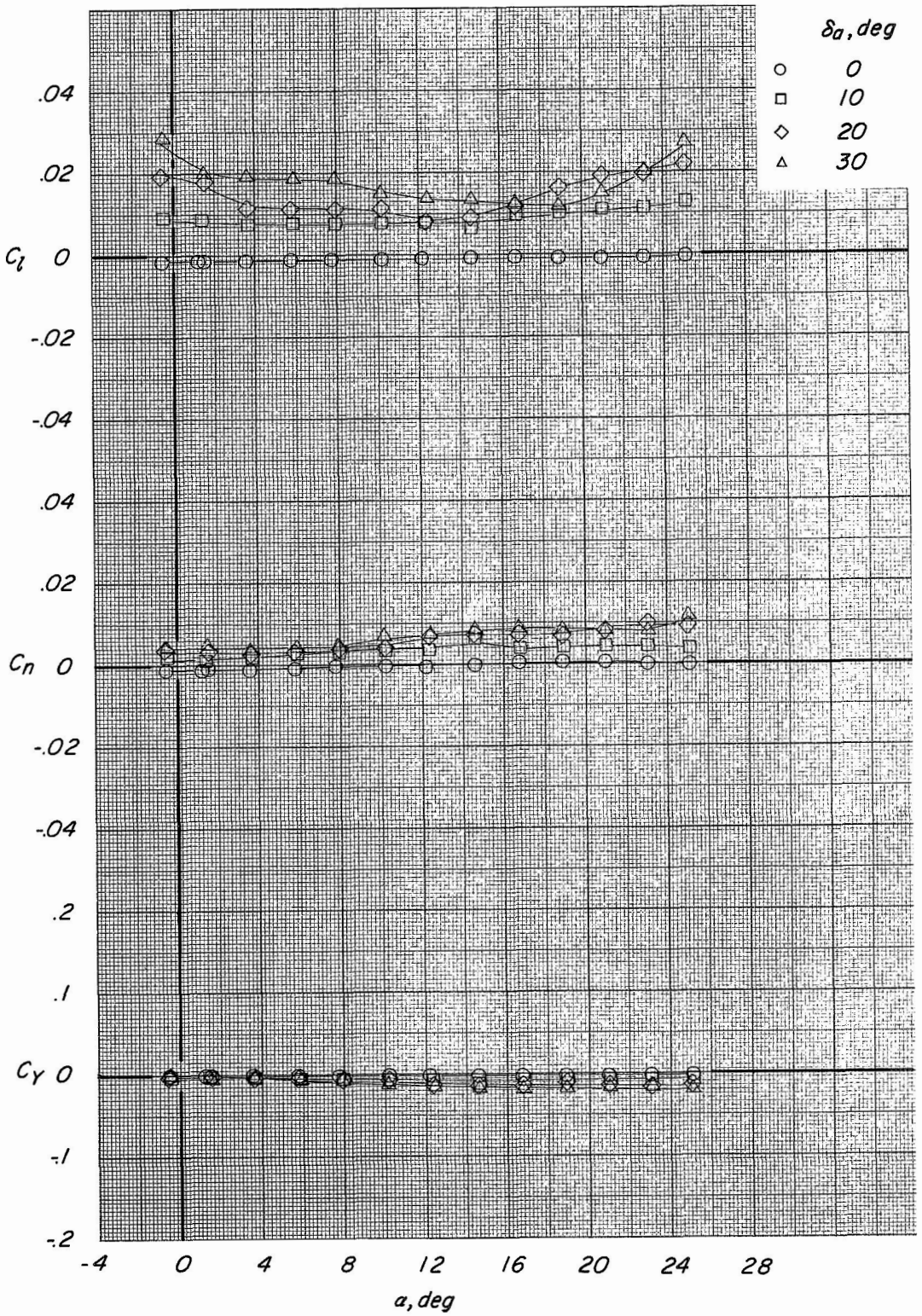
(j) $\delta_e = -10^o$; M = 0.80.

Figure 11.- Continued.



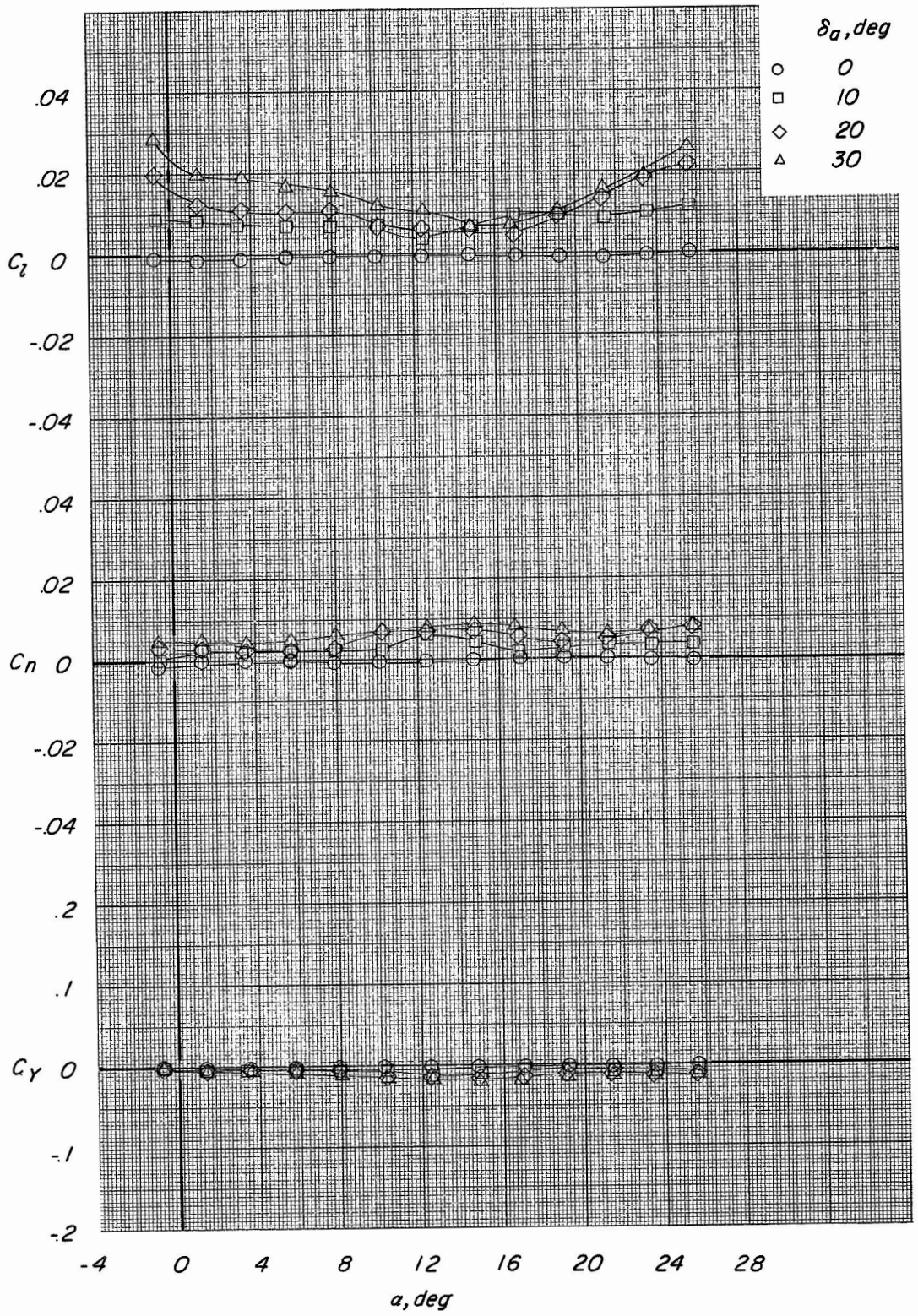
(k) $\delta_e = -15^o$; M = 0.35.

Figure 11.- Continued.



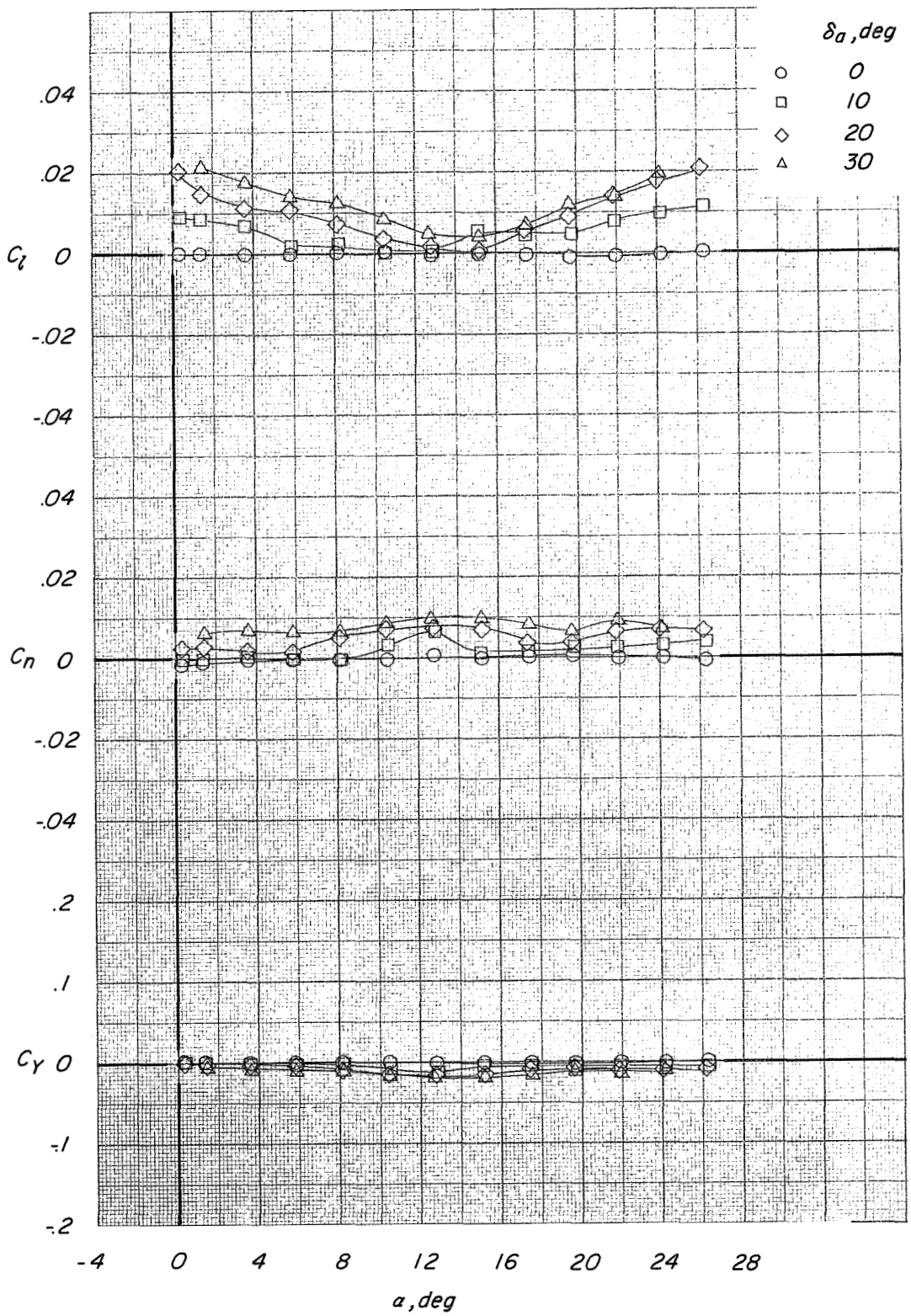
(l) $\delta_e = -15^o$; M = 0.50.

Figure 11.- Continued.



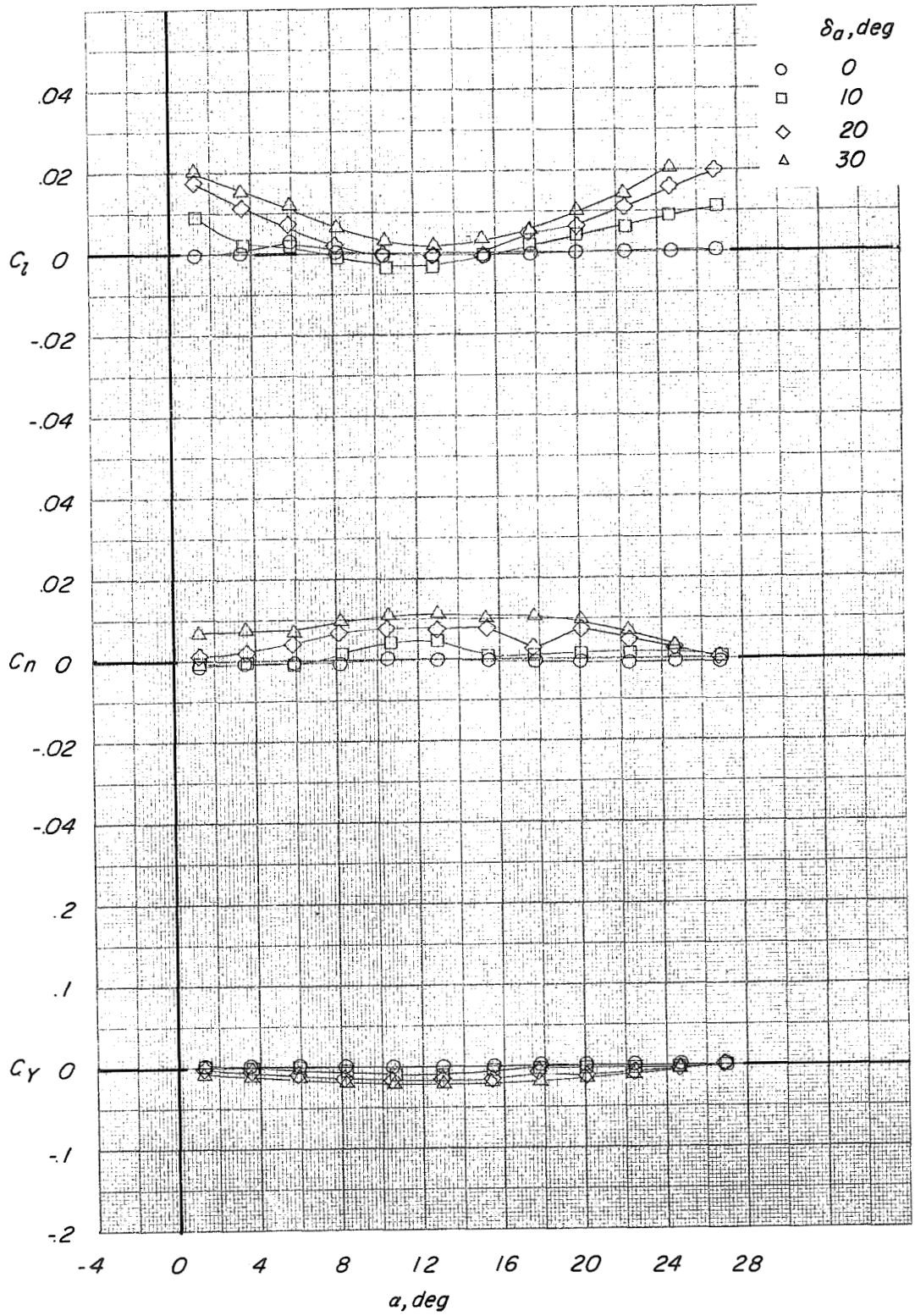
(m) $\delta_e = -15^o$; M = 0.60.

Figure 11.- Continued.



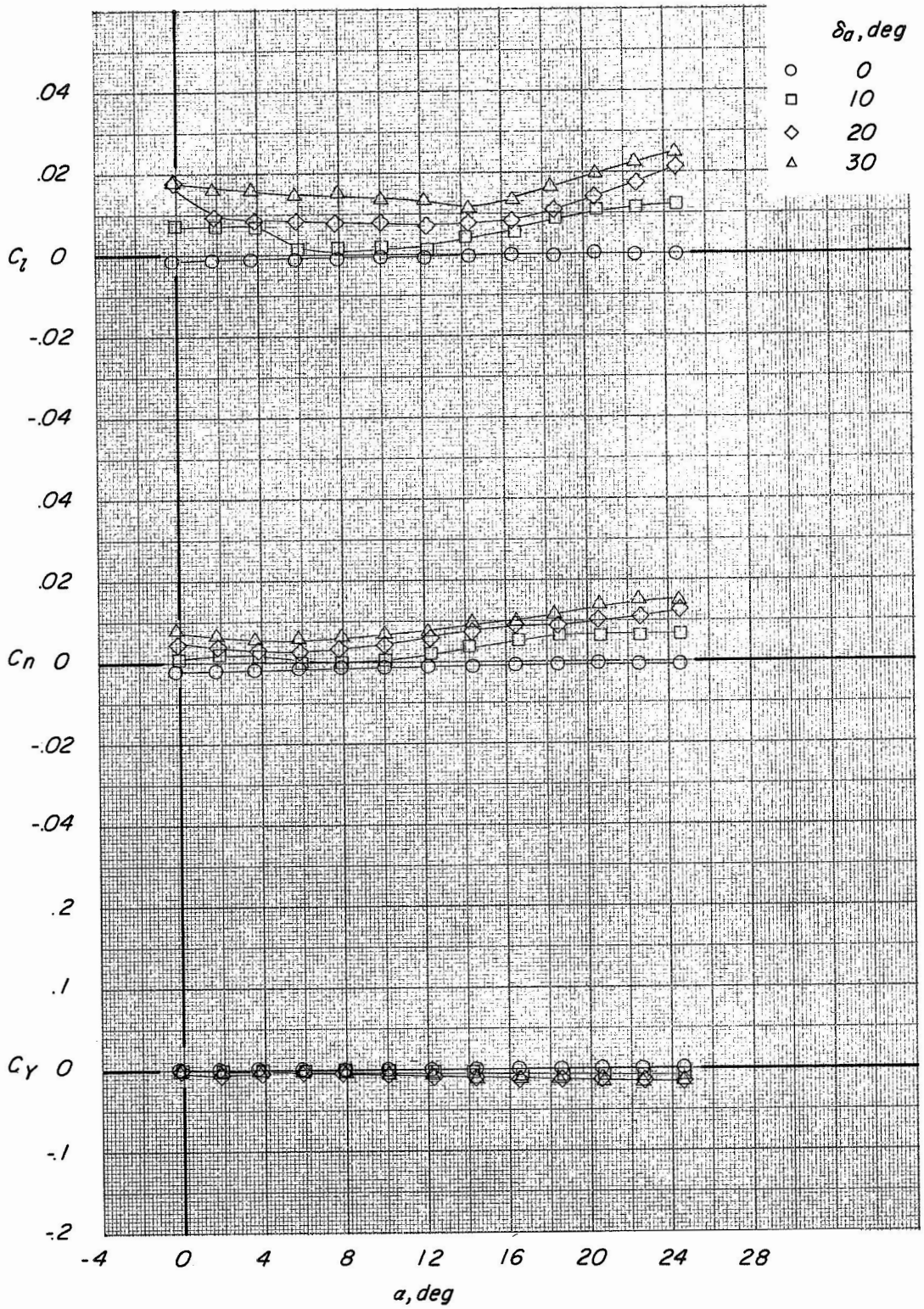
(n) $\delta_e = -15^o$; M = 0.70.

Figure 11.- Continued.



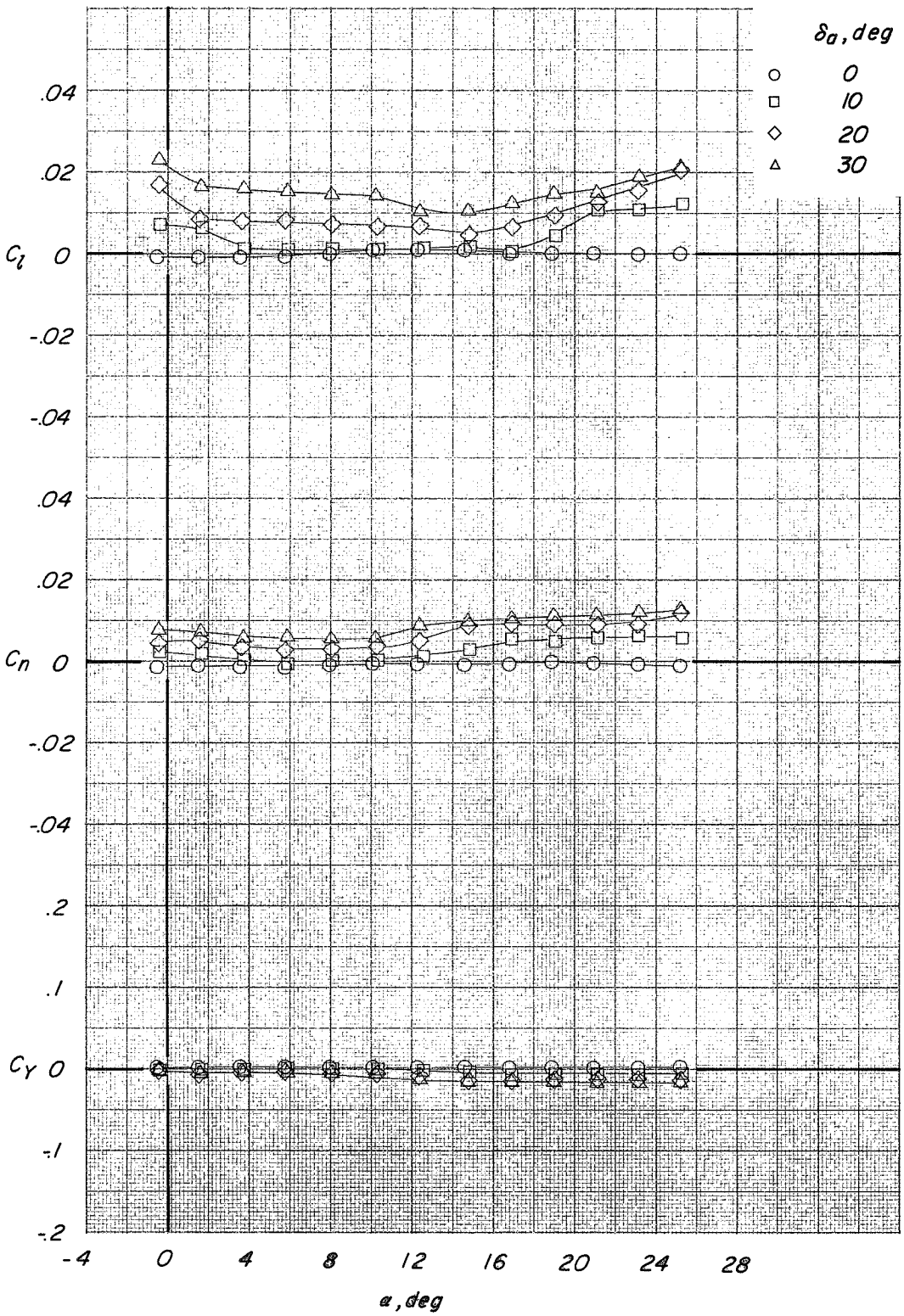
(o) $\delta_e = -15^o$; M = 0.80.

Figure 11.- Continued.



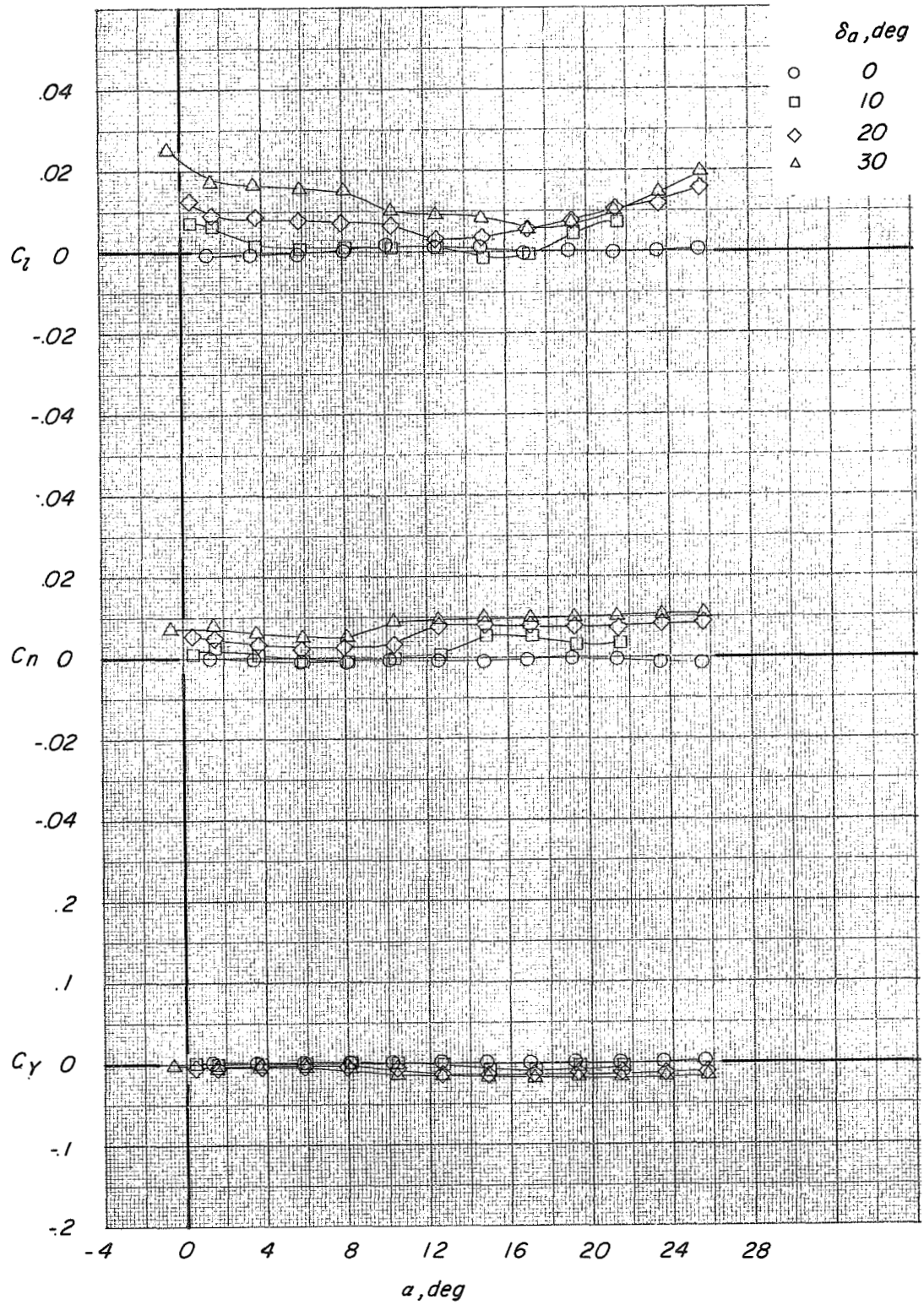
(p) $\delta_e = -20^o$; M = 0.35.

Figure 11.- Continued.



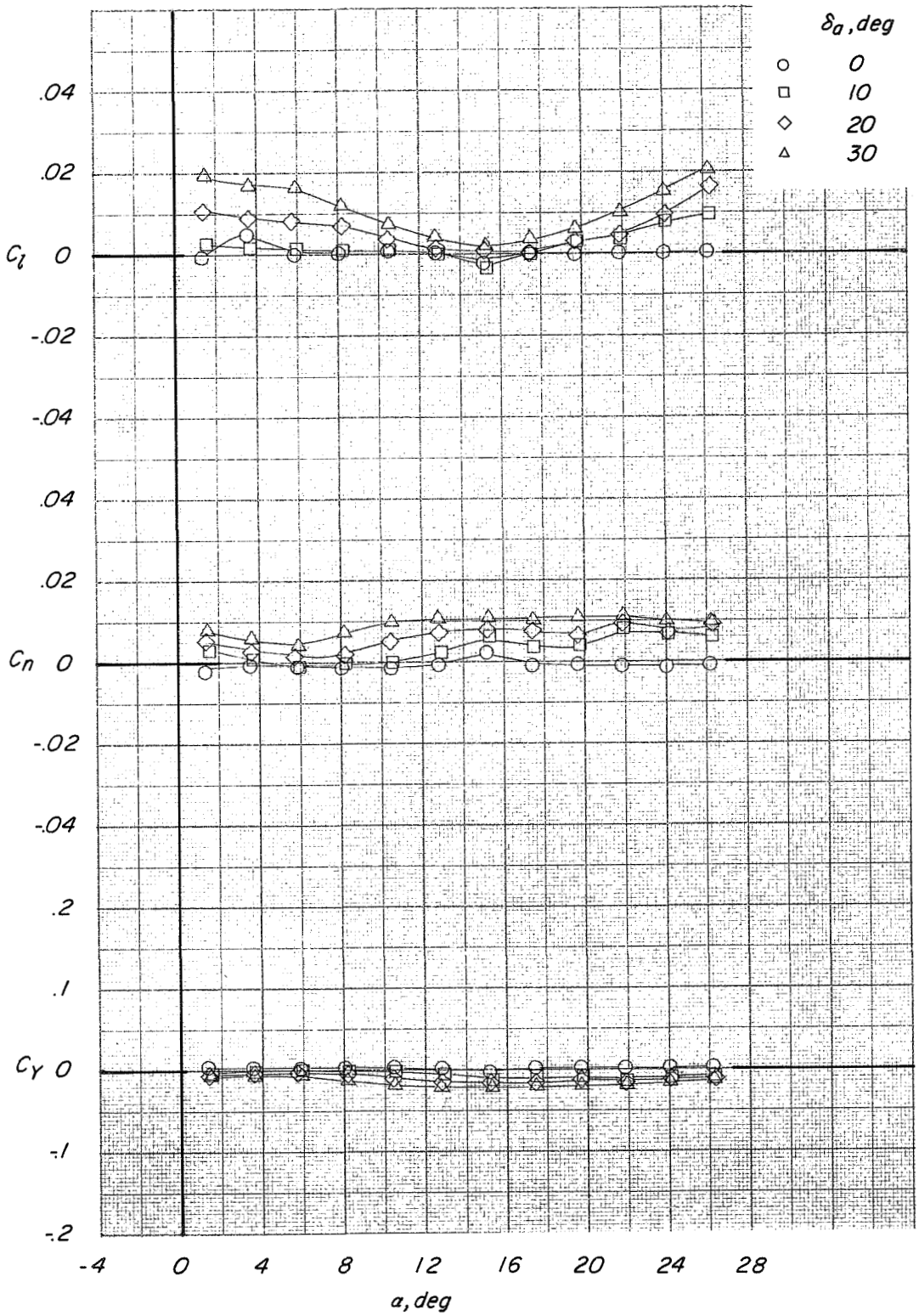
(q) $\delta_e = -20^o$; M = 0.50.

Figure 11.- Continued.



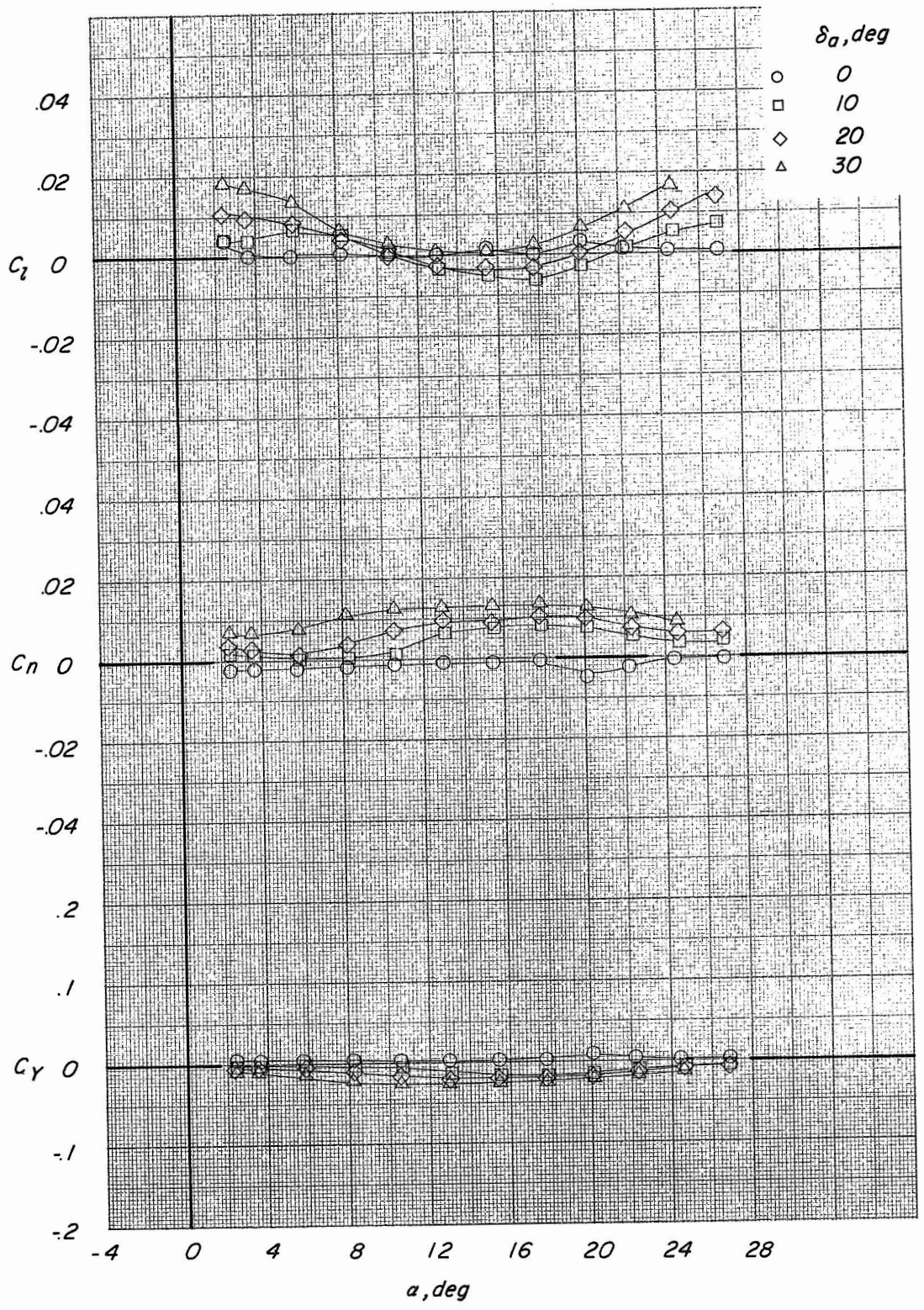
(r) $\delta_e = -20^o$; M = 0.60.

Figure 11.- Continued.



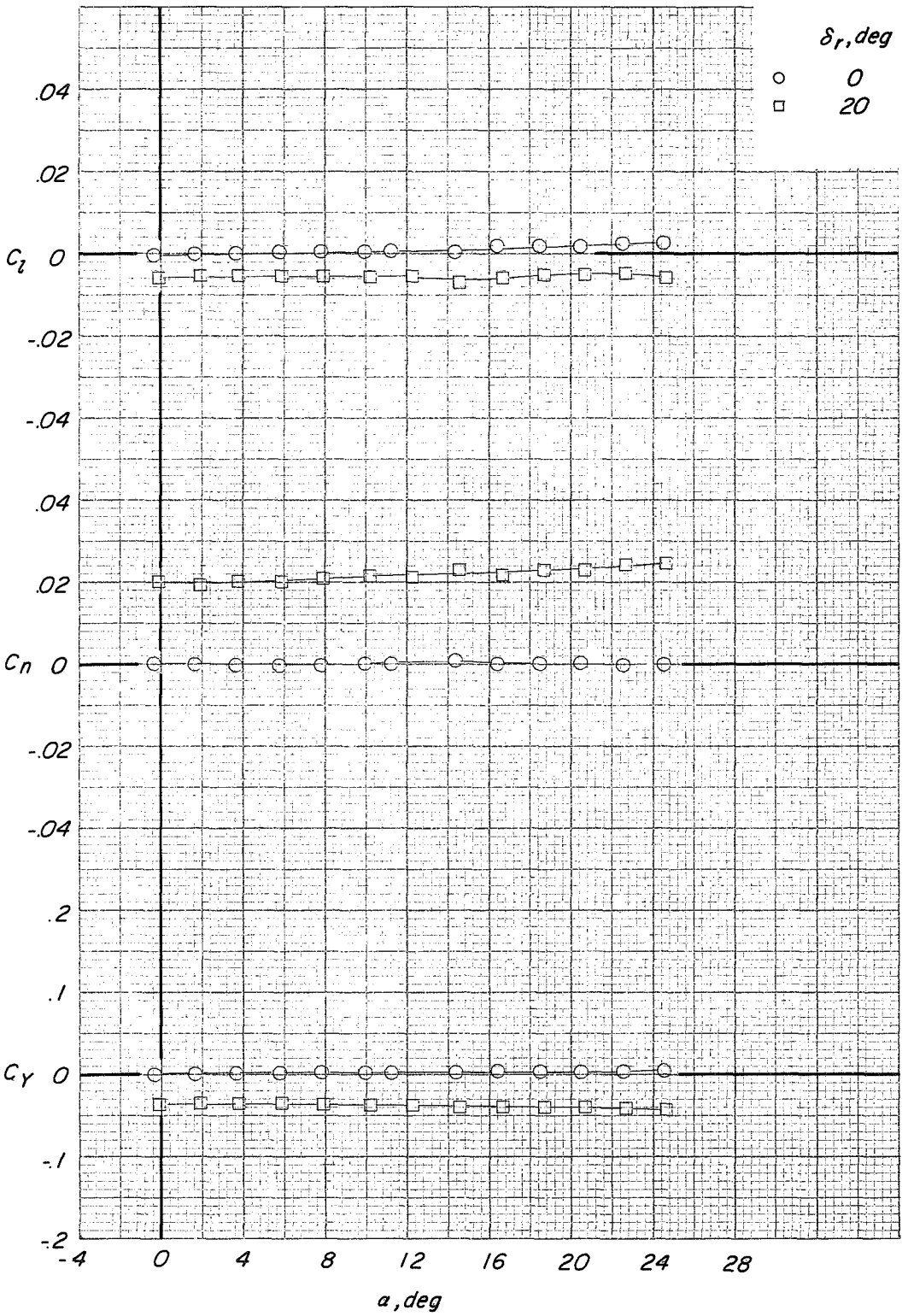
(s) $\delta_e = -20^o$; M = 0.70.

Figure 11.- Continued.



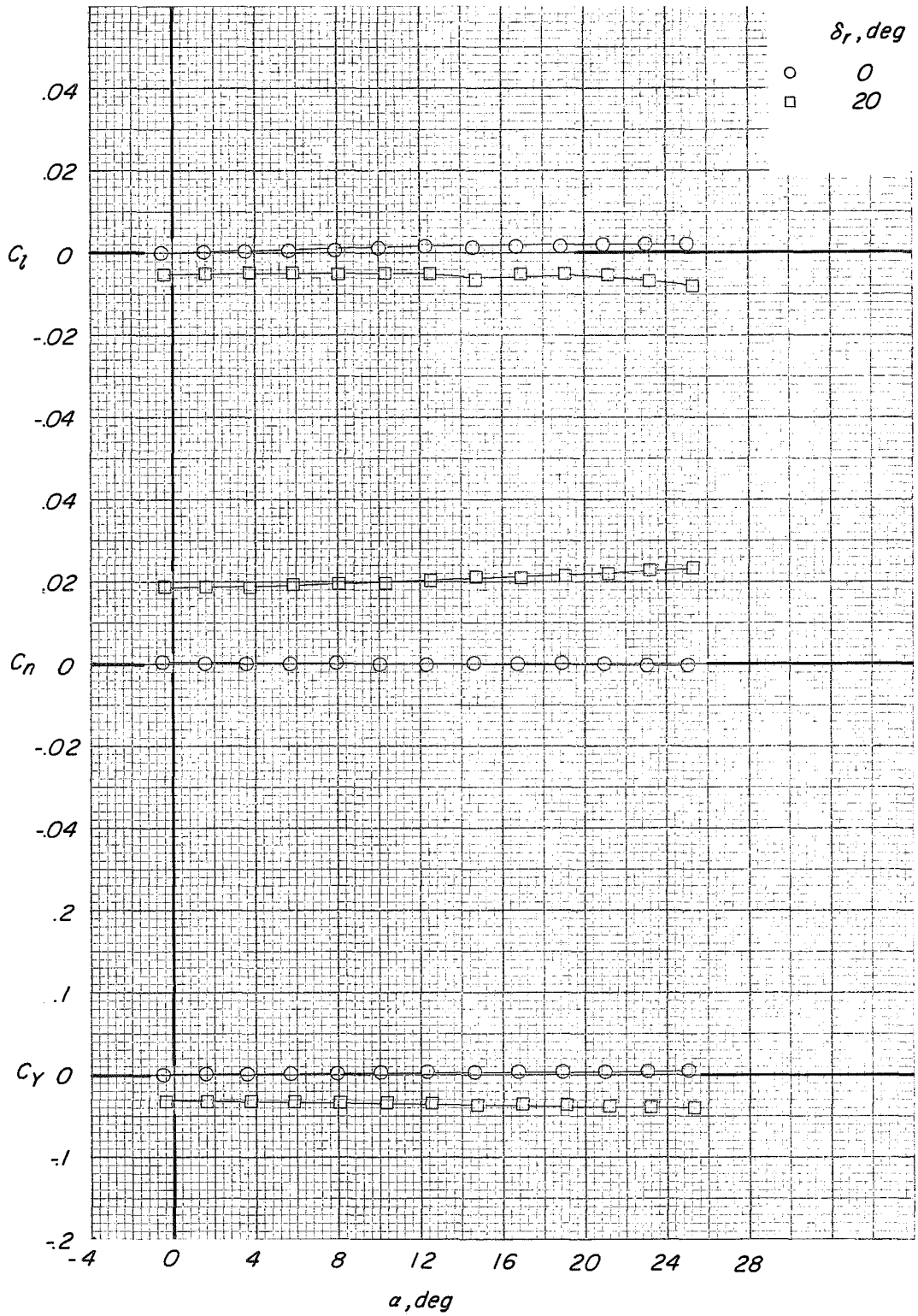
(t) $\delta_e = -20^o$; M = 0.80.

Figure 11.- Concluded.



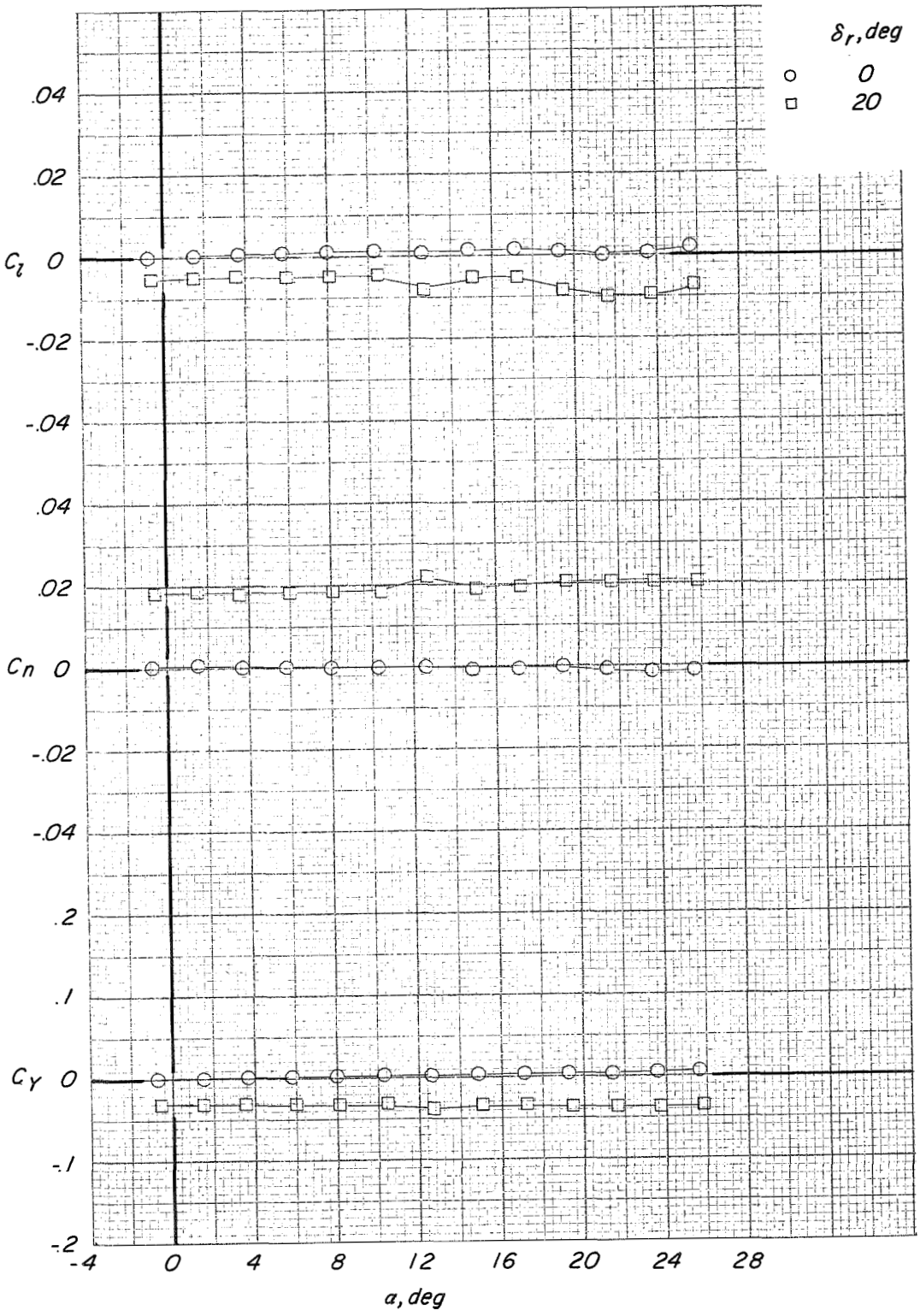
(a) $\delta_e = -10^o$; M = 0.35.

Figure 12.- Effect of rudder deflection on the lateral directional characteristics. Basic fin configuration; auxiliary flaps in the subsonic position; $\beta = \delta_a = 0^o$.



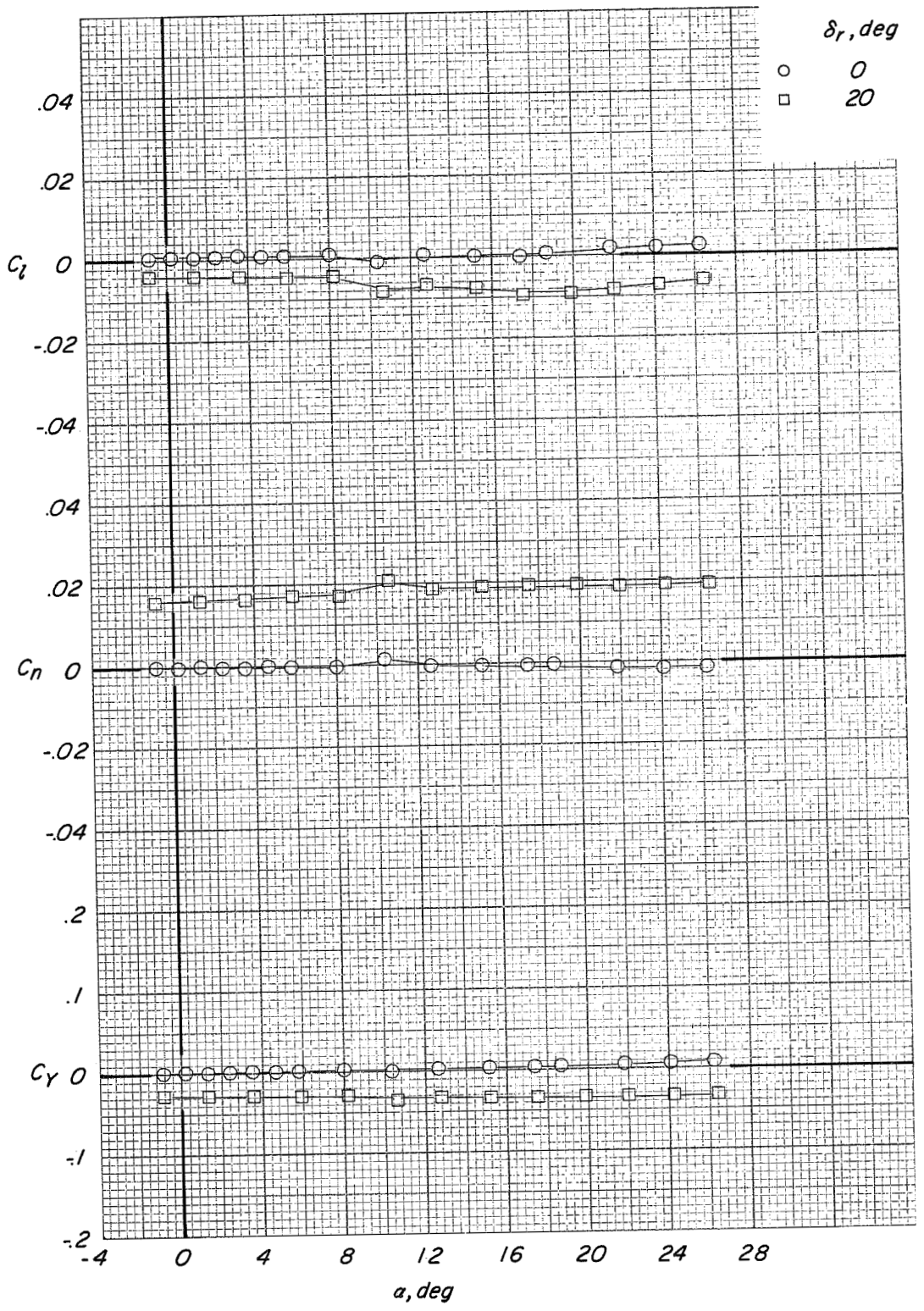
(b) $\delta_e = -10^o$; M = 0.50.

Figure 12.- Continued.



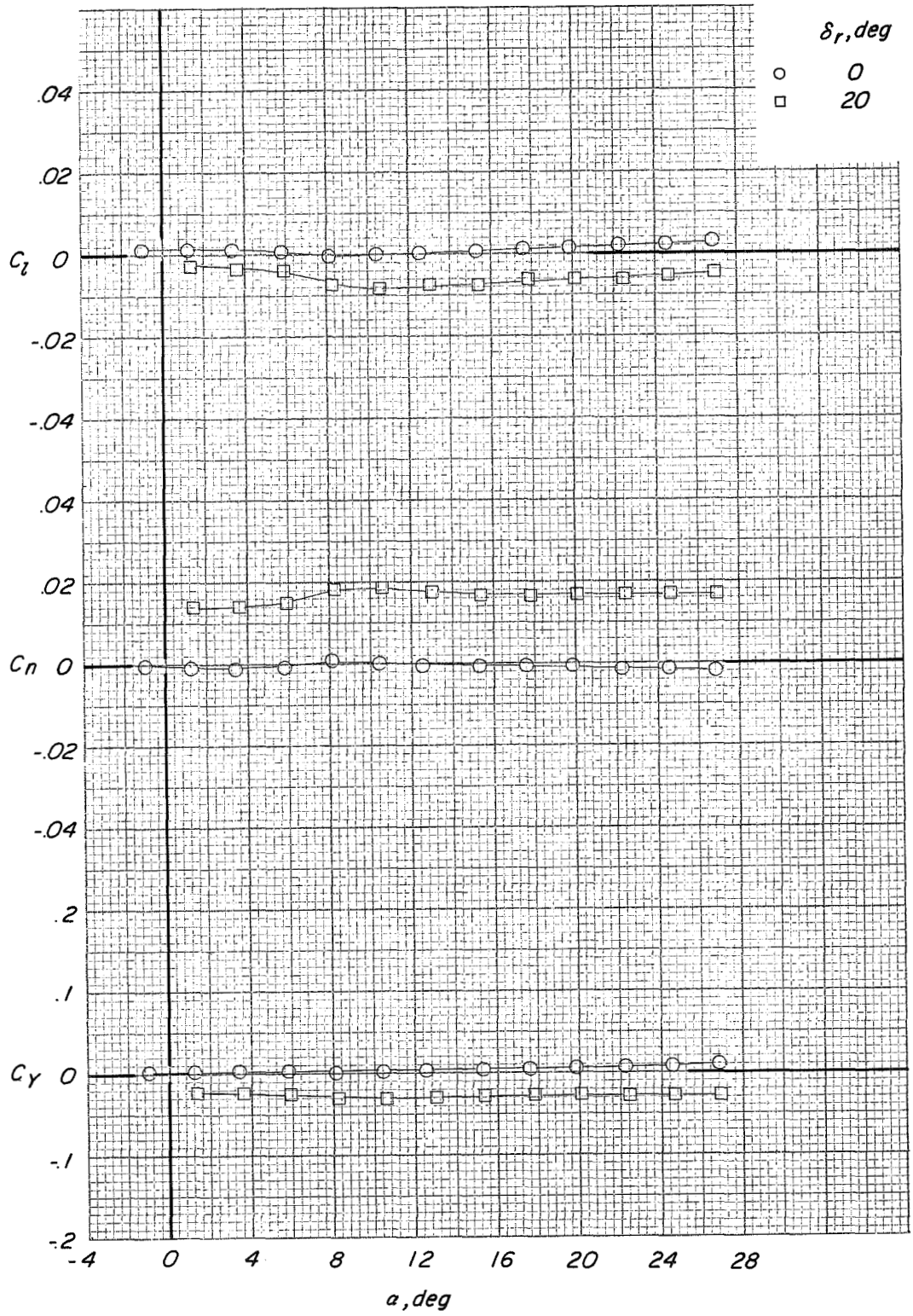
(c) $\delta_e = -10^o$; M = 0.60.

Figure 12.- Continued.



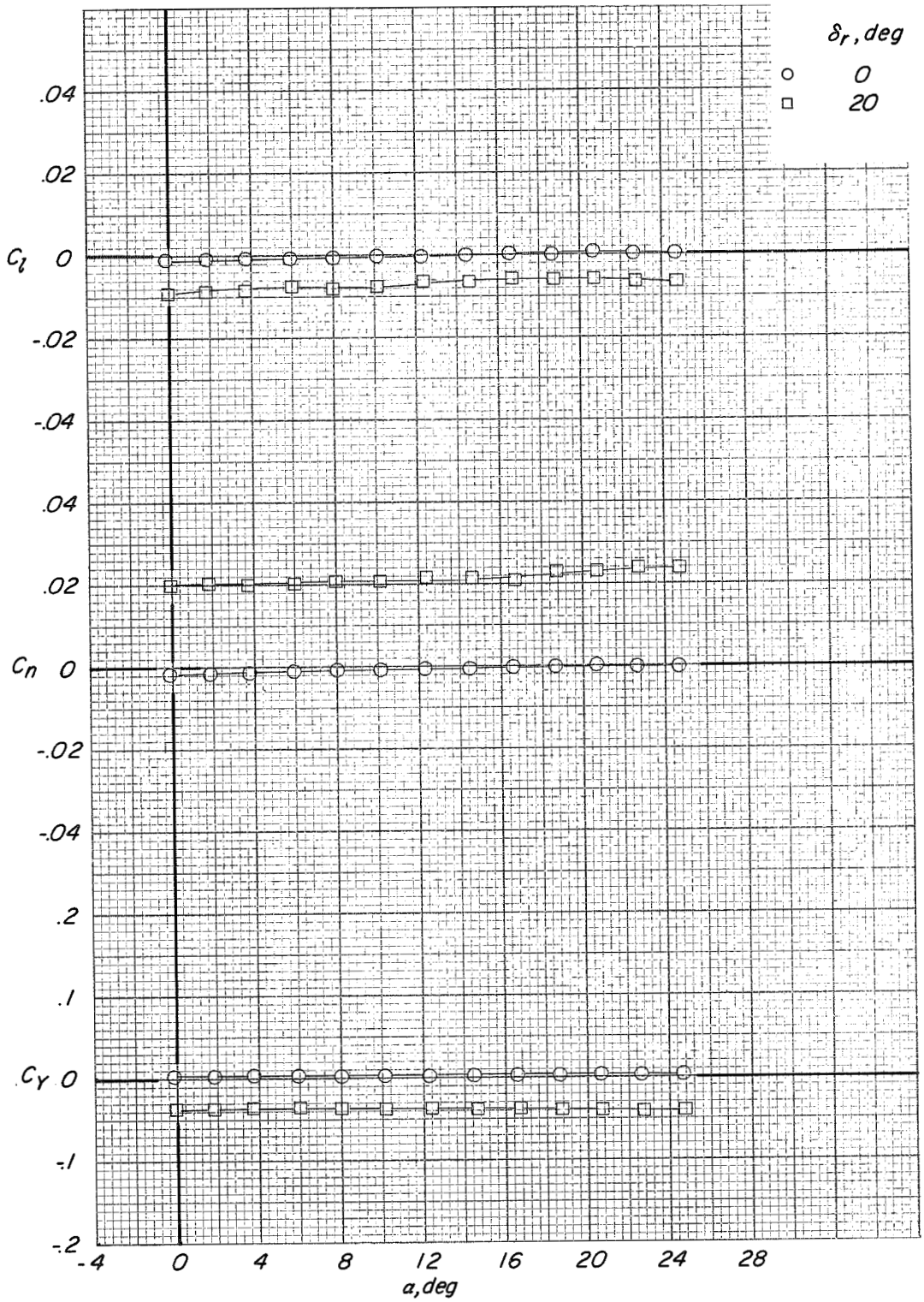
(d) $\delta_e = -10^o$; M = 0.70.

Figure 12.- Continued.



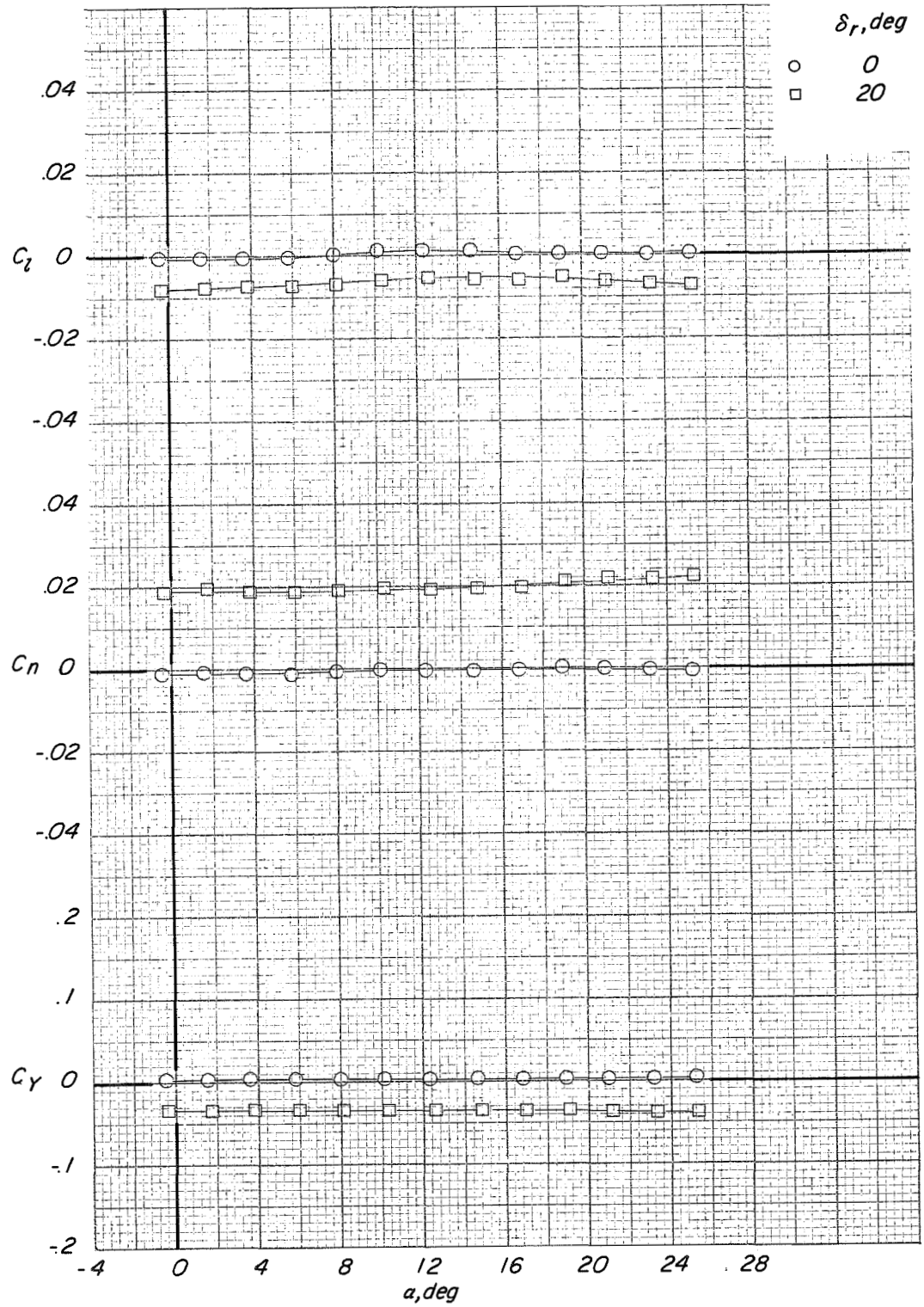
(e) $\delta_e = -10^o$; M = 0.80.

Figure 12.- Continued.



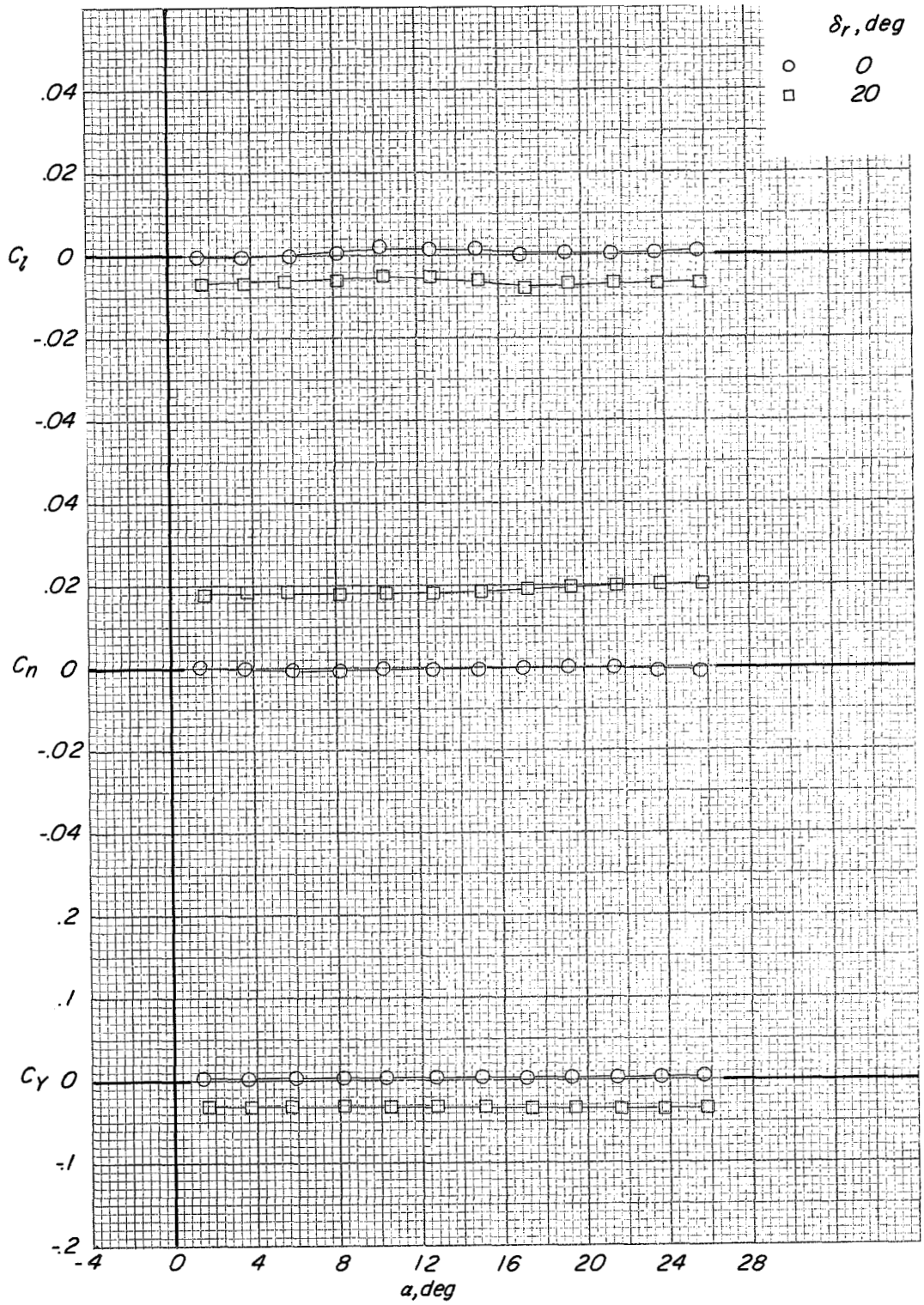
(f) $\delta_e = -15^o$; M = 0.35.

Figure 12.- Continued.



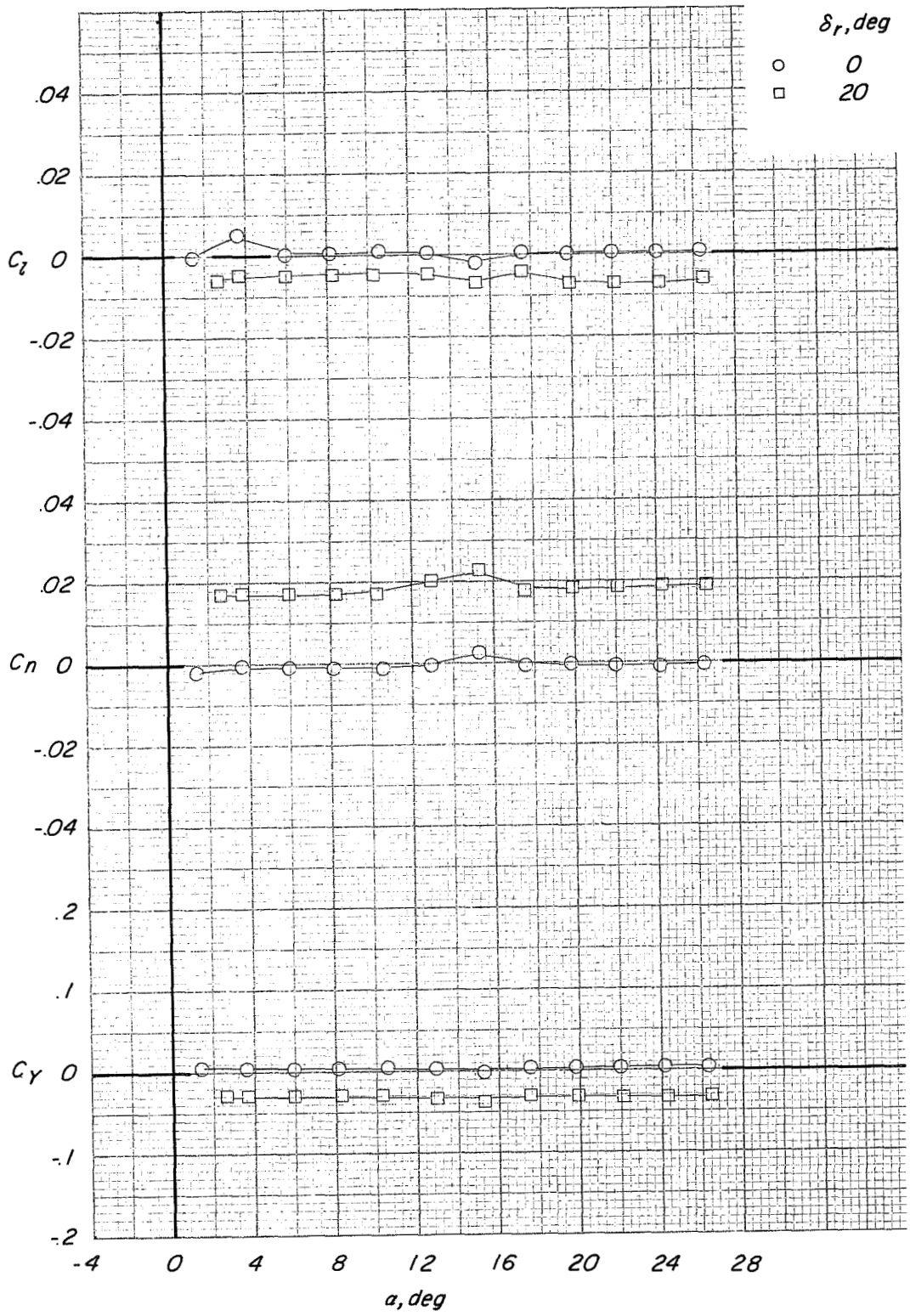
(g) $\delta_e = -15^o$; M = 0.50.

Figure 12.- Continued.



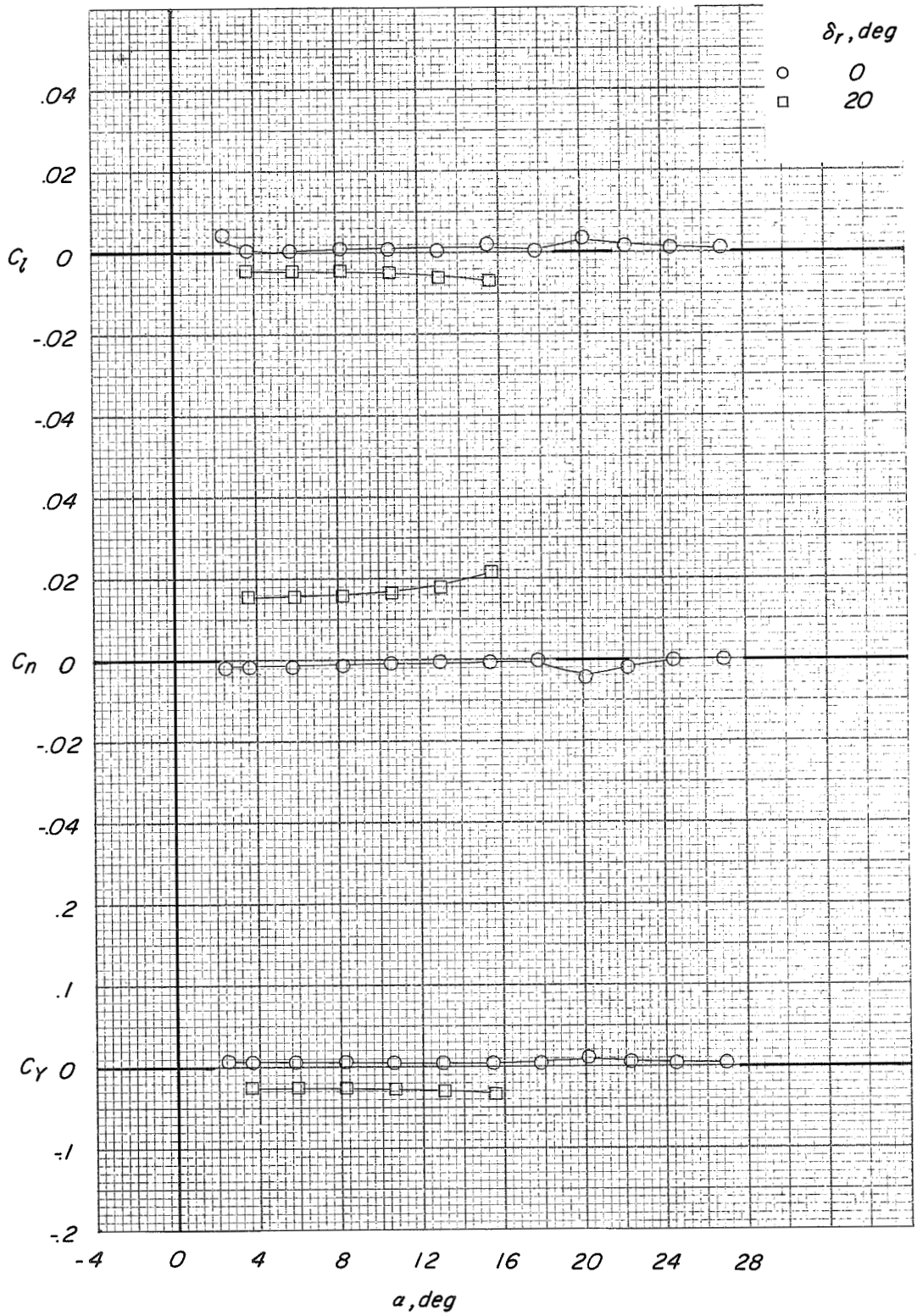
(h) $\delta_e = -15^o$; M = 0.60.

Figure 12.- Continued.



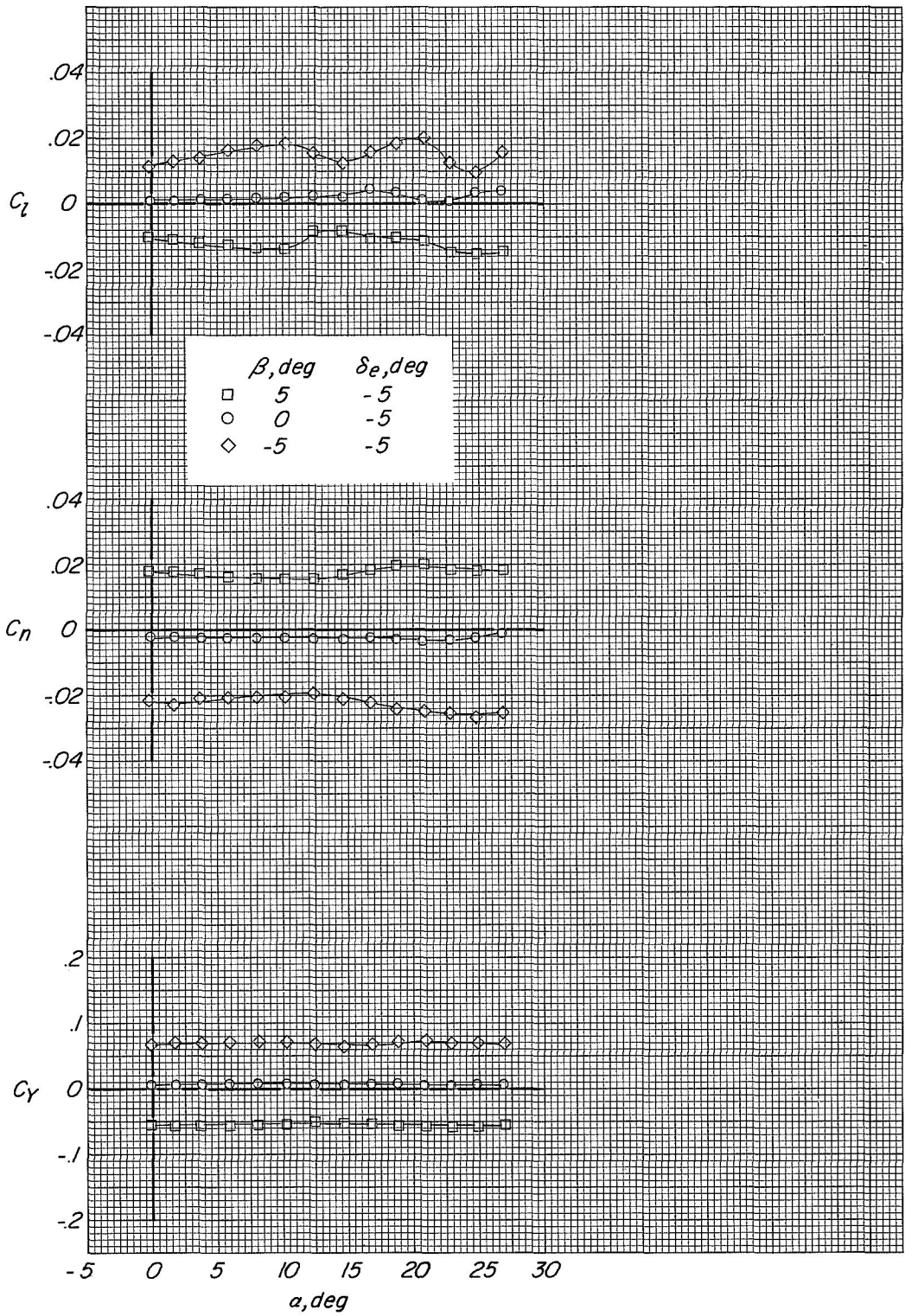
(i) $\delta_e = -15^o$; M = 0.70.

Figure 12.- Continued.



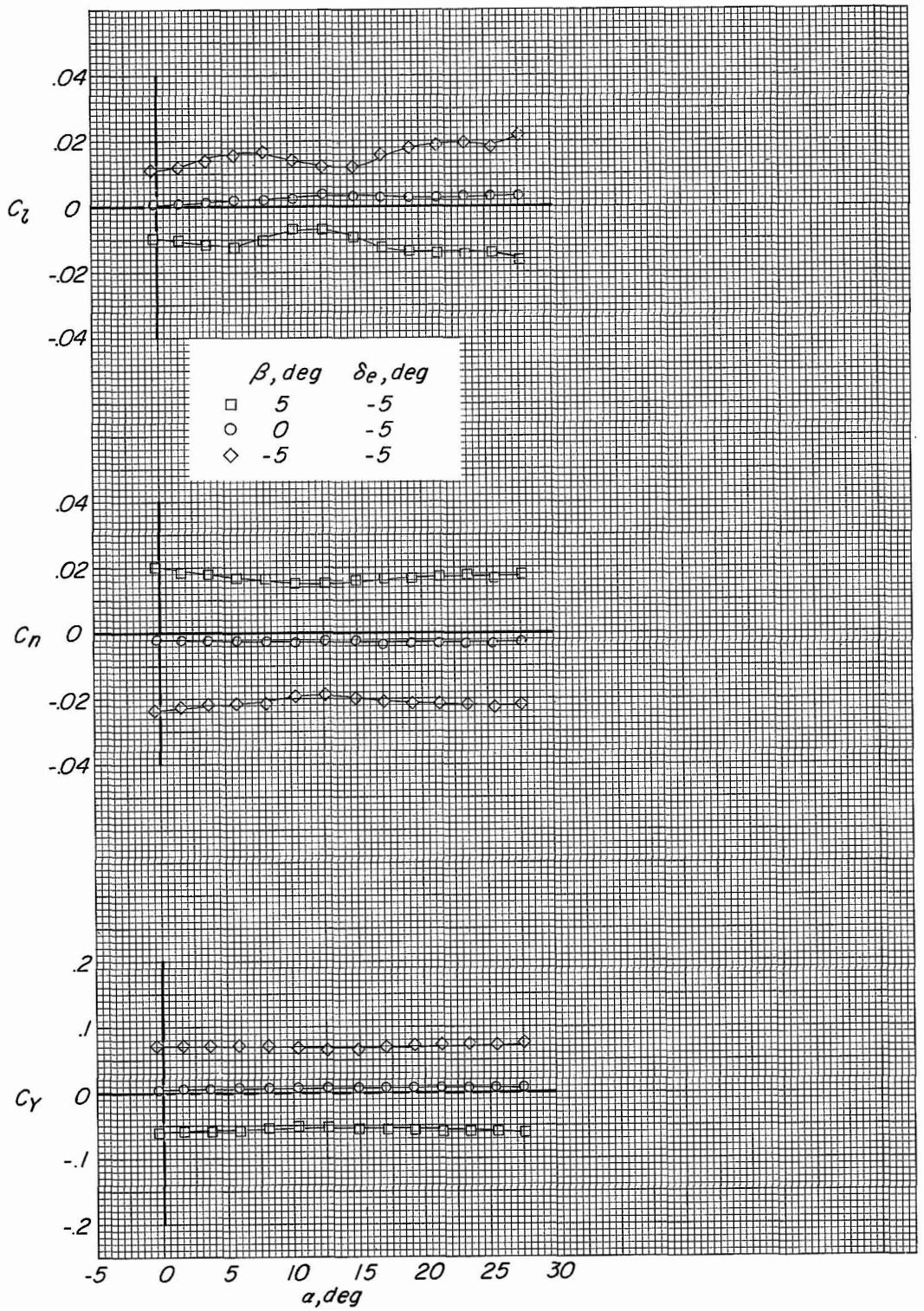
(j) $\delta_e = -15^o$; M = 0.80.

Figure 12.- Concluded.



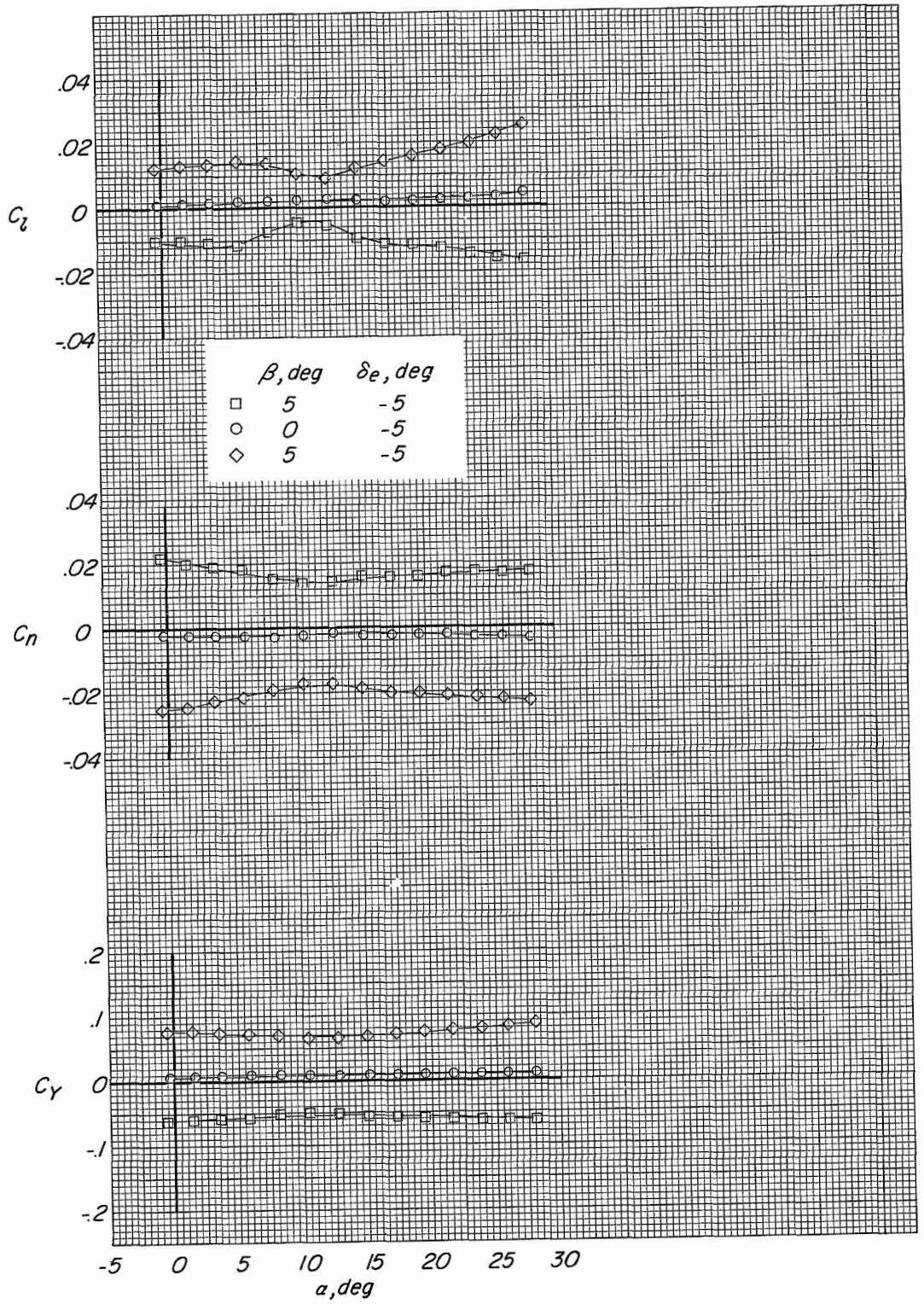
(a) $\delta_e = -5^o$; M = 0.35.

Figure 13.- Effect of sideslip on the lateral directional characteristics. Basic fin configuration; auxiliary flaps in subsonic position.



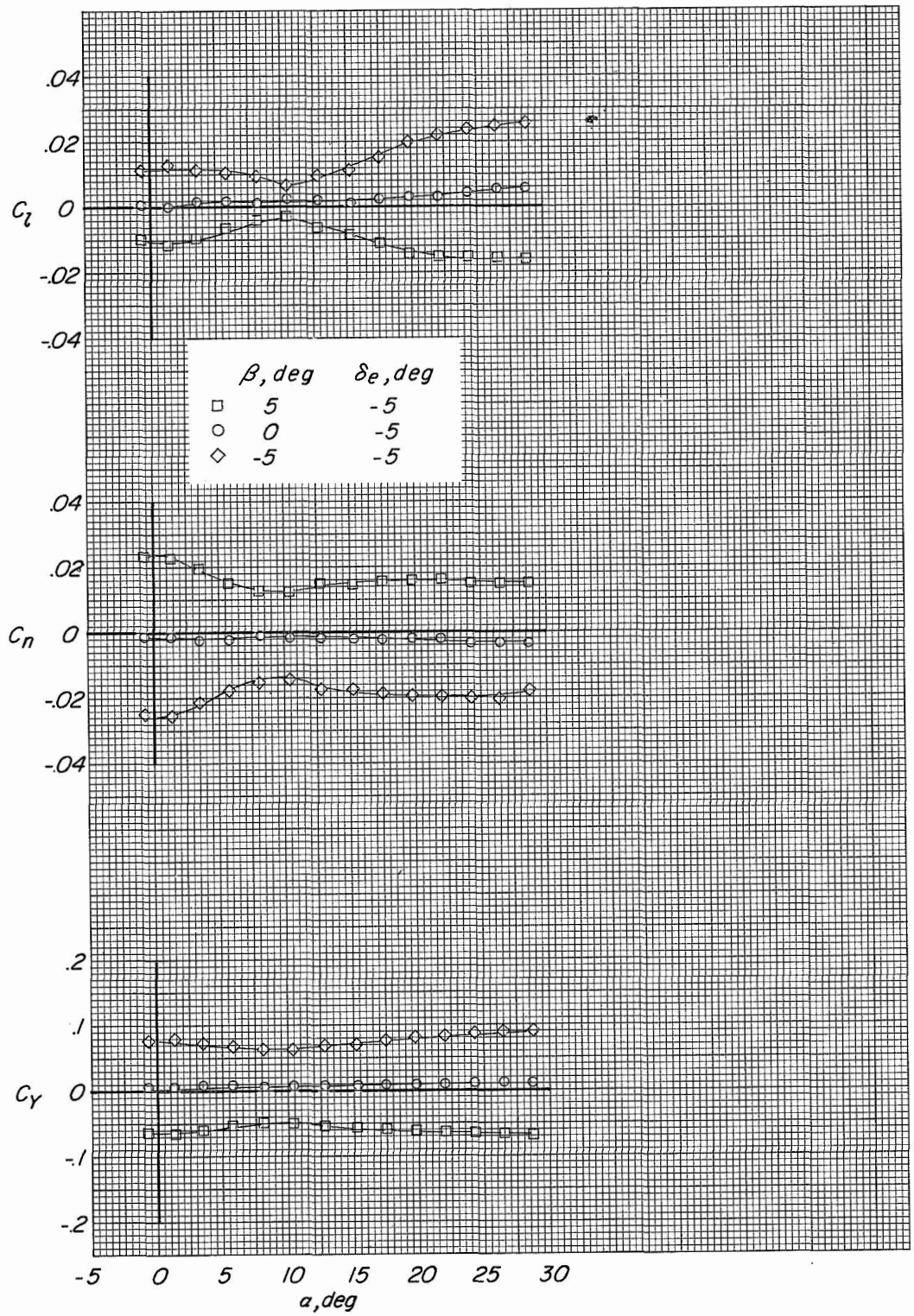
(b) $\delta_e = -5^o$; M = 0.50.

Figure 13.- Continued.



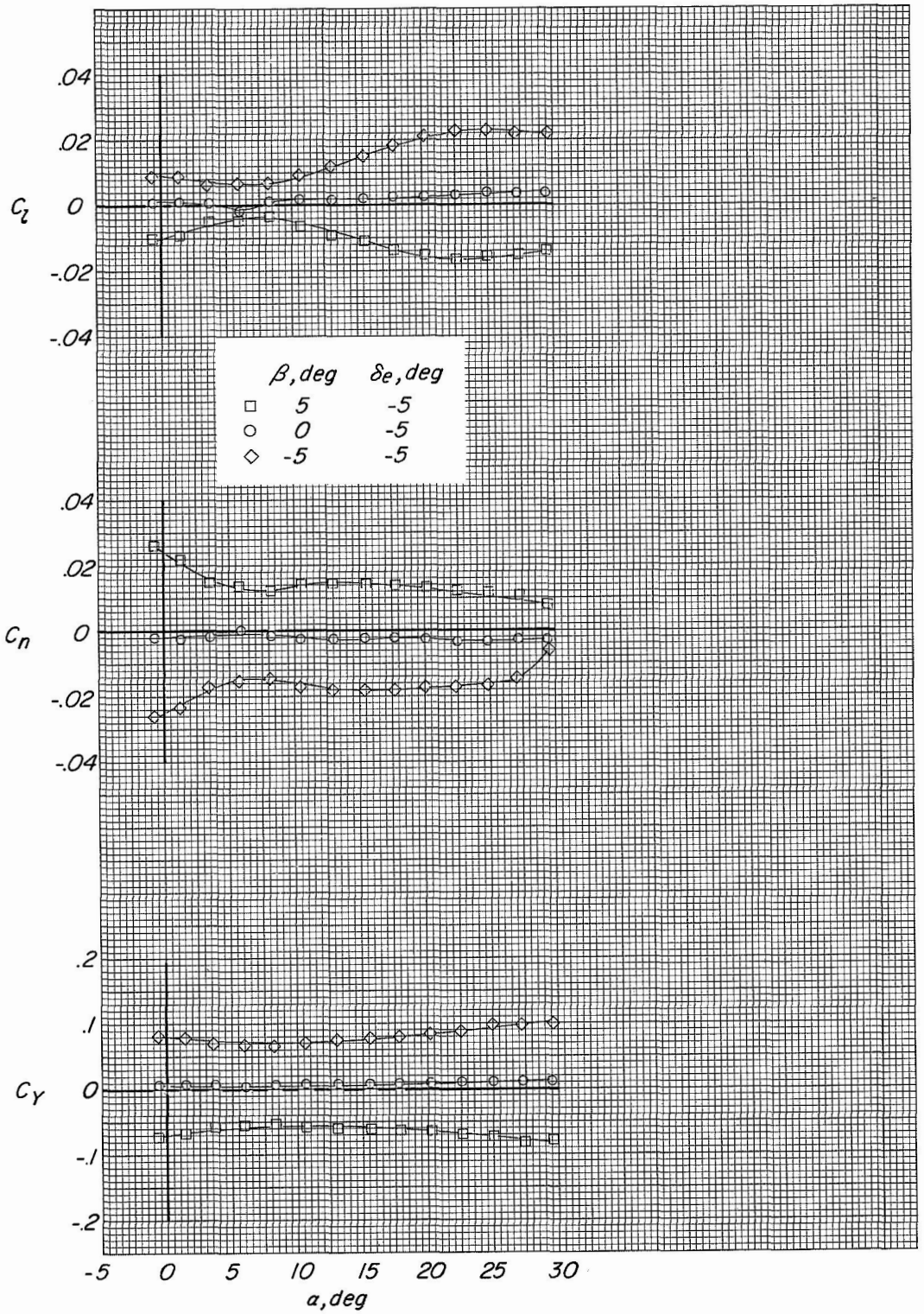
(c) $\delta_e = -5^o$; M = 0.60.

Figure 13.- Continued.



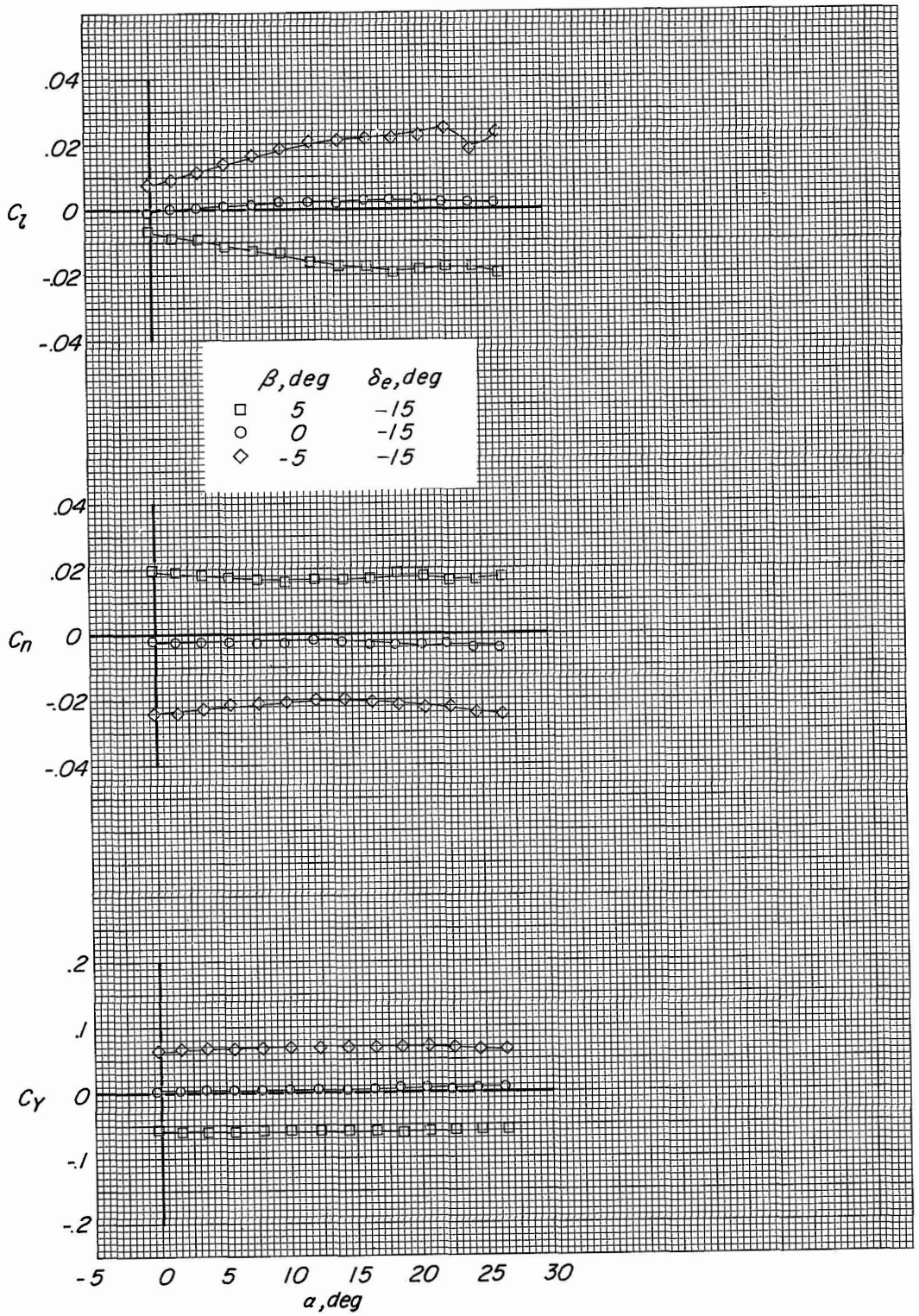
(d) $\delta_e = -5^o$; M = 0.70.

Figure 13.- Continued.



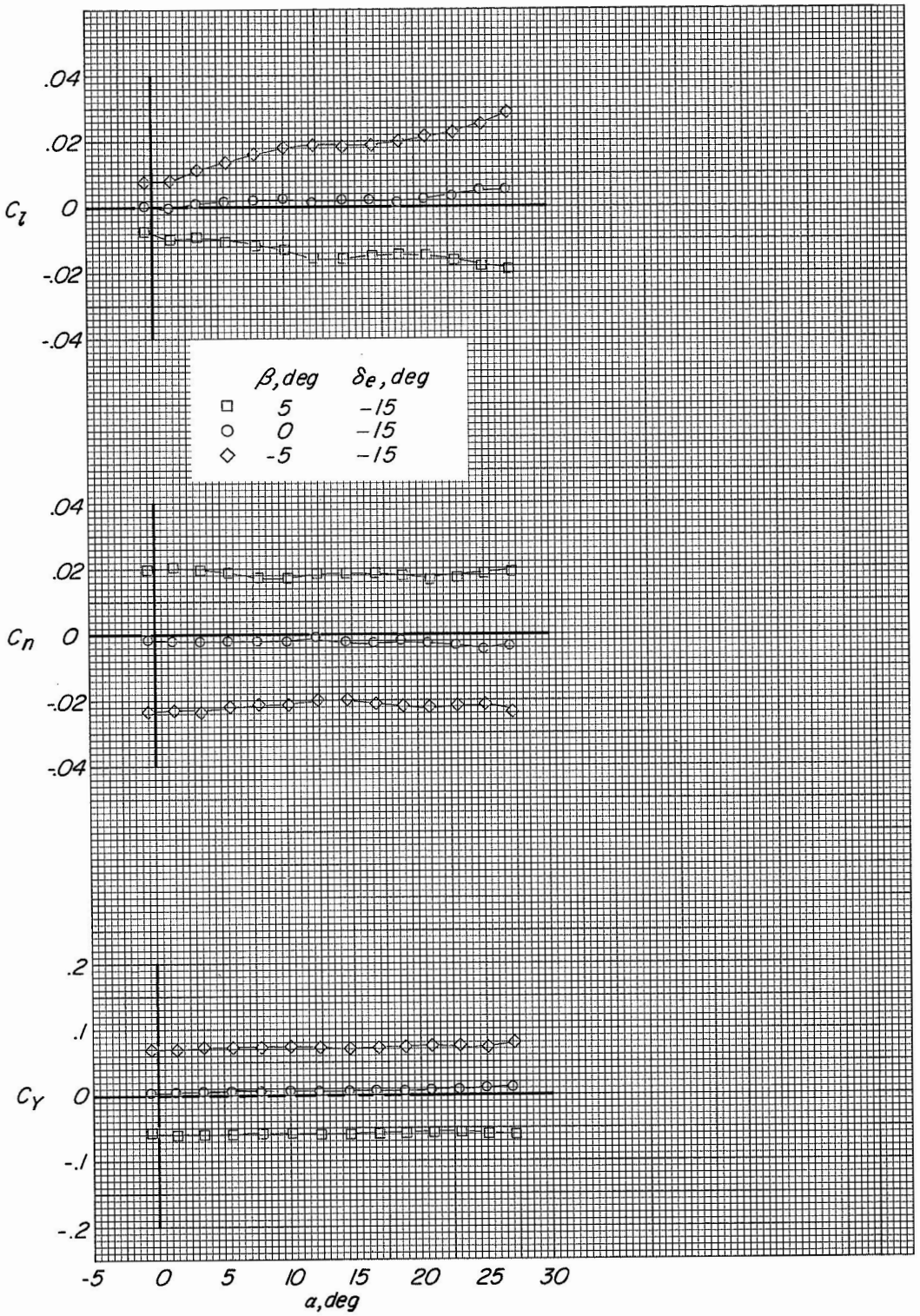
(e) $\delta_e = -5^o$; M = 0.80.

Figure 13.- Continued.



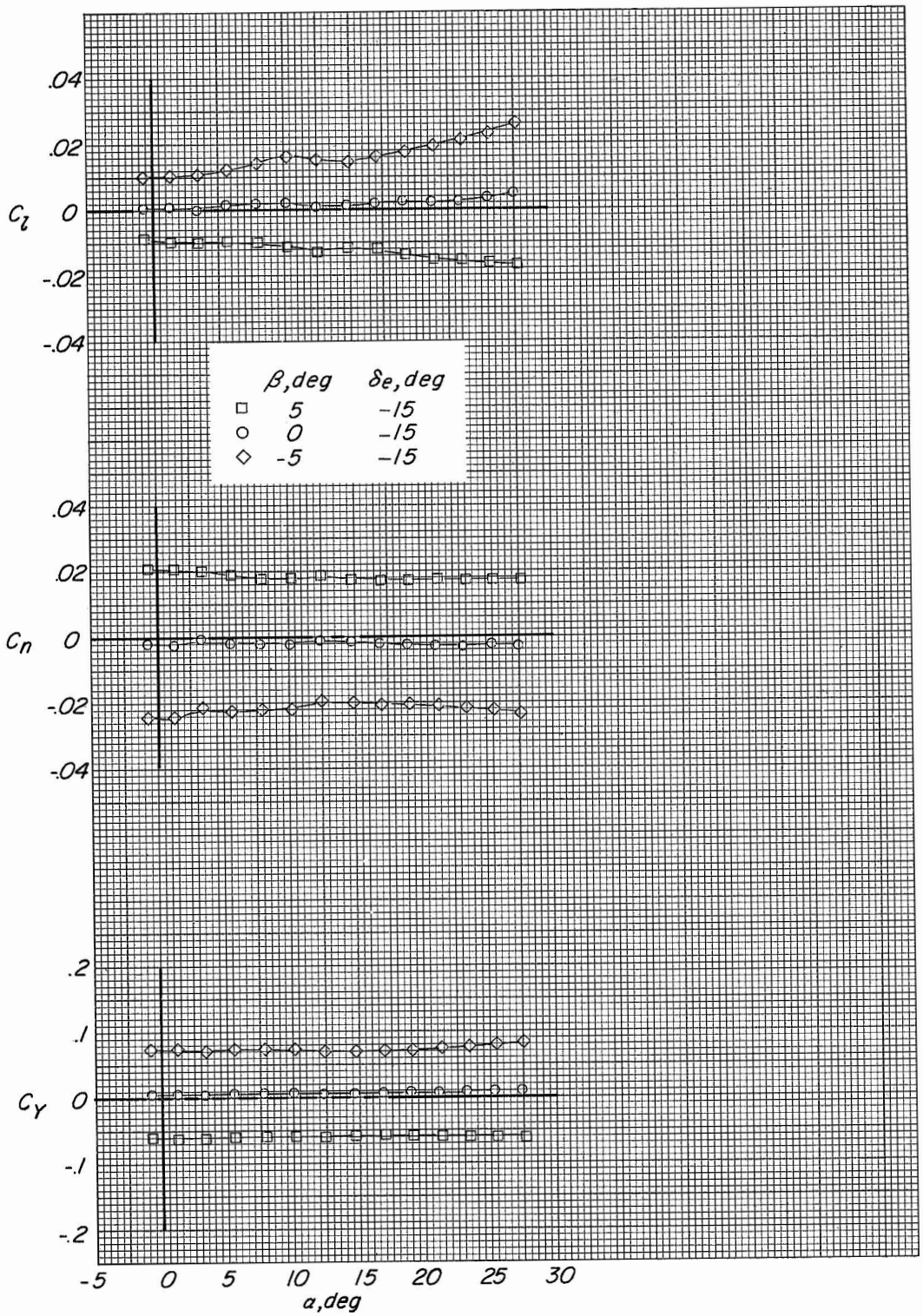
(f) $\delta_e = -15^o$; M = 0.35.

Figure 13.- Continued.



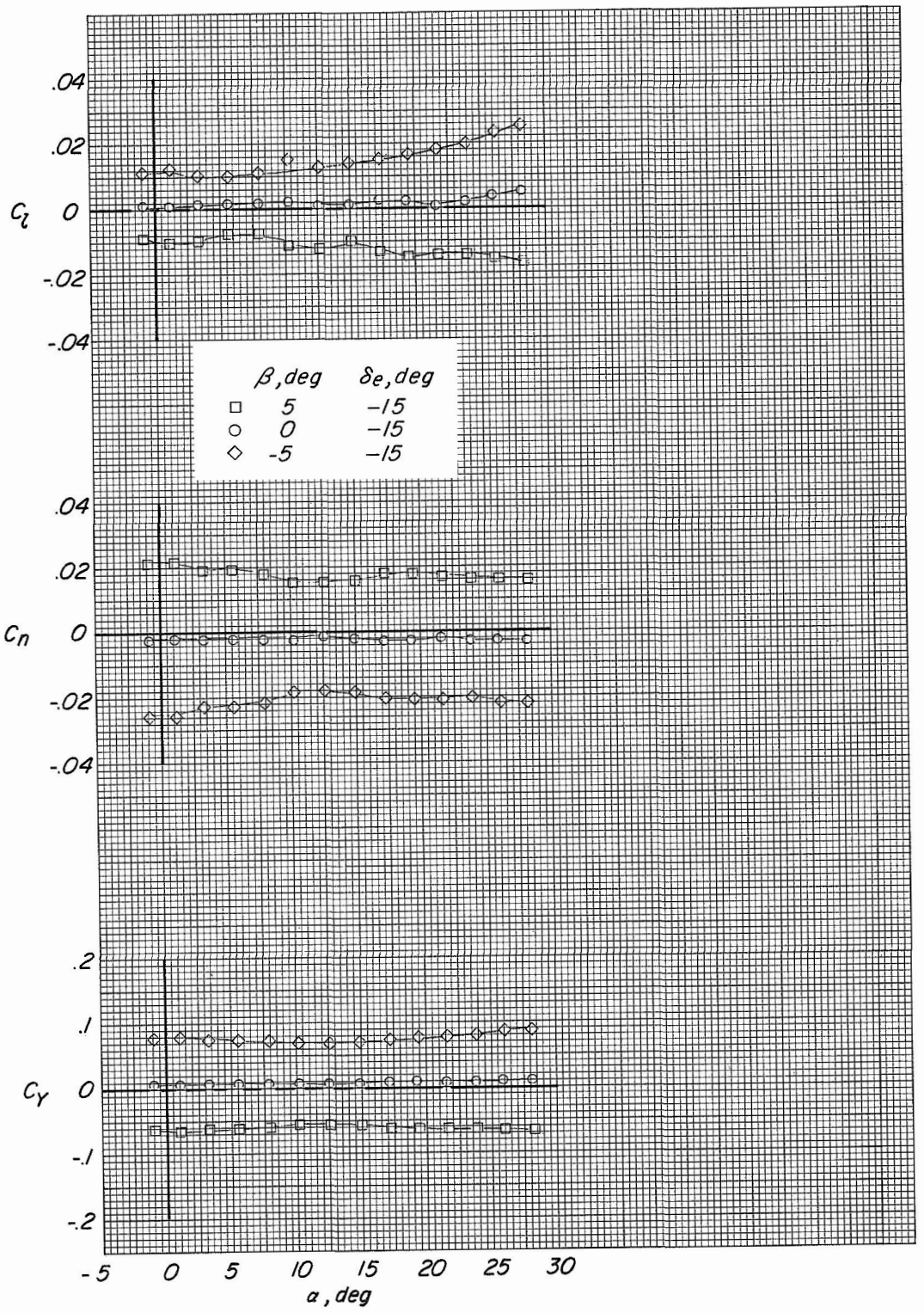
(g) $\delta_e = -15^o$; M = 0.50.

Figure 13.- Continued.



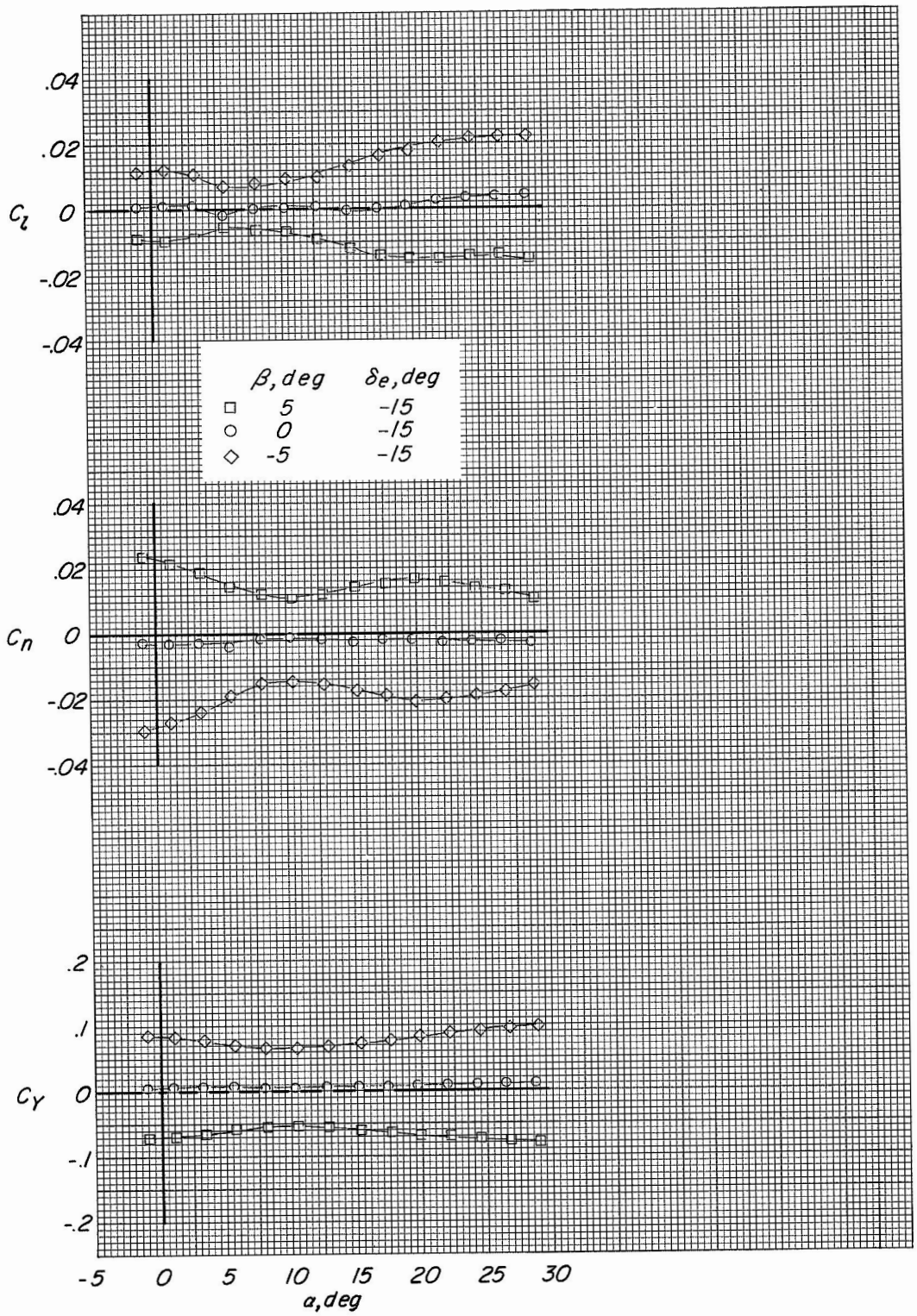
(h) $\delta_e = -15^o$; M = 0.60.

Figure 13.- Continued.



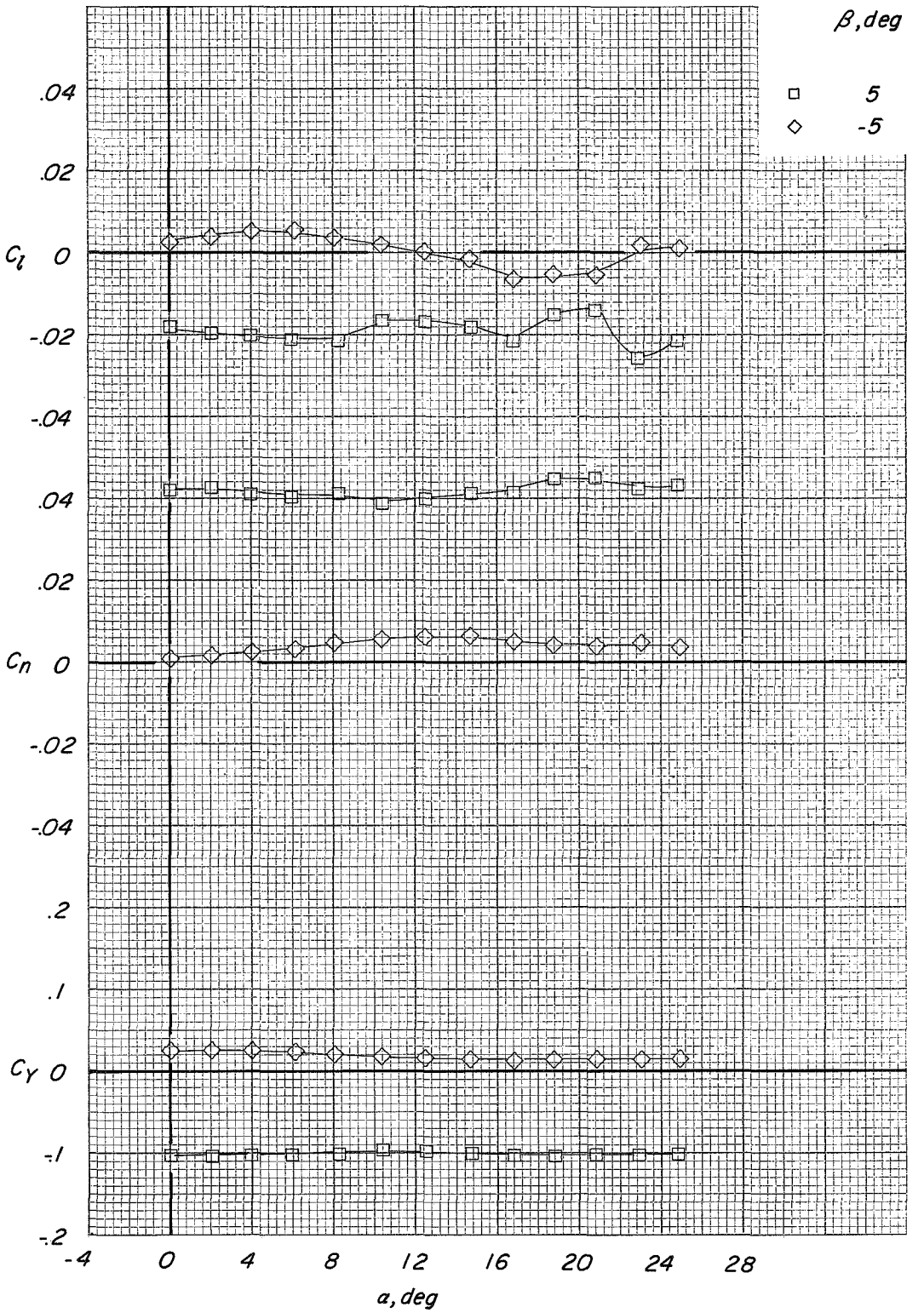
(i) $\delta_e = -15^o$; M = 0.70.

Figure 13.- Continued.



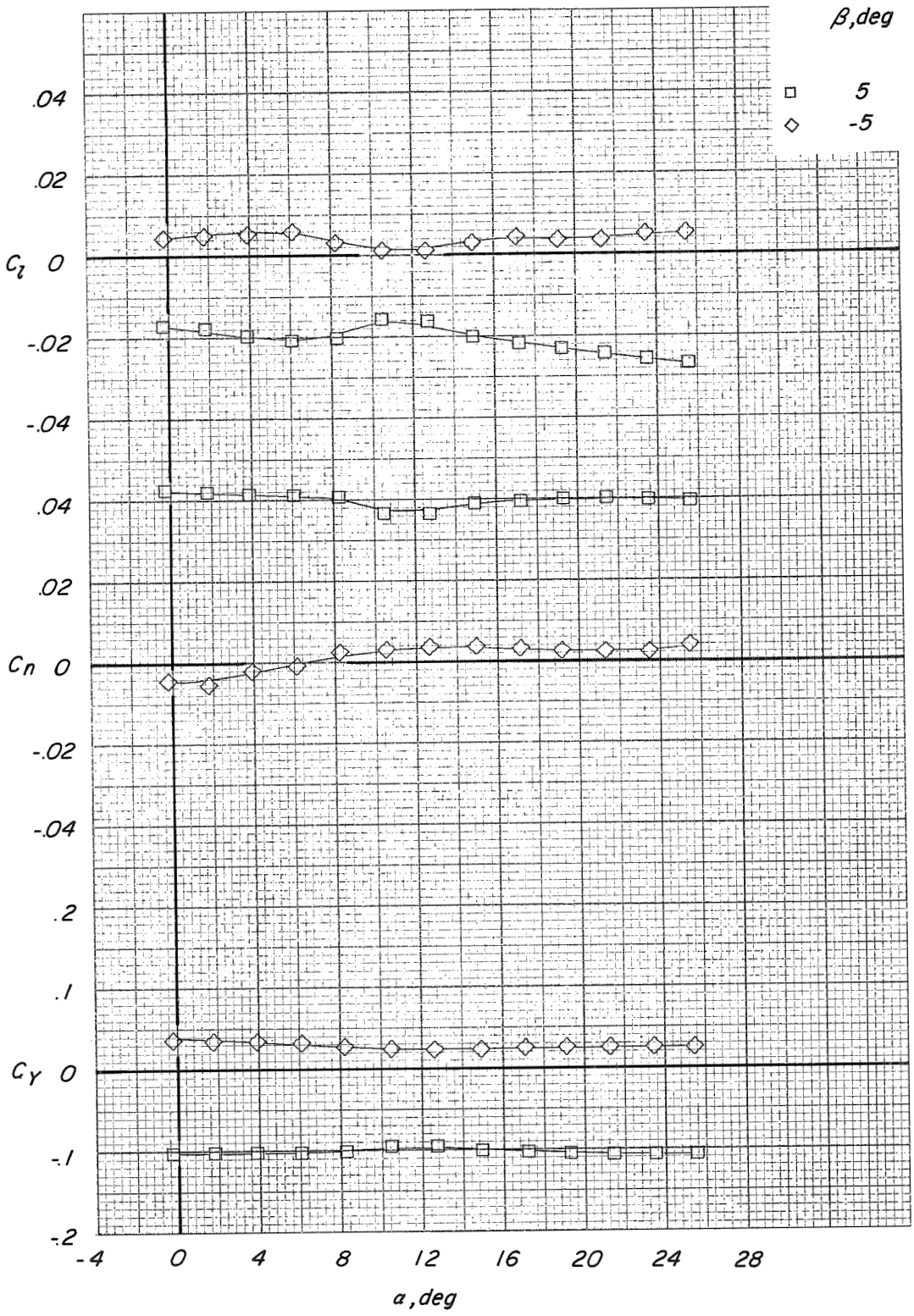
(j) $\delta_e = -15^o$; M = 0.80.

Figure 13.- Concluded.



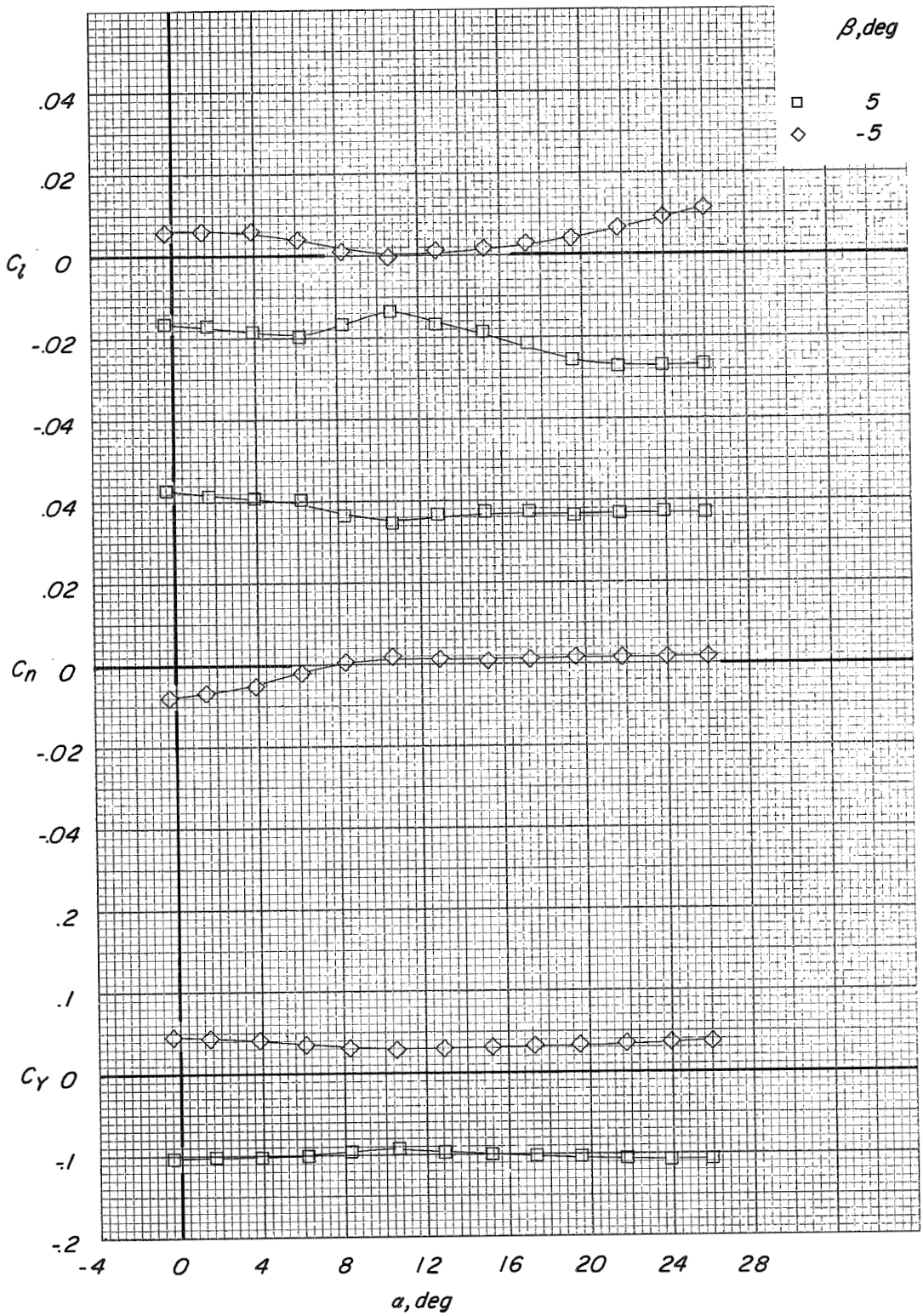
(a) $\delta_e = -5^o$; M = 0.35.

Figure 14.- Effect of combined rudder deflection and sideslip on the lateral directional characteristics. Basic fin configuration; auxiliary flaps in the subsonic position; $\delta_r = 20^o$; $\beta = \delta_a = 0^o$.



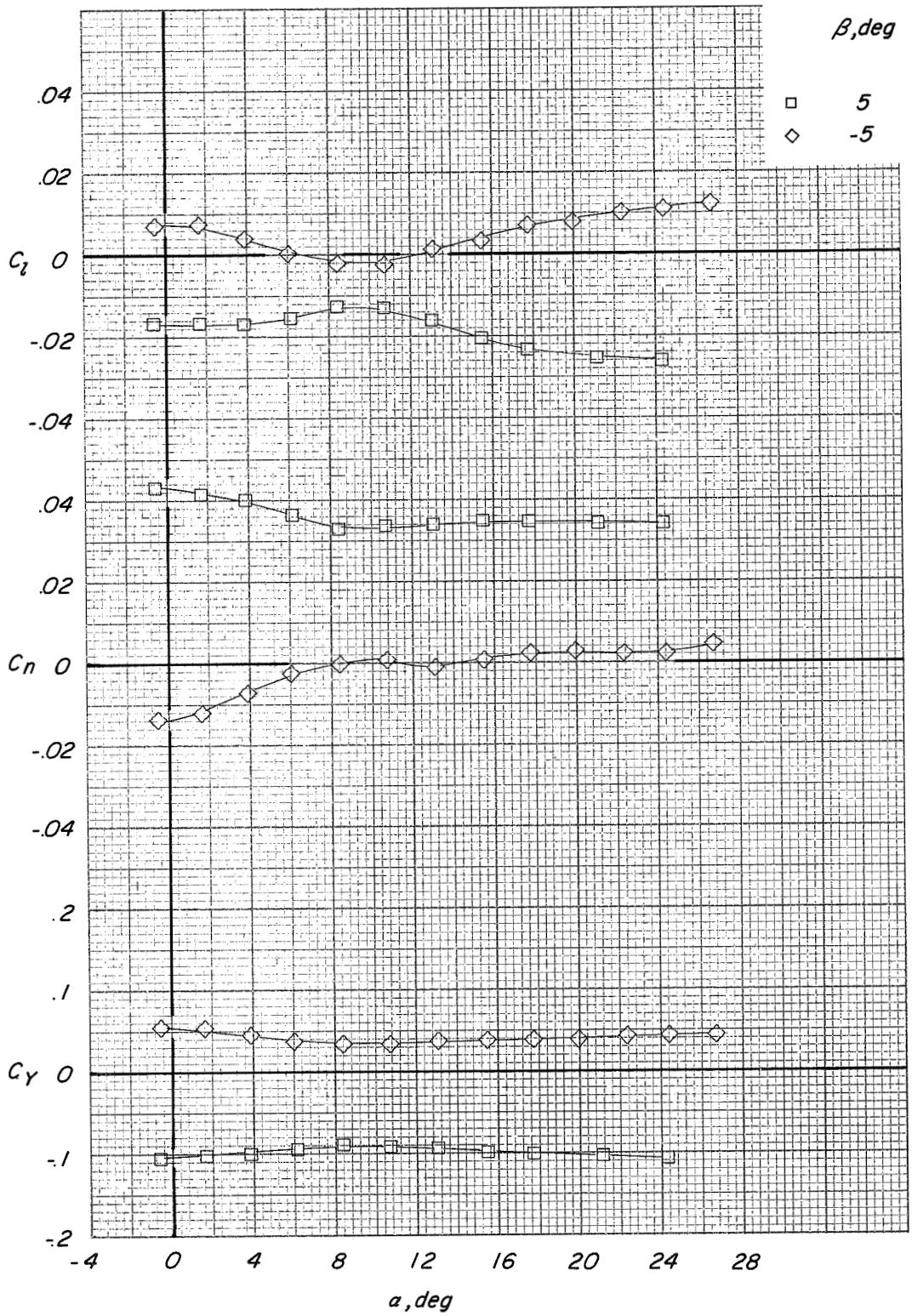
(b) $\delta_e = -5^o$; M = 0.50.

Figure 14.- Continued.



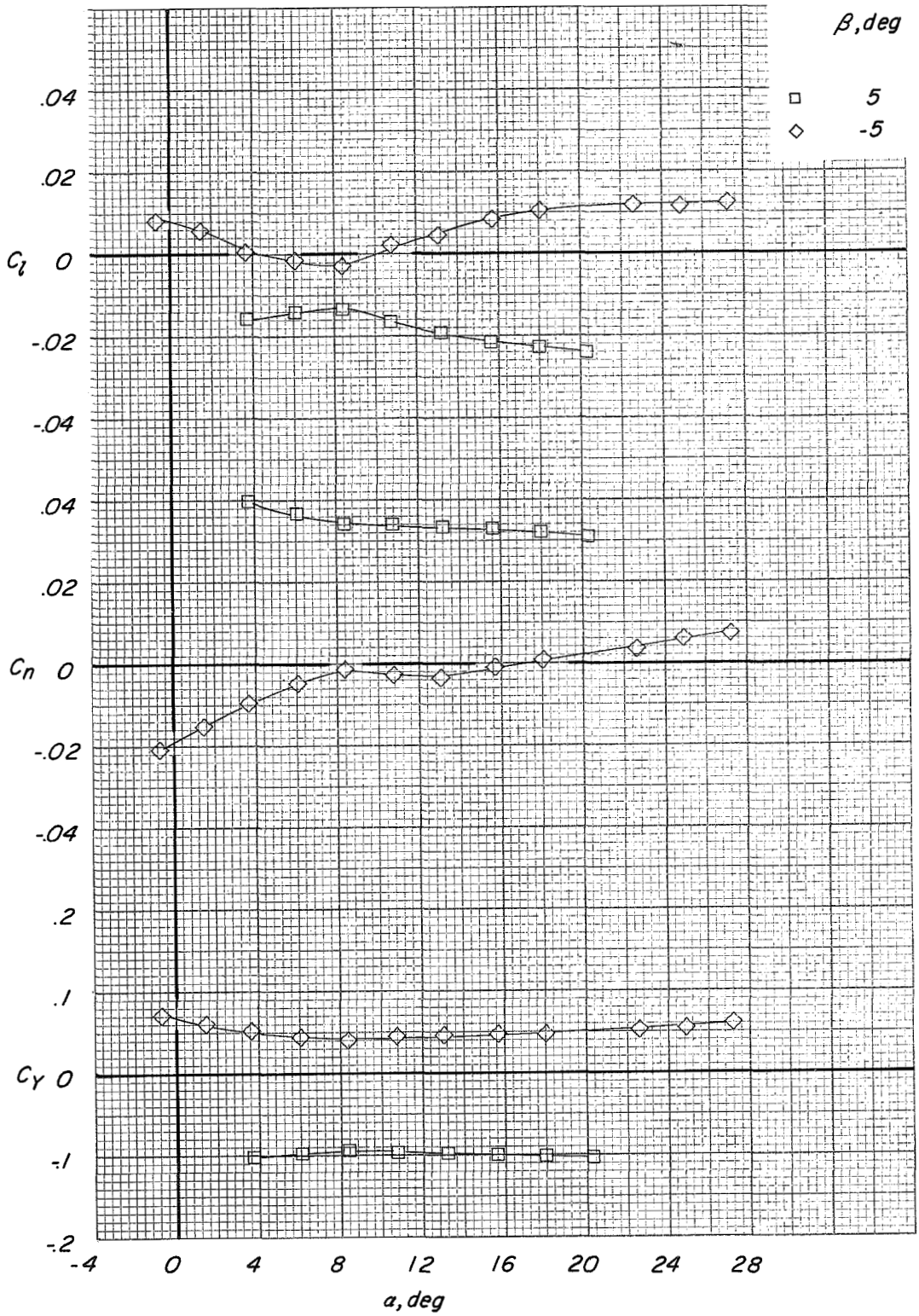
(c) $\delta_e = -5^o$; M = 0.60.

Figure 14.- Continued.



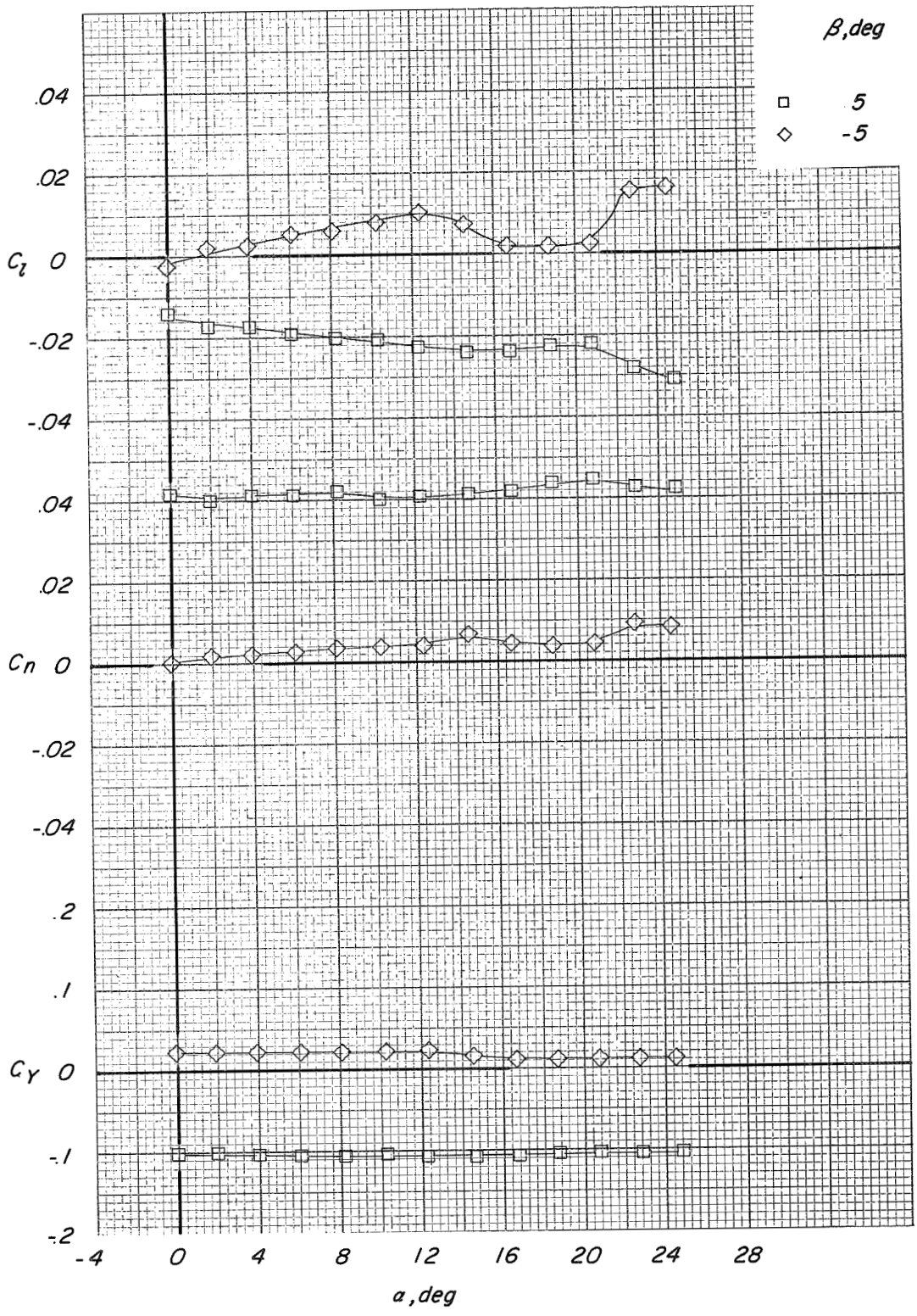
(d) $\delta_e = -5^o$; M = 0.70.

Figure 14.- Continued.



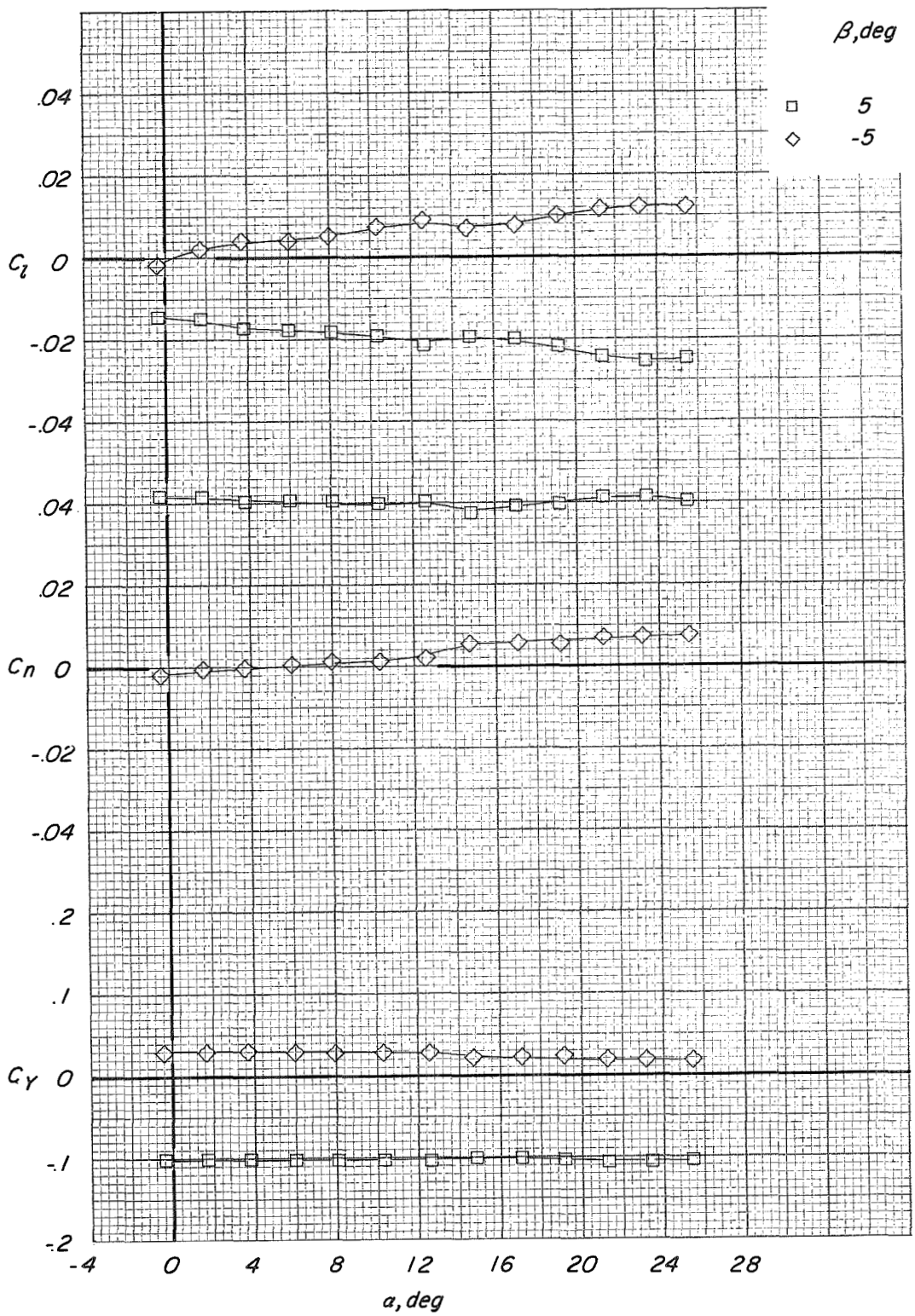
(e) $\delta_e = -5^o$; M = 0.80.

Figure 14.- Continued.



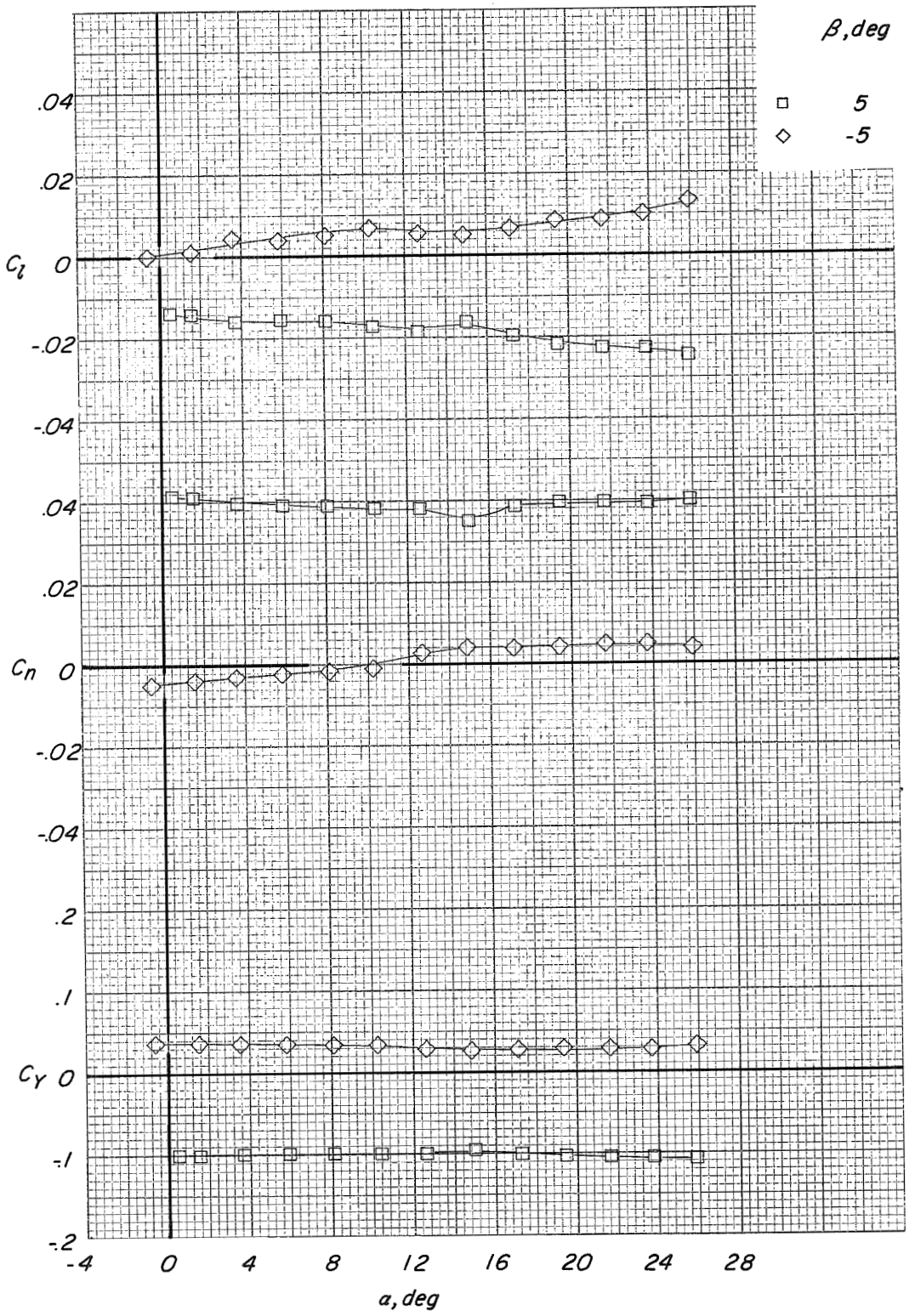
(f) $\delta_e = -15^o$; M = 0.35.

Figure 14.- Continued.



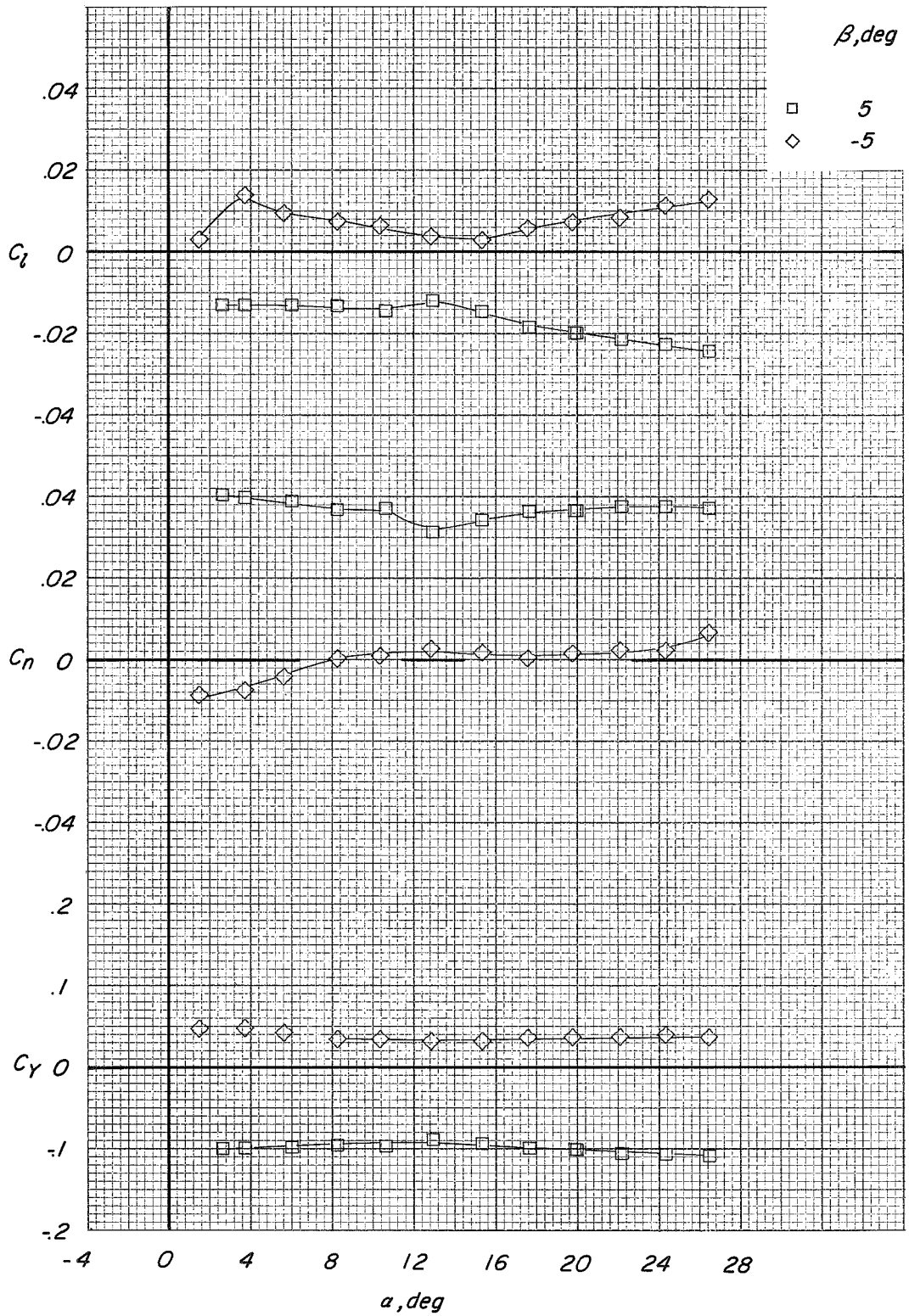
(g) $\delta_e = -15^o$; M = 0.50.

Figure 14.- Continued.



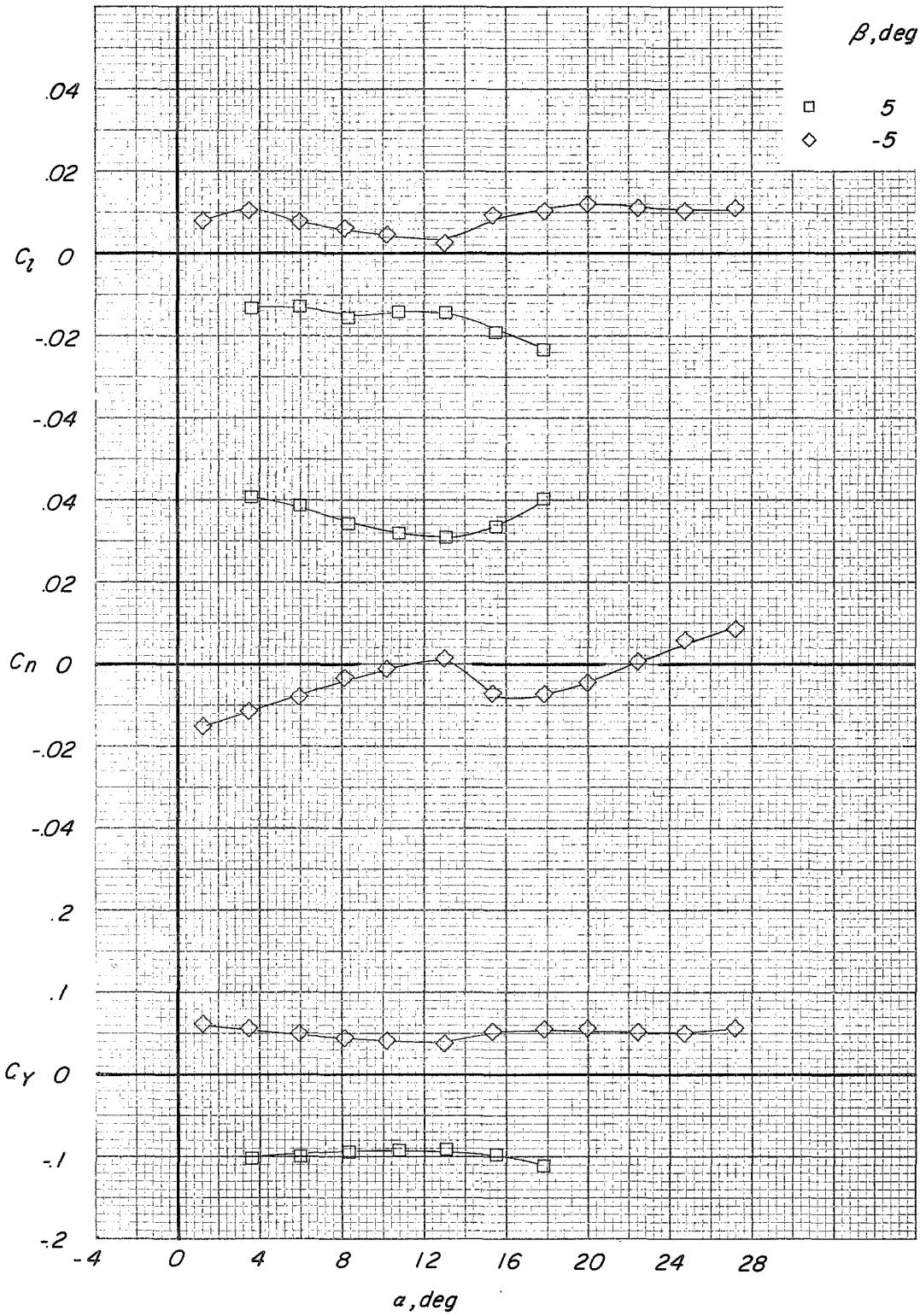
(h) $\delta_e = -15^o$; M = 0.60.

Figure 14.- Continued.



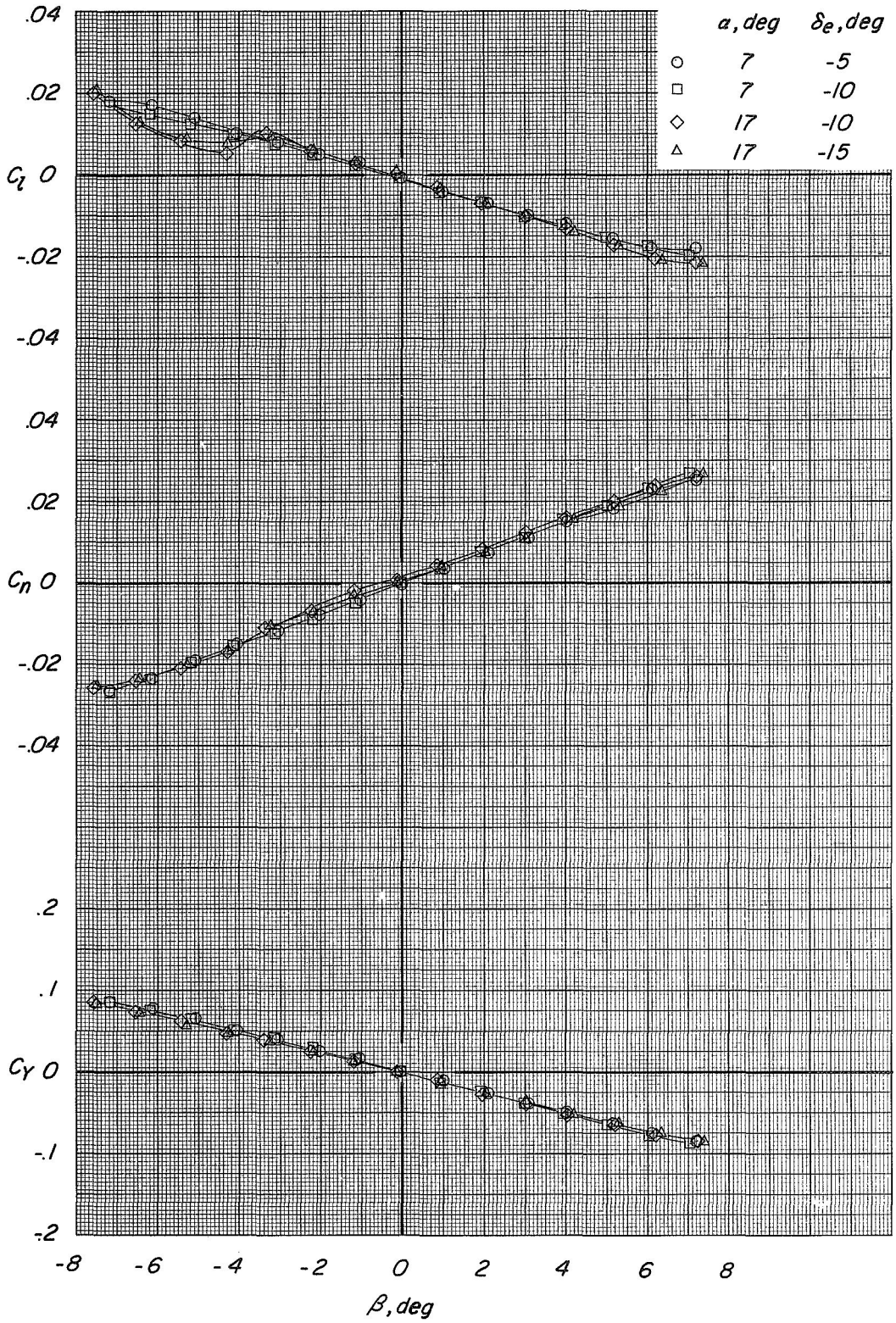
(i) $\delta_e = -15^o$; M = 0.70.

Figure 14.- Continued.



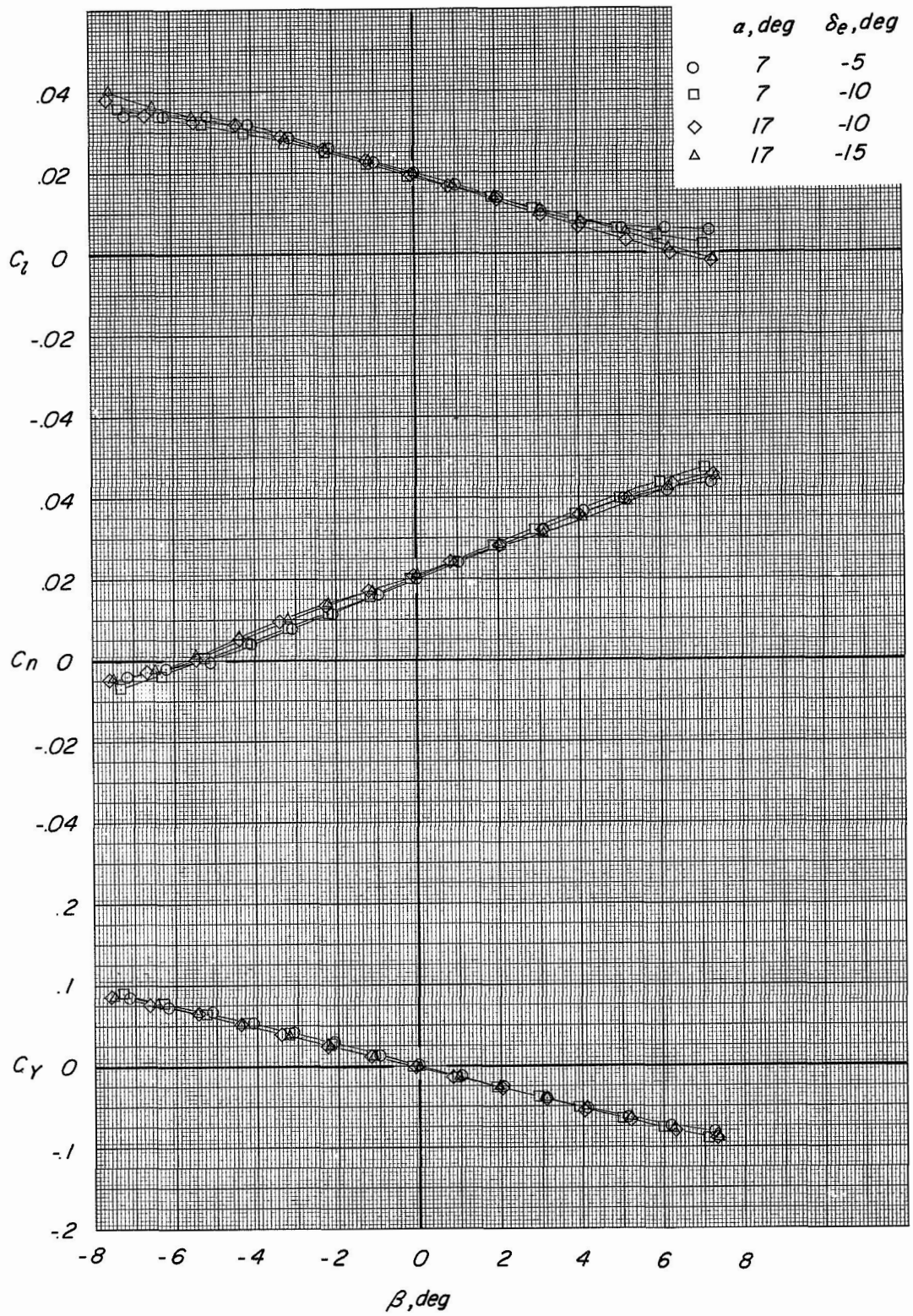
(j) $\delta_e = -15^o$; M = 0.80.

Figure 14.- Concluded.



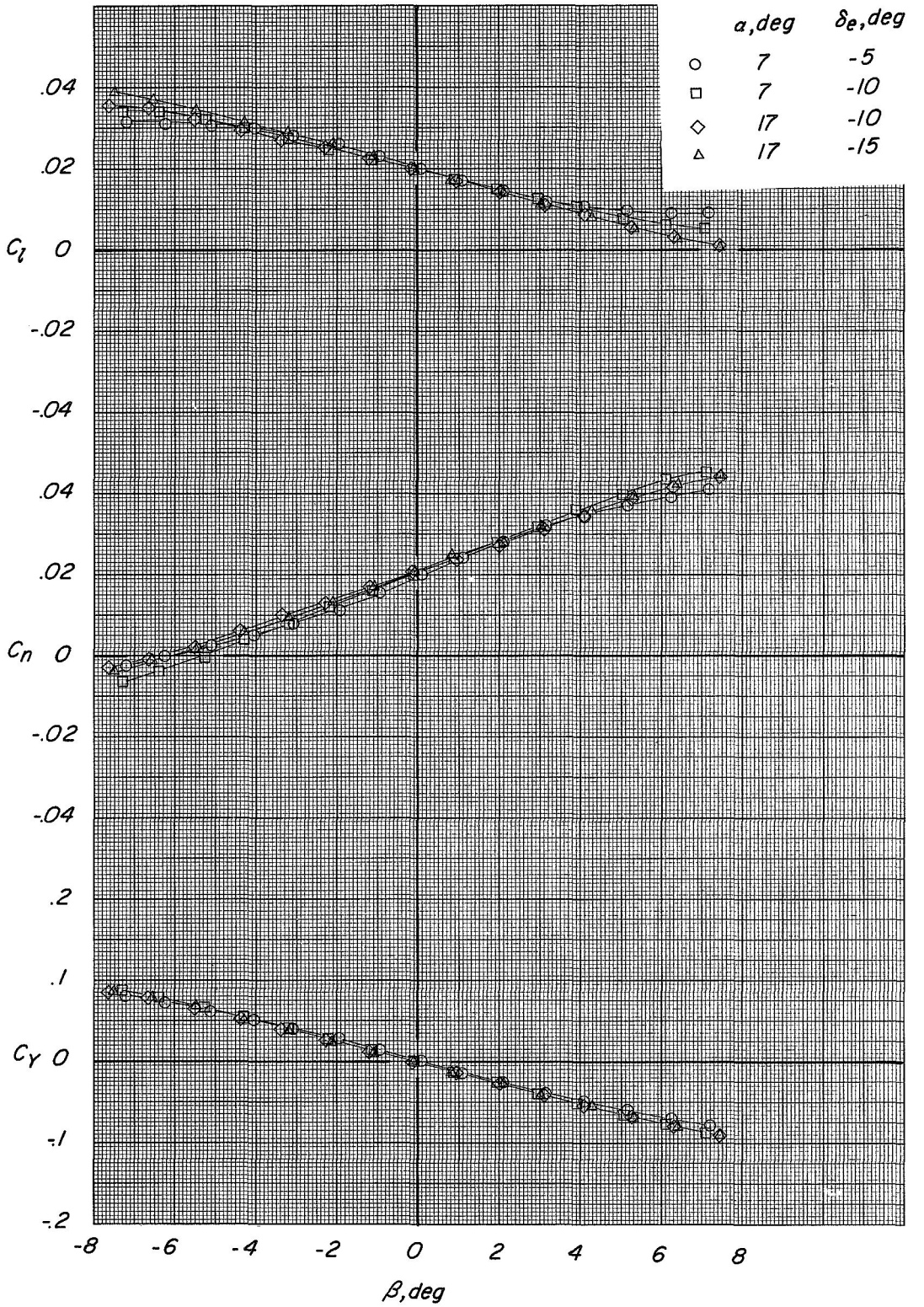
(a) M = 0.35.

Figure 15.- Variation of lateral force and moment coefficients with sideslip angle. Basic fin configuration; auxiliary flaps in the subsonic position; $\delta_a = 0^o$.



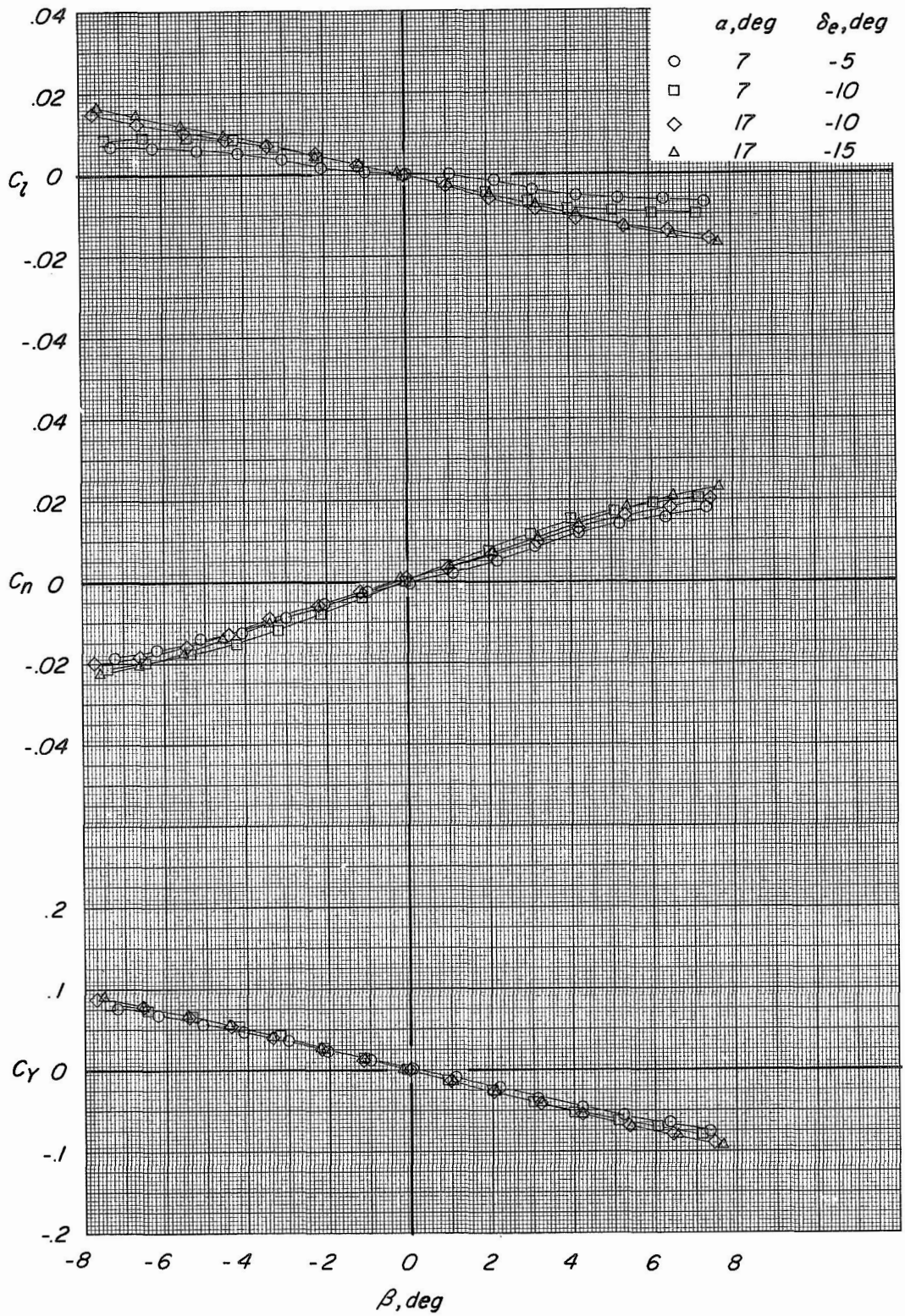
(b) M = 0.50.

Figure 15.- Continued.



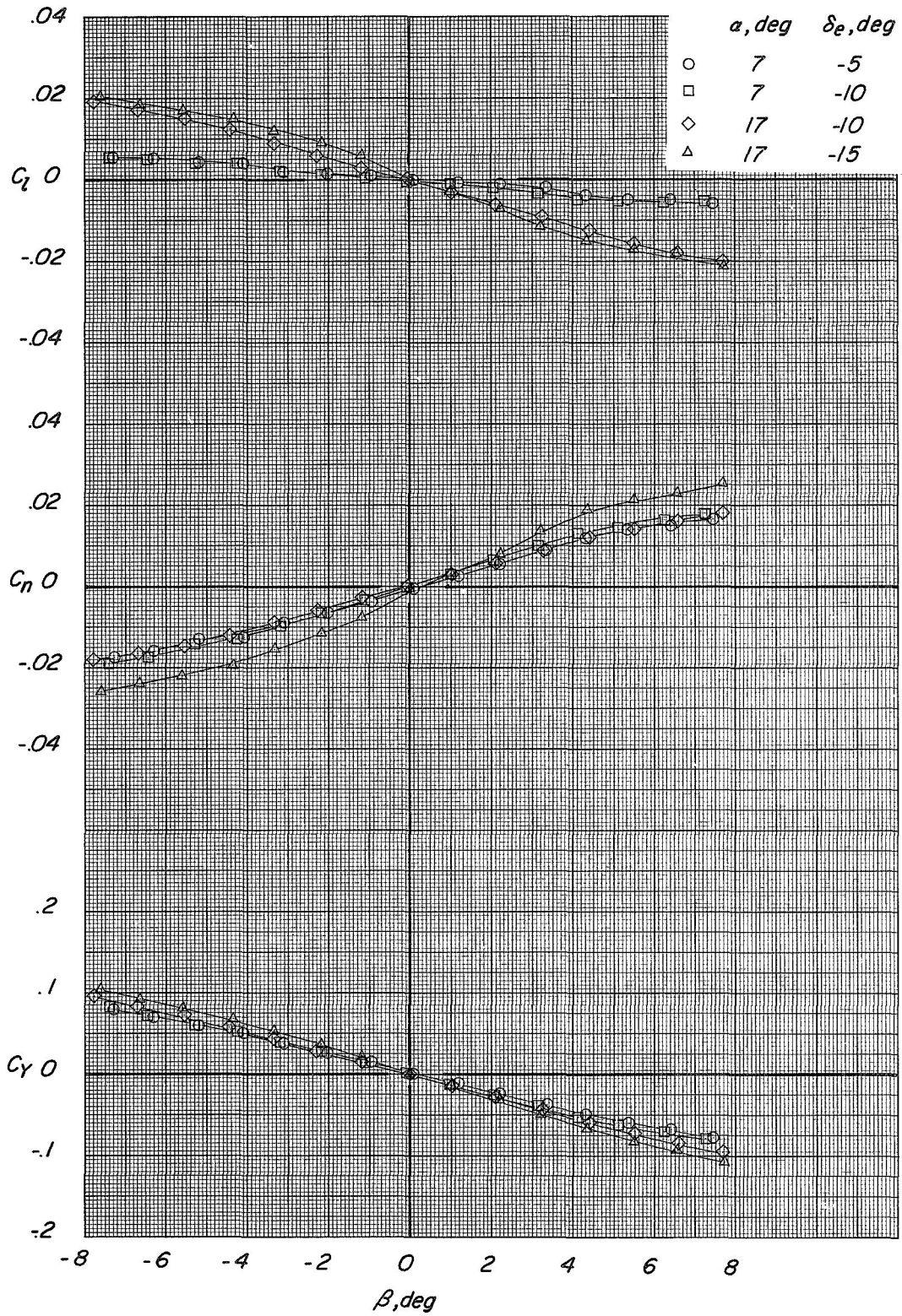
(c) M = 0.60.

Figure 15.- Continued.



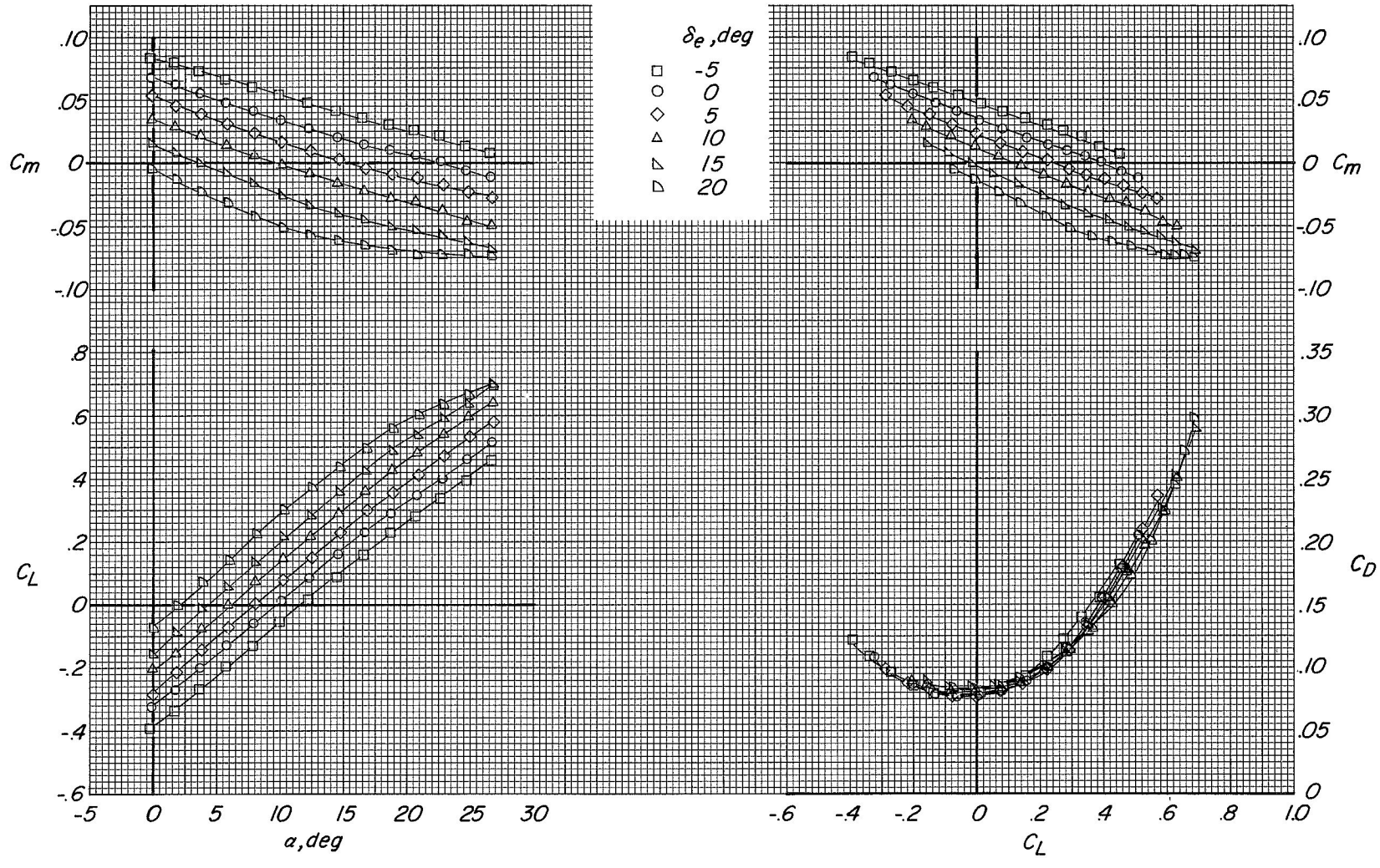
(d) M = 0.70.

Figure 15.- Continued.



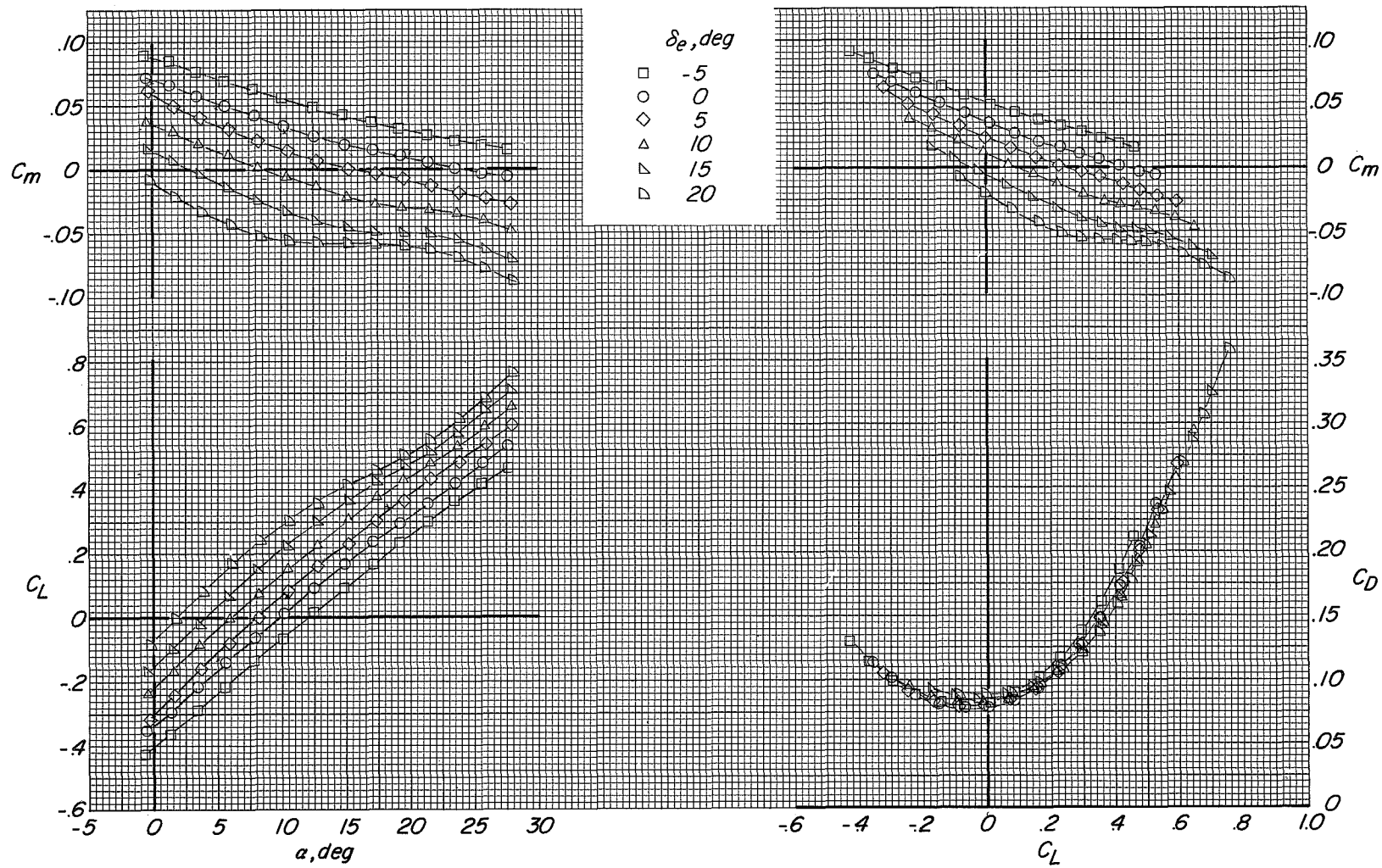
(e) M = 0.80.

Figure 15.- Concluded.



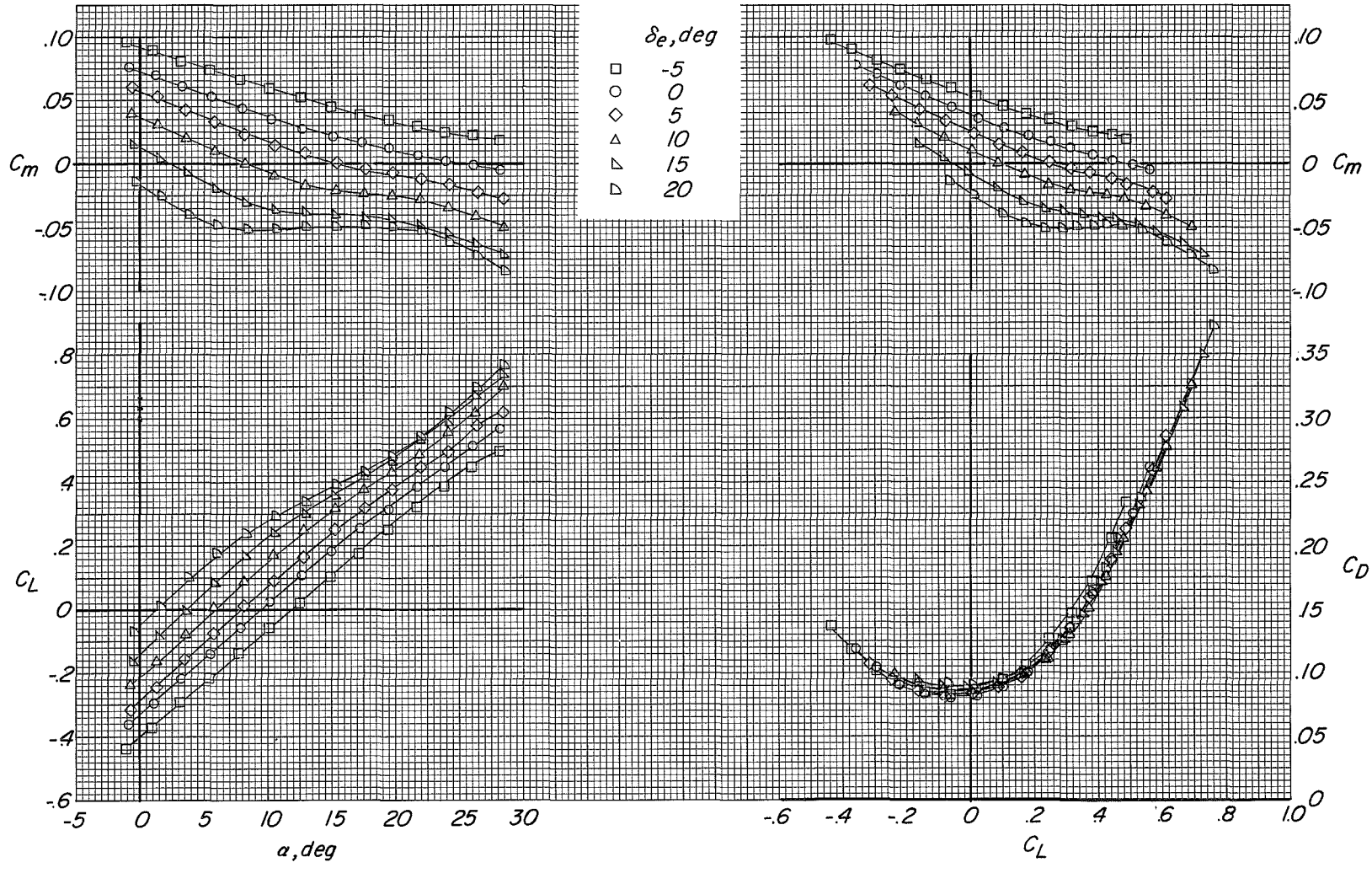
(a) M = 0.40.

Figure 16.- Longitudinal characteristics of HL-10 with basic fin configuration. Auxiliary flaps in transonic position; $\delta_a = \beta = 0^o$.



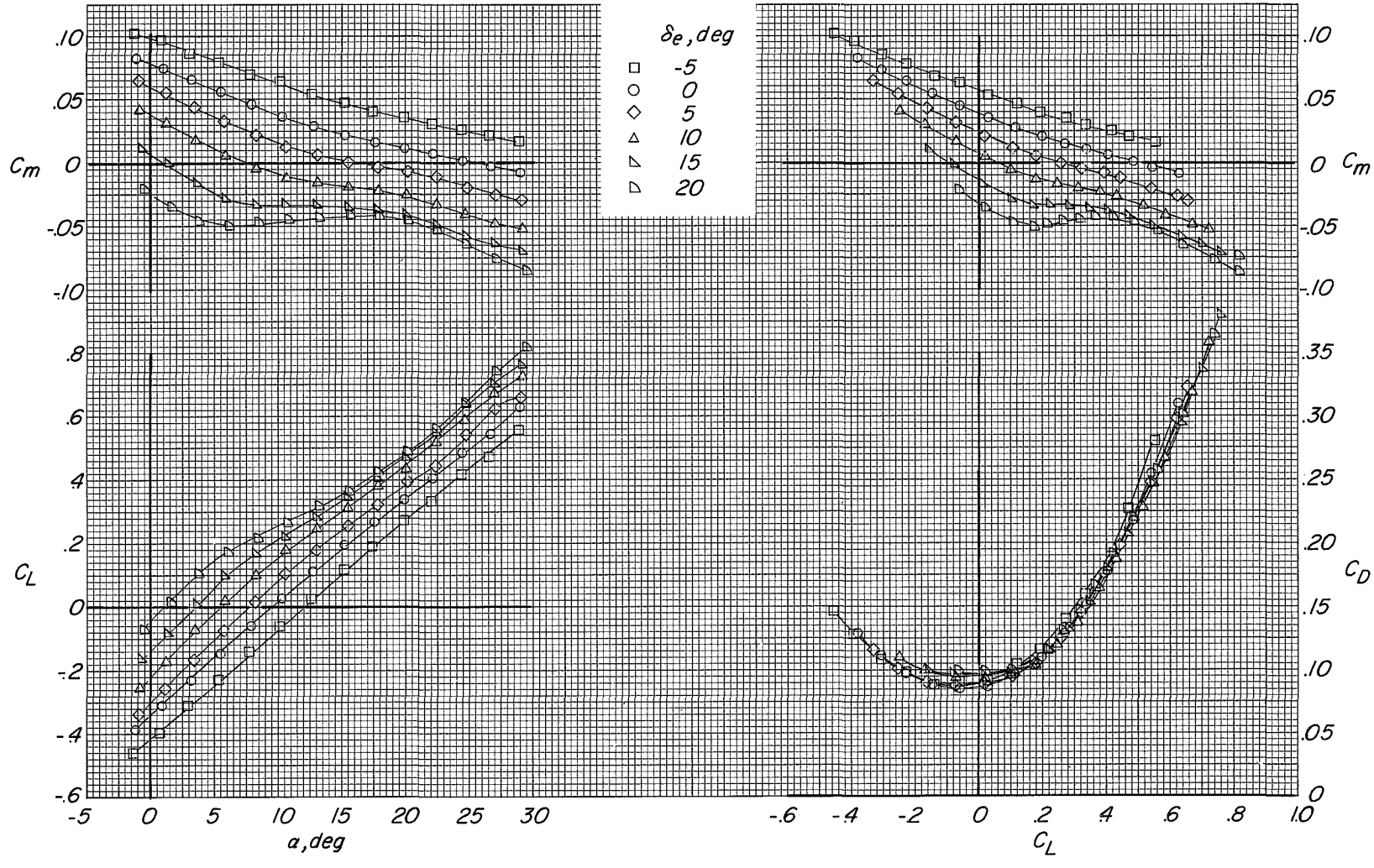
(b) M = 0.60.

Figure 16.- Continued.



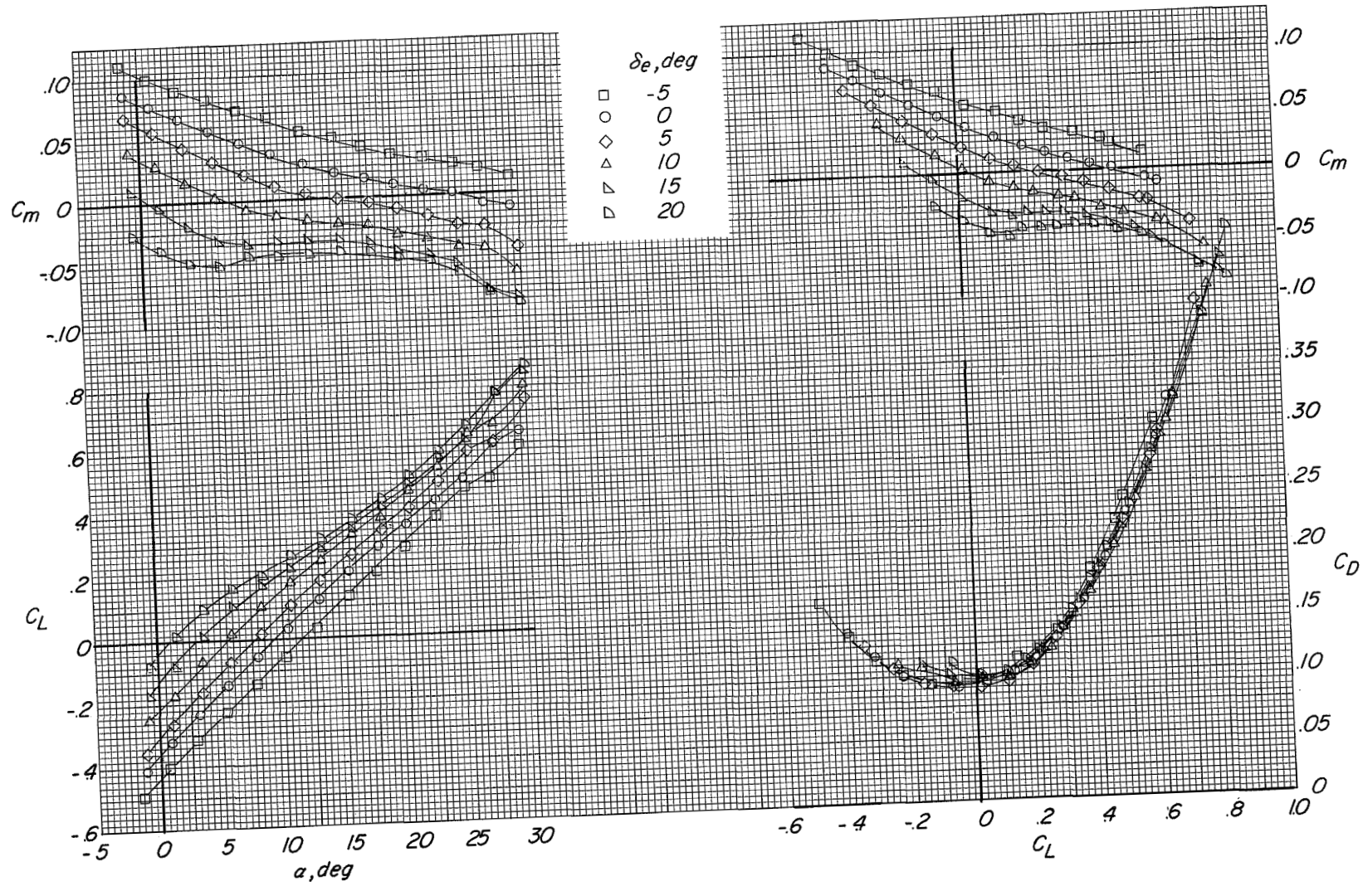
(c) M = 0.70.

Figure 16.- Continued.



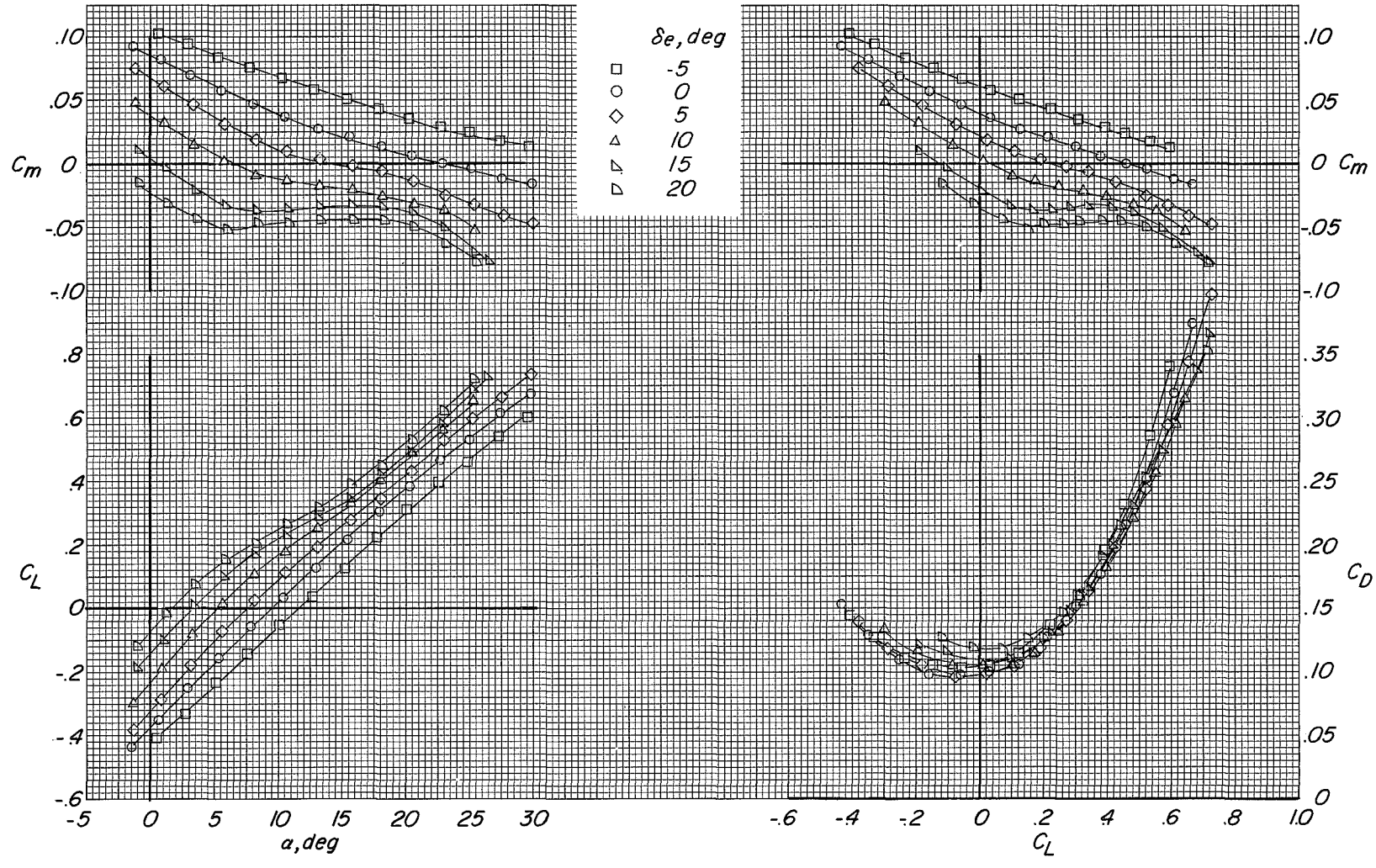
(d) M = 0.80.

Figure 16.- Continued.



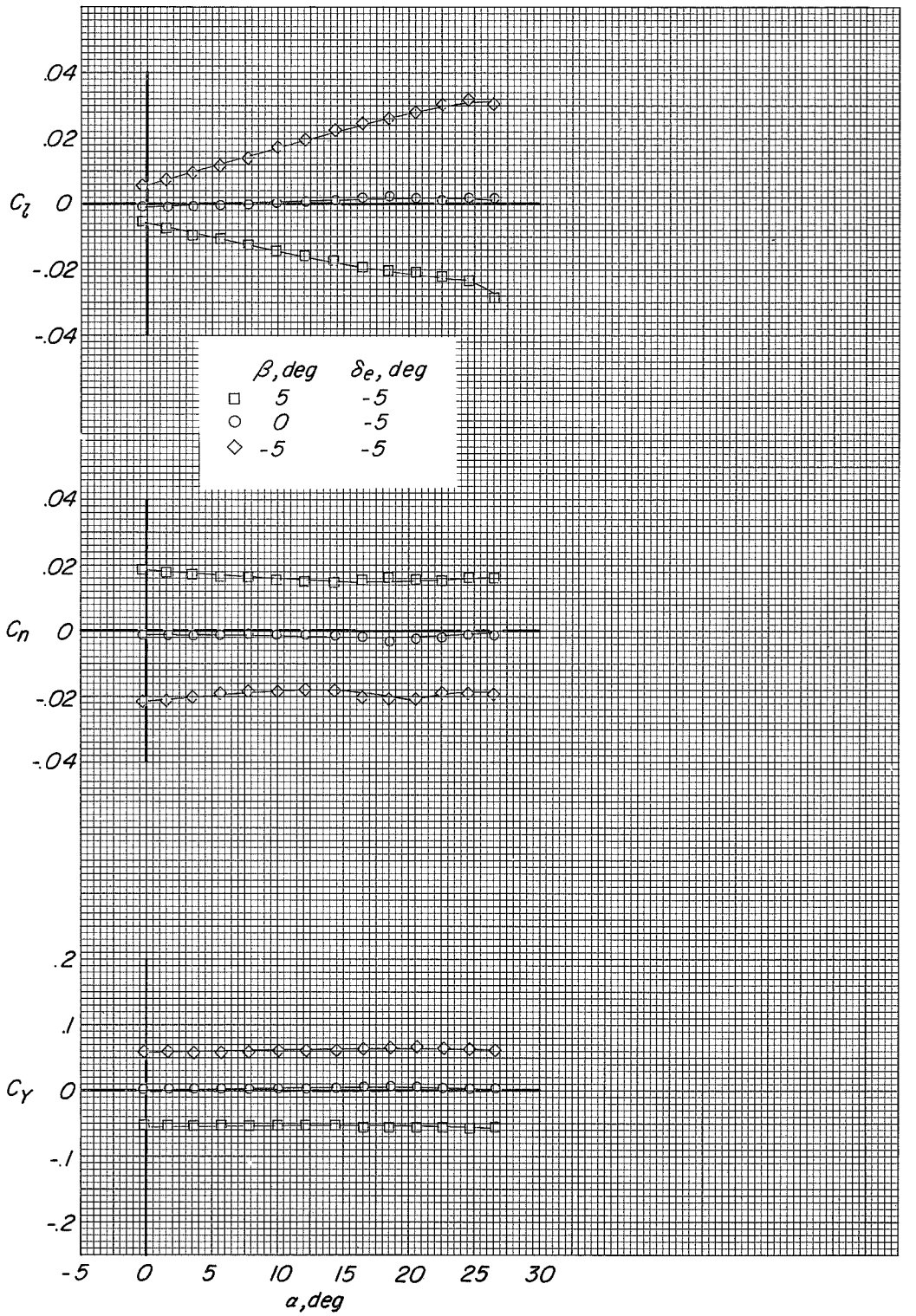
(e) M = 0.85.

Figure 16.- Continued.



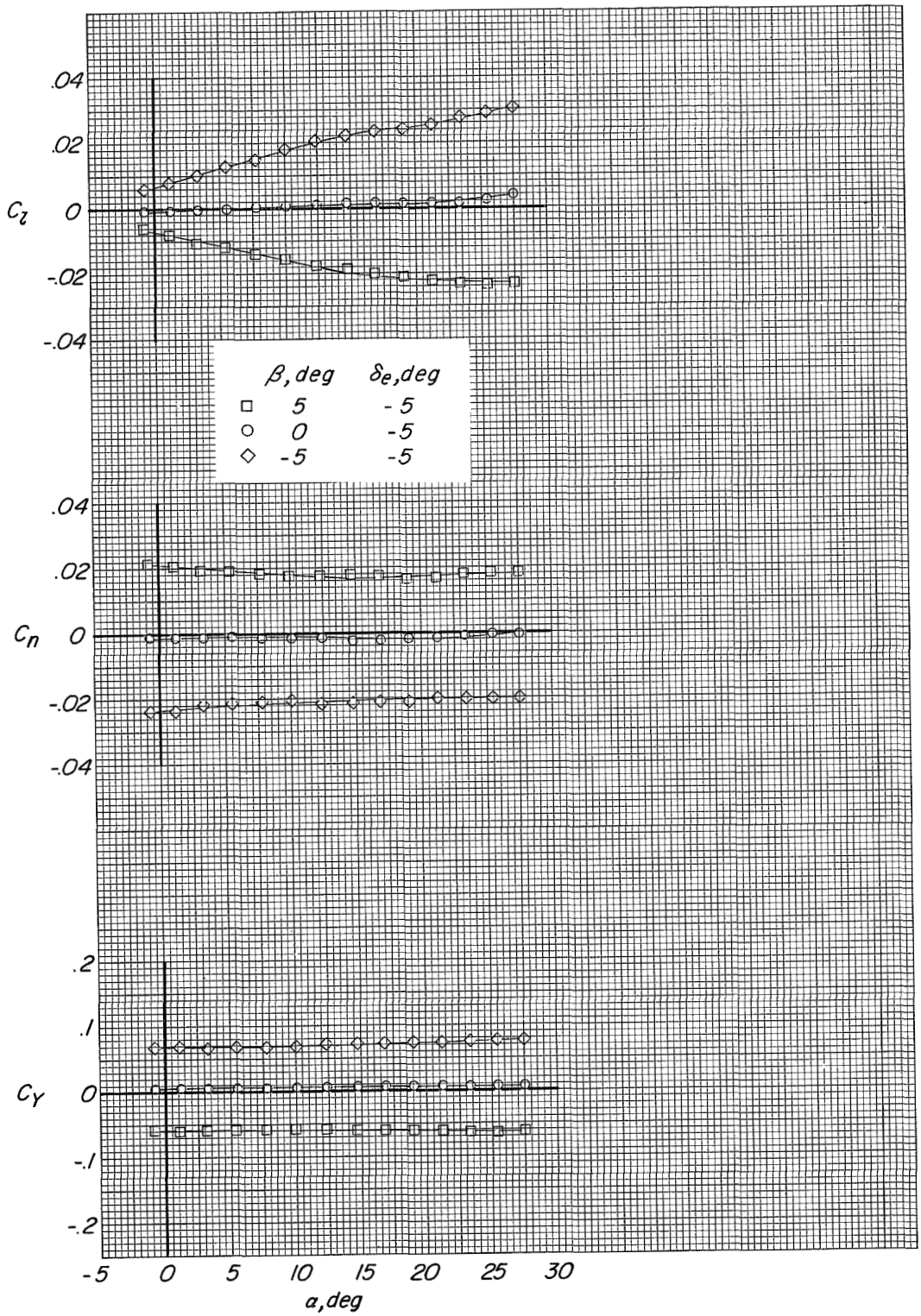
(f) M = 0.90.

Figure 16.- Concluded.



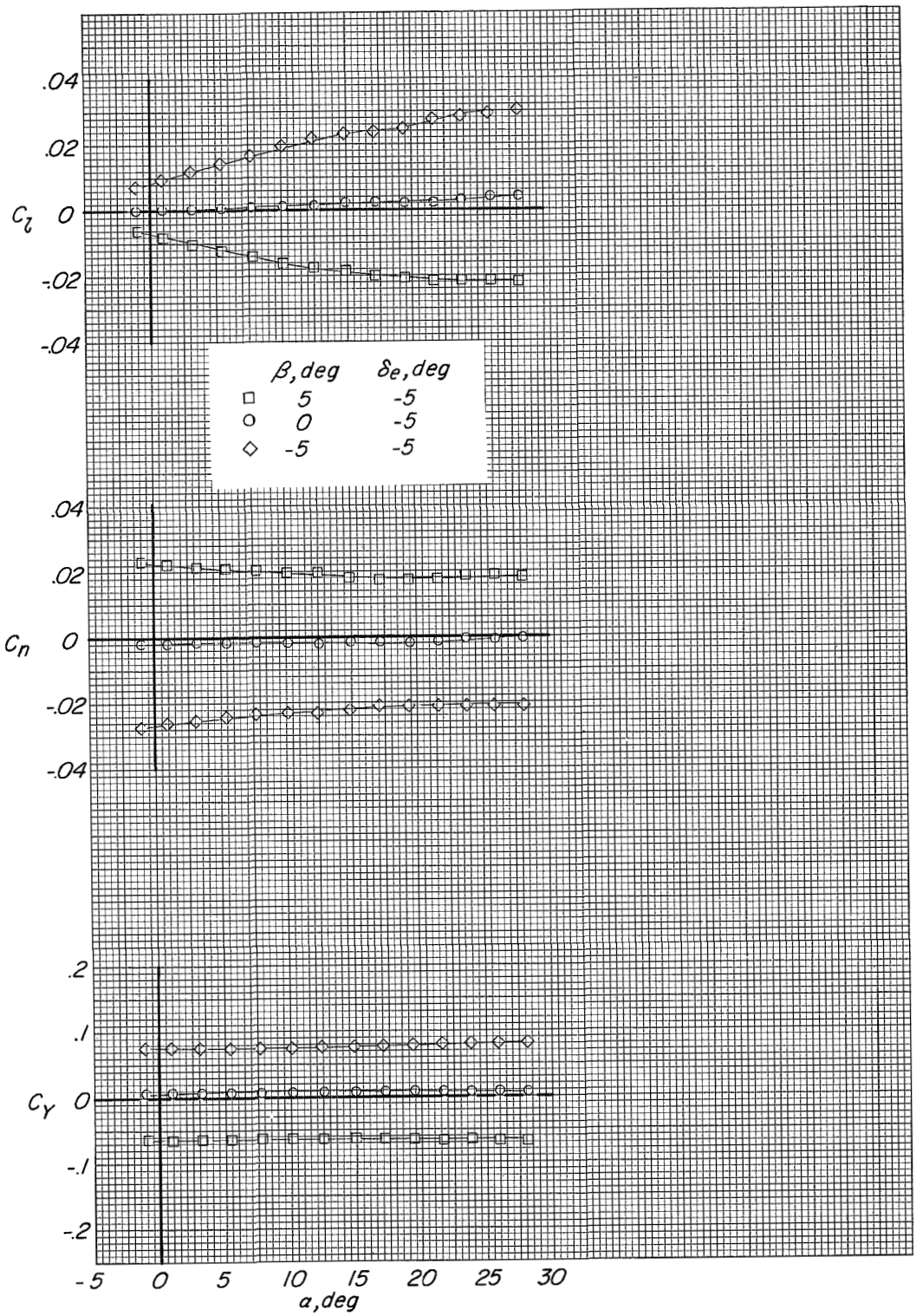
(a) $\delta_e = -5^o$; M = 0.40.

Figure 17.- Effect of sideslip on the lateral directional characteristics. Basic fin configuration; auxiliary flaps in the transonic position; $\delta_a = 0^o$.



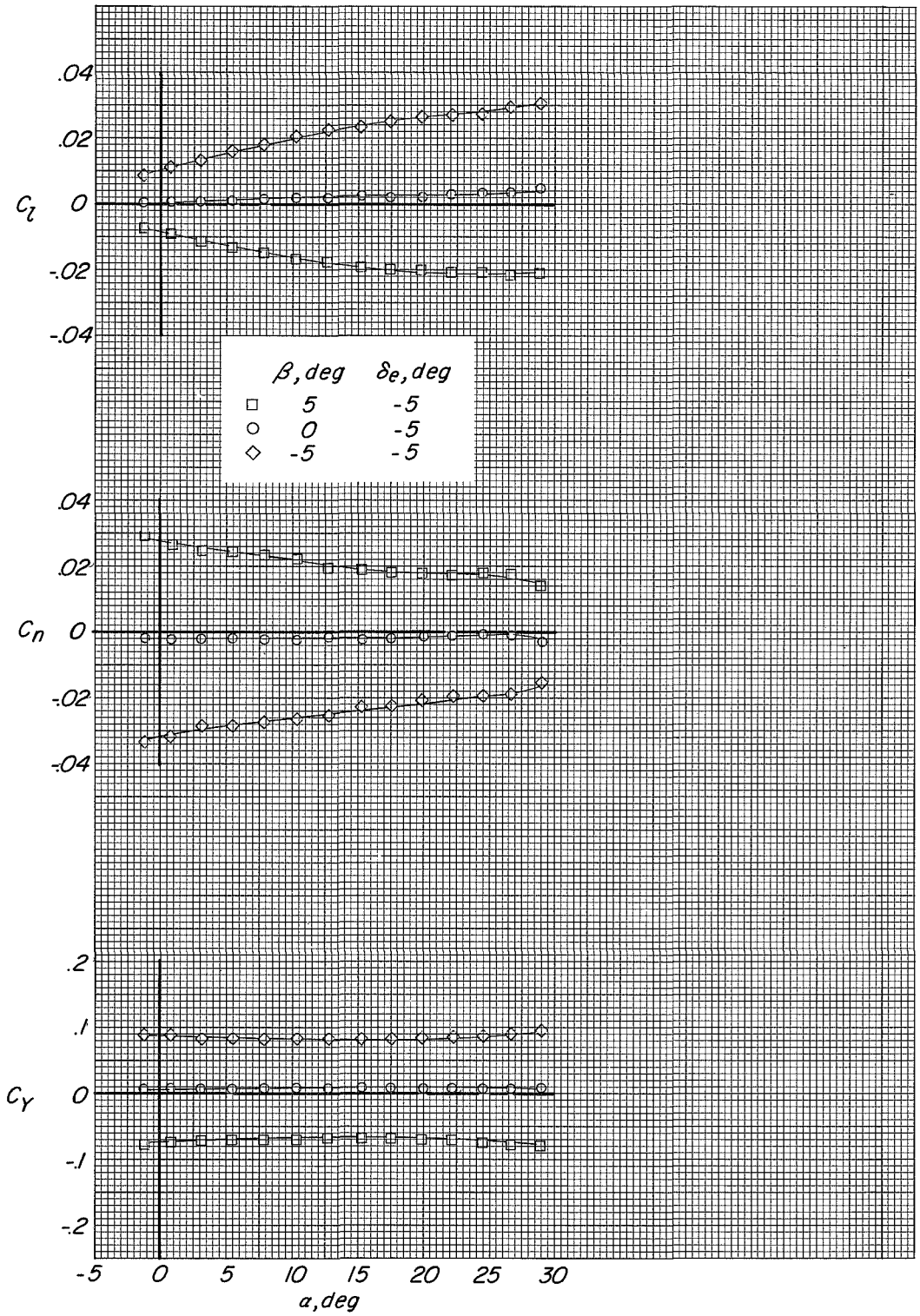
(b) $\delta_e = -5^o$; M = 0.60.

Figure 17.- Continued.



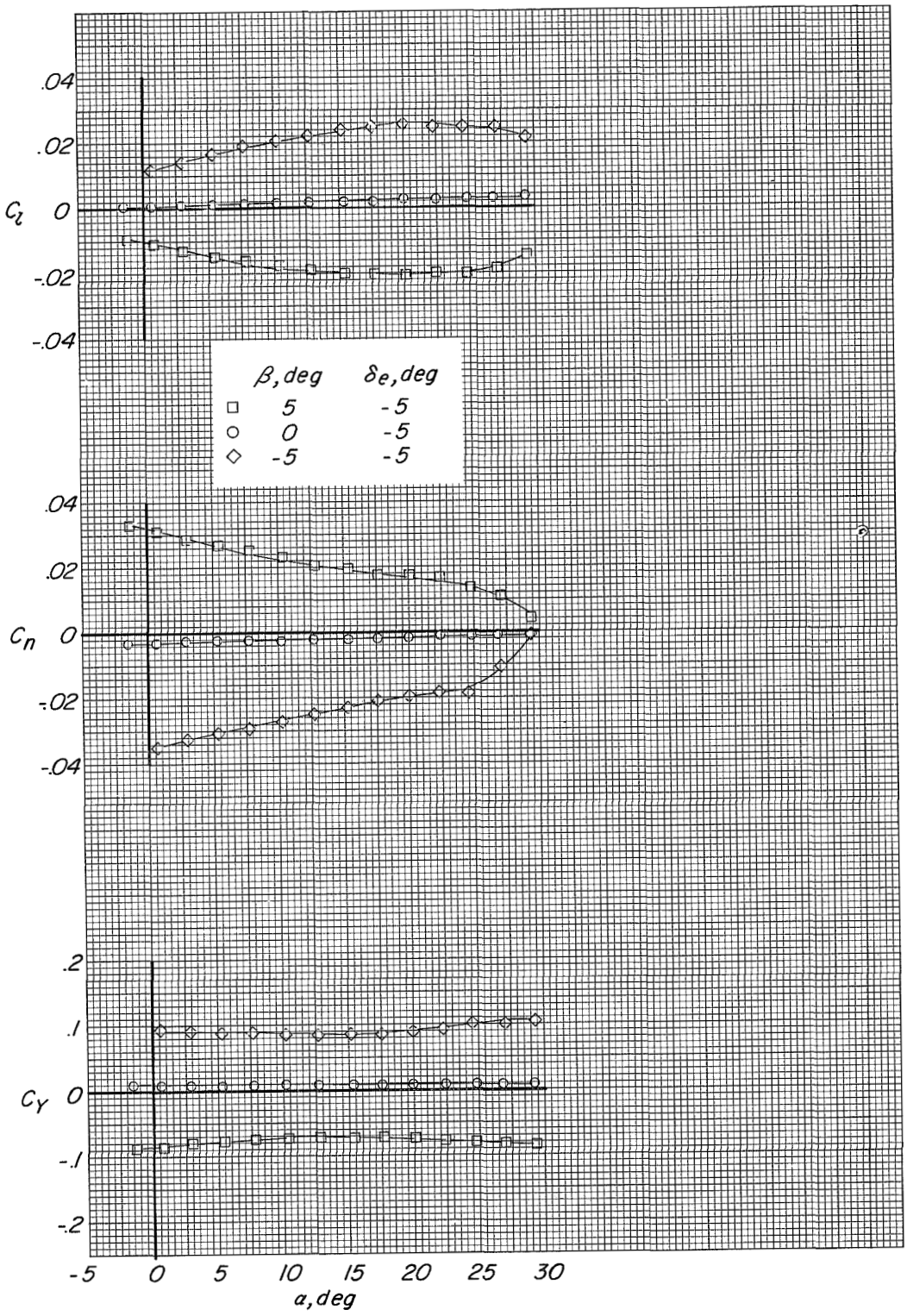
(c) $\delta_e = -5^o$; M = 0.70.

Figure 17.- Continued.



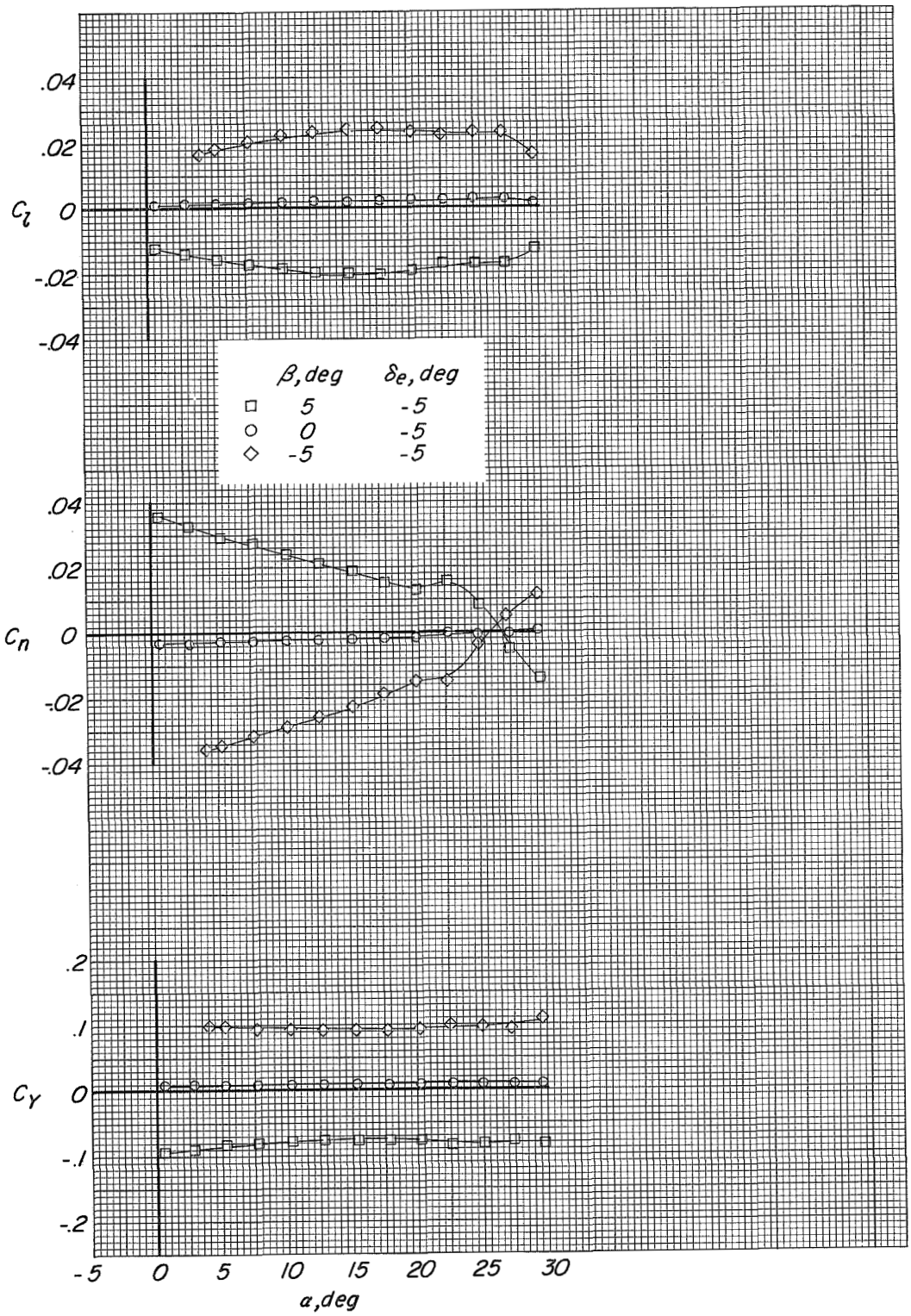
(d) $\delta_e = -5^o$; M = 0.80.

Figure 17.- Continued.



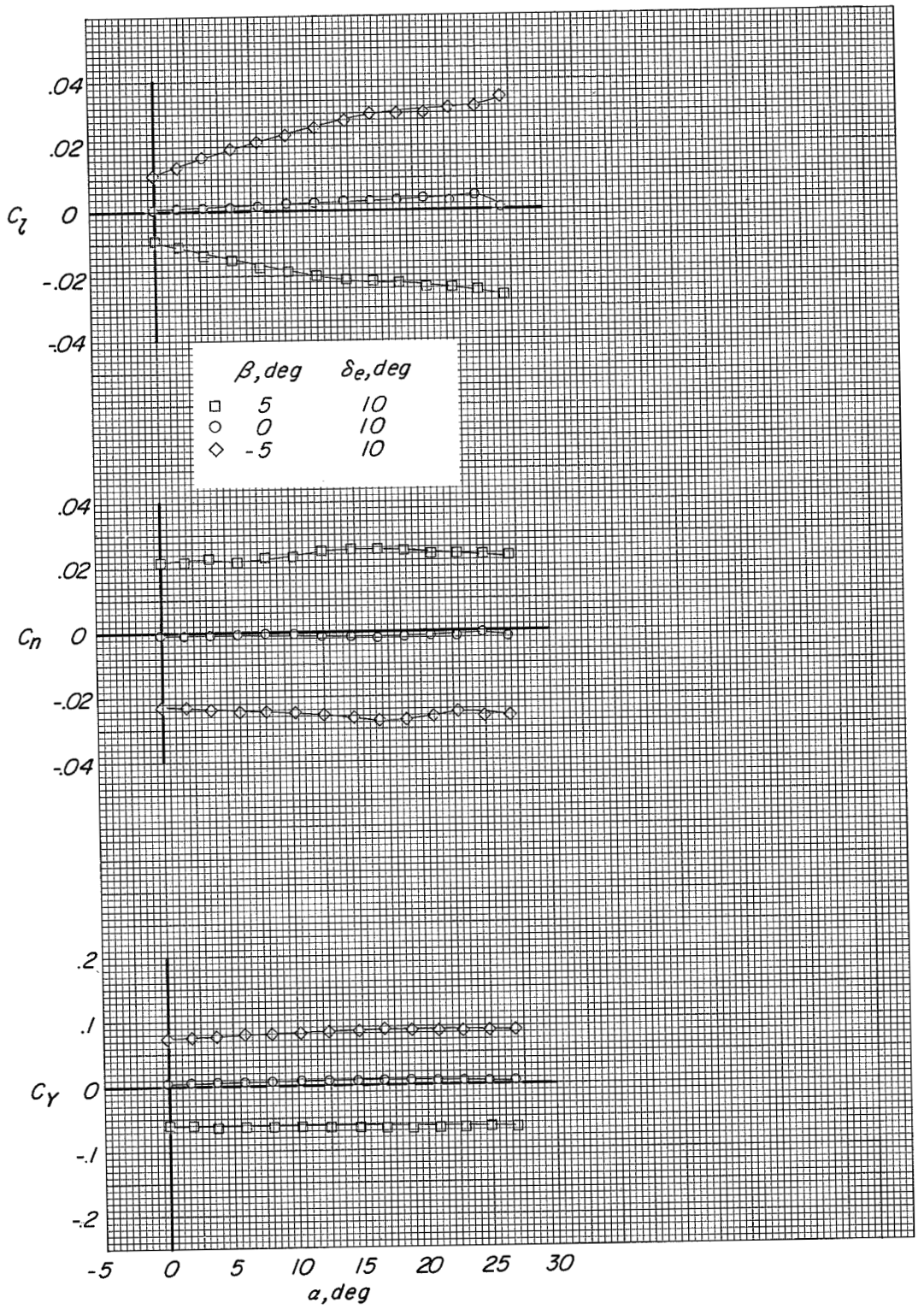
(e) $\delta_e = -5^o$; M = 0.85.

Figure 17.- Continued.



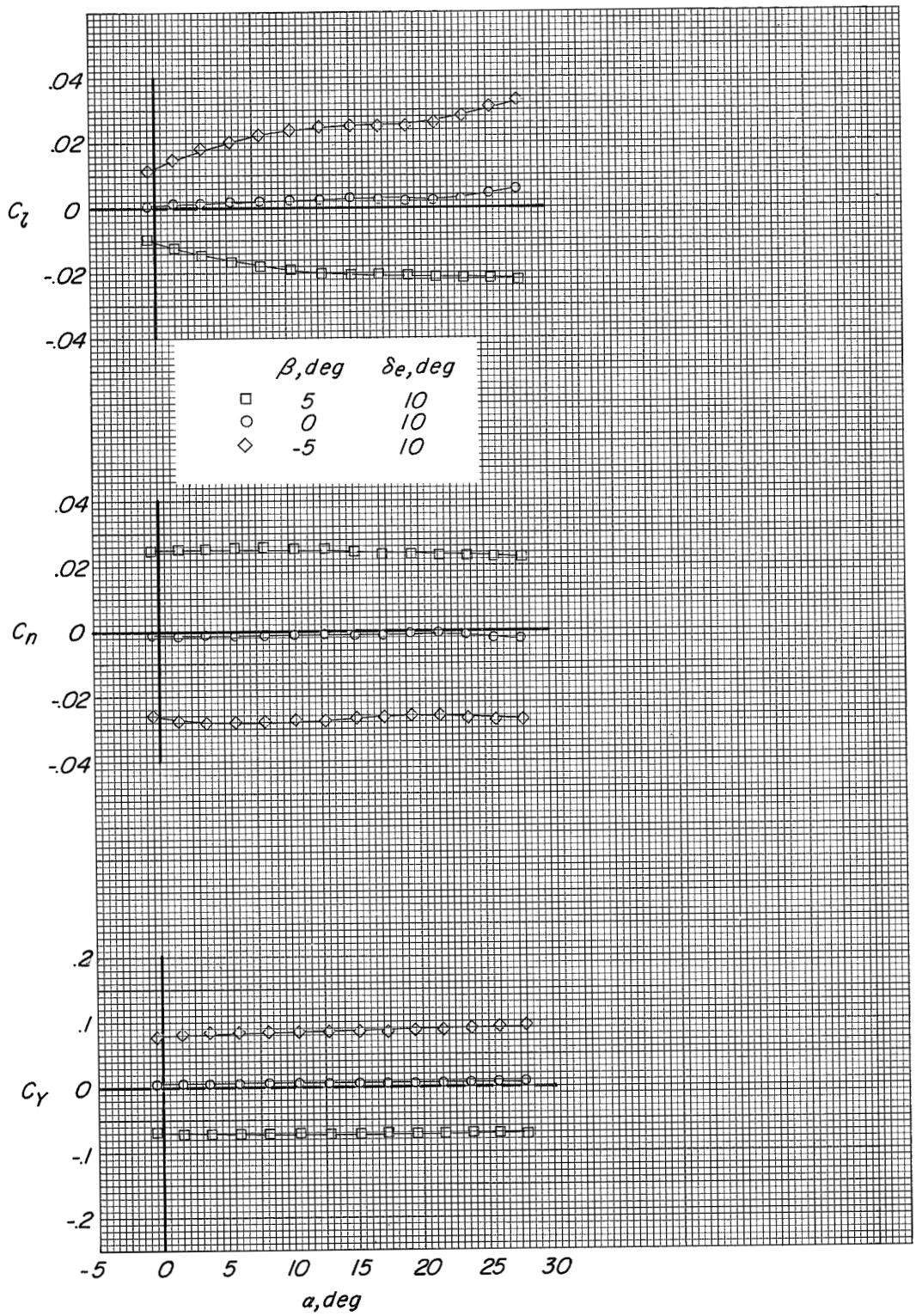
(f) $\delta_e = -5^o$; M = 0.90.

Figure 17.- Continued.



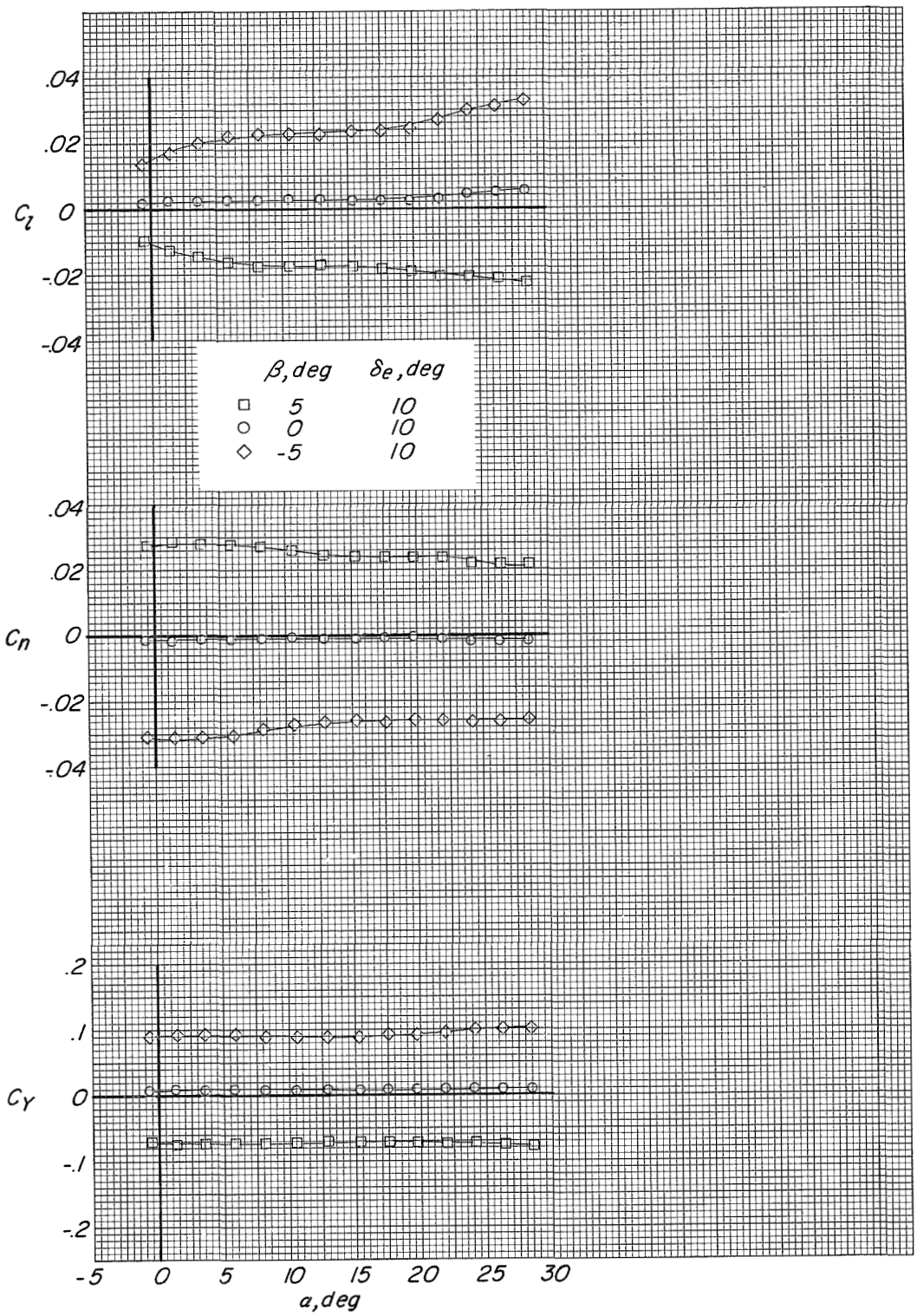
(g) $\delta_e = 10^o$; M = 0.40.

Figure 17.- Continued.



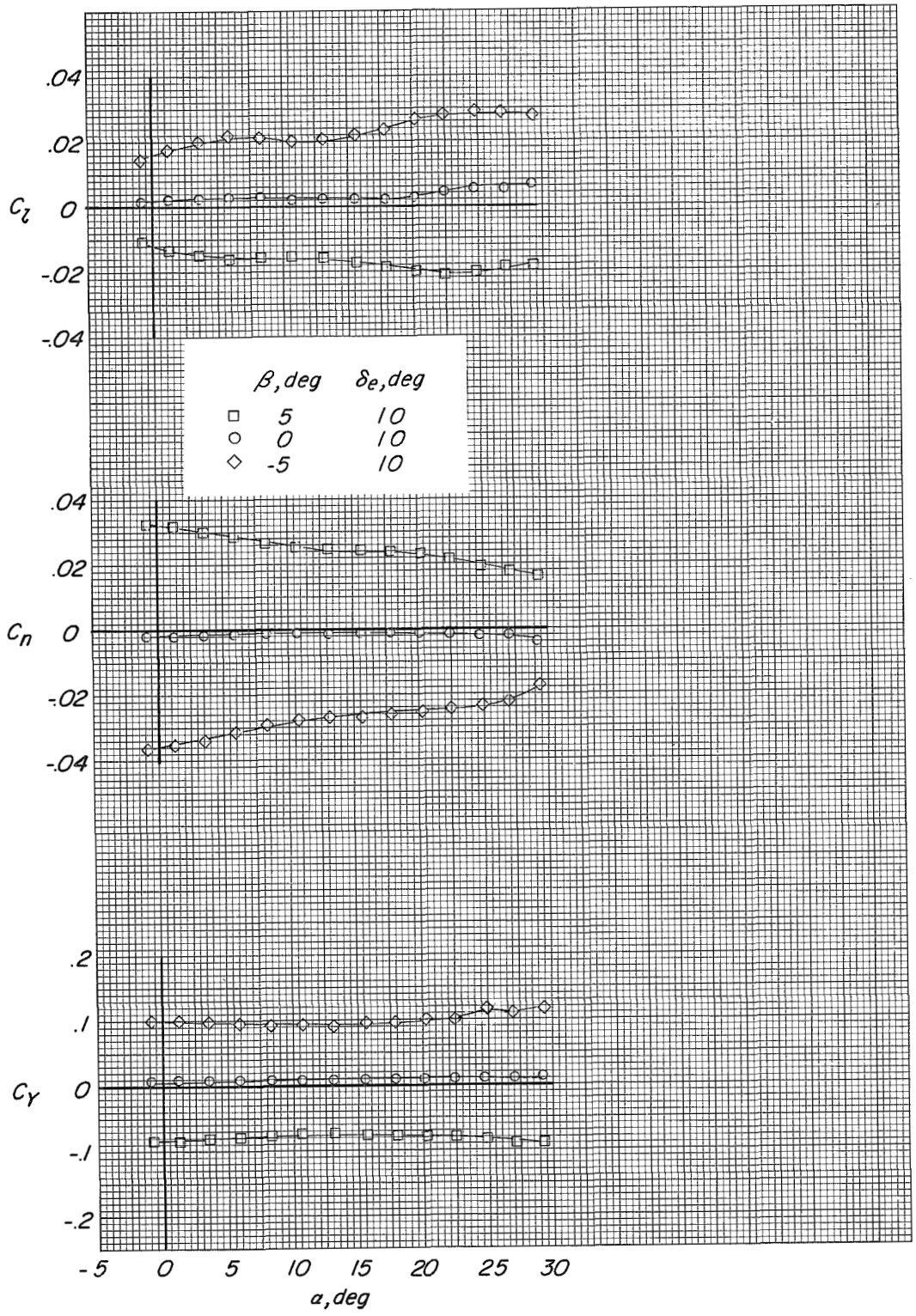
(h) $\delta_e = 10^o$; M = 0.60.

Figure 17.- Continued.



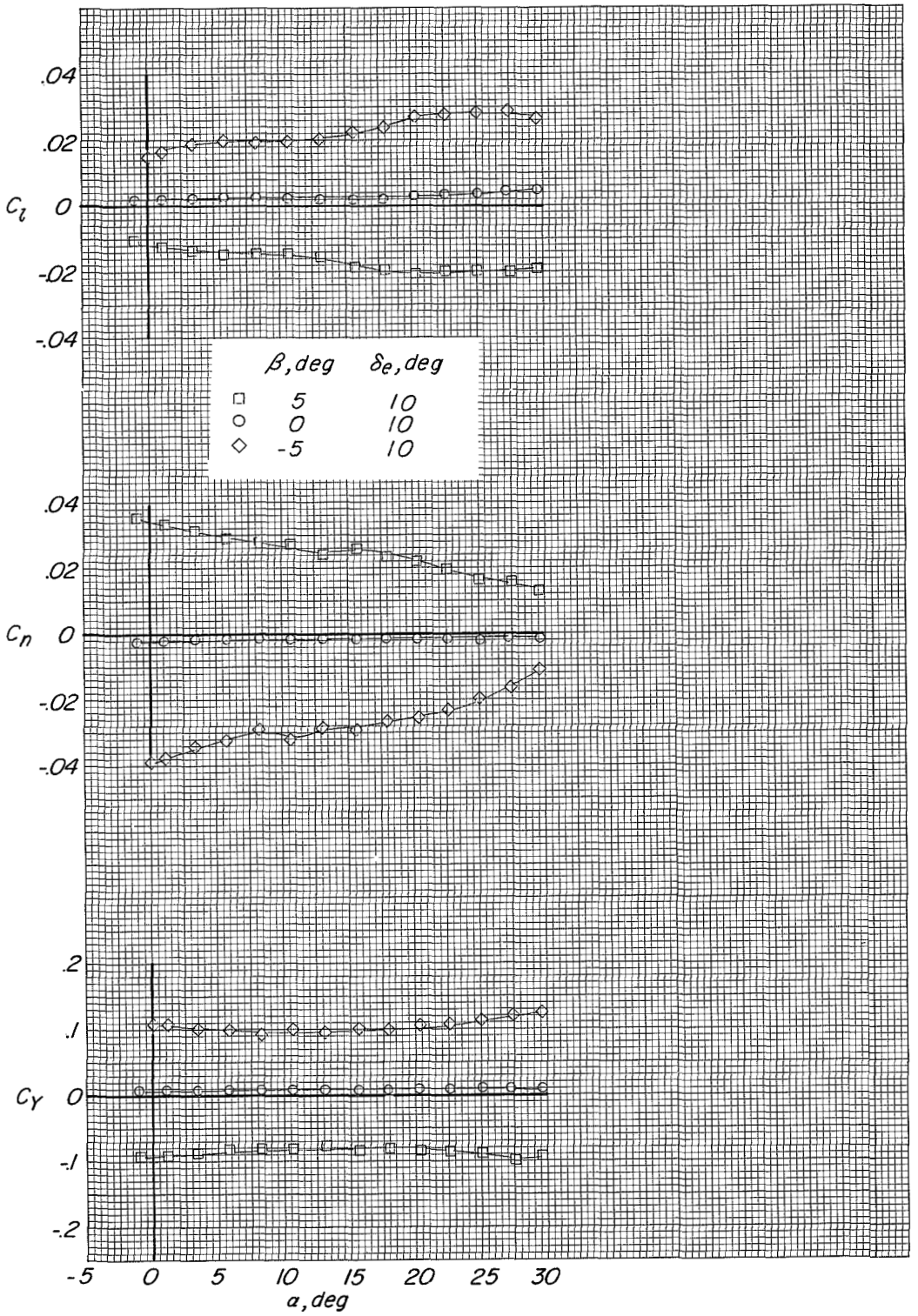
(i) $\delta_e = 10^o$; M = 0.70.

Figure 17.- Continued.



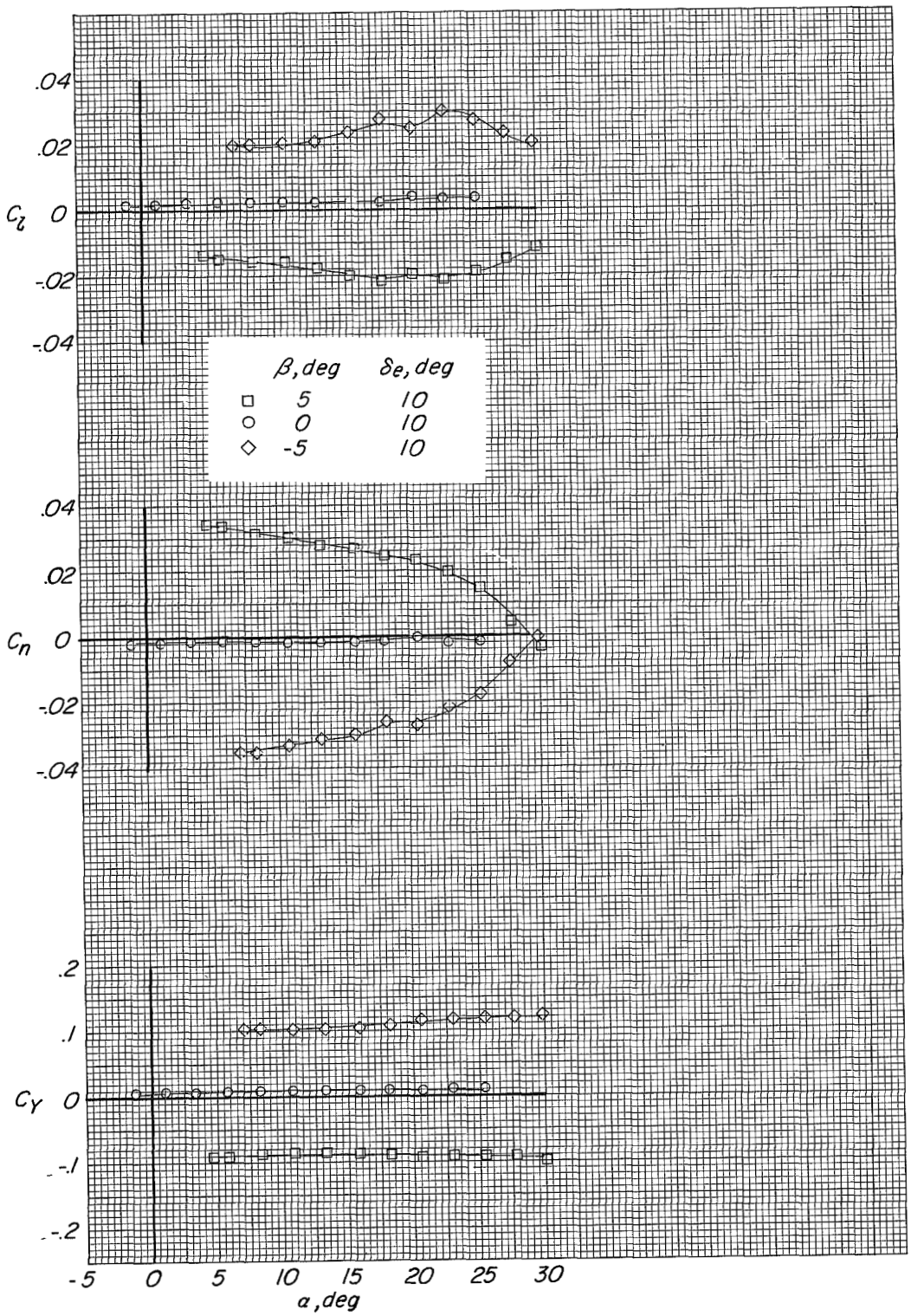
(j) $\delta_e = 10^o$; M = 0.80.

Figure 17.- Continued.



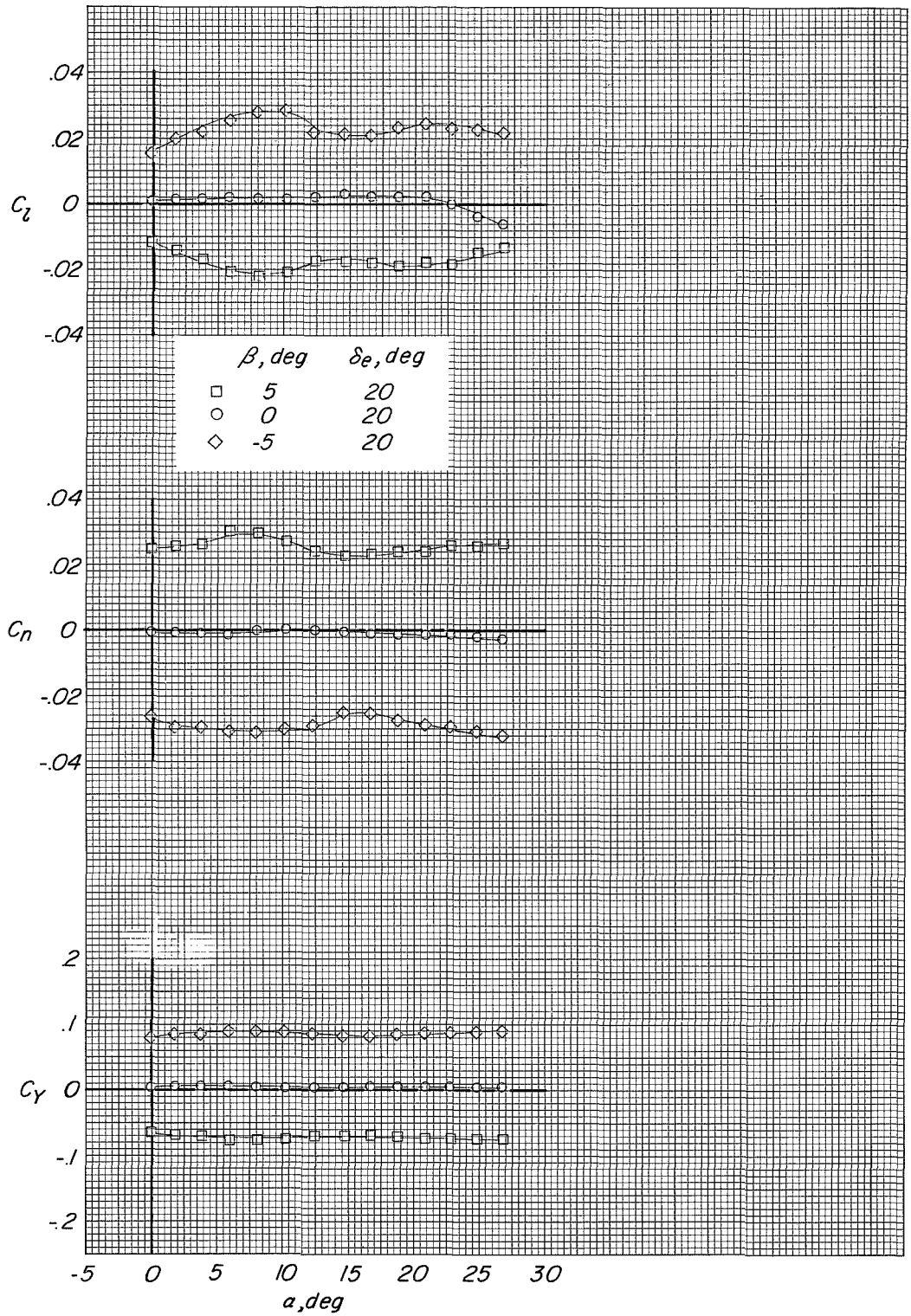
(k) $\delta_e = 10^o$; M = 0.85.

Figure 17.- Continued.



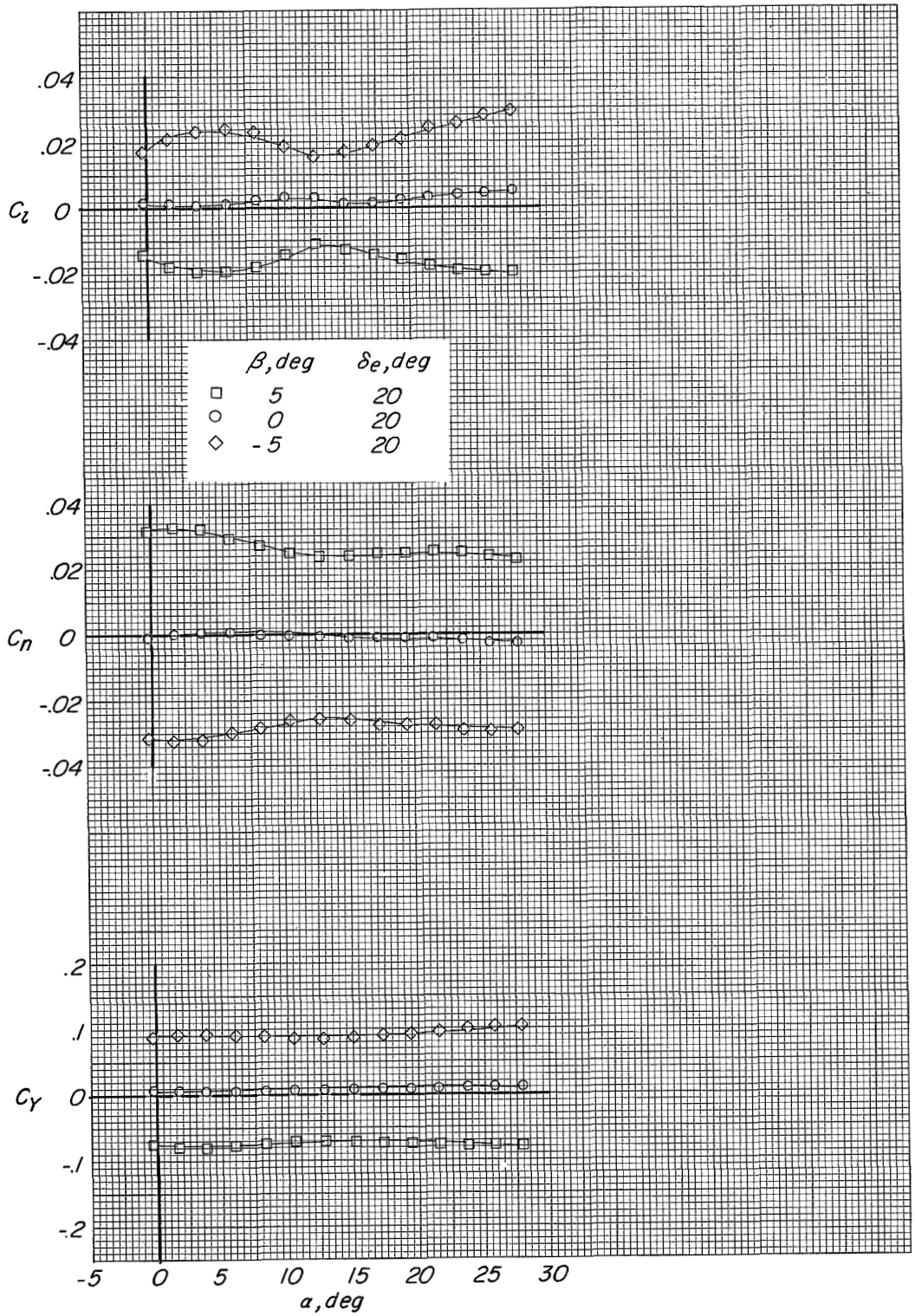
(l) $\delta_e = 10^o$; M = 0.90.

Figure 17.- Continued.



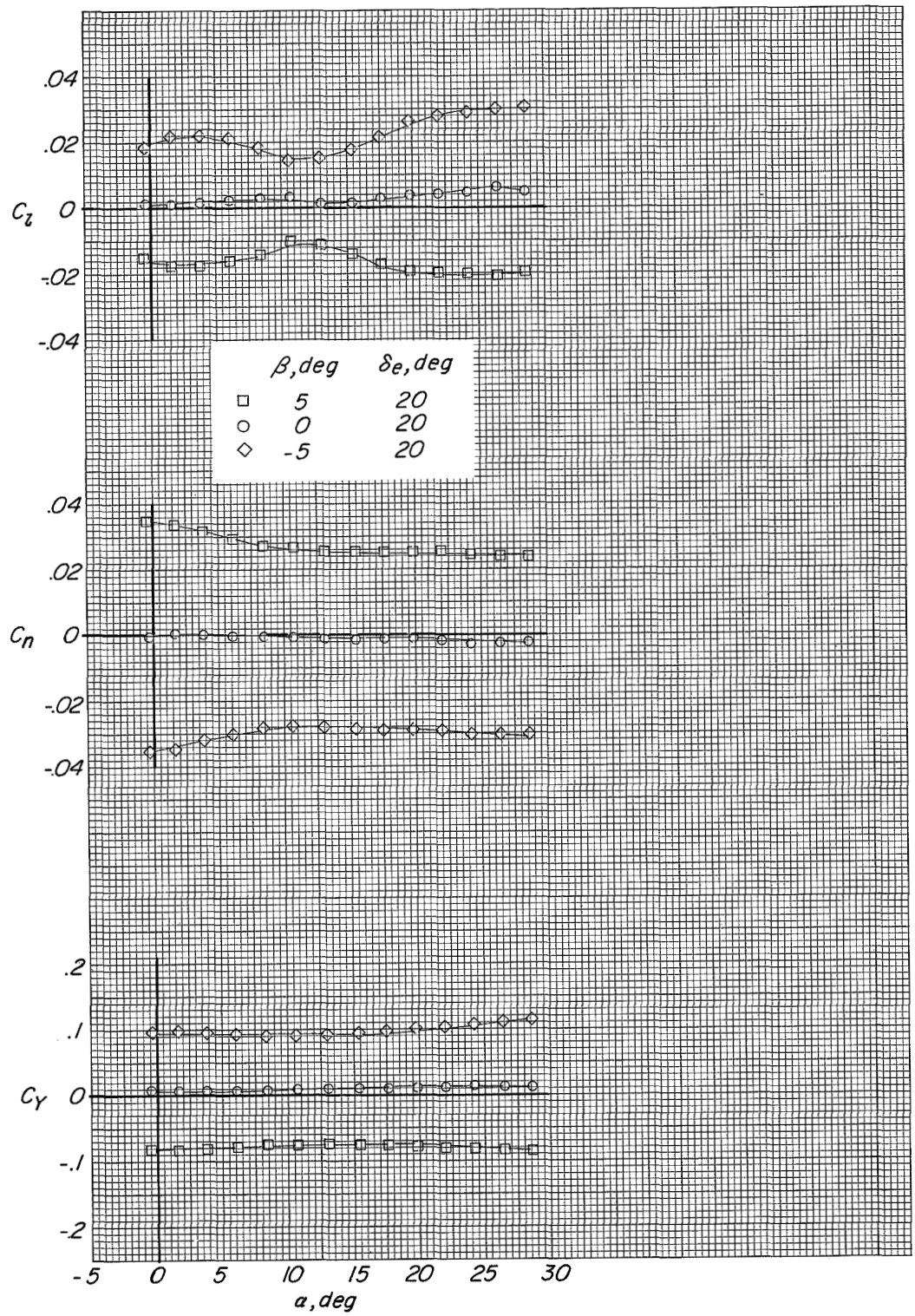
(m) $\delta_e = 20^o$; M = 0.40.

Figure 17.- Continued.



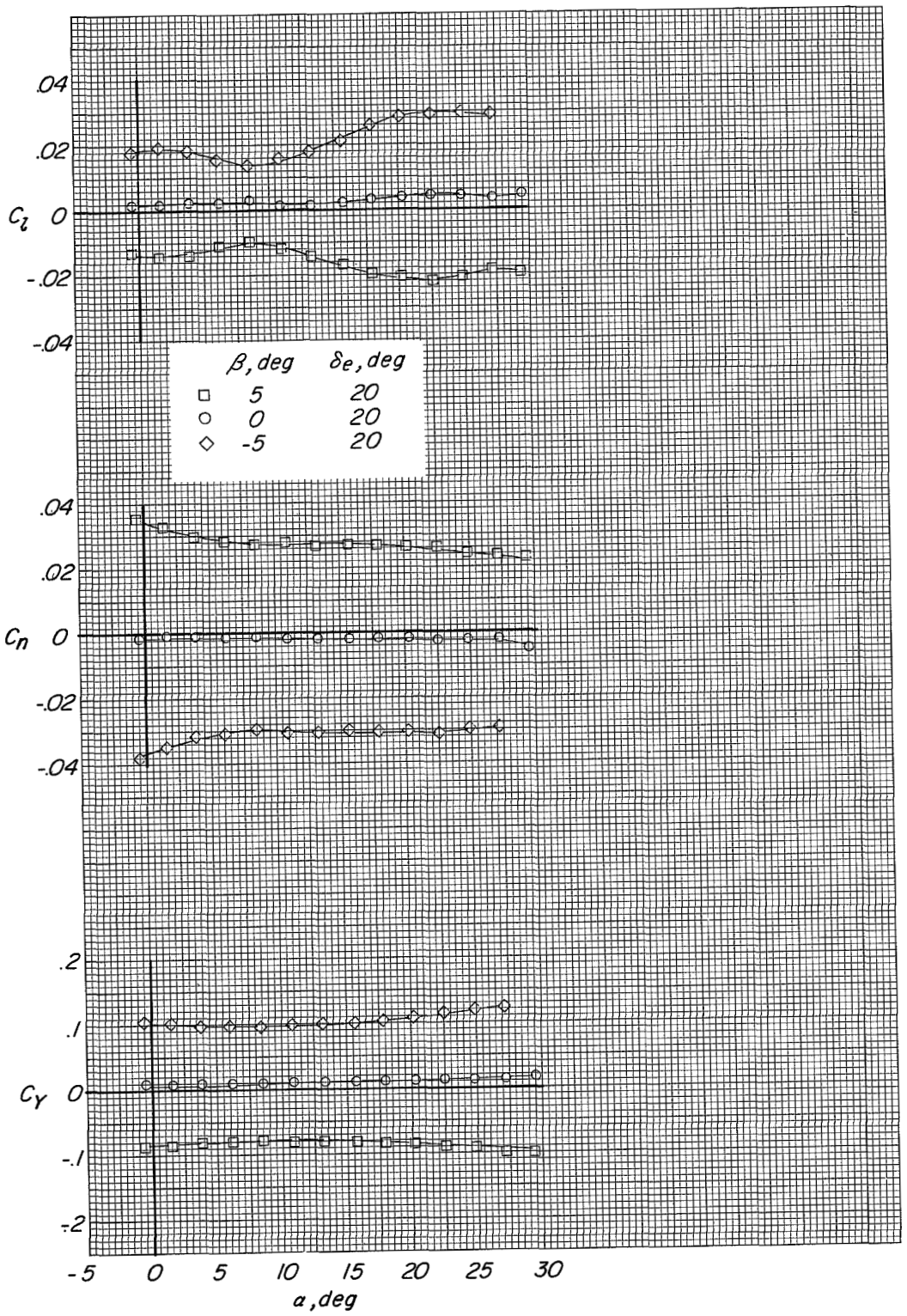
(n) $\delta_e = 20^o$; M = 0.60.

Figure 17.- Continued.



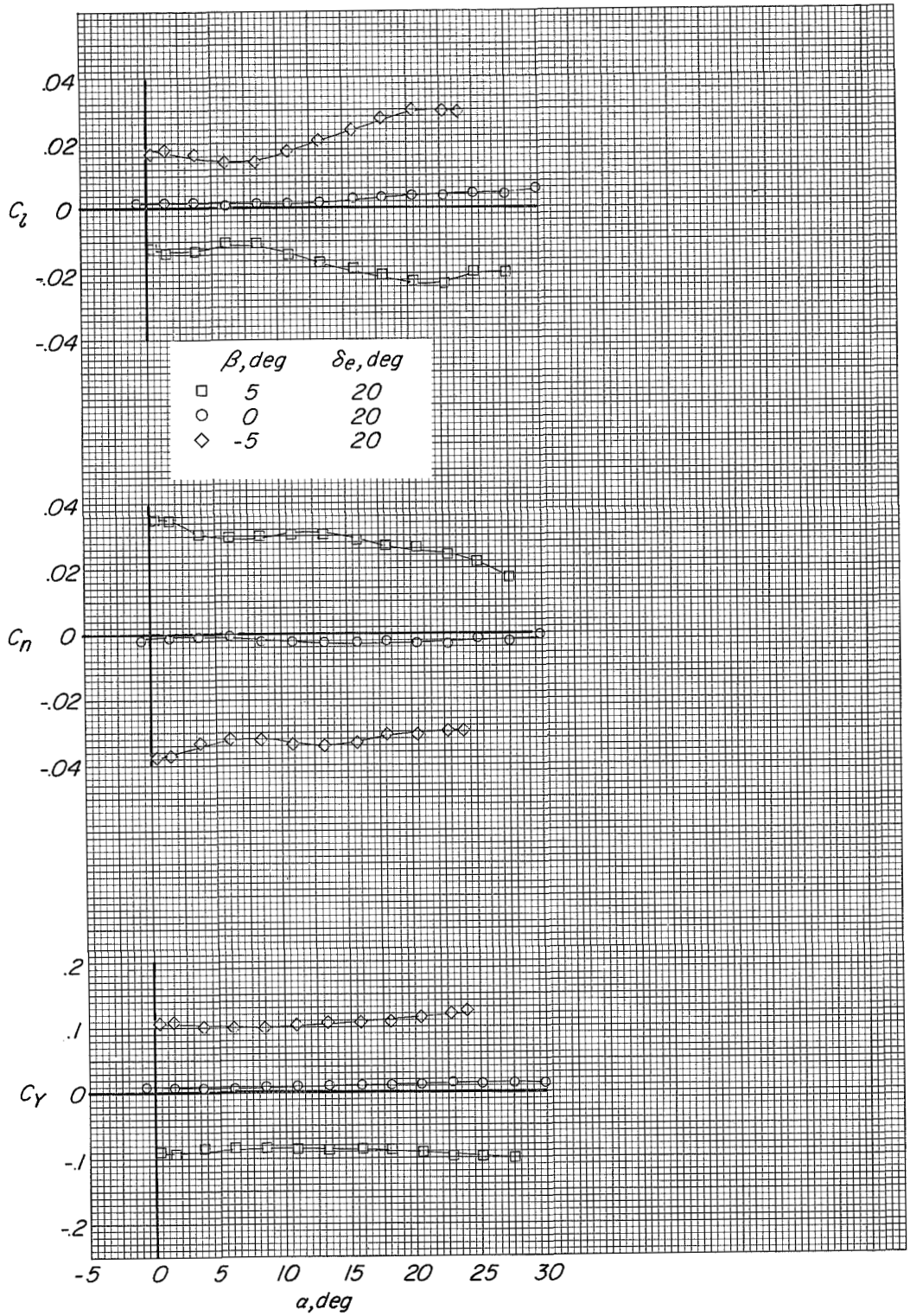
(o) $\delta_e = 20^o$; M = 0.70.

Figure 17.- Continued.



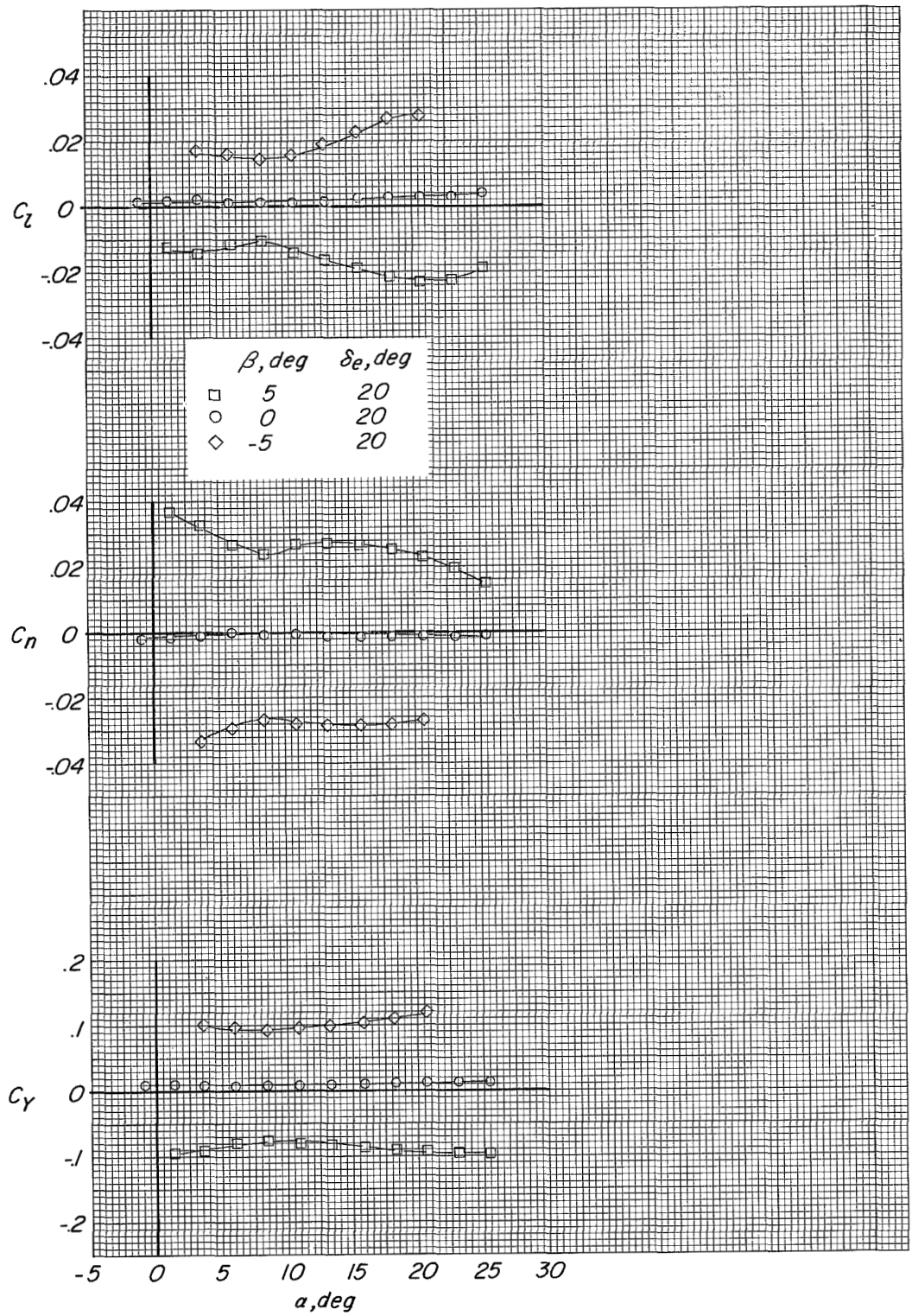
(p) $\delta_e = 20^o$; M = 0.80.

Figure 17.- Continued.



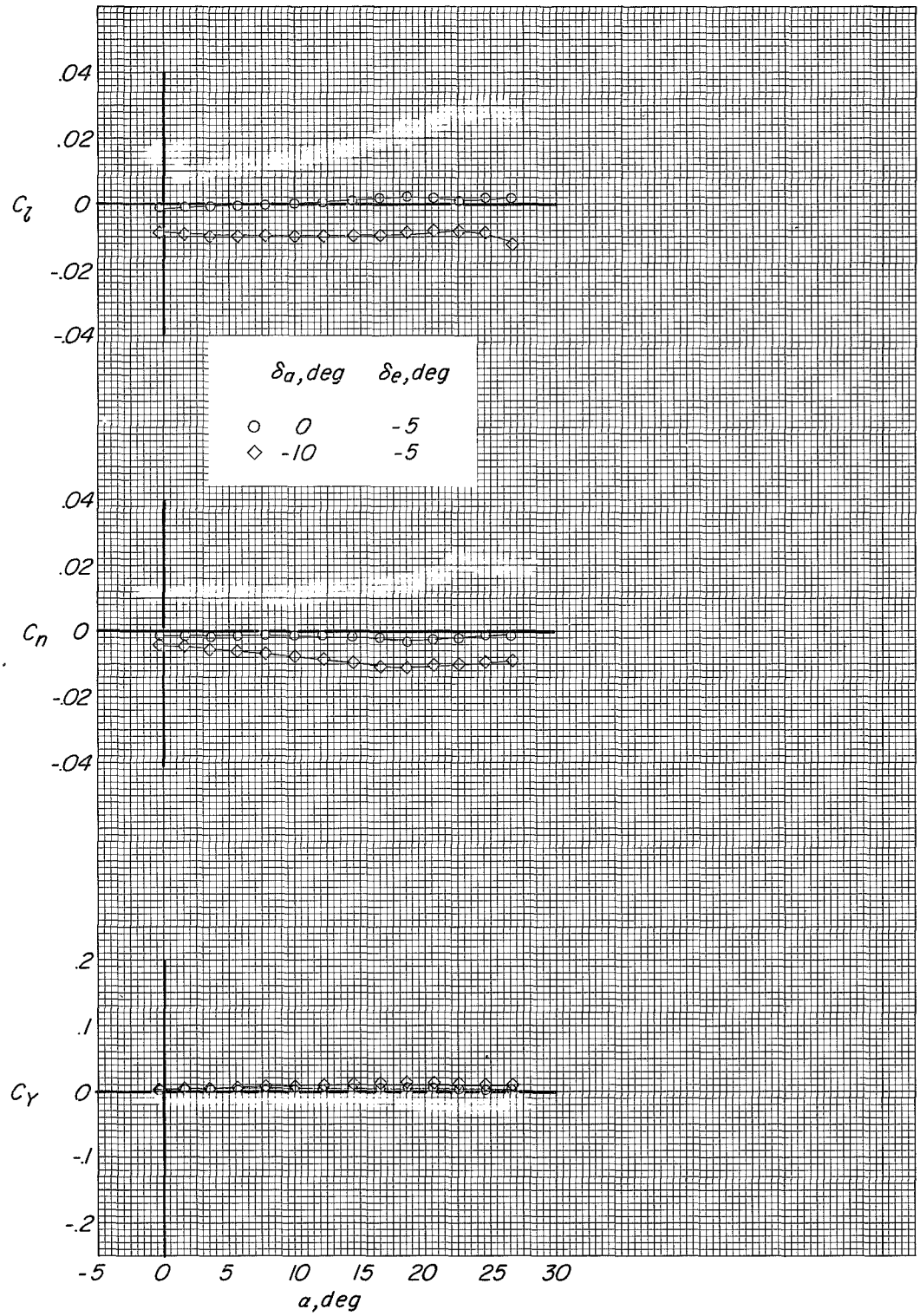
(q) $\delta_e = 20^o$; M = 0.85.

Figure 17.- Continued.



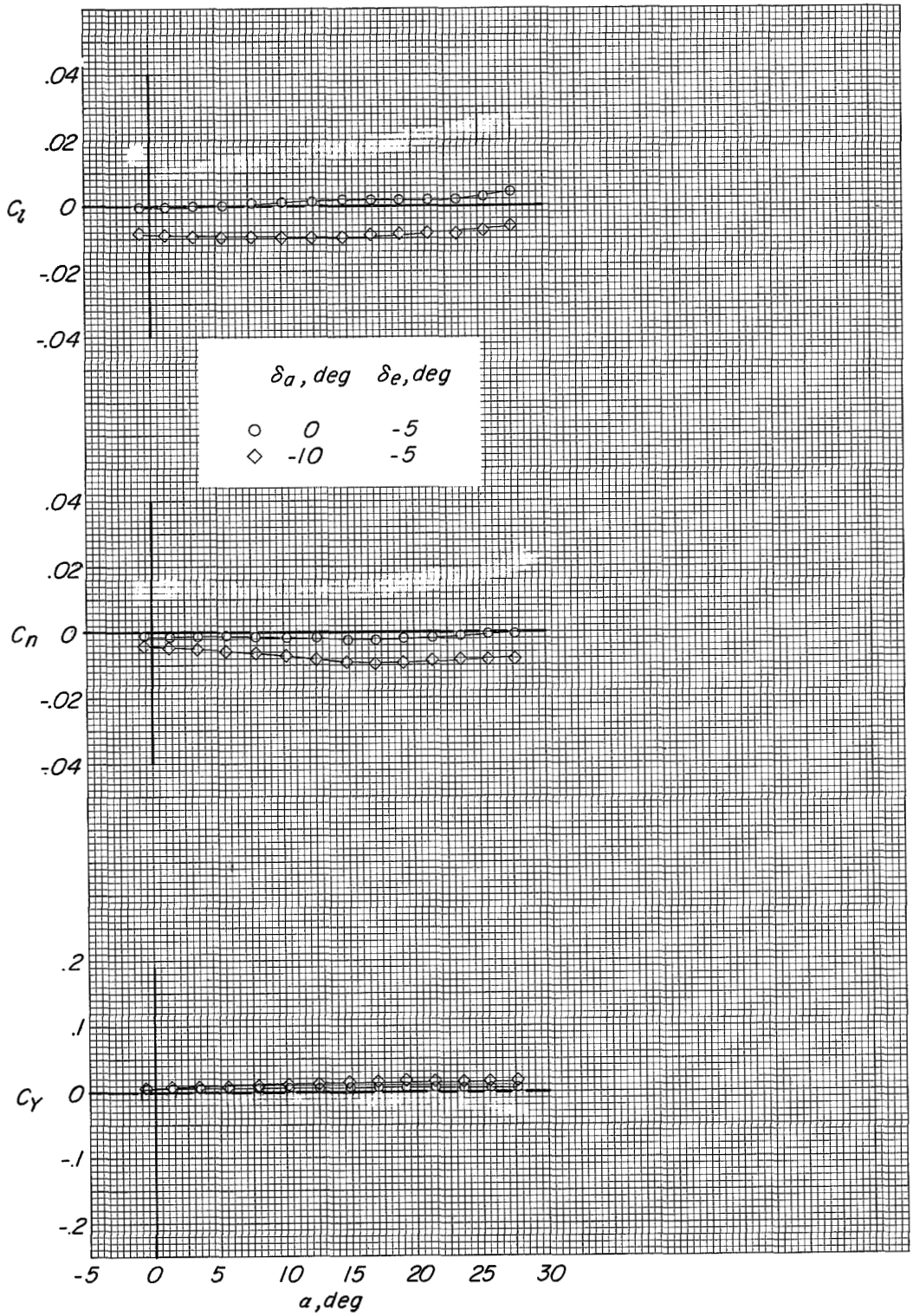
(r) $\delta_e = 20^o$; M = 0.90.

Figure 17.- Concluded.



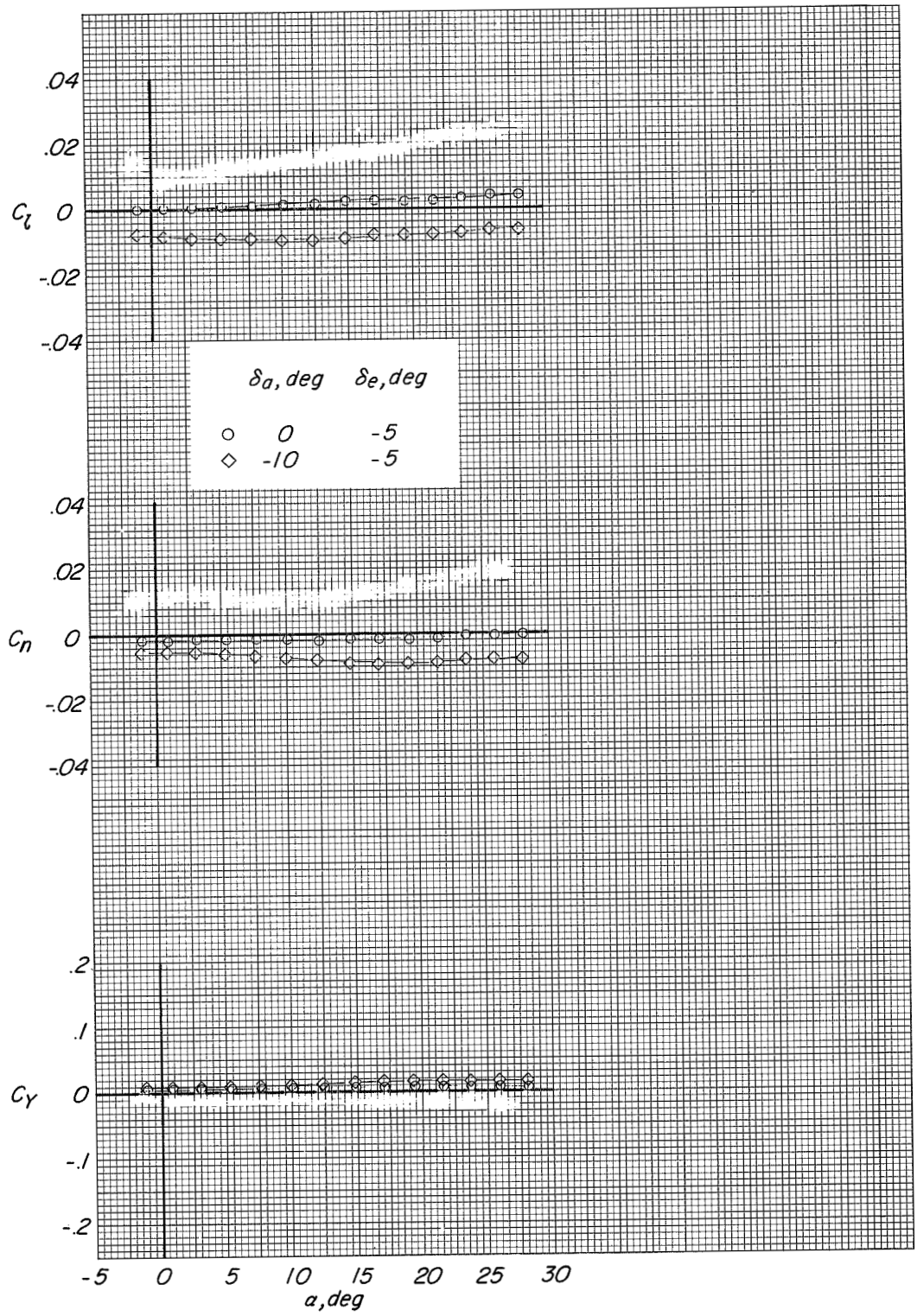
(a) $\delta_e = -5^o$; M = 0.40.

Figure 18.- Effect of aileron deflection on the lateral force and moment characteristics. Basic fin configuration; auxiliary flaps in the transonic position; $\beta = 0^o$.



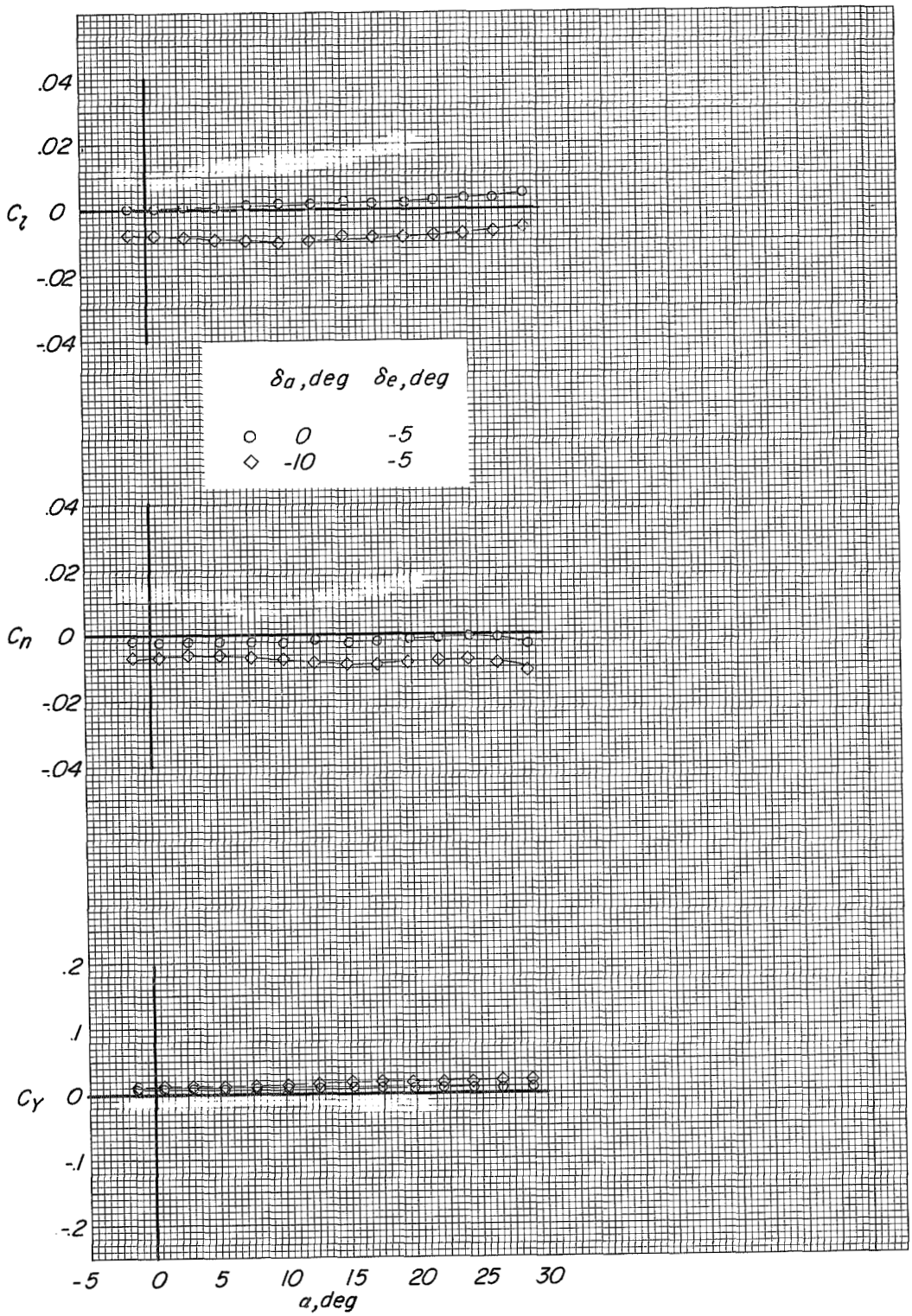
(b) $\delta_e = -5^o$; M = 0.60.

Figure 18.- Continued.



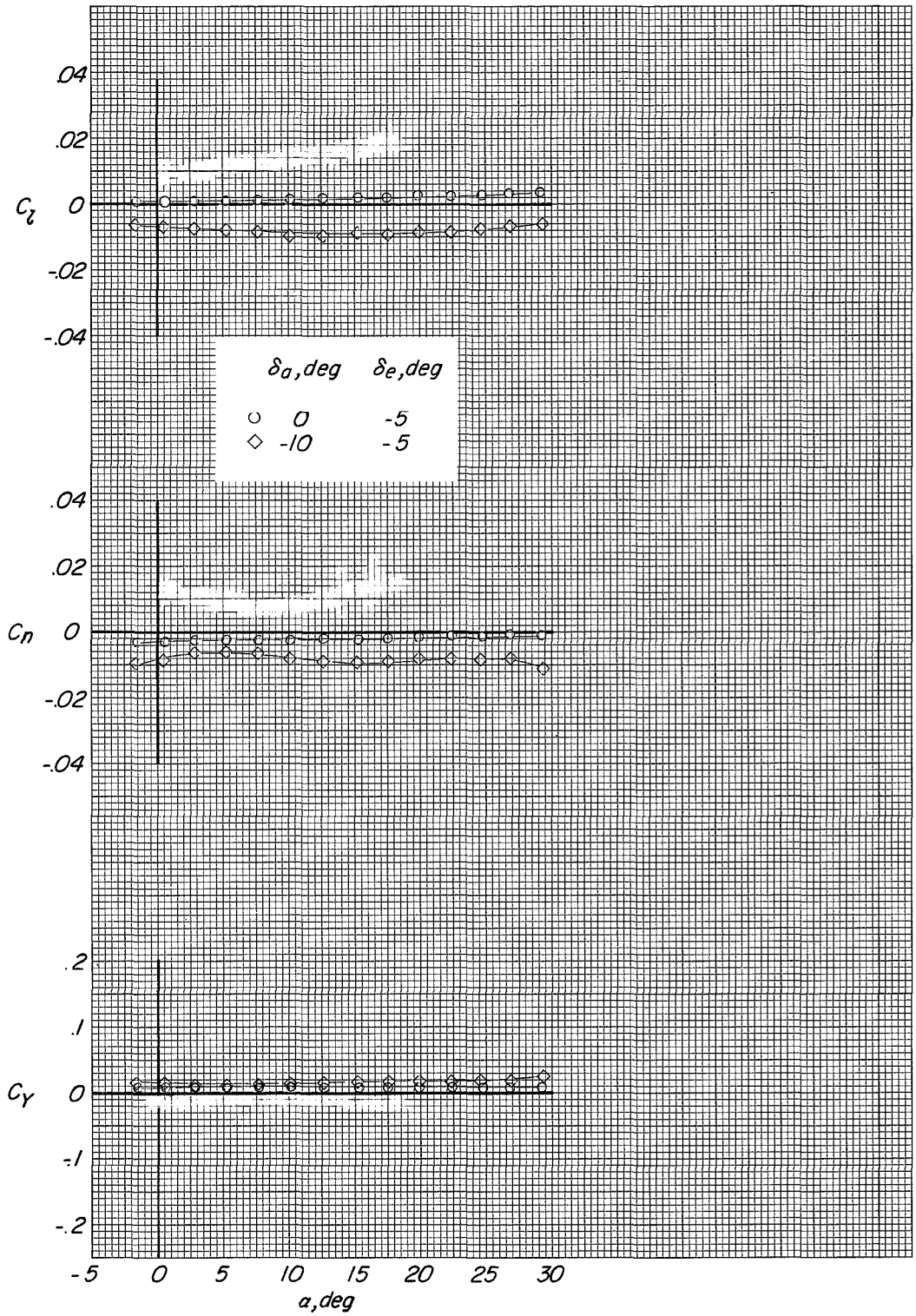
(c) $\delta_e = -5^o$; M = 0.70.

Figure 18.- Continued.



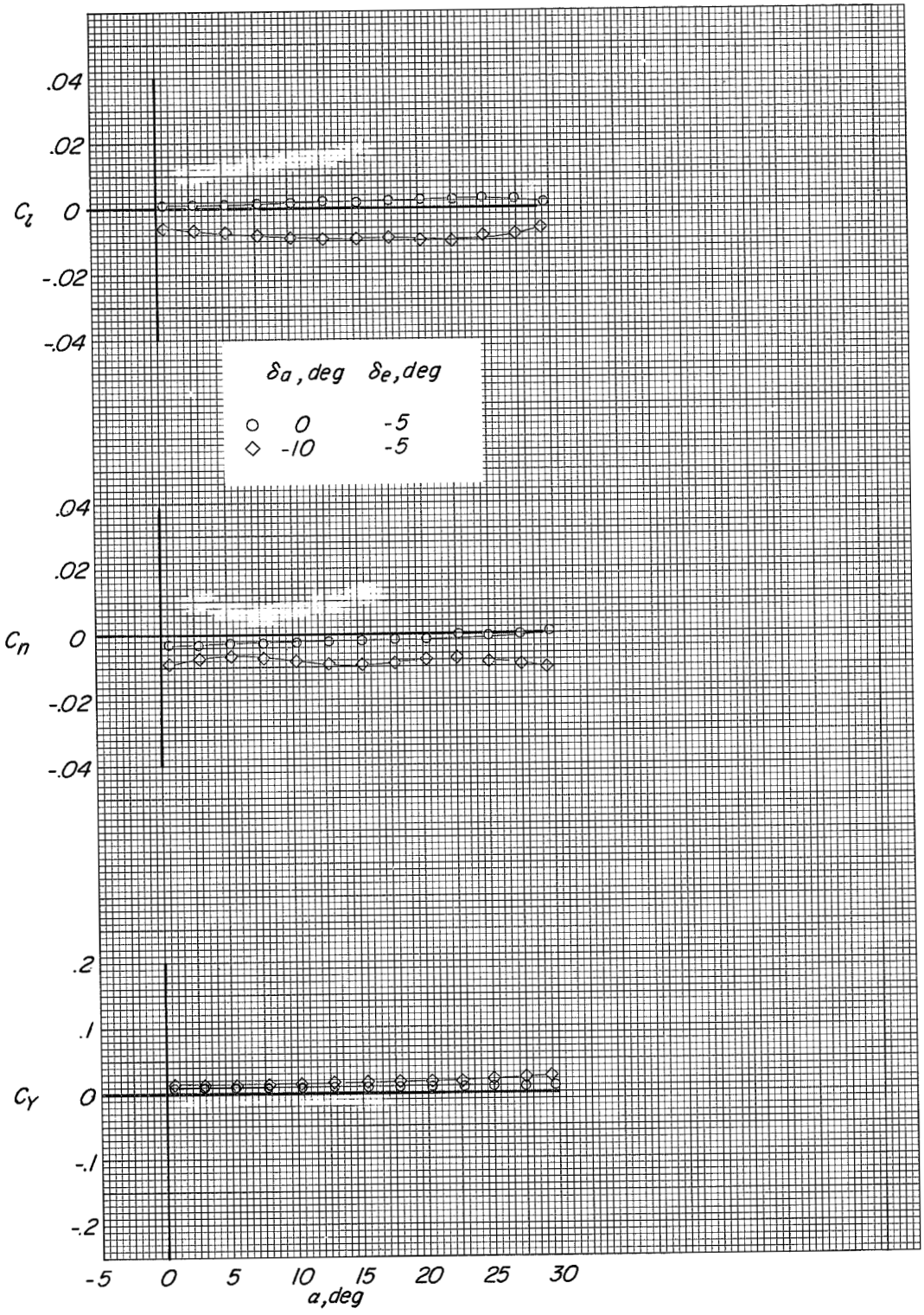
(d) $\delta_e = -5^o$; M = 0.80.

Figure 18.- Continued.



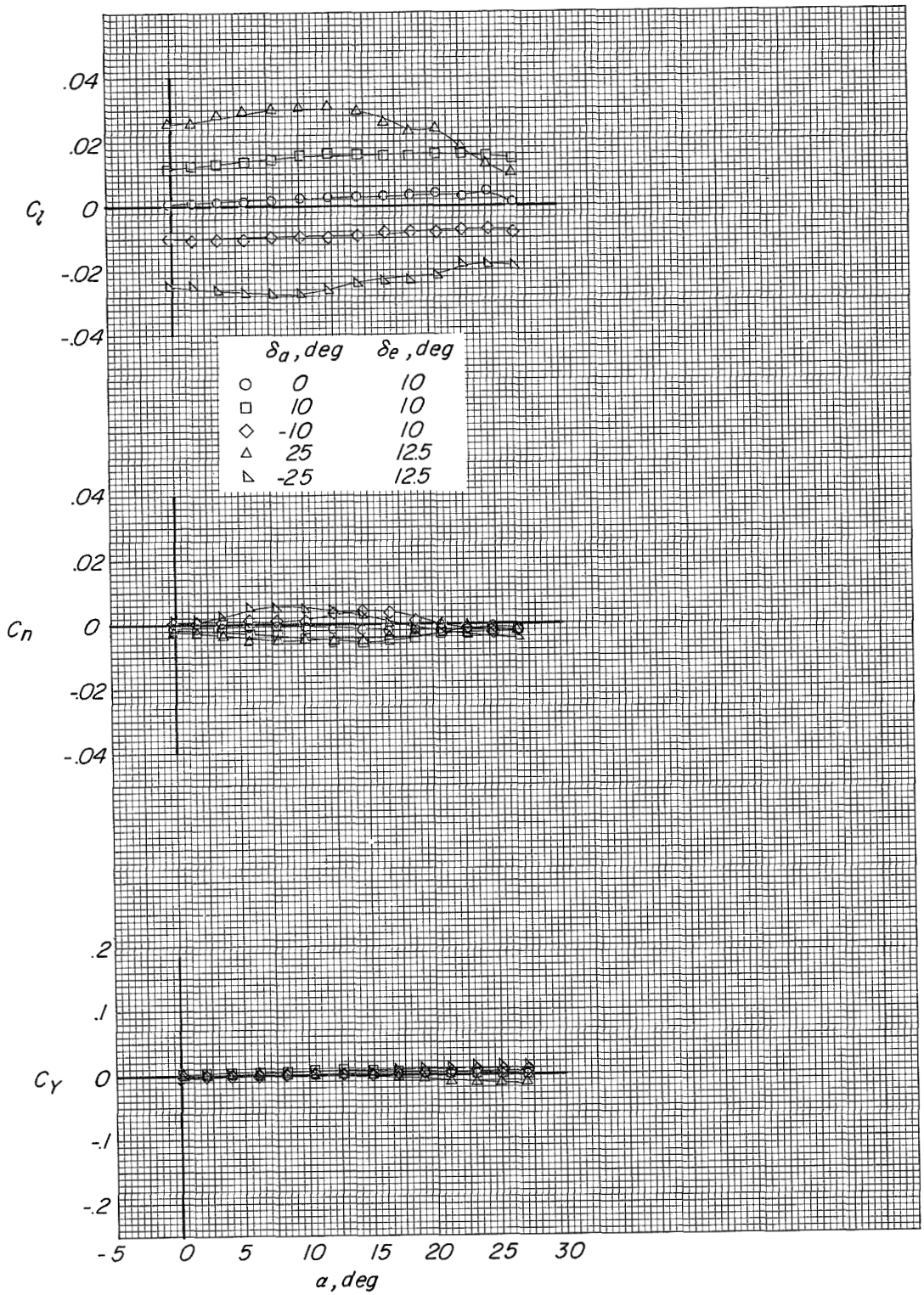
(e) $\delta_e = -5^o$; M = 0.85.

Figure 18.- Continued.



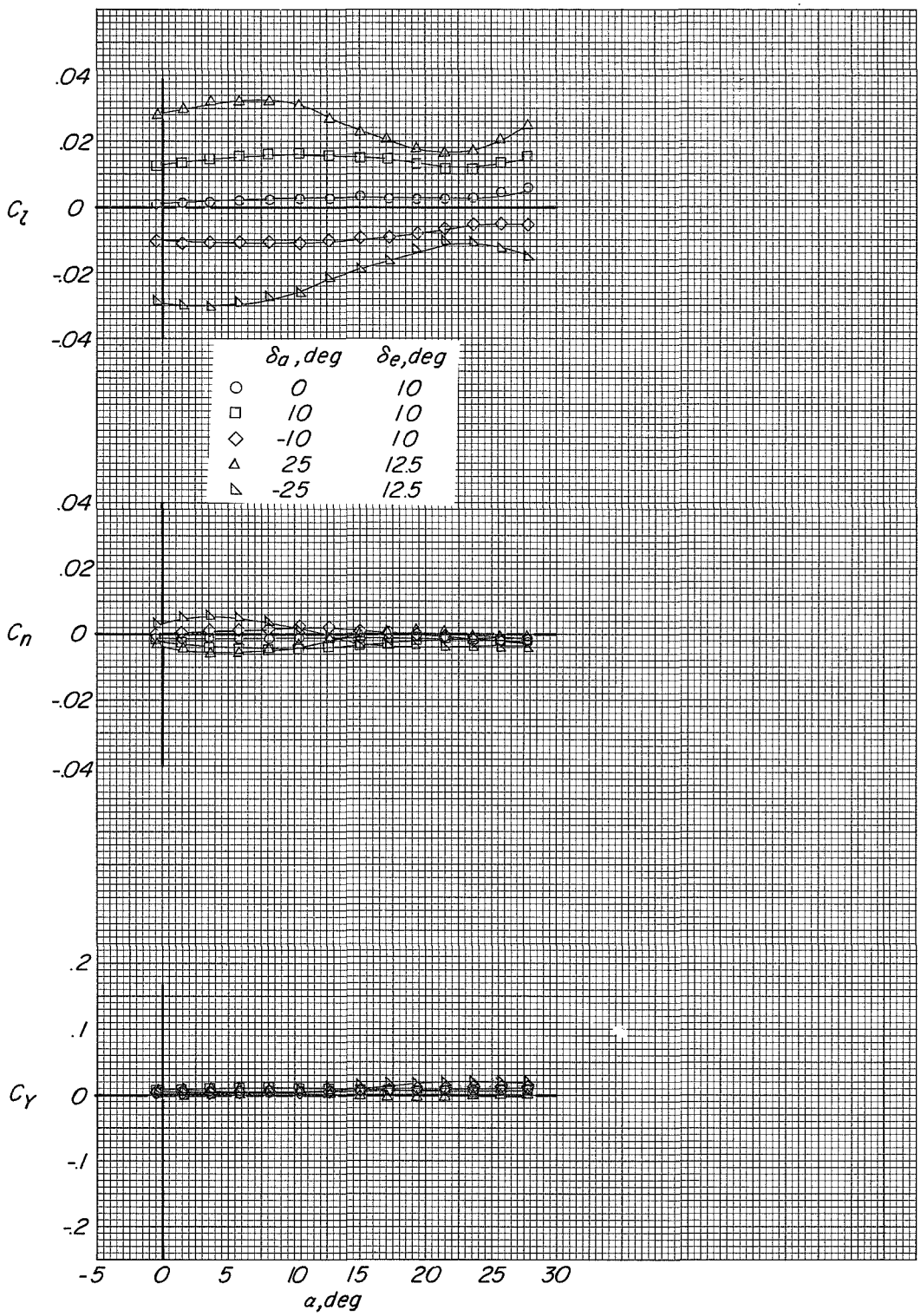
(f) $\delta_e = -5^o$; M = 0.90.

Figure 18.- Continued.



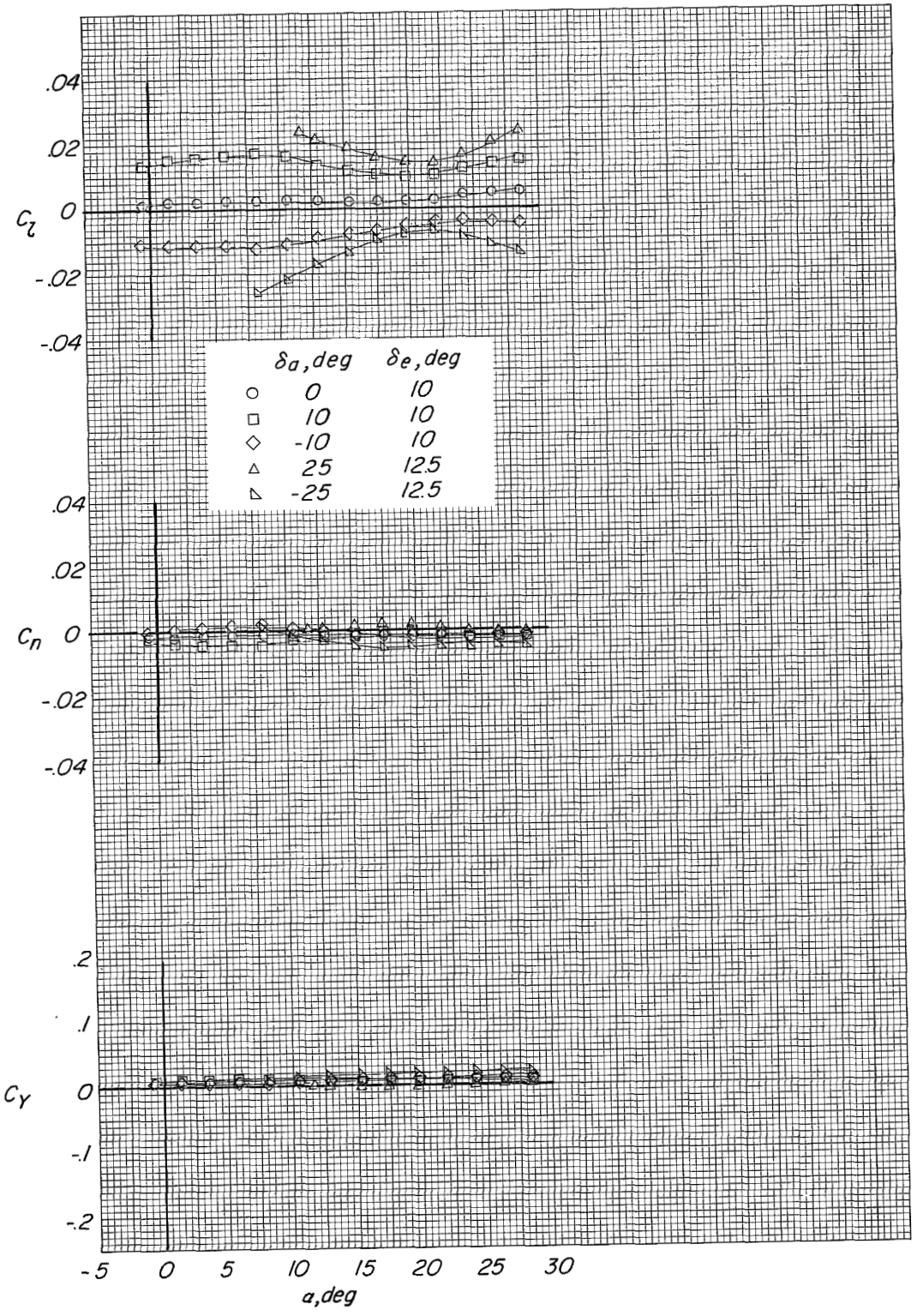
(g) M = 0.40.

Figure 18.- Continued.



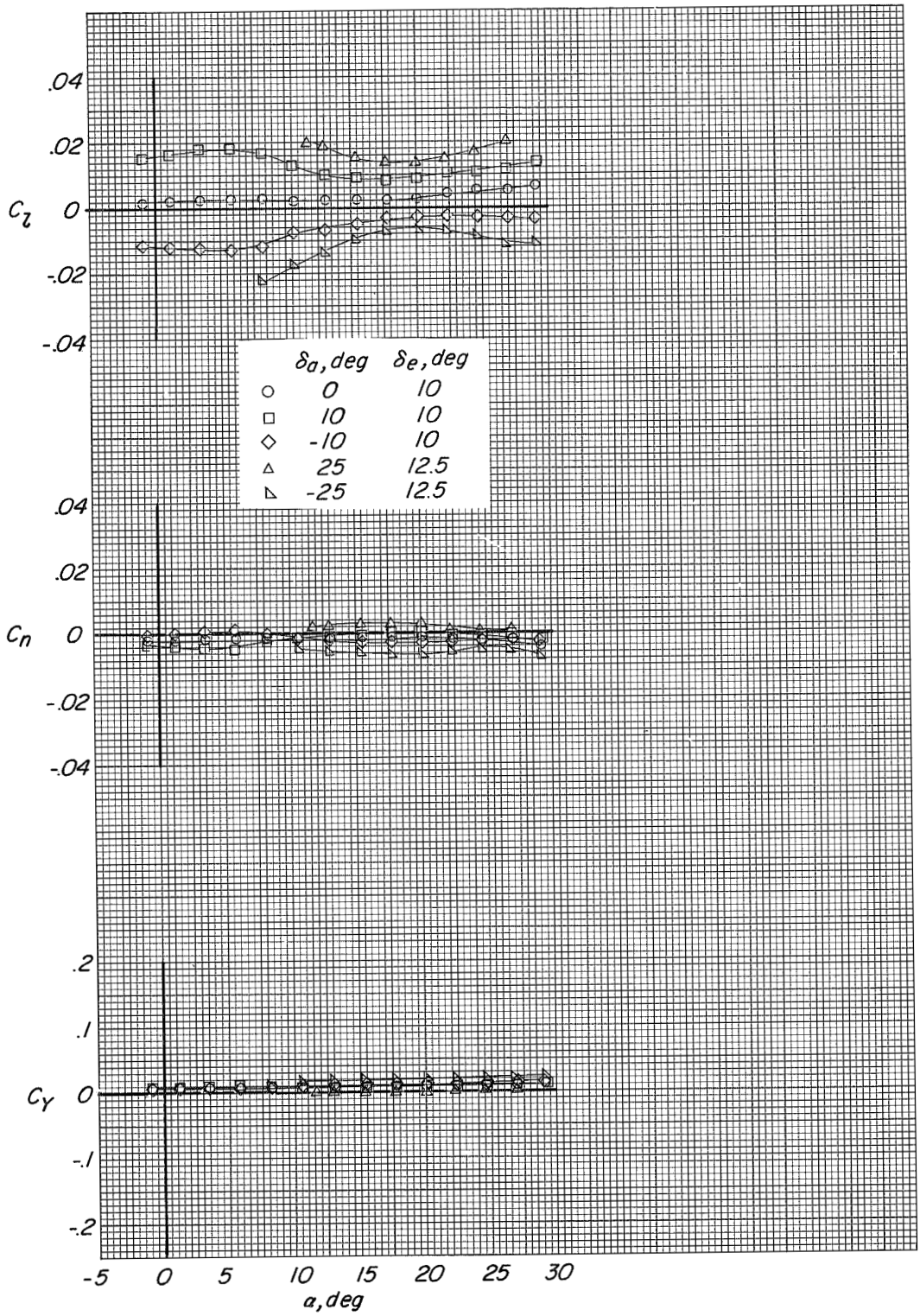
(h) M = 0.60.

Figure 18.- Continued.



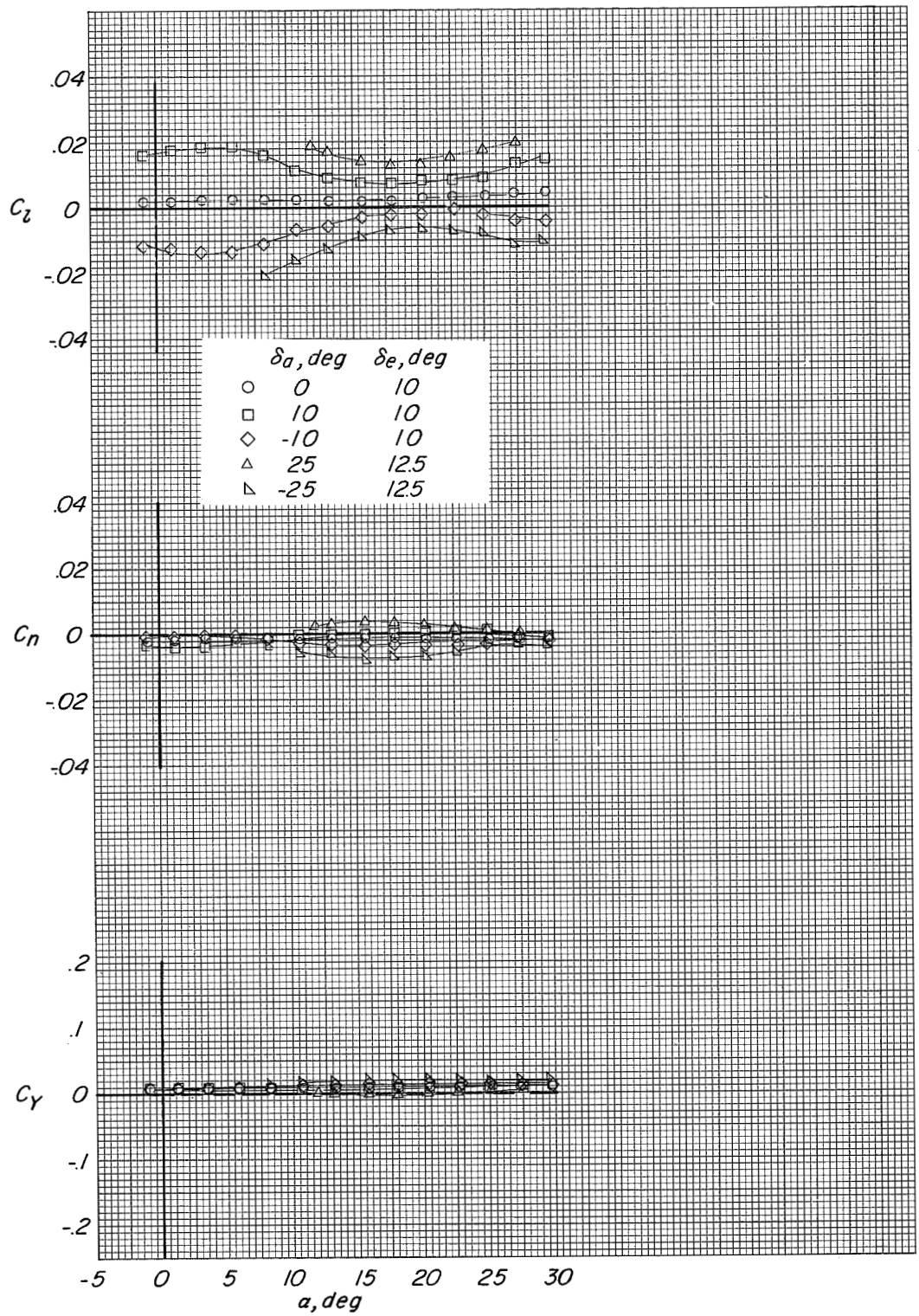
(i) M = 0.70.

Figure 18.- Continued.



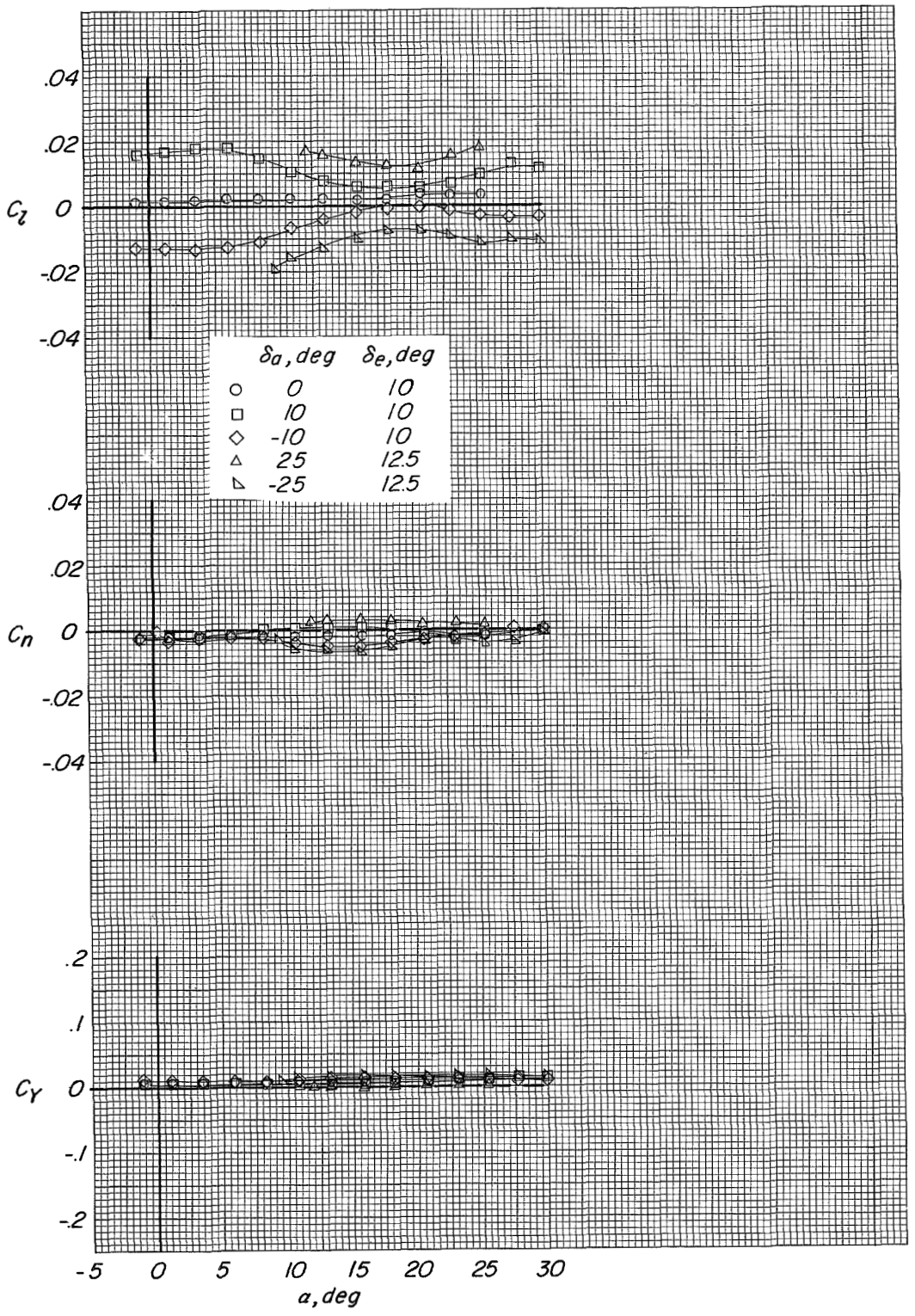
(j) M = 0.80.

Figure 18.- Continued.



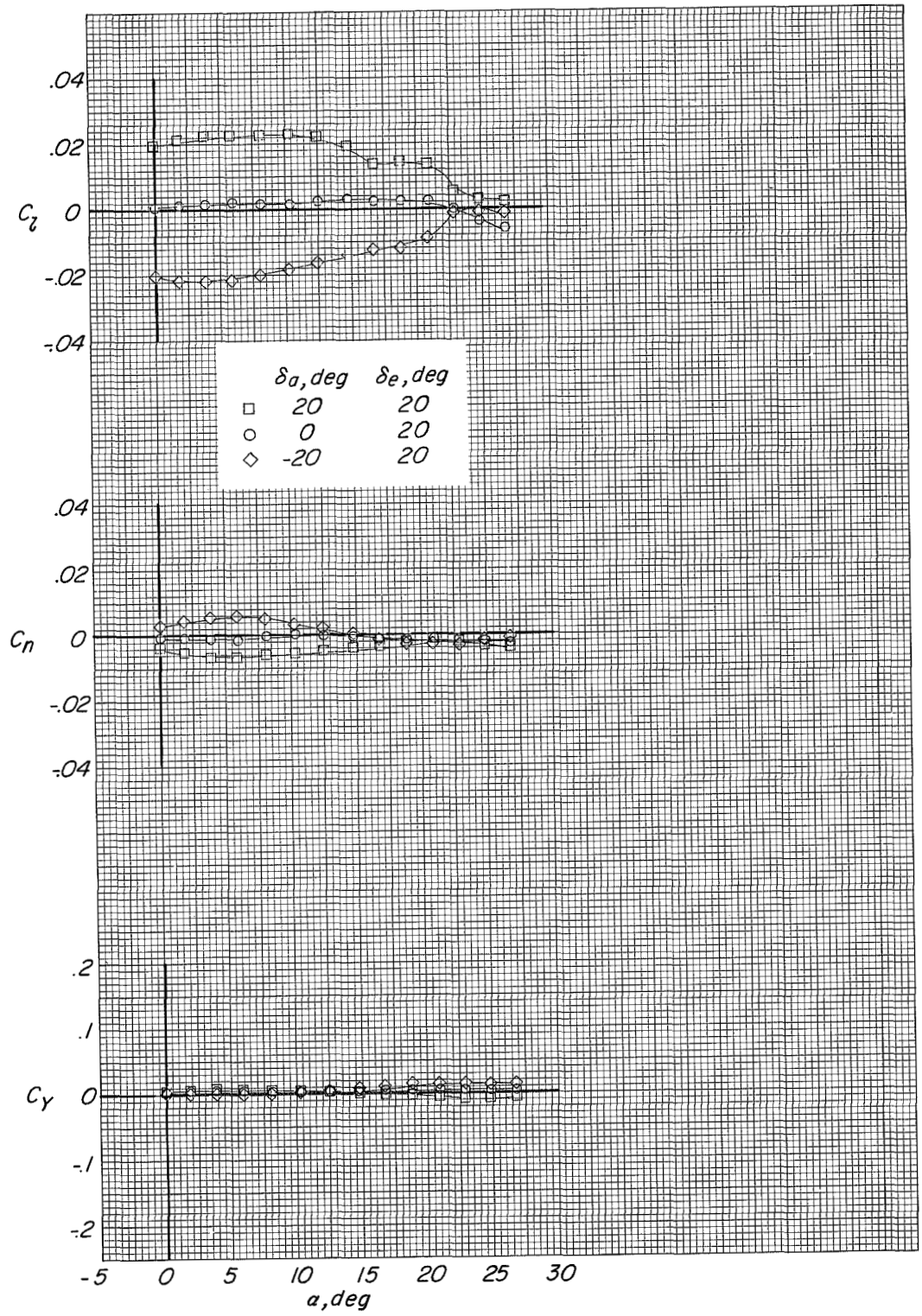
(k) M = 0.85.

Figure 18.- Continued.



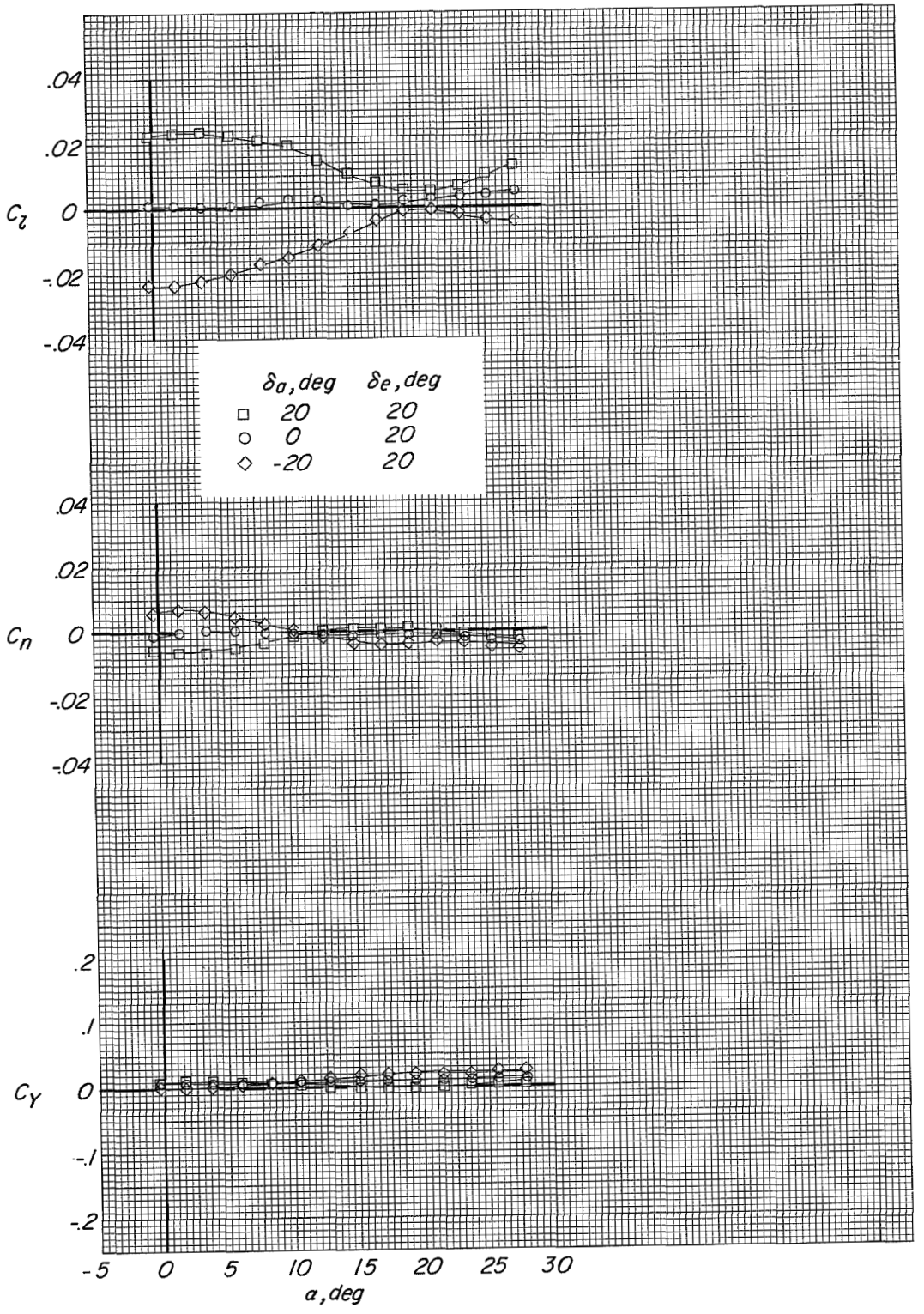
(l) M = 0.90.

Figure 18.- Continued.



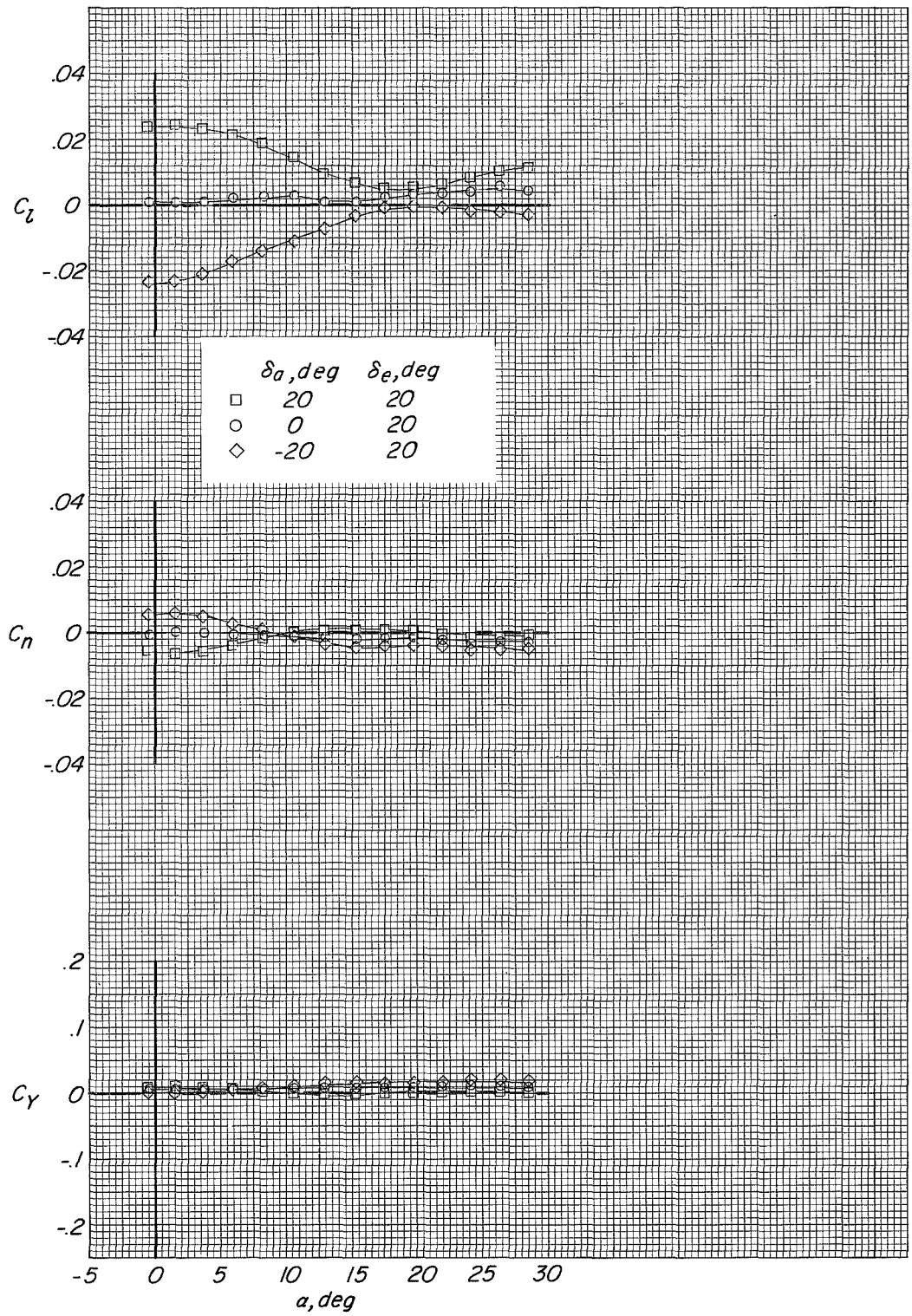
(m) $\delta_e = 20^o$; M = 0.40.

Figure 18.- Continued.



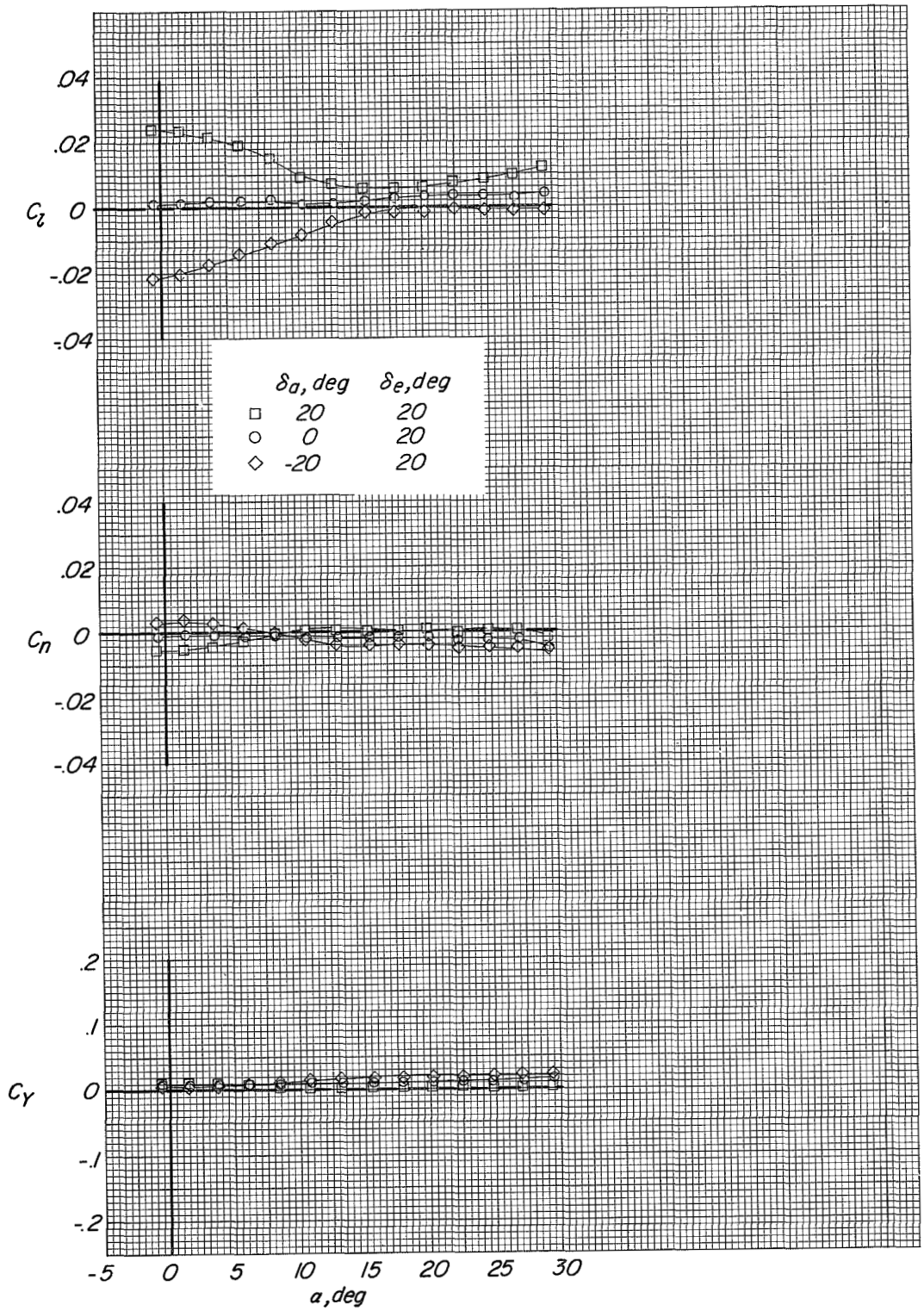
(n) $\delta_e = 20^o$; M = 0.60.

Figure 18.- Continued.



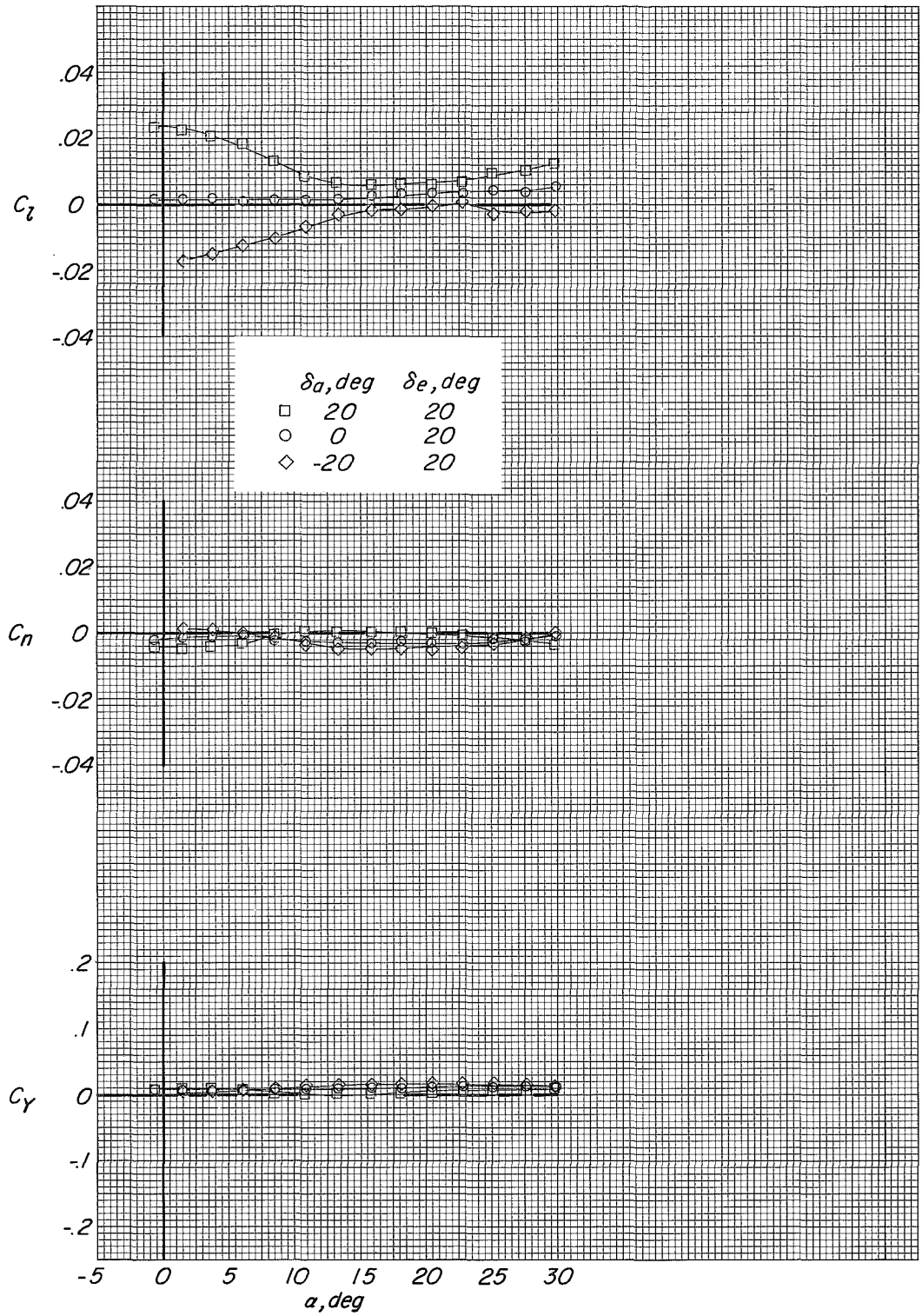
(o) $\delta_e = 20^o$; M = 0.70.

Figure 18.- Continued.



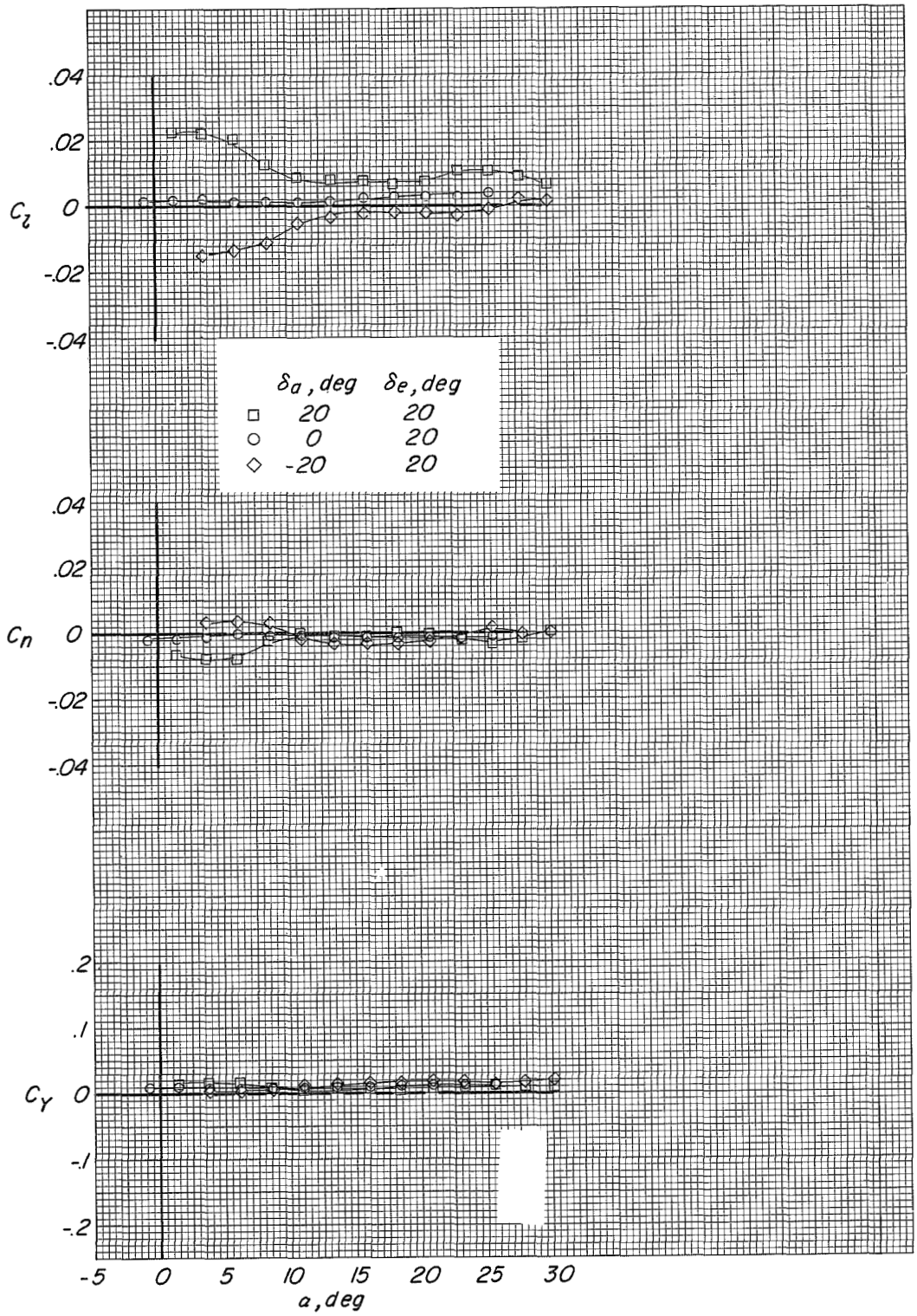
(p) $\delta_e = 20^o$; M = 0.80.

Figure 18.- Continued.



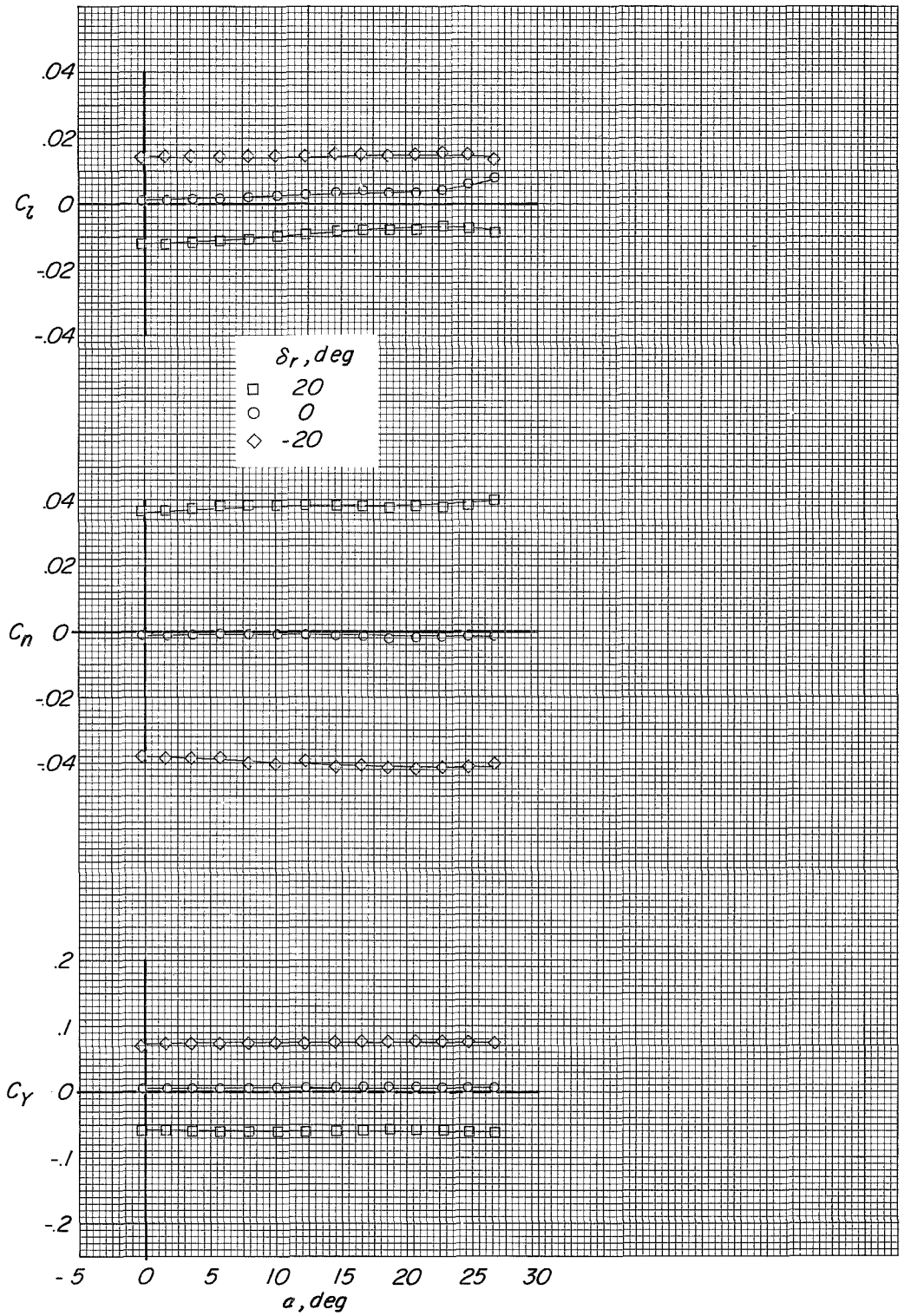
(q) $\delta_e = 20^o$; M = 0.85.

Figure 18.- Continued.



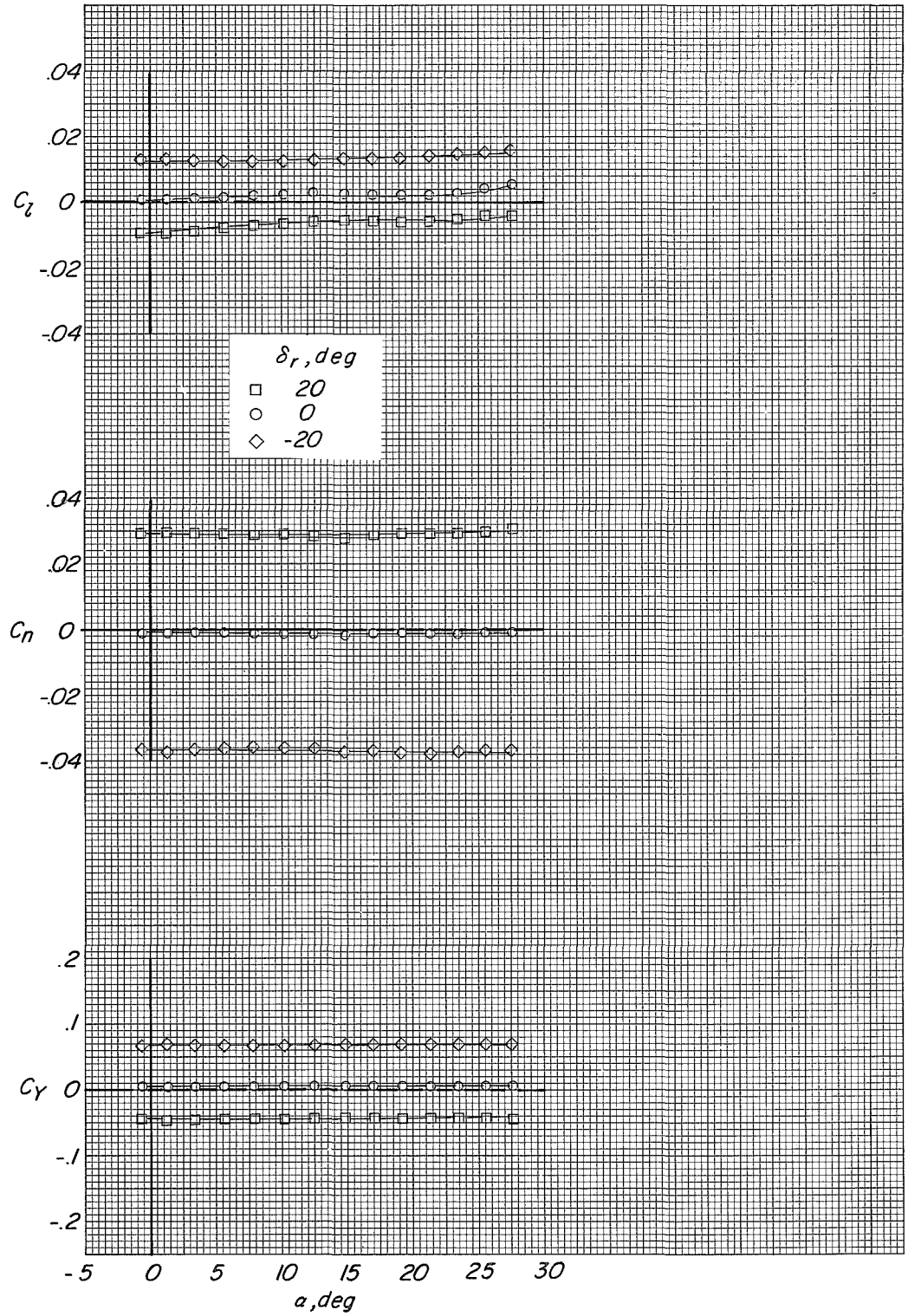
(r) $\delta_e = 20^o$; M = 0.90.

Figure 18.- Concluded.



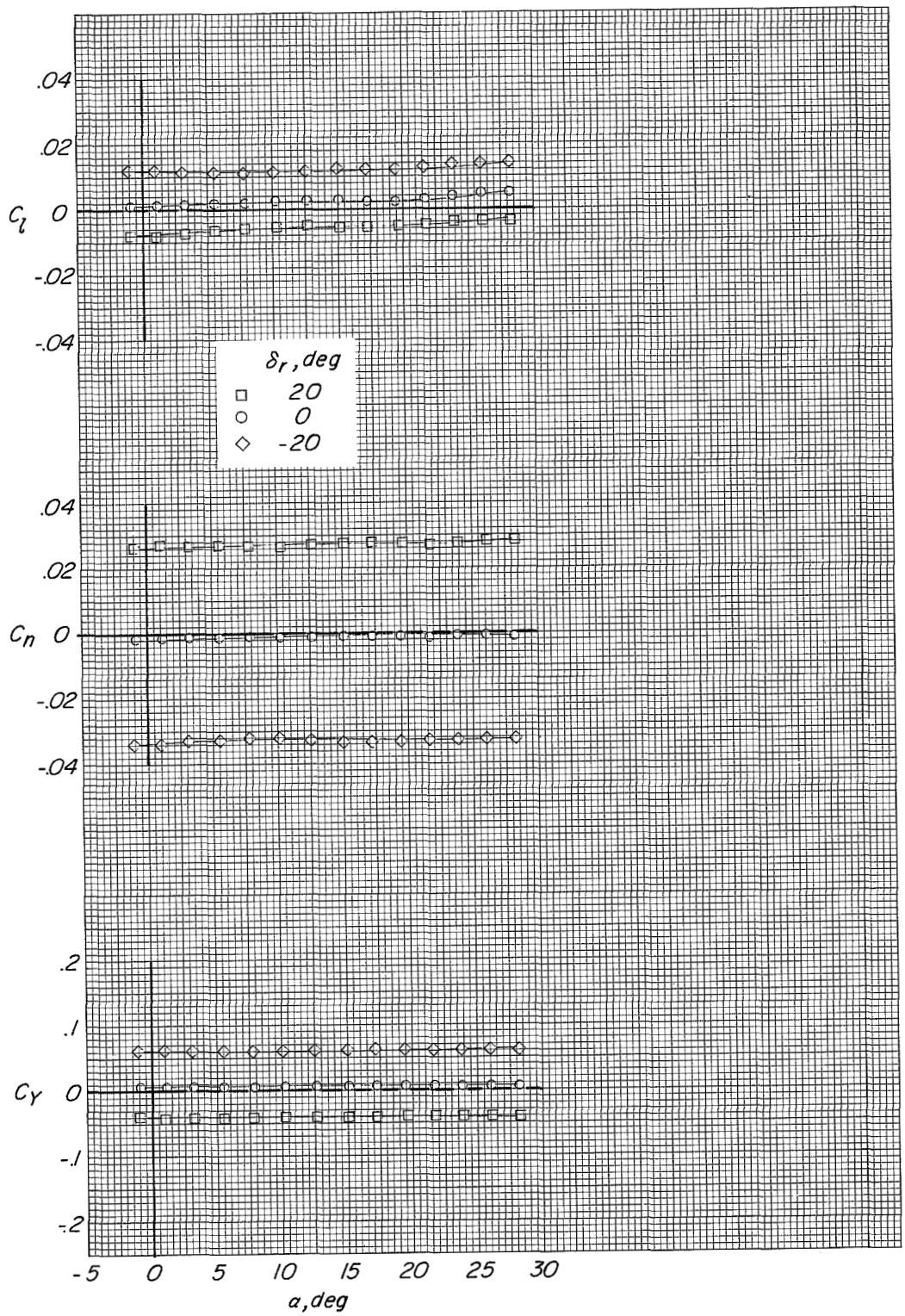
(a) M = 0.40.

Figure 19.- Effect of rudder deflection on the lateral force and moment characteristics Basic fin configuration; auxiliary flaps in the transonic position; $\beta = \delta_a = 0^o$; $\delta_e = 0^o$.



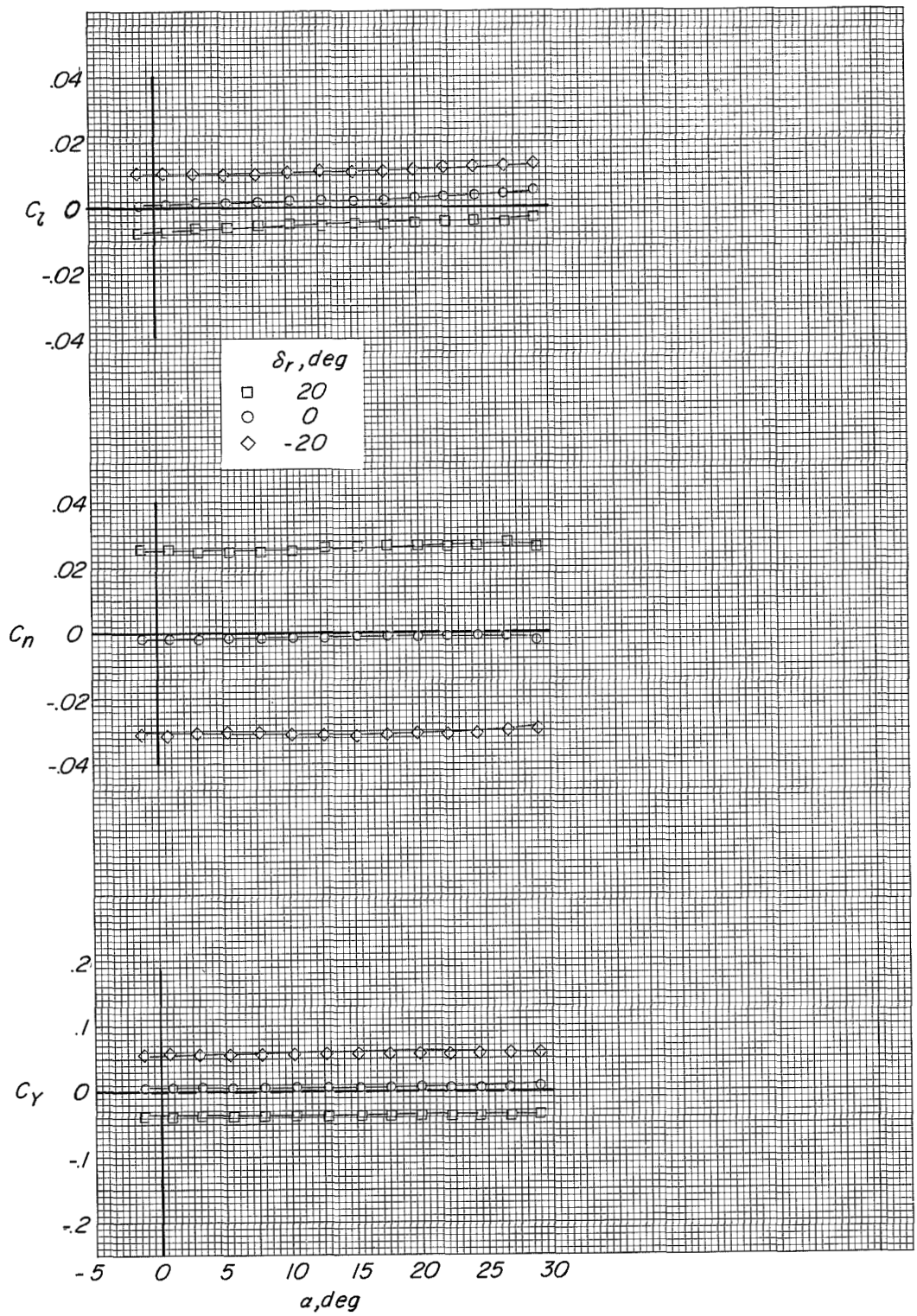
(b) M = 0.60.

Figure 19.- Continued.



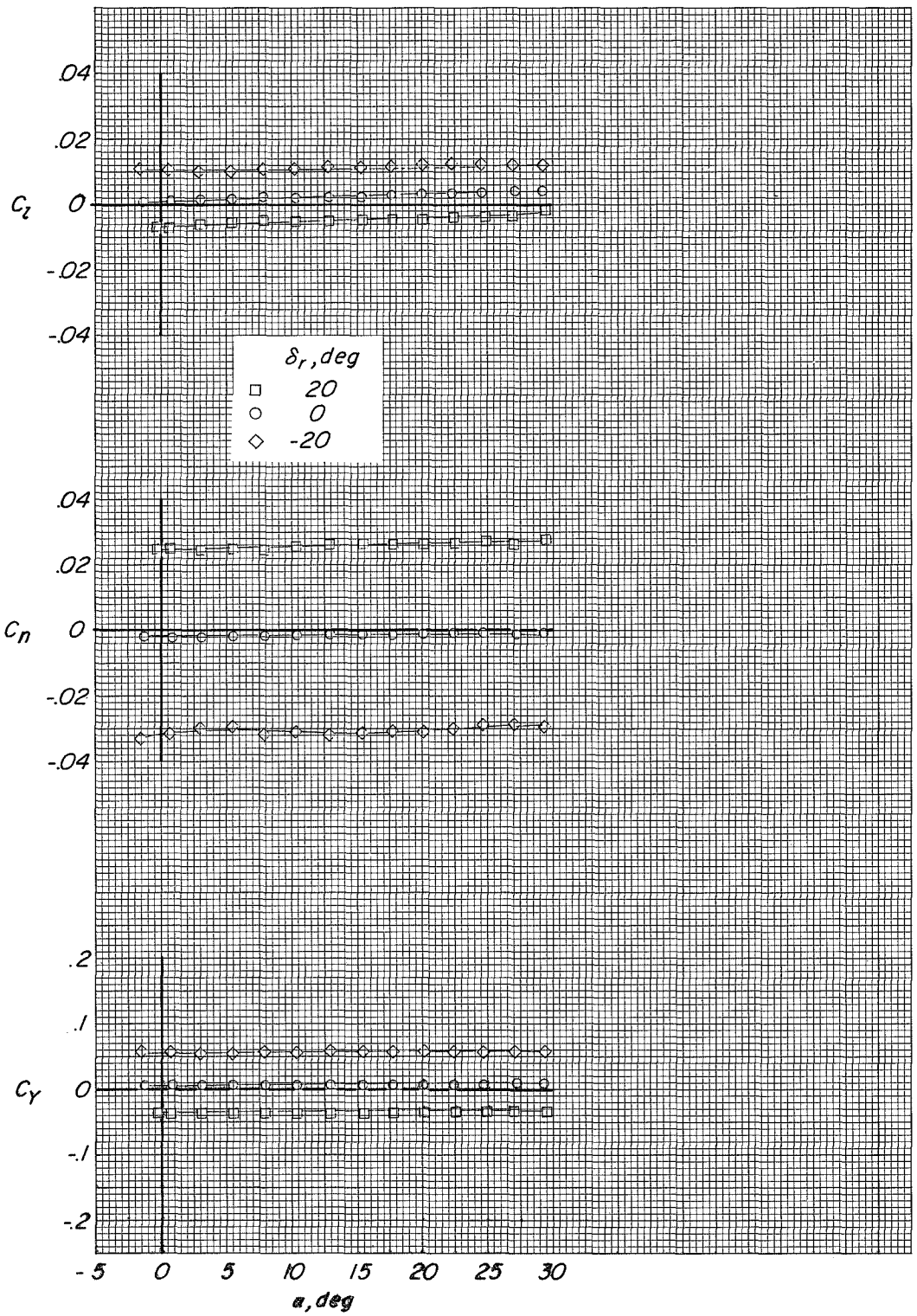
(c) M = 0.70.

Figure 19.- Continued.



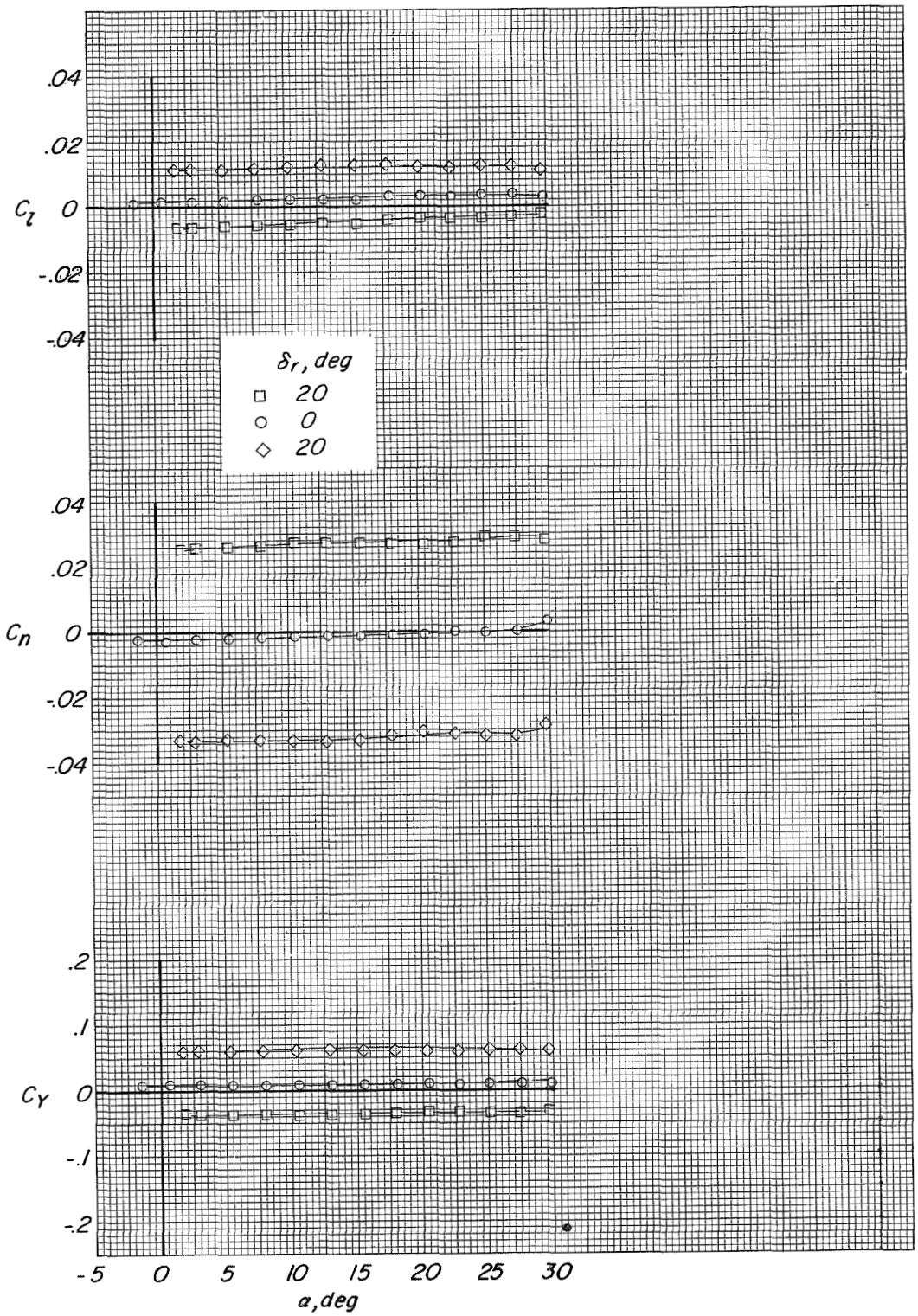
(d) M = 0.80.

Figure 19.- Continued.



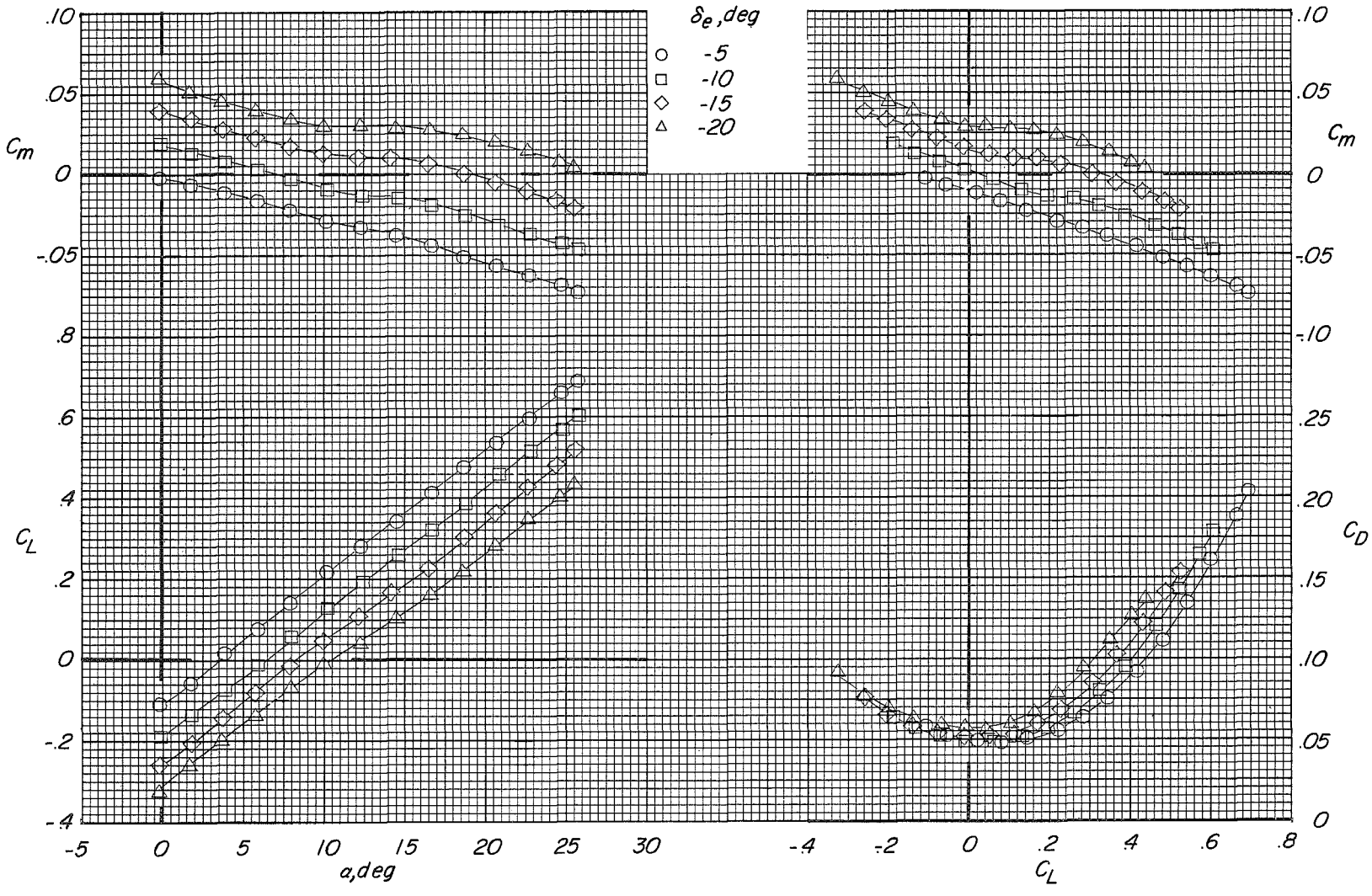
(e) M = 0.85.

Figure 19.- Continued.



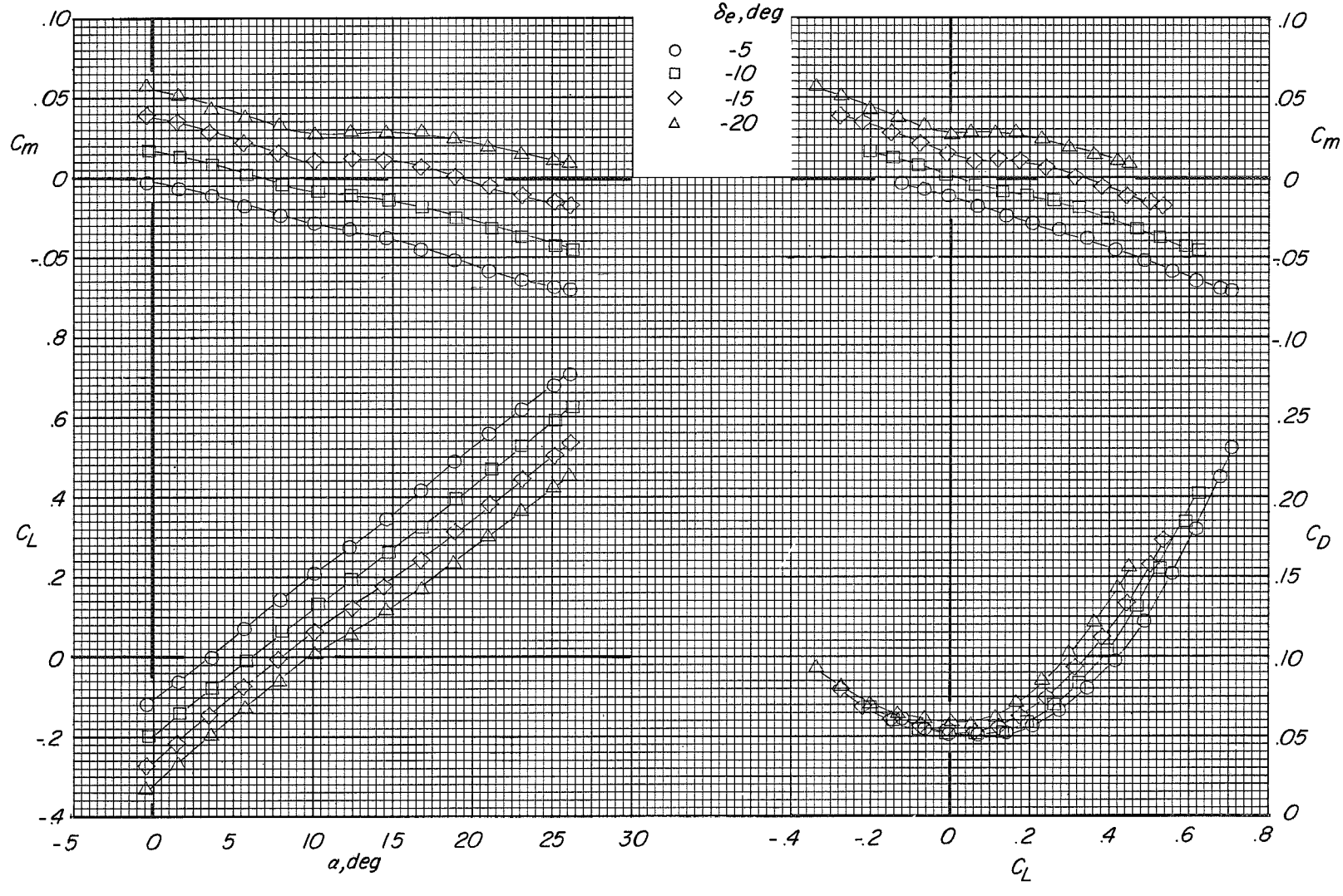
(f) M = 0.90.

Figure 19.- Concluded.



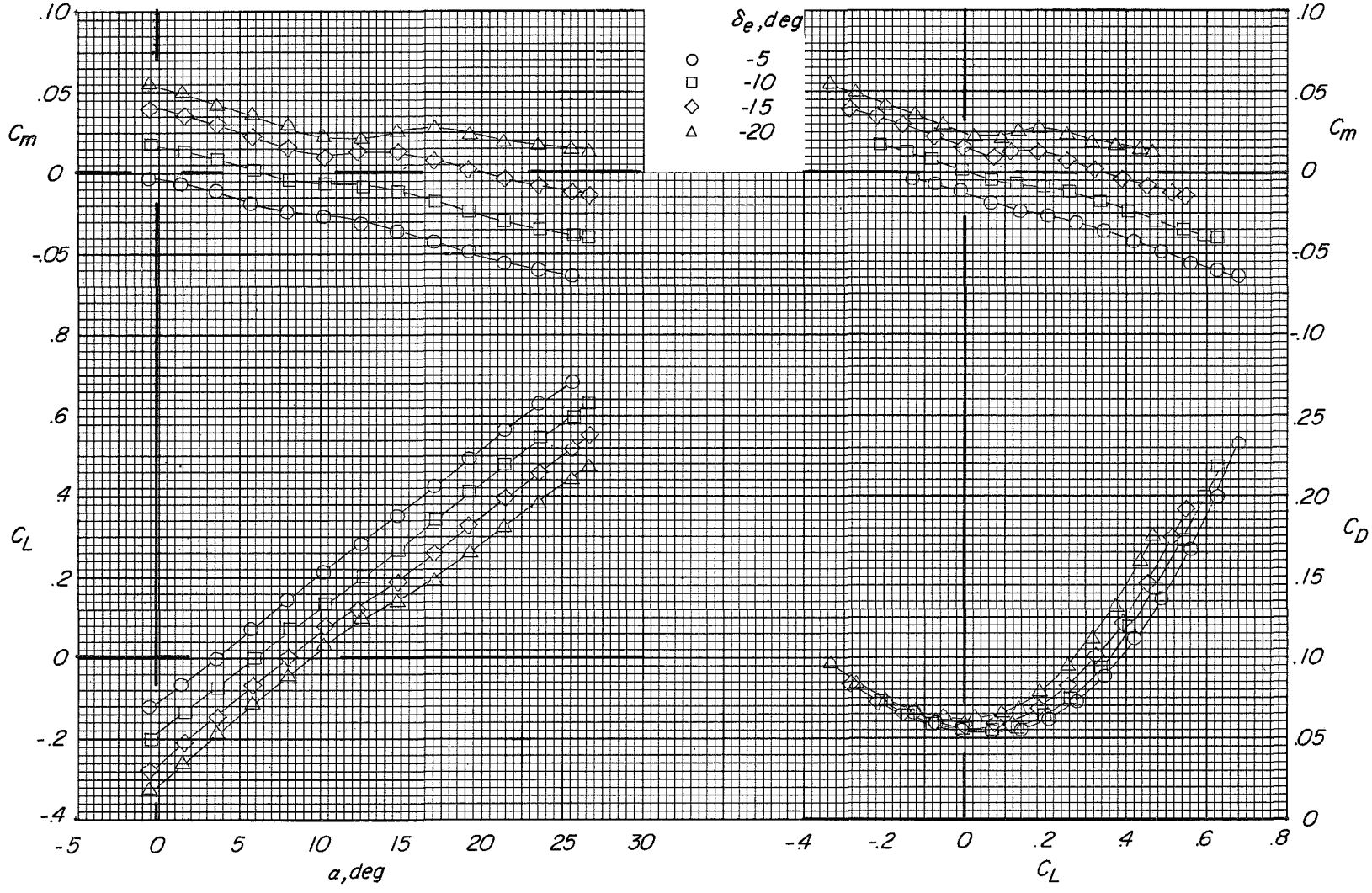
(a) M = 0.35.

Figure 20.- Longitudinal characteristics. Modification I fin configuration; auxiliary flaps in the subsonic position; $\delta_a = \beta = 0^o$.



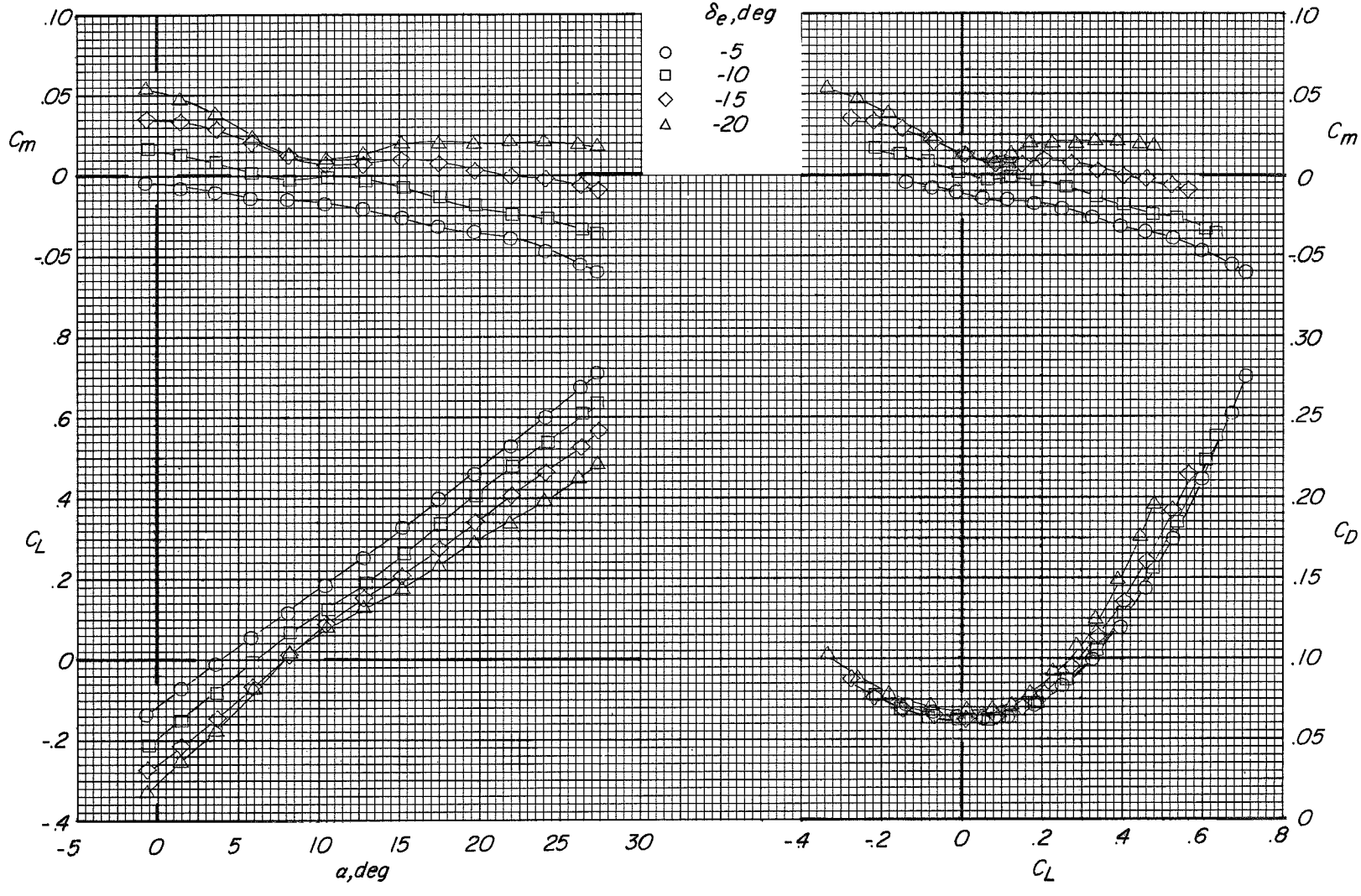
(b) M = 0.50.

Figure 20.- Continued.



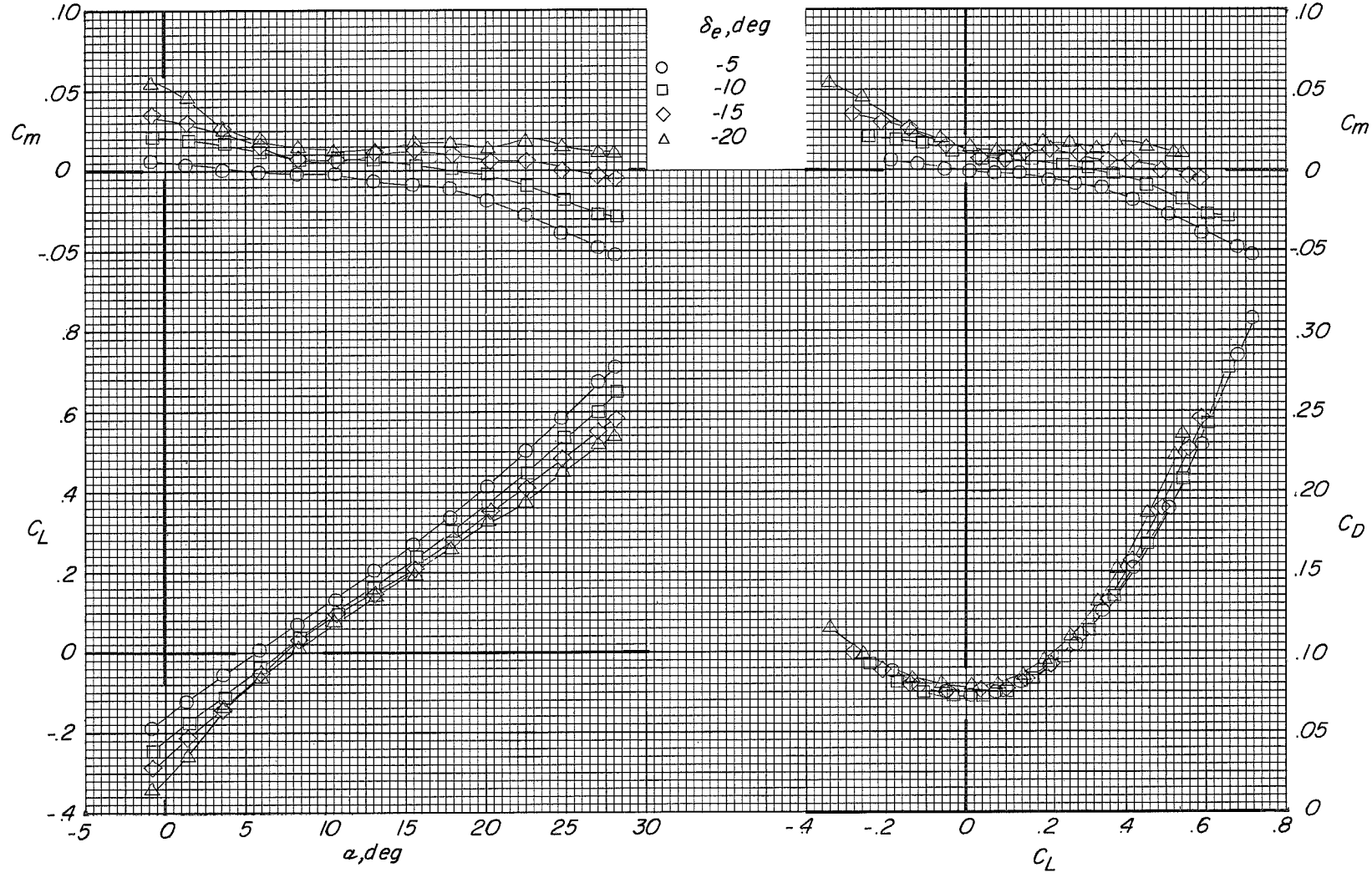
(c) M = 0.60.

Figure 20.- Continued.



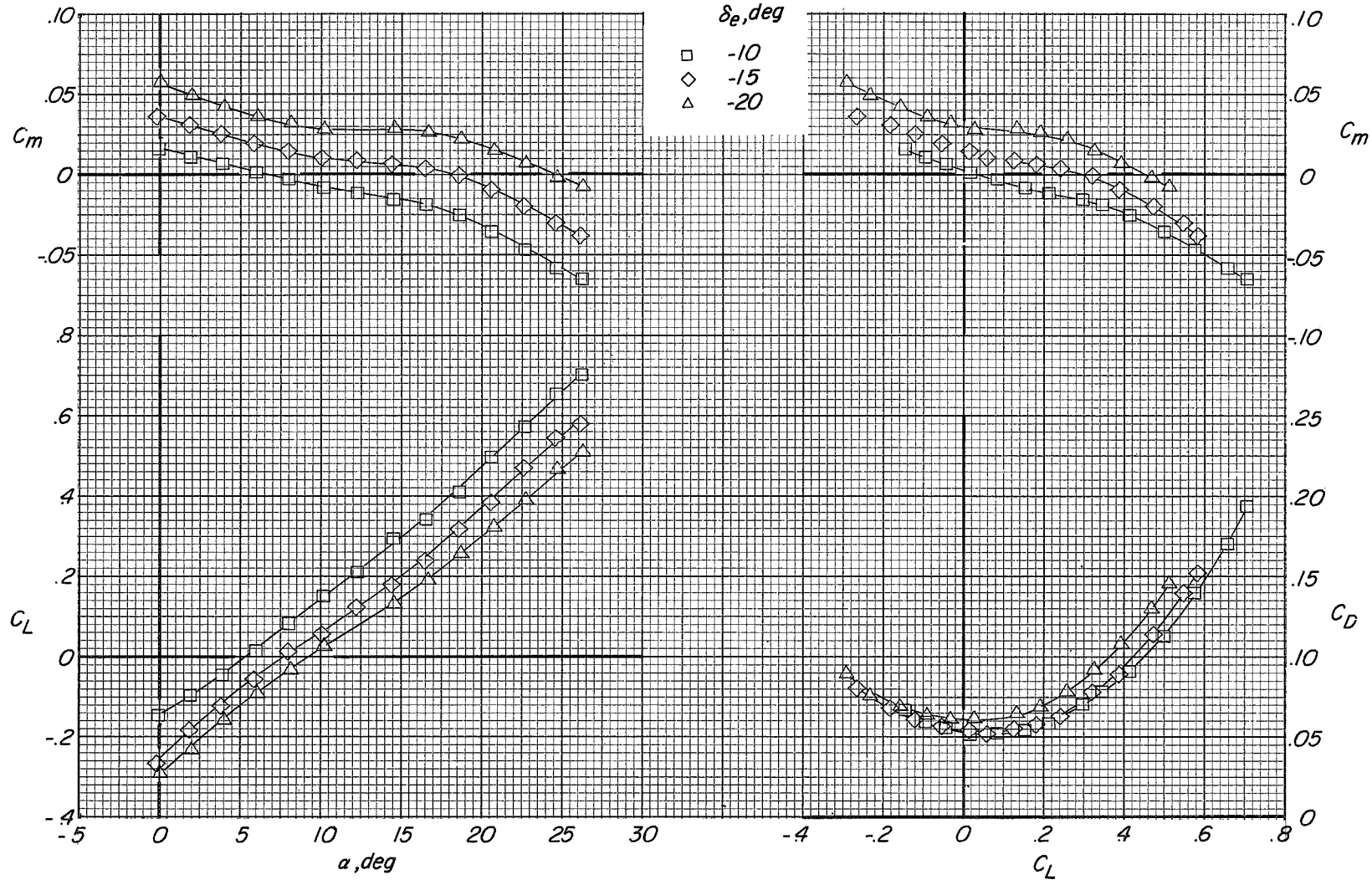
(d) M = 0.70.

Figure 20.- Continued.



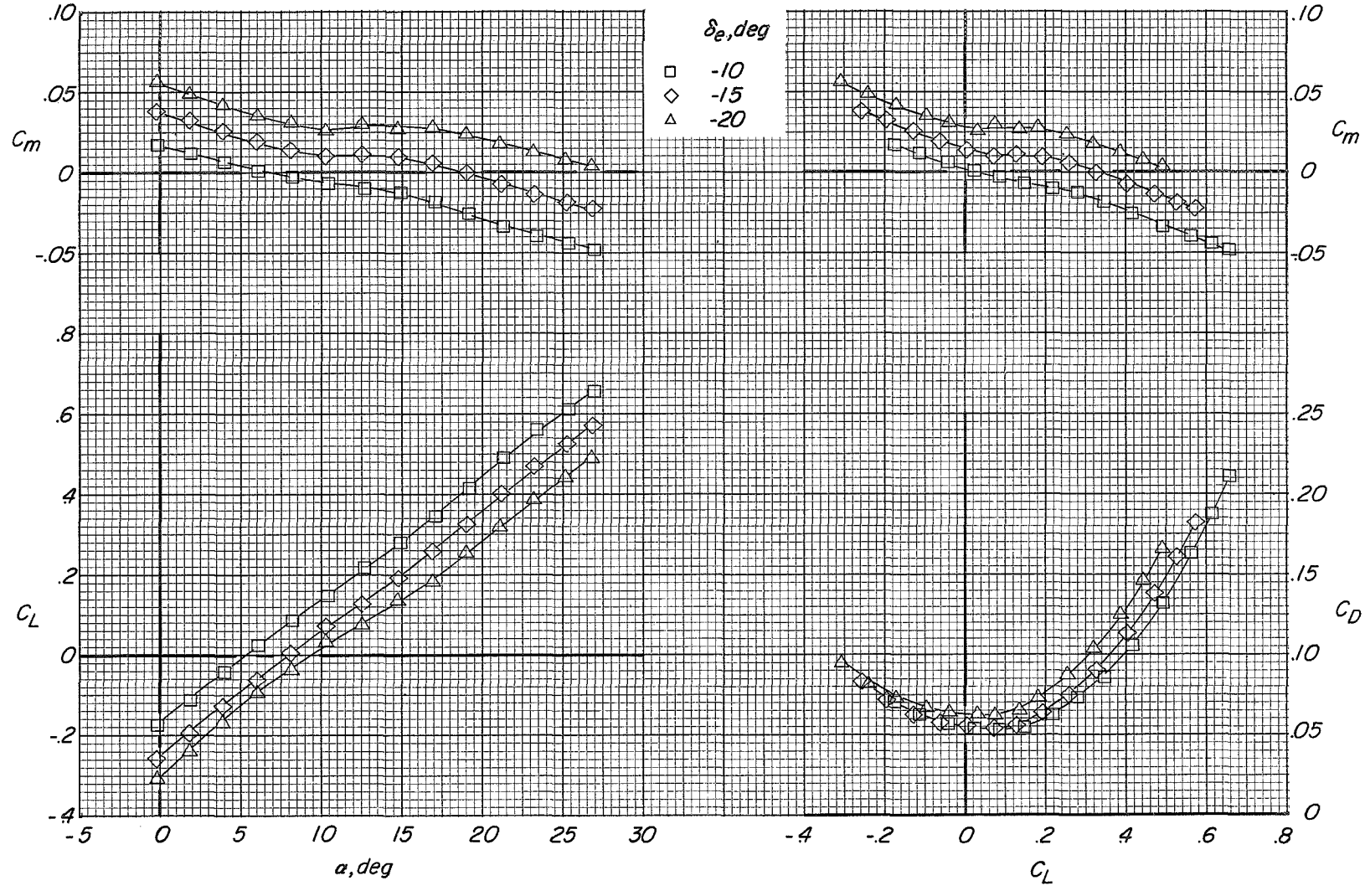
(e) M = 0.80.

Figure 20.- Concluded.



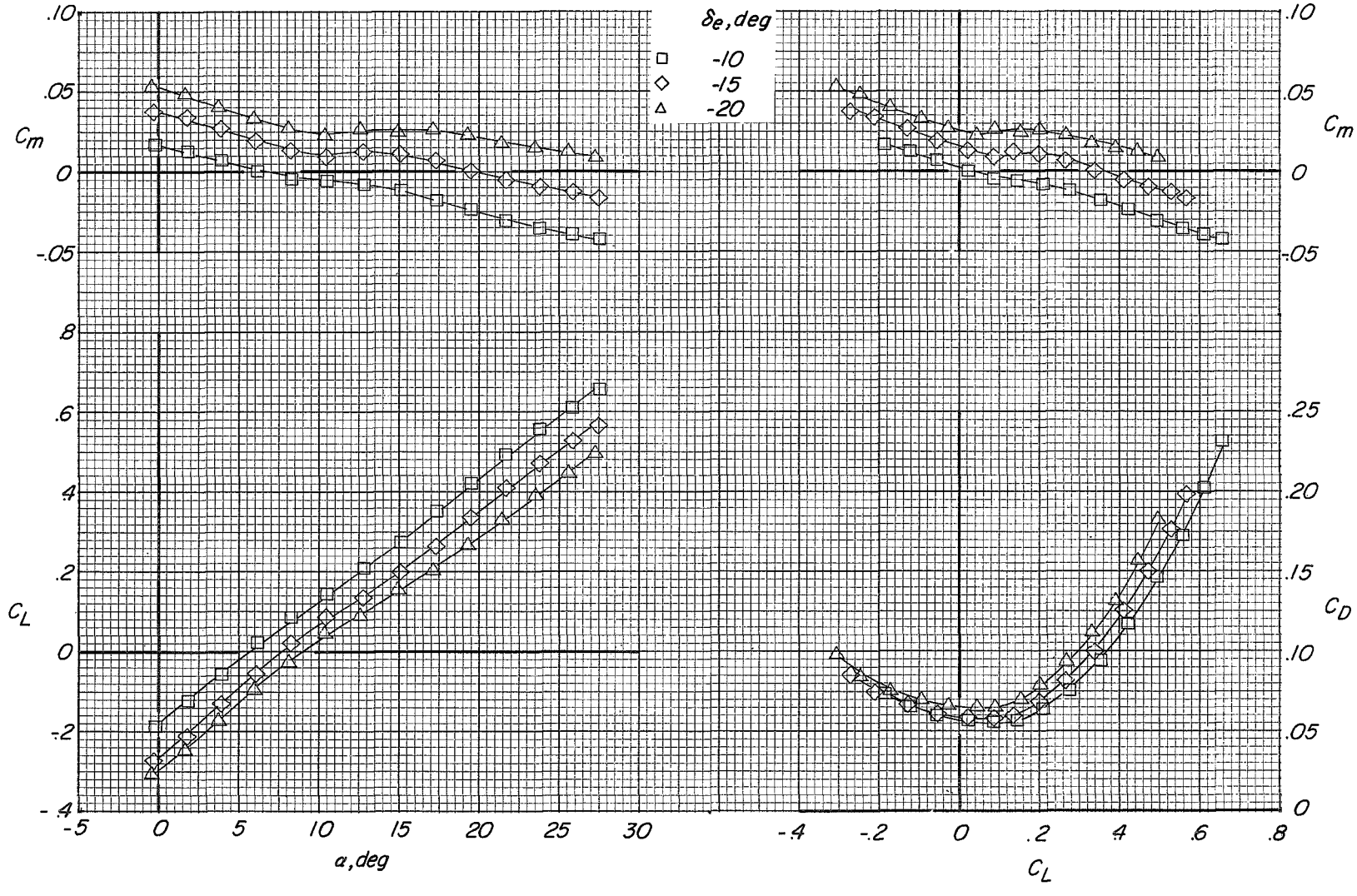
(a) $\beta = 2.3^{o}$; M = 0.35.

Figure 21.- Longitudinal characteristics at sideslip. Modification I fin configuration; auxiliary flaps in the subsonic position; $\delta_a = 0^{o}$.



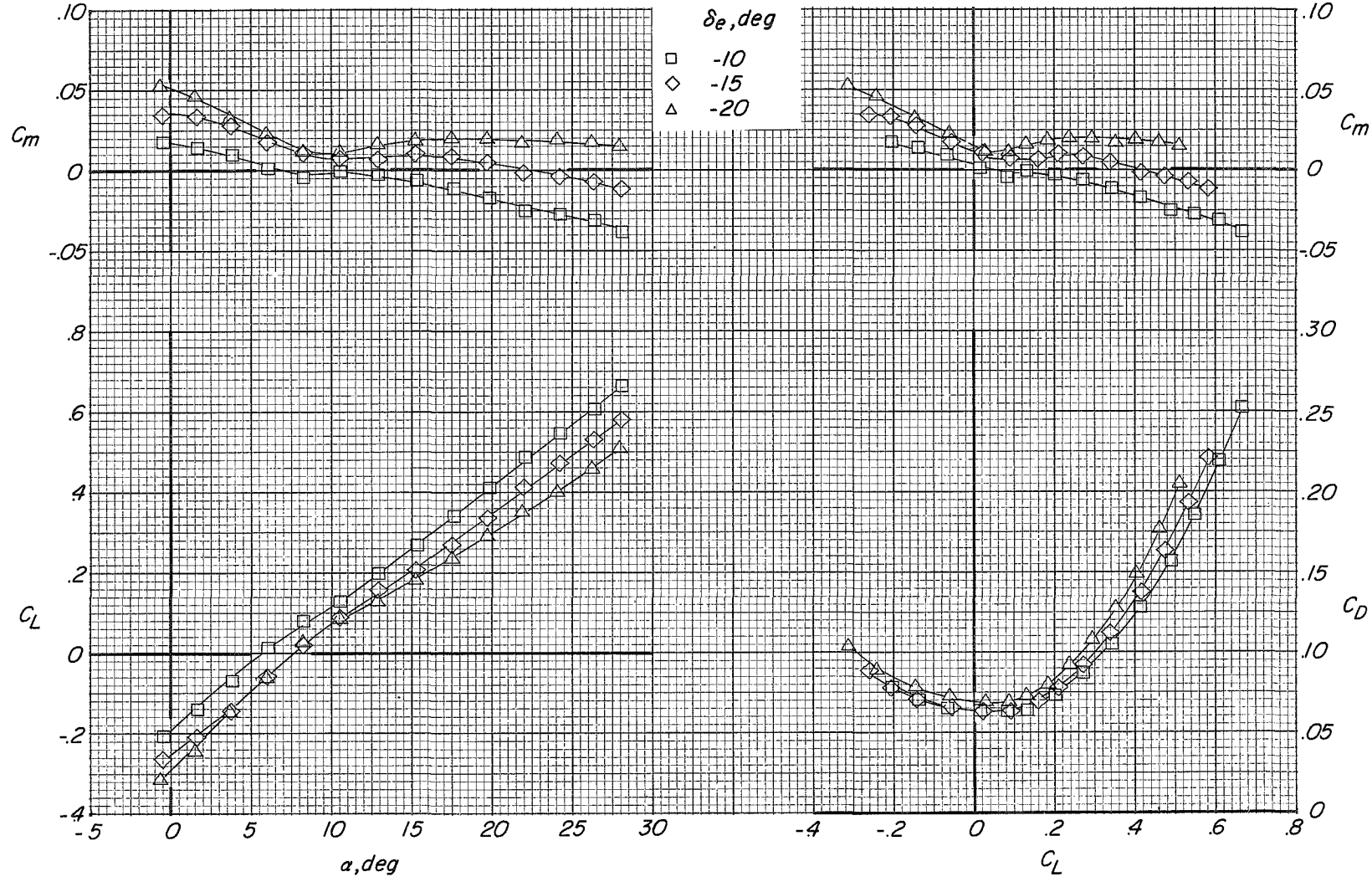
(b) $\beta = 2.3^{o}$; M = 0.50.

Figure 21.- Continued.



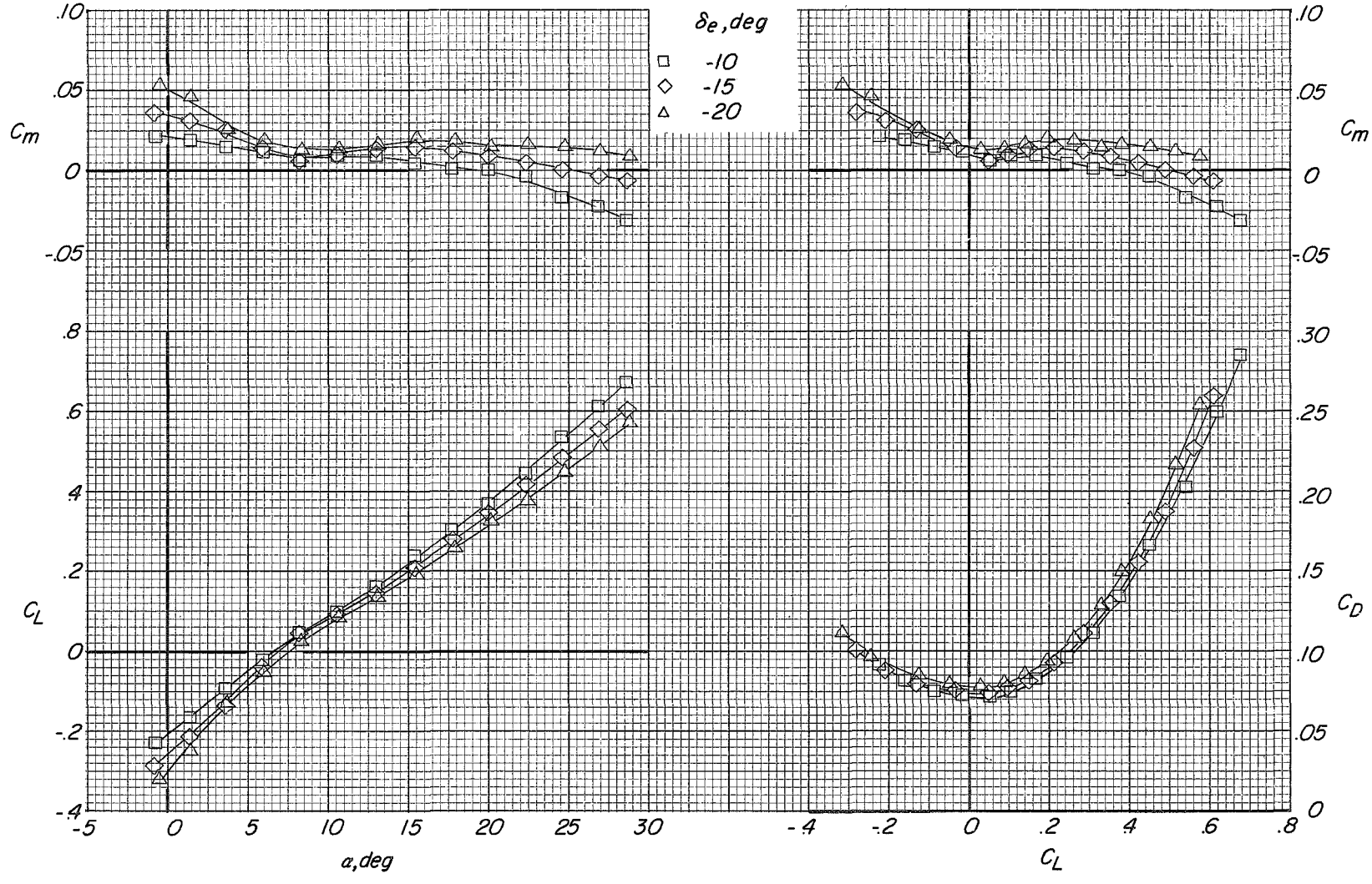
(c) $\beta = 2.3^{o}$; M = 0.60.

Figure 21.- Continued.



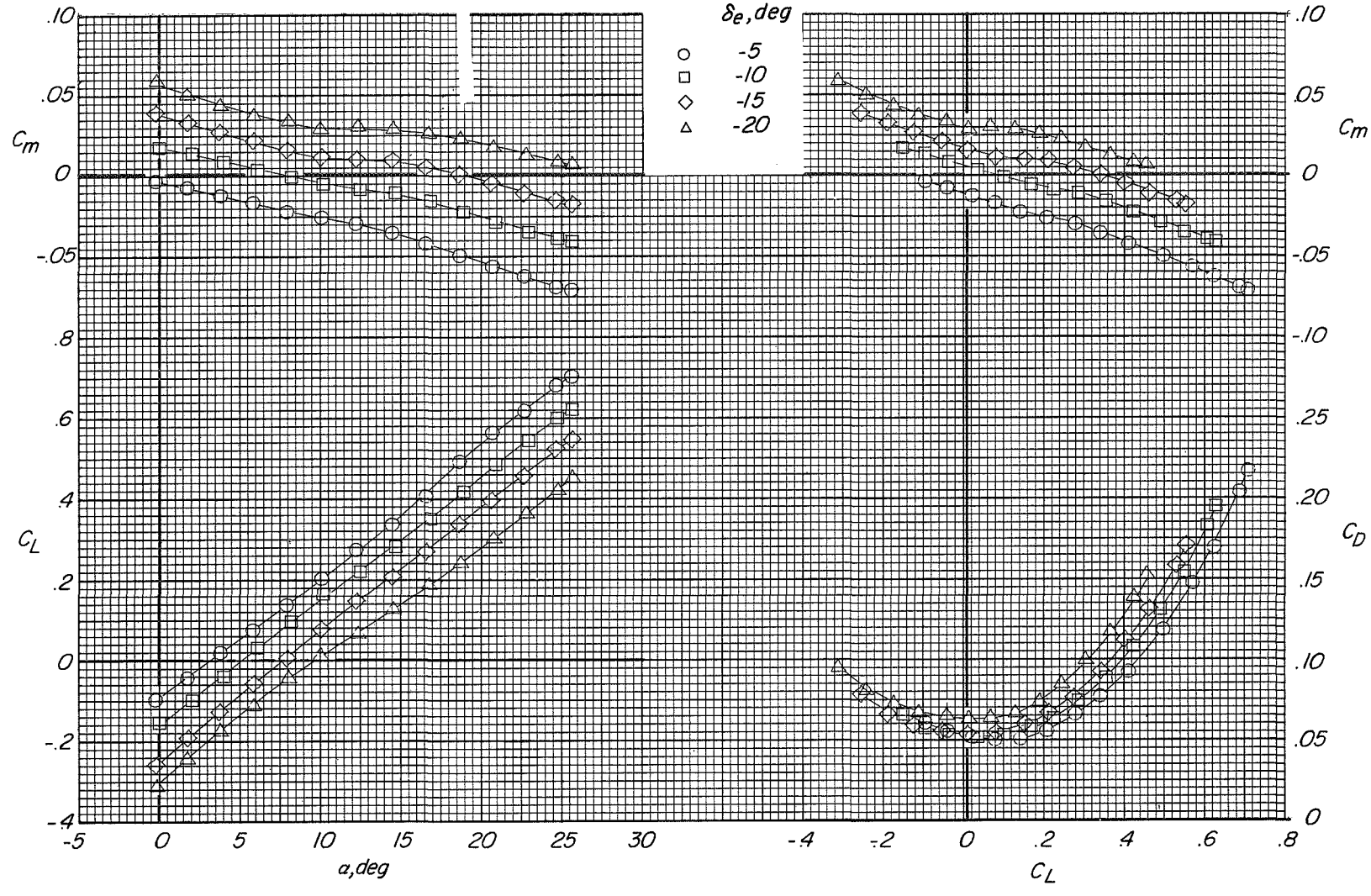
(d) $\beta = 2.3^{o}$; M = 0.70.

Figure 21.- Continued.



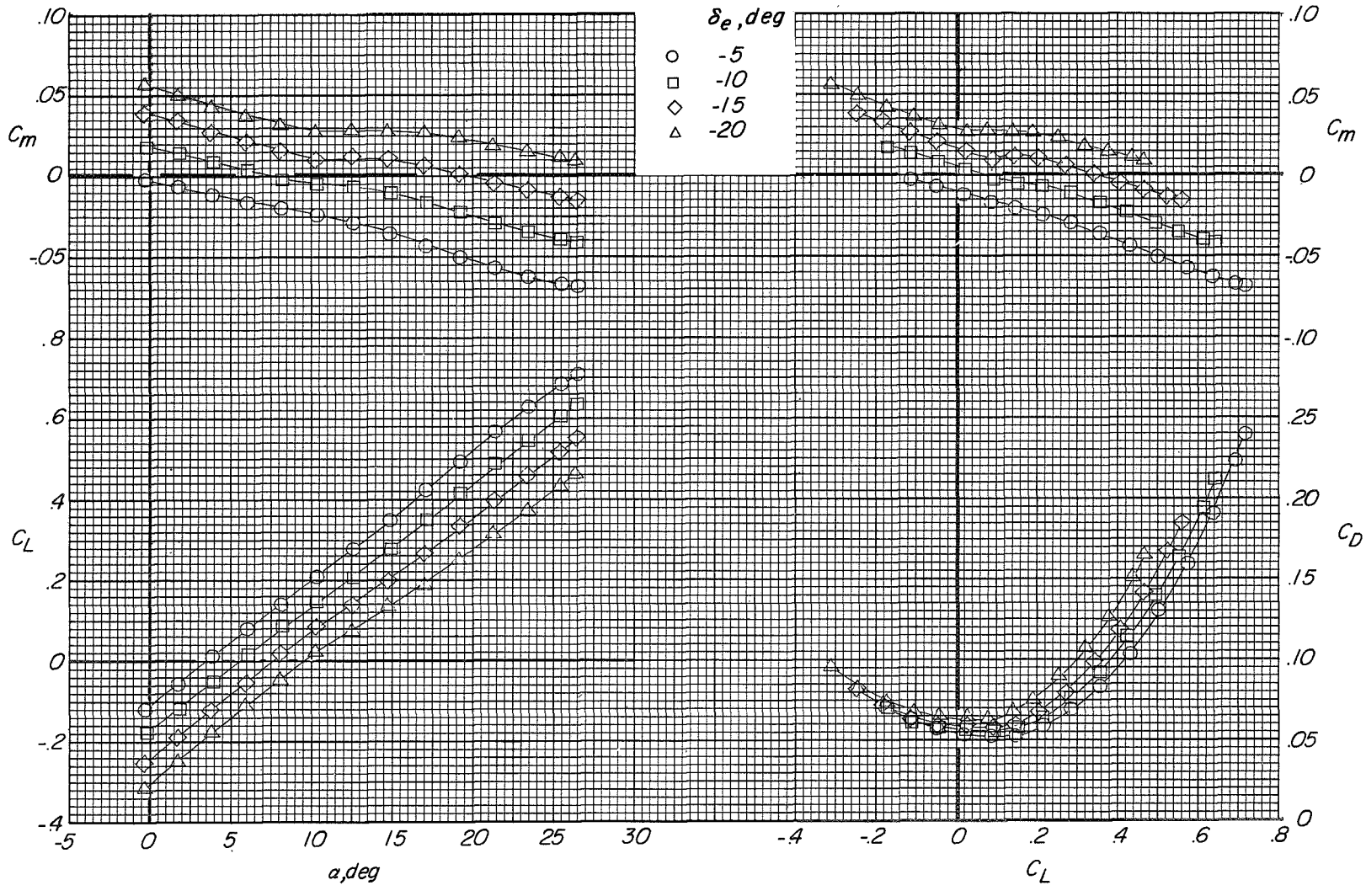
(e) $\beta = 2.3^{o}$; M = 0.80.

Figure 21.- Continued.



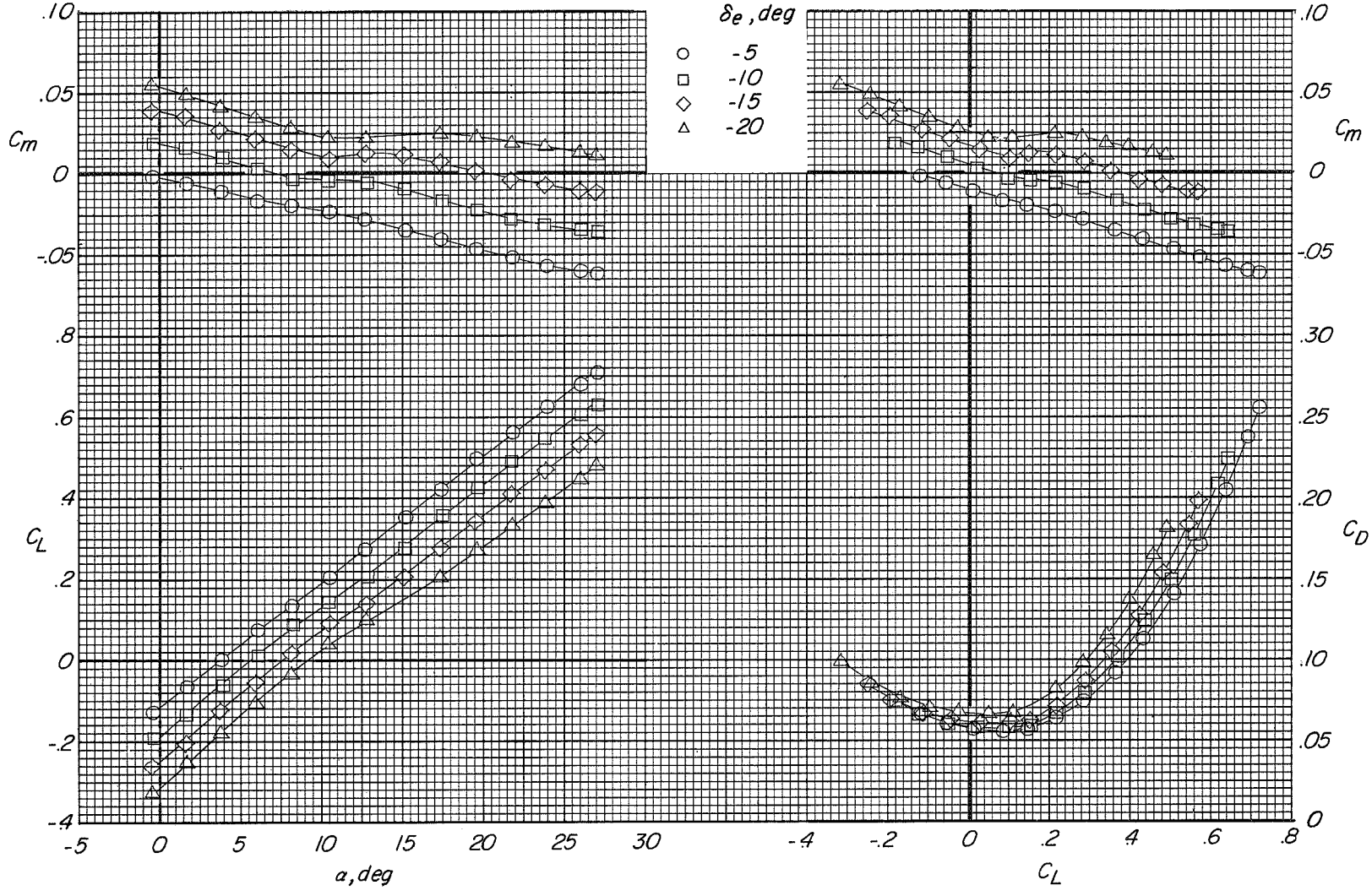
(f) $\beta = -2.3^{o}$; M = 0.35.

Figure 21.- Continued.



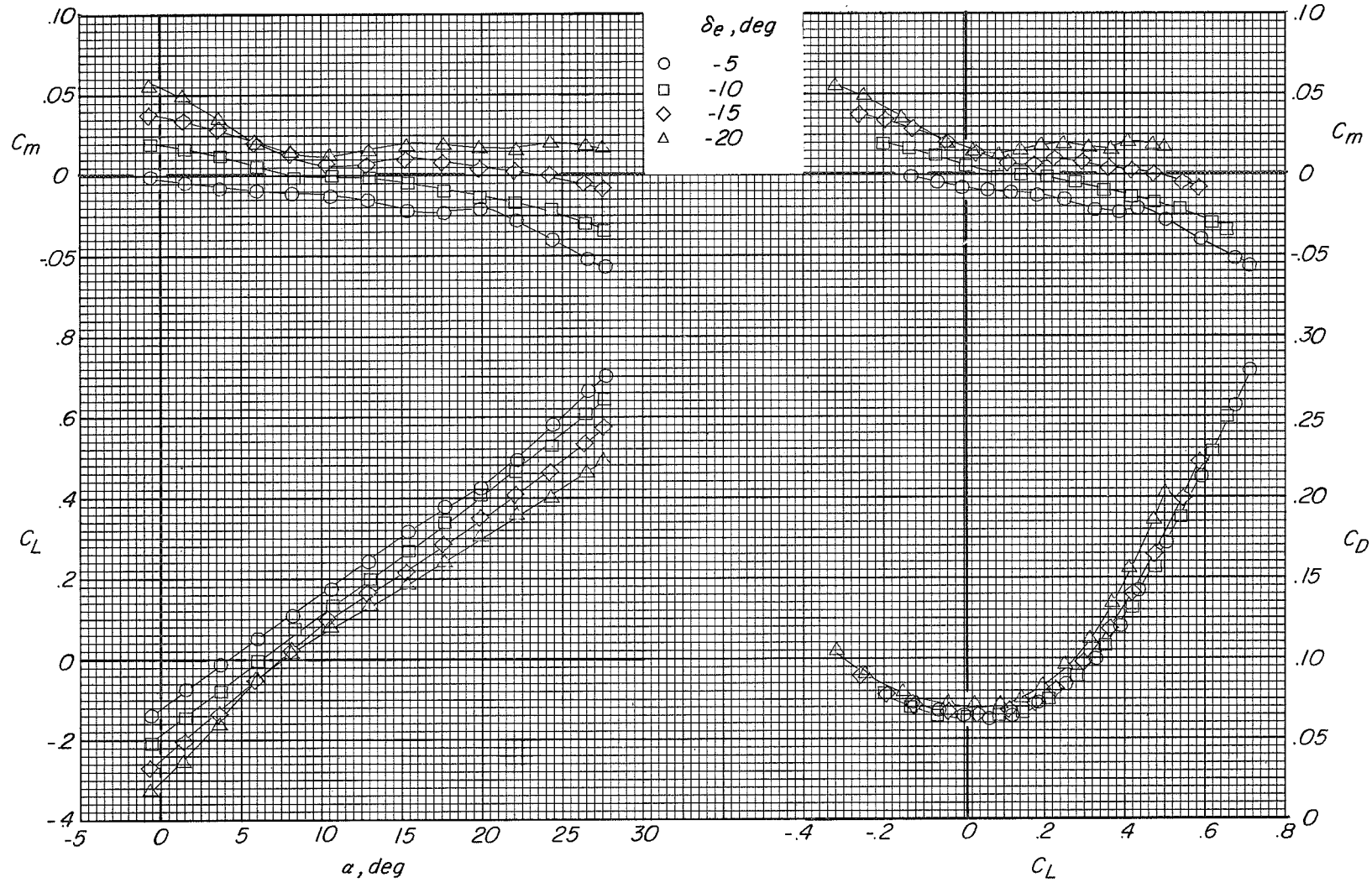
(g) $\beta = -2.3^{o}$; M = 0.50.

Figure 21.- Continued.



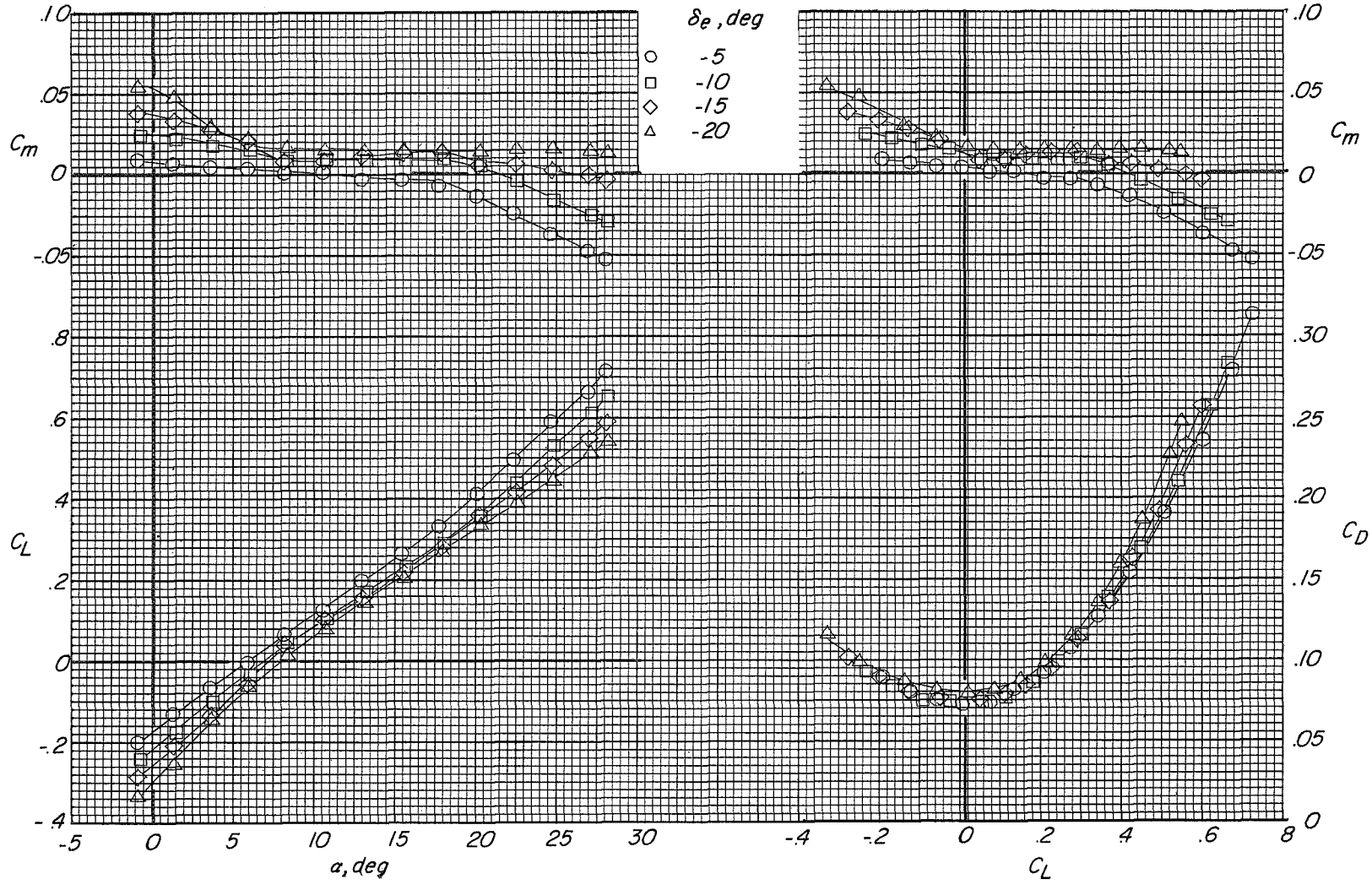
(h) $\beta = -2.3^{o}$; M = 0.60.

Figure 21.- Continued.



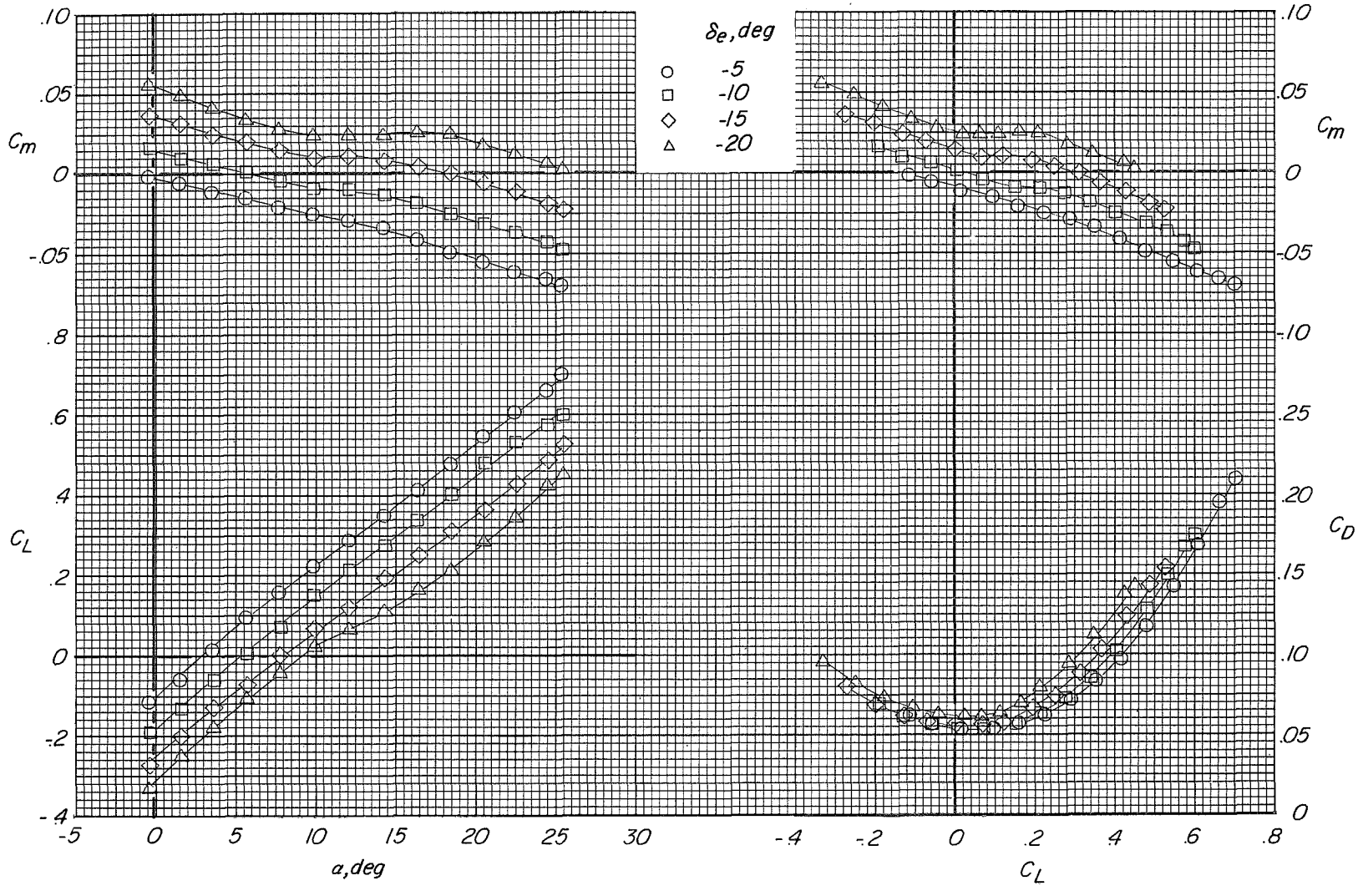
(i) $\beta = -2.3^{o}$; M = 0.70.

Figure 21.- Continued.



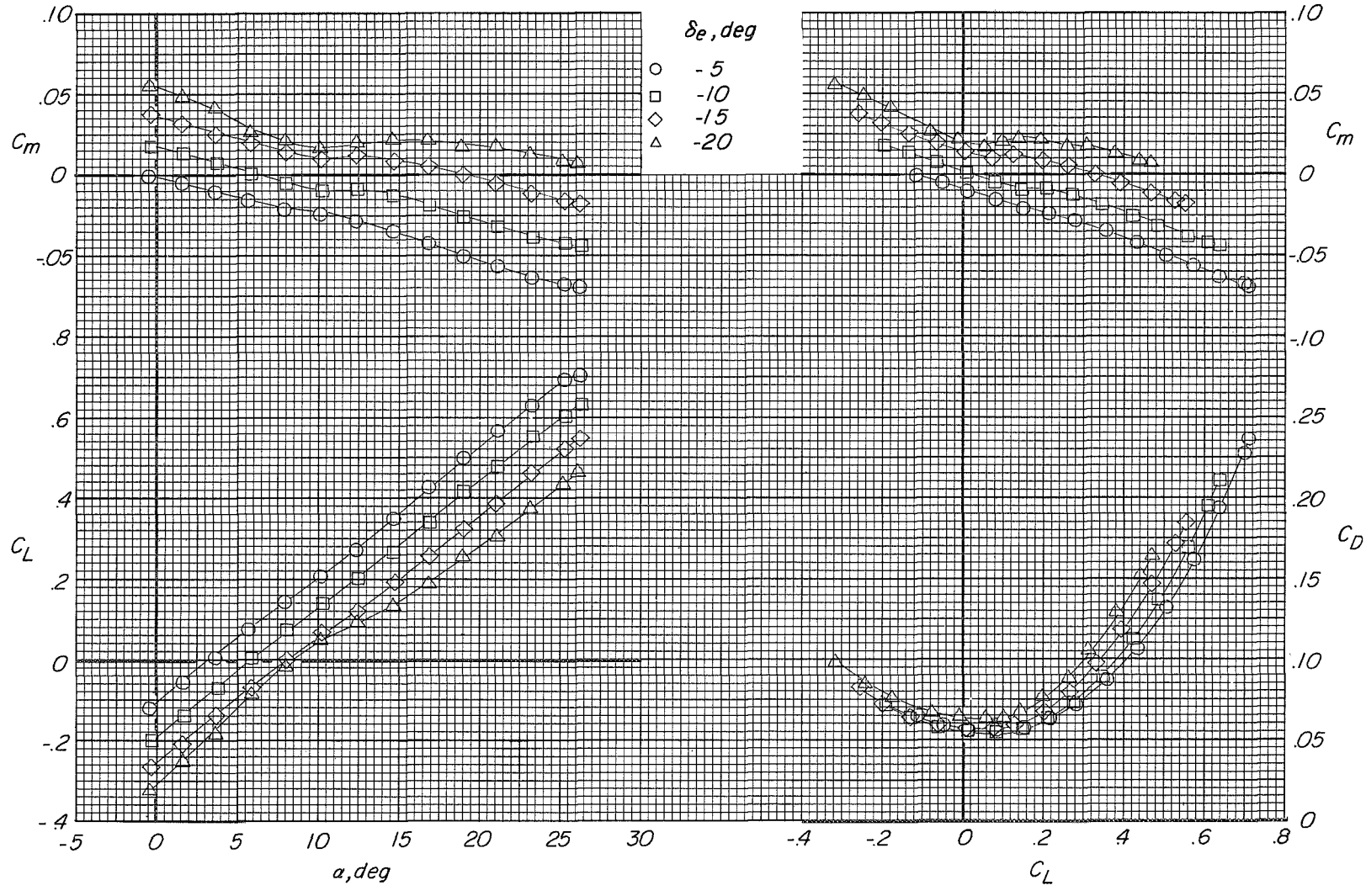
(j) $\beta = -2.3^{o}$; M = 0.80.

Figure 21.- Concluded.



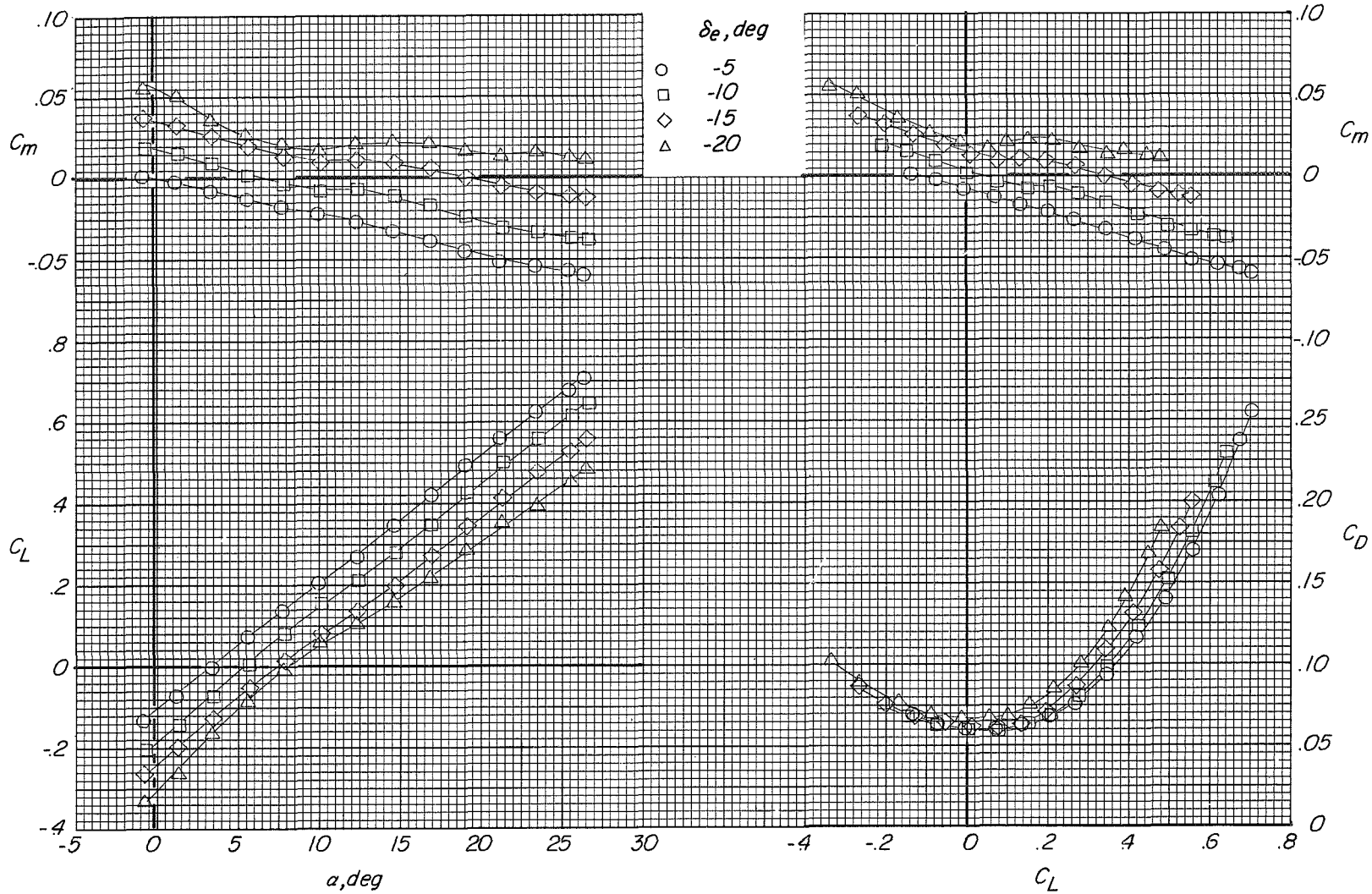
(a) $\delta_a = 10^o$; M = 0.35.

Figure 22.- Longitudinal characteristics with ailerons deflected. Modification I fin configuration; auxiliary flaps in subsonic position; $\beta = 0^o$.



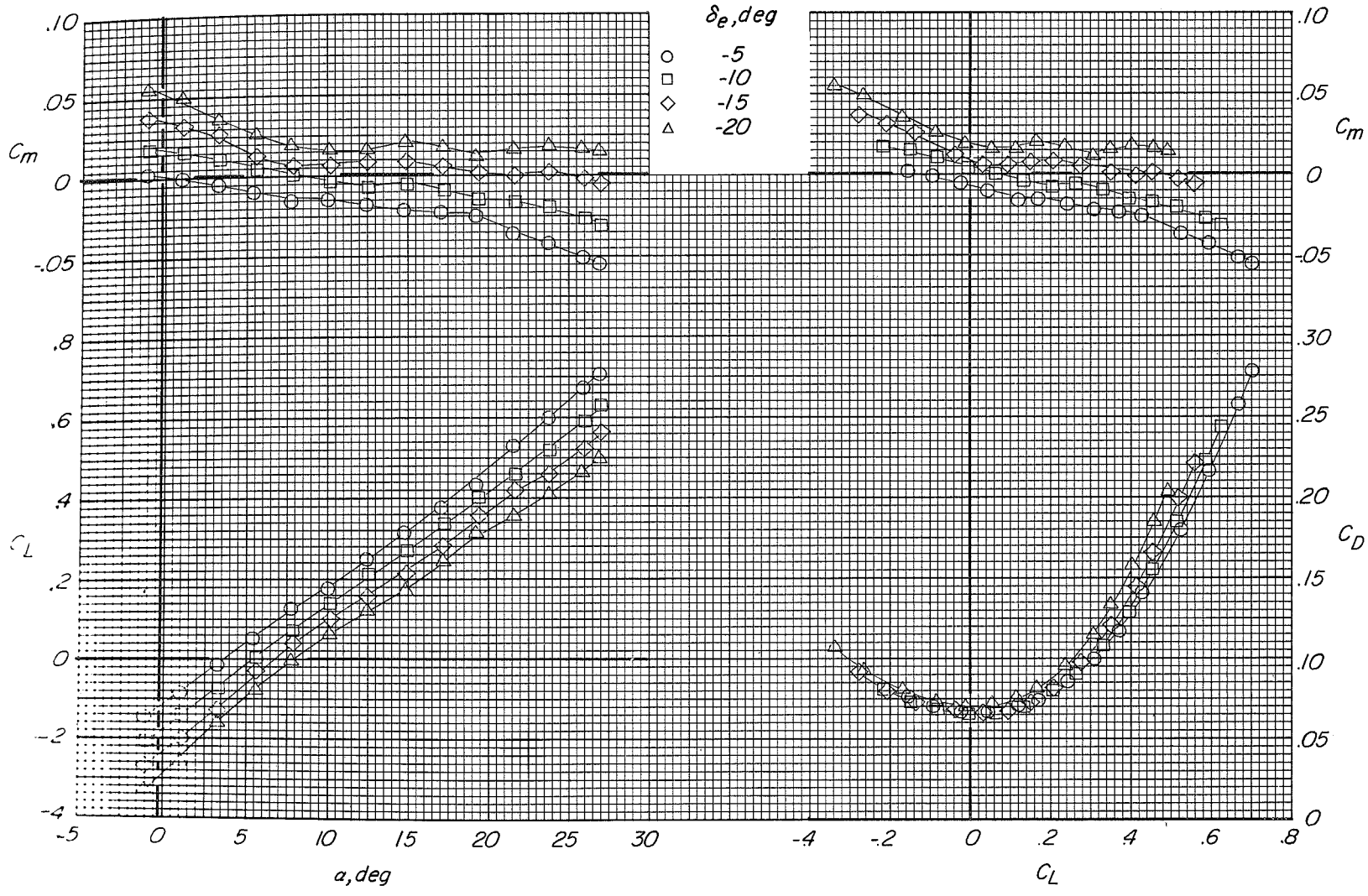
(b) $\delta_a = 10^o$; M = 0.50.

Figure 22.- Continued.



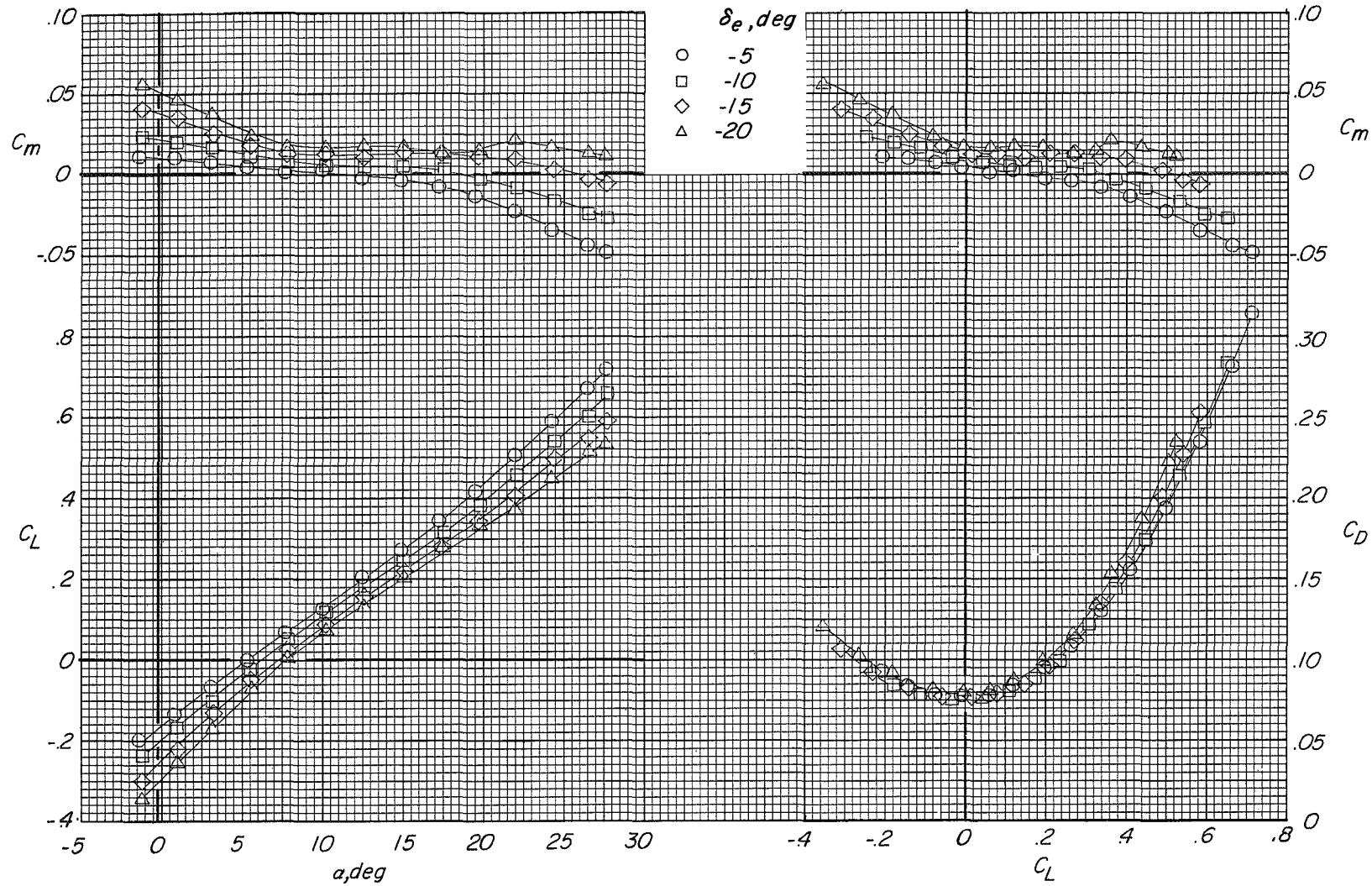
(c) $\delta_a = 10^o$; M = 0.60.

Figure 22.- Continued.



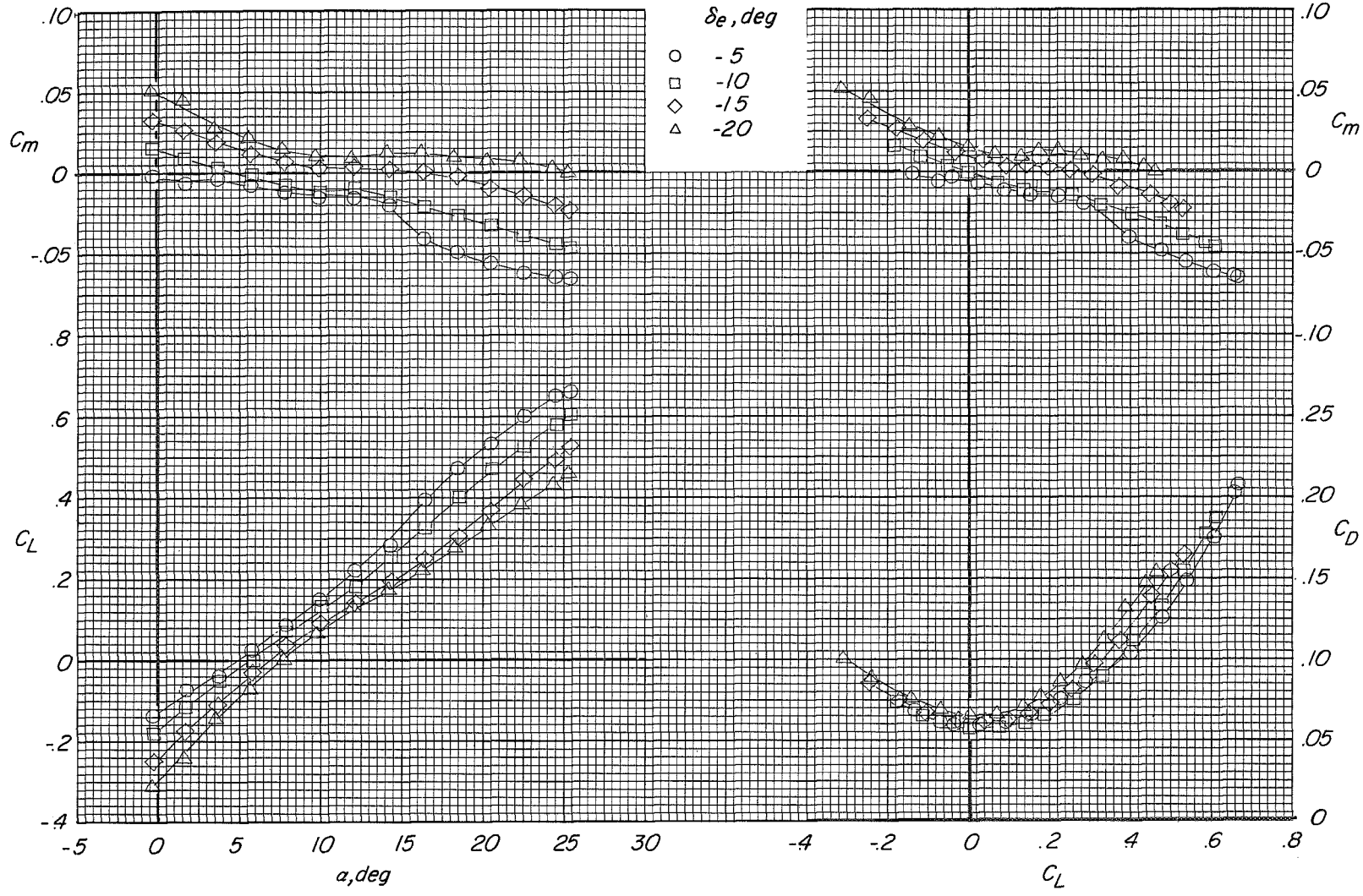
(d) $\delta_a = 10^o$; M = 0.70.

Figure 22.- Continued.



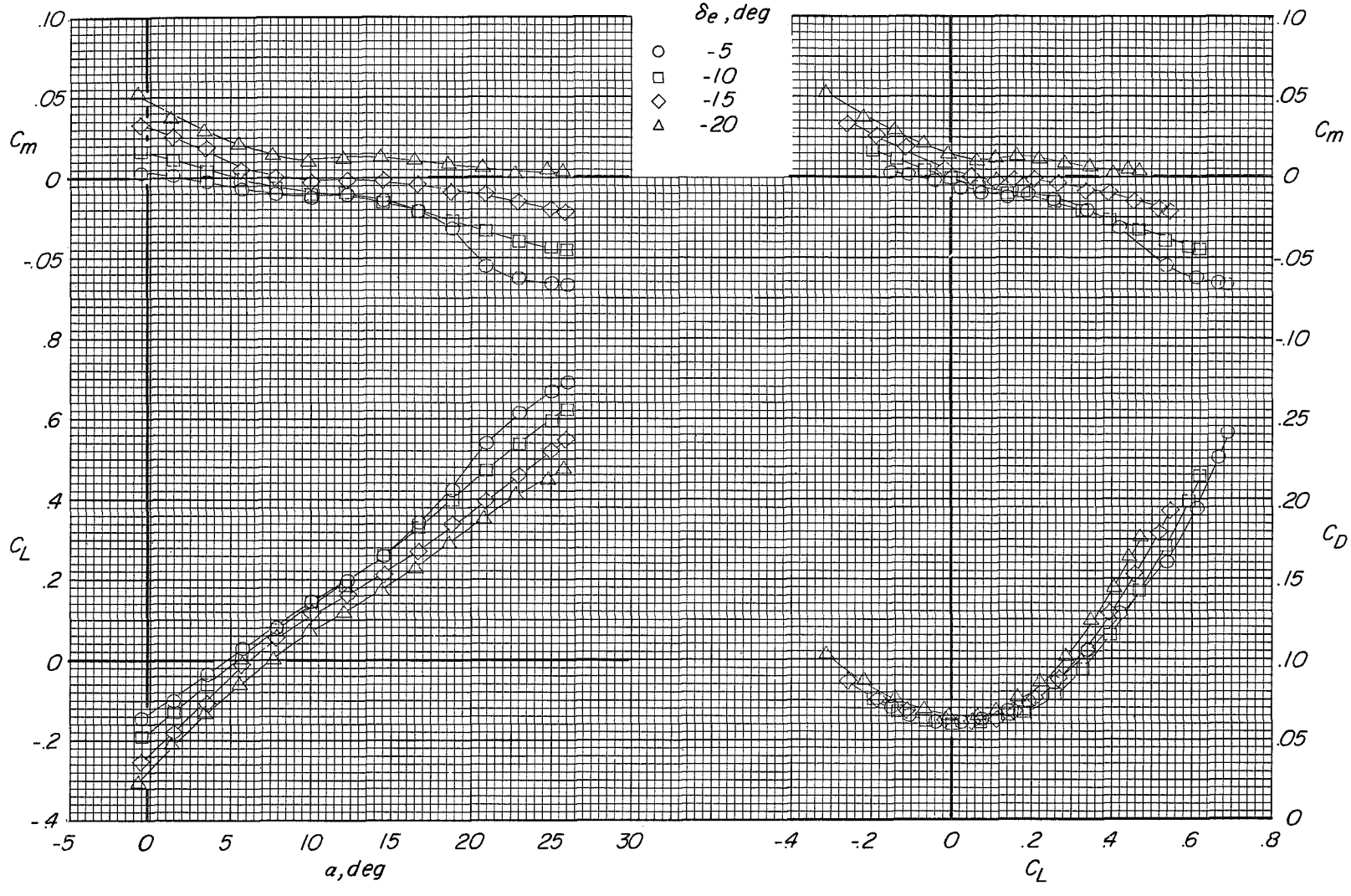
(e) $\delta_a = 10^o$; M = 0.80.

Figure 22.- Continued.



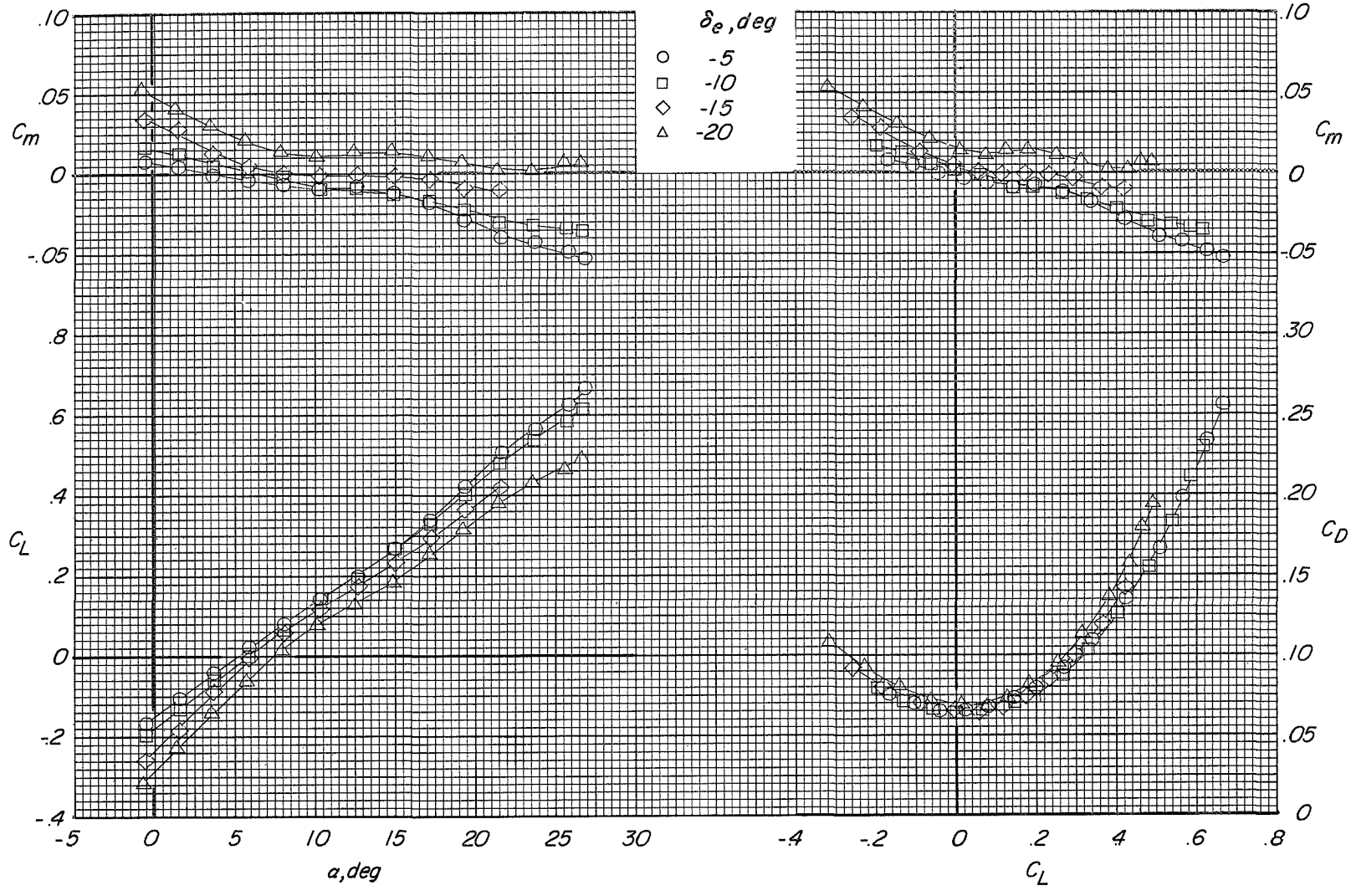
(f) $\delta_a = 20^U$; M = 0.35.

Figure 22.- Continued.



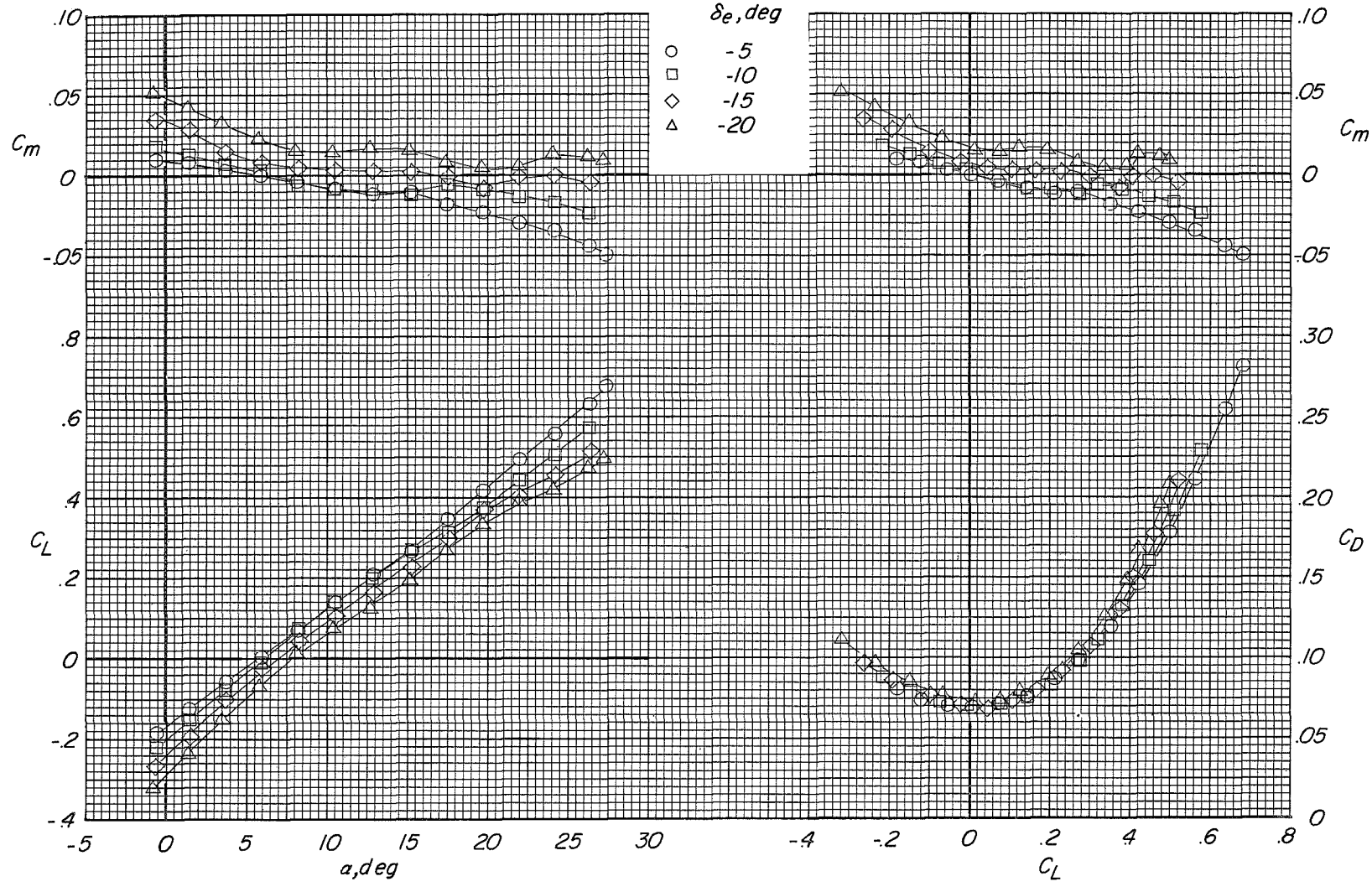
(g) $\delta_a = 20^o$; M = 0.50.

Figure 22.- Continued.



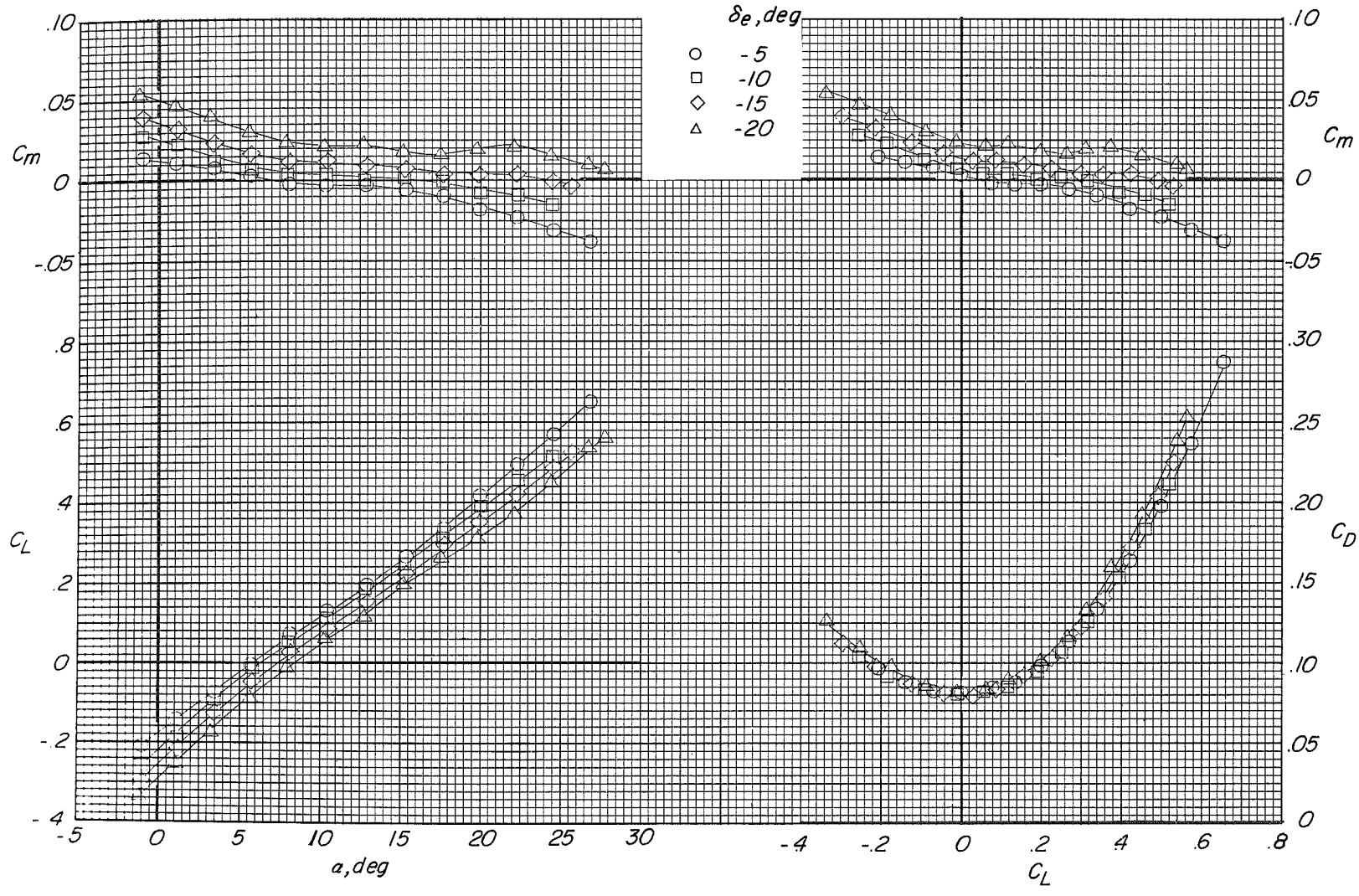
(h) $\delta_a = 20^o$; M = 0.60.

Figure 22.- Continued.



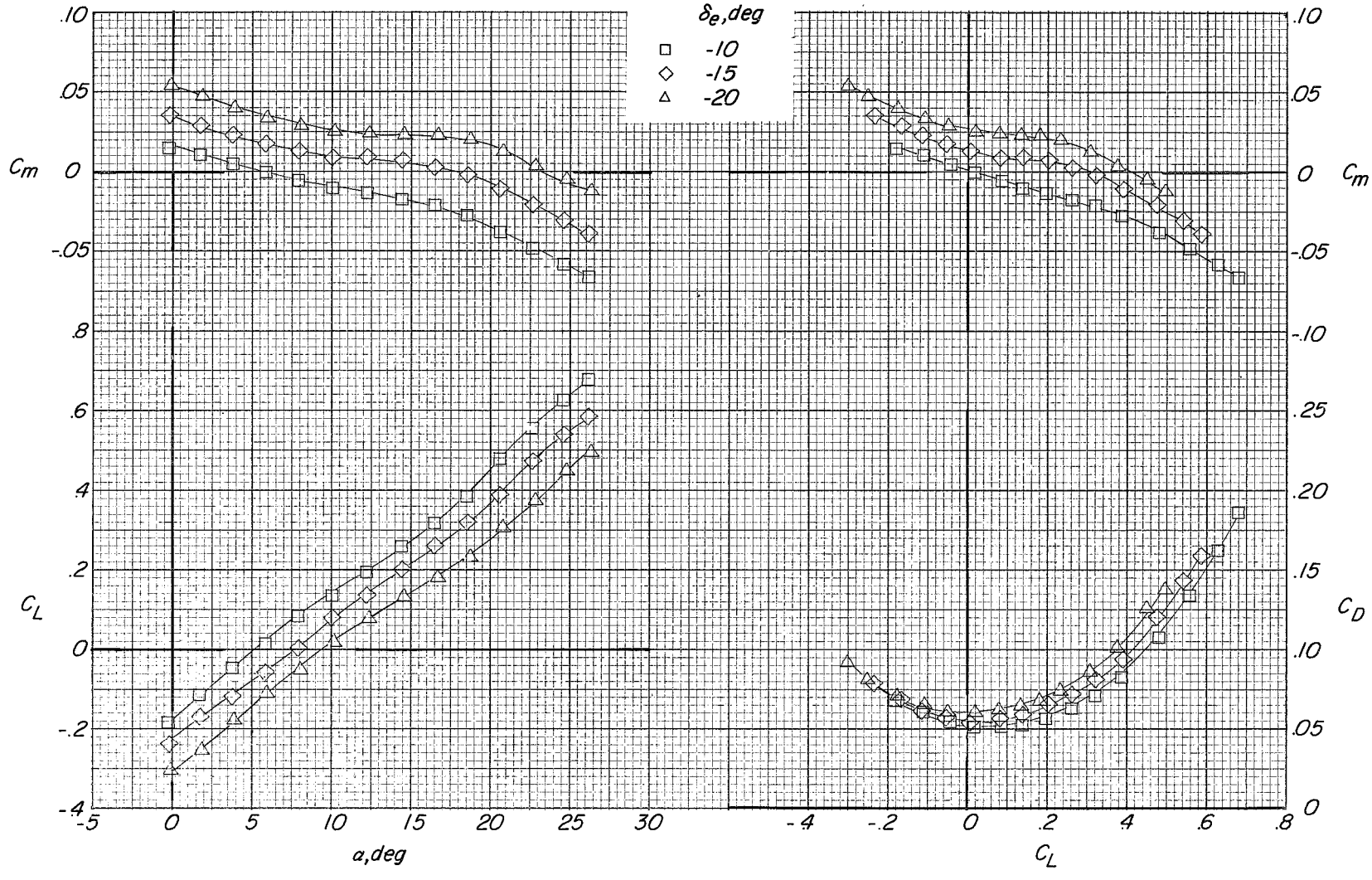
(i) $\delta_a = 20^o$; M = 0.70.

Figure 22.- Continued.



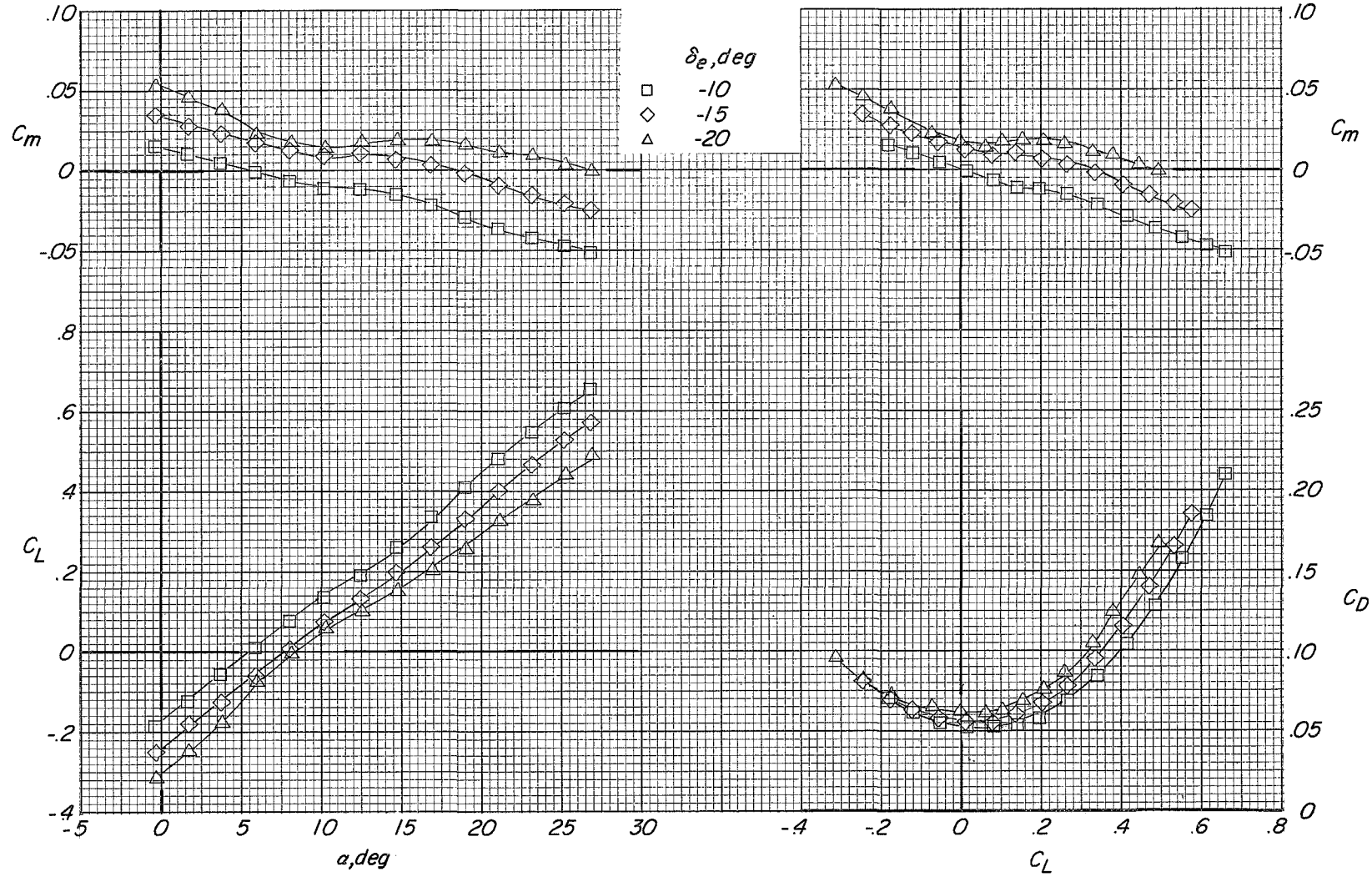
(j) $\delta_a = 20^o$; M = 0.80.

Figure 22.- Concluded.



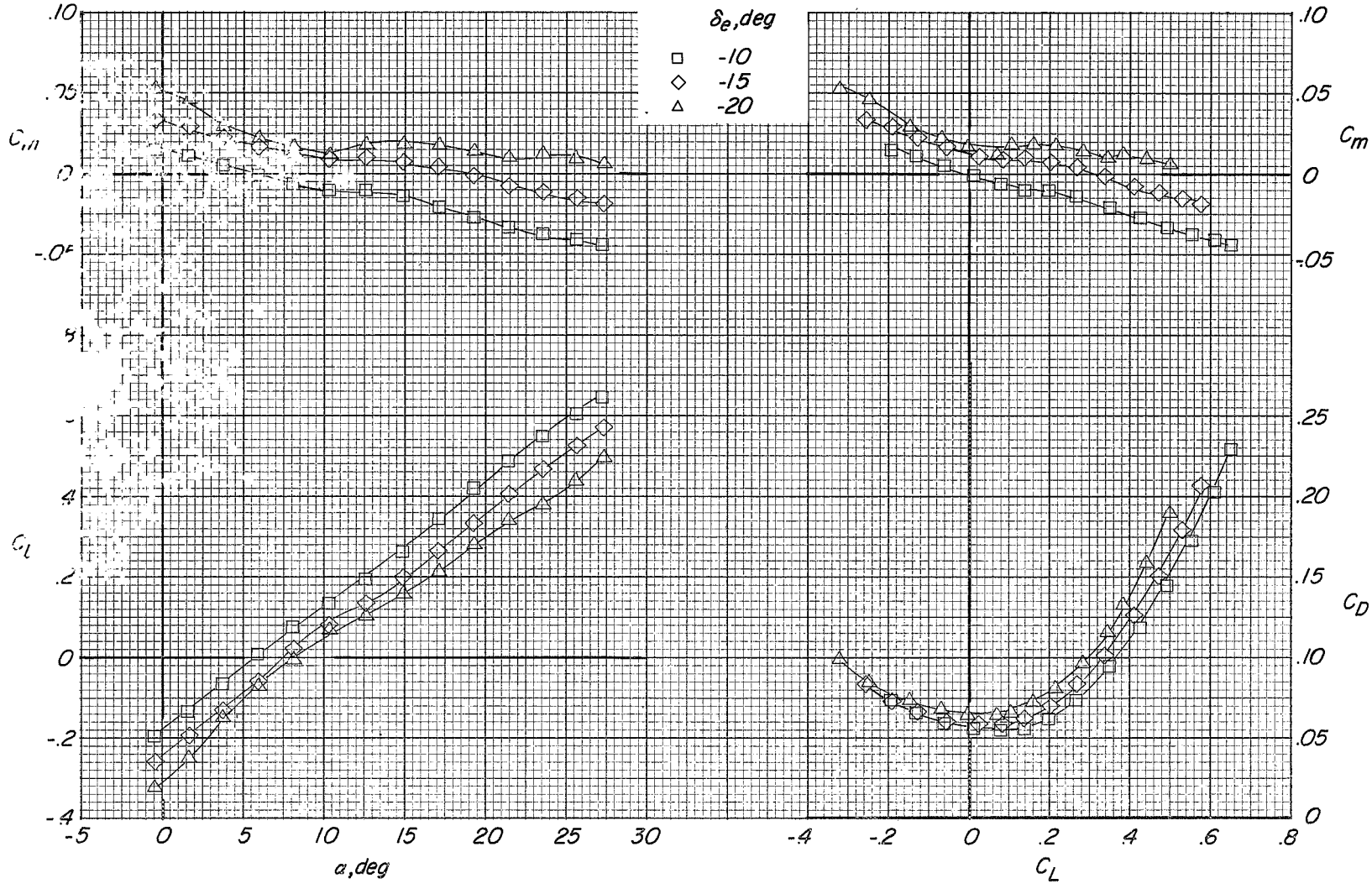
(a) $\beta = 2.3^{o}$; $\delta_a = 10^{o}$; M = 0.35.

Figure 23.- Longitudinal characteristics with combined aileron deflection and sideslip. Modification I fin configuration; auxiliary flaps in subsonic position.



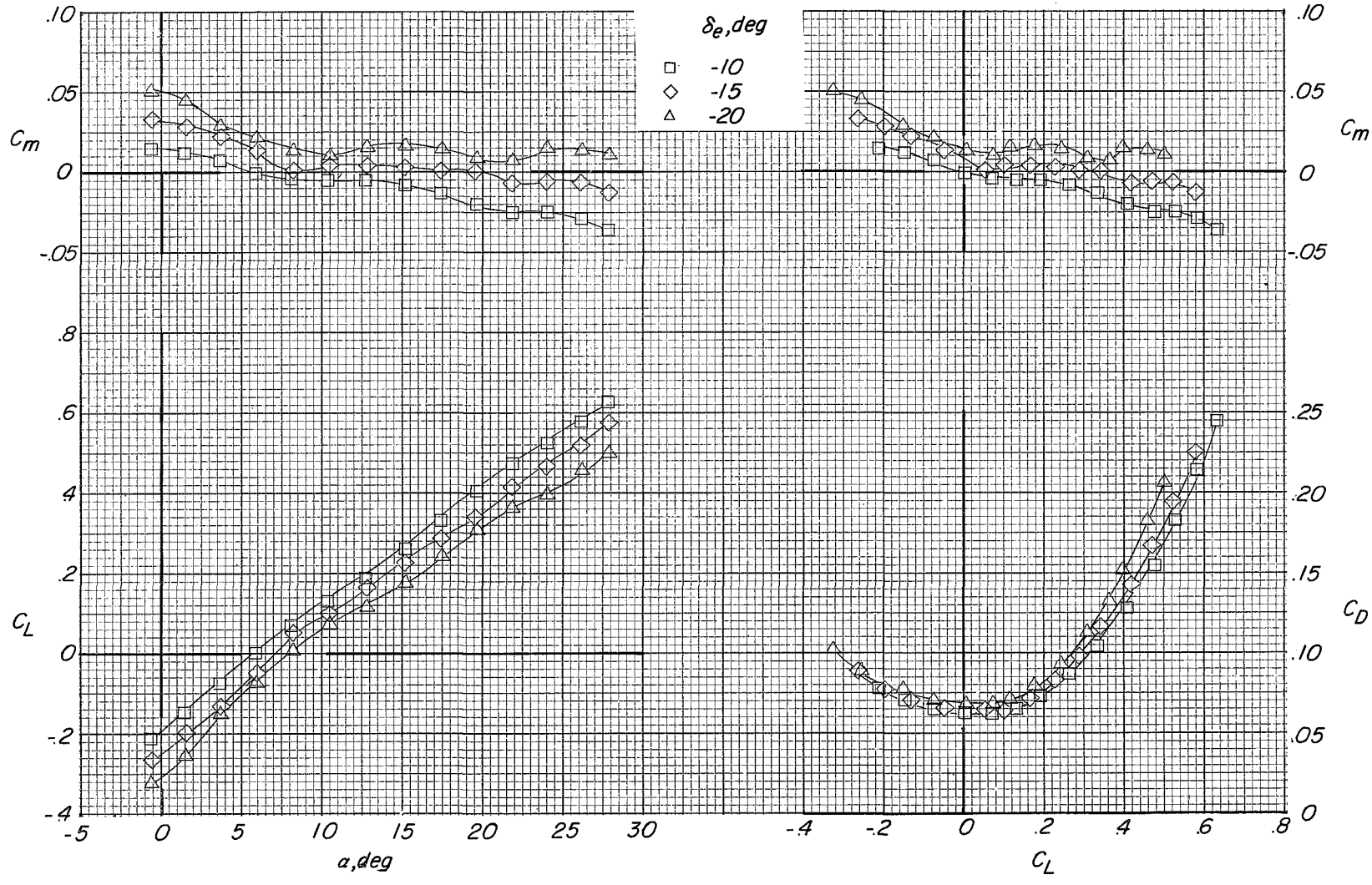
(b) $\beta = 2.3^{o}$; $\delta_a = 10^{o}$; M = 0.50.

Figure 23.- Continued.



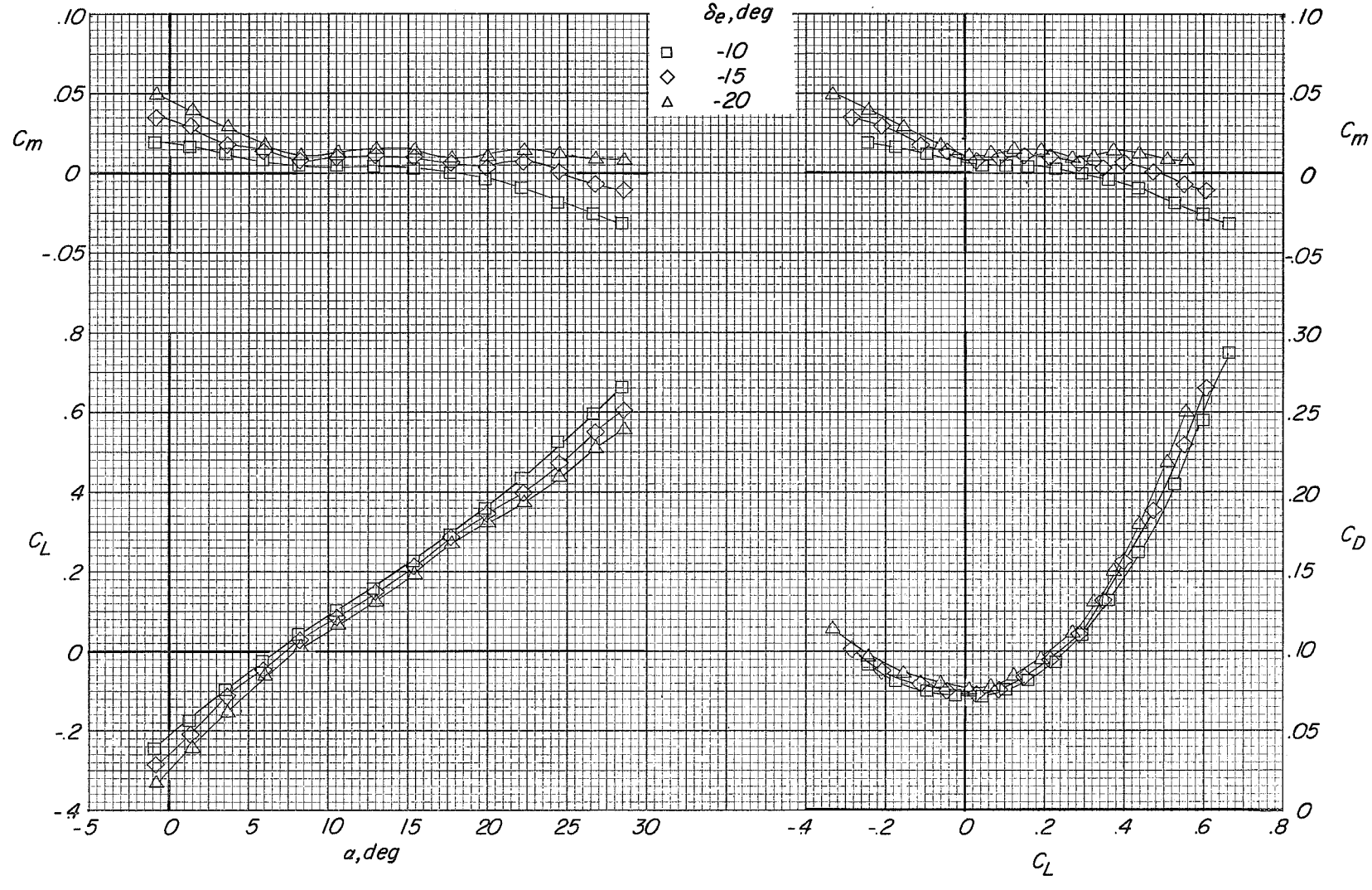
(c) $\beta = 2.3^{o}$; $\delta_a = 10^{o}$; M = 0.60.

Figure 23.- Continued.



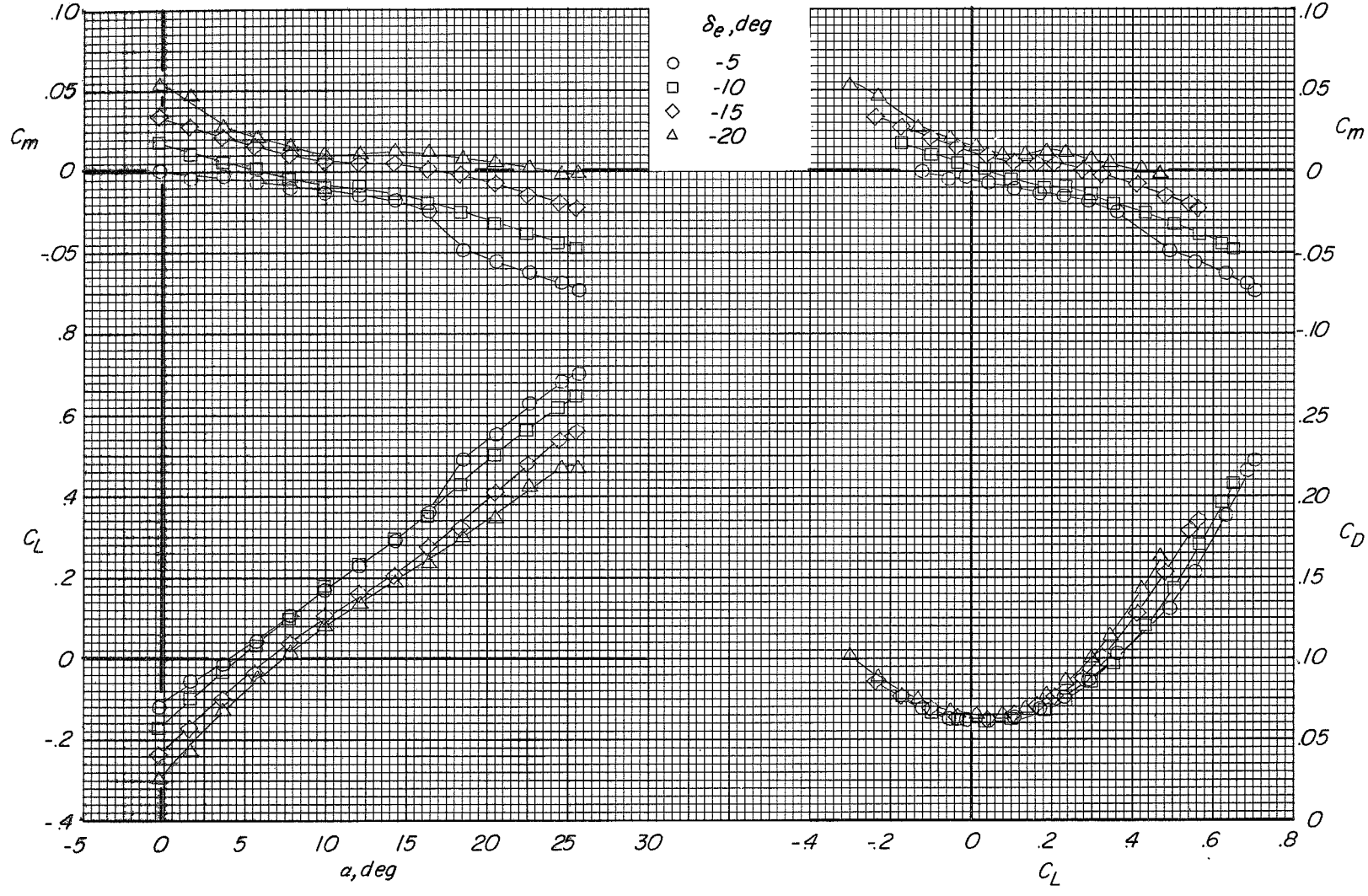
(d) $\beta = 2.3^{o}$; $\delta_a = 10^{o}$; M = 0.70.

Figure 23.- Continued.



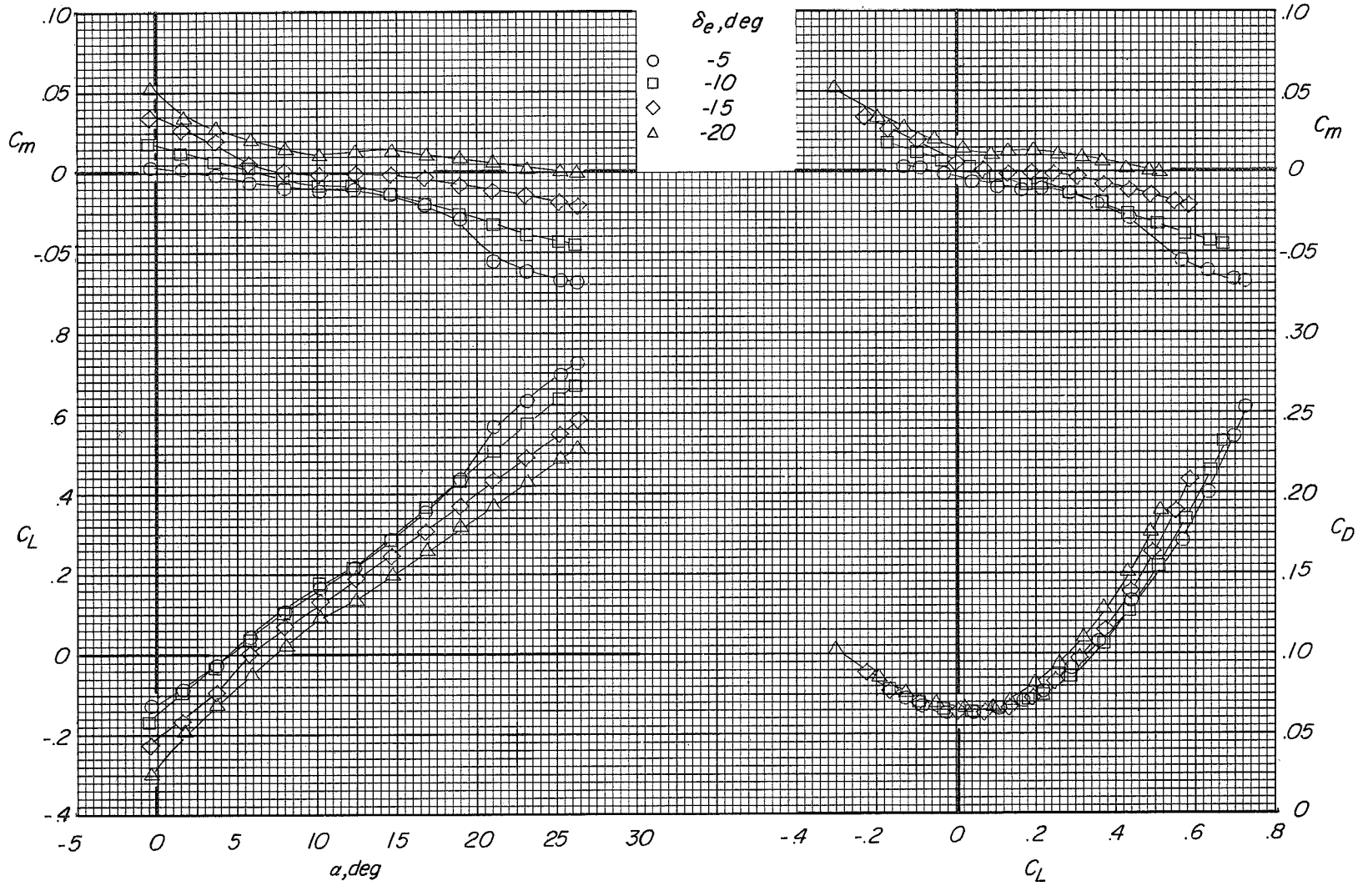
(e) $\beta = 2.3^{o}$; $\delta_a = 10^{o}$; M = 0.80.

Figure 23.- Continued.



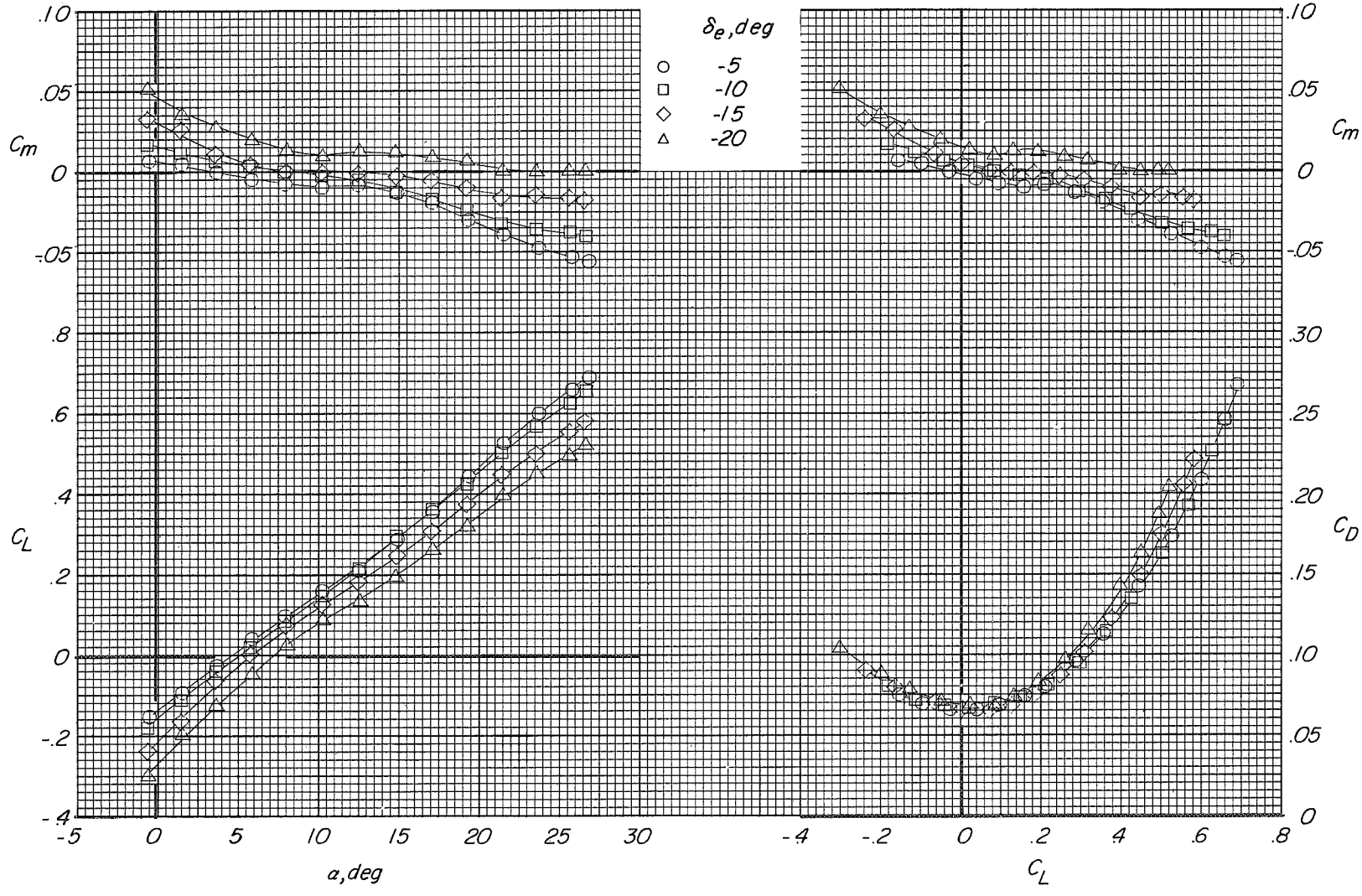
(f) $\beta = 2.3^{\circ}$; $\delta_a = 20^{\circ}$; M = 0.35.

Figure 23.- Continued.



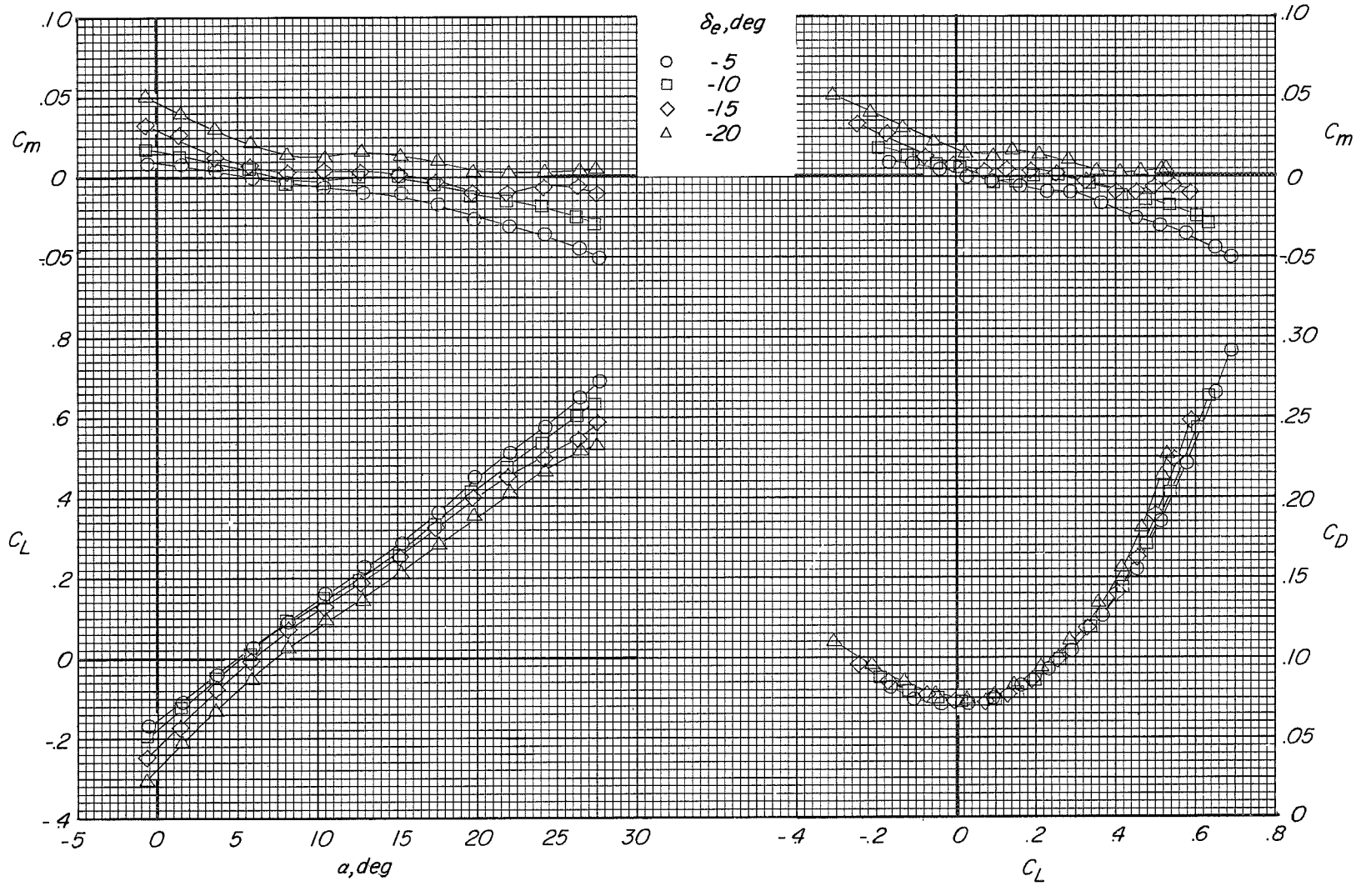
(g) $\beta = 2.3^{o}$; $\delta_a = 20^{o}$; M = 0.50.

Figure 23.- Continued.



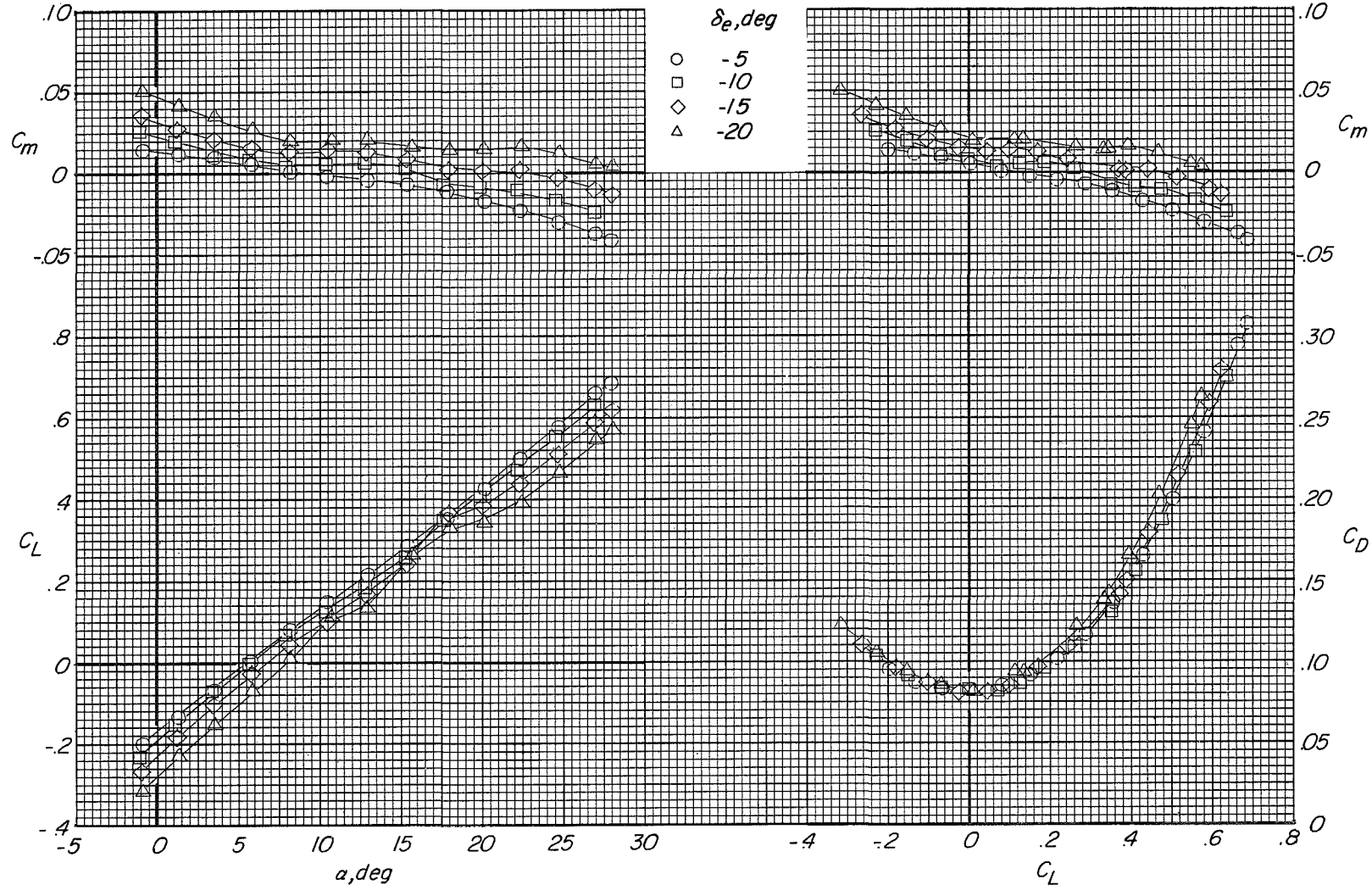
(h) $\beta = 2.3^{\circ}$; $\delta_a = 20^{\circ}$; M = 0.60.

Figure 23.- Continued.



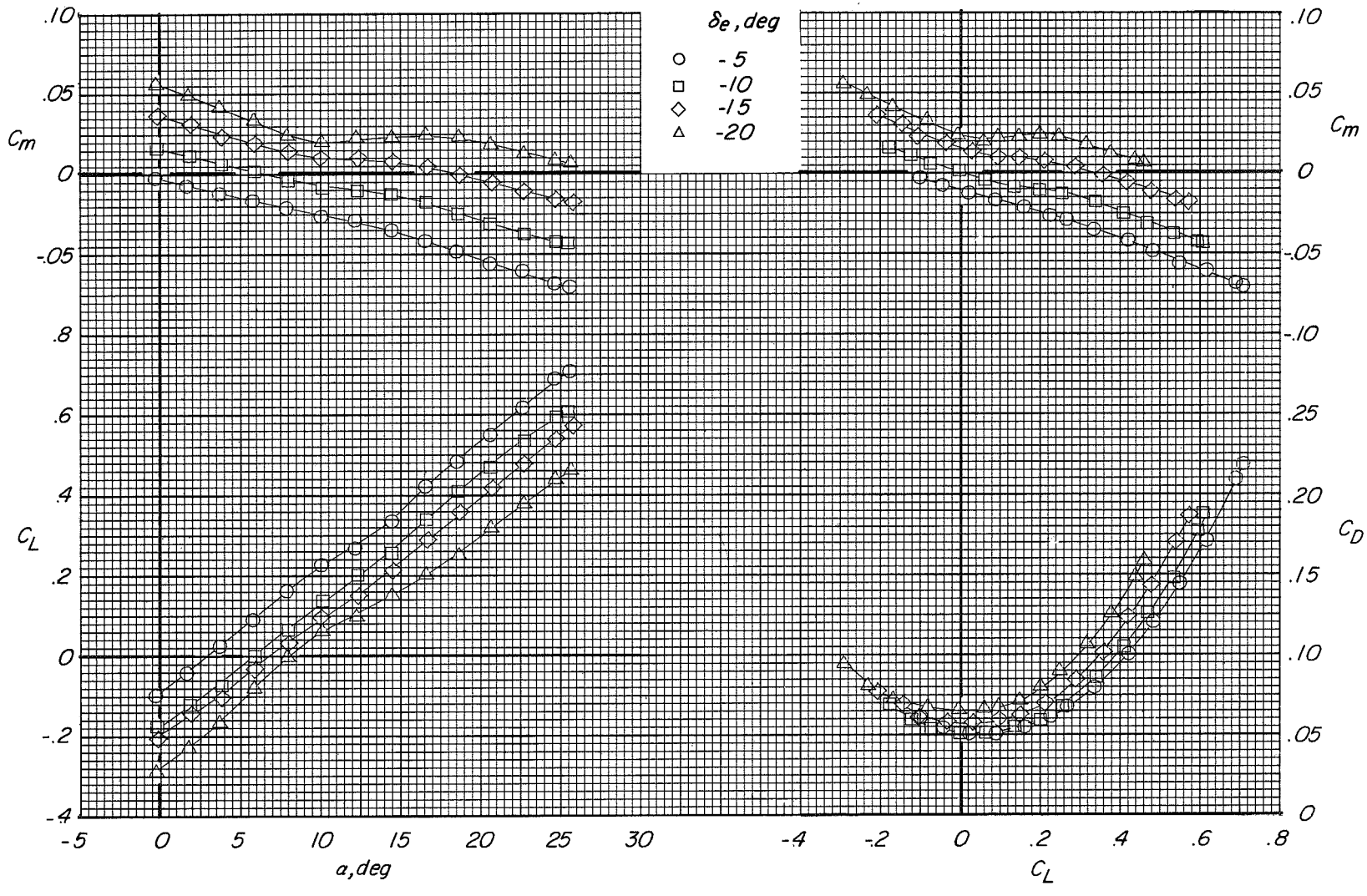
(i) $\beta = 2.3^{o}$; $\delta_a = 20^{o}$; M = 0.70.

Figure 23.- Continued.



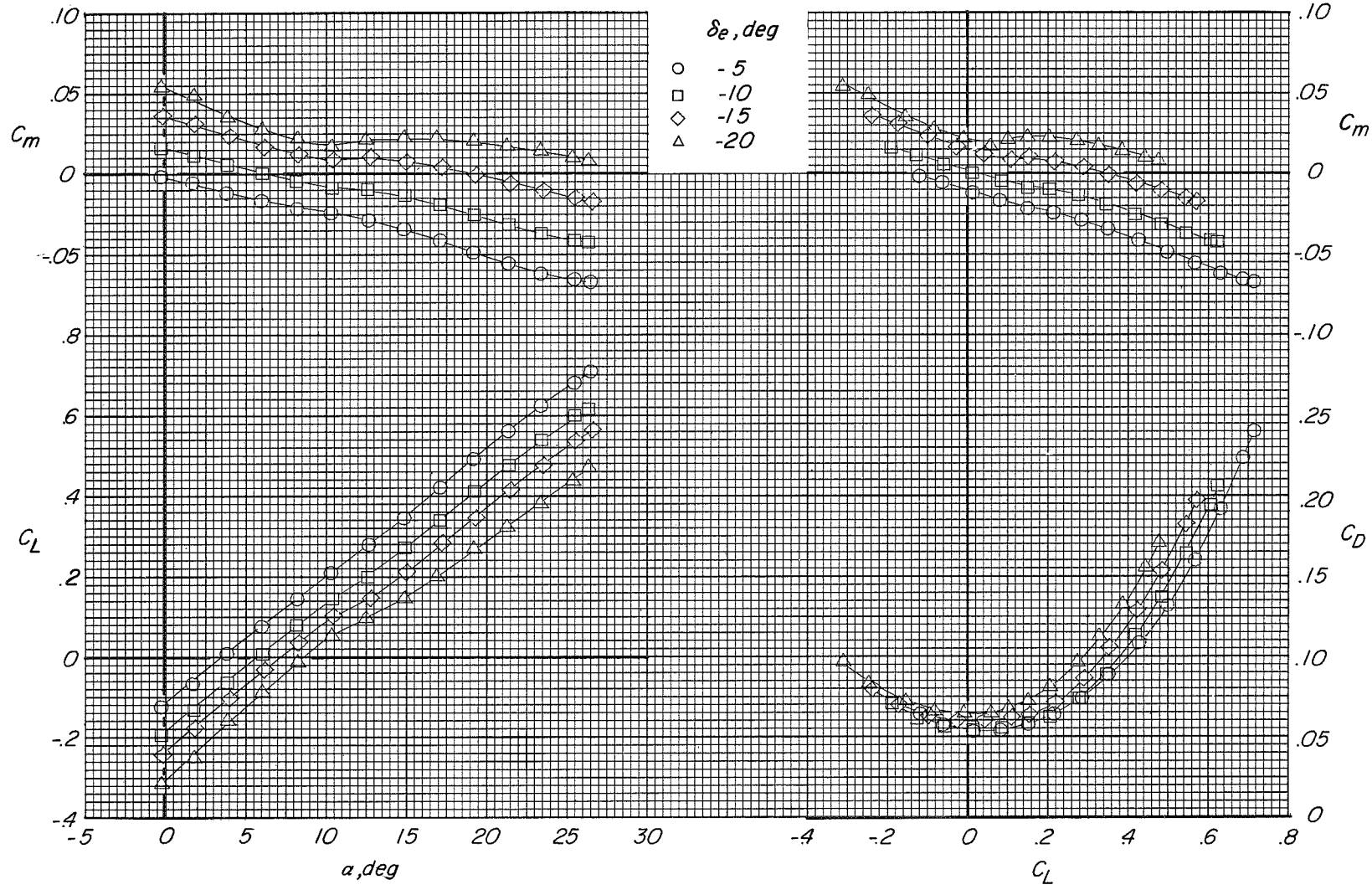
(j) $\beta = 2.3^{o}$; $\delta_a = 20^{o}$; M = 0.80.

Figure 23.- Continued.



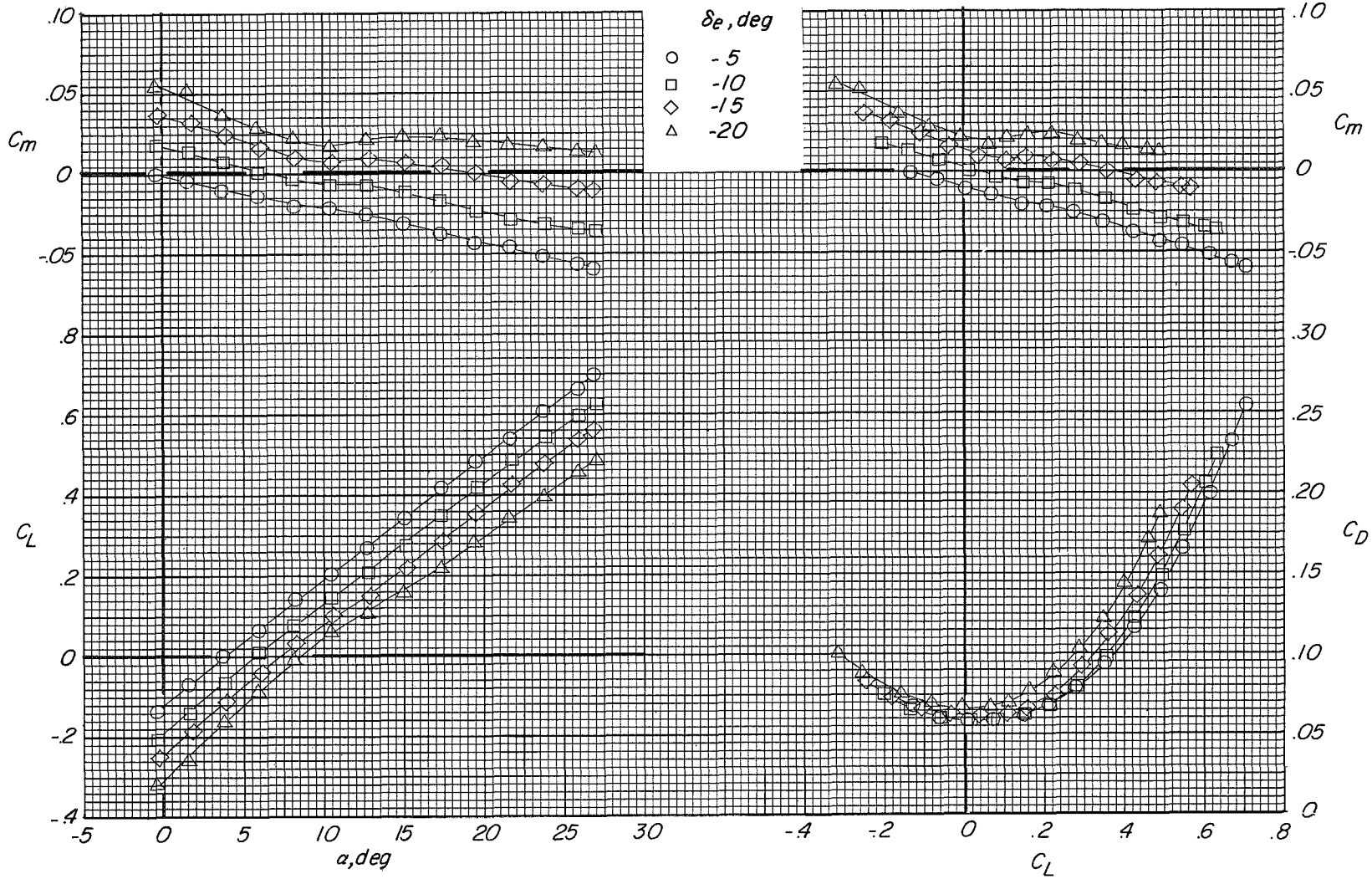
(k) $\beta = -2.3^{o}$; $\delta_a = 10^{o}$; M = 0.35.

Figure 23.- Continued.



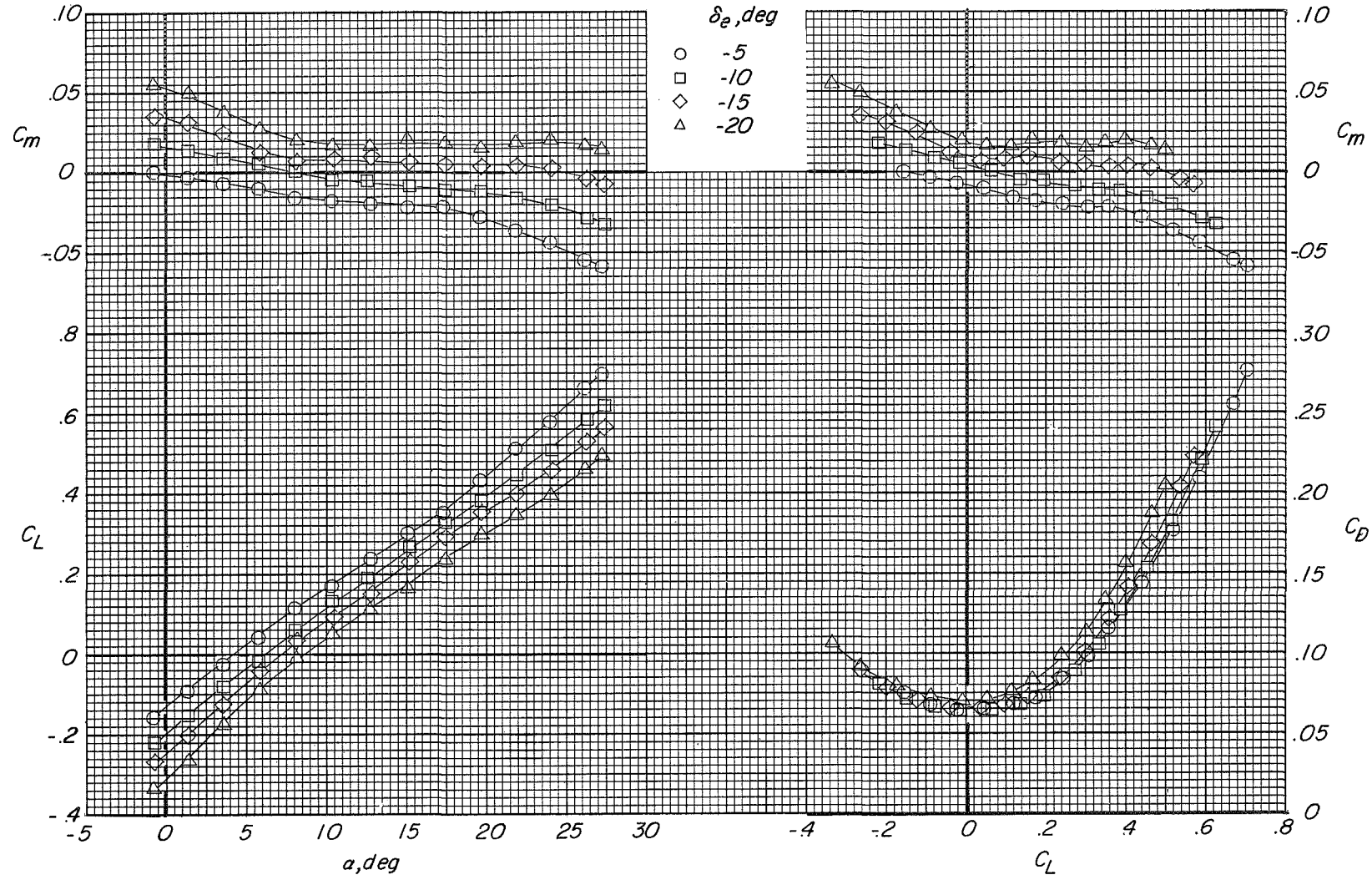
(l) $\beta = -2.3^{o}$; $\delta_a = 10^{o}$; M = 0.50.

Figure 23.- Continued.



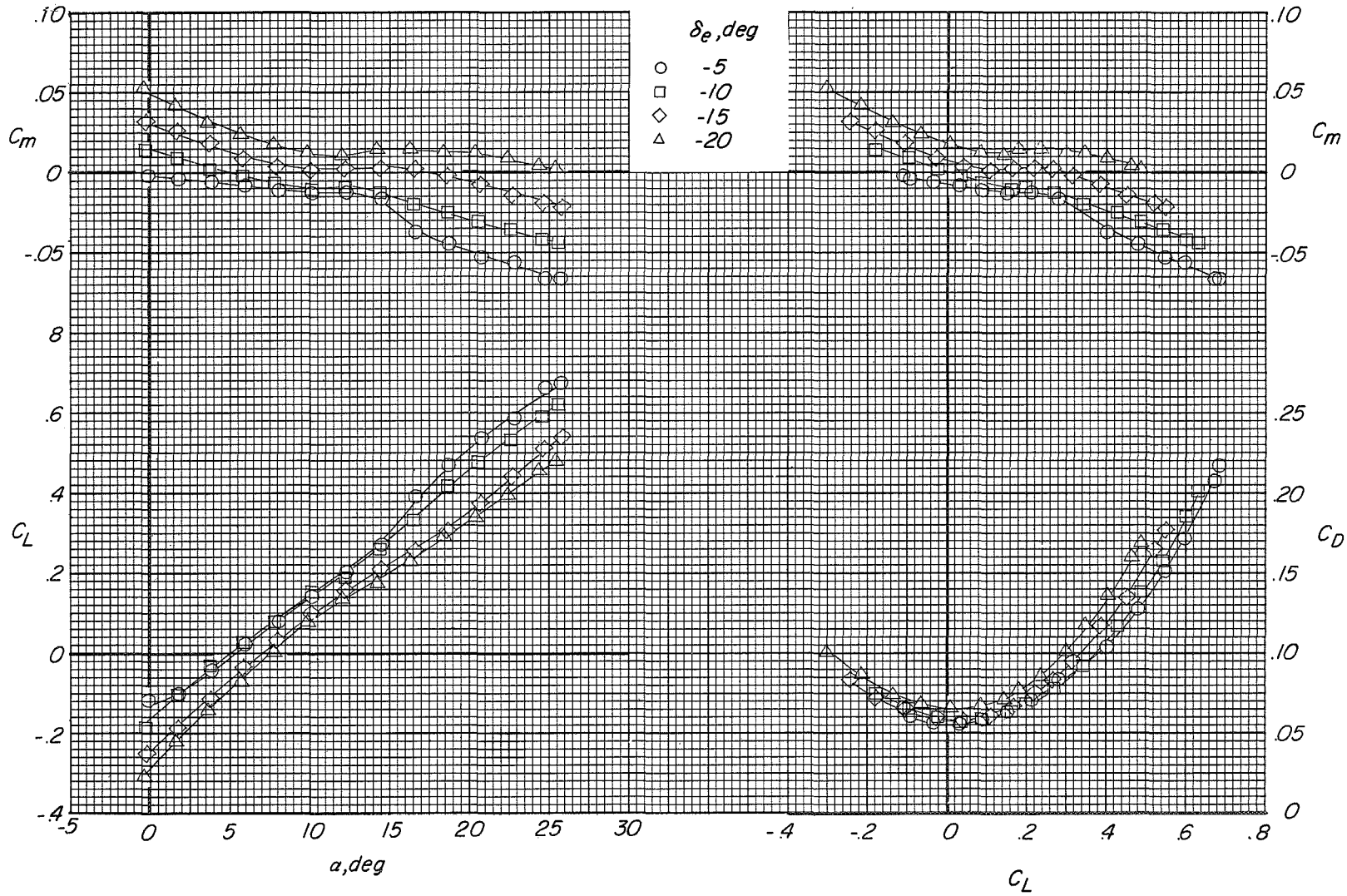
(m) $\beta = -2.3^{o}$; $\delta_a = 10^{o}$; M = 0.60.

Figure 23.- Continued.



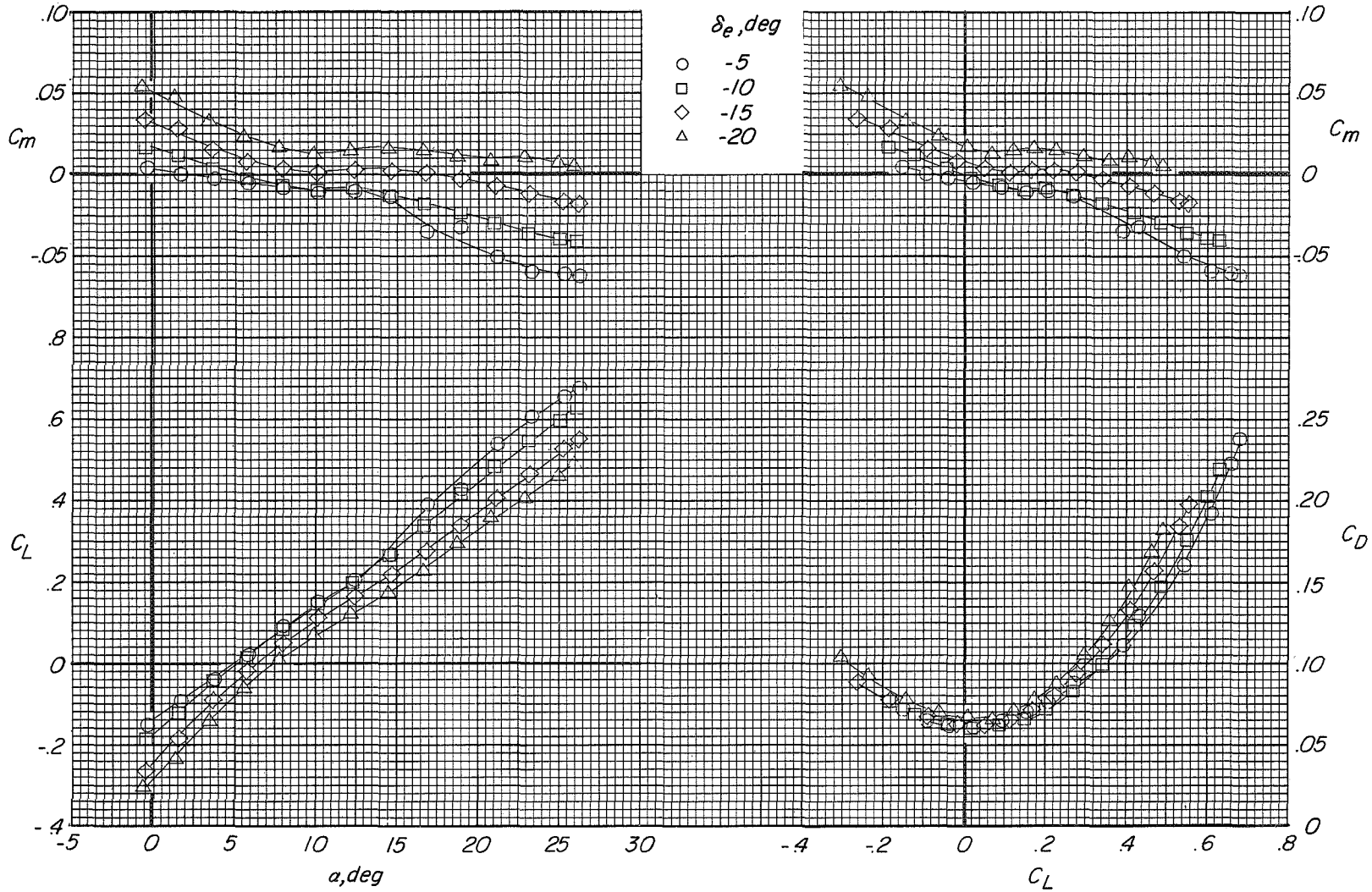
(n) $\beta = -2.3^{o}$; $\delta_a = 10^{o}$; M = 0.70.

Figure 23.- Continued.



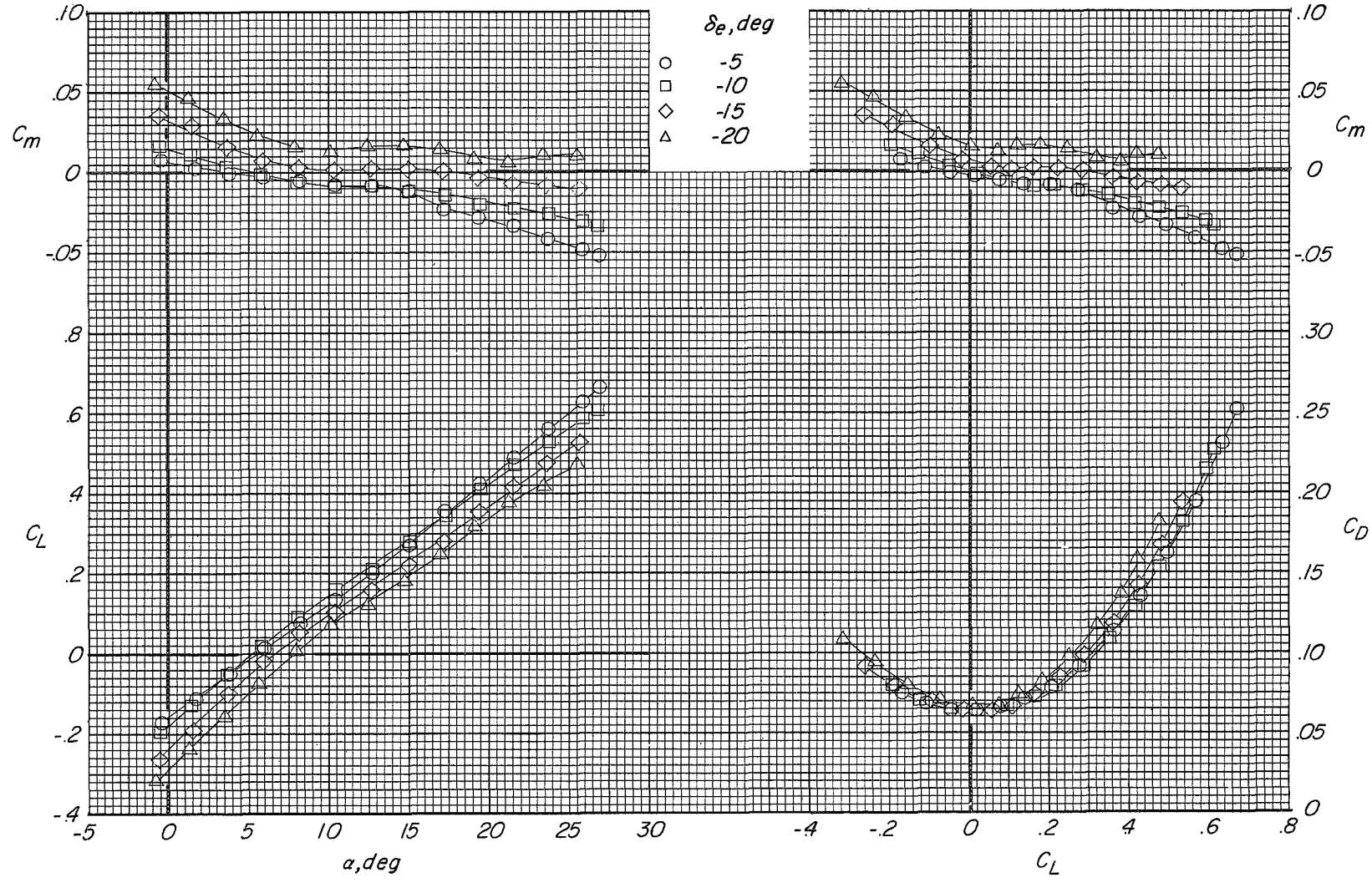
(o) $\beta = -2.3^{o}$; $\delta_a = 20^{o}$; $M = 0.35$.

Figure 23.- Continued.



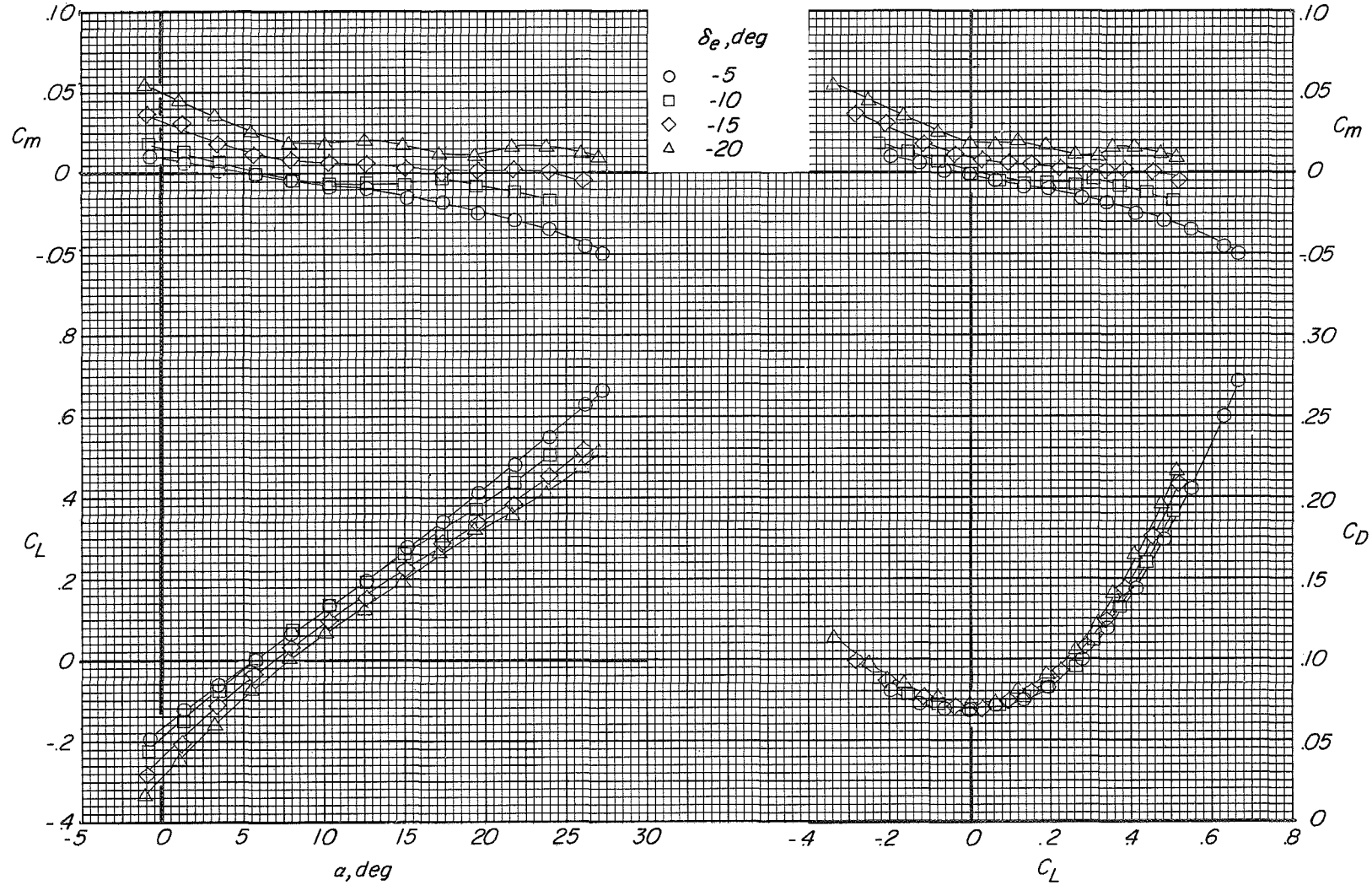
(p) $\beta = -2.3^{\circ}$; $\delta_a = 20^{\circ}$; M = 0.50.

Figure 23.- Continued.



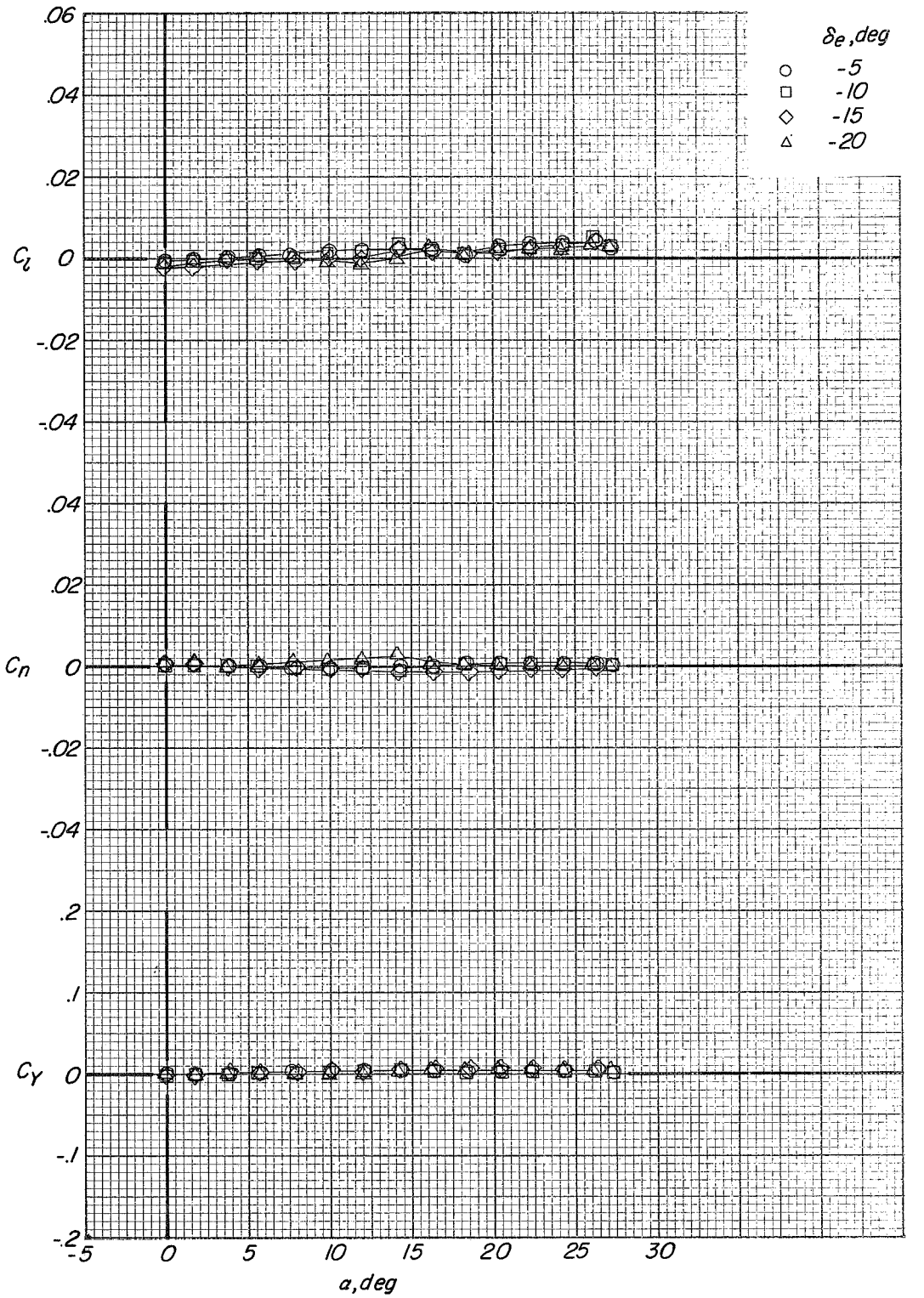
(q) $\beta = -2.3^{o}$; $\delta_a = 20^{o}$; M = 0.60.

Figure 23.- Continued.



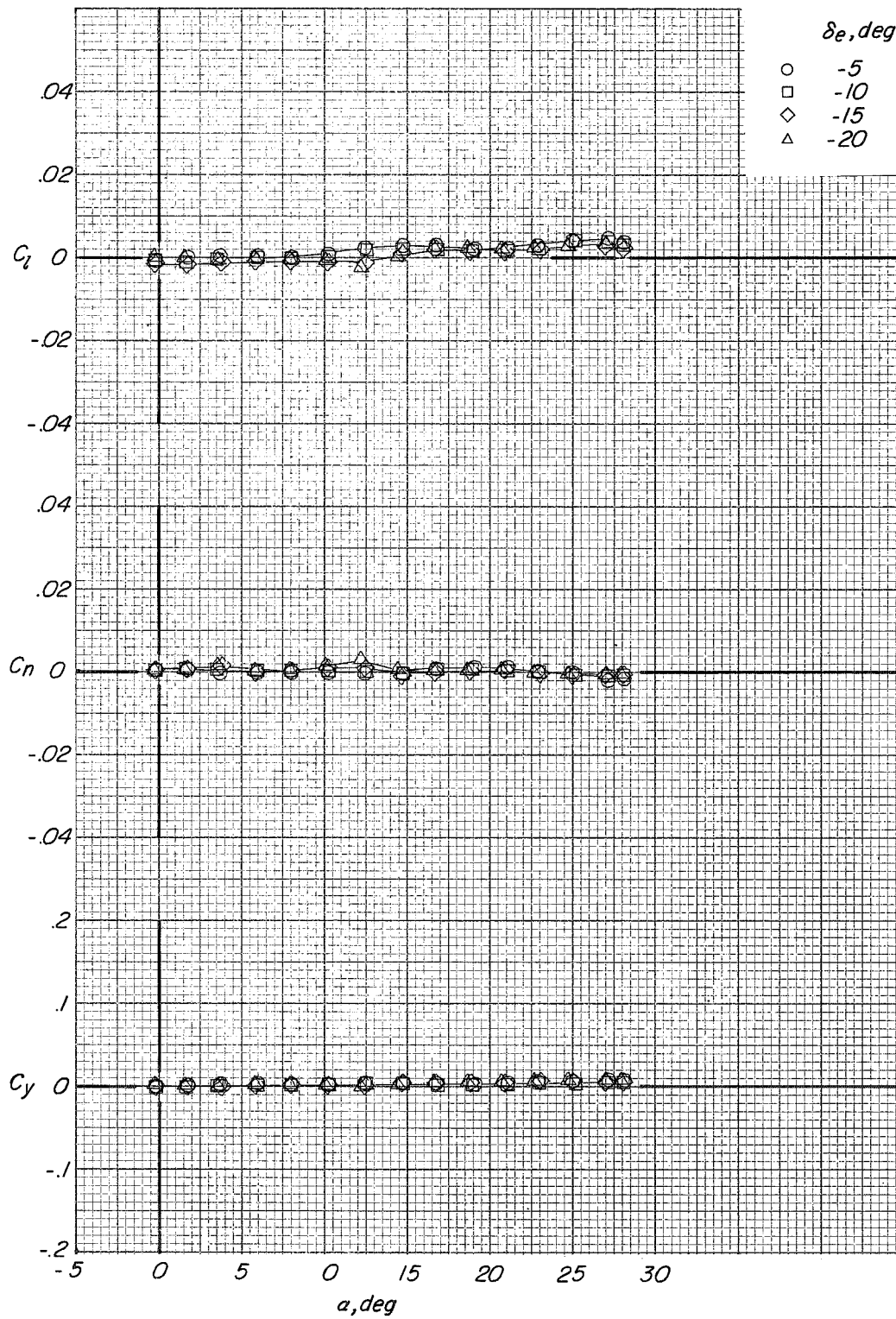
(r) $\beta = -2.3^{o}$; $\delta_a = 20^{o}$; M = 0.70.

Figure 23.- Concluded.



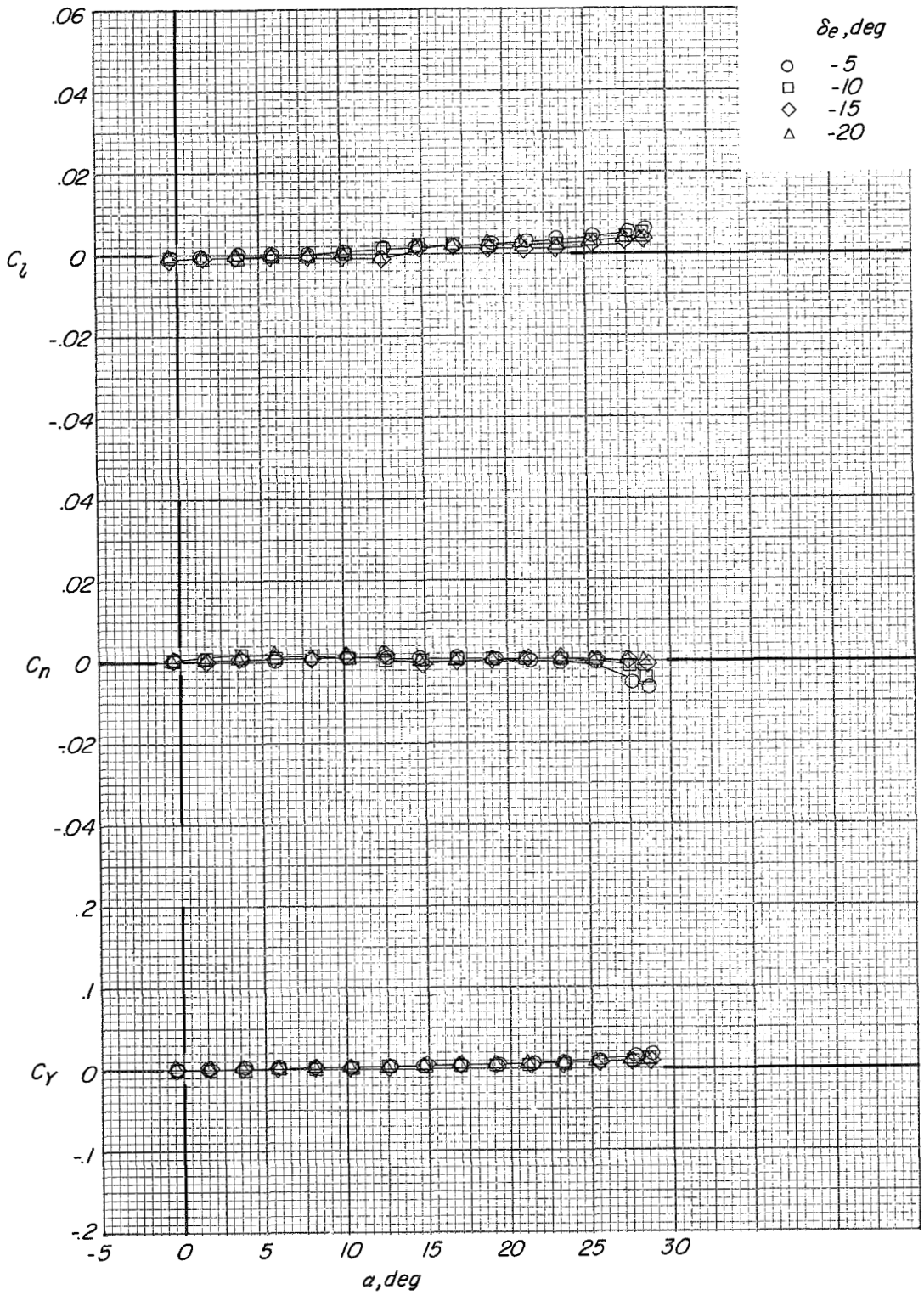
(a) $\delta_a = 0^o$; M = 0.35.

Figure 24.- Variation of the lateral force and moment coefficients with angle of attack for several aileron deflections. Modification I fin configuration; auxiliary flaps in the subsonic position; $\beta = 0^o$.



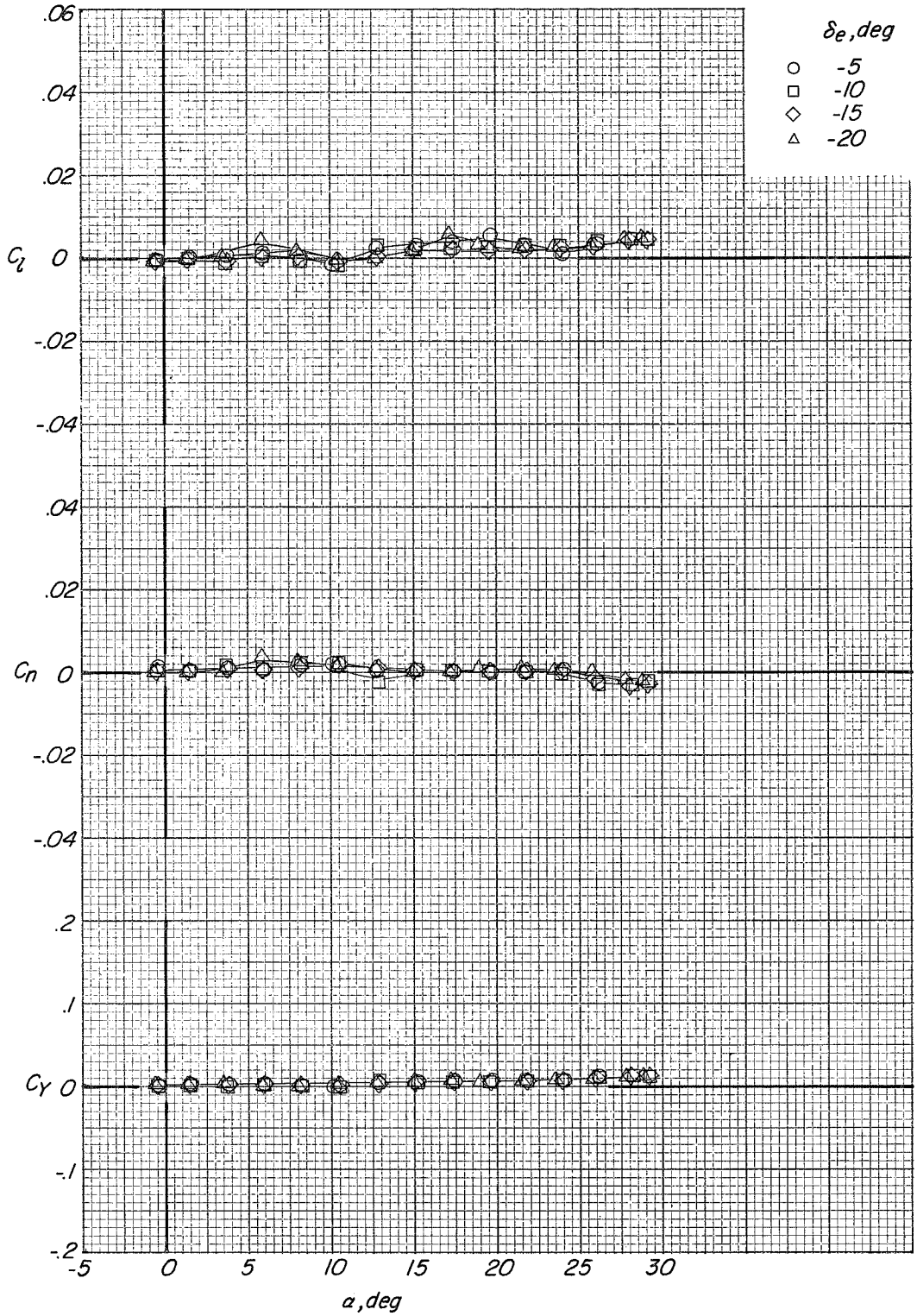
(b) $\delta_a = 0^o$; M = 0.50.

Figure 24.- Continued.



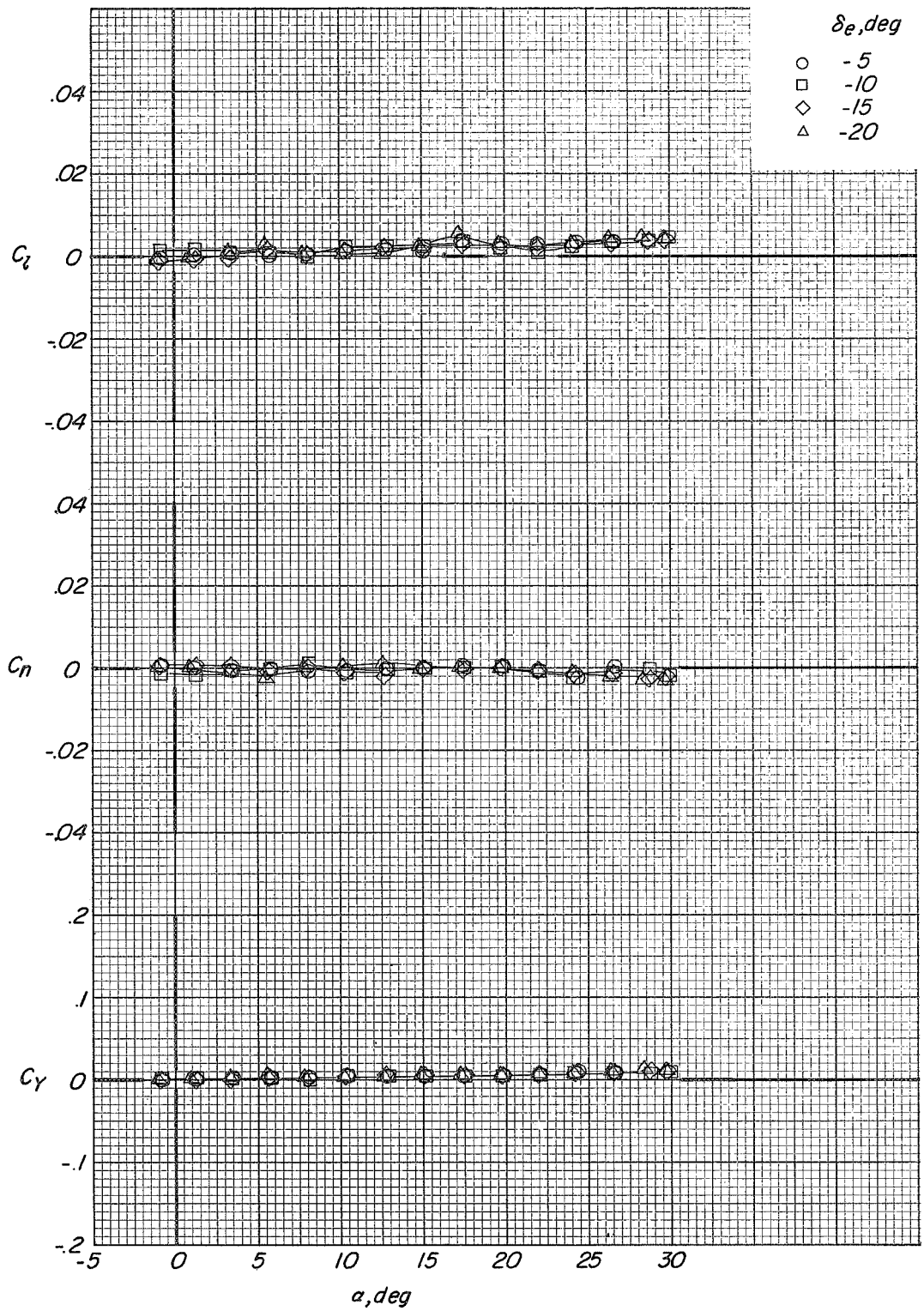
(c) $\delta_a = 0^o$; M = 0.60.

Figure 24.- Continued.



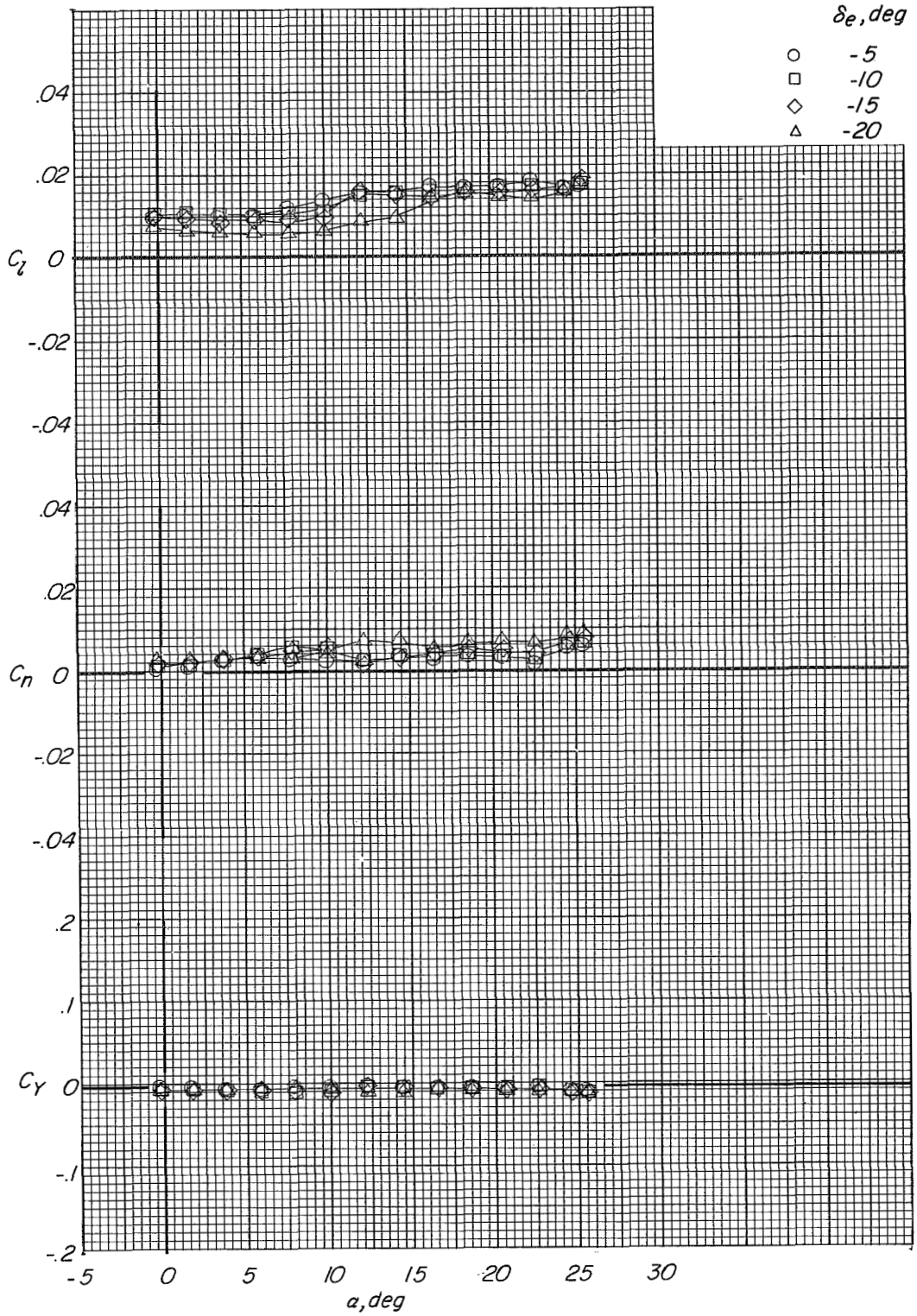
(d) $\delta_a = 0^o$; M = 0.70.

Figure 24.- Continued.



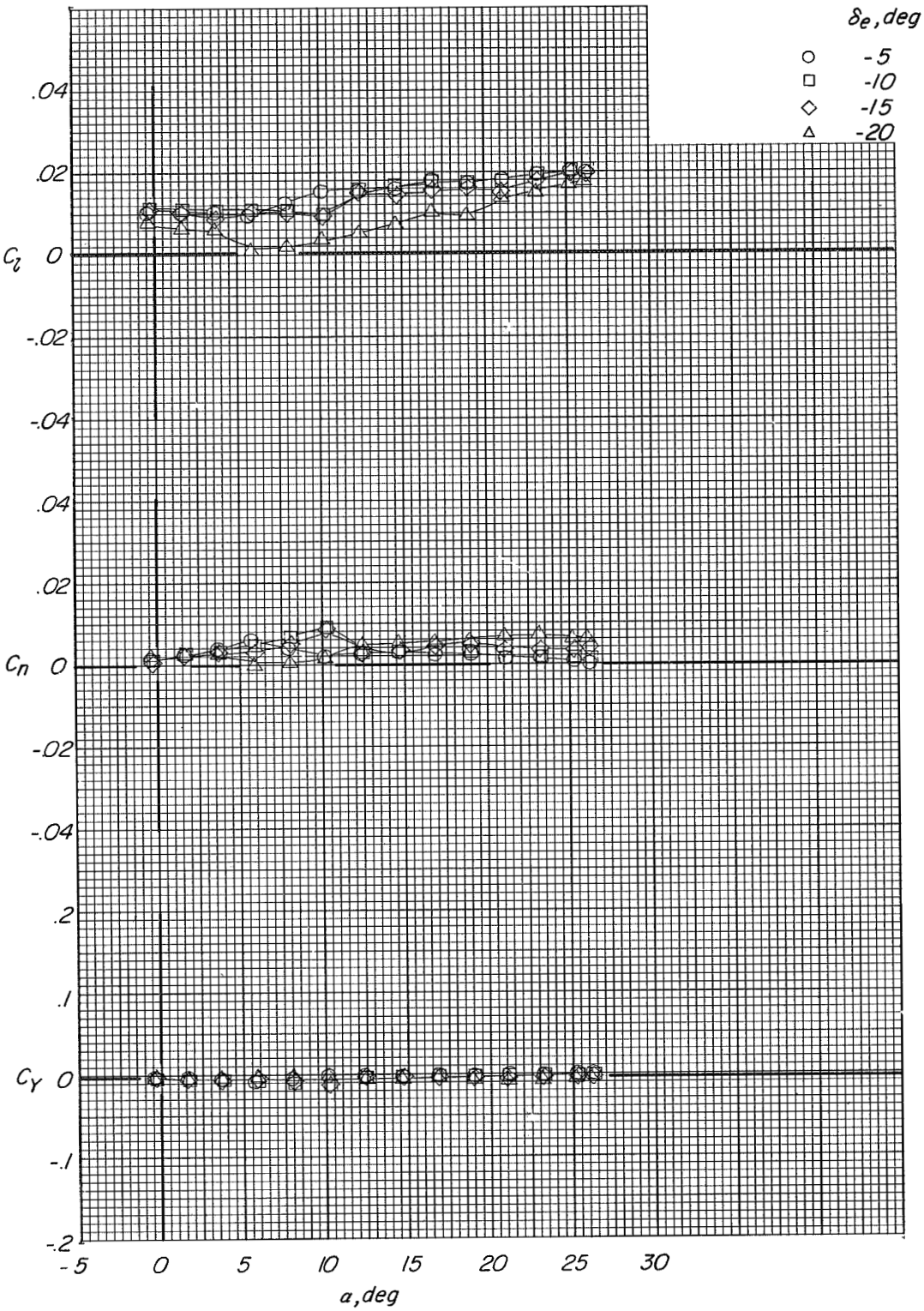
(e) $\delta_a = 0^o$; M = 0.80.

Figure 24.- Continued.



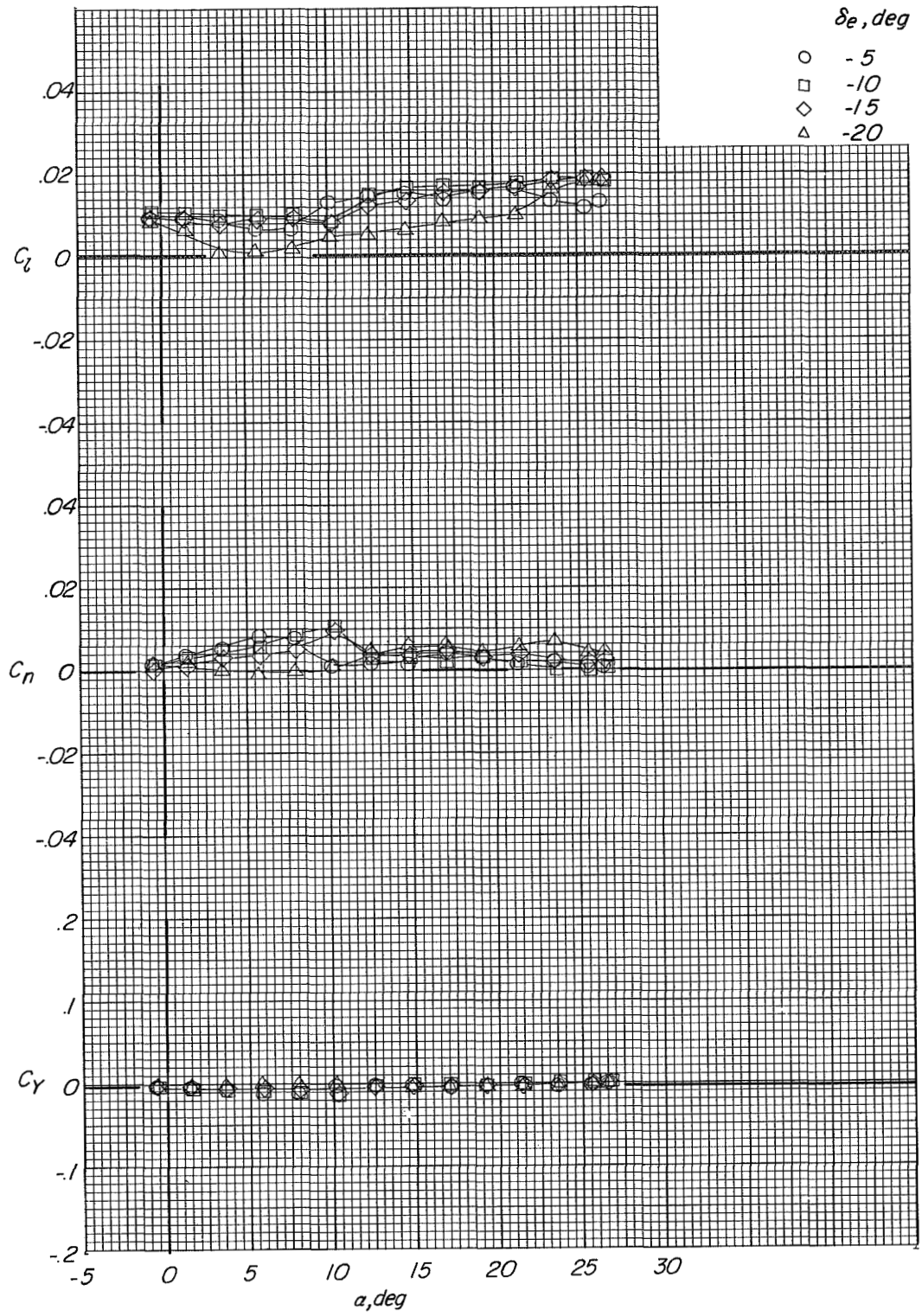
(f) $\delta_a = 10^o$; M = 0.35.

Figure 24.- Continued.



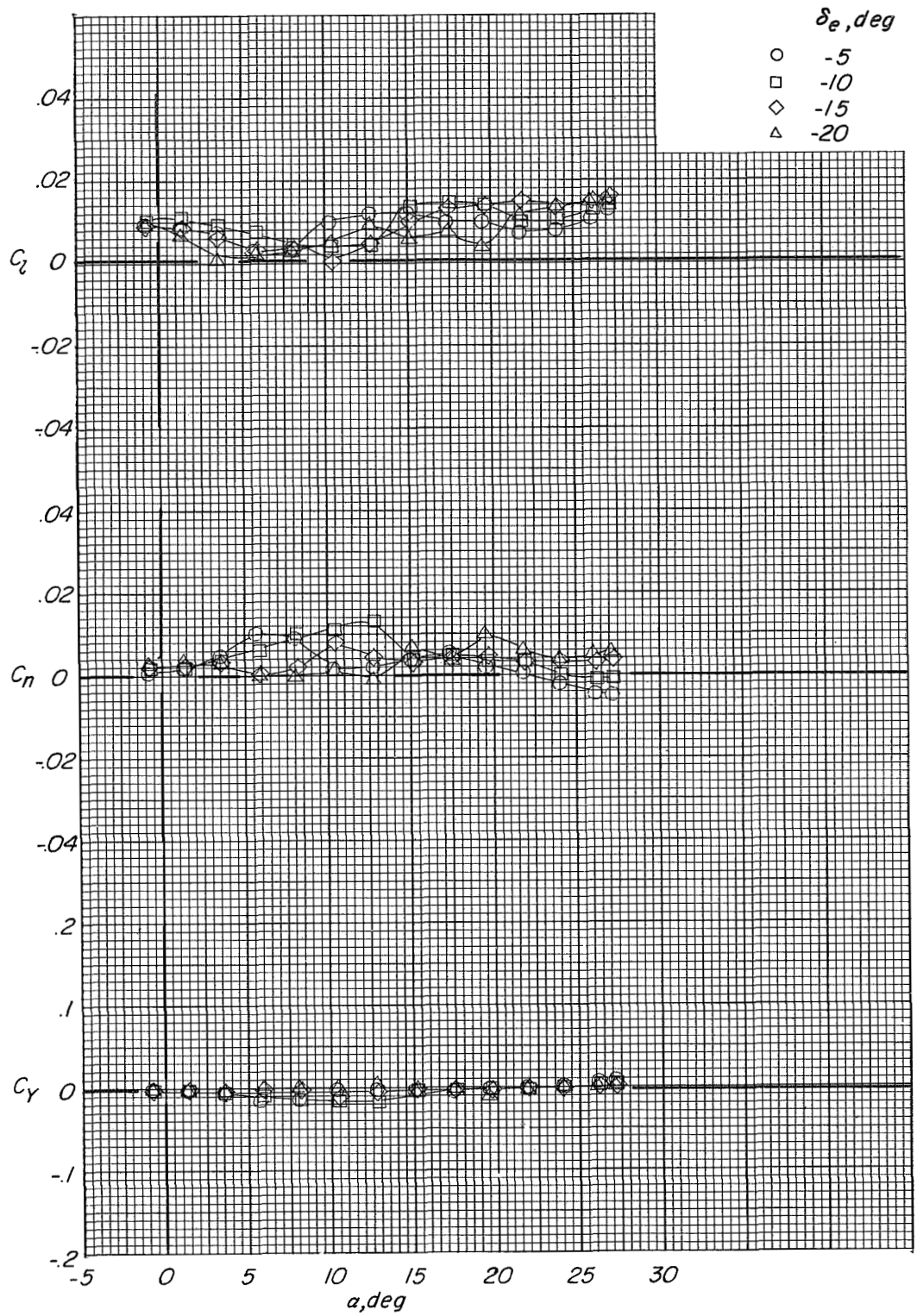
(g) $\delta_a = 10^o$; M = 0.50.

Figure 24.- Continued.



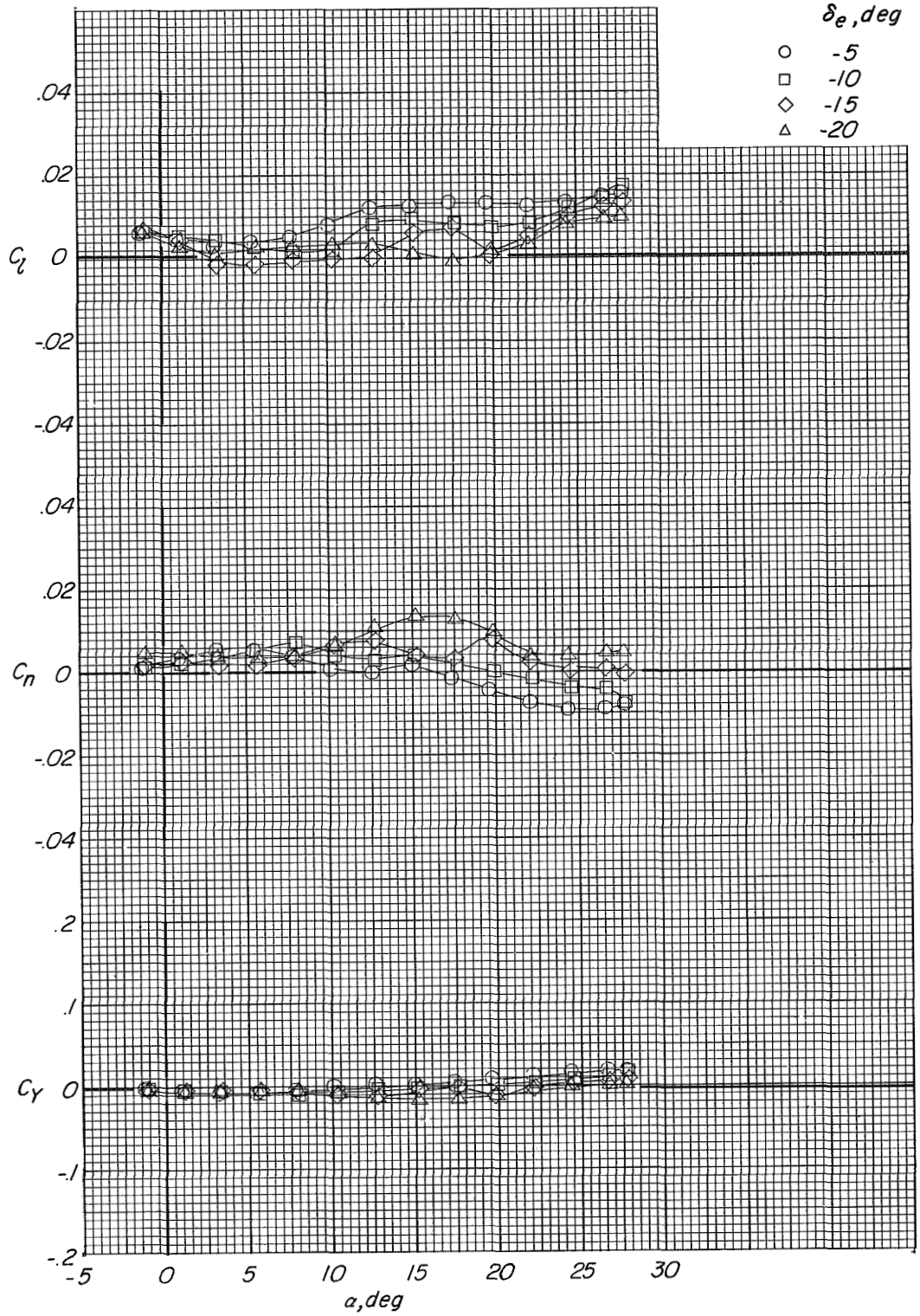
(h) $\delta_a = 10^o$; M = 0.60.

Figure 24.- Continued.



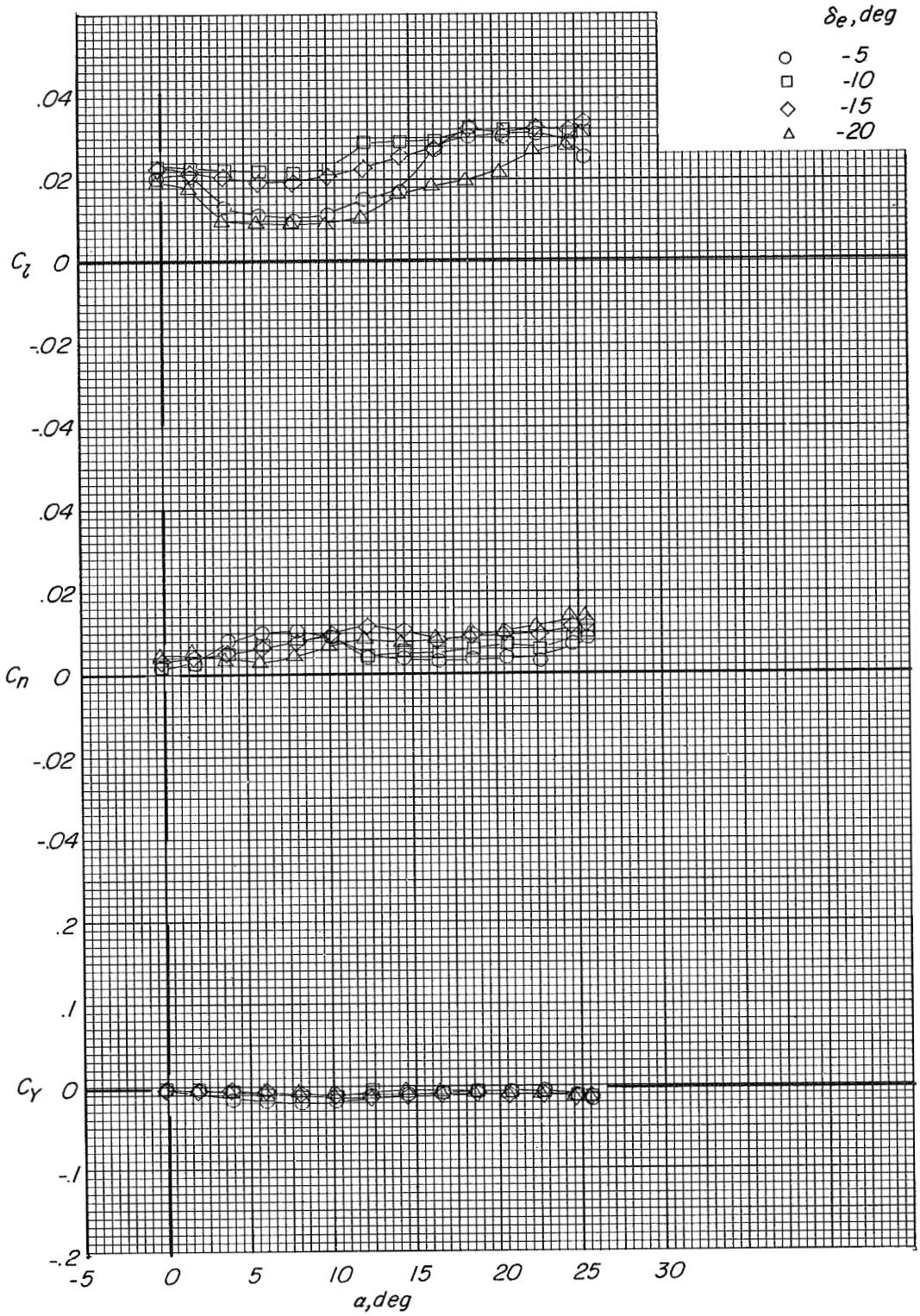
(i) $\delta_a = 10^o$; M = 0.70.

Figure 24.- Continued.



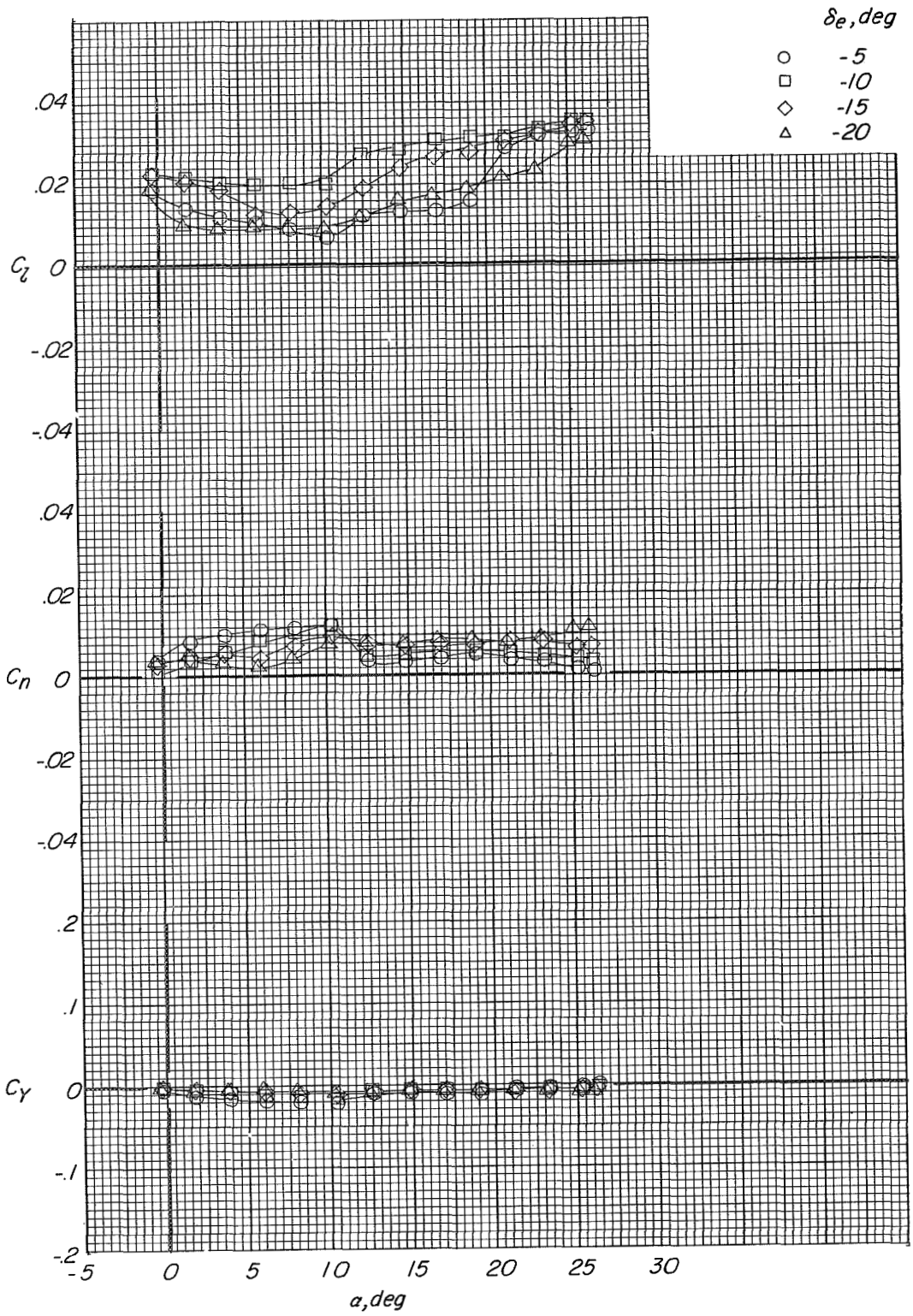
(j) $\delta_a = 10^o$; M = 0.80.

Figure 24.- Continued.



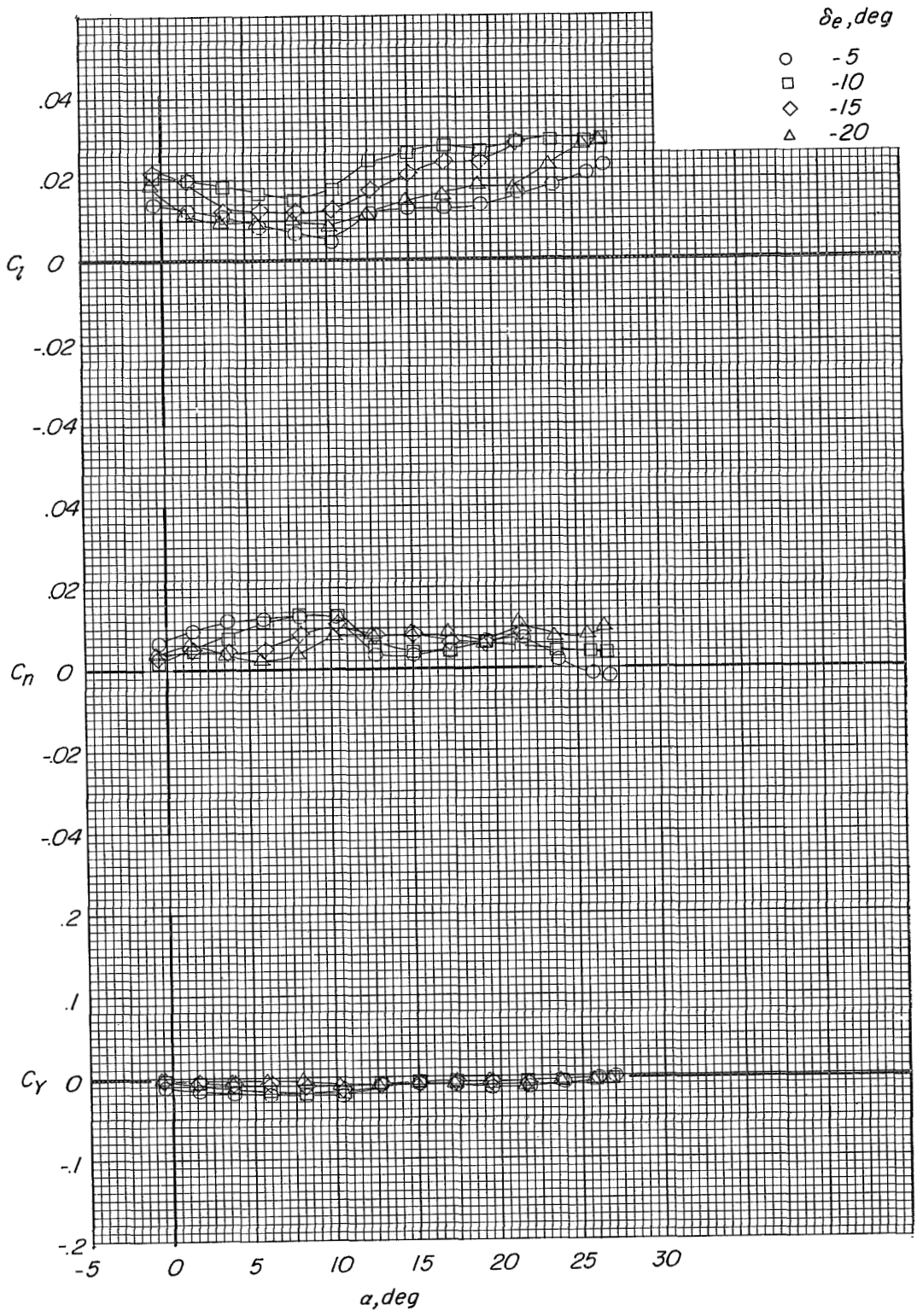
(k) $\delta_a = 20^o$; M = 0.35.

Figure 24.- Continued.



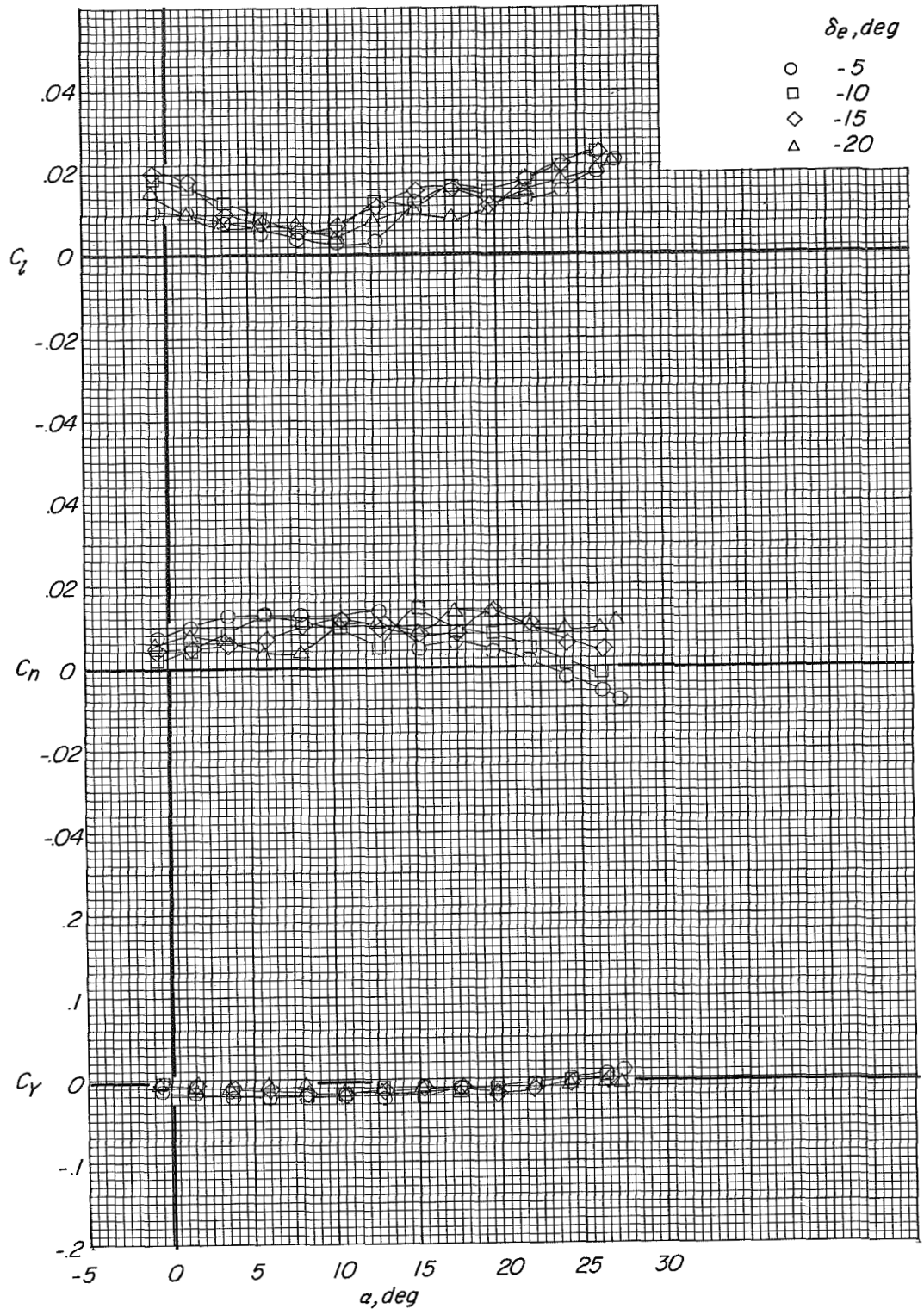
(l) $\delta_a = 20^o$; M = 0.50.

Figure 24.- Continued.



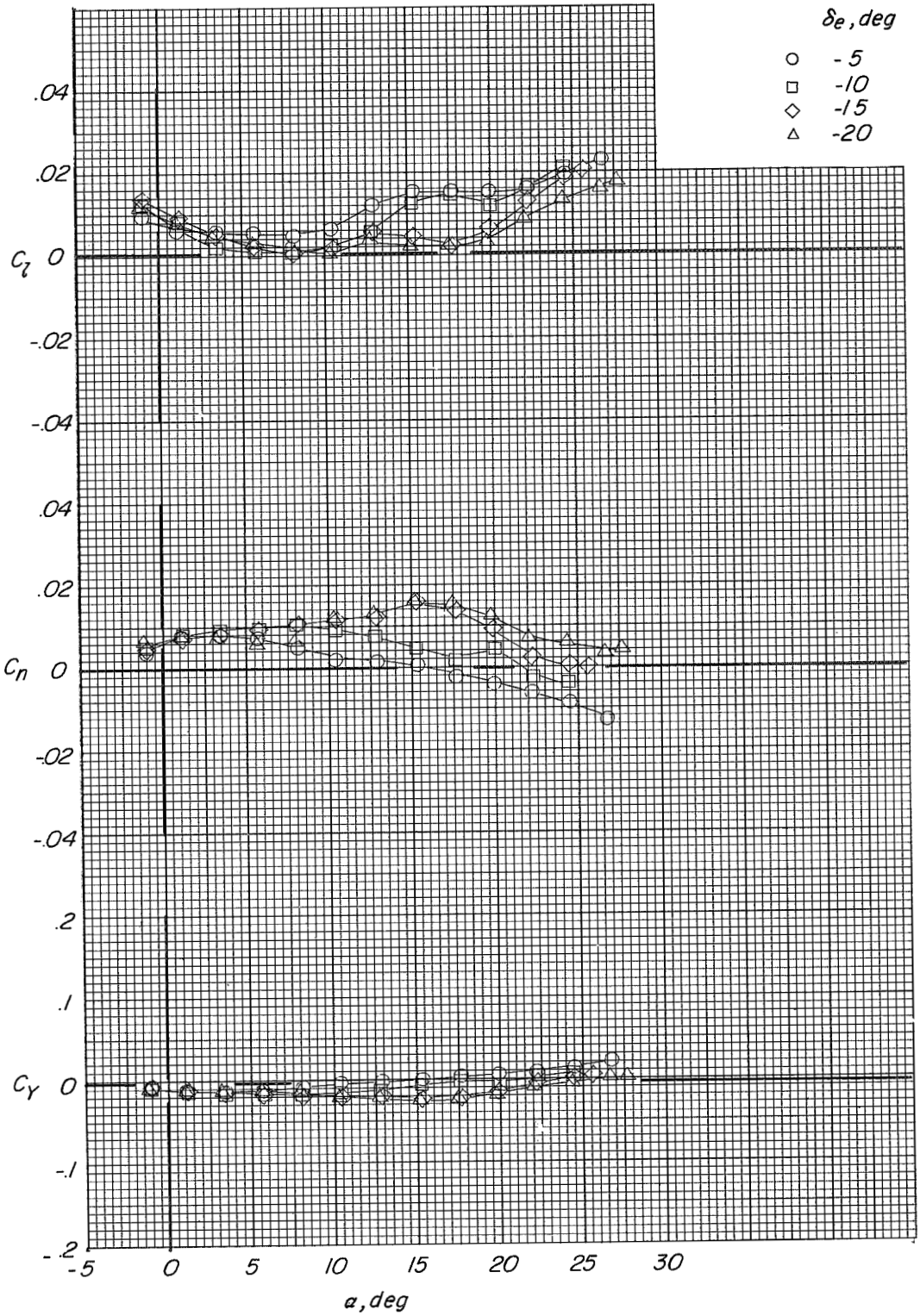
(m) $\delta_a = 20^o$; M = 0.60.

Figure 24.- Continued.



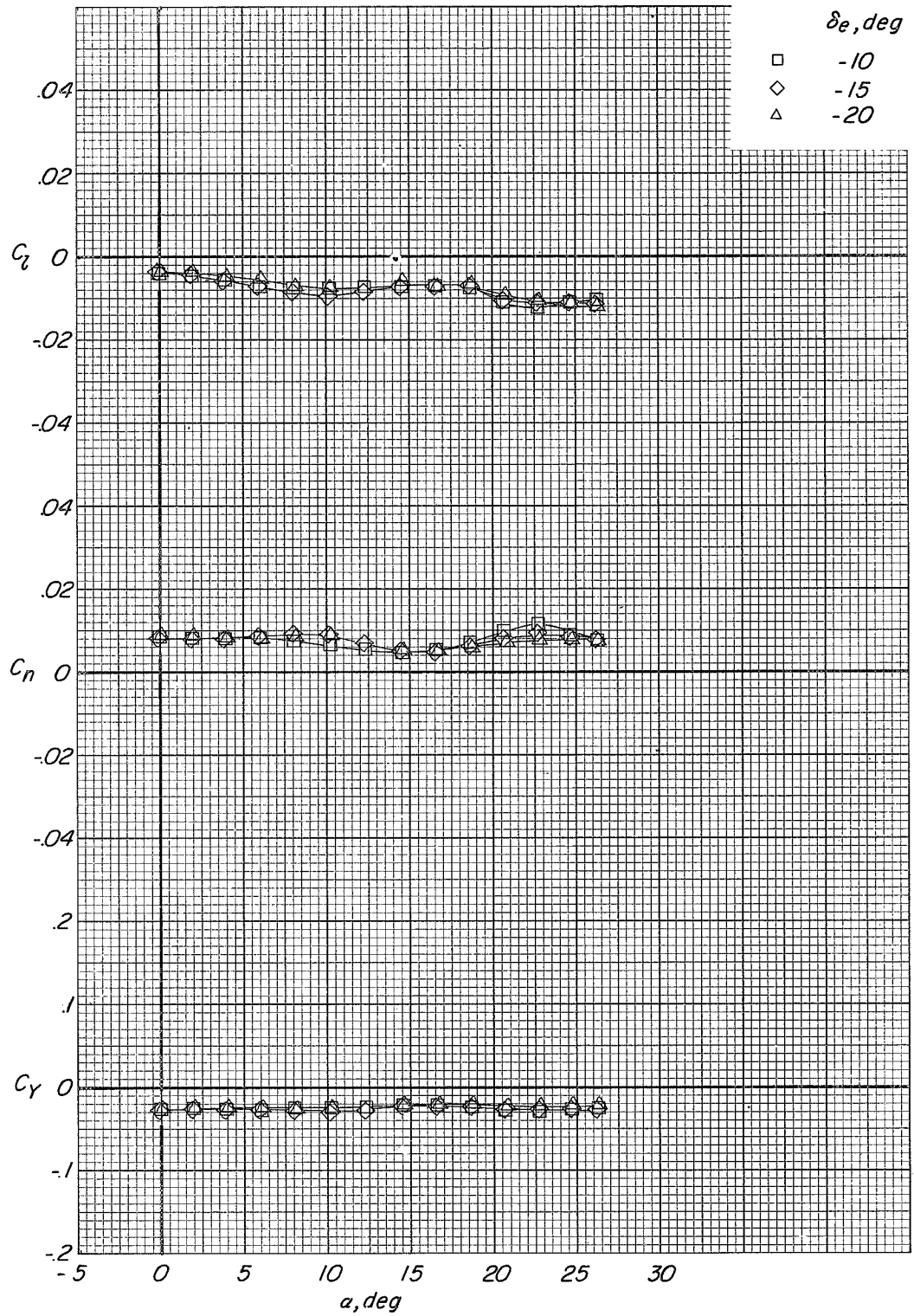
(n) $\delta_a = 20^o$; M = 0.70.

Figure 24.- Continued.



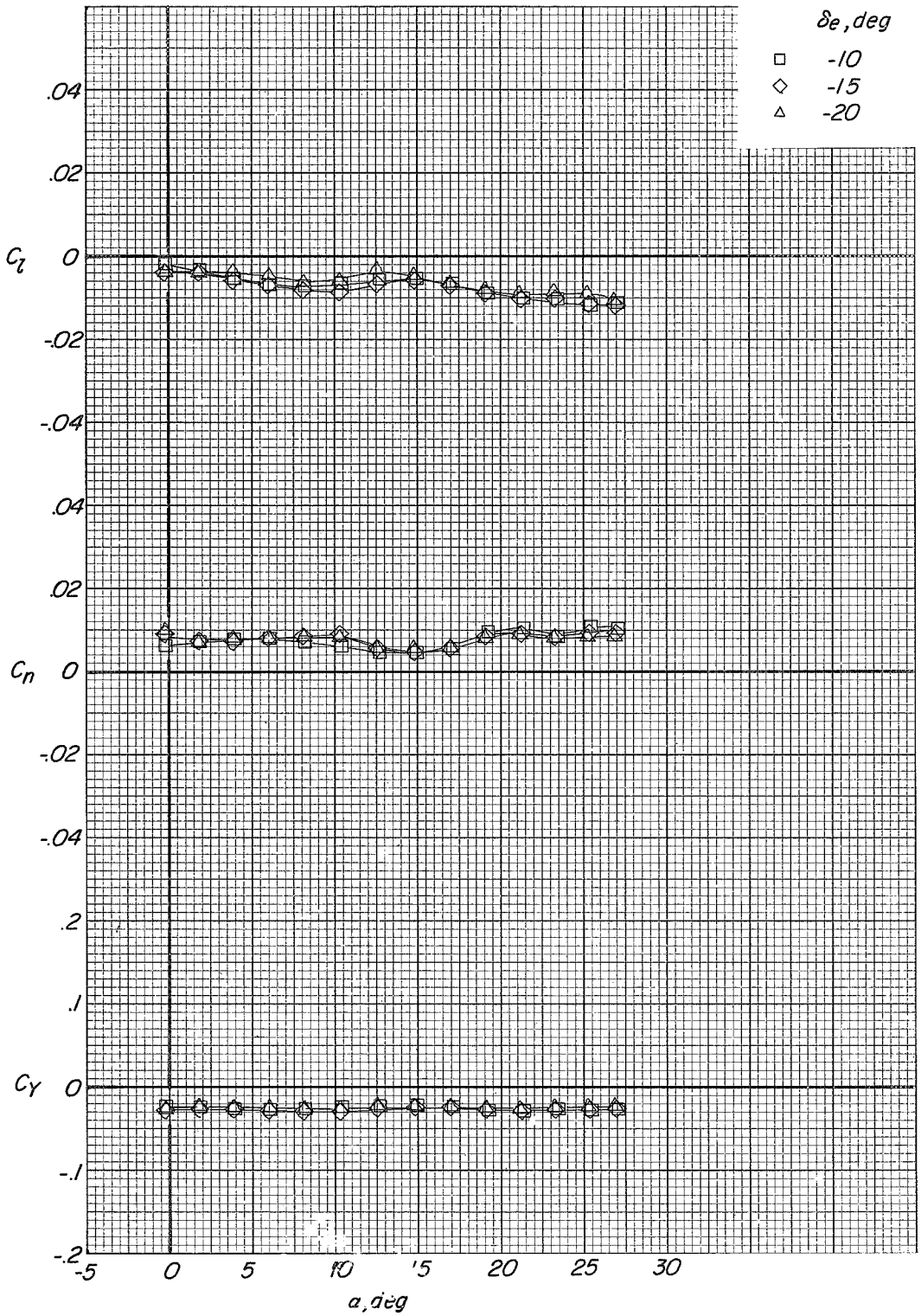
(o) $\delta_a = 20^o$; M = 0.80.

Figure 24.- Concluded.



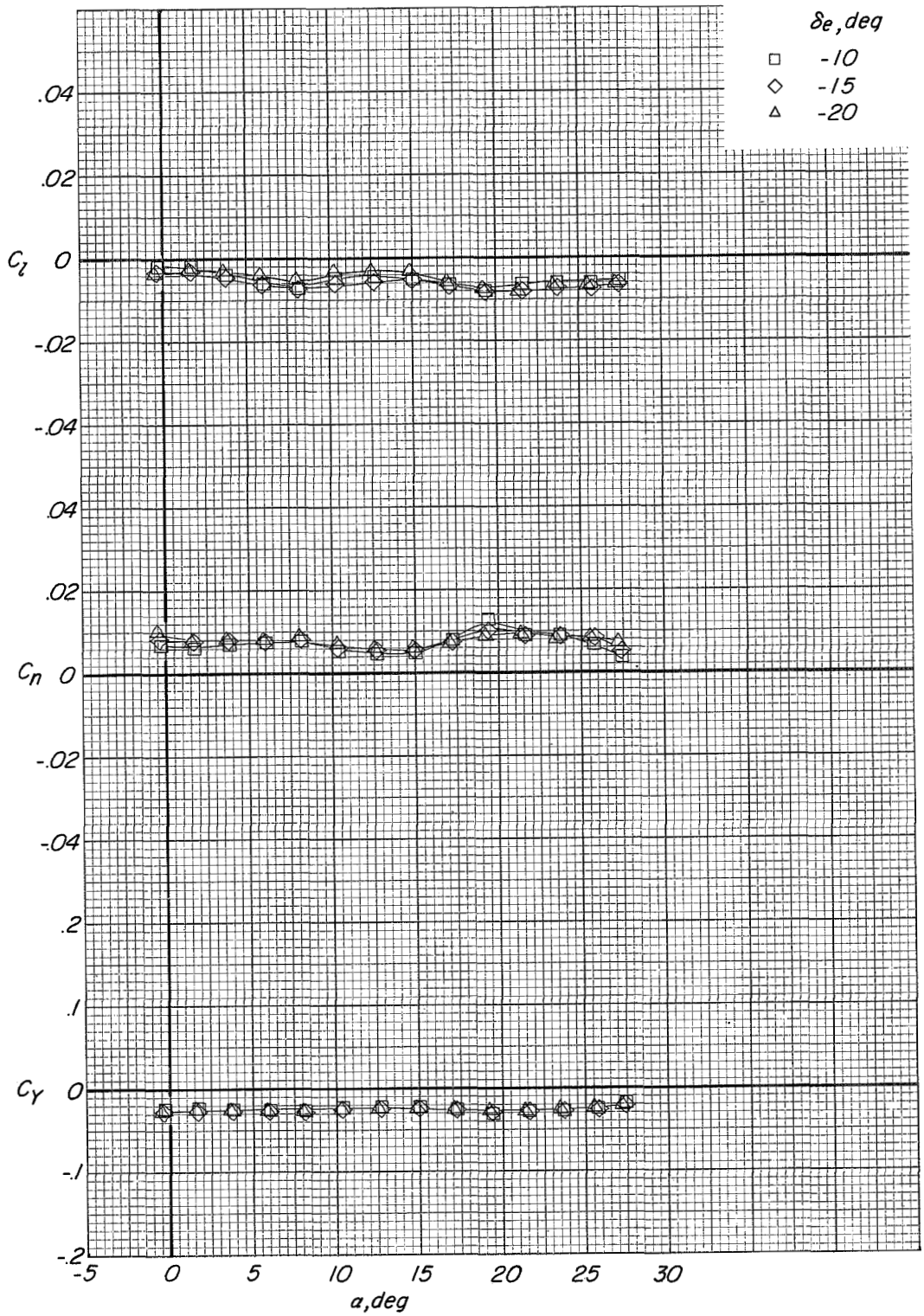
(a) $\beta = 2.3^{o}$; M = 0.35.

Figure 25.- Variation of the lateral force and moment coefficients with angle of attack for sideslipped conditions. Modification I fin configuration; auxiliary flaps in the subsonic position; $\delta_a = 0^{o}$.



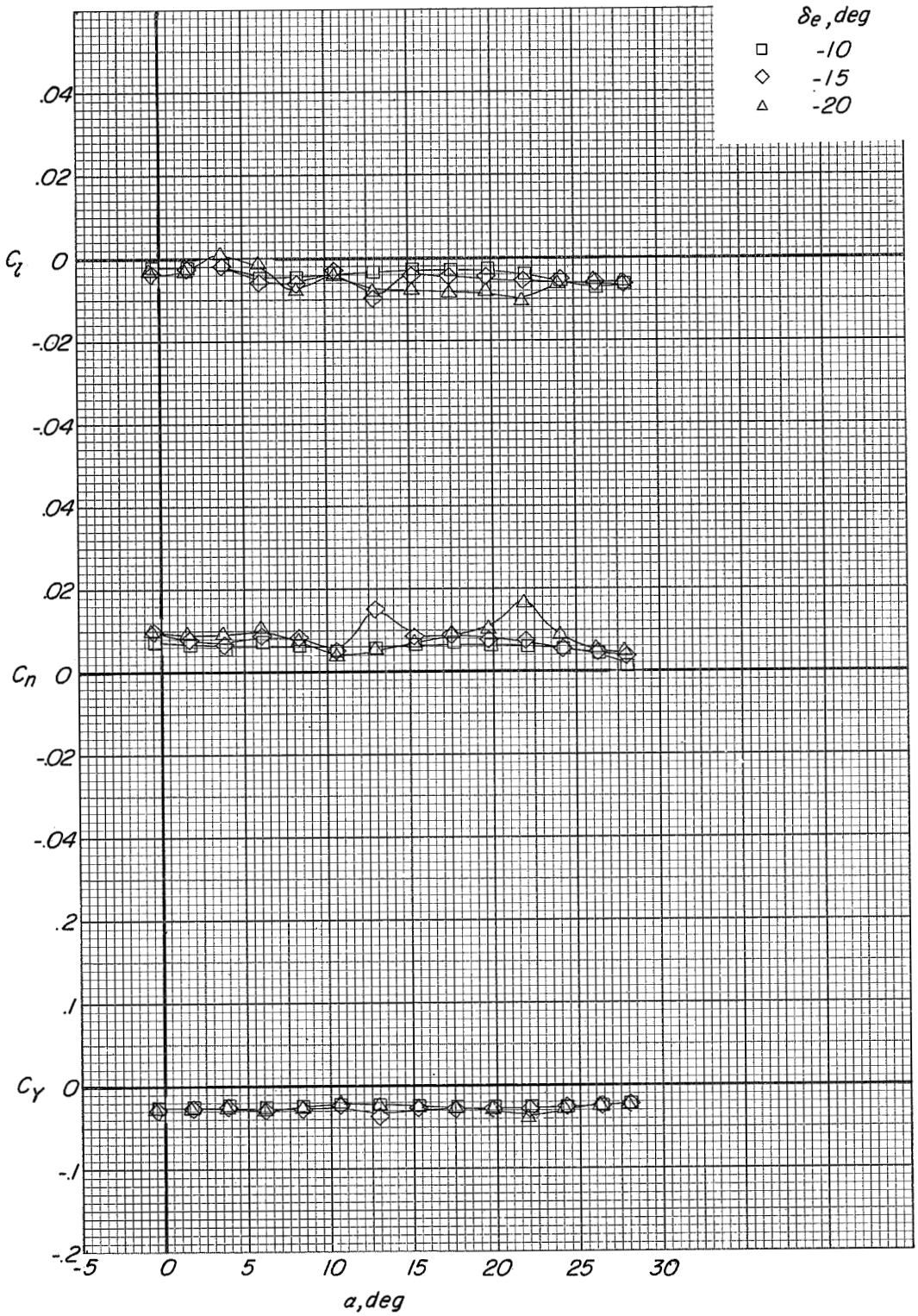
(b) $\beta = 2.3^{\circ}$; M = 0.50.

Figure 25.- Continued.



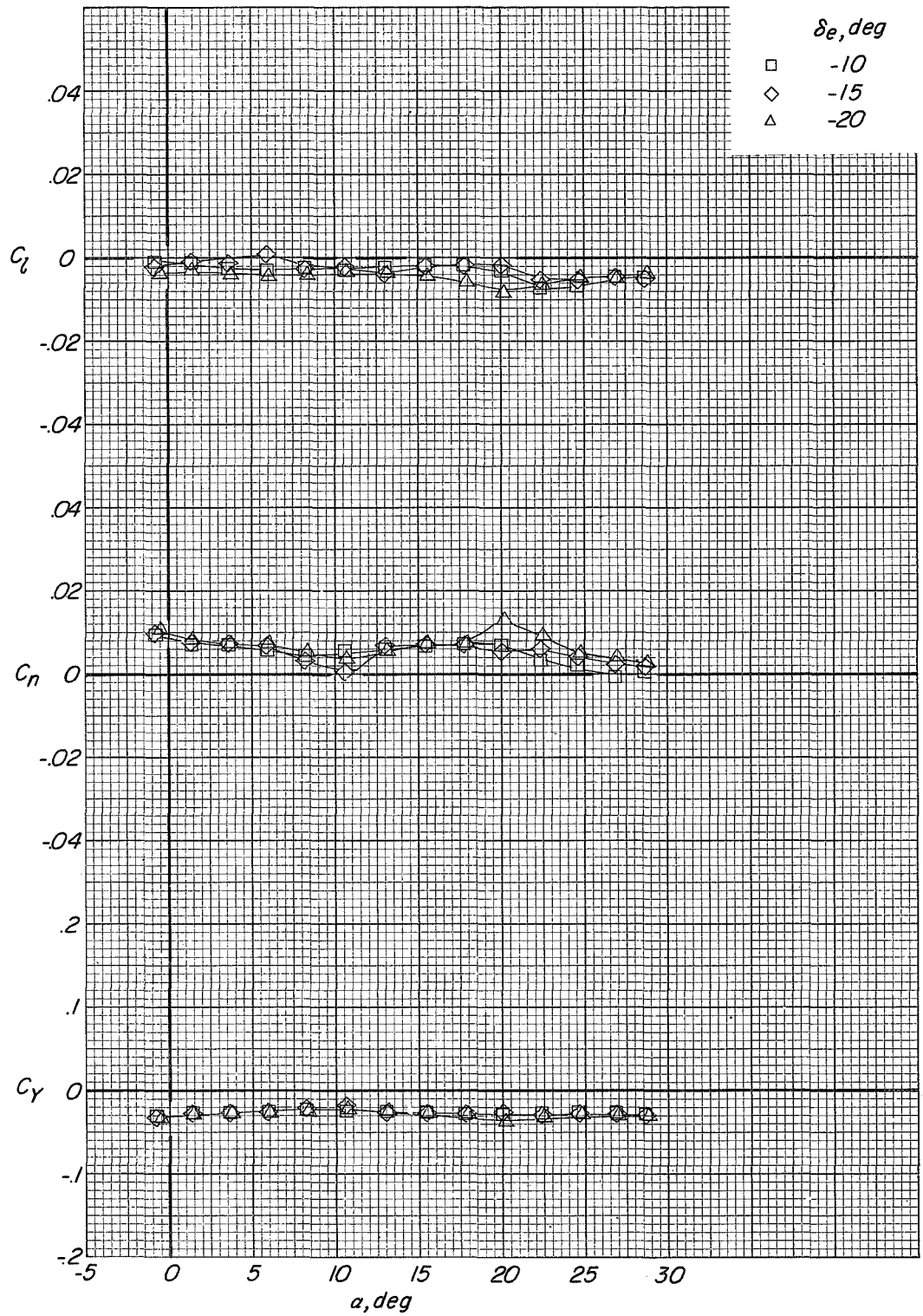
(c) $\beta = 2.3^{o}$; M = 0.60.

Figure 25.- Continued.



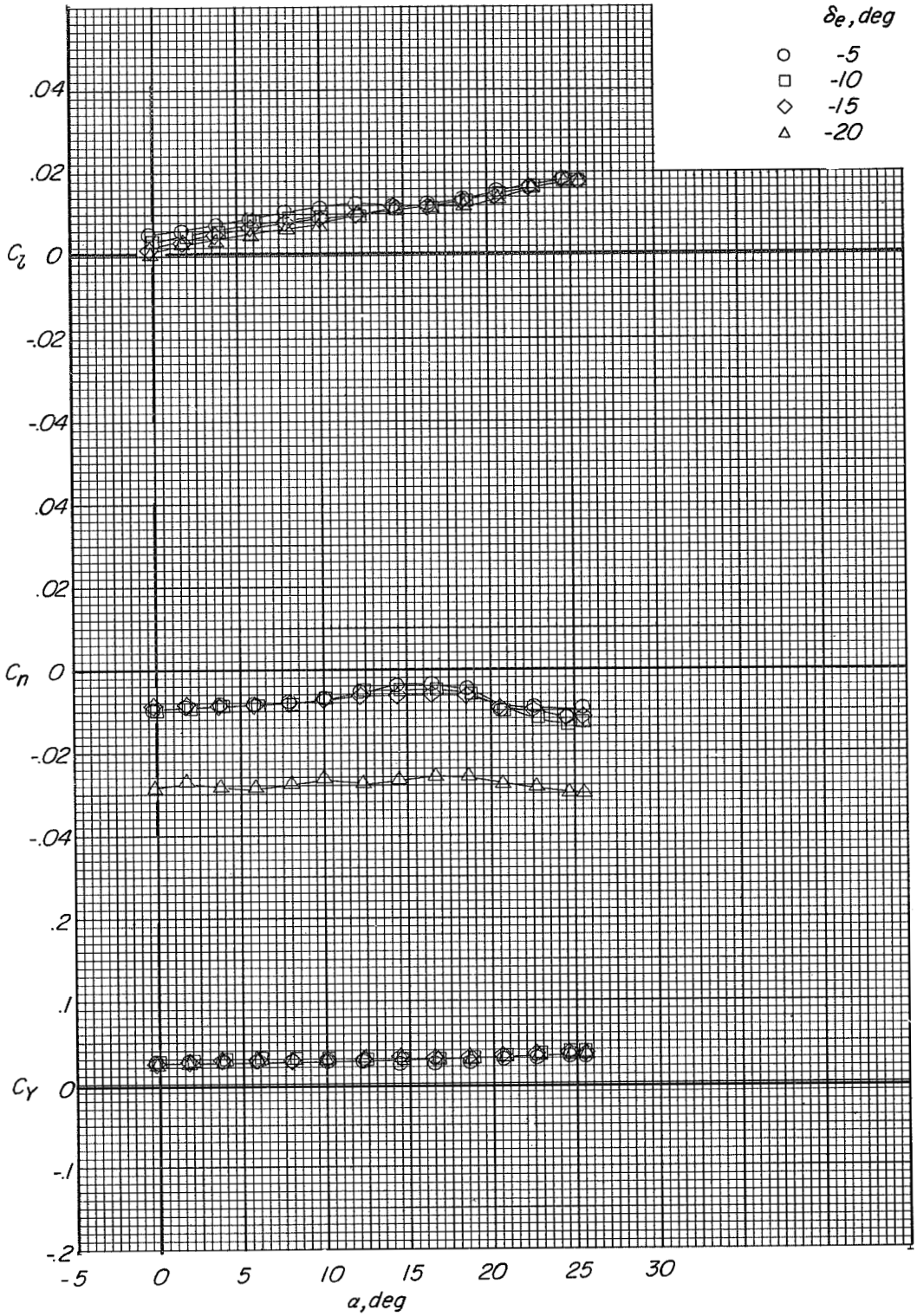
(d) $\beta = 2.3^{o}$; M = 0.70.

Figure 25.- Continued.



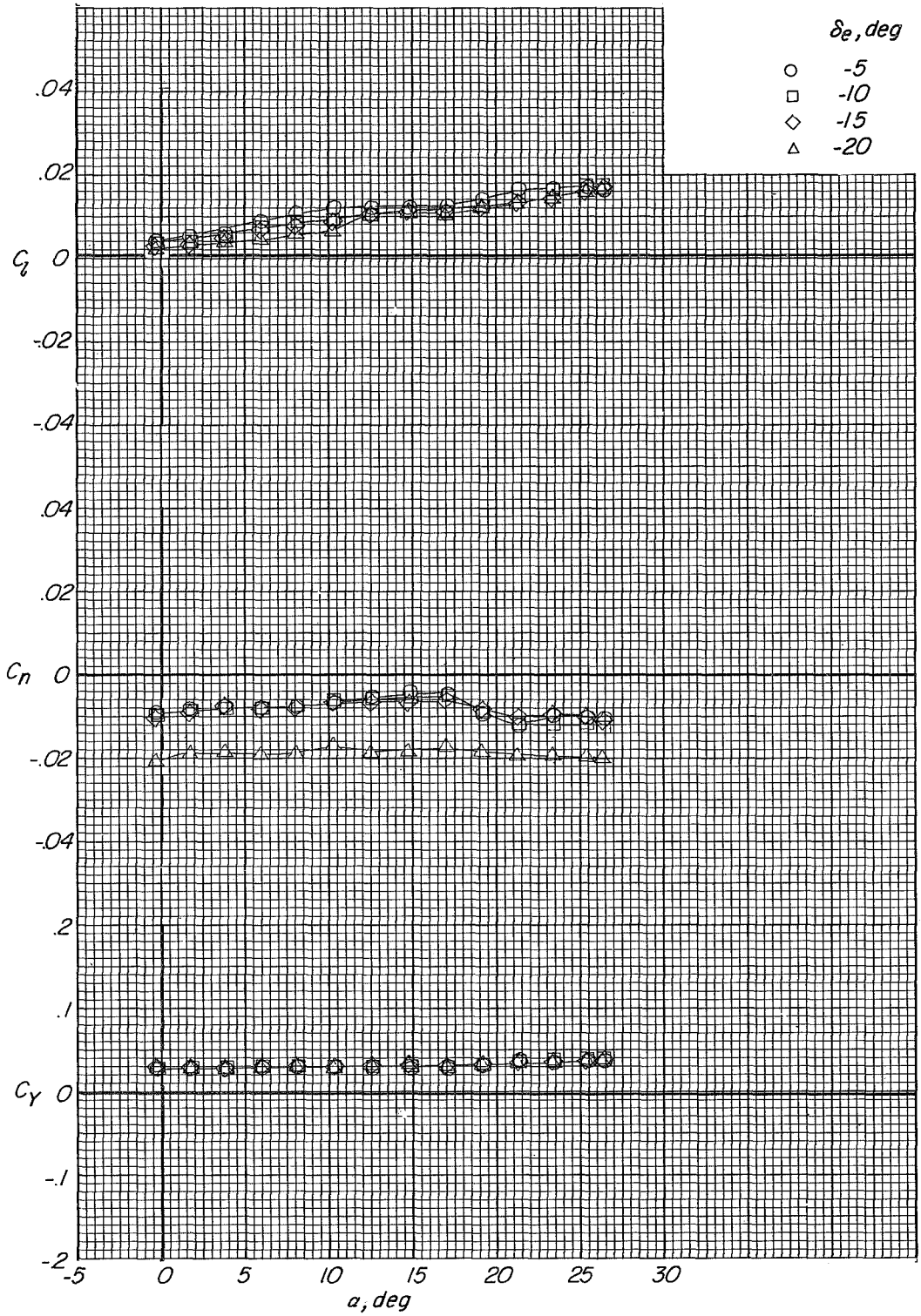
(e) $\beta = 2.3^{o}$; M = 0.80.

Figure 25.- Continued.



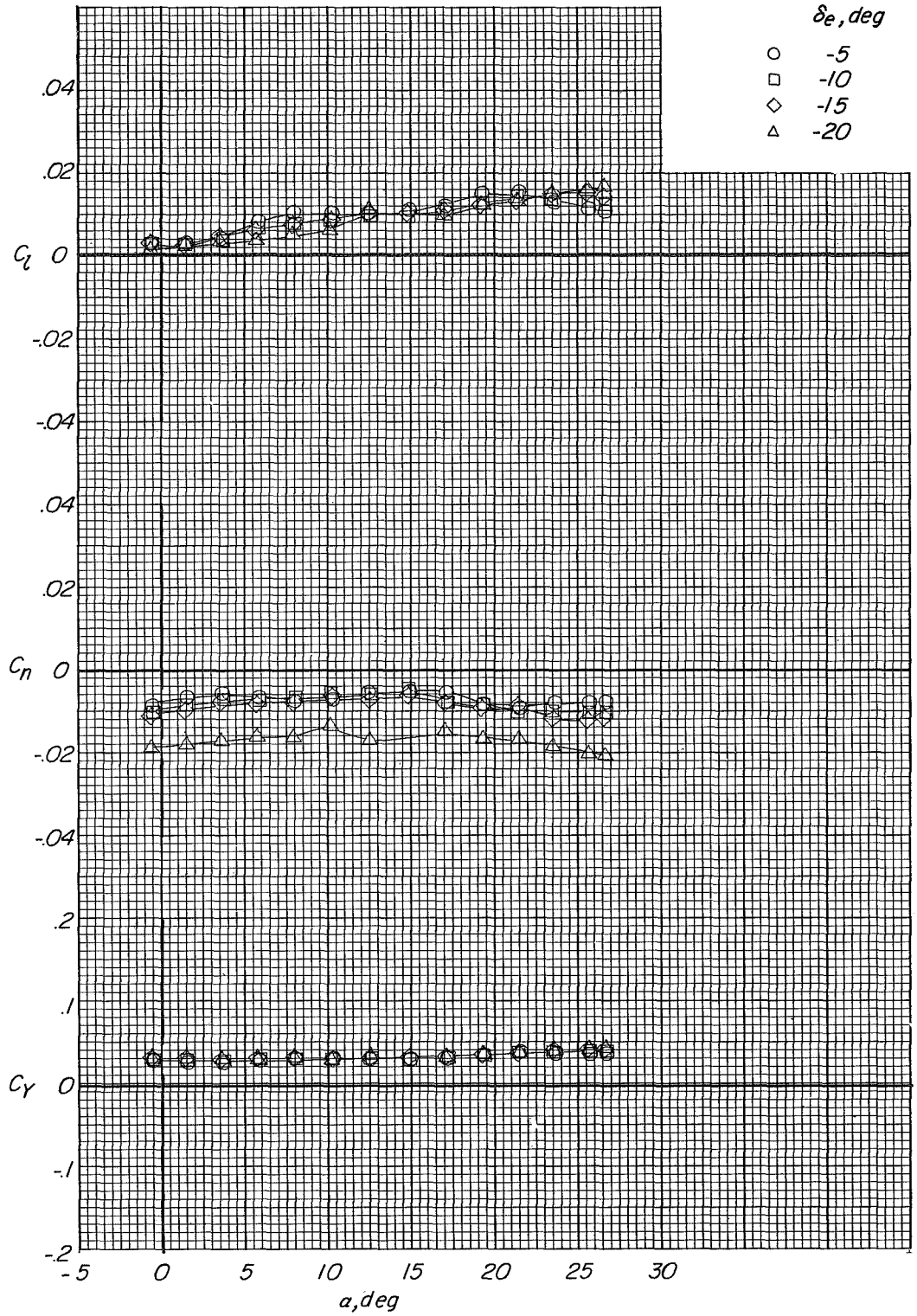
(f) $\beta = -2.3^{o}$; M = 0.35.

Figure 25.- Continued.



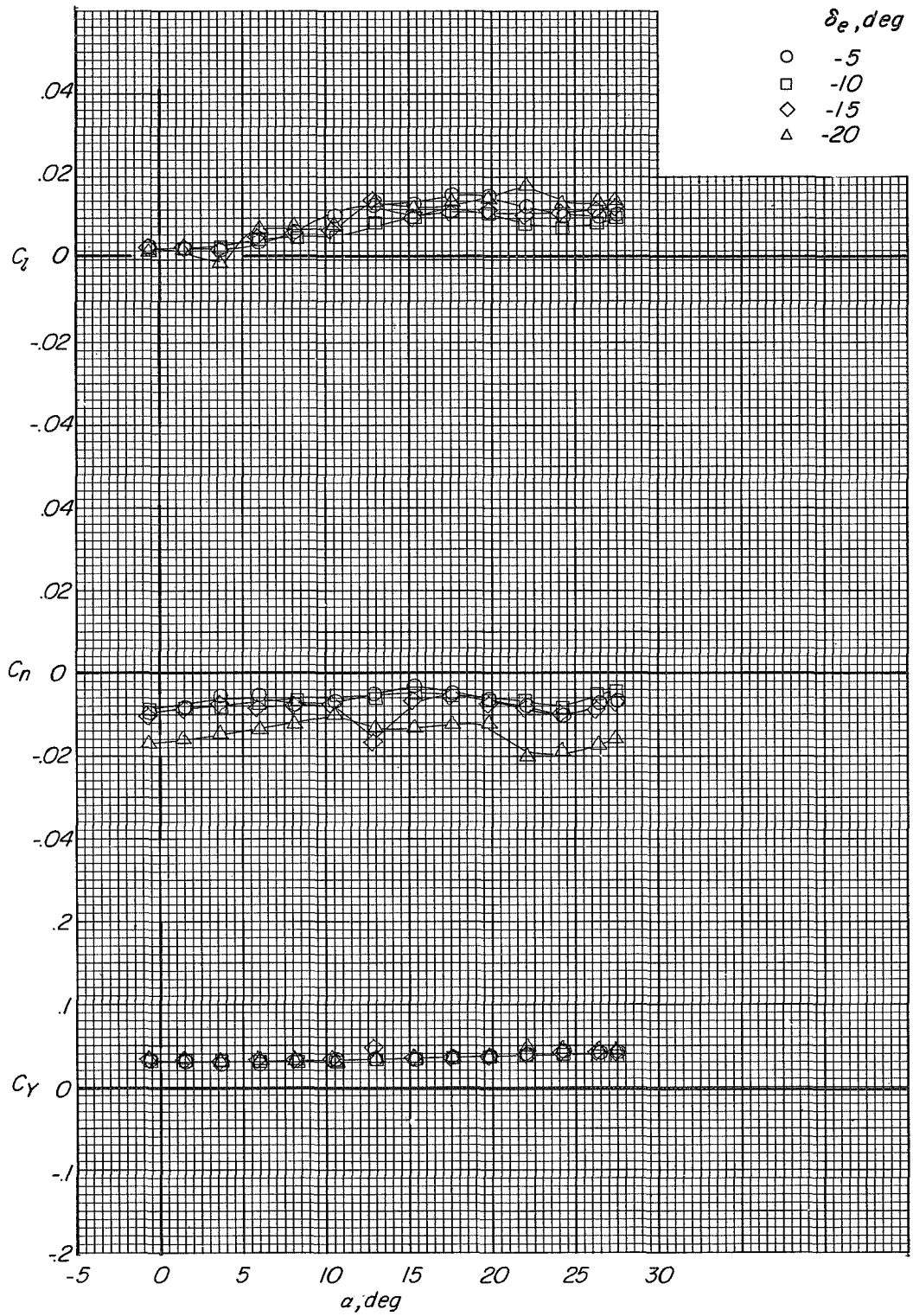
(g) $\beta = -2.3^{\circ}$; M = 0.50.

Figure 25.- Continued.



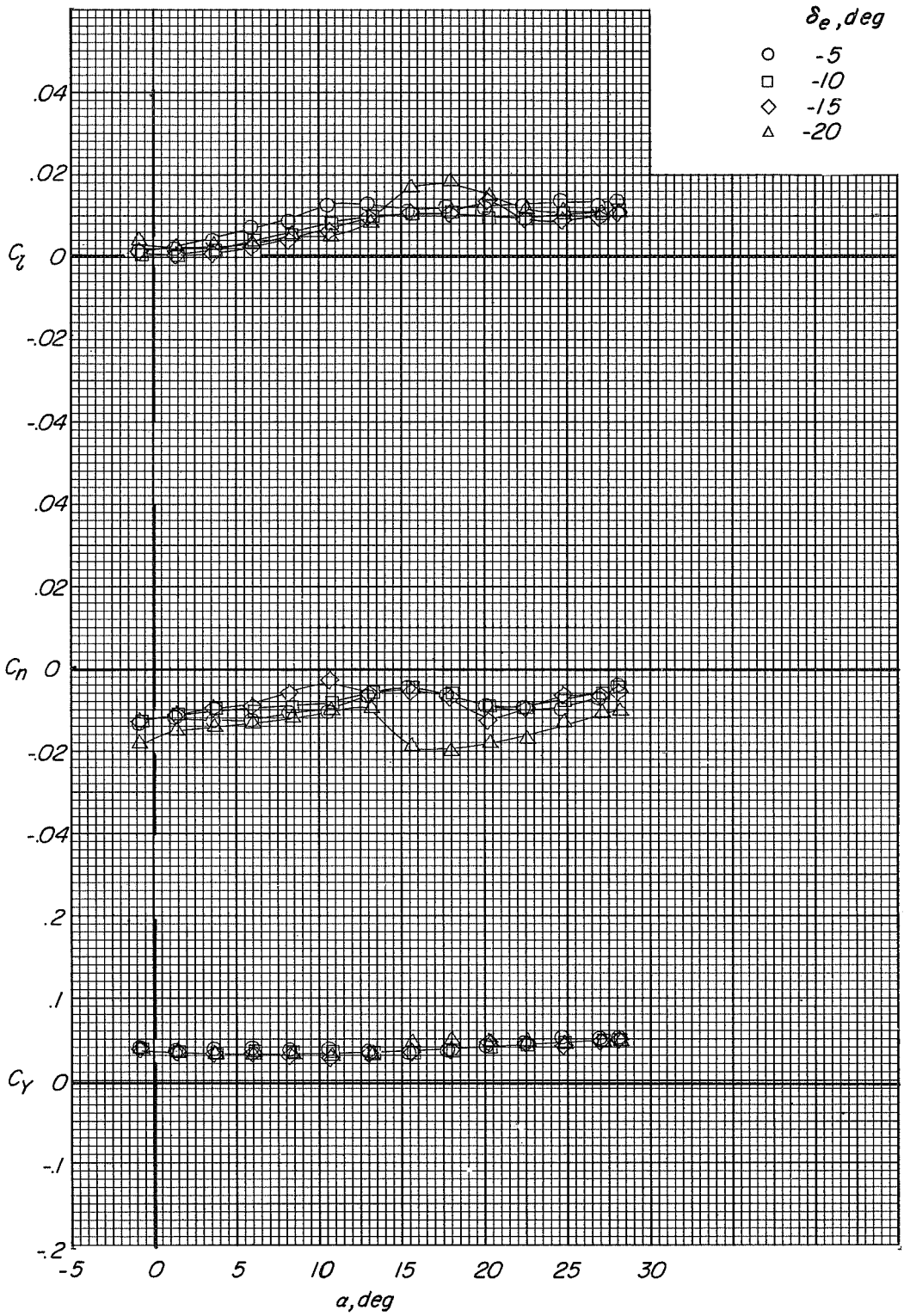
(h) $\beta = -2.3^{o}$; M = 0.60.

Figure 25.- Continued.



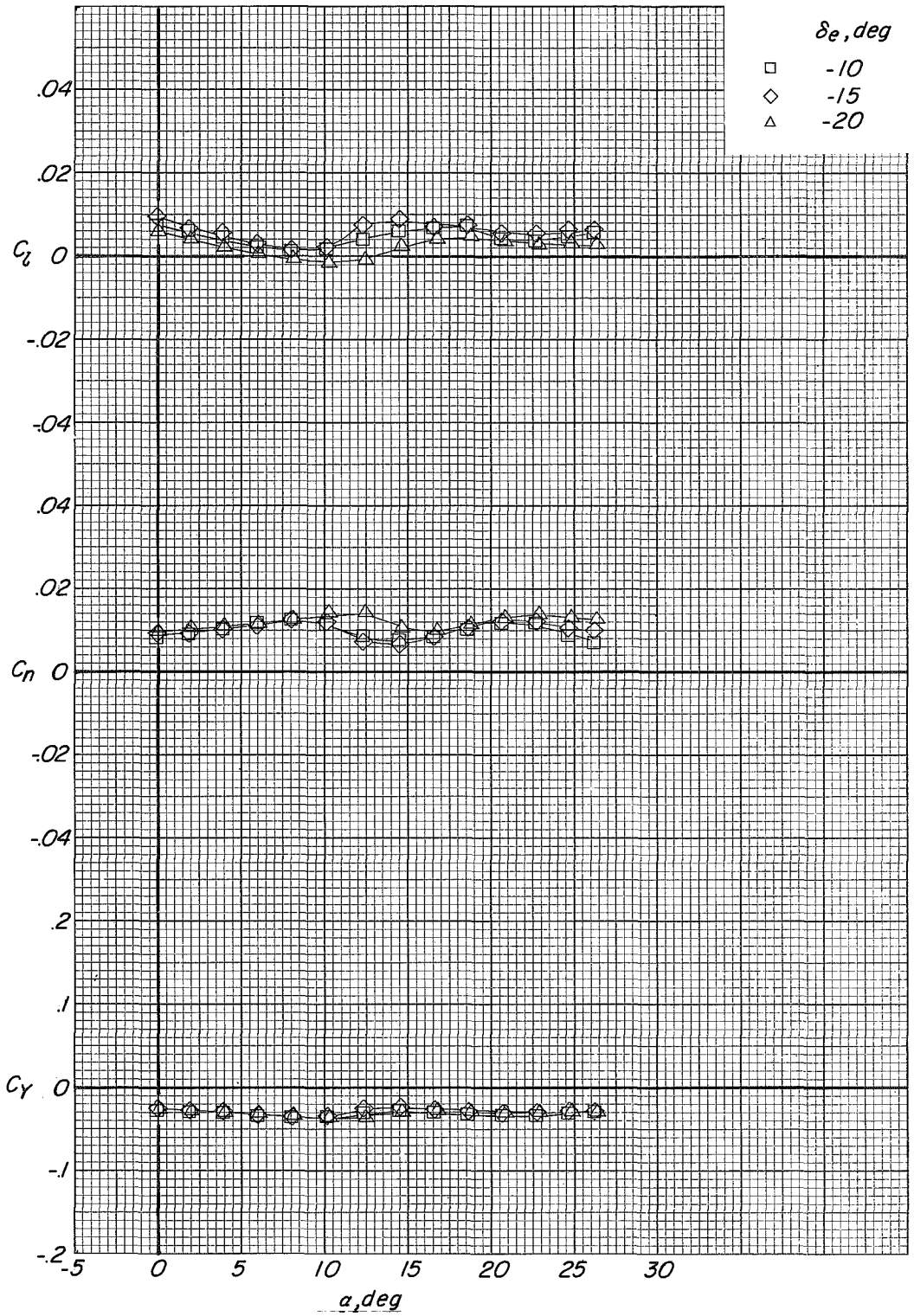
(i) $\beta = -2.3^{o}$; M = 0.70.

Figure 25.- Continued.



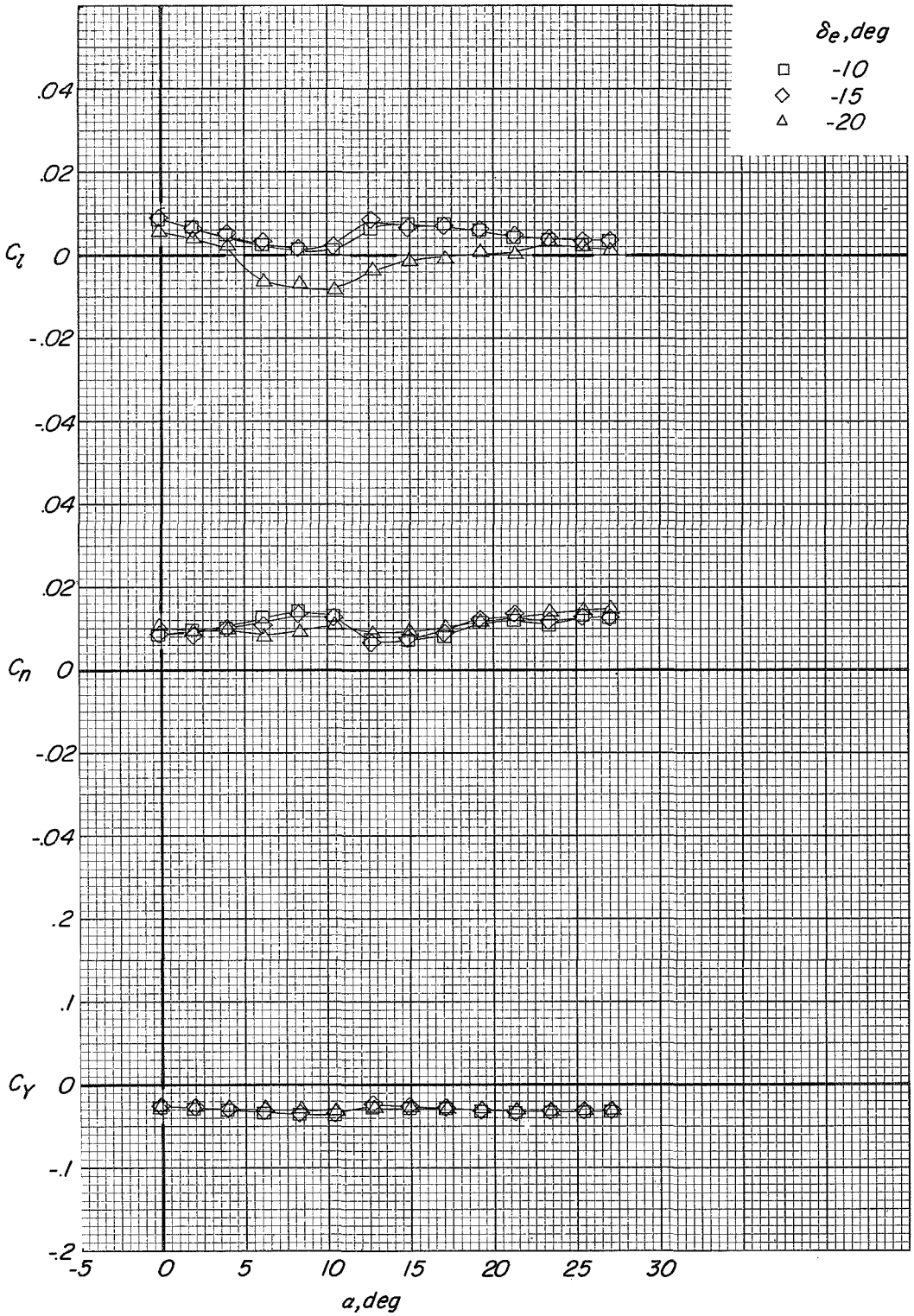
(j) $\beta = -2.3^{o}$; M = 0.80.

Figure 25.- Concluded.



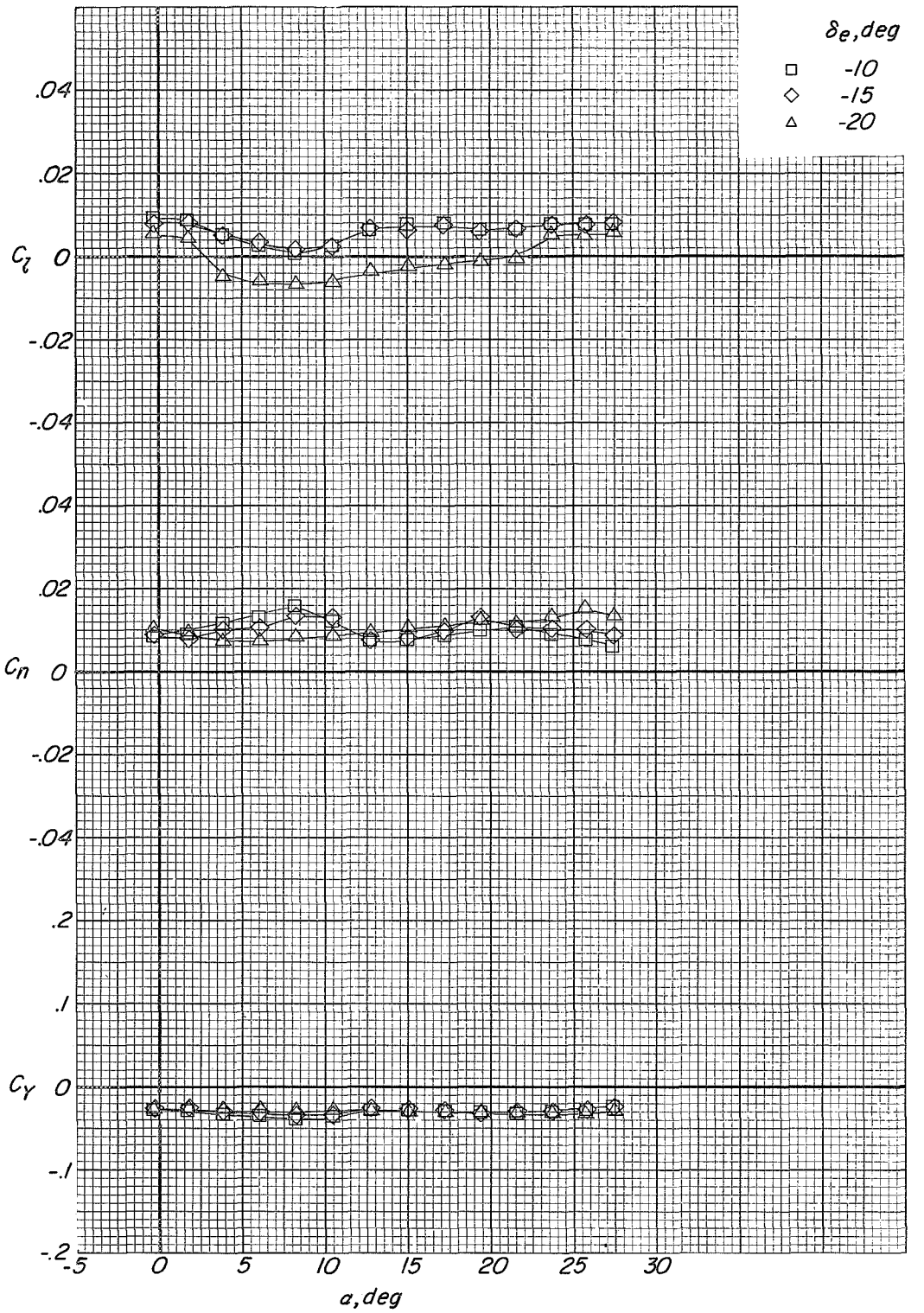
(a) $\beta = 2.3^{o}$; $\delta_a = 10^{o}$; M = 0.35.

Figure 26.- Variation of the lateral force and moment coefficients with angle of attack for combined aileron deflection and sideslip. Modification I fin configuration; auxiliary flaps in the subsonic position.



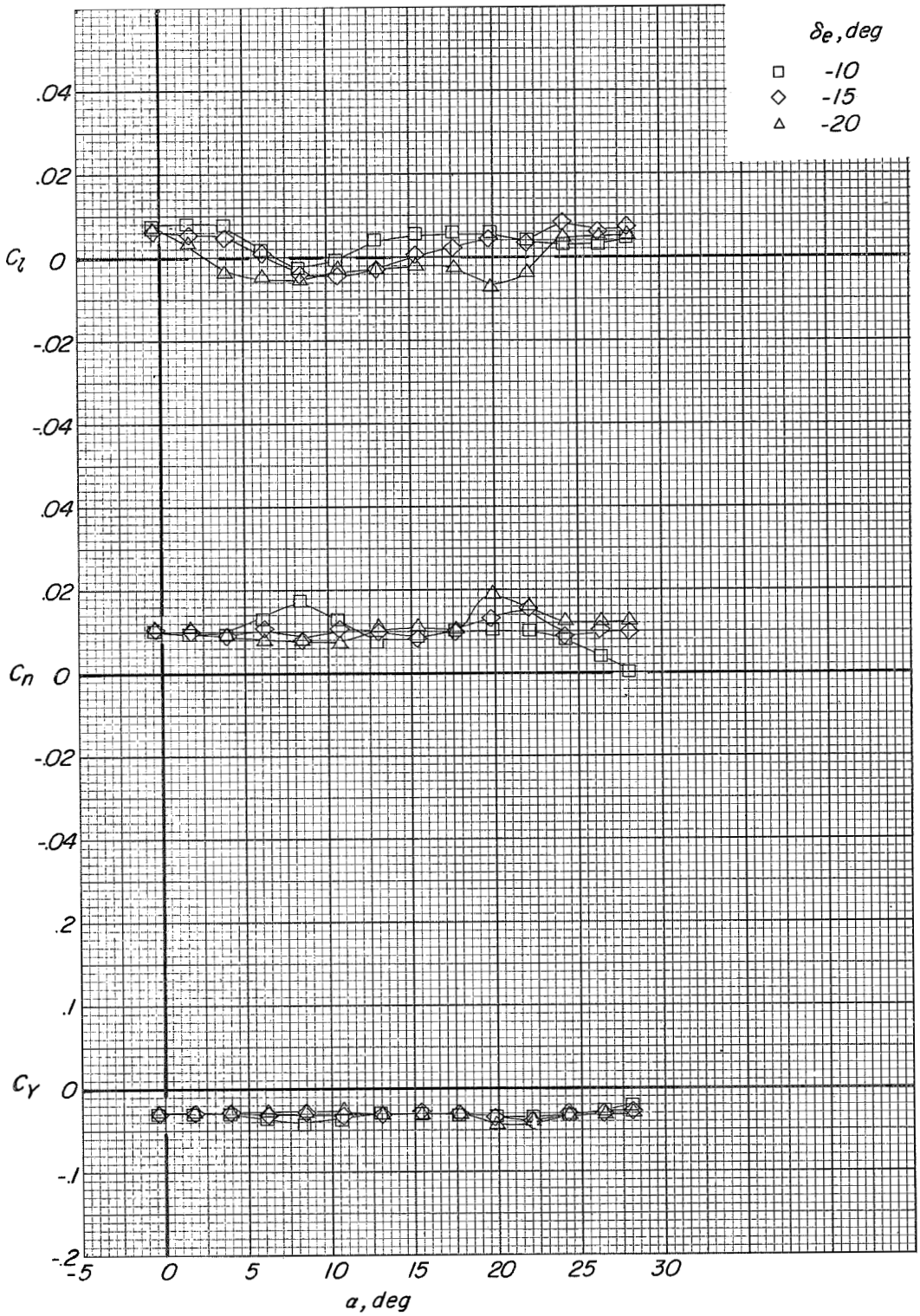
(b) $\beta = 2.3^{o}$; $\delta_a = 10^{o}$; M = 0.50.

Figure 26.- Continued.



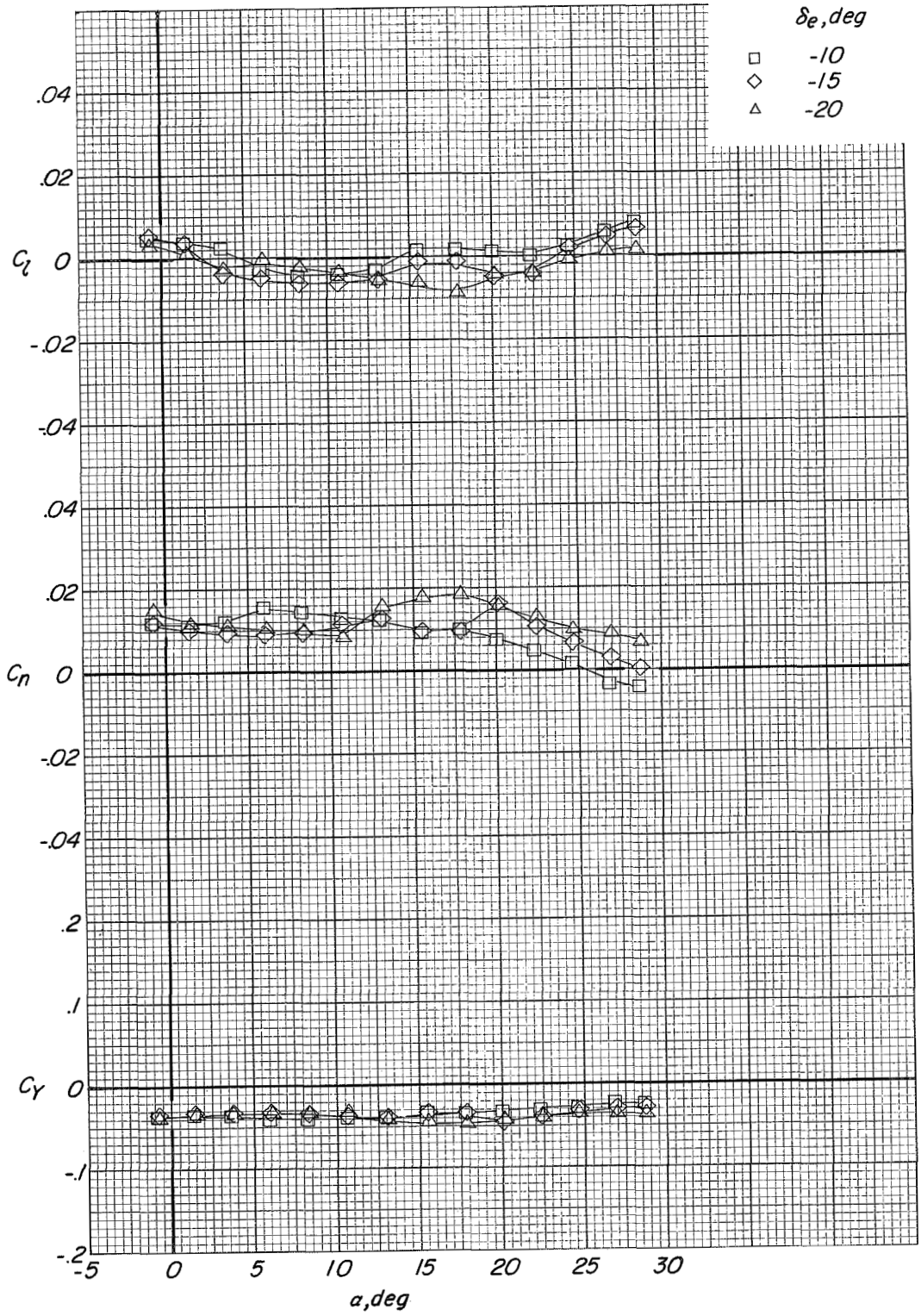
(c) $\beta = 2.3^{o}$; $\delta_a = 10^{o}$; M = 0.60.

Figure 26.- Continued.



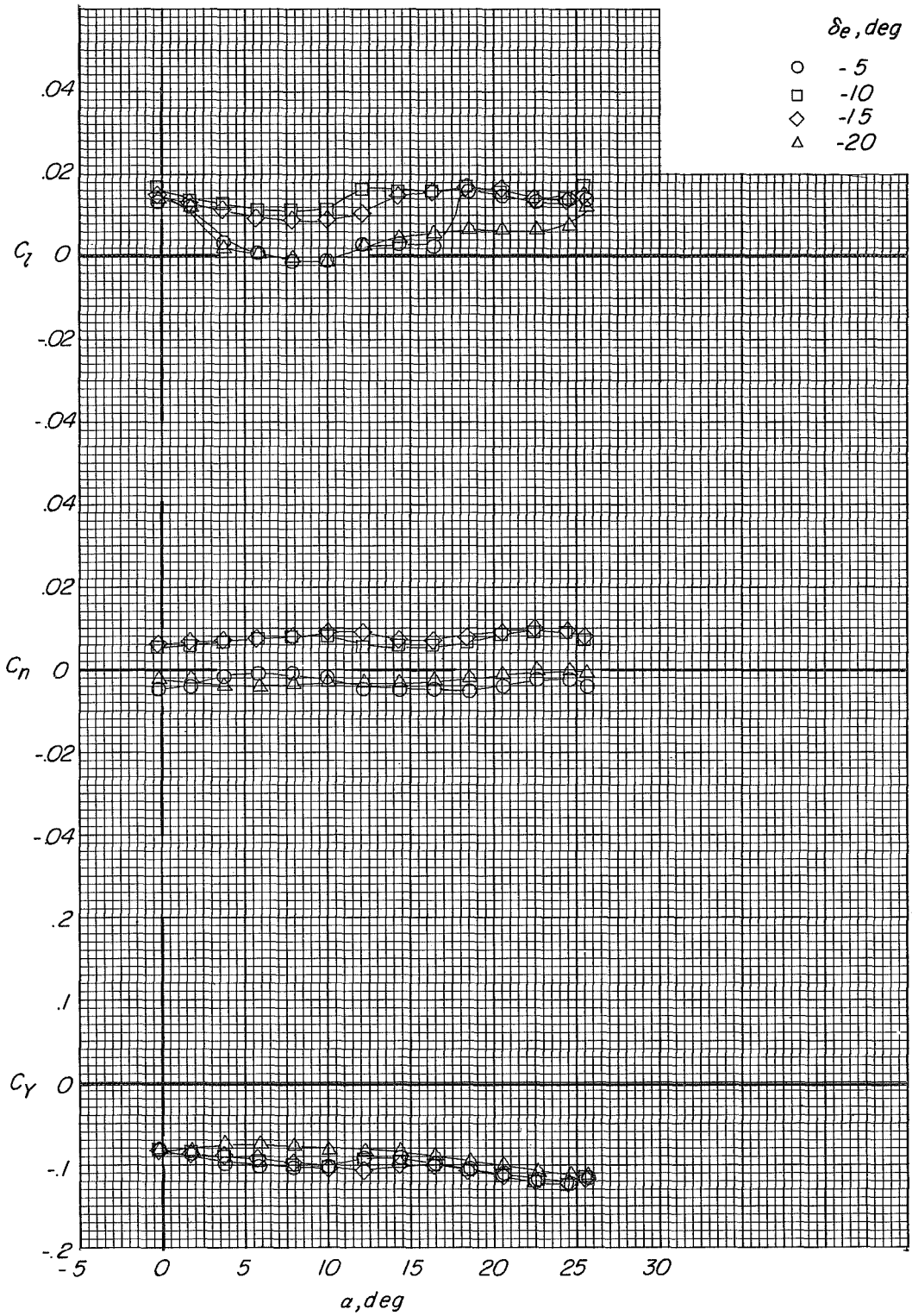
(d) $\beta = 2.3^{o}$; $\delta_a = 10^{o}$; M = 0.70.

Figure 26.- Continued.



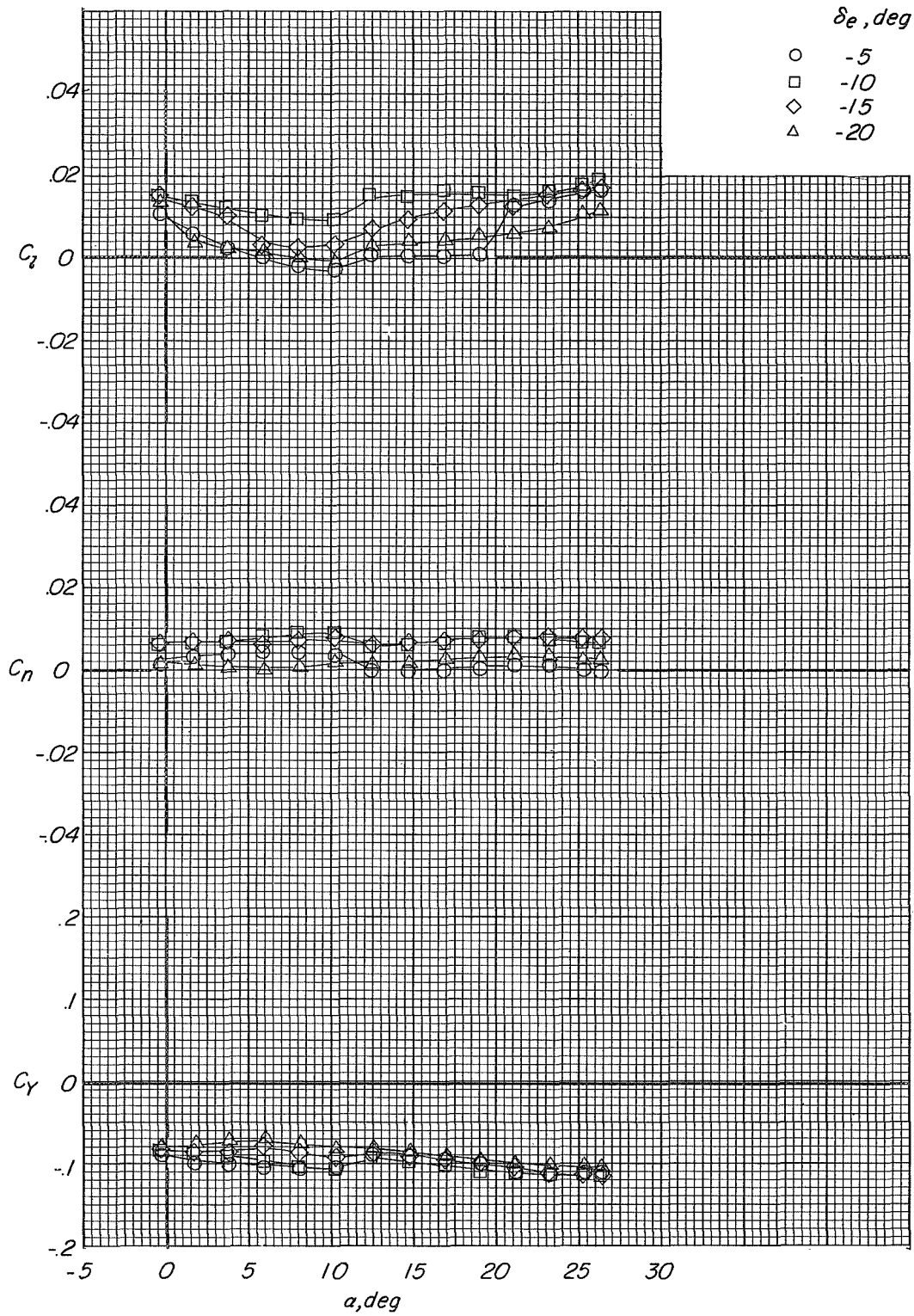
(e) $\beta = 2.3^{o}$; $\delta_a = 10^{o}$; M = 0.80.

Figure 26.- Continued.



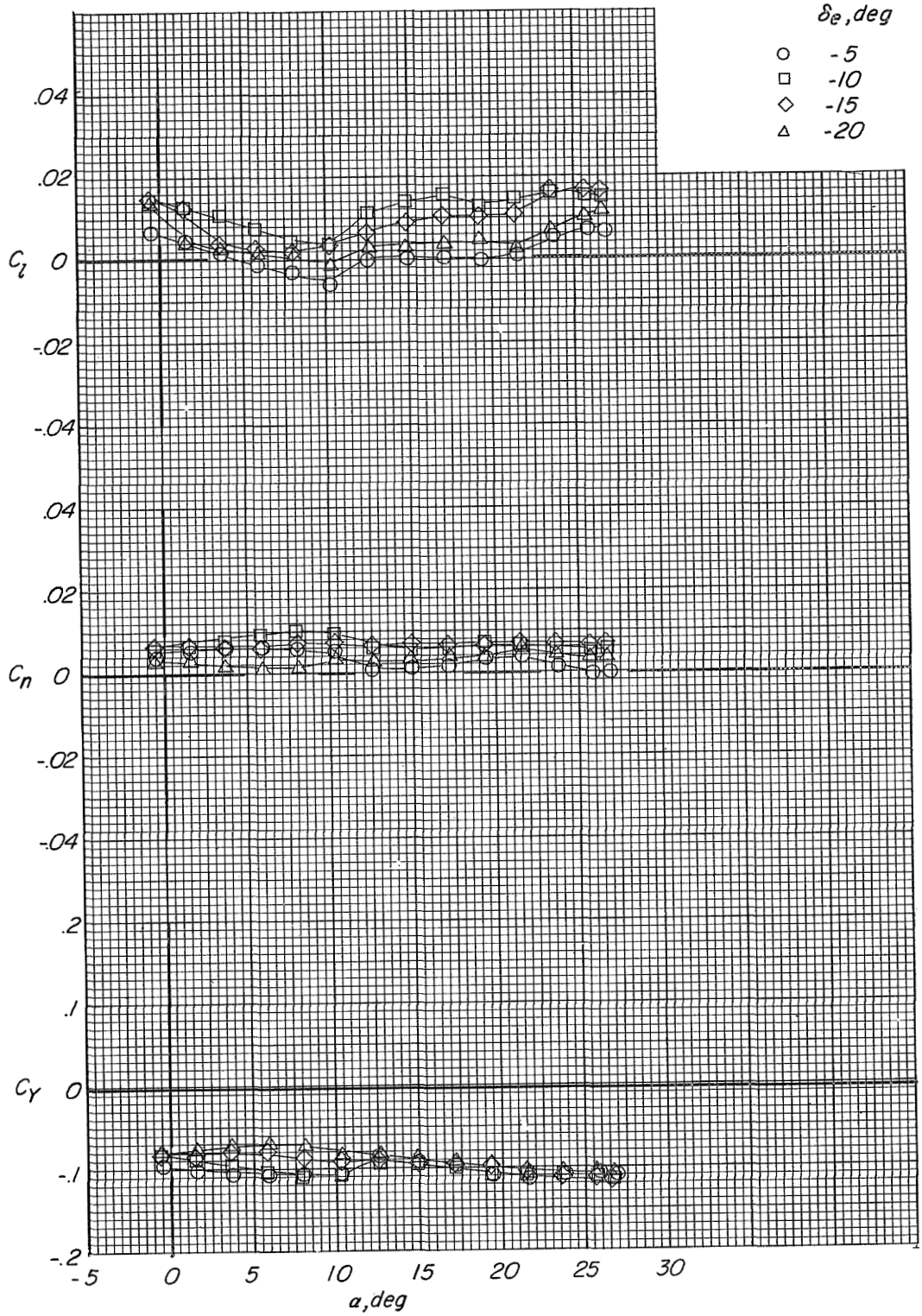
(f) $\beta = 2.3^{\circ}$; $\delta_a = 20^{\circ}$; M = 0.35.

Figure 26.- Continued.



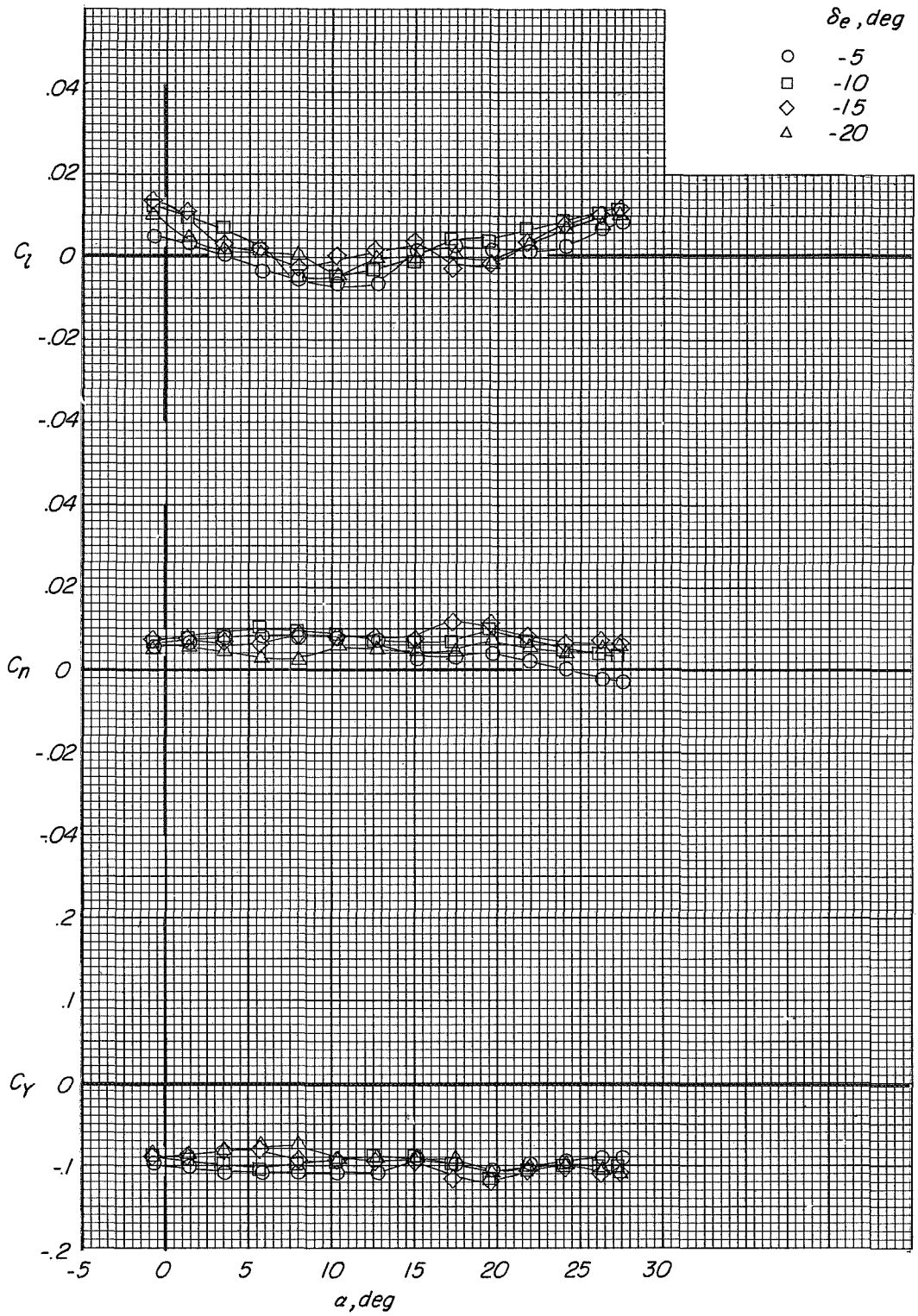
(g) $\beta = 2.3^{o}$; $\delta_a = 20^{o}$; M = 0.50.

Figure 26.- Continued.



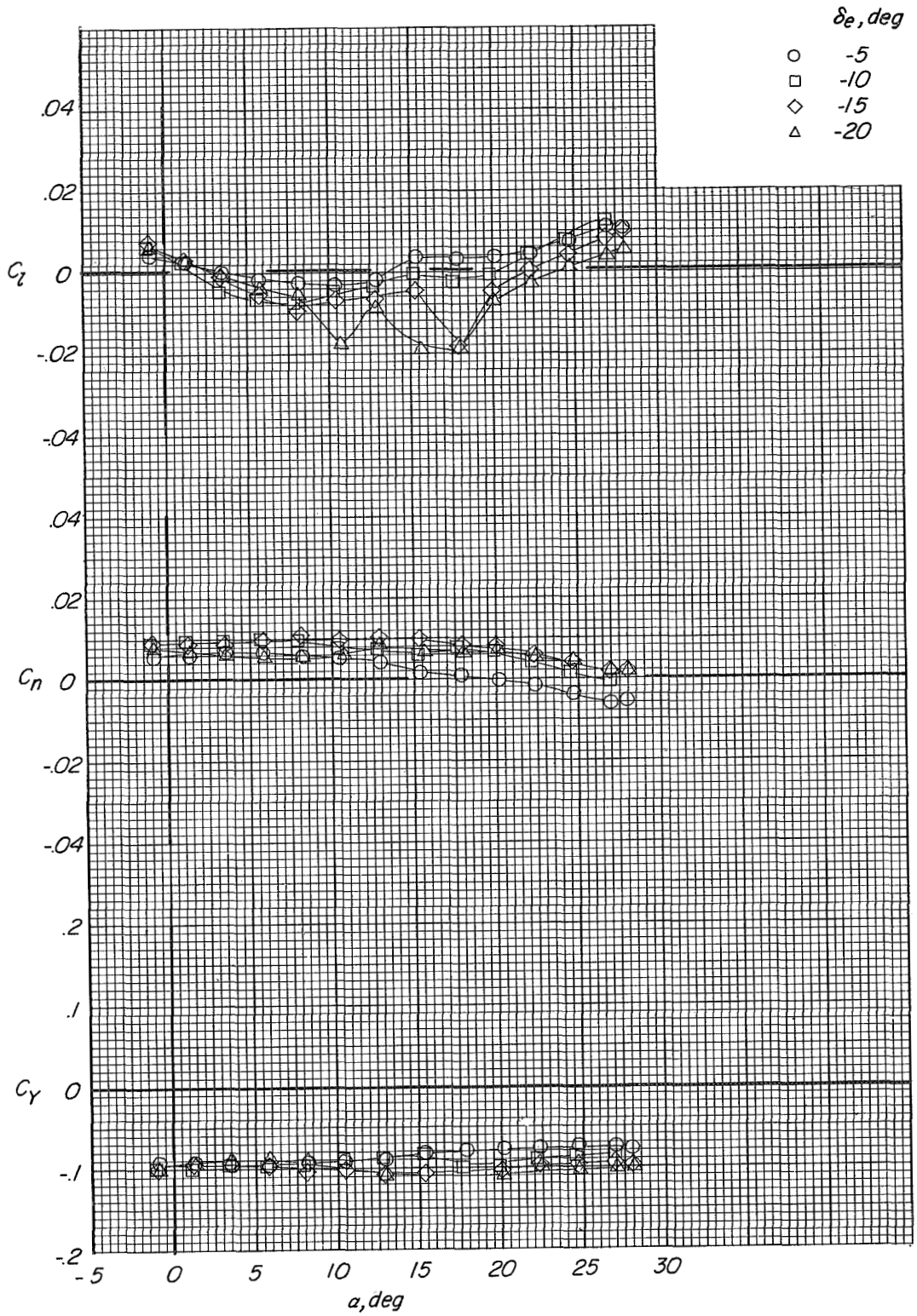
(h) $\beta = 2.3^{o}$; $\delta_a = 20^{o}$; M = 0.60.

Figure 26.- Continued.



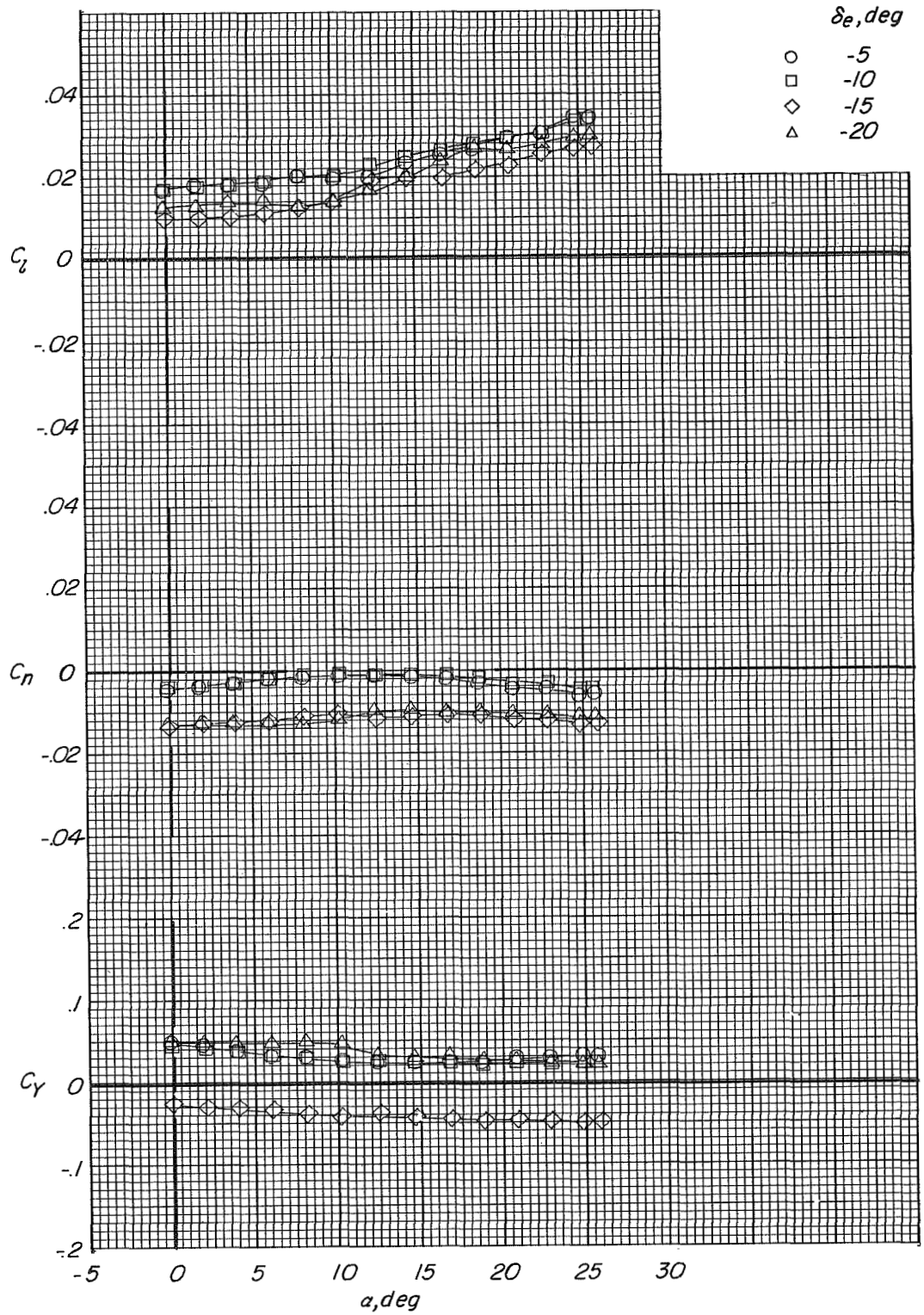
(i) $\beta = 2.3^{O}$; $\delta_a = 20^{O}$; M = 0.70.

Figure 26.- Continued.



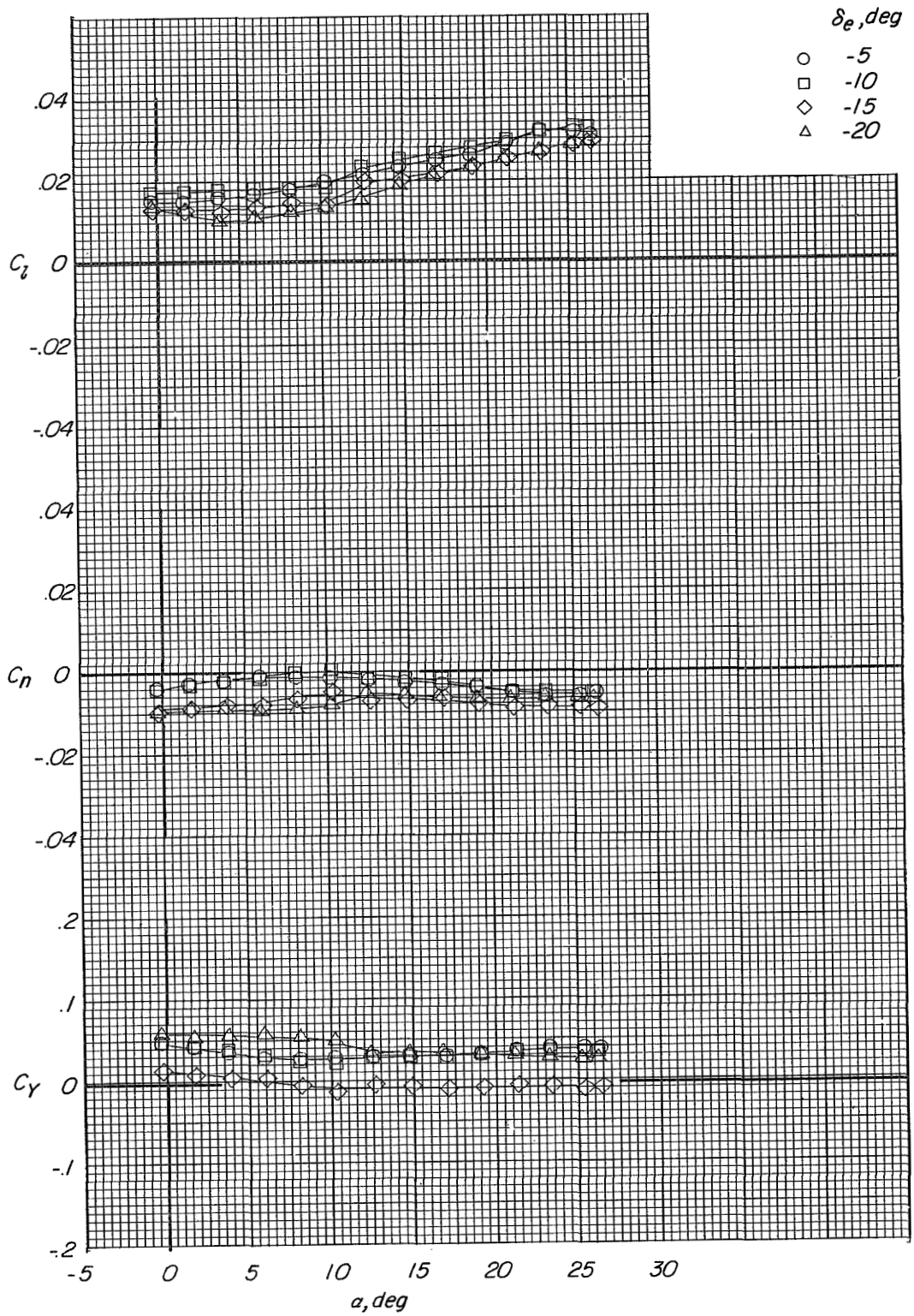
(j) $\beta = 2.3^{o}$; $\delta_a = 20^{o}$; M = 0.80.

Figure 26.- Continued.



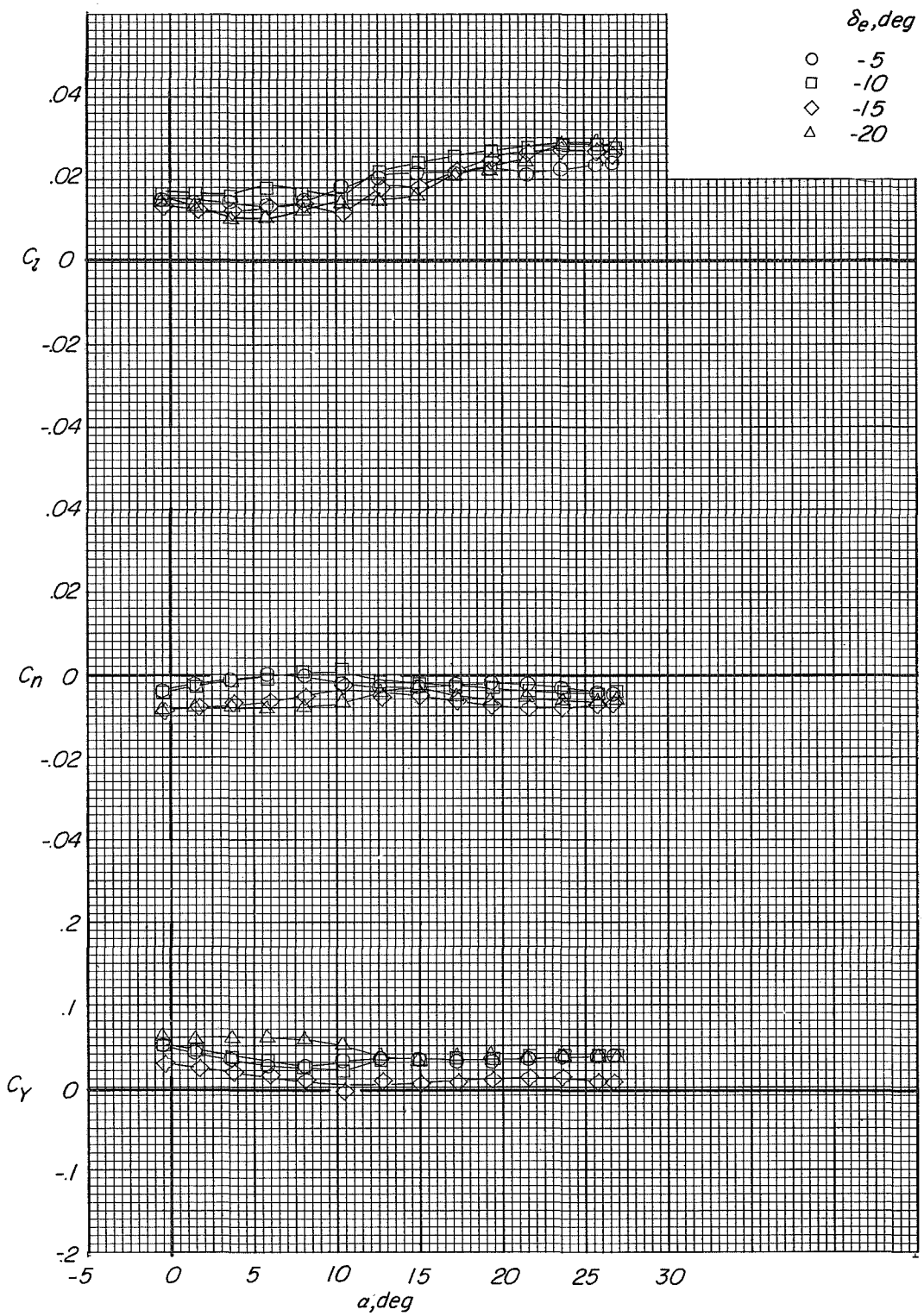
(k) $\beta = -2.3^{o}$; $\delta_a = 10^{o}$; M = 0.35.

Figure 26.- Continued.



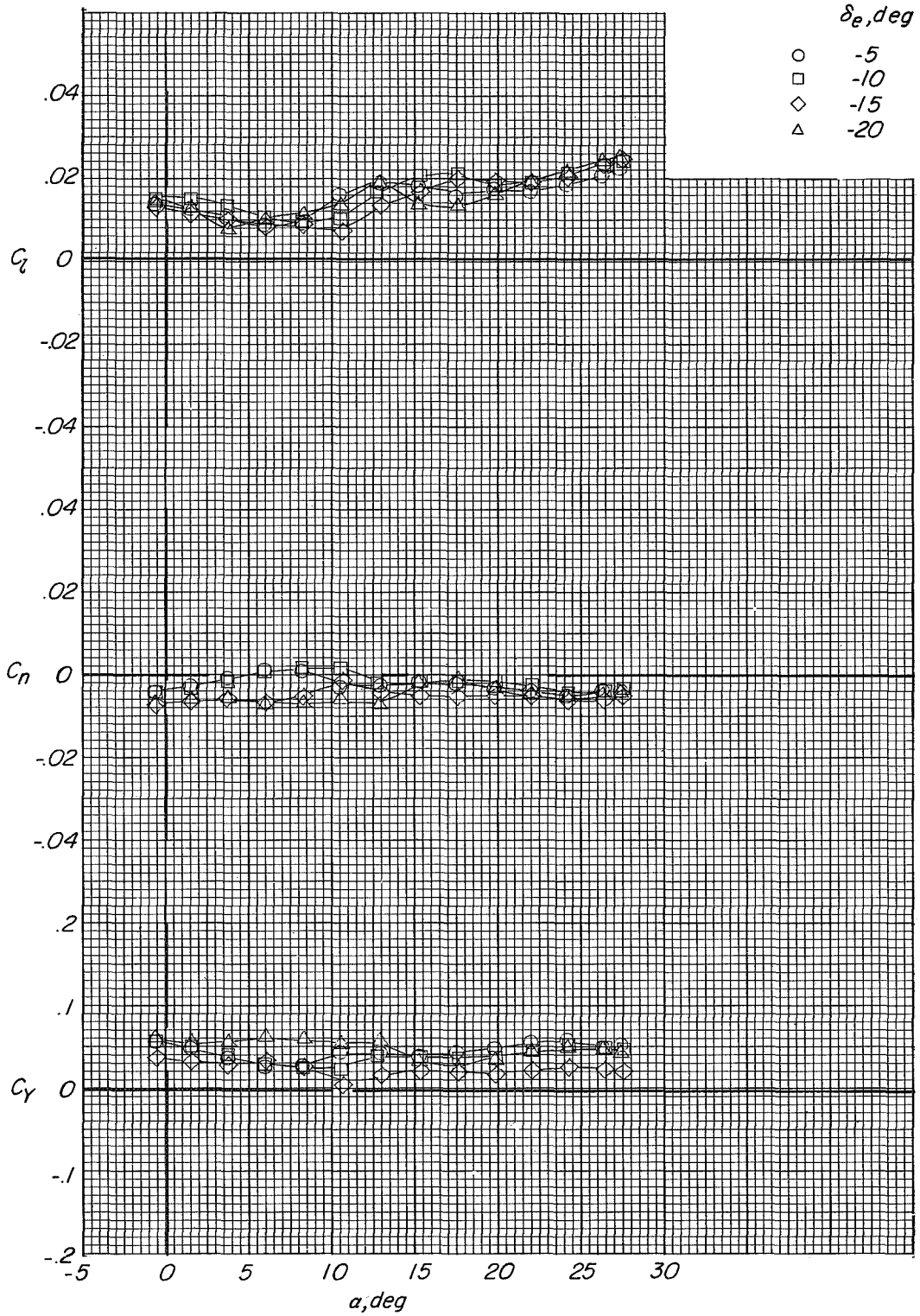
(l) $\beta = -2.3^{o}$; $\delta_a = 10^{o}$; M = 0.50.

Figure 26.- Continued.



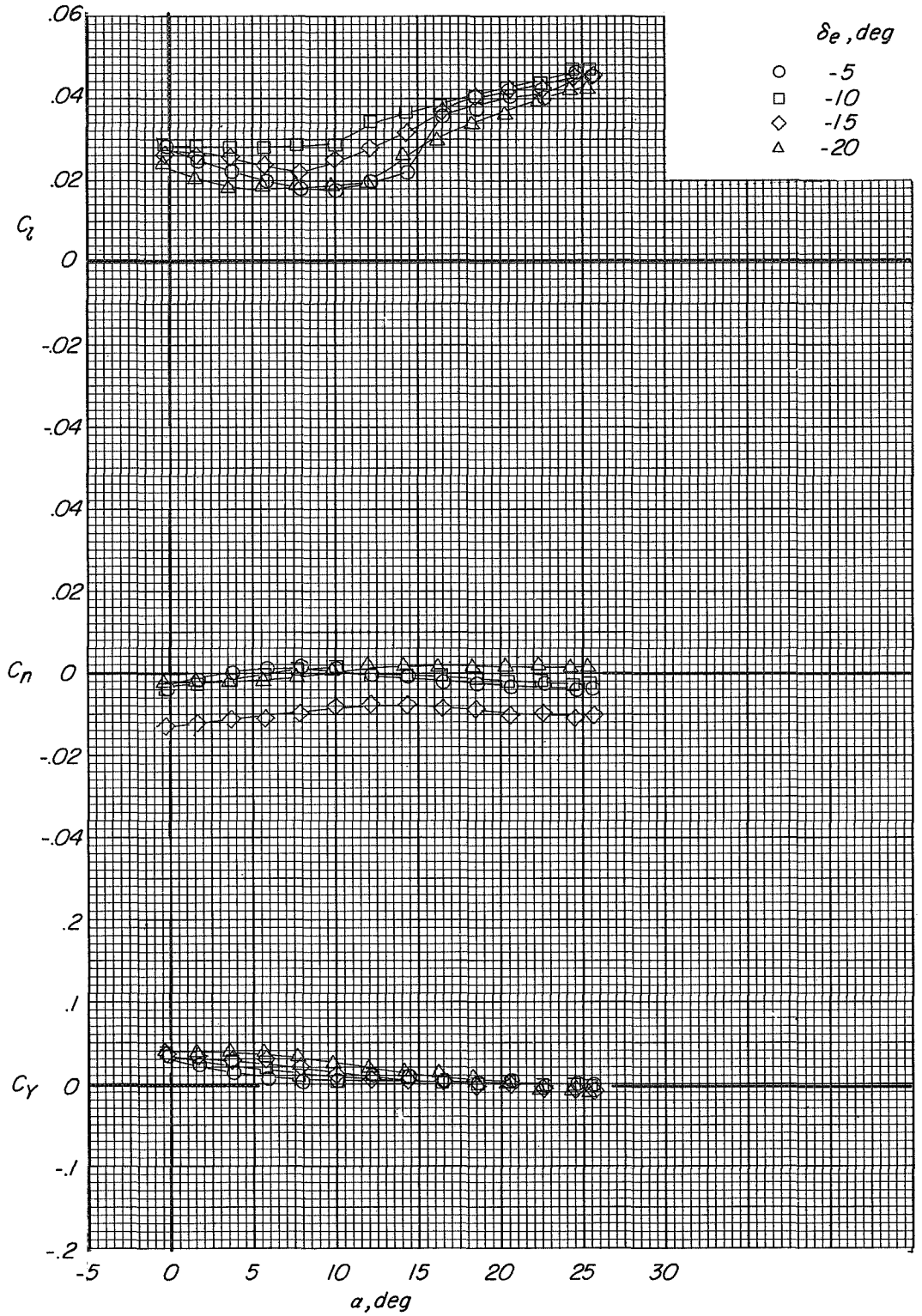
(m) $\beta = -2.3^{o}$; $\delta_a = 10^{o}$; M = 0.60.

Figure 26.- Continued.



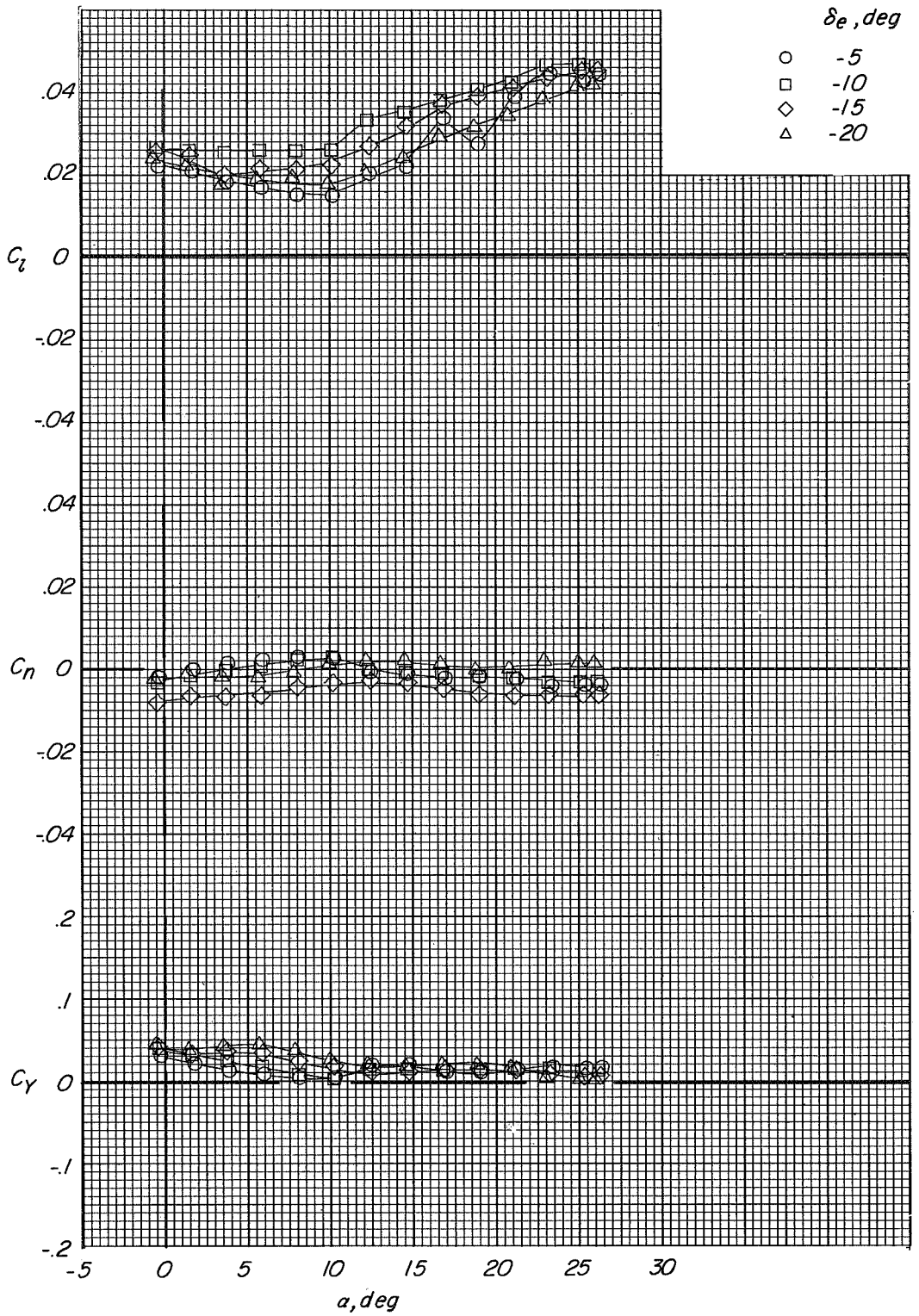
(n) $\beta = -2.3^{o}$; $\delta_a = 10^{o}$; M = 0.70.

Figure 26.- Continued.



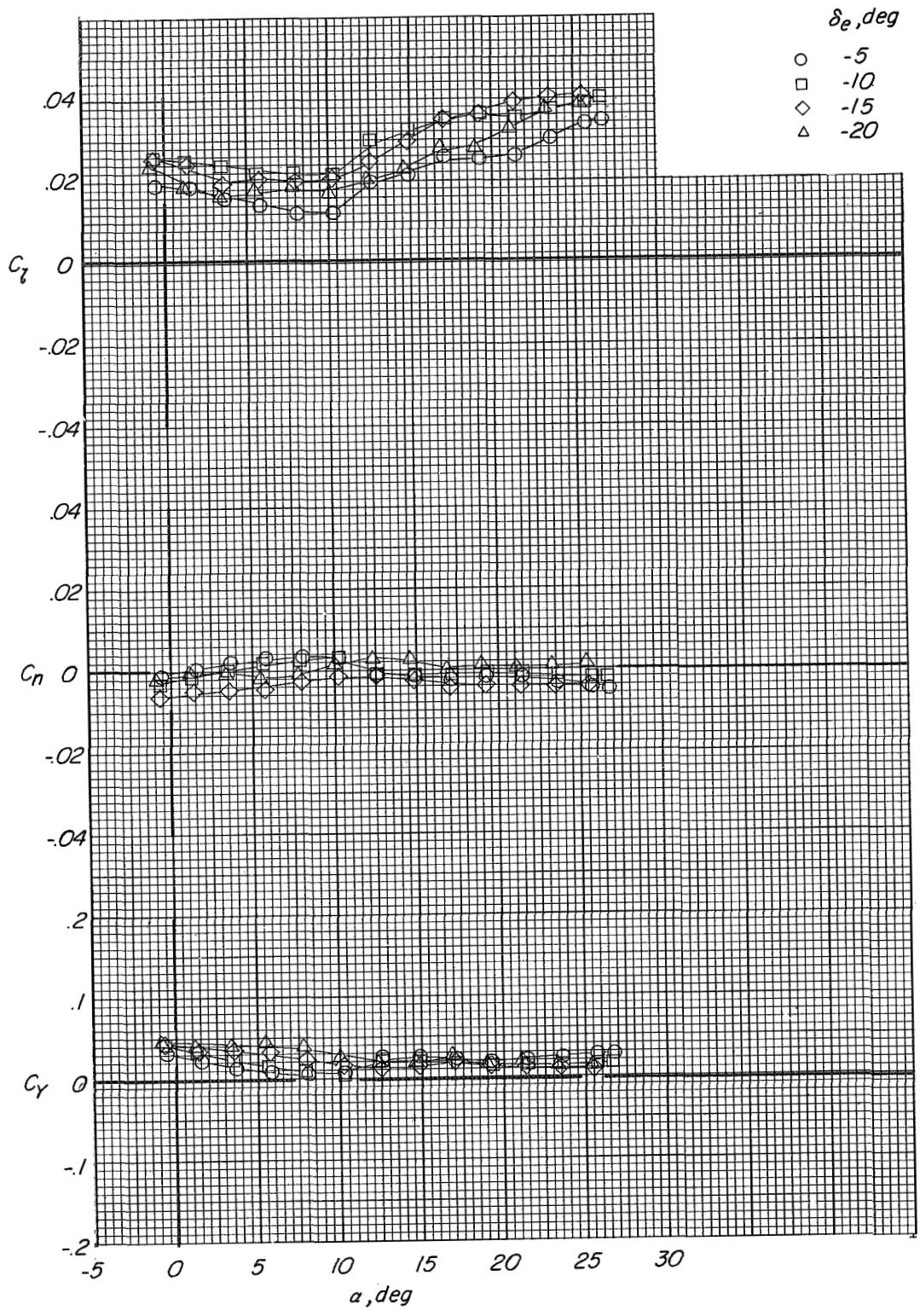
(o) $\beta = -2.3^{o}$; $\delta_a = 20^{o}$; M = 0.35.

Figure 26.- Continued.



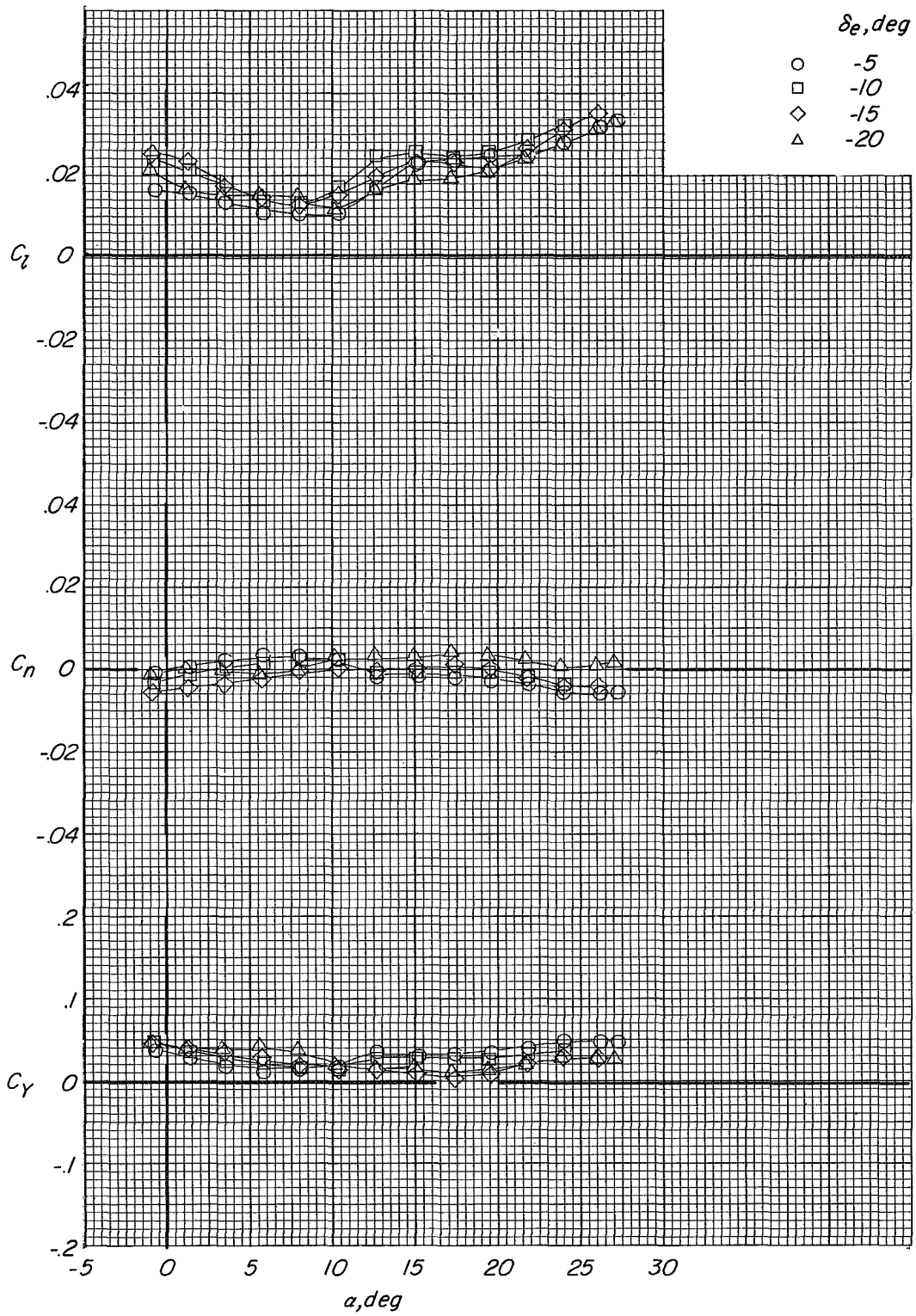
(p) $\beta = -2.3^{o}$; $\delta_a = 20^{o}$; M = 0.50.

Figure 26.- Continued.



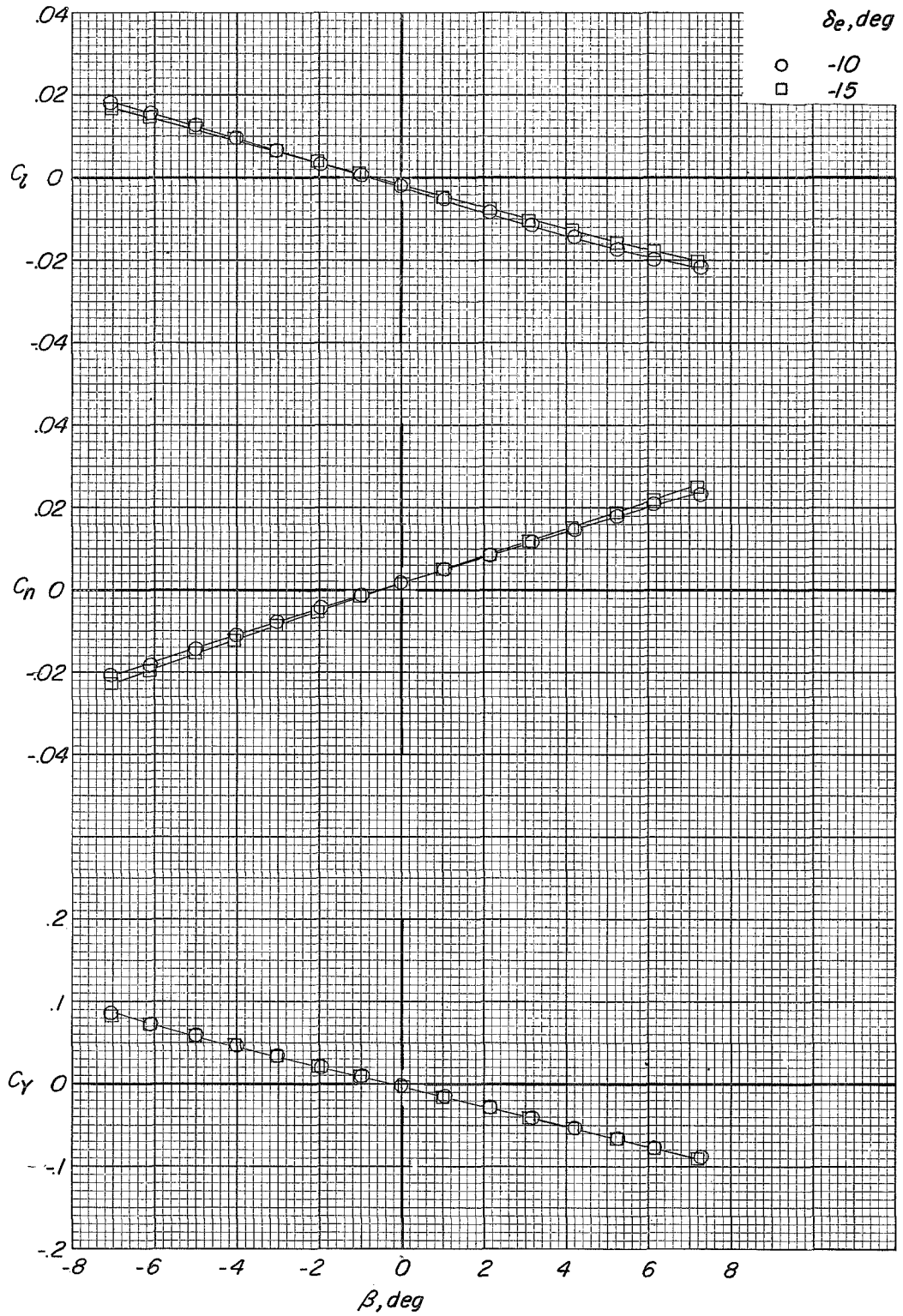
(q) $\beta = -2.3^{o}$; $\delta_a = 20^{o}$; M = 0.60.

Figure 26.- Continued.



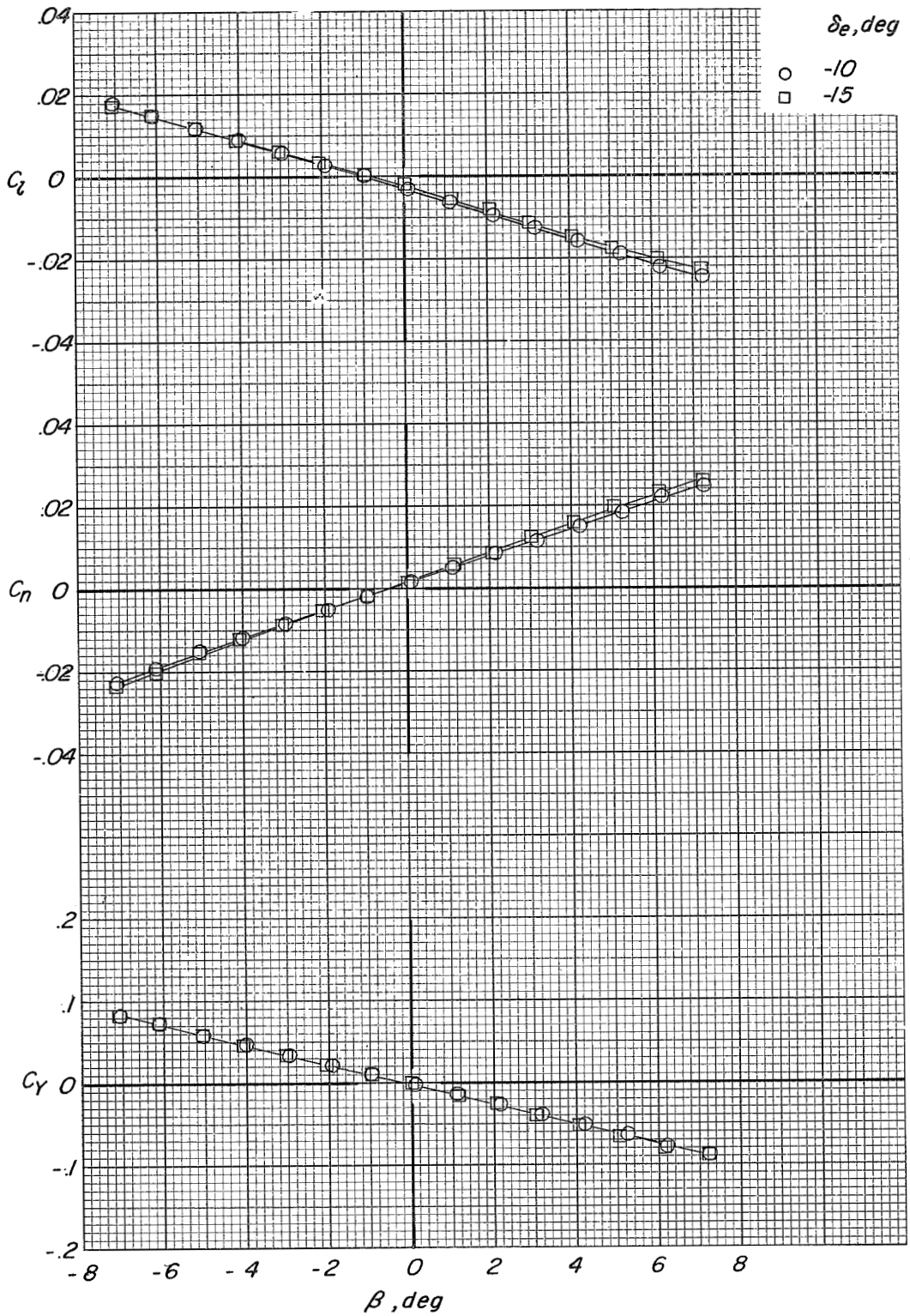
(r) $\beta = -2.3^{o}$; $\delta_a = 20^{o}$; M = 0.70.

Figure 26.- Concluded.



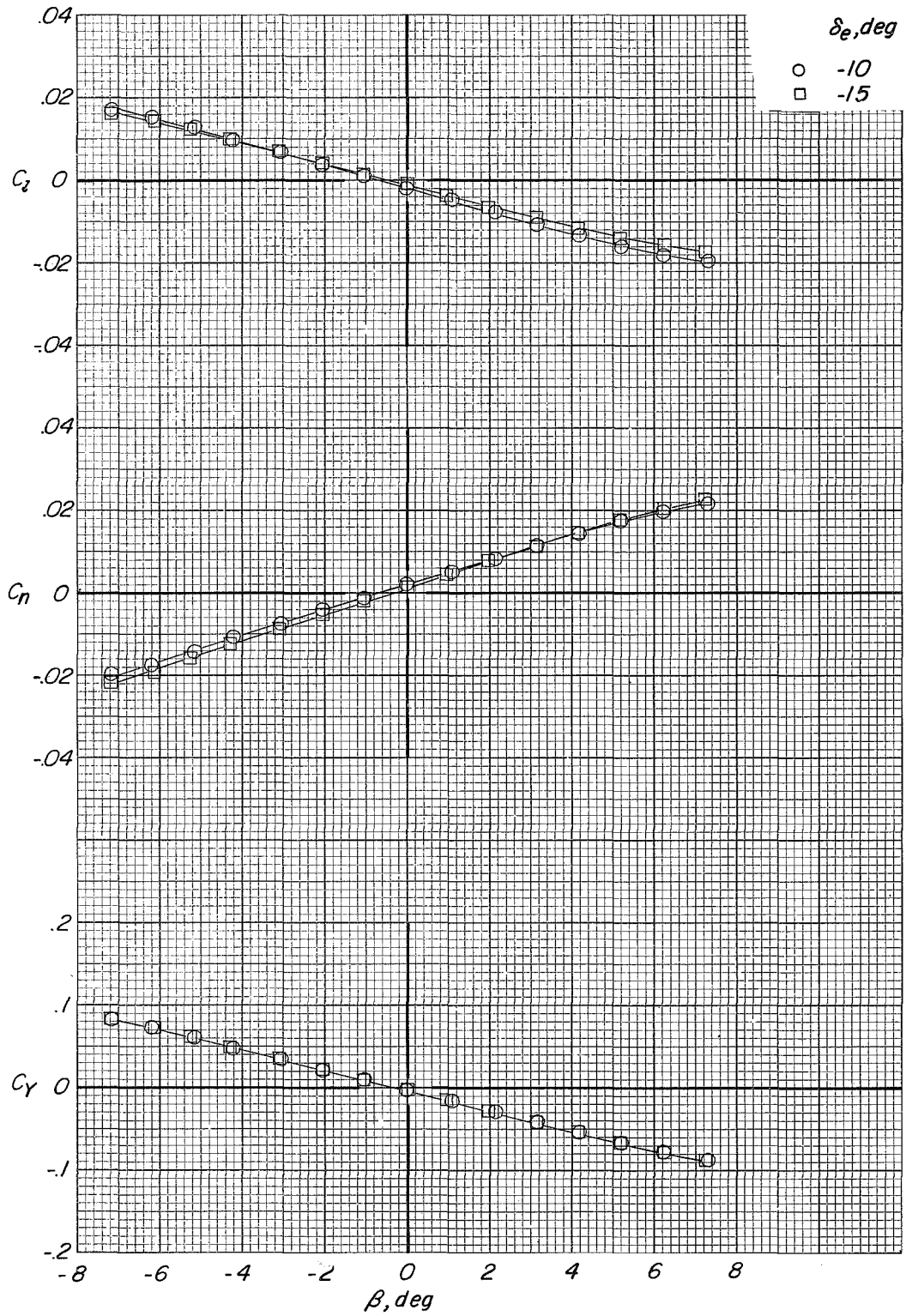
(a) $\delta_a = 0^o$; M = 0.35.

Figure 27.- Variation of the lateral force and moment coefficients with sideslip angle. Modification I fin configuration; auxiliary flaps in the subsonic position; $\alpha = 7^o$.



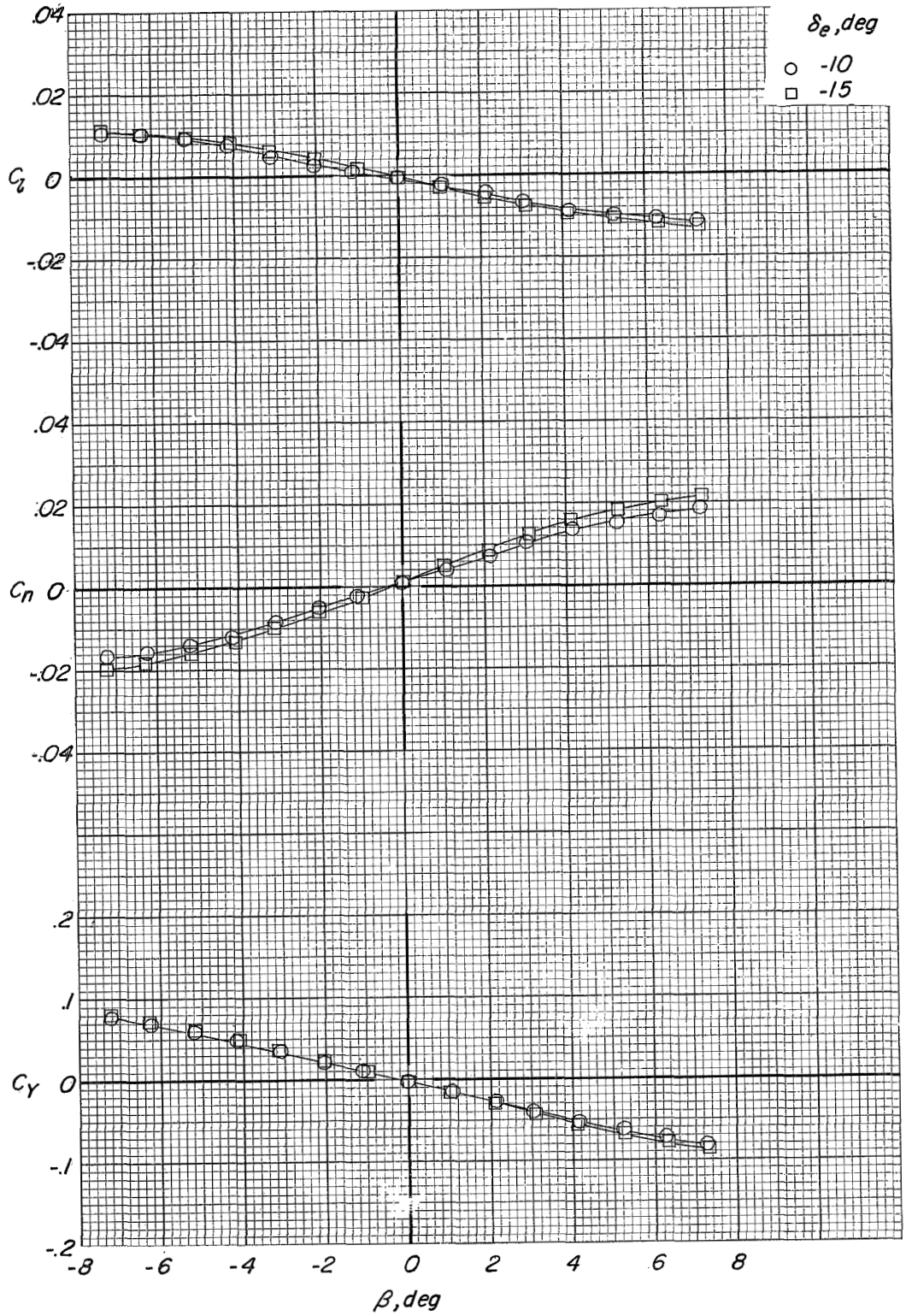
(b) $\delta_a = 0^o$; M = 0.50.

Figure 27.- Continued.



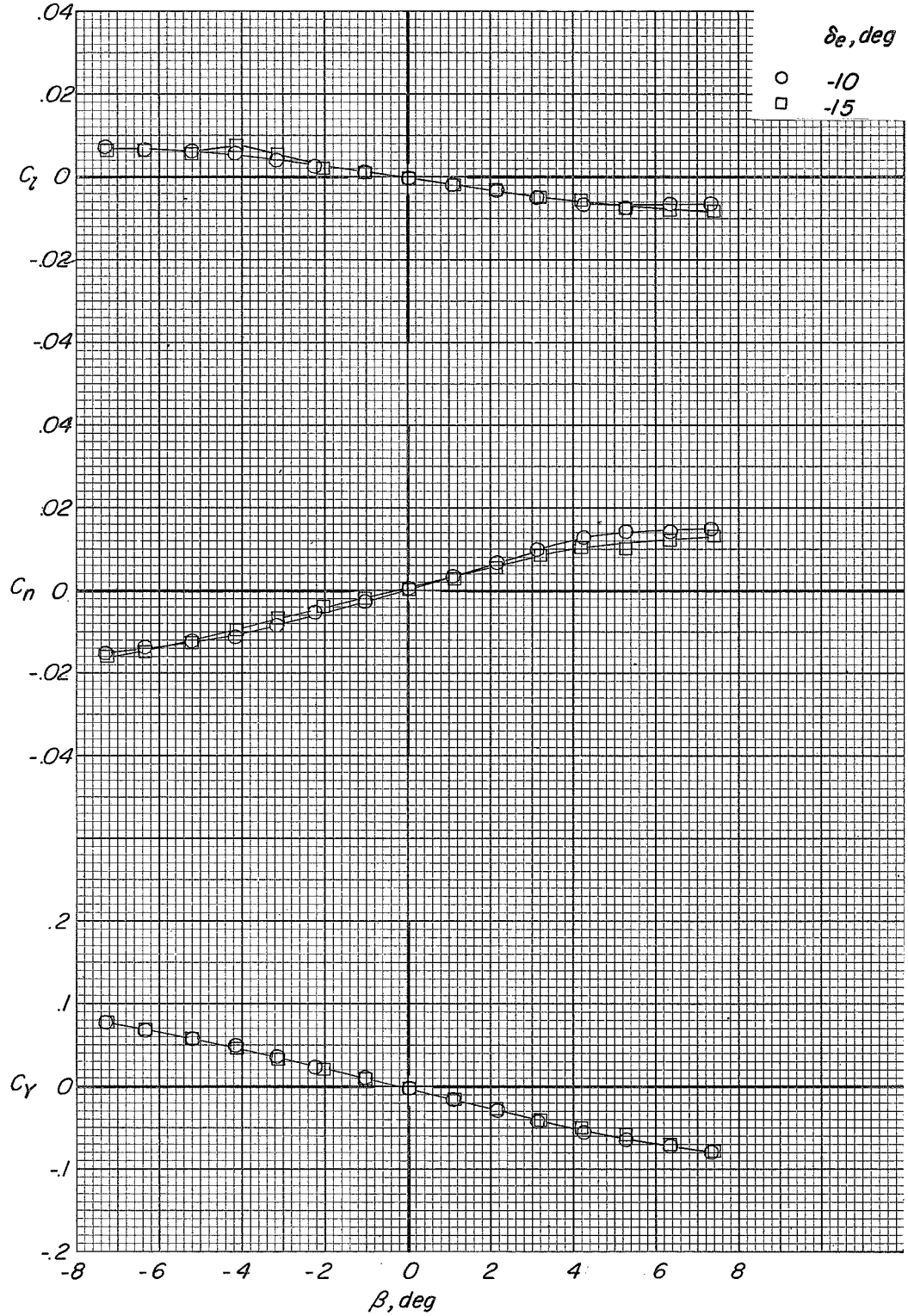
(c) $\delta_a = 0^o$; M = 0.60.

Figure 27.- Continued.



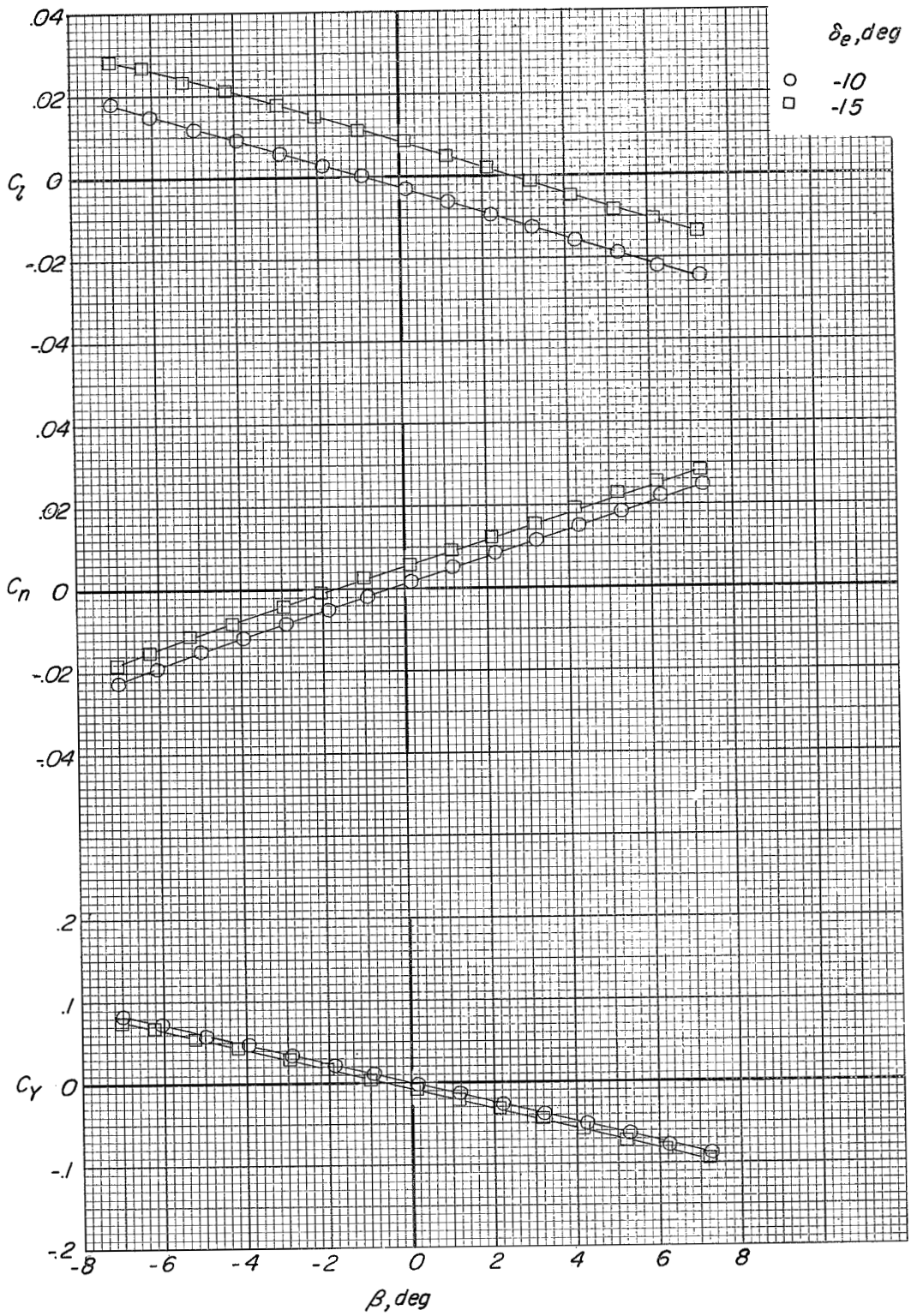
(d) $\delta_a = 0^o$; M = 0.70.

Figure 27.- Continued.



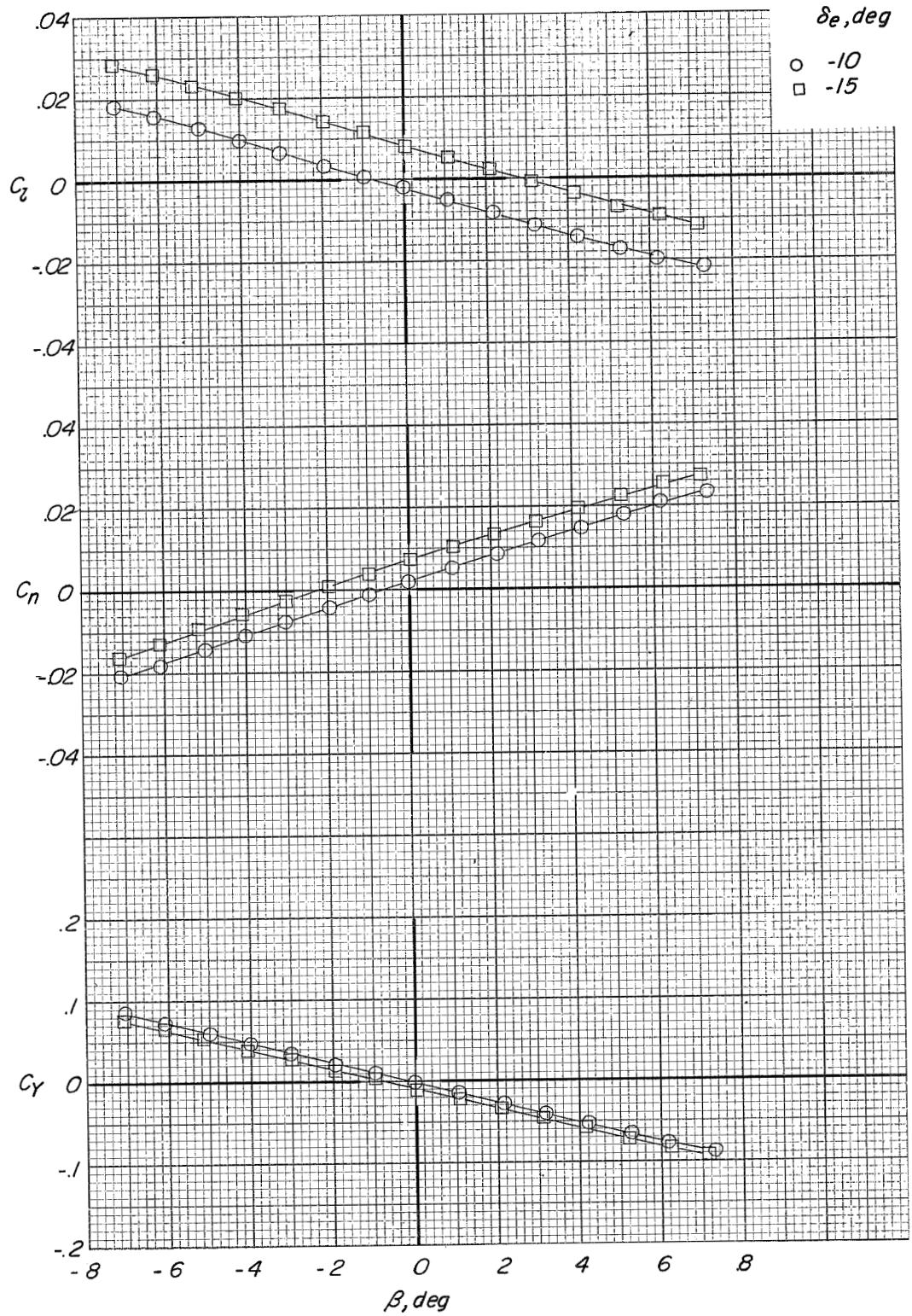
(e) $\delta_a = 0^o$; M = 0.80.

Figure 27.- Continued.



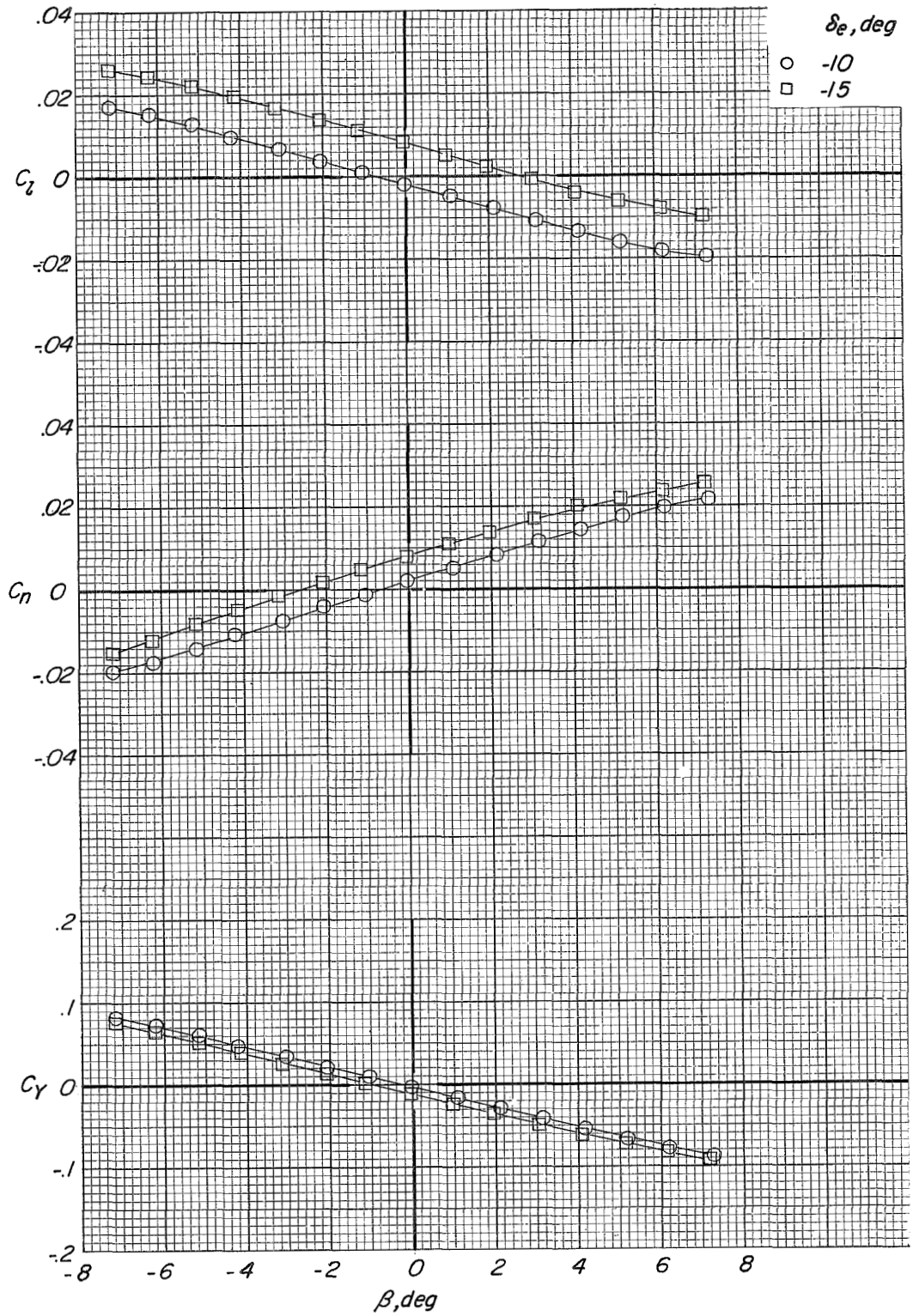
(f) $\delta_a = 10^o$; M = 0.35.

Figure 27.- Continued.



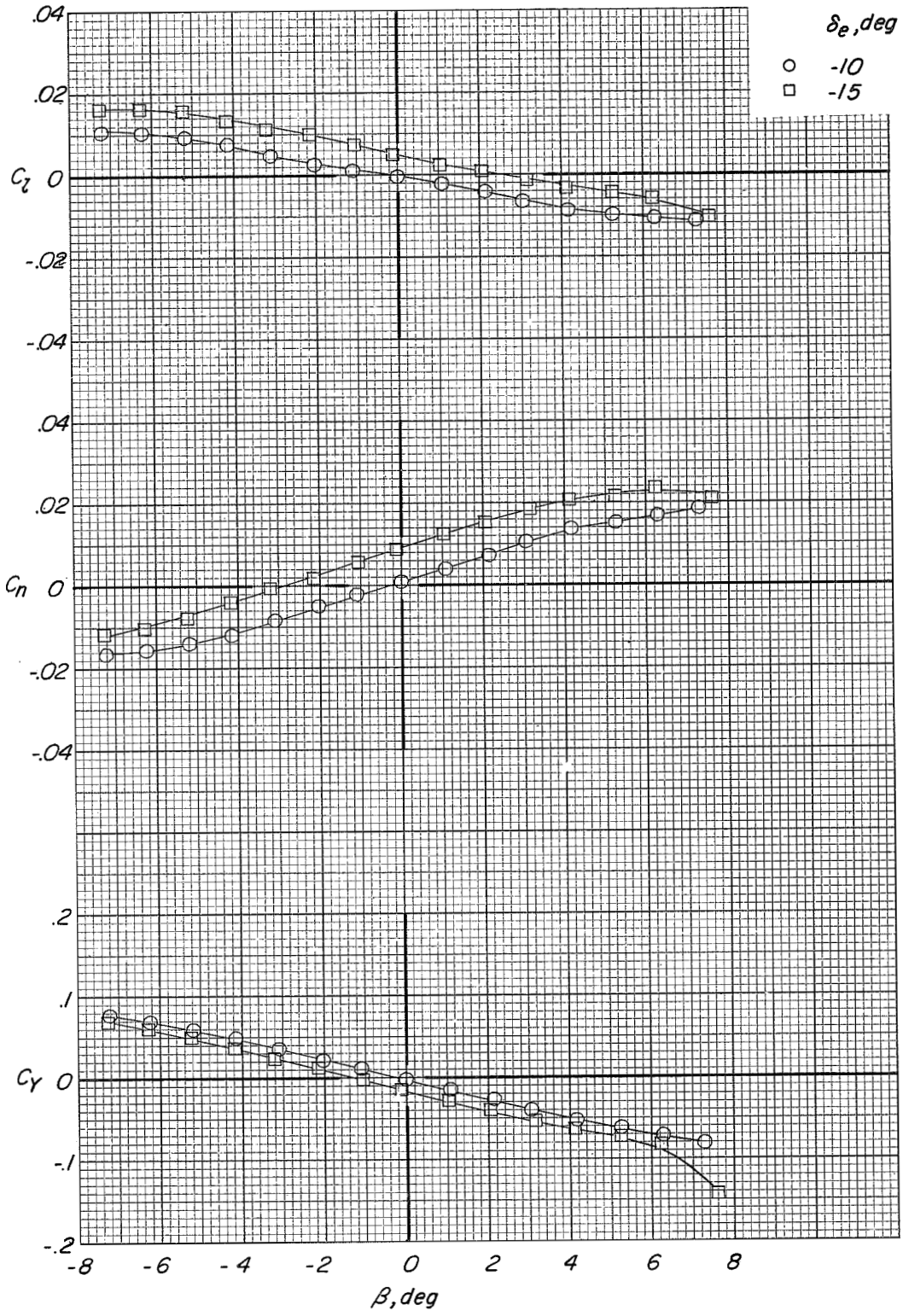
(g) $\delta_a = 10^o$; M = 0.50.

Figure 27.- Continued.



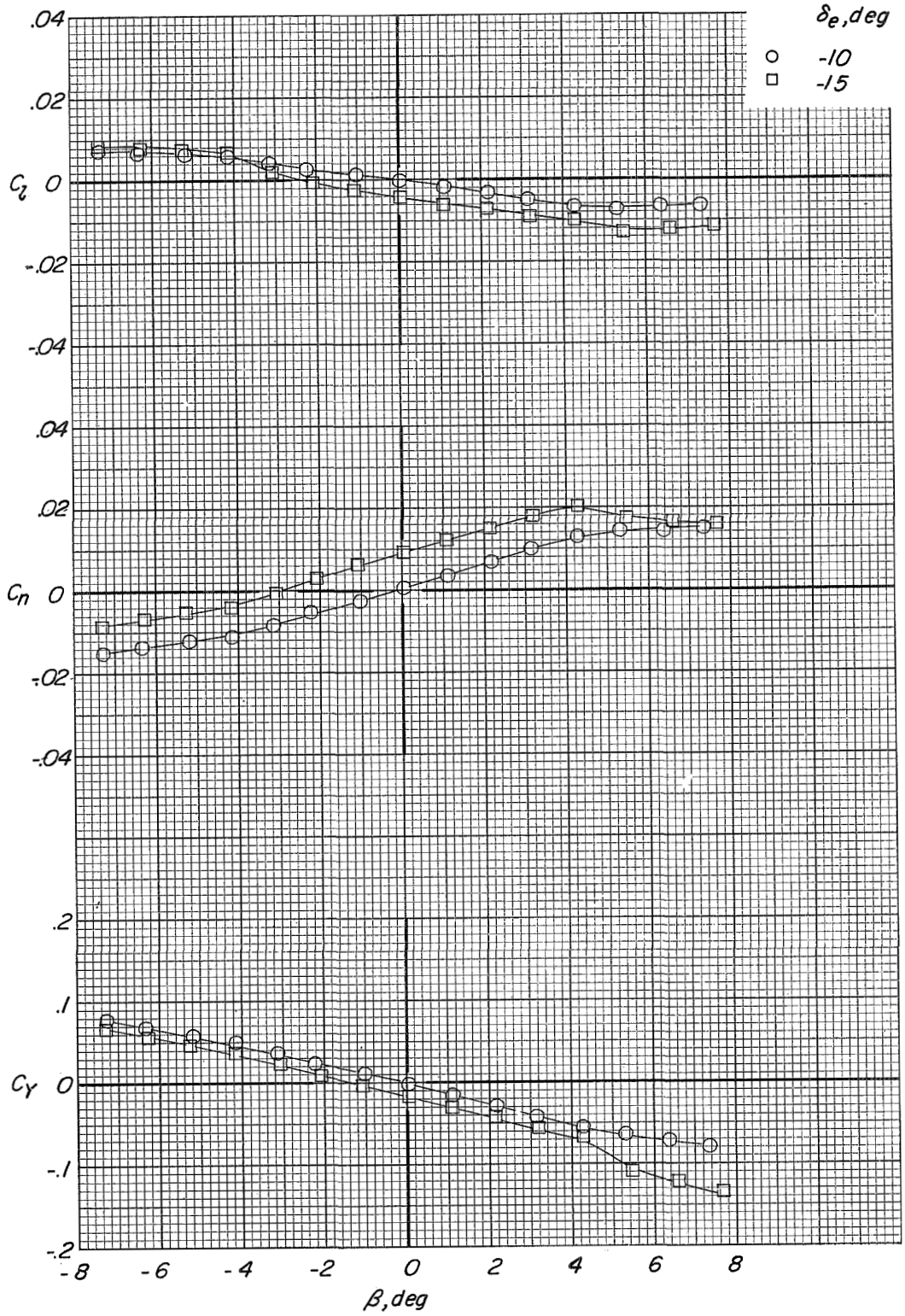
(h) $\delta_a = 10^o$; M = 0.60.

Figure 27.- Continued.



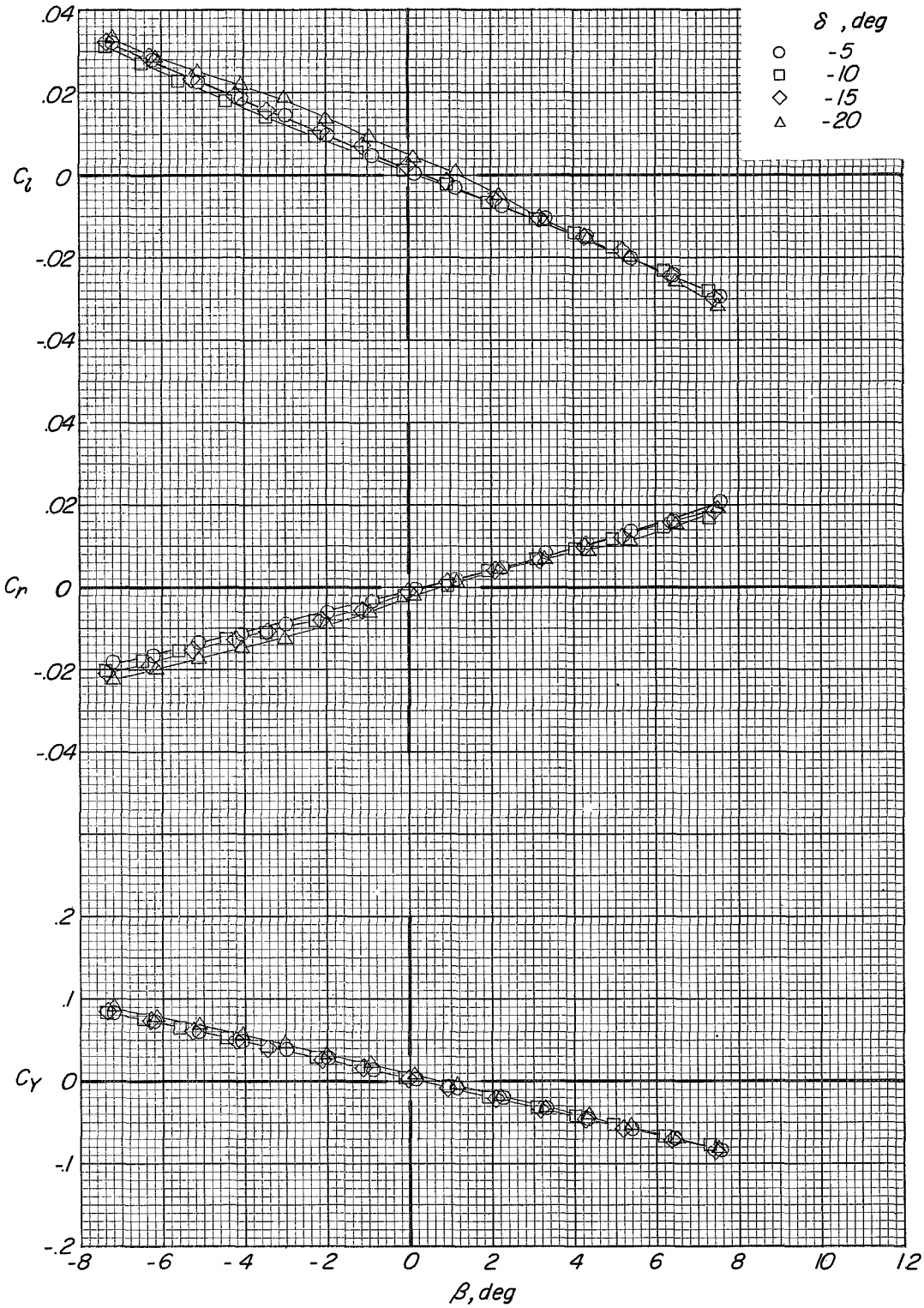
(i) $\delta_a = 10^o$; M = 0.70.

Figure 27.- Continued.



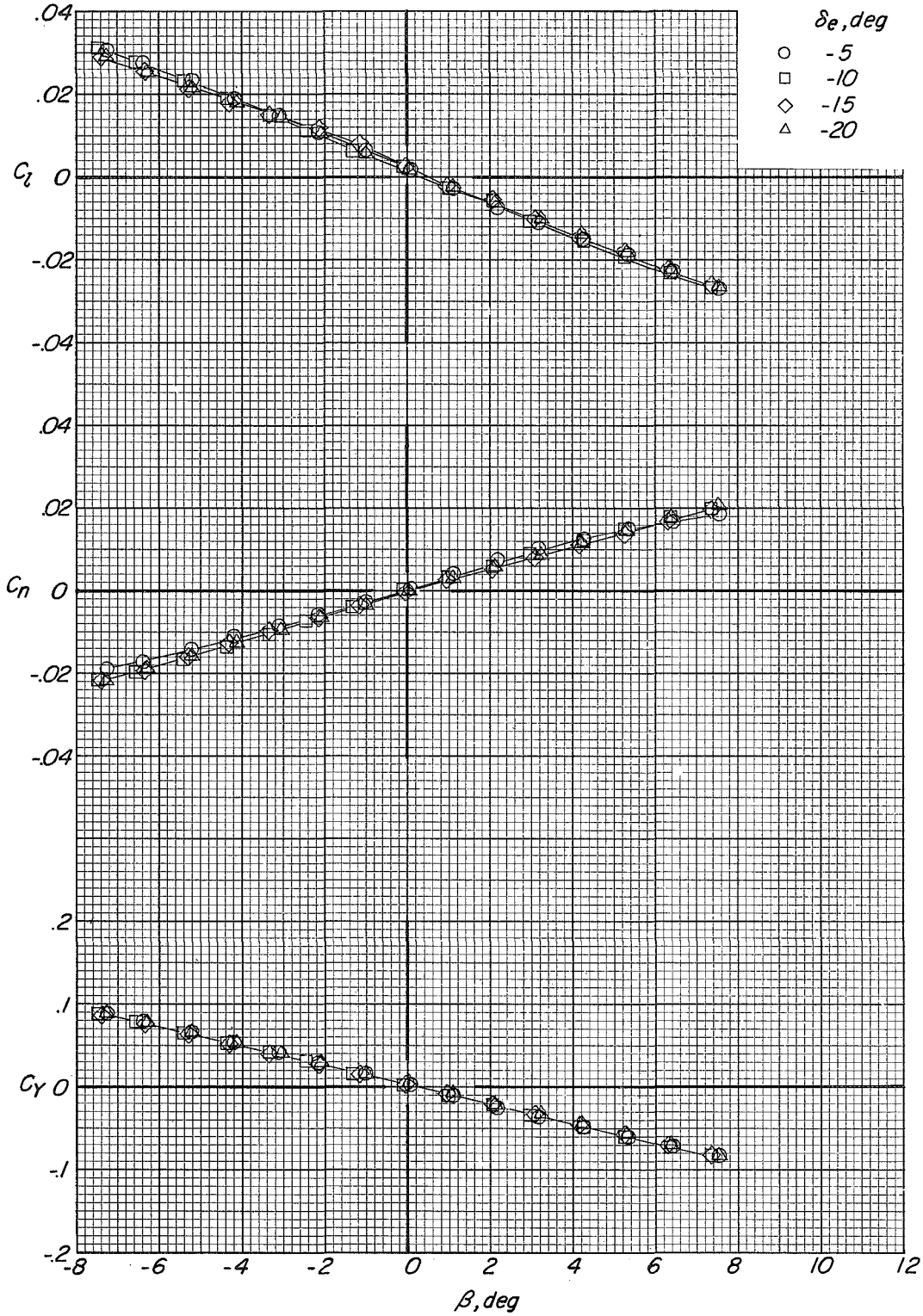
(j) $\delta_a = 10^o$; M = 0.80.

Figure 27.- Concluded.



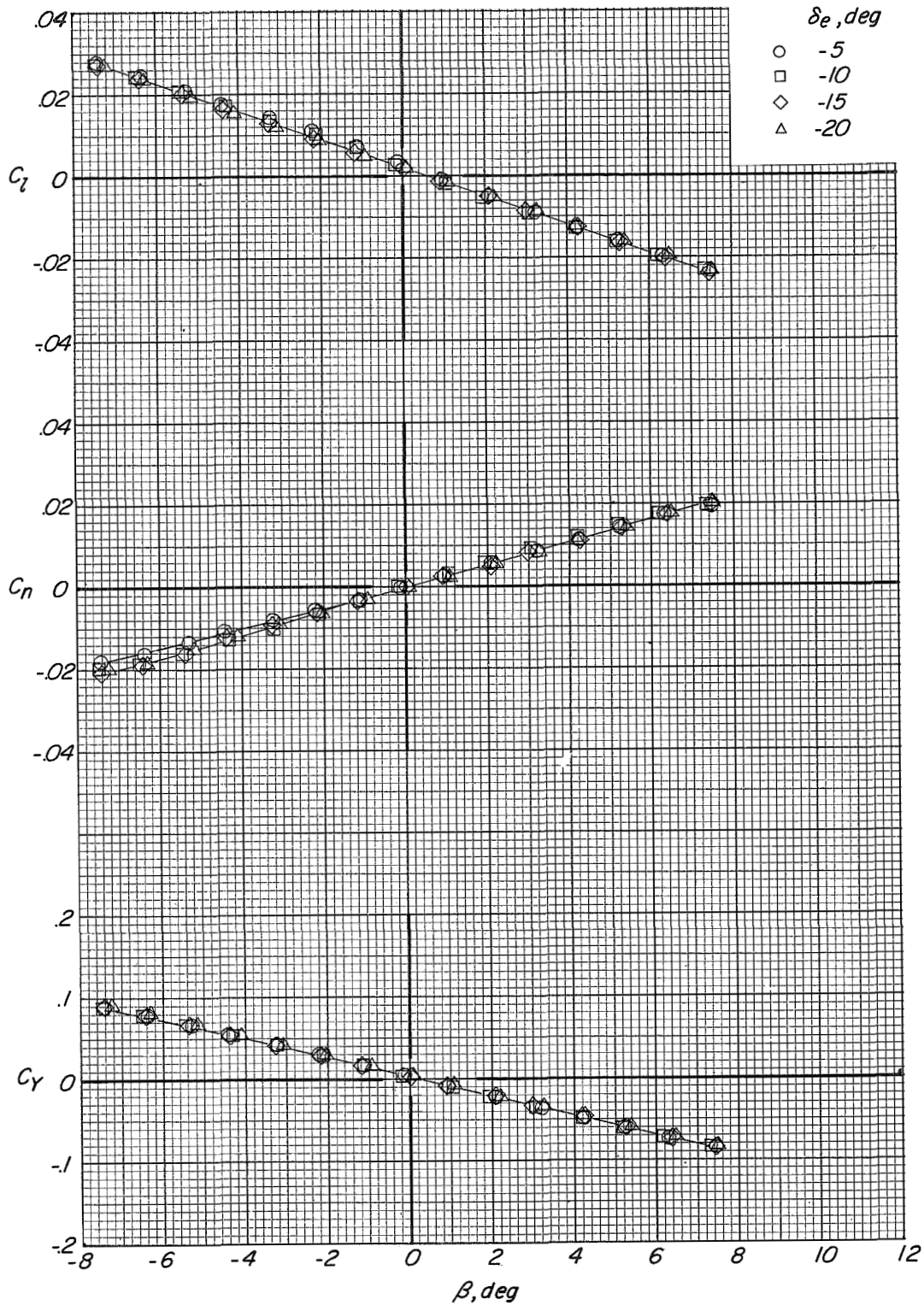
(a) $\delta_a = 0^o$; M = 0.35.

Figure 28.- Variation of the lateral force and moment coefficients with sideslip angle. Modification I fin configuration; auxiliary flaps in the subsonic position; $\alpha = 17^o$.



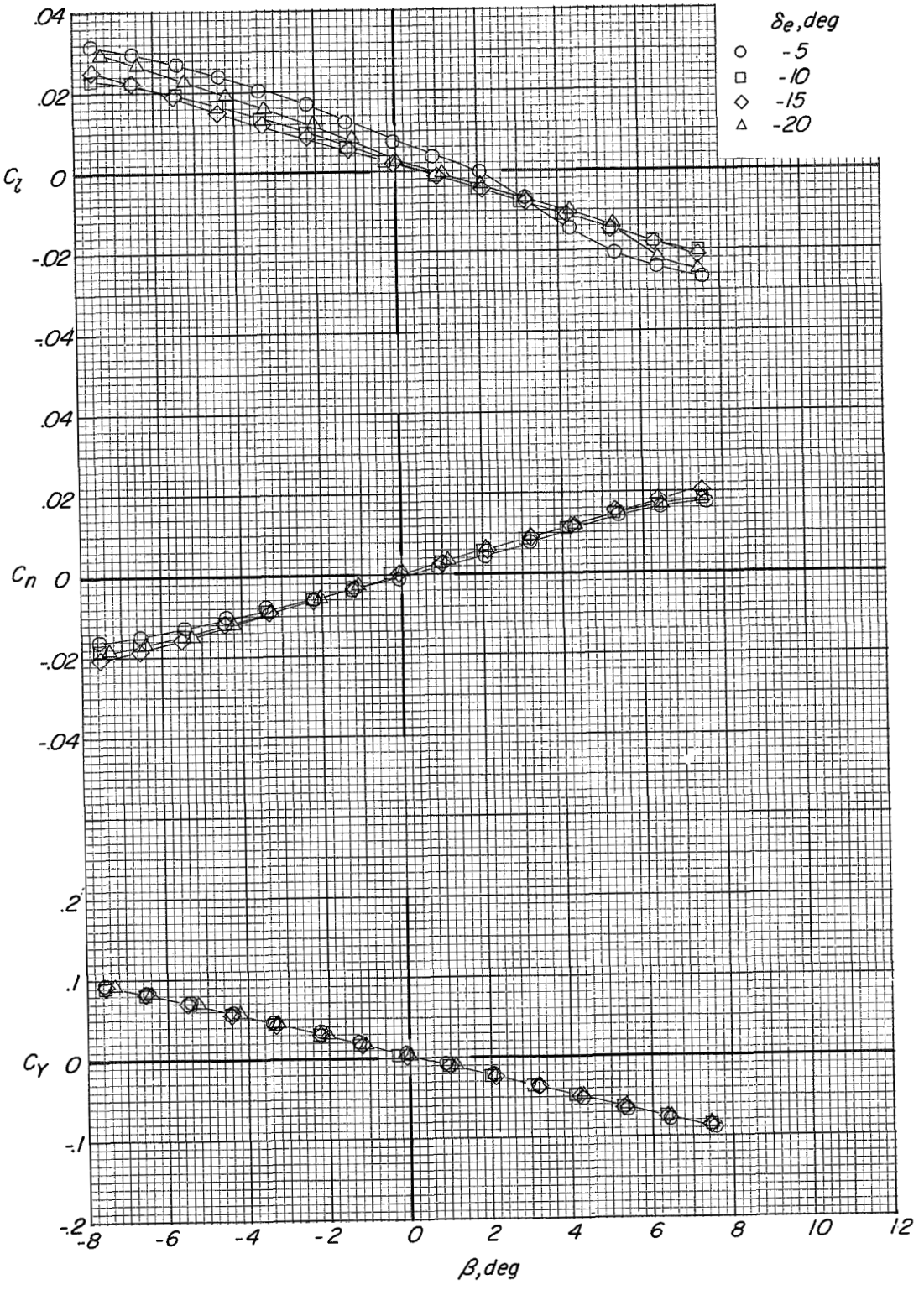
(b) $\delta_a = 0^o$; M = 0.50.

Figure 28.- Continued.



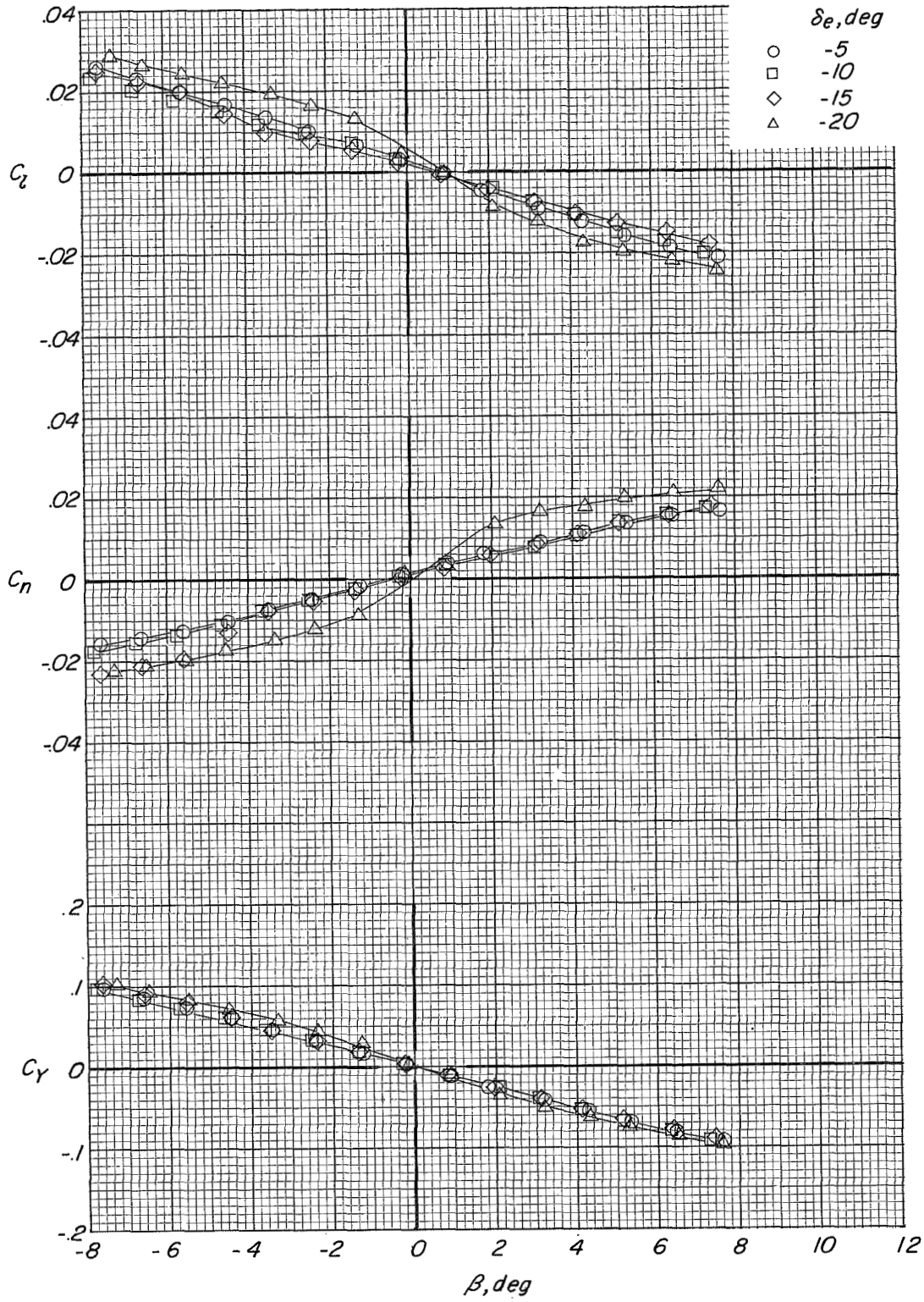
(c) $\delta_a = 0^o$; M = 0.60.

Figure 28.- Continued.



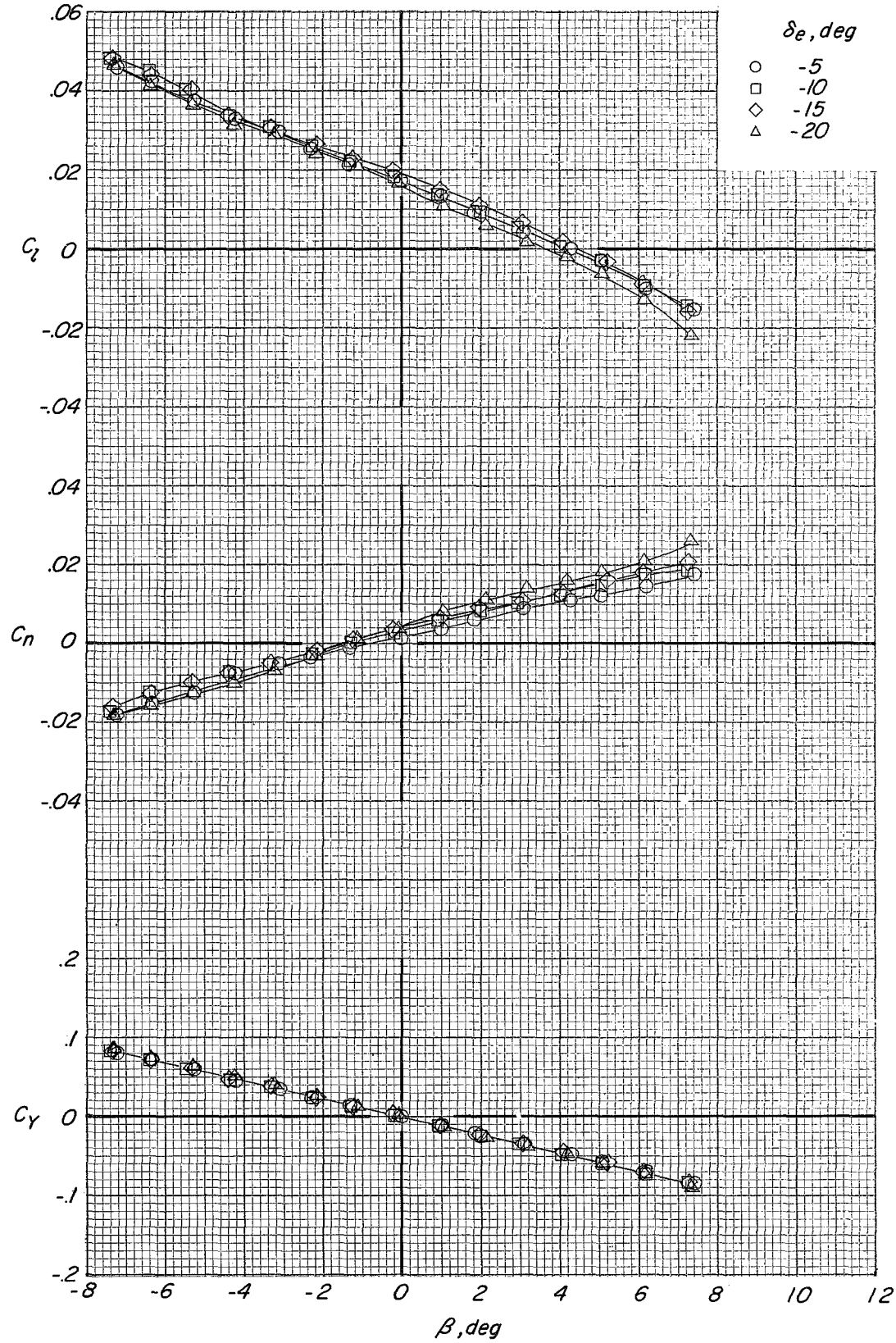
(d) $\delta_a = 0^o$; M = 0.70.

Figure 28.- Continued.



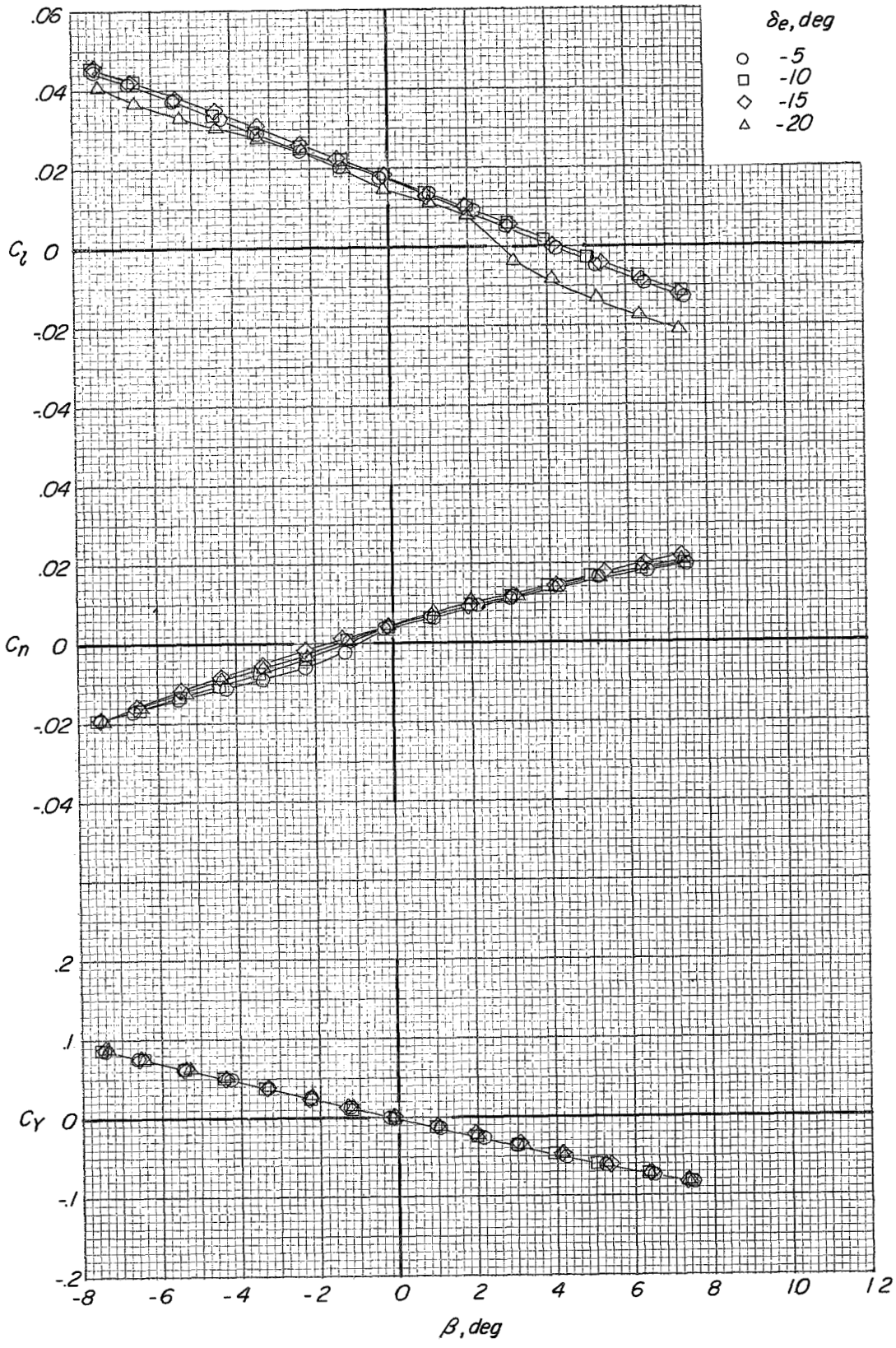
(e) $\delta_a = 0^o$; M = 0.80.

Figure 28.- Continued.



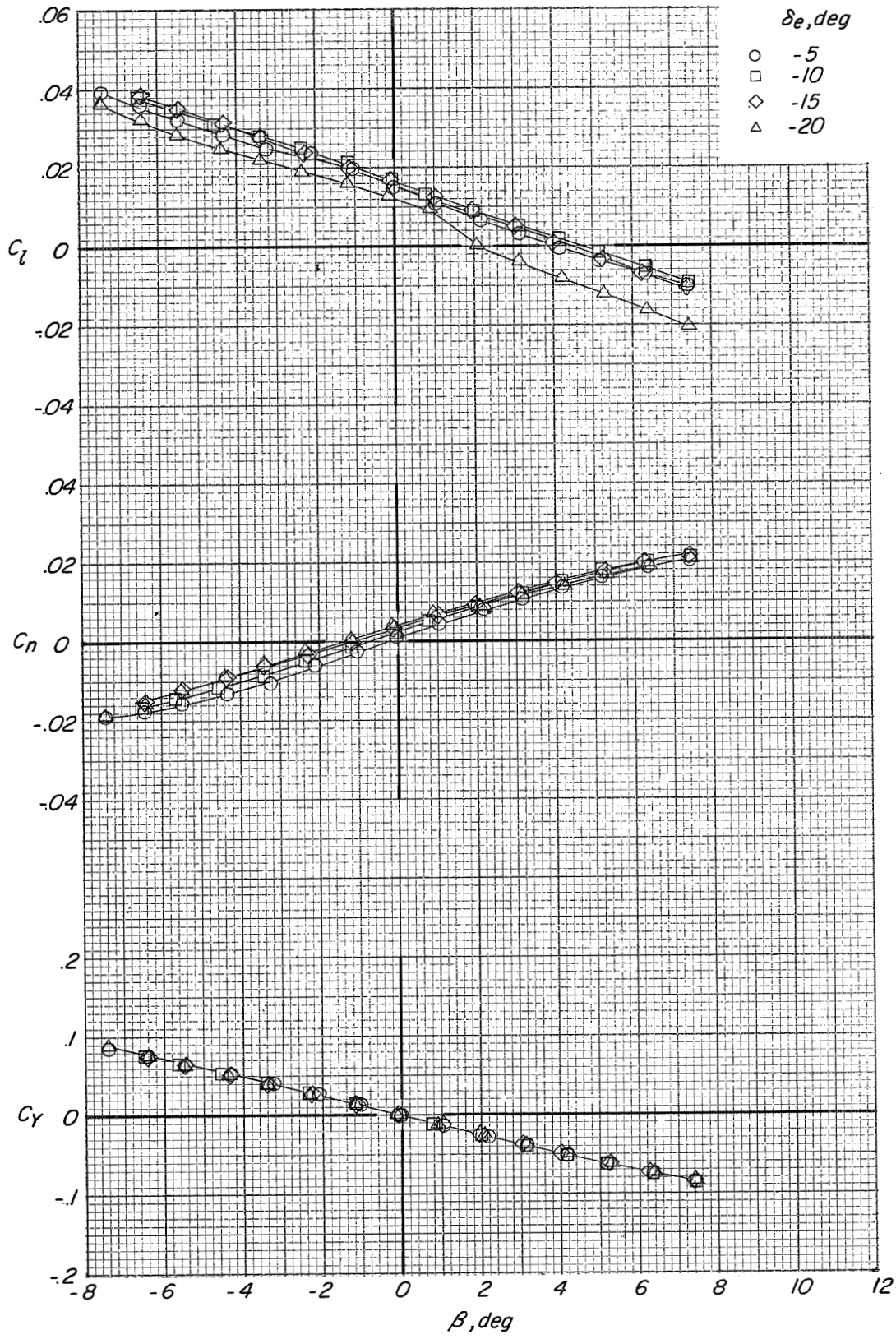
(f) $\delta_a = 10^o$; M = 0.35.

Figure 28.- Continued.



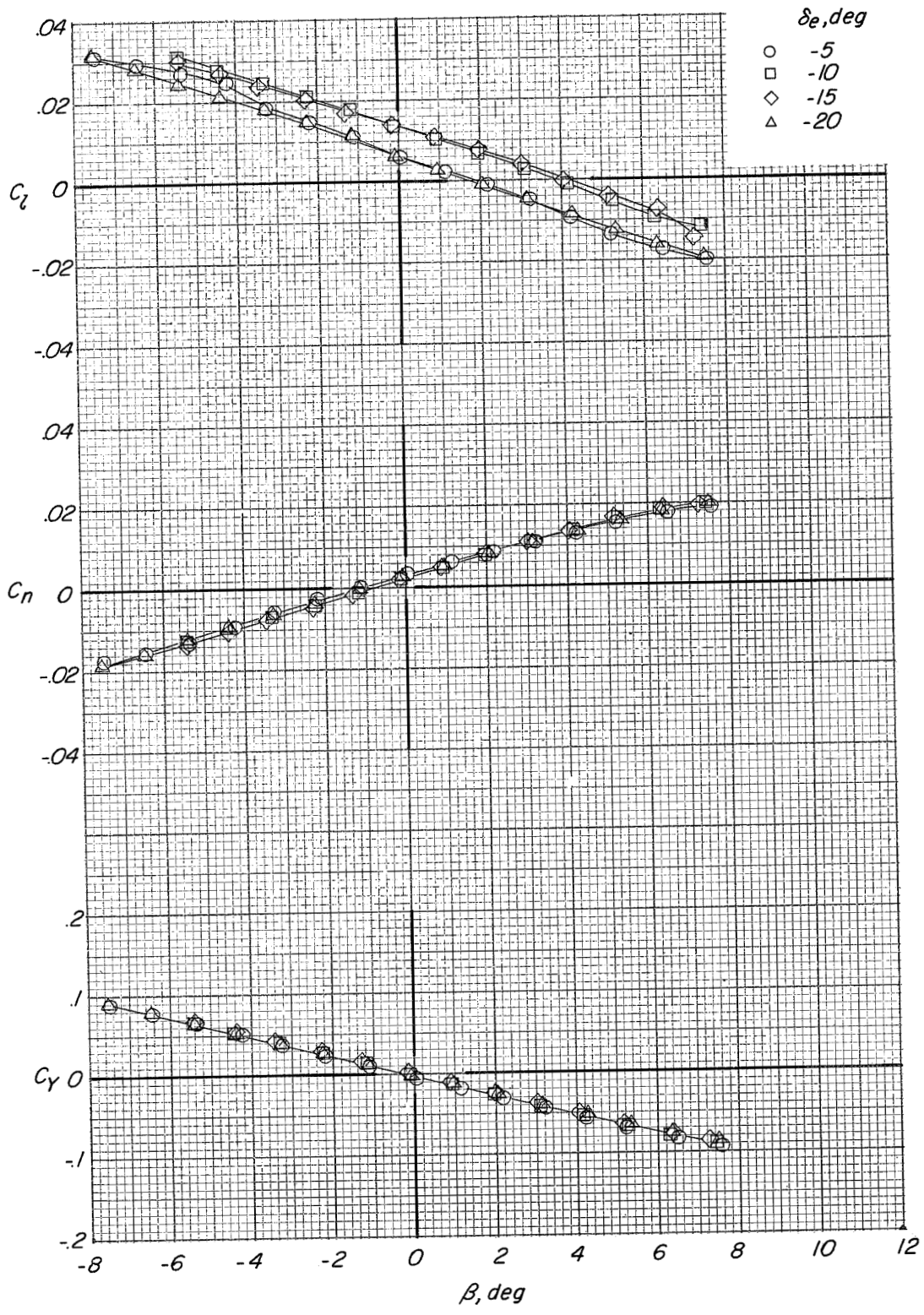
(g) $\delta_a = 10^o$; M = 0.50.

Figure 28.- Continued.



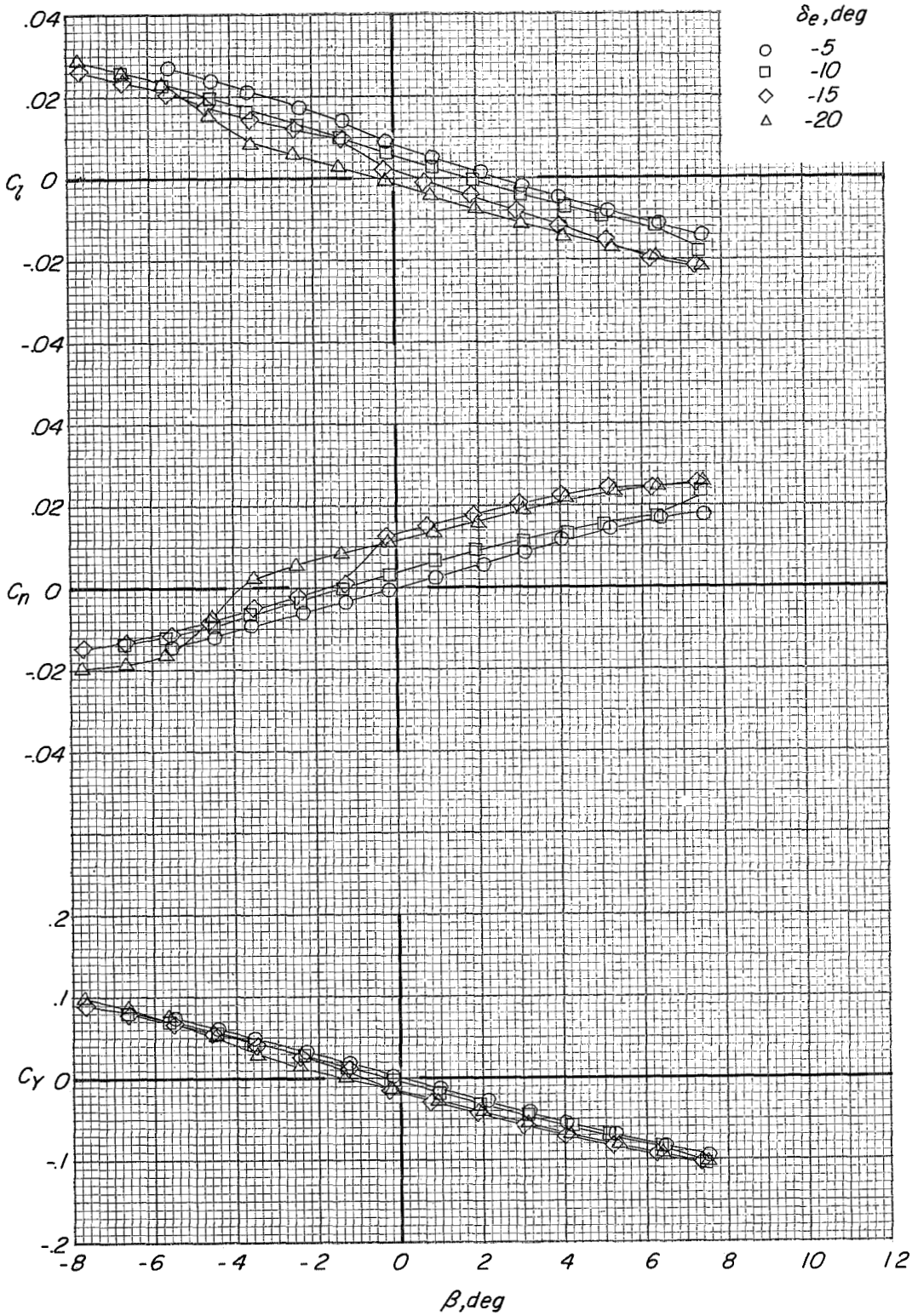
(h) $\delta_a = 10^o$; M = 0.60.

Figure 28.- Continued.



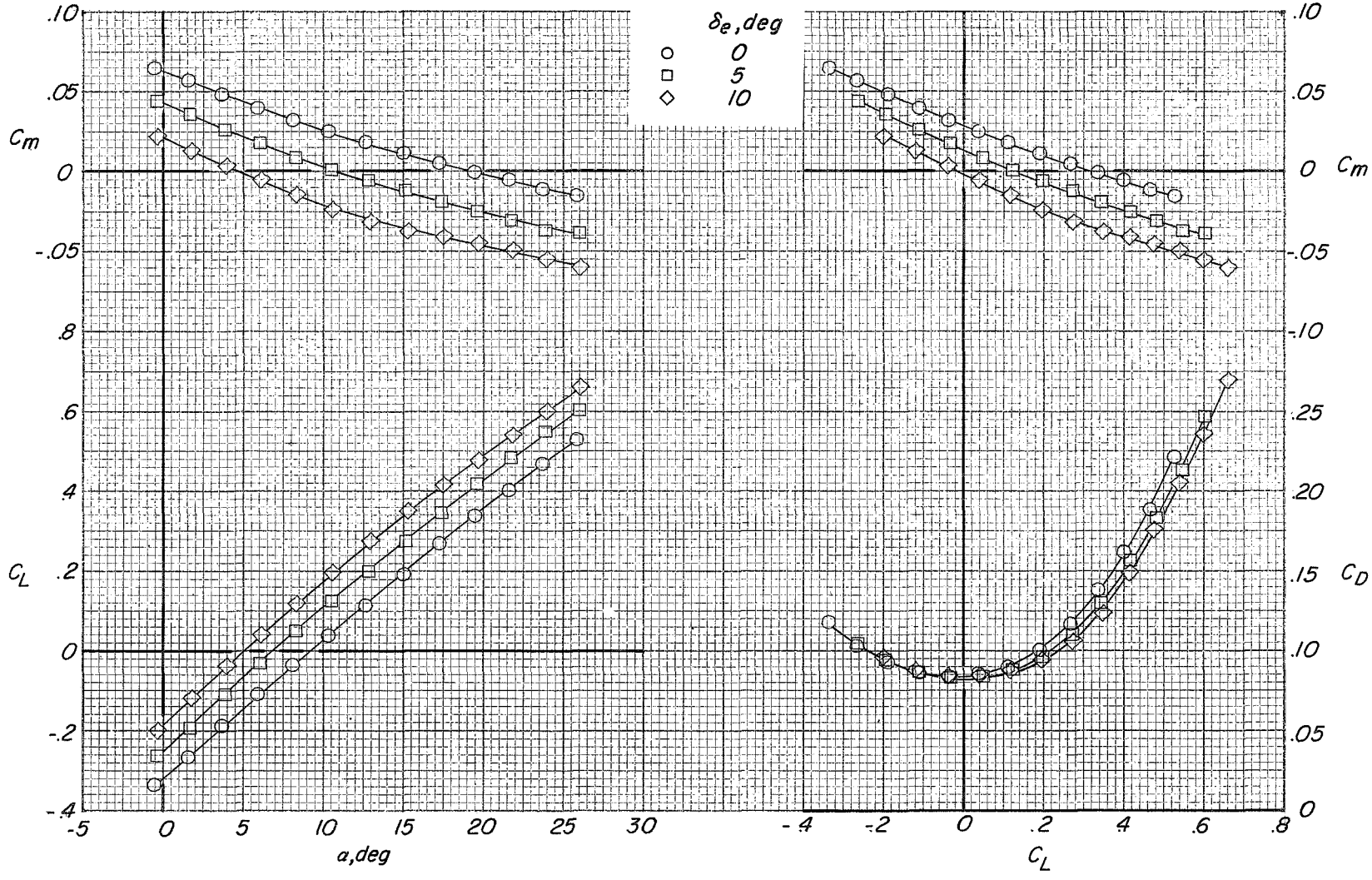
(i) $\delta_a = 10^o$; M = 0.70.

Figure 28.- Continued.



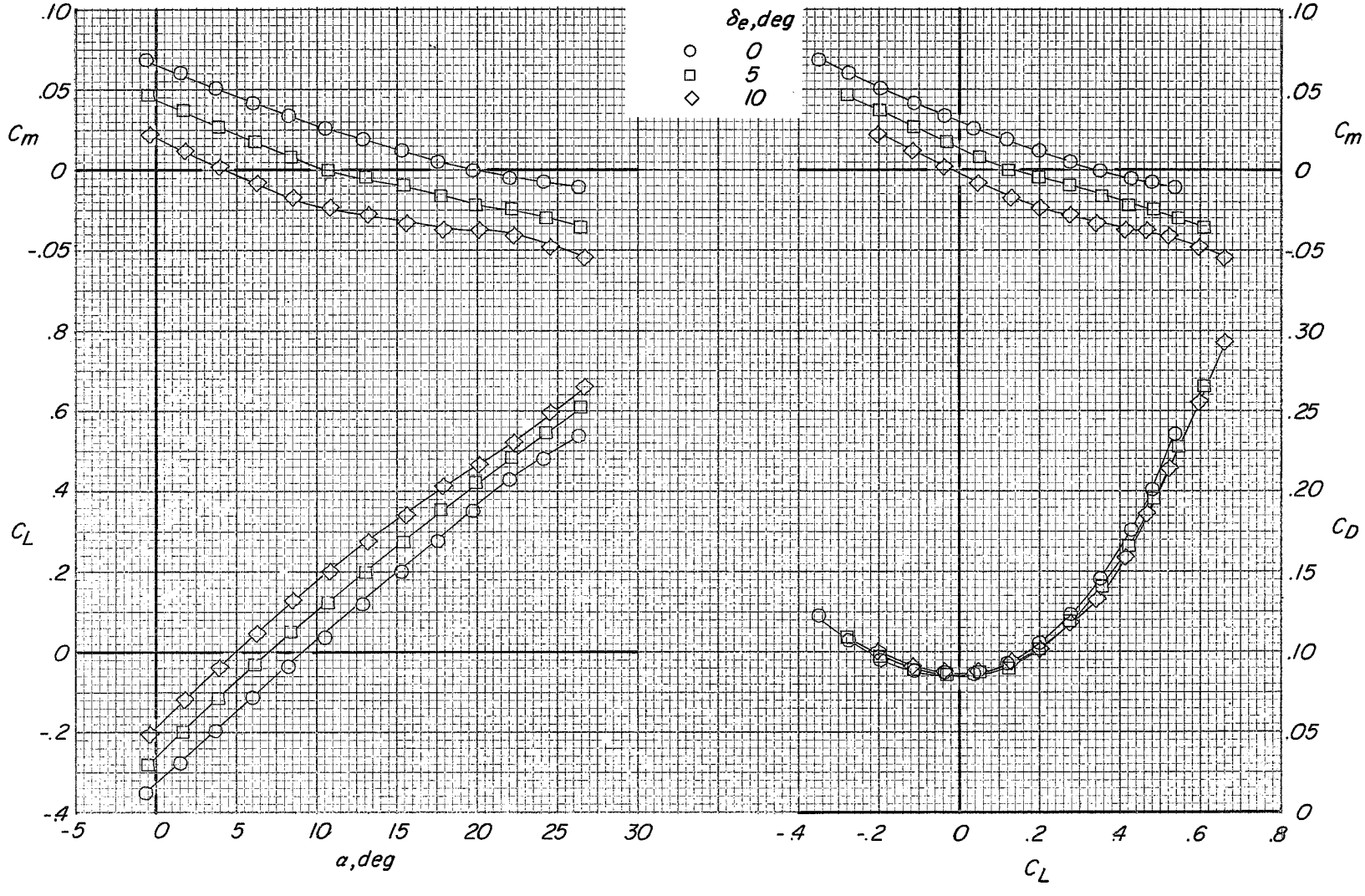
(j) $\delta_a = 10^o$; M = 0.80.

Figure 28.- Concluded.



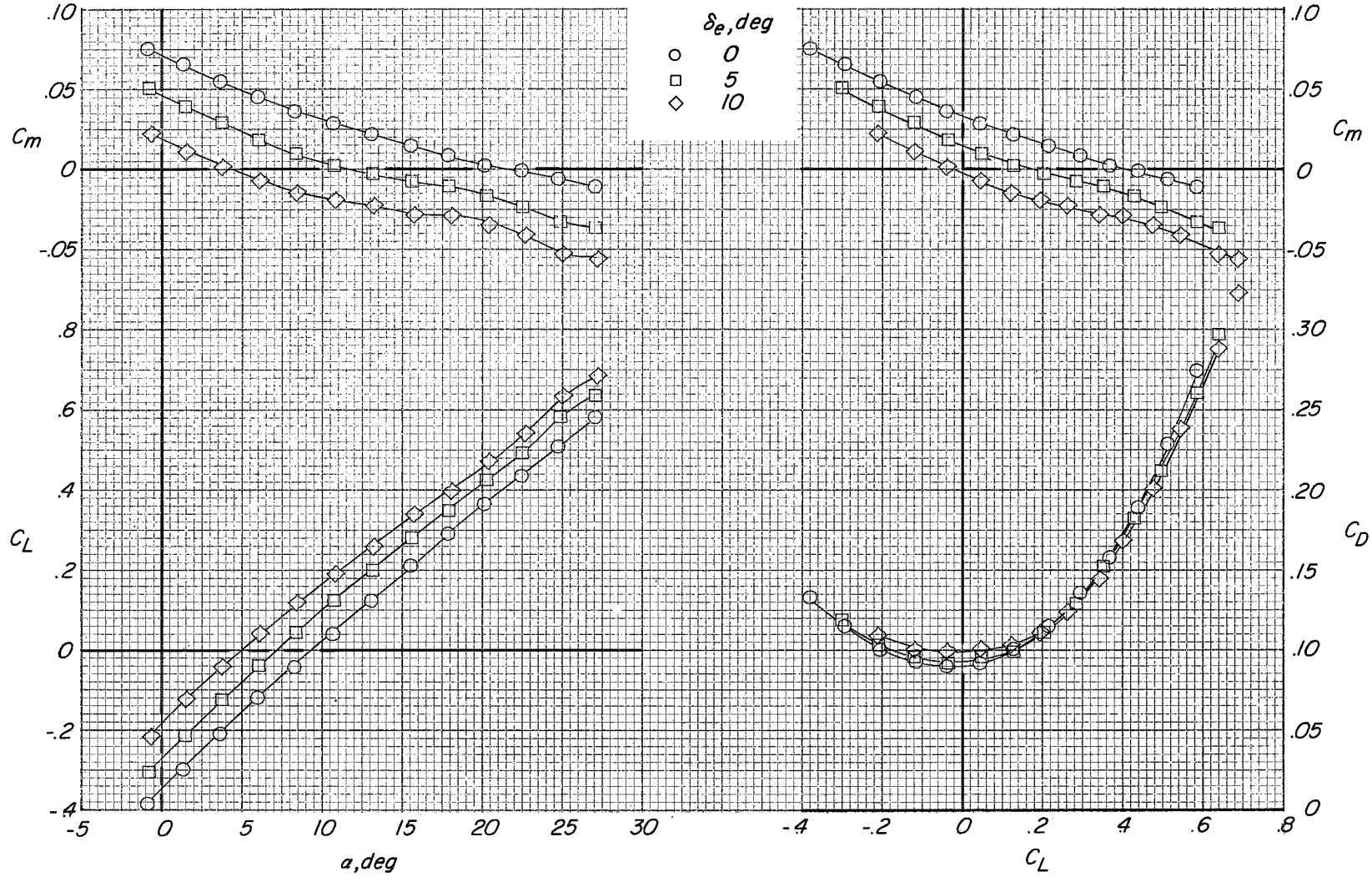
(a) M = 0.60.

Figure 29.- Longitudinal characteristics with modification I fin configuration. Auxiliary flaps in transonic position: $\delta_a = 0.00$



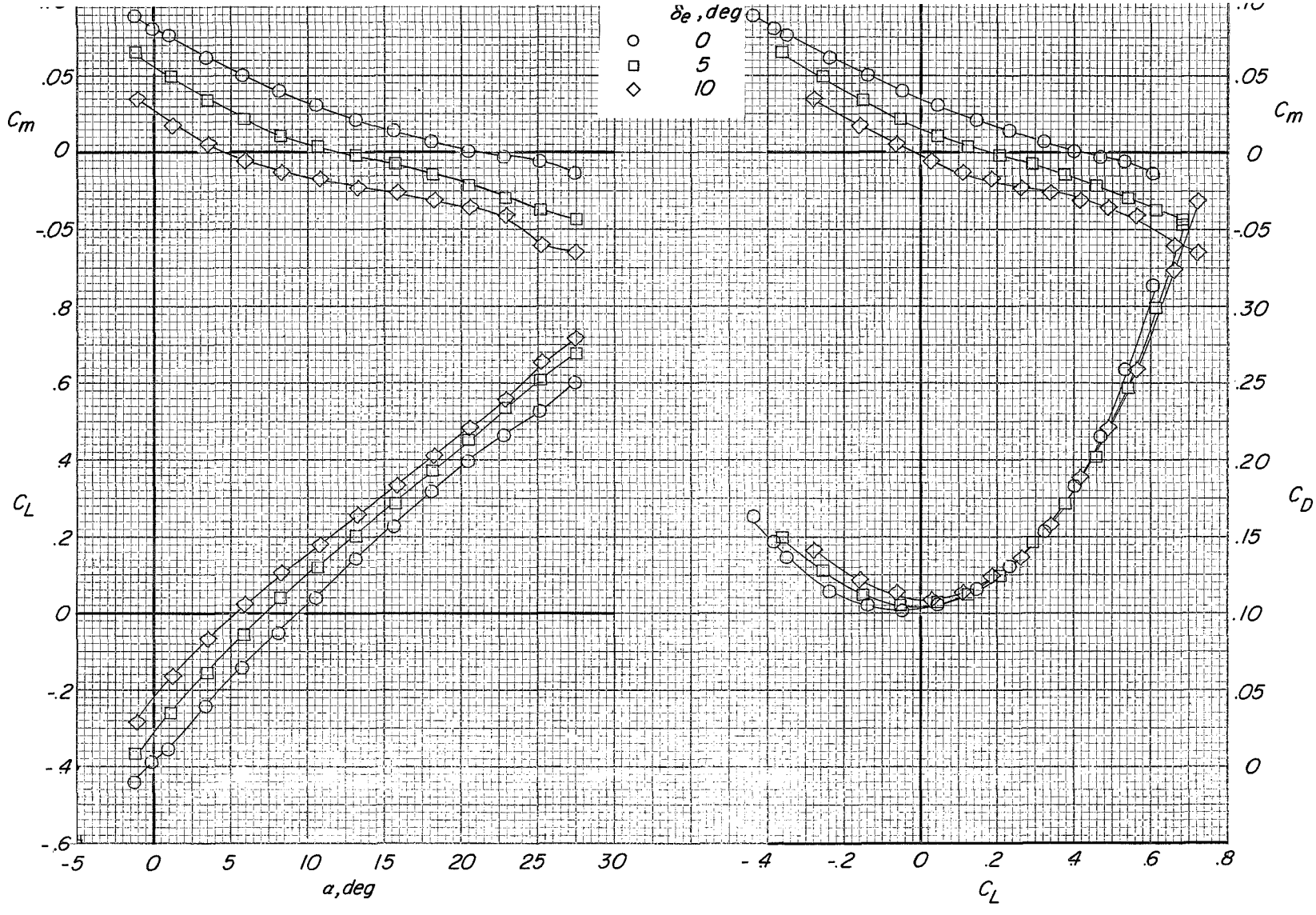
(b) M = 0.70.

Figure 29.- Continued.



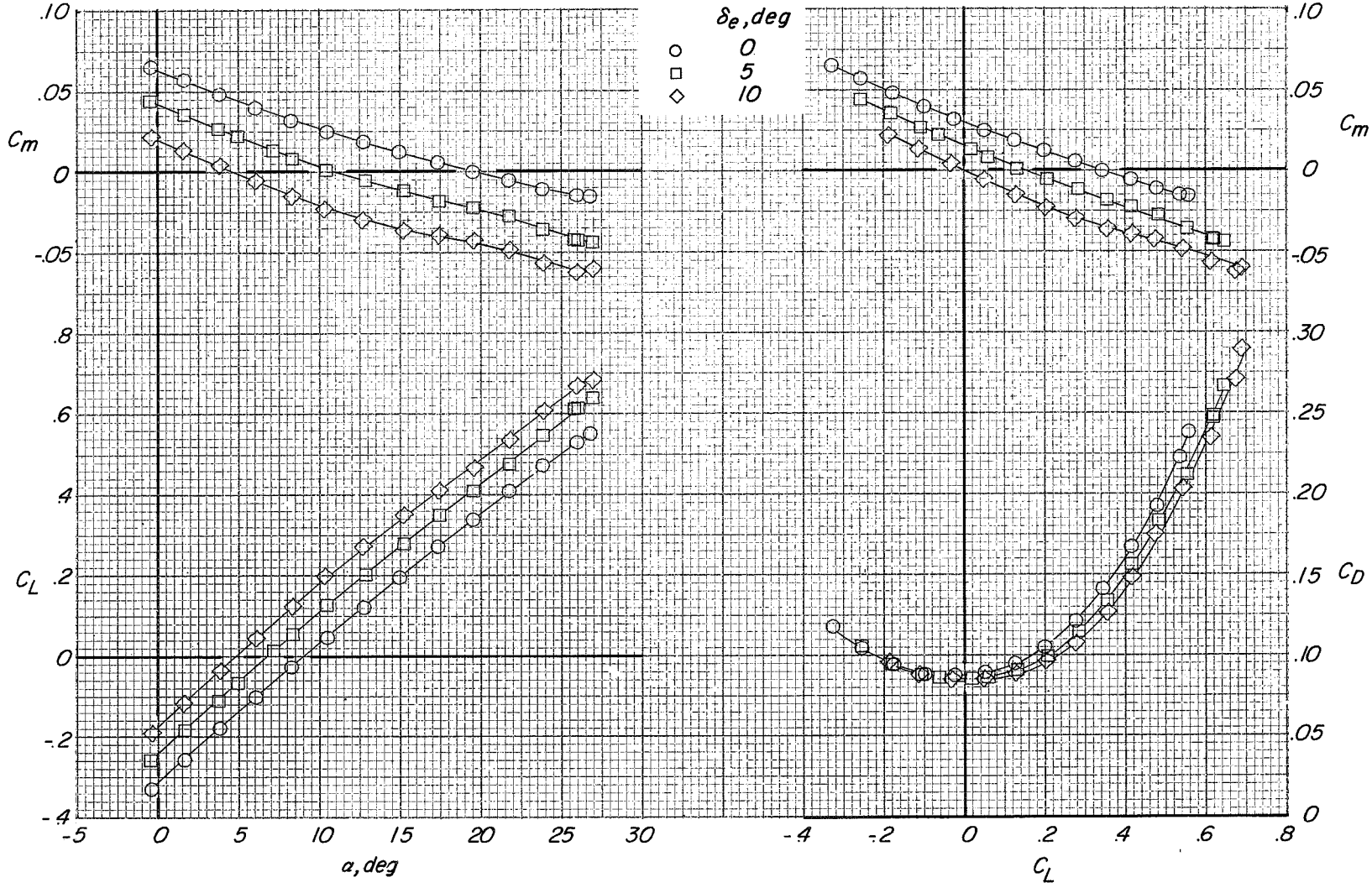
(c) M = 0.80.

Figure 29.- Continued.



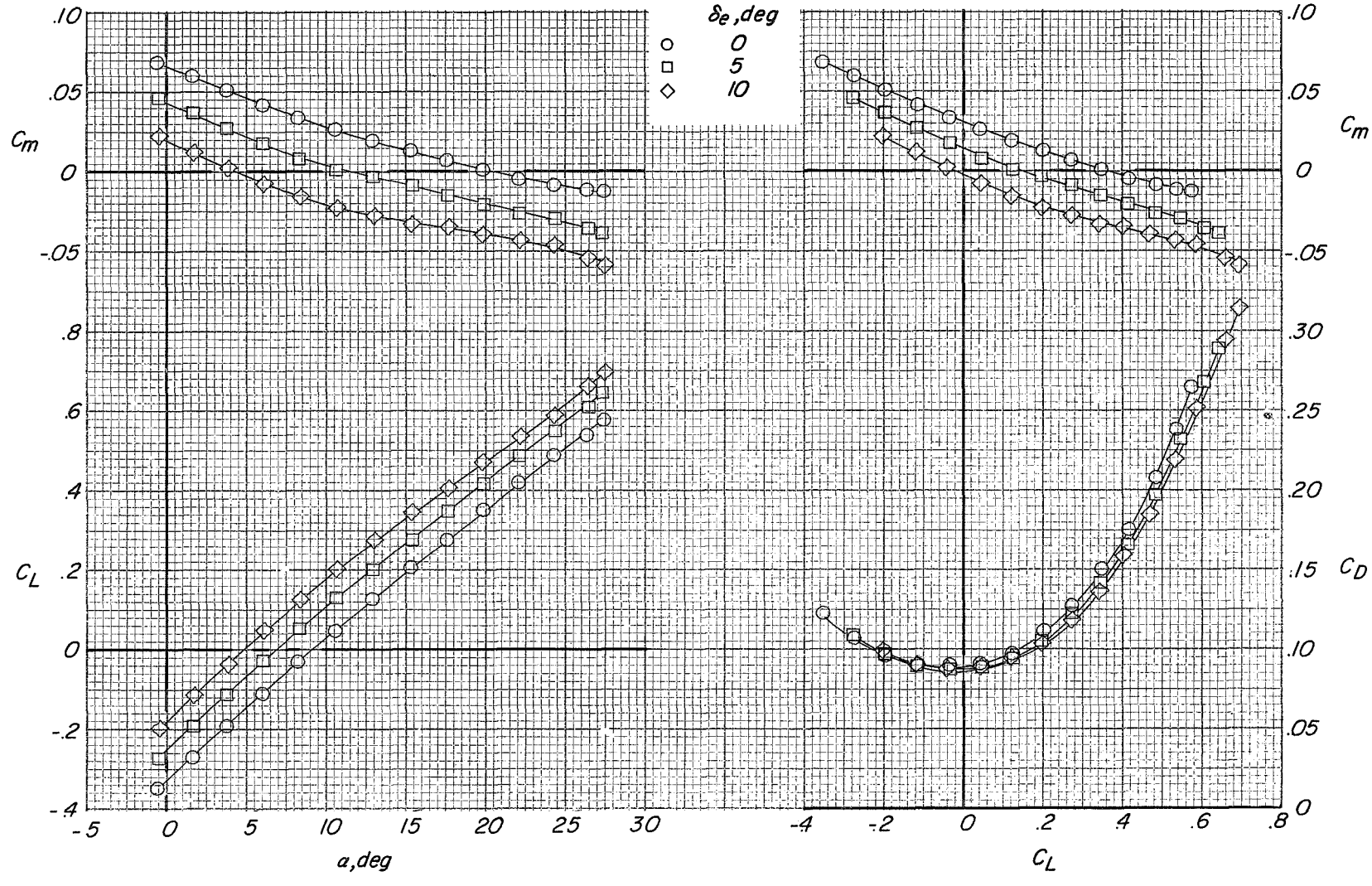
(d) M = 0.90.

Figure 29.- Concluded.



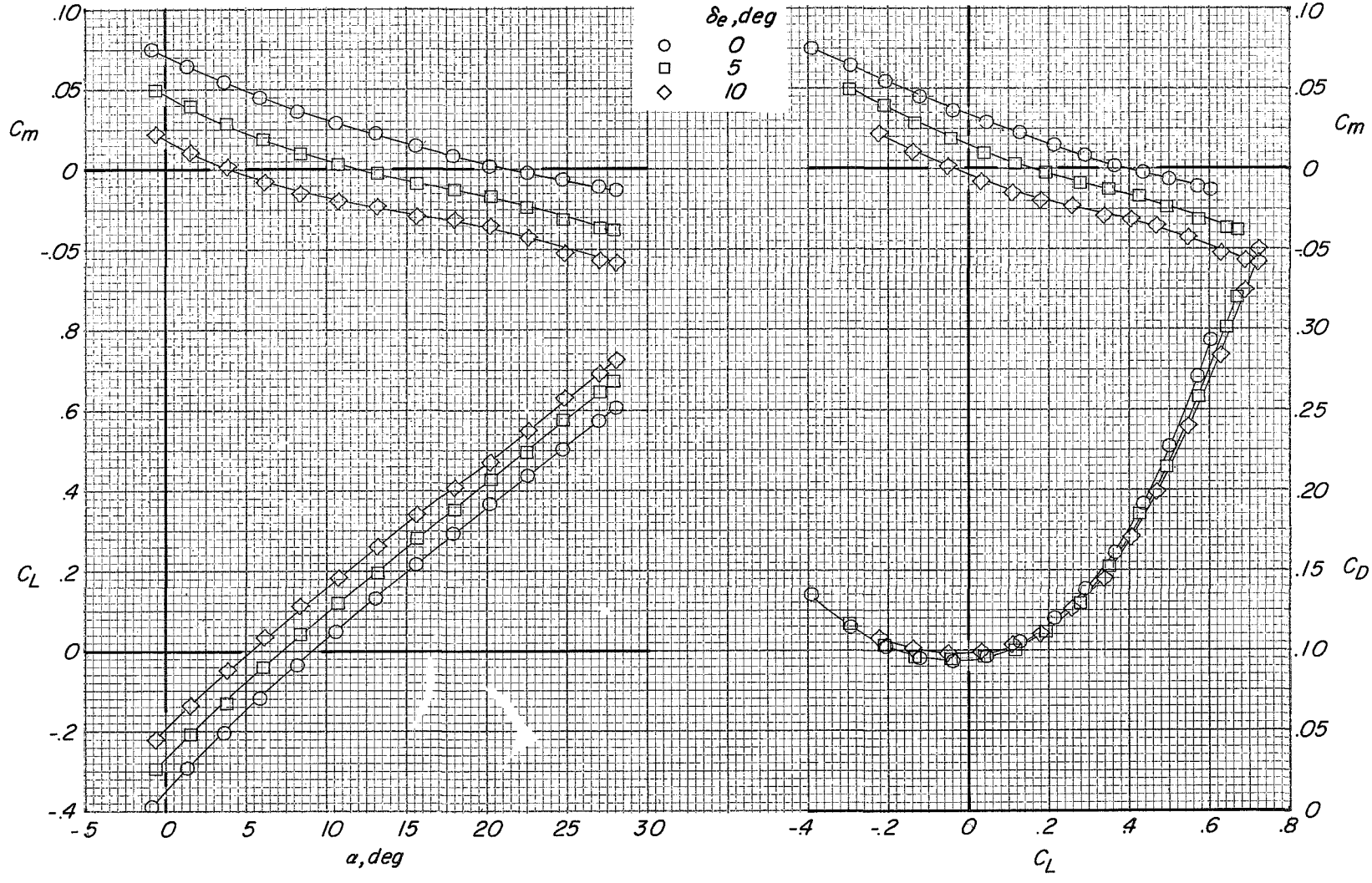
(a) $\beta = 2.3^{o}$; M = 0.60.

Figure 30.- Longitudinal characteristics at sideslip. Modification I fin configuration; auxiliary flaps in transonic configuration; $\delta_a = 0^{o}$.



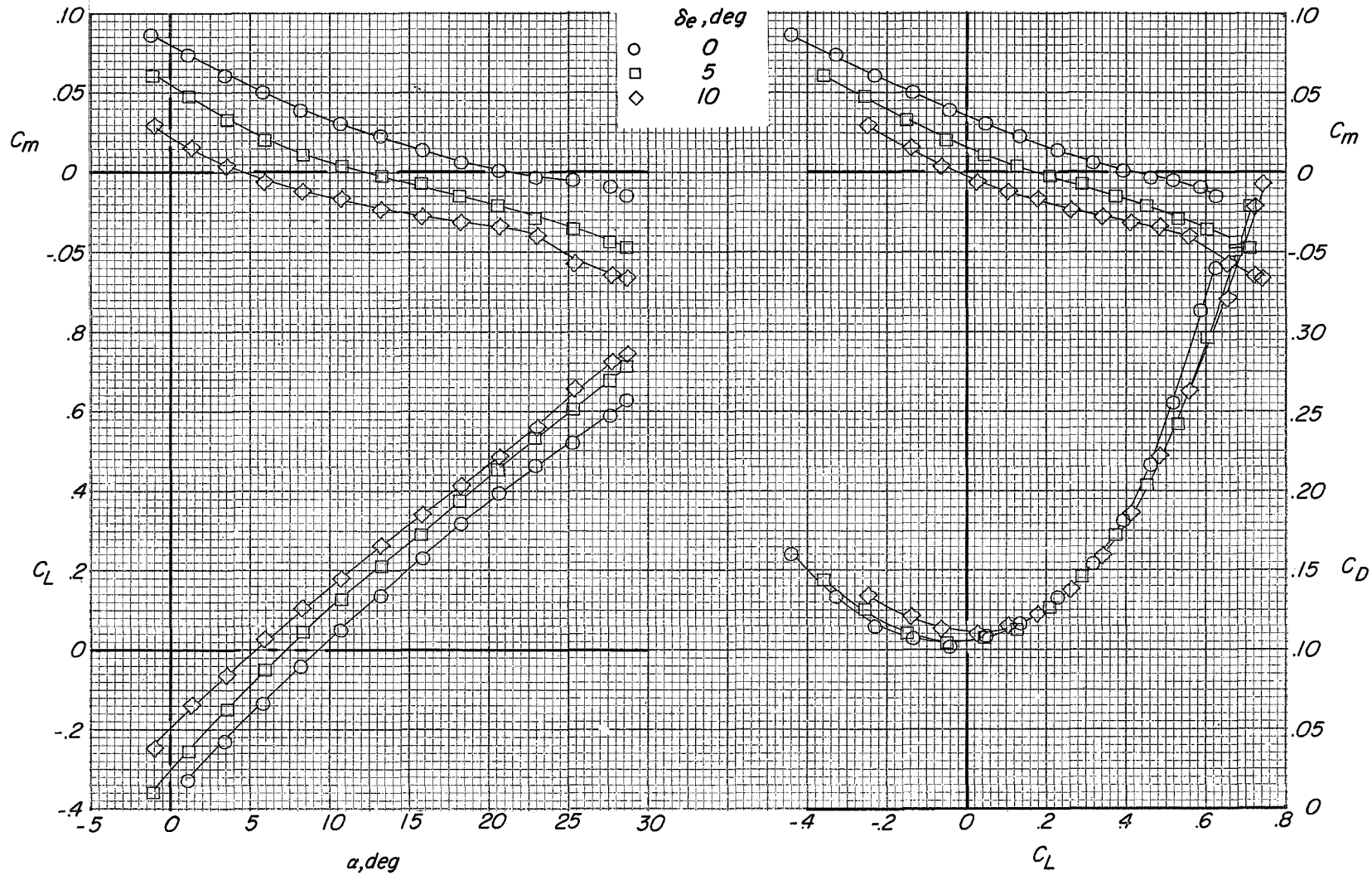
(b) $\beta = 2.3^{o}$; M = 0.70.

Figure 30.- Continued.



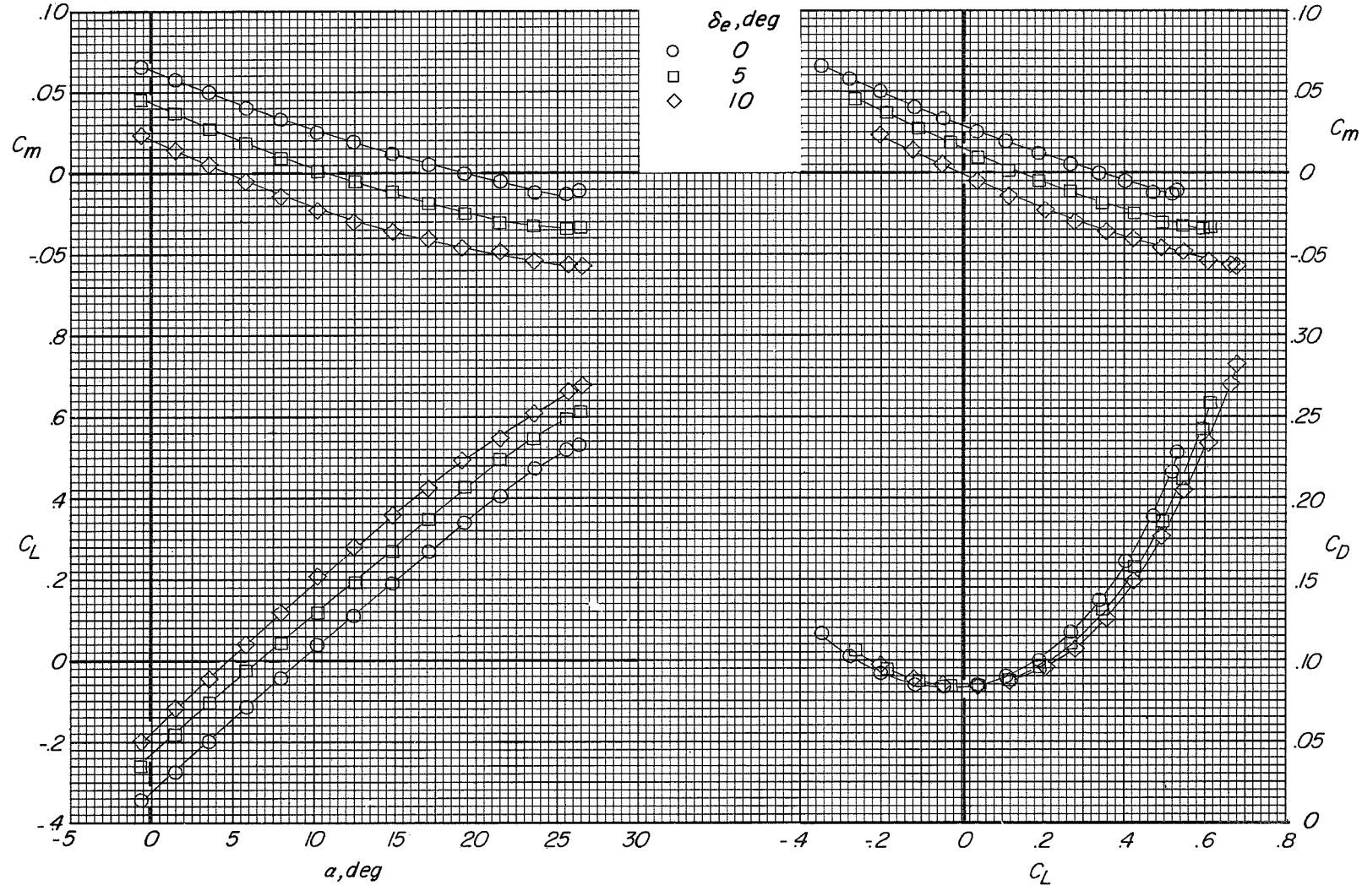
(c) $\beta = 2.3^{o}$; M = 0.80.

Figure 30.- Continued.



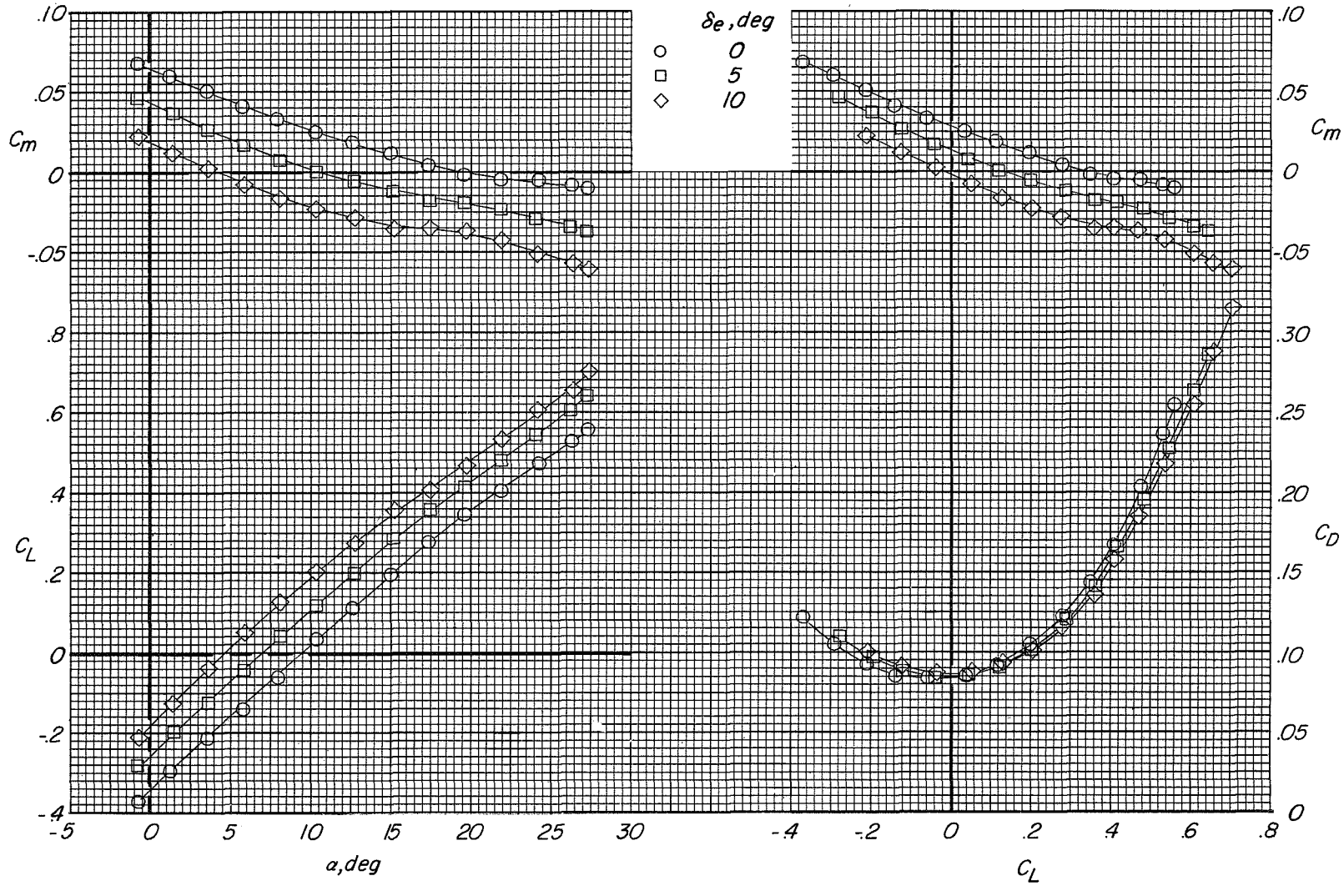
(d) $\beta = 2.3^{o}$; M = 0.90.

Figure 30.- Continued.



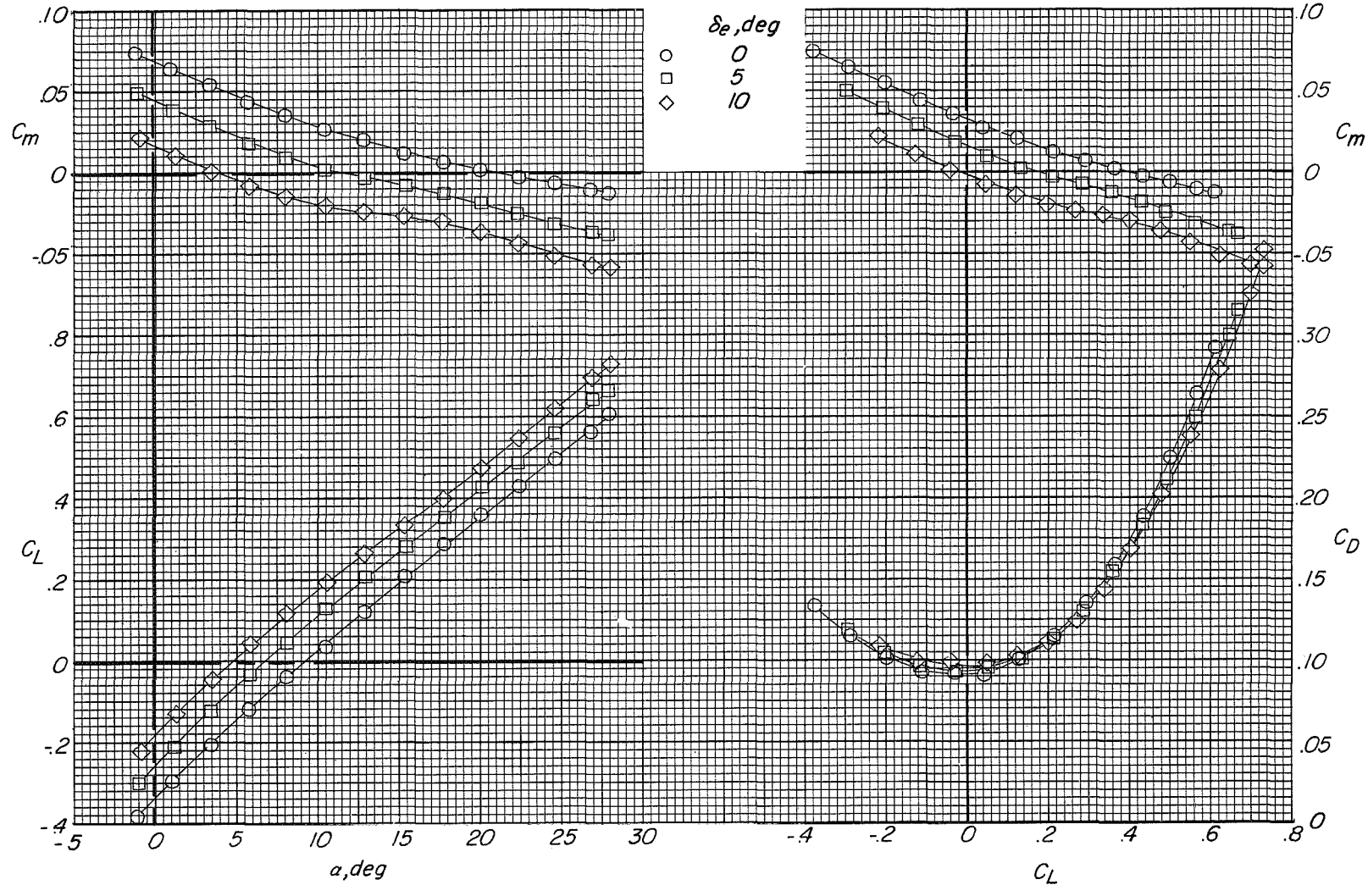
(e) $\beta = -2.3^{o}$; M = 0.60.

Figure 30.- Continued.



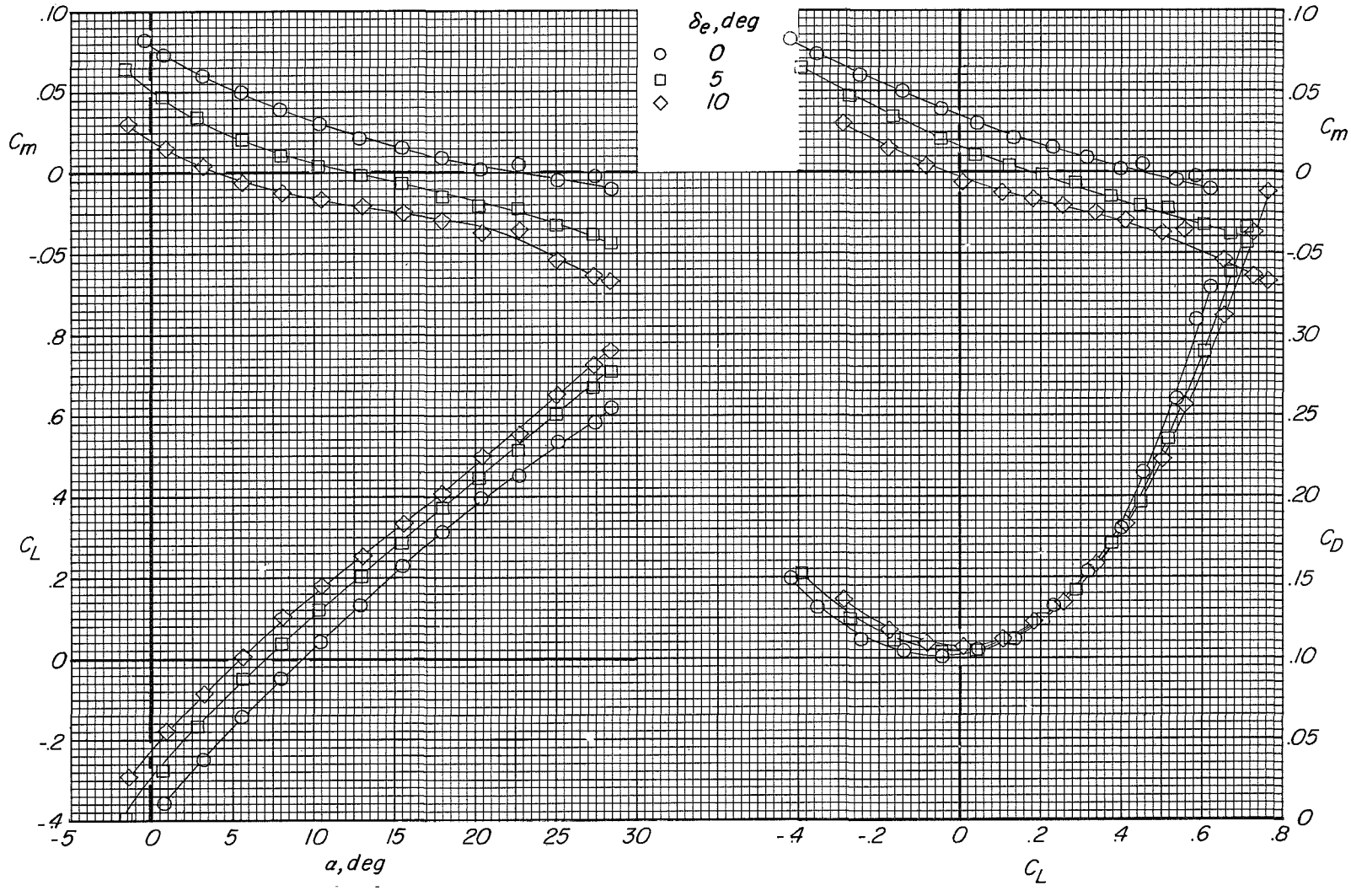
(f) $\beta = -2.3^{o}$; M = 0.70.

Figure 30.- Continued.



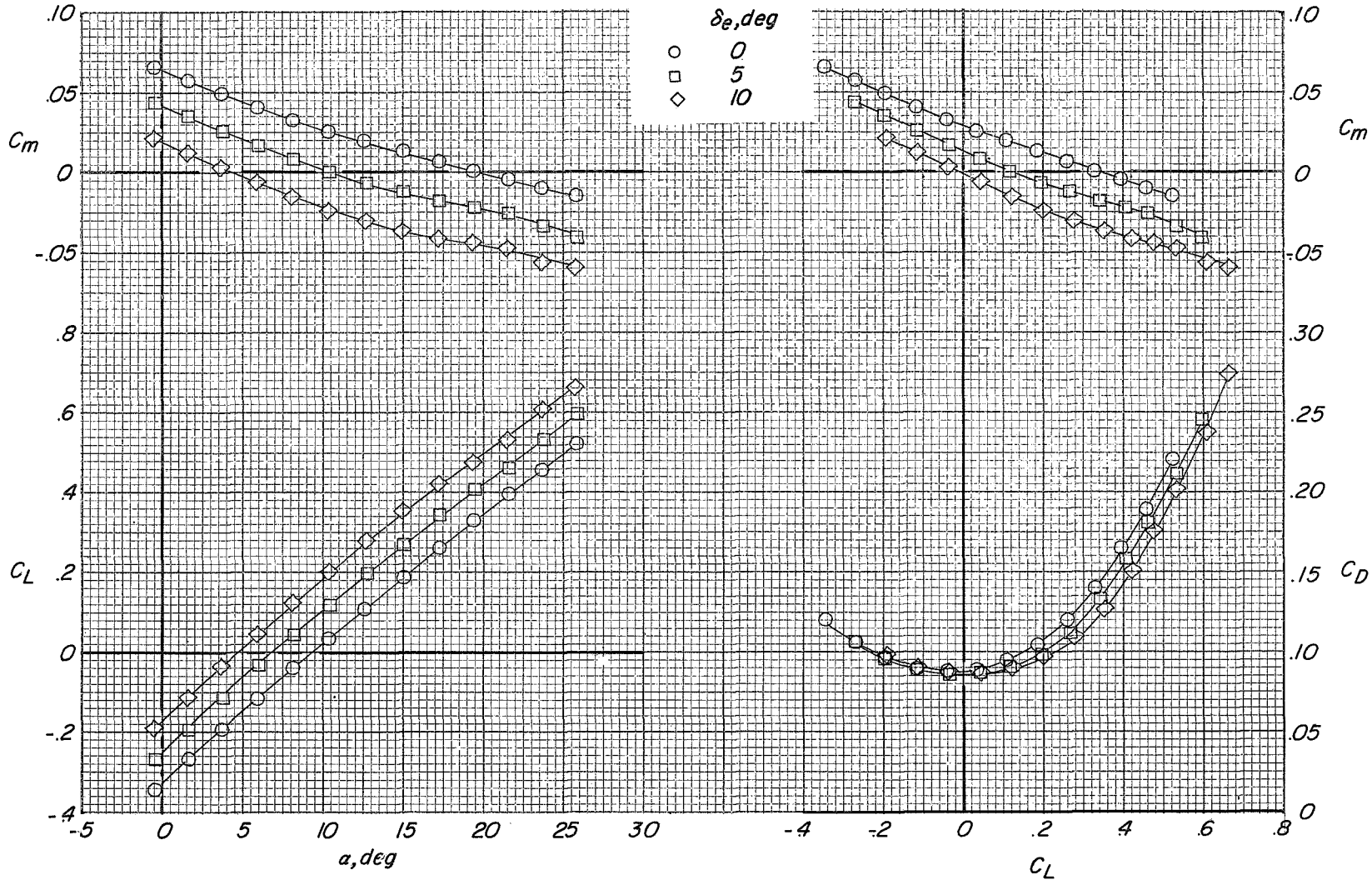
(g) $\beta = -2.3^{o}$; M = 0.80.

Figure 30.- Continued.



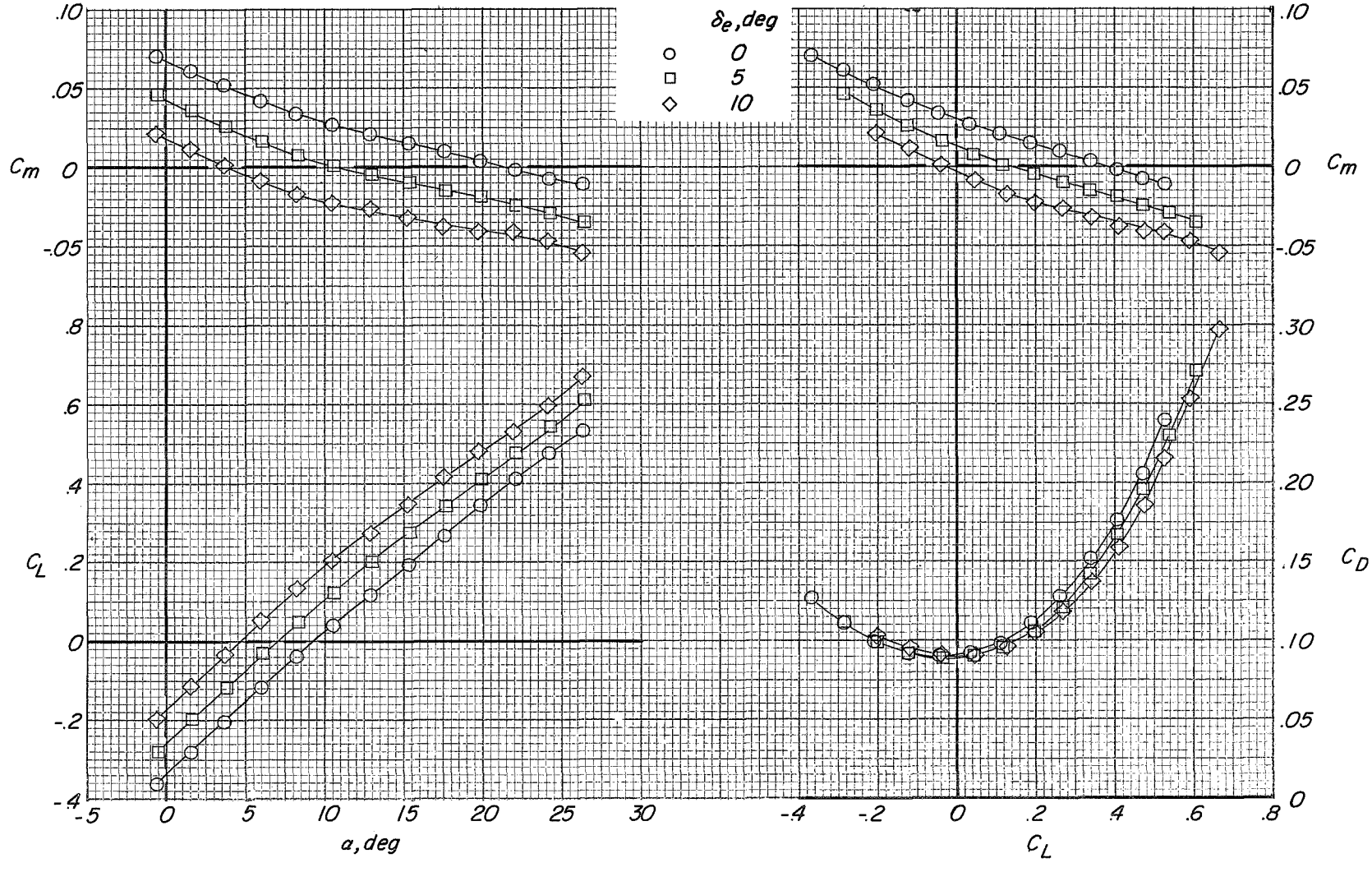
(h) $\beta = -2.3^{o}$; M = 0.90.

Figure 30.- Concluded.



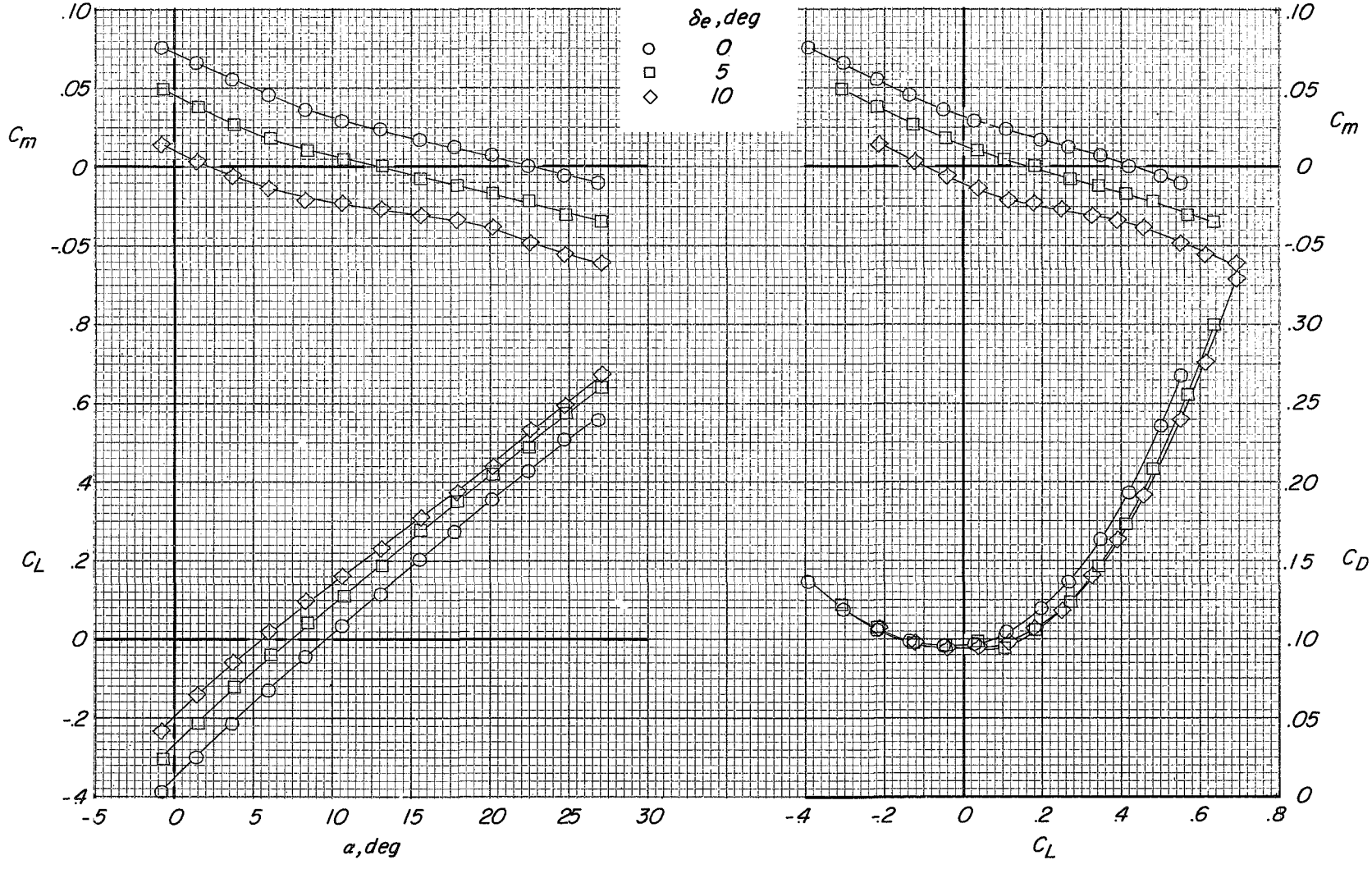
(a) M = 0.60.

Figure 31.- Longitudinal characteristics with ailerons deflected 10^{o}. Modification I fin configuration; auxiliary flaps in transonic position; $\beta = 0^{o}$.



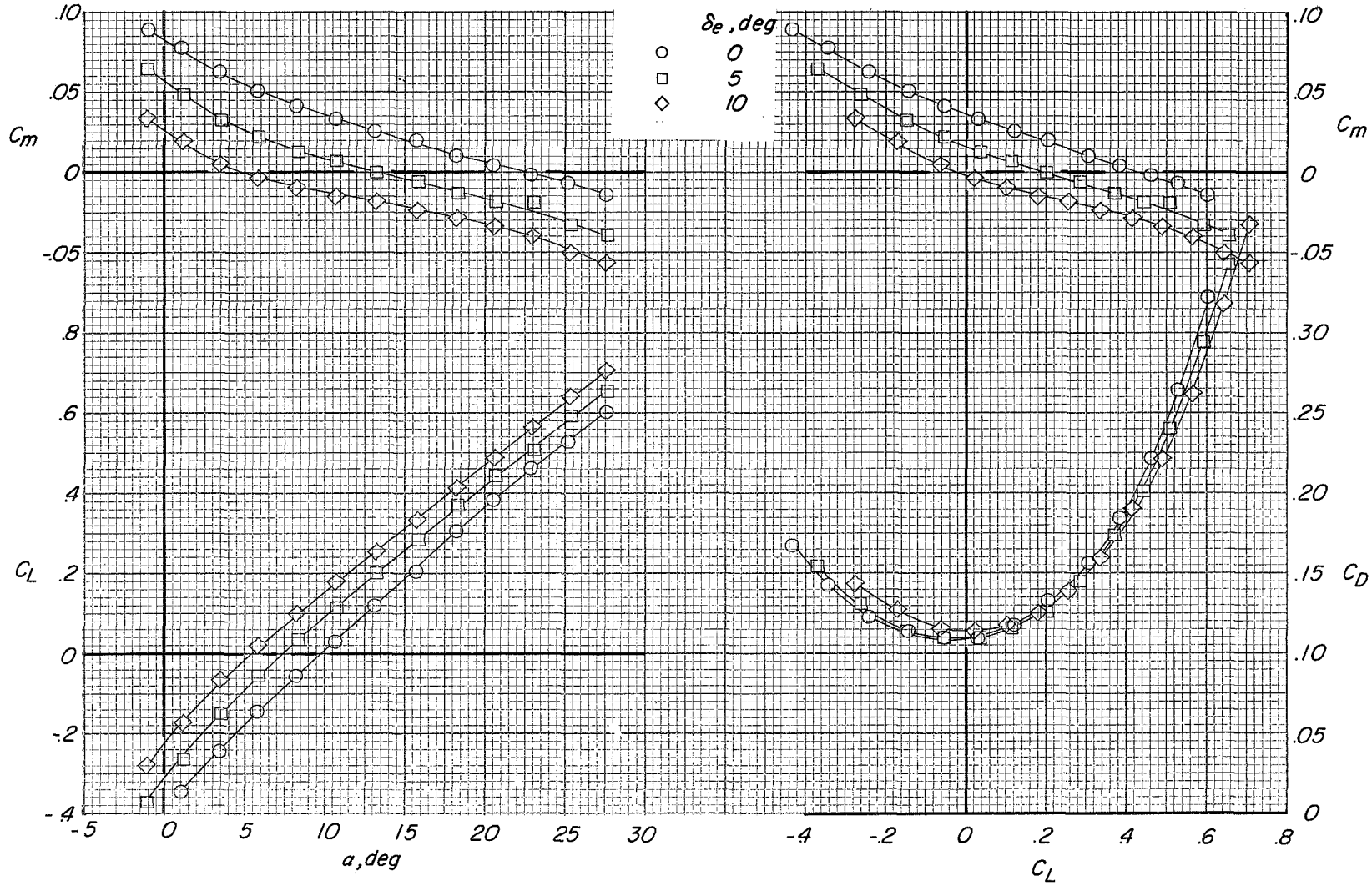
(b) M = 0.70.

Figure 31.- Continued.



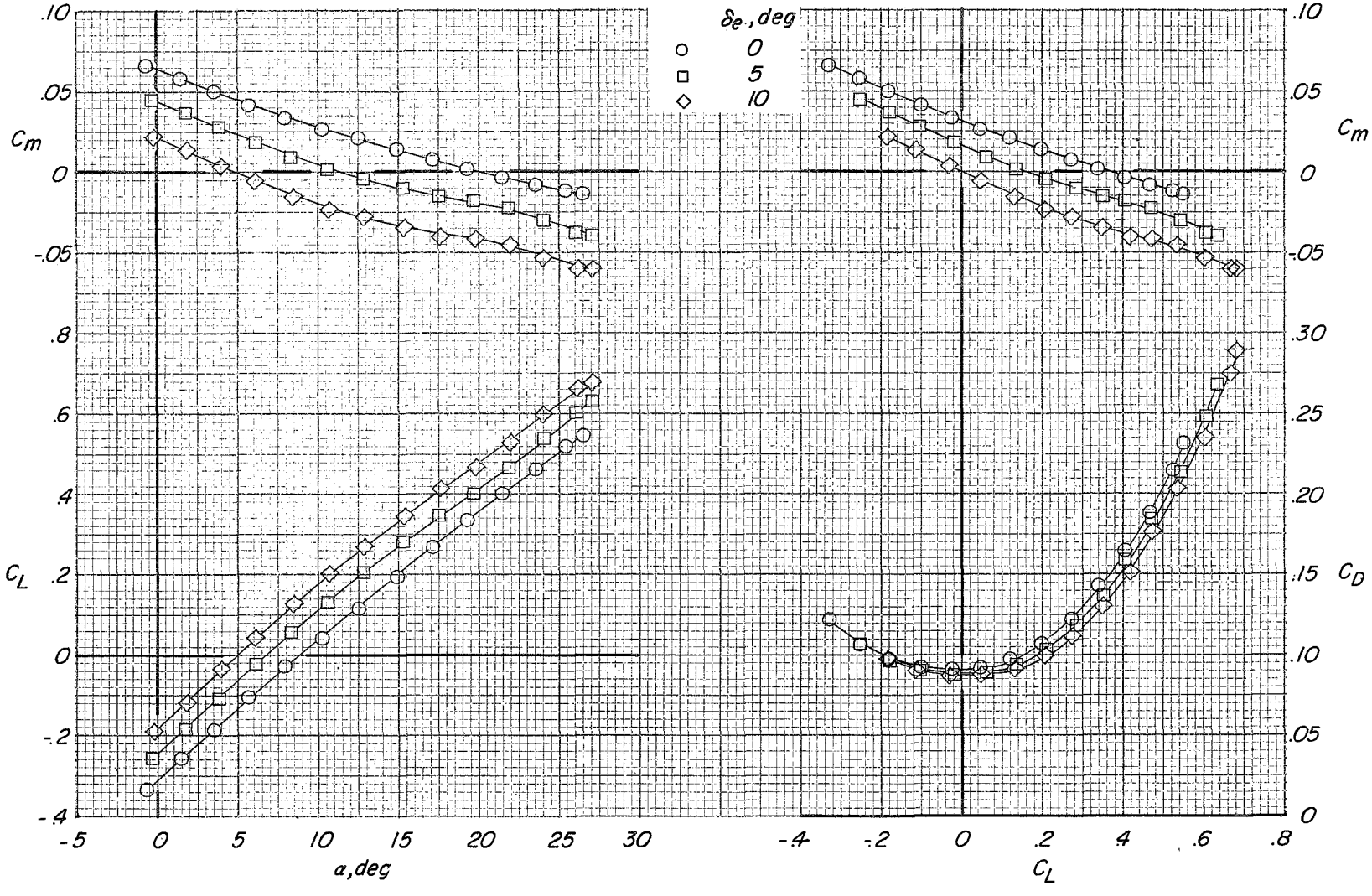
(c) M = 0.80.

Figure 31.- Continued.



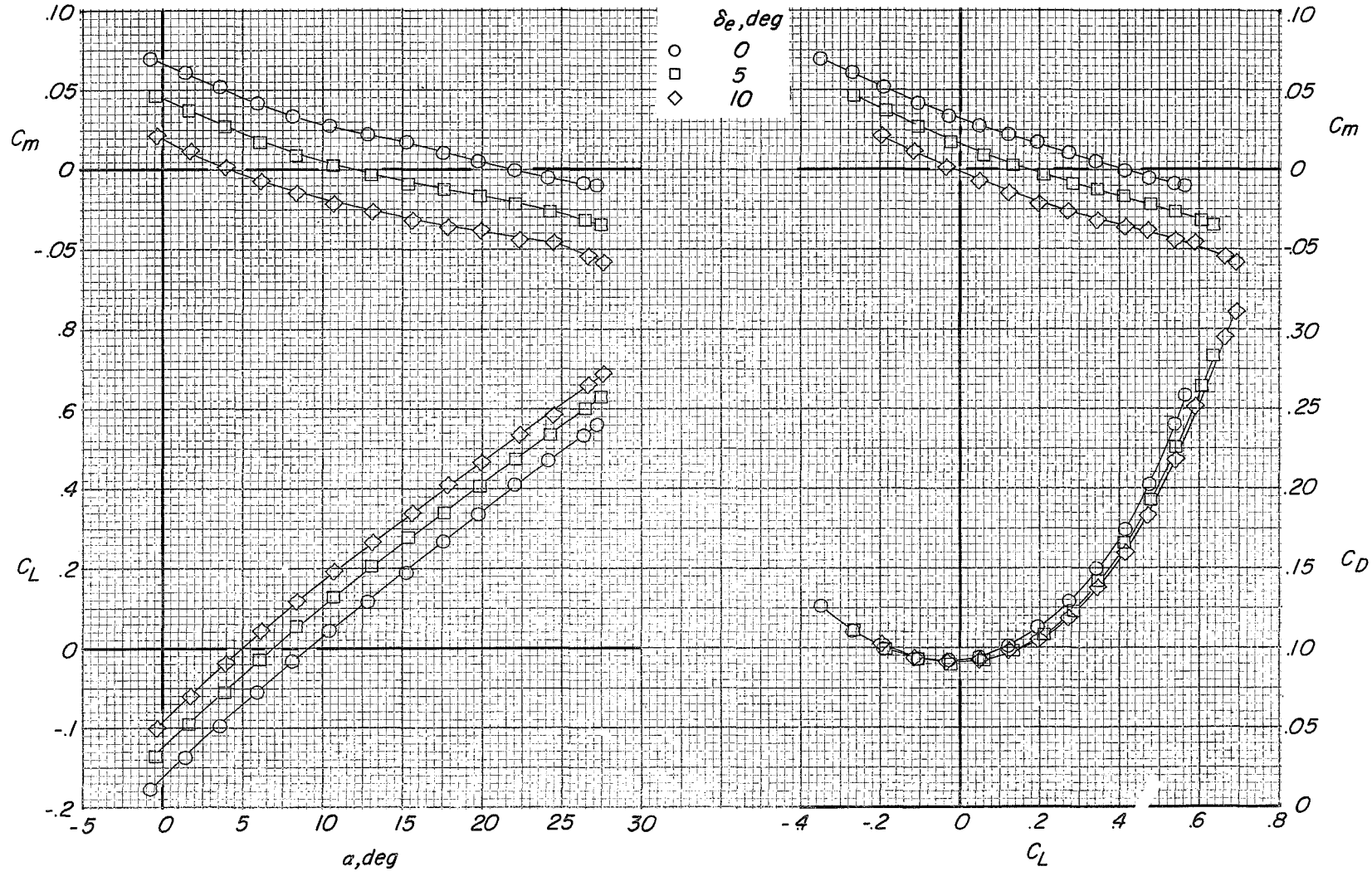
(d) M = 0.90.

Figure 31.- Concluded.



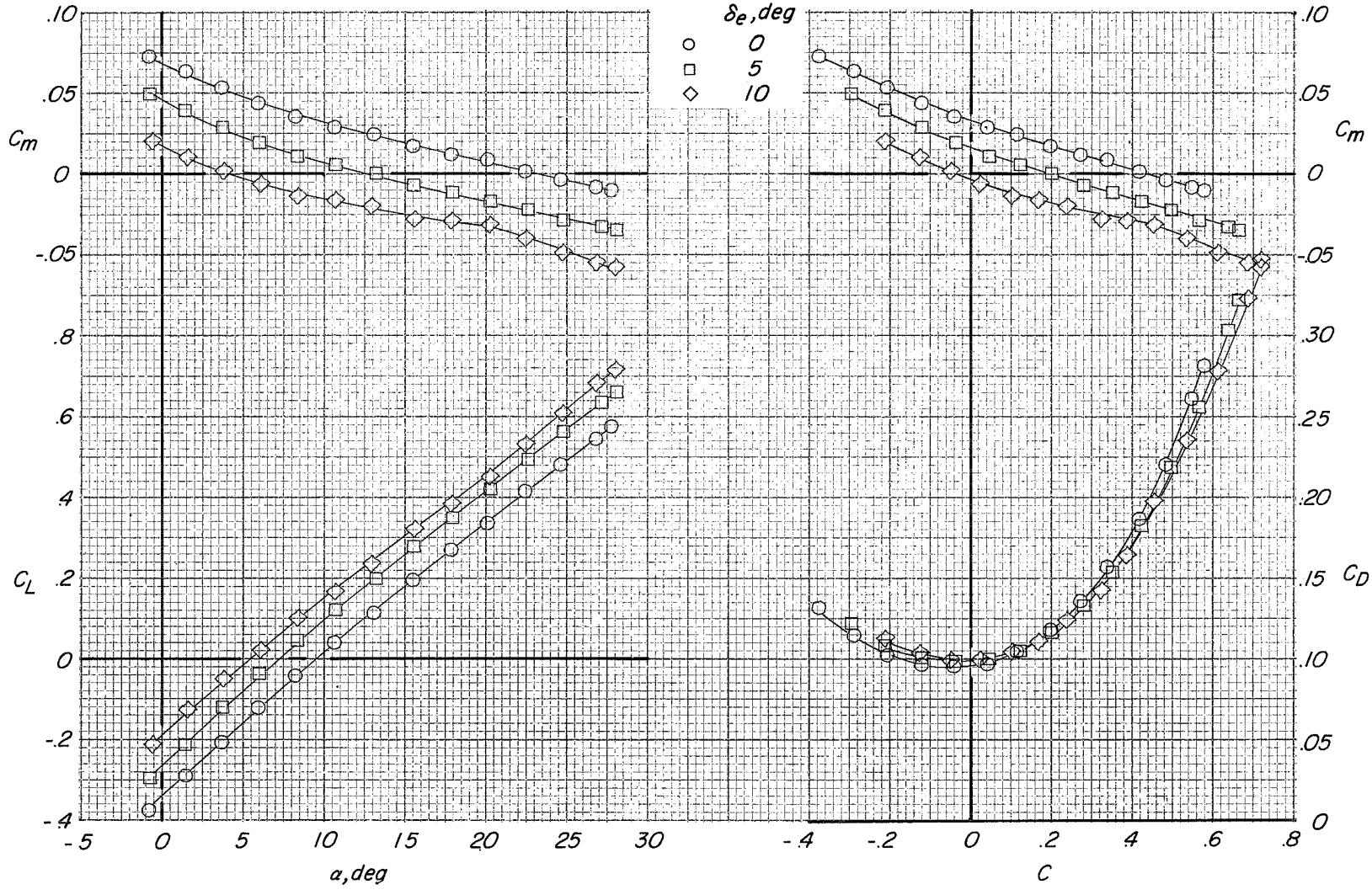
(a) $\beta = 2.3^{o}$; $\delta_a = 10^{o}$; M = 0.60.

Figure 32.- Longitudinal characteristics with combined aileron deflection and sideslip angle. Modification I fin configuration; auxiliary flaps in transonic position.



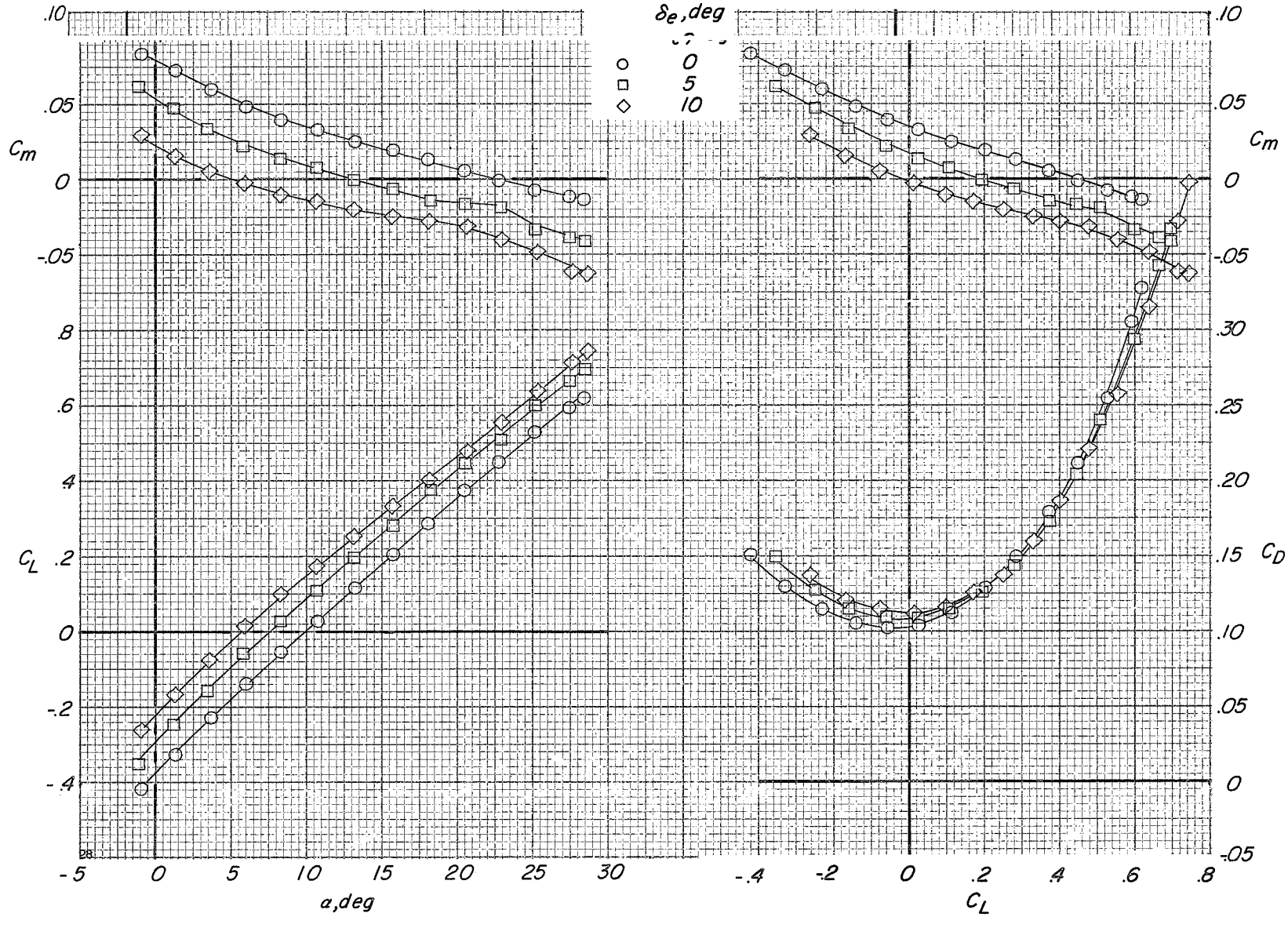
(b) $\beta = 2.3^{\circ}$; $\delta_a = 10^{\circ}$; M = 0.70.

Figure 32.- Continued.



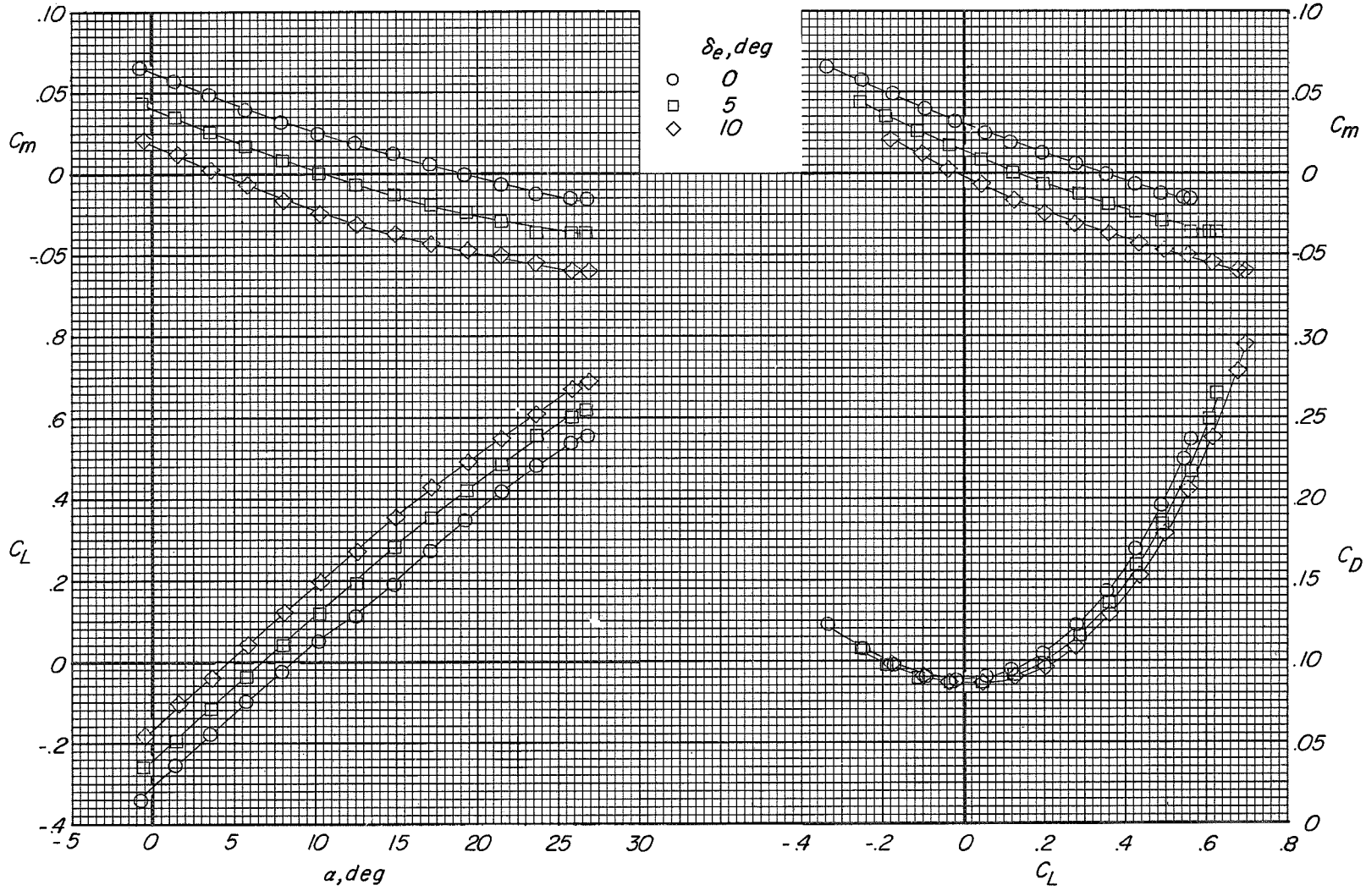
(c) $\beta = 2.3^{o}$; $\delta_a = 10^{o}$; M = 0.80.

Figure 32.- Continued.



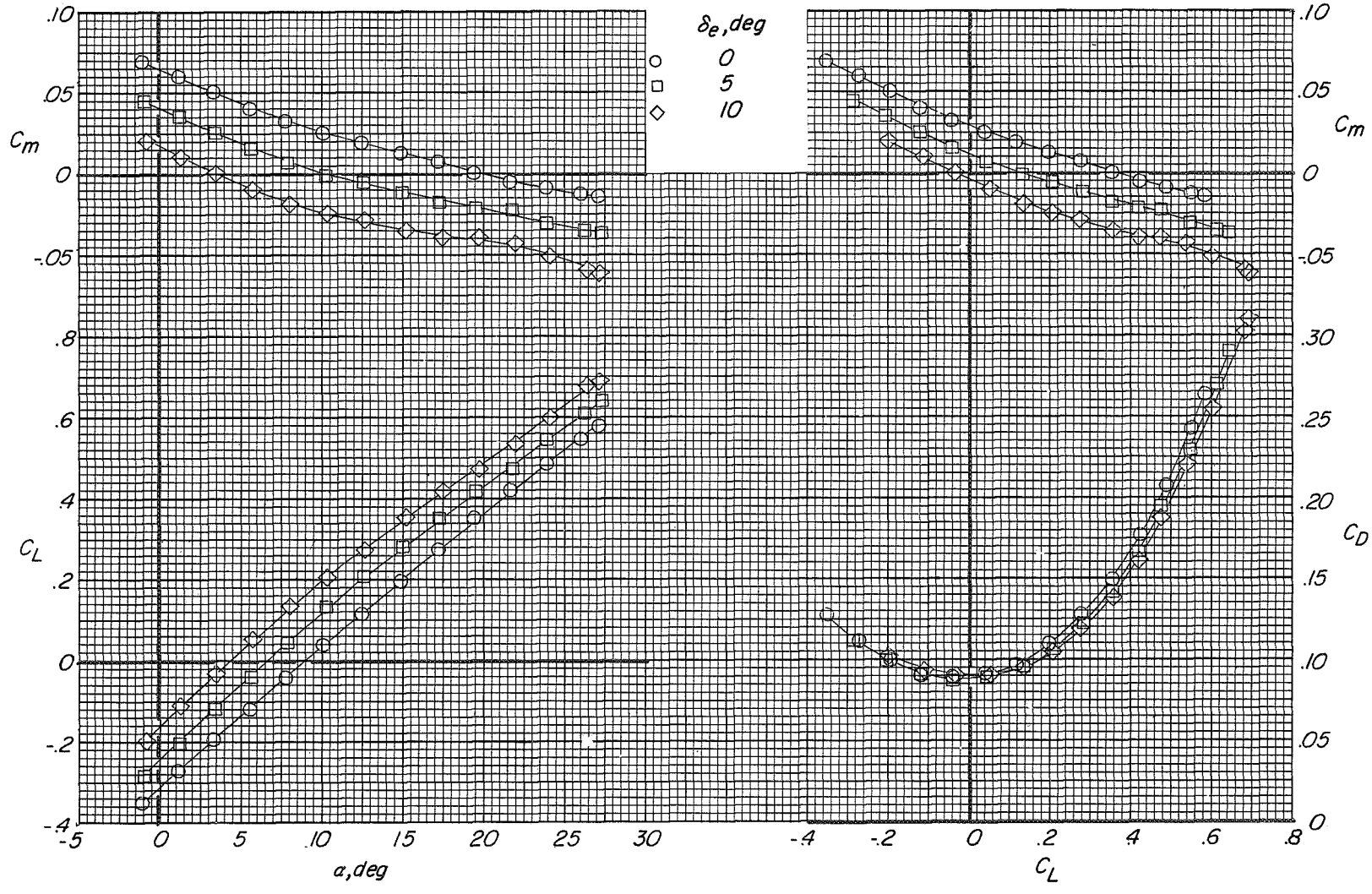
(d) $\beta = 2.3^{o}$; $\delta_a = 10^{o}$; M = 0.90.

Figure 32.- Continued.



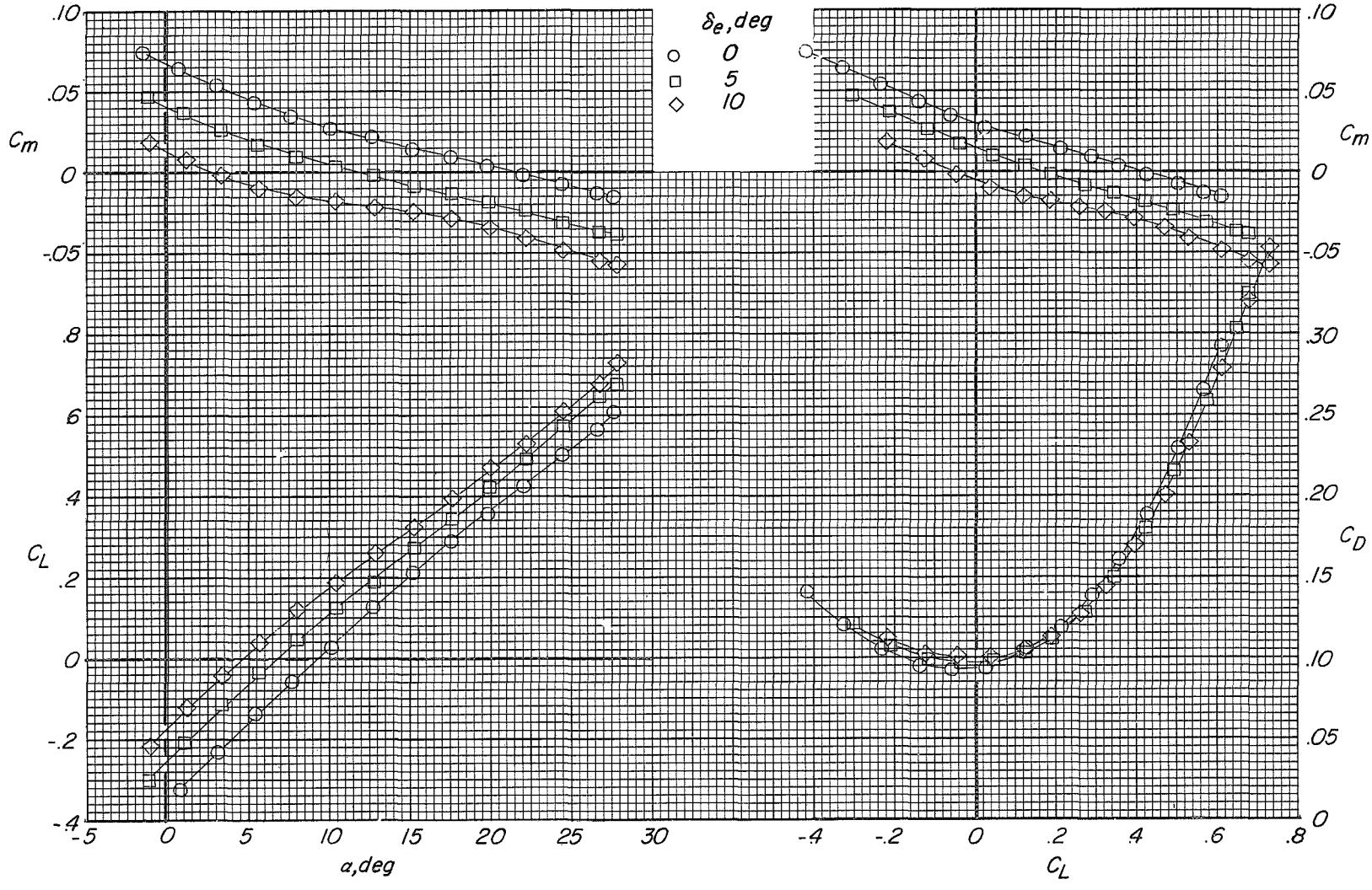
(e) $\beta = -2.3^{o}$; $\delta_a = 10^{o}$; M = 0.60.

Figure 32.- Continued.



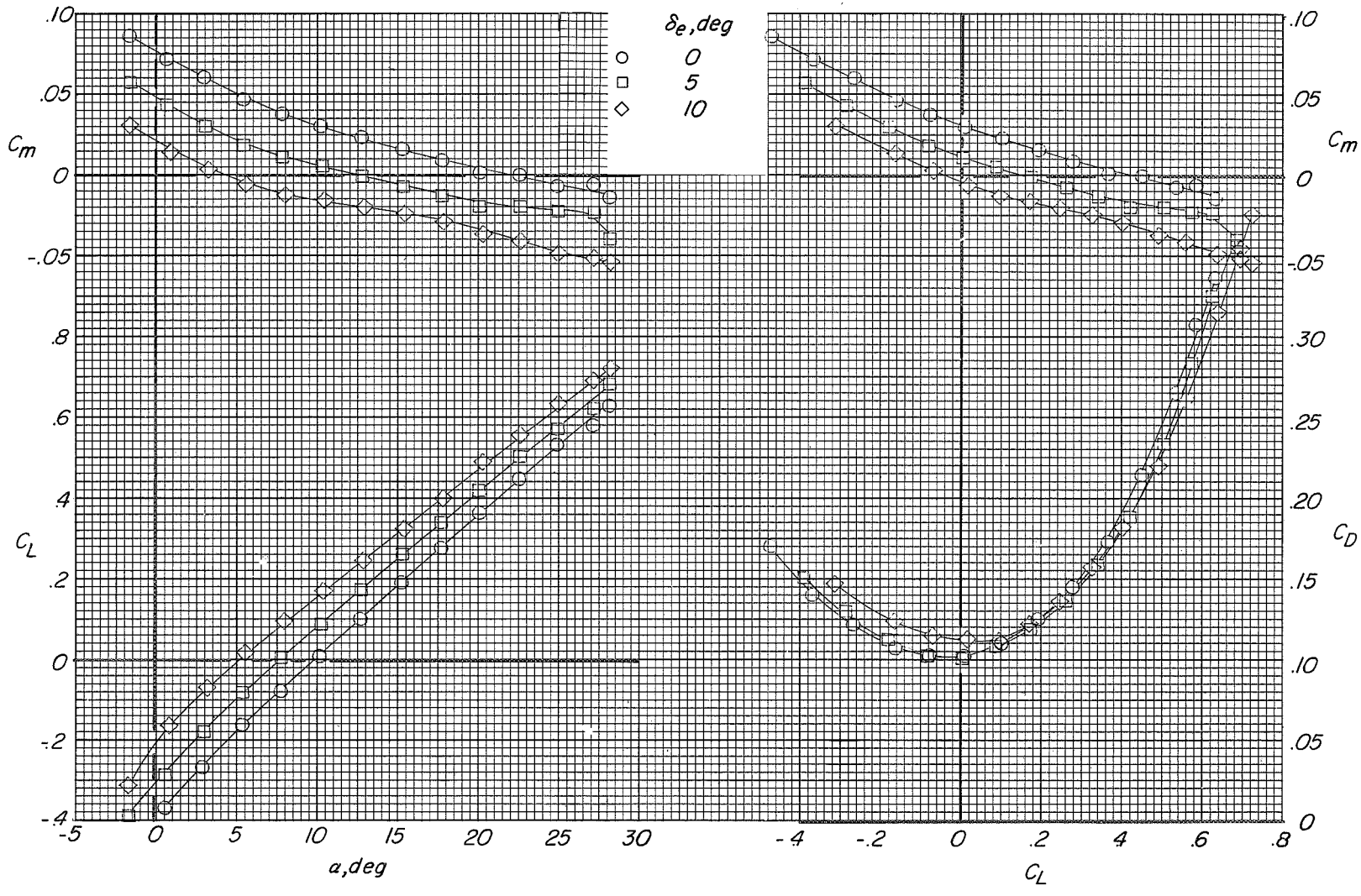
(f) $\beta = -2.3^{o}$; $\delta_a = 10^{o}$; M = 0.70.

Figure 32.- Continued.



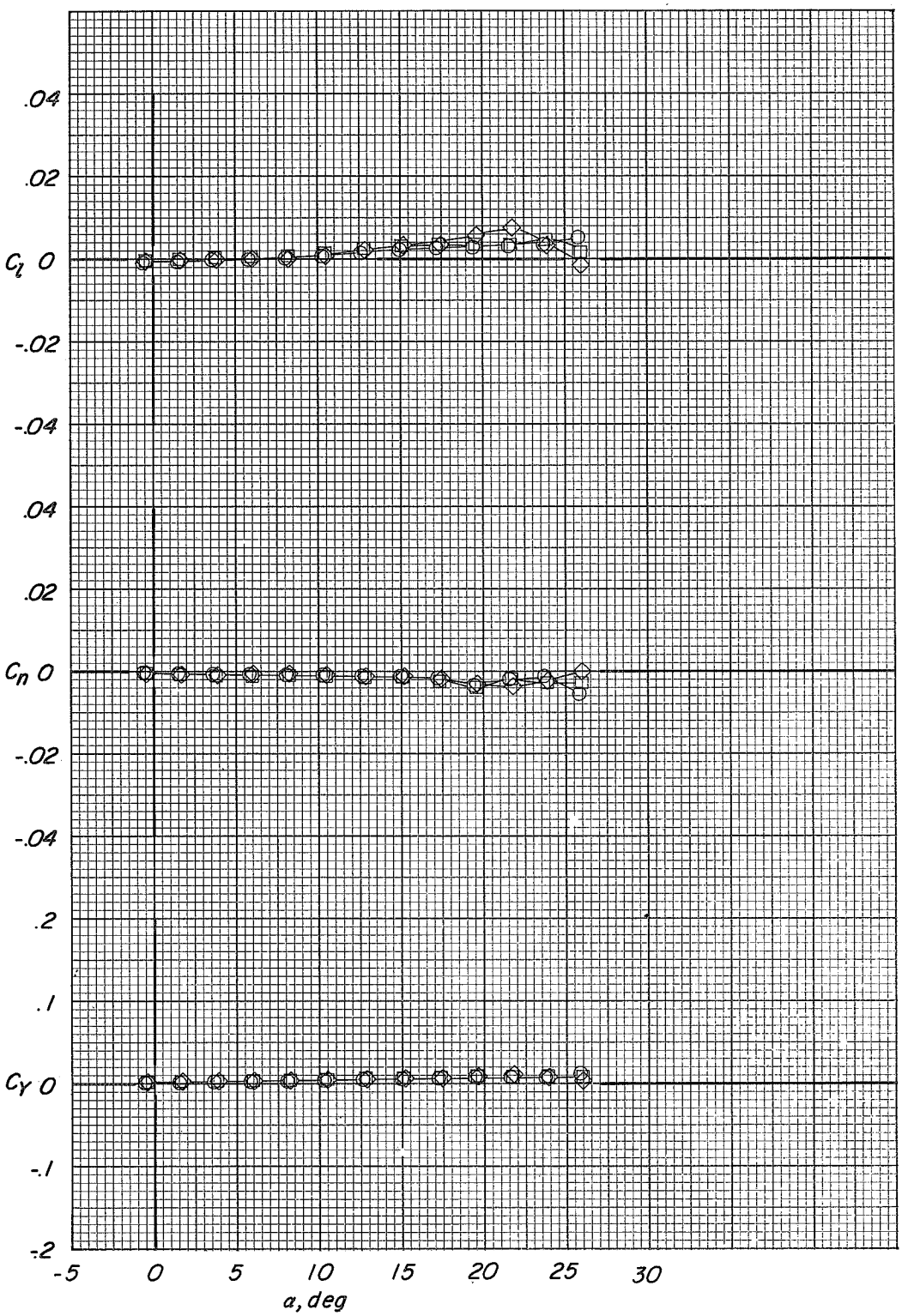
(g) $\beta = -2.3^{o}$; $\delta_a = 10^{o}$; M = 0.80.

Figure 32.- Continued.



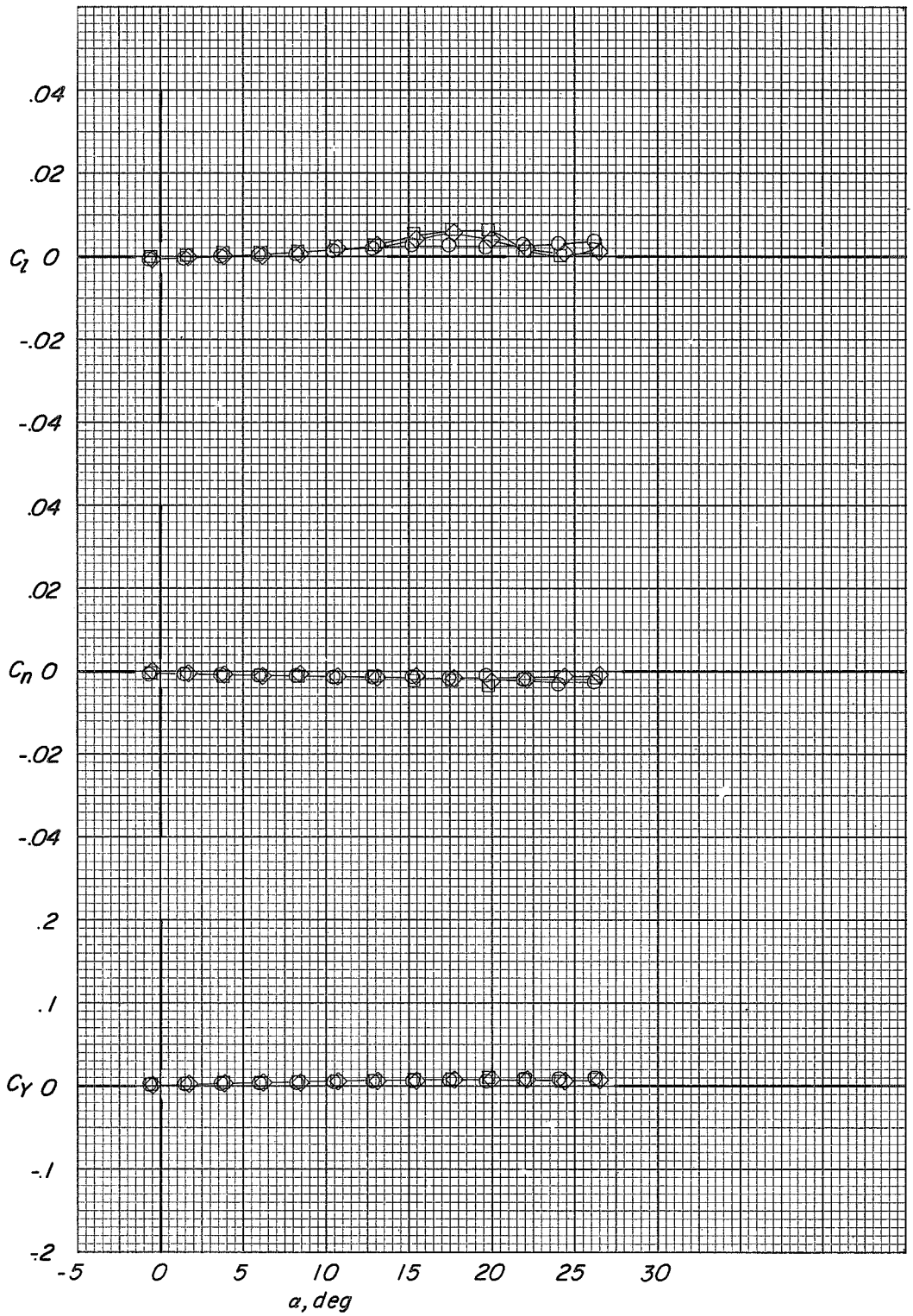
(h) $\beta = -2.3^{o}$; $\delta_a = 10^{o}$; M = 0.90.

Figure 32.- Concluded.



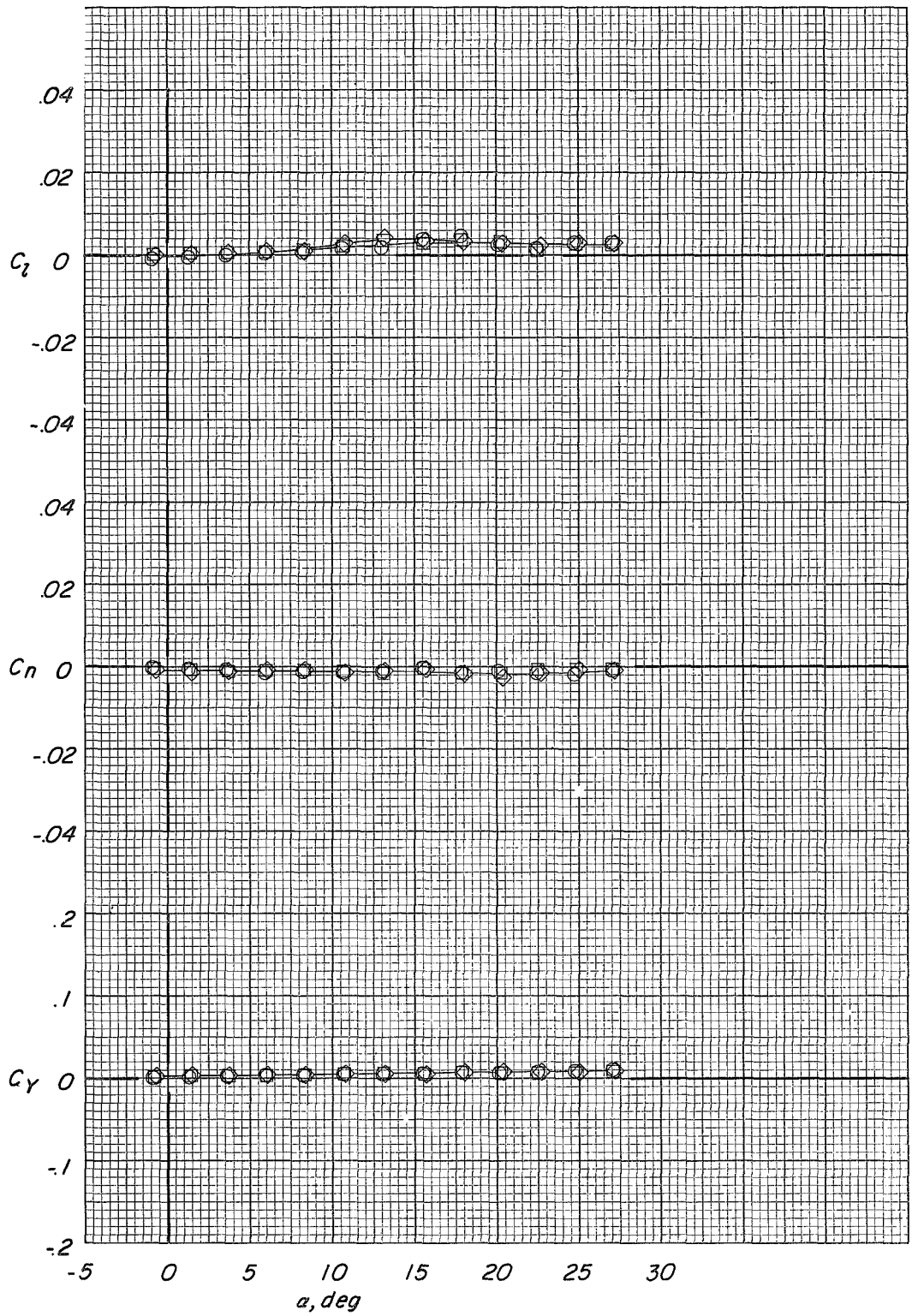
(a) $\delta_a = 0^o$; M = 0.60.

Figure 33.- Variation of the lateral force and moment coefficients with angle of attack for several aileron deflections. Modification I fin configuration; auxiliary flaps in the transonic position; $\beta = 0^o$.



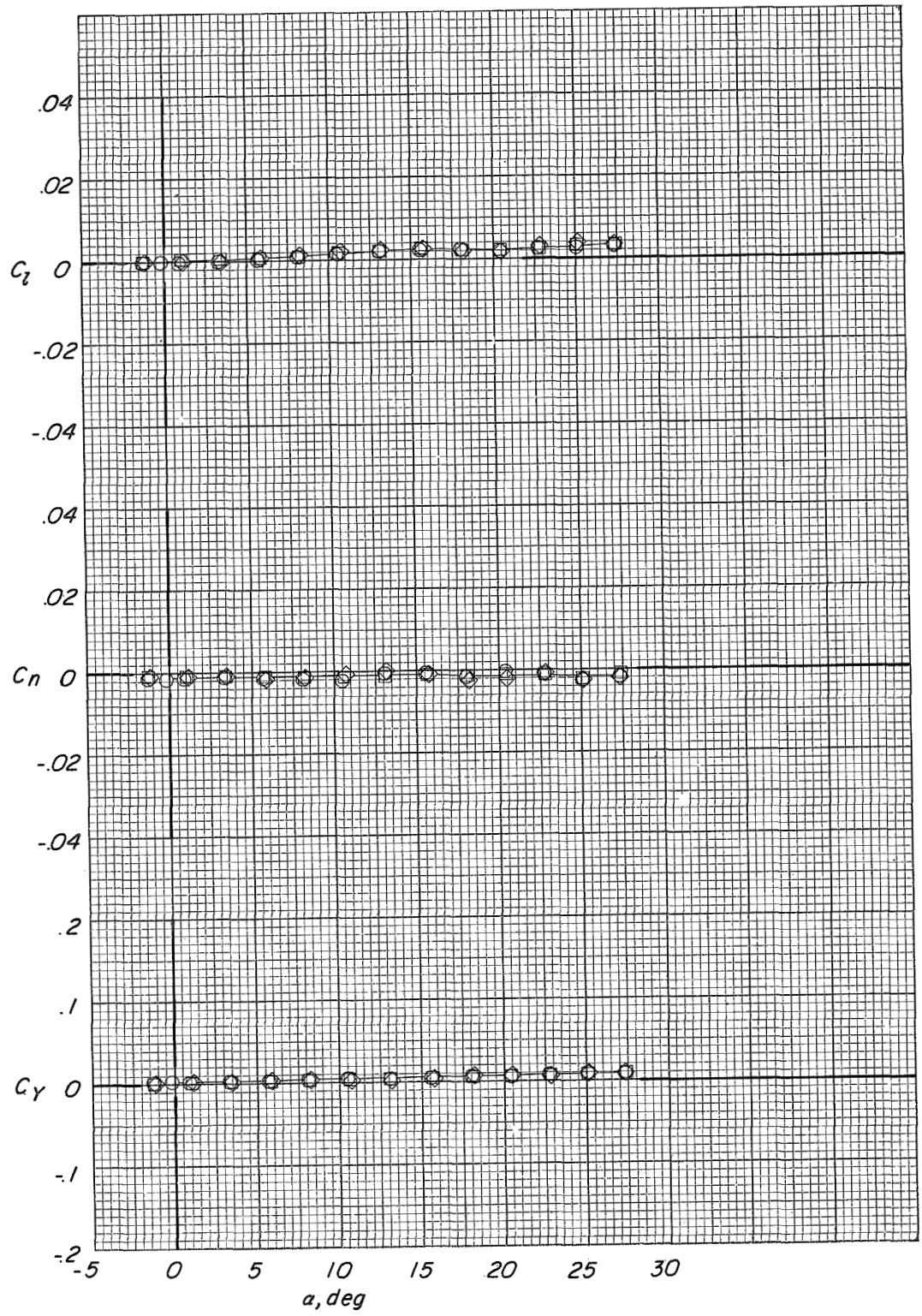
(b) $\delta_a = 0^o$; M = 0.70.

Figure 33.- Continued.



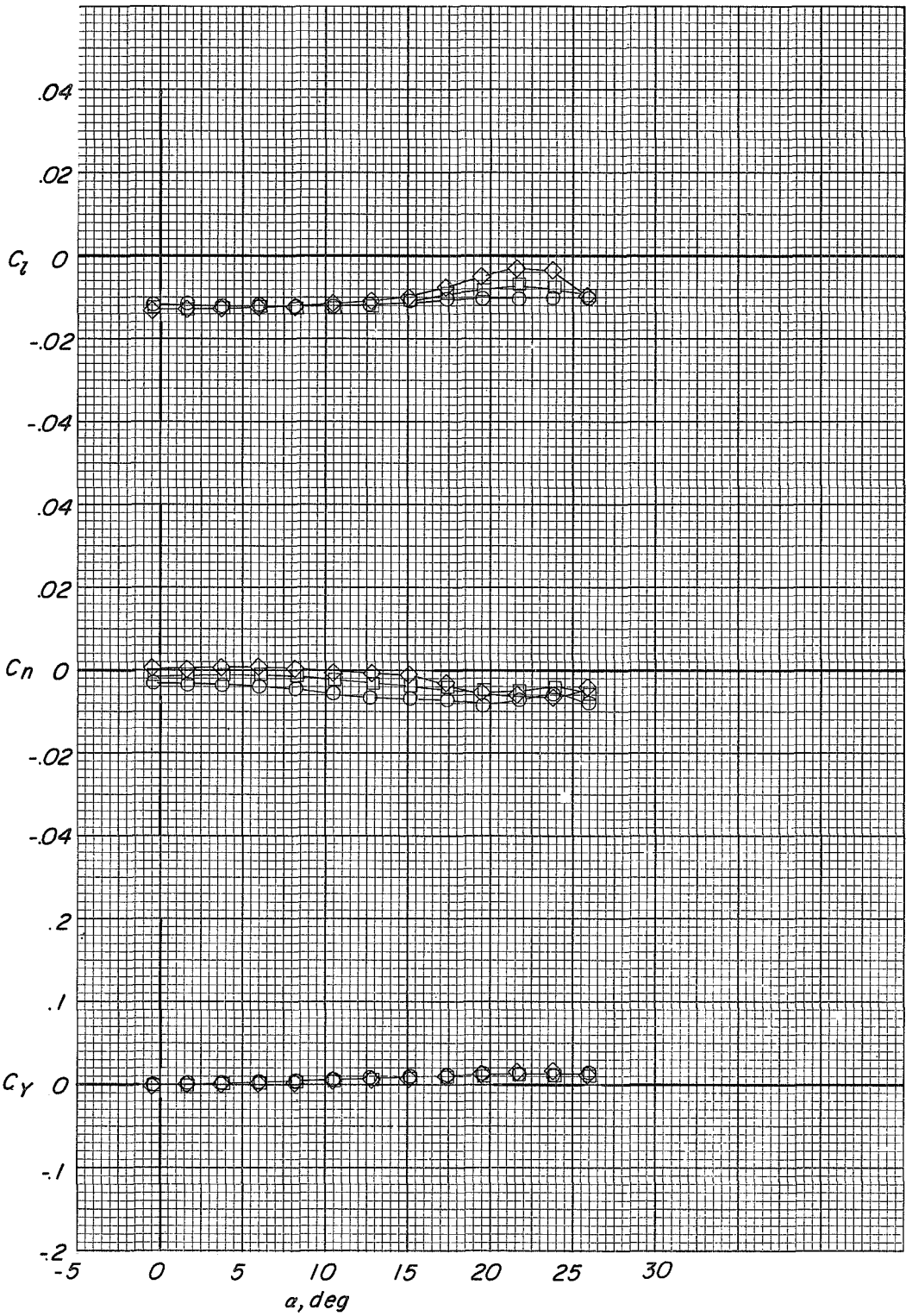
(c) $\delta_a = 0^o$; M = 0.80.

Figure 33.- Continued.



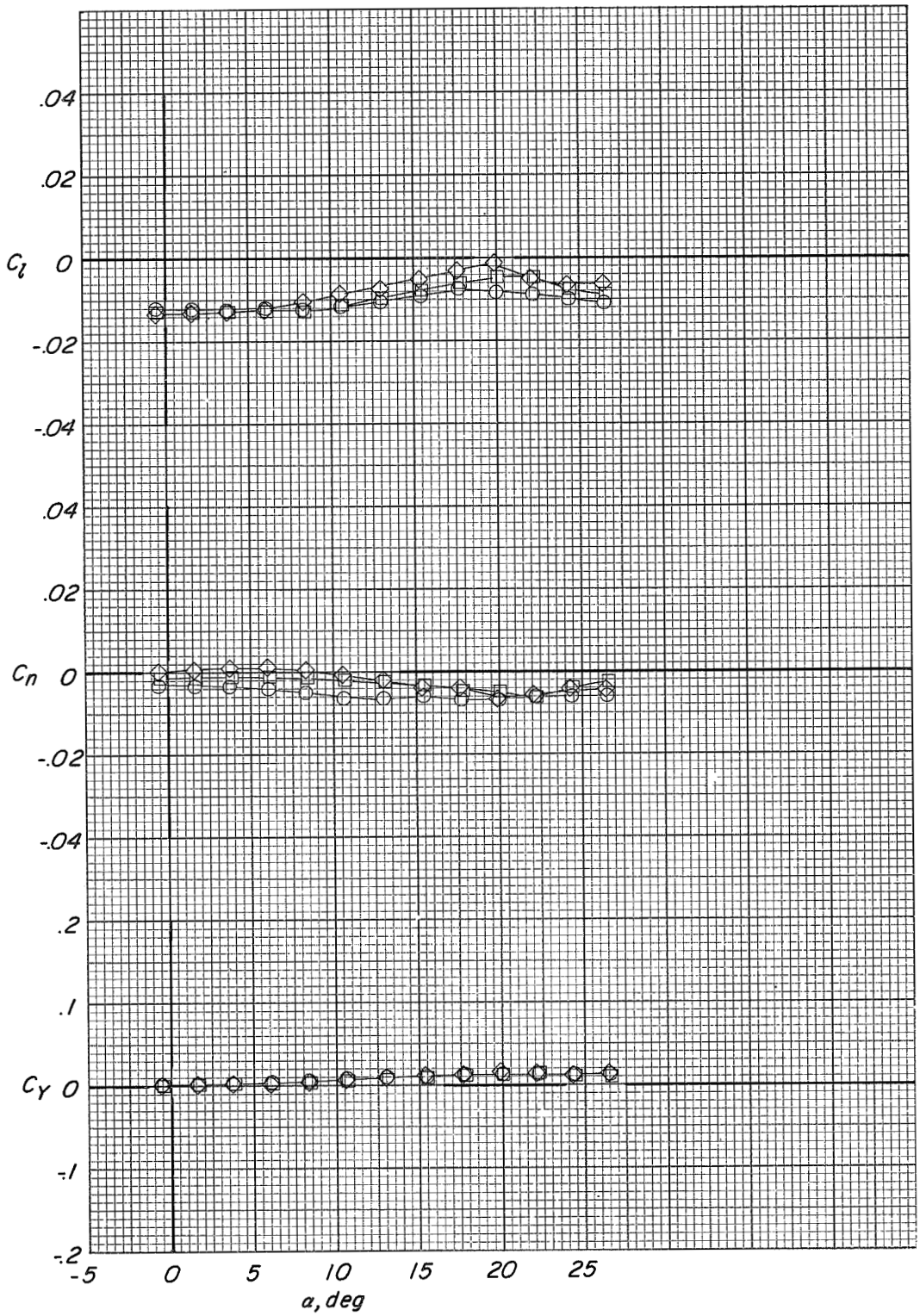
(d) $\delta_a = 0^o$; M = 0.90.

Figure 33.- Continued.



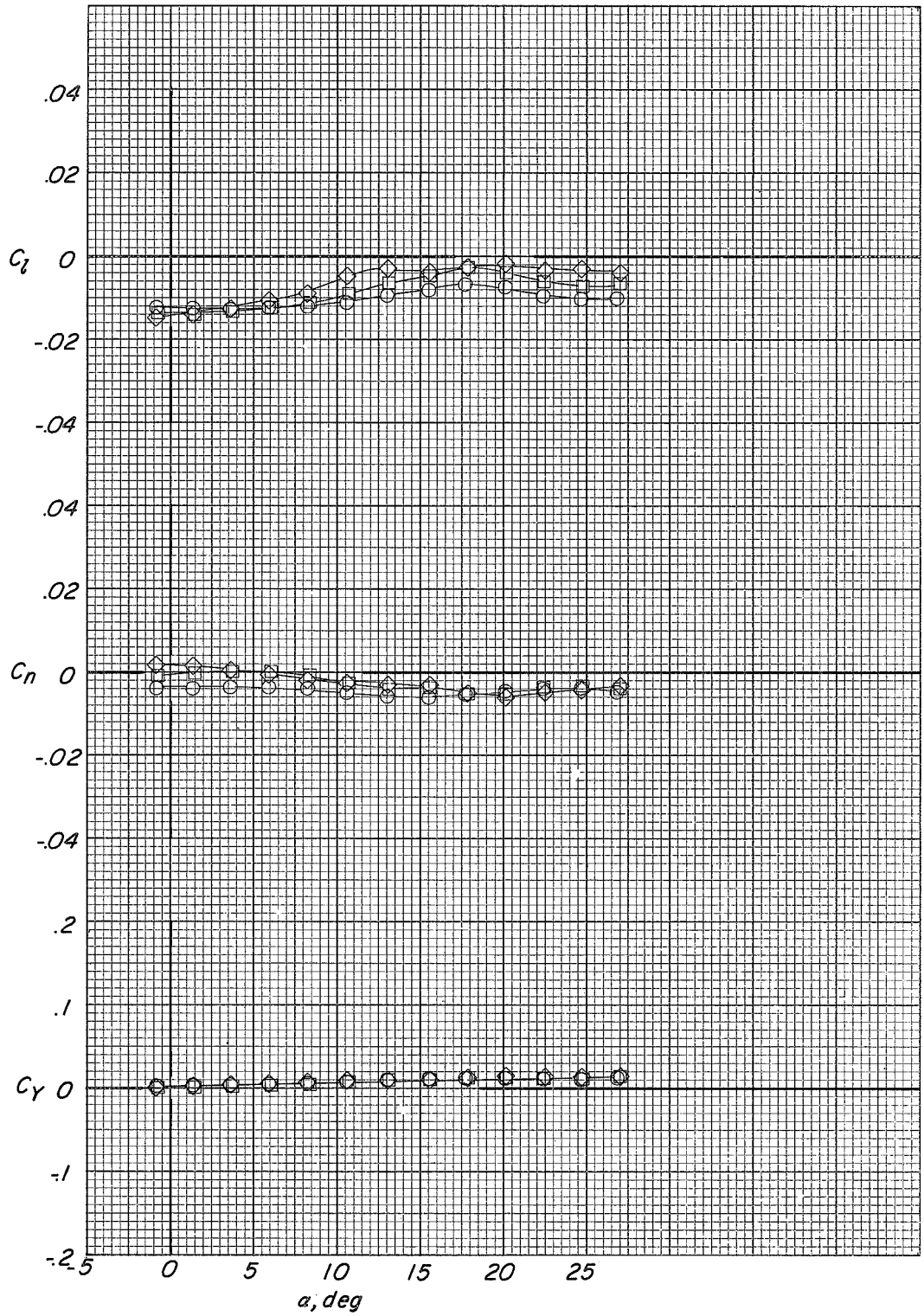
(e) $\delta_a = 10^o$; M = 0.60.

Figure 33.- Continued.



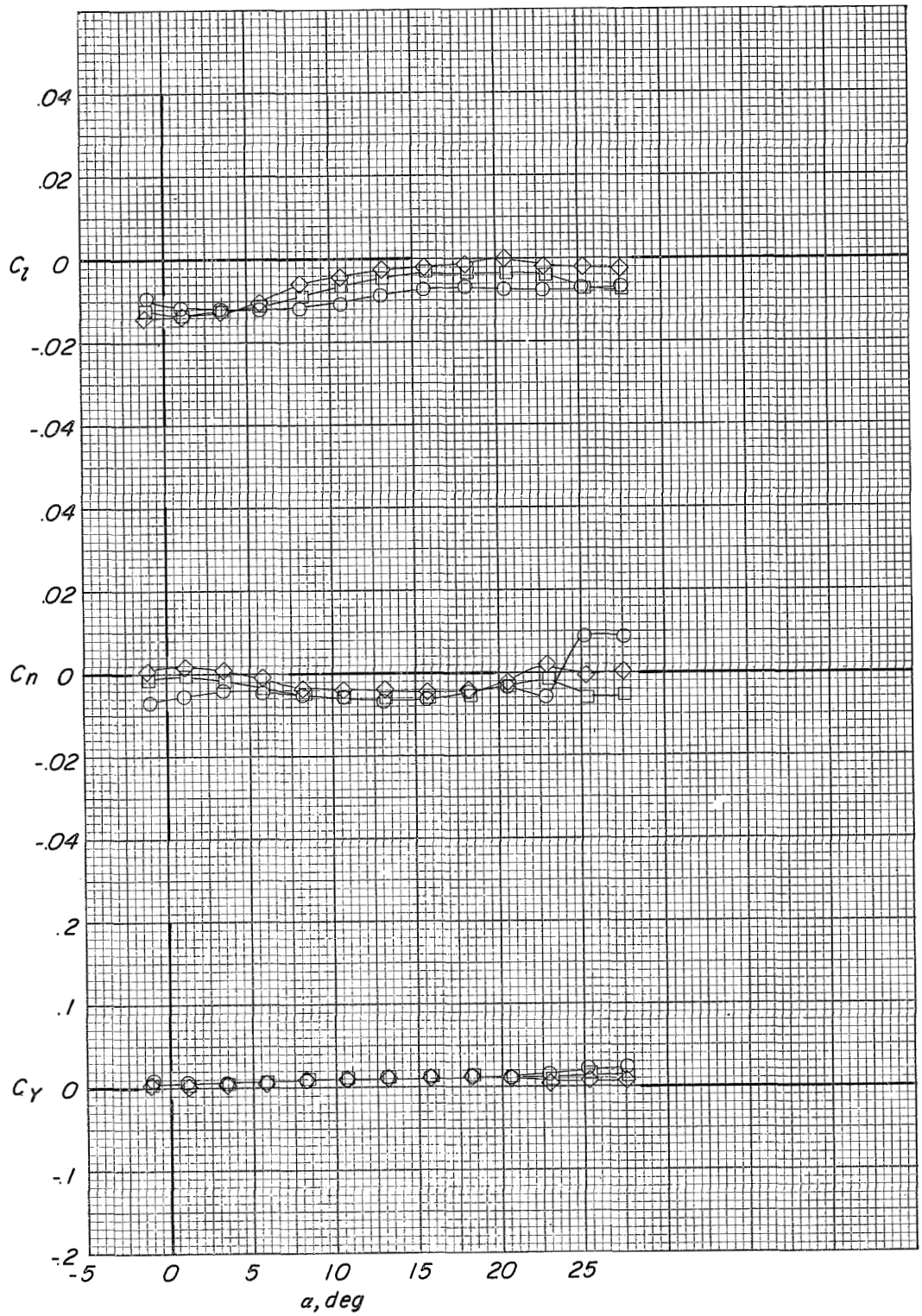
(f) $\delta_a = 10^o$; M = 0.70.

Figure 33.- Continued.



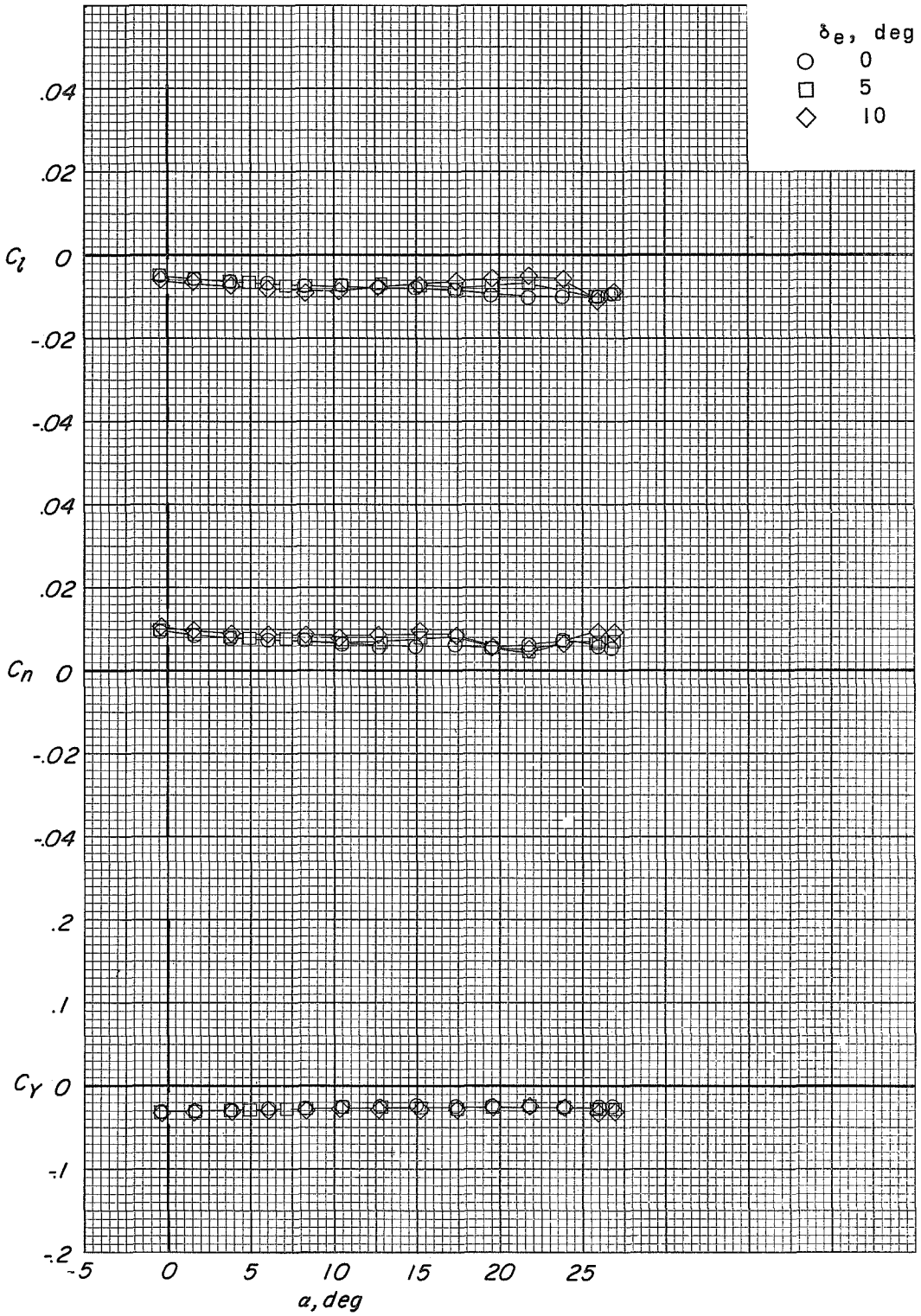
(g) $\delta_a = 10^o$; M = 0.80.

Figure 33.- Continued.



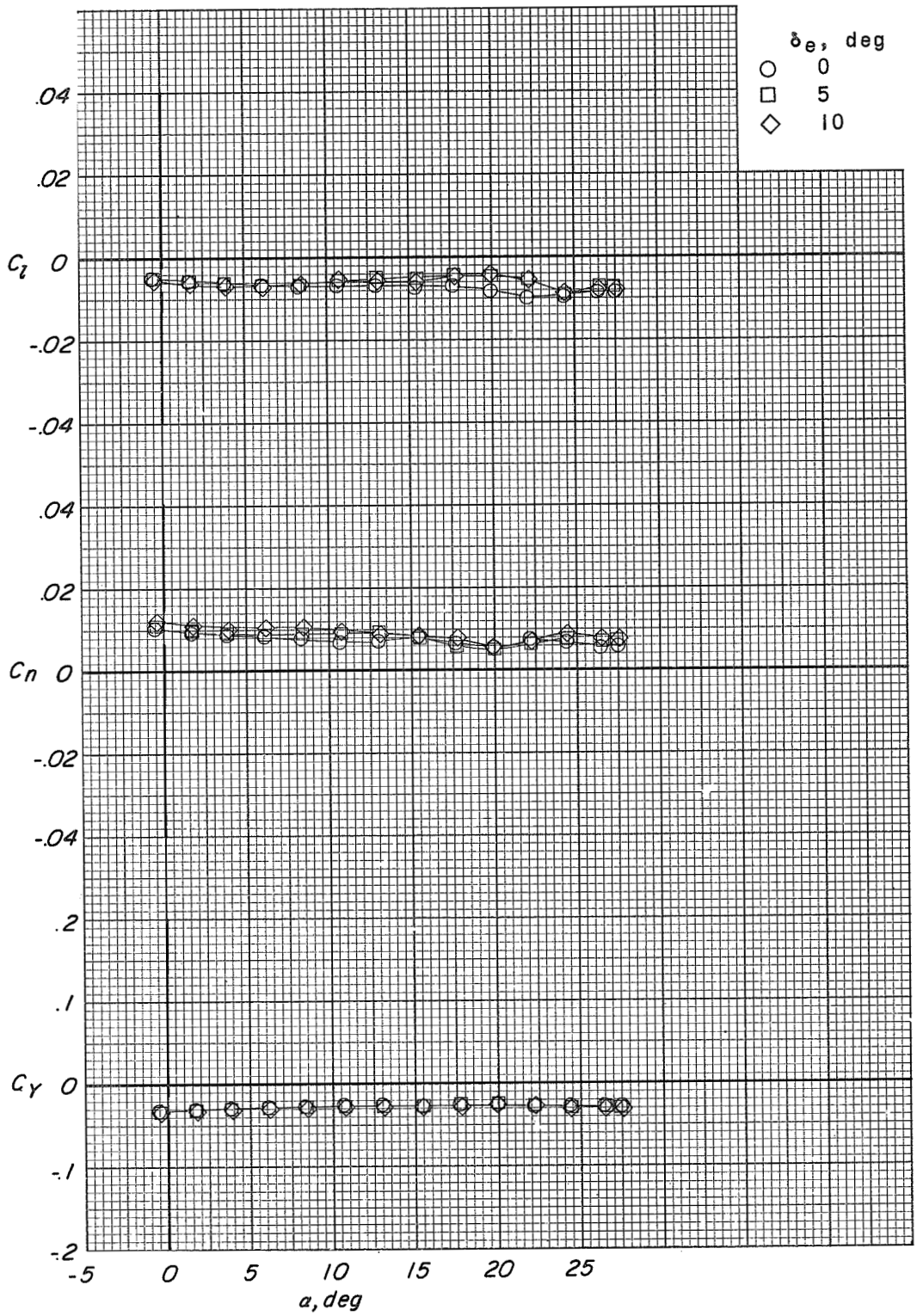
(h) $\delta_a = 10^o$; M = 0.90.

Figure 33.- Concluded.



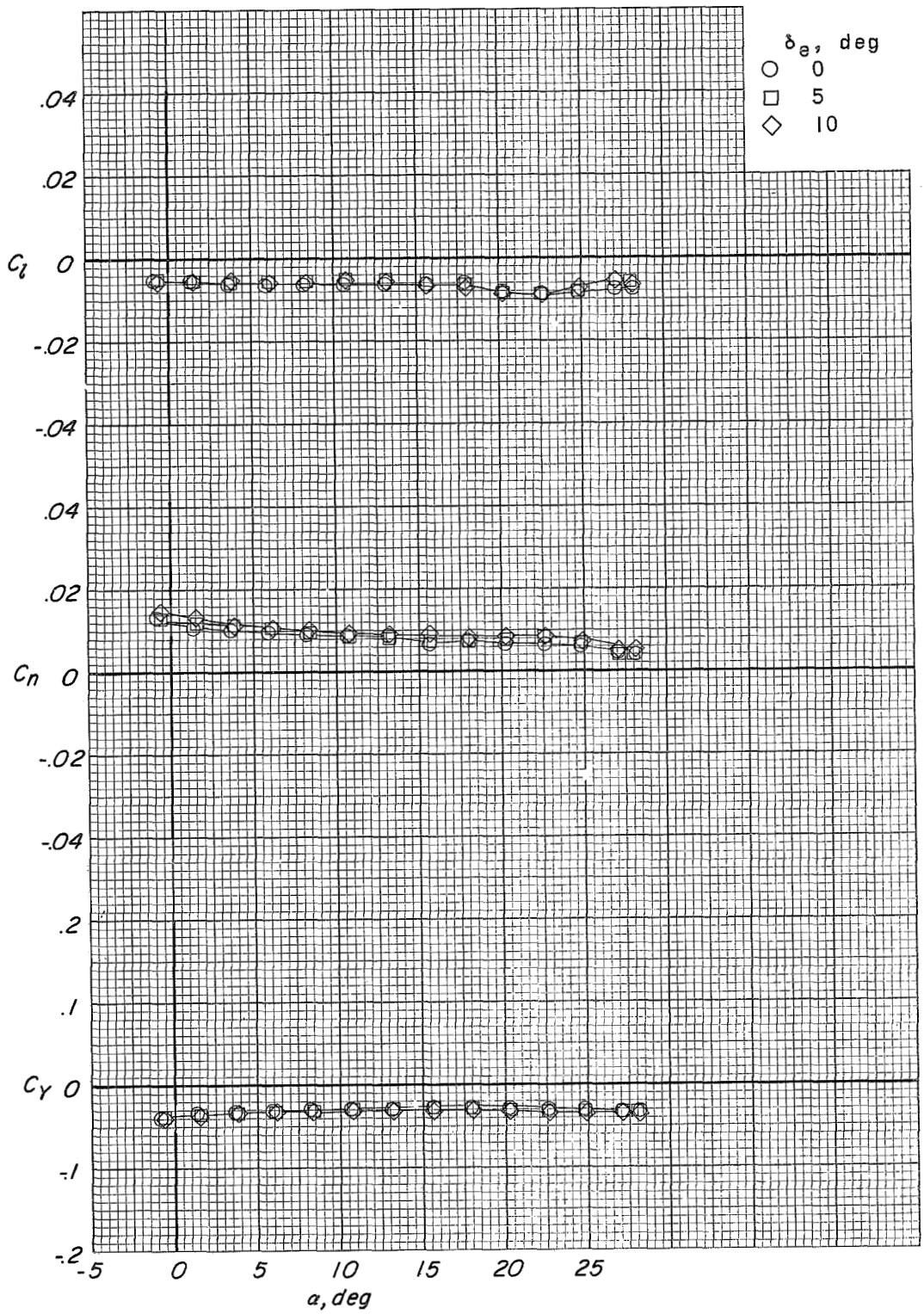
(a) $\beta = 2.3^{o}$; M = 0.60.

Figure 34.- Variation of the lateral force and moment coefficients with angle of attack for sideslipped conditions. Modification I fin configuration; auxiliary flaps in the transonic position; $\delta_a = 0^{o}$.



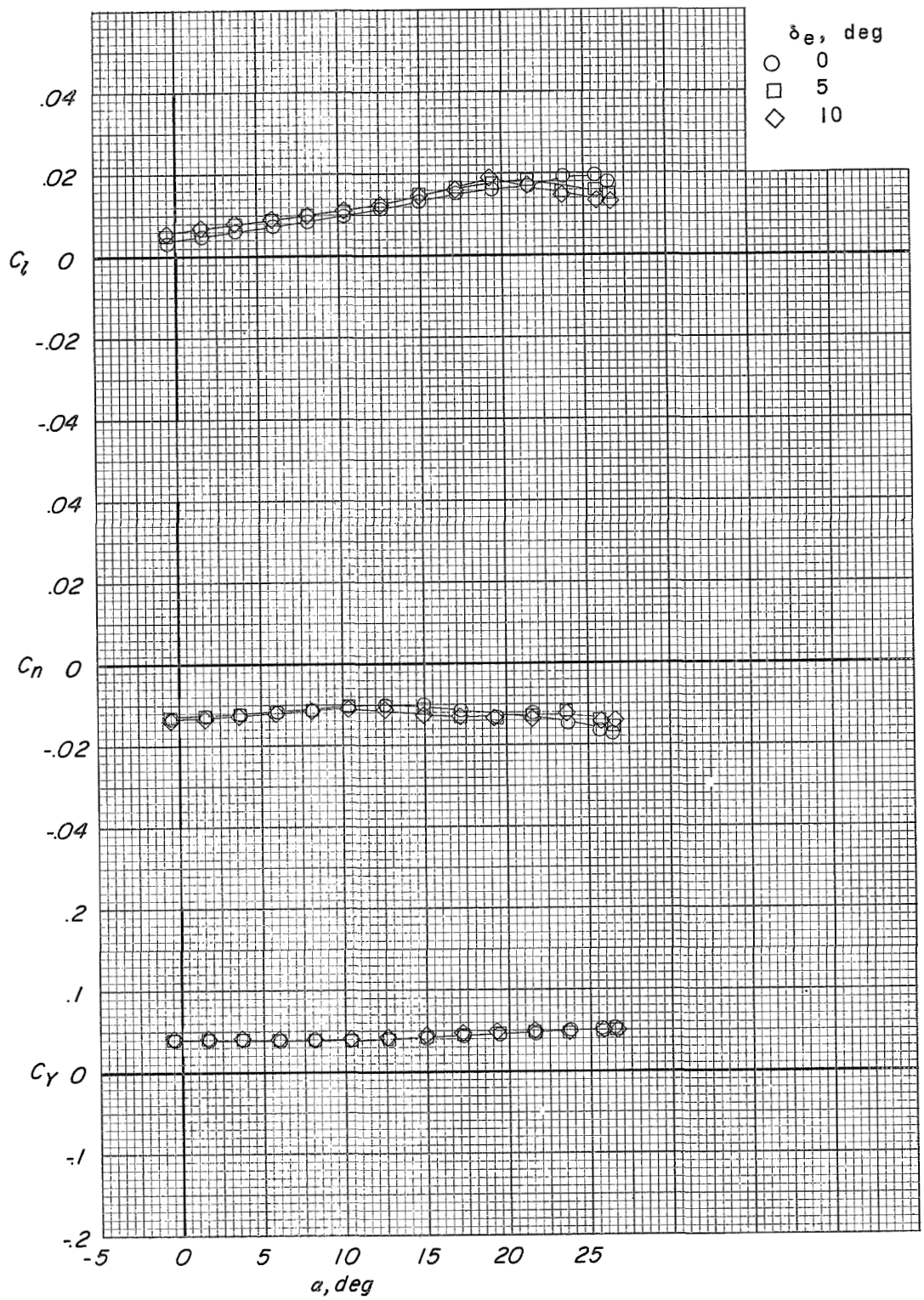
(b) $\beta = 2.3^{o}$; M = 0.70.

Figure 34.- Continued.



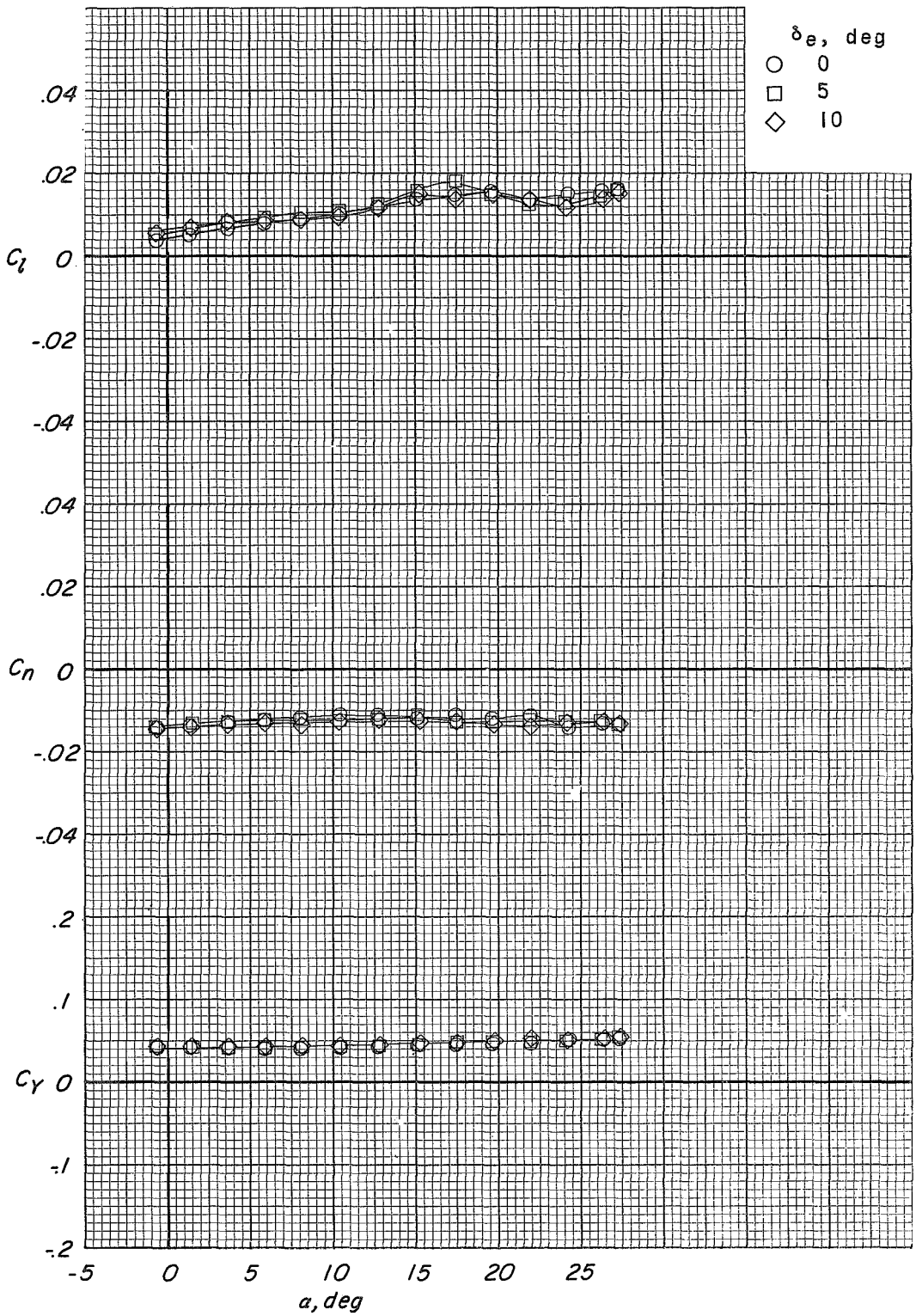
(c) $\beta = 2.3^{\circ}$; M = 0.80.

Figure 34.- Continued.



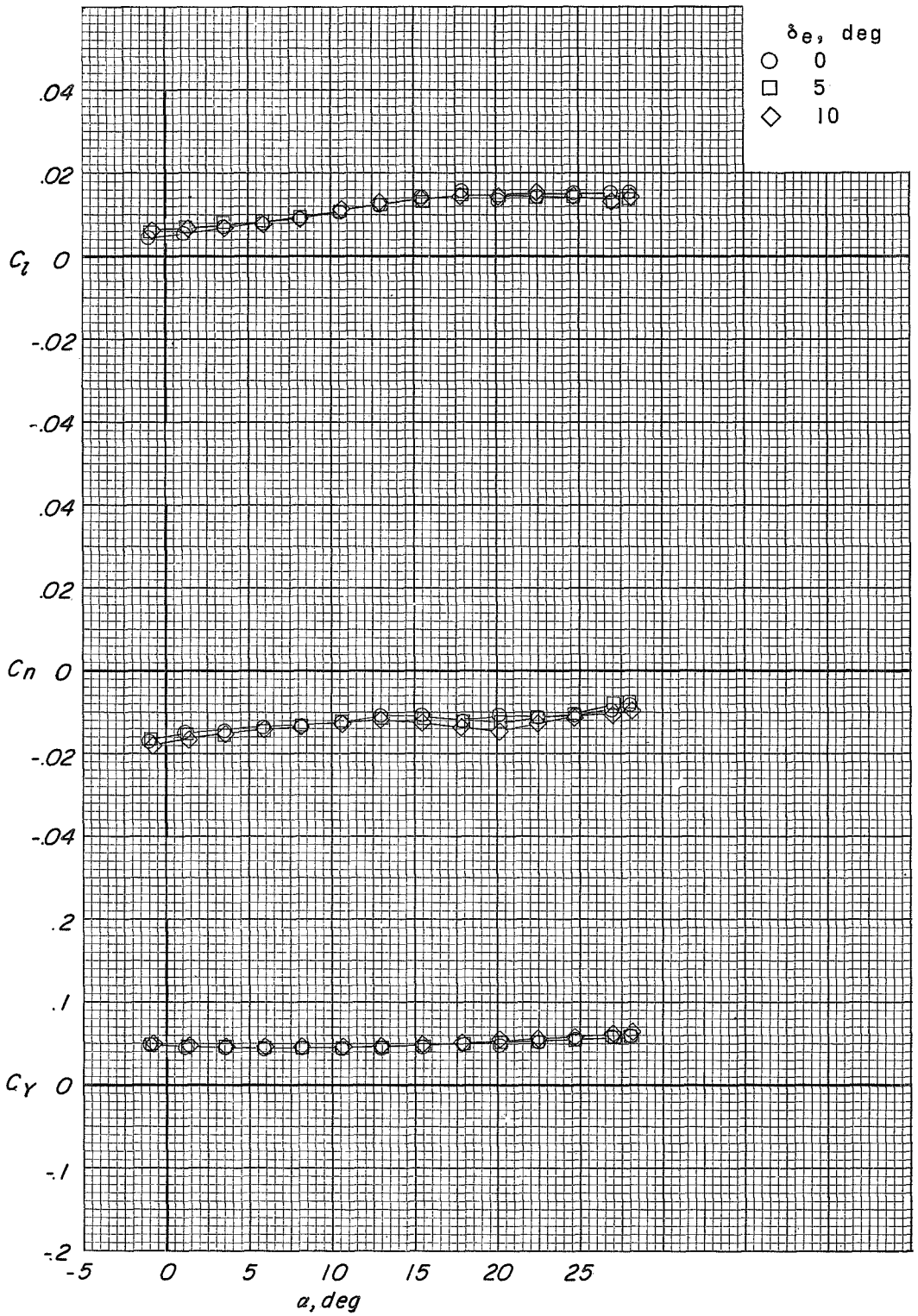
(d) $\beta = -2.3^{o}$; M = 0.60.

Figure 34.- Continued.



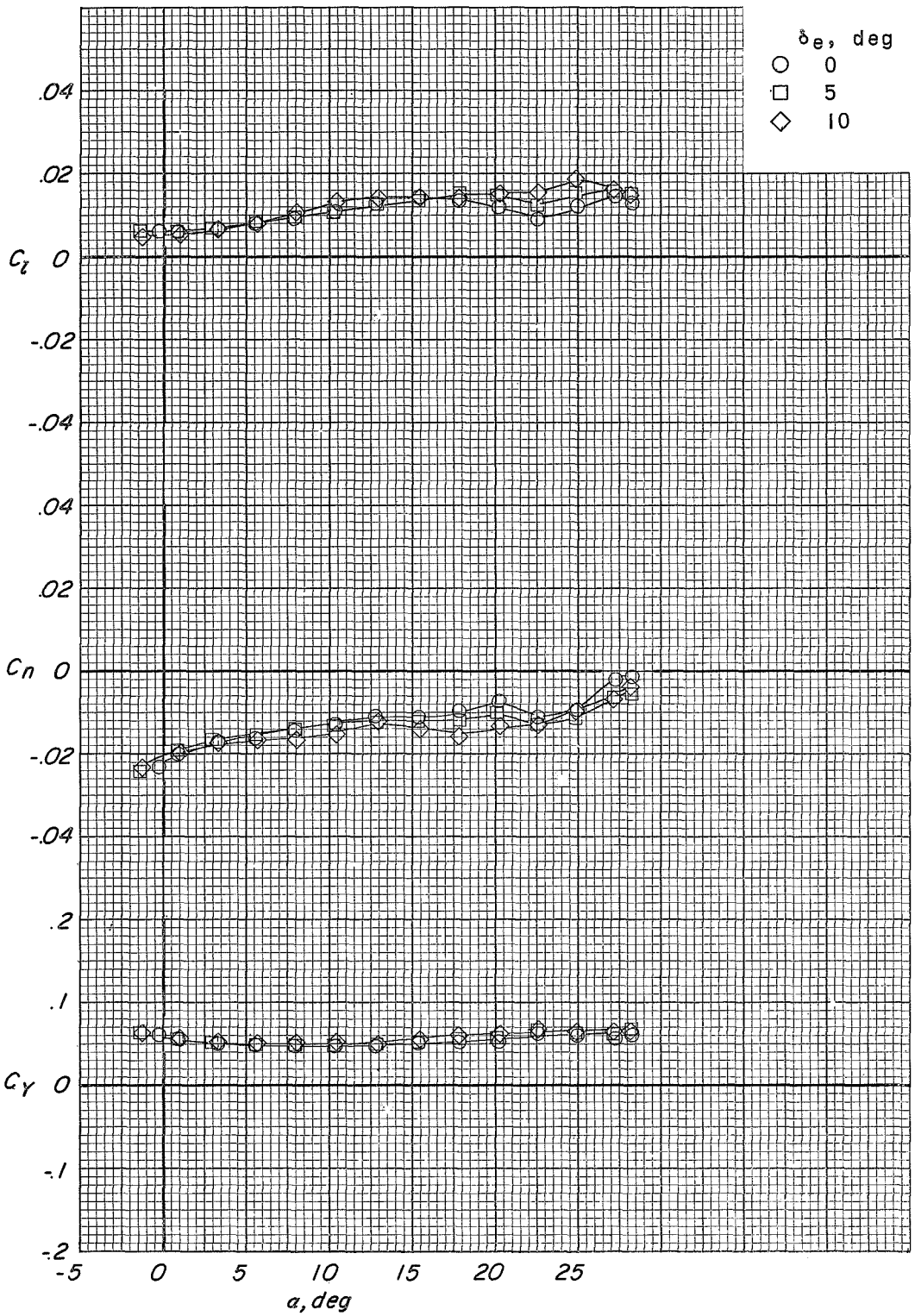
(e) $\beta = -2.3^{\circ}$; M = 0.70.

Figure 34.- Continued.



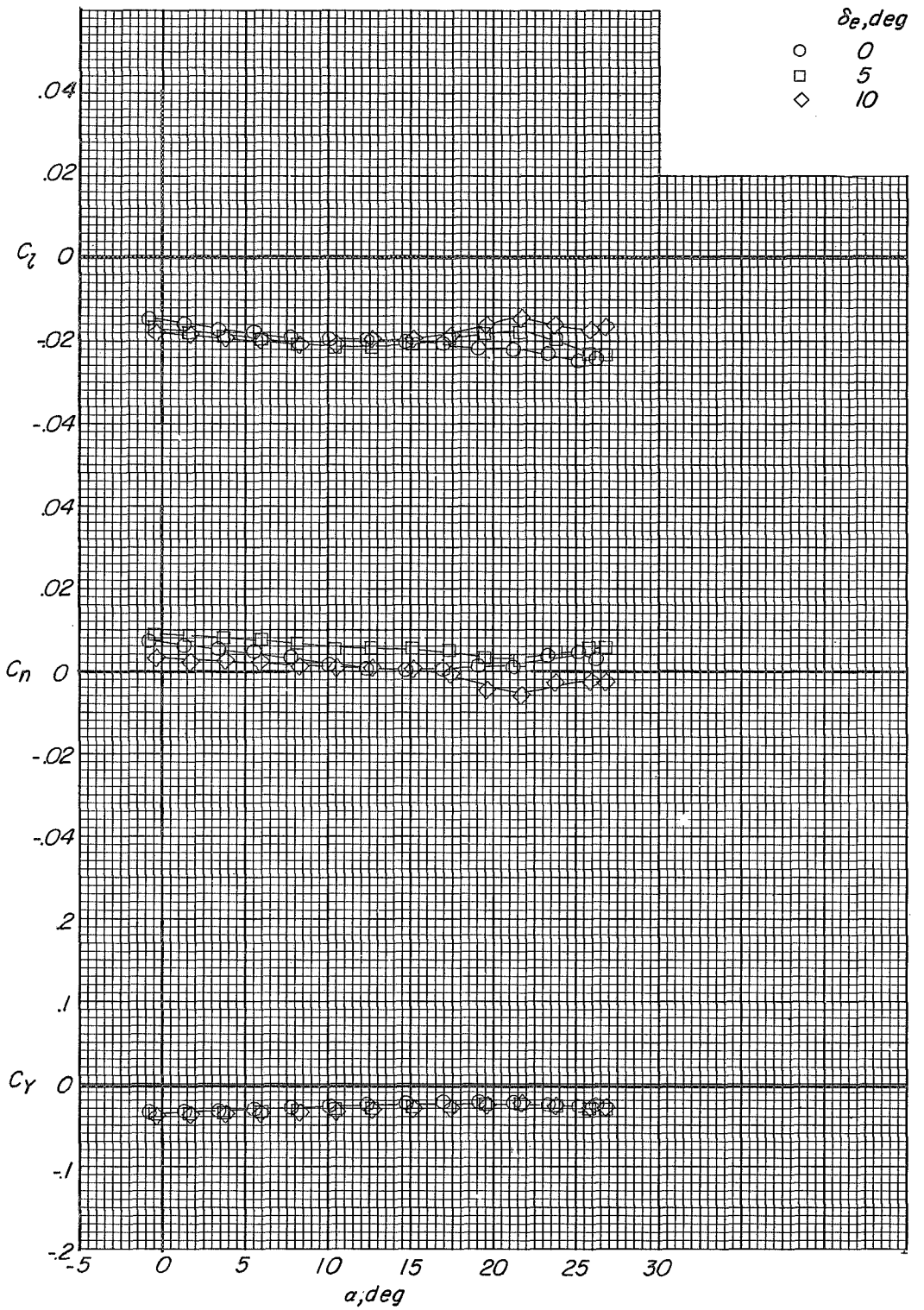
(f) $\beta = -2.3^{\circ}$; M = 0.80.

Figure 34.- Continued.



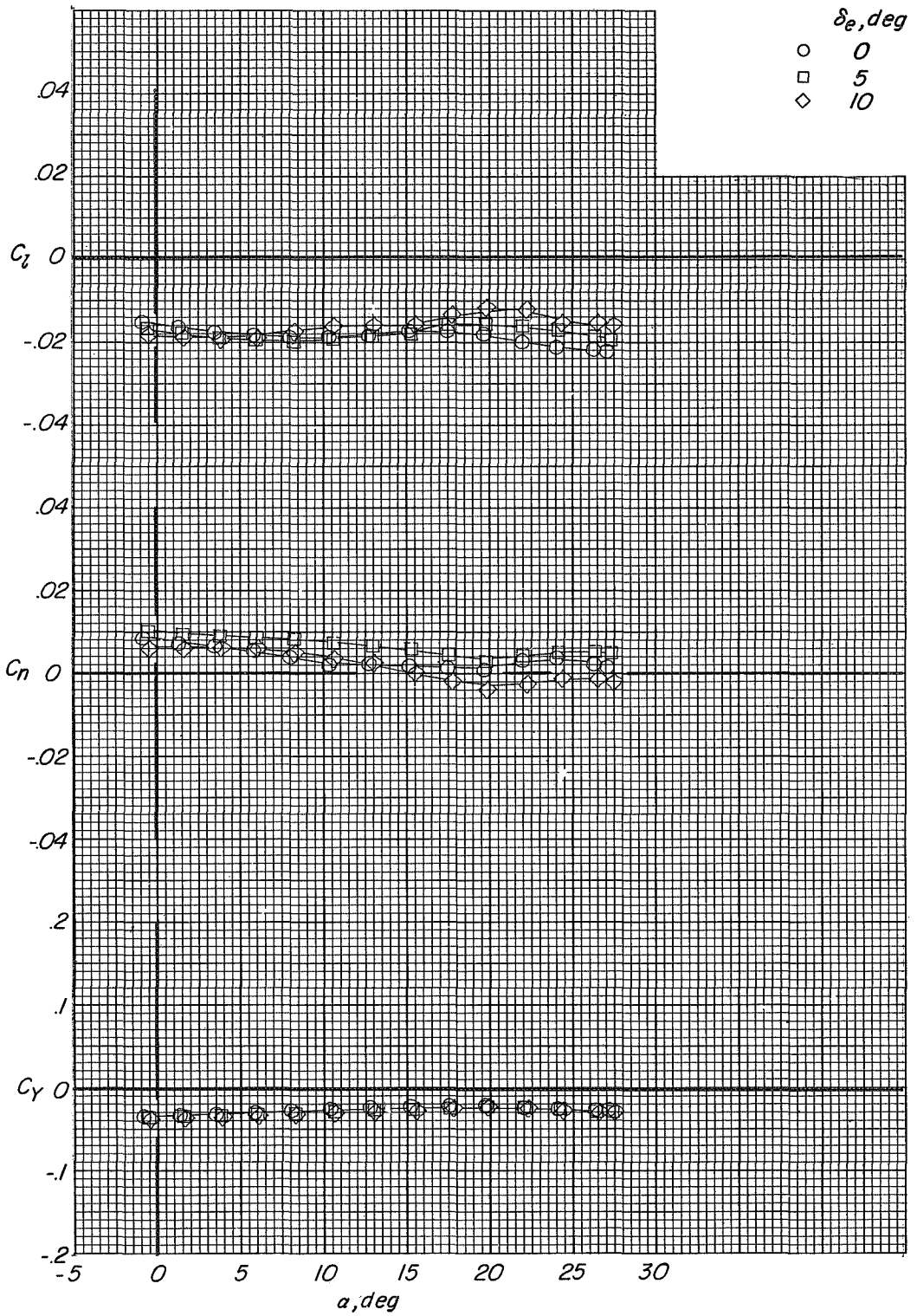
(g) $\beta = -2.3^{o}$; M = 0.90.

Figure 34.- Concluded.



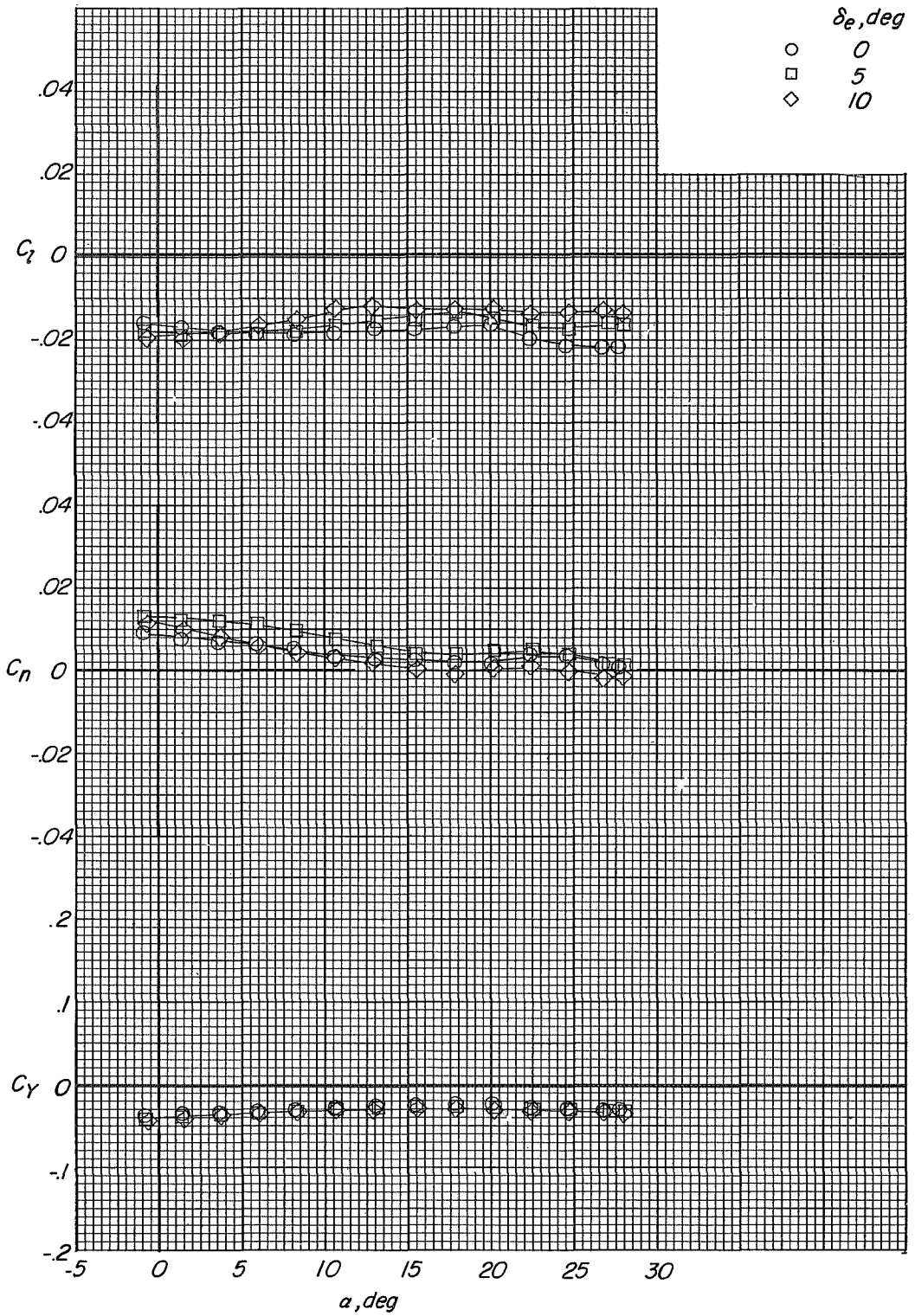
(a) $\beta = 2.3^{\circ}$; $\delta_a = 10^{\circ}$; M = 0.60.

Figure 35.- Variation of the lateral force and moment coefficients with angle of attack for combined aileron deflection and sideslip. Modification I fin configuration; auxiliary flaps in the transonic position.



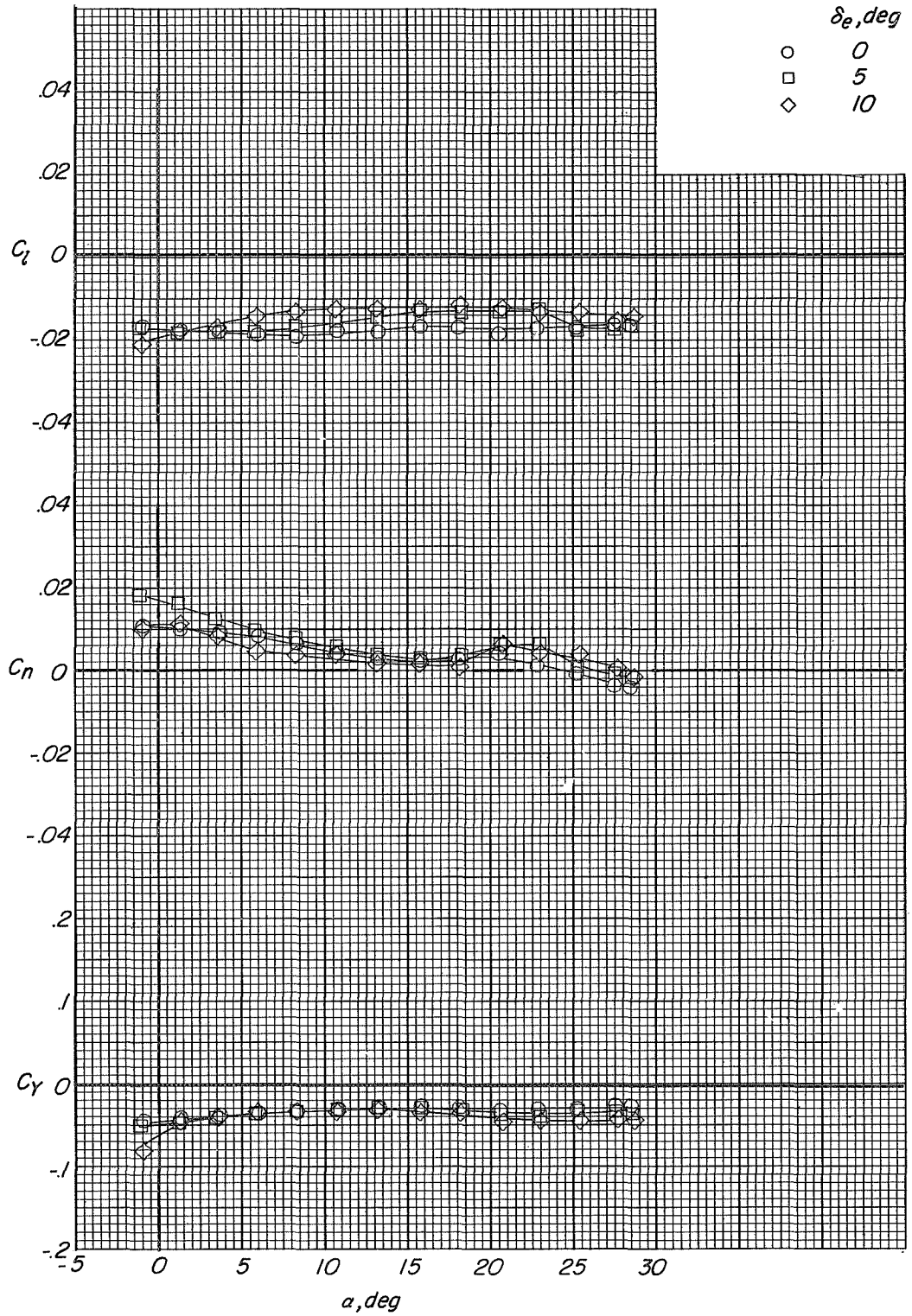
(b) $\beta = 2.3^{o}$; $\delta_a = 10^{o}$; M = 0.70.

Figure 35.- Continued.



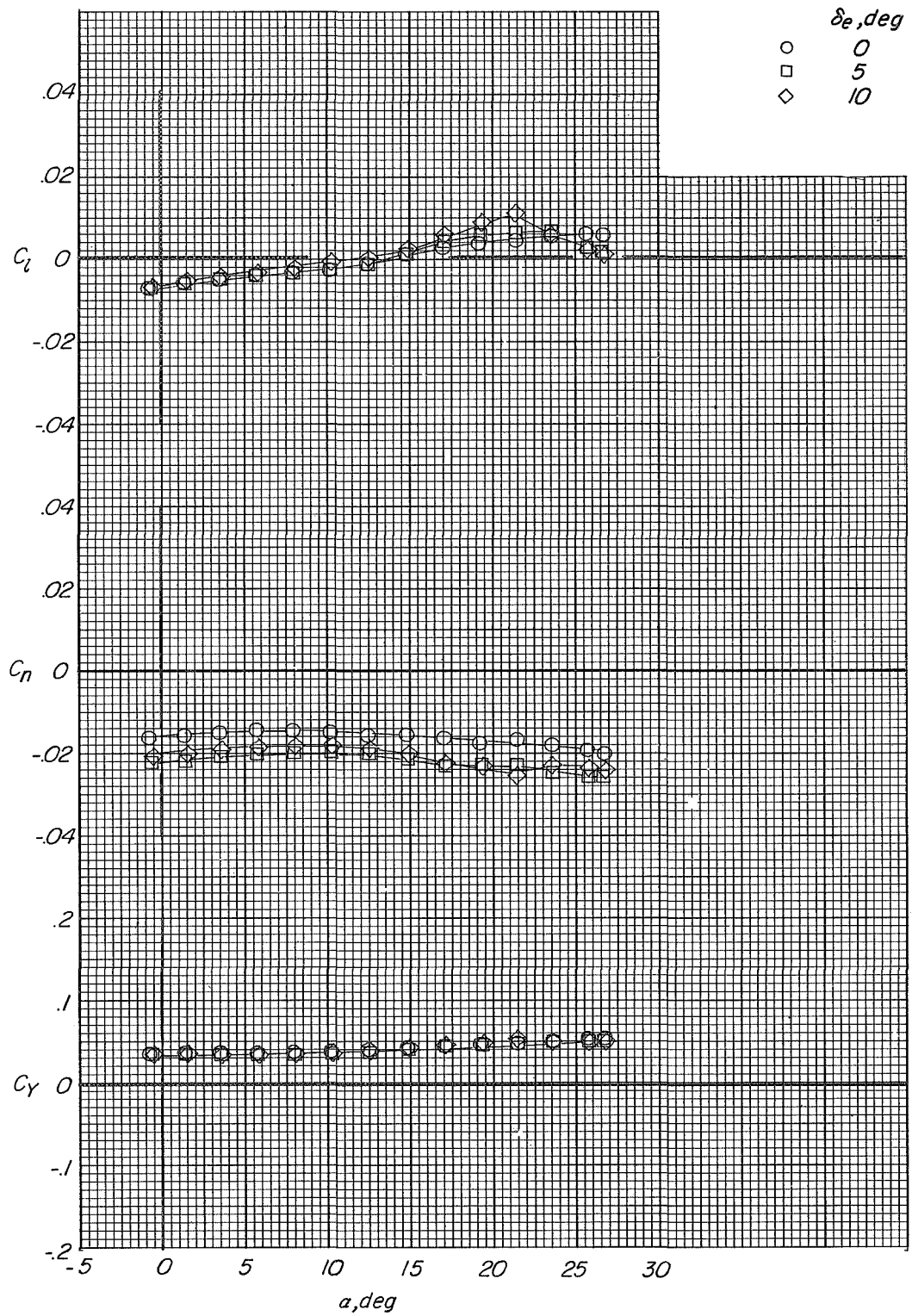
(c) $\beta = 2.3^{o}$; $\delta_a = 10^{o}$; M = 0.80.

Figure 35.- Continued.



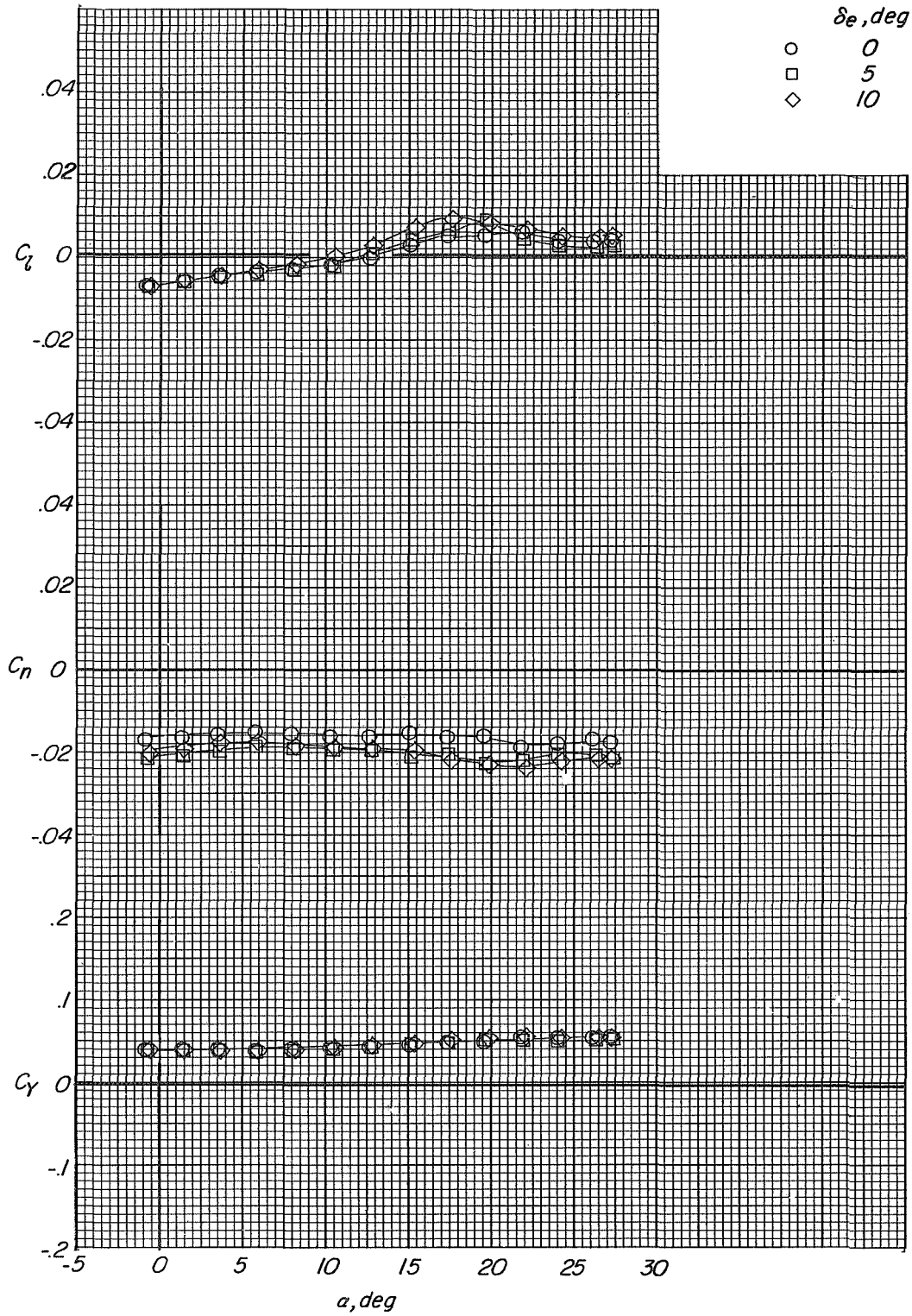
(d) $\beta = 2.3^{o}$; $\delta_a = 10^{o}$; M = 0.90.

Figure 35.- Continued.



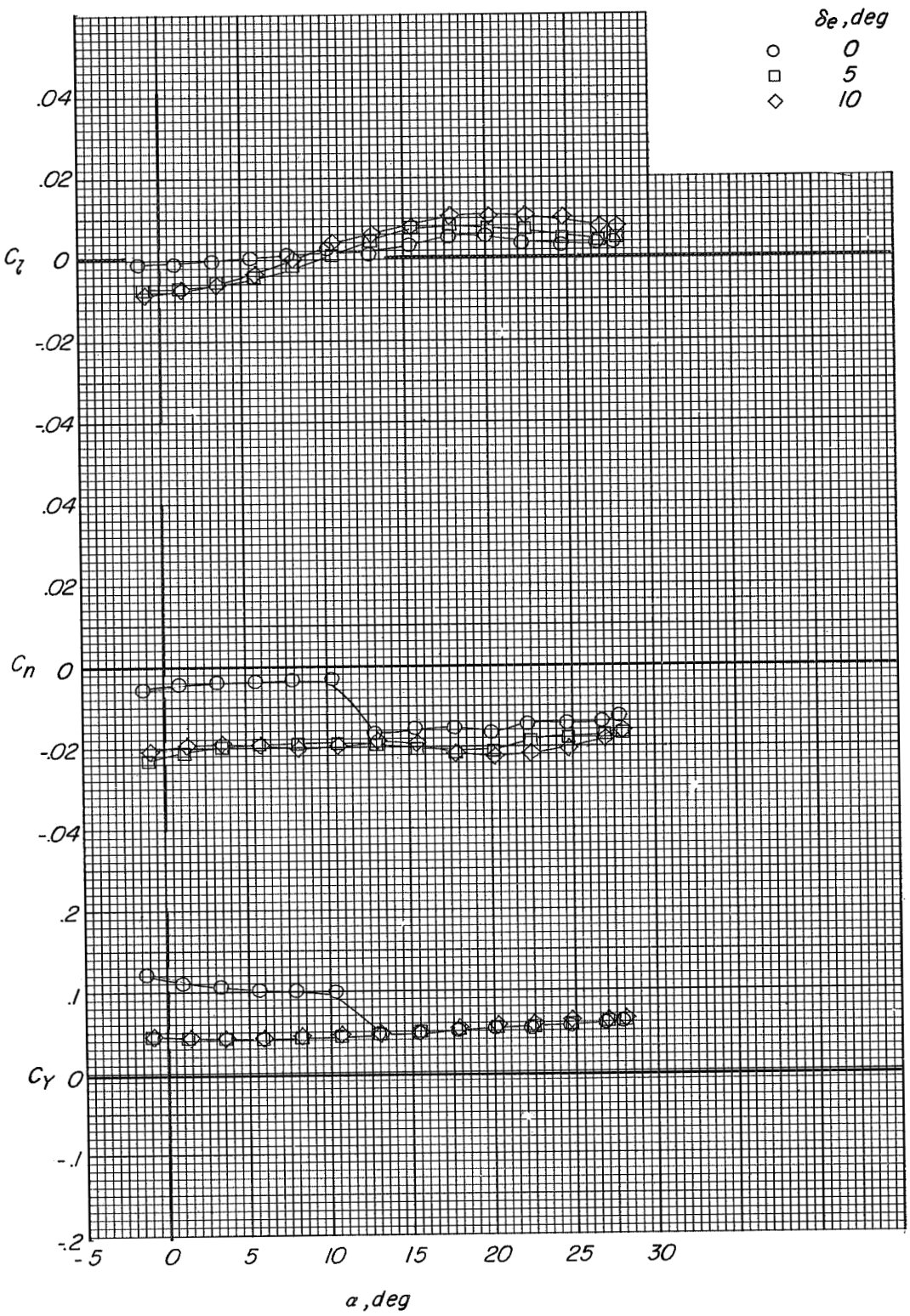
(e) $\beta = -2.3^{\circ}$; $\delta_a = 10^{\circ}$; M = 0.60.

Figure 35.- Continued.



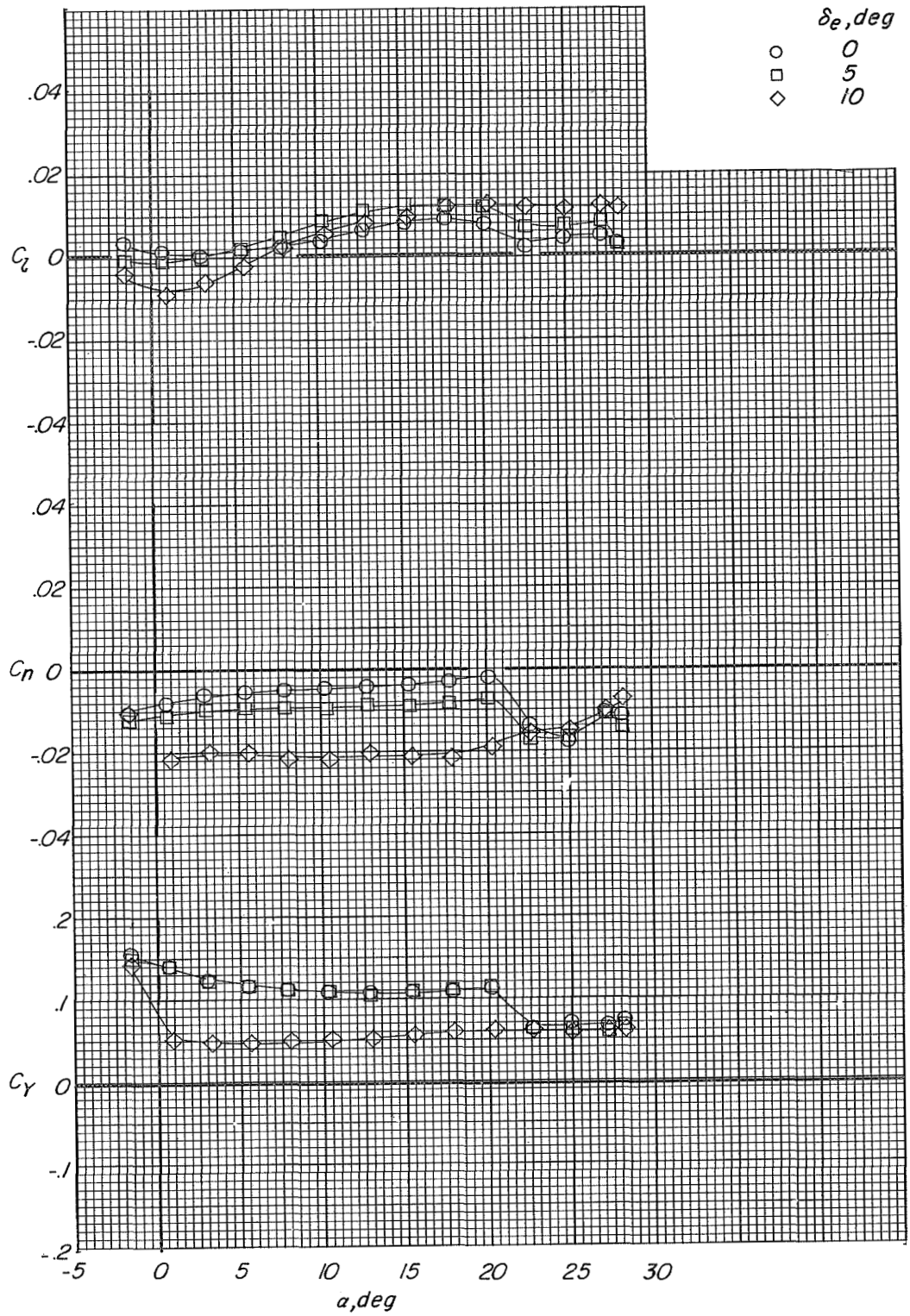
(f) $\beta = -2.3^o$; $\delta_a = 10^o$; M = 0.70.

Figure 35.- Continued.



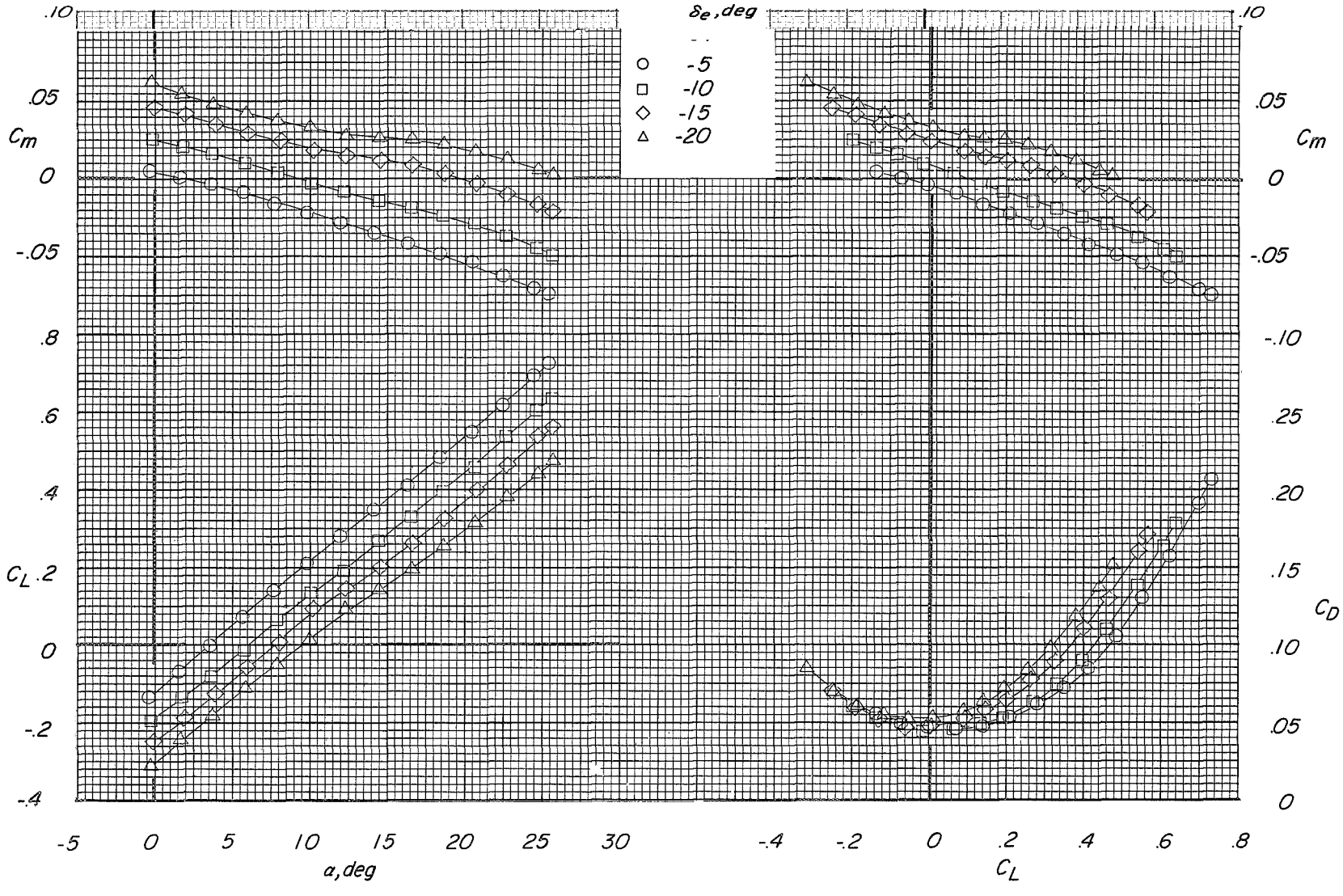
(g) $\beta = -2.3^{o}$; $\delta_a = 10^{o}$; M = 0.80.

Figure 35.- Continued.



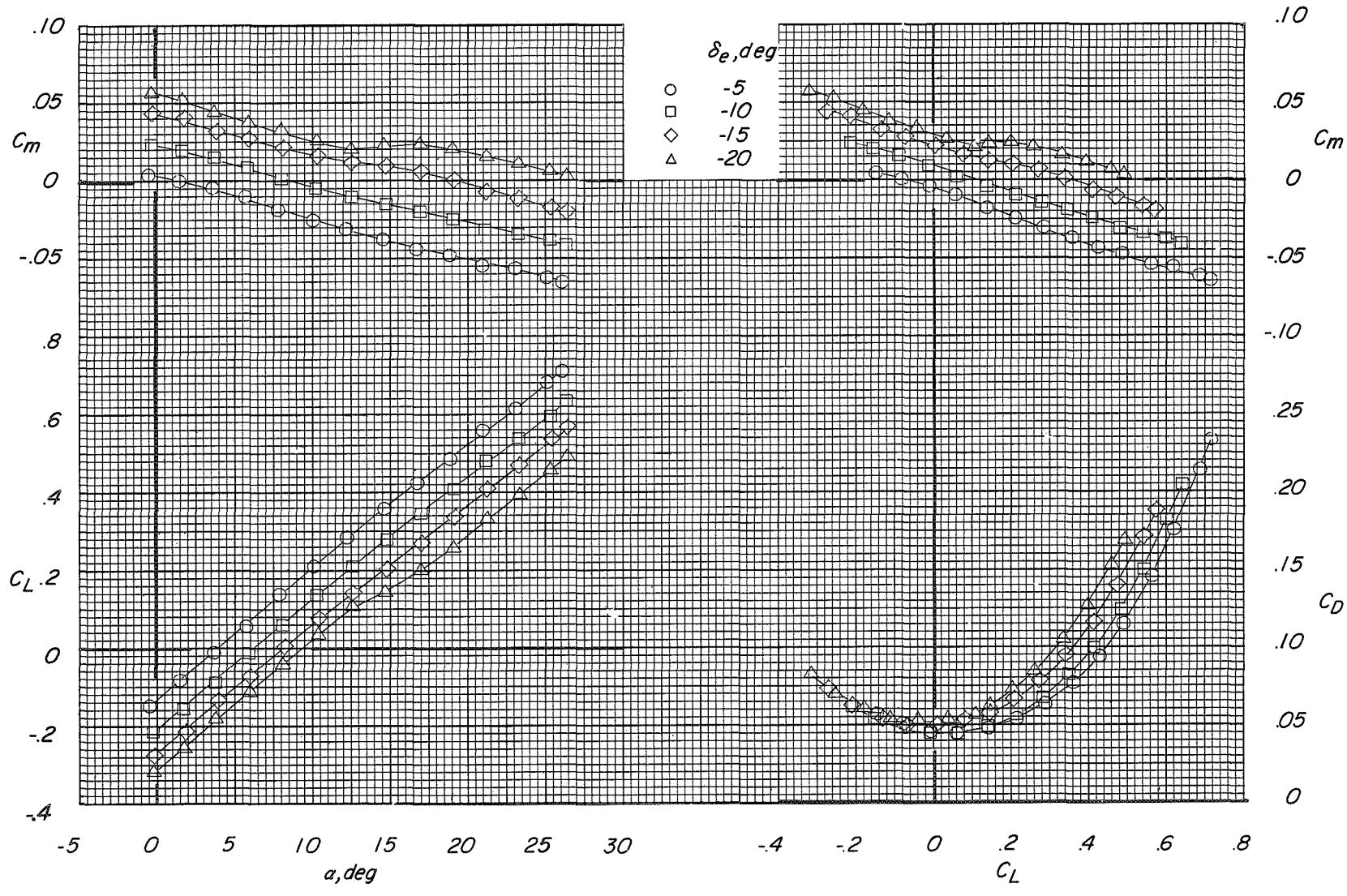
(h) $\beta = -2.3^{o}$; $\delta_a = 10^{o}$; M = 0.90.

Figure 35.- Concluded.



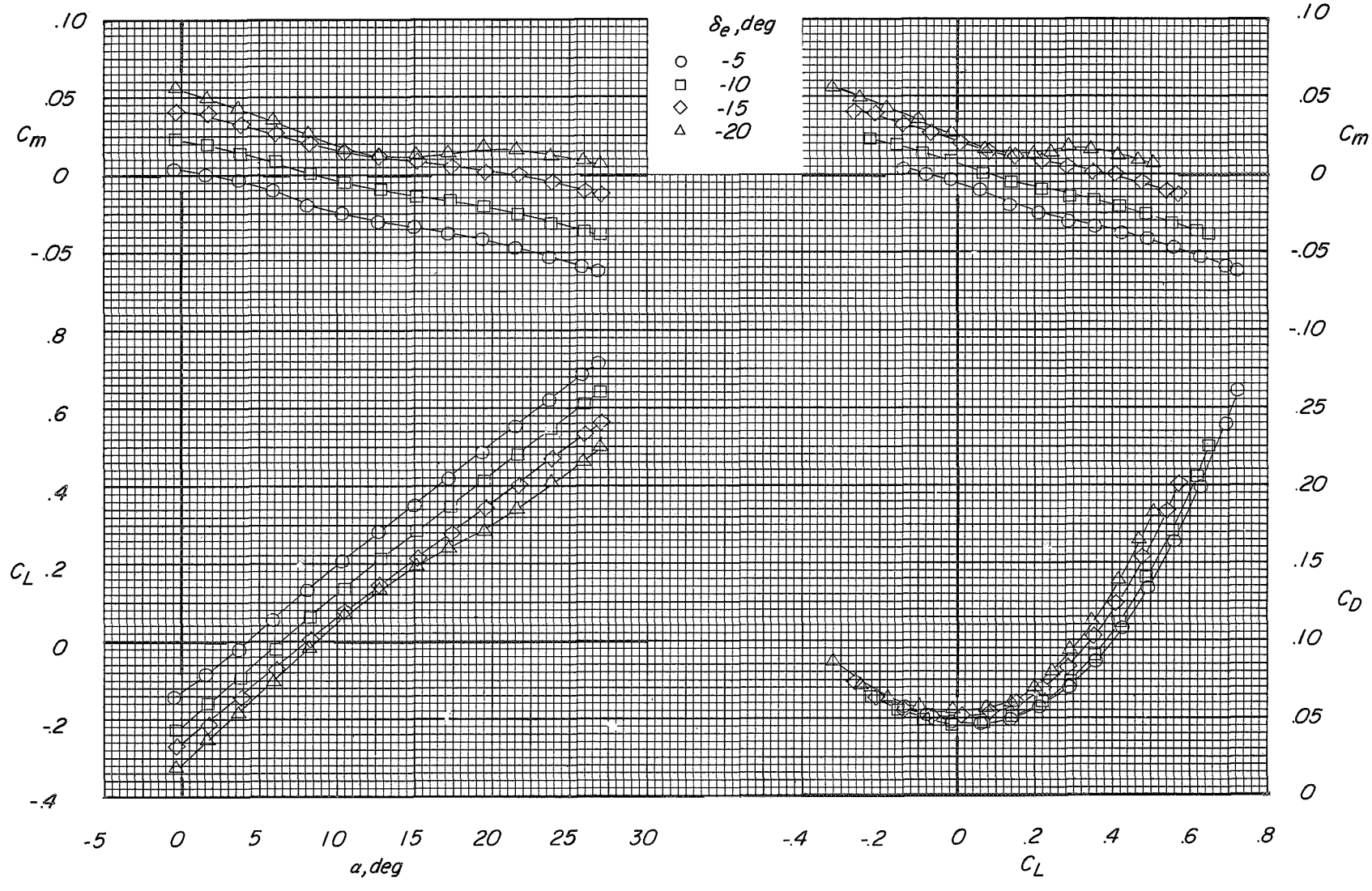
(a) M = 0.35.

Figure 36.- Longitudinal characteristics modification II fin configuration. Auxiliary flaps in the subsonic position; $\delta_a = \beta = 0^o$.



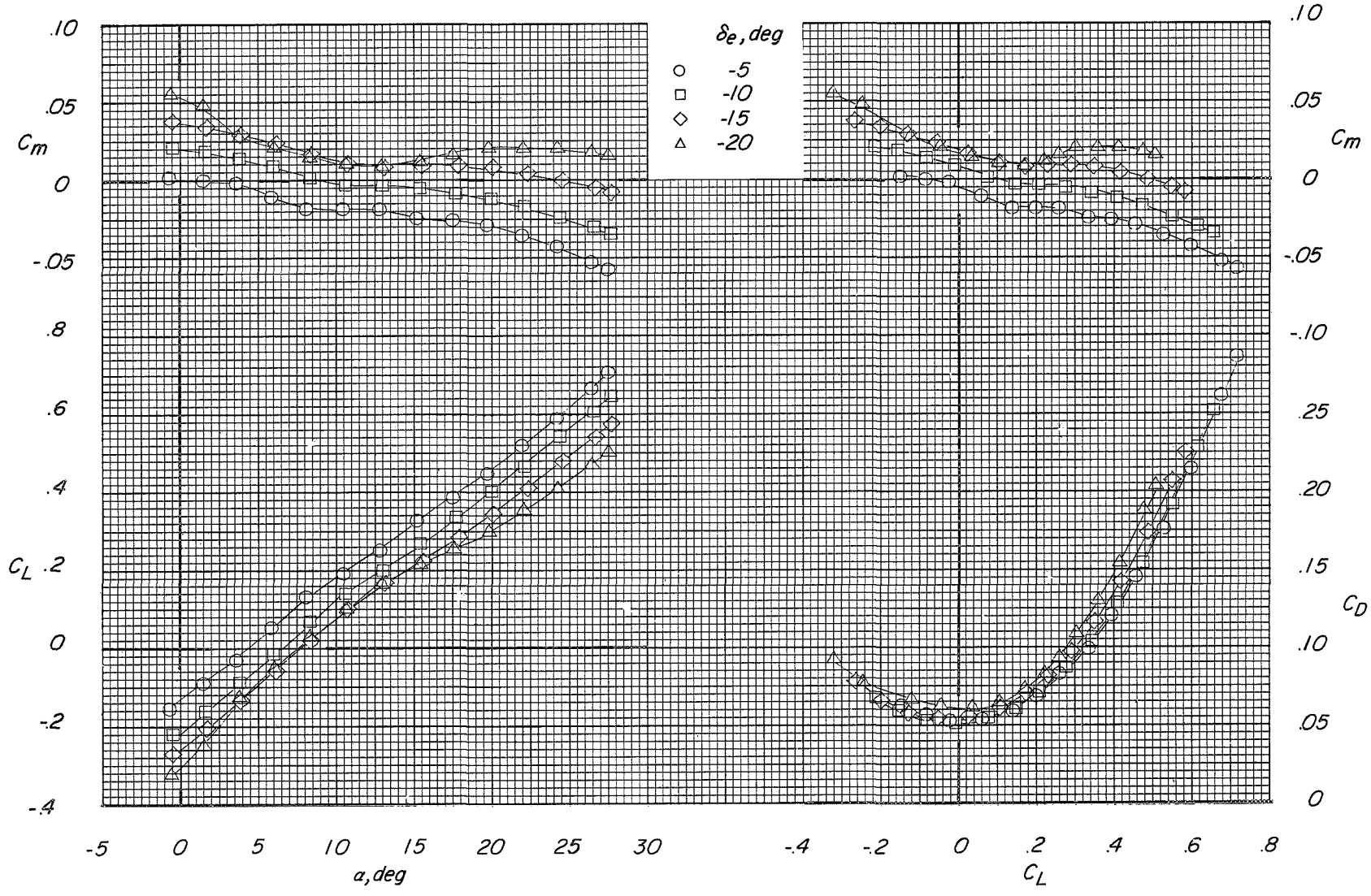
(b) M = 0.50.

Figure 36.- Continued.



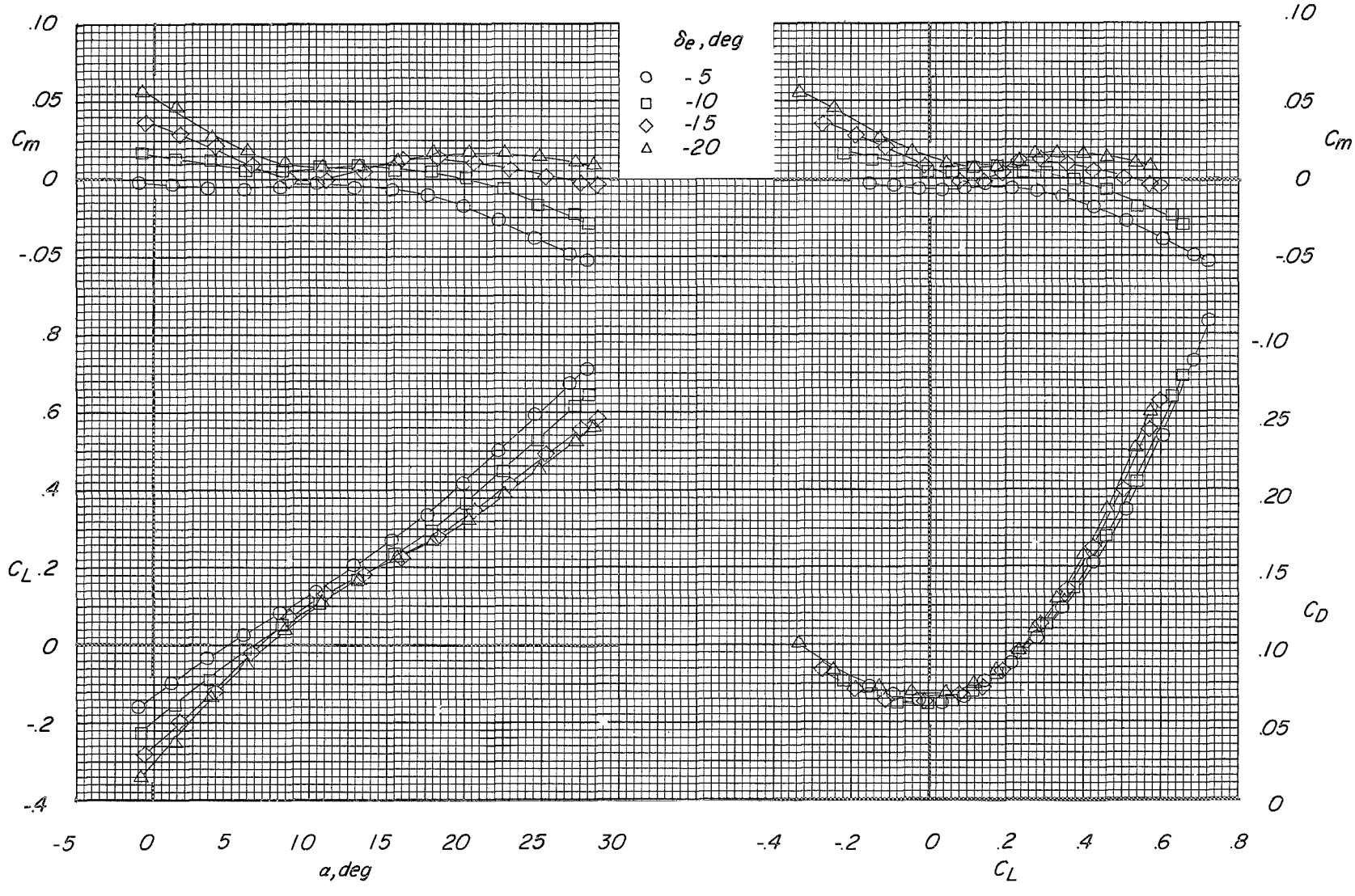
(c) M = 0.60.

Figure 36.- Continued.



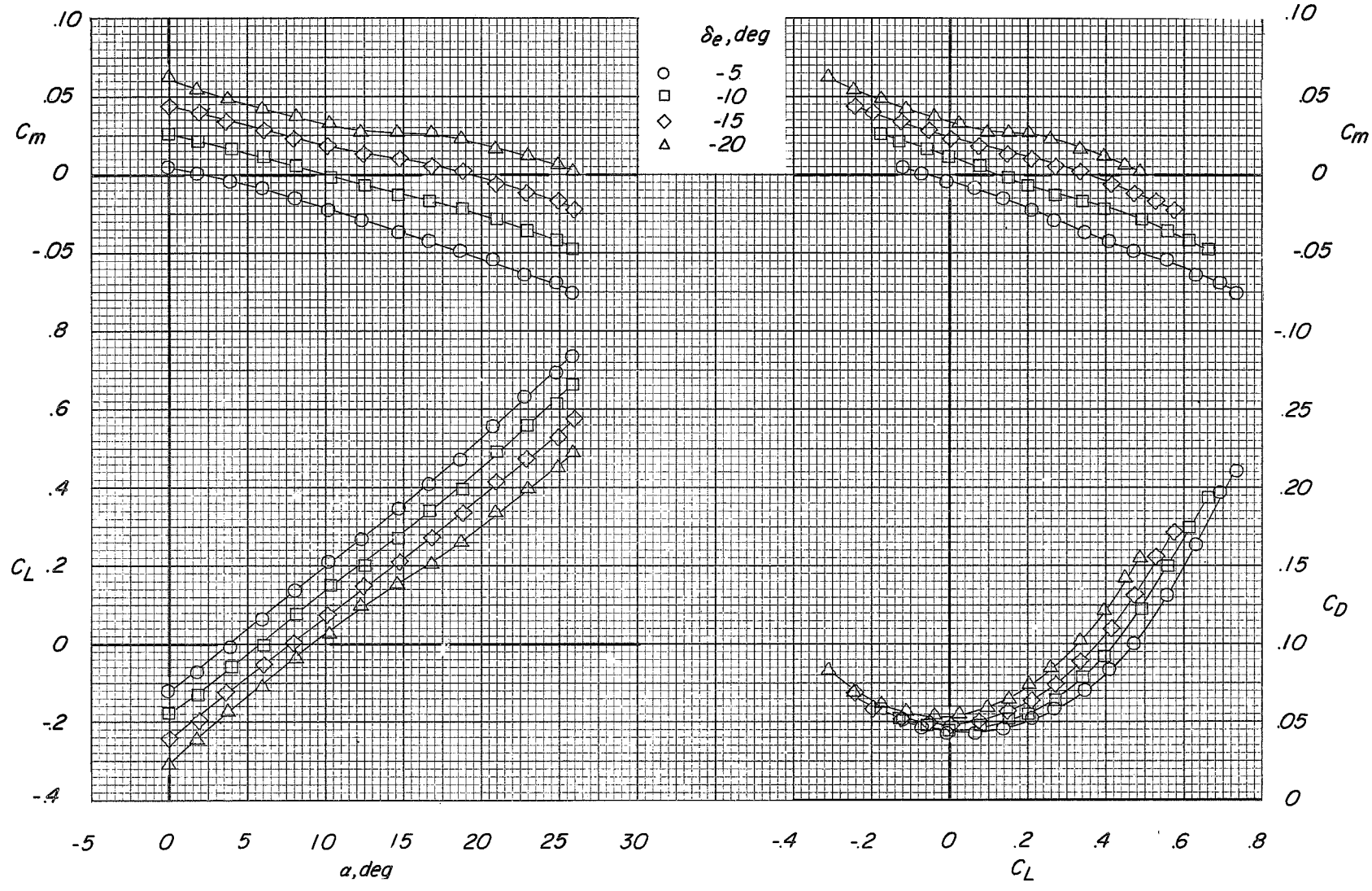
(d) M = 0.70.

Figure 26. Continued



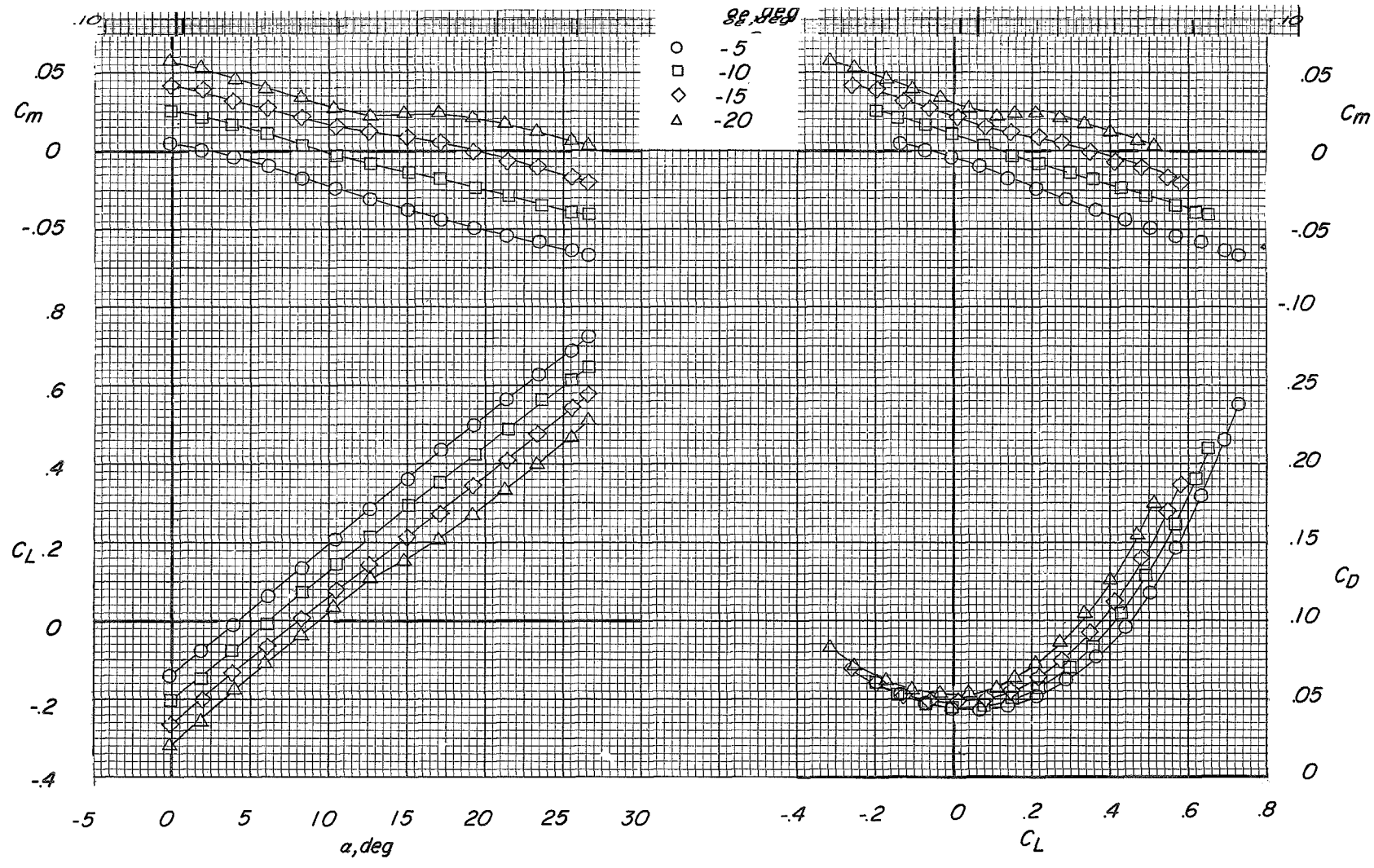
(e) M = 0.80.

Figure 36.- Concluded.



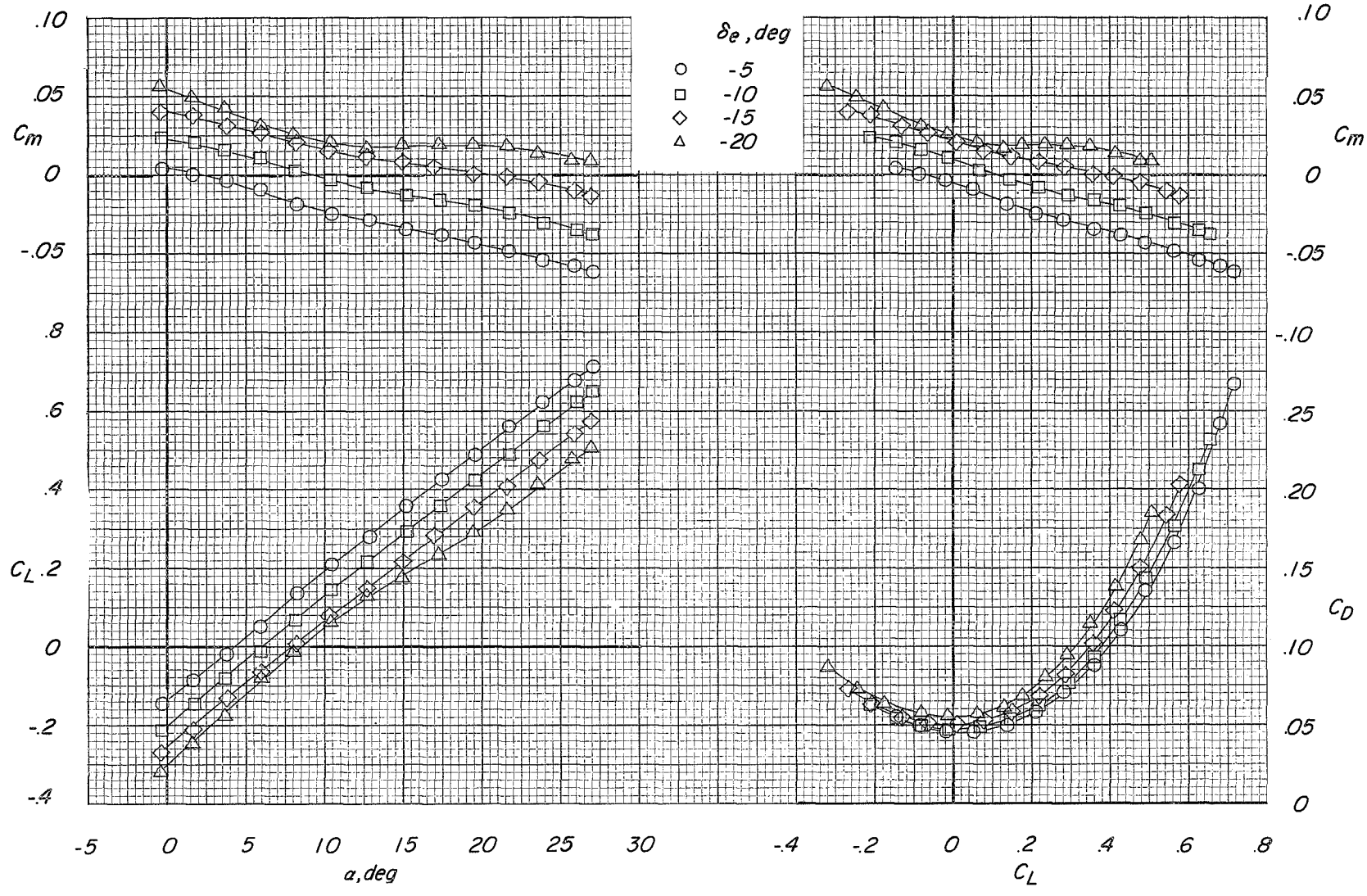
(a) $\beta = 2.3^{o}$; M = 0.35.

Figure 37.- Longitudinal characteristics at sideslip. Modification II fin configuration; auxiliary flaps in the subsonic position; $\delta_a = 0^{o}$.



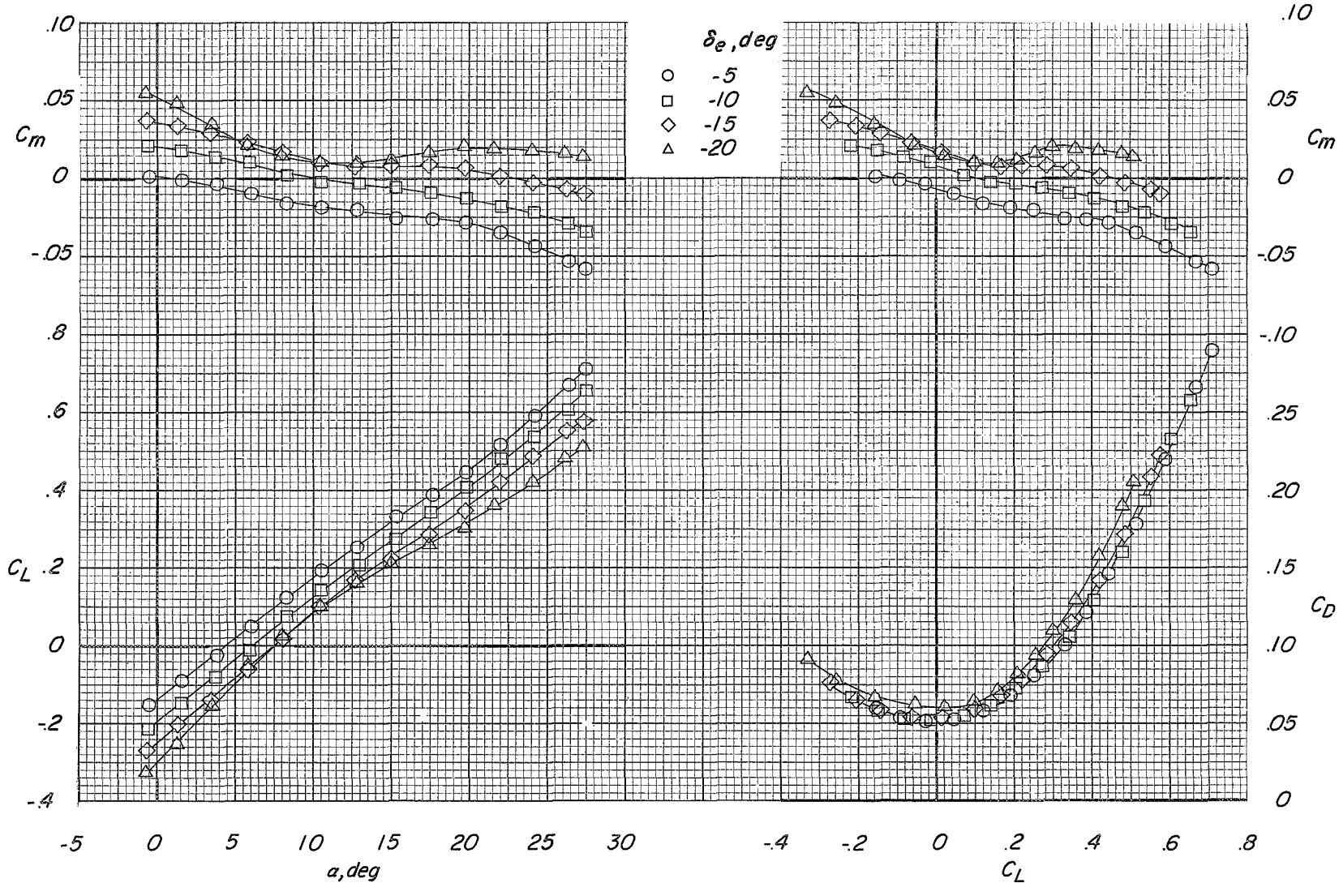
(b) $\beta = 2.3^{o}$; M = 0.50.

Figure 37.- Continued.



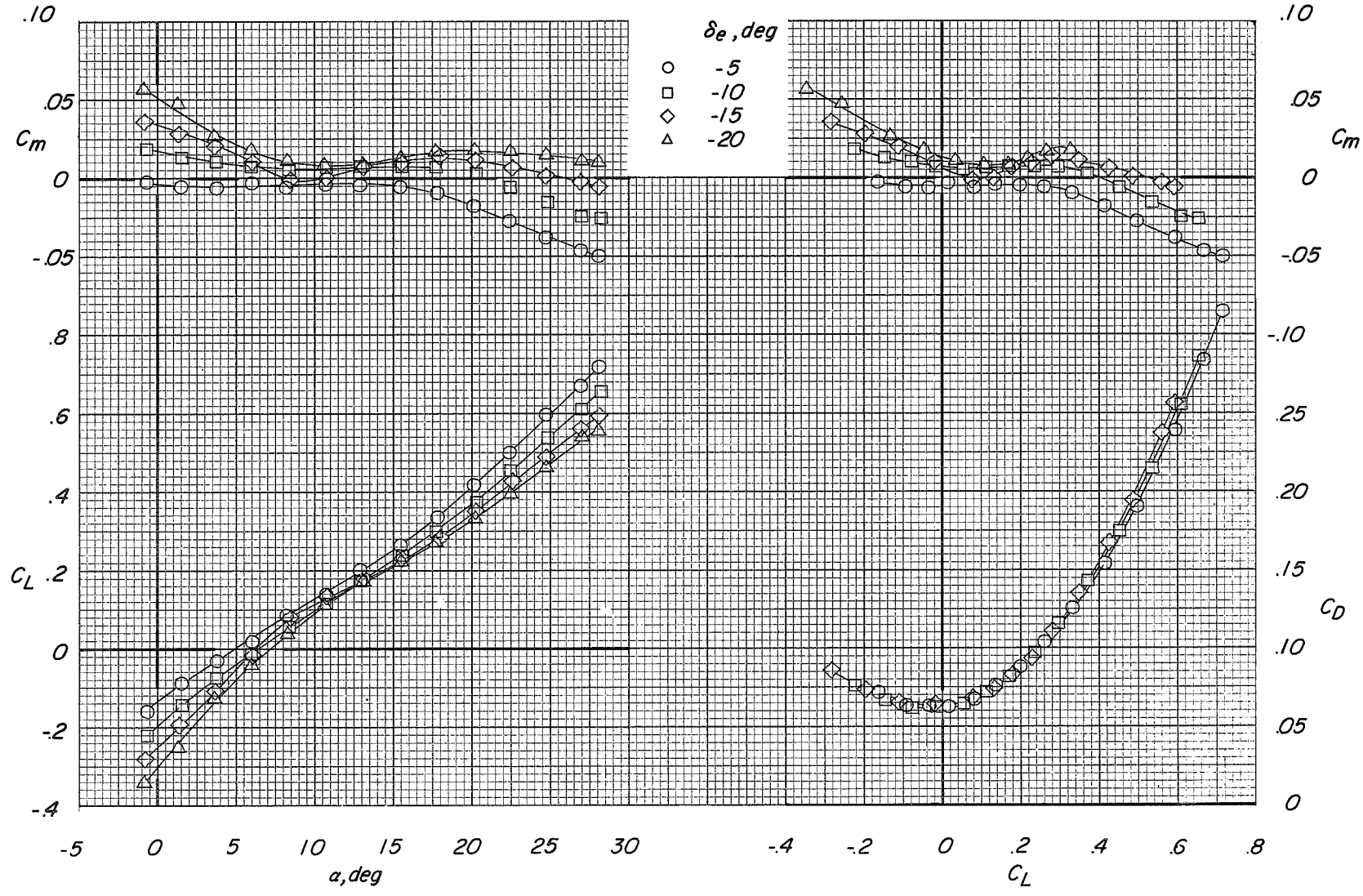
(c) $\beta = 2.3^{o}$; M = 0.60.

Figure 37.- Continued.



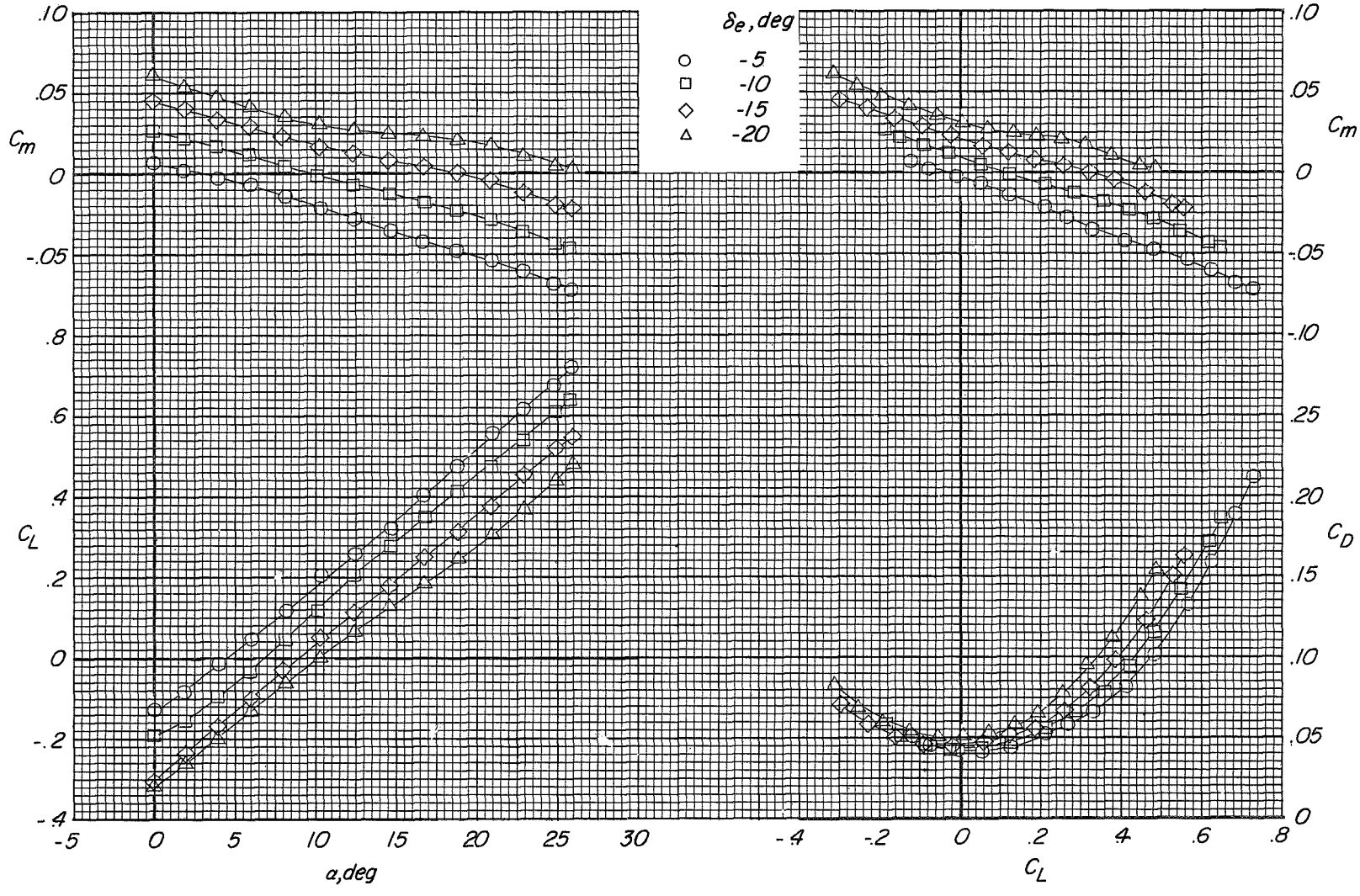
(d) $\beta = 2.3^{o}$; M = 0.70.

Figure 37.- Continued.



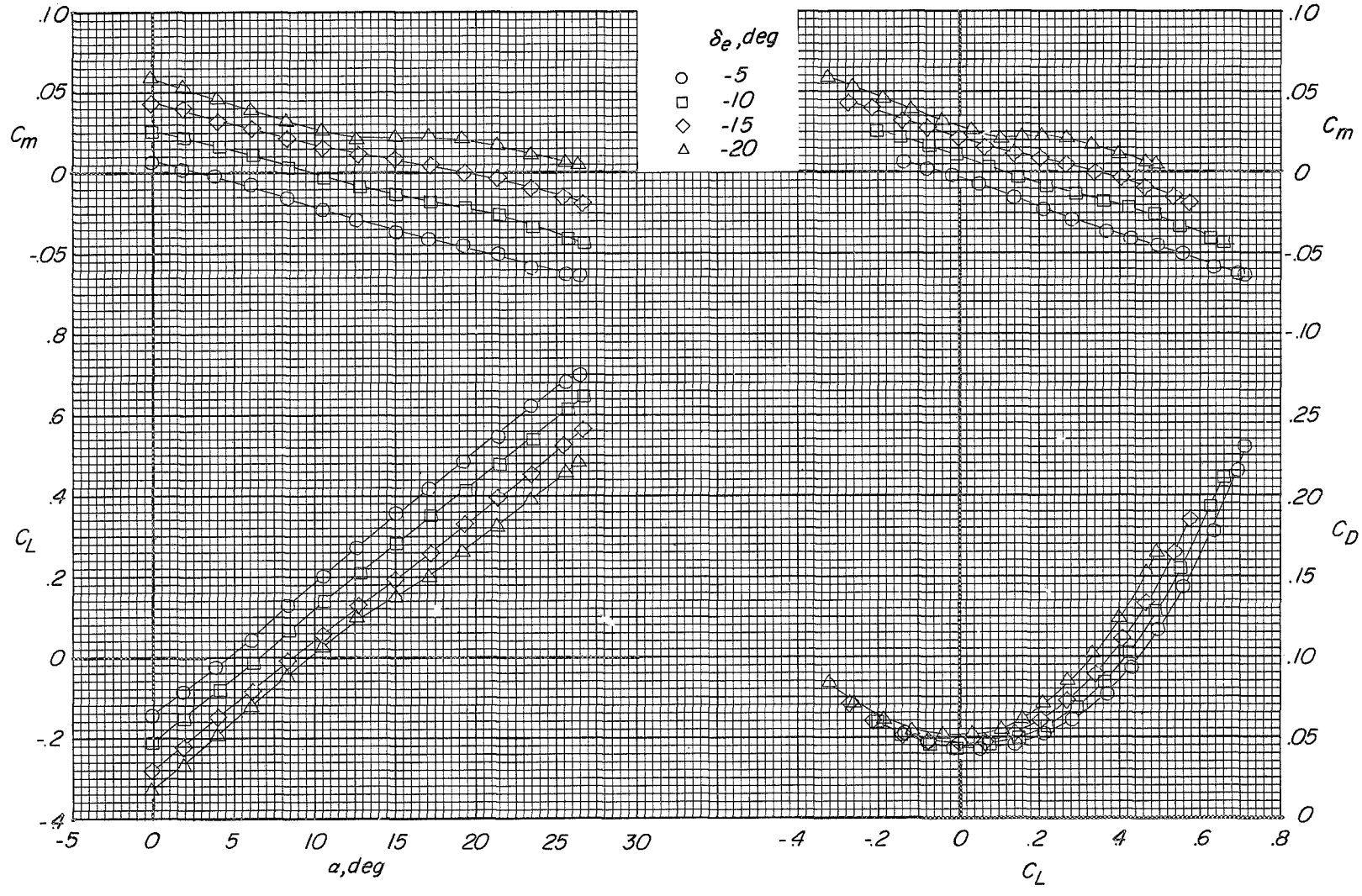
(e) $\beta = 2.3^{\circ}$; M = 0.80.

Figure 37.- Continued.



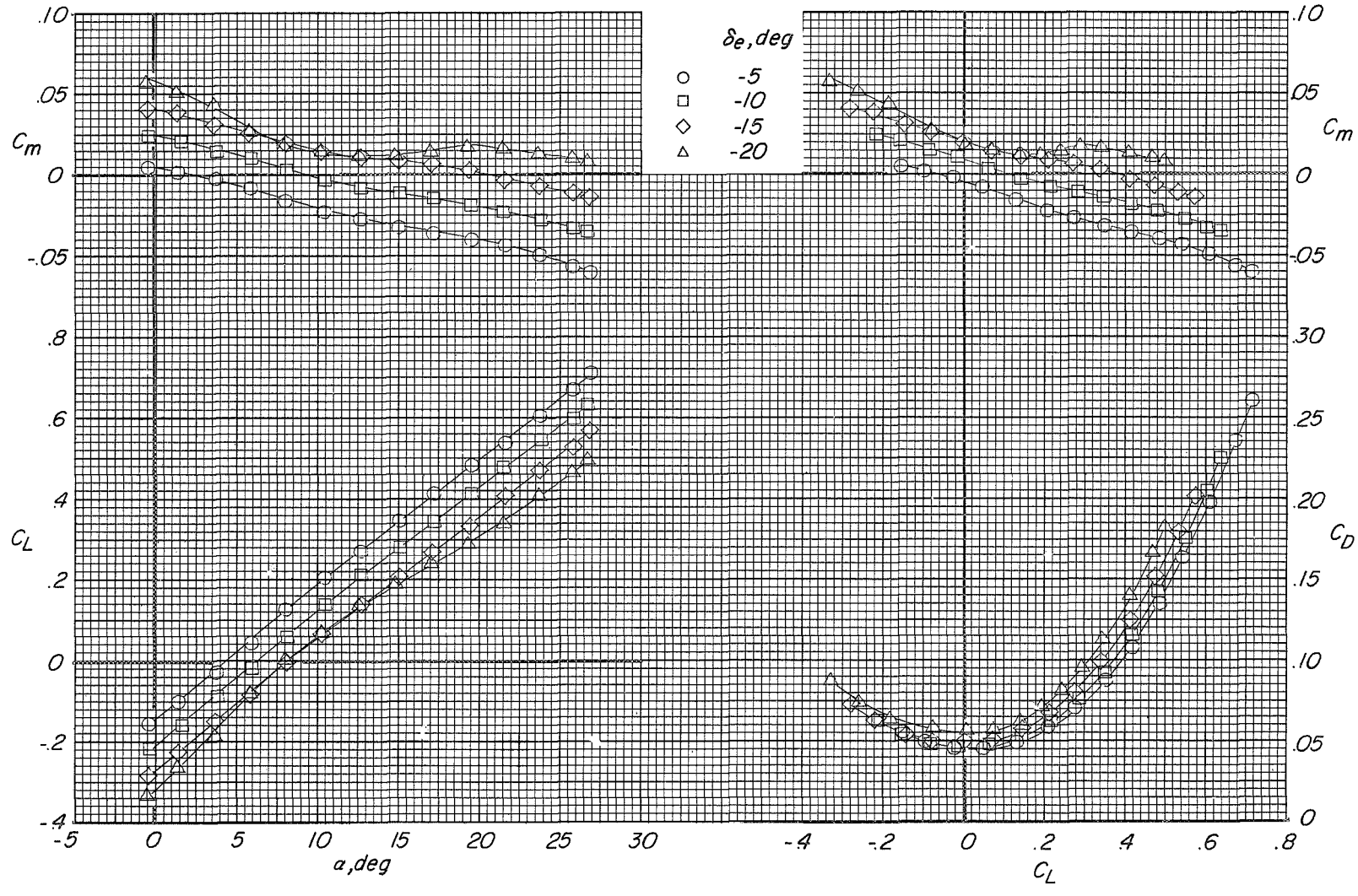
(f) $\beta = -2.3^{o}$; M = 0.35.

Figure 37.- Continued.



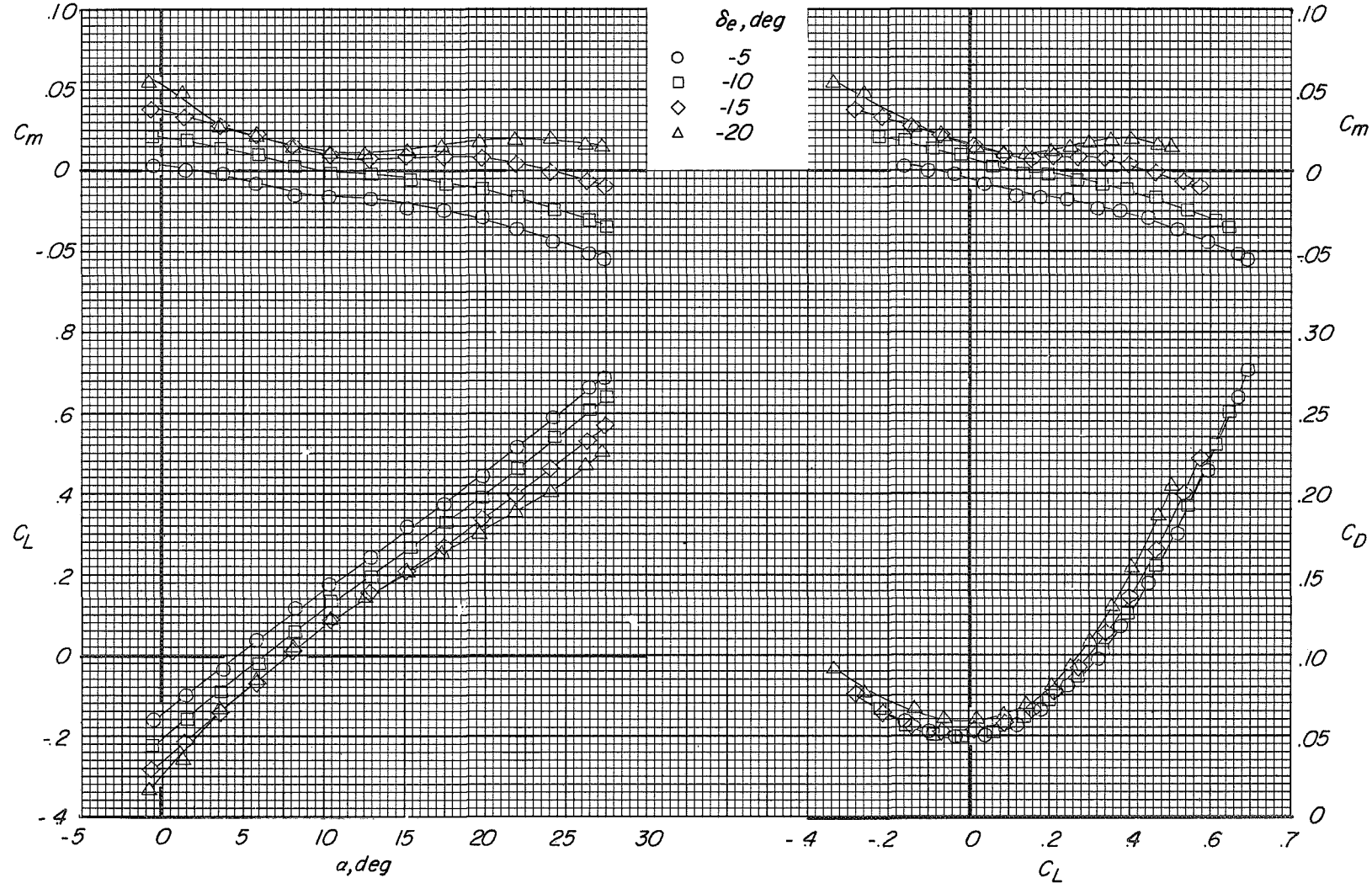
(g) $\beta = -2.3^{o}$; M = 0.50.

Figure 37.- Continued.



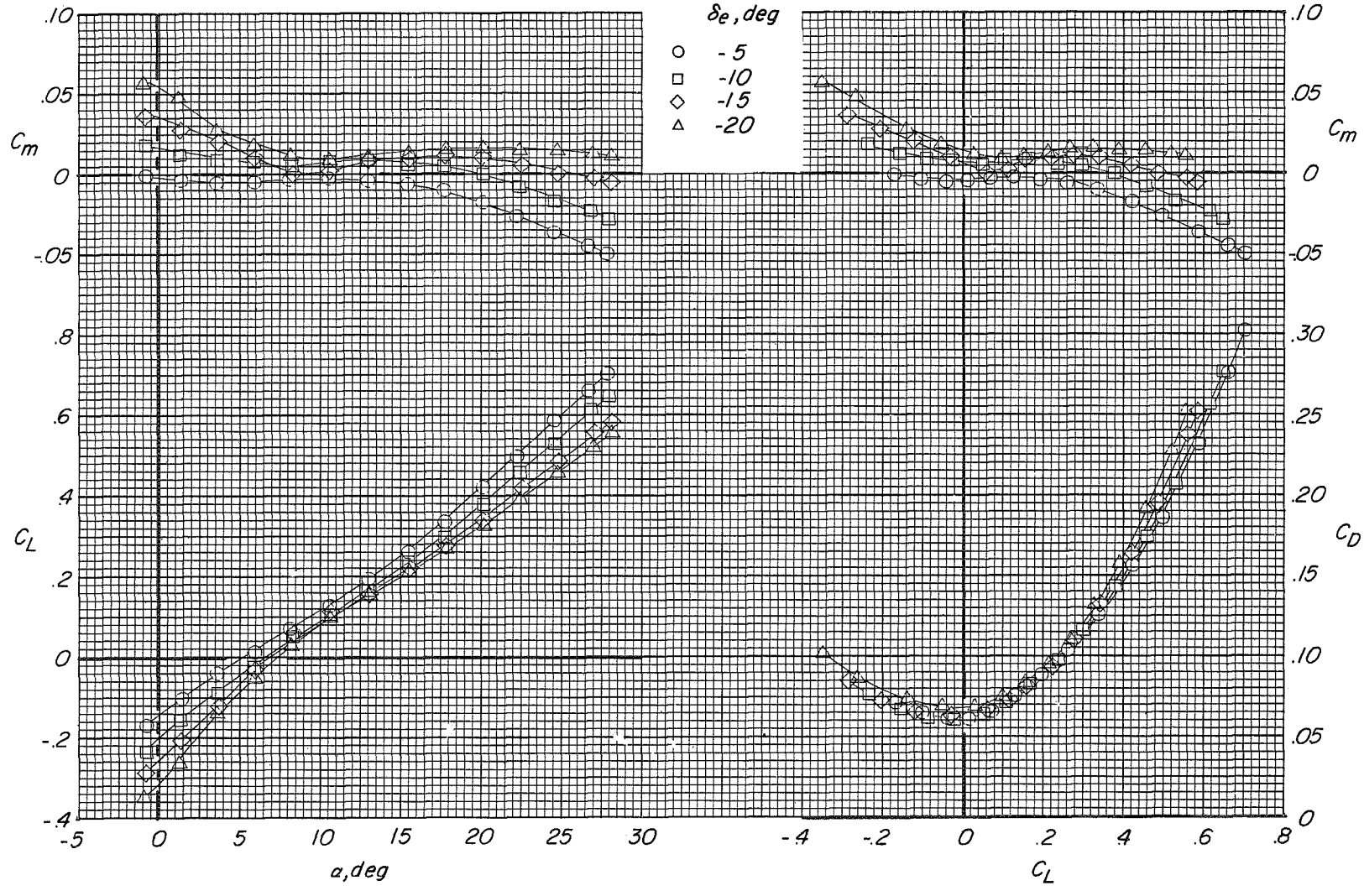
(h) $\beta = -2.3^{o}$; M = 0.60.

Figure 37.- Continued.



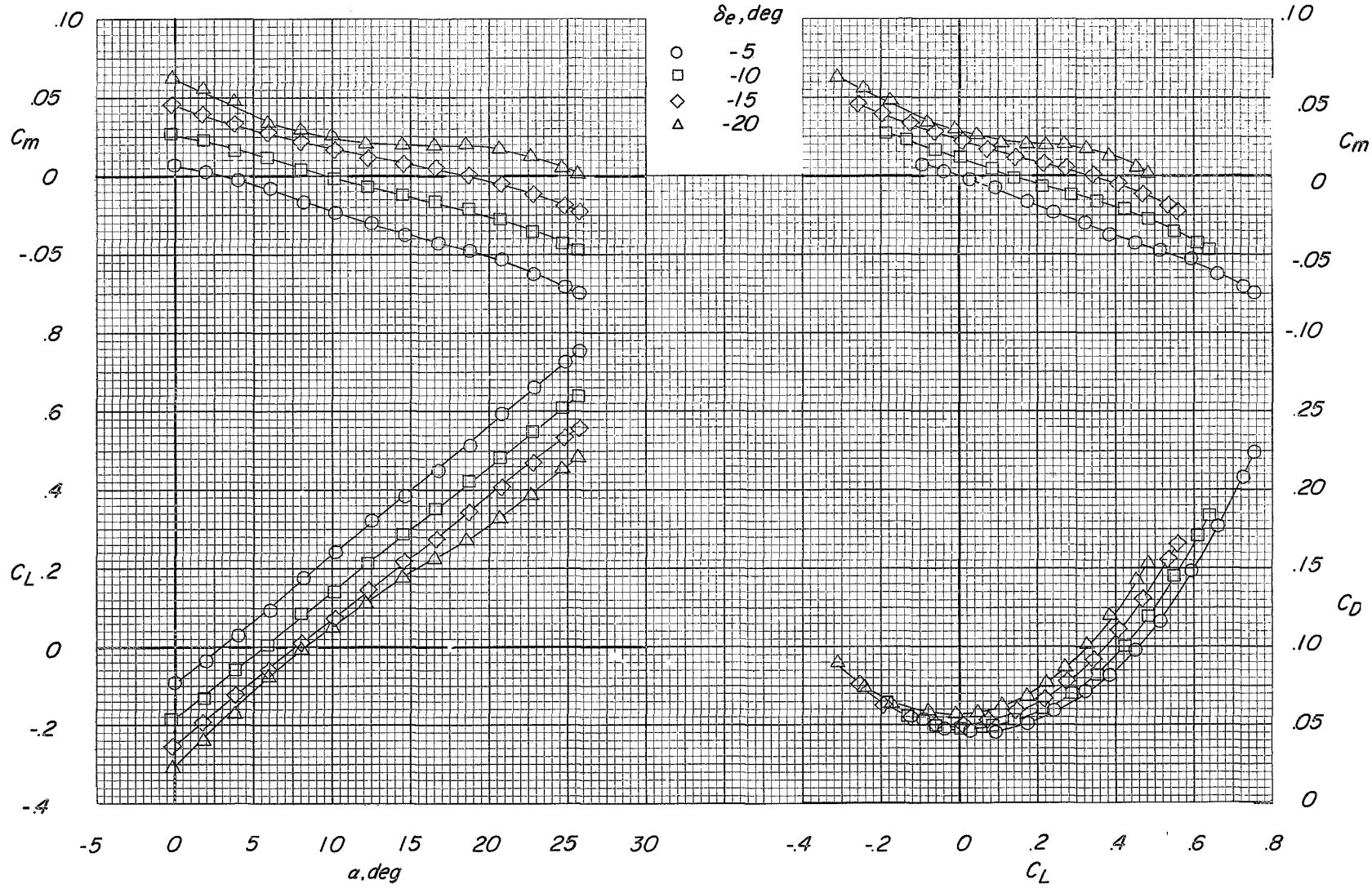
(i) $\beta = -2.3^{o}$; M = 0.70.

Figure 37.- Continued.



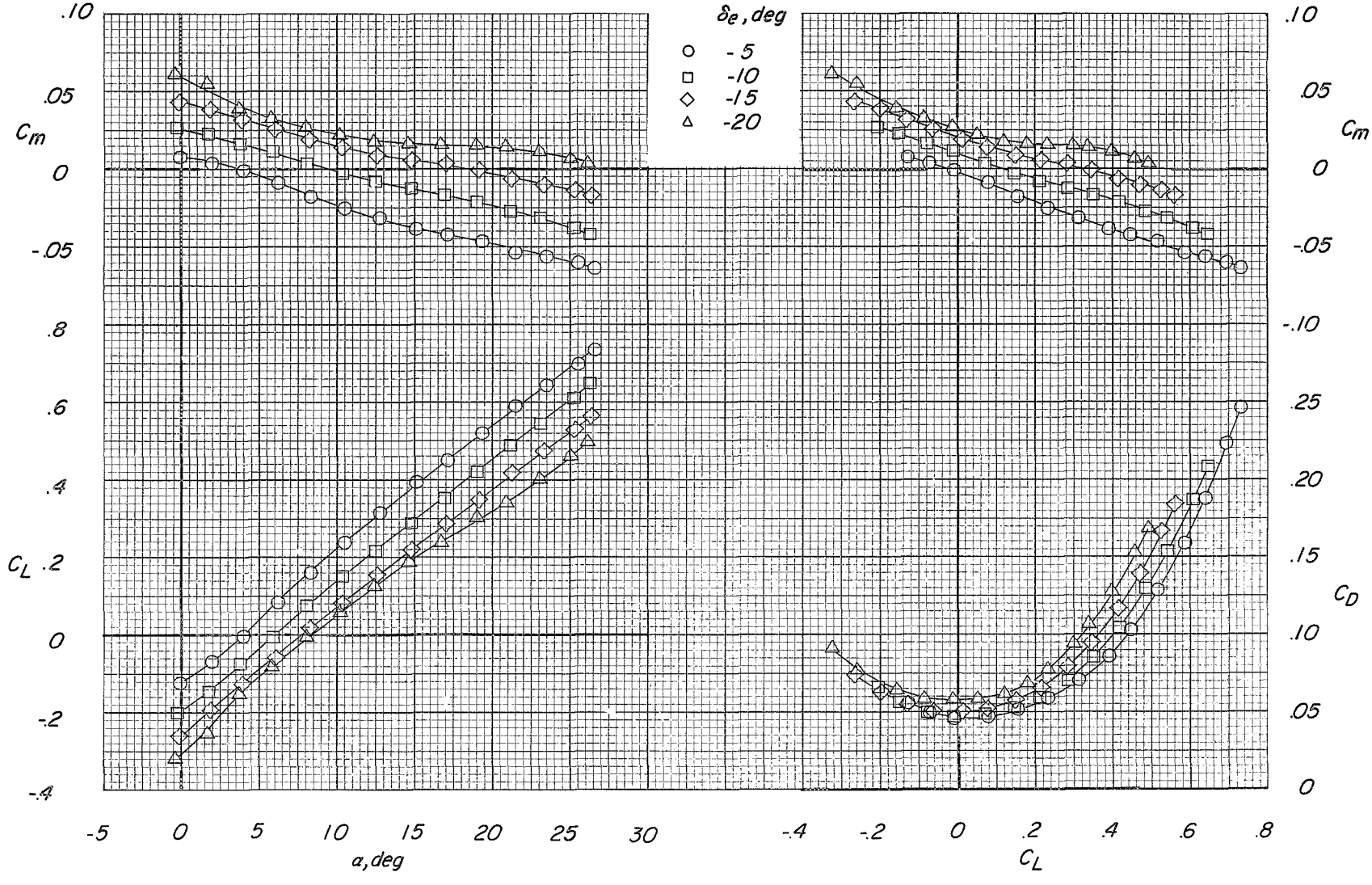
(j) $\beta = -2.3^{o}$; M = 0.80.

Figure 37.- Concluded.



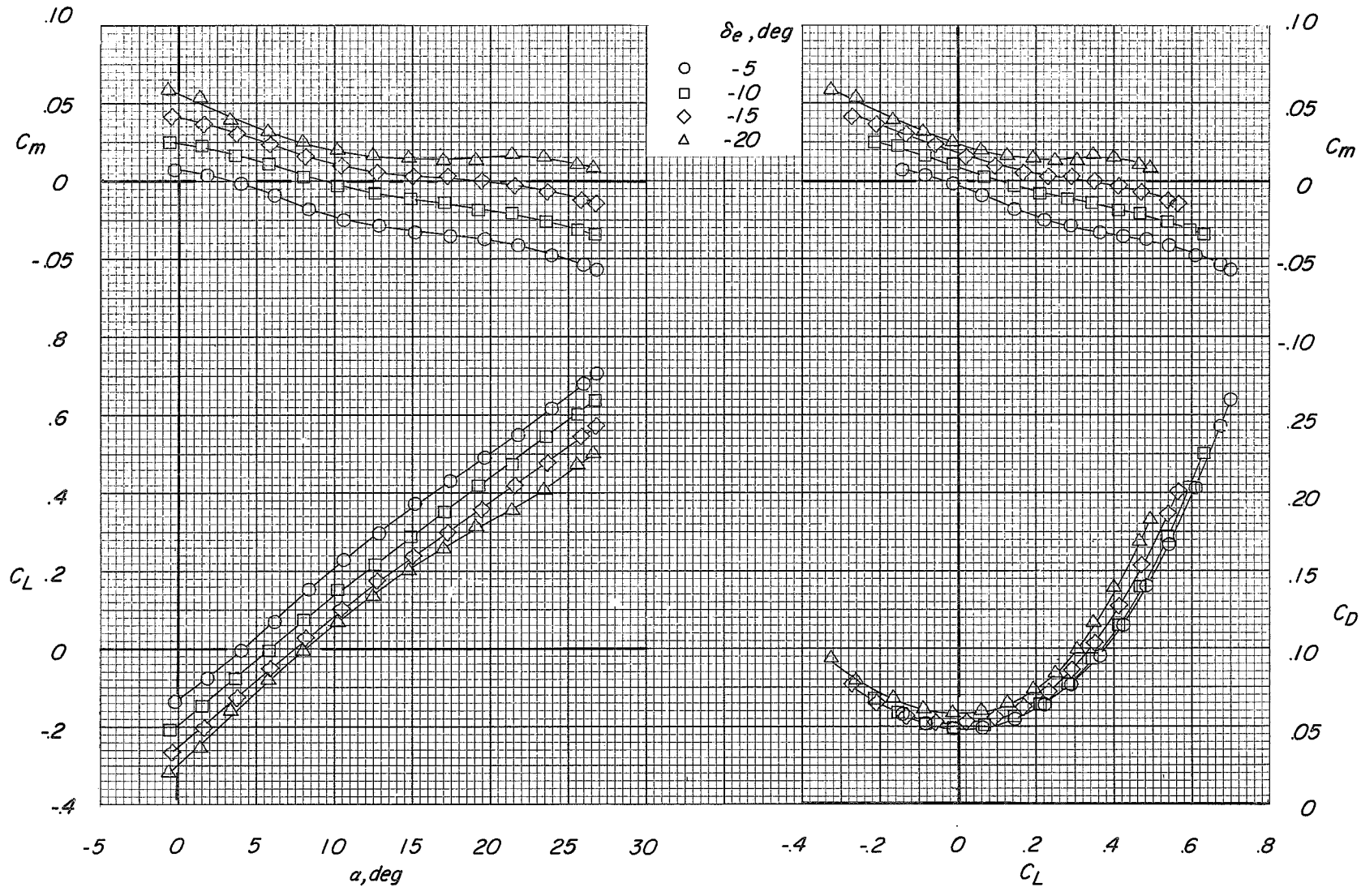
(a) $\delta_a = 10^o$; M = 0.35.

Figure 38.- Longitudinal characteristics with ailerons deflected. Modification II fin configuration; auxiliary flaps in the subsonic position. $\beta = 0^o$.



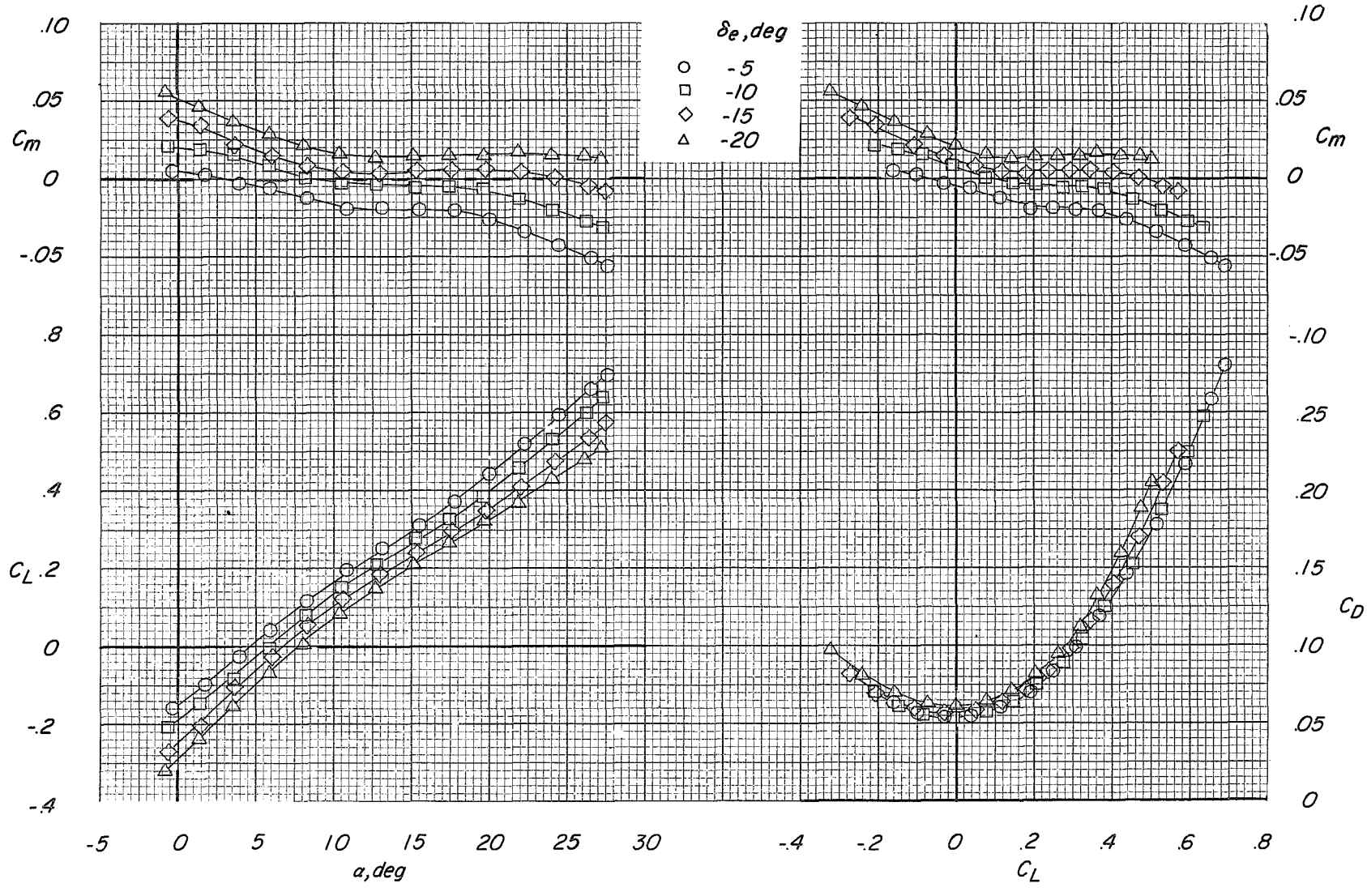
(b) $\delta_a = 10^o$; M = 0.50.

Figure 38.- Continued.



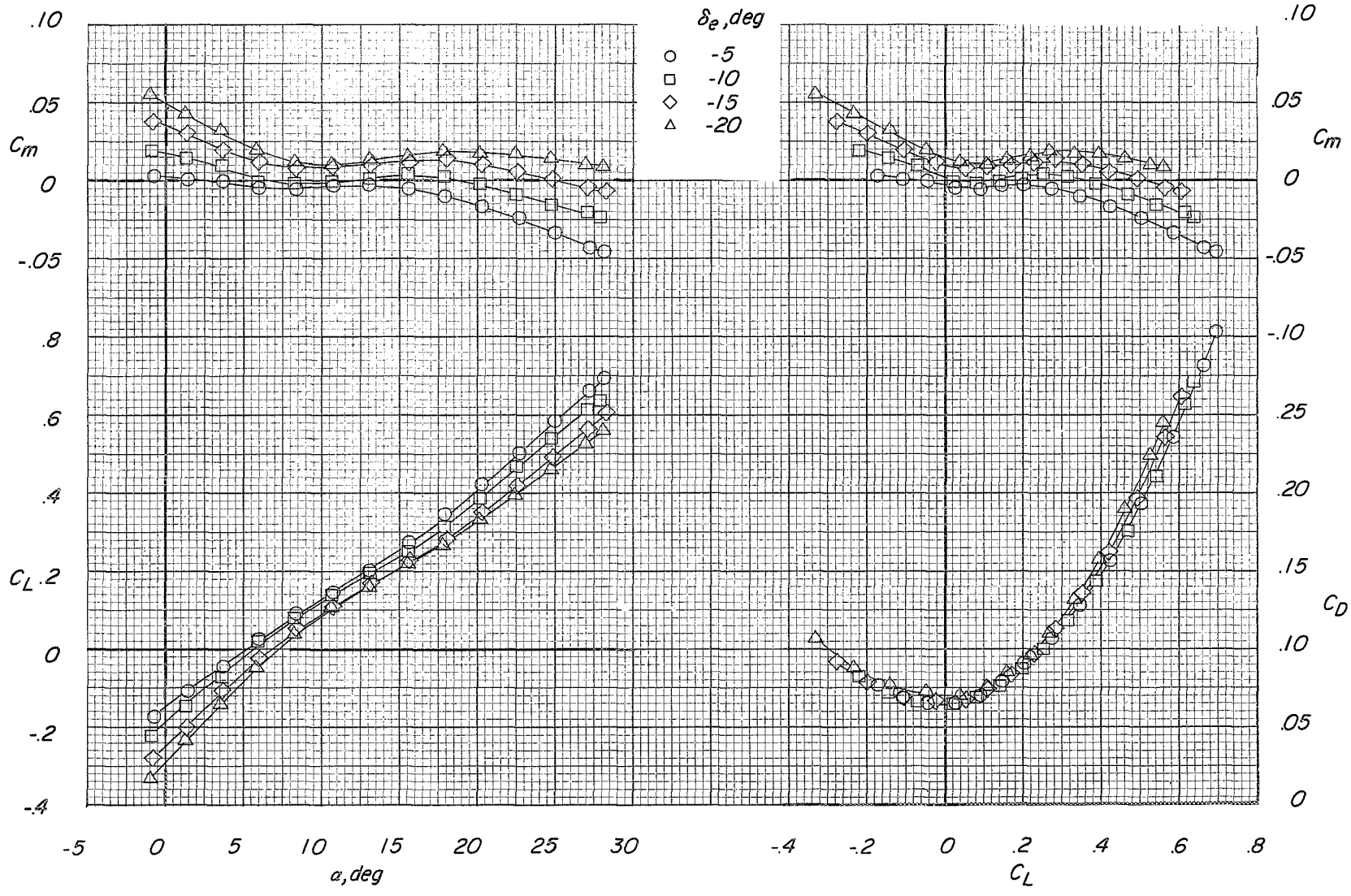
(c) $\delta_a = 10^o$; M = 0.60.

Figure 38.- Continued.



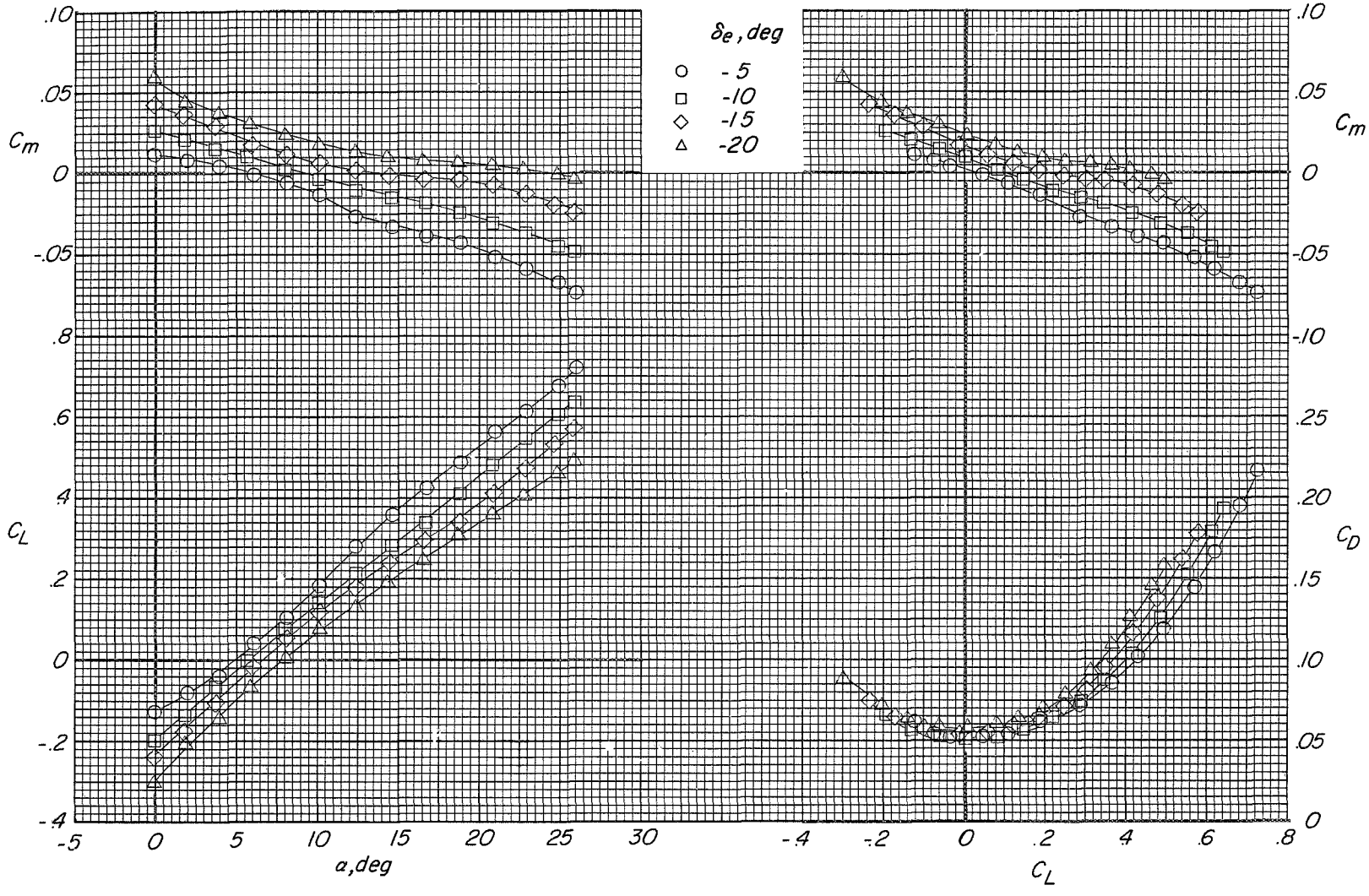
(d) $\delta_a = 10^o$; M = 0.70.

Figure 38.- Continued.



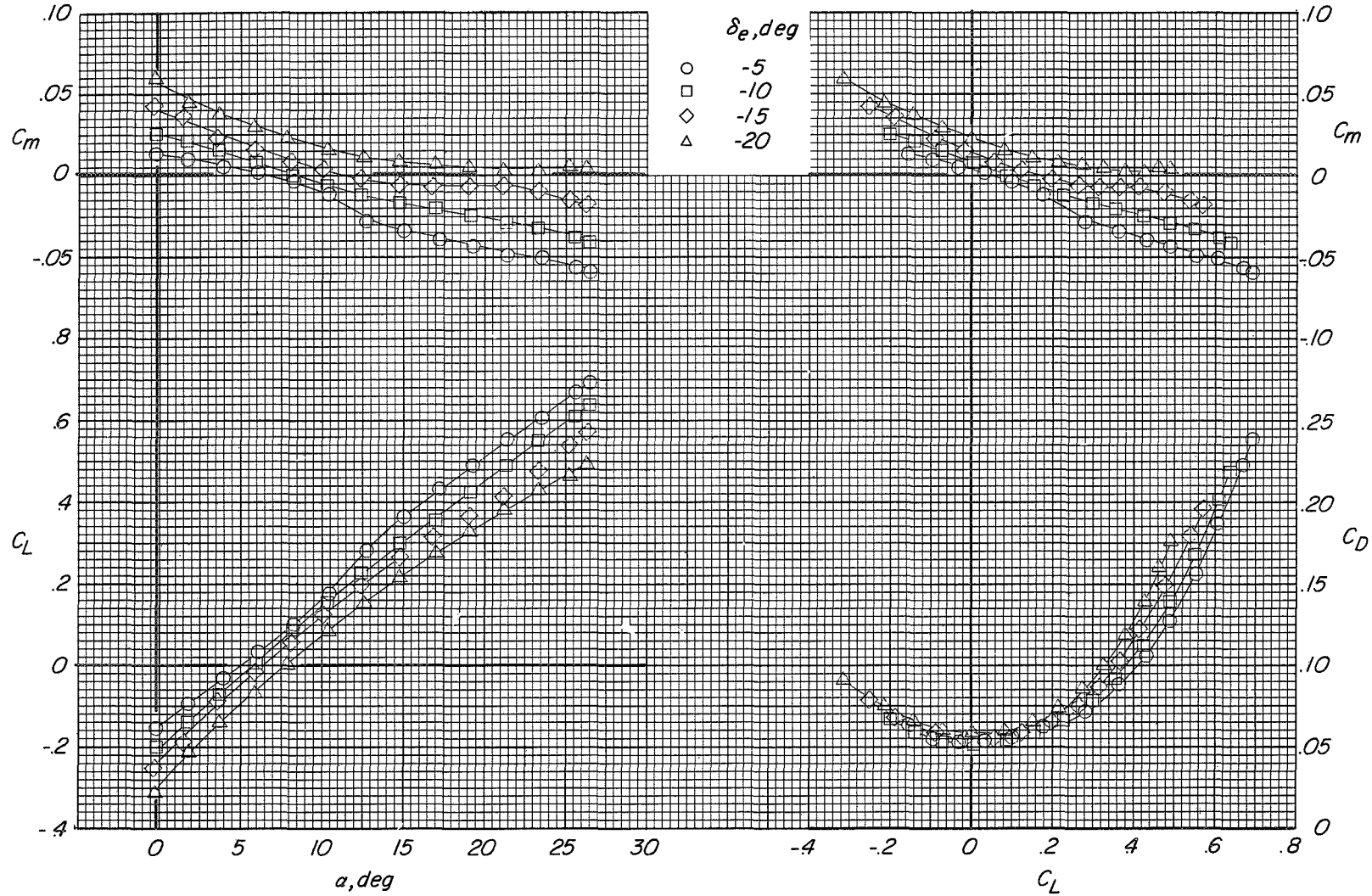
(e) $\delta_a = 10^o$; M = 0.80.

Figure 38 - Continued



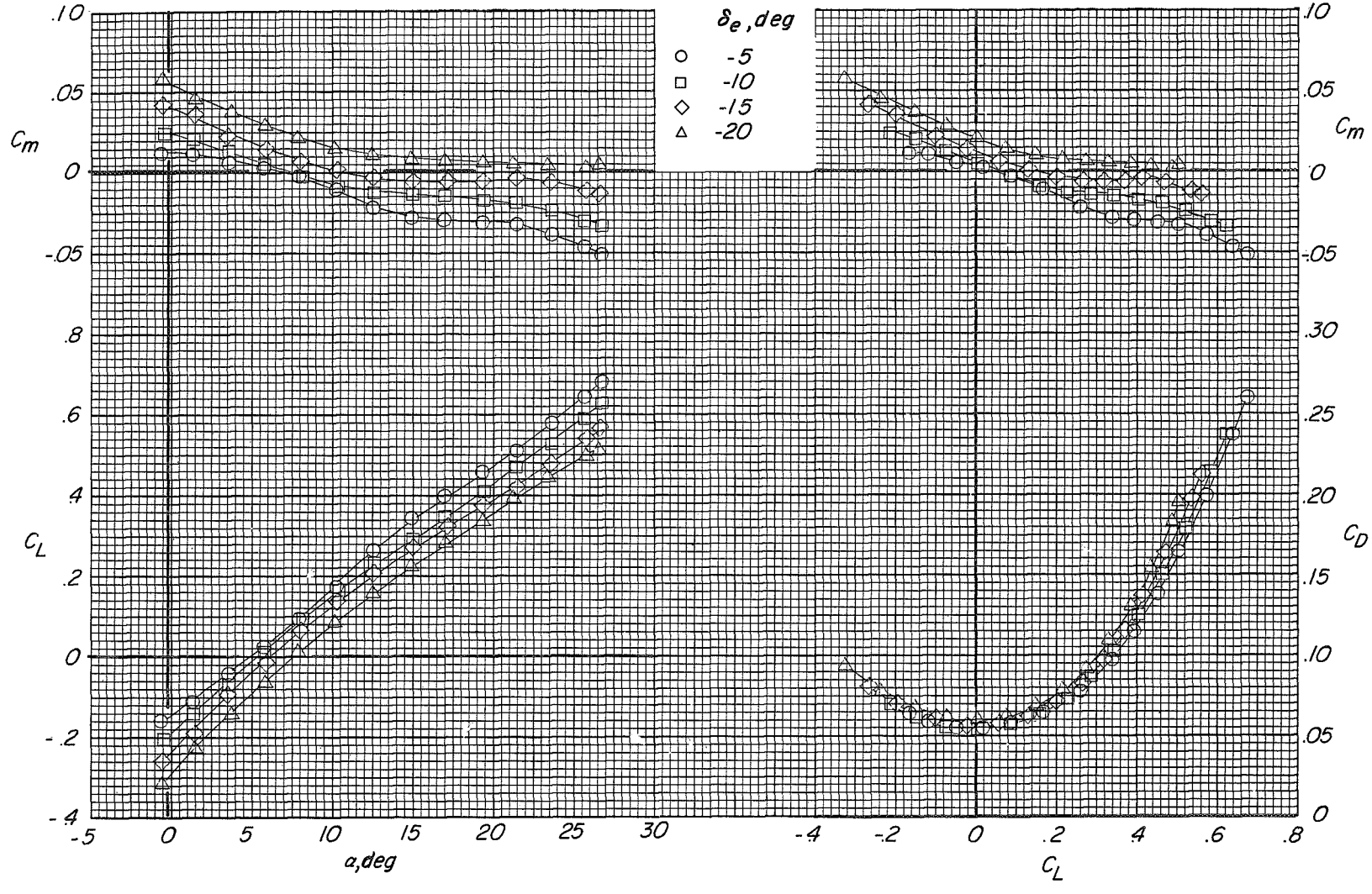
(f) $\delta_a = 20^o$; M = 0.35.

Figure 38.- Continued.



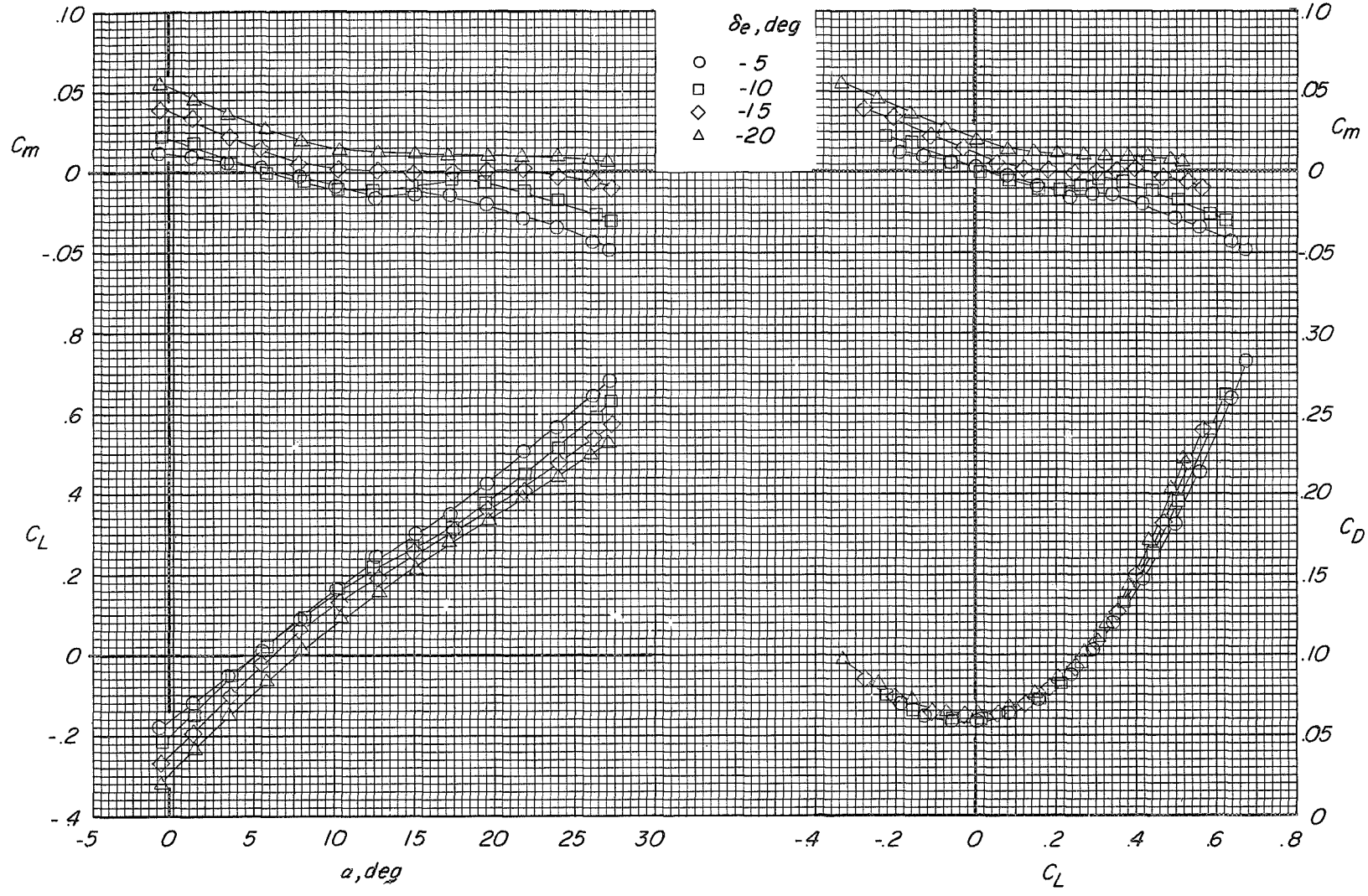
(g) $\delta_a = 20^o$; M = 0.50.

Figure 38.- Continued.



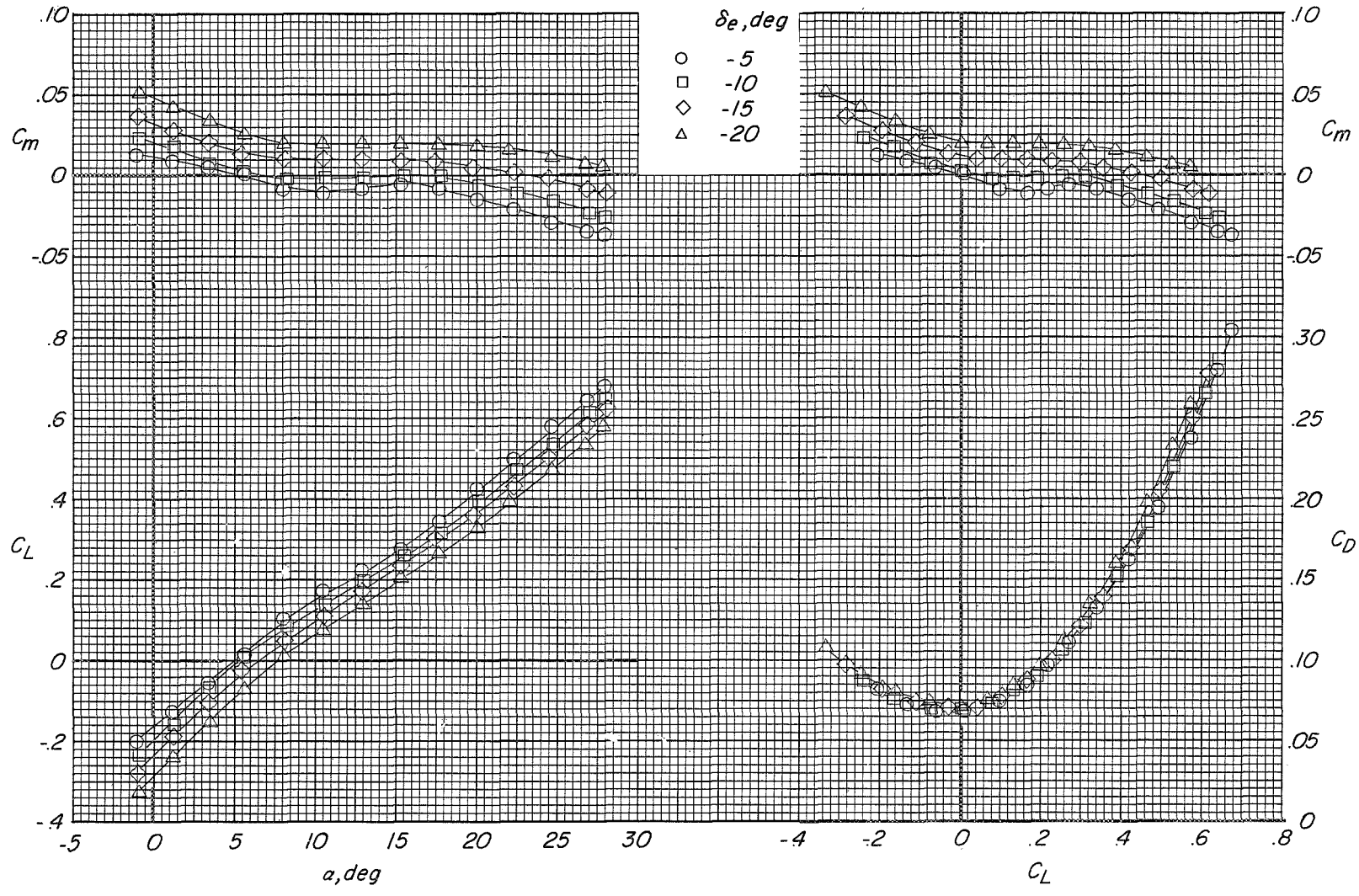
(h) $\delta_a = 20^o$; M = 0.60.

Figure 38.- Continued.



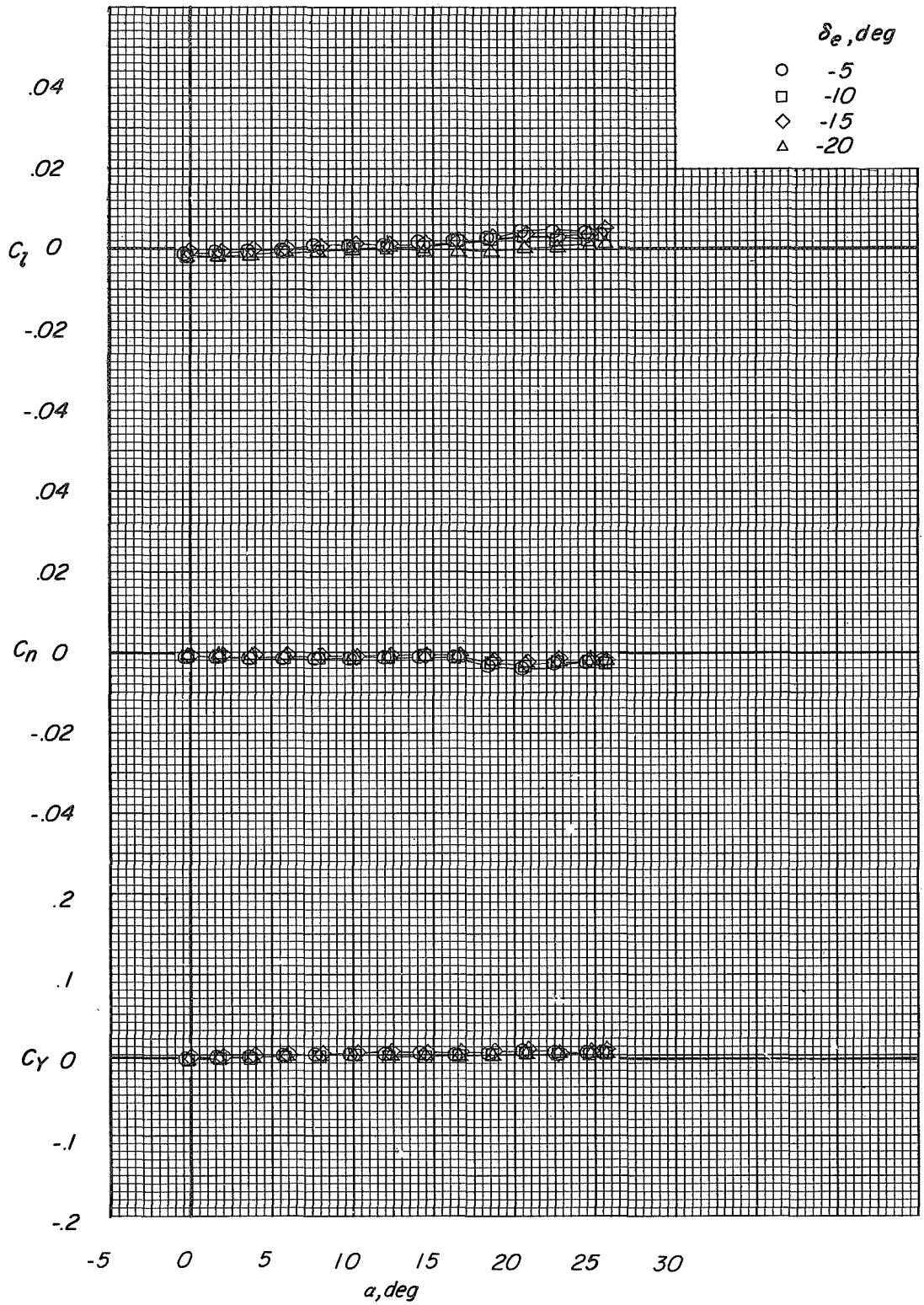
(i) $\delta_a = 20^o$; M = 0.70.

Figure 38.- Continued.



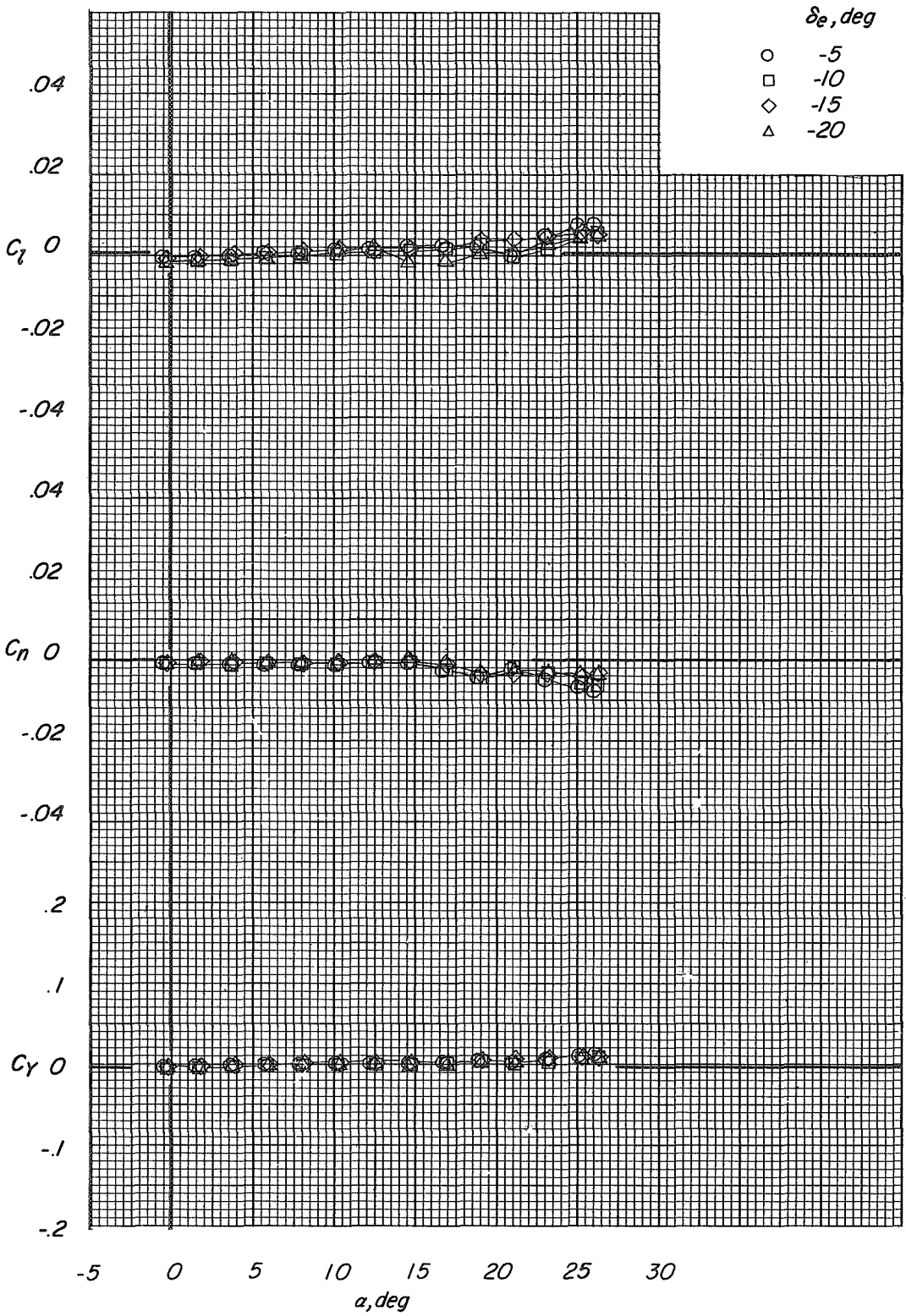
(j) $\delta_a = 20^o$; M = 0.80.

Figure 38.- Concluded.



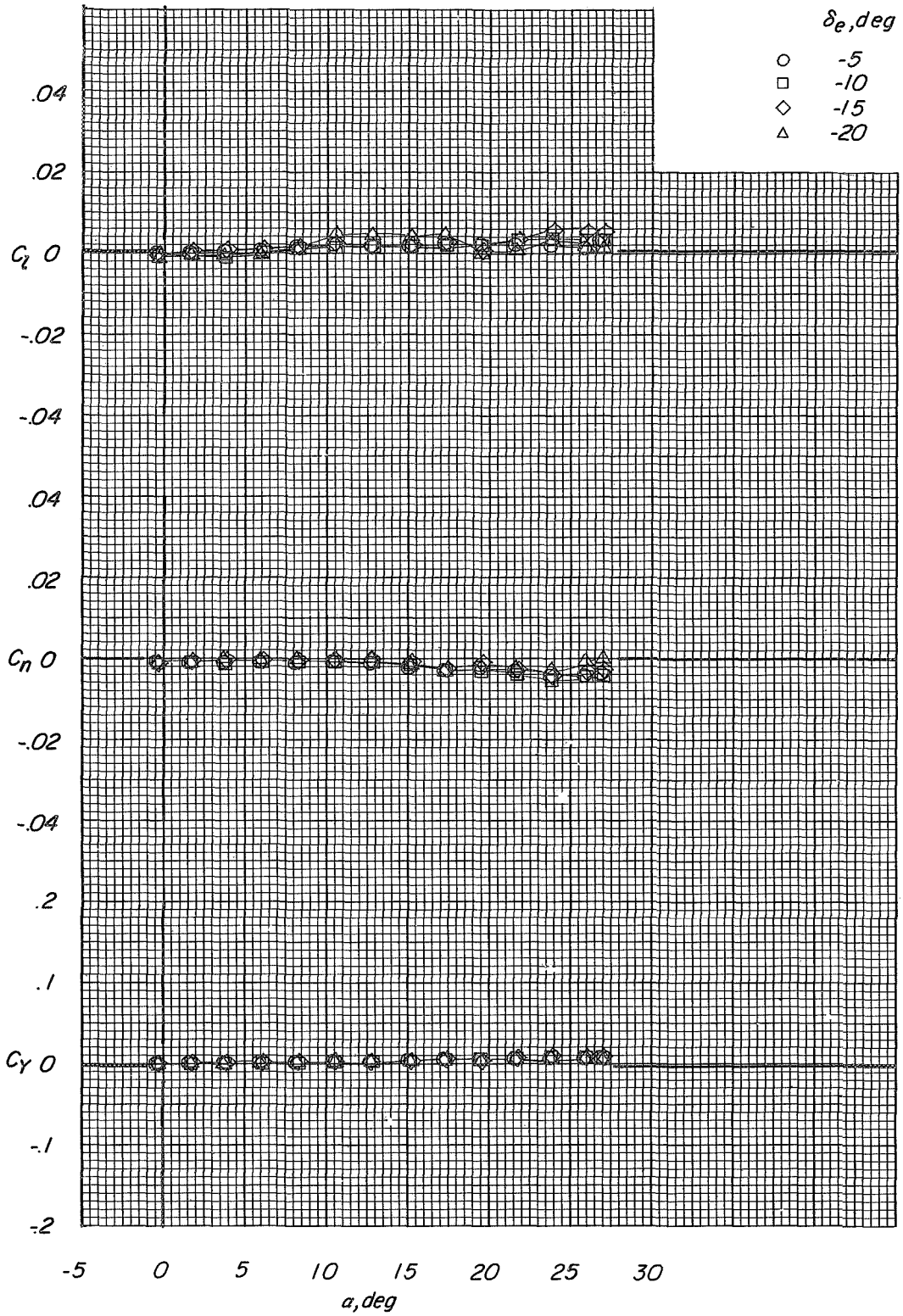
(a) $\delta_a = 0^o$; M = 0.35.

Figure 39.- Variation of the lateral force and moment coefficients with angle of attack for several aileron deflections. Modification II fin configuration; auxiliary flaps in the subsonic position; $\beta = 0^o$.



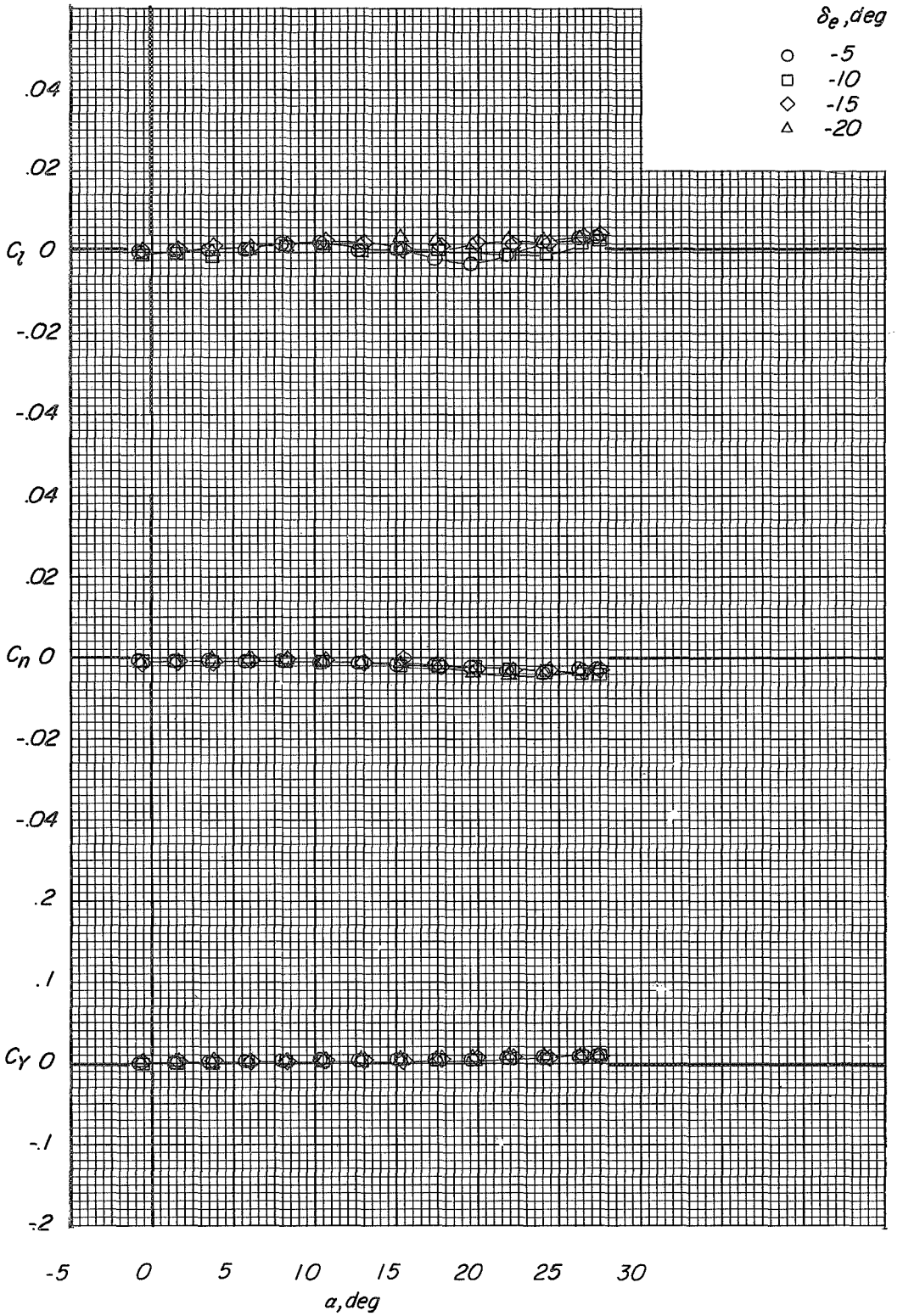
(b) $\delta_a = 0^o$; M = 0.50.

Figure 39.- Continued.



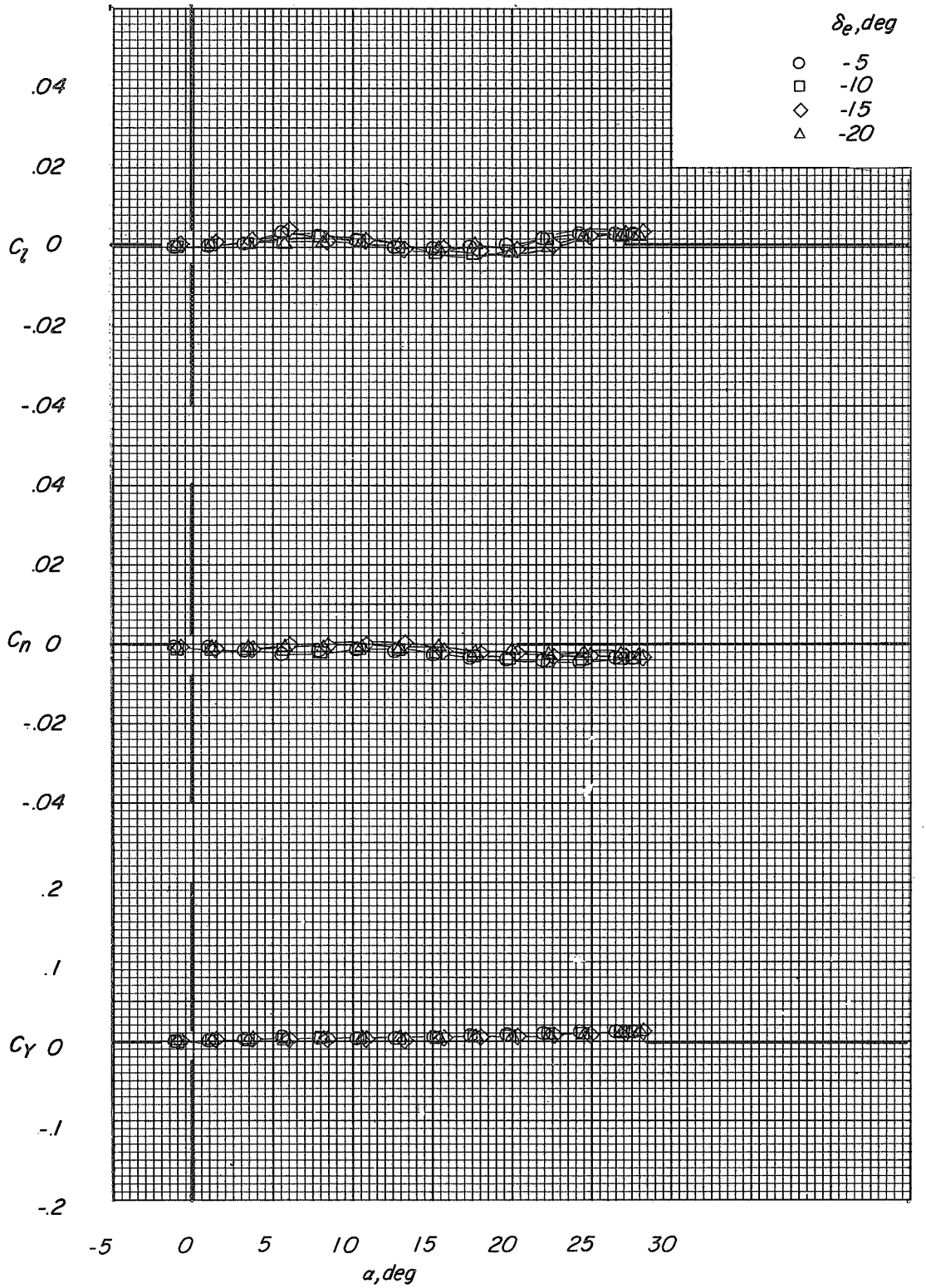
(c) $\delta_a = 0^o$; M = 0.60.

Figure 39.- Continued.



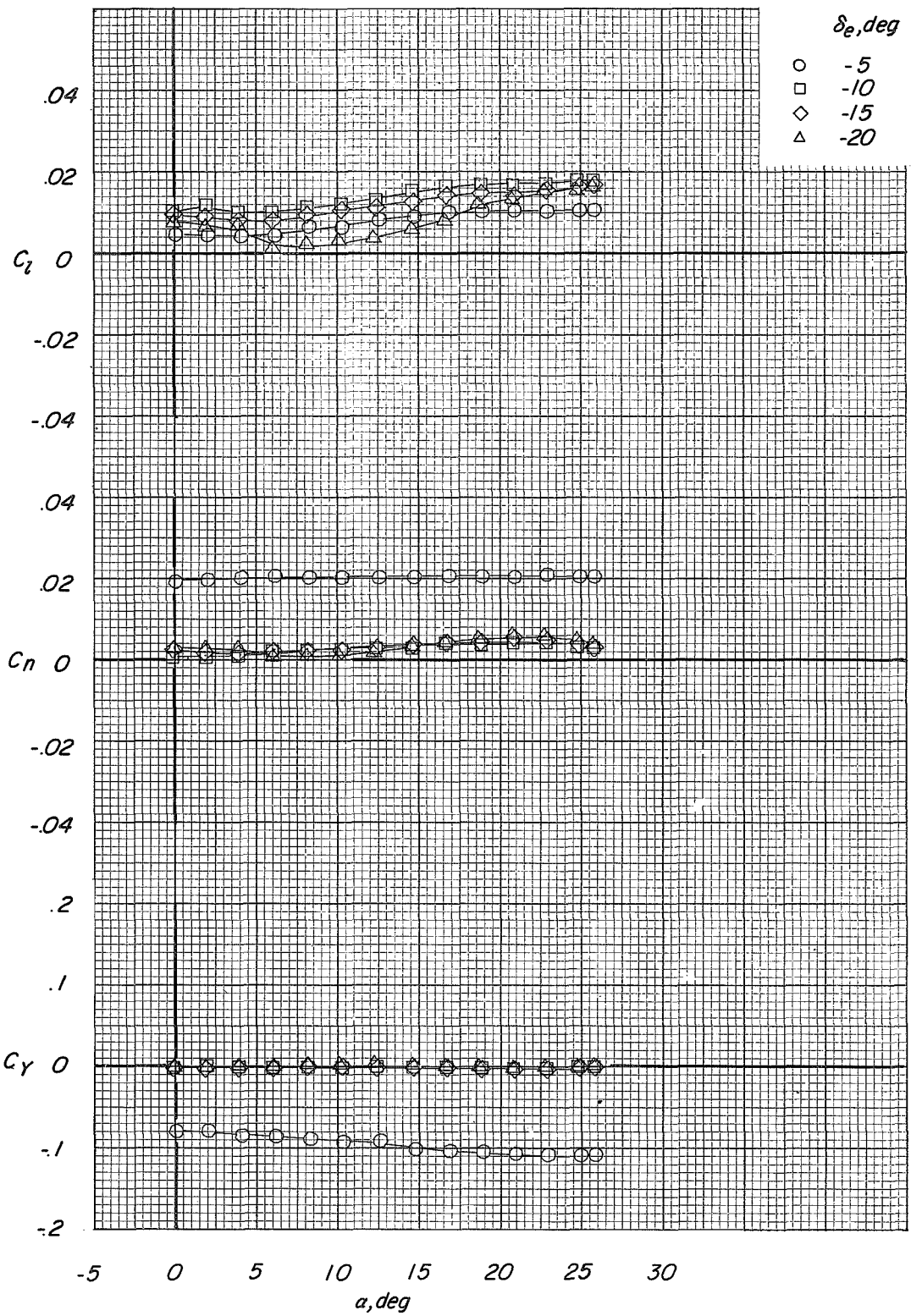
(d) $\delta_a = 0^o$; M = 0.70.

Figure 39.- Continued.



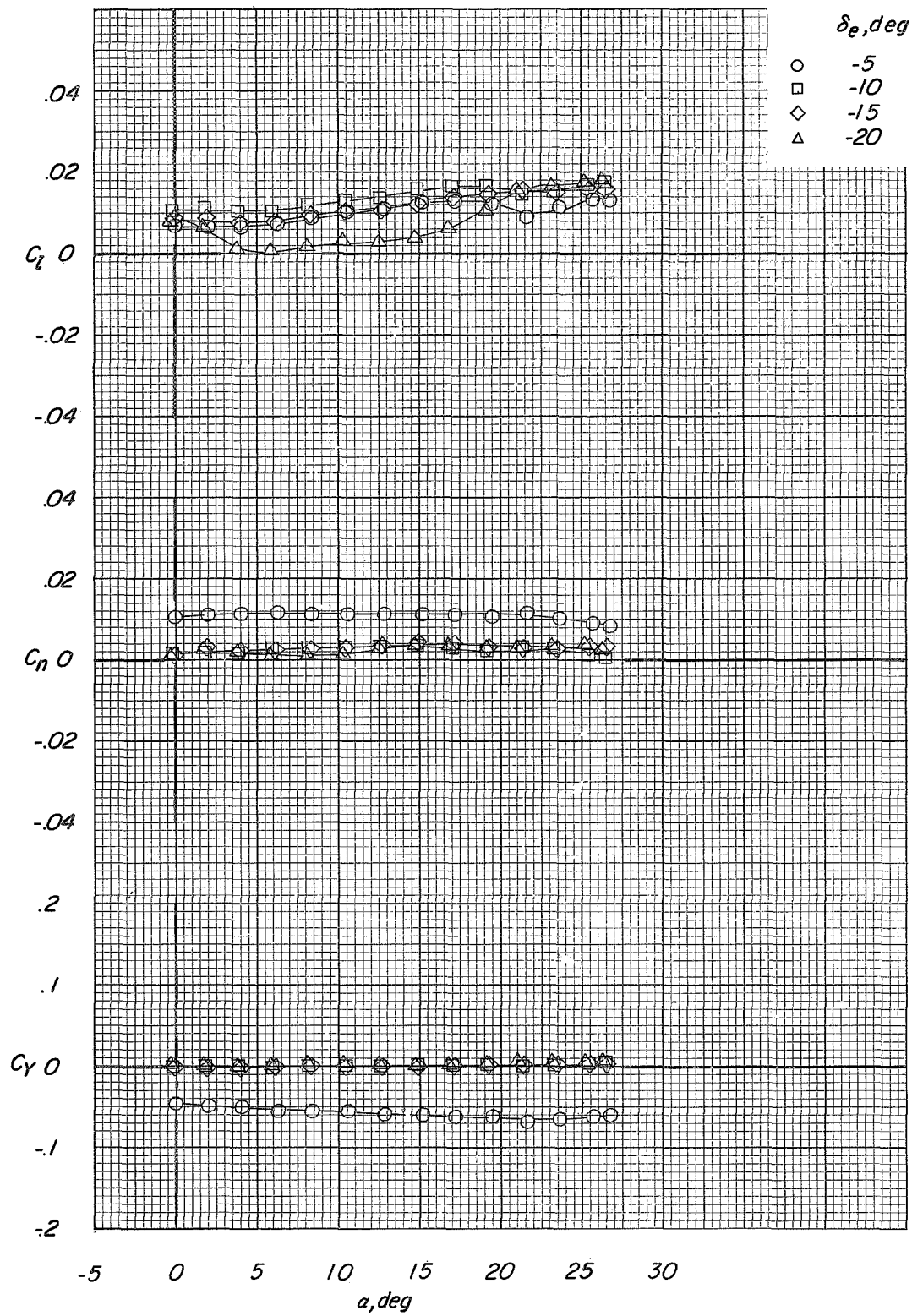
(e) $\delta_a = 0^o$; M = 0.80.

Figure 39.- Continued.



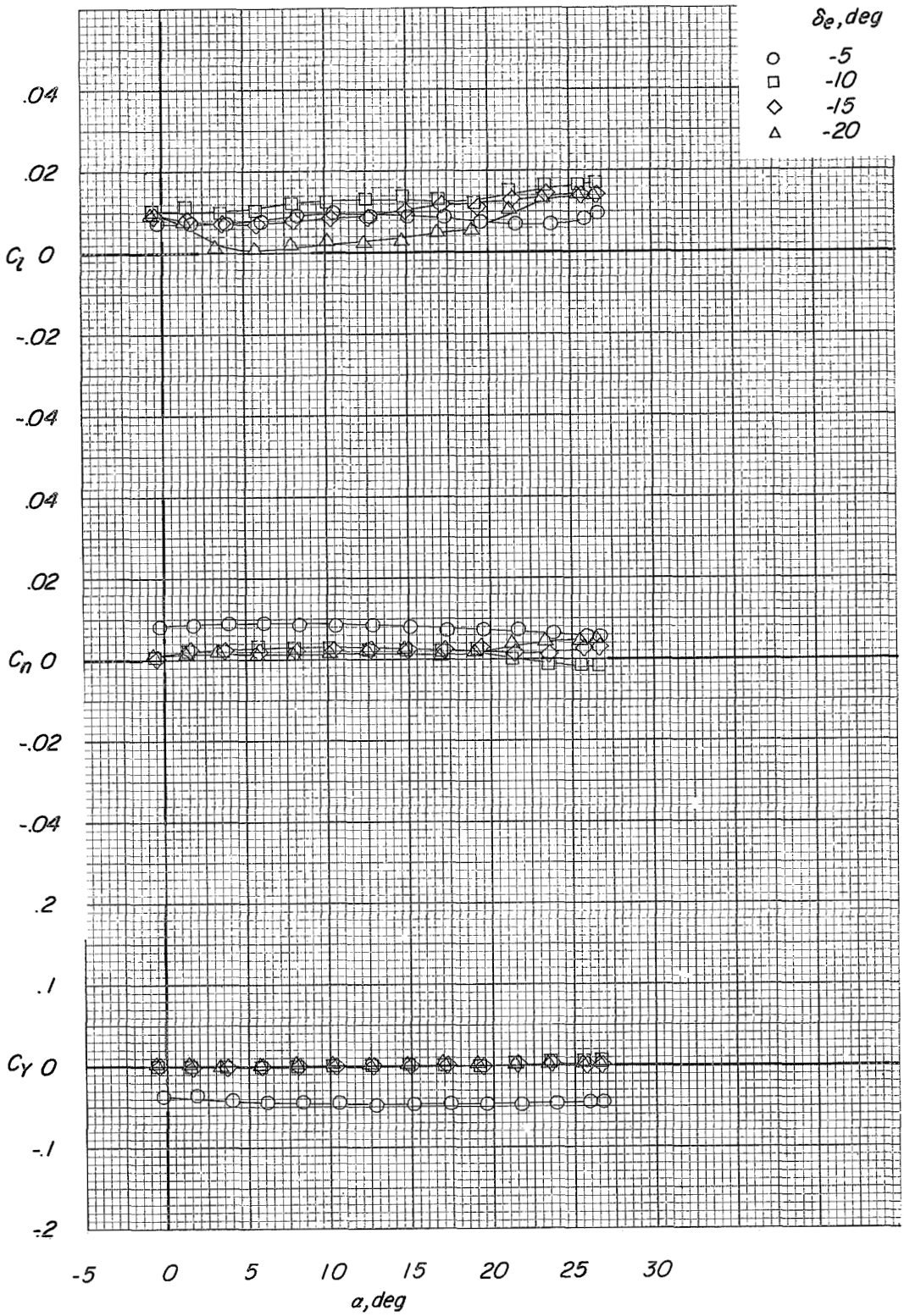
(f) $\delta_a = 10^o$; M = 0.35.

Figure 39.- Continued.



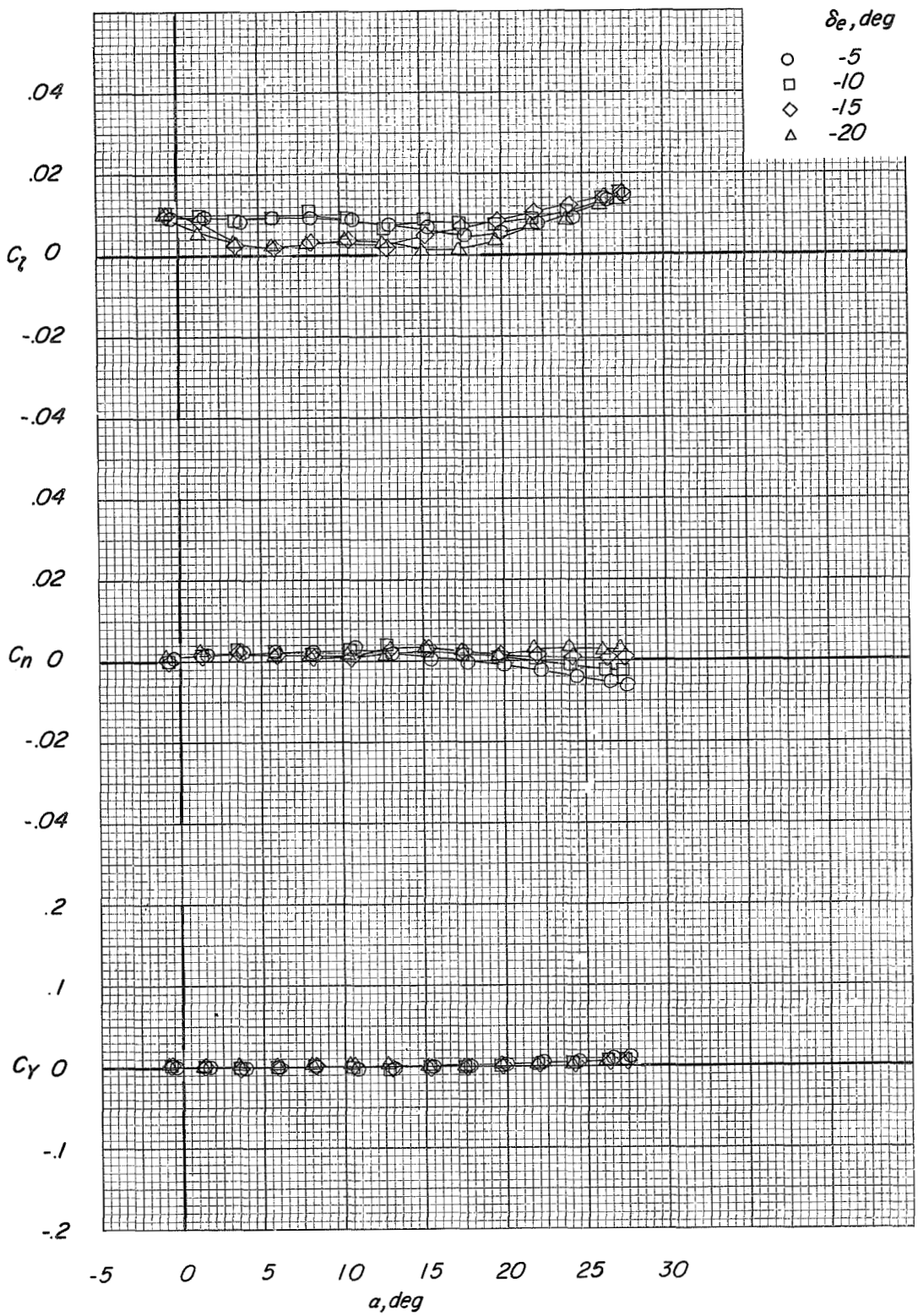
(g) $\delta_a = 10^o$; M = 0.50.

Figure 39.- Continued.



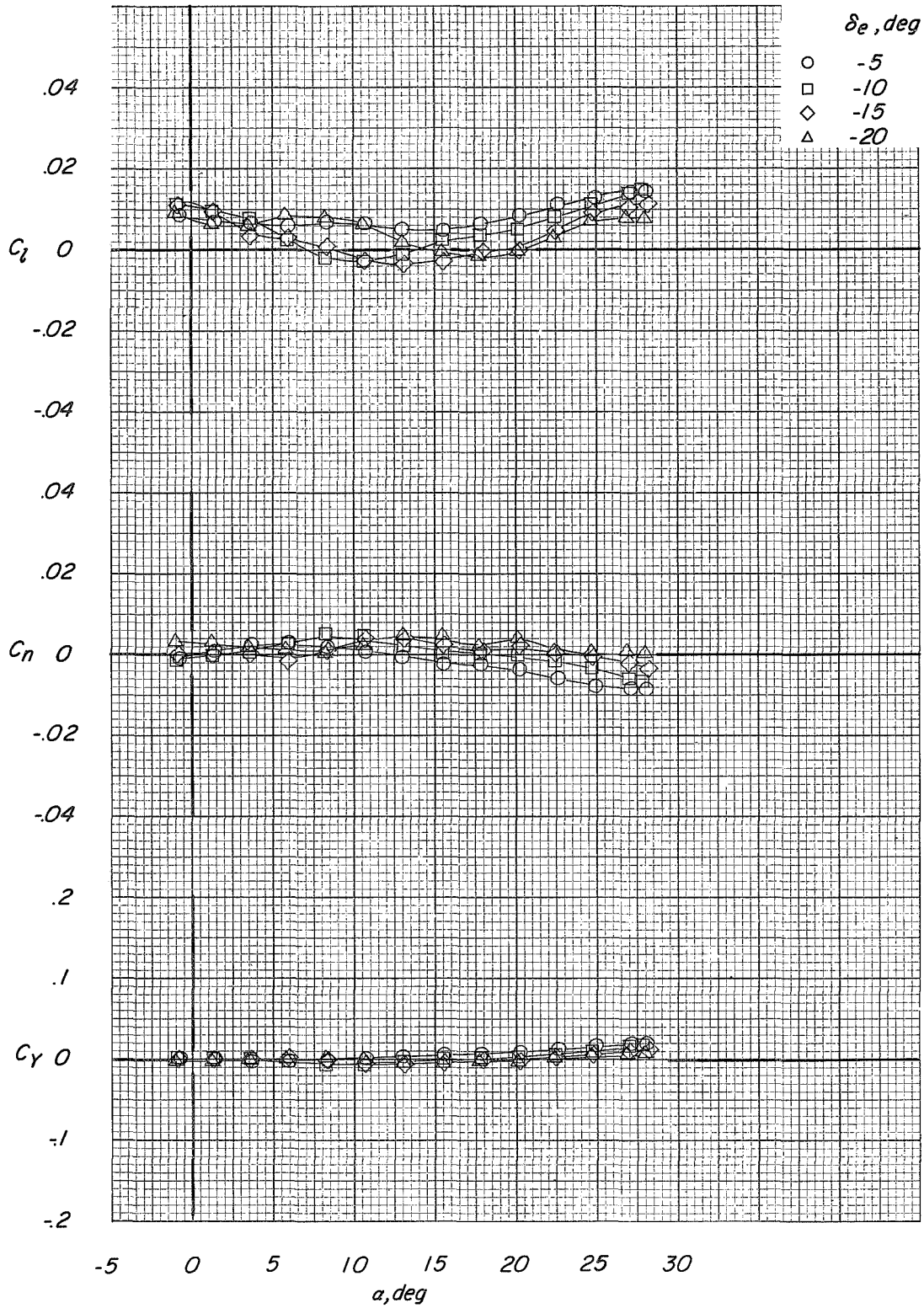
(h) $\delta_a = 10^o$; M = 0.60.

Figure 39.- Continued.



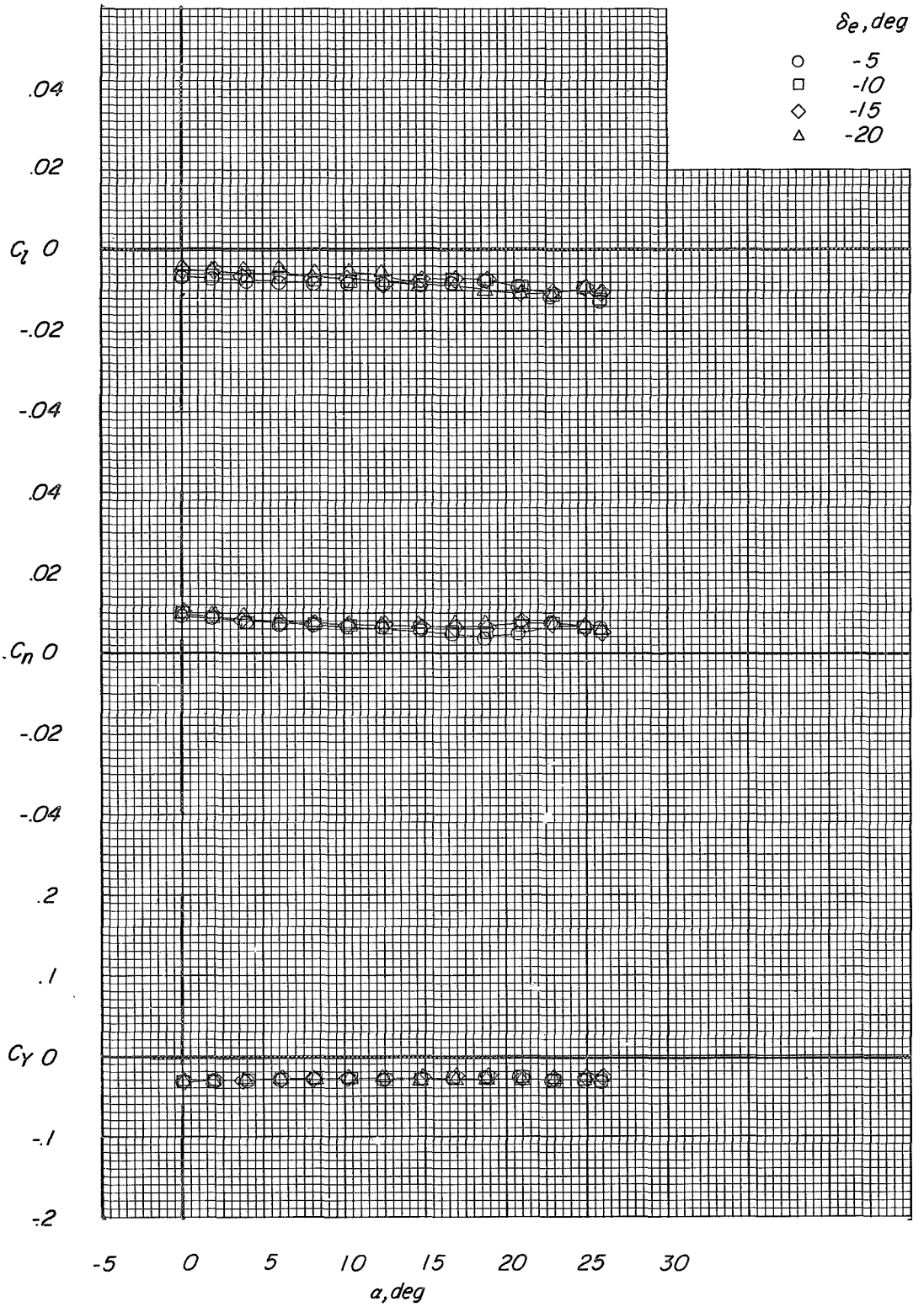
(i) $\delta_a = 10^o$; M = 0.70.

Figure 39.- Continued.



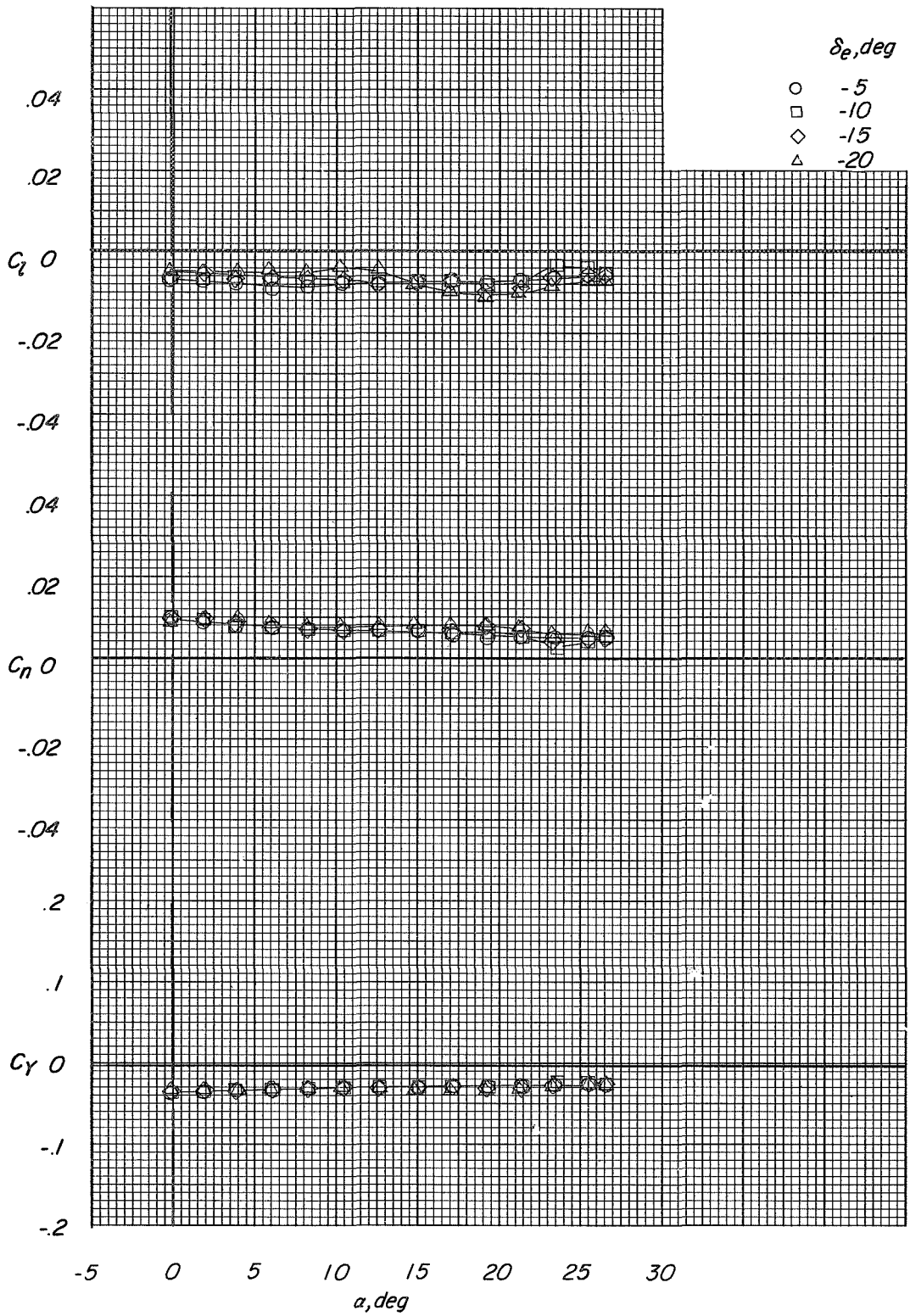
(j) $\delta_a = 10^o$; M = 0.80.

Figure 39.- Concluded.



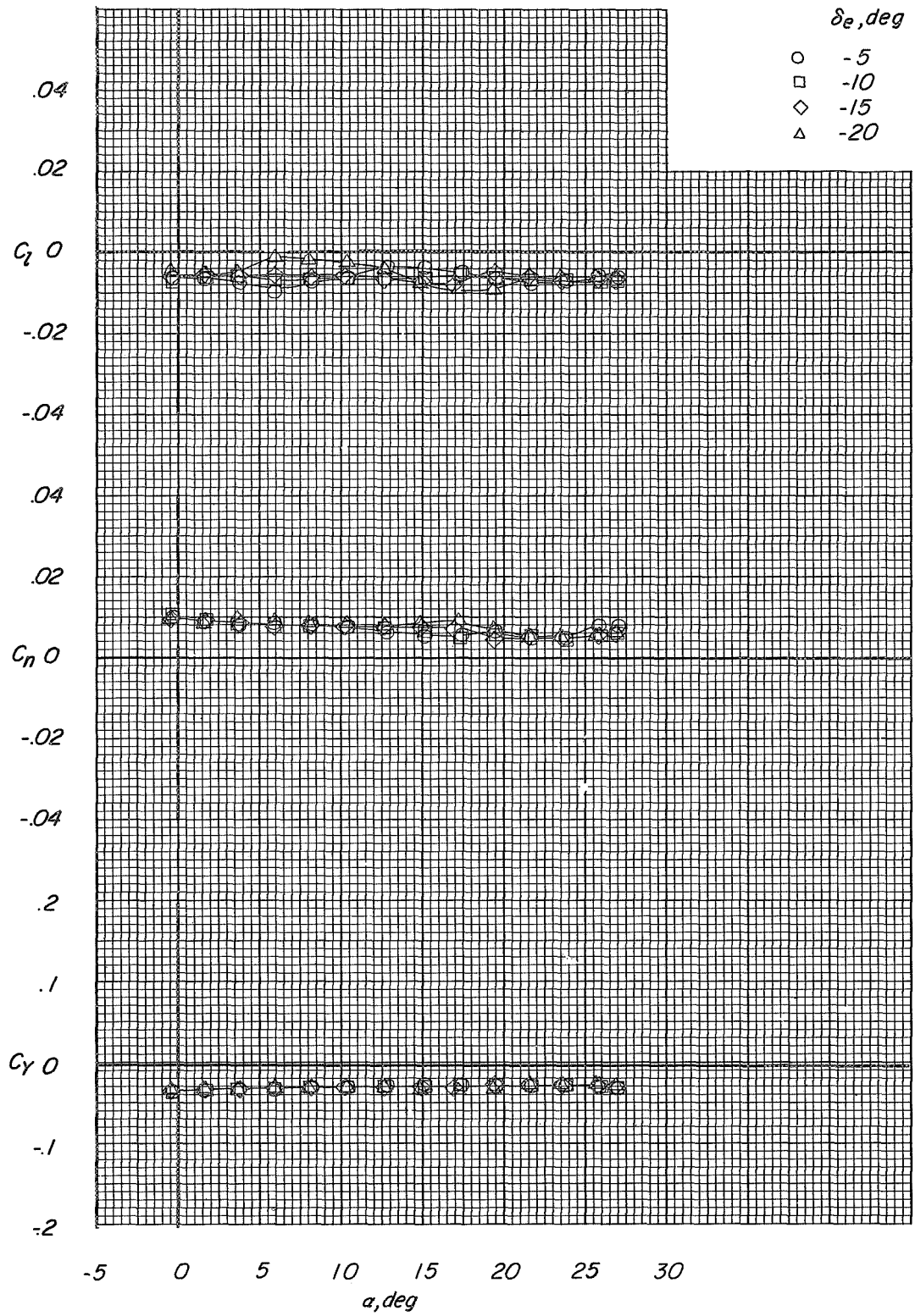
(a) $\beta = 2.3^{o}$; M = 0.35.

Figure 40.- Variation of the lateral force and moment coefficients with angle of attack for sideslipped conditions. Modification II fin configuration; auxiliary flaps in the subsonic position; $\delta_a = 0^{o}$.



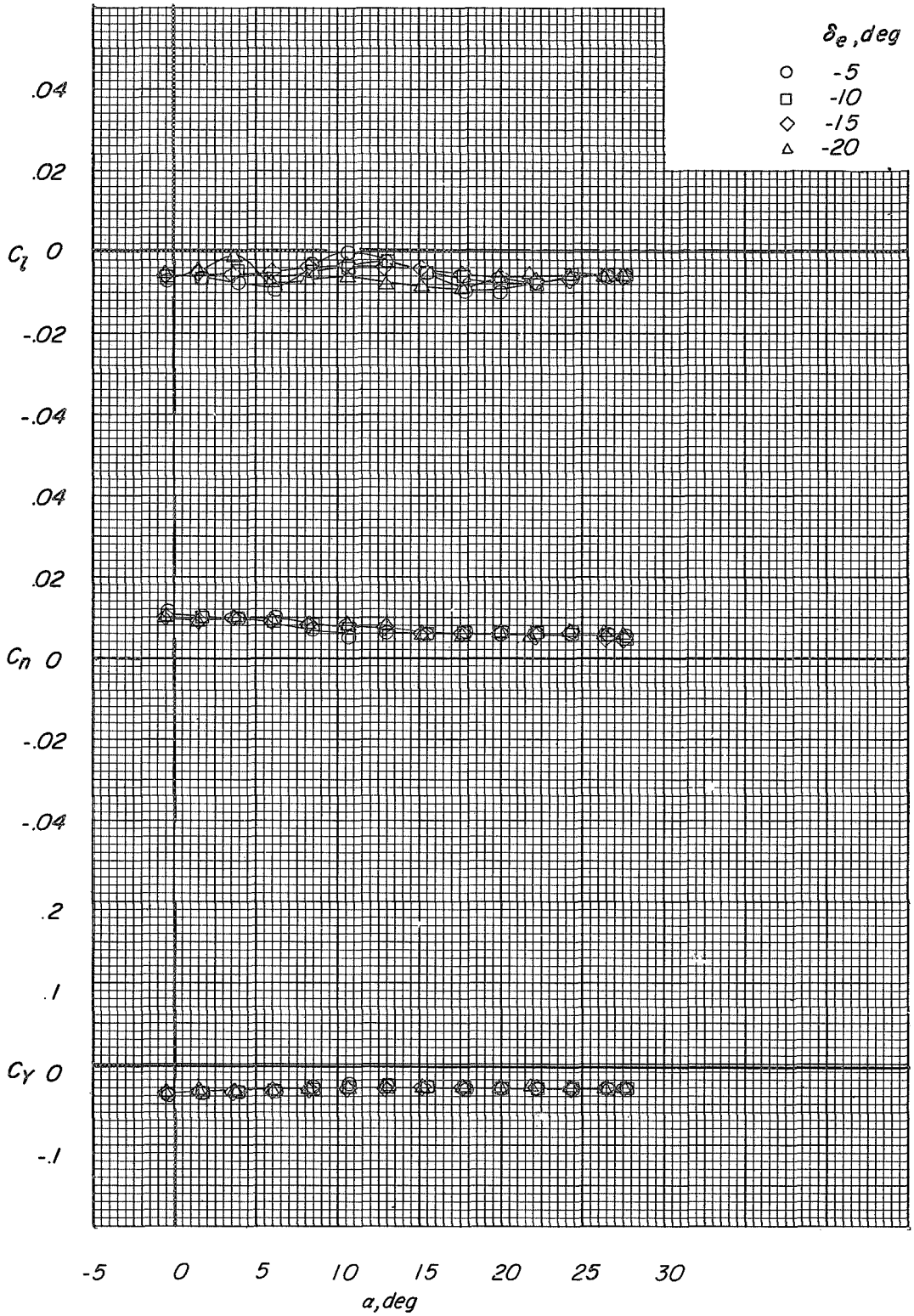
(b) $\beta = 2.3^{o}$; $M = 0.50$.

Figure 40.- Continued.



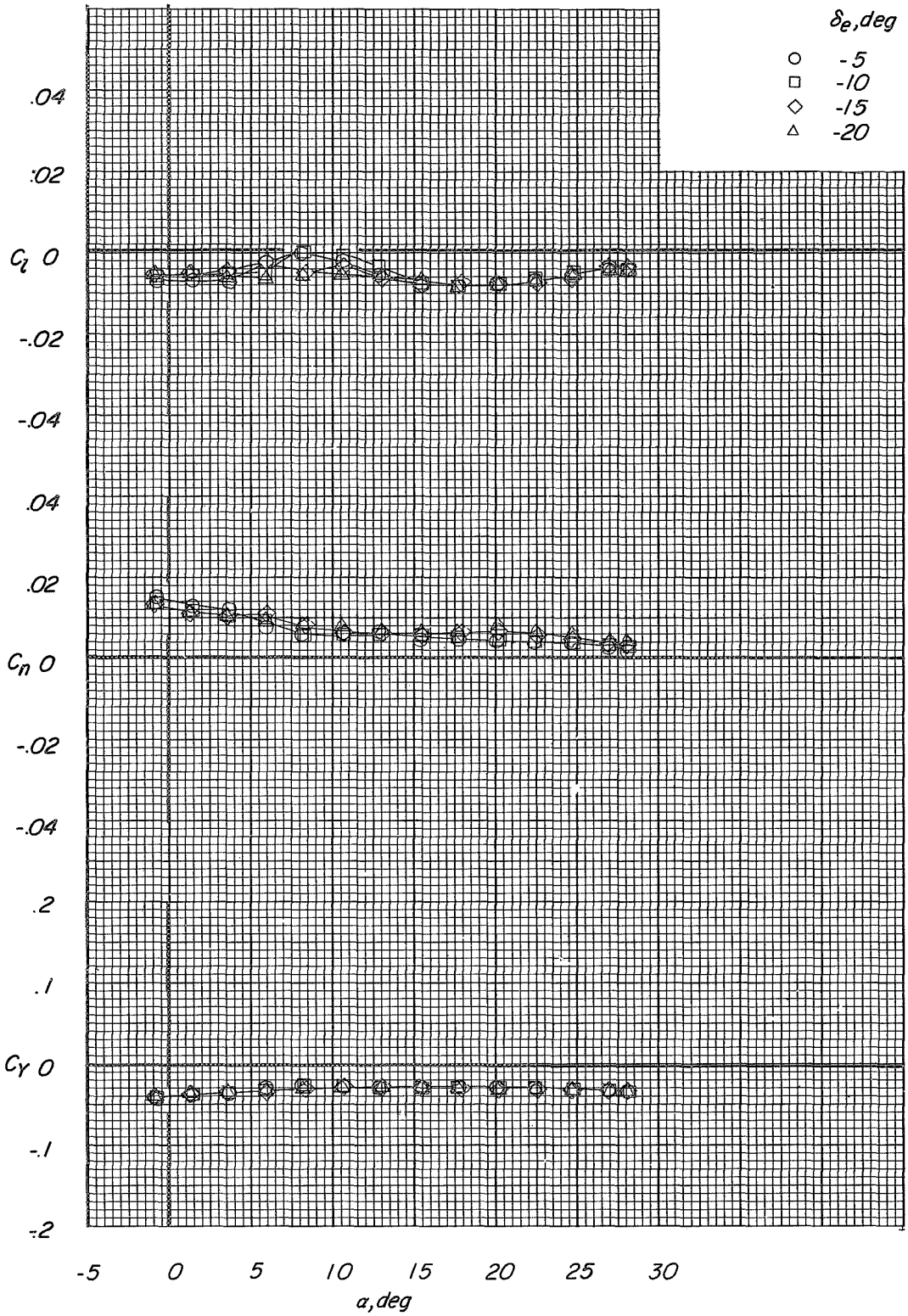
(c) $\beta = 2.3^{\circ}$; M = 0.60.

Figure 40.- Continued.



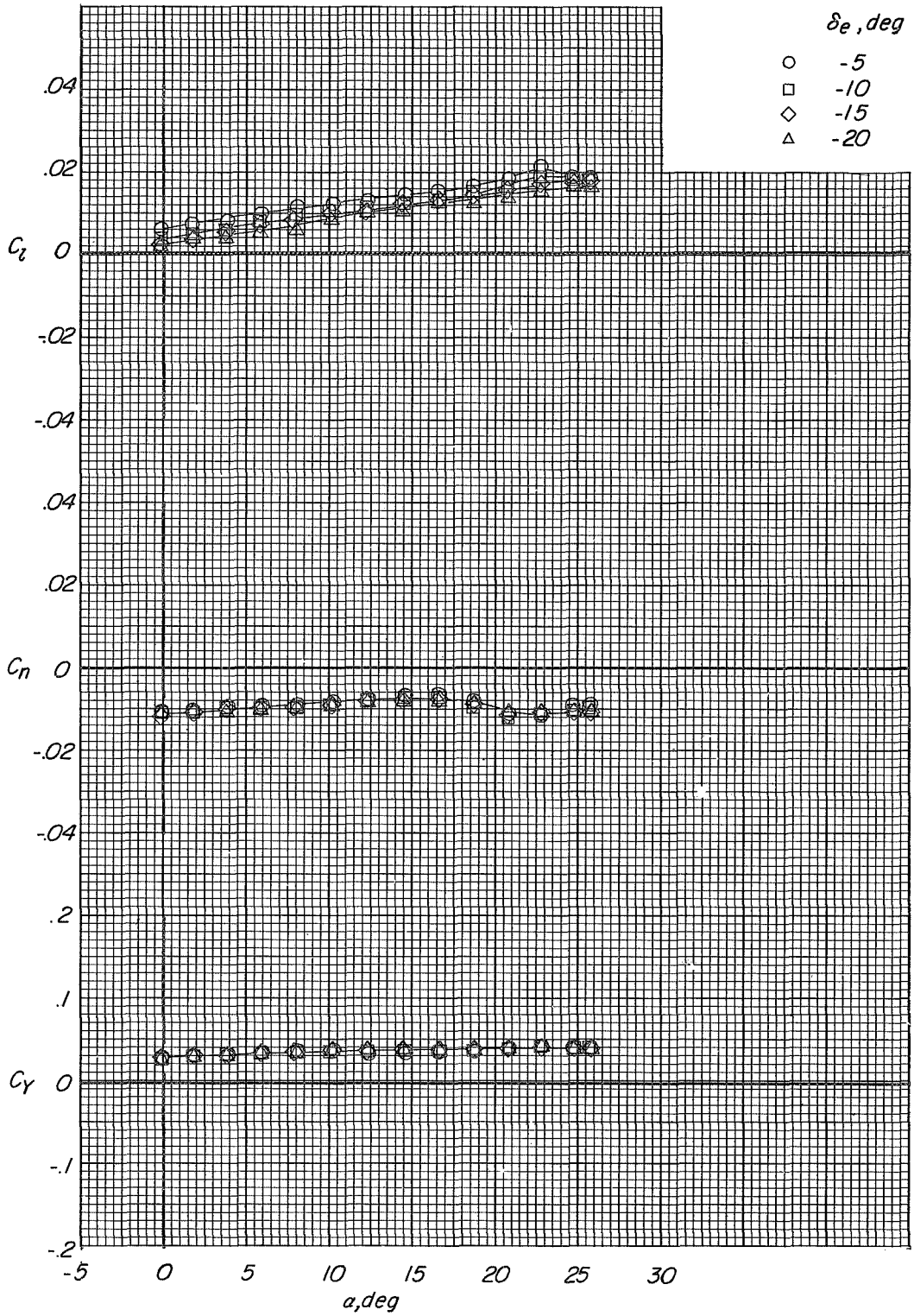
(d) $\beta = 2.3^{o}$; M = 0.70.

Figure 40.- Continued.



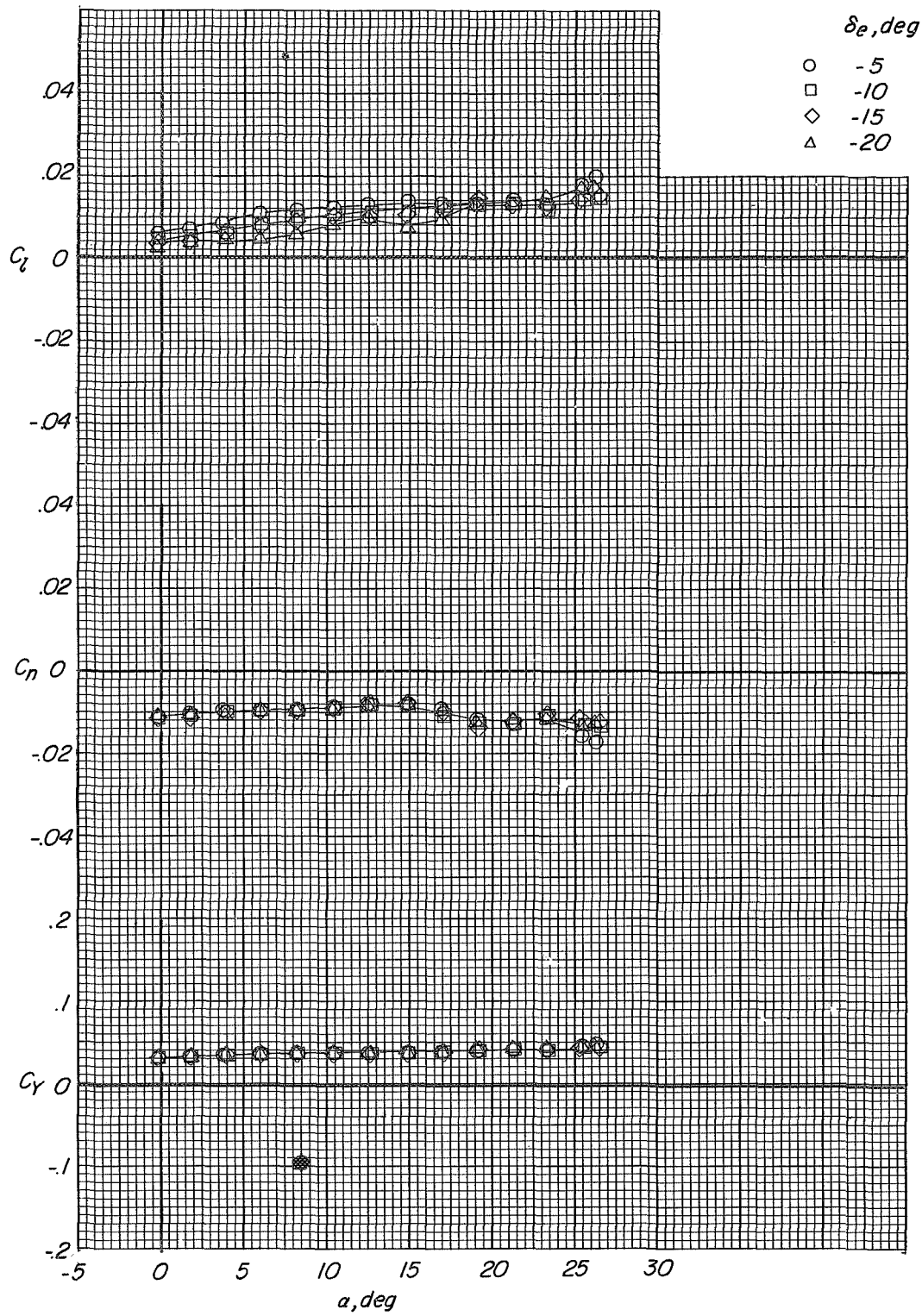
(e) $\beta = 2.3^{o}$; M = 0.80.

Figure 40.- Continued.



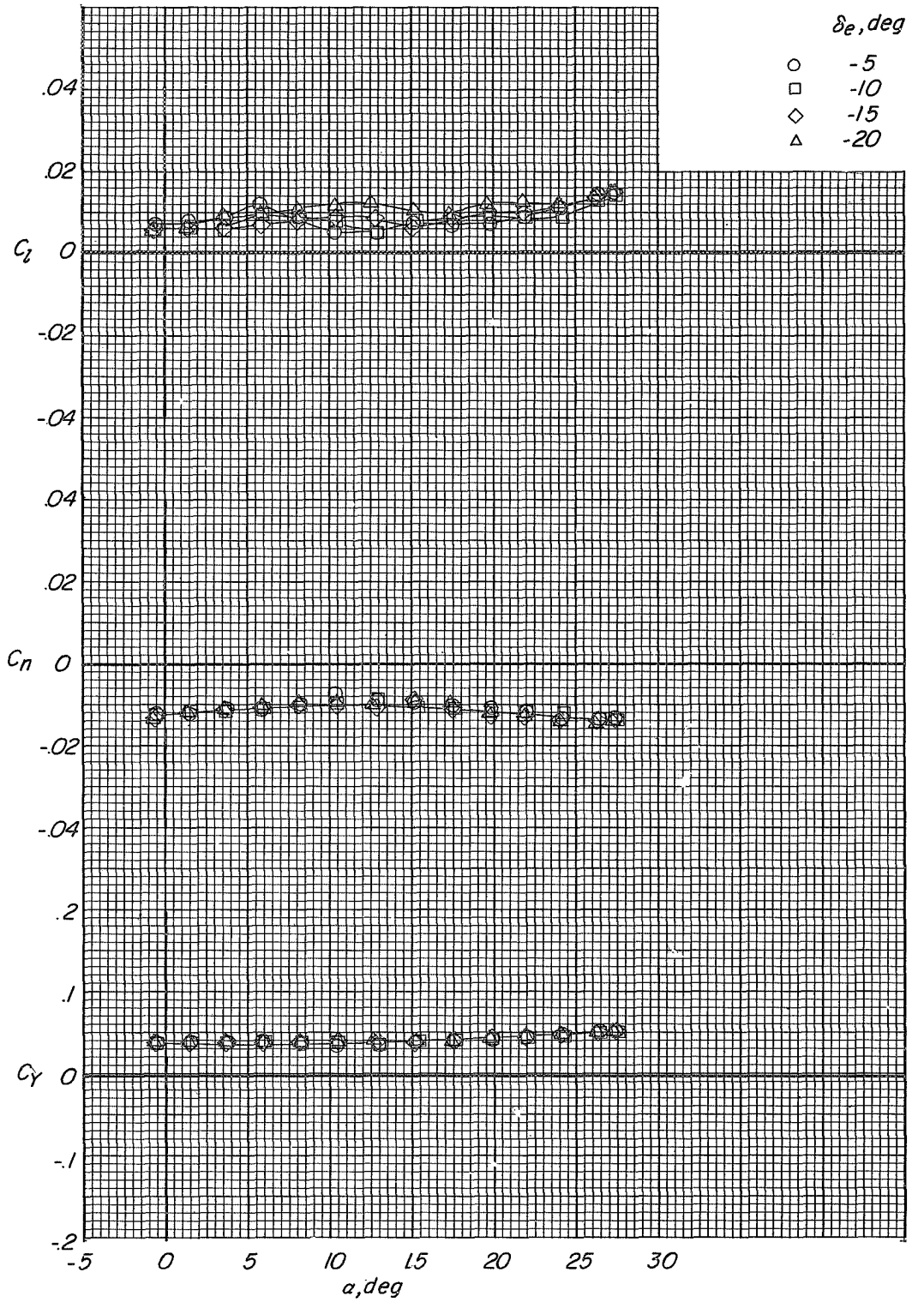
(f) $\beta = -2.3^{\circ}$; M = 0.35.

Figure 40.- Continued.



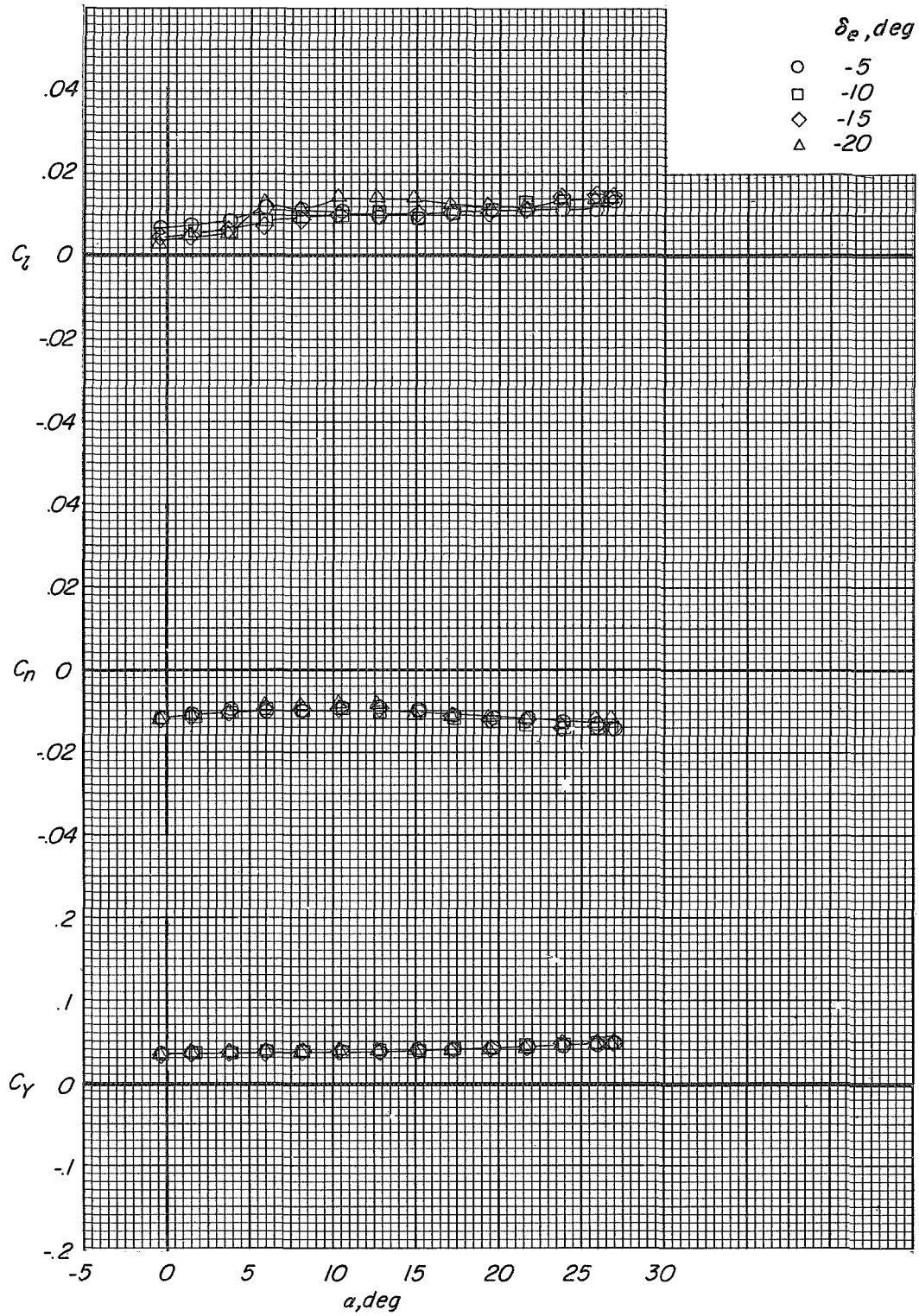
(g) $\beta = -2.3^{o}$; M = 0.50.

Figure 40.- Continued.



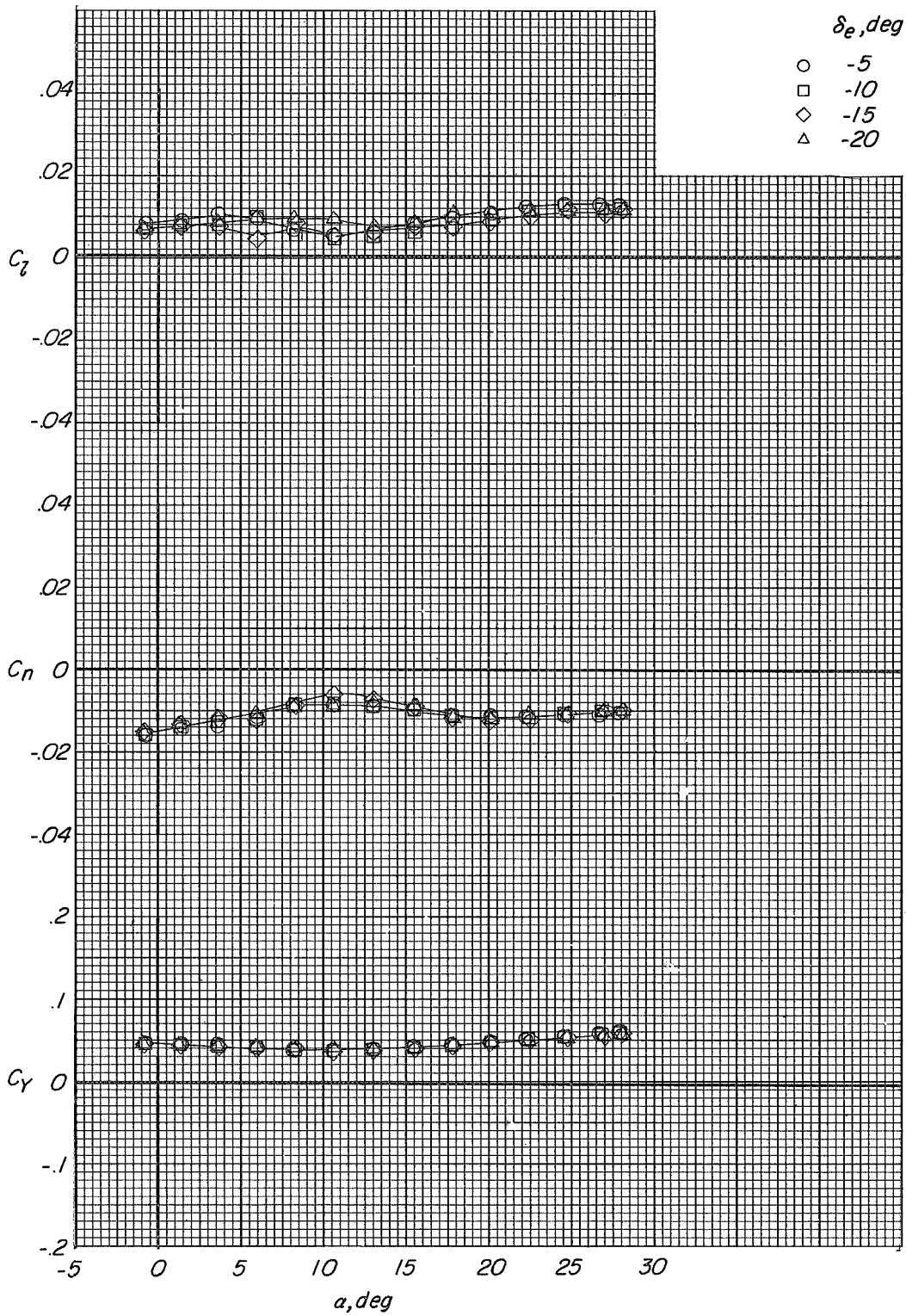
(h) $\beta = -2.3^{\circ}$; M = 0.60.

Figure 40.- Continued.



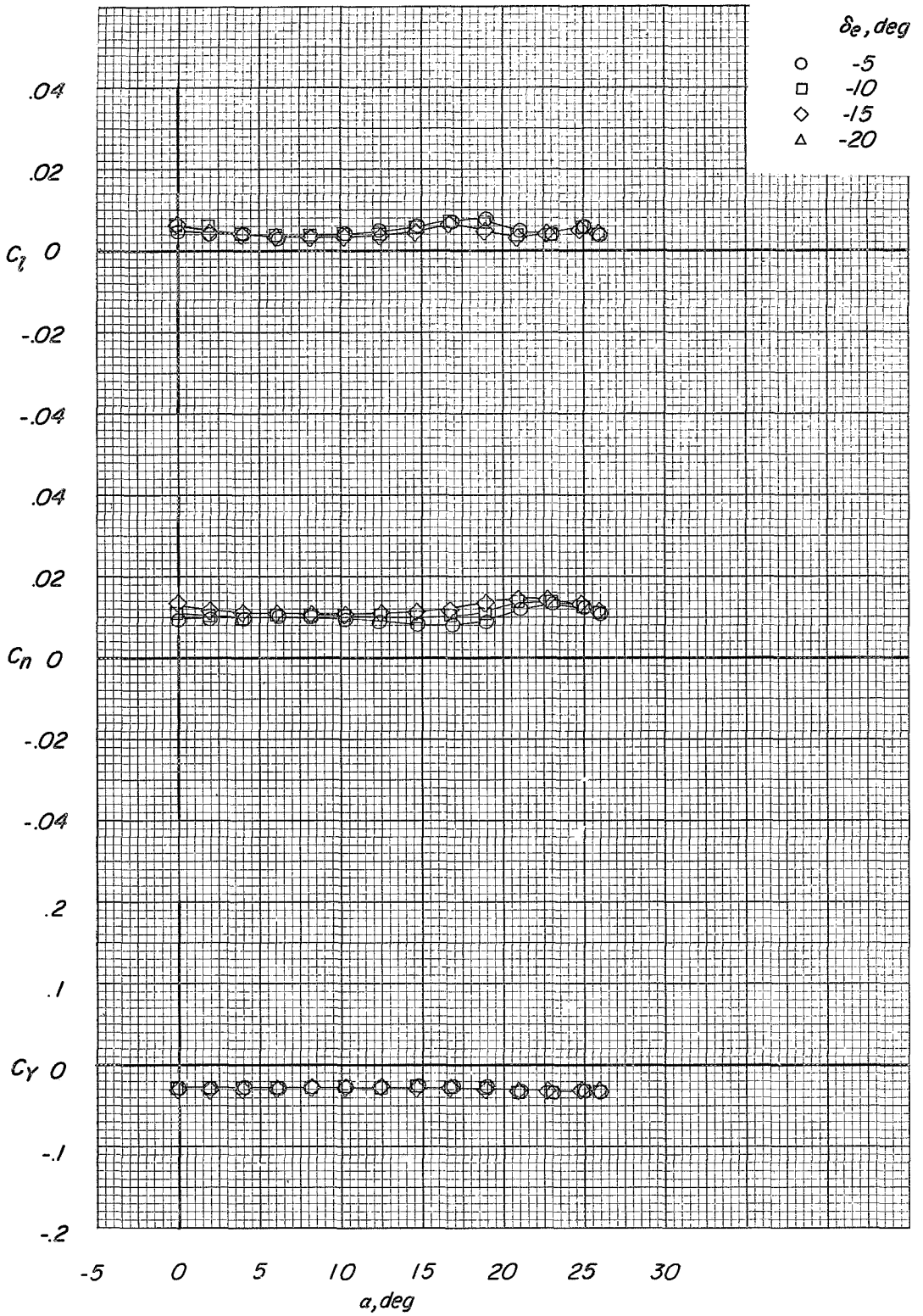
(i) $\beta = -2.3^{o}$; M = 0.70.

Figure 40.- Continued.



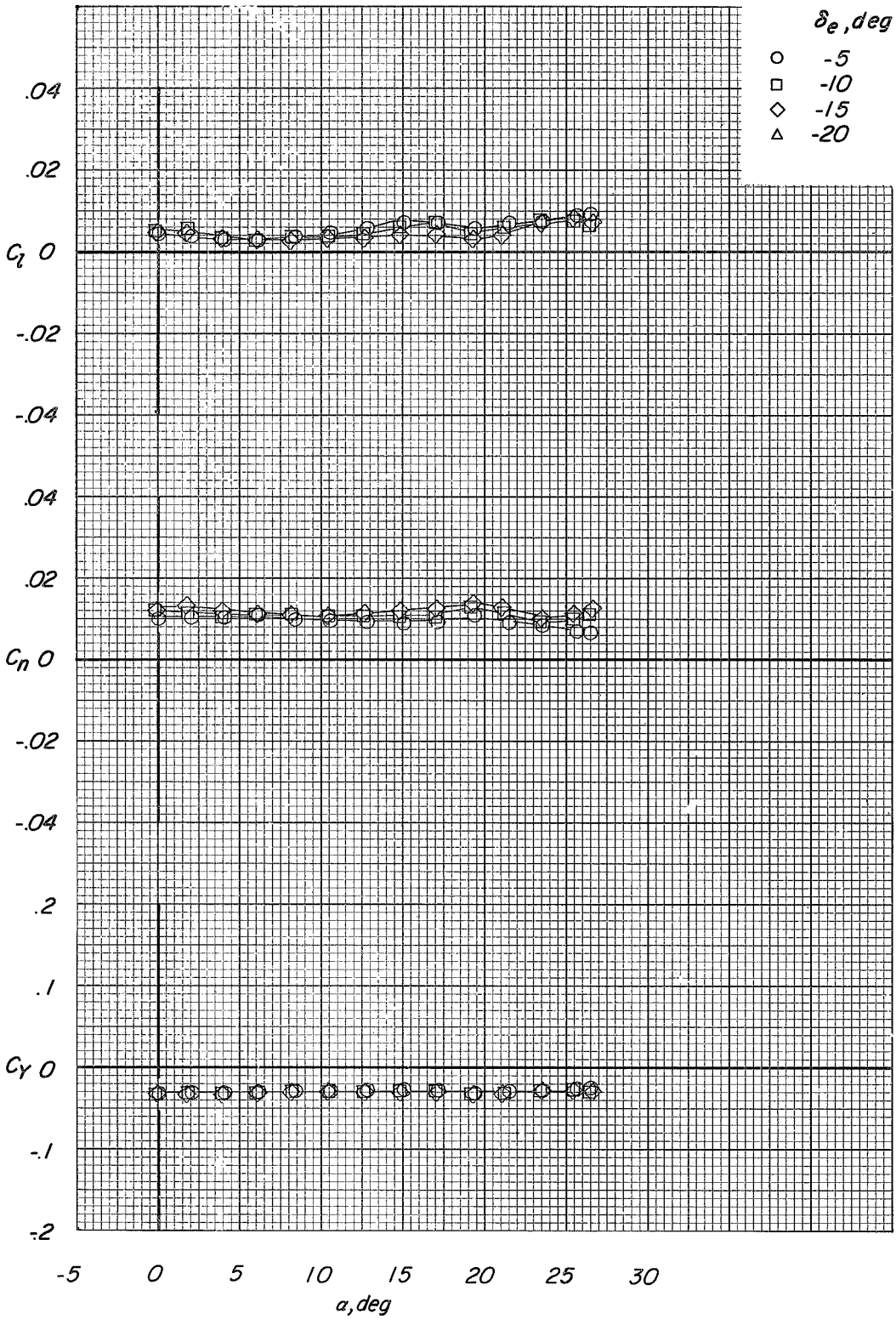
(j) $\beta = -2.3^{o}$; M = 0.80.

Figure 40.- Concluded.



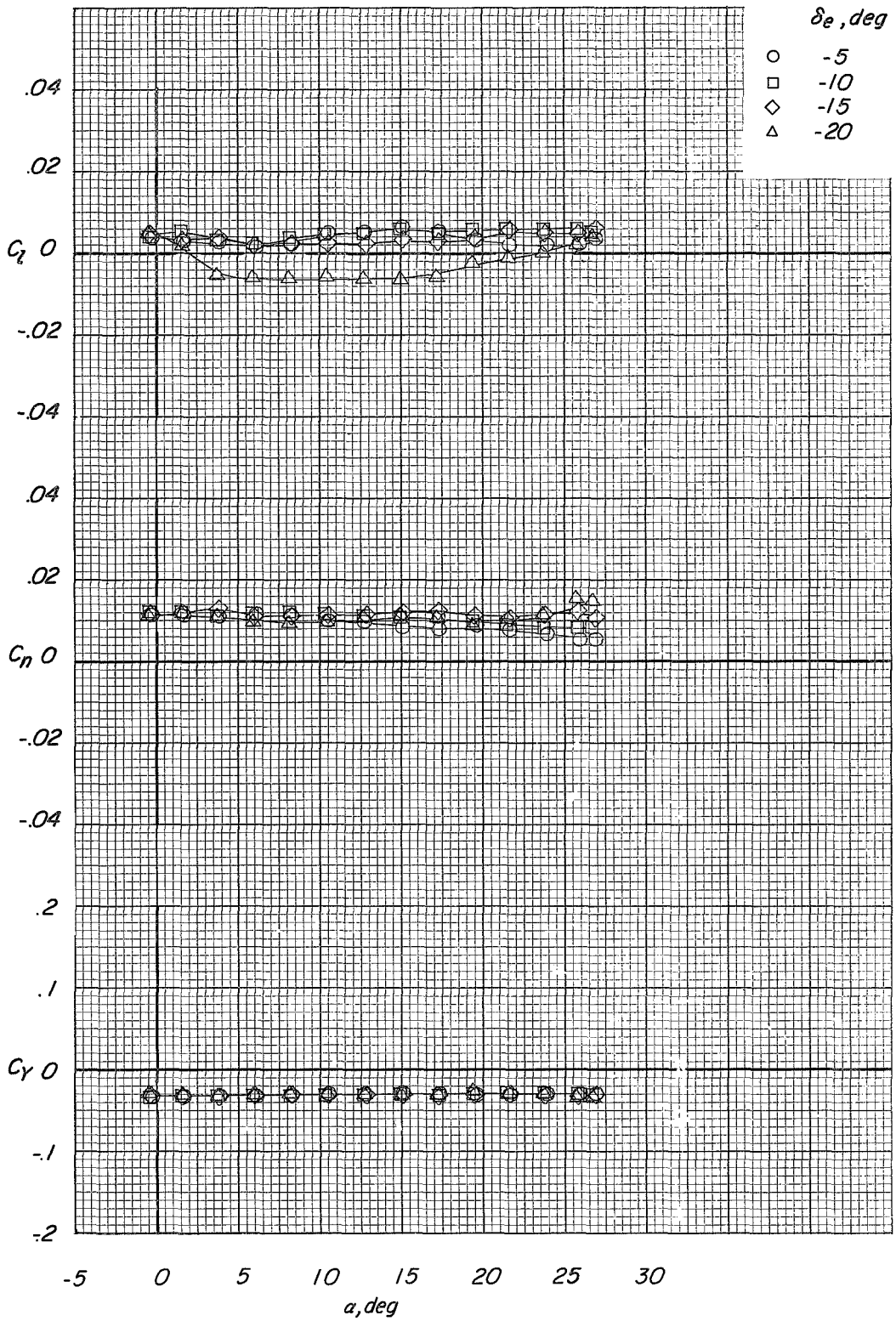
(a) $\beta = 2.3^{\circ}$; $\delta_a = 10^{\circ}$; $M = 0.35$.

Figure 41.- Variation of the lateral force and moment coefficients with angle of attack for combined aileron deflection and sideslip. Modification II fin configuration; auxiliary flaps in the subsonic position.



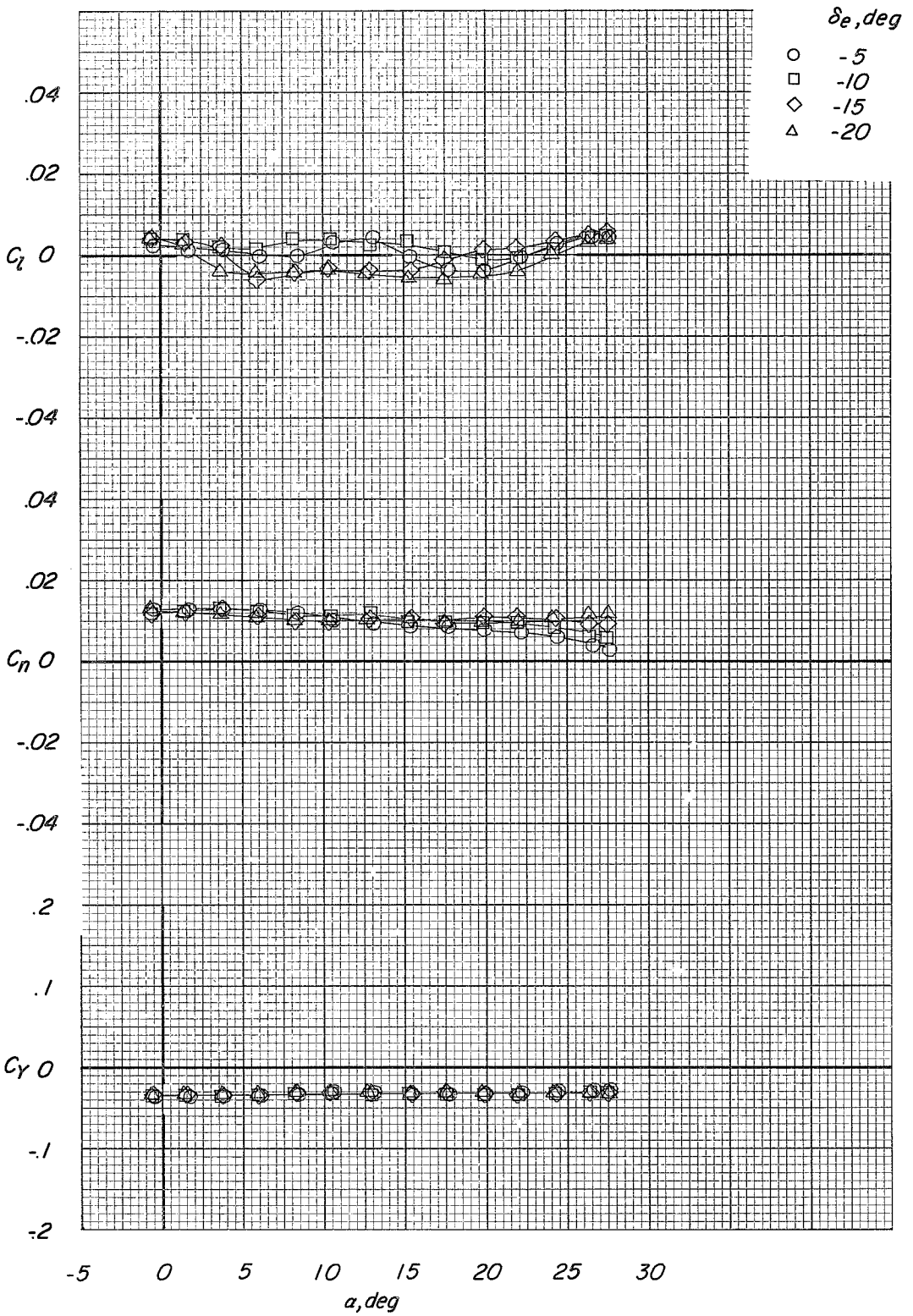
(b) $\beta = 2.3^{o}$; $\delta_a = 10^{o}$; M = 0.50.

Figure 41.- Continued.



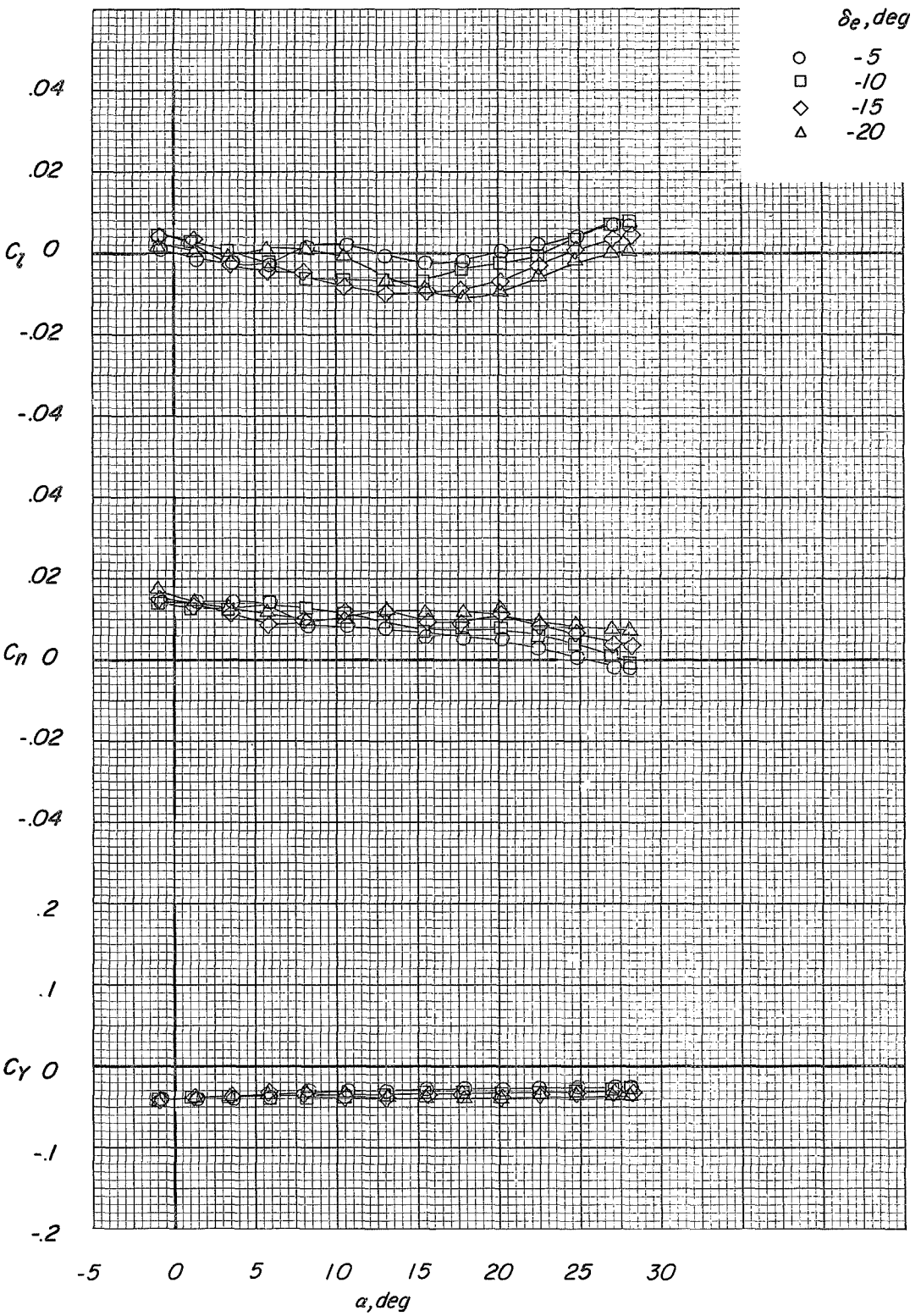
(c) $\beta = 2.3^{o}$; $\delta_a = 10^{o}$; M = 0.60.

Figure 41.- Continued.



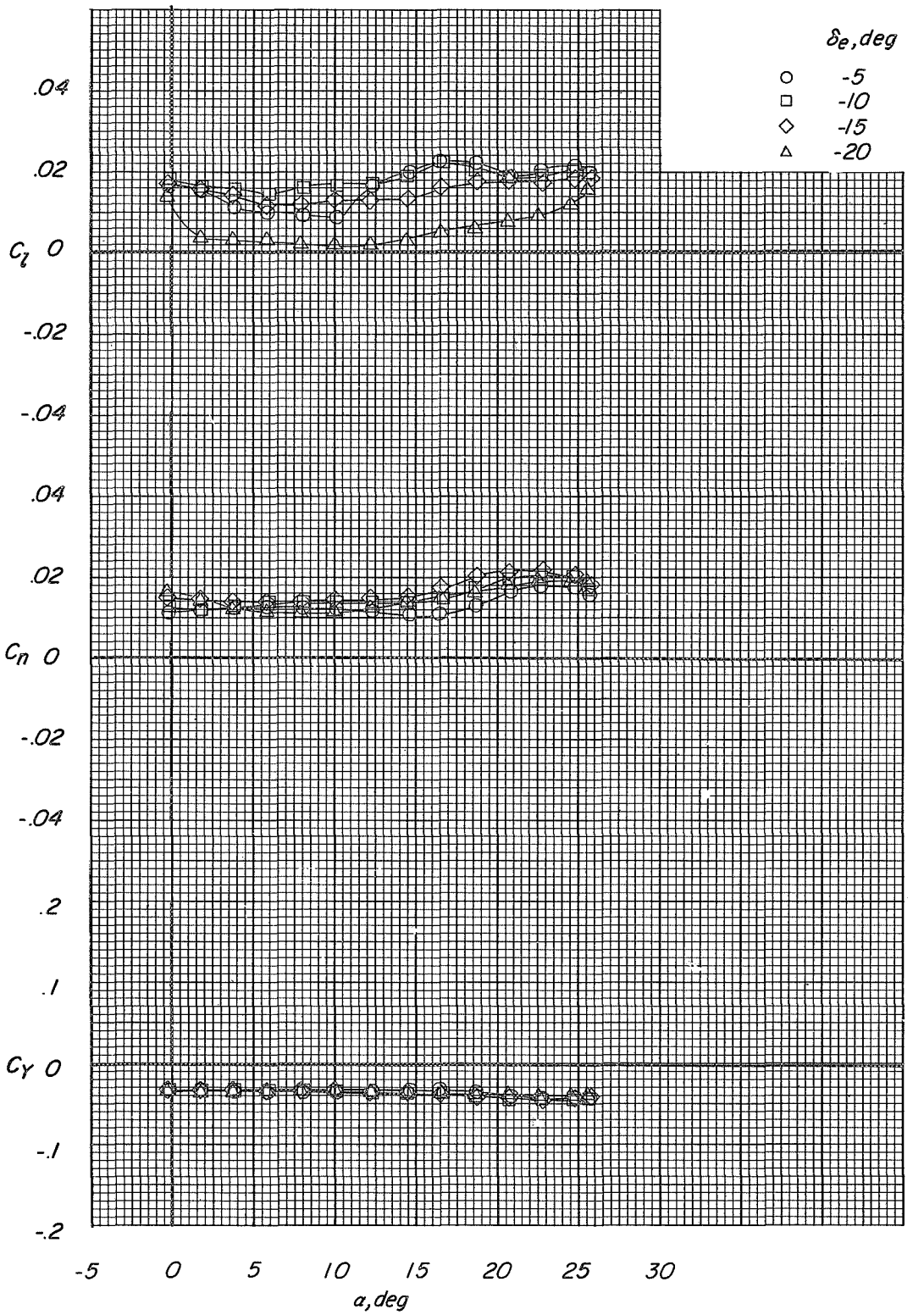
(d) $\beta = 2.3^{o}$; $\delta_a = 10^{o}$; M = 0.70.

Figure 41.- Continued.



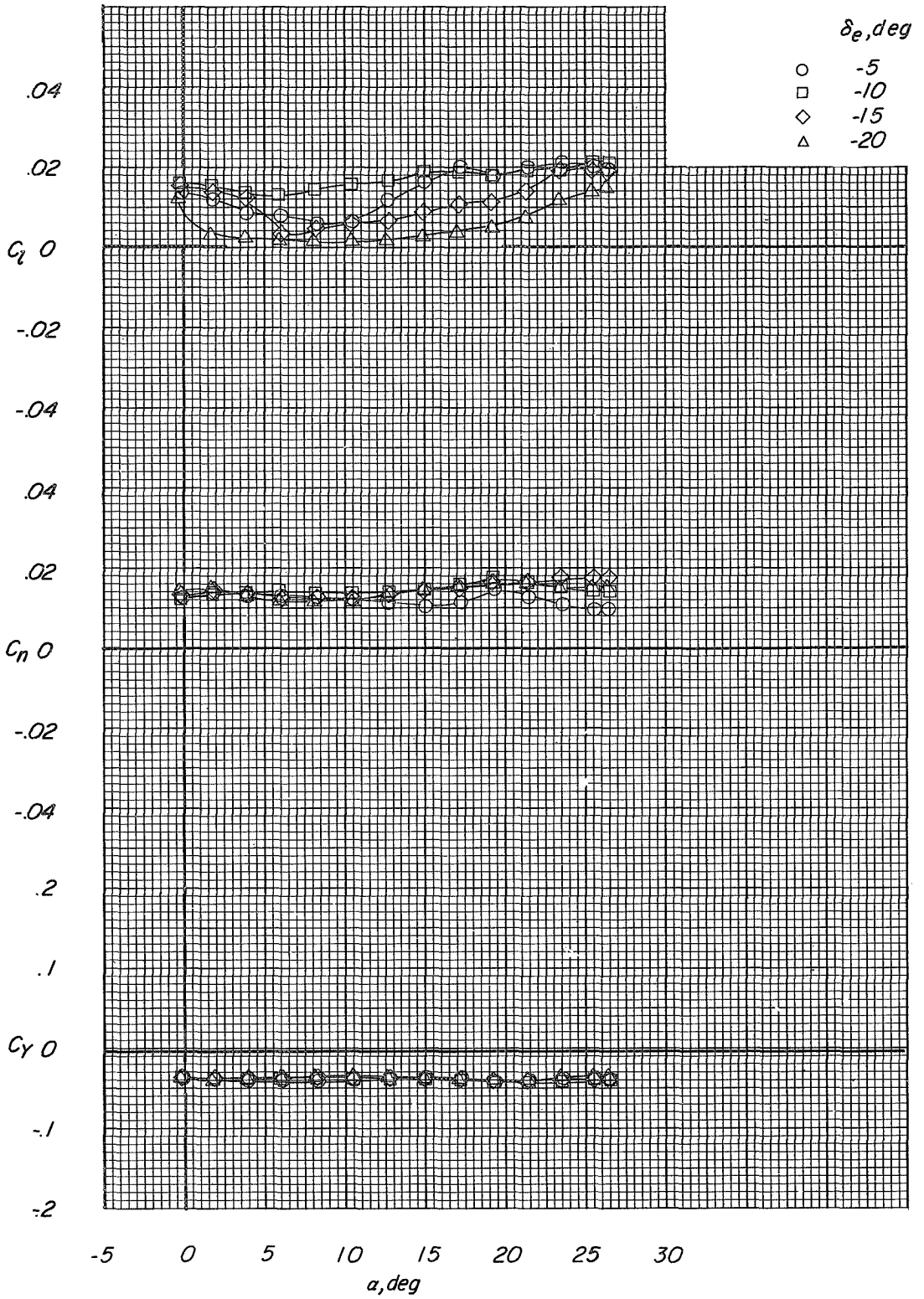
(e) $\beta = 2.3^{o}$; $\delta_a = 10^{o}$; M = 0.80.

Figure 41.- Continued.



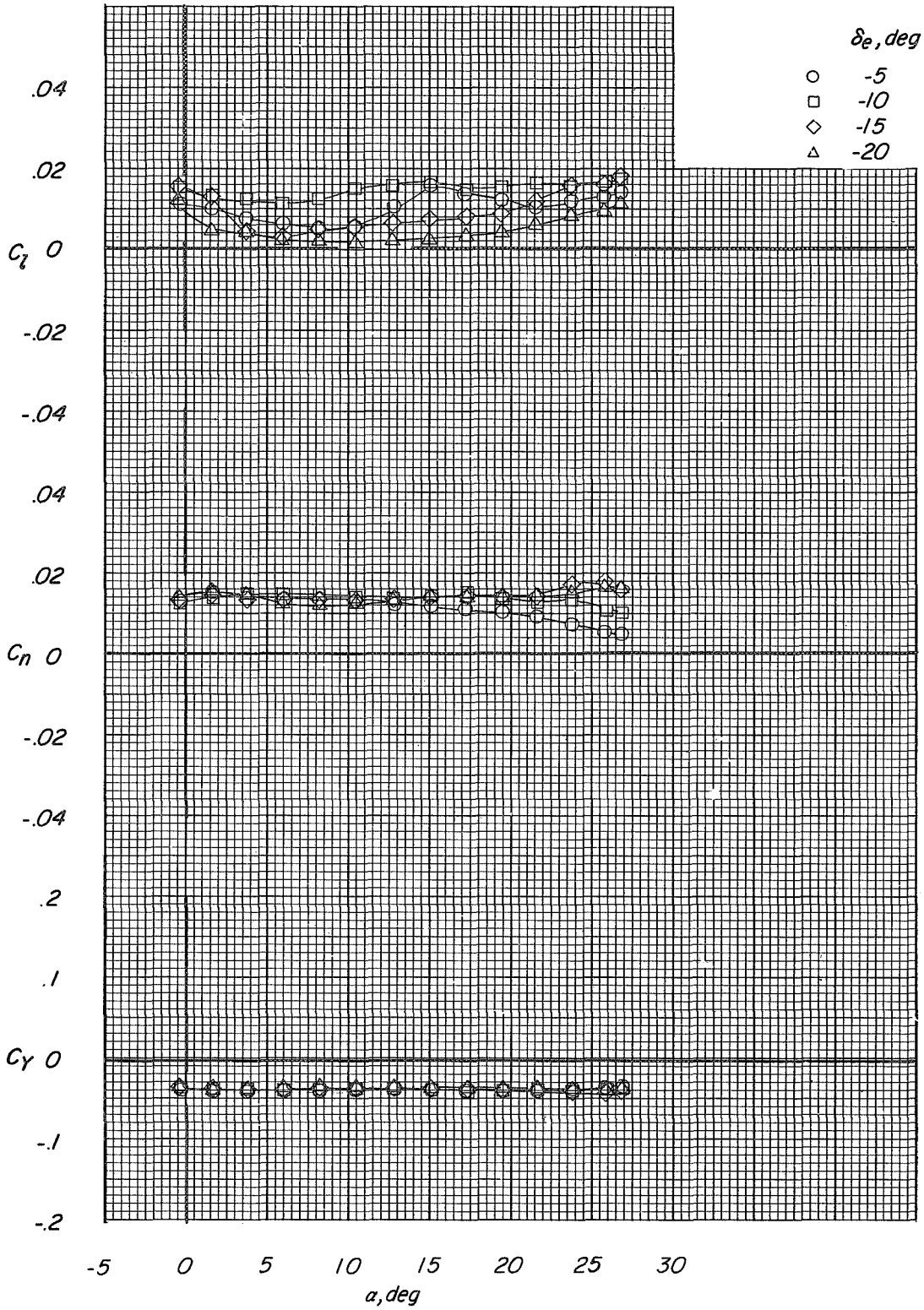
(f) $\beta = 2.3^{\circ}$; $\delta_a = 20^{\circ}$; M = 0.35.

Figure 41.- Continued.



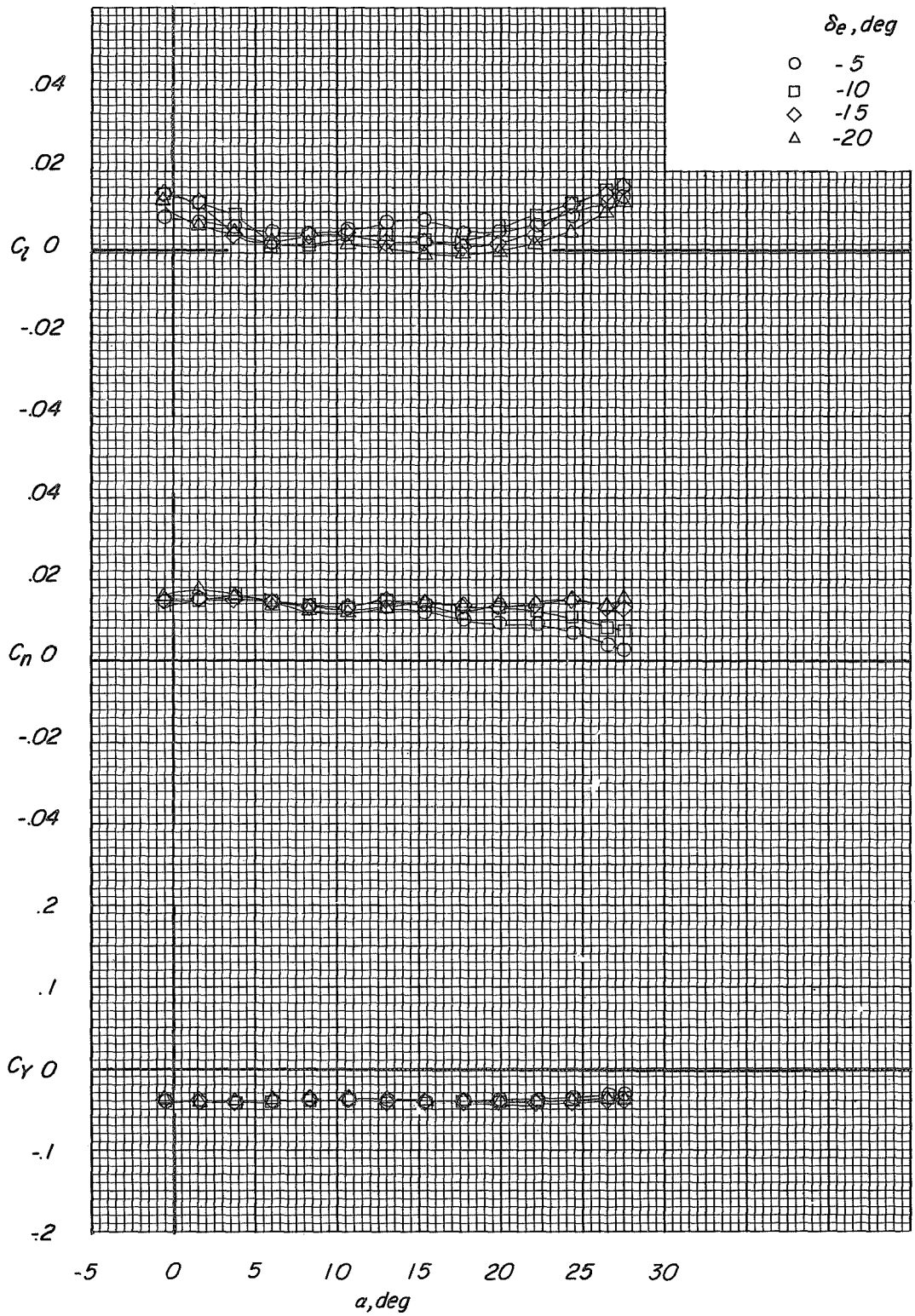
(g) $\beta = 2.3^{o}$; $\delta_a = 20^{o}$; M = 0.50.

Figure 41.- Continued.



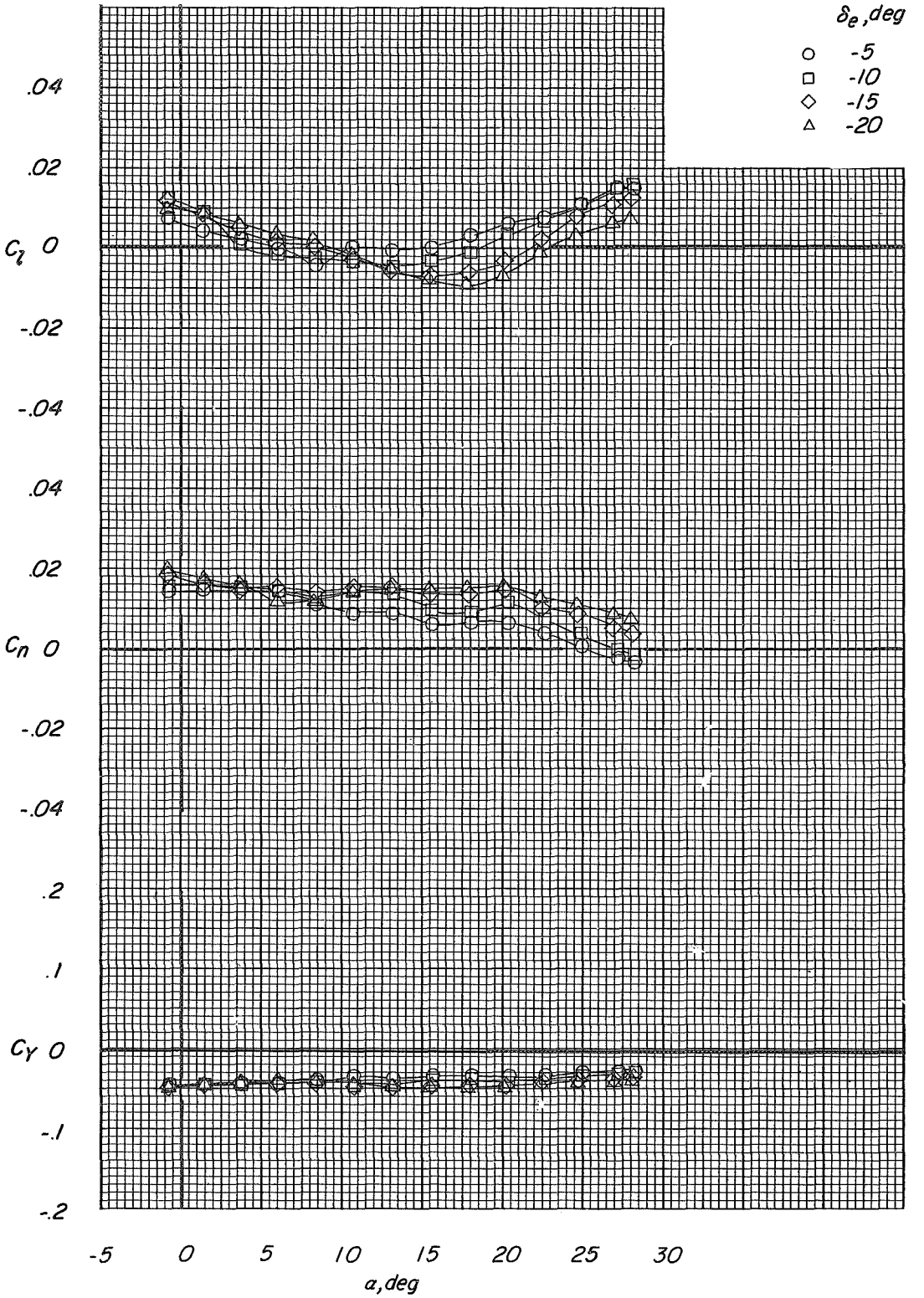
(h) $\beta = 2.3^{o}$; $\delta_a = 20^{o}$; M = 0.60.

Figure 41.- Continued.



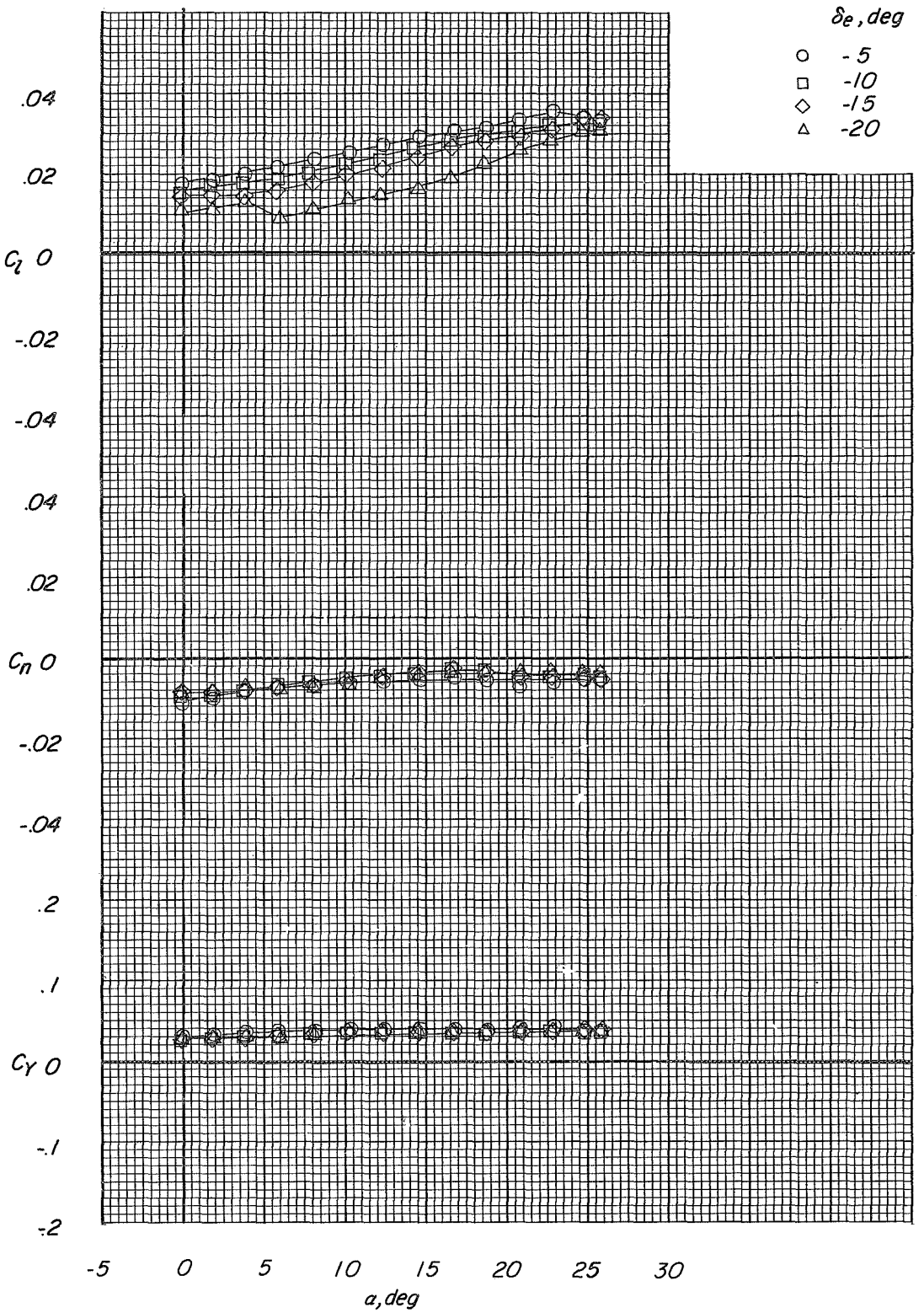
(i) $\beta = 2.3^{\circ}$; $\delta_a = 20^{\circ}$; M = 0.70.

Figure 41.- Continued.



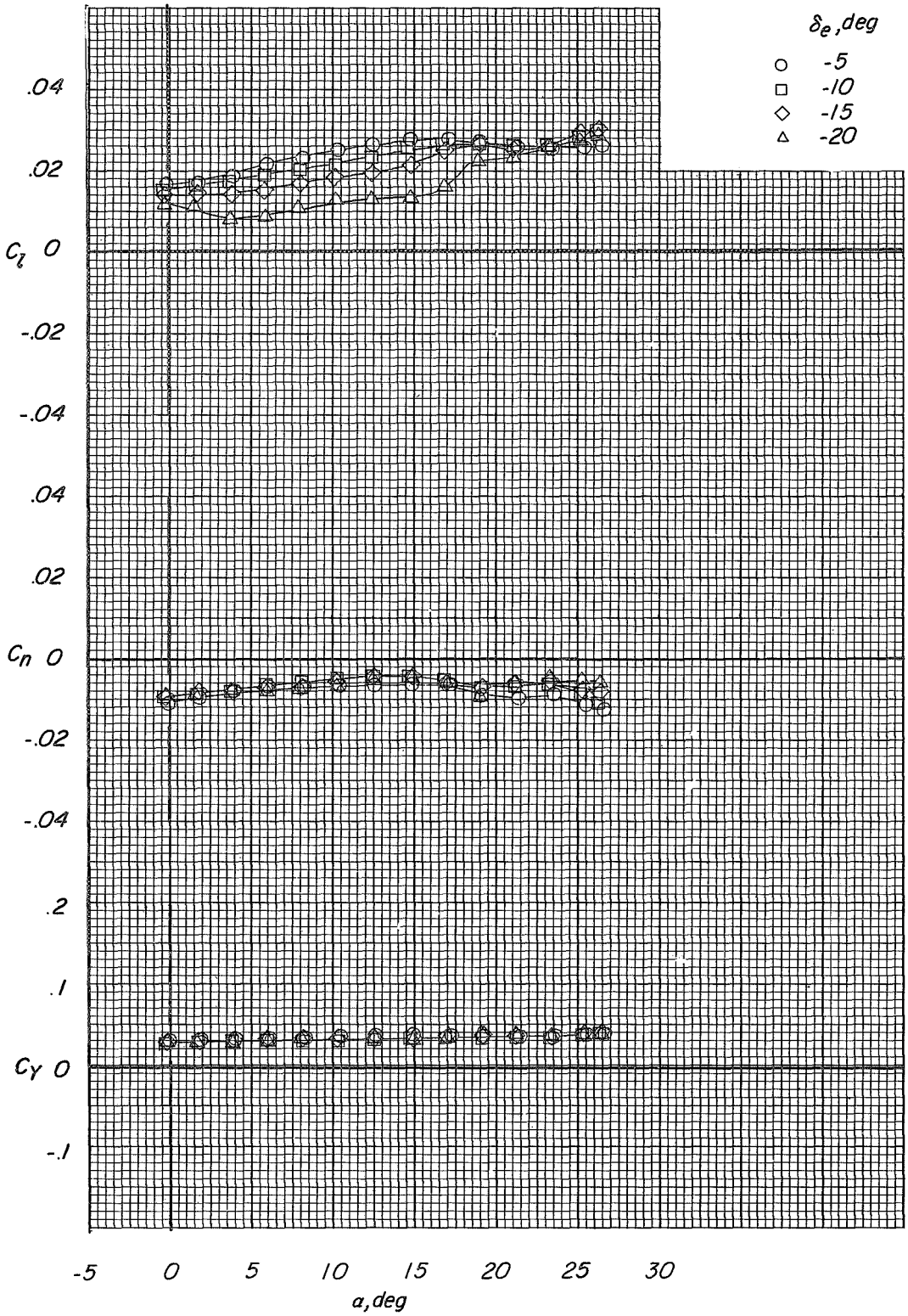
(j) $\beta = 2.3^{\circ}$; $\delta_a = 20^{\circ}$; M = 0.80.

Figure 41.- Continued.



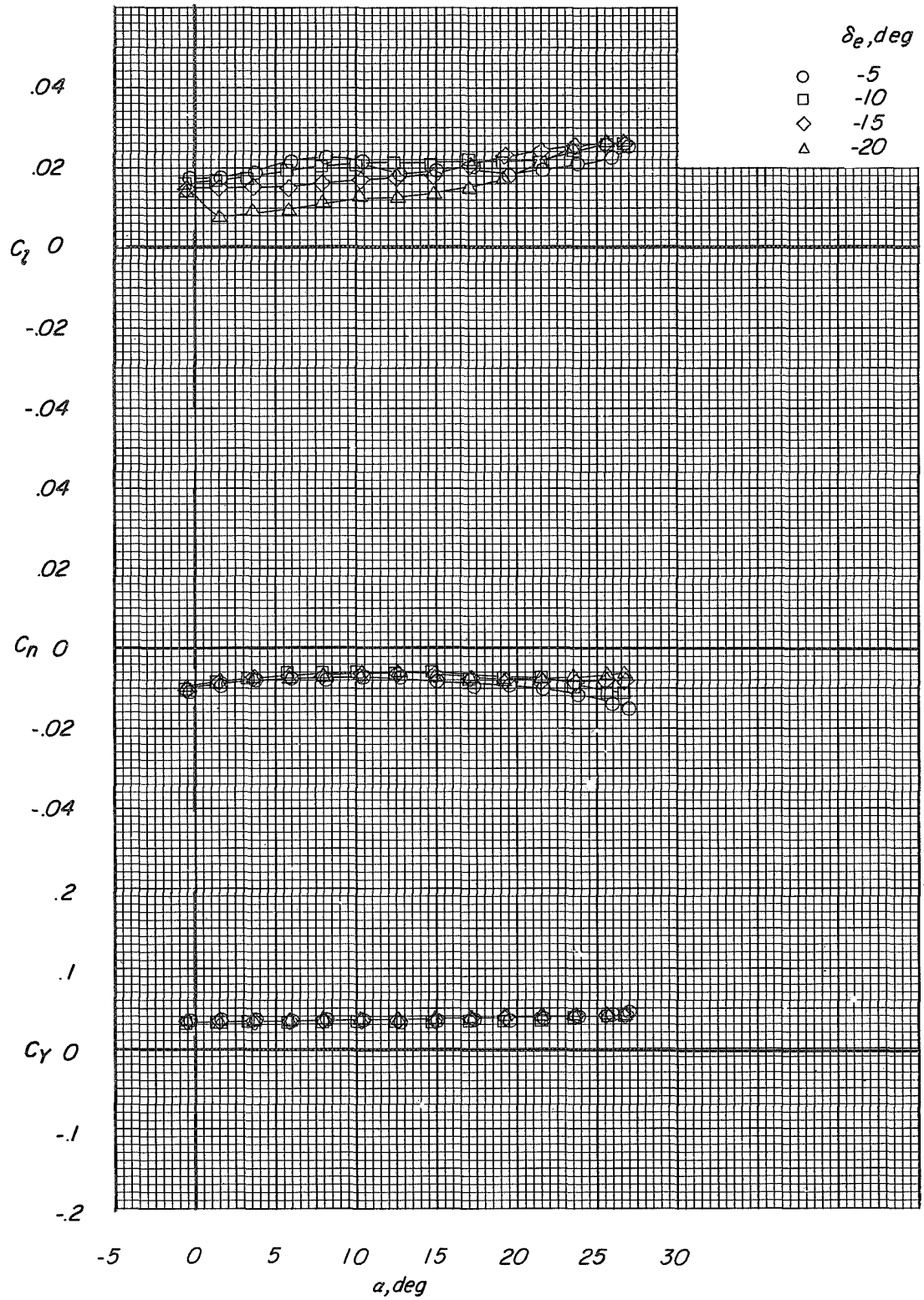
(k) $\beta = -2.3^{o}$; $\delta_a = 10^{o}$; $M = 0.35$.

Figure 41.- Continued.



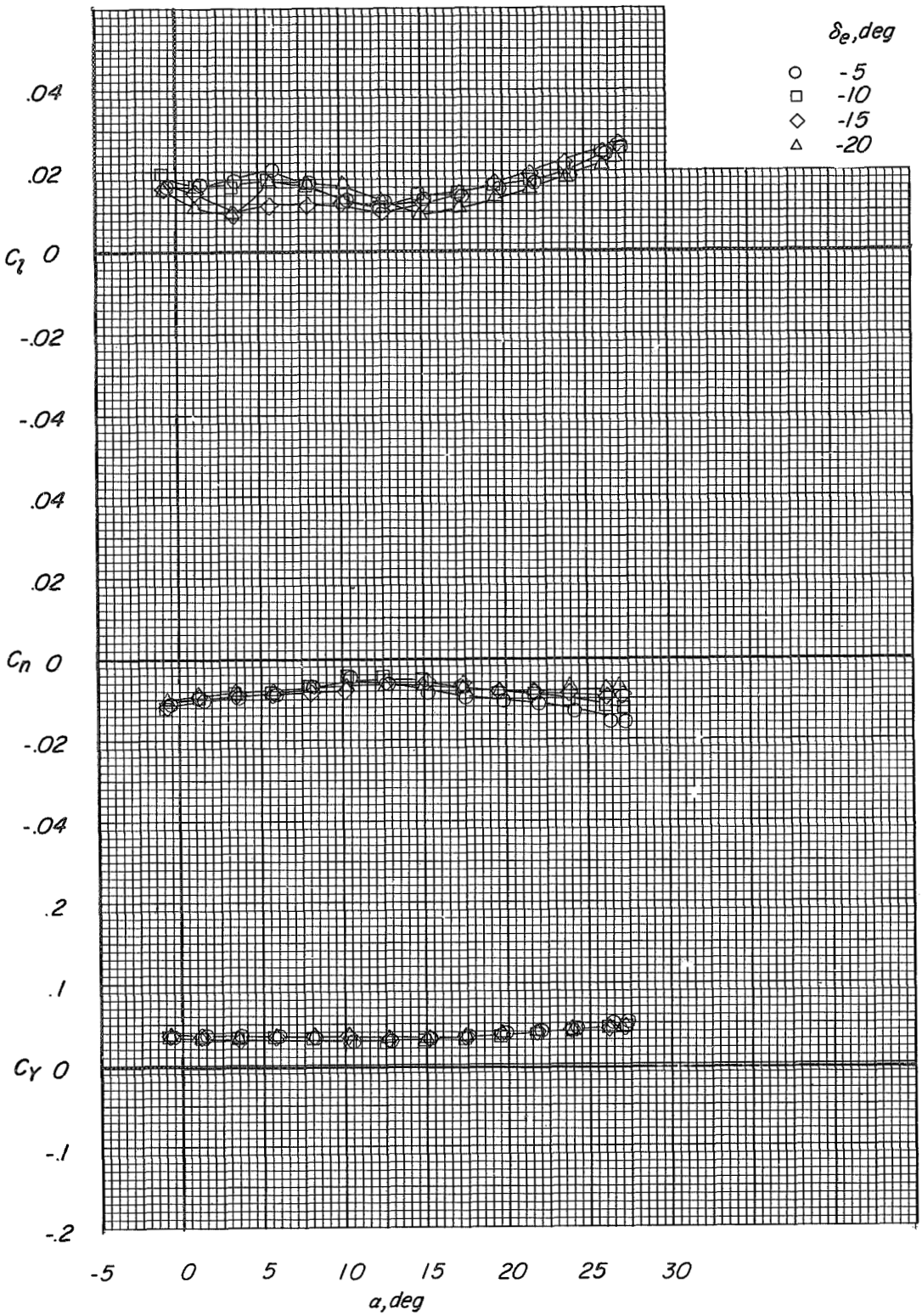
(l) $\beta = -2.3^{o}$; $\delta_a = 10^{o}$; M = 0.50.

Figure 41.- Continued.



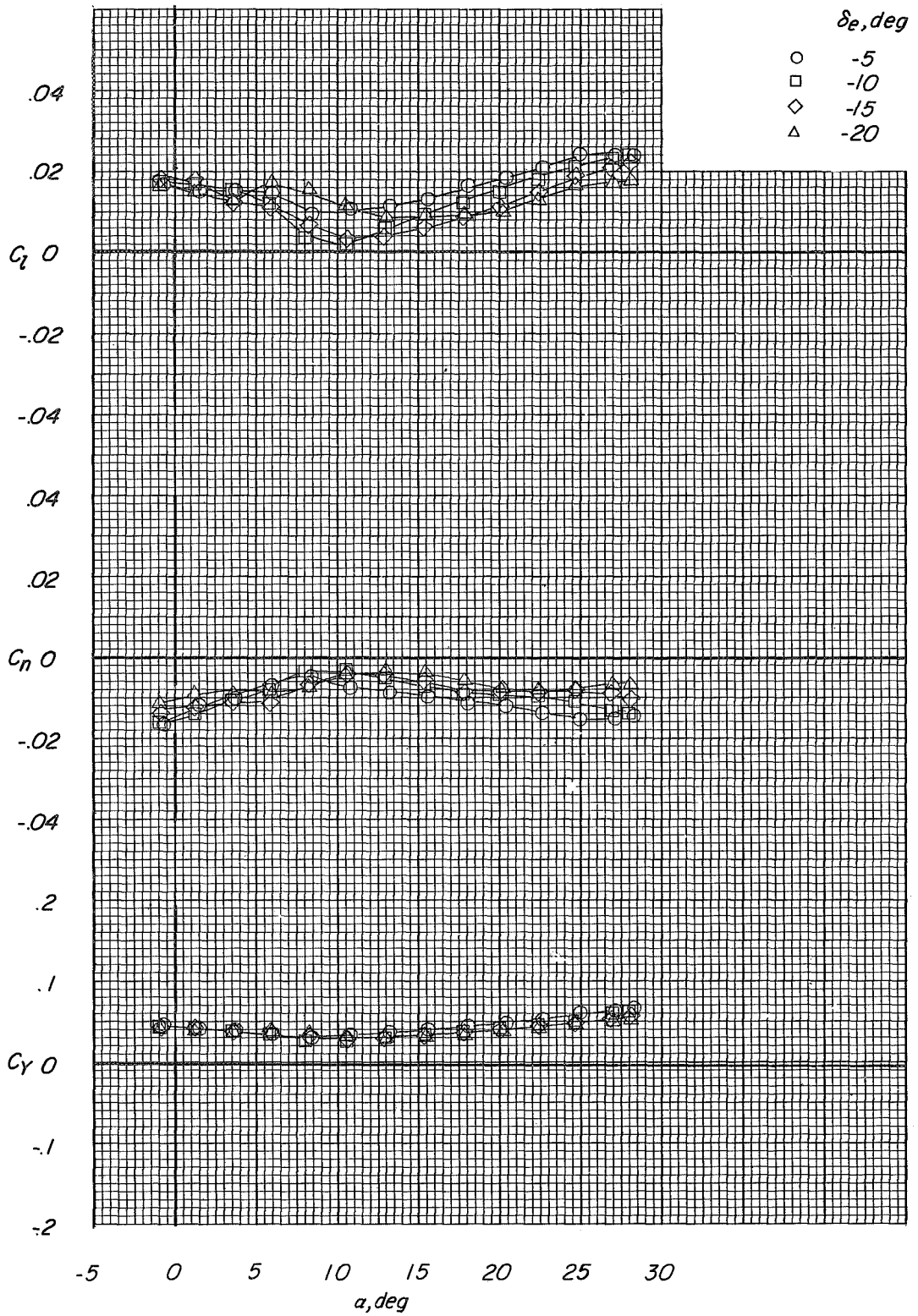
(m) $\beta = -2.3^{o}$; $\delta_a = 10^{o}$; M = 0.60.

Figure 41.- Continued.



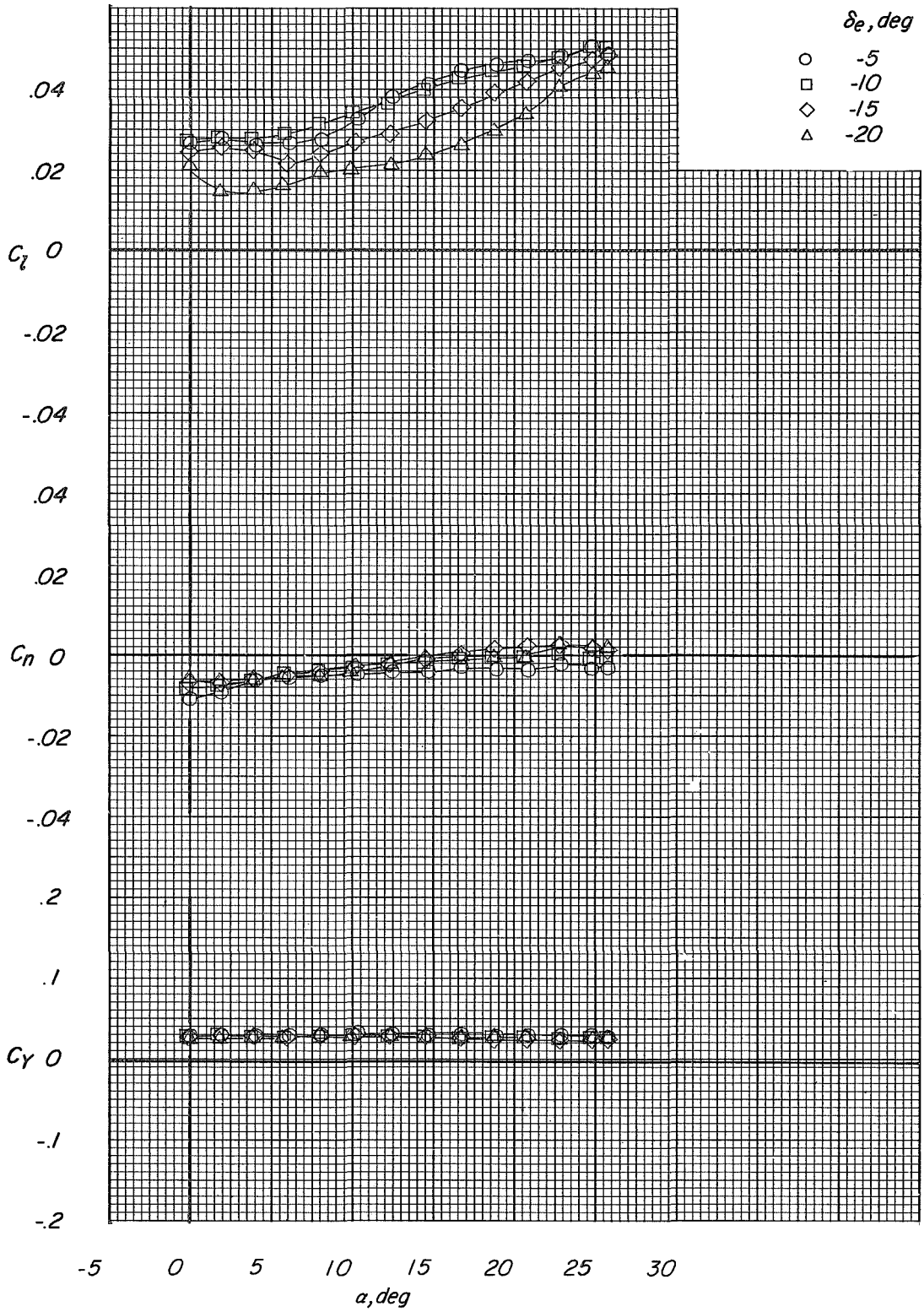
(n) $\beta = -2.3^{\circ}$; $\delta_a = 10^{\circ}$; $M = 0.70$.

Figure 41.- Continued.



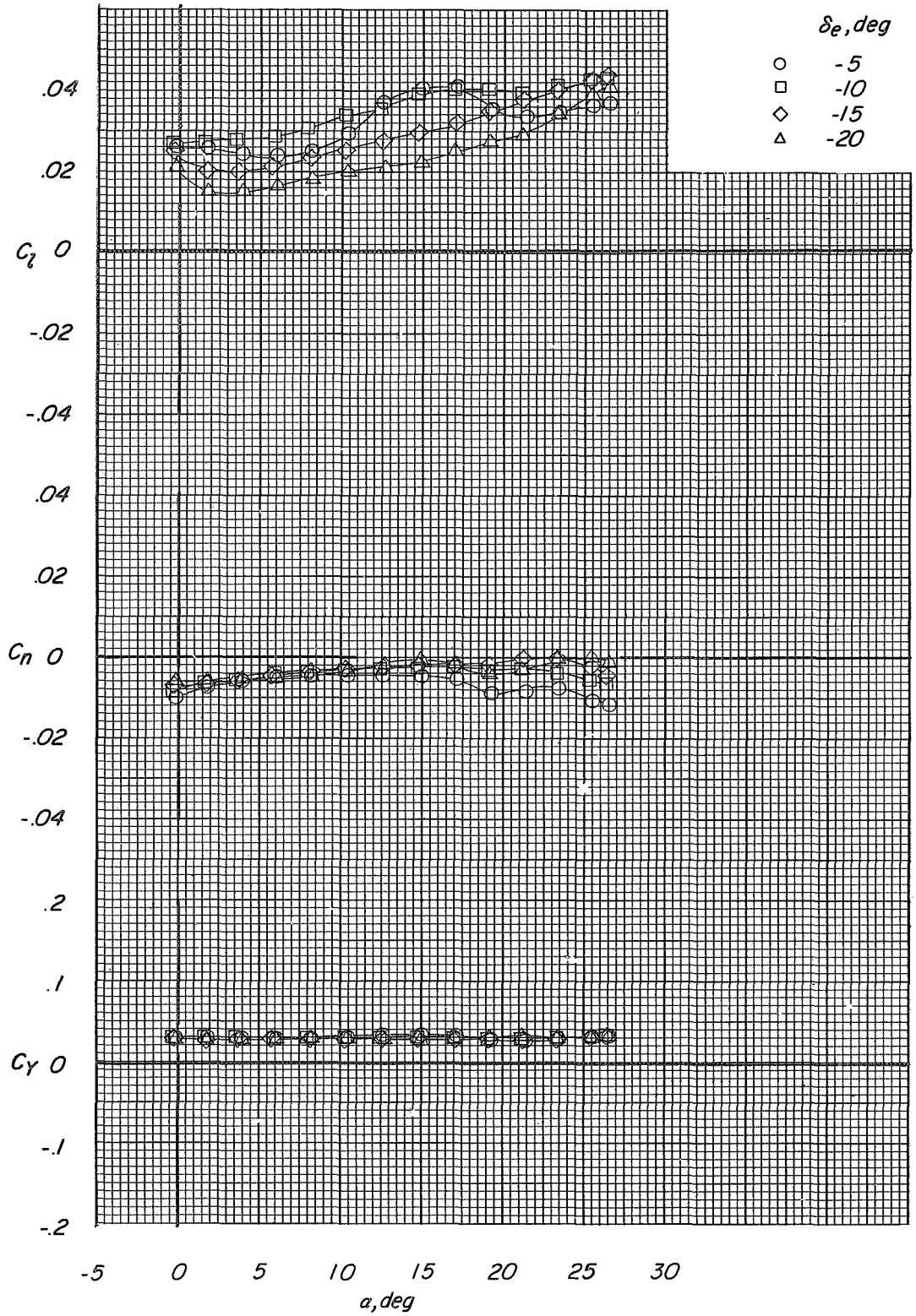
(o) $\beta = -2.3^{o}$; $\delta_a = 10^{o}$; M = 0.80.

Figure 41.- Continued.



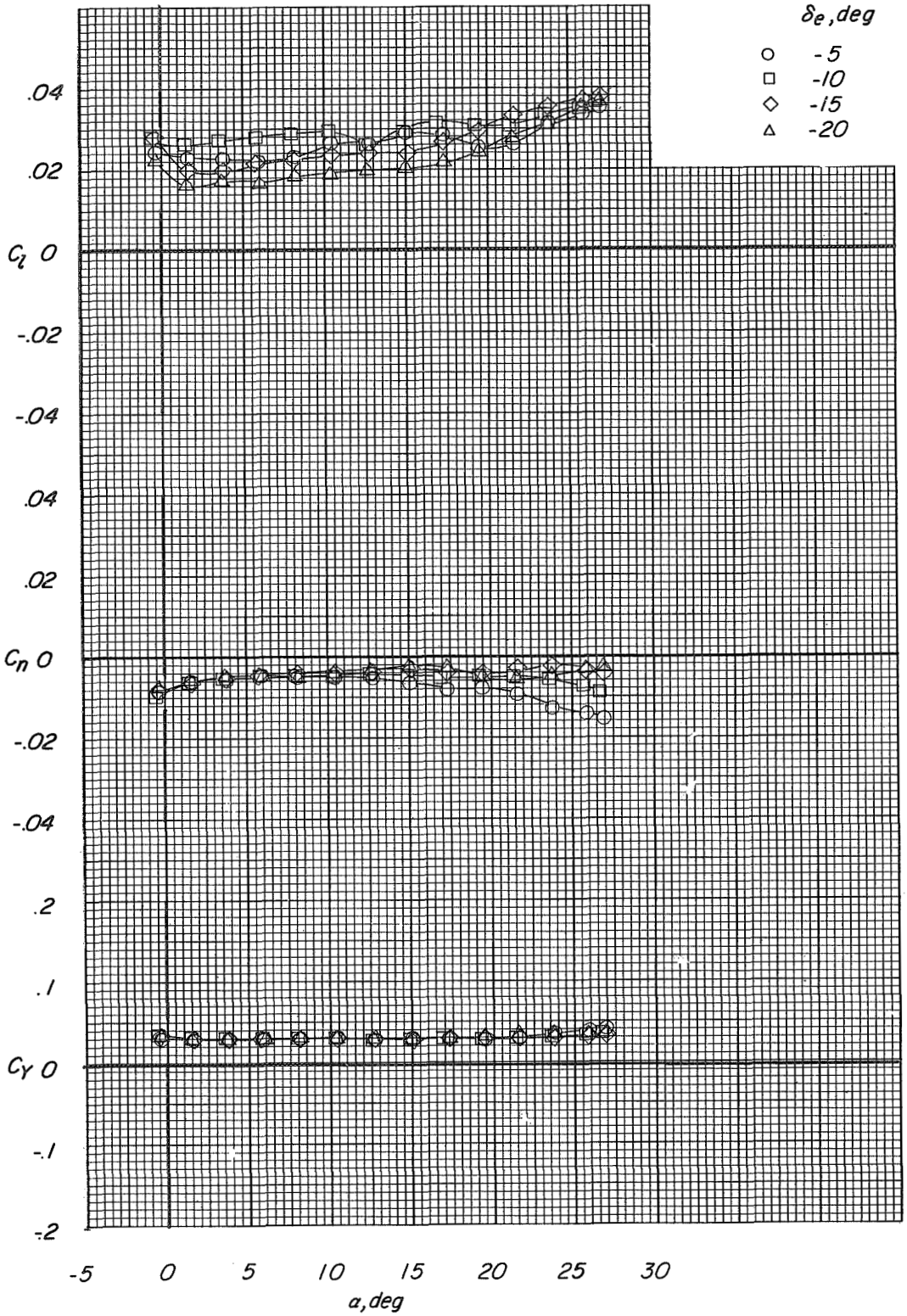
(p) $\beta = -2.3^{o}$; $\delta_a = 20^{o}$; M = 0.35.

Figure 41.- Continued.



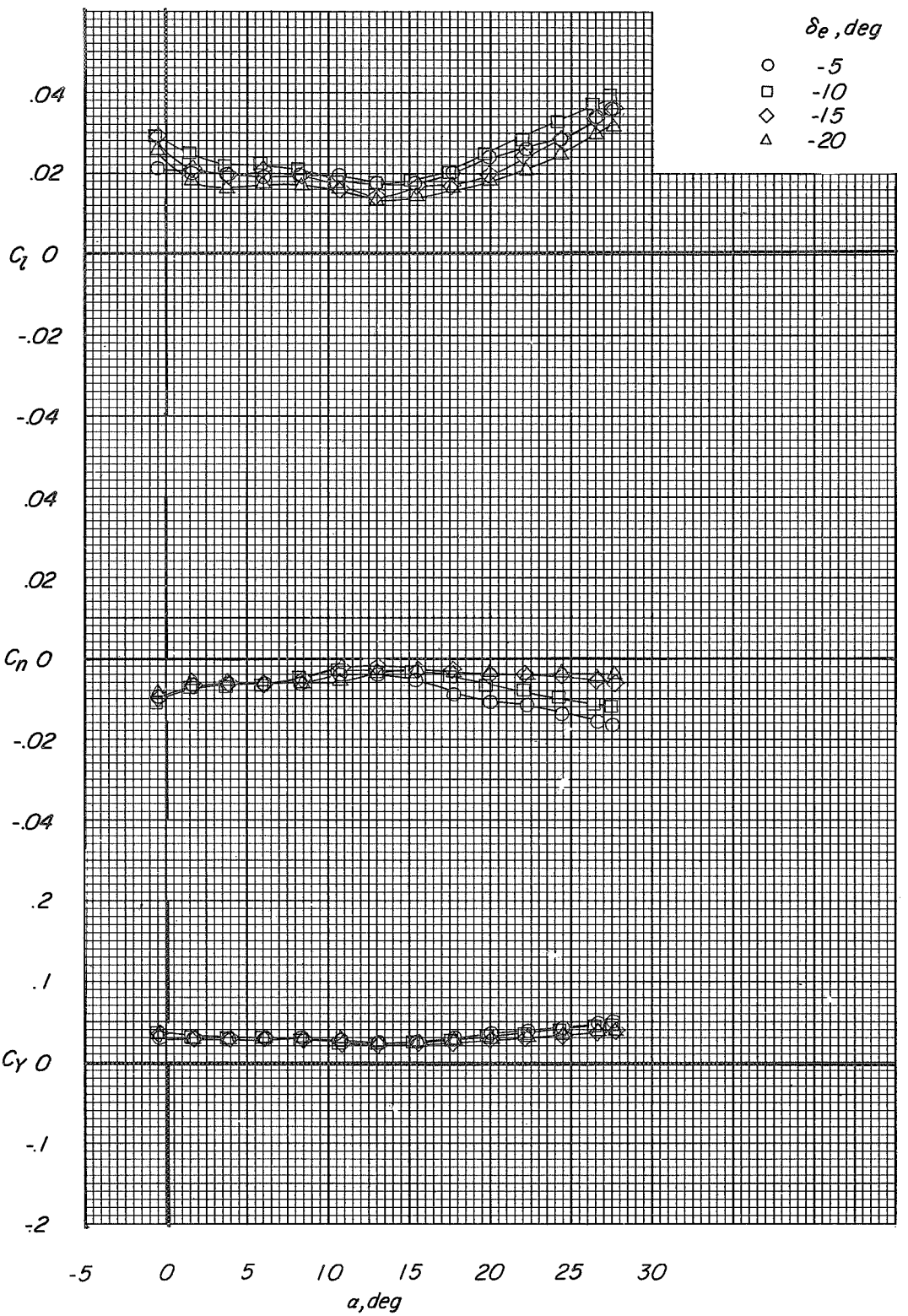
(q) $\beta = -2.3^{\circ}$; $\delta_a = 20^{\circ}$; M = 0.50.

Figure 41.- Continued.



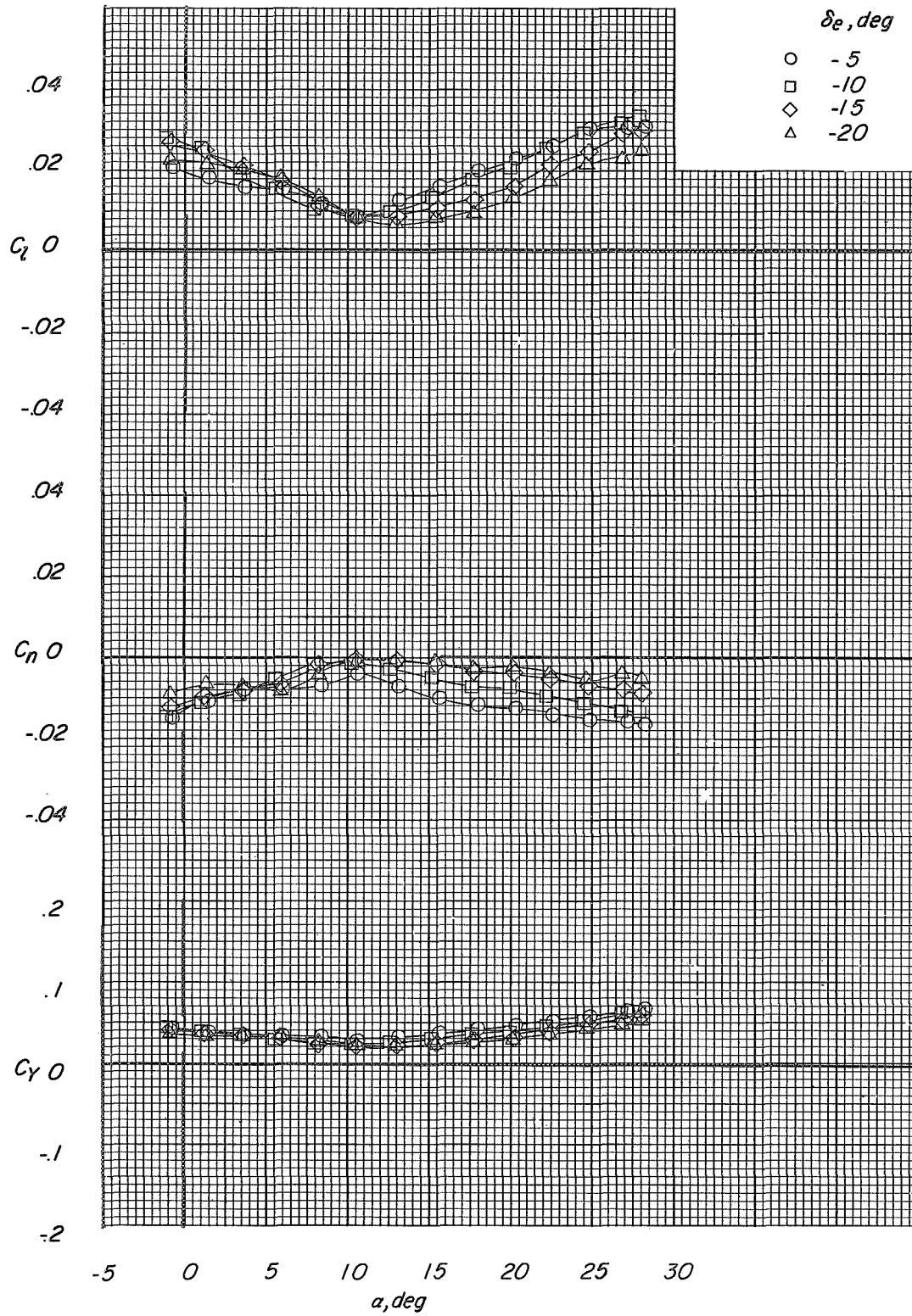
(r) $\beta = -2.3^{o}$; $\delta_a = 20^{o}$; M = 0.60.

Figure 41.- Continued.



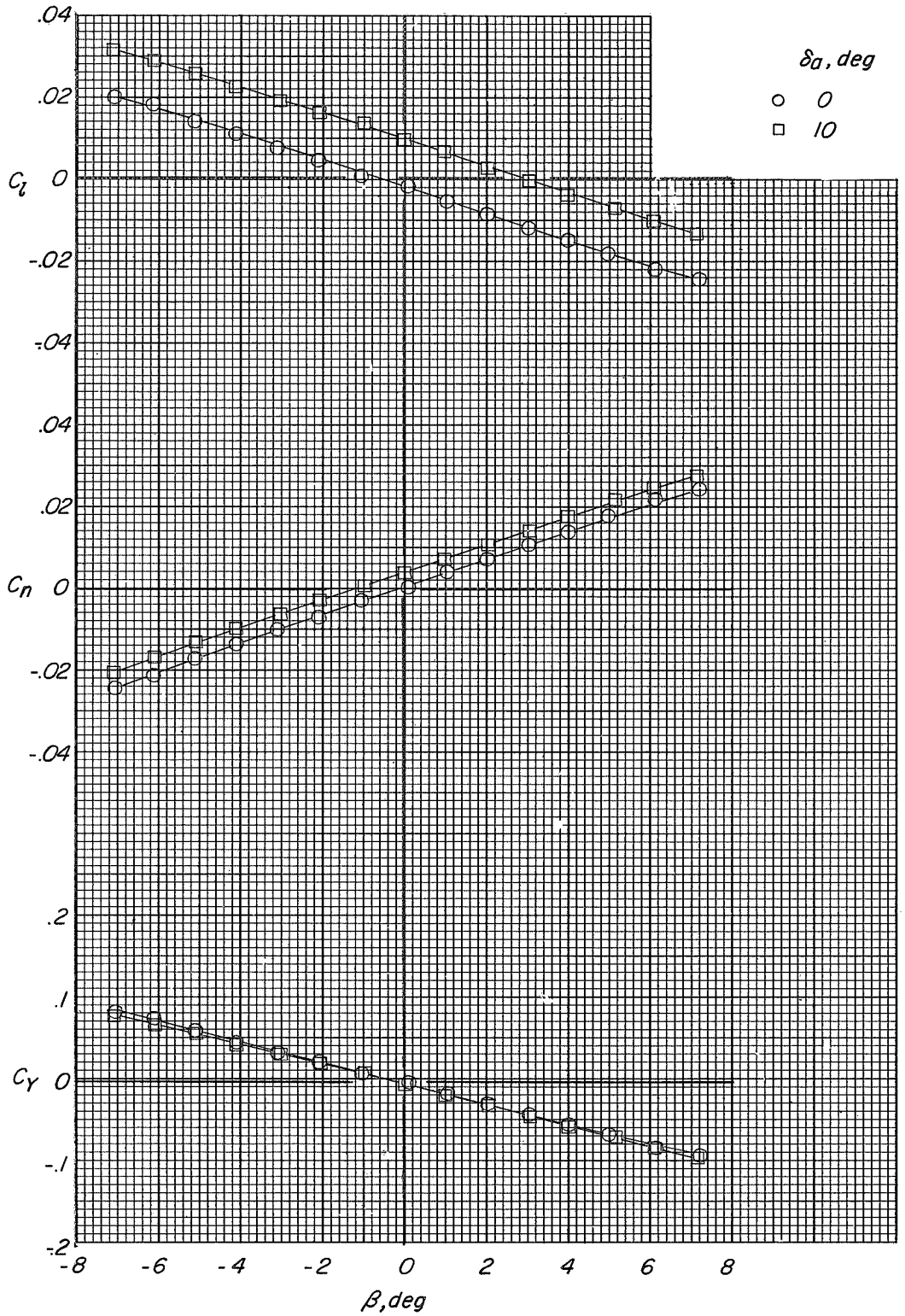
(s) $\beta = -2.3^{o}$; $\delta_a = 20^{o}$; M = 0.70.

Figure 41.- Continued.



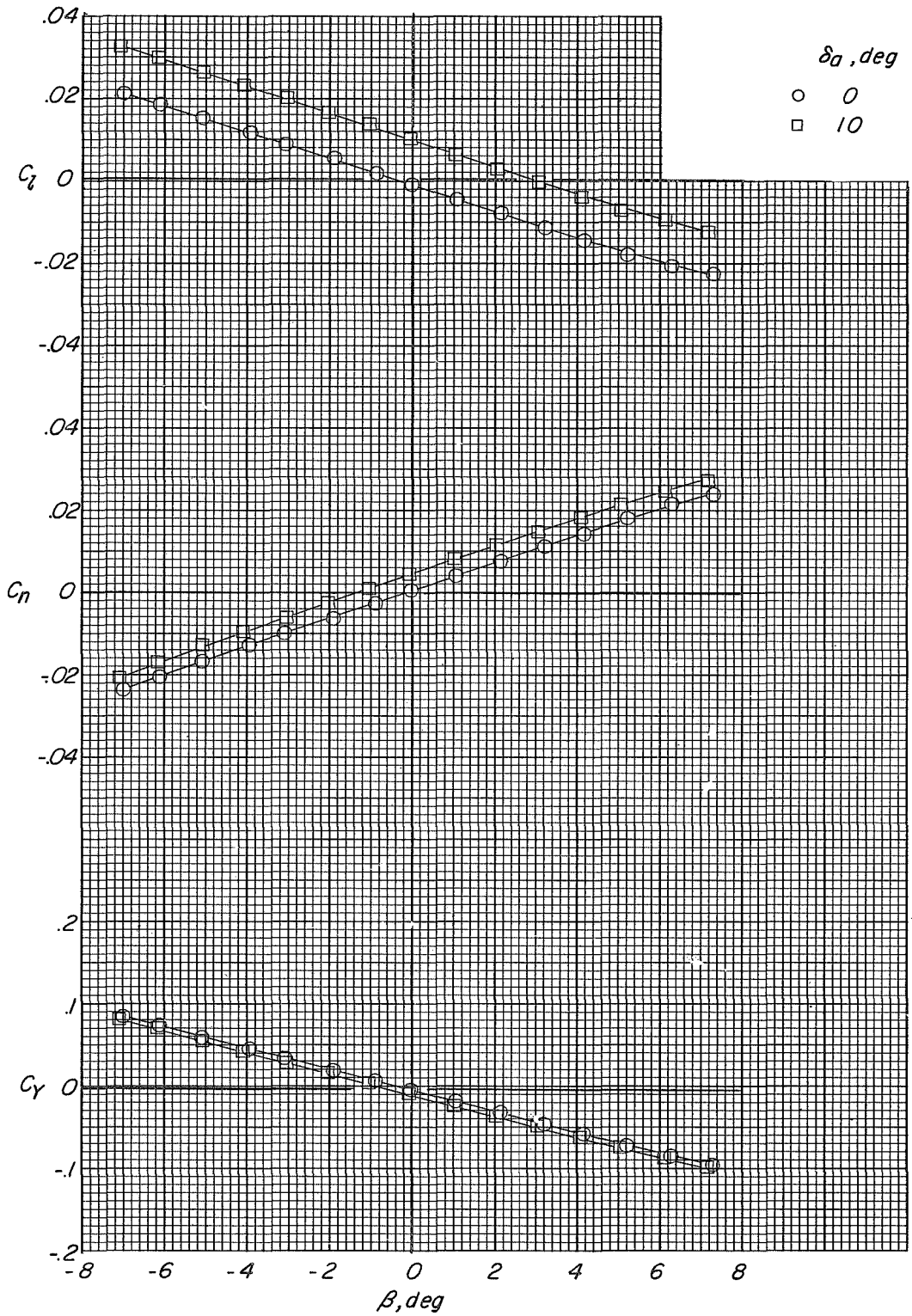
(t) $\beta = -2.3^{o}$; $\delta_a = 20^{o}$; M = 0.80.

Figure 41.- Concluded.



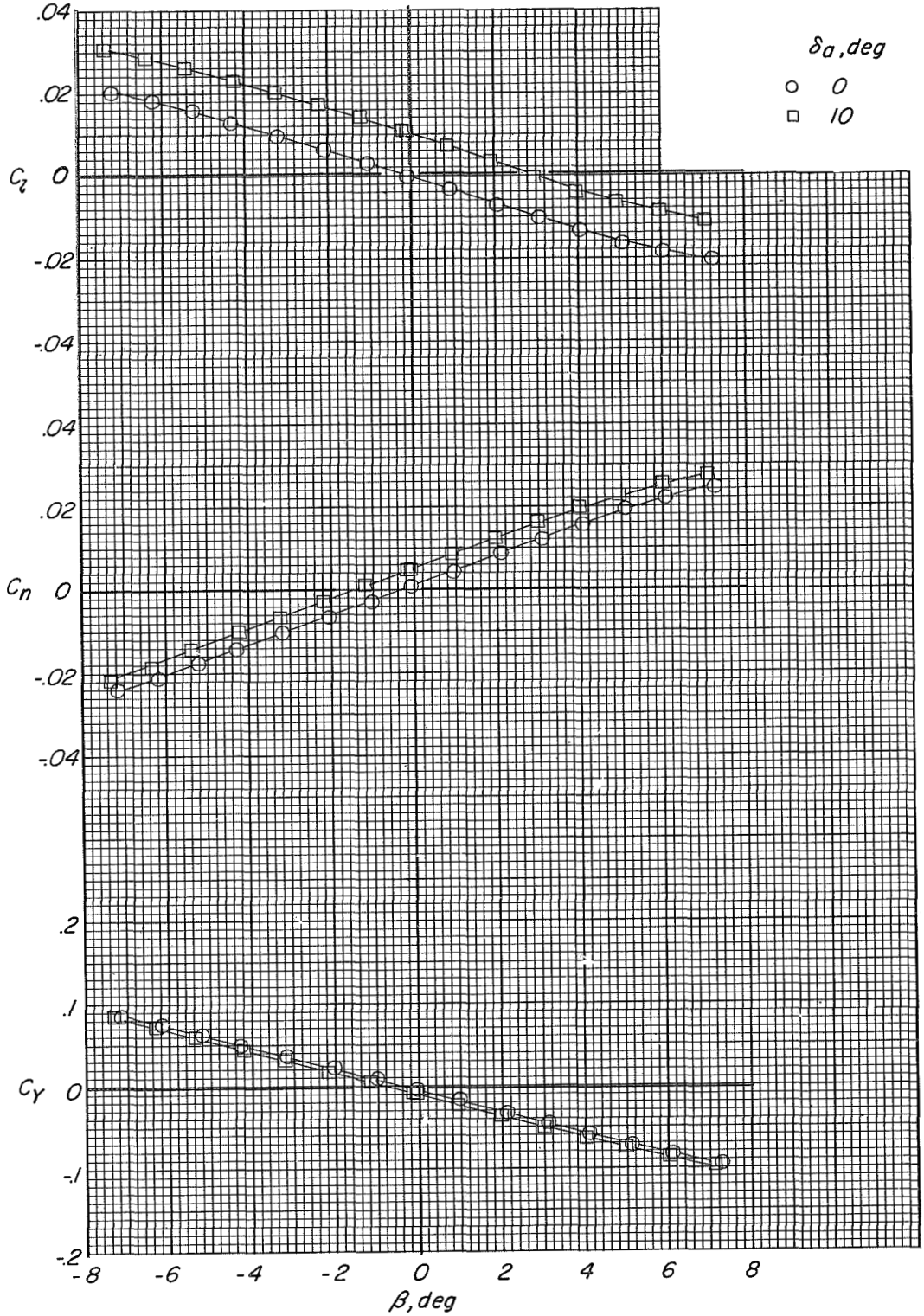
(a) M = 0.35.

Figure 42.- Variation of the lateral force and moment coefficients with sideslip angle. Modification II fin configuration; auxiliary flaps in the subsonic position; $\alpha = 7^{o}$; $\delta_e = -10^{o}$.



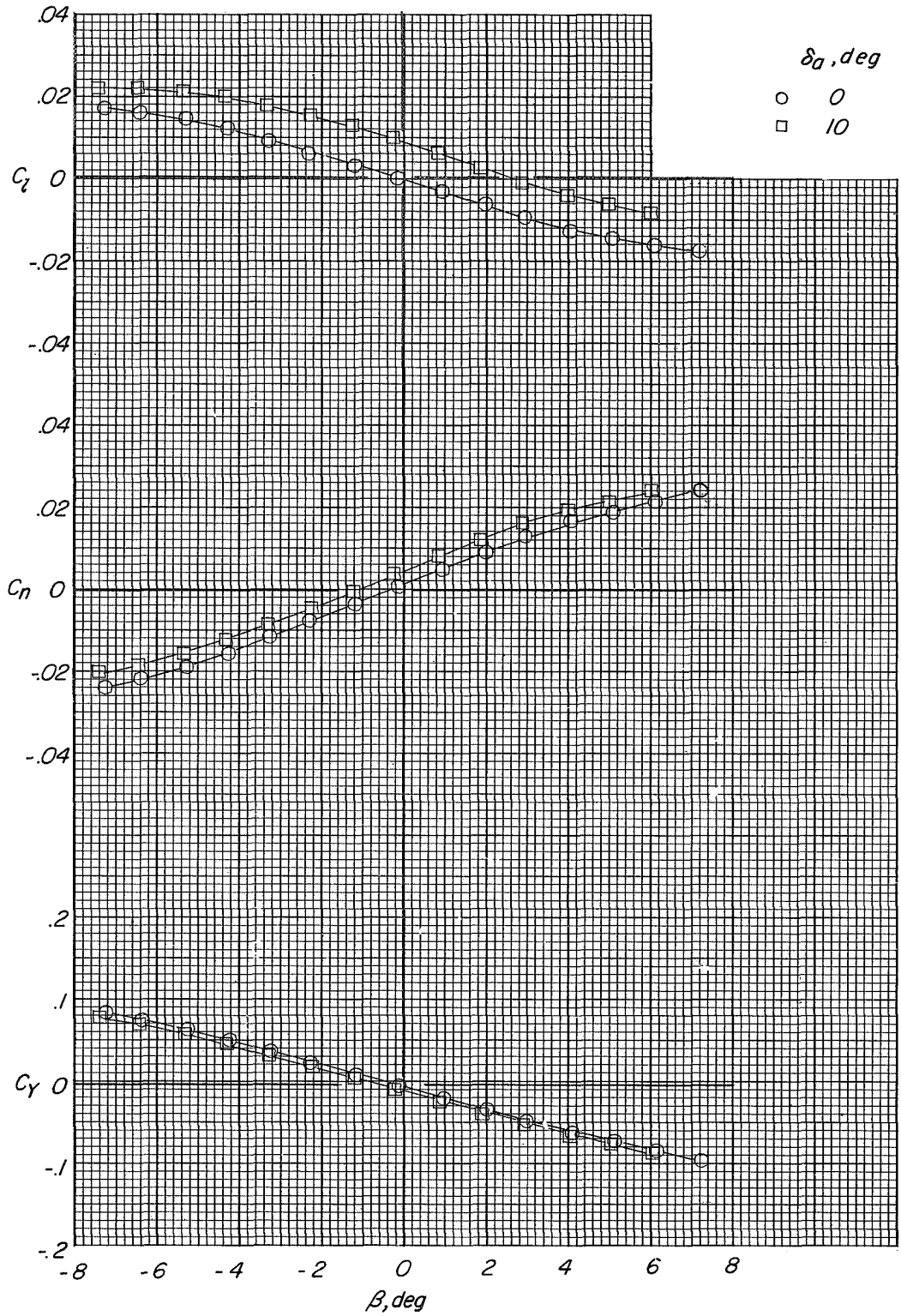
(b) M = 0.50.

Figure 42.- Continued.



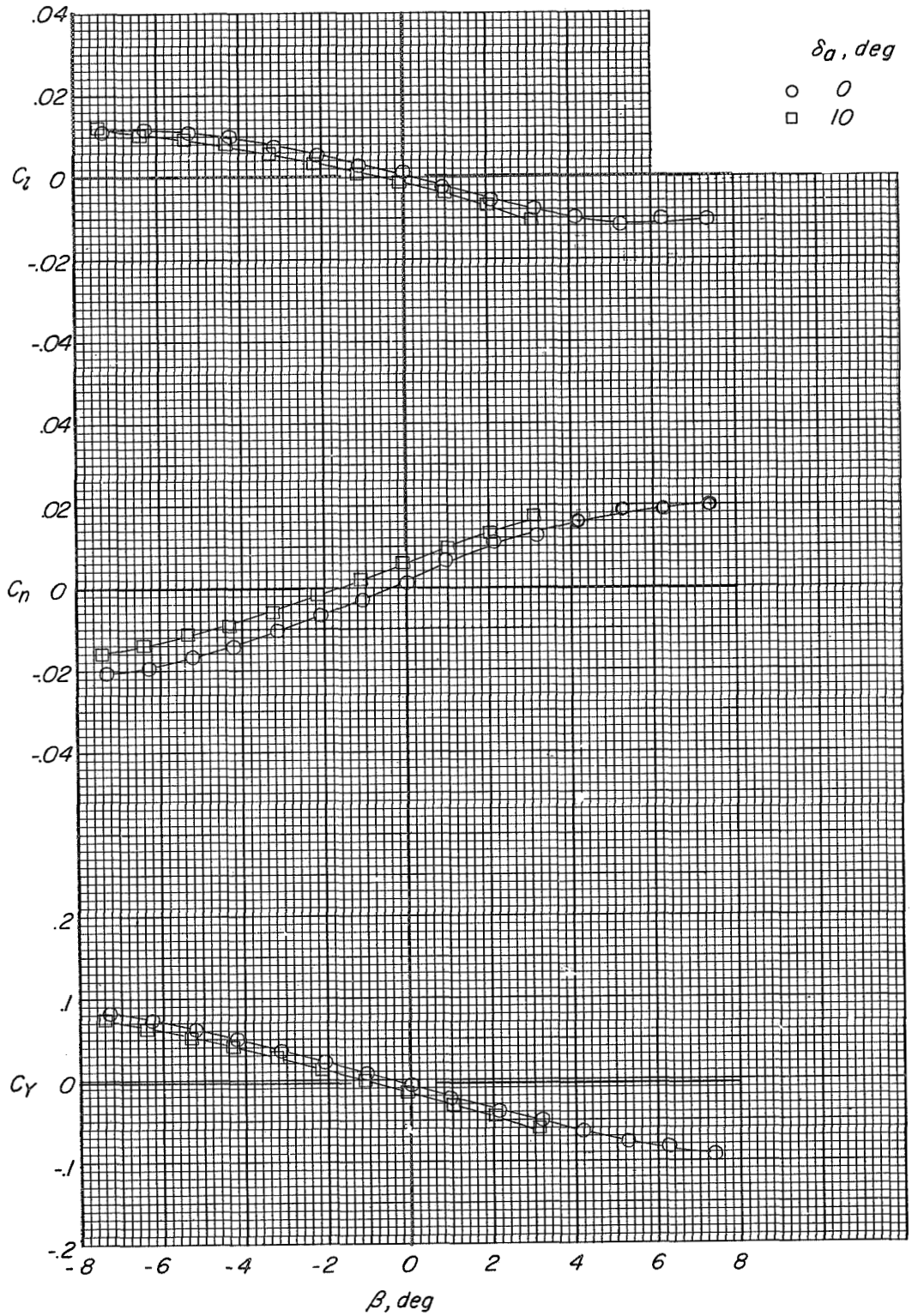
(c) M = 0.60.

Figure 42.- Continued.



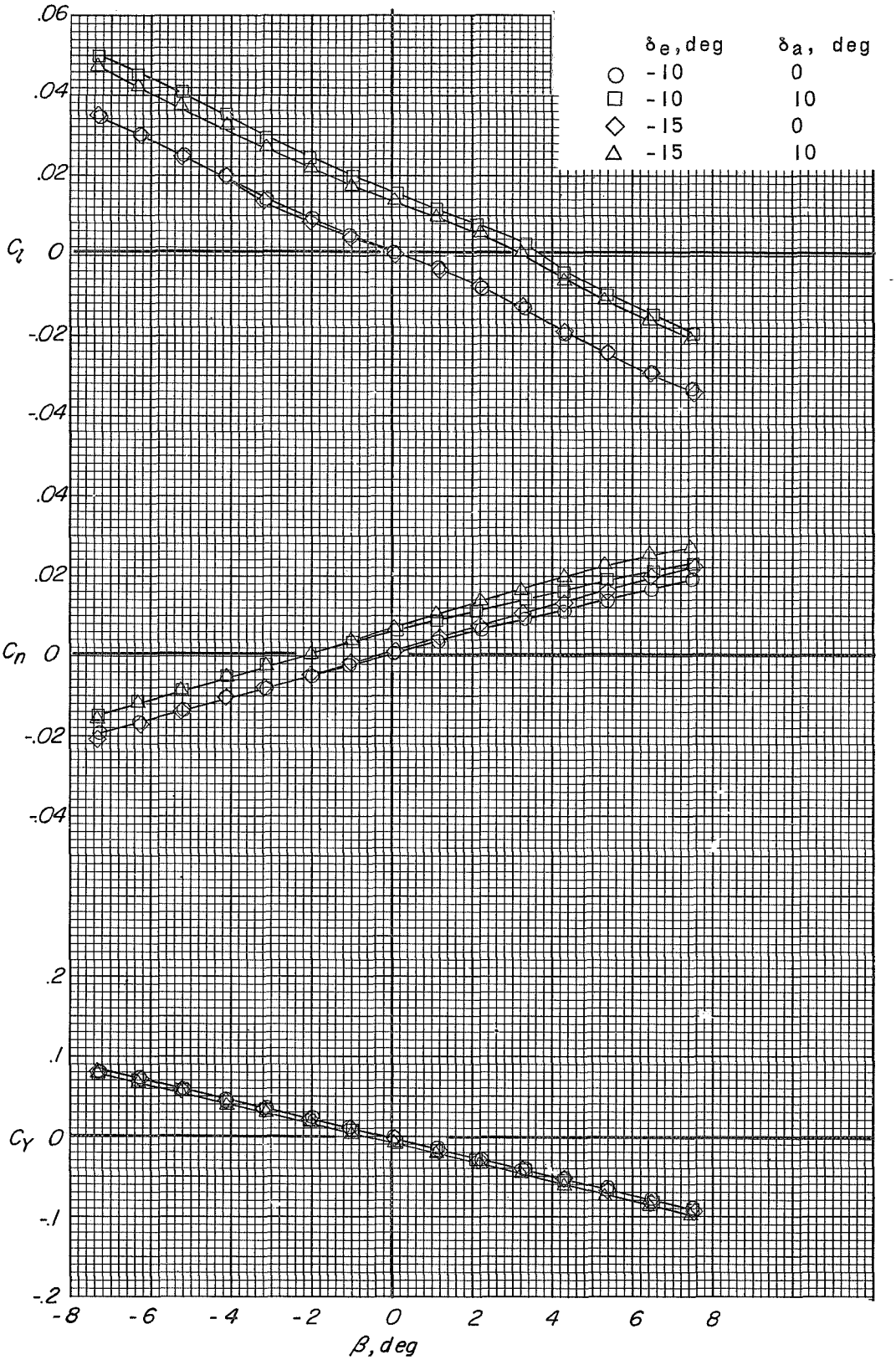
(d) M = 0.70.

Figure 42.- Continued.



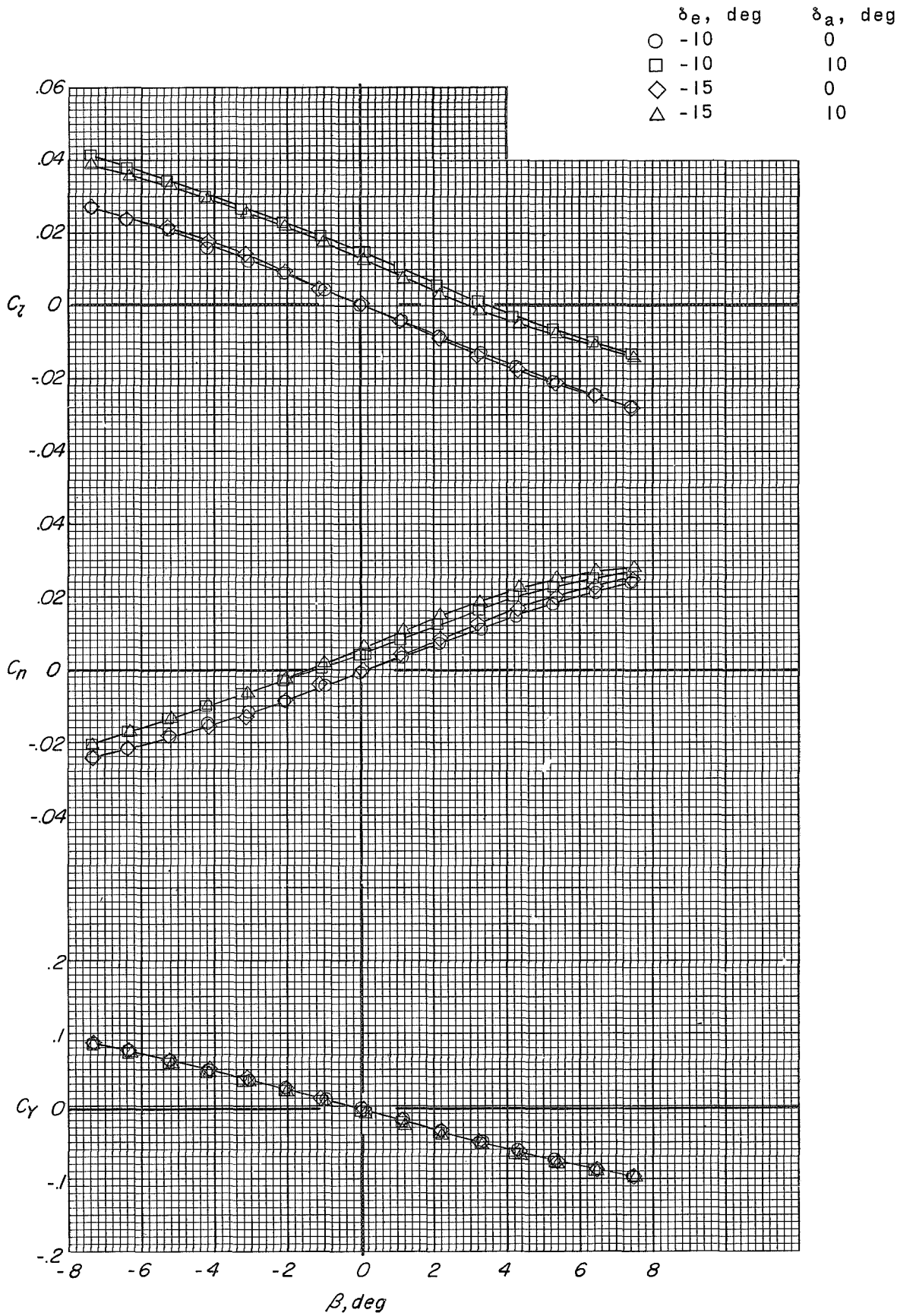
(e) M = 0.80.

Figure 42.- Concluded.



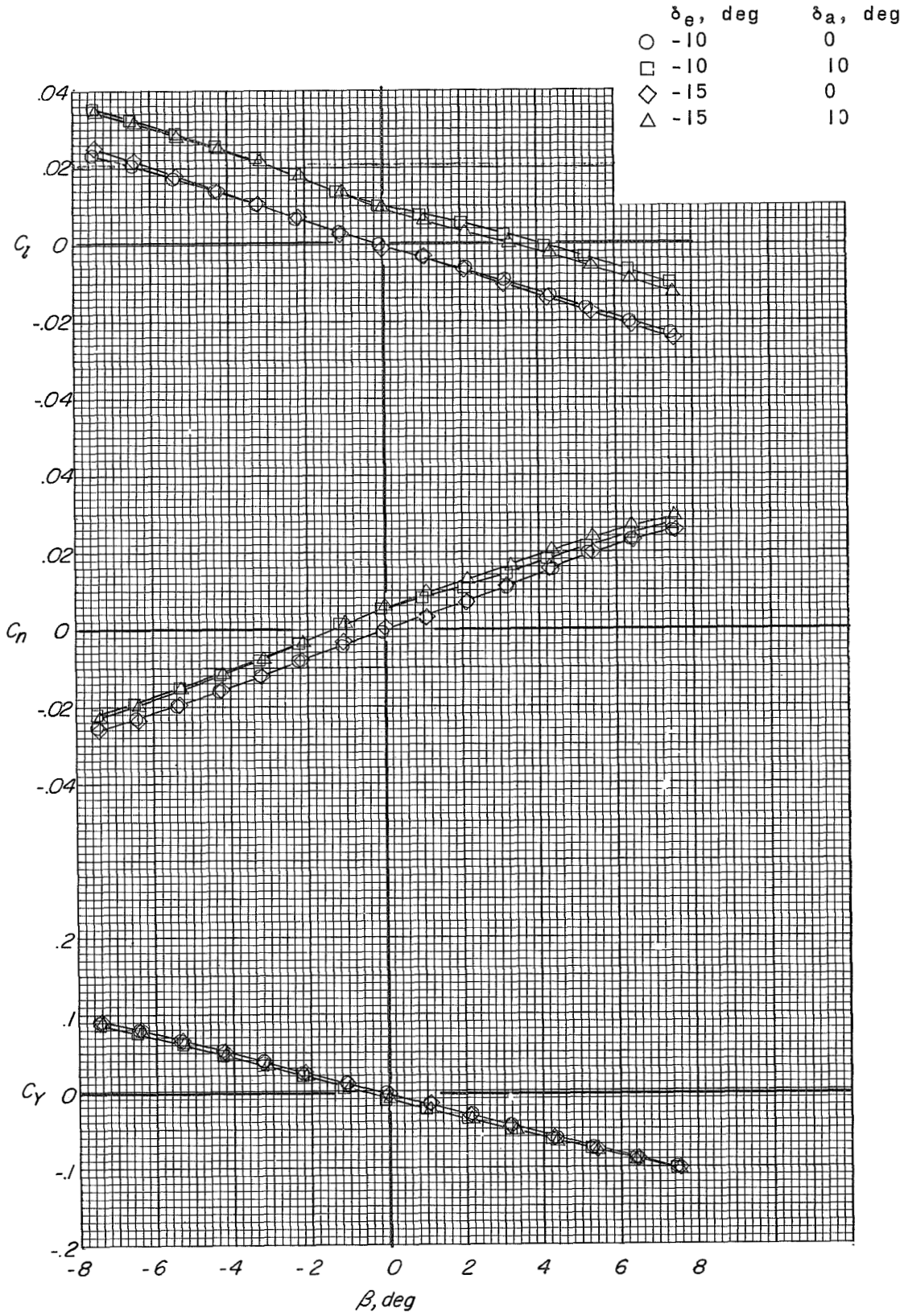
(a) M = 0.35.

Figure 43.- Variation of the lateral force and moment coefficients with sideslip angle. Modification II fin configuration; auxiliary flaps in the subsonic position; $\alpha = 17^{o}$.



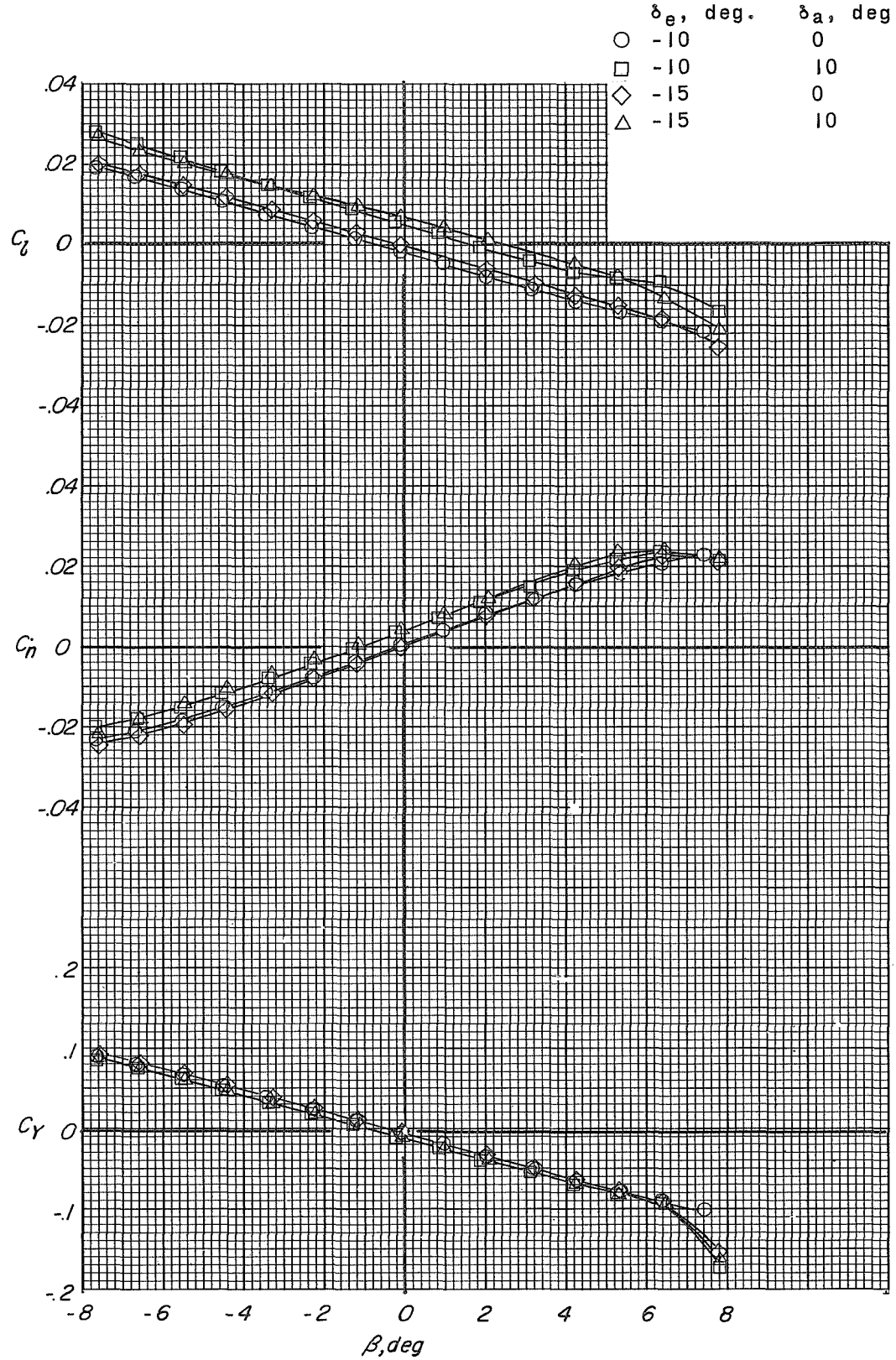
(b) M = 0.50.

Figure 43.- Continued.



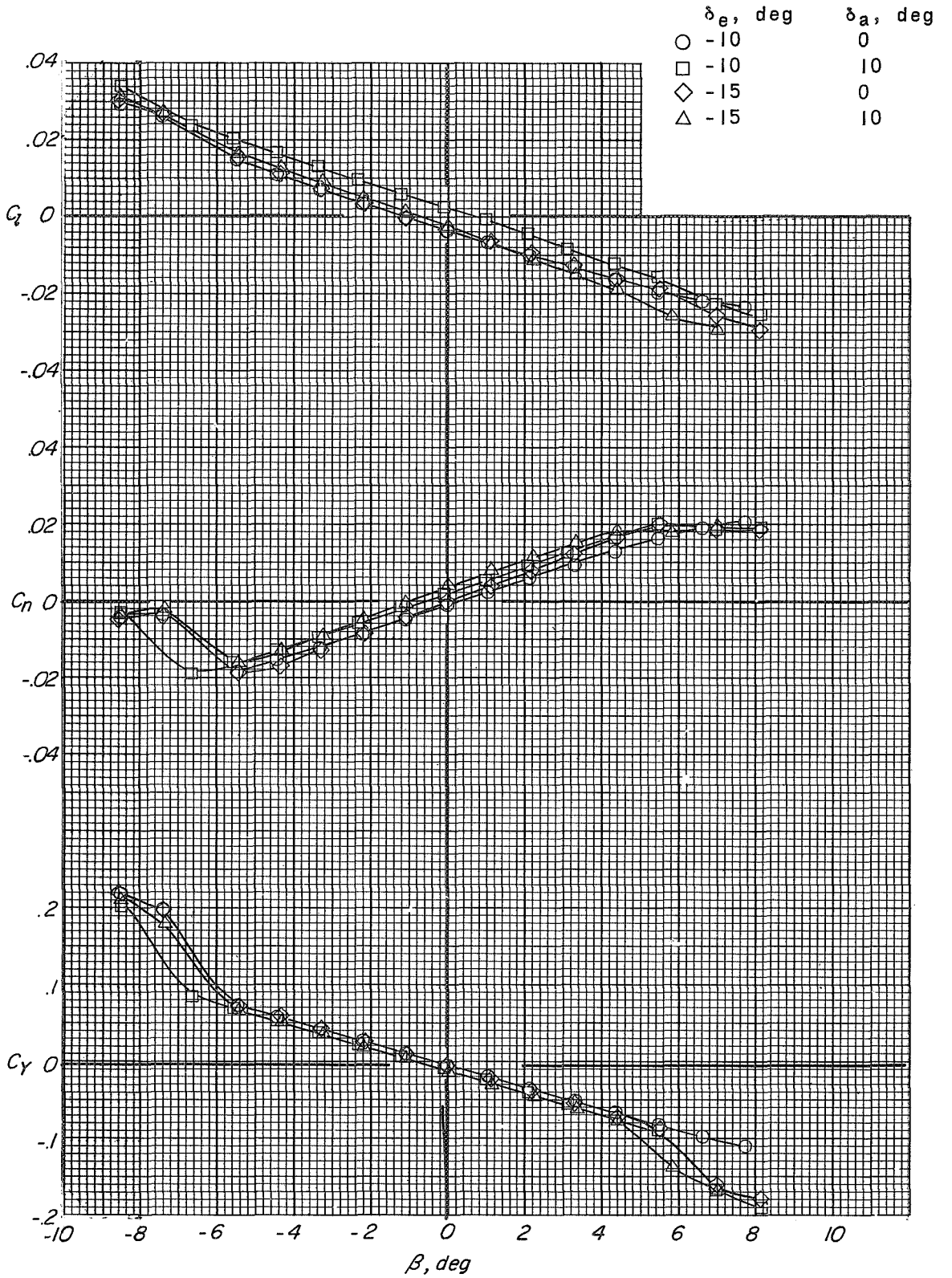
(c) M = 0.60.

Figure 43.- Continued.



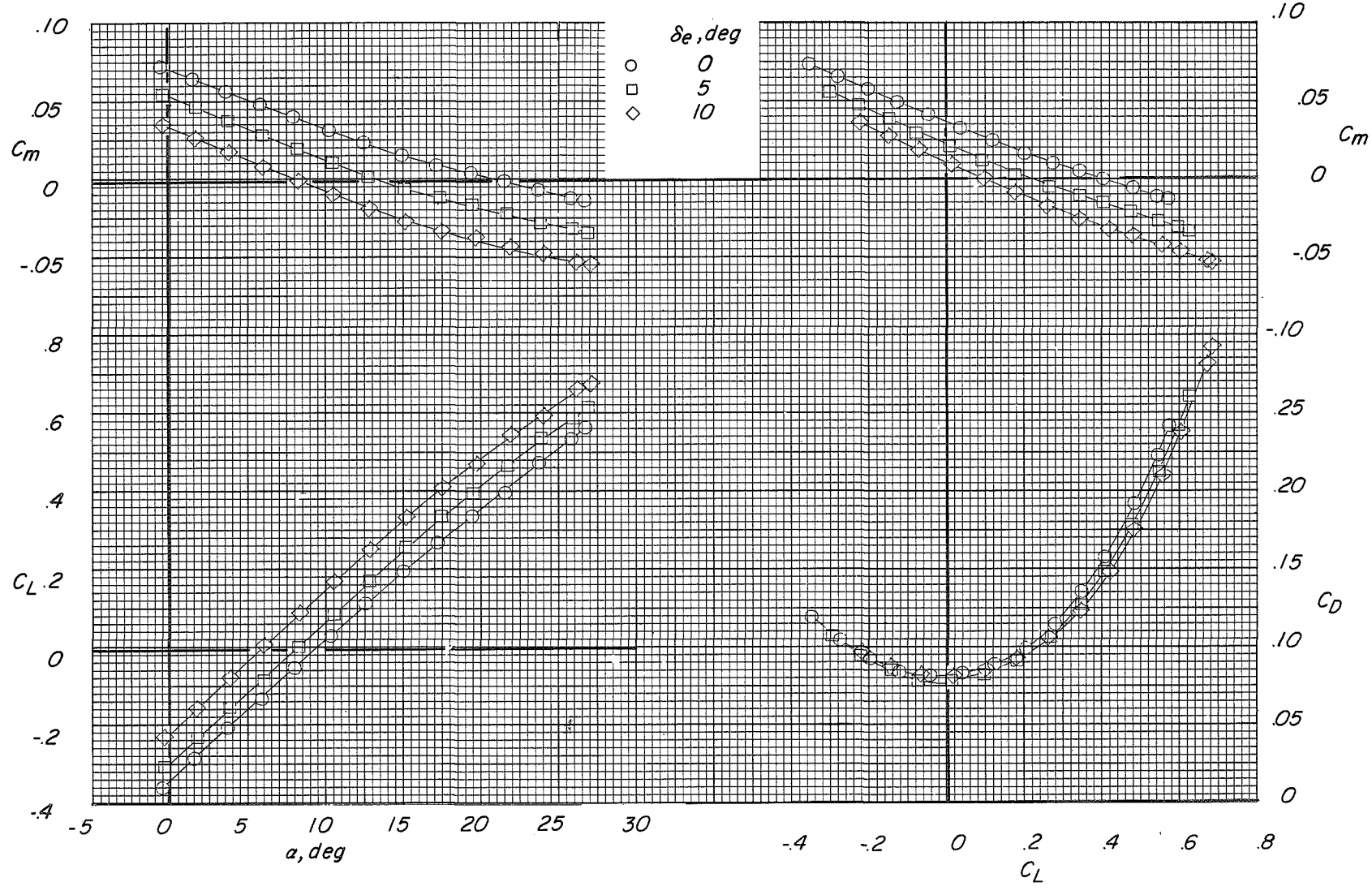
(d) M = 0.70.

Figure 43.- Continued.



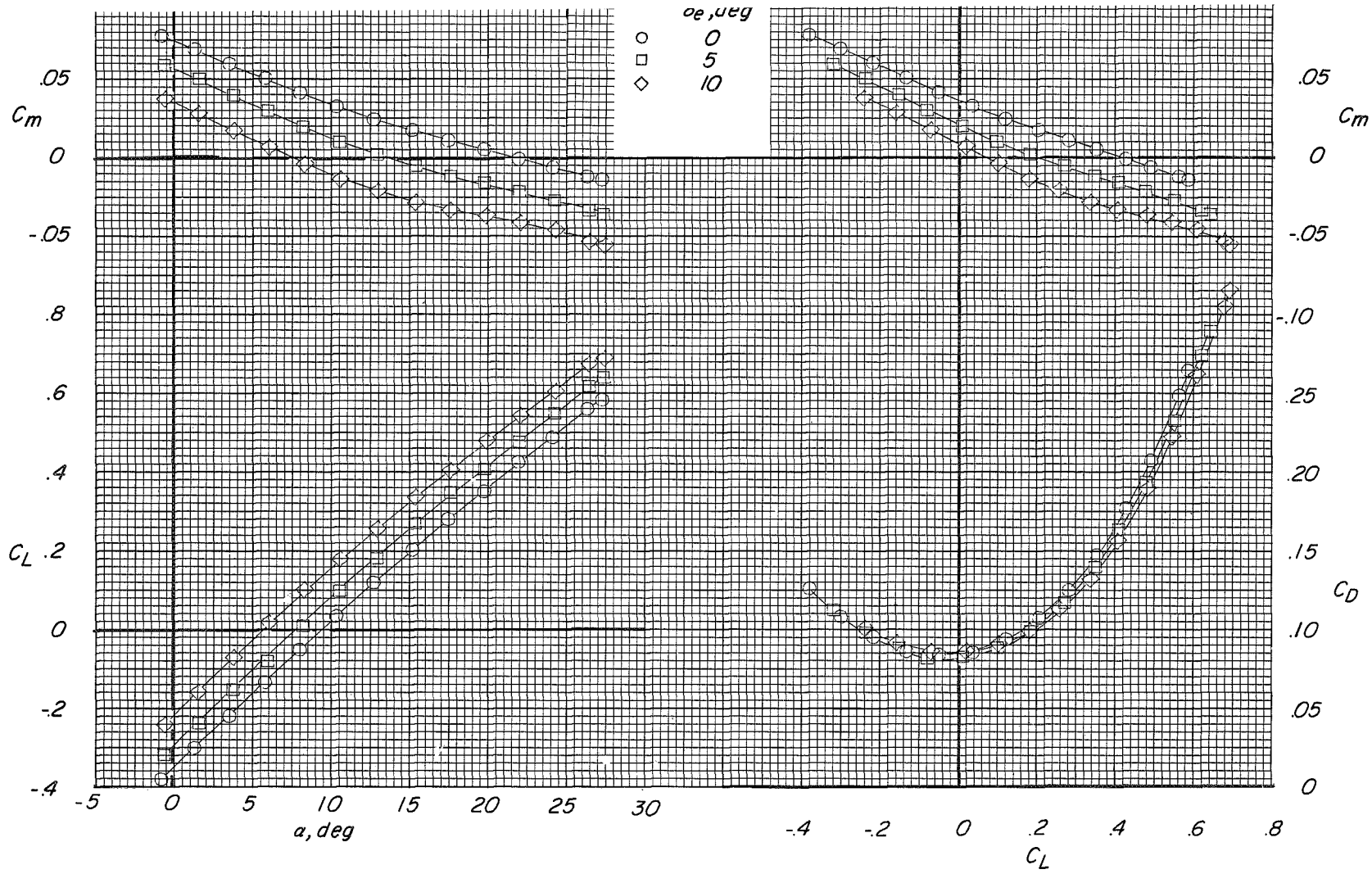
(e) M = 0.80.

Figure 43.- Concluded.



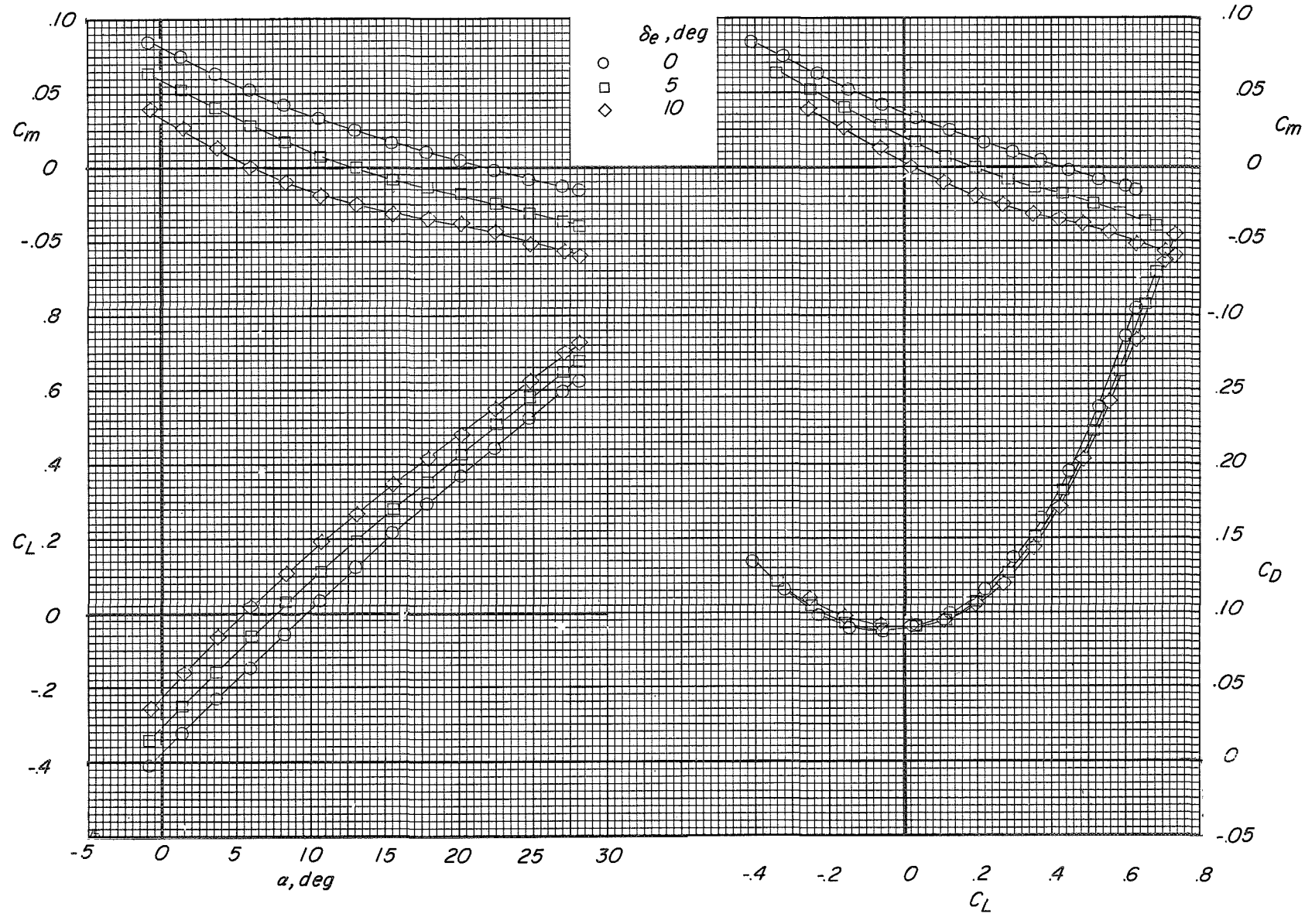
(a) M = 0.60.

Figure 44.- Longitudinal characteristics with modification II fin configuration. Auxiliary flaps in transonic position; $\beta = \delta_a = 0^o$.

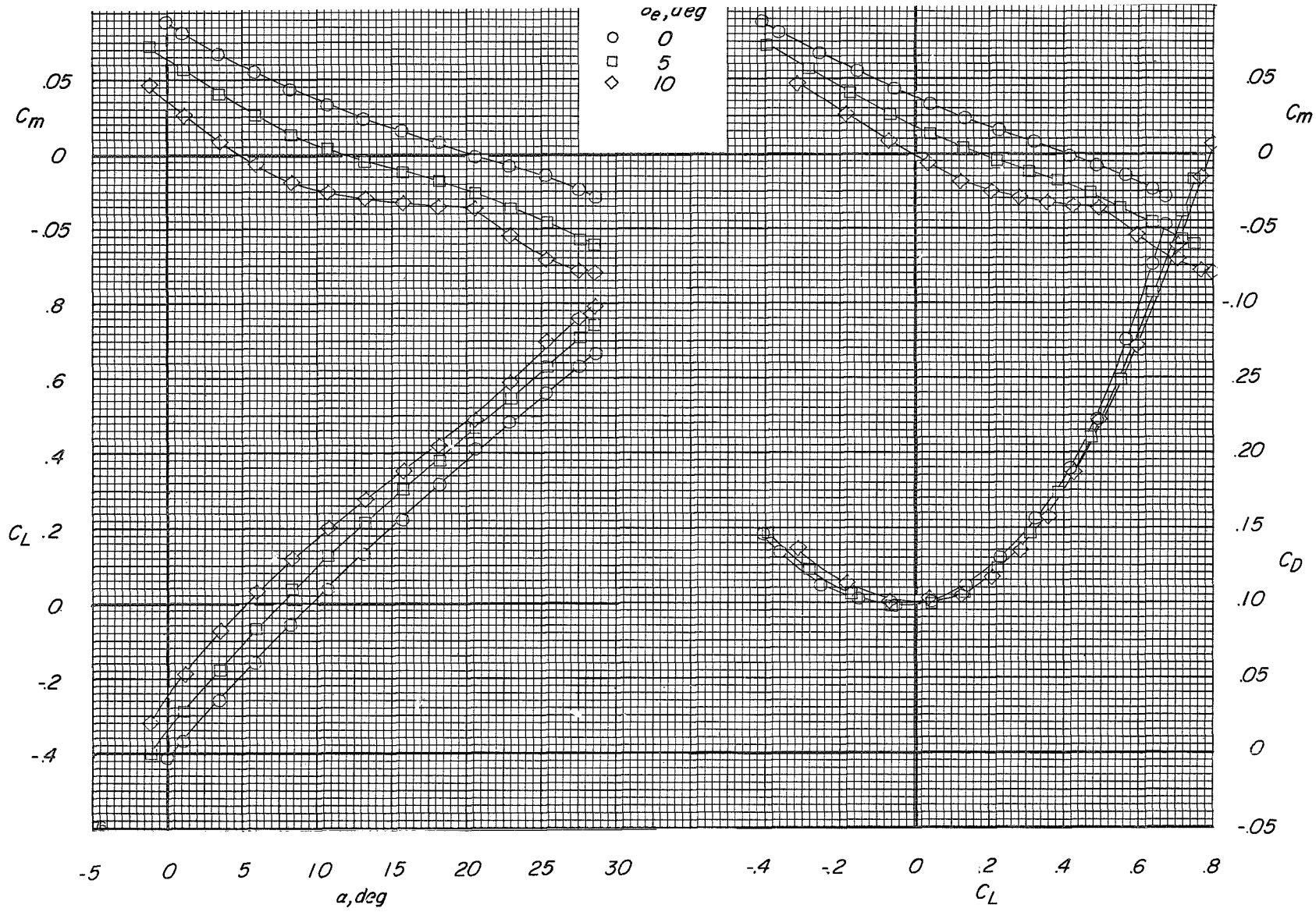


(b) M = 0.70.

Figure 44.- Continued.

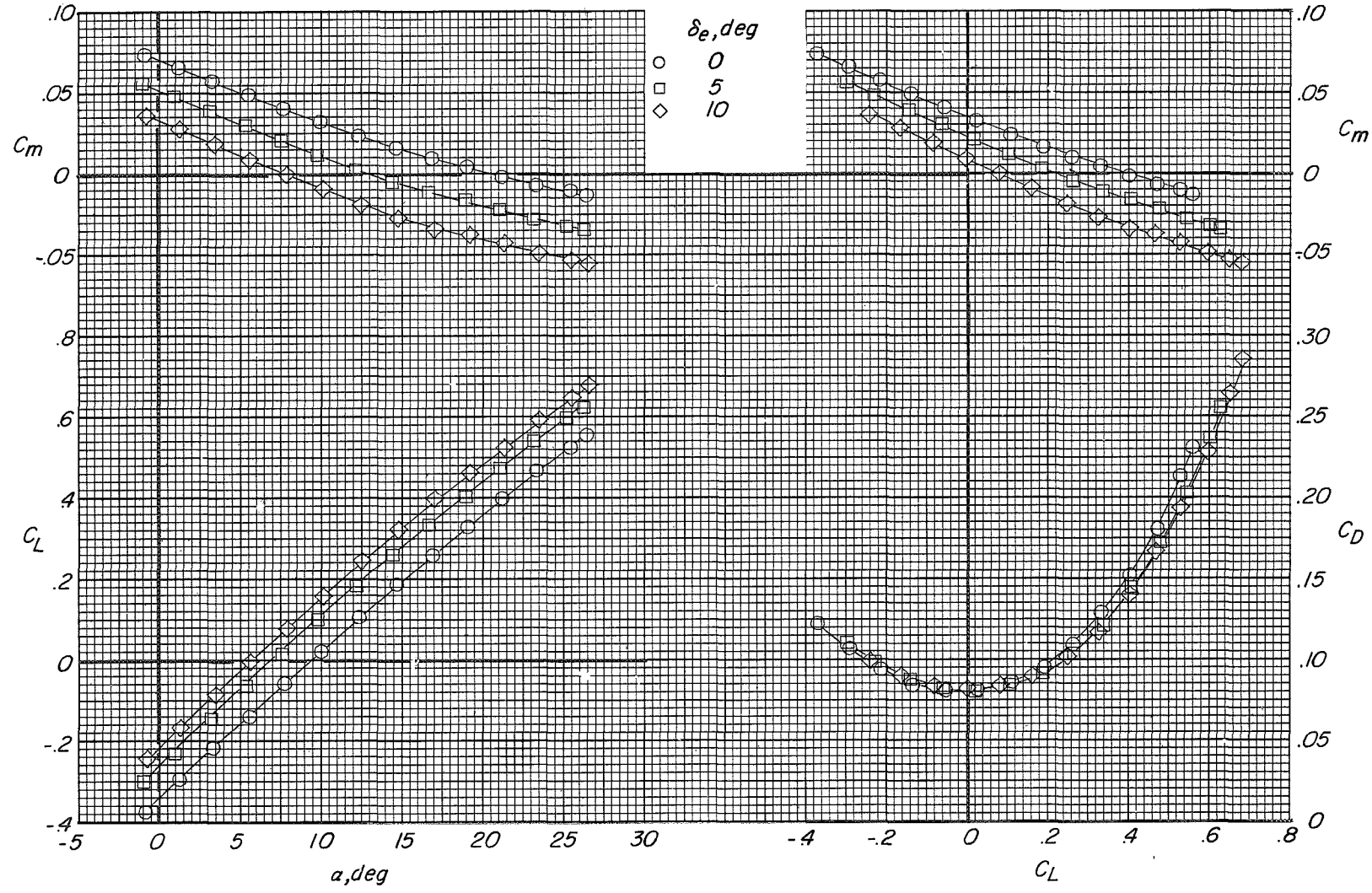

δ_e, deg
0
5
10
C_m
C_L
C_D
α, deg
.10
.05
0
-.05
.8
.6
.4
.2
-.2
-.4
-5
0
5
10
15
20
25
30
.25
.20
.15
.10
.05
-.10

(c) M = 0.80.



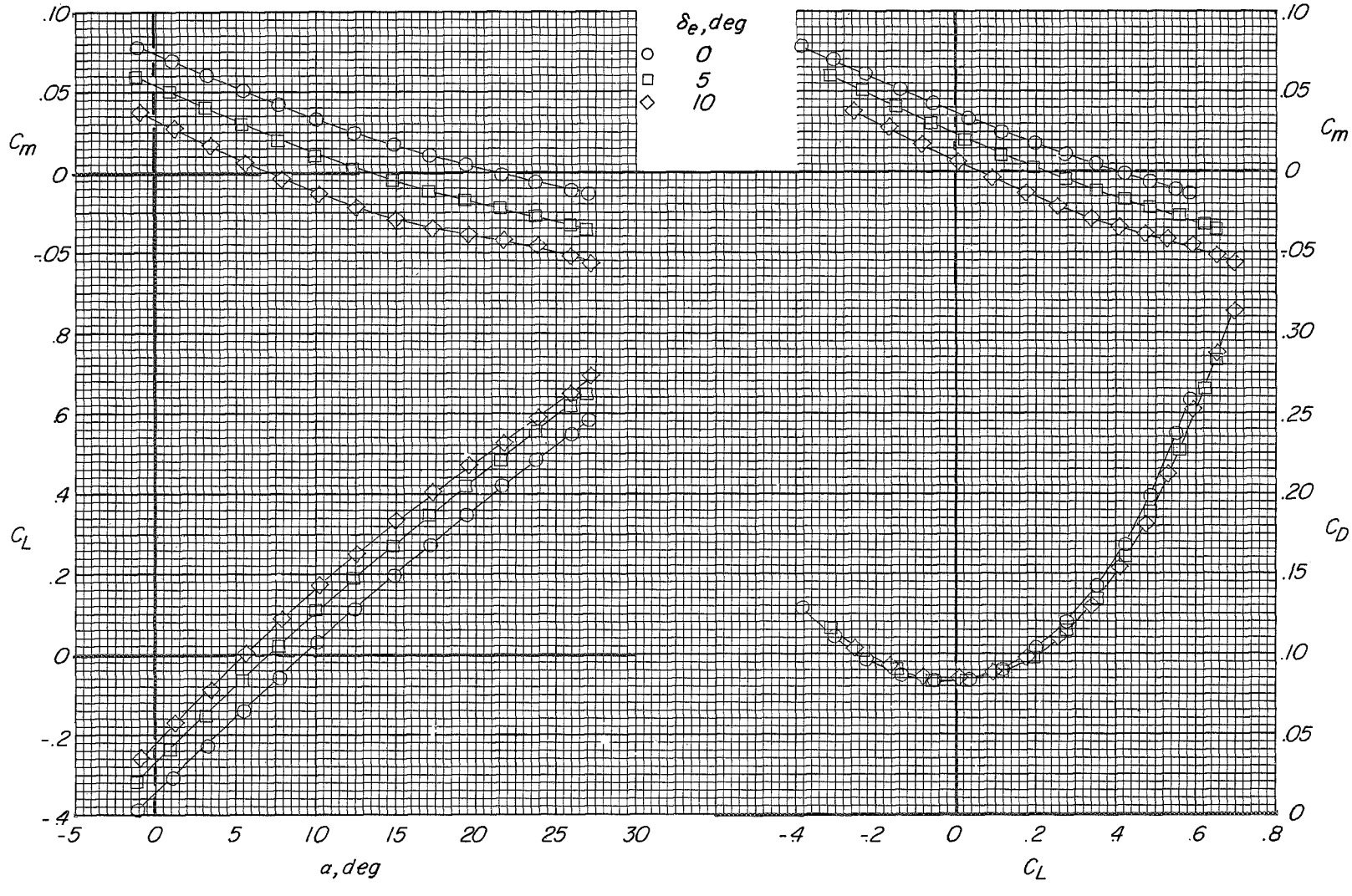
(d) M = 0.90.

Figure 44.- Concluded.



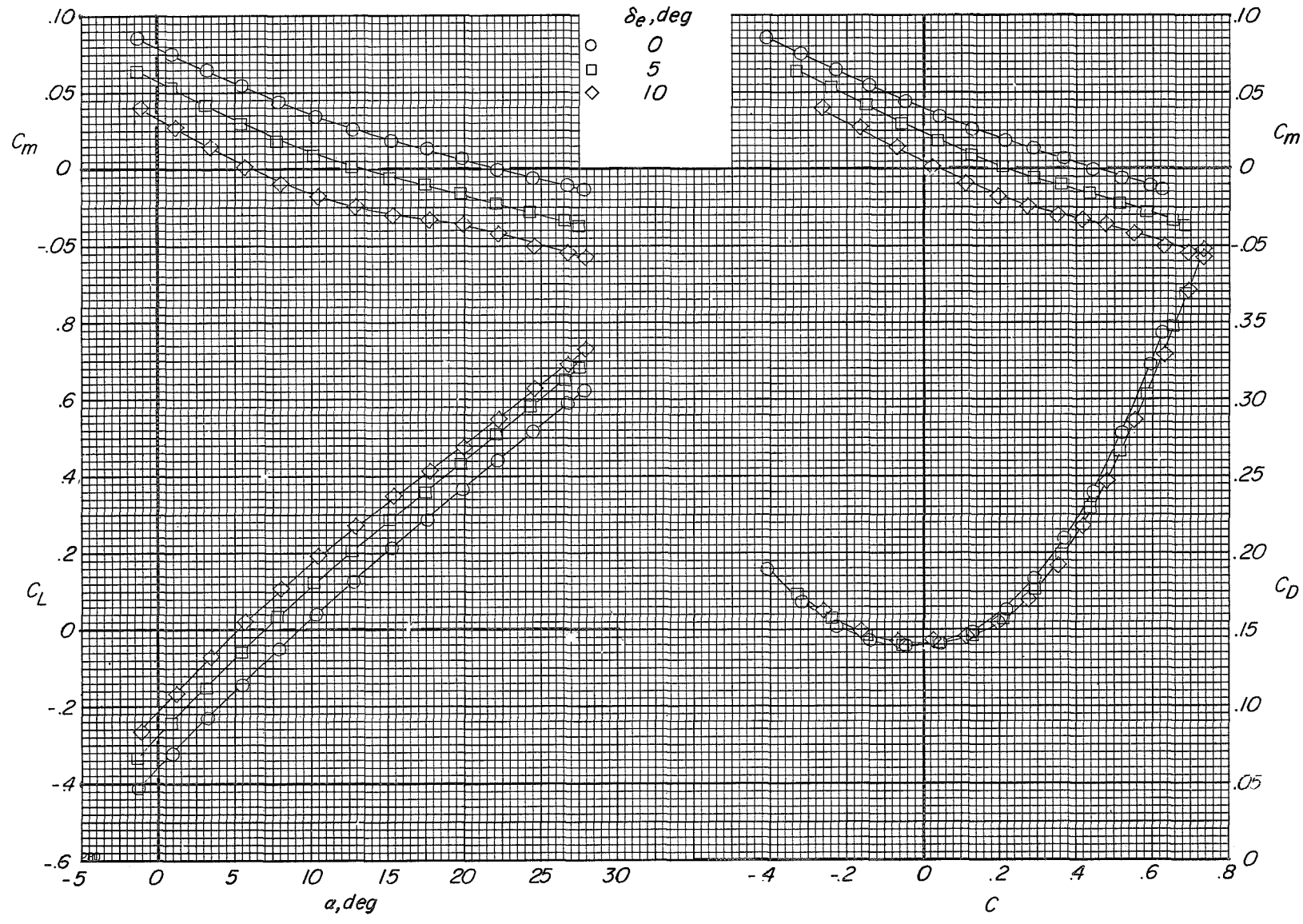
(a) $\beta = 2.3^{o}$; M = 0.60.

Figure 45.- Longitudinal characteristics at sideslip. Modification II fin configuration; auxiliary flaps in transonic configuration; $\delta_a = 0^{o}$.



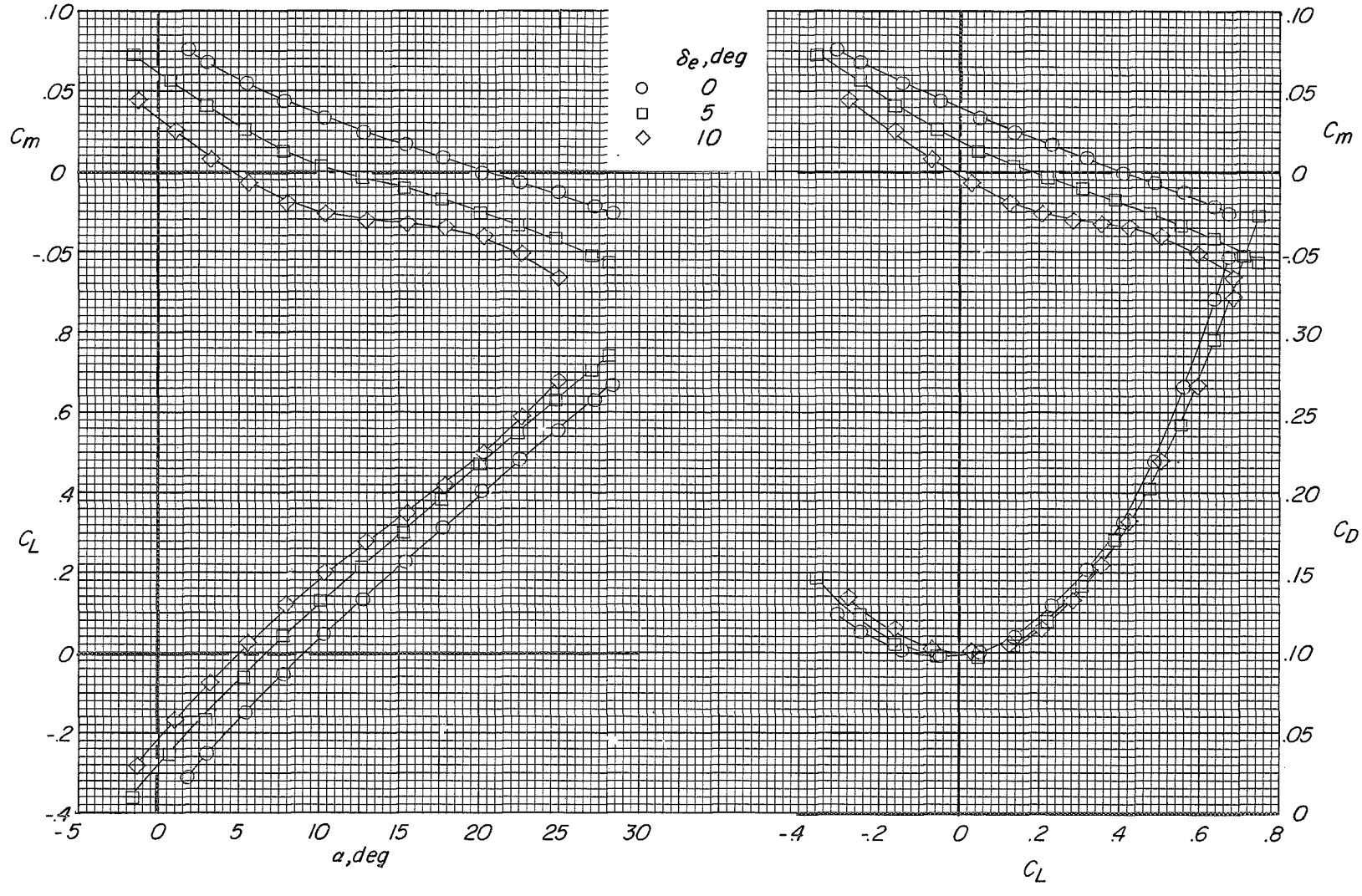
(b) $\beta = 2.3^{o}$; M = 0.70.

Figure 45.- Continued.



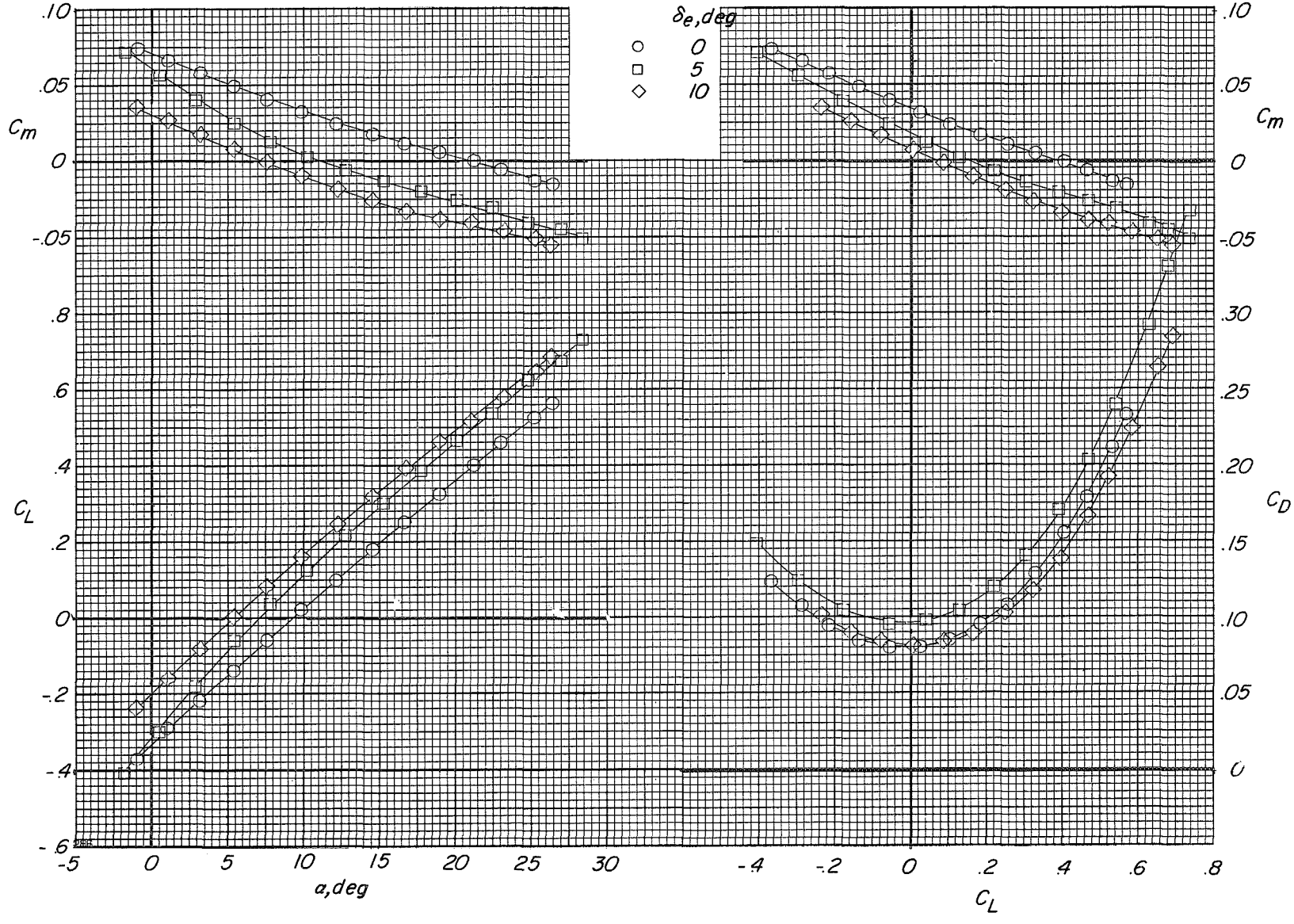
(c) $\beta = 2.3^{o}$; M = 0.80.

Figure 45 - Continued



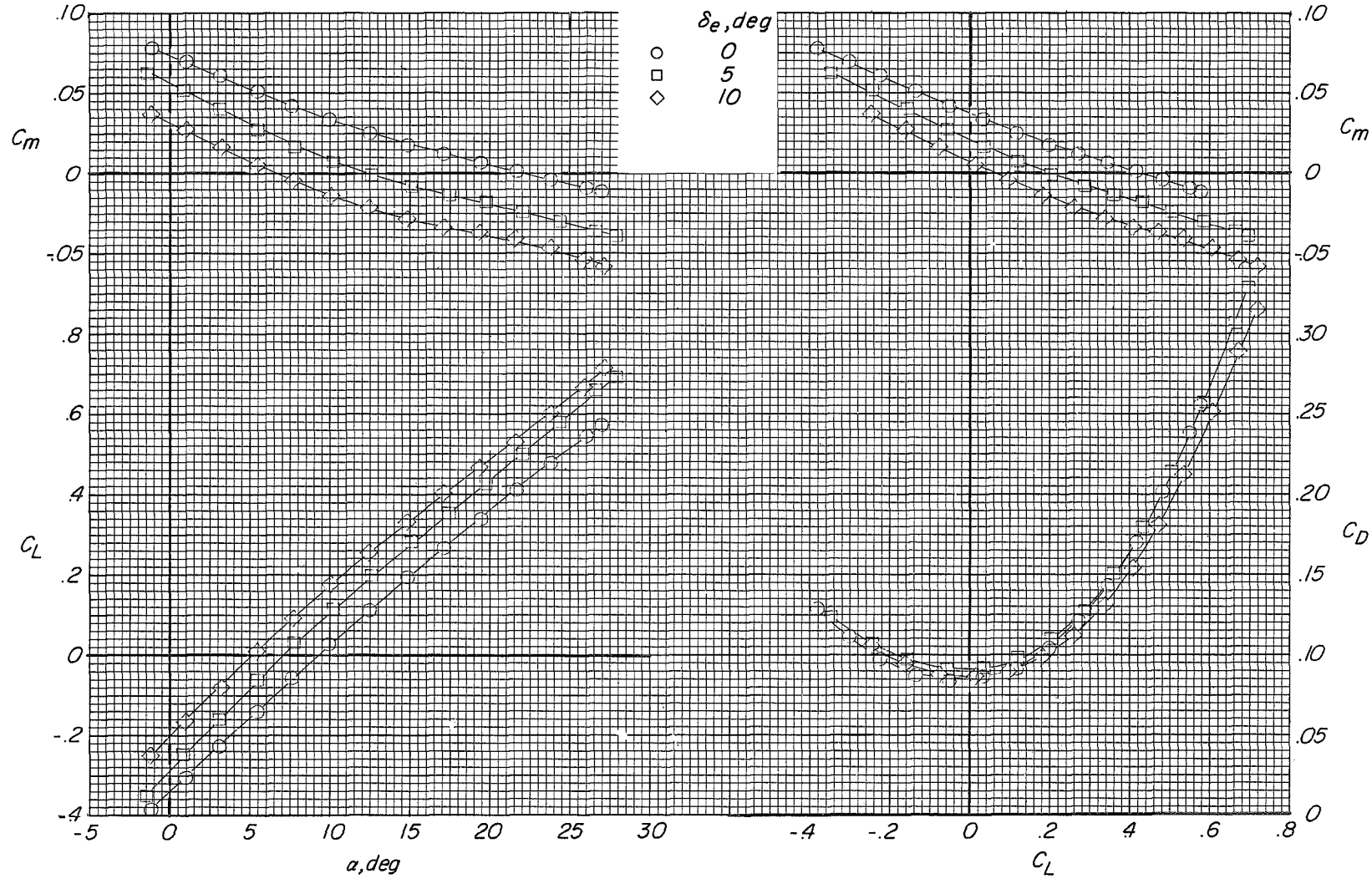
(d) $\beta = 2.3^{\circ}$; M = 0.90.

Figure 45.- Continued.



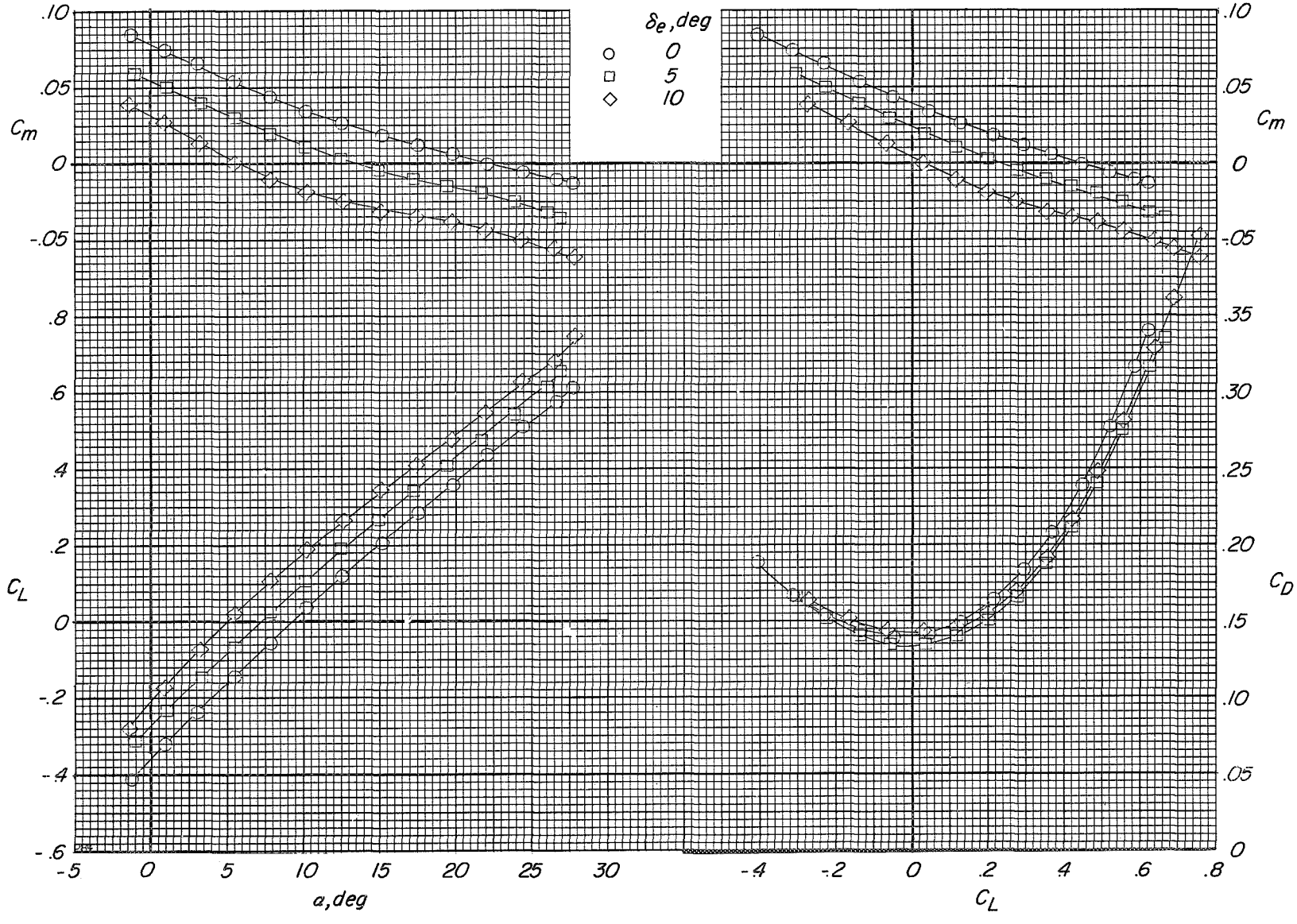
(e) $\beta = -2.3^{o}$; M = 0.60.

Figure 45. Continued



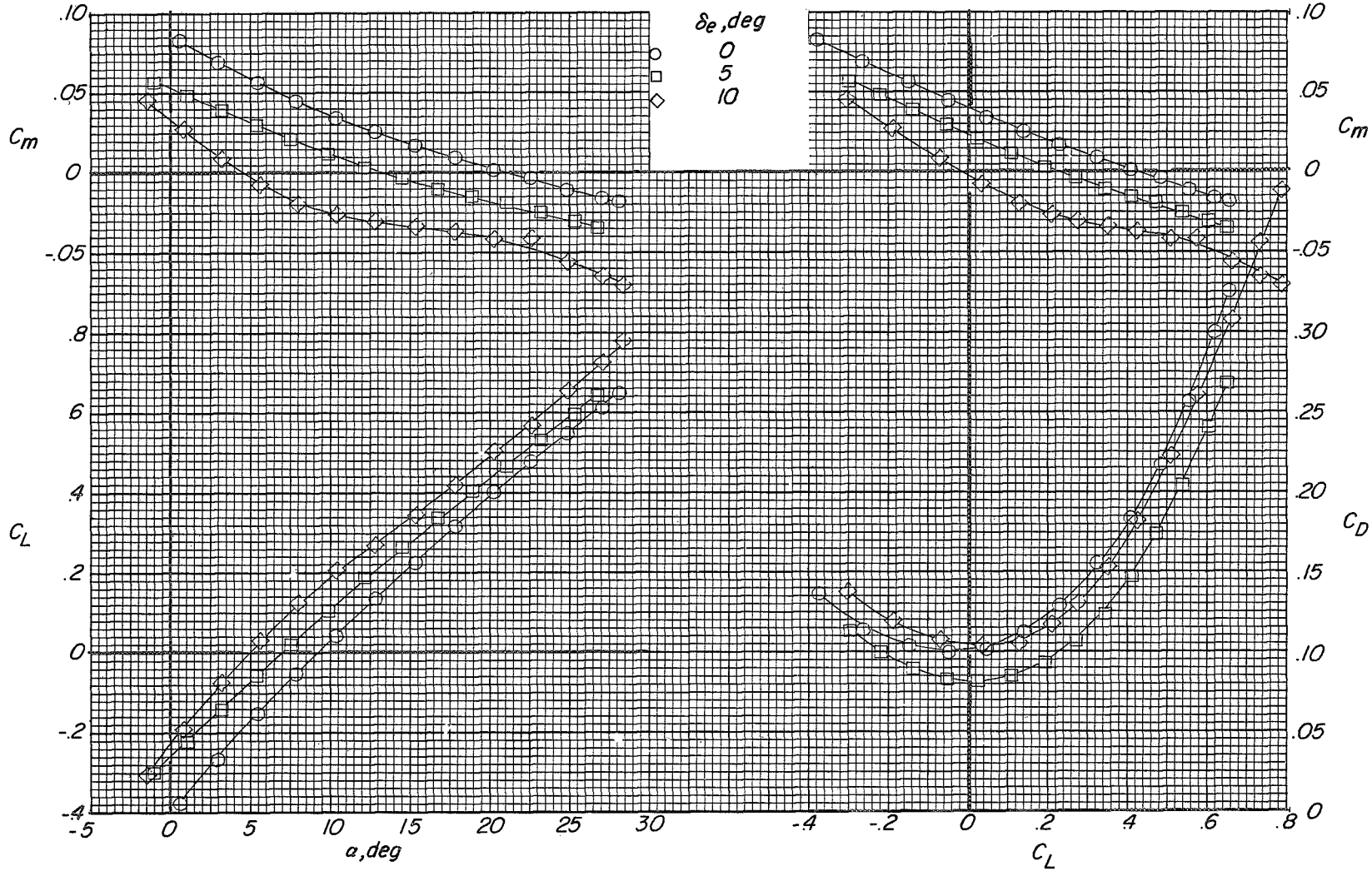
(f) $\beta = -2.3^{o}$; M = 0.70.

Figure 45.- Continued.



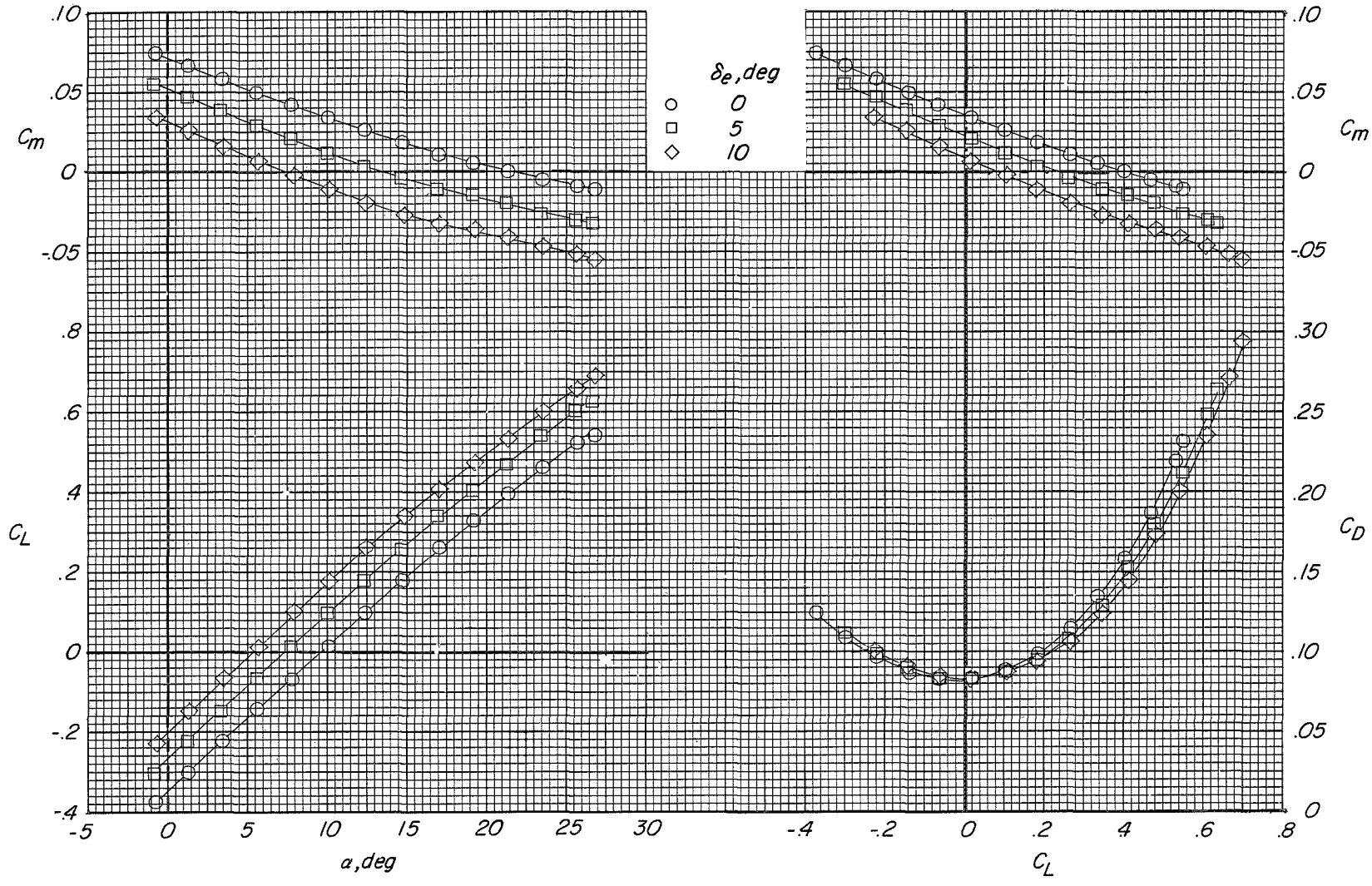
(g) $\beta = -2.3^{o}$; M = 0.80.

Figure 45 - Continued



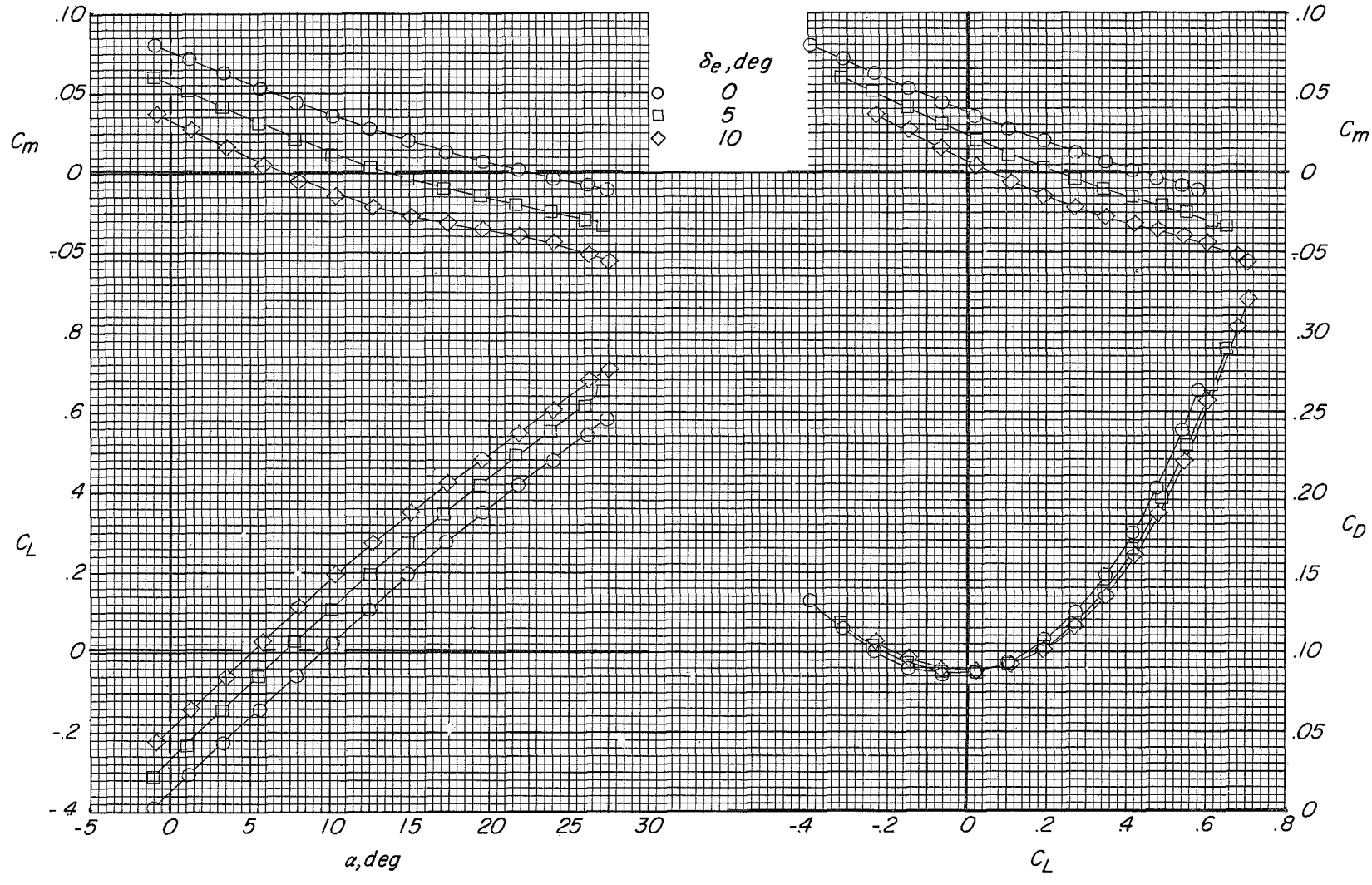
(h) $\beta = -2.3^{\circ}$; M = 0.90.

Figure 45.- Concluded.



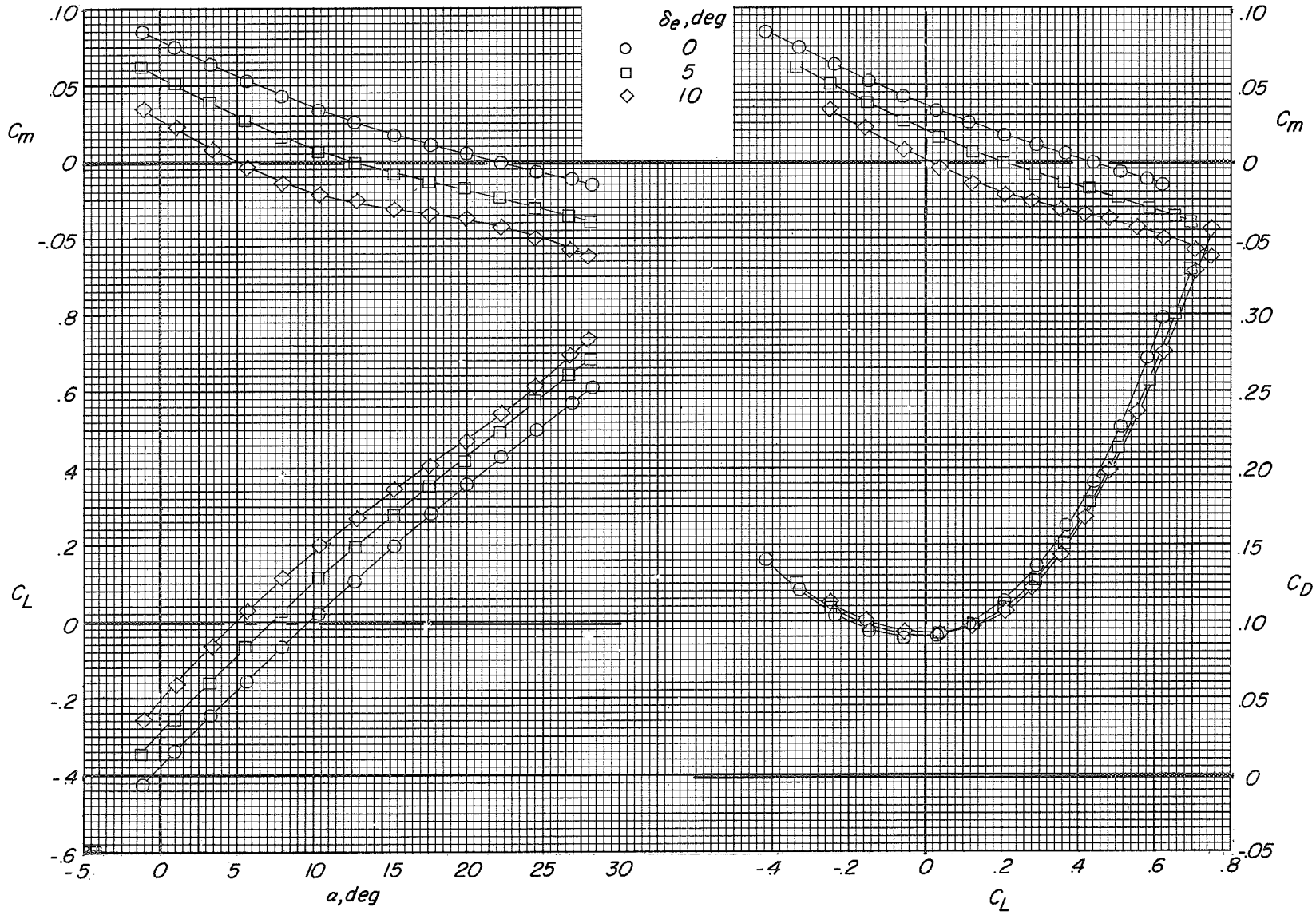
(a) M = 0.60.

Figure 46.- Longitudinal characteristics with ailerons deflected 10°. Modification II fin configuration; auxiliary flaps in transonic position; $\beta = 0°$.



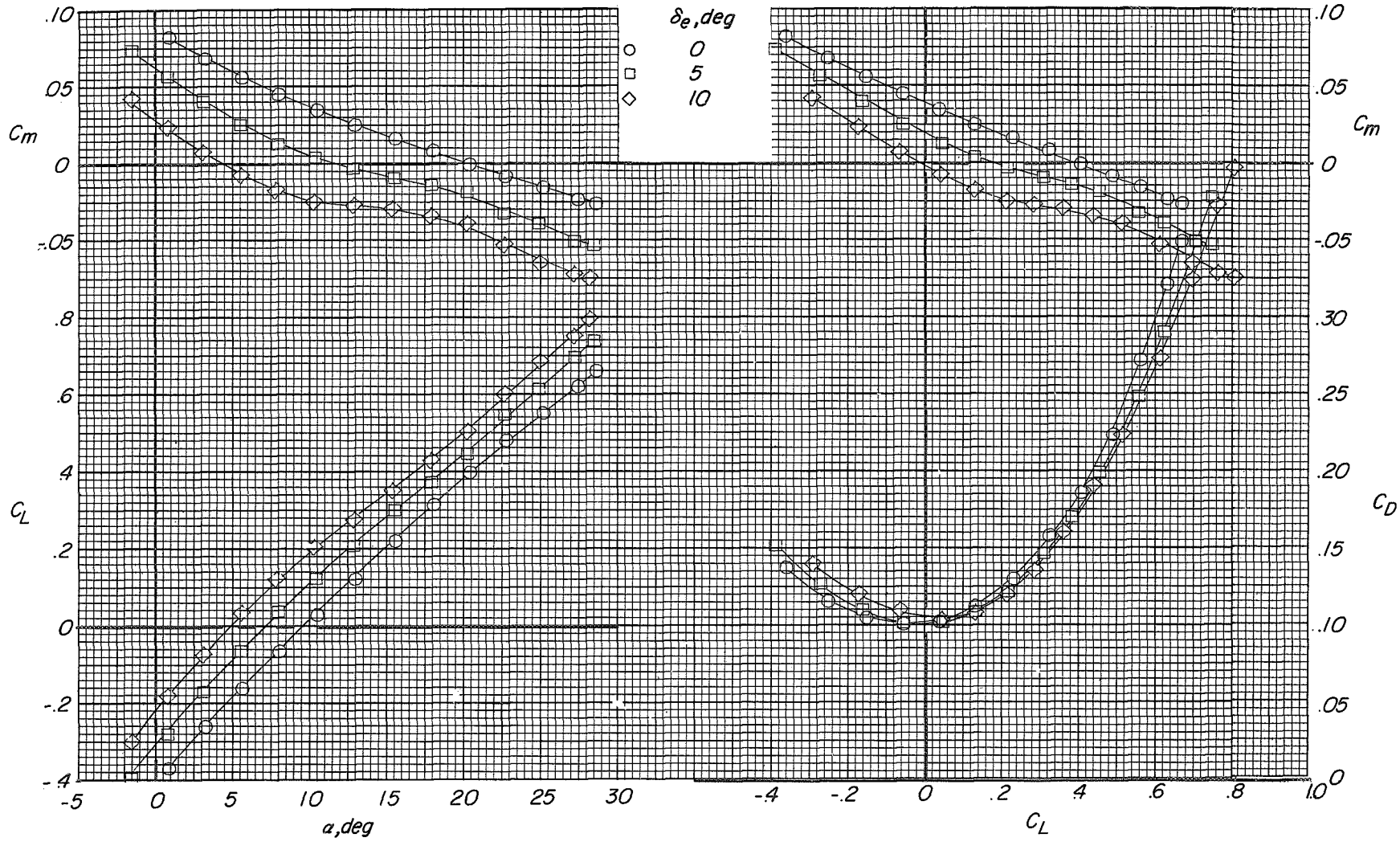
(b) M = 0.70.

Figure 46.- Continued.



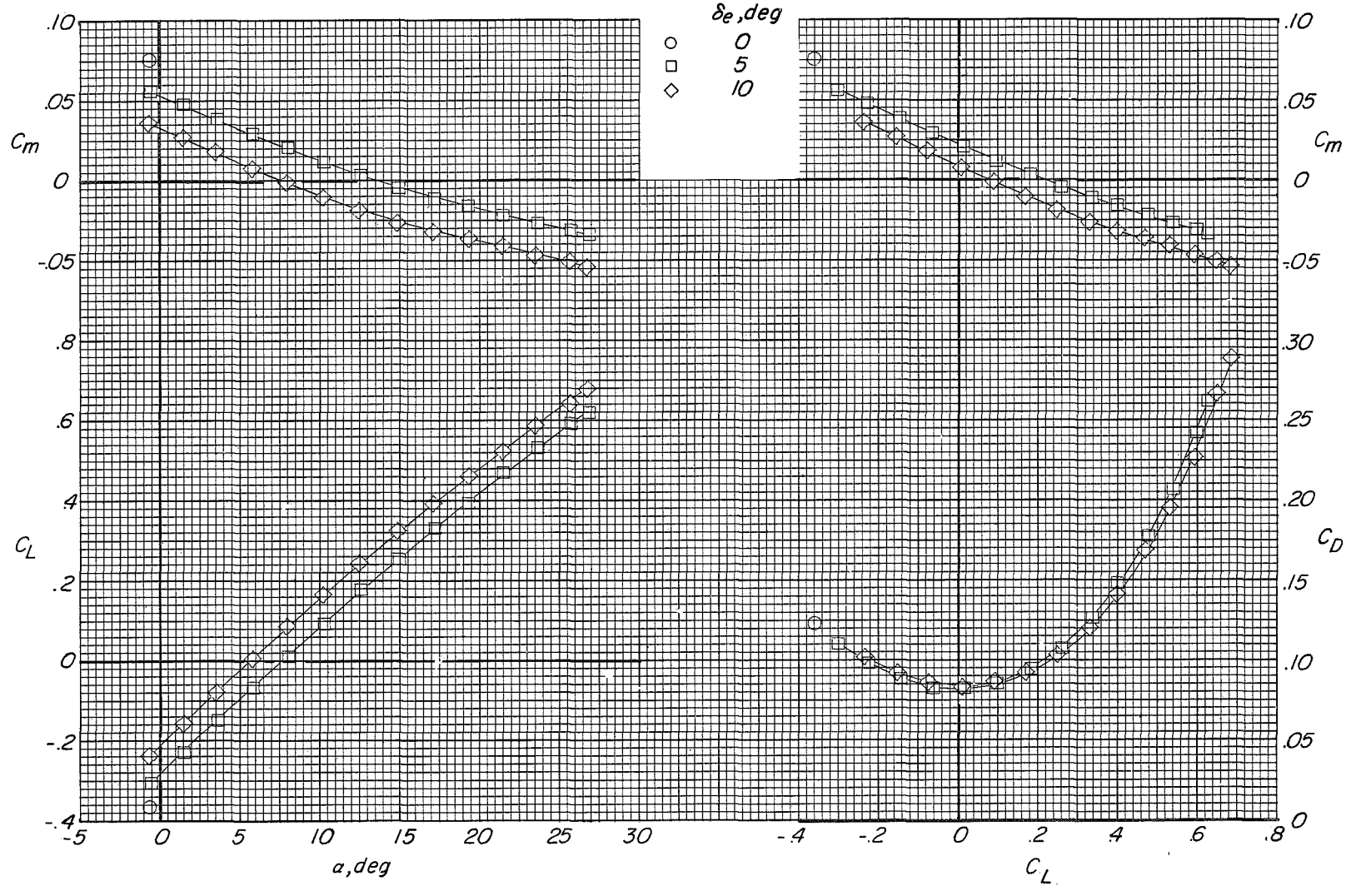
(c) M = 0.80.

Figure 46 - Continued



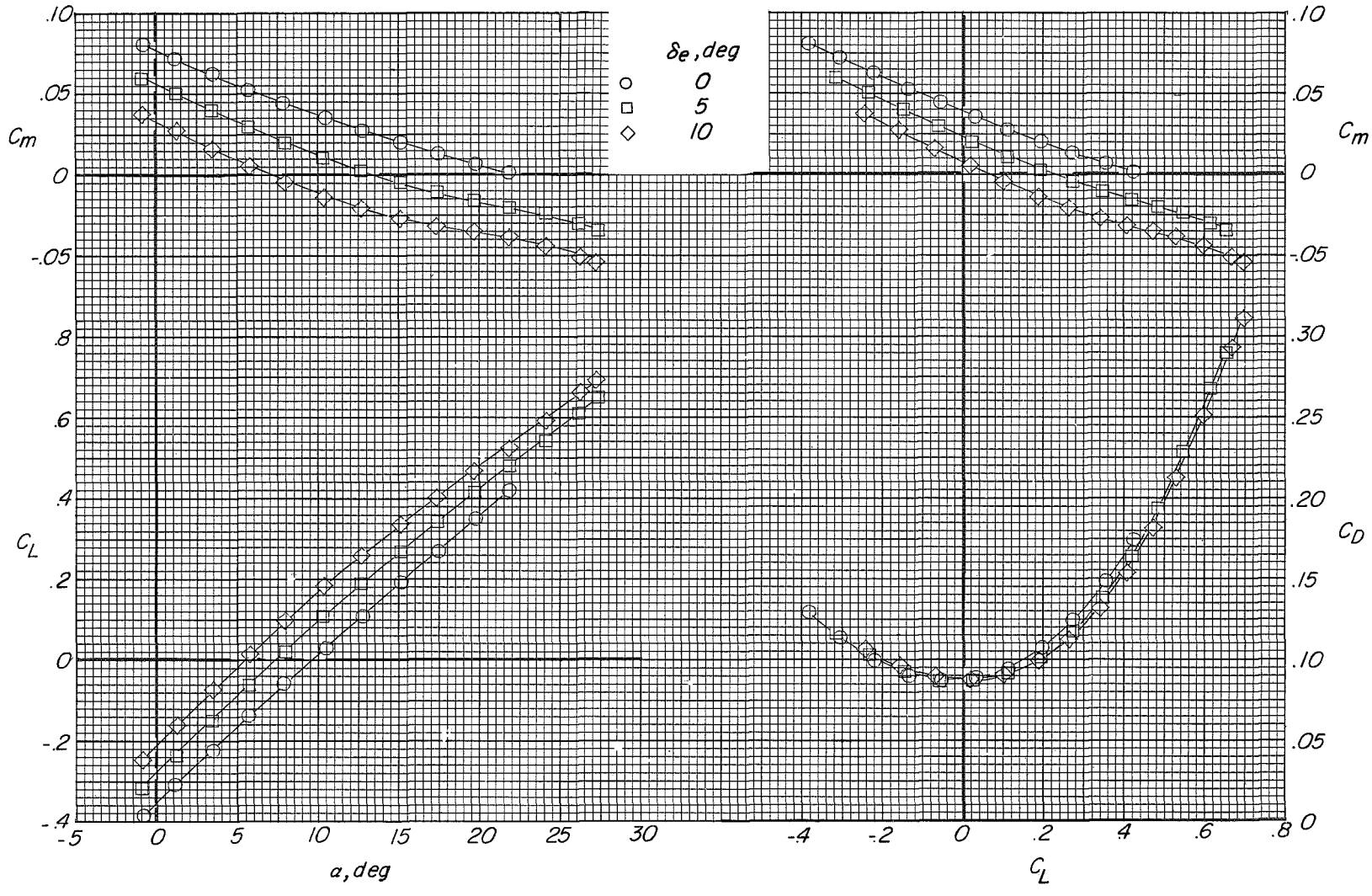
(d) M = 0.90.

Figure 46.- Concluded.



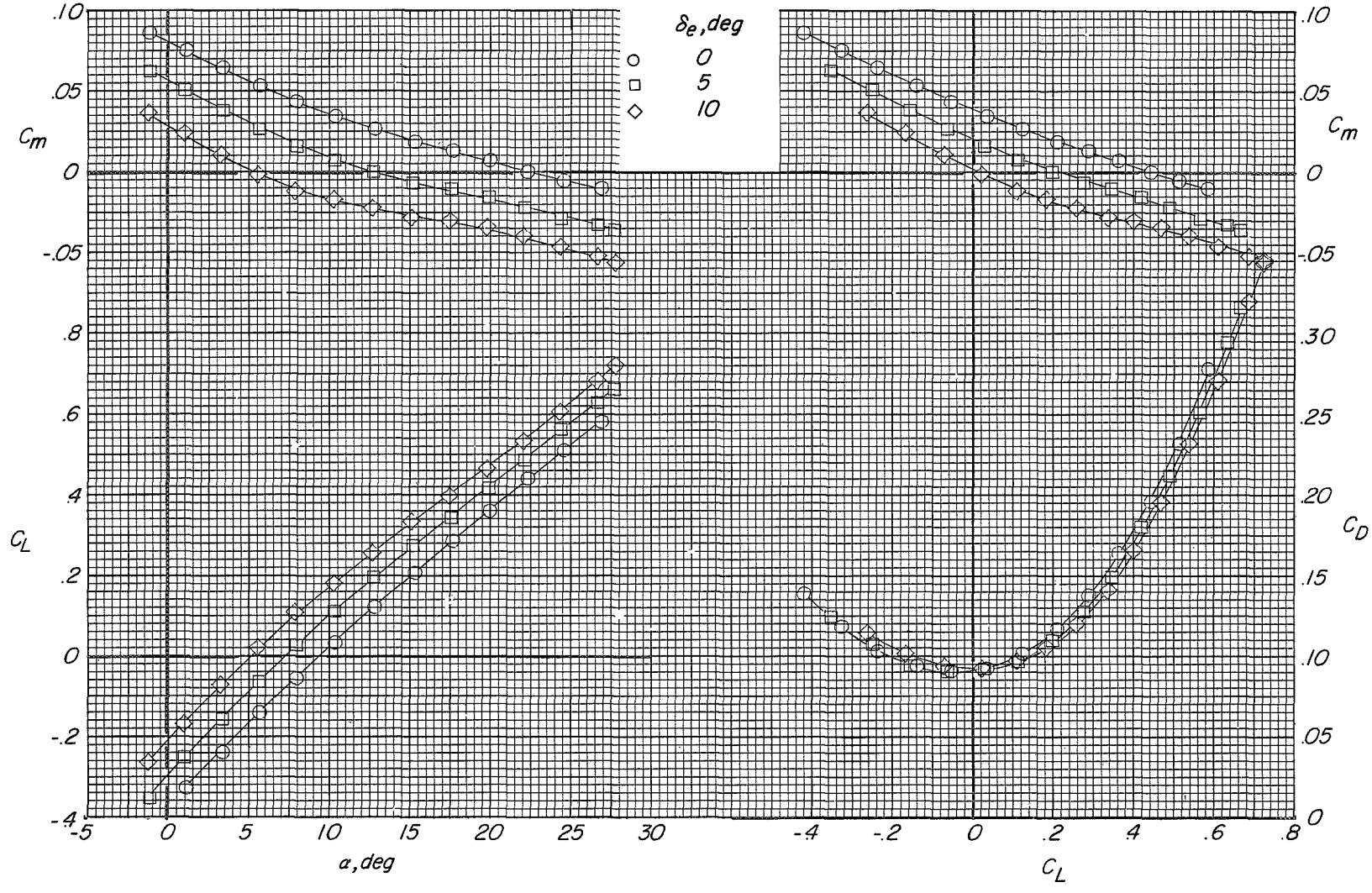
(a) $\beta = 2.3^{o}$; $\delta_a = 10^{o}$; M = 0.60.

Figure 47.- Longitudinal characteristics with combined aileron deflection and sideslip angle. Modification II fin configuration; auxiliary flaps in transonic position.



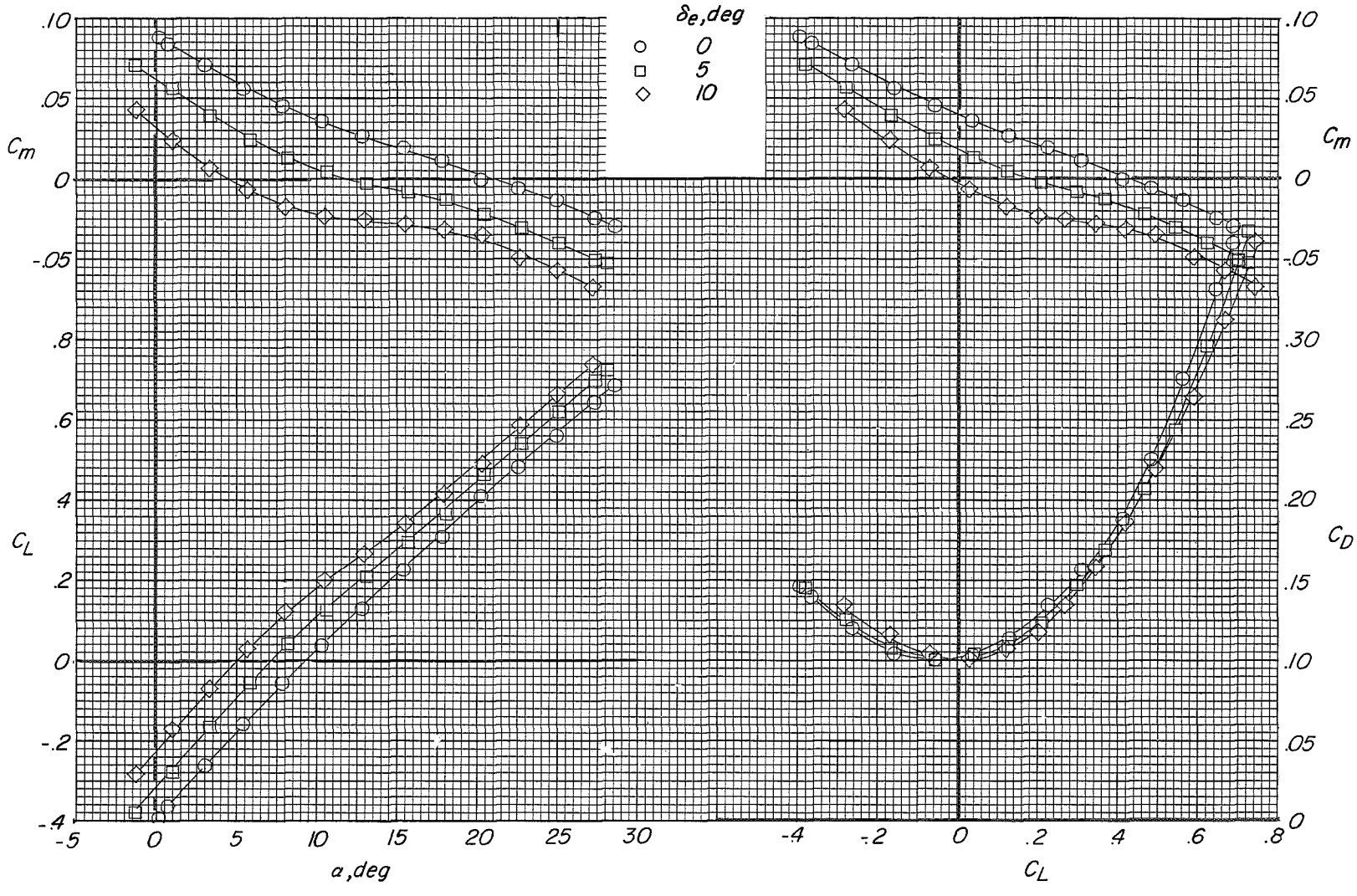
(b) $\beta = 2.3^{o}$; $\delta_a = 10^{o}$; M = 0.70.

Figure 47.- Continued.



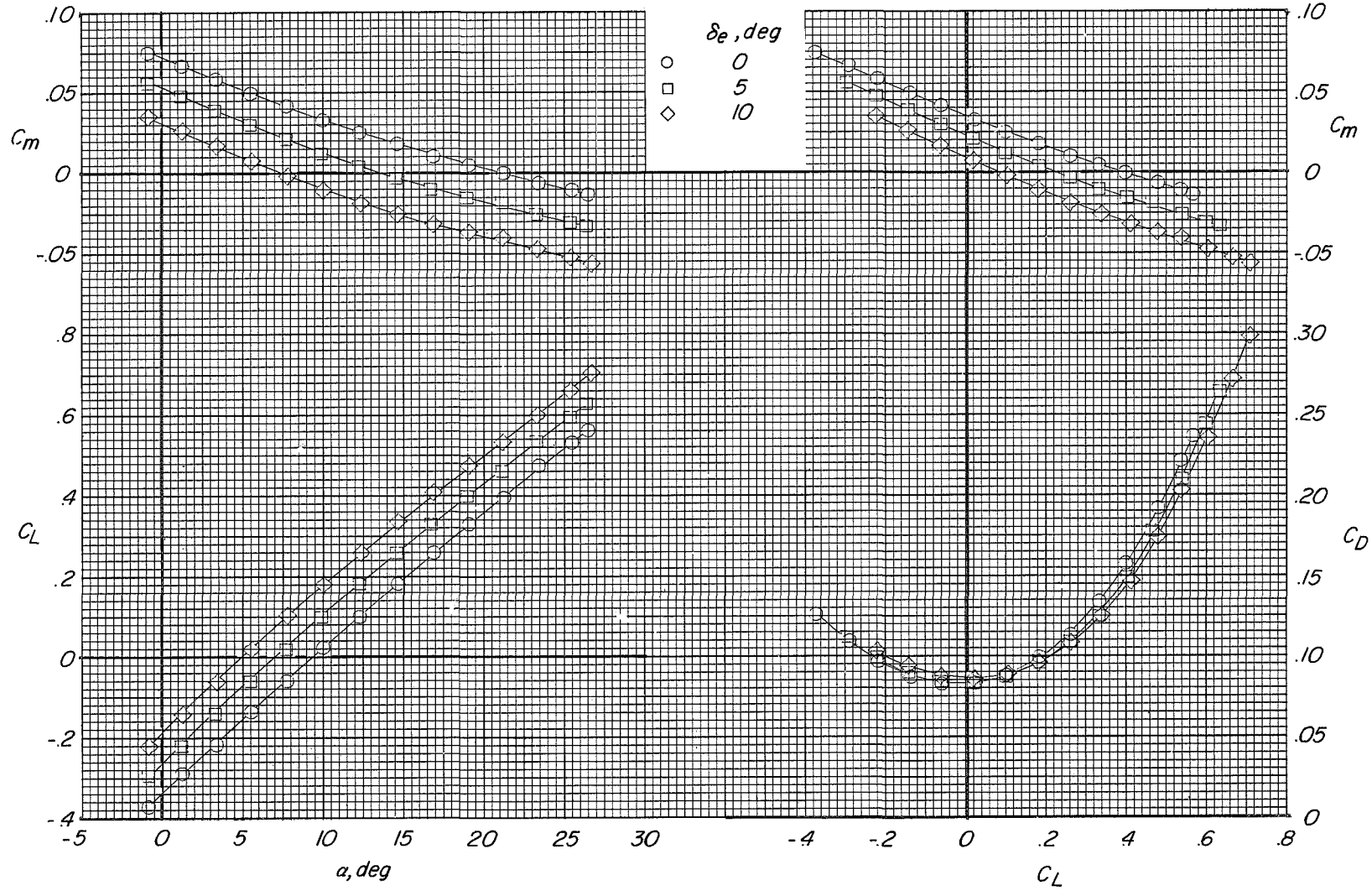
(c) $\beta = 2.3^{o}$; $\delta_a = 10^{o}$; M = 0.80.

Figure 47.- Continued.



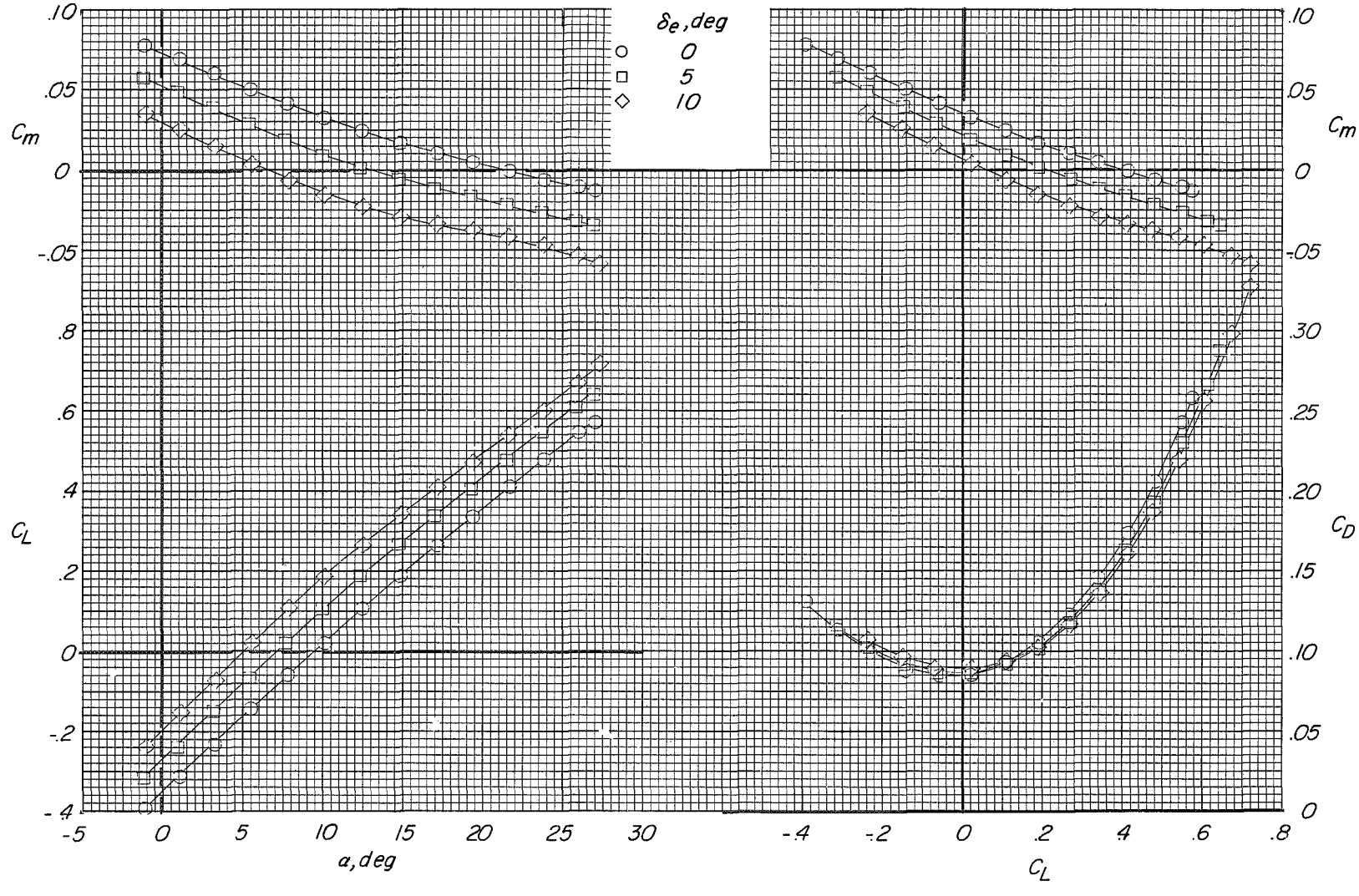
(d) $\beta = 2.3^{o}$; $\delta_a = 10^{o}$; M = 0.90.

Figure 47.- Continued.



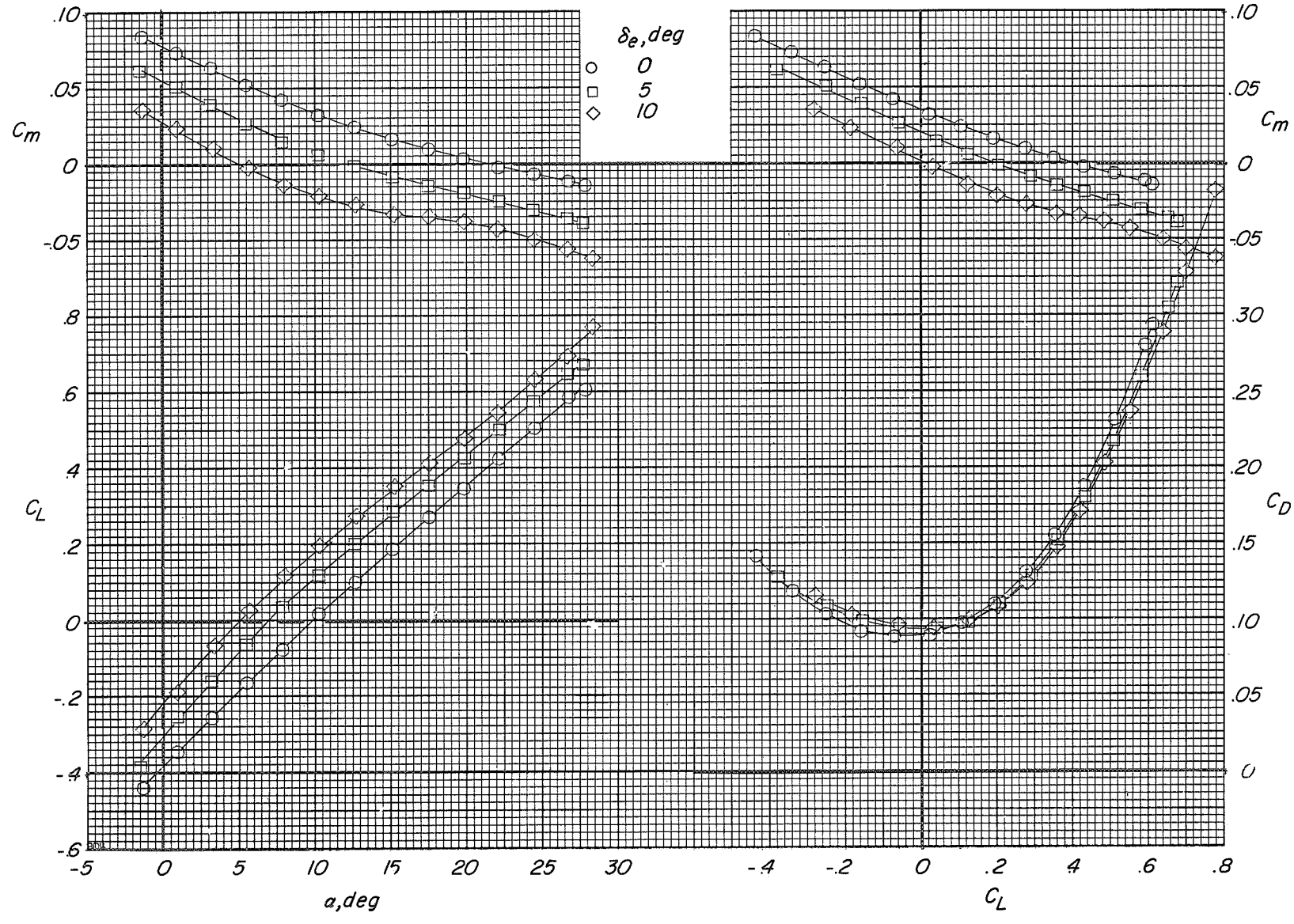
(e) $\beta = -2.3^{o}$; $\delta_a = 10^{o}$; M = 0.60.

Figure 47.- Continued.

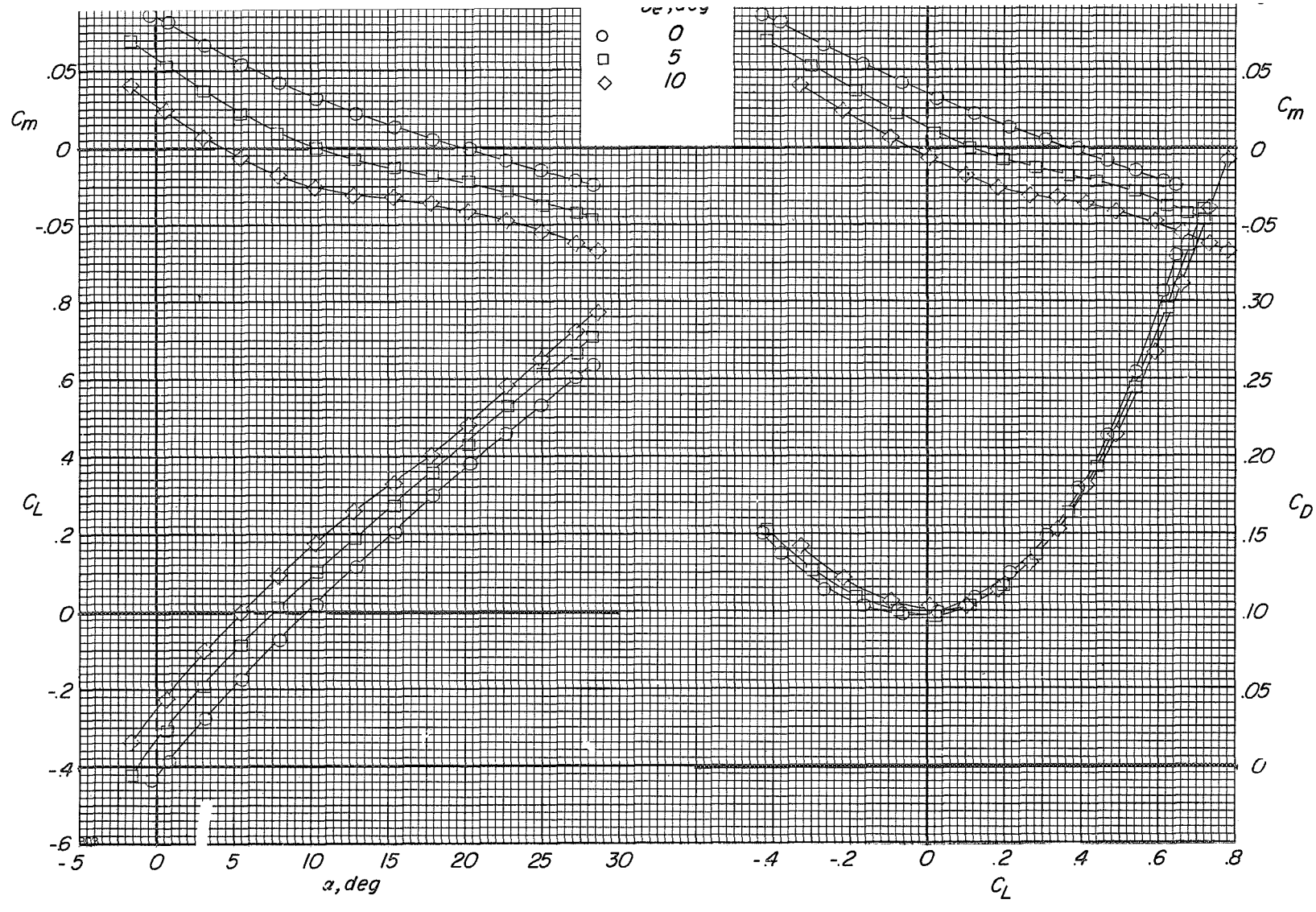


(f) $\beta = -2.3^{o}$; $\delta_a = 10^{o}$; M = 0.70.

Figure 47.- Continued.

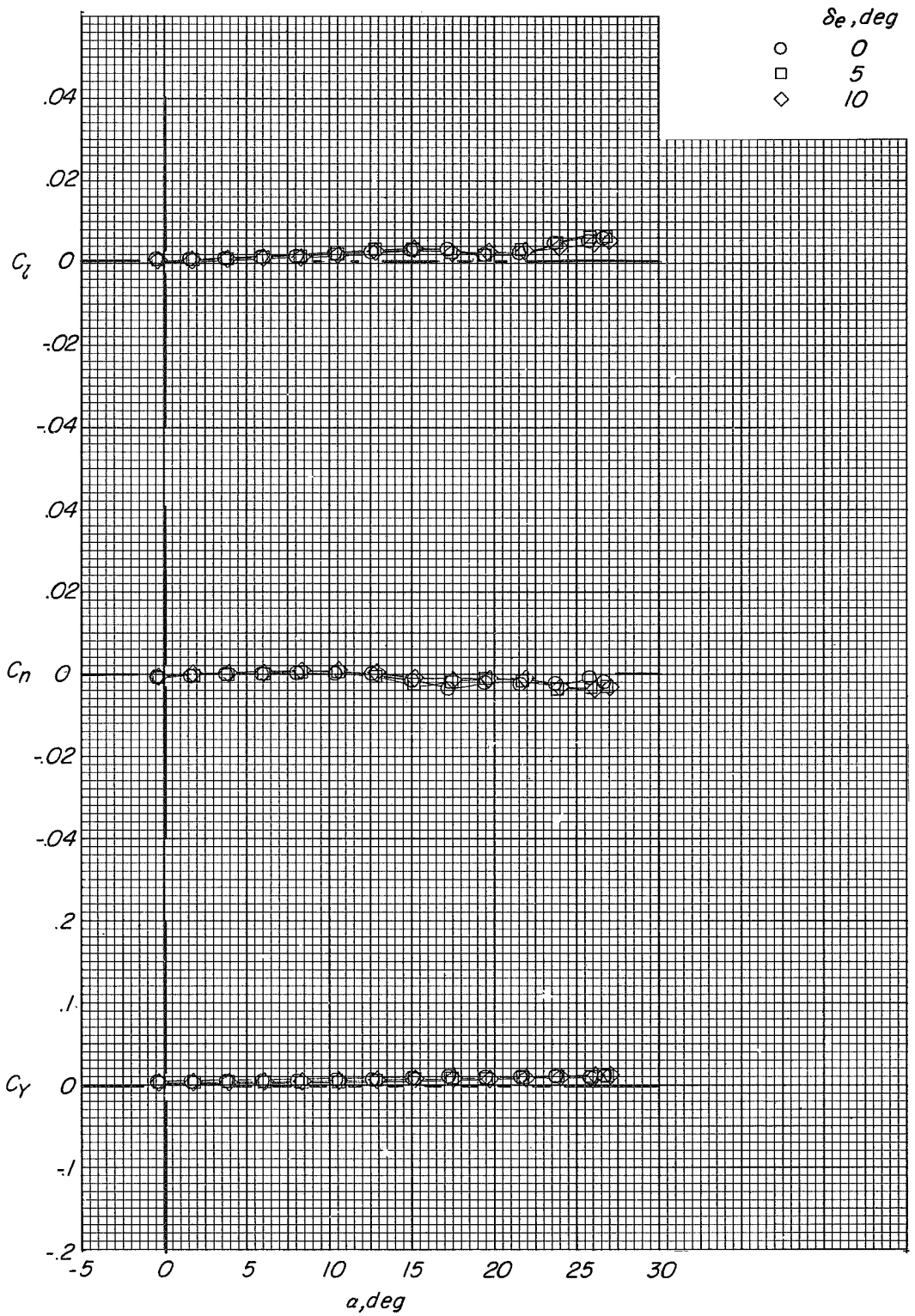


(g) $\beta = -2.3^{o}$; $\delta_a = 10^{o}$; M = 0.80.



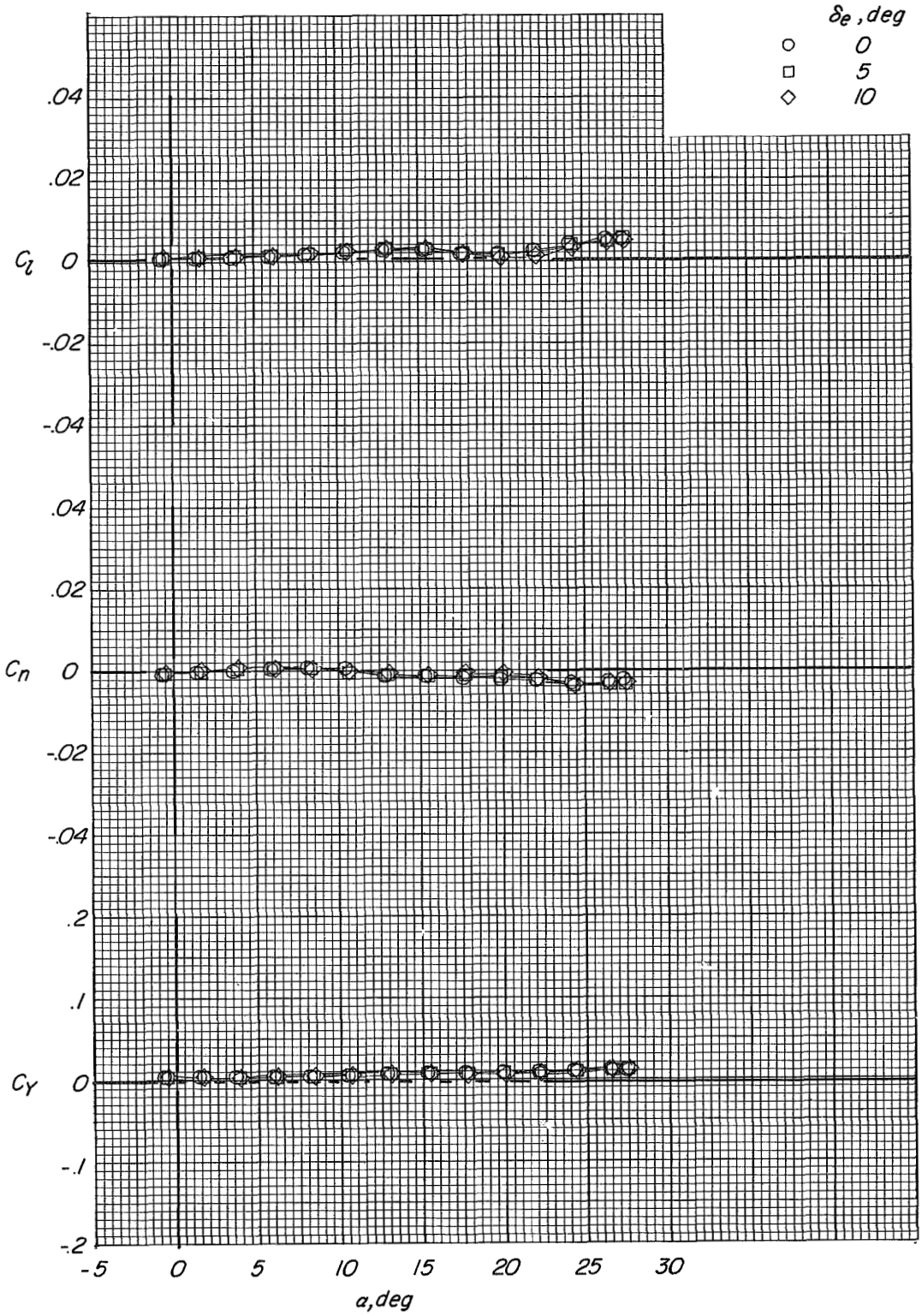
(h) $\beta = -2.3^{o}$; $\delta_a = 10^{o}$; M = 0.90.

Figure 47.- Concluded.



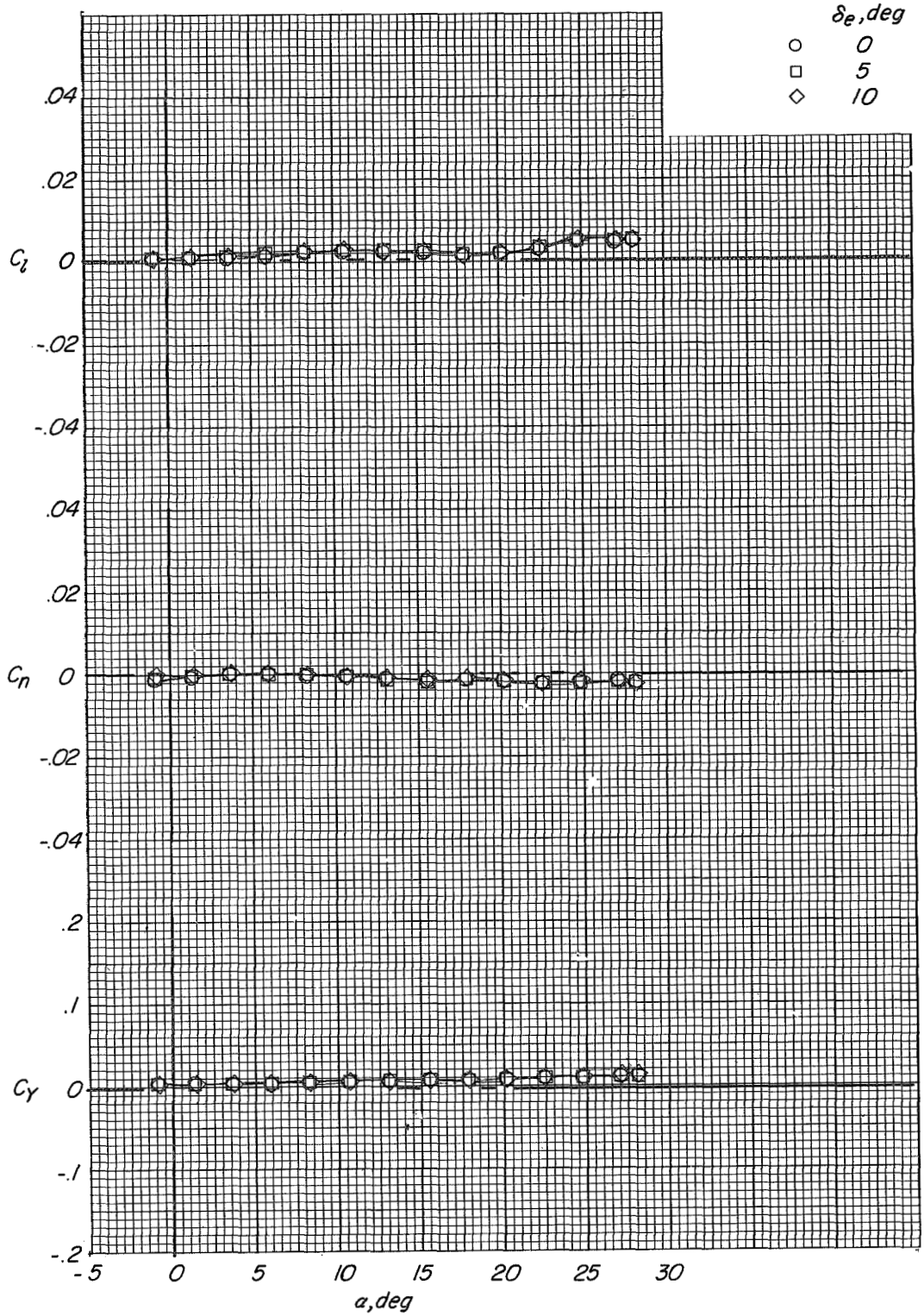
(a) $\delta_a = 0^o$; M = 0.60.

Figure 48.- Variation of the lateral force and moment coefficients with angle of attack for several aileron deflections. Modification II fin configuration; auxiliary flaps in the transonic position; $\beta = 0^o$.



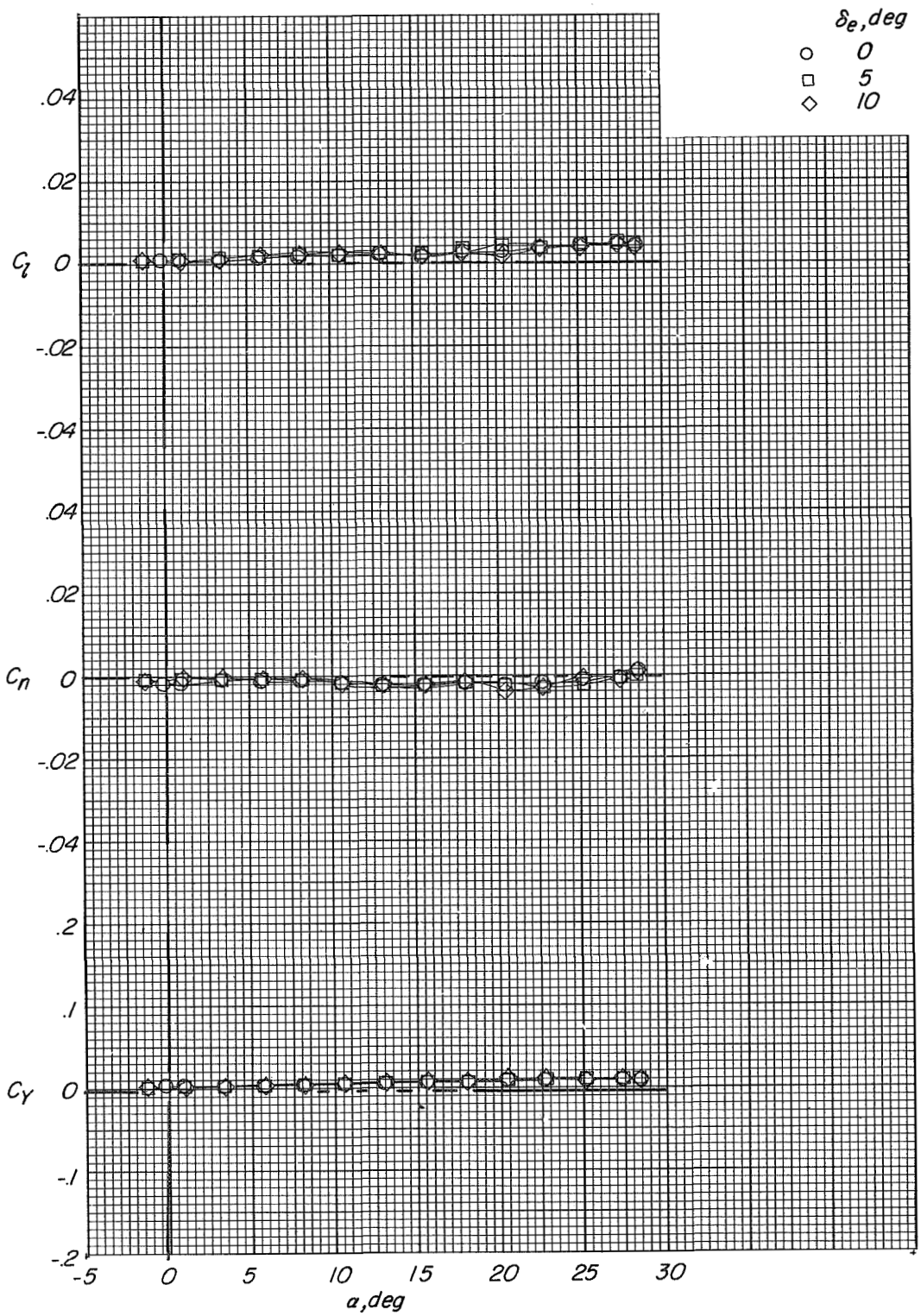
(b) $\delta_a = 0^o$; M = 0.70.

Figure 48.- Continued.



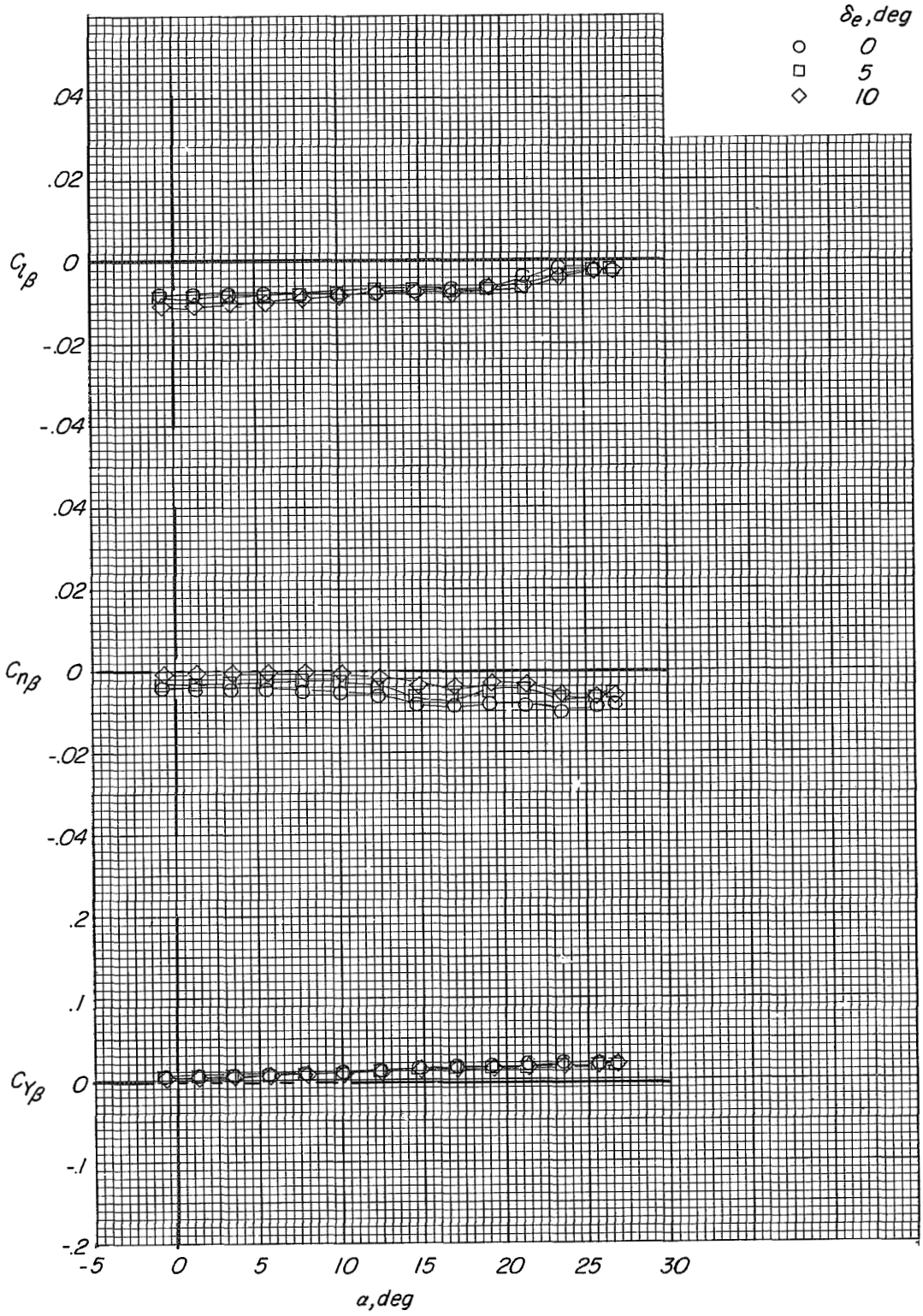
(c) $\delta_a = 0^o$; M = 0.80.

Figure 48.- Continued.



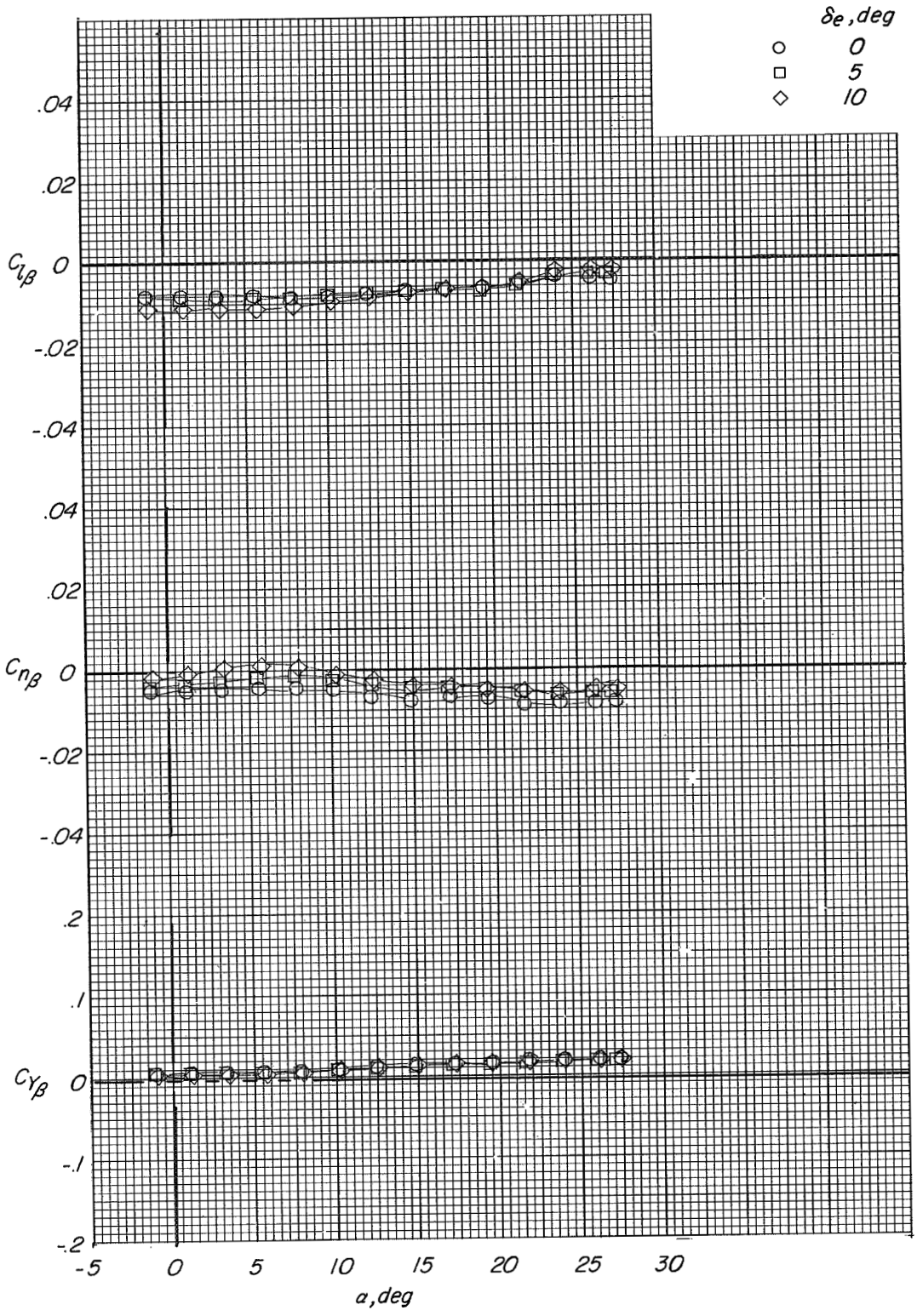
(d) $\delta_a = 0^o$; M = 0.90.

Figure 48.- Continued.



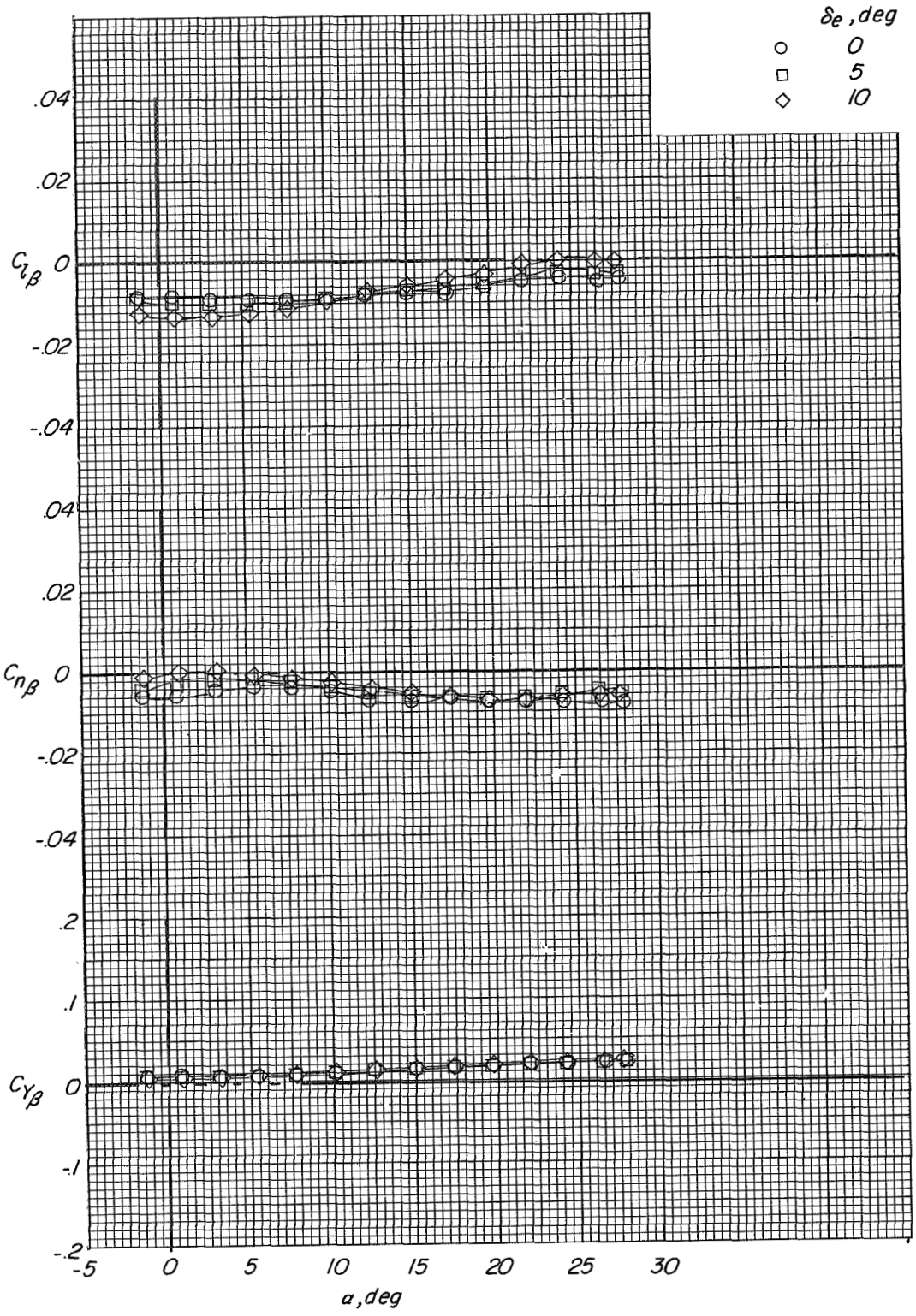
(e) $\delta_a = 10^o$; M = 0.60.

Figure 48.- Continued.



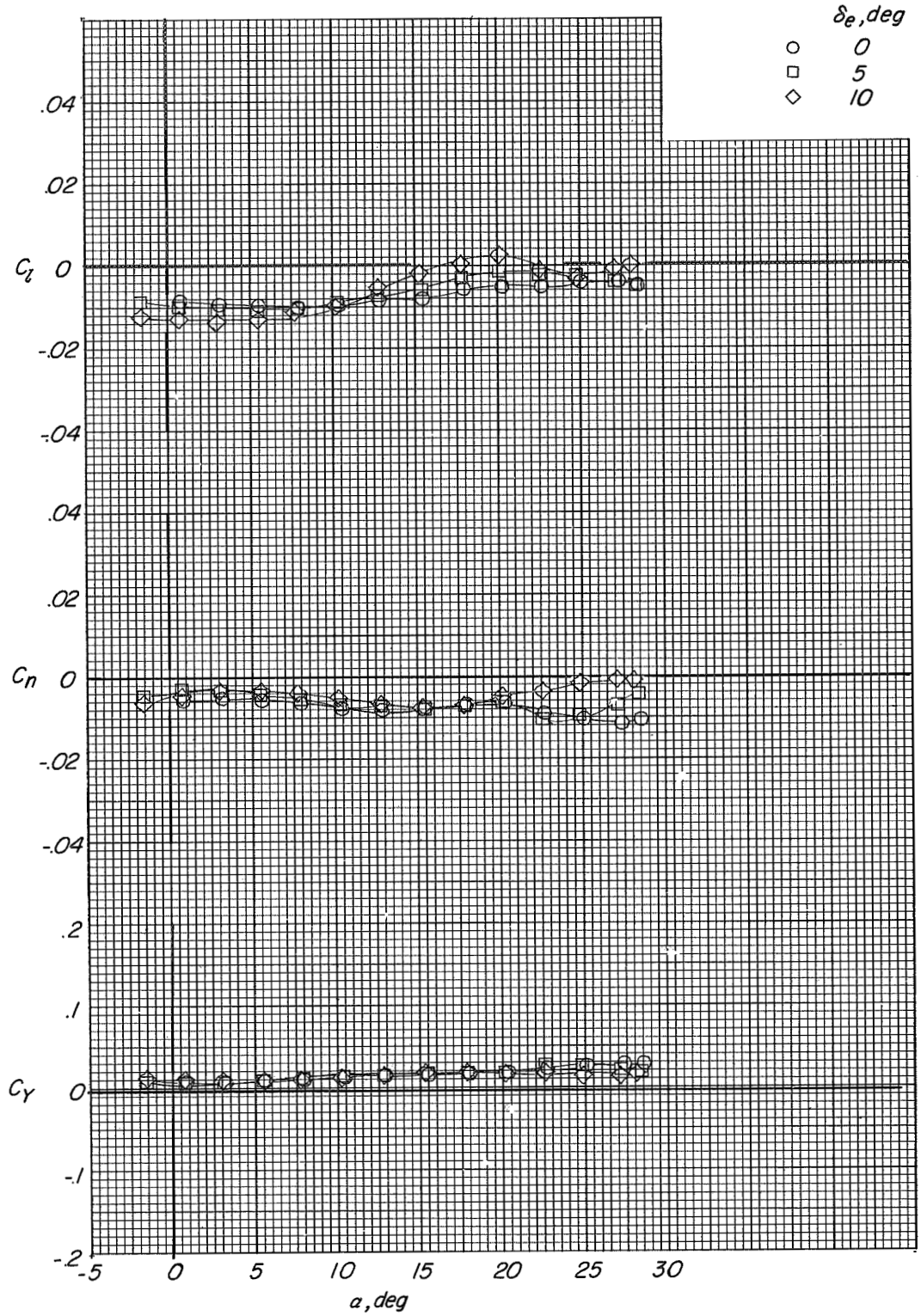
(f) $\delta_a = 10^o$; M = 0.70.

Figure 48.- Continued.



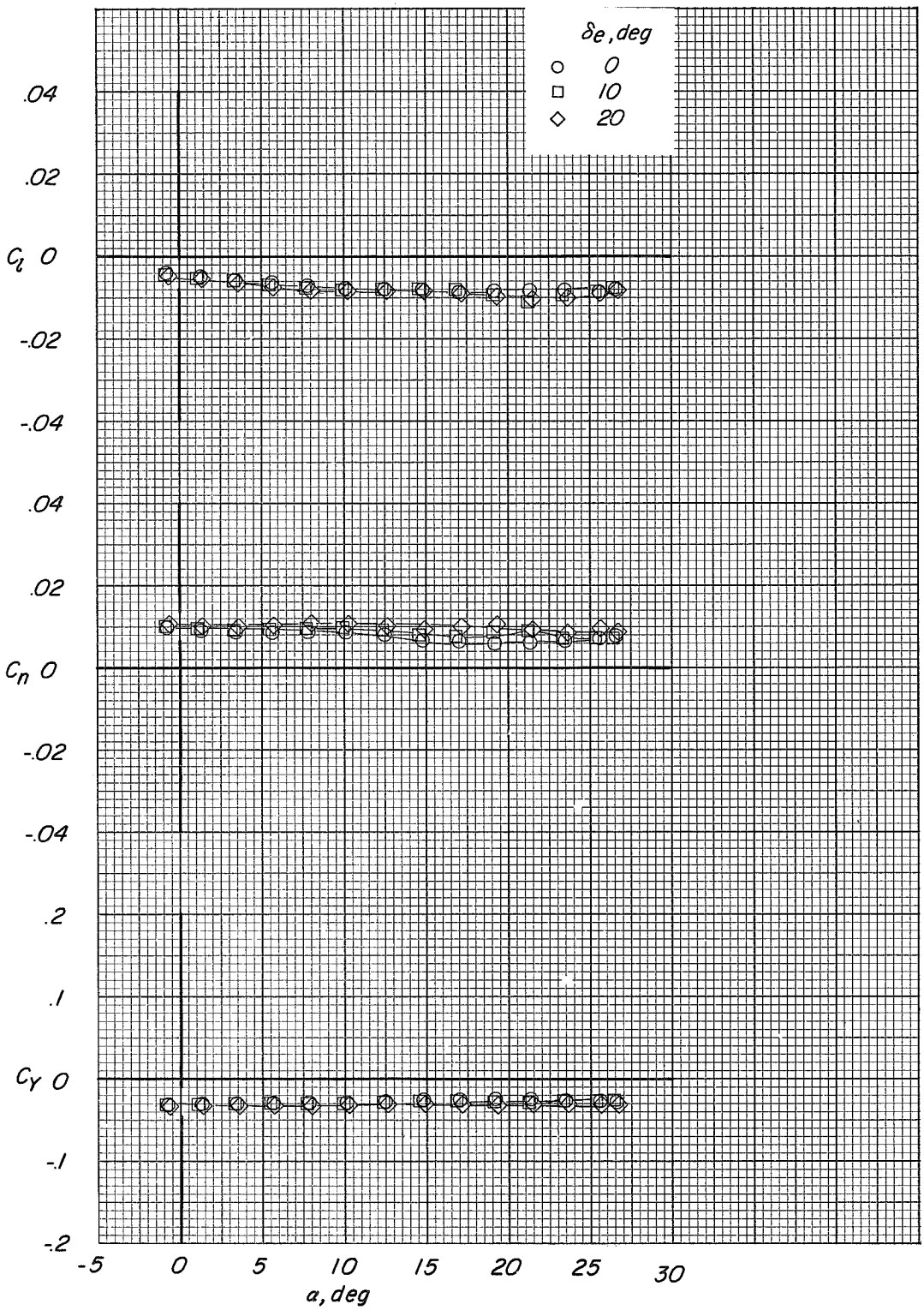
(g) $\delta_a = 10^o$; M = 0.80.

Figure 48.- Continued.



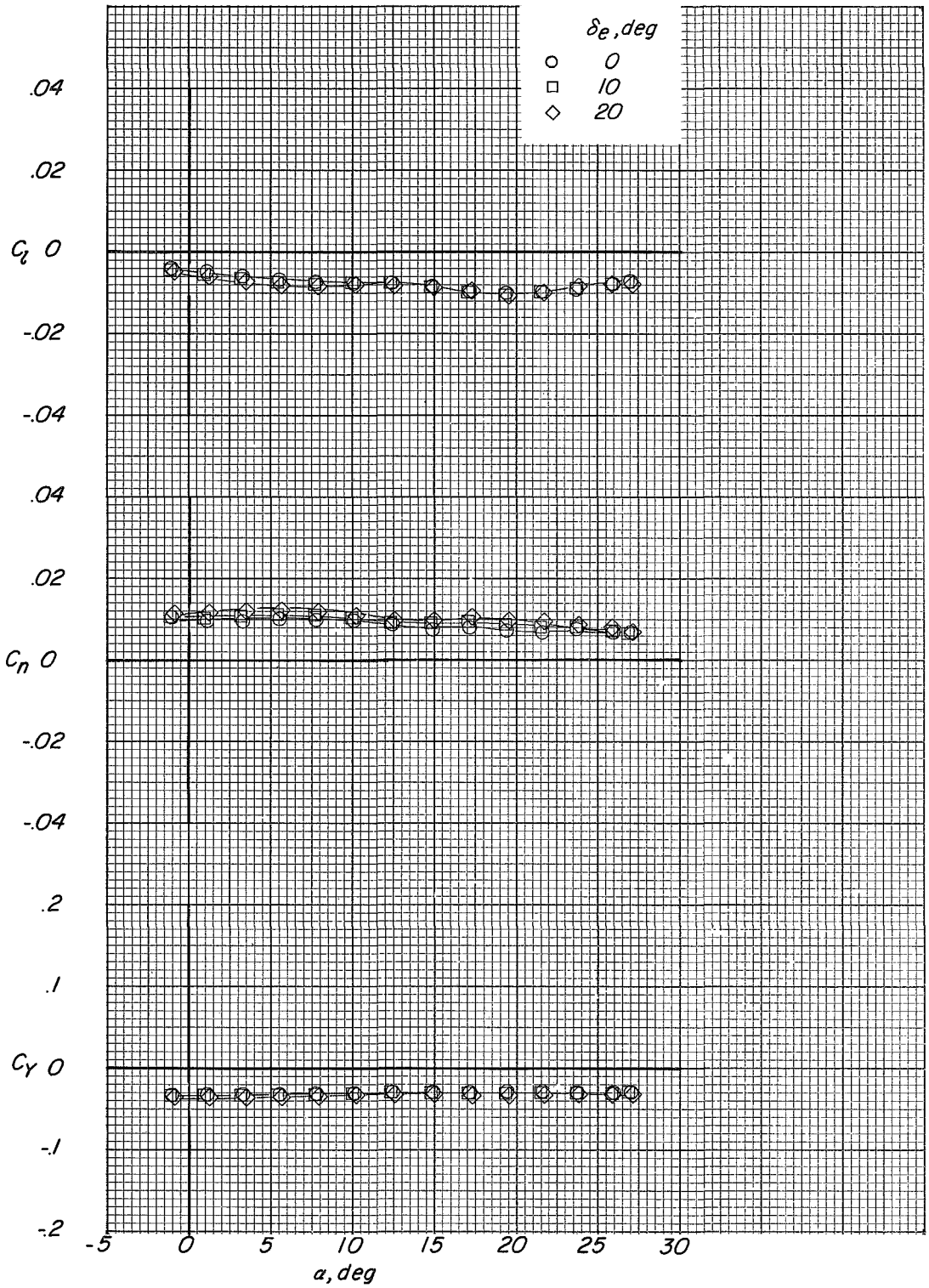
(h) $\delta_a = 10^o$; M = 0.90.

Figure 48.- Concluded.



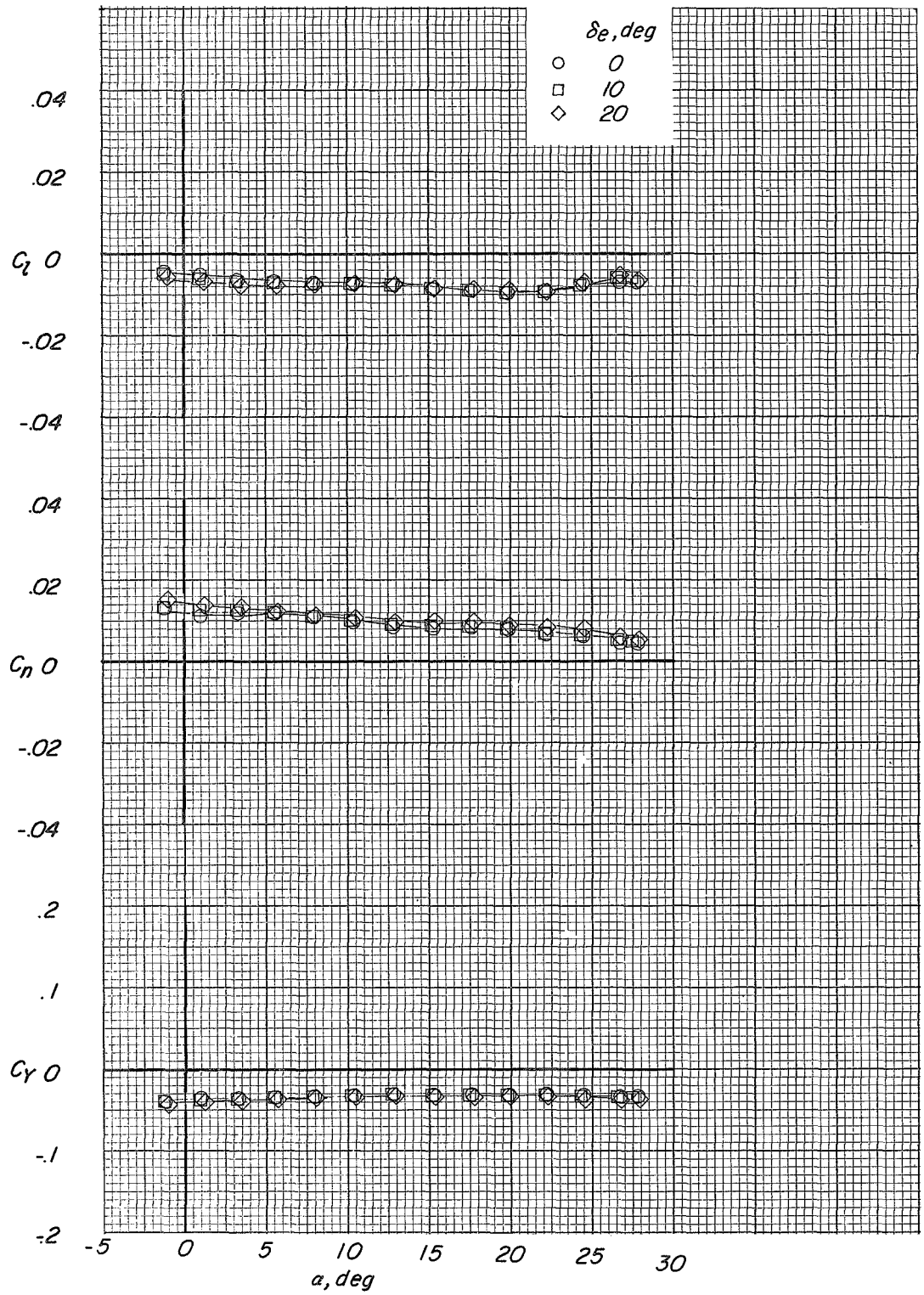
(a) $\beta = 2.3^{\circ}$; M = 0.60.

Figure 49.- Variation of the lateral force and moment coefficients with angle of attack for sideslipped conditions. Modification II fin configuration; auxiliary flaps in the transonic position; $\delta_a = 0^{\circ}$.



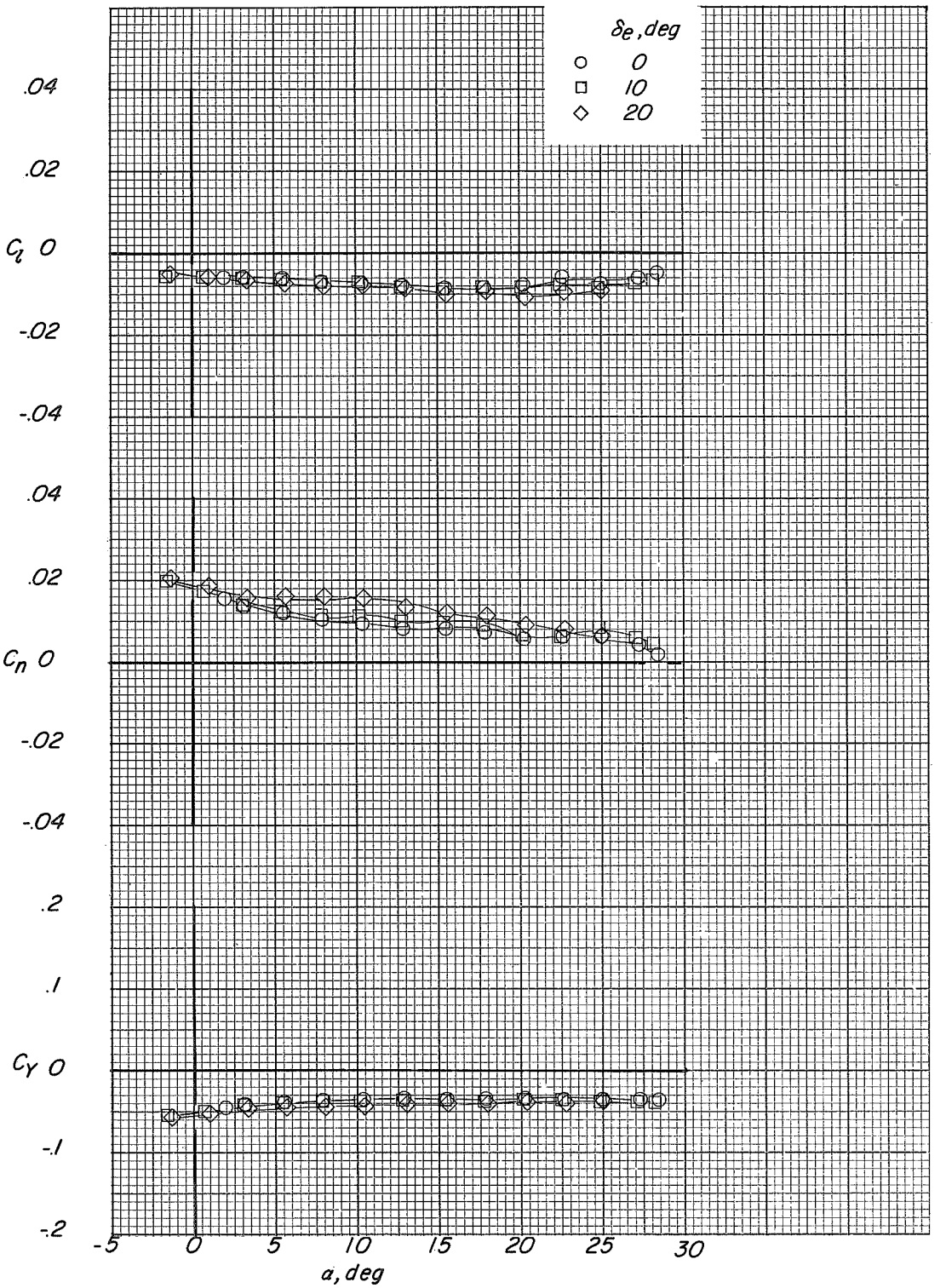
(b) $\beta = 2.3^{\circ}$; M = 0.70.

Figure 49.- Continued.



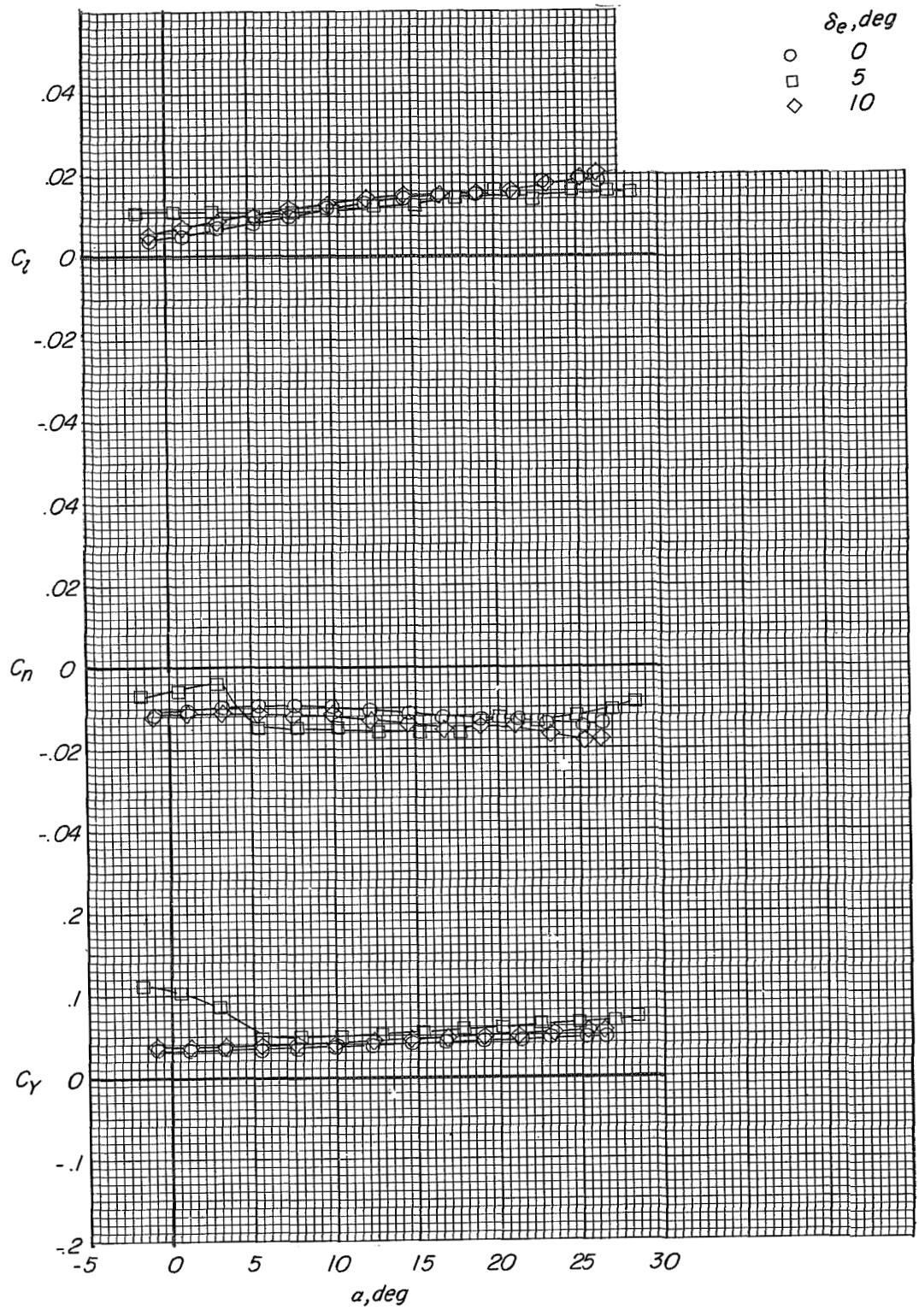
(c) $\beta = 2.3^{\circ}$; M = 0.80.

Figure 49.- Continued.



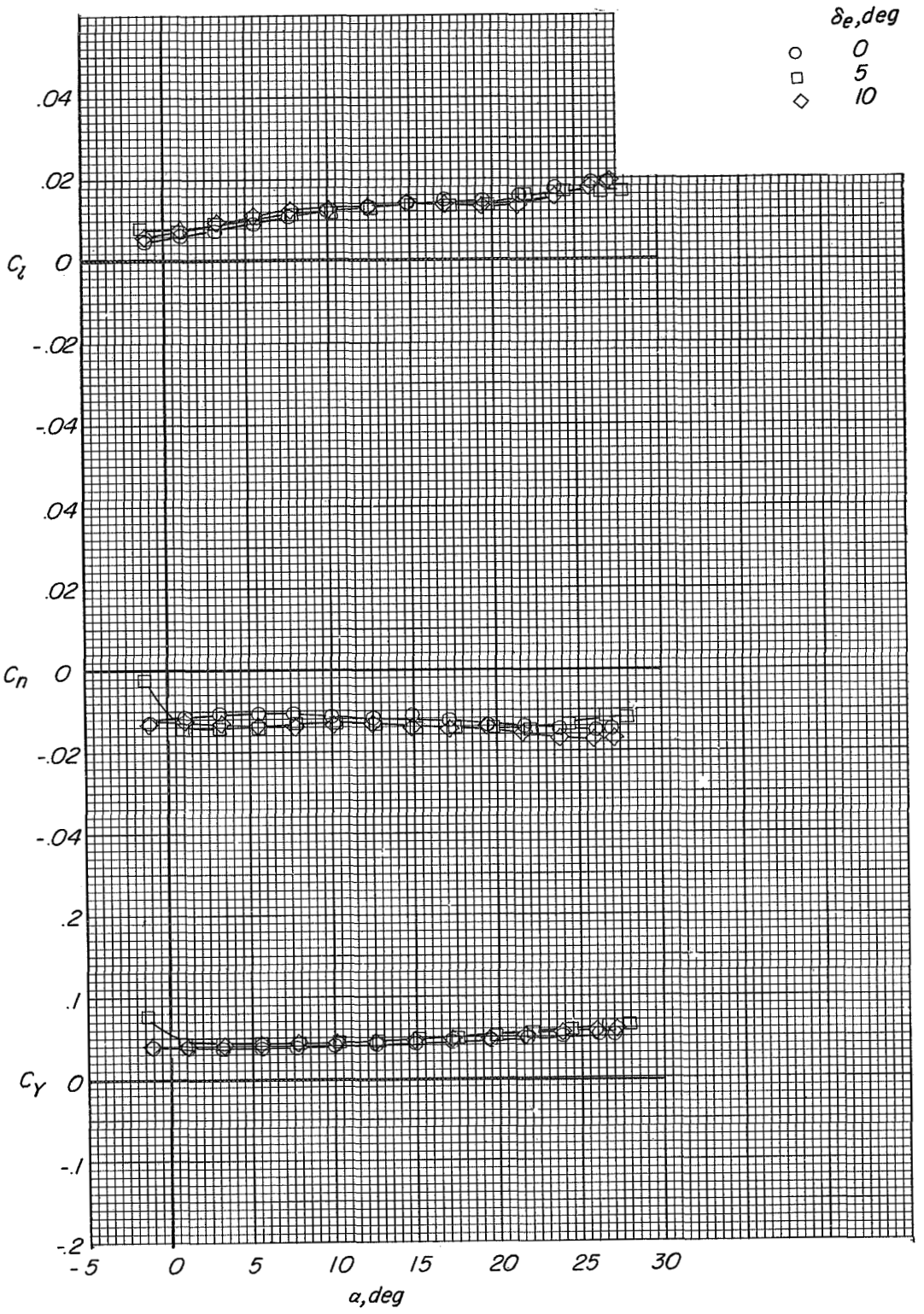
(d) $\beta = 2.3^{o}$; M = 0.90.

Figure 49.- Continued.



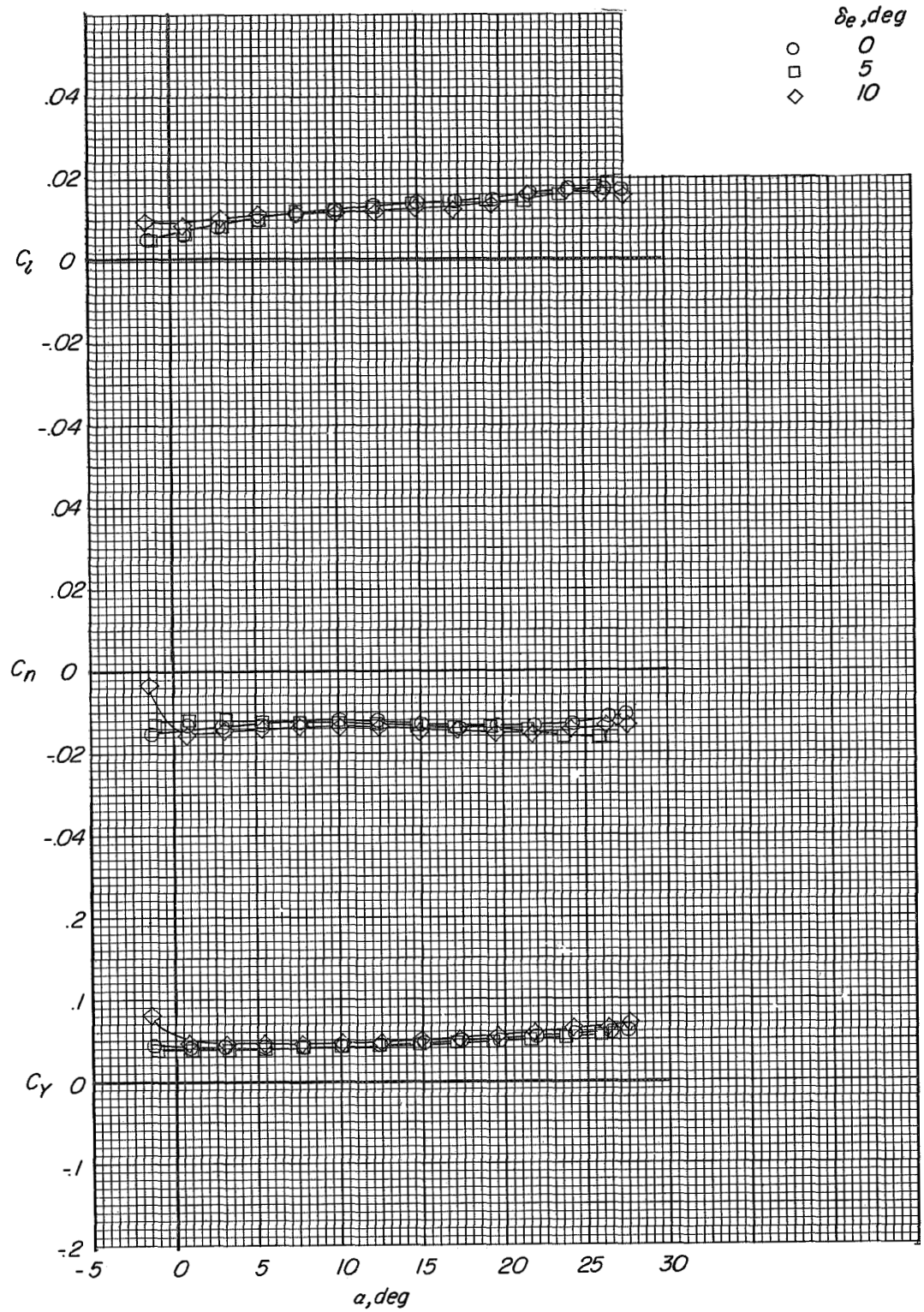
(e) $\beta = -2.3^{o}$; M = 0.60.

Figure 49.- Continued.



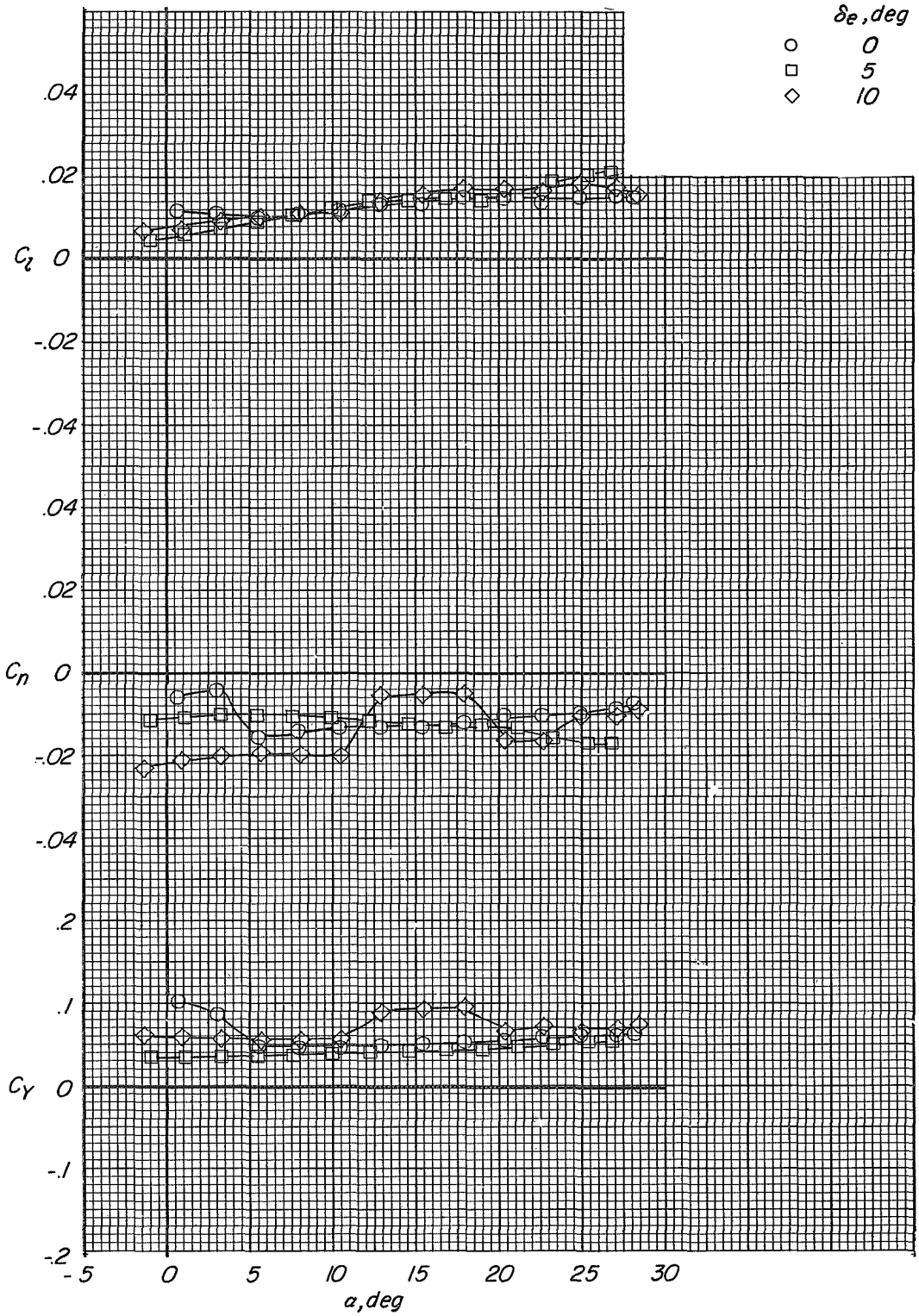
(f) $\beta = -2.3^{o}$; M = 0.70.

Figure 49.- Continued.



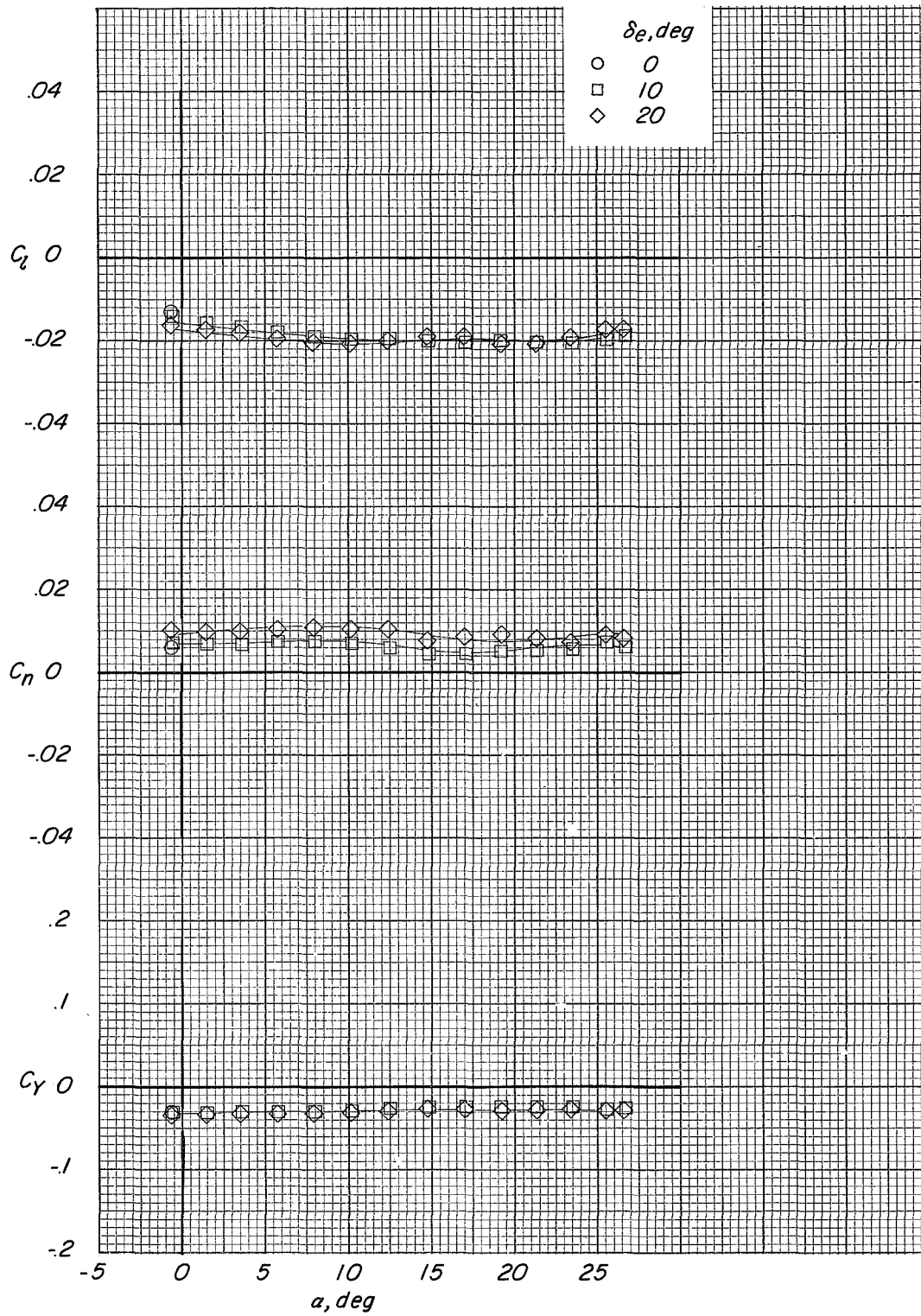
(g) $\beta = -2.3^{o}$; M = 0.80.

Figure 49.- Continued.



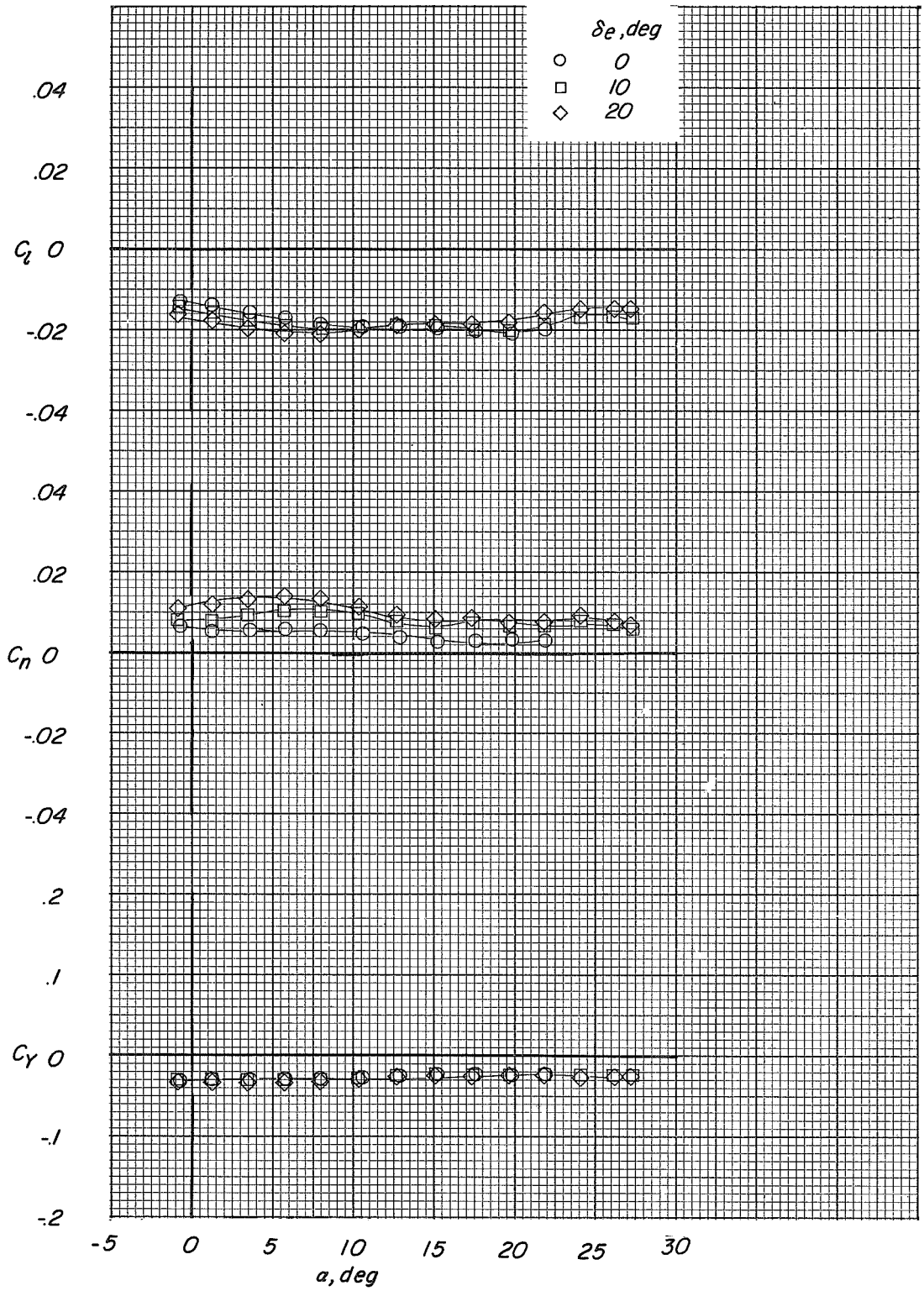
(h) $\beta = -2.3^{\circ}$; M = 0.90.

Figure 49.- Concluded.



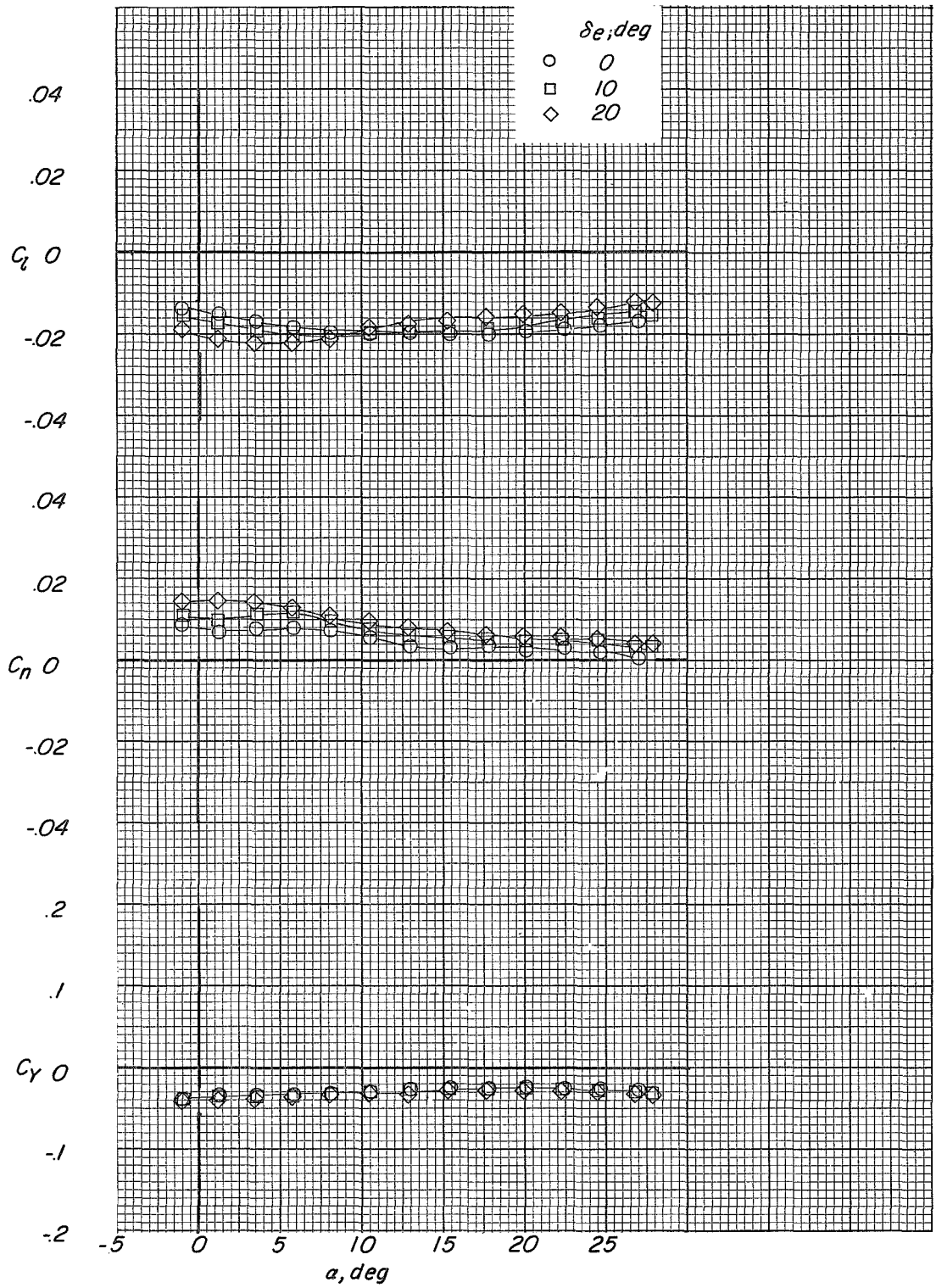
(a) $\beta = 2.3^{o}$; $\delta_a = 10^{o}$; M = 0.60.

Figure 50.- Variation of the lateral force and moment coefficients with angle of attac for combined aileron deflection and sideslip angle. Modification II fin configuration; auxiliary flaps in the transonic position.



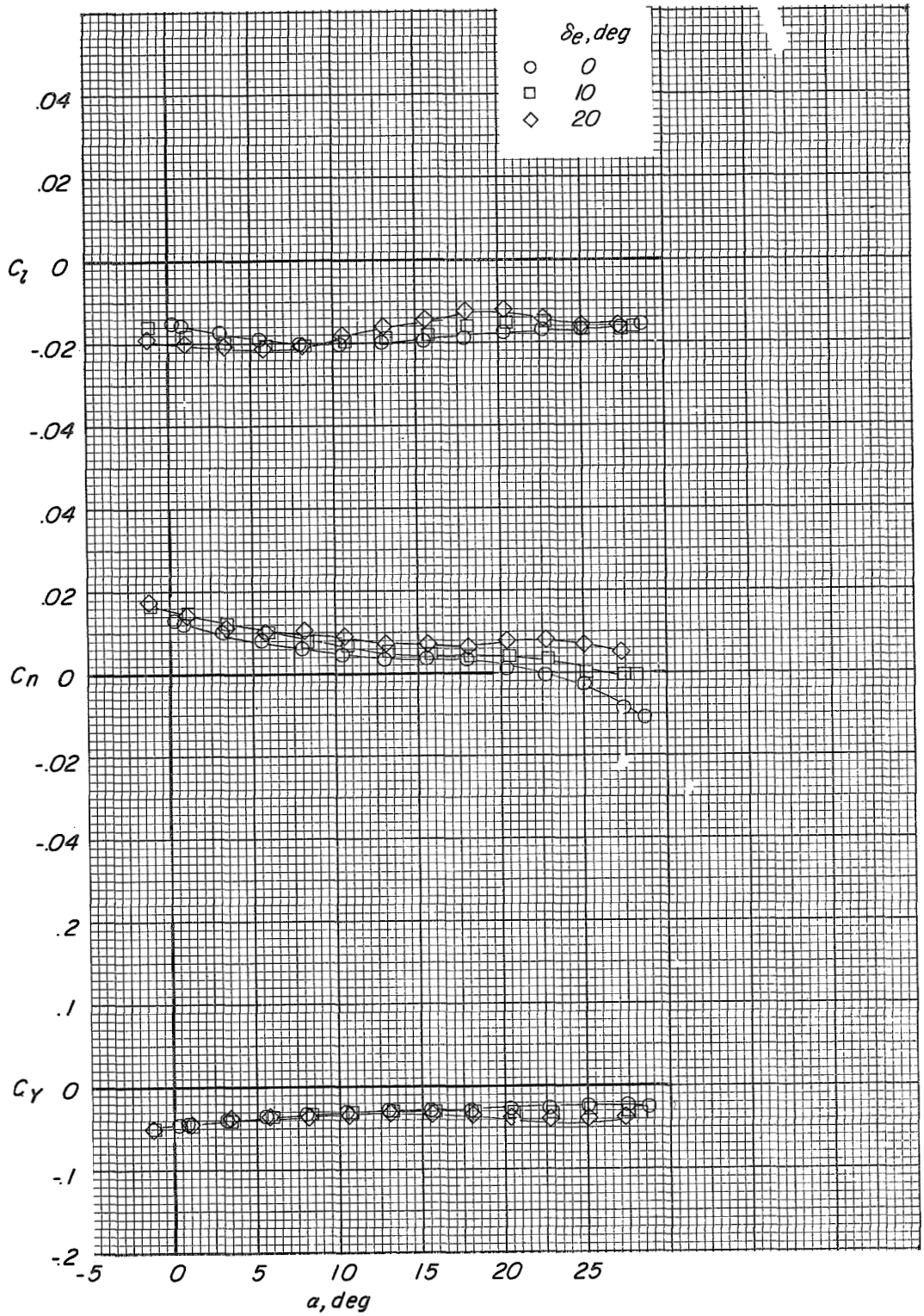
(b) $\beta = 2.3^{o}$; $\delta_a = 10^{o}$; M = 0.70.

Figure 50.- Continued.



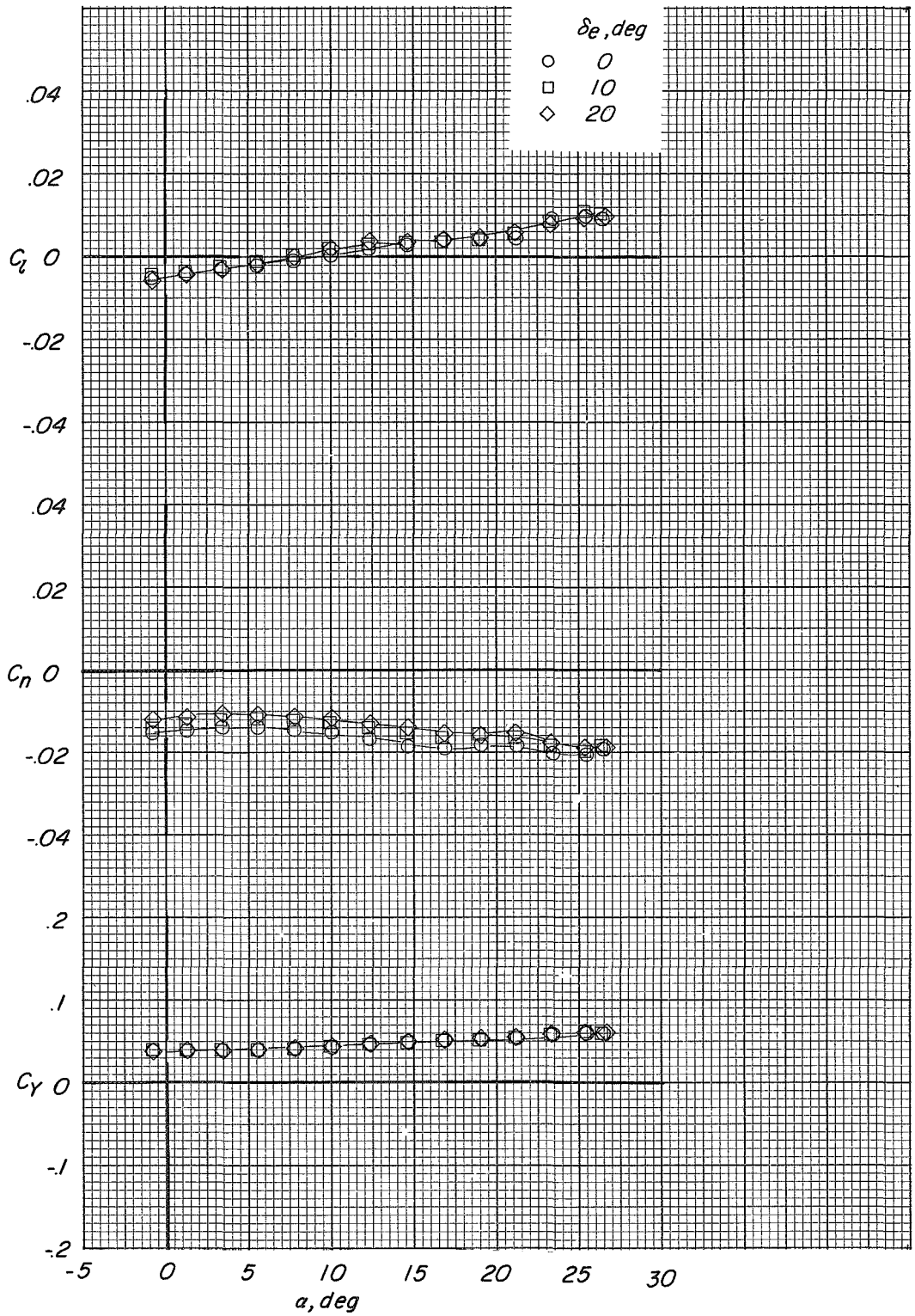
(c) $\beta = 2.3^{\circ}$; $\delta_a = 10^{\circ}$; M = 0.80.

Figure 50.- Continued.



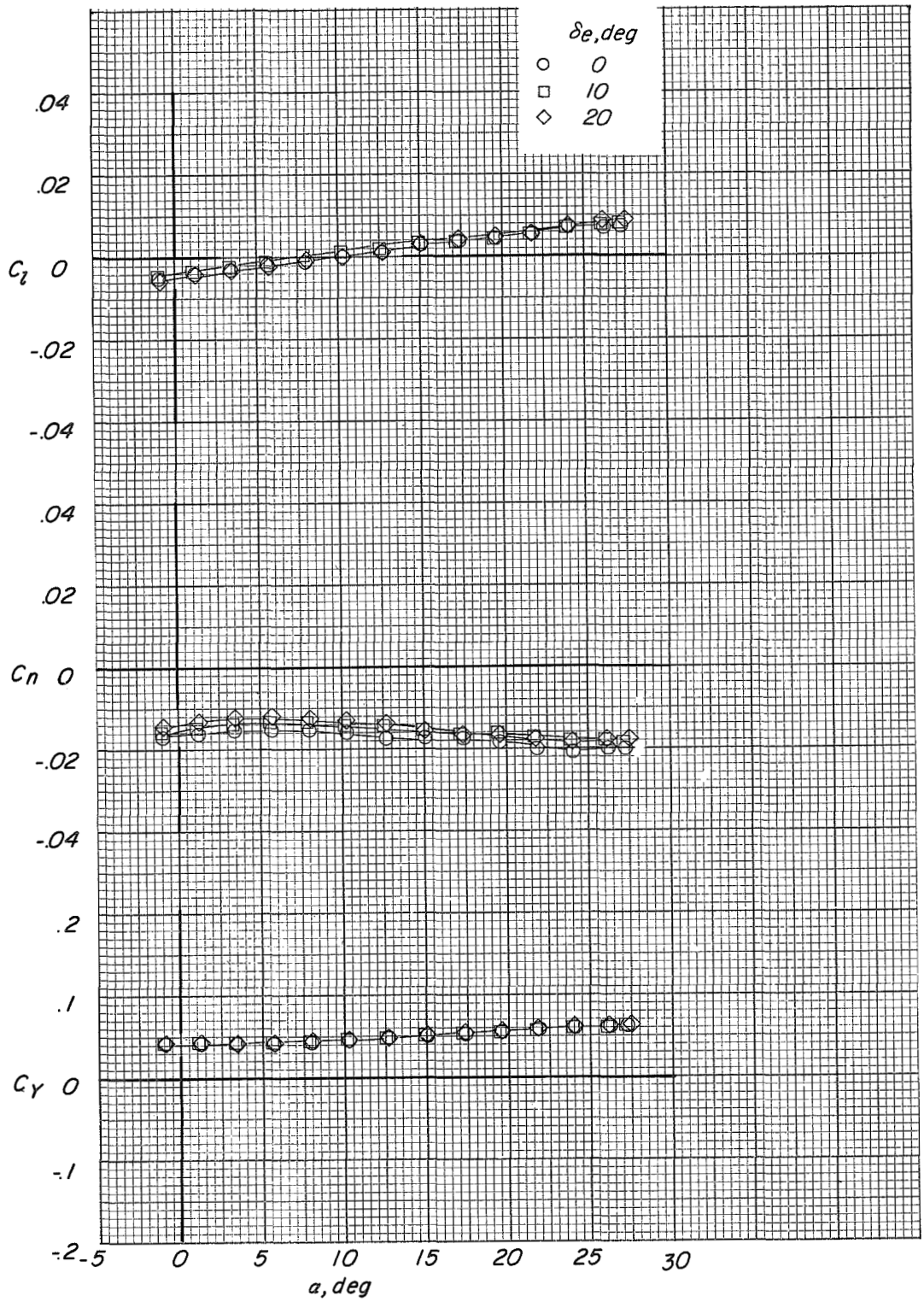
(d) $\beta = 2.3^{o}$; $\delta_a = 10^{o}$; M = 0.90.

Figure 50.- Continued.



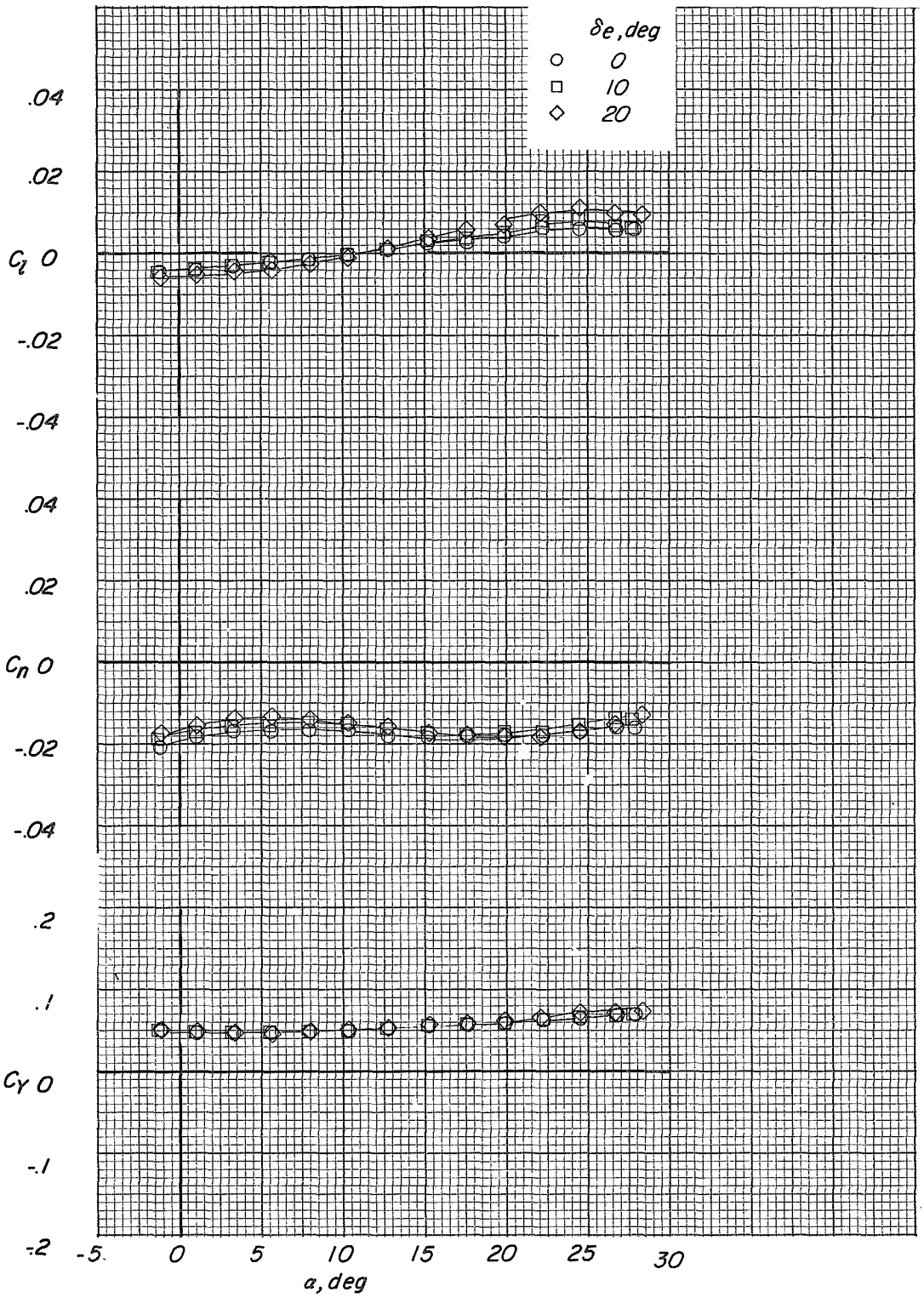
(e) $\beta = -2.3^{o}$; $\delta_a = 10^{o}$; M = 0.60.

Figure 50.- Continued.



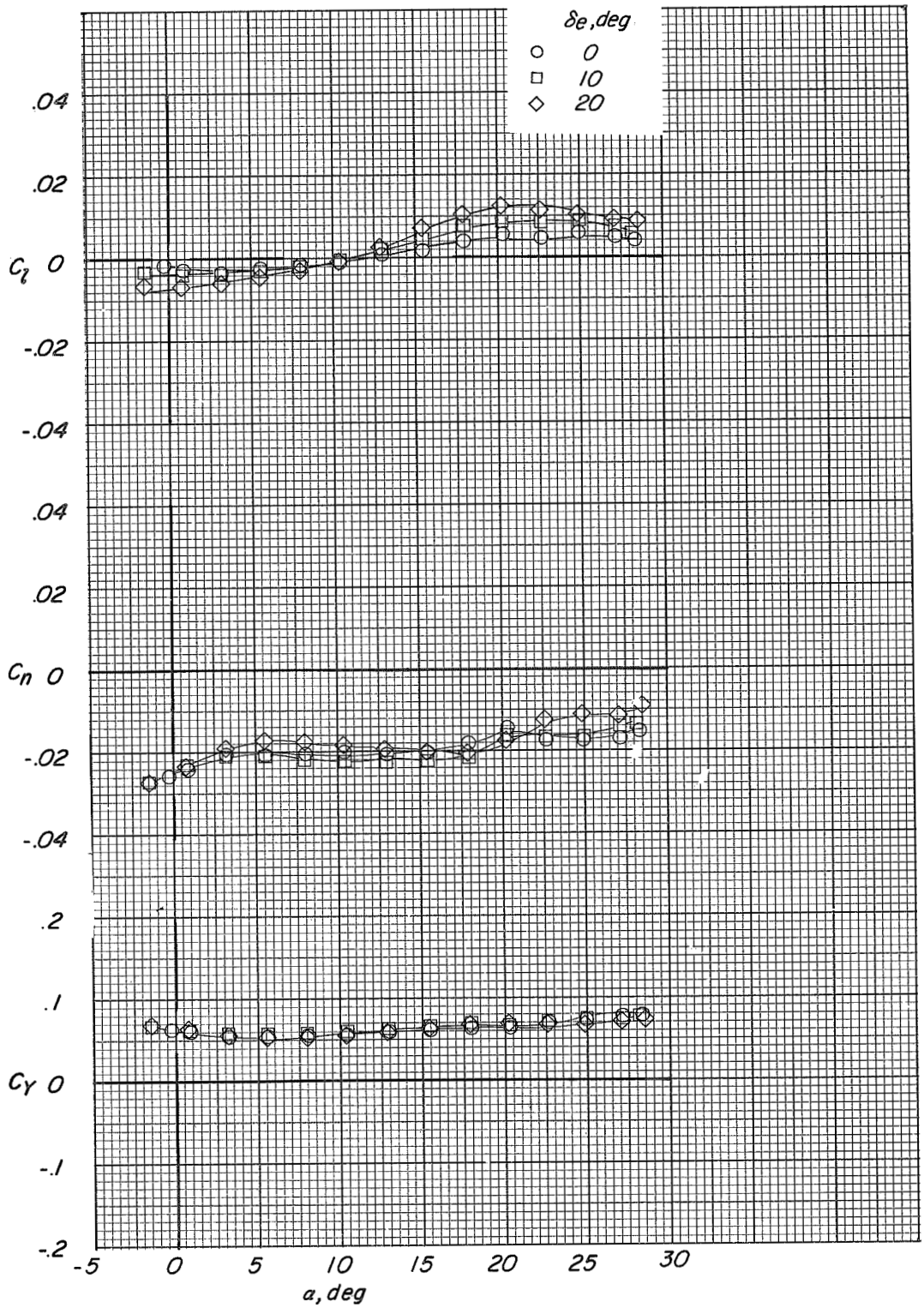
(f) $\beta = -2.3^{o}$; $\delta_a = 10^{o}$; M = 0.70.

Figure 50.- Continued.



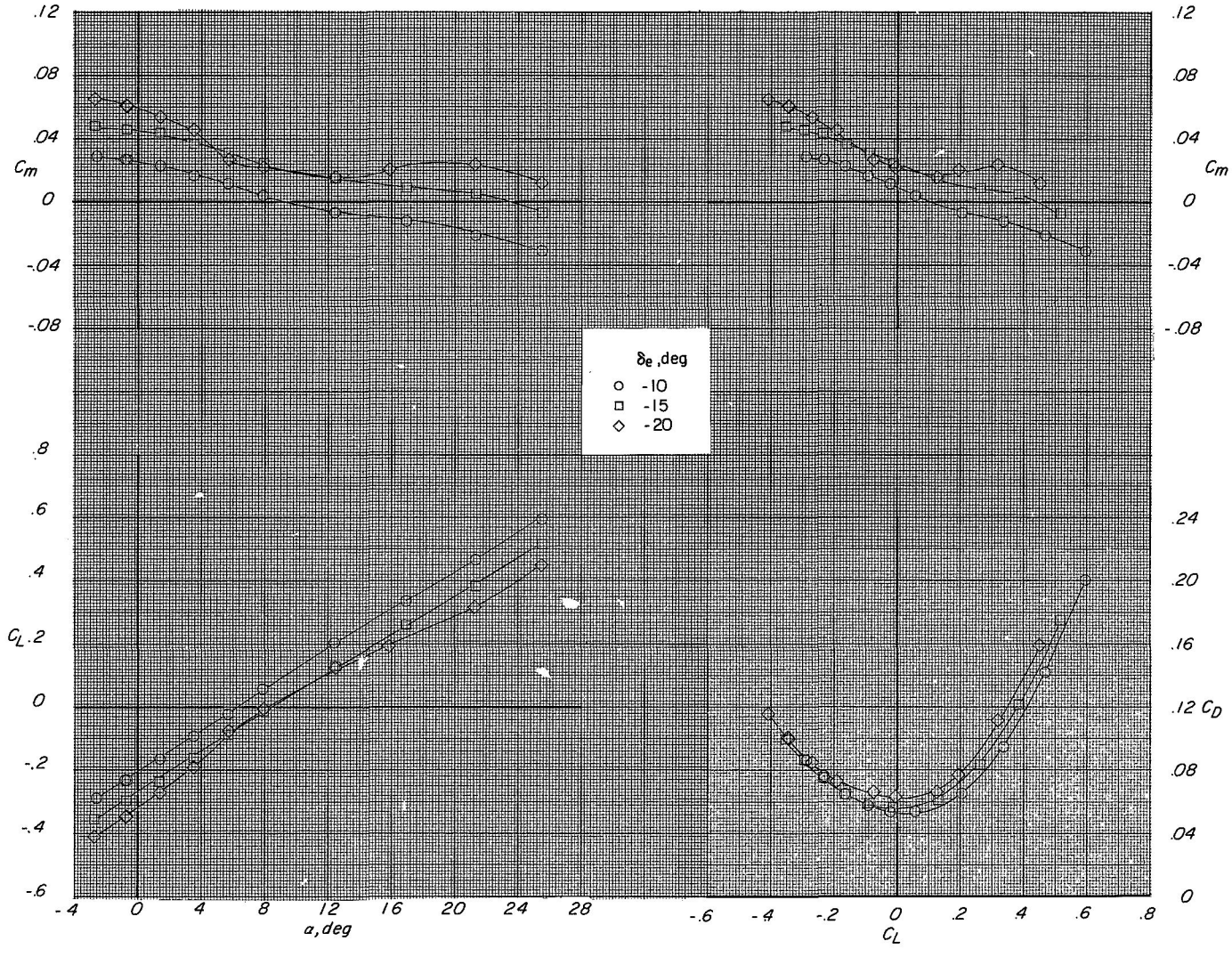
(g) $\beta = -2.3^{O}$; $\delta_a = 10^{O}$; M = 0.80.

Figure 50.- Continued.



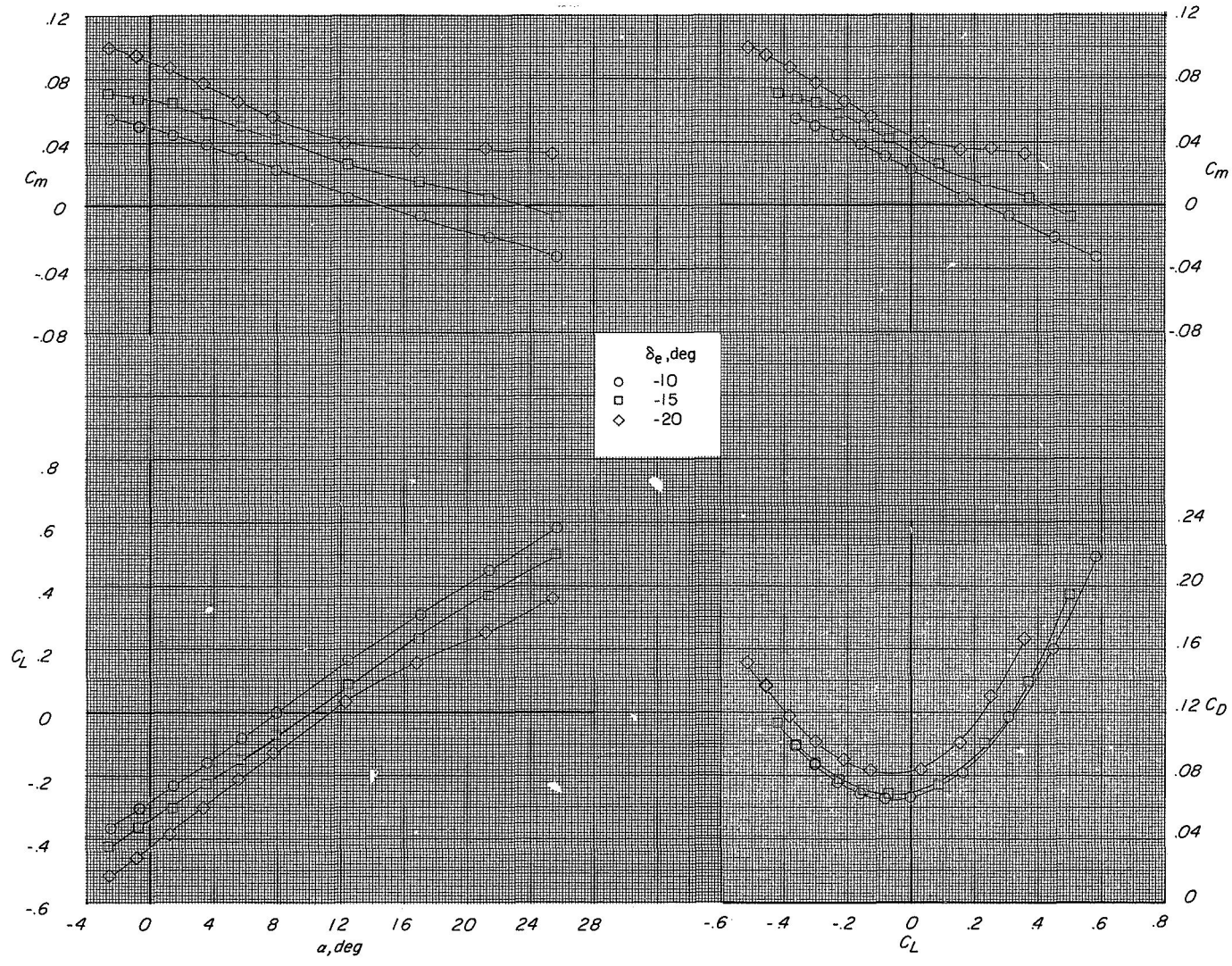
(h) $\beta = -2.3^{\circ}$; $\delta_a = 10^{\circ}$; M = 0.90.

Figure 50.- Concluded.



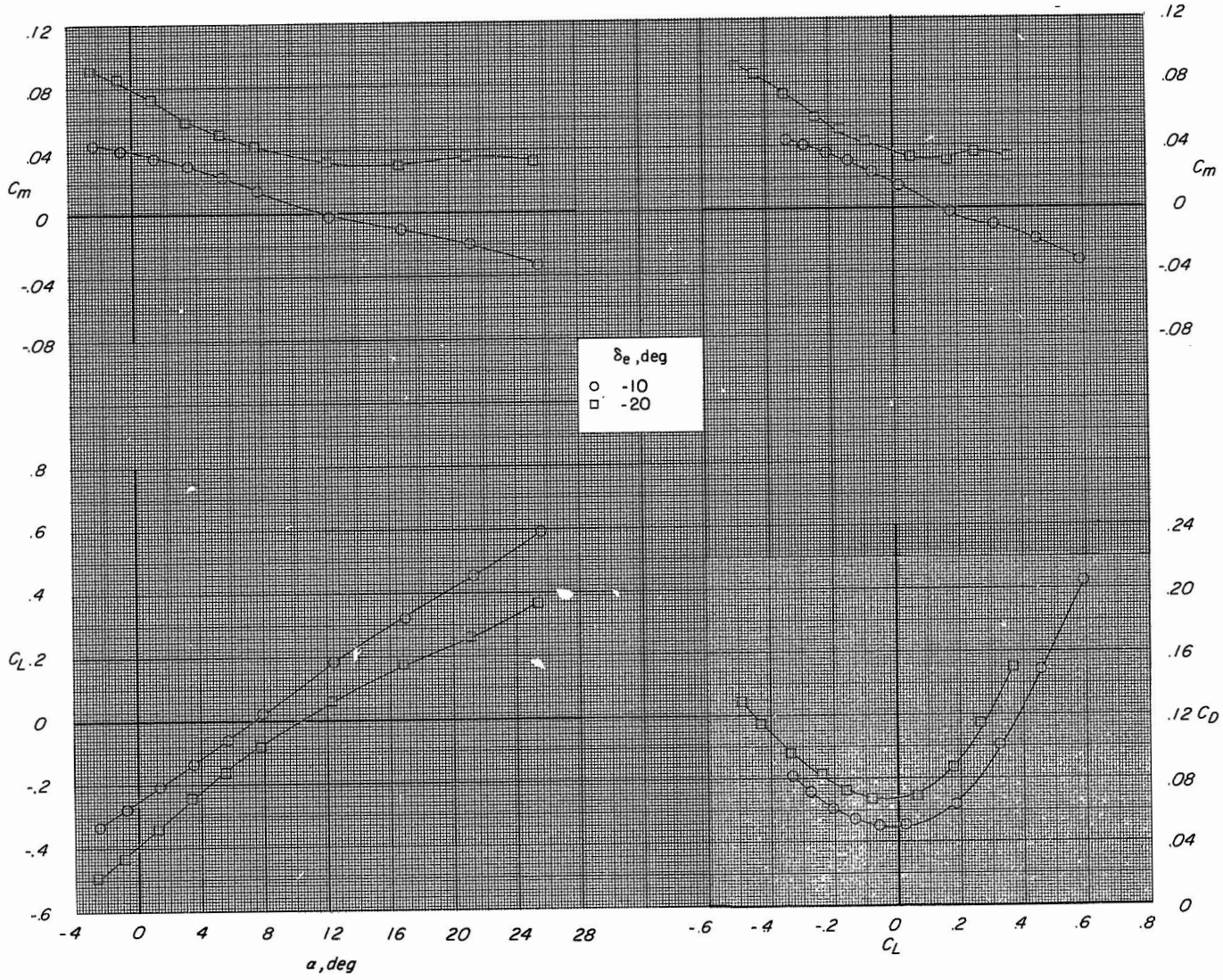
(a) $\delta_{ef} = -8^{o}$; $\delta_{if} = 0^{o}$; $\delta_{of} = 32^{o}$.

Figure 51.- Longitudinal aerodynamic characteristics of the HL-10 with various degrees of deflection on the auxiliary flaps. Modification II fin configuration; $\delta_a = \beta = 0^{o}$; M = 0.60.



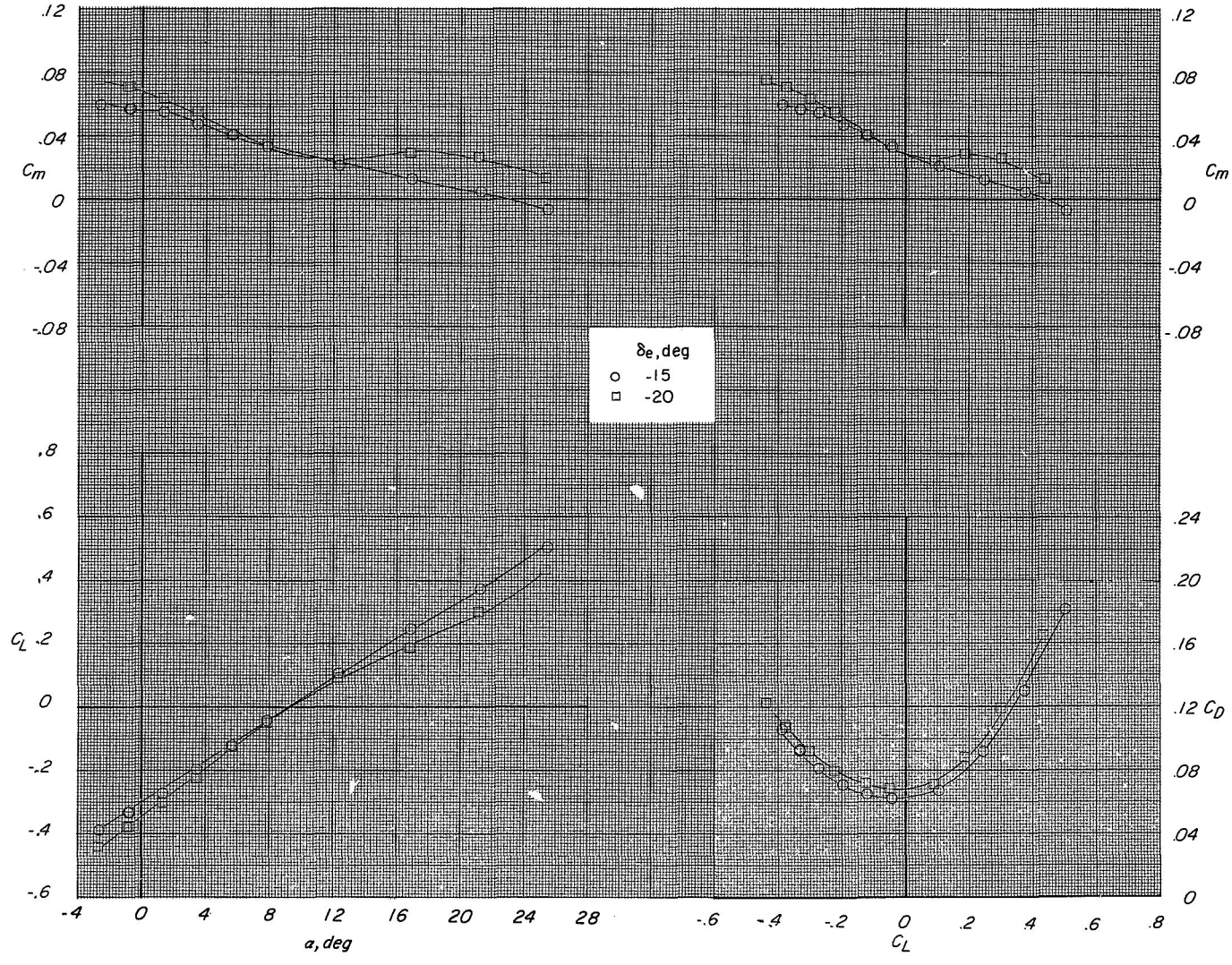
(b) $\delta_{ef} = -8^o$; $\delta_{if} = 32^o$; $\delta_{of} = 0^o$.

Figure 51.- Continued.



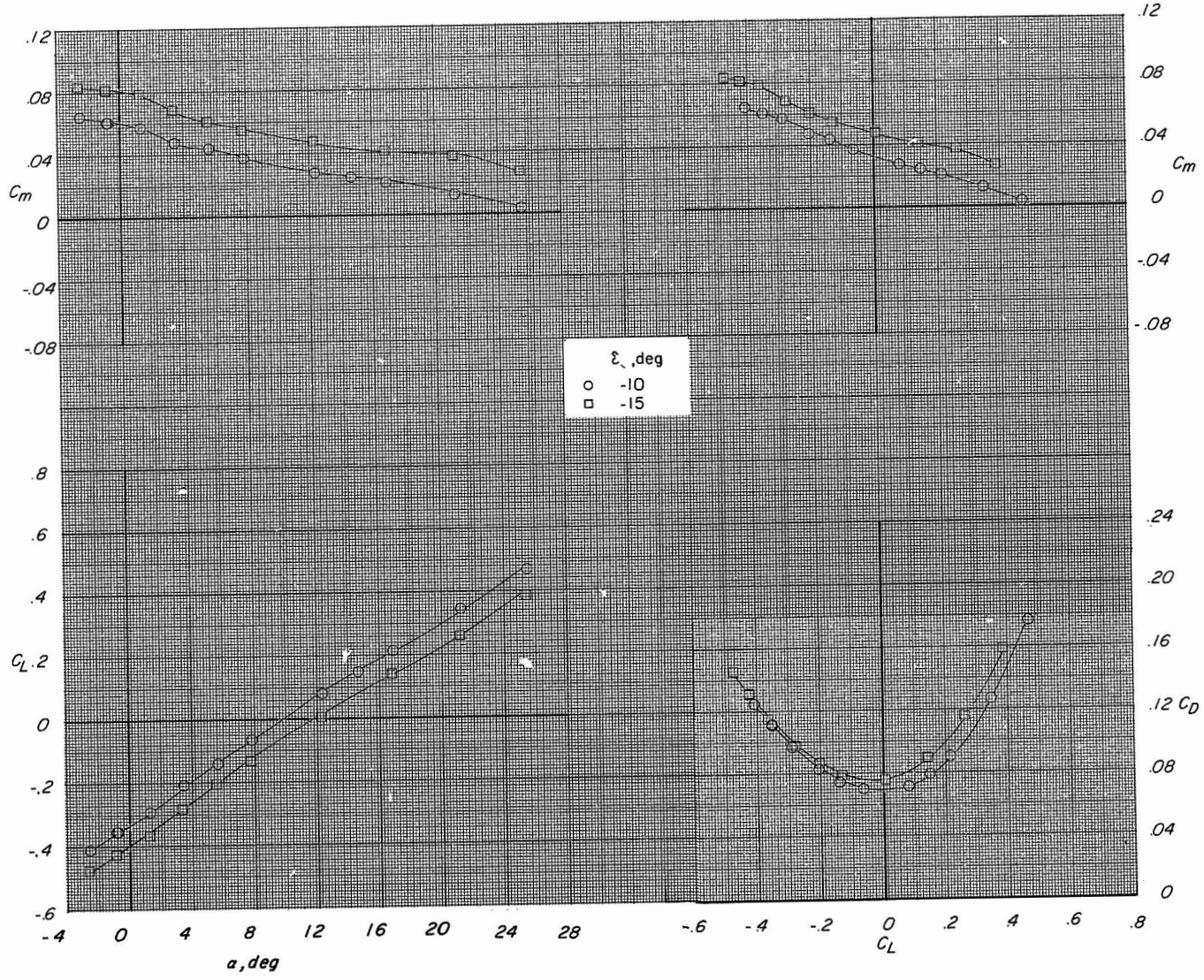
(c) $\delta_{ef} = -8^{o}$; $\delta_{if} = \delta_{of} = 16^{o}$.

Figure 51.- Continued.



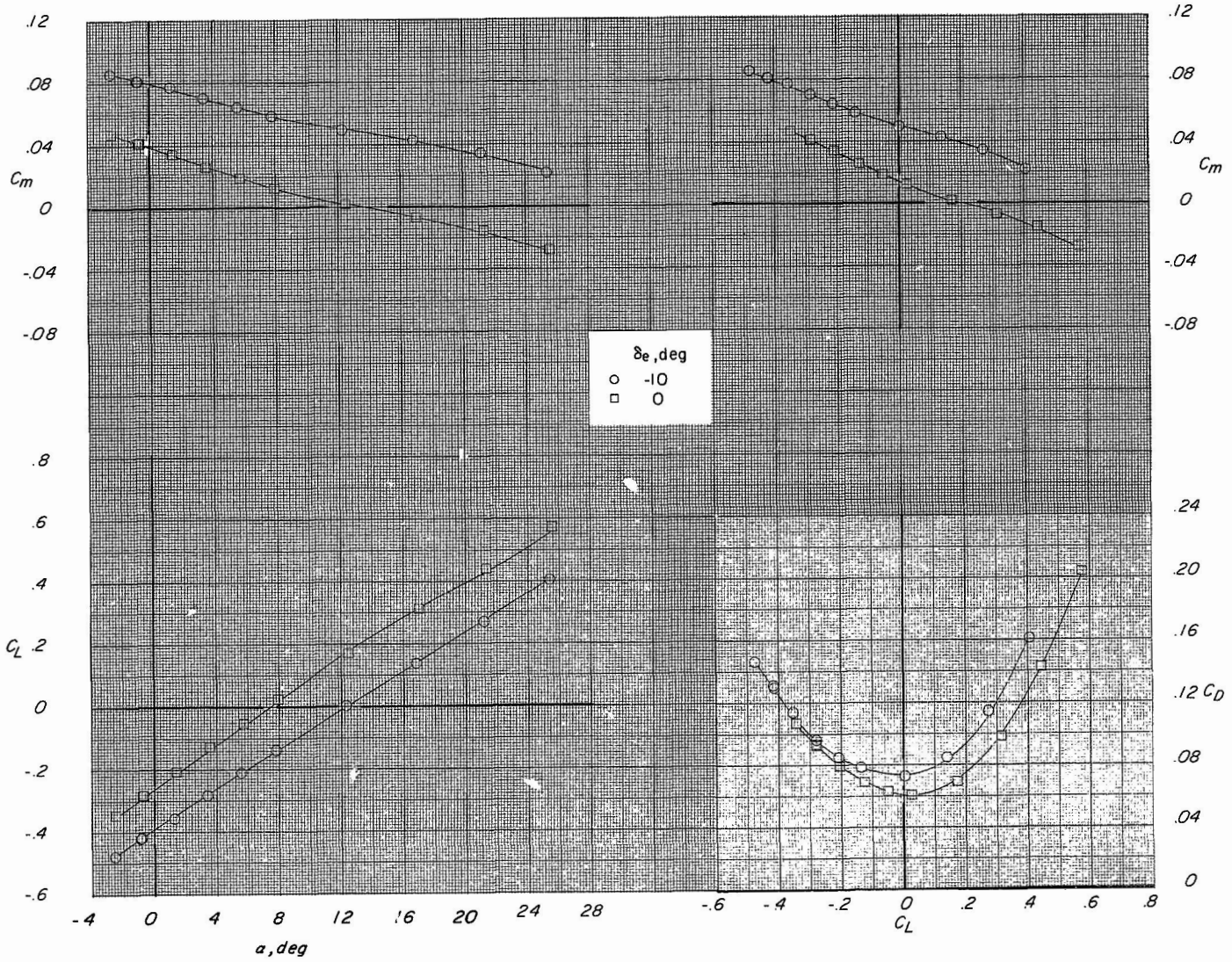
(d) $\delta_{ef} = -8^{o}$; $(\delta_{if})_L = (\delta_{of})_R = 0^{o}$; $(\delta_{if})_R = (\delta_{of})_L = 32^{o}$.

Figure 51.- Continued.



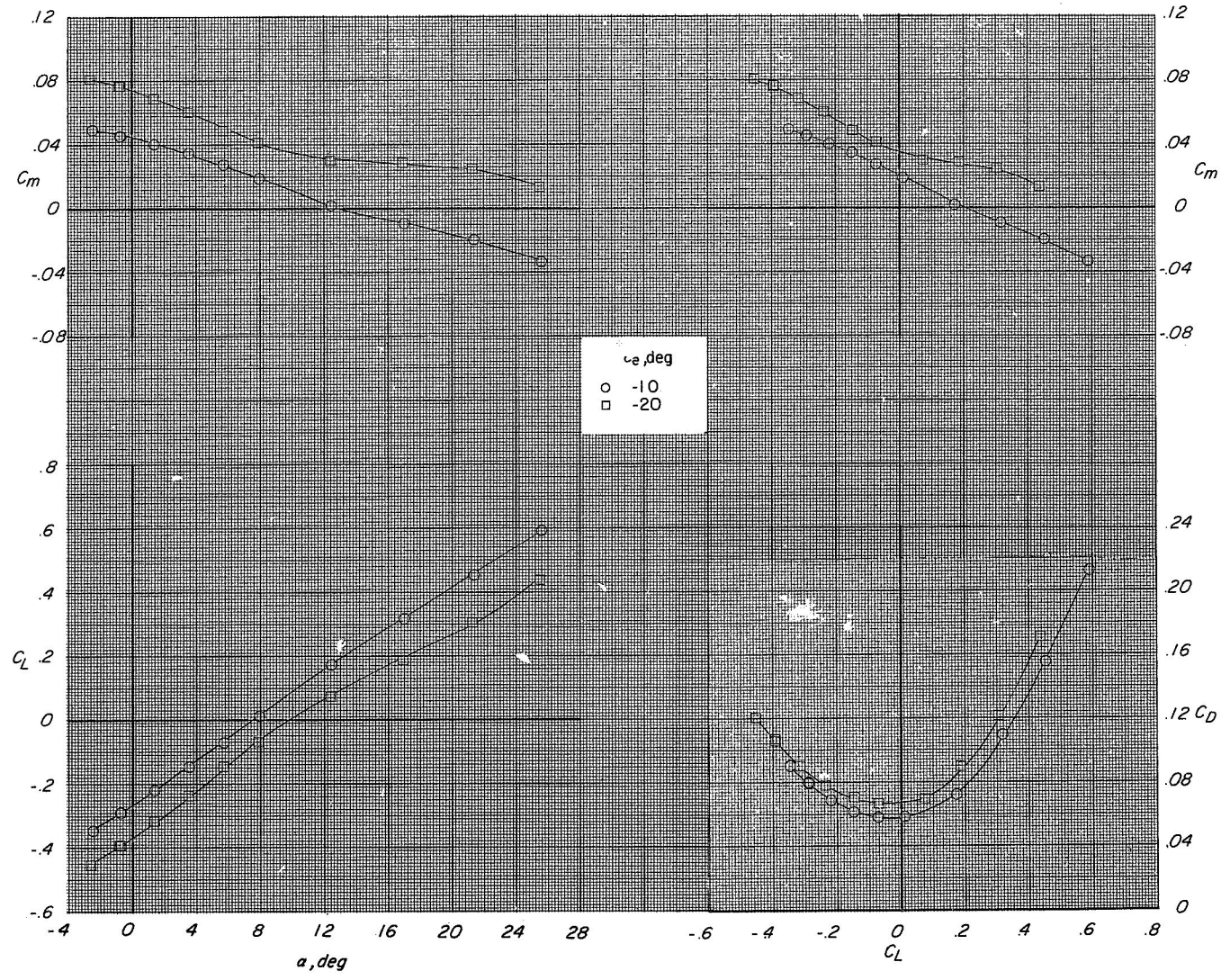
(e) $(\delta_{ef})_L = -8^o$; $(\delta_{ef})_R = 13^o$; $\delta_{if} = 0^o$; $\delta_{of} = 32^o$.

Figure 51.- Continued.

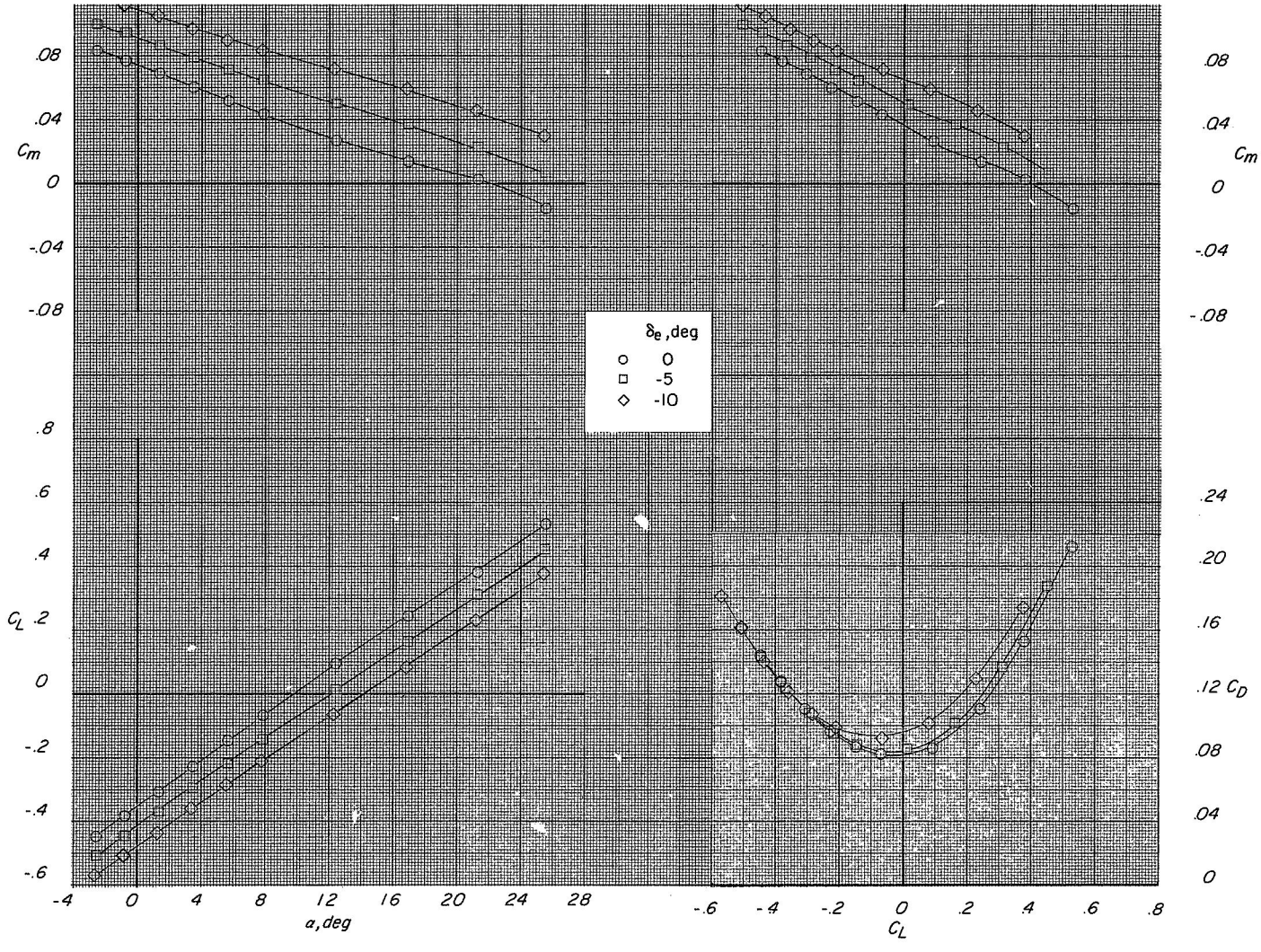


(f) $(\delta_{ef})_L = 3^o$; $(\delta_{ef})_R = 13^o$; $\delta_{if} = 0^o$; $\delta_{of} = 32^o$.

Figure 51.- Continued.

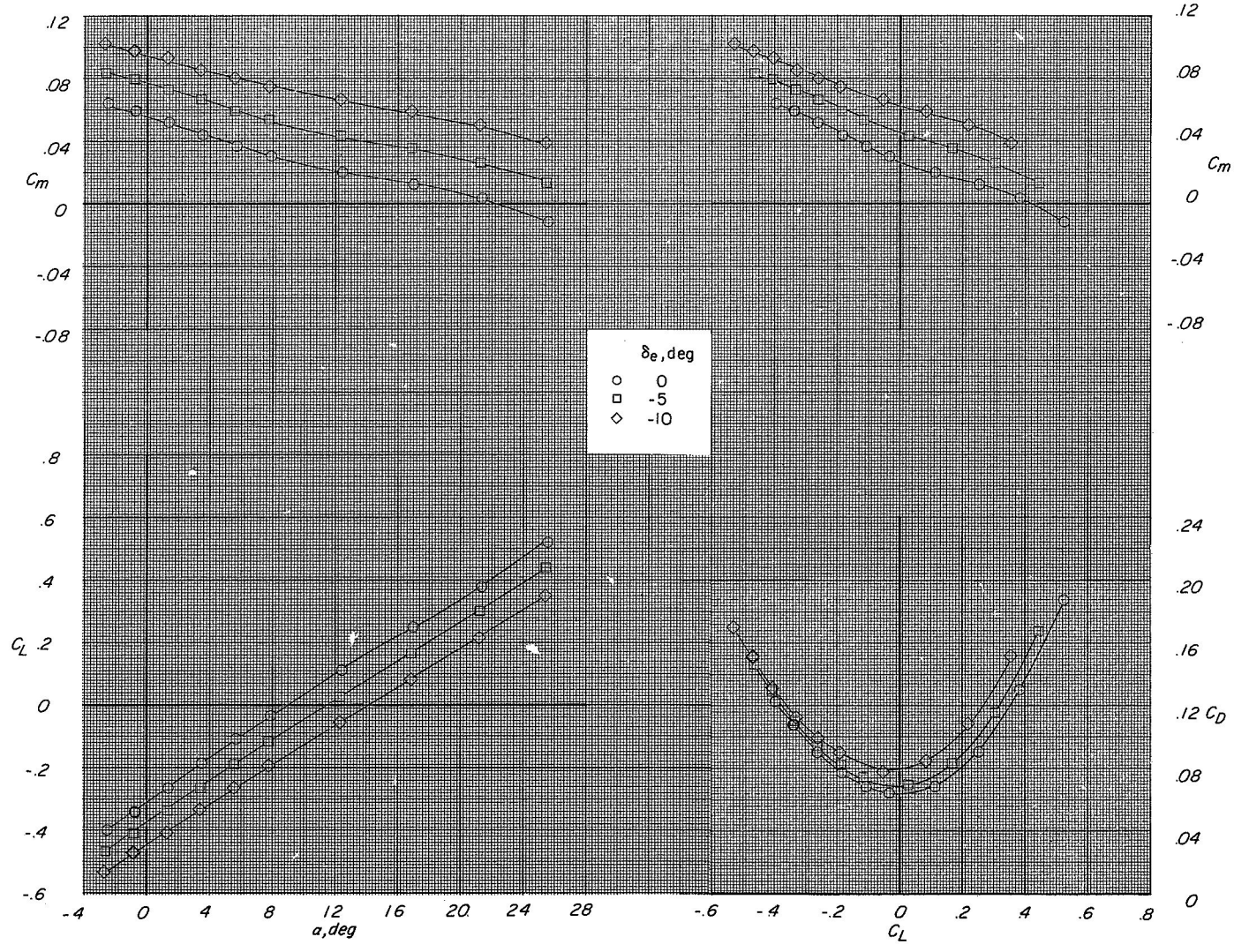


(g) $\delta_{ef} = 0^{o}$; $(\delta_{if})_L = (\delta_{of})_L = 16^{o}$; $(\delta_{if})_R = 32^{o}$; $(\delta_{of})_R = 16^{o}$.



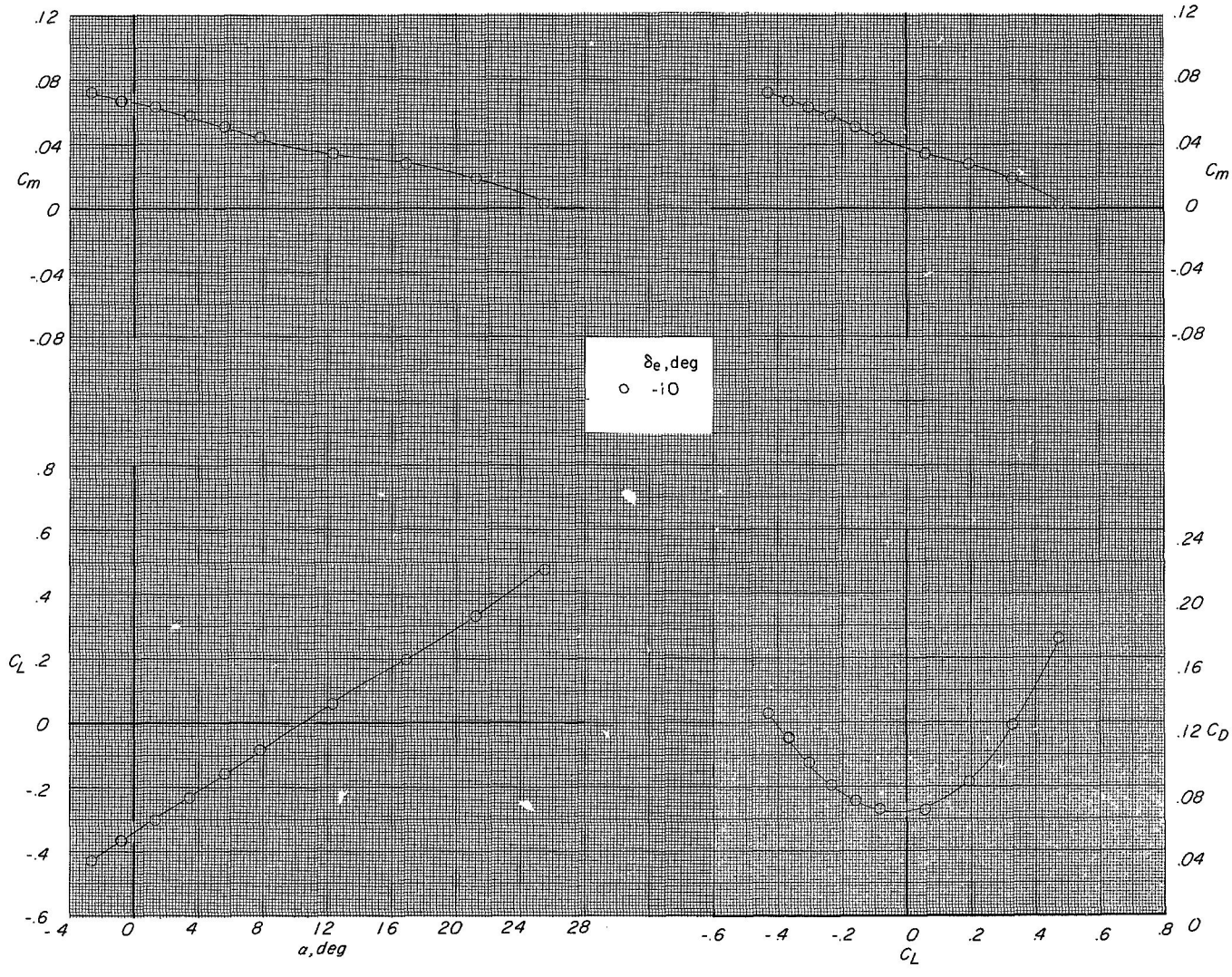
(a) $\delta_{ef} = 13^o$; $\delta_{if} = 32^o$; $\delta_{of} = 0^o$.

Figure 52.- Longitudinal aerodynamic characteristics of the HL-10 with modification II fin configuration. $\delta_a = \beta = 0^o$; M = 0.60.



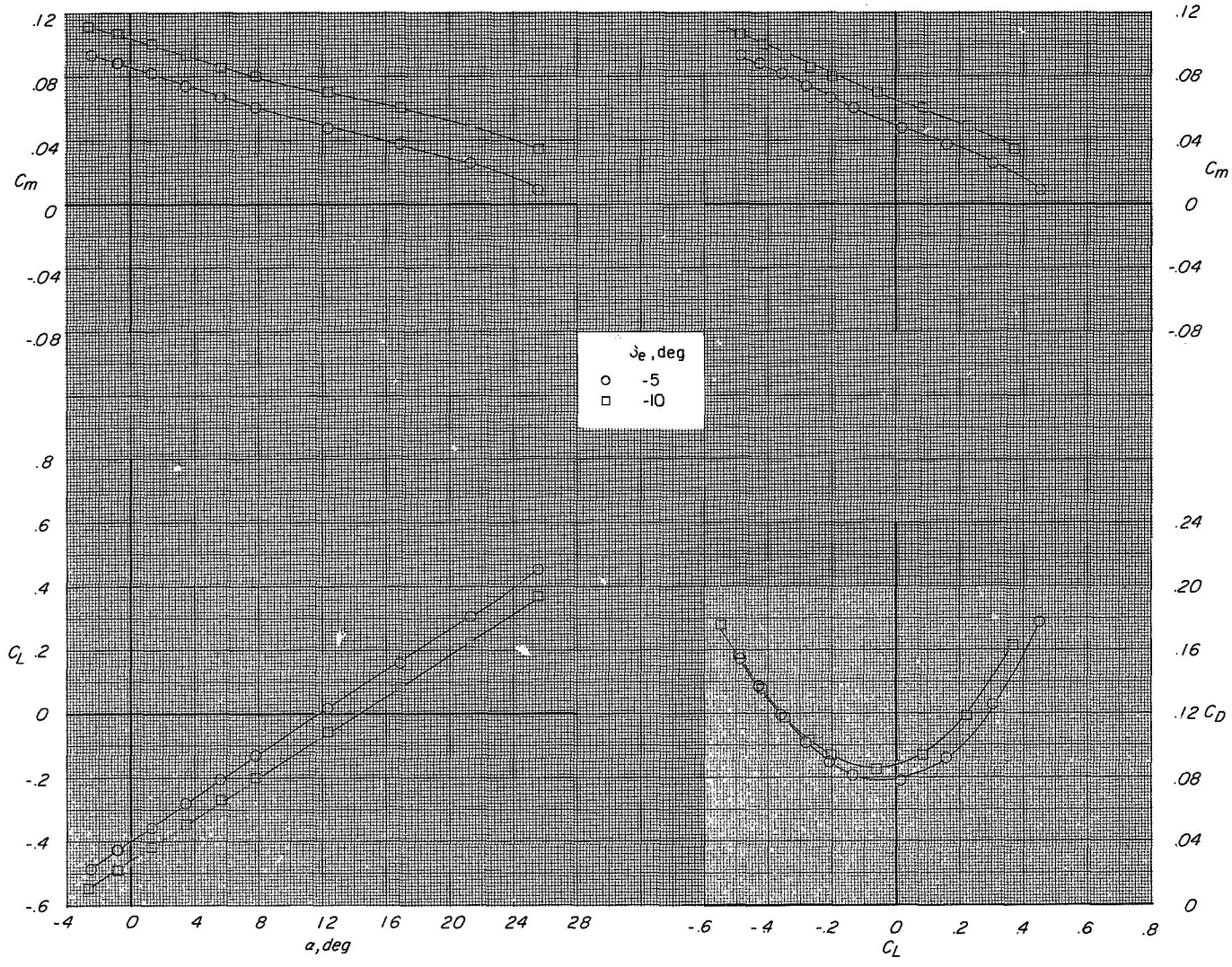
(b) $\delta_{ef} = 13^o$; $\delta_{if} = 0^o$; $\delta_{of} = 32^o$.

Figure 52.- Continued.



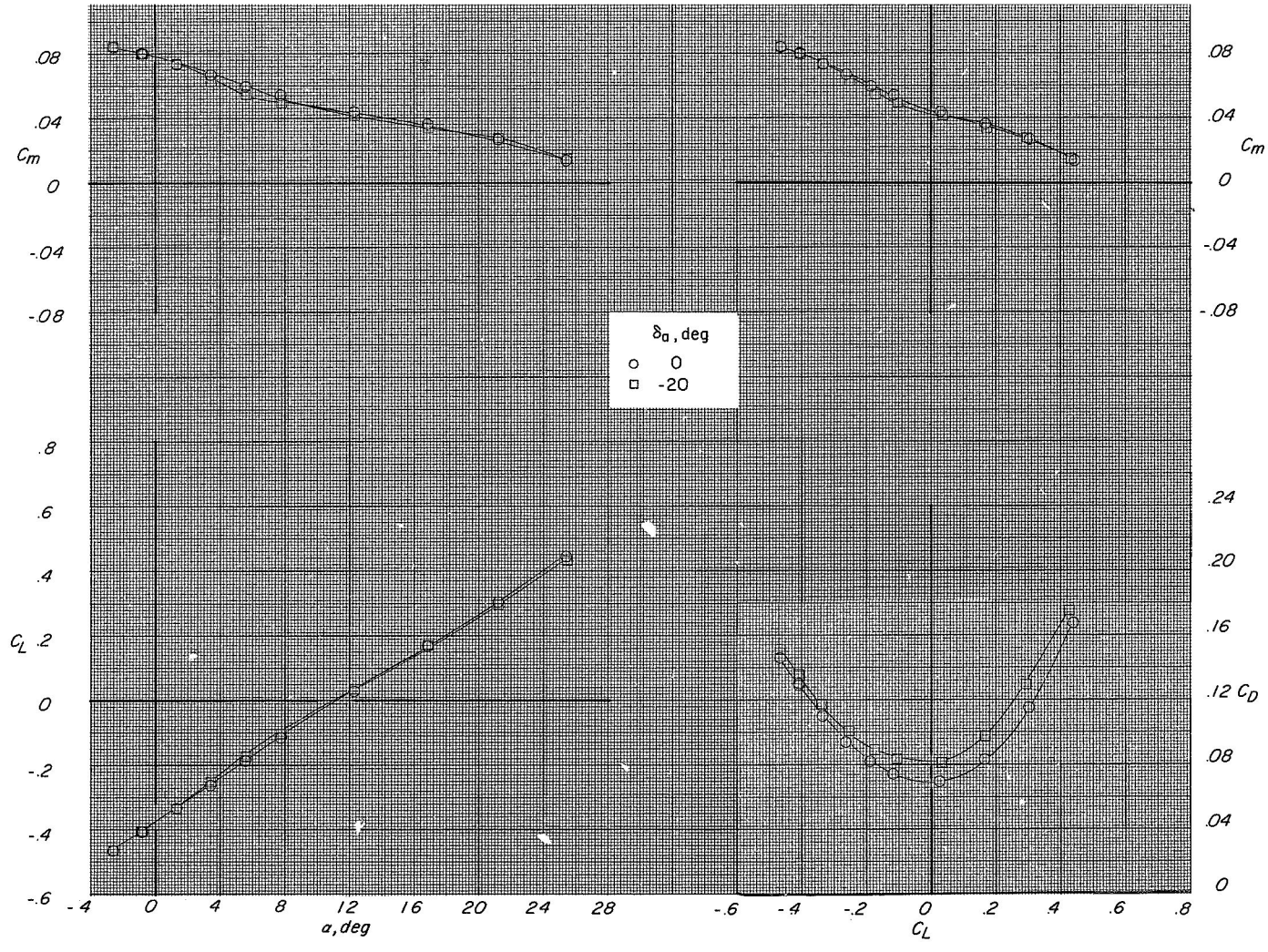
(c) $\delta_{ef} = 3^o$; $\delta_{if} = 0^o$; $\delta_{of} = 32^o$.

Figure 52.- Continued.



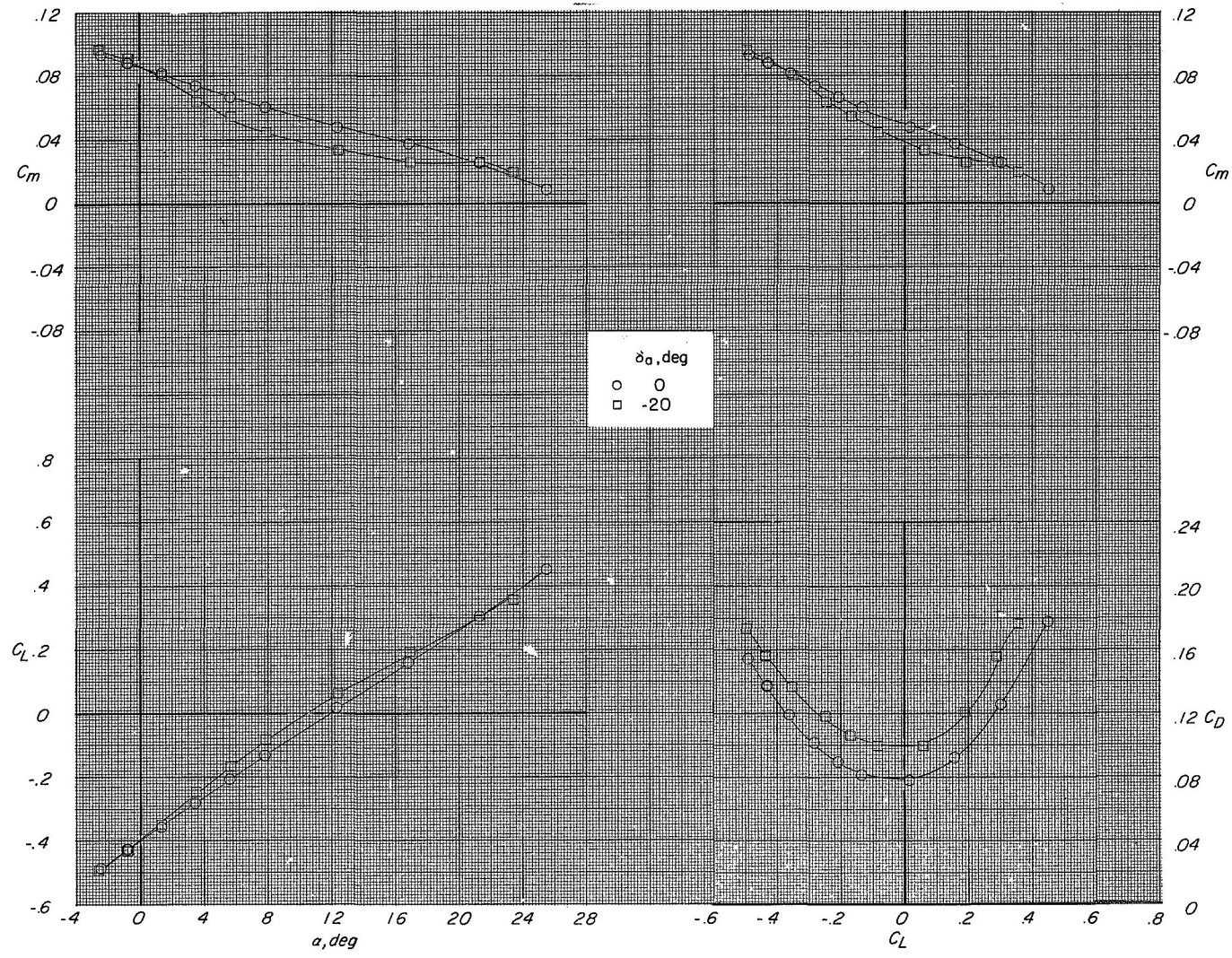
(d) $\delta_{ef} = 13^{o}$; $(\delta_{if})_L = (\delta_{of})_R = 0^{o}$; $(\delta_{if})_R = (\delta_{of})_L = 32^{o}$.

Figure 52.- Concluded.



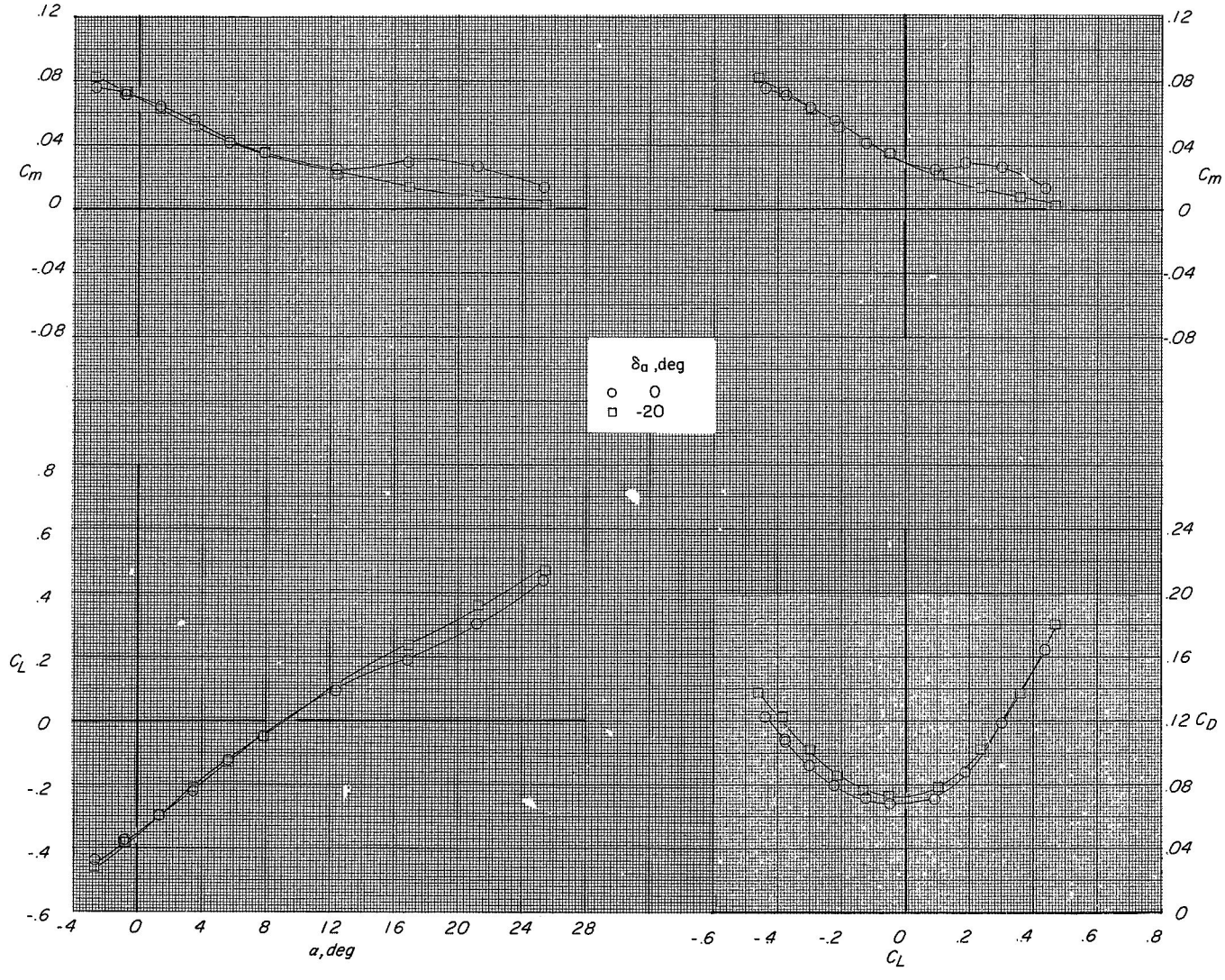
(a) $\delta_{ef} = 13^o$; $\delta_{if} = 0^o$; $\delta_{of} = 32^o$; $\delta_e = -5^o$.

Figure 53.- Longitudinal characteristics of the HL-10 for several aileron deflections with asymmetric deflection of auxiliary flaps. Modification II fin configuration; $\beta = 0^o$; M = 0.60.



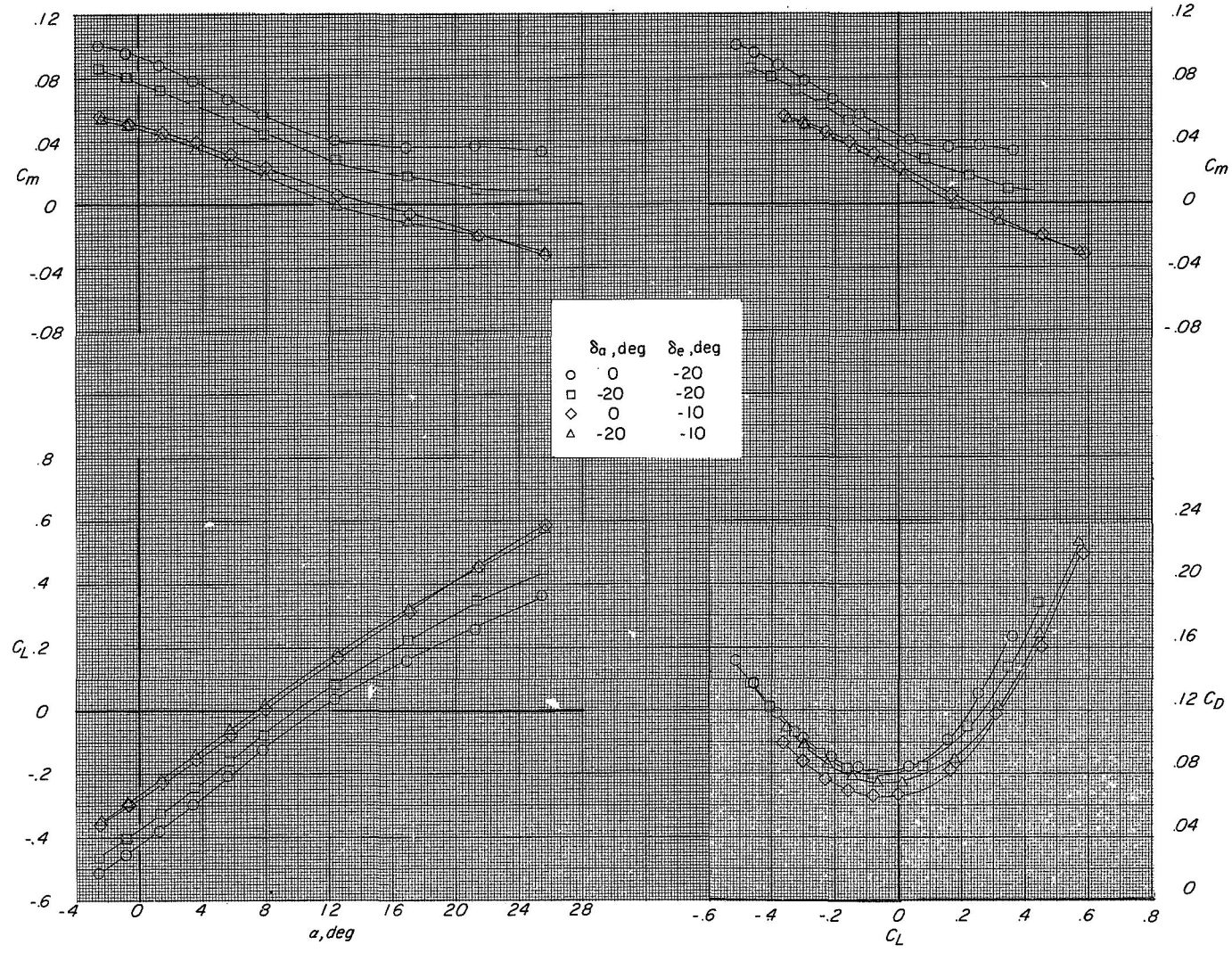
(b) $\delta_{ef} = 13^{o}$; $(\delta_{if})_L = (\delta_{of})_R = 0^{o}$; $(\delta_{if})_R = (\delta_{of})_L = 32^{o}$; $\delta_e = -5^{o}$.

Figure 53.- Continued.



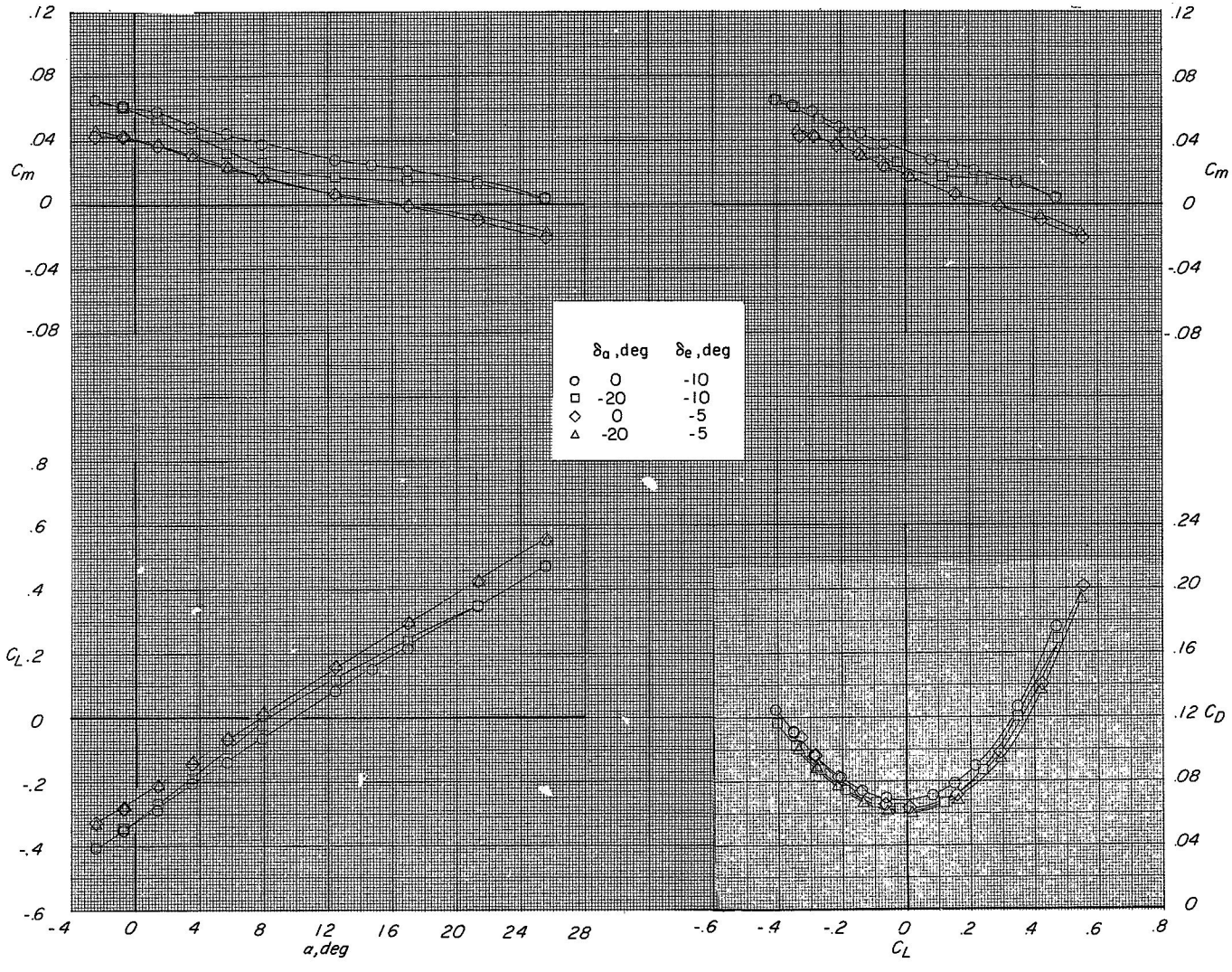
(c) $\delta_{ef} = -8^{o}$; $(\delta_{if})_L = (\delta_{of})_R = 0^{o}$; $(\delta_{if})_R = (\delta_{of})_L = 32^{o}$; $\delta_e = -10^{o}$.

Figure 53.- Concluded.



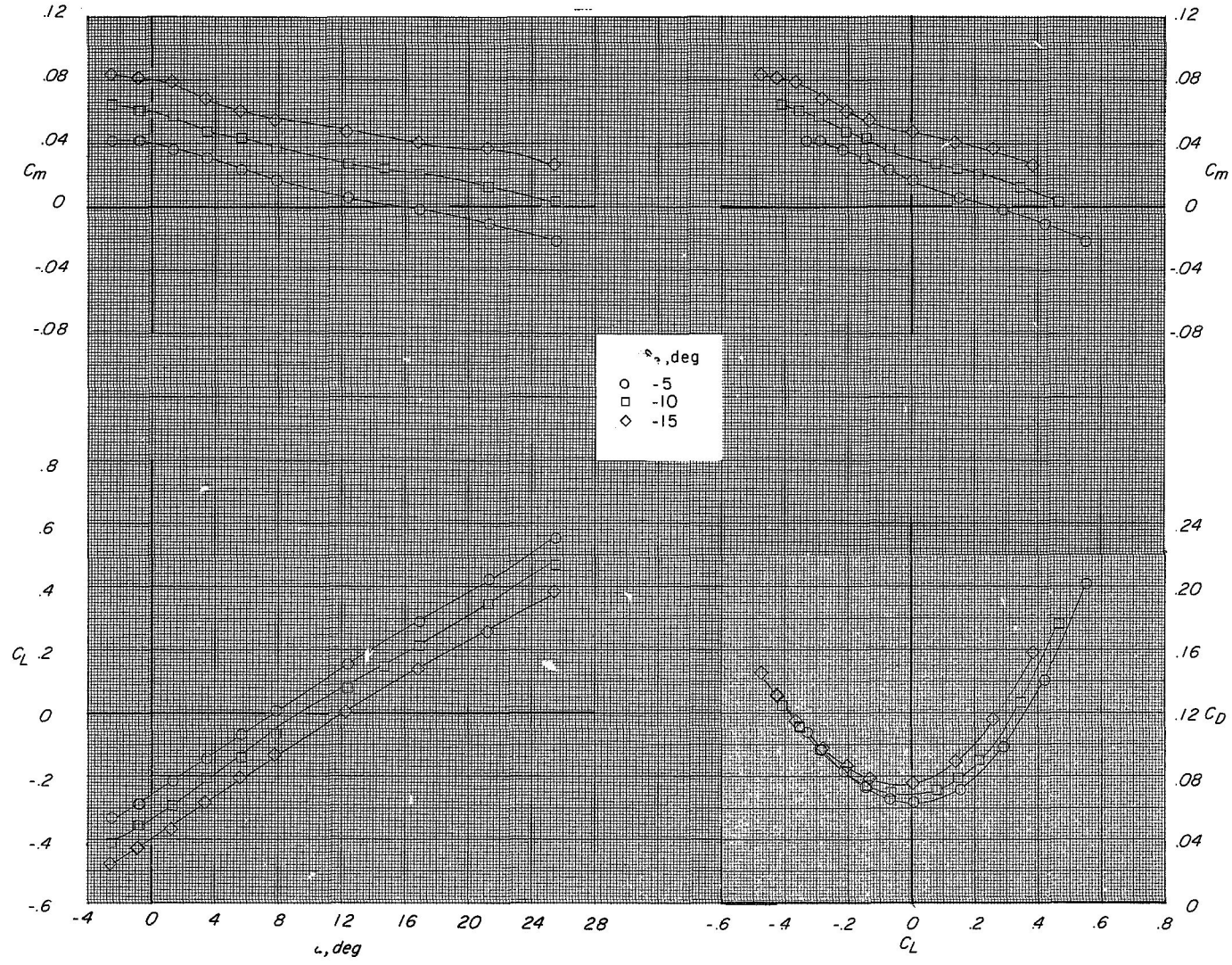
(a) $\delta_{ef} = -8^o$; $\delta_{if} = 32^o$; $\delta_{of} = 0^o$.

Figure 54.- Effect of aileron deflection on the longitudinal characteristics of the HL-10 for several elevon deflections with asymmetric deflection of auxiliary flaps. Modification H fin configuration; $\beta = 0^o$



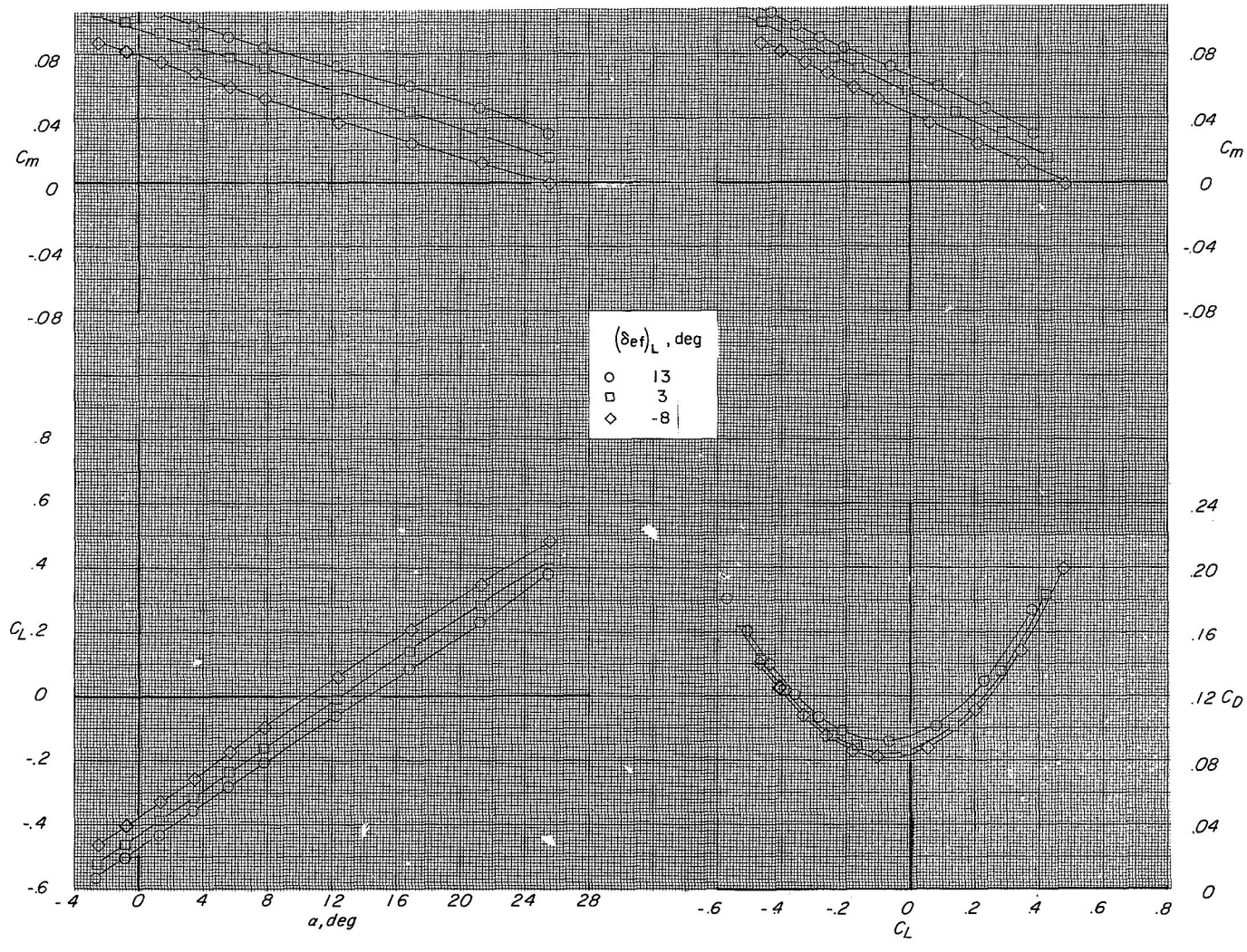
(b) $(\delta_{ef})_L = -8^o$; $(\delta_{ef})_R = 13^o$; $\delta_{if} = 0^o$; $\delta_{of} = 32^o$.

Figure 54.- Continued.



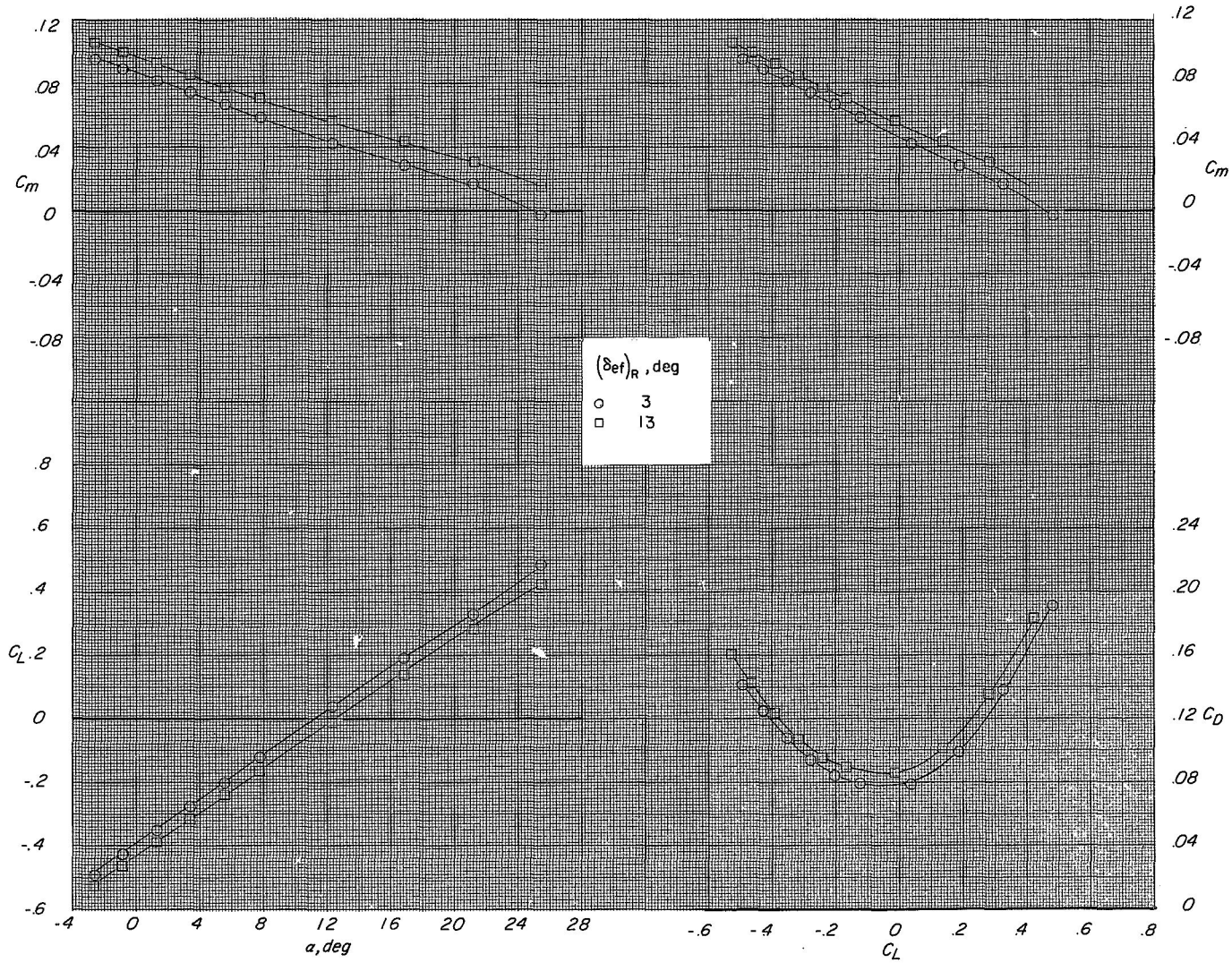
(c) $(\delta_{ef})_L = -8^o$; $(\delta_{ef})_R = 13^o$; $\delta_{if} = 0^o$; $\delta_{of} = 32^o$.

Figure 54.- Concluded.



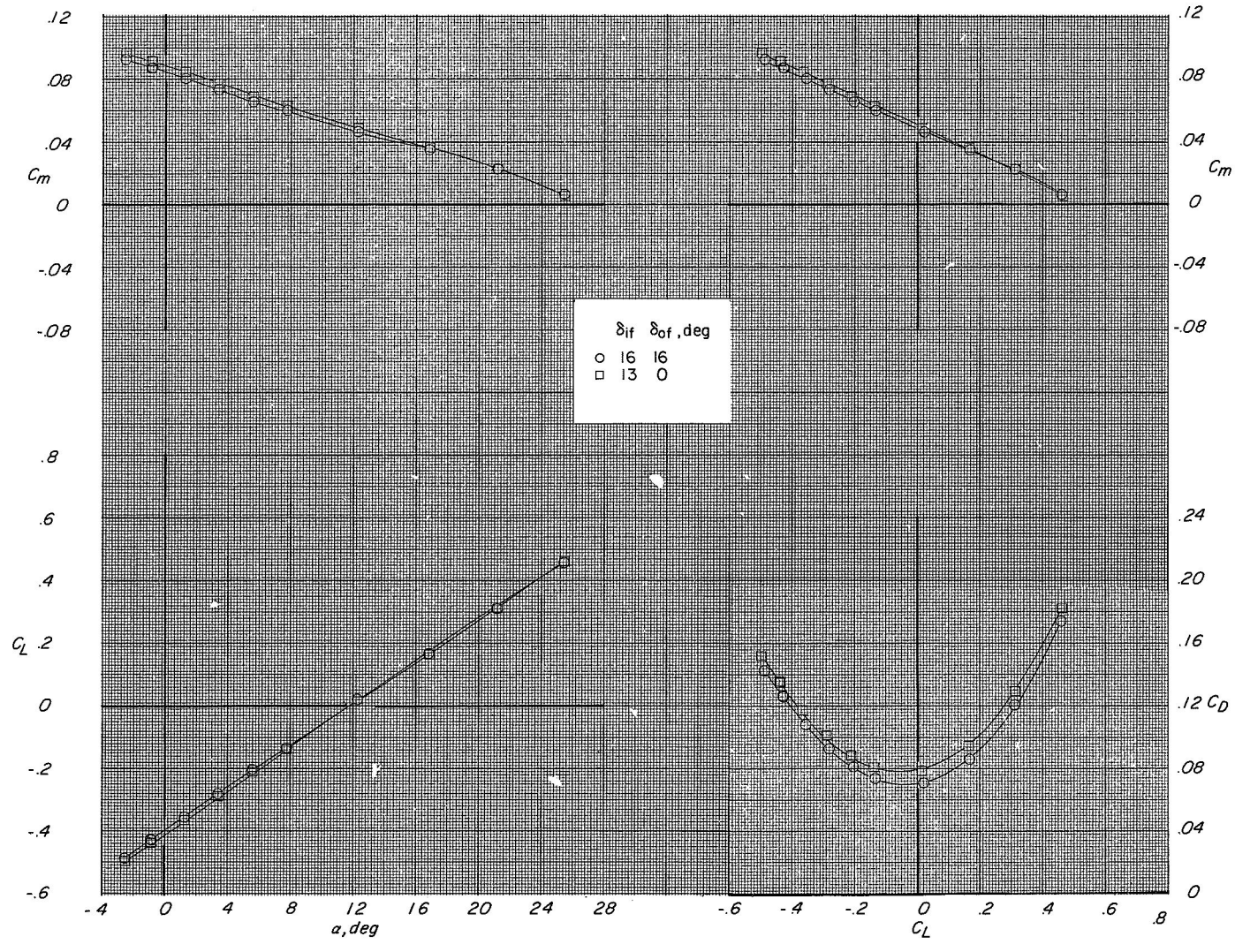
(a) $(\delta_{ef})_R = 13^o$; $\delta_{if} = 32^o$; $\delta_{of} = 0^o$; $\delta_e = -10^o$.

Figure 55.- Effect of deflecting one of the elevon flaps on the longitudinal characteristics of the HL-10. Modification II fin configuration; $\beta = 0^o$; M = 0.60.



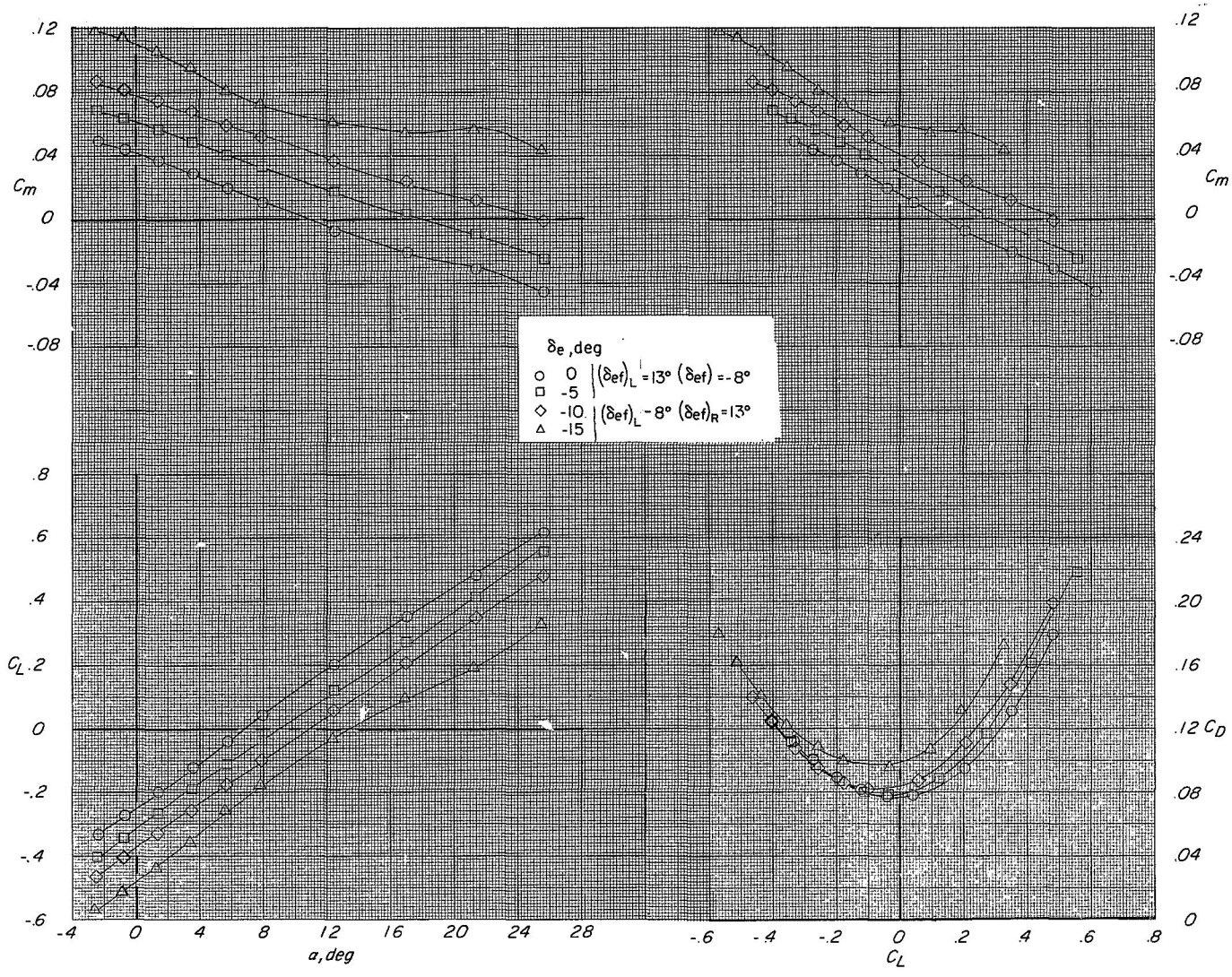
(b) $(\delta_{ef})_L = 3^o$; $\delta_{if} = 32^o$; $\delta_{of} = 0^o$; $\delta_e = -10^o$.

Figure 55 - Continued.



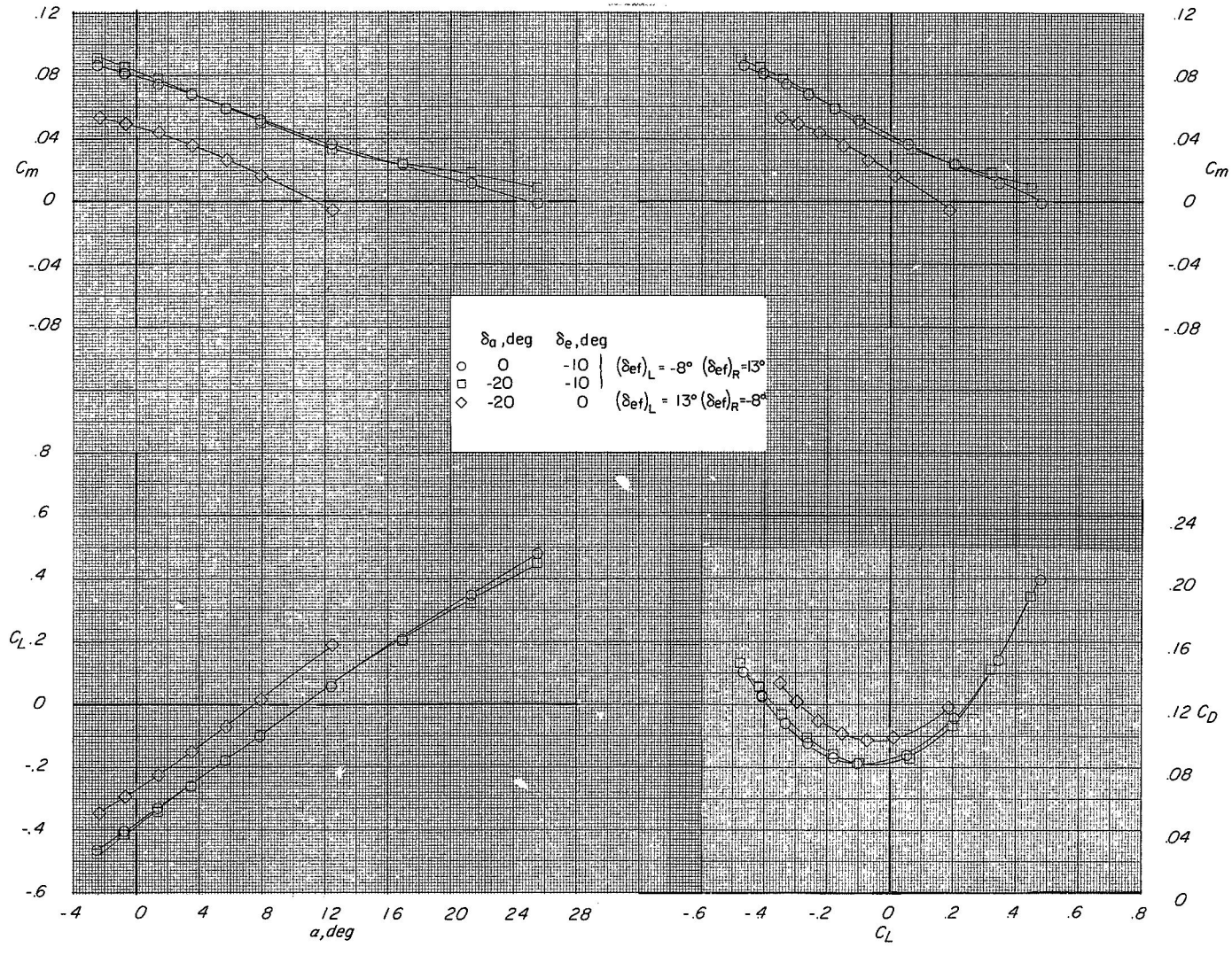
(c) $\delta_{ef} = 13^{o}$; $(\delta_{if})_L = (\delta_{of})_L = 16^{o}$; $\delta_e = -5^{o}$.

Figure 55.- Concluded.



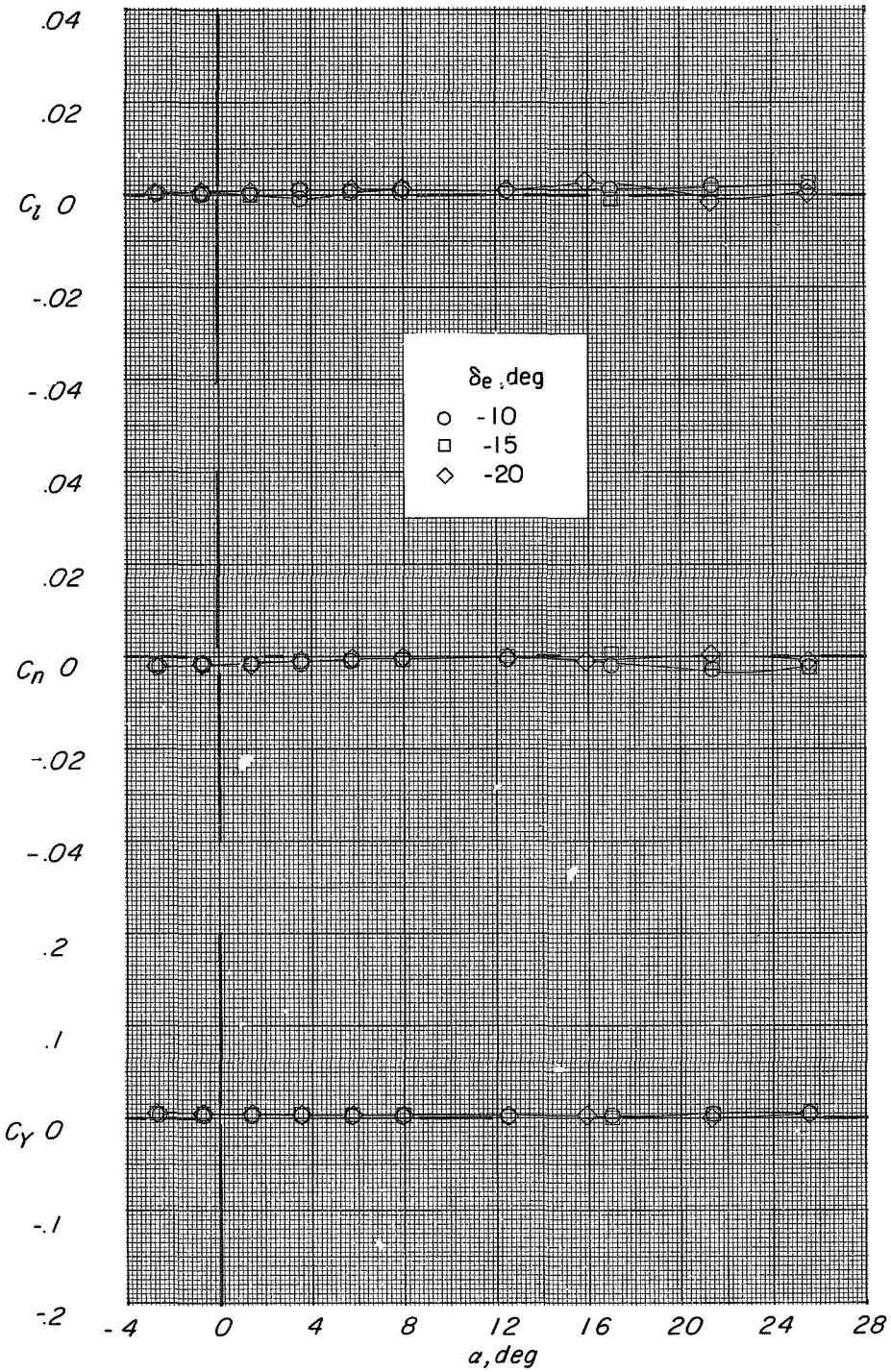
(a) $\delta_{if} = 32^{o}$; $\delta_{of} = 32^{o}$.

Figure 56.- Effect of combined aileron and elevon deflection on the longitudinal characteristics of HL-10 for several auxiliary flap deflections. Modification II fin configuration: $\beta = 0^{o}$; $M = 0.60$



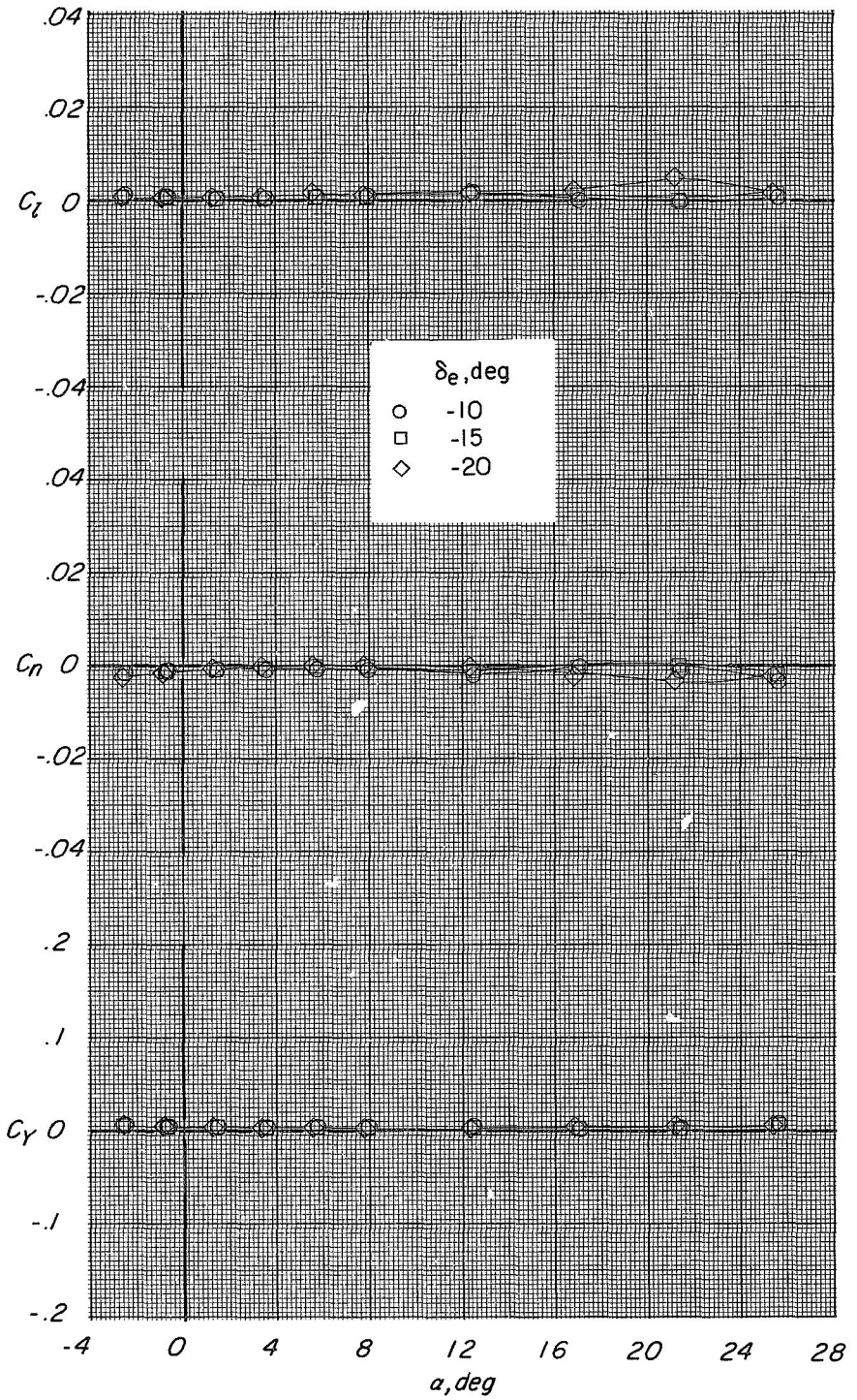
(b) $\delta_{if} = 32^o$; $\delta_{of} = 0^o$; $\delta_a = 0^o$.

Figure 56.- Concluded.



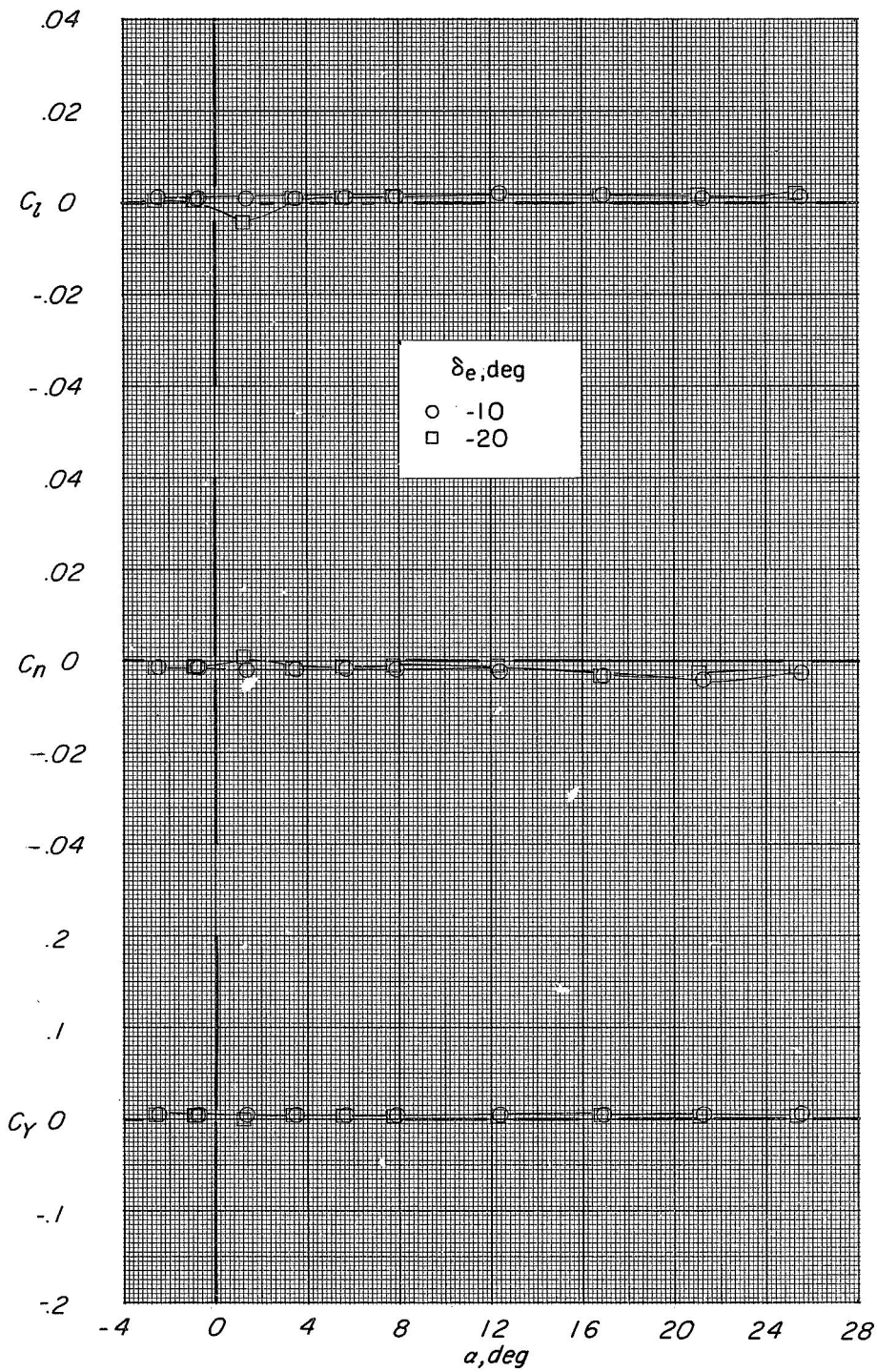
(a) $\delta_{ef} = -8^{o}$; $\delta_{if} = 0^{o}$; $\delta_{of} = 32^{o}$.

Figure 57.- Lateral aerodynamic characteristics of the HL-10 with various degrees of deflection on the auxiliary flaps. Modification II fin configuration; $\delta_a = \beta = 0^{o}$; M = 0.60.



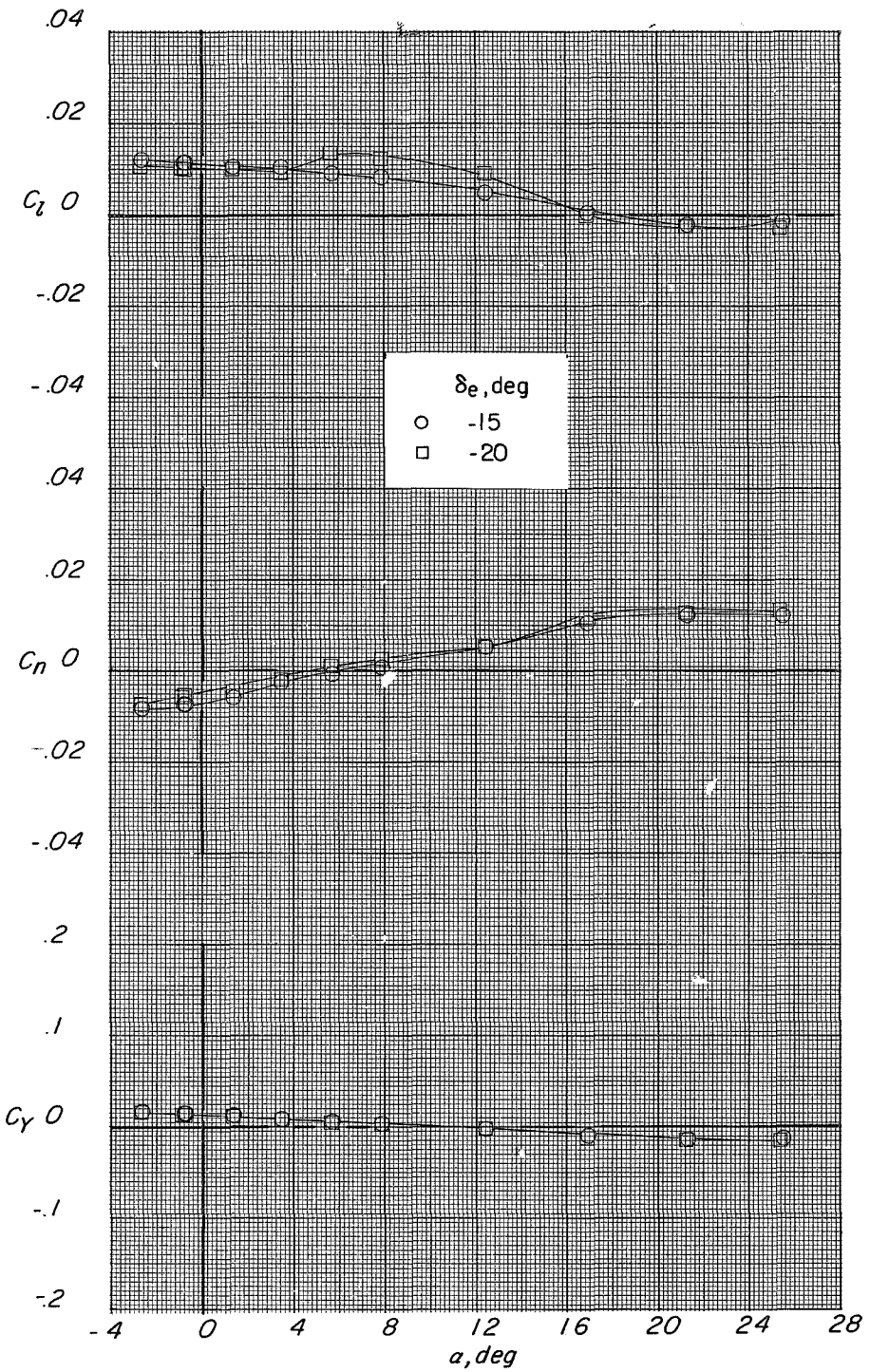
(b) $\delta_{ef} = -8^o$; $\delta_{if} = 32^o$; $\delta_{of} = 0^o$.

Figure 57.- Continued.



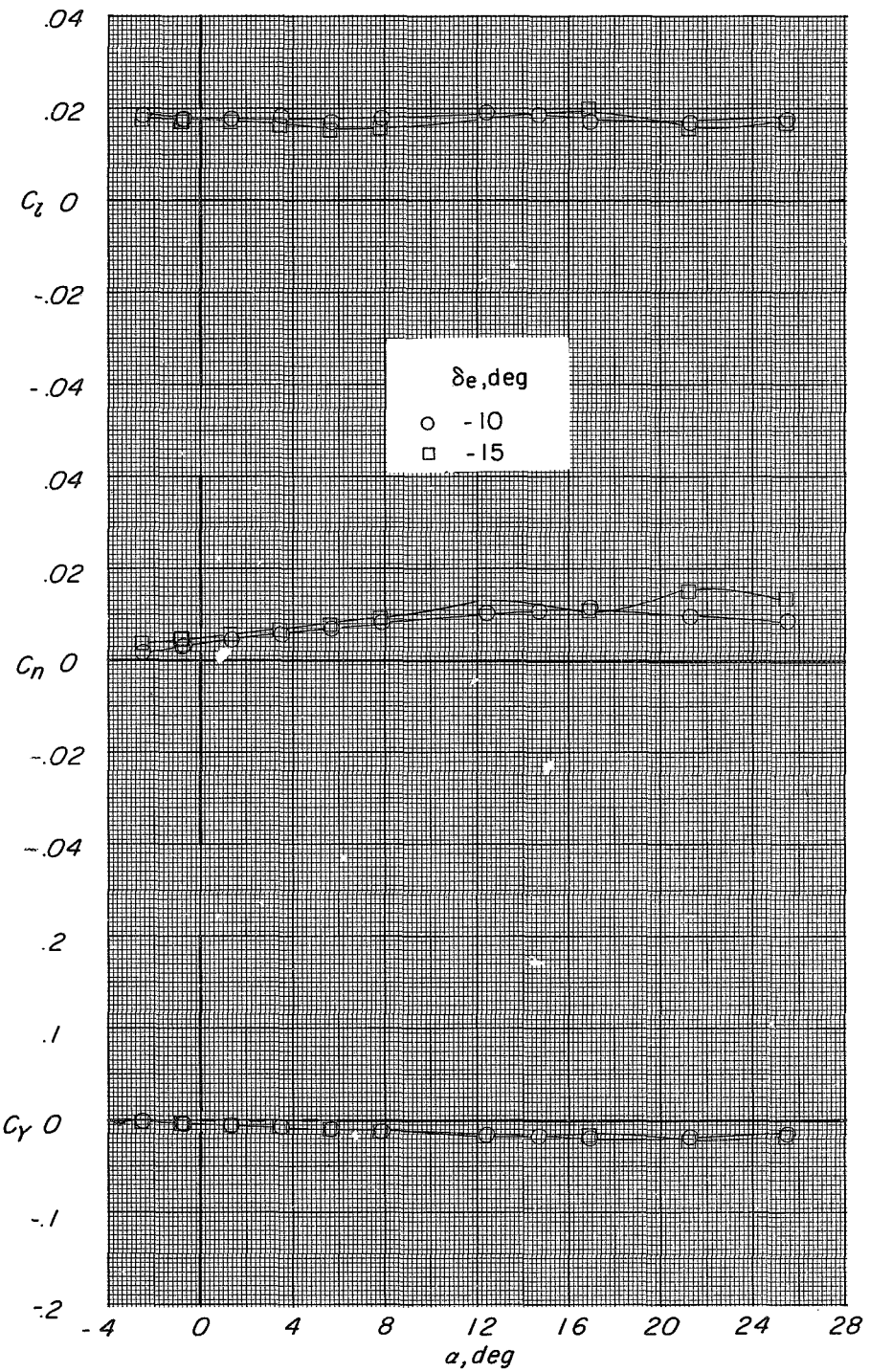
(c) $\delta_{ef} = -8^{o}$; $\delta_{if} = 16^{o}$; $\delta_{of} = 16^{o}$.

Figure 57.- Continued.



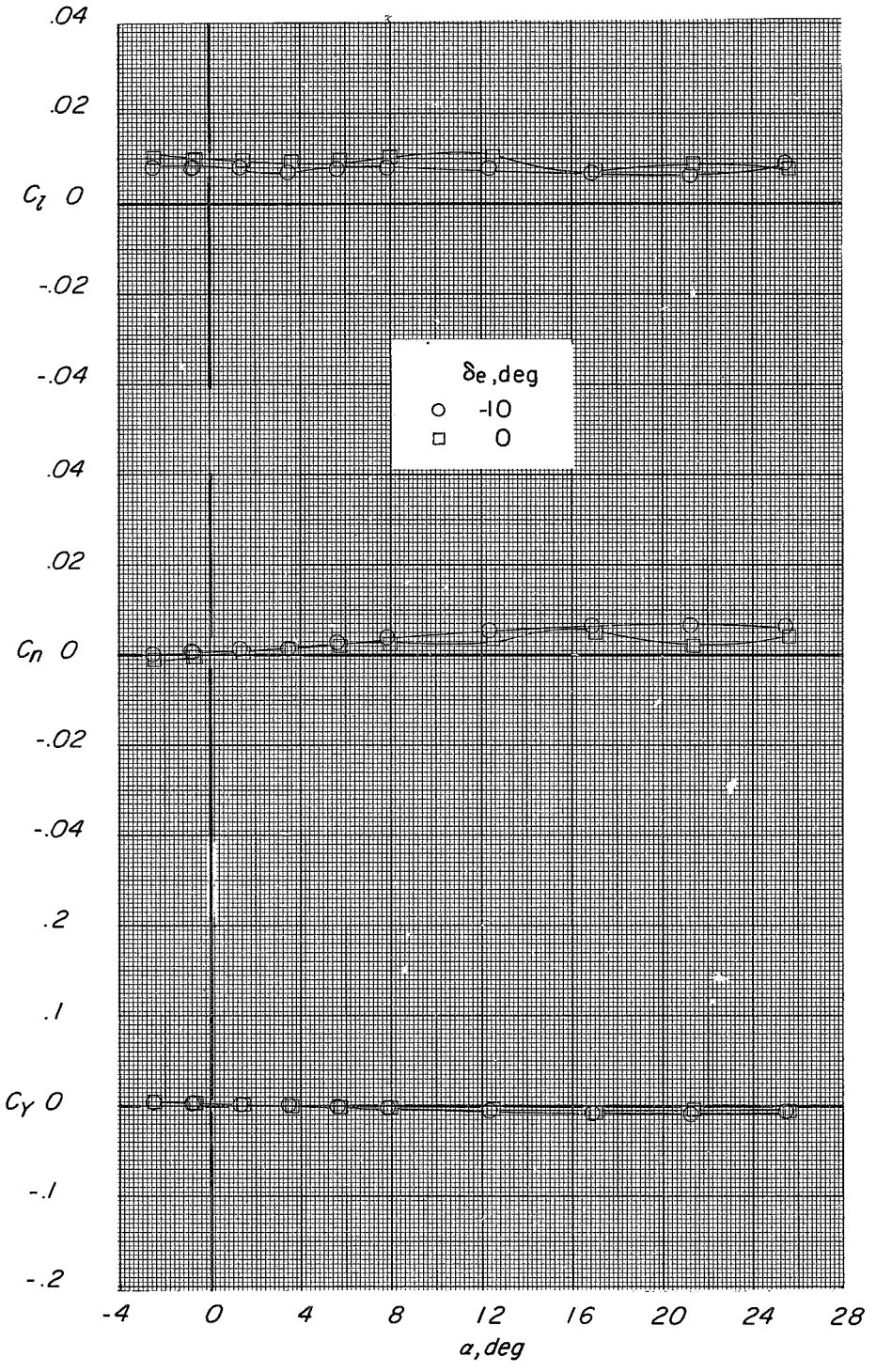
(d) $\delta_{ef} = -8^{o}$; $(\delta_{if})_L = (\delta_{of})_R = 0^{o}$; $(\delta_{if})_R = (\delta_{of})_L = 32^{o}$.

Figure 57.- Continued.



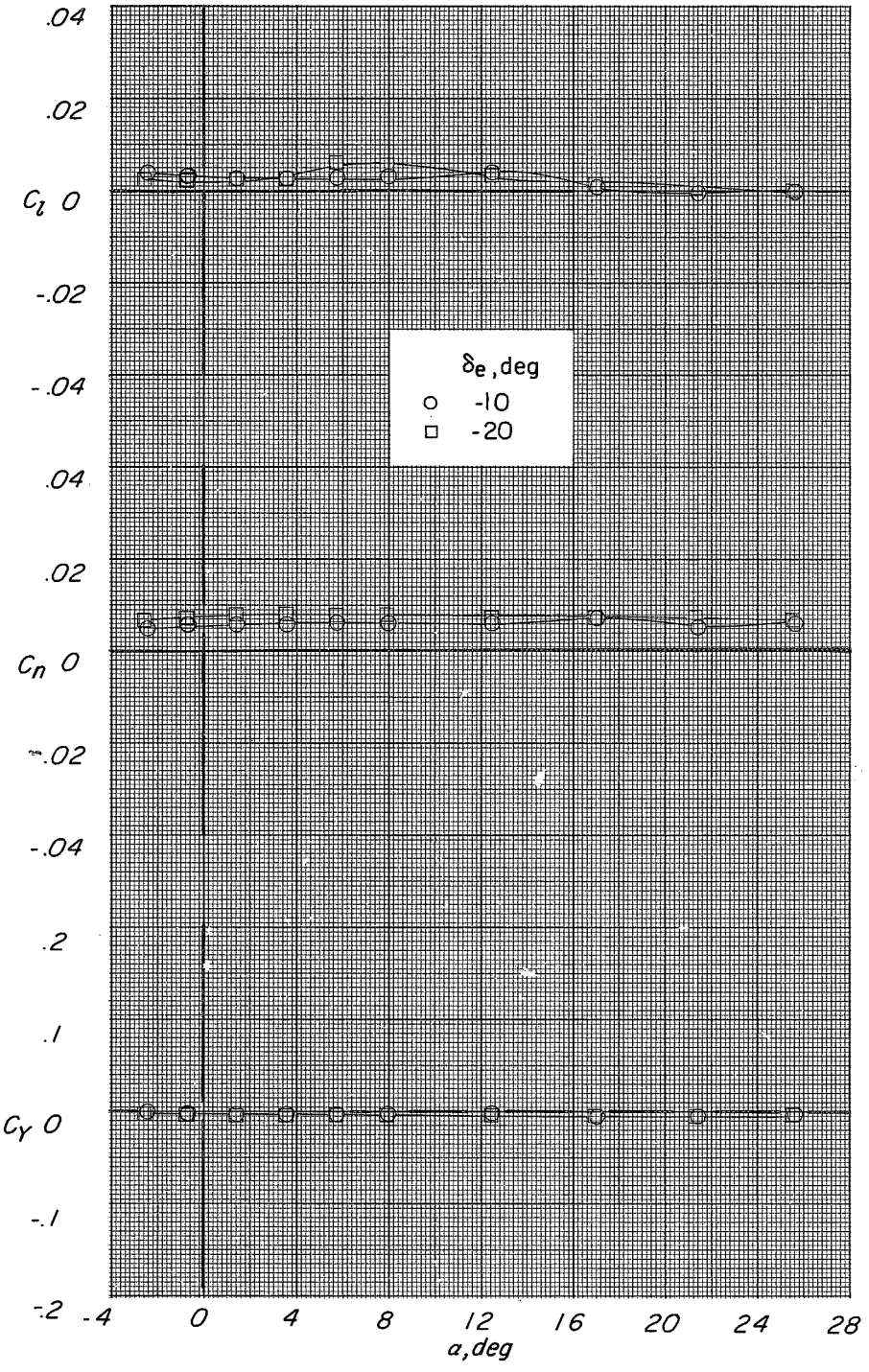
(e) $(\delta_{ef})_L = -8^o$; $(\delta_{ef})_R = 13^o$; $\delta_{if} = 0^o$; $\delta_{of} = 32^o$.

Figure 57.- Continued.



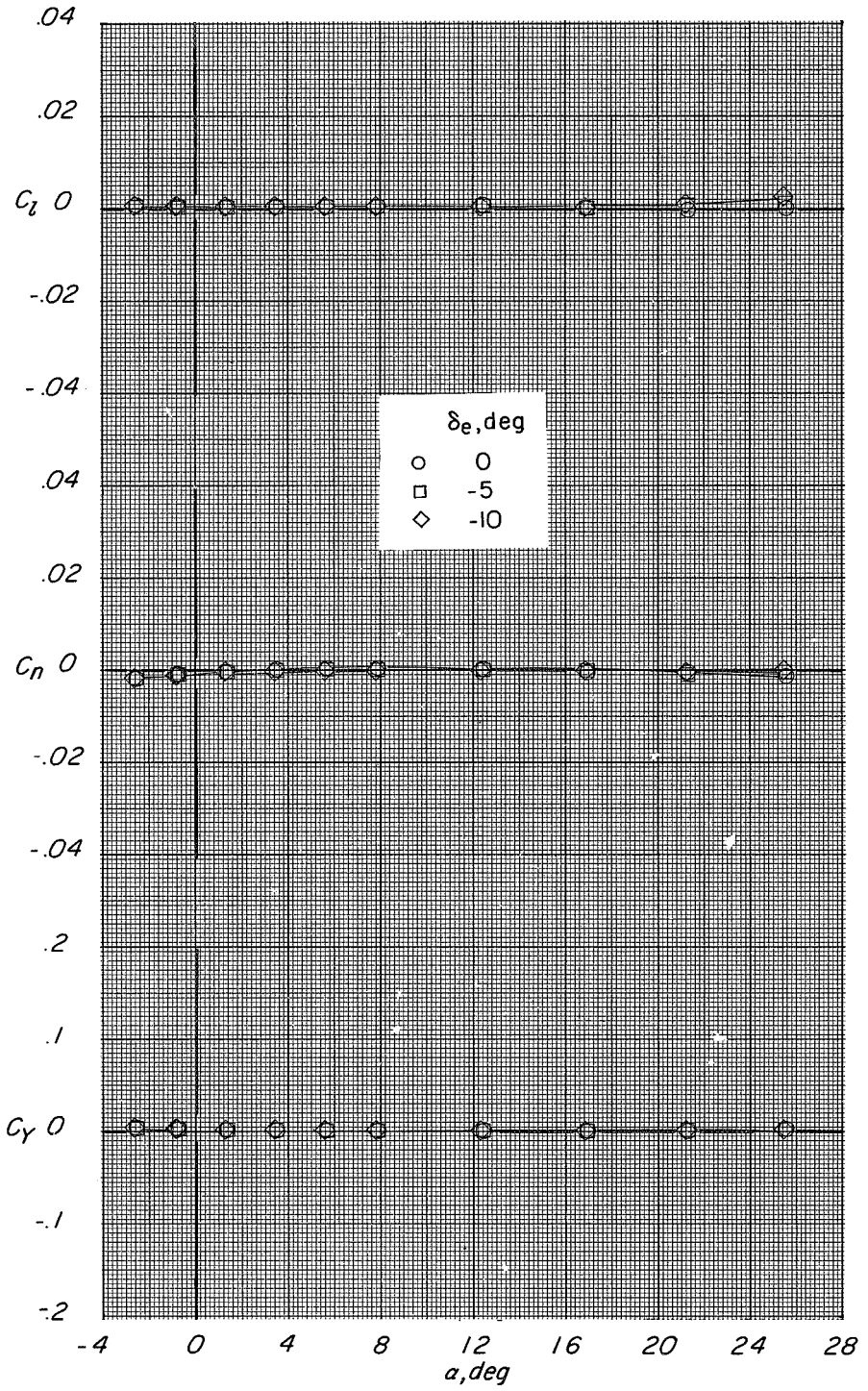
(f) $(\delta_{ef})_L = 3^o$; $(\delta_{ef})_R = 13^o$; $\delta_{if} = 0^o$; $\delta_{of} = 32^o$.

Figure 57.- Continued.



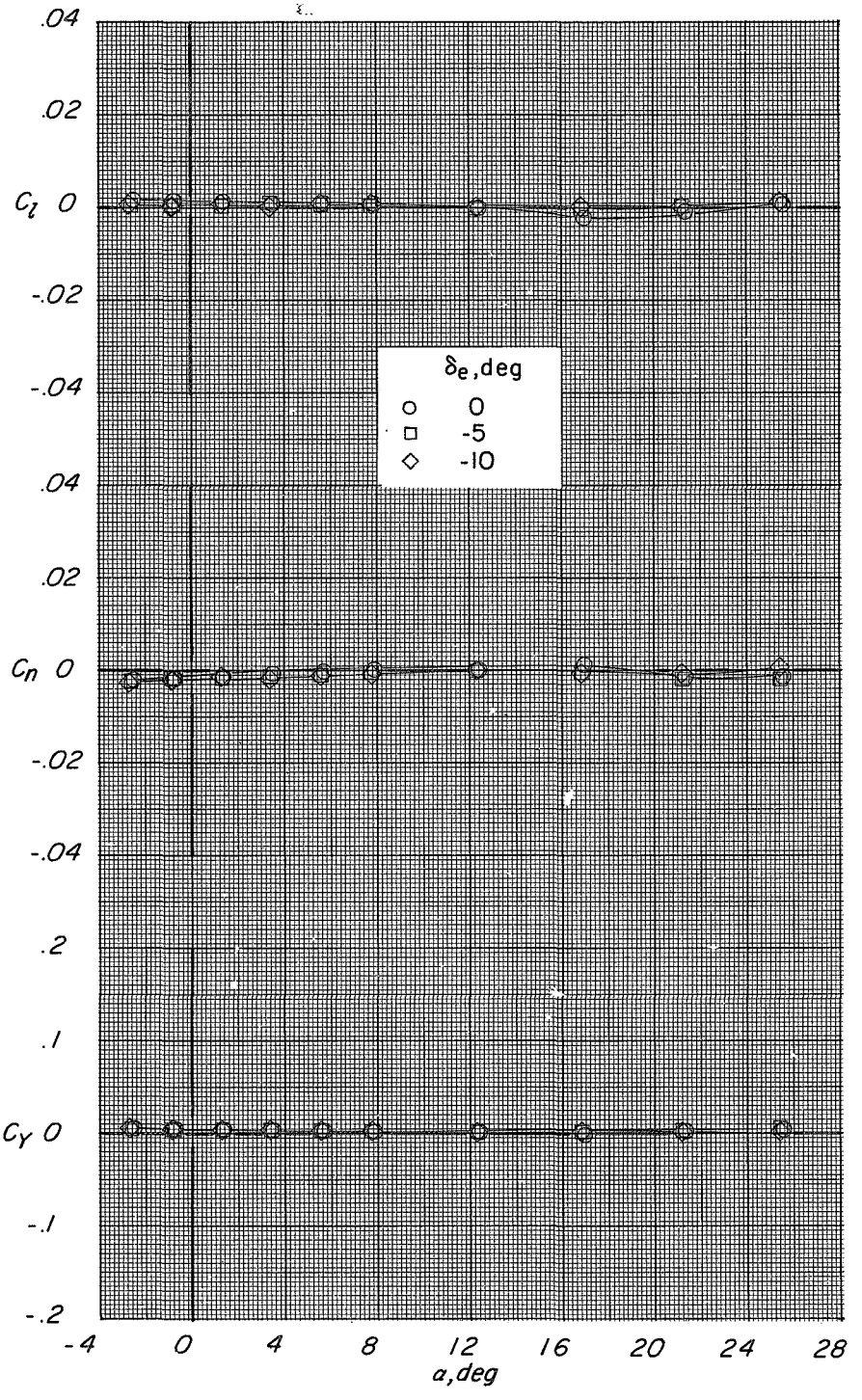
(g) $\delta_{ef} = -8^{o}$; $(\delta_{if})_L = (\delta_{of})_L = 16^{o}$; $(\delta_{if})_R = 32^{o}$; $(\delta_{of})_R = 0^{o}$.

Figure 57.- Concluded.



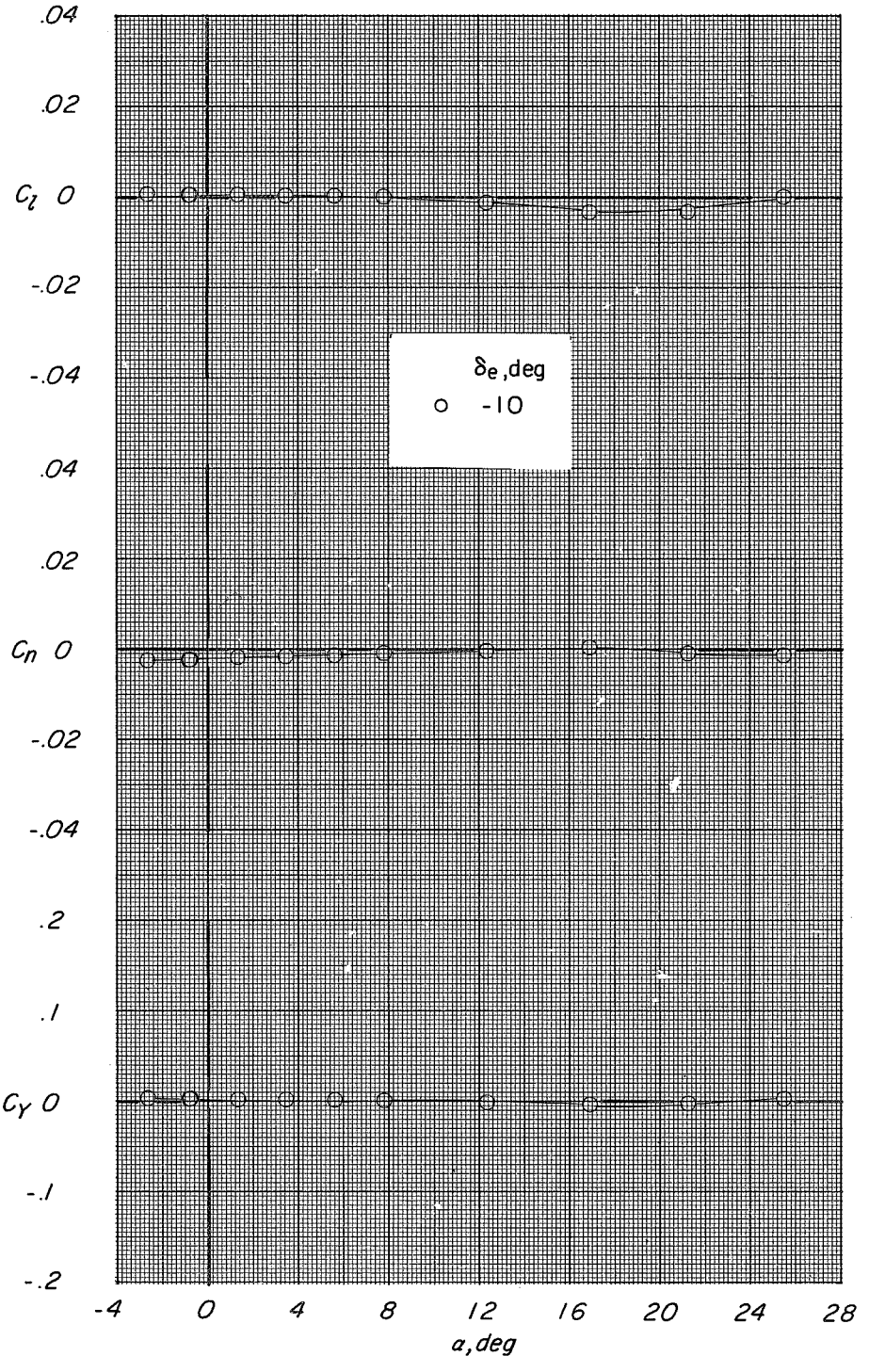
(a) $\delta_{ef} = 13^o$; $\delta_{if} = 32^o$; $\delta_{of} = 0^o$.

Figure 58.- Lateral aerodynamic characteristics of HL-10 with modification II fin configuration. $\delta_a = \beta = 0^o$; M = 0.60.



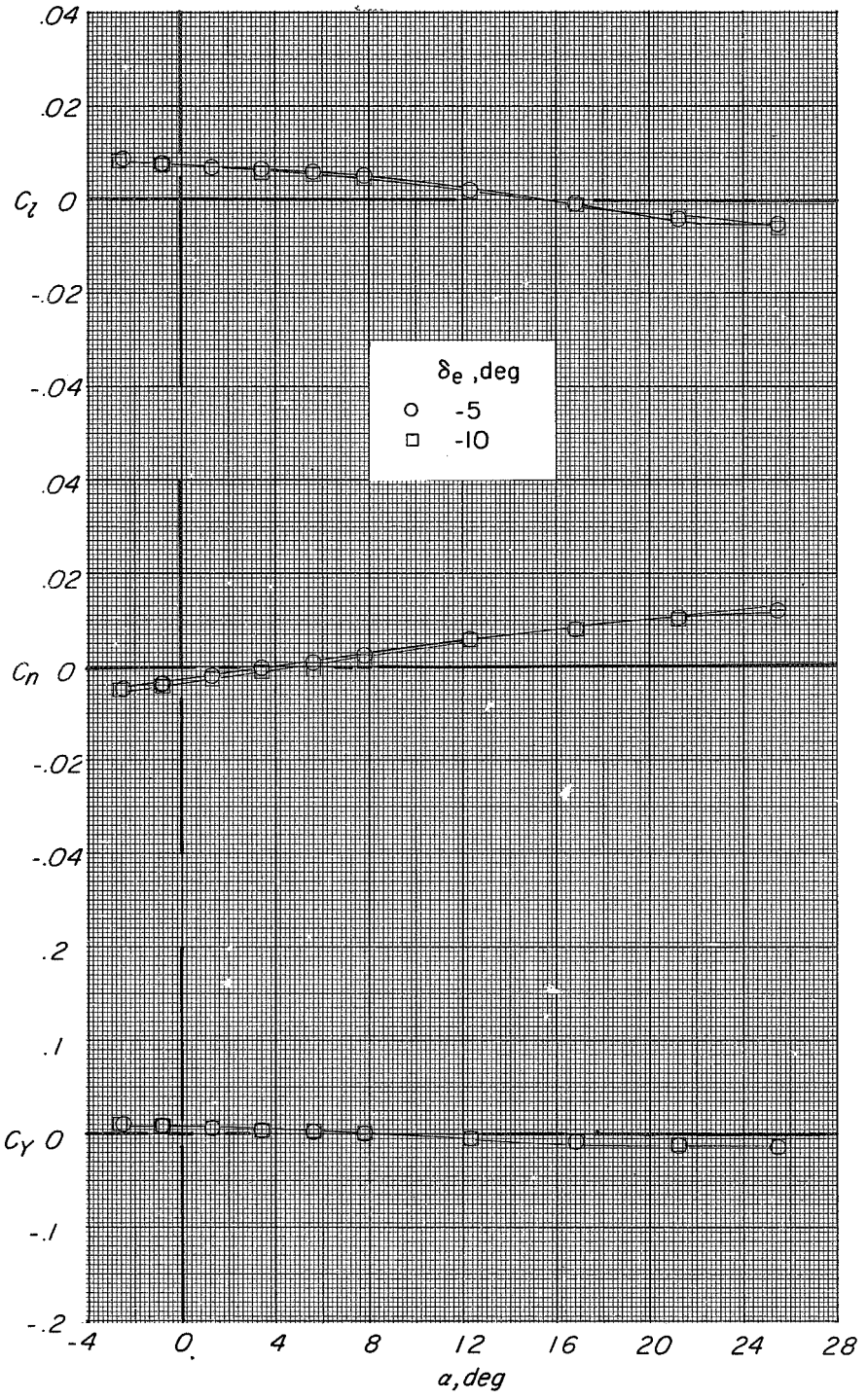
(b) $\delta_{ef} = 13^o$; $\delta_{if} = 0^o$; $\delta_{of} = 32^o$.

Figure 58.- Continued.



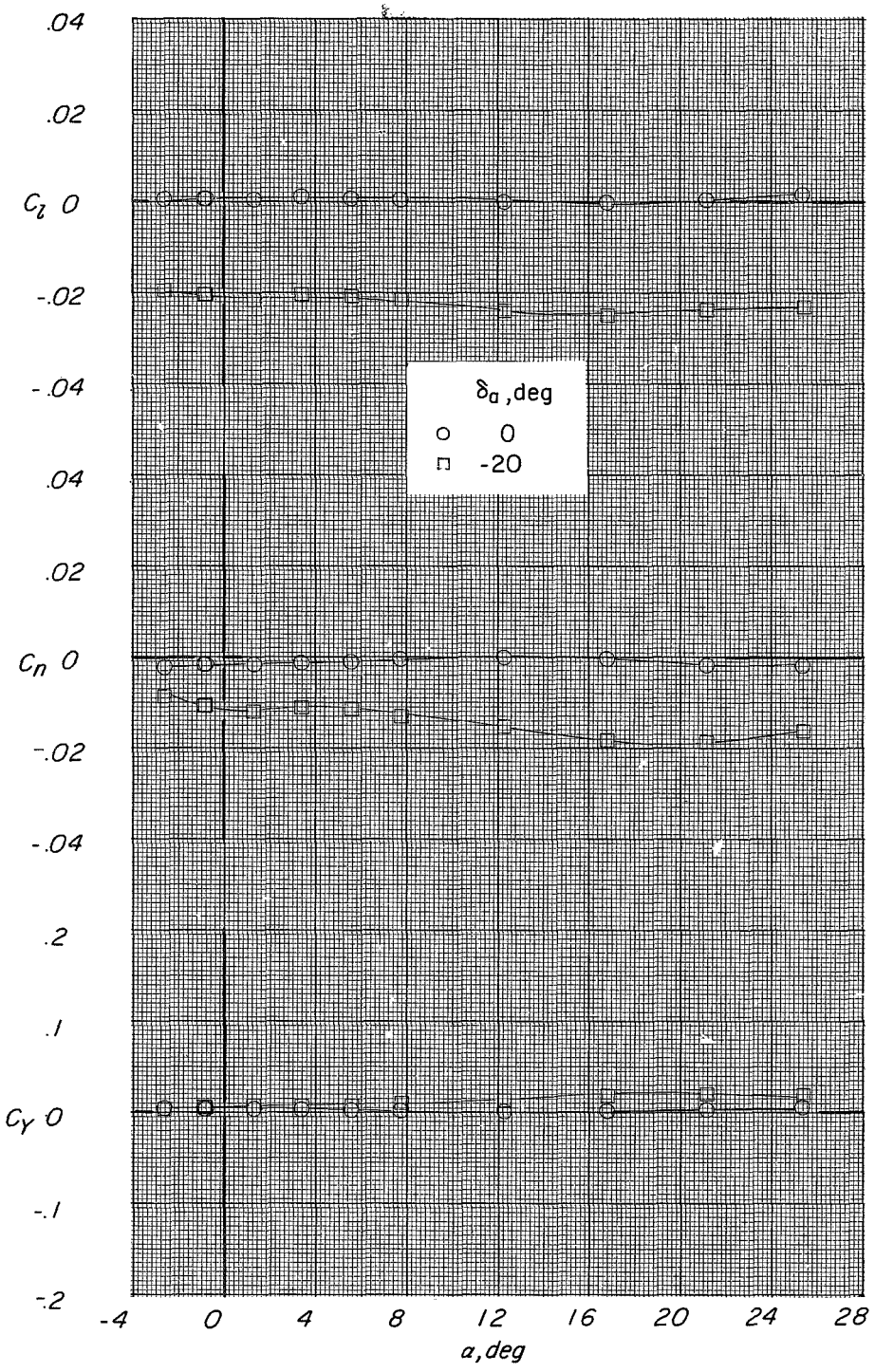
(c) $\delta_{ef} = 3^o$; $\delta_{if} = 0^o$; $\delta_{of} = 32^o$.

Figure 58.- Continued.



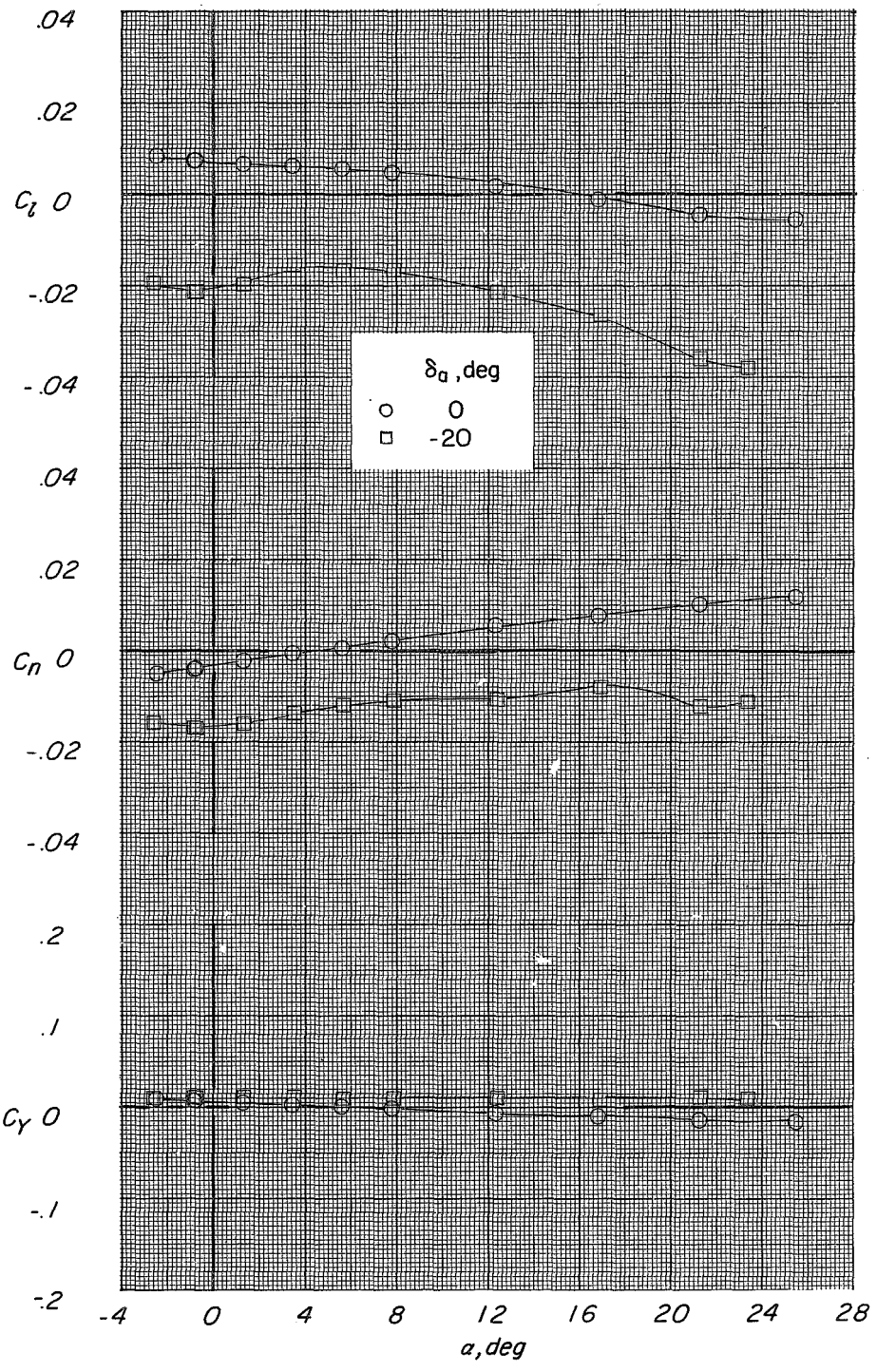
(d) $\delta_{ef} = 13^{o}$; $(\delta_{if})_L = (\delta_{of})_R = 0^{o}$; $(\delta_{if})_R = (\delta_{of})_L = 32^{o}$.

Figure 58.- Concluded.



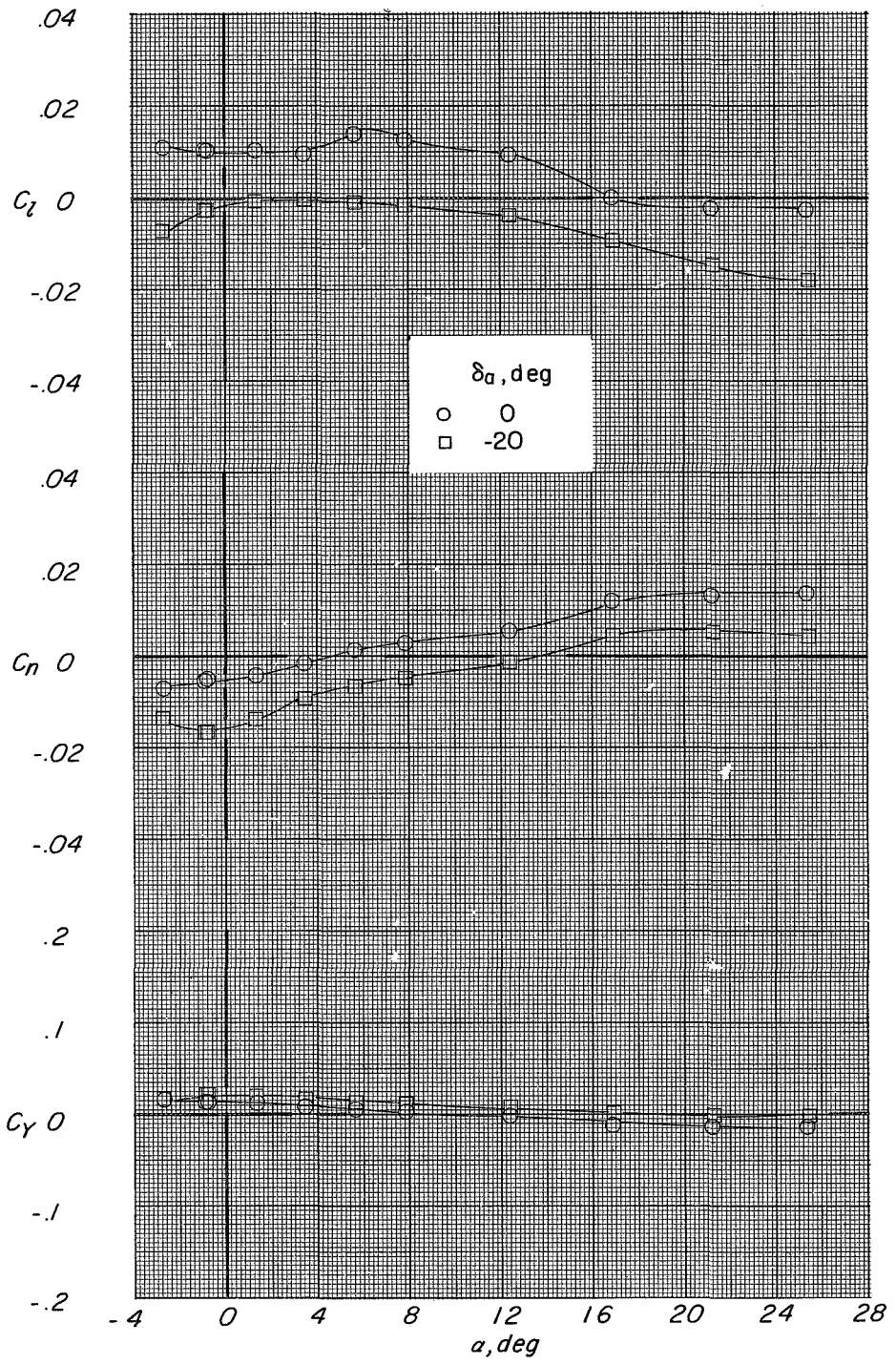
(a) $\delta_{ef} = 13^{o}$; $\delta_{if} = 0^{o}$; $\delta_{of} = 32^{o}$; $\delta_{e} = -5^{o}$.

Figure 59.- Lateral characteristics of the HL-10 for several aileron deflections with asymmetric auxiliary flap deflections. Modification II fin configuration; $\beta = 0^{o}$; M = 0.60.



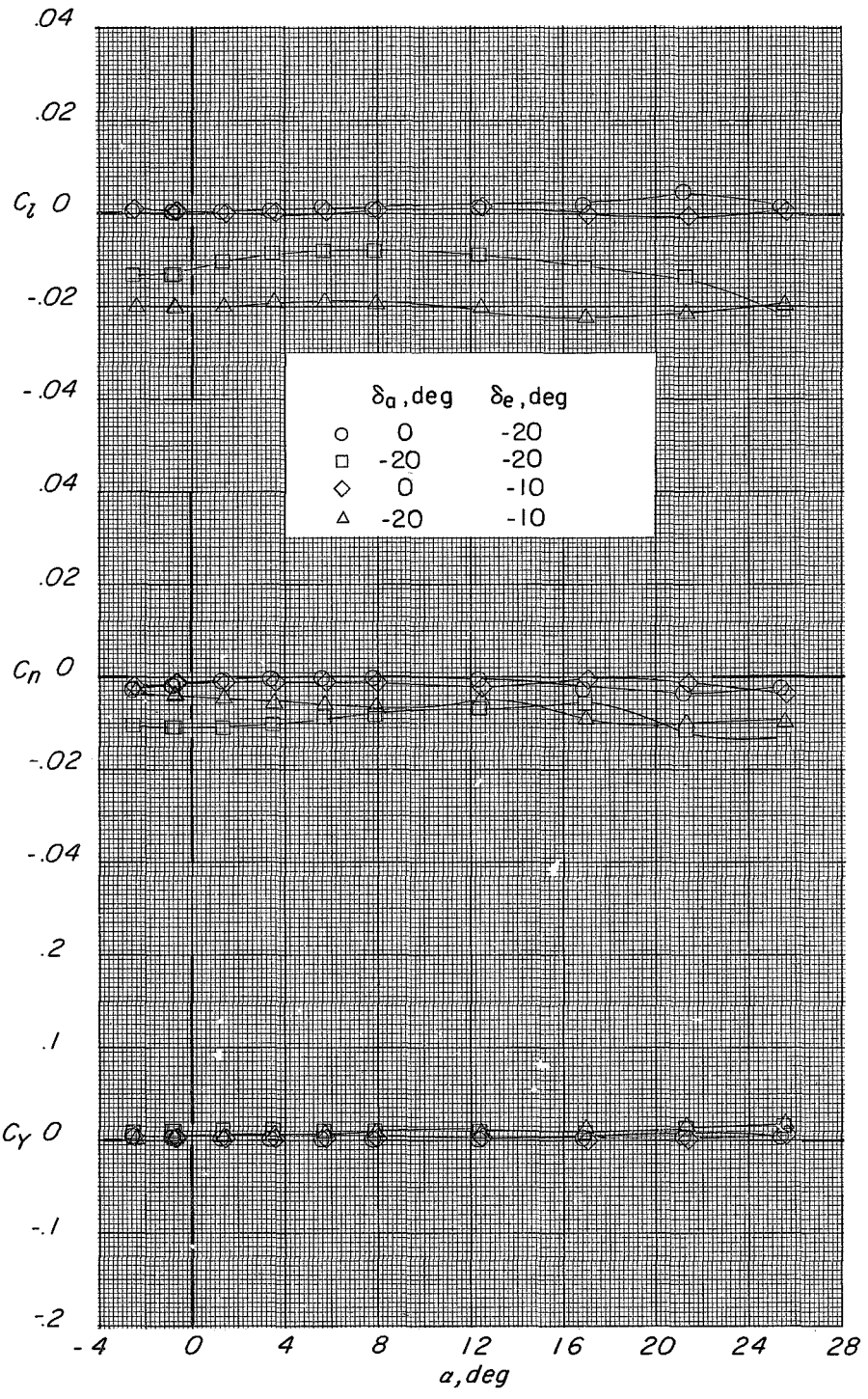
(b) $\delta_{ef} = 13^o$; $(\delta_{if})_L = (\delta_{of})_R = 0^o$; $(\delta_{if})_R = (\delta_{of})_L = 32^o$; $\delta_e = -5^o$.

Figure 59.- Continued.



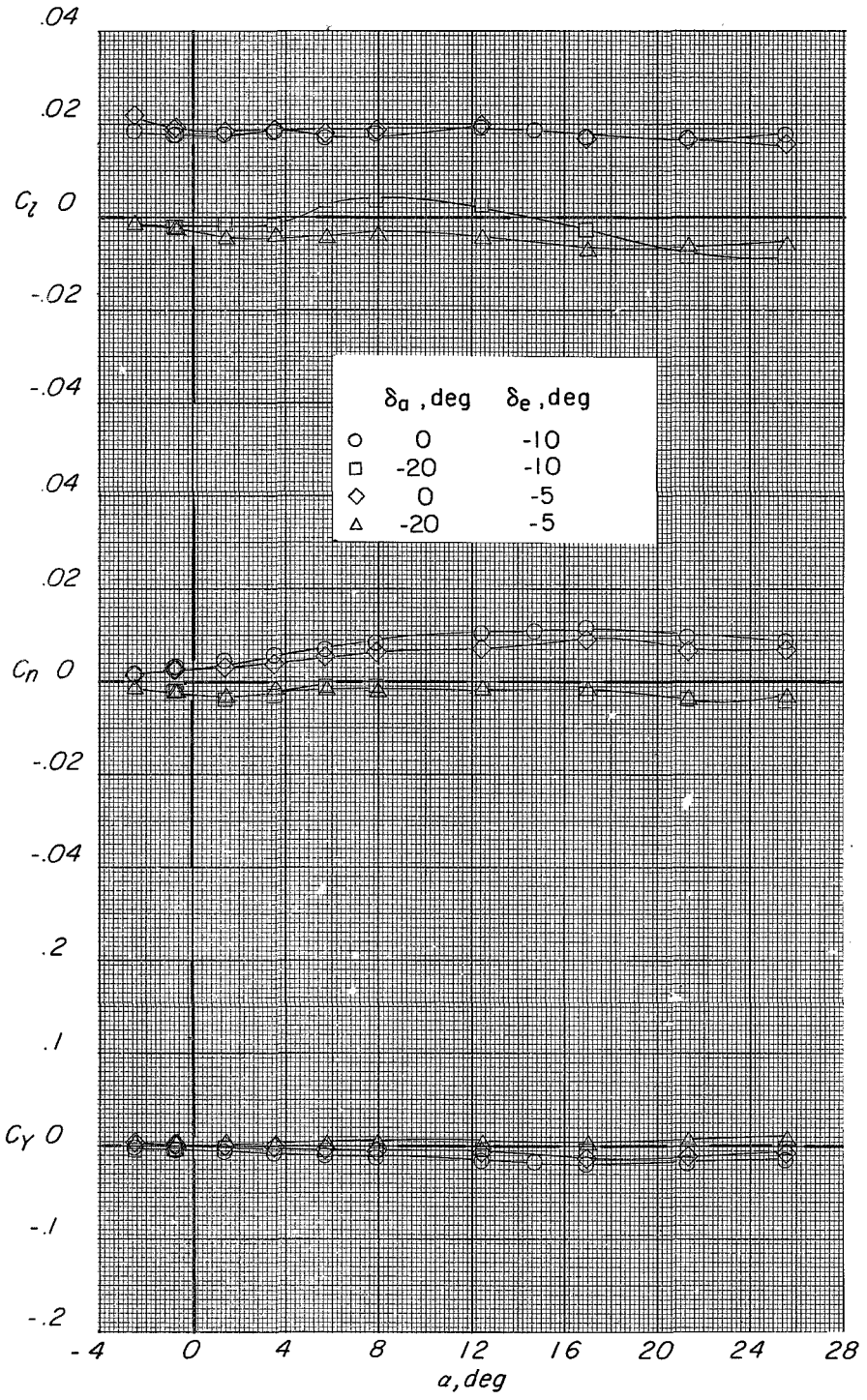
(c) $\delta_{ef} = -8^o$; $(\delta_{if})_L = (\delta_{of})_R = 0^o$; $(\delta_{if})_R = (\delta_{of})_L = 32^o$; $\delta_e = -10^o$.

Figure 59.- Concluded.



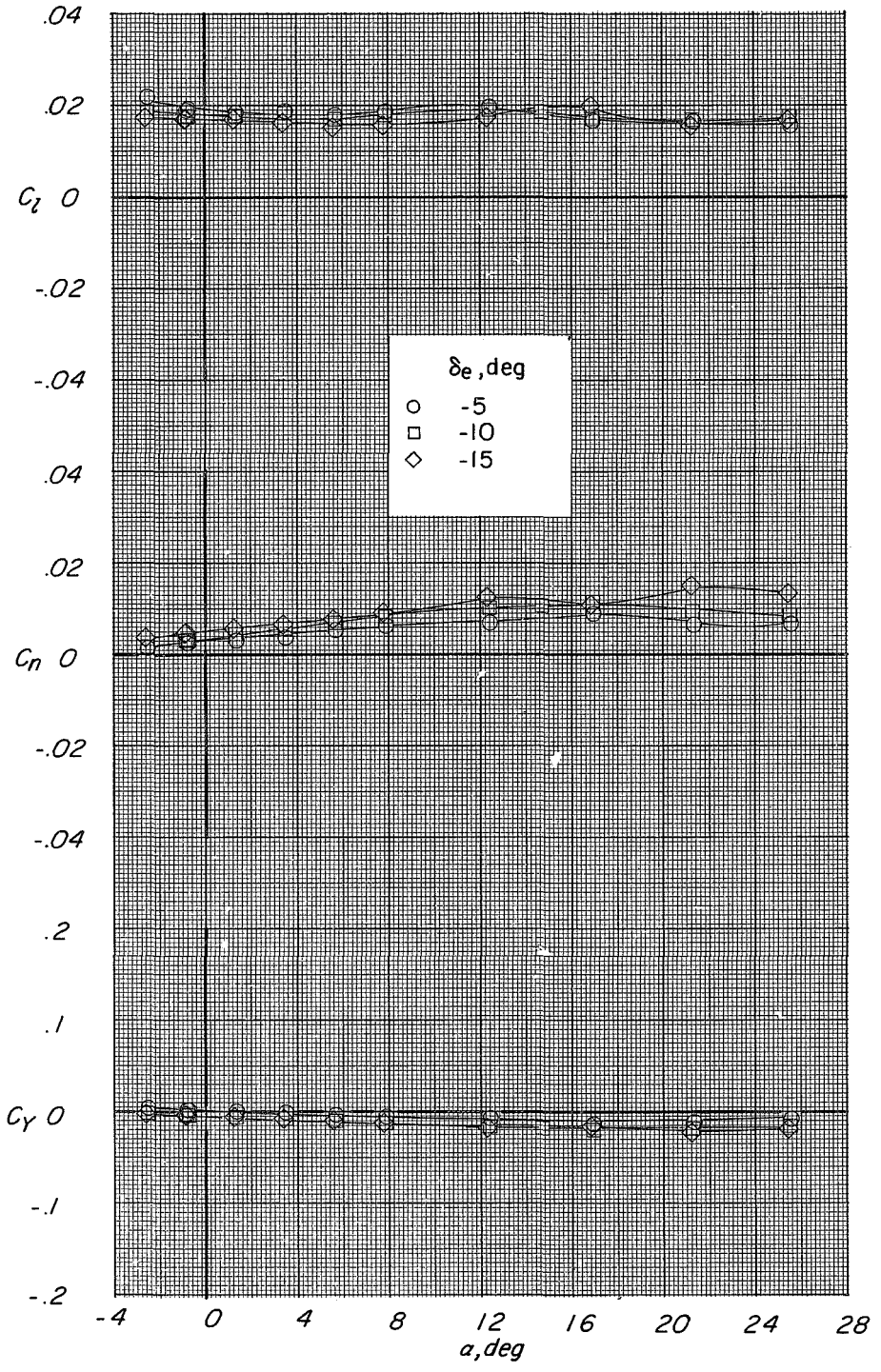
(a) $\delta_{ef} = -8^{o}$; $\delta_{if} = 32^{o}$; $\delta_{of} = 0^{o}$.

Figure 60.- Effect of aileron deflection on the lateral characteristics of the HL-10 for several elevon deflections with asymmetric deflection of auxiliary flaps. Modification II fin configuration; $\beta = 0^{o}$; M = 0.60.



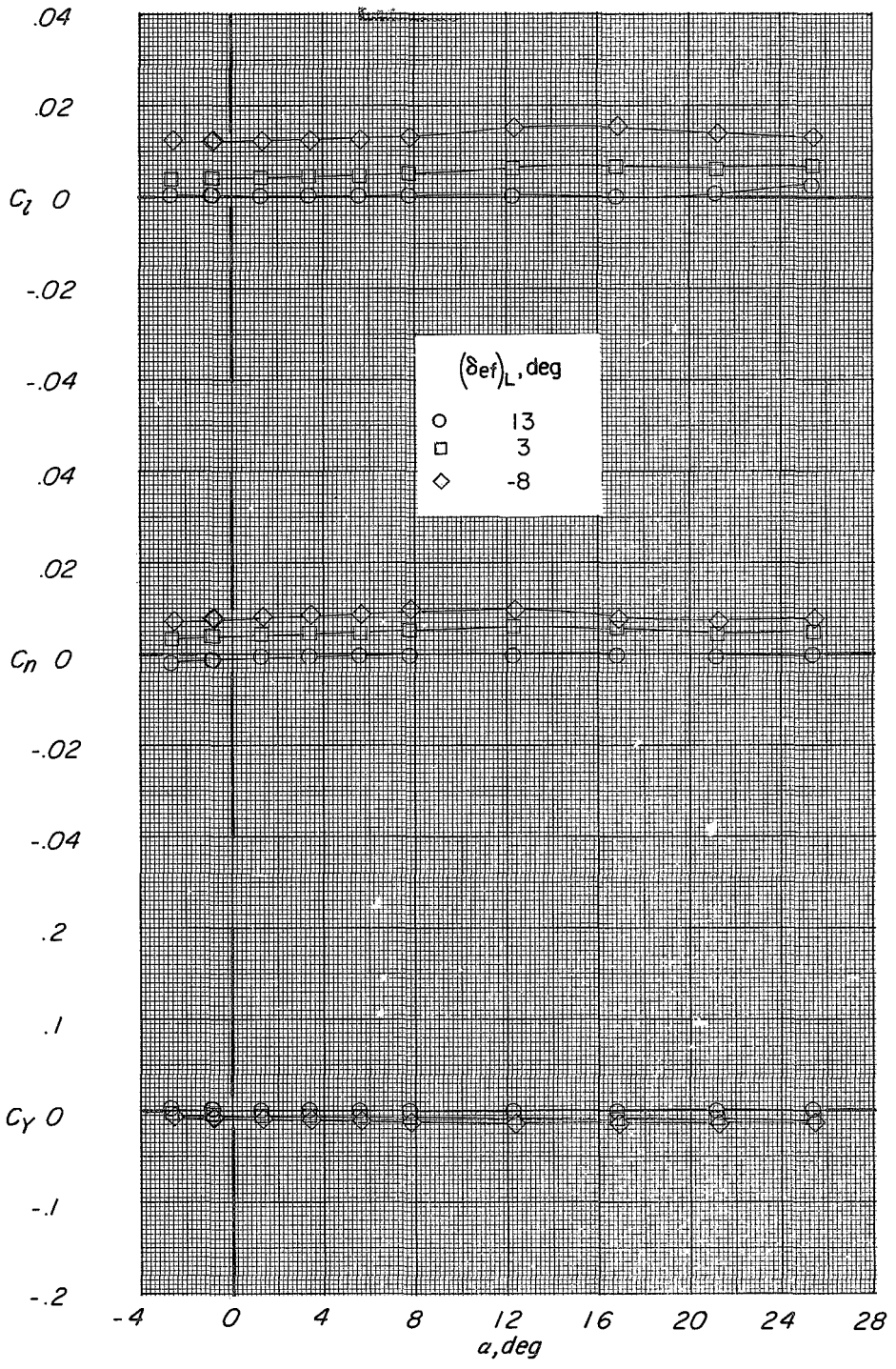
(b) $(\delta_{ef})_L = -8^o$; $(\delta_{ef})_R = 13^o$; $\delta_{if} = 0^o$; $\delta_{of} = 32^o$.

Figure 60.- Continued.



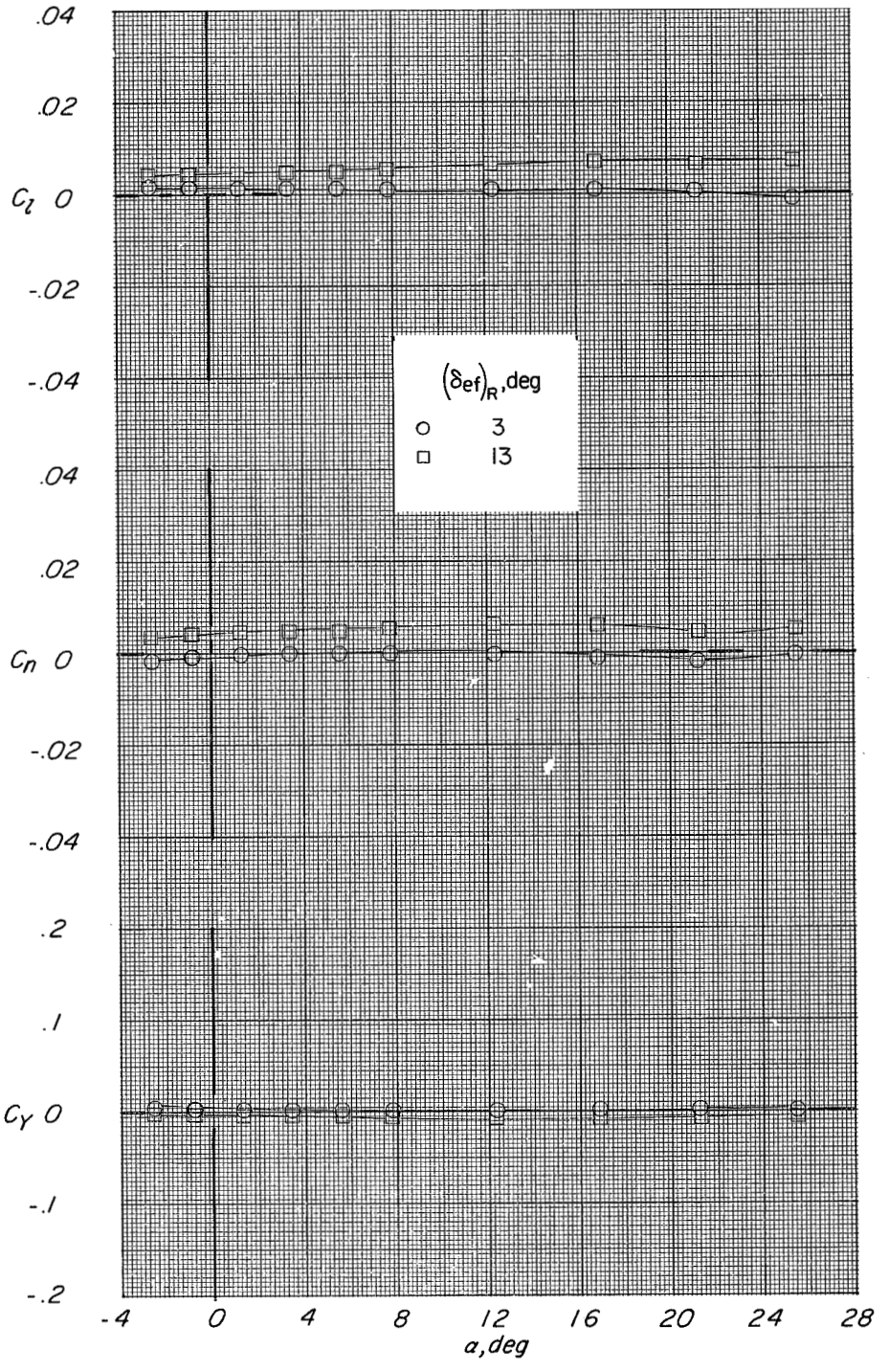
(c) $(\delta_{ef})_L = -8^o$; $(\delta_{ef})_R = 13^o$; $\delta_{if} = 0^o$; $\delta_{of} = 32^o$.

Figure 60.- Concluded.



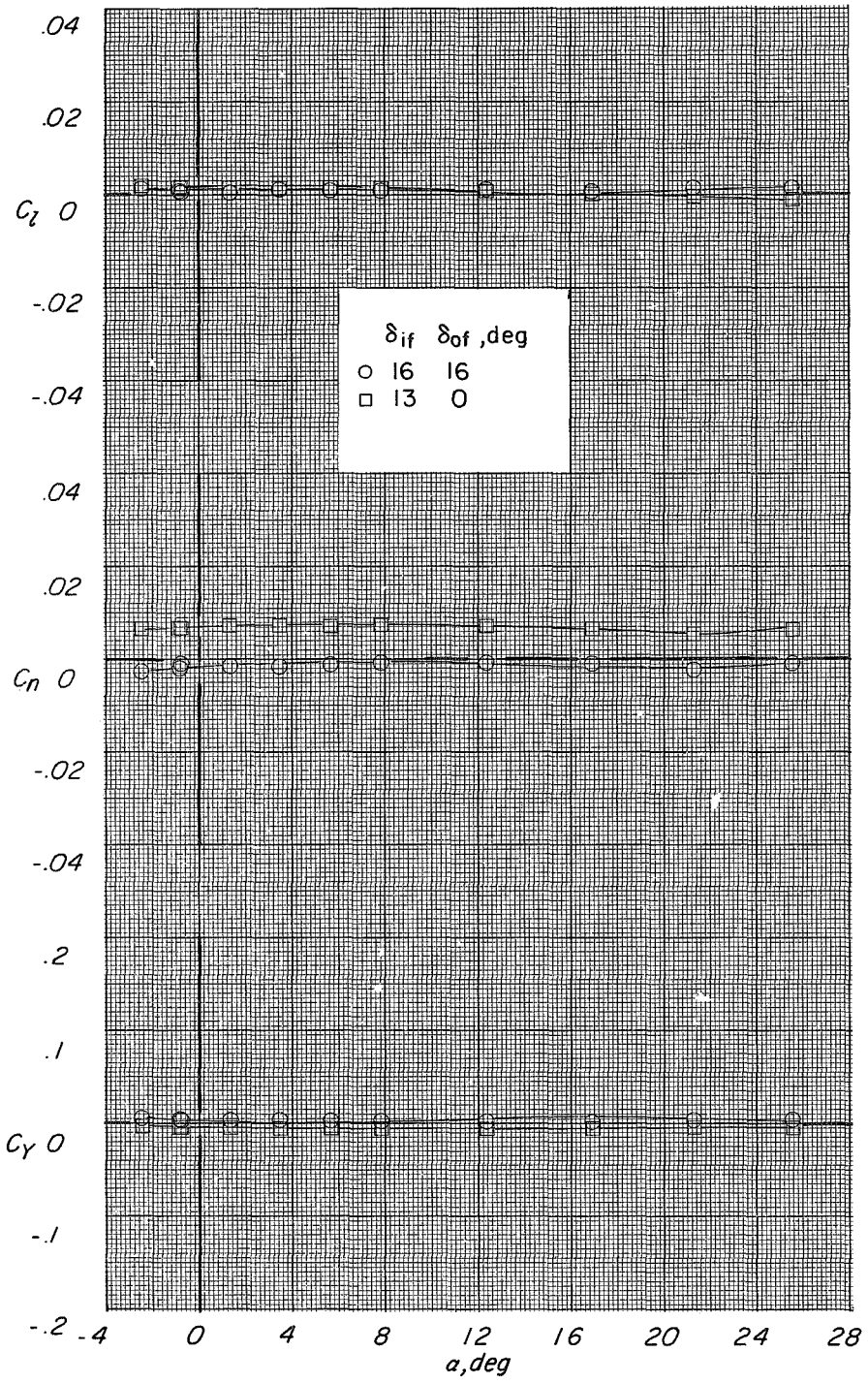
(a) $(\delta_{ef})_R = 13^o$; $\delta_{if} = 32^o$; $\delta_{of} = 0^o$; $\delta_e = 10^o$.

Figure 61.- Effect of deflecting one of the elevon flaps on the lateral characteristics of the HL-10. Modification II fin configuration; $\beta = 0^o$; M = 0.60.



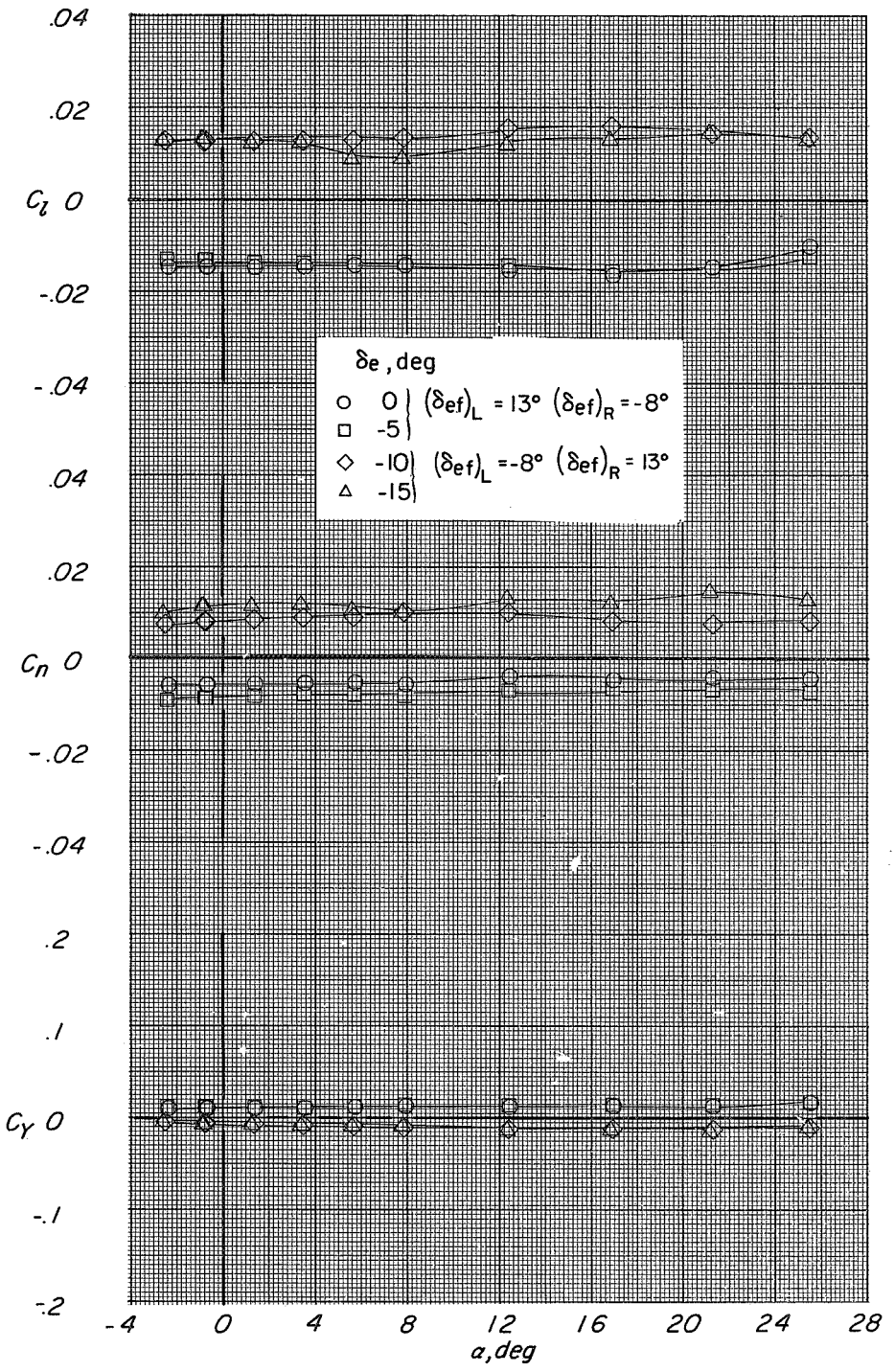
(b) $(\delta_{ef})_L = 3^o$; $\delta_{if} = 32^o$; $\delta_{of} = 0^o$; $\delta_e = -10^o$.

Figure 61.- Continued.



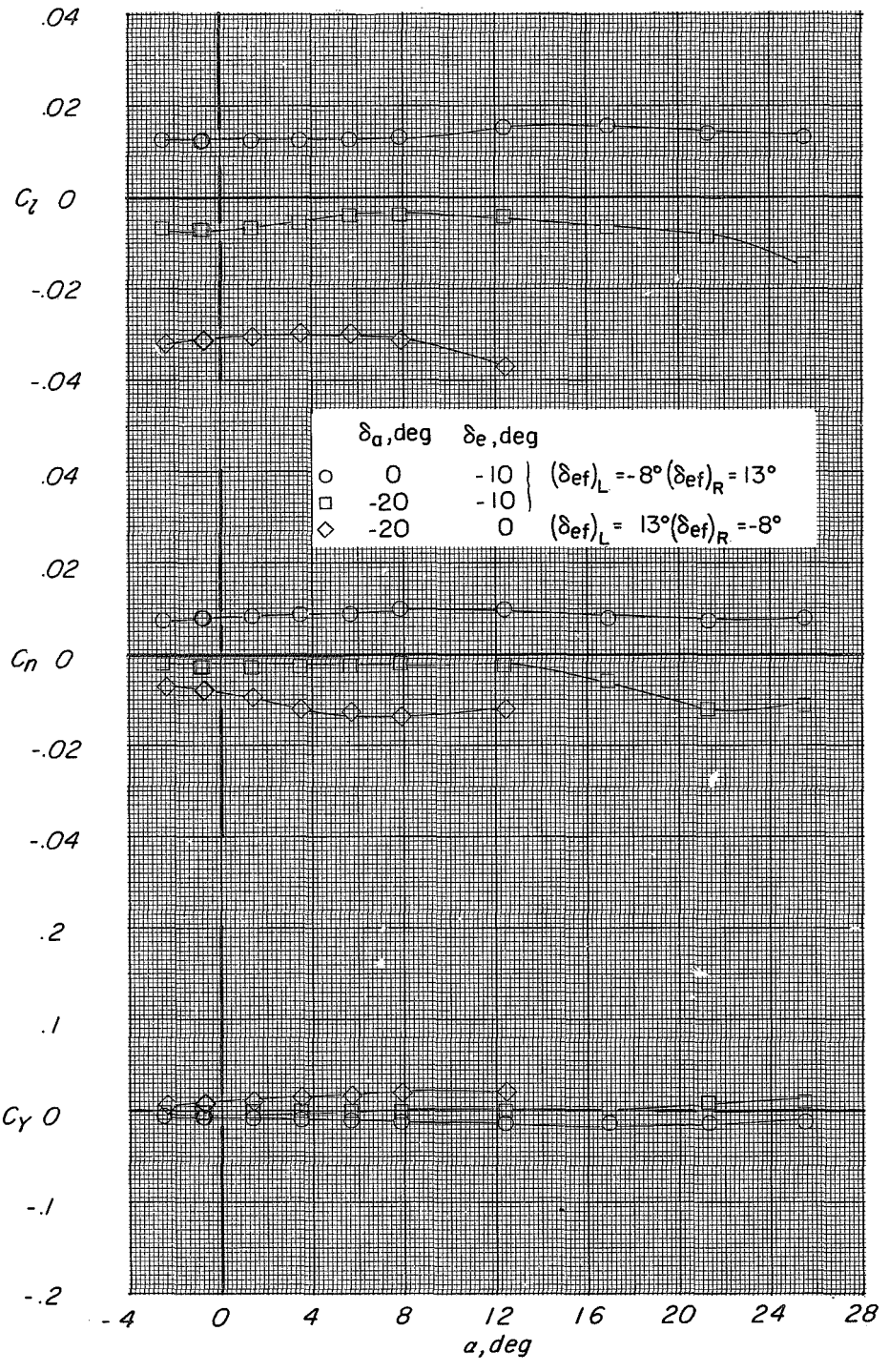
(c) $\delta_{ef} = 13^{o}$; $(\delta_{if})_L = (\delta_{of})_L = 16^{o}$; $\delta_e = -5^{o}$.

Figure 61.- Concluded.



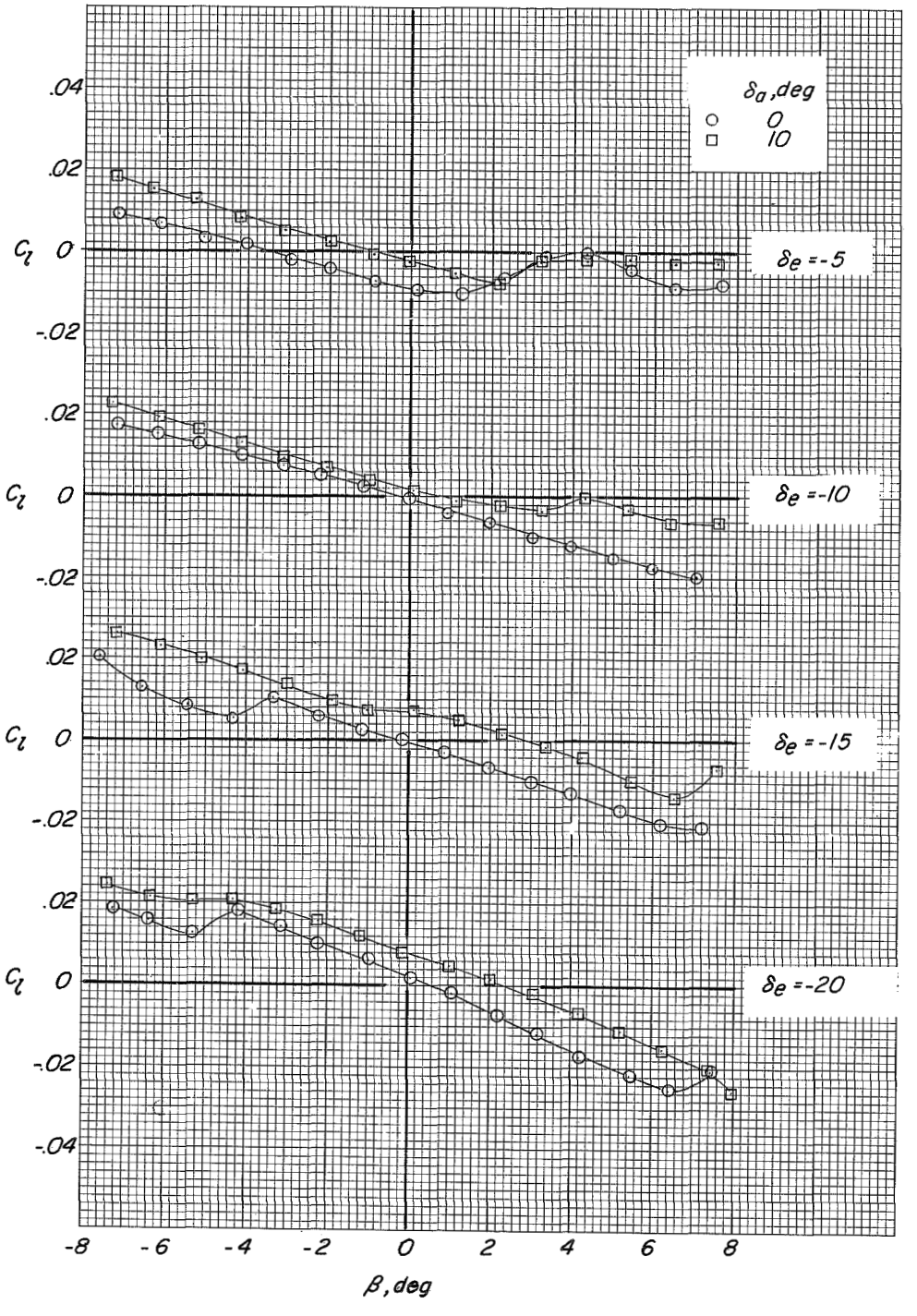
(a) $\delta_{if} = 32^{o}$; $\delta_{of} = 0^{o}$.

Figure 62.- Effect of combined aileron and elevon deflection on the lateral characteristics of the model for several auxiliary flap deflections. Modification II fin configuration; $\beta = 0^{o}$; M = 0.60.



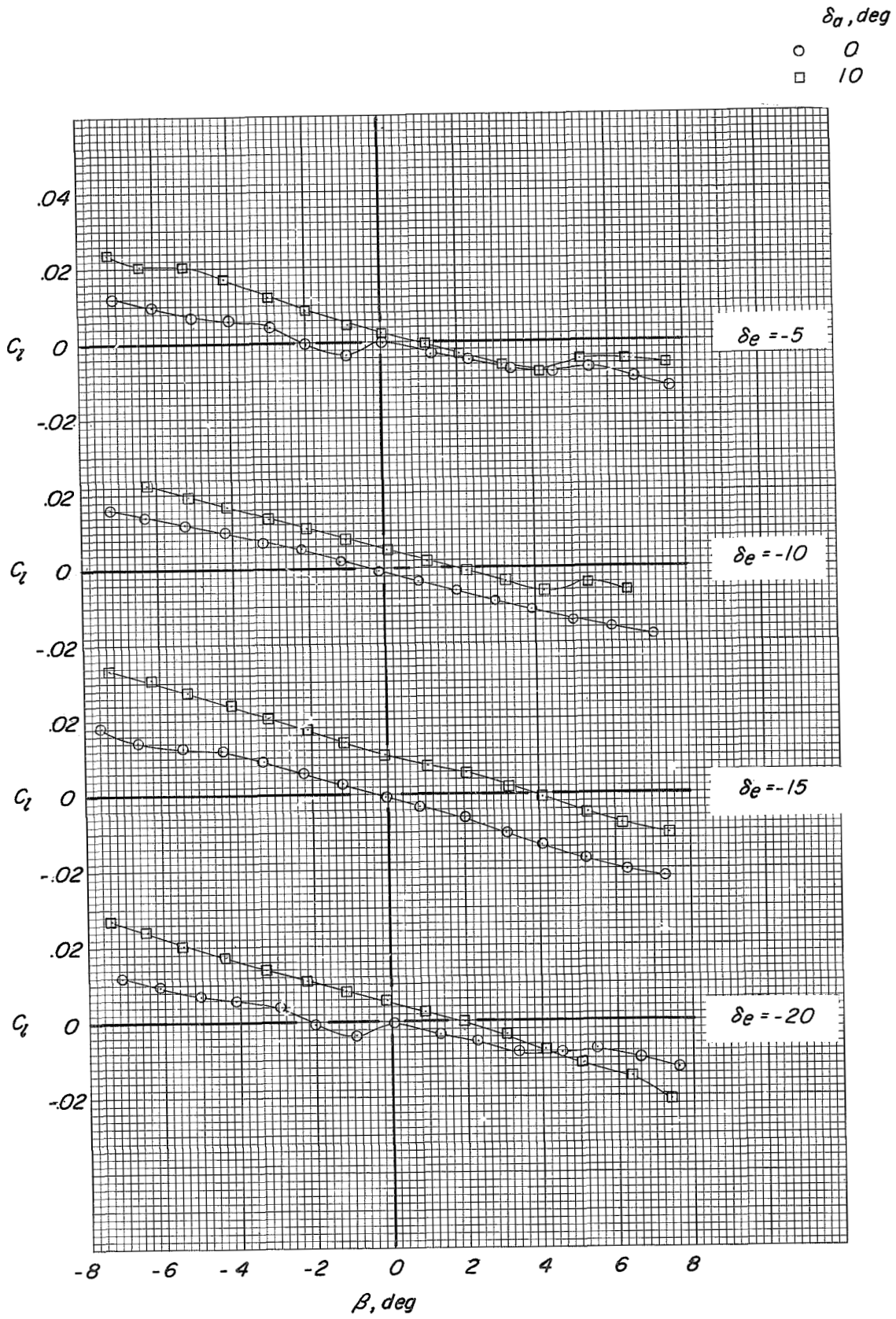
(b) $\delta_{if} = 32^{o}$; $\delta_{of} = 0^{o}$.

Figure 62.- Concluded.



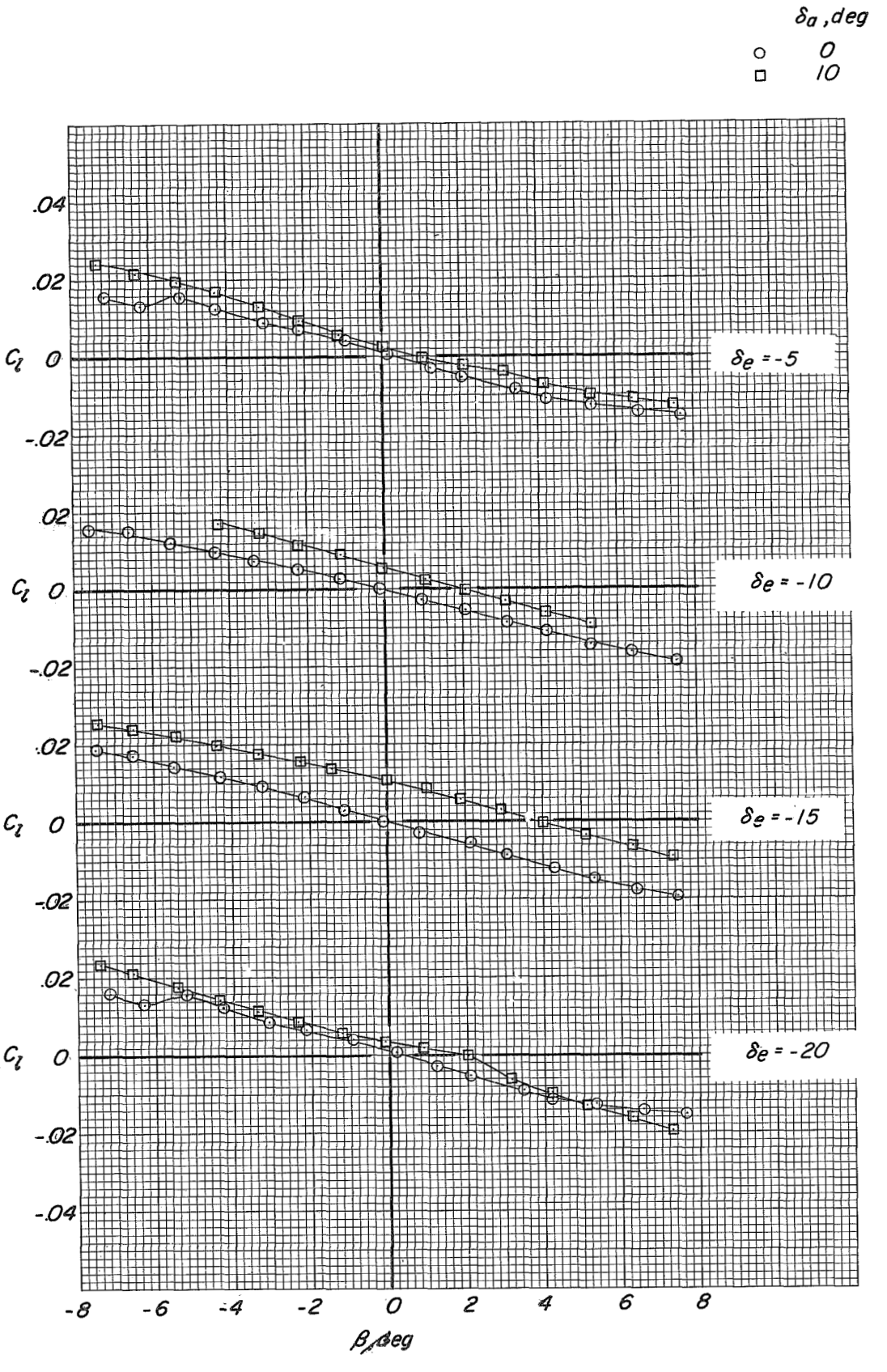
(a) M = 0.35.

Figure 63.- Variation of rolling-moment coefficient with sideslip angle for several elevator angles on the basic configuration of the HL-10 at angles of attack of $\alpha = 17^{\circ}$. Subsonic configuration.



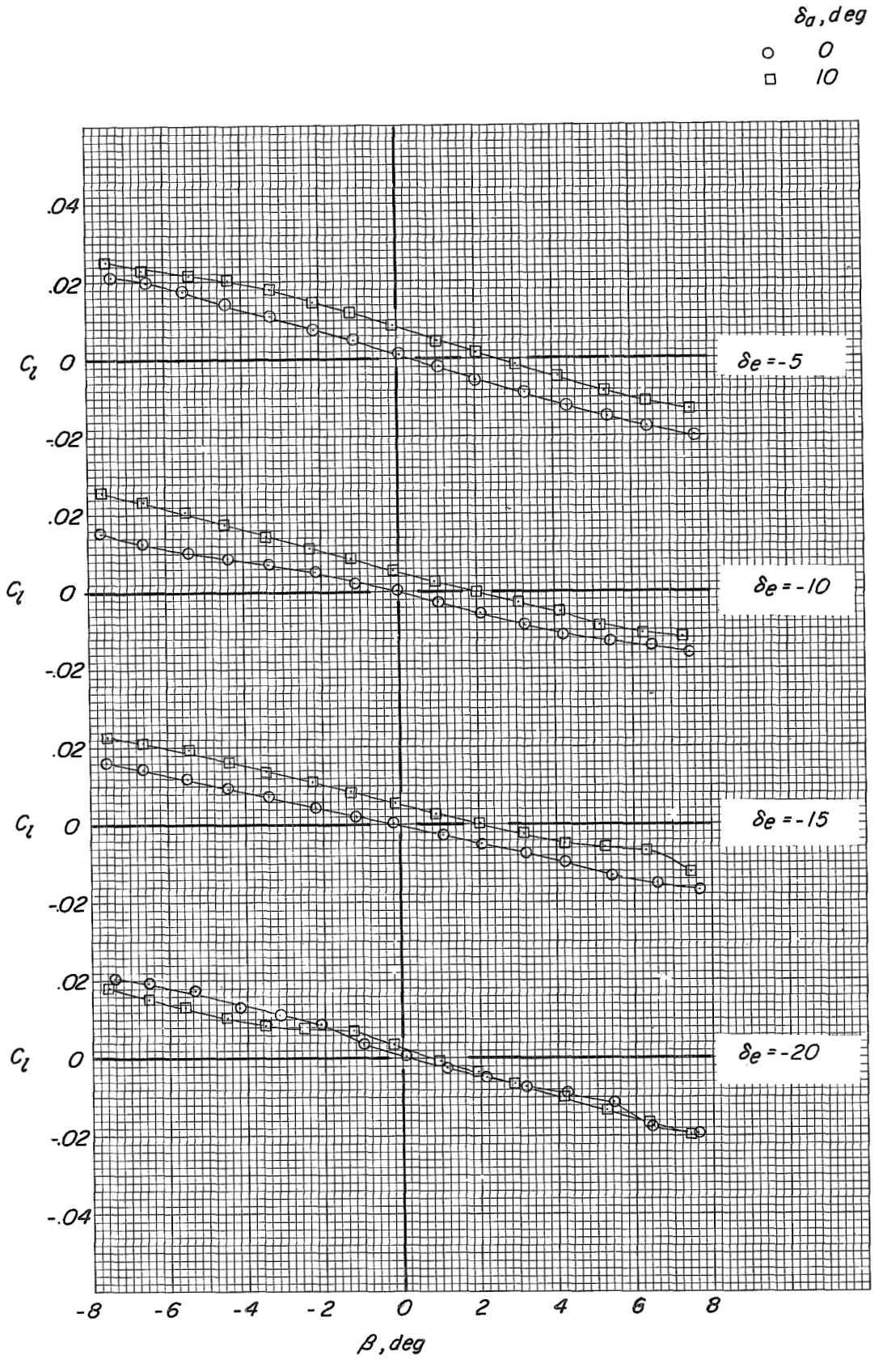
(b) M = 0.50.

Figure 63.- Continued.



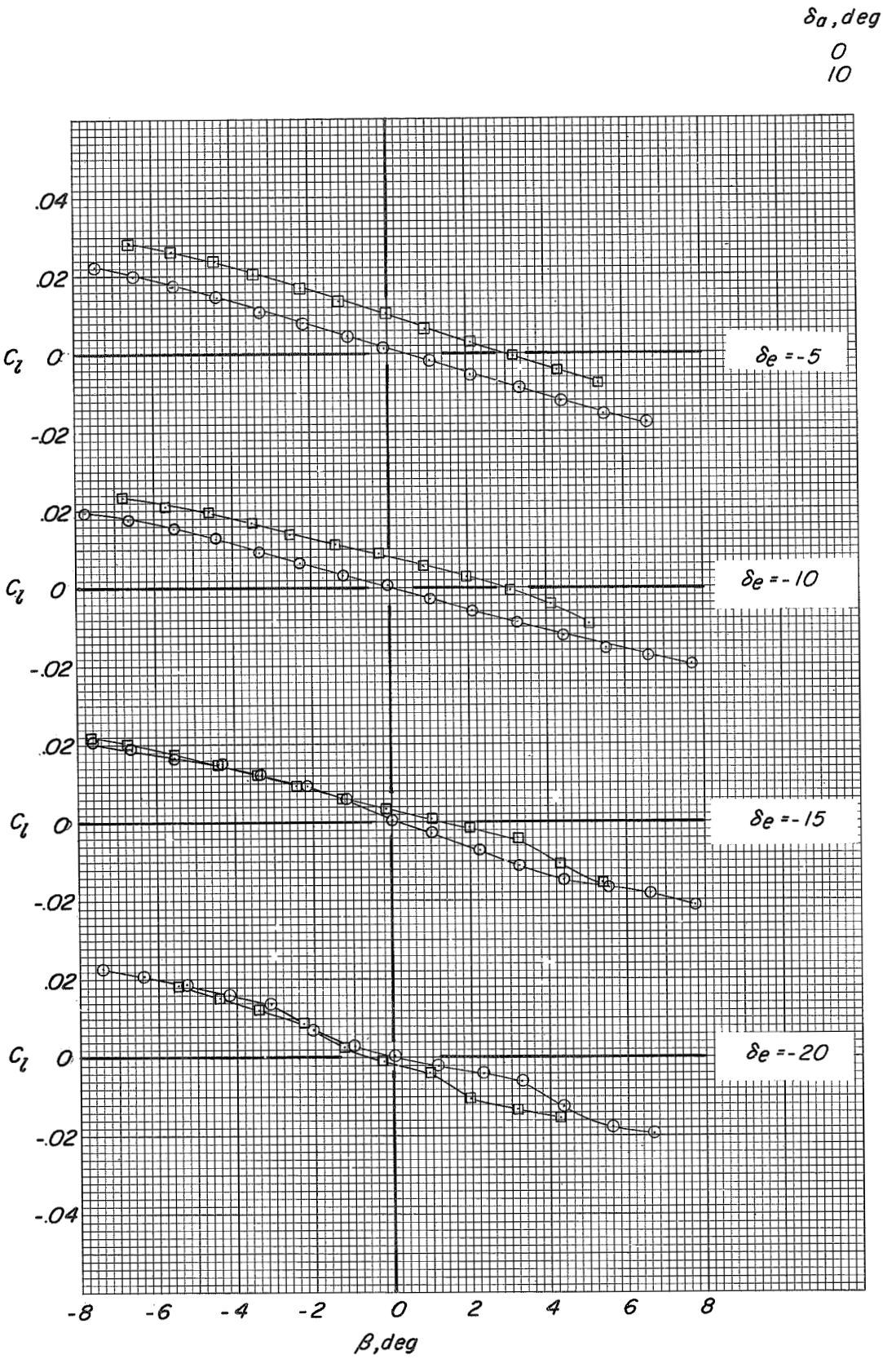
(c) M = 0.60.

Figure 63.- Continued.



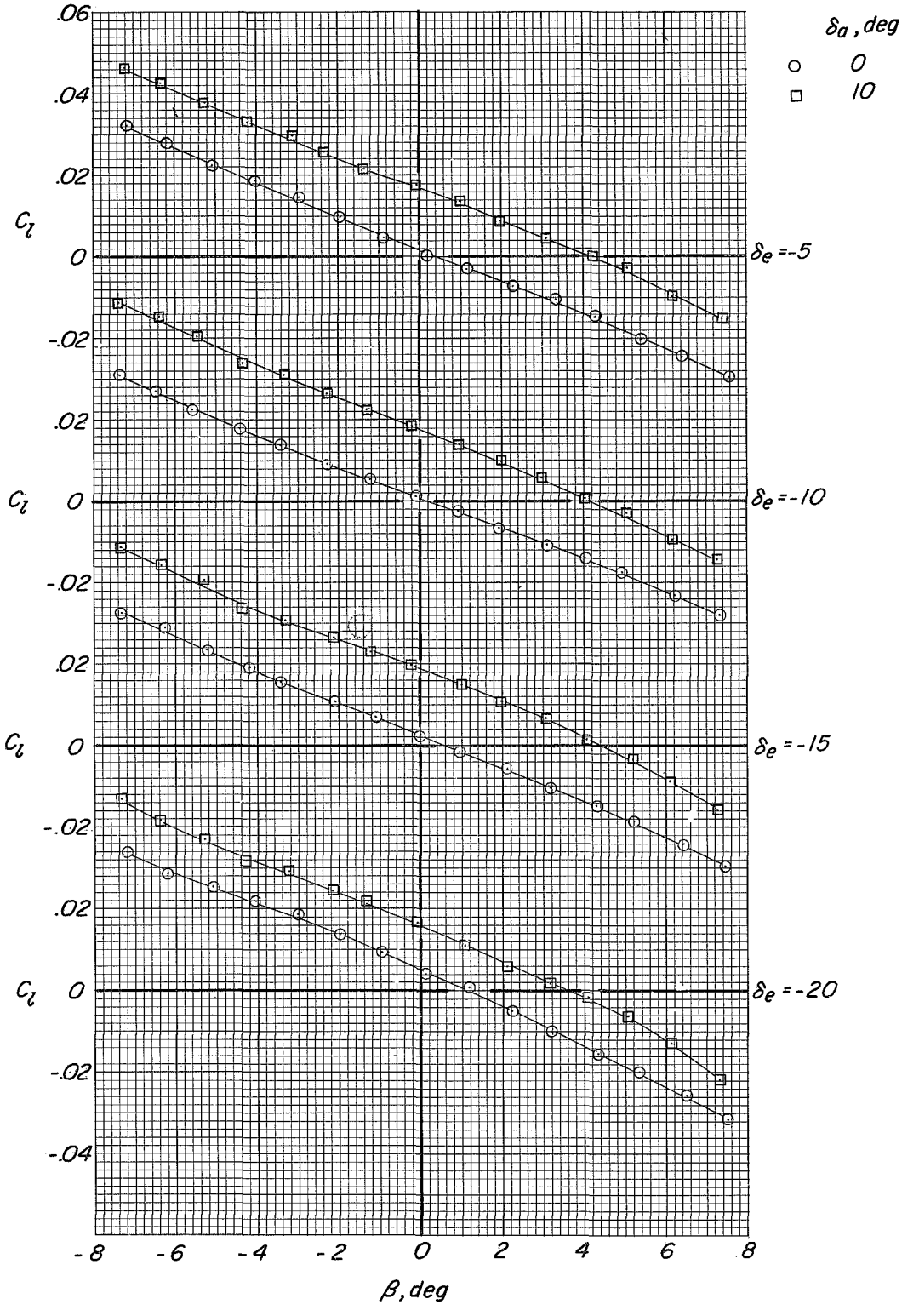
(d) M = 0.70.

Figure 63.- Continued.



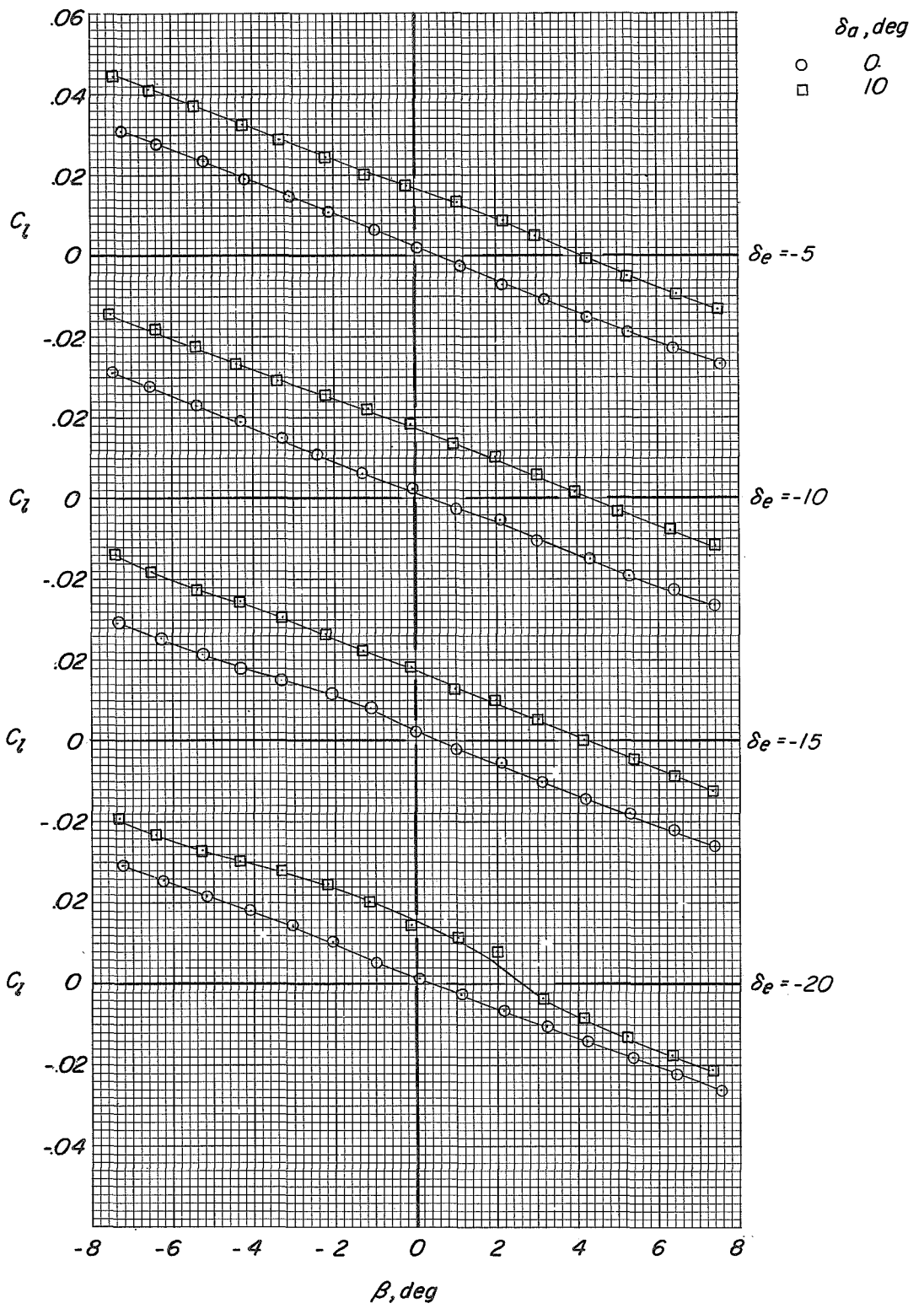
(e) M = 0.80.

Figure 63.- Concluded.



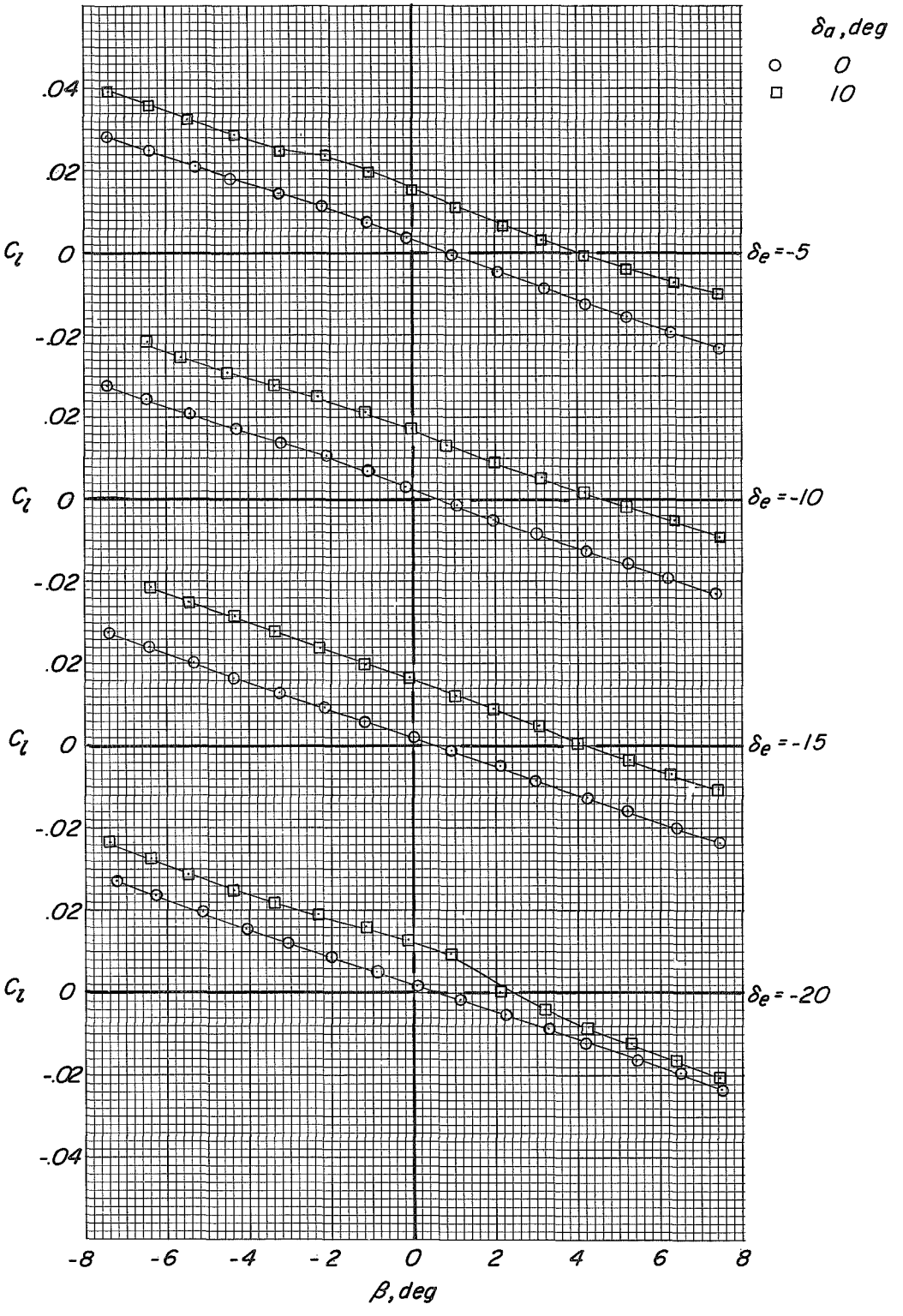
(a) Variation of C_l with β. M = 0.35.

Figure 64.- Variation of rolling- and yawing-moment coefficients with sideslip angle for several elevon angles on modification I of the HL-10 at an angle of attack of $\alpha = 17^{o}$. Subsonic configuration.



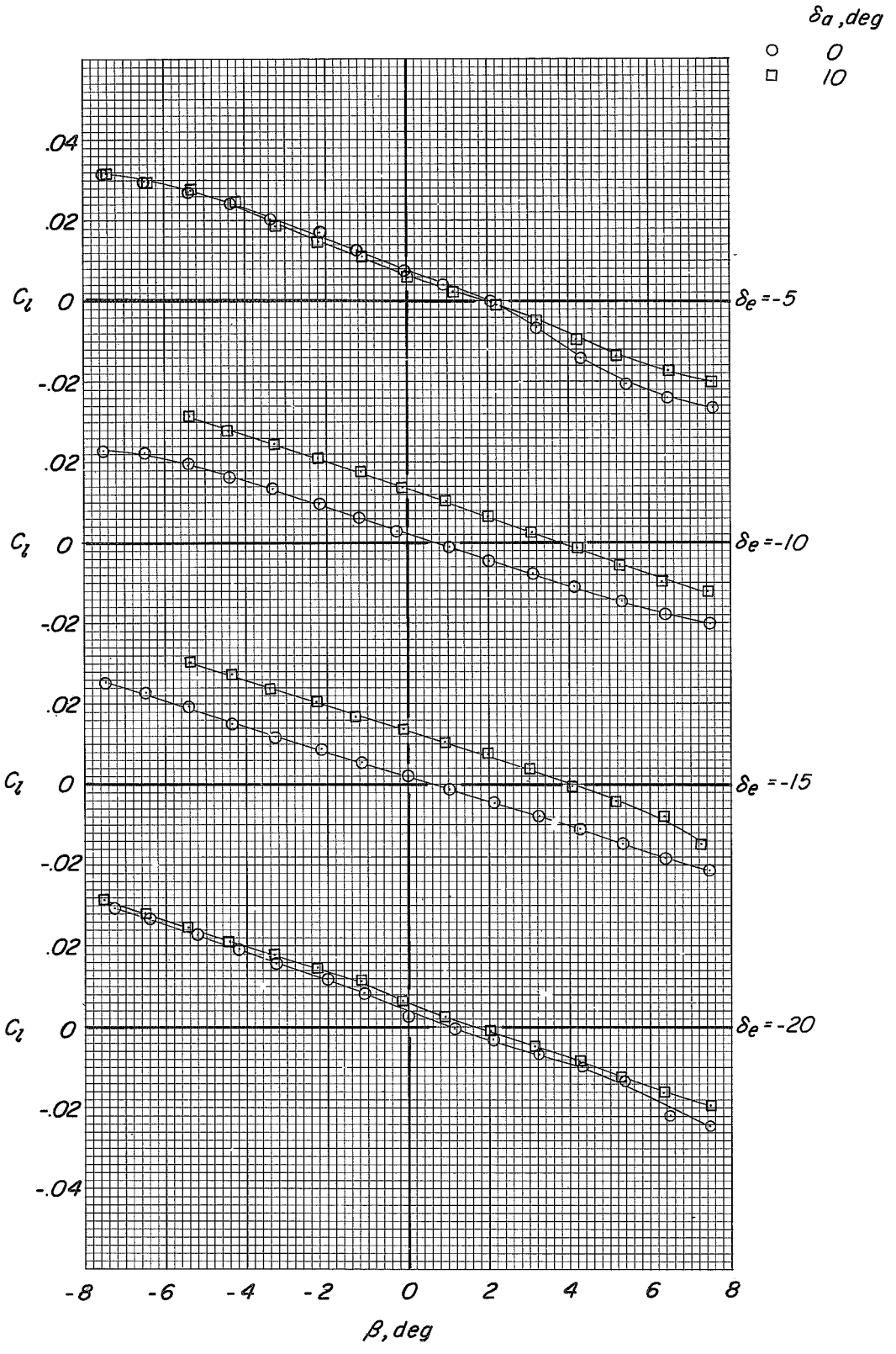
(b) Variation of C_l with β. M = 0.50.

Figure 64.- Continued.



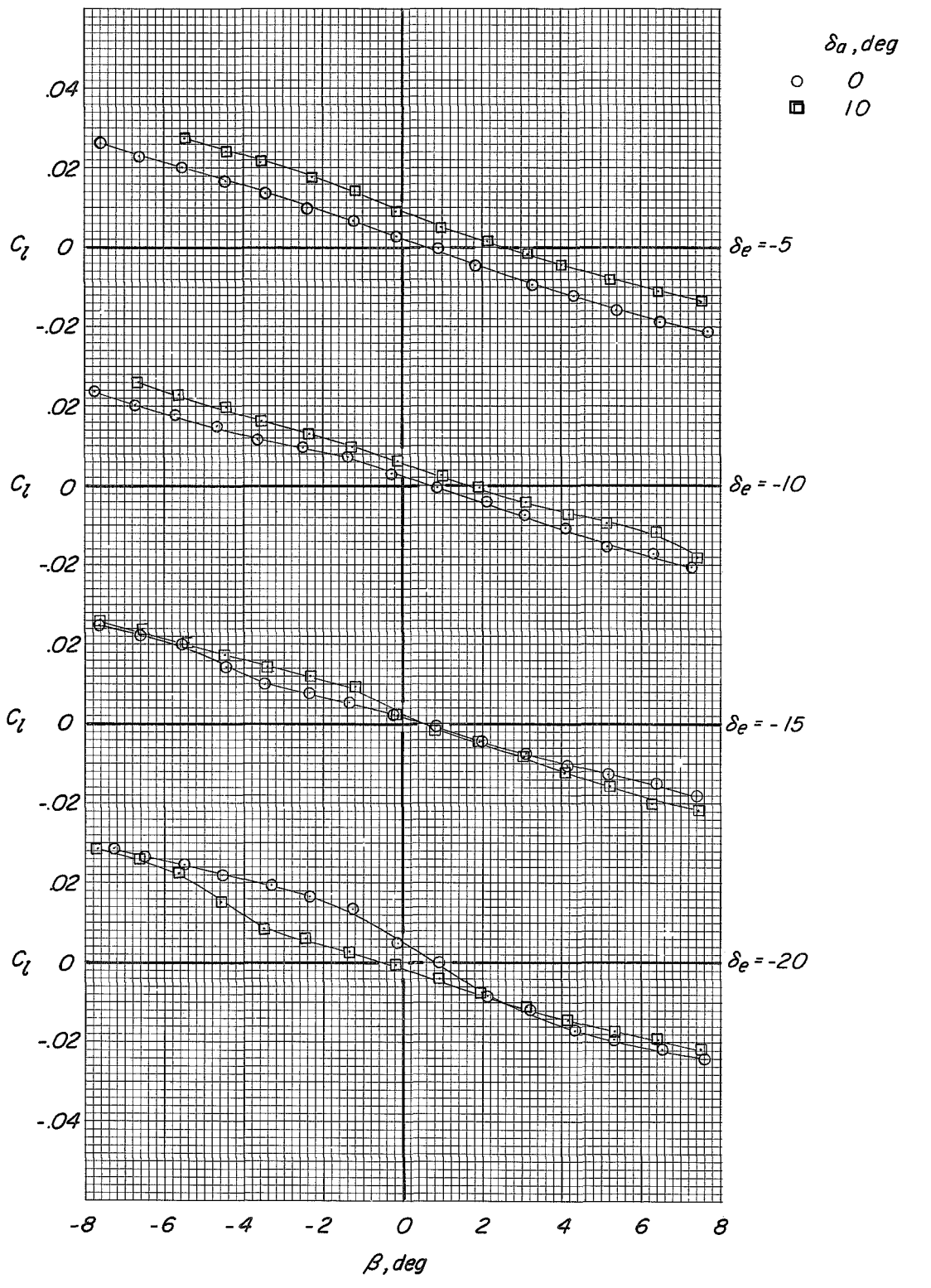
(c) Variation of C_l with β. M = 0.60.

Figure 64.- Continued.



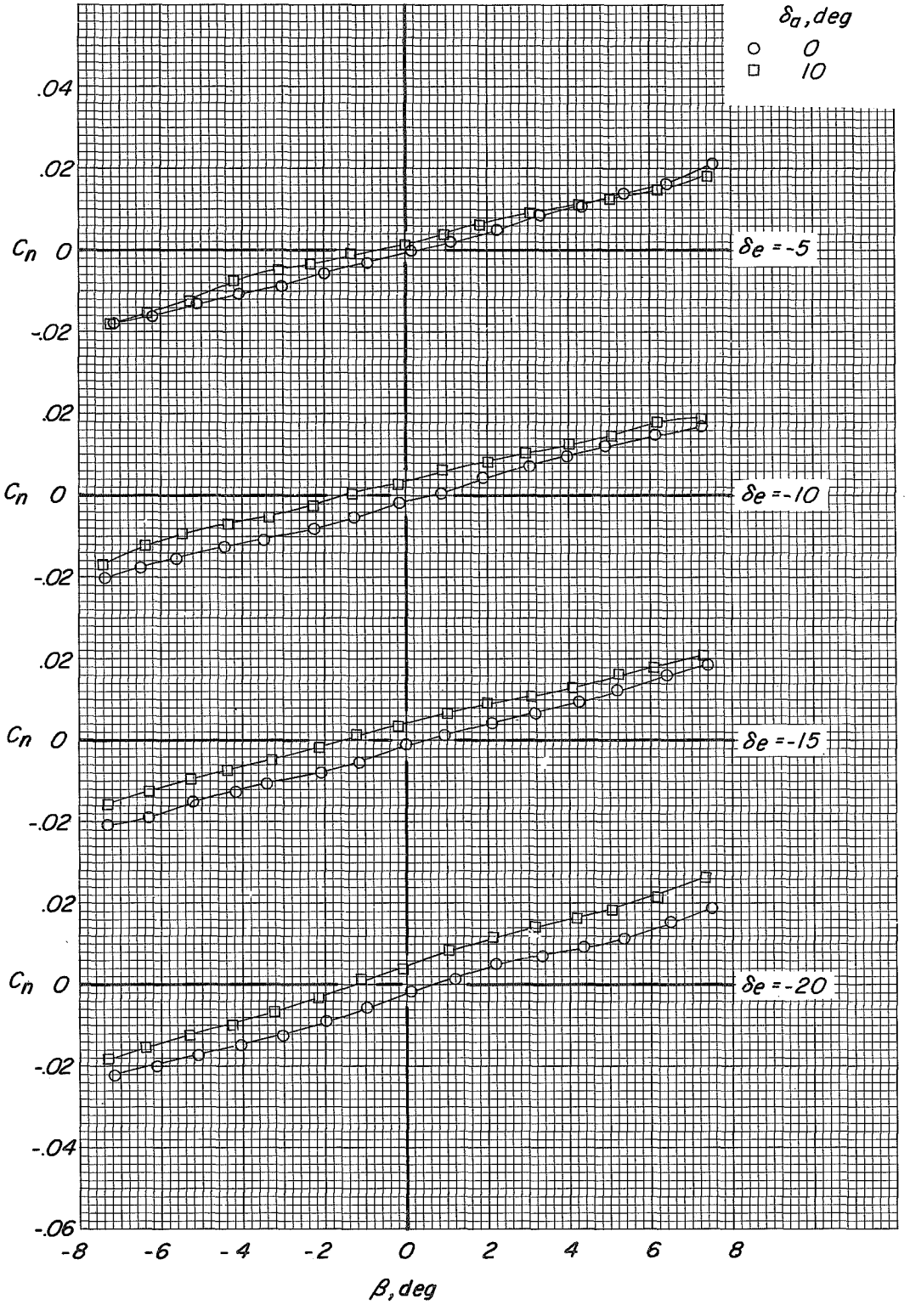
(d) Variation of C_l with β. M = 0.70.

Figure 64.- Continued.



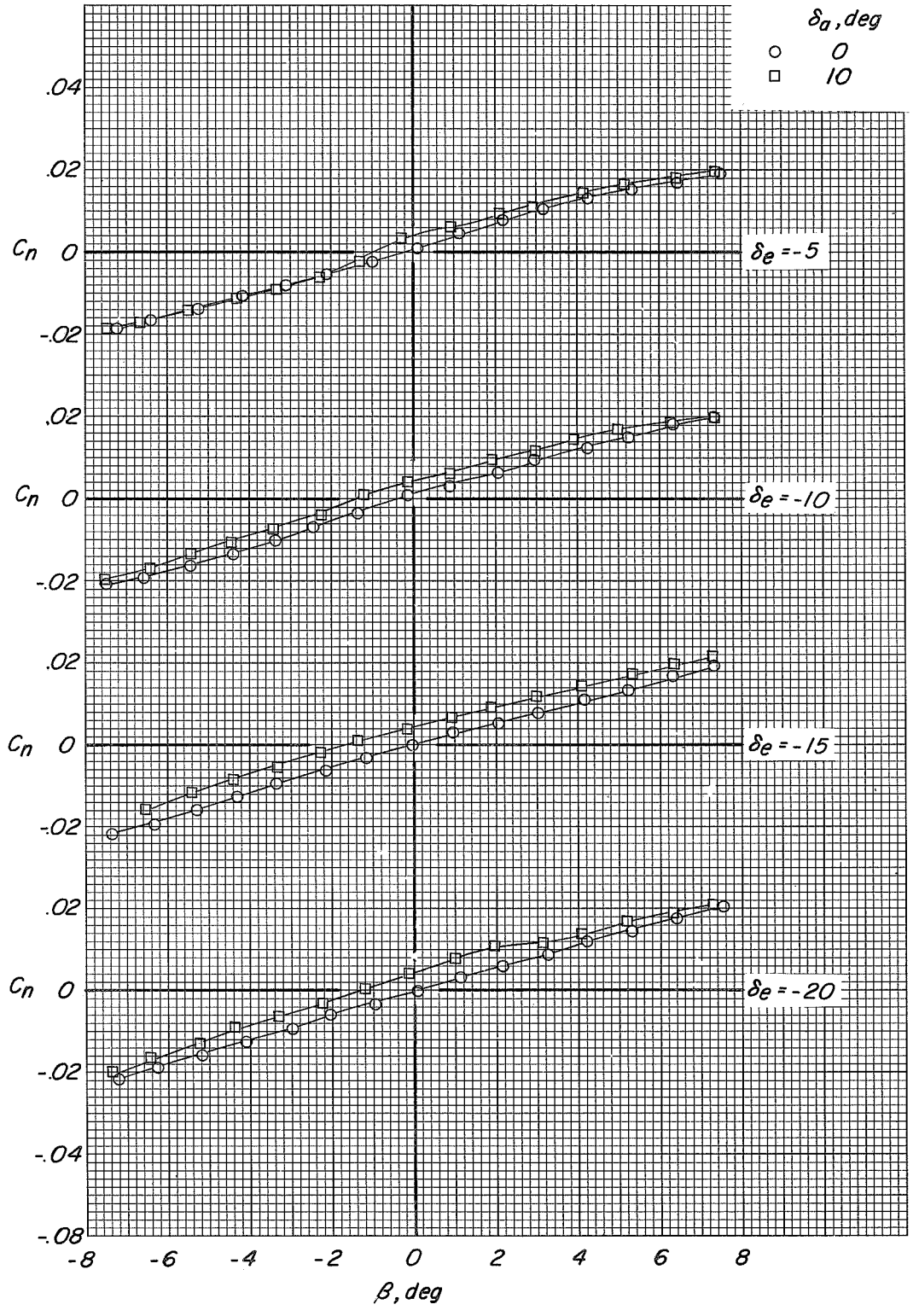
(e) Variation of C_l with β. M = 0.80.

Figure 64.- Continued.



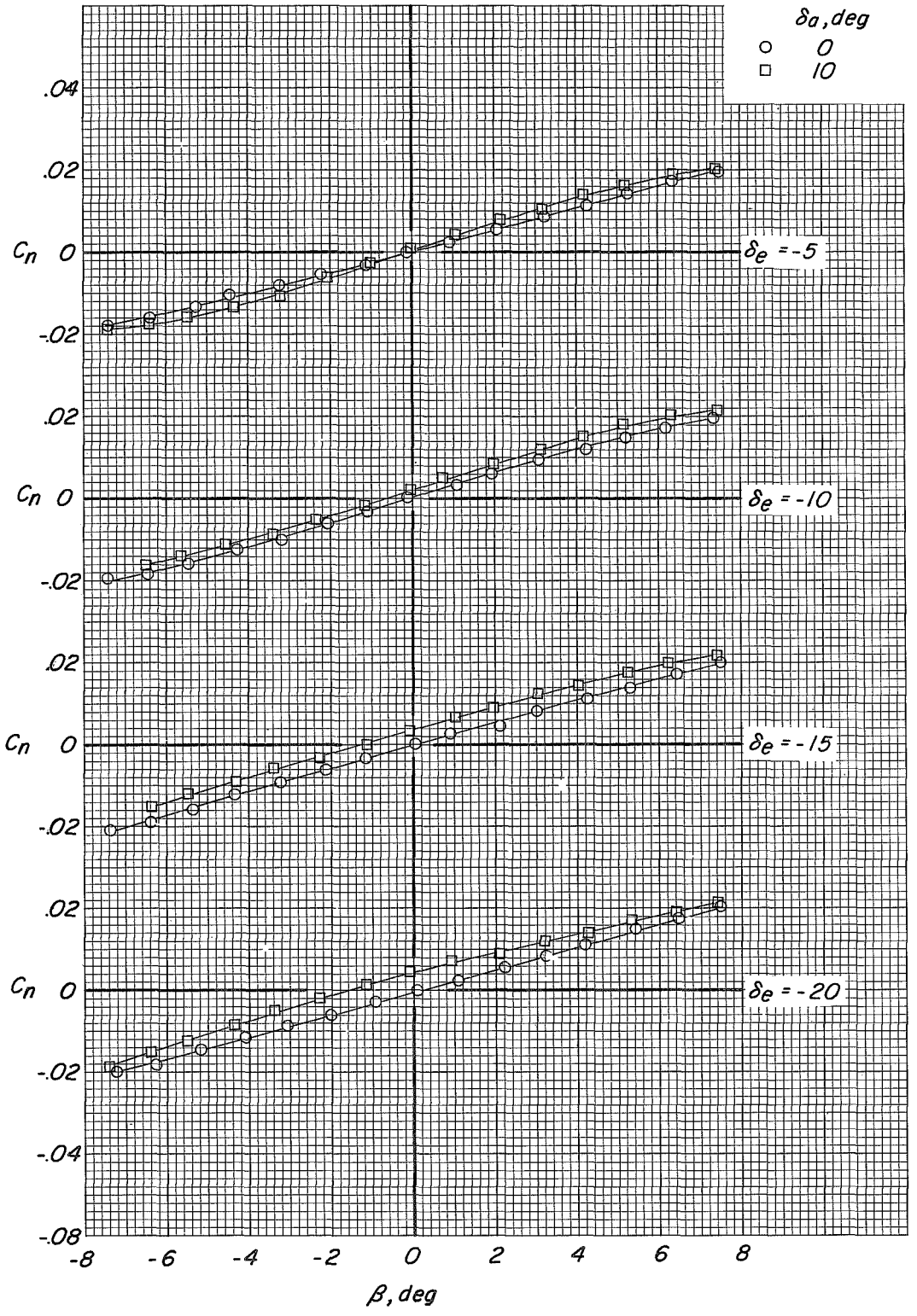
(f) Variation of C_n with β. M = 0.35.

Figure 64.- Continued.



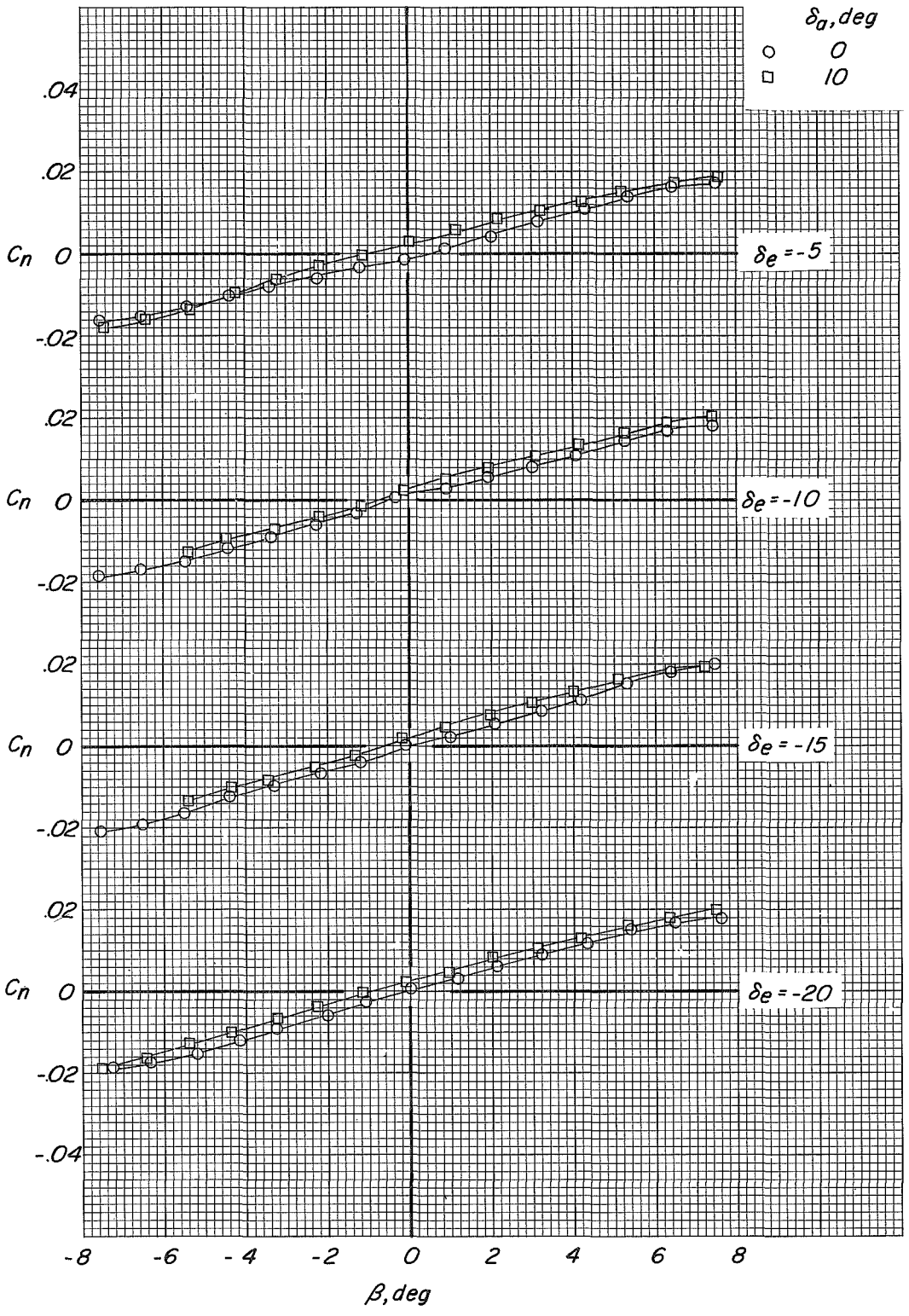
(g) Variation of C_n with β. M = 0.50.

Figure 64.- Continued.



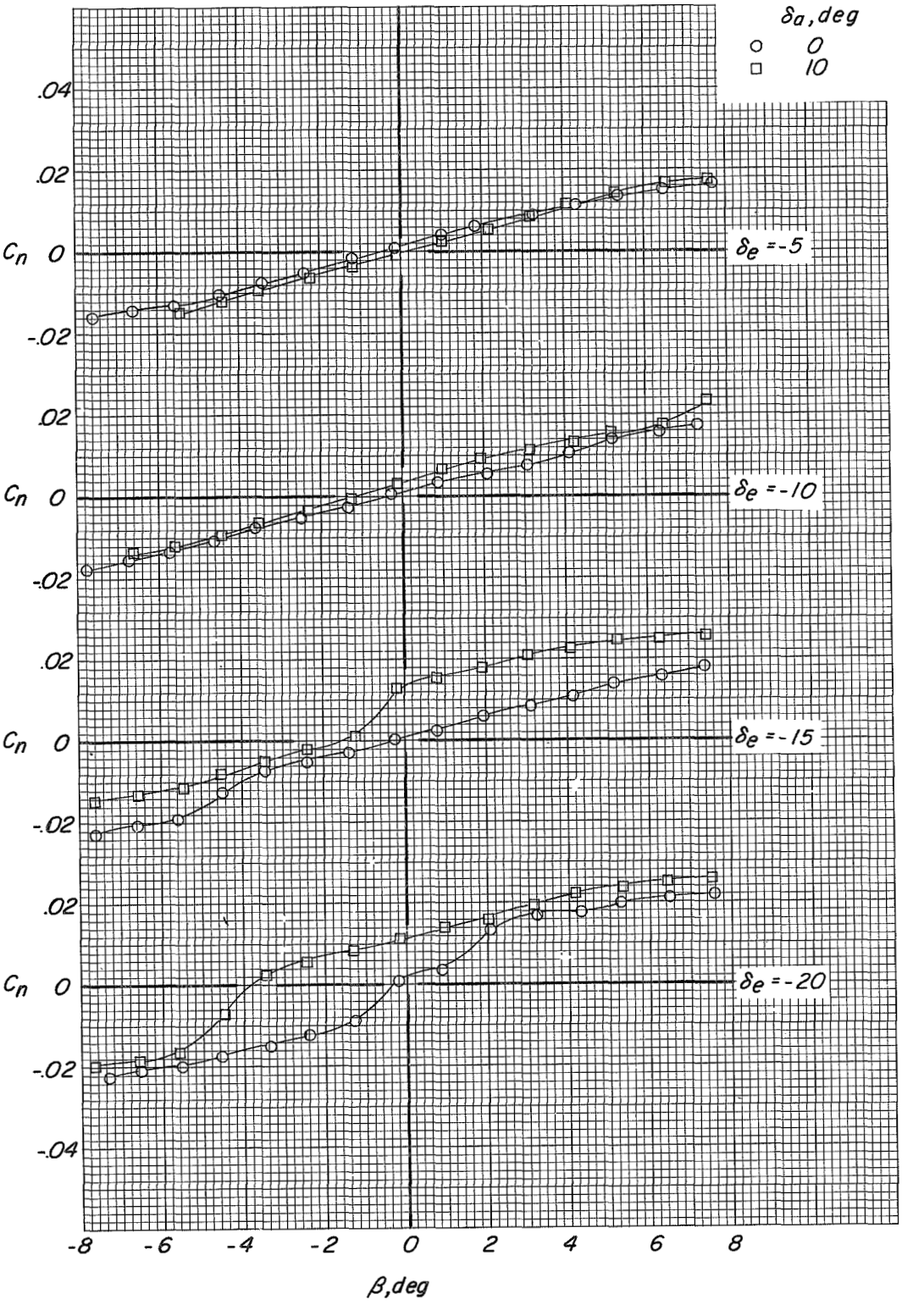
(h) Variation of C_n with β. M = 0.60.

Figure 64.- Continued.



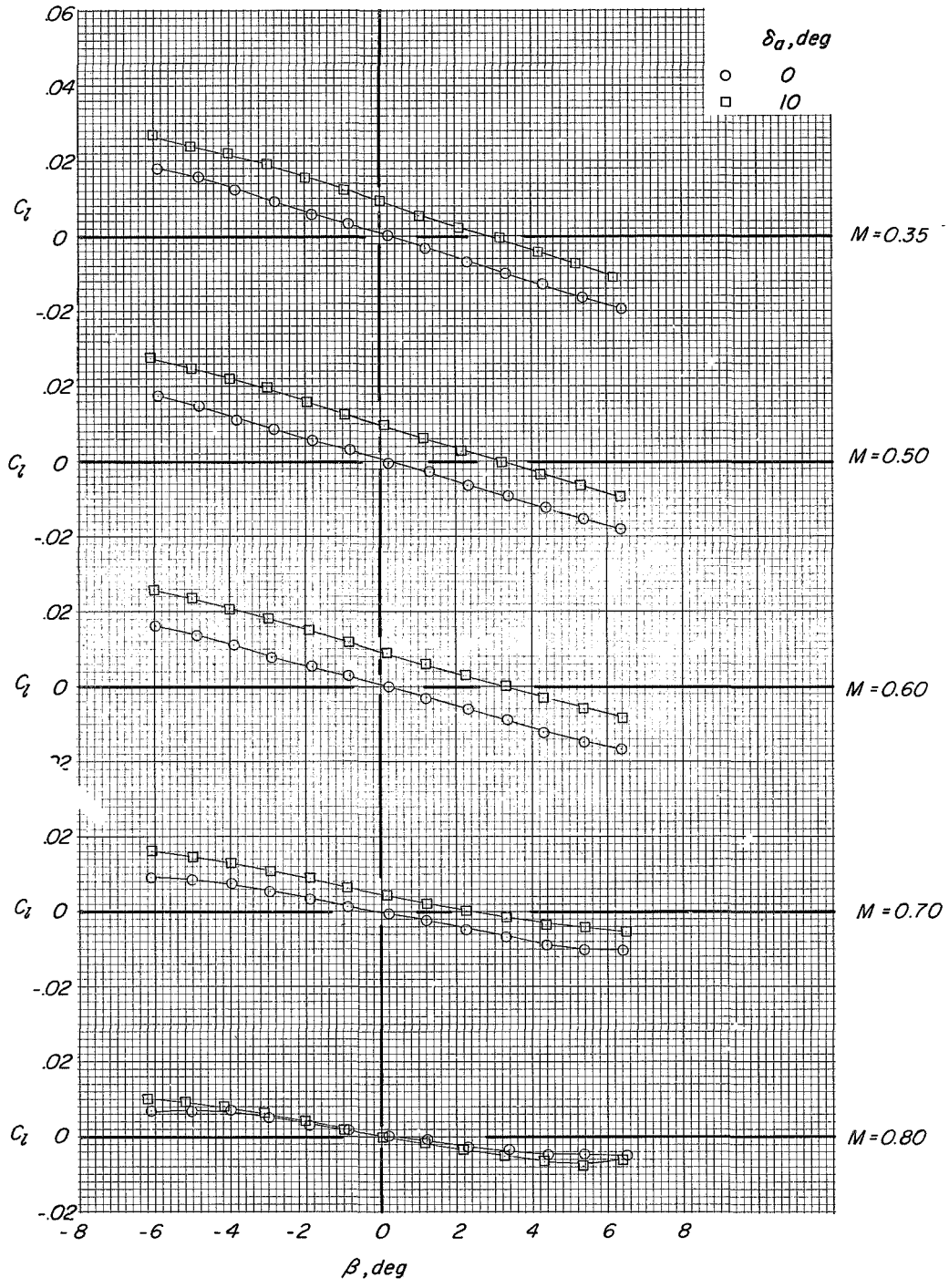
(i) Variation of C_n with β. M = 0.70.

Figure 64.- Continued.



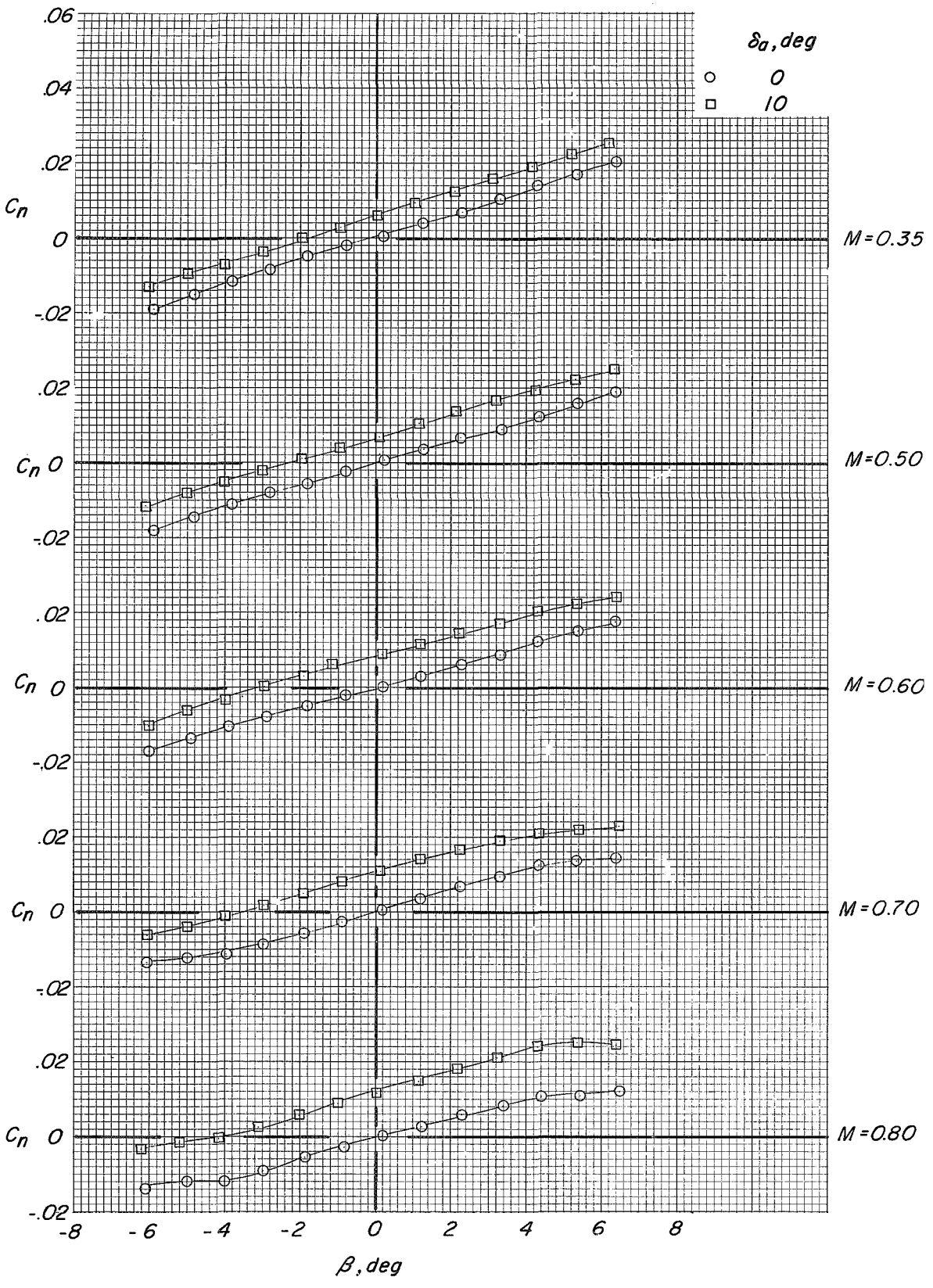
(j) Variation of C_n with β. M = 0.80.

Figure 64.- Concluded.



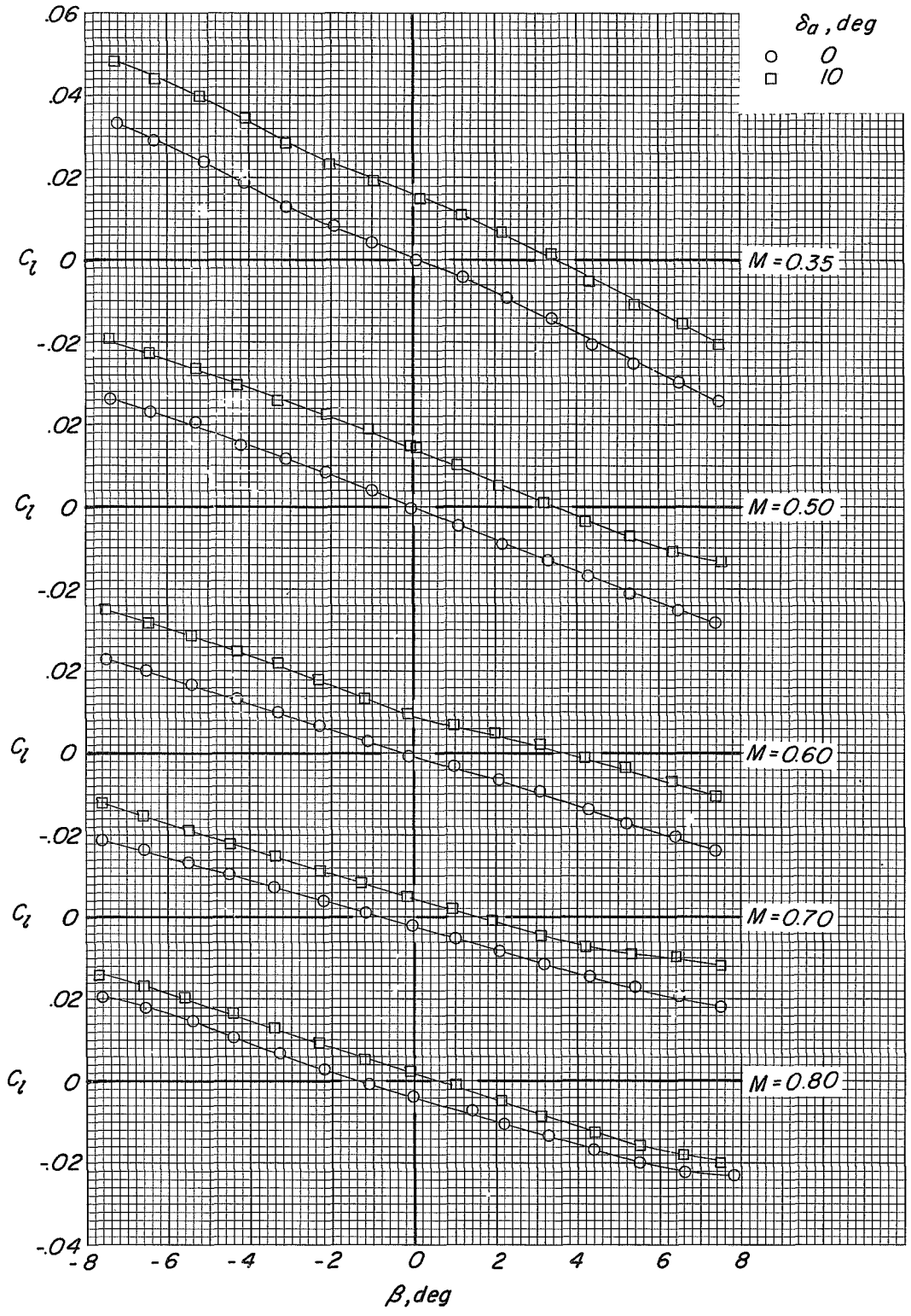
(a) Variation of C_l with β.

Figure 65.- Variation of rolling- and yawing-moment coefficients with sideslip angle for an elevon angle $\delta_e = -10^o$ and an angle of attack $\alpha = 7^o$. Modification I; subsonic configuration.



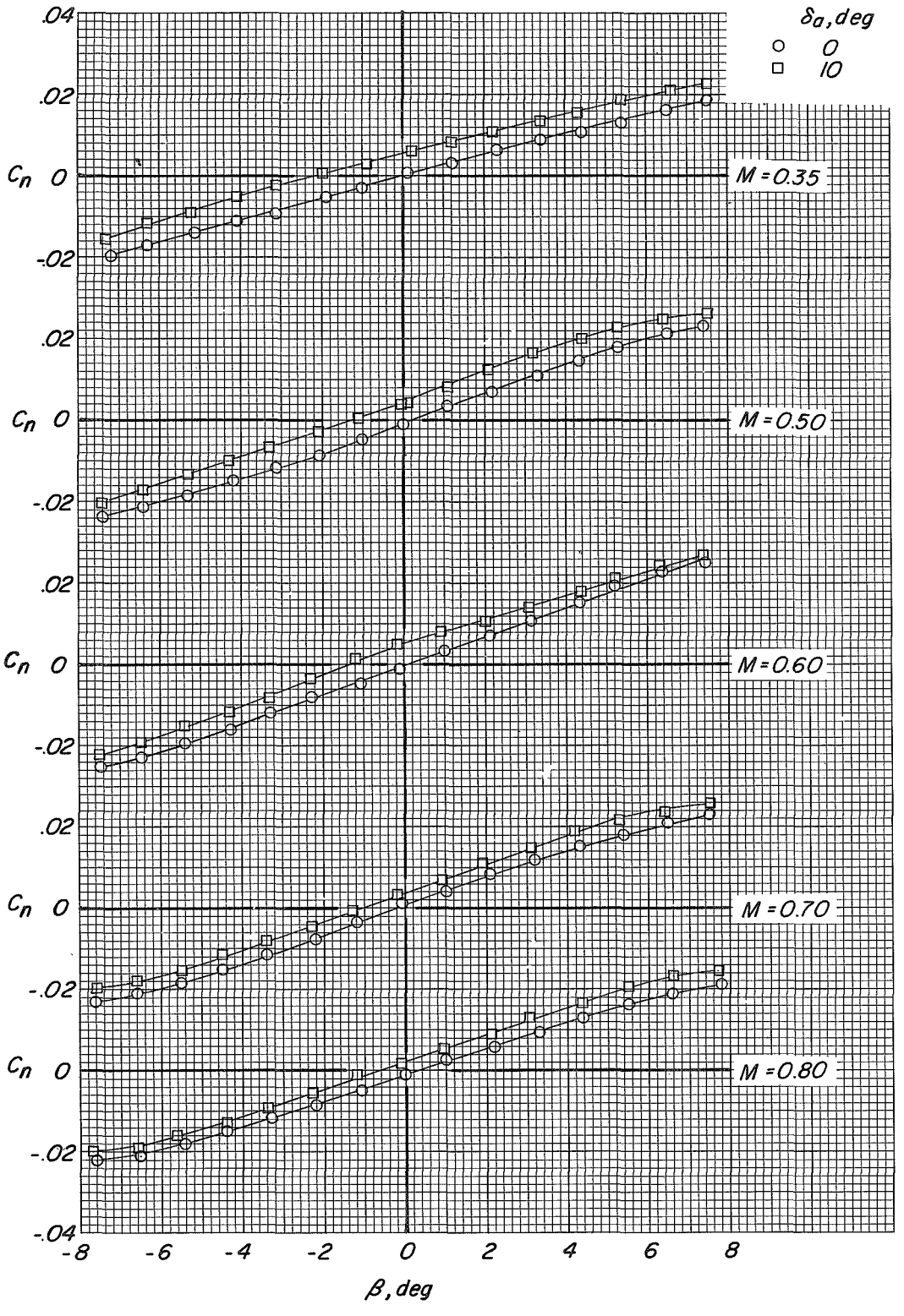
(b) Variation of C_n with β.

Figure 65.- Concluded.



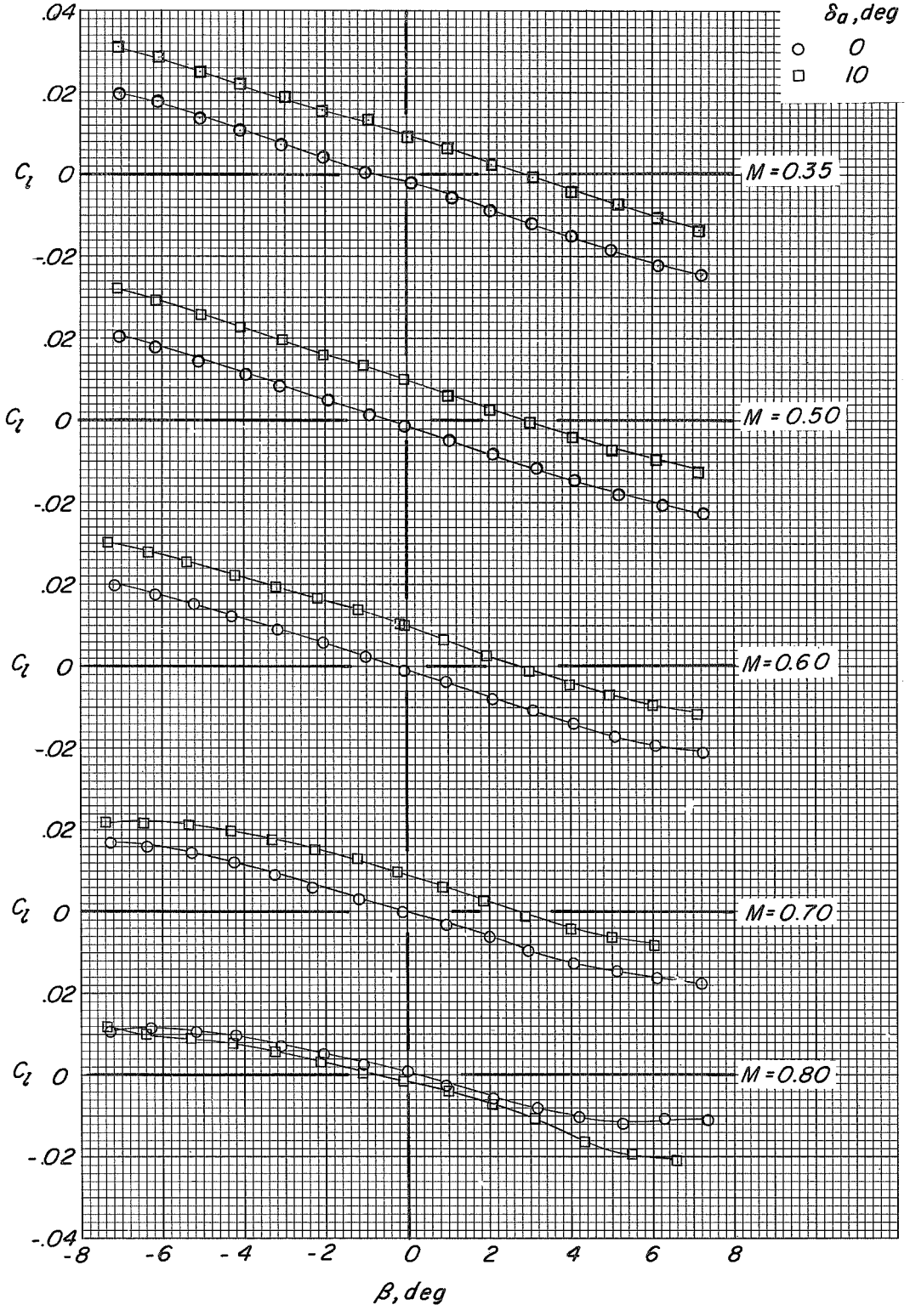
(a) Variation of C_l with β.

Figure 66.- Variation of rolling- and yawing-moment coefficients with sideslip angle for an elevon angle of $\delta_e = -15^o$ and an angle of attack of $\alpha = 17^o$. Modification II; subsonic configuration.



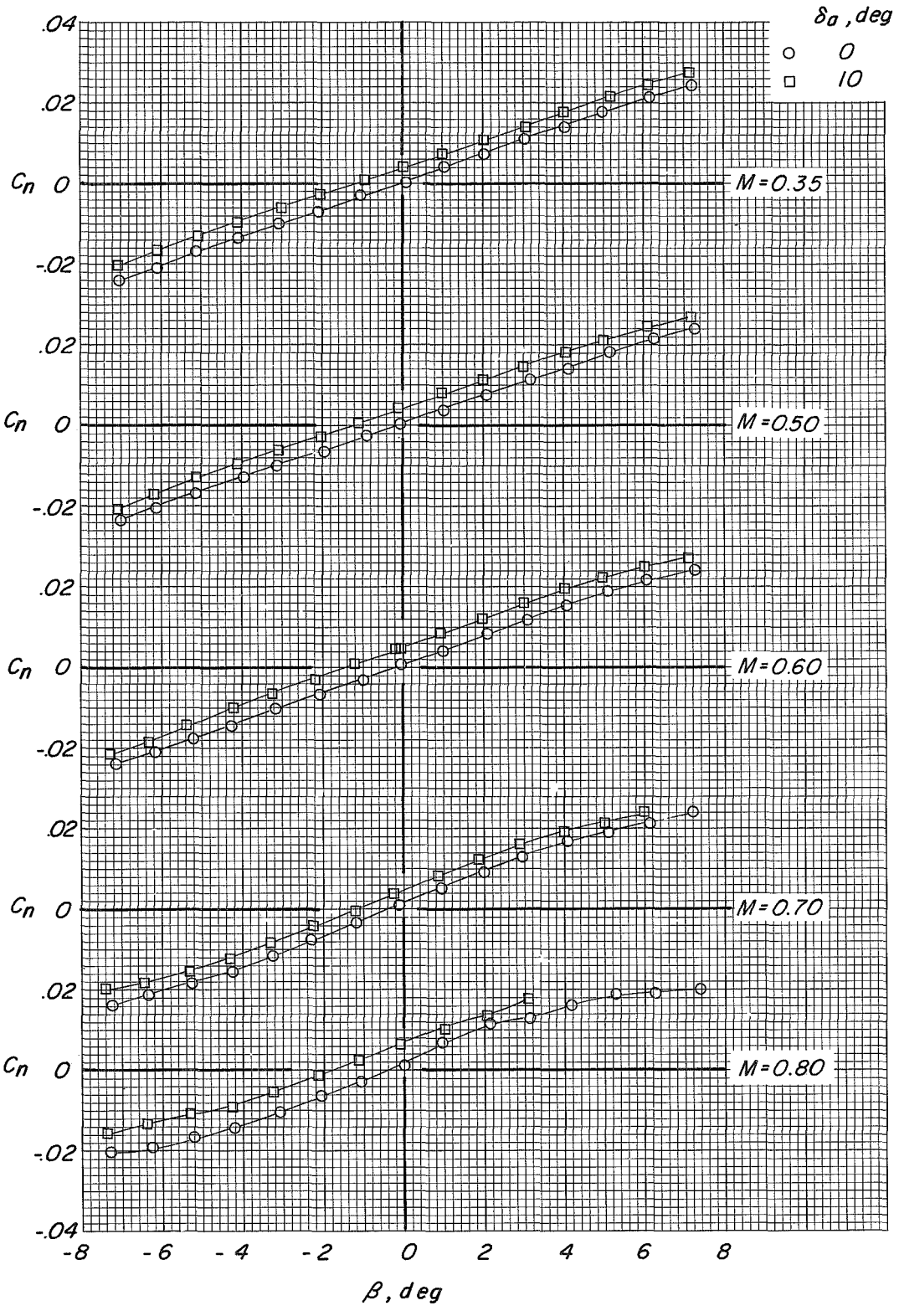
(b) Variation of C_n with β.

Figure 66.- Concluded.



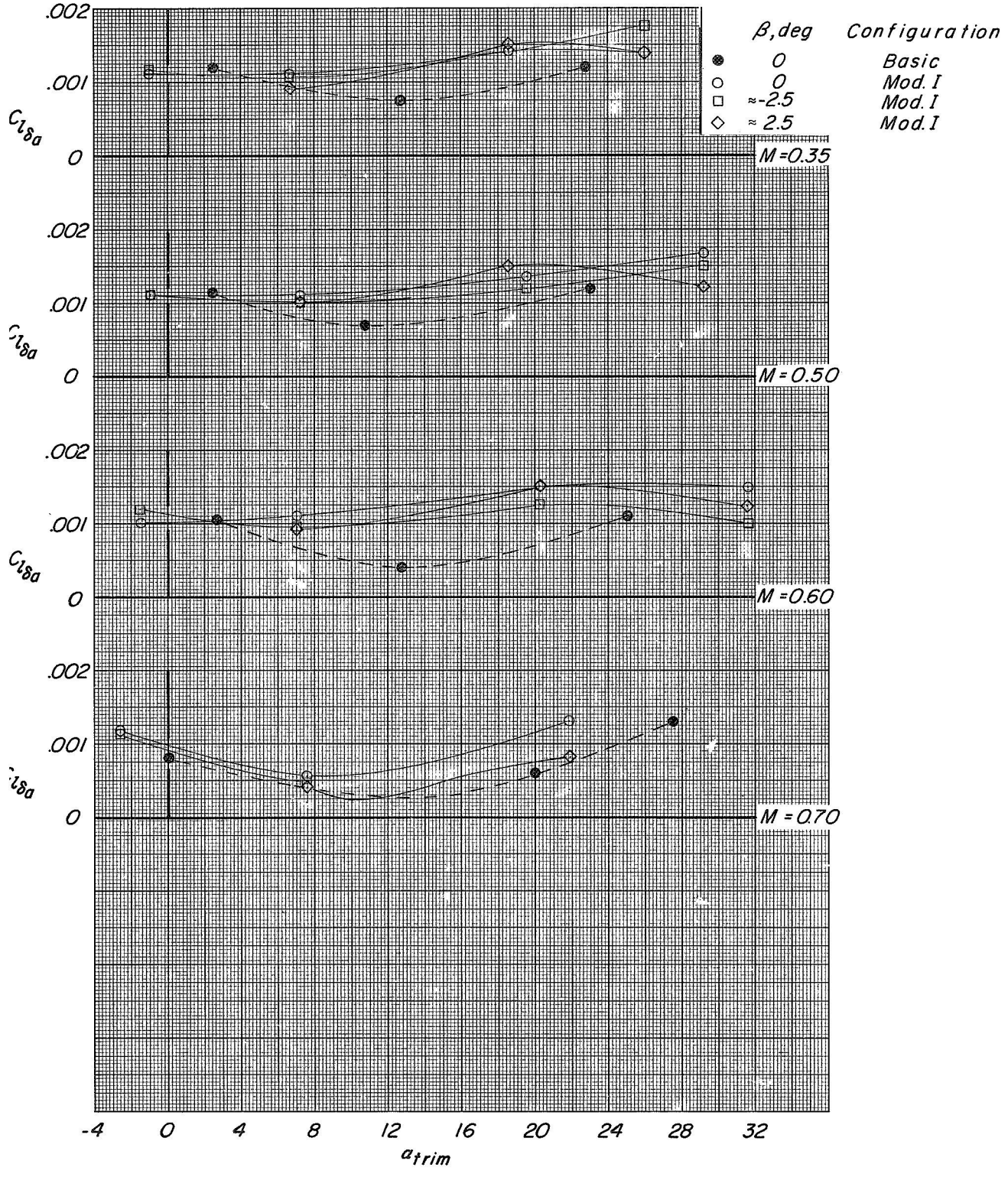
(a) Variation of C_l with β.

Figure 67.- Variation of rolling- and yawing-moment coefficients with sideslip angle for an elevon angle of $\delta_e = -10^o$ and an angle of attack of $\alpha = 7^o$. Modification II; subsonic configuration.



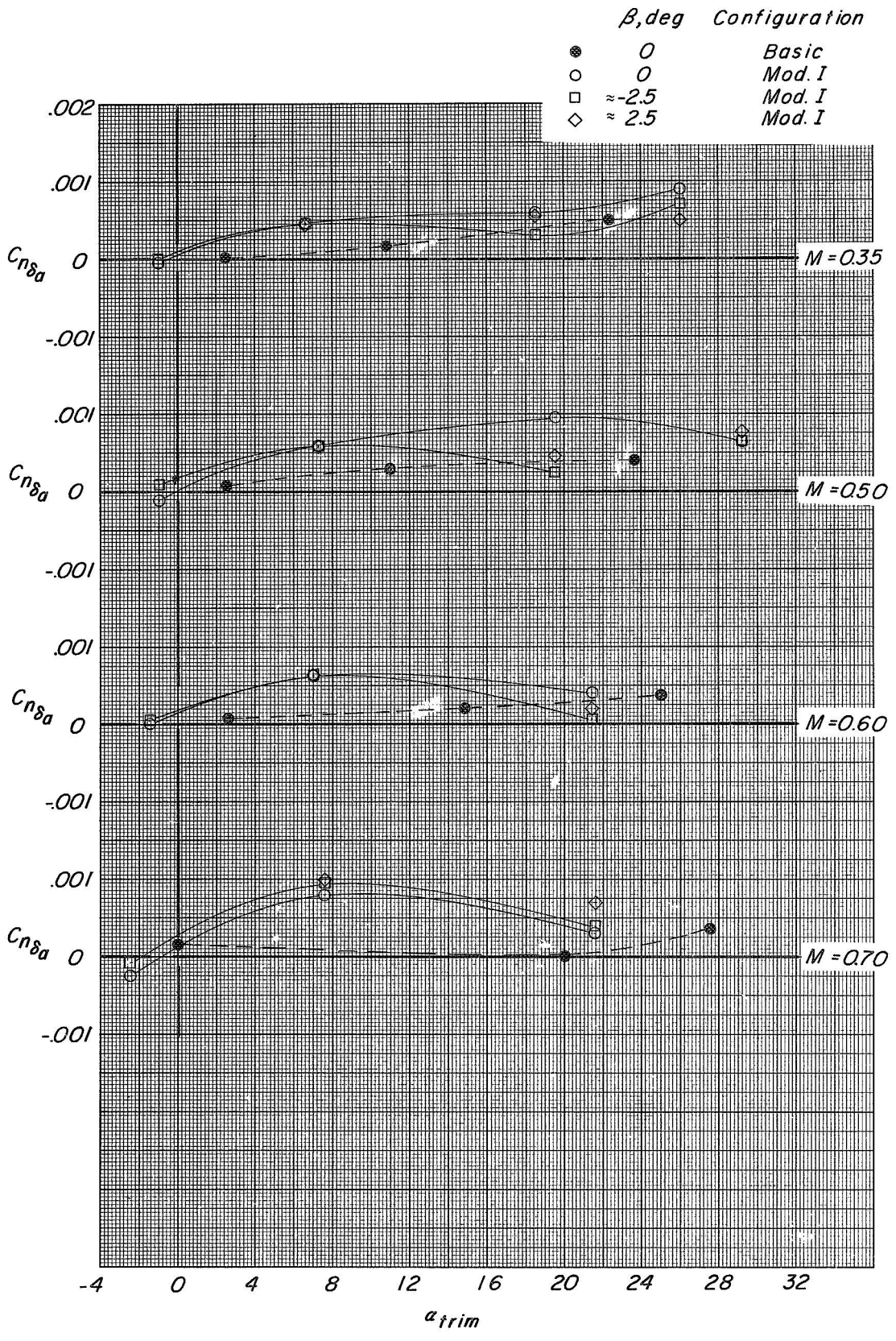
(b) Variation of C_n with β.

Figure 67.- Concluded.



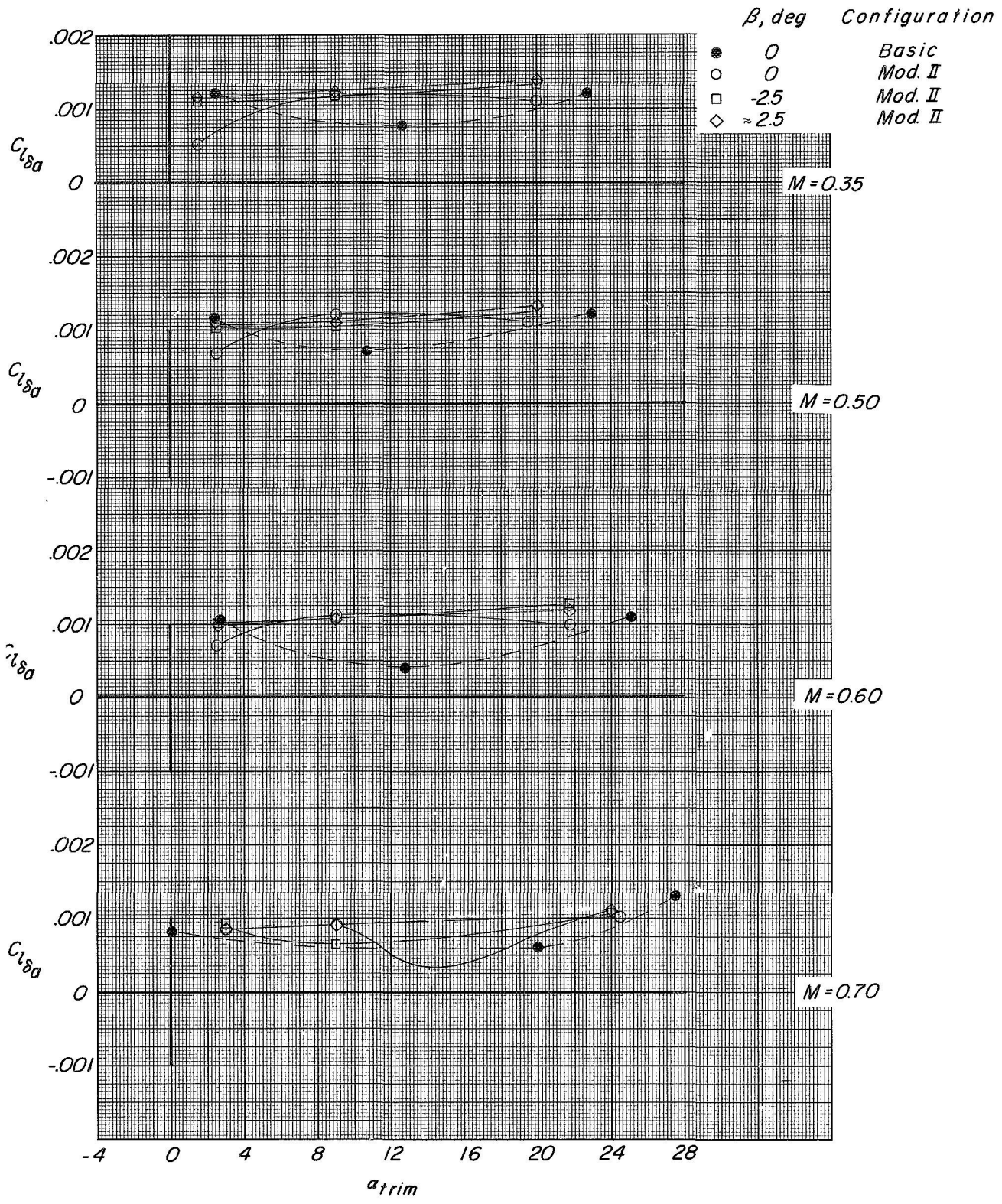
(a) Variation of $C_{l_{\delta_a}}$ with α_{trim}. Modification I.

Figure 68.- Summary of the effect of modifications I and II on the lateral control characteristics of the HL-10 as a function of trimmed angle of attack. Subsonic configuration.



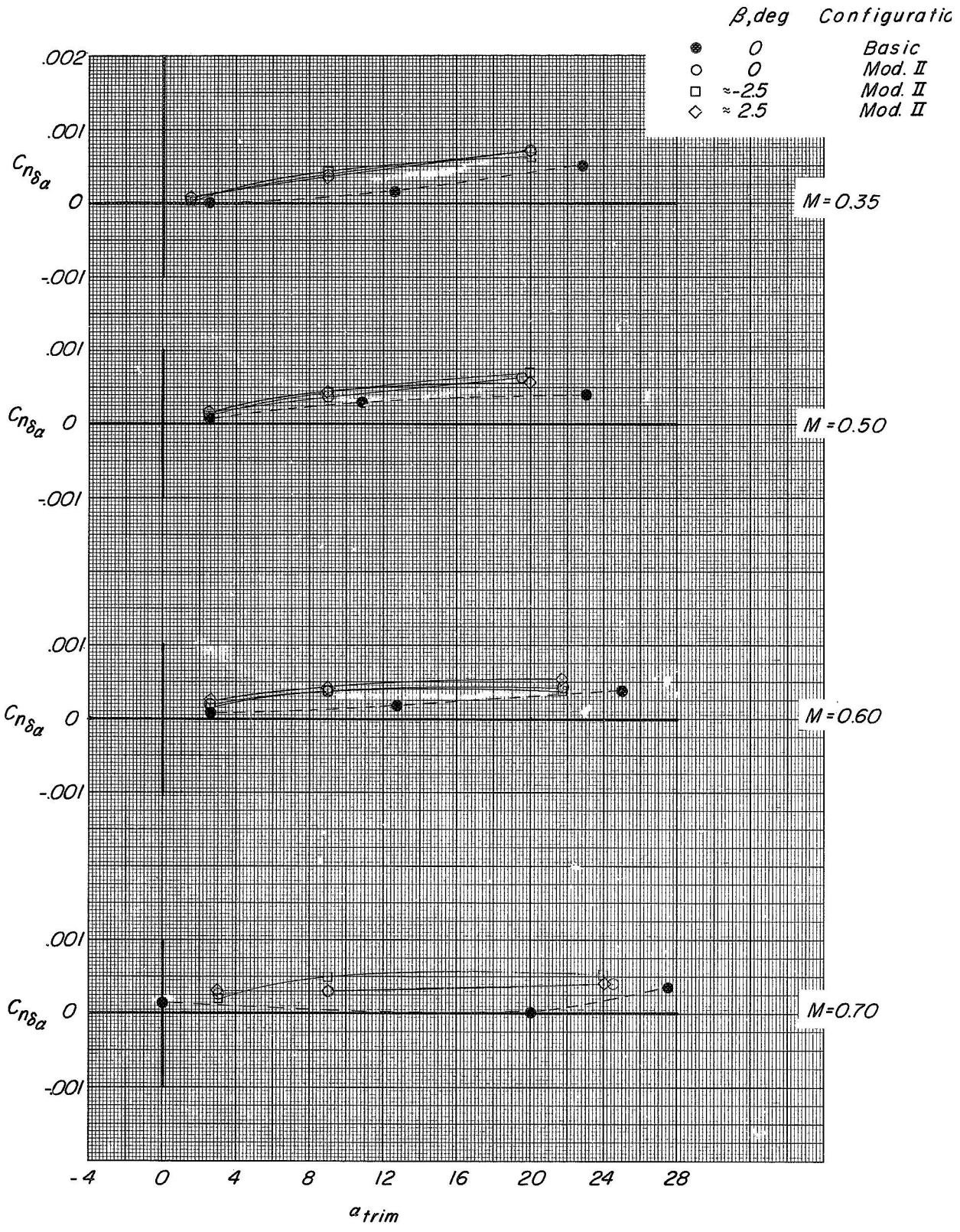
(b) Variation of $C_{n_{\delta_a}}$ with α_{trim}. Modification I.

Figure 68.- Continued.



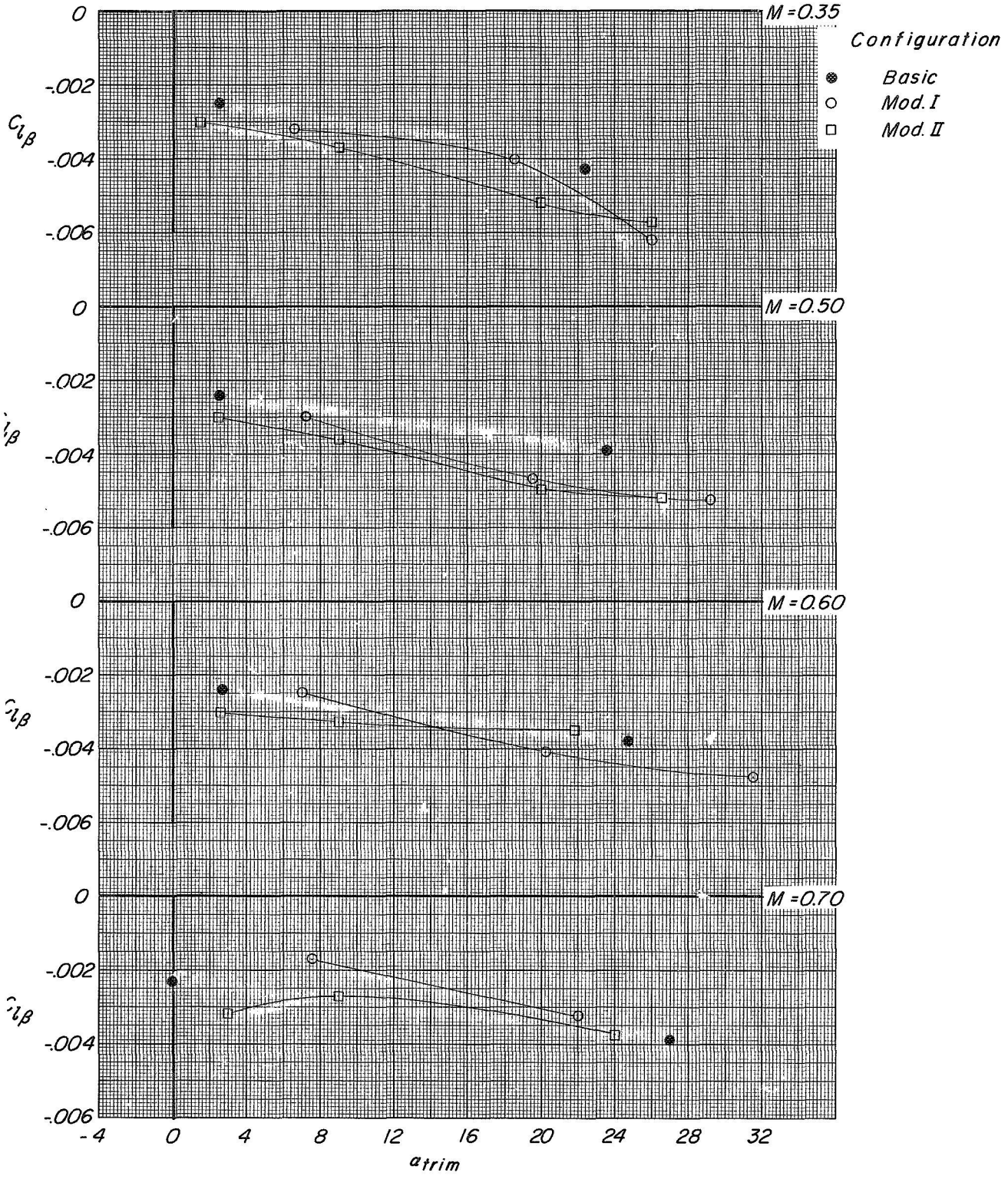
(c) Variation of $C_{l_{\delta_a}}$ with α_{trim}. Modification II.

Figure 68.- Continued.



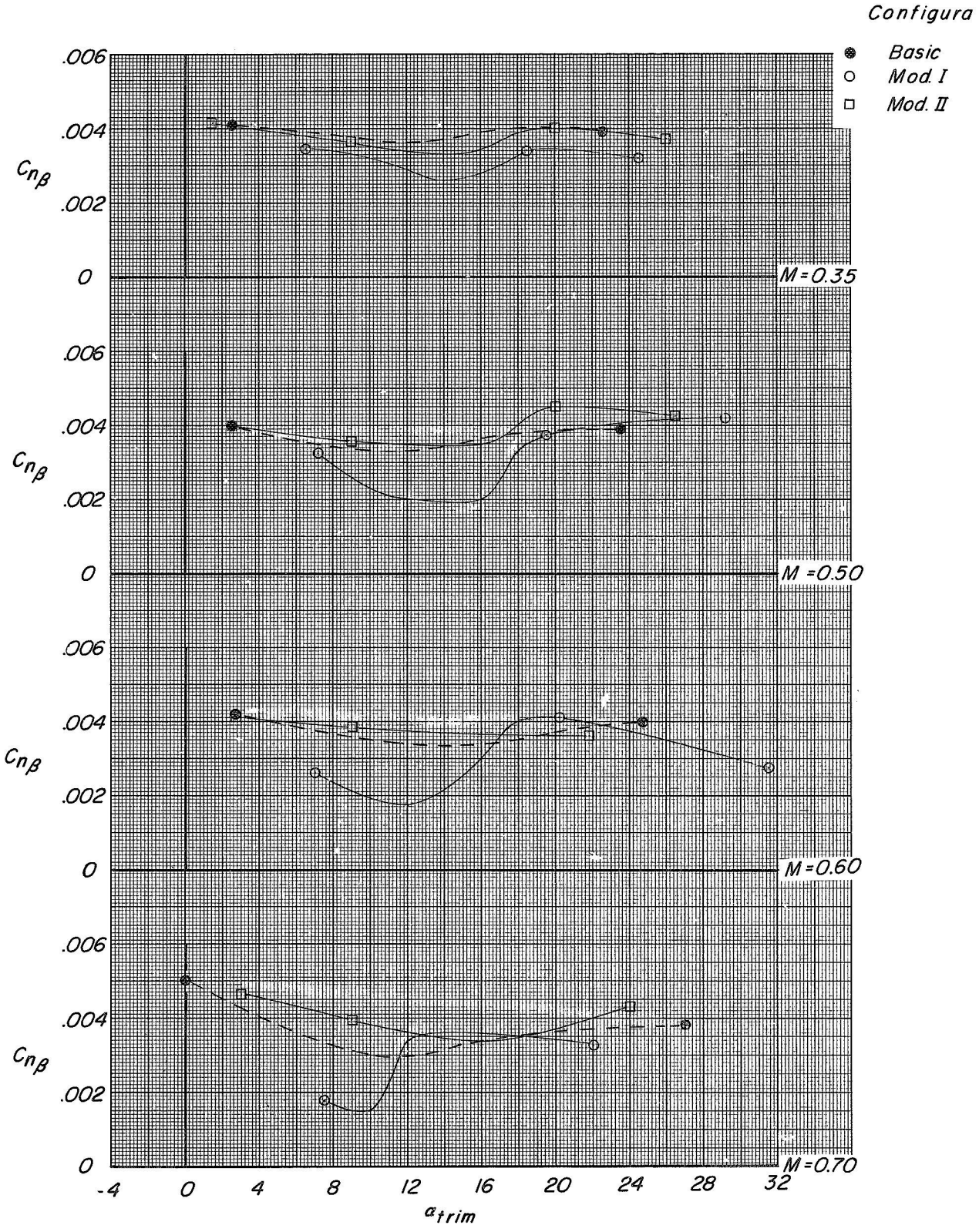
(d) Variation of $C_{n_{\delta a}}$ with α_{trim}. Modification II.

Figure 68.- Concluded.



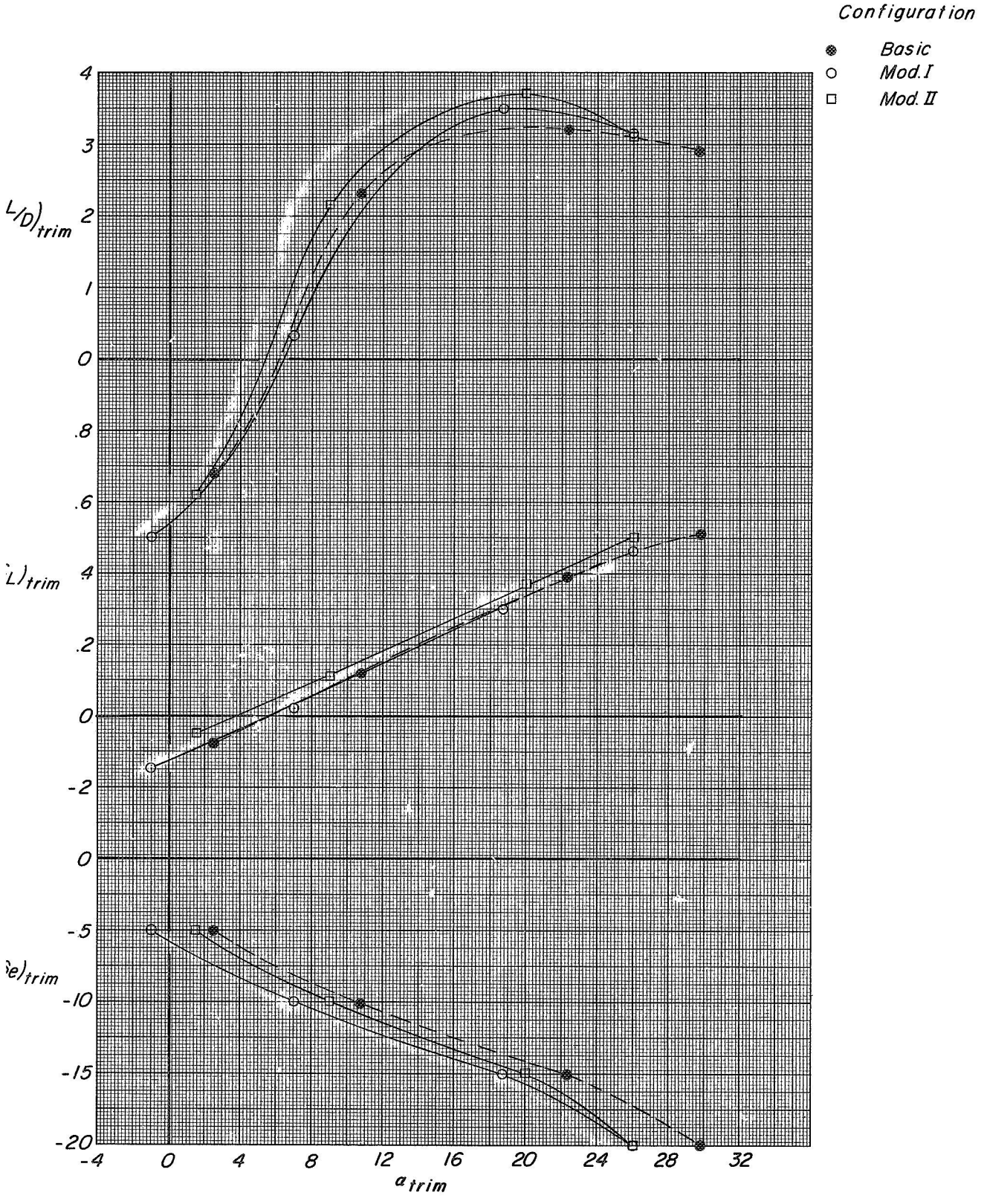
(a) Variation of C_{l_β} with α_{trim}.

Figure 69.- Summary of the effect of modifications I and II on the lateral directional characteristics of the HL-10 as a function of trimmed angle of attack.



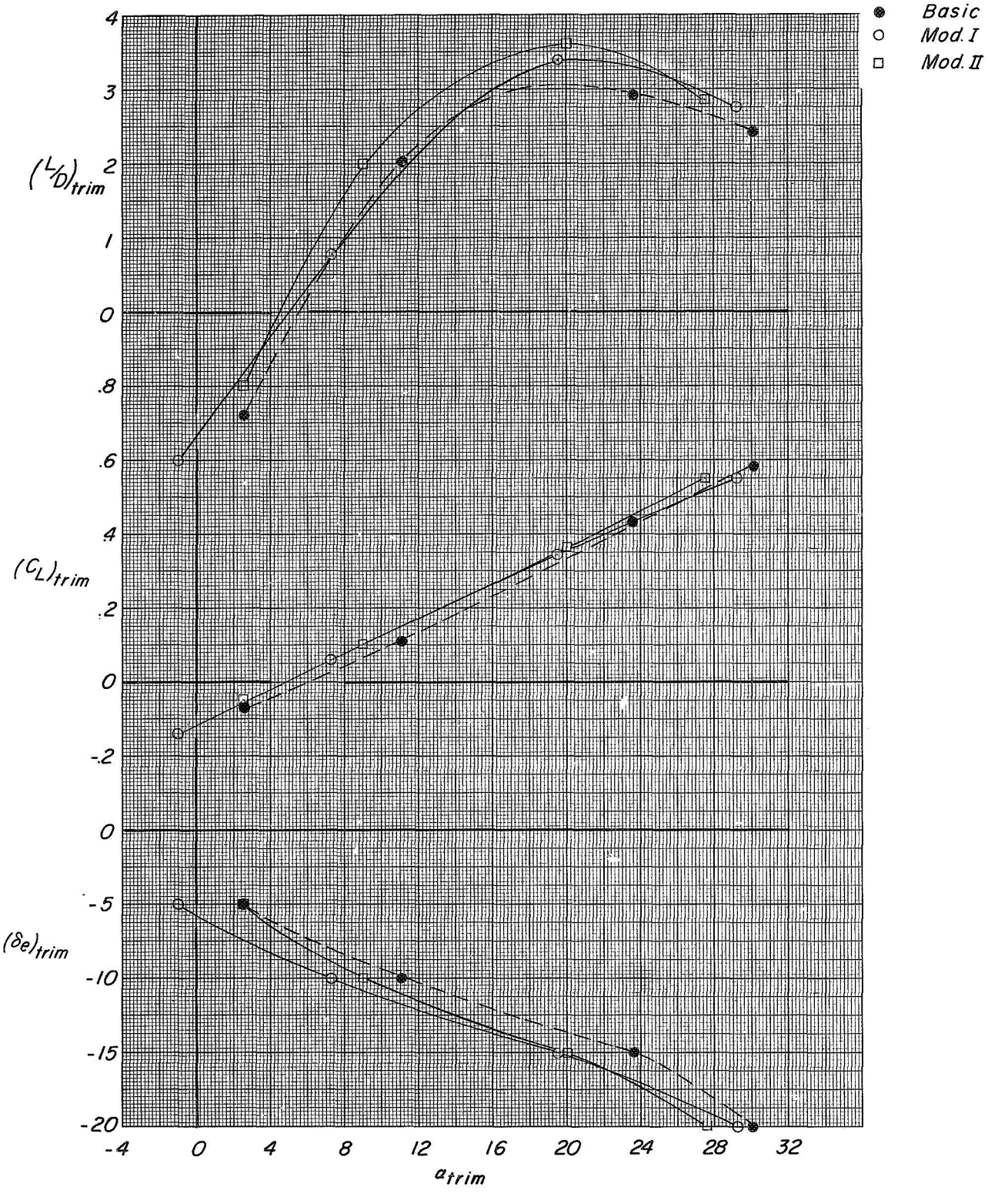
(b) Variation of C_{n_β} with α_{trim}.

Figure 69.- Concluded.



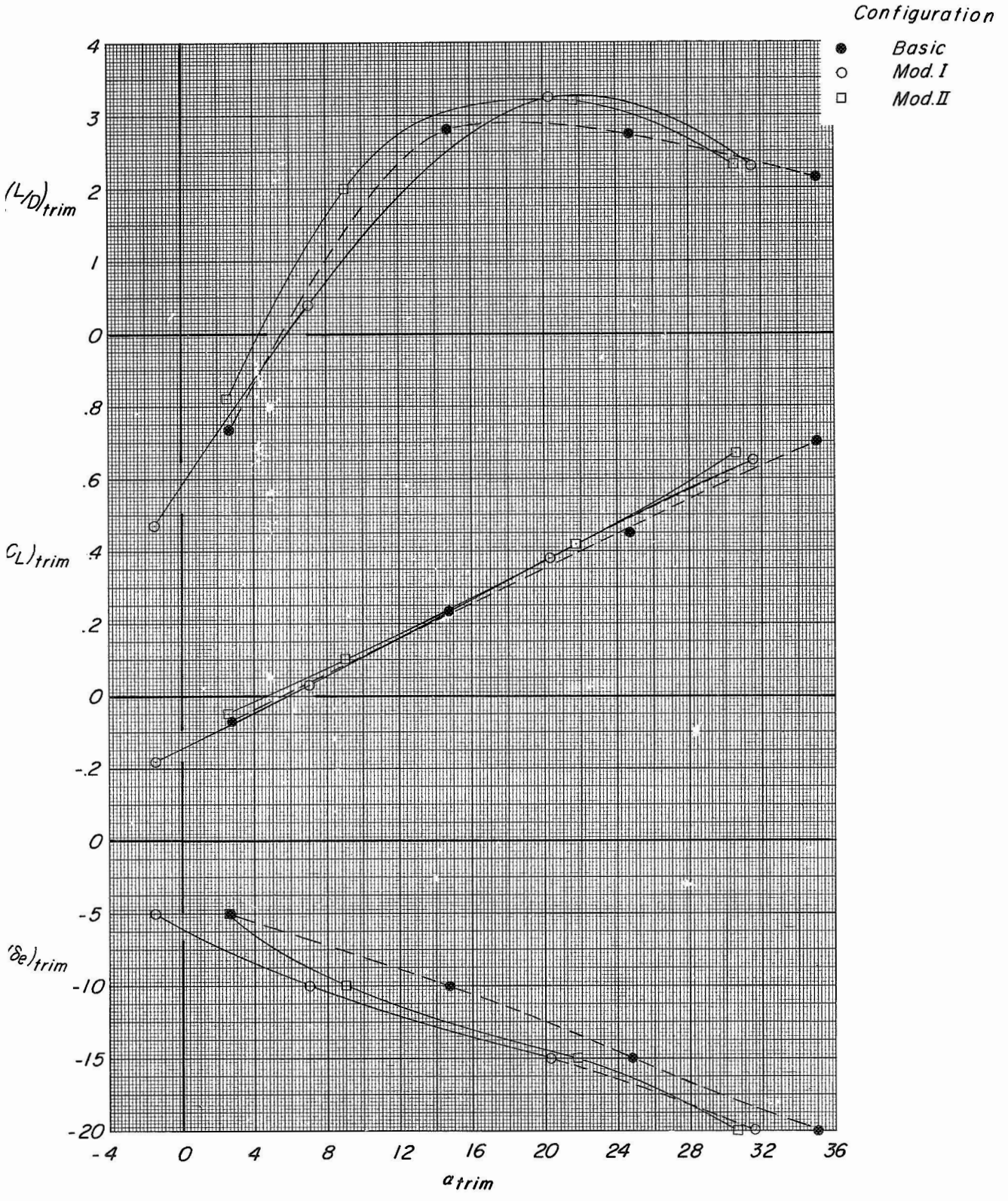
(a) M = 0.35.

Figure 70.- Summary of the longitudinal aerodynamic characteristics of modifications I and II compared with the basic HL-10. Subsonic configuration.



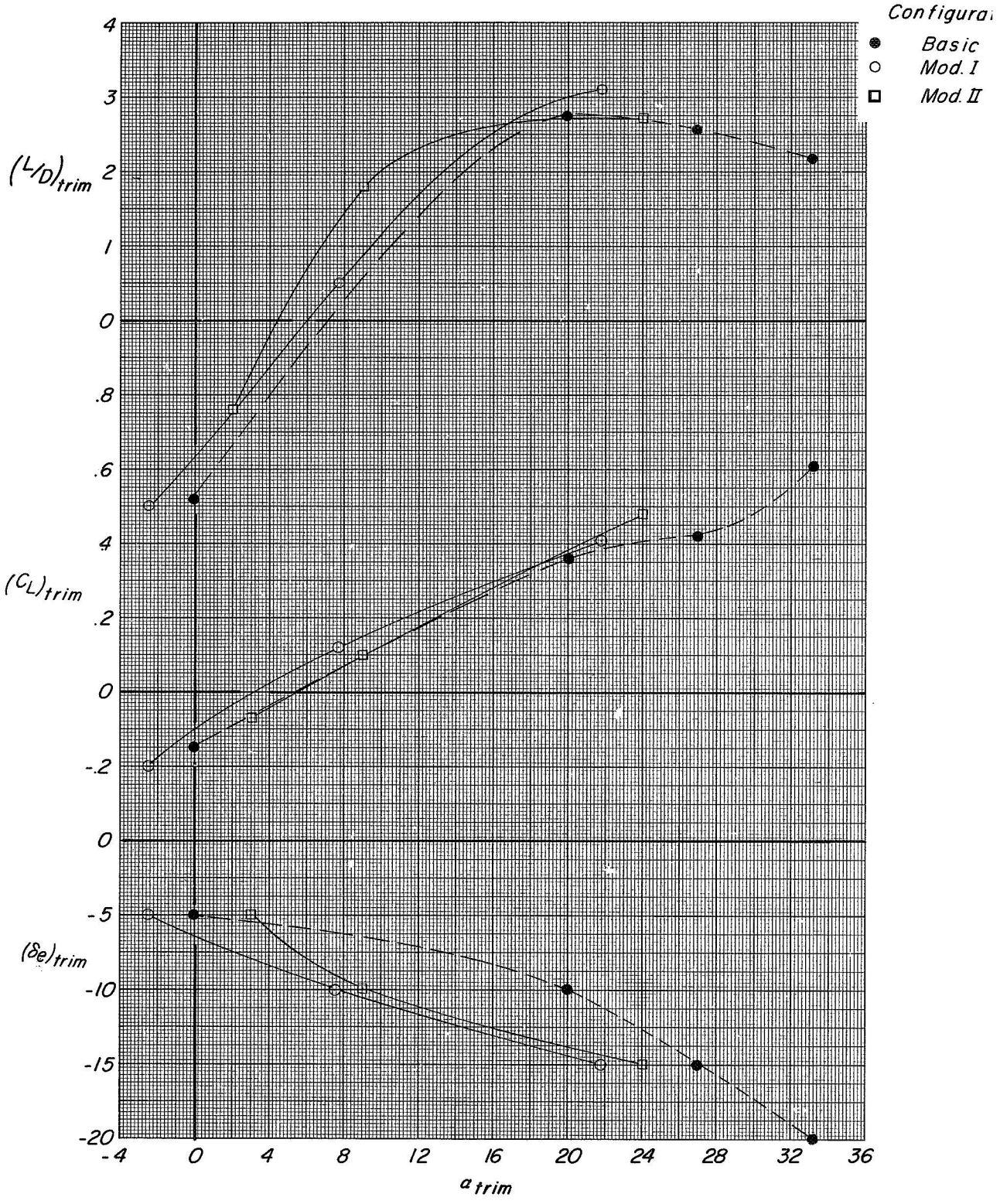
(b) M = 0.50.

Figure 70.- Continued.



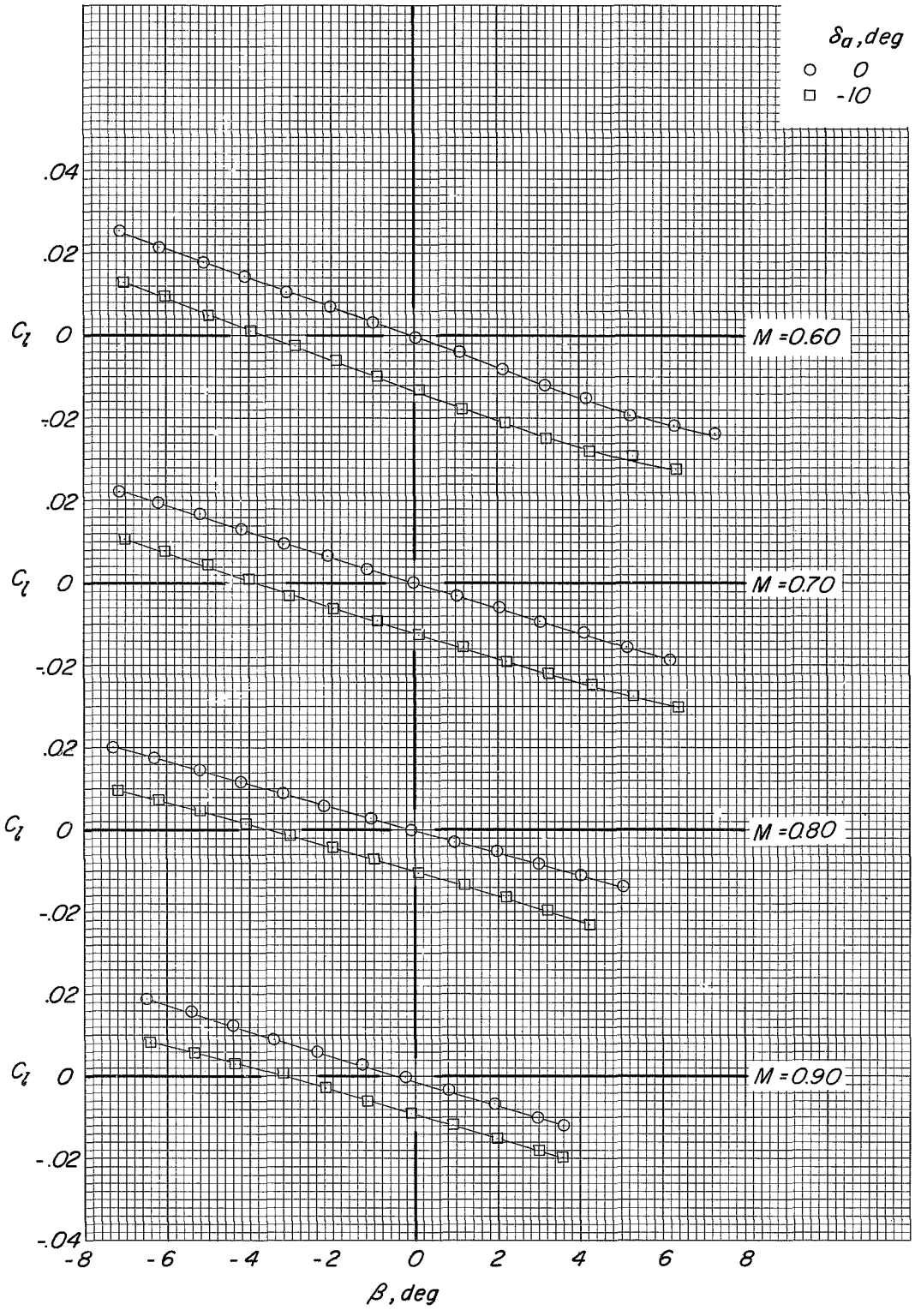
(c) M = 0.60.

Figure 70.- Continued.



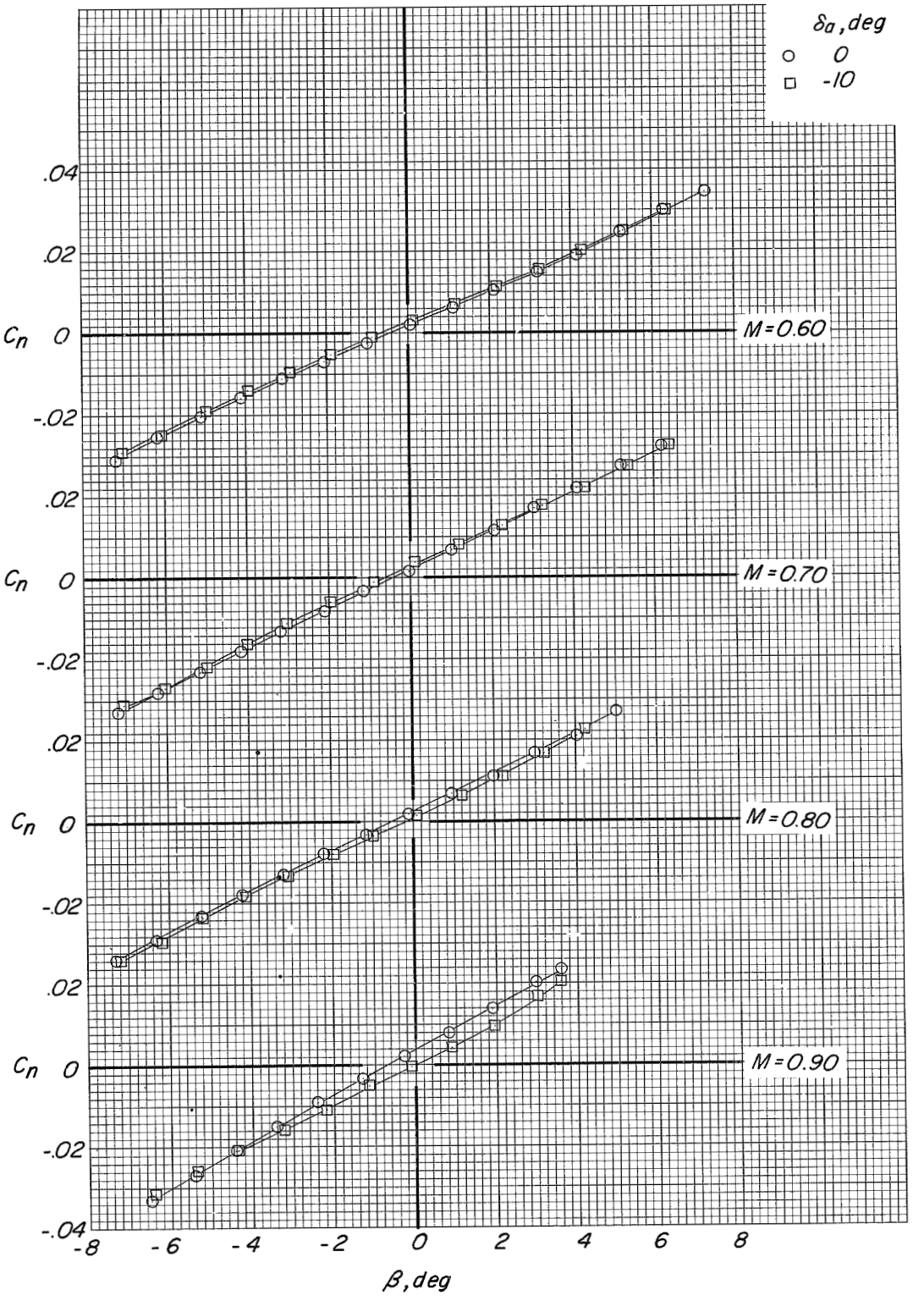
(d) M = 0.70.

Figure 70.- Concluded.



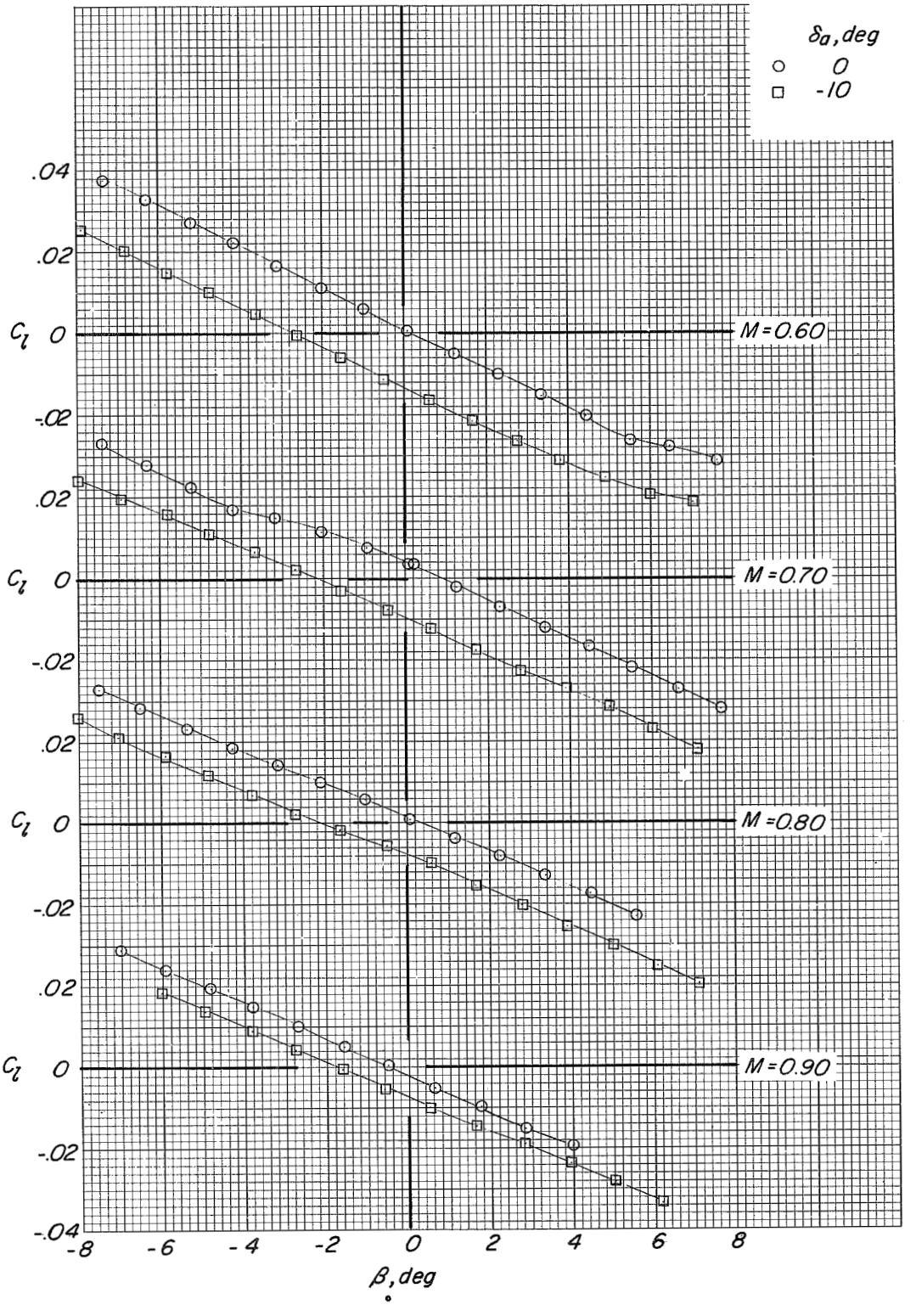
(a) $\alpha = 7^{o}$; $\delta_e = 10^{o}$.

Figure 71.- Variation of rolling- and yawing-moment coefficients with sideslip angle. Modification I; transonic configuration.



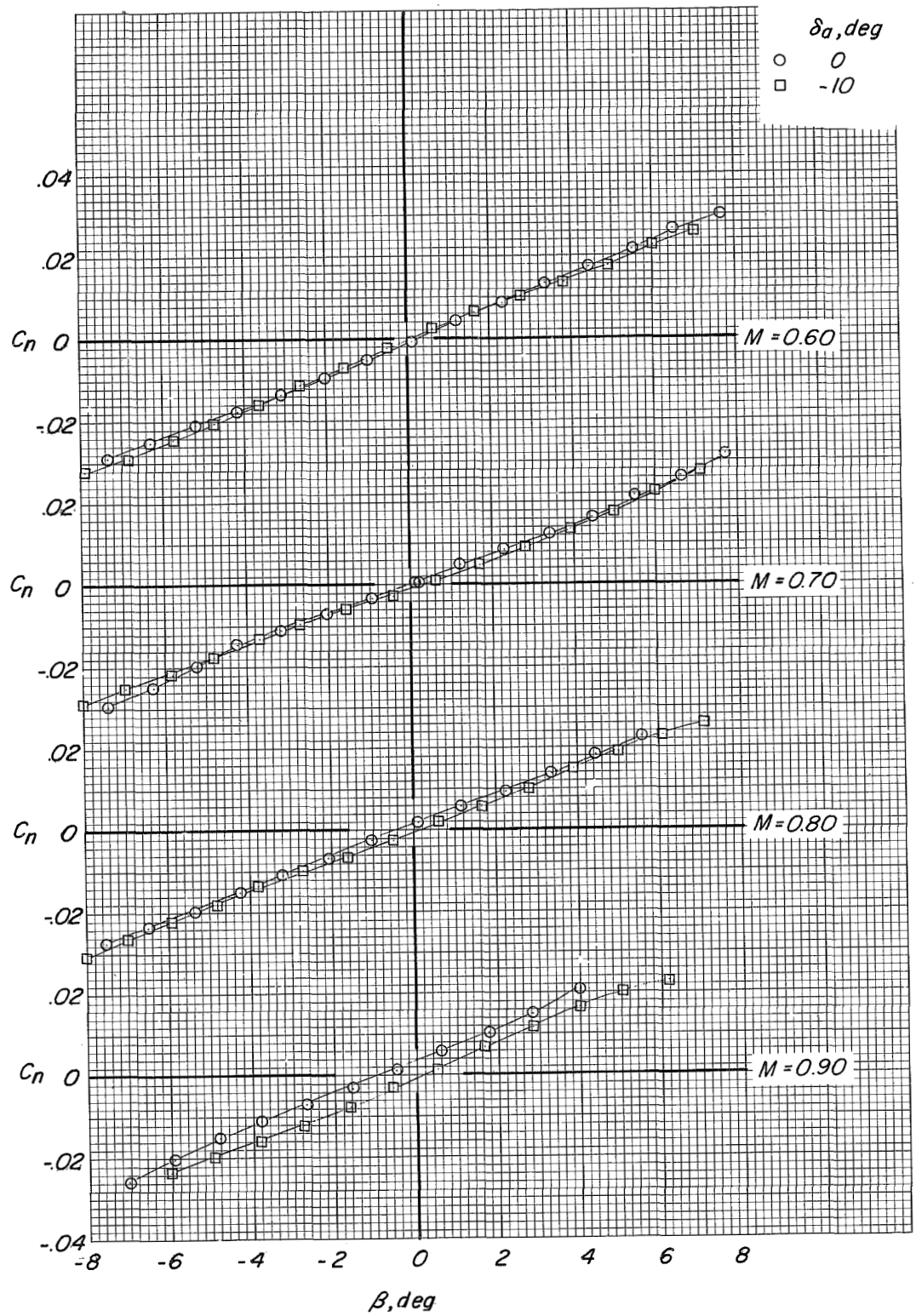
(a) Concluded.

Figure 71.- Continued.



(b) $\alpha = 17^{\circ}$; $\delta_e = 5^{\circ}$.

Figure 71.- Continued.



(b) Concluded.

Figure 71.- Concluded.

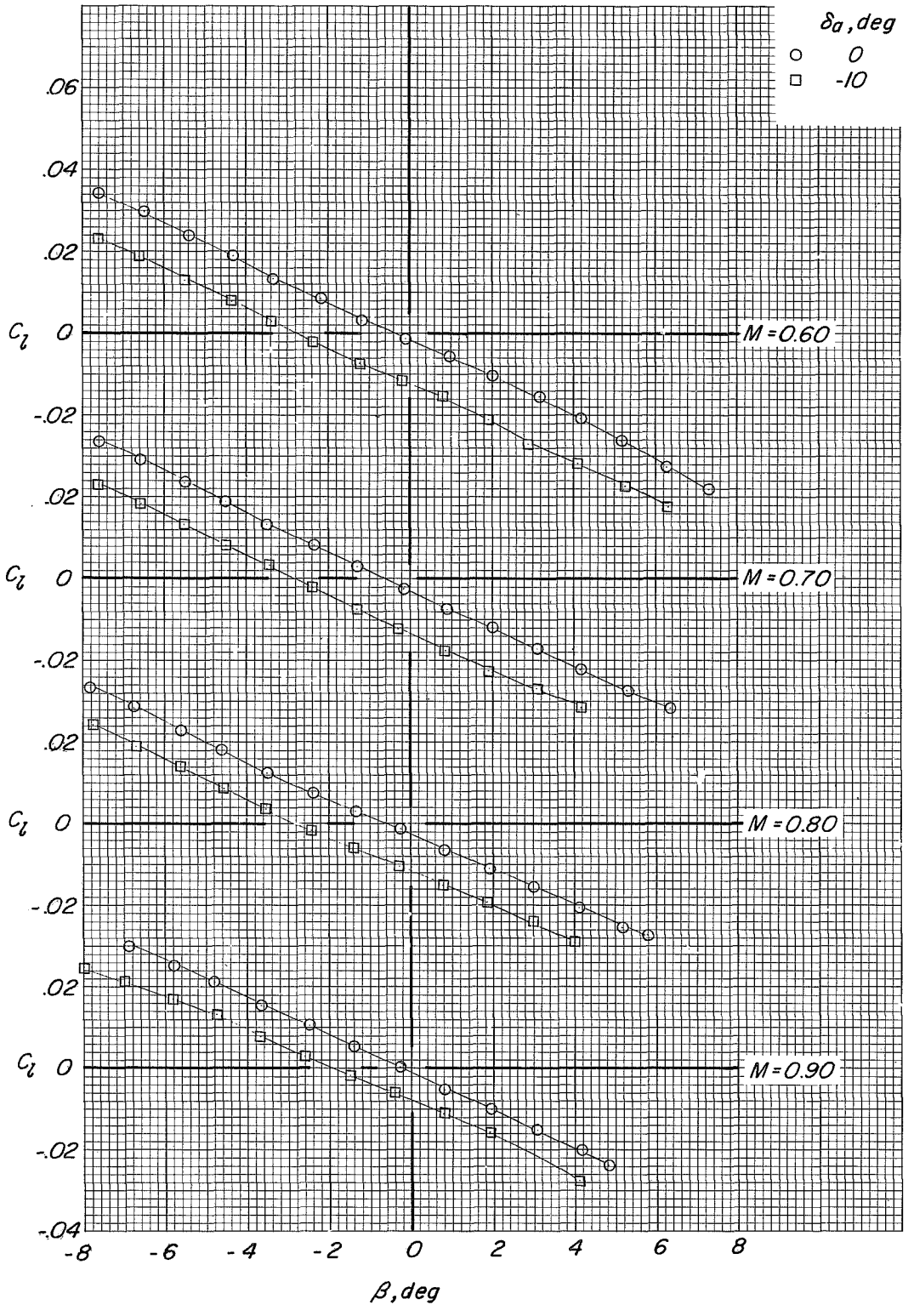


Figure 72.- Variation of rolling- and yawing-moment coefficients with sideslip angle. Modification II; transonic configuration; $\alpha = 17^{o}$; $\delta_e = 5^{o}$.

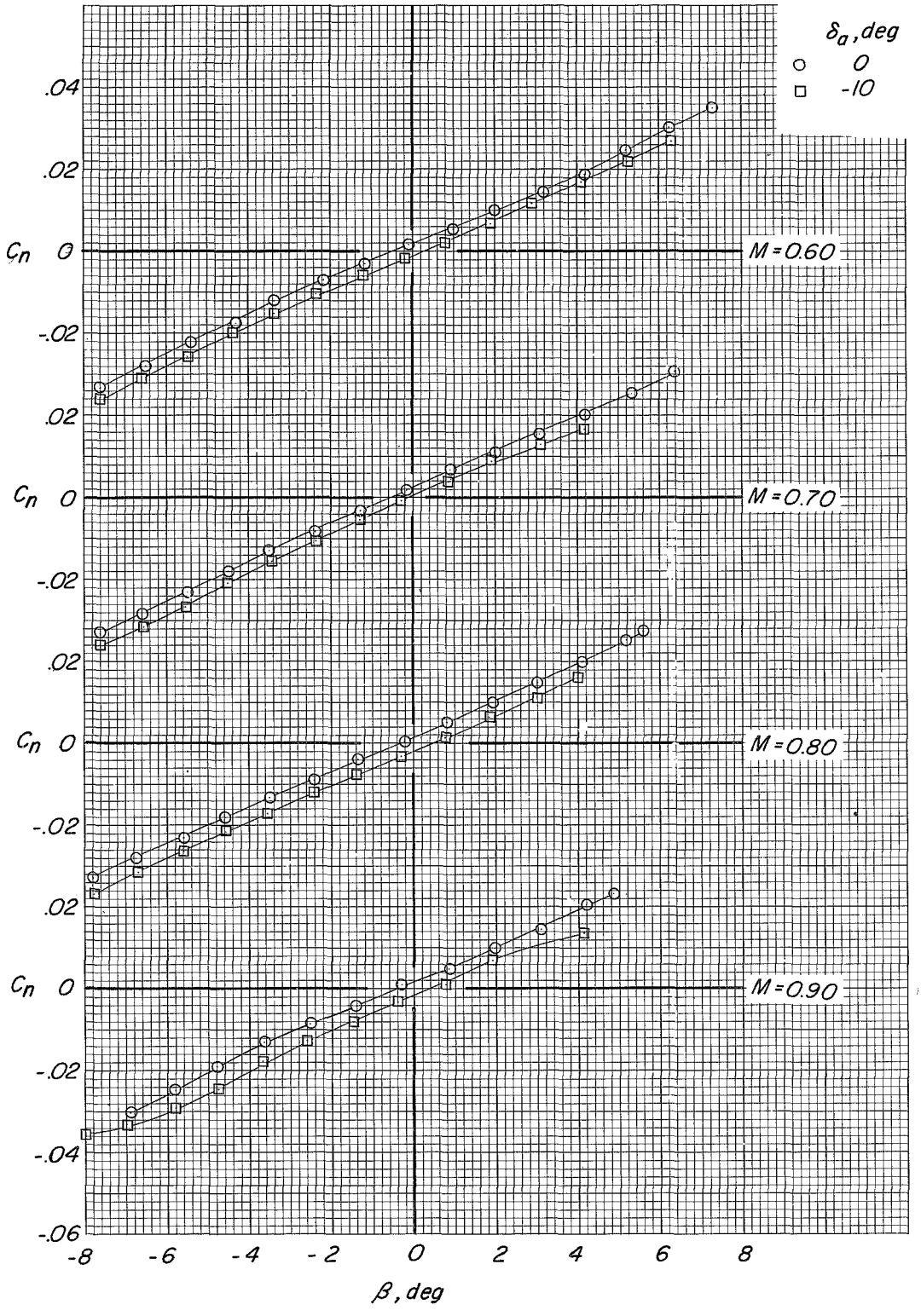
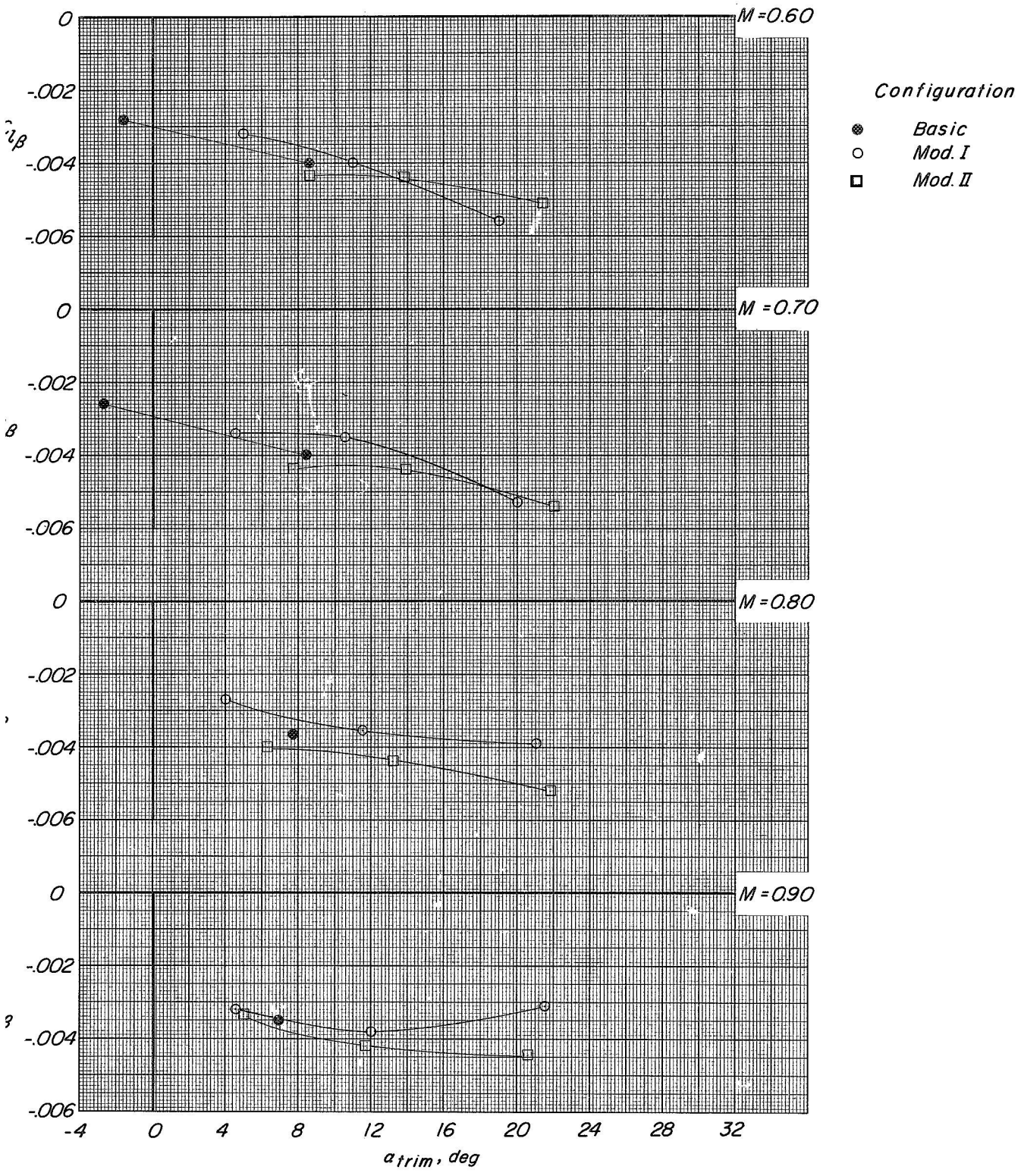
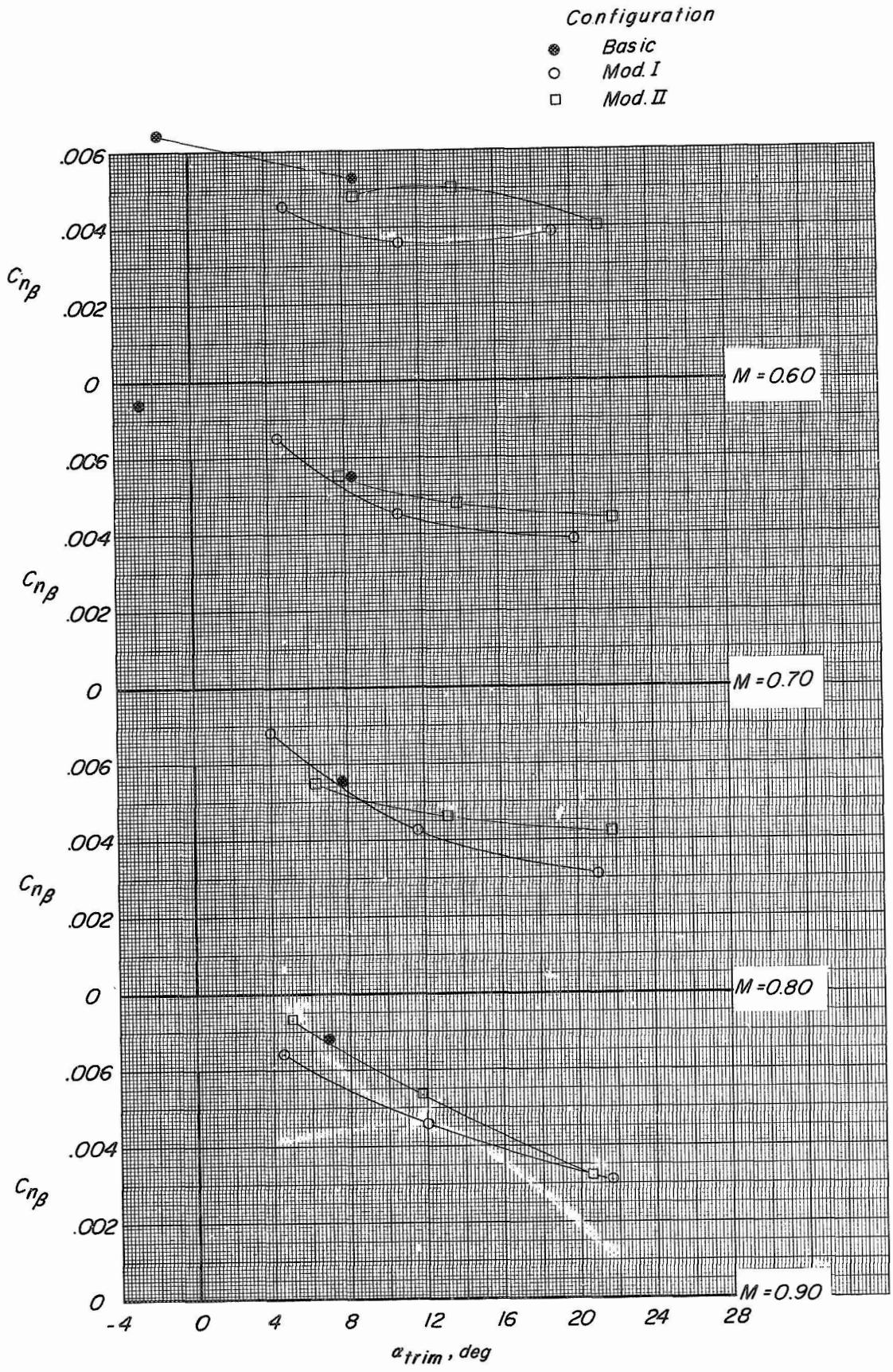


Figure 72.- Concluded.



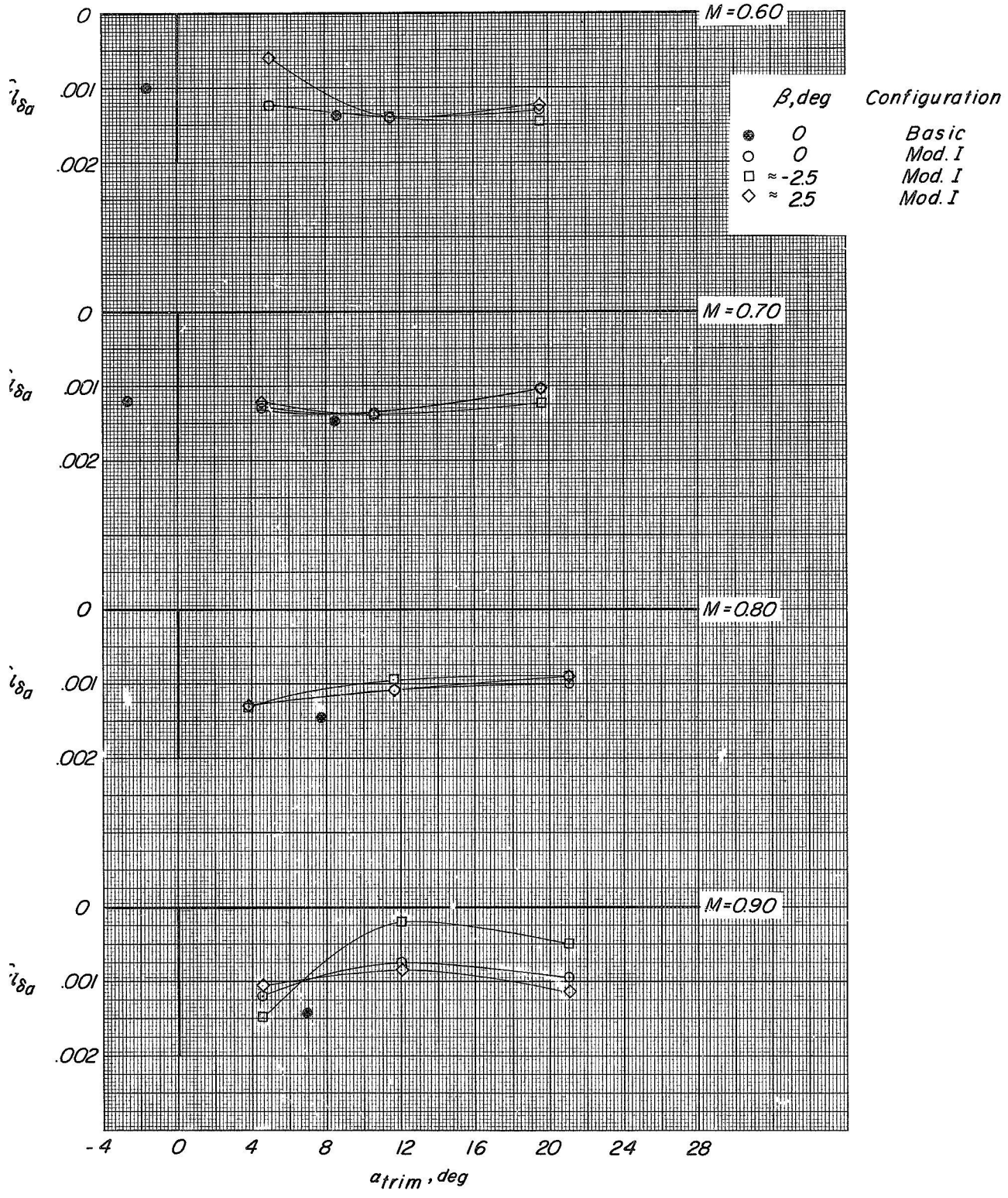
(a) Variation of C_{l_β} with α.

Figure 73.- Summary of the effects of modifications I and II on the lateral directional characteristics of the HL-10 as a function of trimmed angle of attack. Transonic configuration.



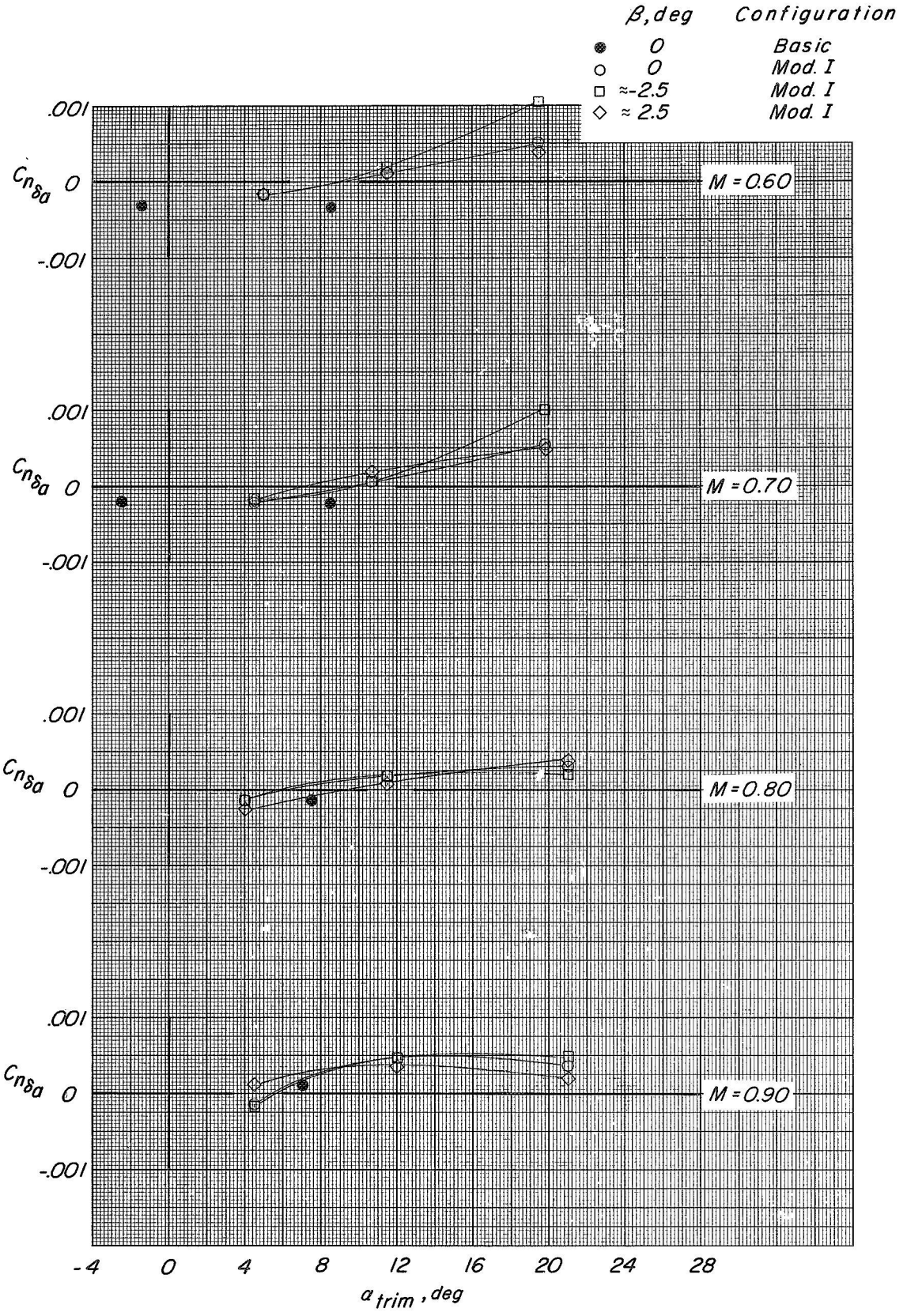
(b) Variation of C_{n_β} with α.

Figure 73.- Concluded.



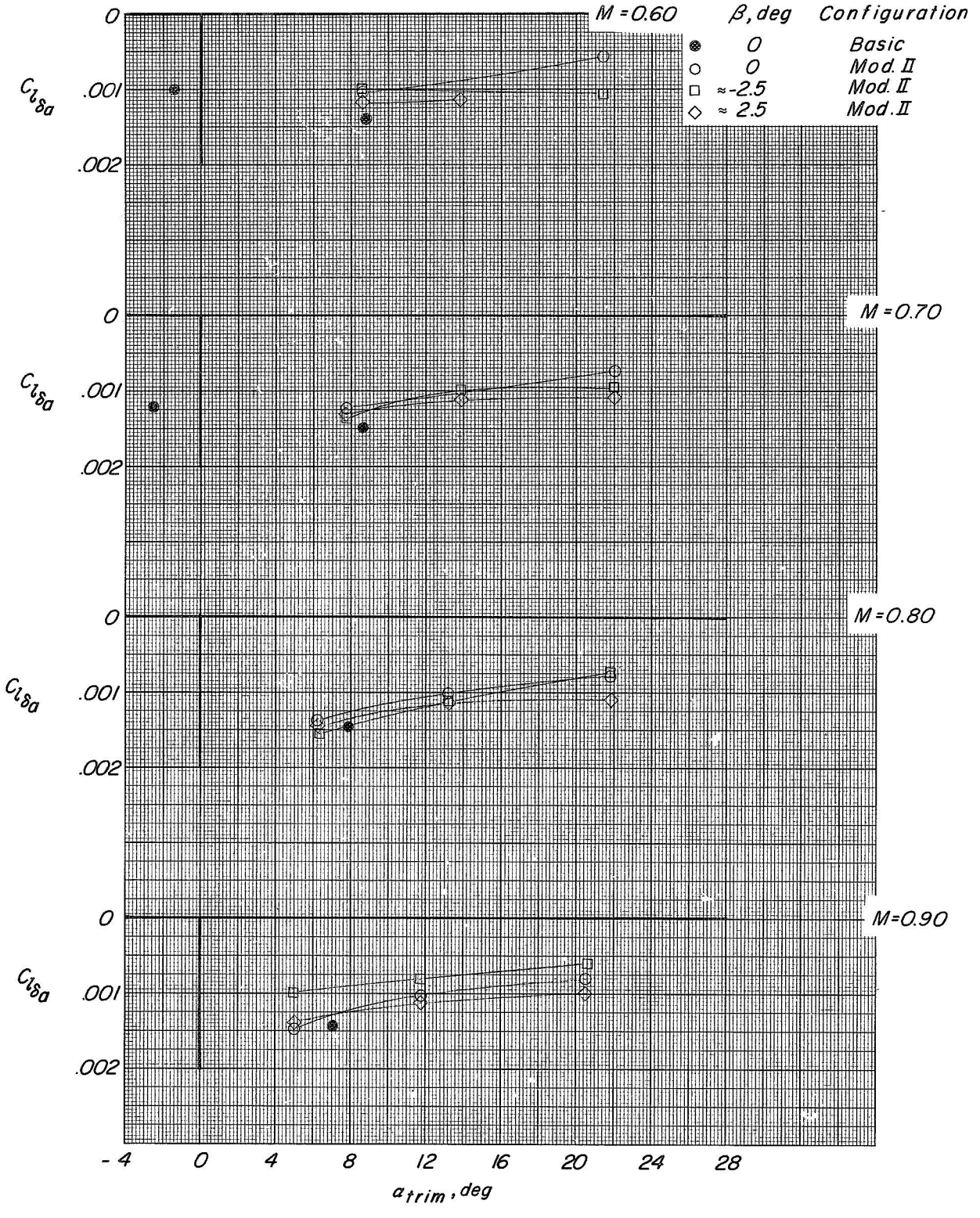
(a) Variation of $C_{l_{\delta_a}}$ with α. Modification I.

Figure 74.- Summary of the effects of modifications I and II on the lateral directional control characteristics of the HL-10 as a function of trimmed angle of attack. Transonic configuration.



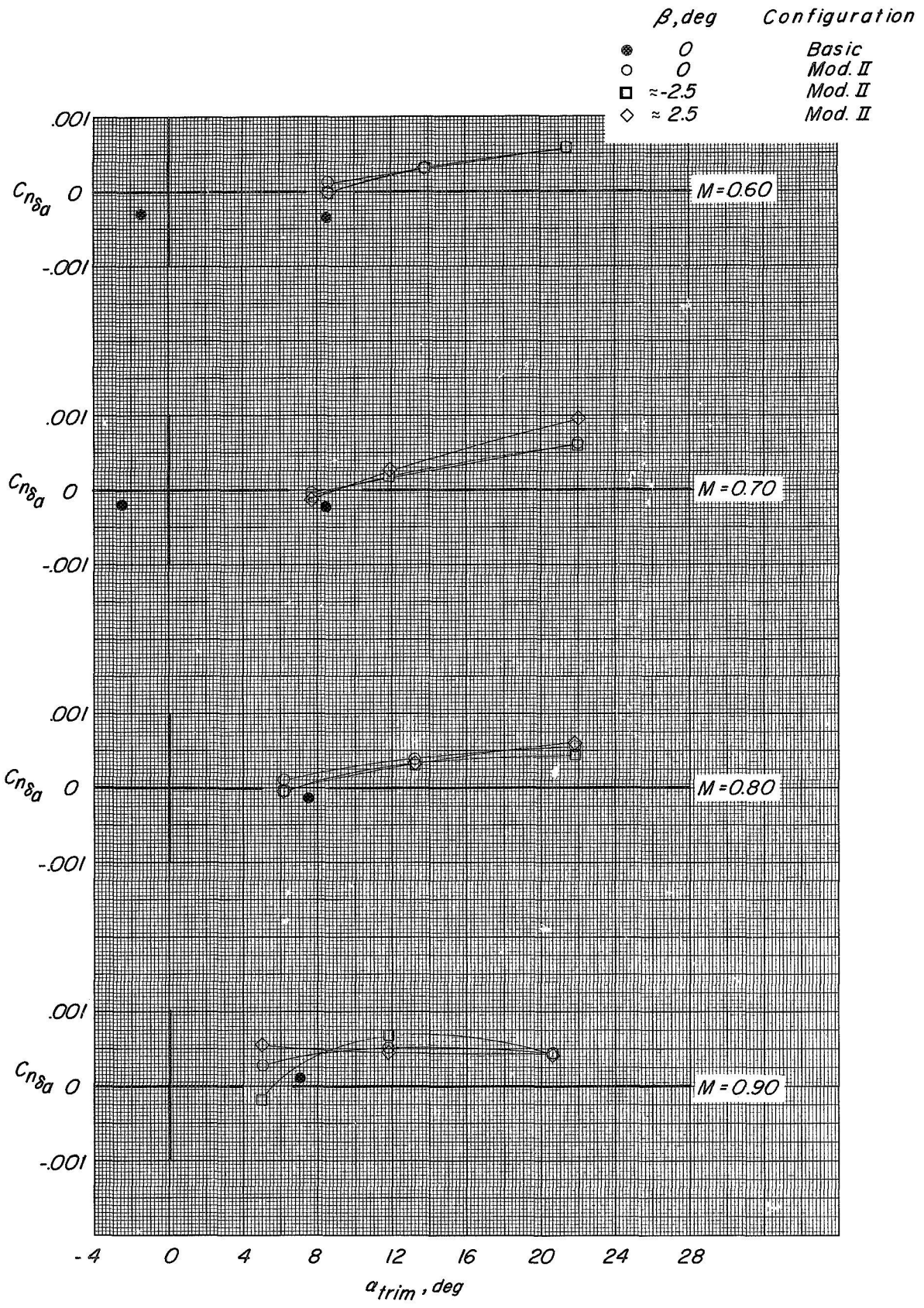
(b) Variation of $C_{n_{\delta a}}$ with α. Modification I.

Figure 74.- Continued.



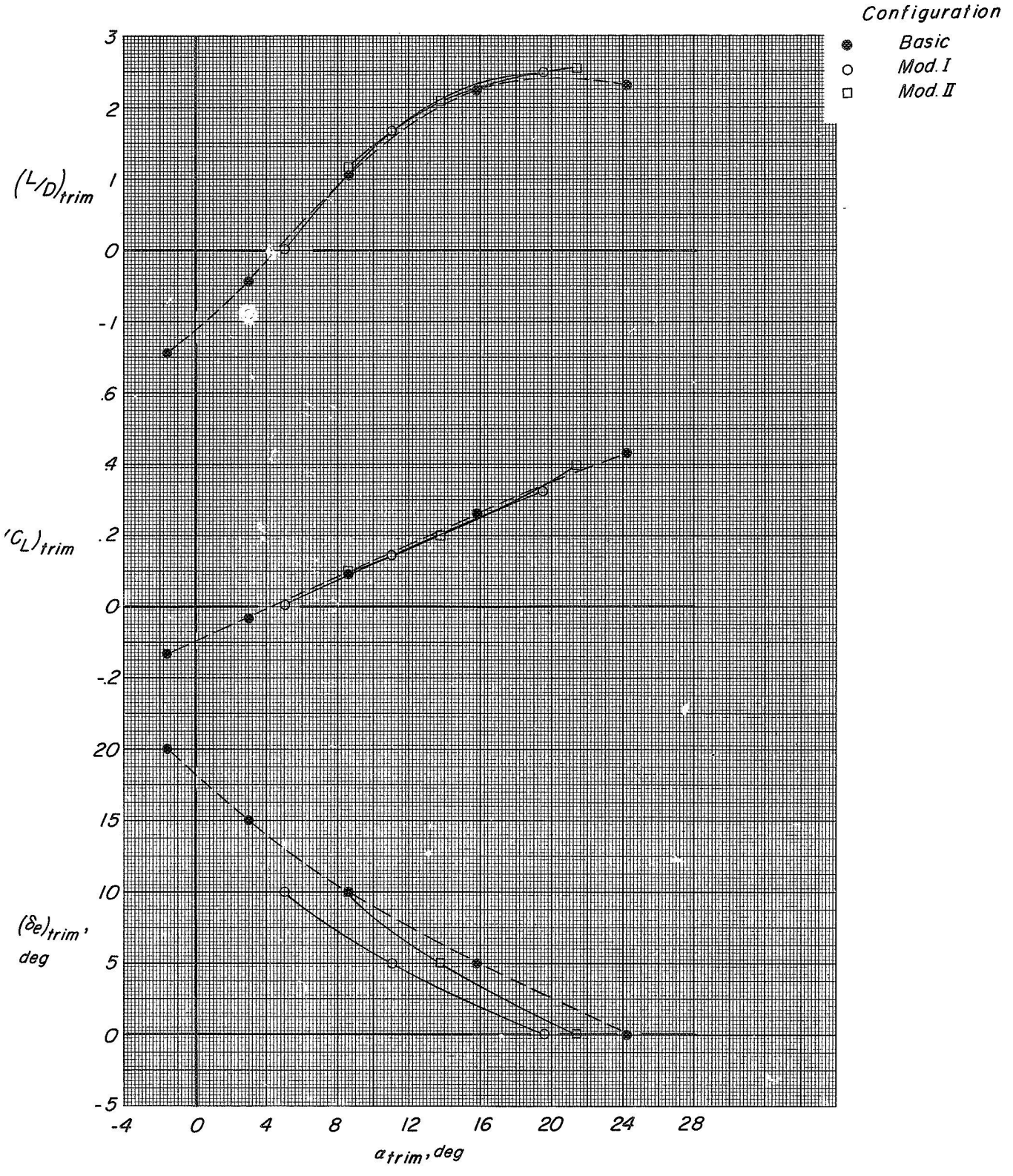
(c) Variation of $C_{l_{\delta a}}$ with α. Modification II.

Figure 74.- Continued.



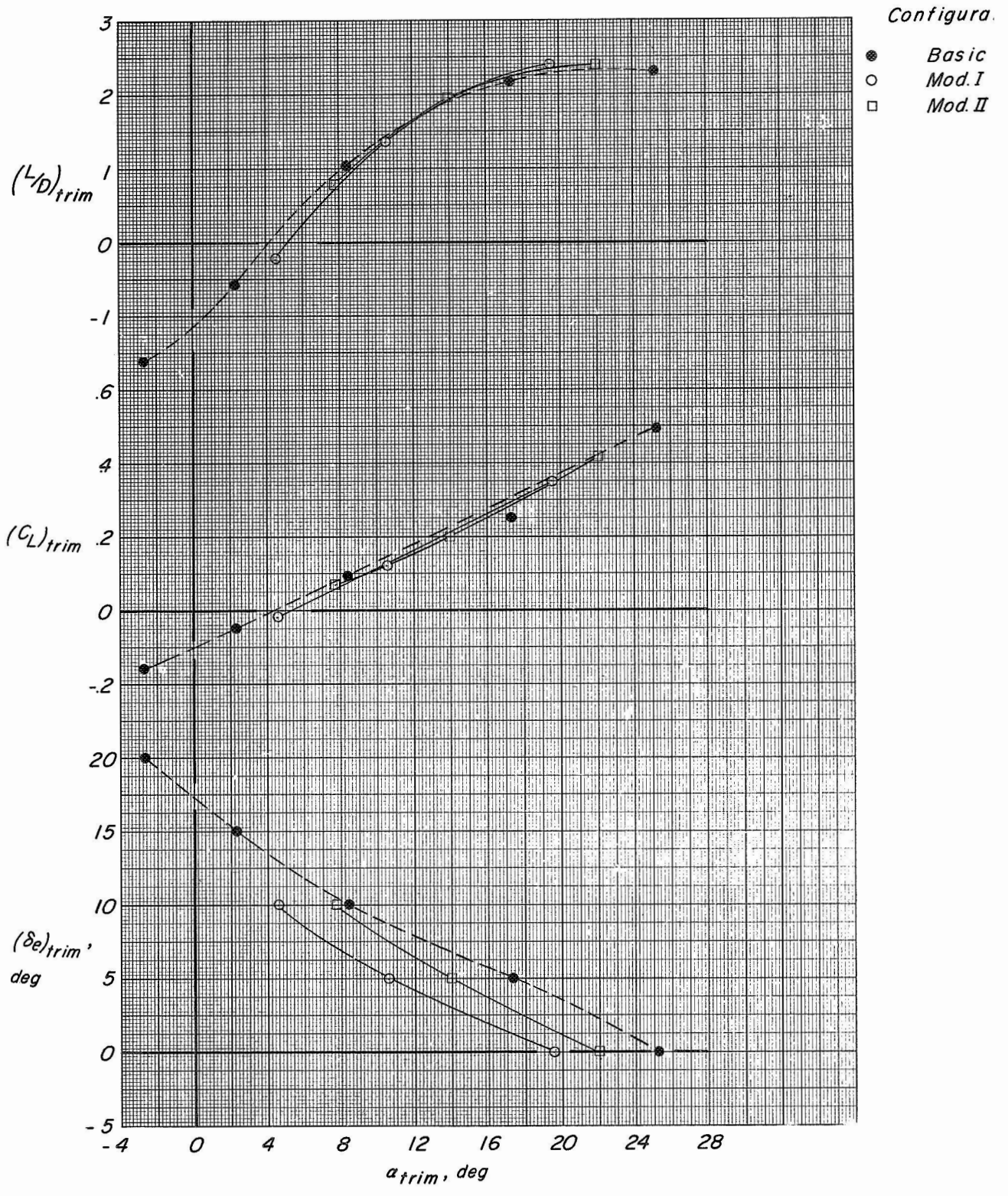
(d) Variation of $C_{n_{\delta a}}$ with α. Modification II.

Figure 74.- Concluded.



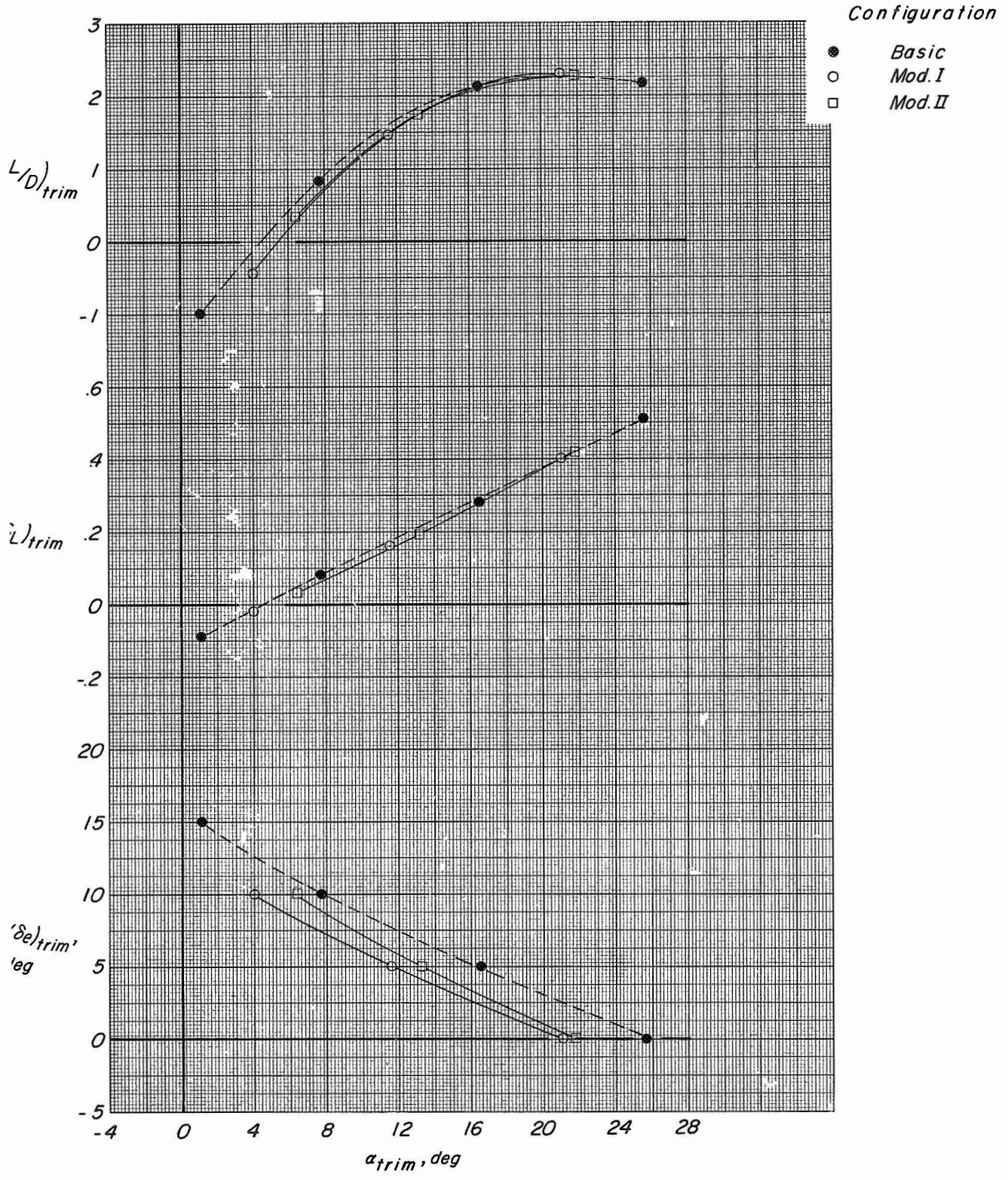
(a) M = 0.60.

Figure 75.- Summary of the effect of modifications I and II on the longitudinal characteristics. Transonic configuration.



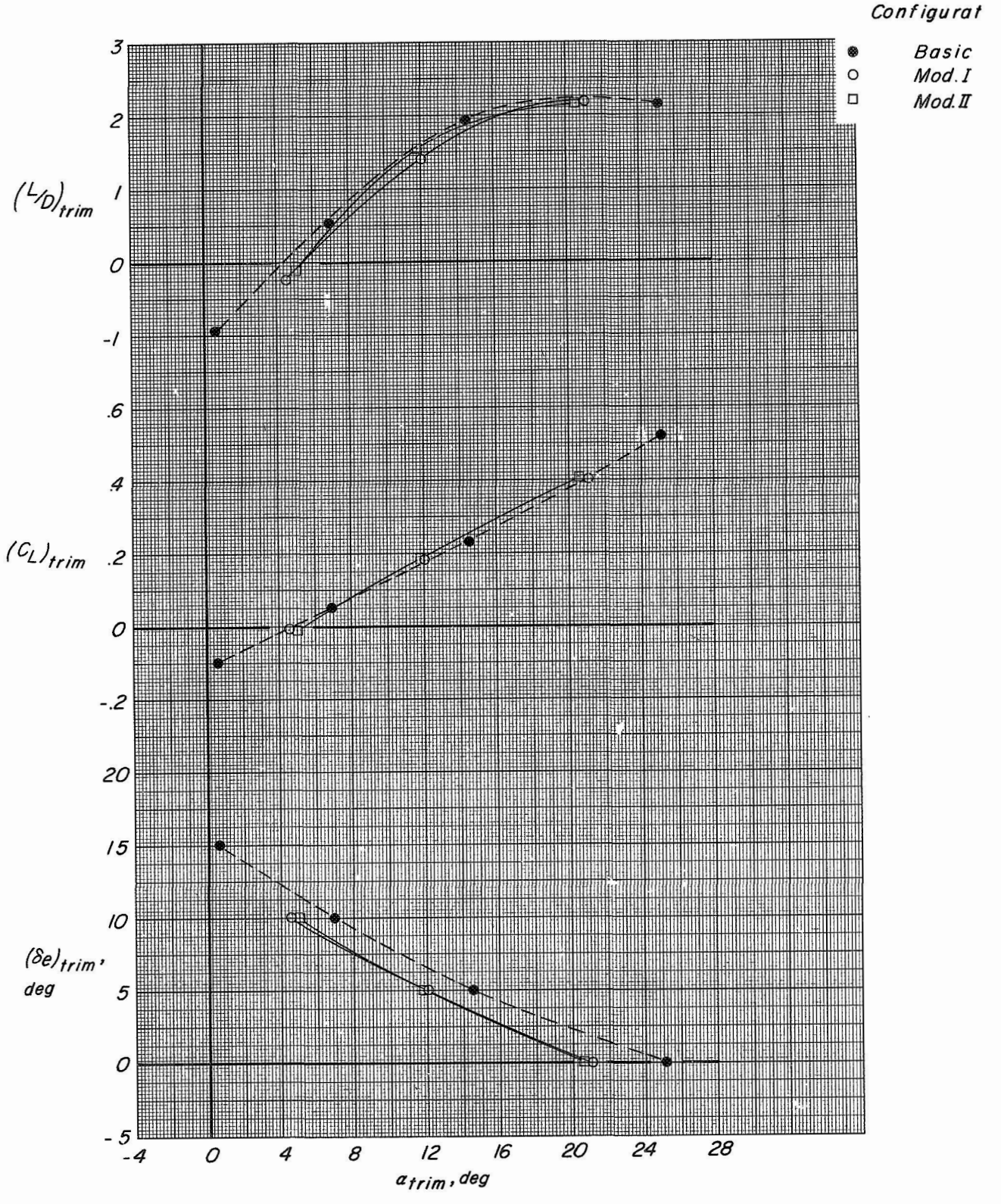
(b) M = 0.70.

Figure 75.- Continued.



(c) M = 0.80.

Figure 75.- Continued.



(d) M = 0.90.

Figure 75.- Concluded.

NASA-Langley, 1971 —— 1 L-743

NATIONAL AERONAUTICS AND SPACE ADMINISTRATION
WASHINGTON, D. C. 20546
OFFICIAL BUSINESS

FIRST CLASS MAIL

POSTAGE AND FE
NATIONAL AERONAU
SPACE ADMINISTR

POSTMASTER: If Undeliverable (Se
Postal Manual) Do

"The aeronautical and space activities of the United States shall be conducted so as to contribute . . . to the expansion of human knowledge of phenomena in the atmosphere and space. The Administration shall provide for the widest practicable and appropriate dissemination of information concerning its activities and the results thereof."

—NATIONAL AERONAUTICS AND SPACE ACT OF 1958

NASA SCIENTIFIC AND TECHNICAL PUBLICATIONS

TECHNICAL REPORTS: Scientific and technical information considered important, complete, and a lasting contribution to existing knowledge.

TECHNICAL NOTES: Information less broad in scope but nevertheless of importance as a contribution to existing knowledge.

TECHNICAL MEMORANDUMS: Information receiving limited distribution because of preliminary data, security classification, or other reasons.

CONTRACTOR REPORTS: Scientific and technical information generated under a NASA contract or grant and considered an important contribution to existing knowledge.

TECHNICAL TRANSLATIONS: Information published in a foreign language considered to merit NASA distribution in English.

SPECIAL PUBLICATIONS: Information derived from or of value to NASA activities. Publications include conference proceedings, monographs, data compilations, handbooks, sourcebooks, and special bibliographies.

TECHNOLOGY UTILIZATION PUBLICATIONS: Information on technology used by NASA that may be of particular interest in commercial and other non-aerospace applications. Publications include Tech Briefs, Technology Utilization Reports and Technology Surveys.

Details on the availability of these publications may be obtained from:

SCIENTIFIC AND TECHNICAL INFORMATION DIVISION
NATIONAL AERONAUTICS AND SPACE ADMINISTRATION
Washington, D.C. 20546